# Scientific and Technical Aerospace Reports

## Volume 39
## December 28, 2001

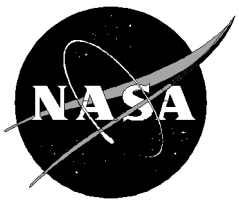


National Aeronautics and Space Administration
**Langley Research Center**

**Scientific and Technical Information Program Office**

# The NASA STI Program Office . . . in Profile

Since its founding, NASA has been dedicated to the advancement of aeronautics and space science. The NASA Scientific and Technical Information (STI) Program Office plays a key part in helping NASA maintain this important role.

The NASA STI Program Office is operated by Langley Research Center, the lead center for NASA's scientific and technical information. The NASA STI Program Office provides access to the NASA STI Database, the largest collection of aeronautical and space science STI in the world. The Program Office is also NASA's institutional mechanism for disseminating the results of its research and development activities. These results are published by NASA in the NASA STI Report Series, which includes the following report types:

- TECHNICAL PUBLICATION. Reports of completed research or a major significant phase of research that present the results of NASA programs and include extensive data or theoretical analysis. Includes compilations of significant scientific and technical data and information deemed to be of continuing reference value. NASA's counterpart of peer-reviewed formal professional papers but has less stringent limitations on manuscript length and extent of graphic presentations.

- TECHNICAL MEMORANDUM. Scientific and technical findings that are preliminary or of specialized interest, e.g., quick release reports, working papers, and bibliographies that contain minimal annotation. Does not contain extensive analysis.

- CONTRACTOR REPORT. Scientific and technical findings by NASA-sponsored contractors and grantees.

- CONFERENCE PUBLICATION. Collected papers from scientific and technical conferences, symposia, seminars, or other meetings sponsored or cosponsored by NASA.

- SPECIAL PUBLICATION. Scientific, technical, or historical information from NASA programs, projects, and missions, often concerned with subjects having substantial public interest.

- TECHNICAL TRANSLATION. English-language translations of foreign scientific and technical material pertinent to NASA's mission.

Specialized services that complement the STI Program Office's diverse offerings include creating custom thesauri, building customized databases, organizing and publishing research results . . . even providing videos.

For more information about the NASA STI Program Office, see the following:

- Access the NASA STI Program Home Page at ***http://www.sti.nasa.gov***

- E-mail your question via the Internet to help@sti.nasa.gov

- Fax your question to the NASA STI Help Desk at (301) 621-0134

- Telephone the NASA STI Help Desk at (301) 621-0390

- Write to:
  NASA STI Help Desk
  NASA Center for AeroSpace Information
  7121 Standard Drive
  Hanover, MD 21076-1320

# Introduction

*Scientific and Technical Aerospace Reports (STAR)* is an electronic abstract journal, listing citations with abstracts for aerospace-related reports obtained from worldwide sources. It is electronically published biweekly and announces documents that have recently been entered into the NASA Scientific and Technical Information (STI) Database. The documents are of the following types:

- NASA, NASA contractor, and NASA grantee reports;
- Reports issued by other U.S. Government agencies, domestic and foreign institutions, universities, and private firms;
- Translations in report form;
- NASA-owned patents and patent applications
- Other U.S. Government agency and foreign patents and patent applications
- Domestic and foreign dissertations and theses.

Also included are two indexes, Subject Term and Personal Author. The Subject Term Index is generated from the *NASA Thesaurus* terms associated and listed with each document.

*STAR* subject coverage includes all aspects of aeronautics and space research and development, supporting basic and applied research, and applications. Aerospace aspects of Earth resources, energy development, conservation, oceanography, environmental protection, urban transportation, and other topics of high national priority are also covered.

Abstracts in *STAR* are categorized by 10 major subject divisions that are divided further into 76 specific subject categories. The subject divisions and categories are listed in the Table of Contents together with a note for each that defines its scope and provides any cross-references.

# *SCAN Goes Electronic!*

If you have electronic mail or if you can access the Internet, you can view biweekly issues of *SCAN* from your desktop absolutely free!

*Electronic SCAN* takes advantage of computer technology to inform you of the latest worldwide, aerospace-related, scientific and technical information that has been published.

No more waiting while the paper copy is printed and mailed to you. You can view *Electronic SCAN* the same day it is released—up to 191 topics to browse at your leisure. When you locate a publication of interest, you can print the announcement. You can also go back to the *Electronic SCAN* home page and follow the ordering instructions to quickly receive the full document.

Start your access to *Electronic SCAN* today. Over 1,000 announcements of new reports, books, conference proceedings, journal articles...and more—available to your computer every two weeks.

For Internet access to *E-SCAN*, use any of the following addresses:

**http://www.sti.nasa.gov**
**ftp.sti.nasa.gov**
**gopher.sti.nasa.gov**

Determine the SCAN topics you wish to receive and send an e-mail to **listserv@sti.nasa.gov**. Leave the subject line blank and enter a subscribe command, denoting which topic you want and your name in the message area, formatted as follows:

**Subscribe SCAN–02–01 Jane Doe**

For additional information, e-mail a message to **help@sti.nasa.gov**.

Phone: (301) 621-0390

Fax: (301) 621-0134

Write: NASA STI Help Desk
NASA Center for AeroSpace Information
7121 Standard Drive
Hanover, MD 21076-1320

**Looking just for *Aerospace Medicine and Biology* reports?**

Although hard copy distribution has been discontinued, you can still receive these vital announcements through your *E-SCAN* subscription. Just **Subscribe SCAN-AEROMED Jane Doe** in the message area of your e-mail to **listserv@sti.nasa.gov**.

# Table of Contents

## Subject Divisions

Document citations are grouped first by the following divisions. Select a division title to view the category-level Table of Contents.


A. Aeronautics
B. Astronautics
C. Chemistry and Materials
D. Engineering
E. Geosciences
F. Life Sciences
G. Mathematical and Computer Sciences
H. Physics
I. Social and Information Sciences
J. Space Sciences
K. General


## Indexes

Two indexes are available. You may use the find command under the tools menu while viewing the PDF file for direct match searching on any text string. You may also select either of the two indexes provided for searching on *NASA Thesaurus* subject terms and personal author names.


Subject Term Index
Personal Author Index


## Document Availability

Select **Availability Info** for important information about NASA Scientific and Technical Information (STI) Program Office products and services, including registration with the NASA Center for AeroSpace Information (CASI) for access to the NASA CASI TRS (Technical Report Server), and availability and pricing information for cited documents.

# Subject Categories of the Division A. Aeronautics

Select a category to view the collection of records cited. N.A. means no abstracts in that category.


## 01 Aeronautics (General) 1

Includes general research topics related to manned and unmanned aircraft and the problems of flight within the Earth's atmosphere. Also includes manufacturing, maintenance, and repair of aircraft. For specific topics in aeronautics see *categories 02 through 09*. For information related to space vehicles see *12 Astronautics*.

## 02 Aerodynamics 2

Includes aerodynamics of flight vehicles, test bodies, airframe components and combinations, wings, and control surfaces. Also includes aerodynamics of rotors, stators, fans and other elements of turbomachinery. For related information, see also *34 Fluid Mechanics and Heat Transfer.*

## 03 Air Transportation and Safety 7

Includes passenger and cargo air transport operations; aircraft ground operations; flight safety and hazards; and aircraft accidents. Systems and hardware specific to ground operations of aircraft and to airport construction are covered in *09 Research and Support Facilities (Air)*. Air traffic control is covered in *04 Aircraft Communications and Navigation*. For related information see also *16 Space Transportation and Safety*; and *85 Technology Utilization and Surface Transportation.*

## 04 Aircraft Communications and Navigation 14

Includes all modes of communication with and between aircraft; air navigation systems (satellite and ground based); and air traffic control. For related information see also *06 Avionics and Aircraft Instrumentation*; *17 Space Communications; Spacecraft Communications, Command and Tracking*, and *32 Communications and Radar.*

## 05 Aircraft Design, Testing and Performance 15

Includes all stages of design of aircraft and aircraft structures and systems. Also includes aircraft testing, performance, and evaluation, and aircraft and flight simulation technology. For related information, see also *18 Spacecraft Design, Testing and Performance* and *39 Structural Mechanics*. For land transportation vehicles, see *85 Technology Utilization and Surface Transportation*.

## 07 Aircraft Propulsion and Power 20

Includes prime propulsion systems and systems components, e.g., gas turbine engines and compressors; and onboard auxiliary power plants for aircraft. For related information see also *20 Spacecraft Propulsion and Power, 28 Propellants and Fuels*, and *44 Energy Production and Conversion.*

## 08 Aircraft Stability and Control 22

Includes flight dynamics, aircraft handling qualities; piloting; flight controls; and autopilots. For related information, see also *05 Aircraft Design, Testing and Performance* and *06 Avionics and Aircraft Instrumentation*.

## 09 Research and Support Facilities (Air) 23

Includes airports, runways, hangers, and aircraft repair and overhaul facilities, wind tunnels, water tunnels, and shock tubes; flight simulators; and aircraft engine test stands. Also includes airport ground equipment and systems. For airport ground operation see *03 Air Transportation and Safety.* For astronautical facilities see *14 Ground Support Systems and Facilities (Space).*

# Subject Categories of the Division B. Astronautics

Select a category to view the collection of records cited. N.A. means no abstracts in that category.

## 12 Astronautics (General) 23

Includes general research topics related to space flight and manned and unmanned space vehicles, platforms or objects launched into, or assembled in, outer space; and related components and equipment. Also includes manufacturing and maintenance of such vehicles or platforms. For specific topics in astronautics see *categories 13 through 20.* For extraterrestrial exploration, see *91 Lunar and Planetary Science and Exploration*.

## 14 Ground Support Systems and Facilities (Space) 27

Includes launch complexes, research and production facilities; ground support equipment, e.g., mobile transporters; and test chambers and simulators. Also includes extraterrestrial bases and supporting equipment. For related information see also *09 Research and Support Facilities (Air).*

## 15 Launch Vehicles and Launch Operations 28

Includes all classes of launch vehicles, launch/space vehicle systems, and boosters; and launch operations. For related information see also *18 Spacecraft Design, Testing, and Performance; and 20 Spacecraft Propulsion and Power.*

## 16 Space Transportation and Safety 29

Includes passenger and cargo space transportation, e.g., shuttle operations; and space rescue techniques. For related information, see also *03 Air Transportation and Safety* and *15 Launch Vehicles and Launch Vehicles,* and *18 Spacecraft Design, Testing and Performance*. For space suits, see *54 Man/System Technology and Life Support*.

## 17 Space Communications, Spacecraft Communications, Command and Tracking 29

Includes space systems telemetry; space communications networks; astronavigation and guidance; and spacecraft radio blackout. For related information, see also *04 Aircraft Communications and Navigation* and *32 Communications and Radar.*

### 18 Spacecraft Design, Testing and Performance 30

Includes satellites; space platforms; space stations; spacecraft systems and components such as thermal and environmental controls; and spacecraft control and stability characteristics. For life support systems, see *54 Man/System Technology and Life Support*. For related information, see also *05 Aircraft Design, Testing and Performance*, *39 Structural Mechanics, and 16 Space Transportation and Safety.*

### 19 Spacecraft Instrumentation and Astrionics 30

Includes the design, manufacture, or use of devices for the purpose of measuring, detecting, controlling, computing, recording, or processing data related to the operation of space vehicles or platforms. For related information, see also *06 Aircraft Instrumentation and Avionics;* For spaceborne instruments not integral to the vehicle itself see *35 Instrumentation and Photography*; For spaceborne telescopes and other astronomical instruments see *89 Astronomy, Instrumentation and Photography*; For spaceborne telescopes and other astronomical instruments see *89 Astronomy.*

### 20 Spacecraft Propulsion and Power 31

Includes main propulsion systems and components, e.g., rocket engines; and spacecraft auxiliary power sources. For related information, see also *07 Aircraft Propulsion and Power; 28 Propellants and Fuels; 15 Launch Vehicles and Launch Operations;* and *44 Energy Production and Conversion*.


## Subject Categories of the Division C. Chemistry and Materials

Select a category to view the collection of records cited. N.A. means no abstracts in that category.


### 23 Chemistry and Materials (General) 32

Includes general research topics related to the composition, properties, structure, and use of chemical compounds and materials as they relate to aircraft, launch vehicles, and spacecraft. For specific topics in chemistry and materials see *categories 24 through 29*. For astrochemistry see category *90 Astrophysics*.

### 24 Composite Materials 49

Includes physical, chemical, and mechanical properties of laminates and other composite materials.

### 25 Inorganic, Organic, and Physical Chemistry 55

Includes the analysis, synthesis, and use inorganic and organic compounds; combustion theory; electrochemistry; and photochemistry. For related information see also *34 Fluid Dynamics and Thermodynamics, For astrochemistry see category 90 Astrophysics*.

### 26 Metals and Metallic Materials 92

Includes physical, chemical, and mechanical properties of metals and metallic materials; and metallurgy.

### 27 Nonmetallic Materials 114

Includes physical, chemical, and mechanical properties of plastics, elastomers, lubricants, polymers, textiles, adhesives, and ceramic materials. For composite materials see *24 Composite Materials.*

### 28 Propellants and Fuels 131

Includes rocket propellants, igniters and oxidizers; their storage and handling procedures; and aircraft fuels. For nuclear fuels see *73 Nuclear Physics*. For related information see also *07 Aircraft Propulsion and Power, 20 Spacecraft Propulsion and Power,* and *44 Energy Production and Conversion*.

### 29 Space Processing 154

Includes space-based development of materials, compounds, and processes for research or commercial application. Also includes the development of materials and compounds in simulated reduced–gravity environments. For legal aspects of space commercialization see *84 Law, Political Science and Space Policy.*


## Subject Categories of the Division D. Engineering

Select a category to view the collection of records cited. N.A. means no abstracts in that category.


### 31 Engineering (General) 155

Includes general research topics to engineering and applied physics, and particular areas of vacuum technology, industrial engineering, cryogenics, and fire prevention. For specific topics in engineering see *categories 32 through 39*.

### 32 Communications and Radar 162

Includes radar; radio, wire, and optical communications; land and global communications; communications theory. For related information see also *04 Aircraft Communications and Navigation;* and *17 Space Communications, Spacecraft Communications, Command and Tracking;* for search and rescue see *03 Air Transportation and Safety,* and *16 Space Transportation and Safety.*

### 33 Electronics and Electrical Engineering 172

Includes development, performance, and maintainability of electrical/electronic devices and components; related test equipment. and microelectronics and integrated circuitry. For related information see also *60 Computer Operations and Hardware;* and *76 Solid-State Physics*. For communications equipment and devices see *32 Communications and Radar.*

### 34 Fluid Mechanics and Thermodynamics 186

Includes fluid dynamics and kinematics and all forms of heat transfer; boundary layer flow; hydrodynamics; hydraulics; fluidics; mass transfer and ablation cooling. For related information see also *02 Aerodynamics.*

## 35 Instrumentation and Photography 200

Includes remote sensors; measuring instruments and gauges; detectors; cameras and photographic supplies; and holography. For aerial photography see *43 Earth Resources and Remote Sensing*. For related information see also *06 Avionics and Aircraft Instrumentation;* and *19 Spacecraft Instrumentation*.

## 36 Lasers and Masers 208

Includes lasing theory, laser pumping techniques, maser amplifiers, laser materials, and the assessment of laser and maser outputs. For cases where the application of the laser or maser is emphasized see also the specific category where the application is treated. For related information see also *76 Solid-State Physics*.

## 37 Mechanical Engineering 213

Includes mechanical devices and equipment; machine elements and processes. For cases where the application of a device or the host vehicle is emphasized see also the specific category where the application or vehicle is treated. For robotics see *63 Cybernetics, Artificial Intelligence, and Robotics*; and *54 Man/System Technology and Life Support*.

## 38 Quality Assurance and Reliability 219

Includes approaches to, and methods for reliability analysis and control, inspection, maintainability, and standardization.

## 39 Structural Mechanics 222

Includes structural element design, analysis and testing; dynamic responses of structures; weight analysis; fatigue and other structural properties; and mechanical and thermal stresses in structure. For applications see *05 Aircraft Design, Testing and Performance* and *18 Spacecraft Design, Testing and Performance*.


# Subject Categories of the Division E. Geosciences

Select a category to view the collection of records cited. N.A. means no abstracts in that category.


## 42 Geosciences (General) 225

Includes general research topics related to the Earth sciences, and the specific areas of petrology, minerology, and general geology. For other specific topics in geosciences see *categories 42 through 48*.

## 43 Earth Resources and Remote Sensing 239

Includes remote sensing of earth features, phenomena and resources by aircraft, balloon, rocket, and spacecraft; analysis or remote sensing data and imagery; development of remote sensing products; photogrammetry; and aerial photographs. For instrumentation see *35 Instrumentation and Photography.*

### 44 Energy Production and Conversion 244

Includes specific energy conversion systems, e.g., fuel cells; and solar, geothermal, windpower, and waterwave conversion systems; energy storage; and traditional power generators. For technologies related to nuclear energy production see *73 Nuclear Physics*. For related information see also *07 Aircraft Propulsion and Power; 20 Spacecraft Propulsion and Power,* and *28 Propellants and Fuels*.

### 45 Environment Pollution 271

Includes atmospheric, water, soil, noise, and thermal pollution.

### 46 Geophysics 287

Includes earth structure and dynamics, aeronomy; upper and lower atmosphere studies; ionospheric and magnetospheric physics; and geomagnetism. For related information see *47 Meteorology and Climatology;* and *93 Space Radiation*.

### 47 Meteorology and Climatology 293

Includes weather observation forecasting and modification.

### 48 Oceanography 303

Includes the physical, chemical and biological aspects of oceans and seas; ocean dynamics, and marine resources. For related information see also *43 Earth Resources and Remote Sensing*.


## Subject Categories of the Division F. Life Sciences

Select a category to view the collection of records cited. N.A. means no abstracts in that category.


### 51 Life Sciences (General) 307

Includes general research topics related to plant and animal biology (non–human); ecology; microbiology; and also the origin, development, structure, and maintenance, of animals and plants in space and related environmental conditions. For specific topics in life sciences see *categories 52 through 55*.

### 52 Aerospace Medicine 320

Includes the biological and physiological effects of atmospheric and space flight (weightlessness, space radiation, acceleration, and altitude stress) on the human being; and the prevention of adverse effects on those environments. For psychological and behavioral effects of aerospace environments see *53 Behavioral Sciences*. For the effects of space on animals and plants see *51 Life Sciences*.

### 53 Behavioral Sciences 327

Includes psychological factors; individual and group behavior; crew training and evaluation; and psychiatric research.

**54 Man/System Technology and Life Support 331**

Includes human factors engineering; bionics, man–machine, life support, space suits and protective clothing. For related information see also *16 Space Transportation* and *52 Aerospace Medicine*.

## Subject Categories of the Division G. Mathematical and Computer Sciences

Select a category to view the collection of records cited. N.A. means no abstracts in that category.

**59 Mathematical and Computer Sciences (General) 335**

Includes general topics and overviews related to mathematics and computer science. For specific topics in these areas see *categories 60 through 67*.

**60 Computer Operations and Hardware 340**

Includes hardware for computer graphics, firmware and data processing. For components see *33 Electronics and Electrical Engineering*. For computer vision see *63 Cybernetics, Artificial Intelligence and Robotics*.

**61 Computer Programming and Software 341**

Includes software engineering, computer programs, routines, algorithms, and specific applications, e.g., CAD/CAM. For computer software applied to specific applications, see also the associated category.

**62 Computer Systems 359**

Includes computer networks and distributed processing systems. For information systems see *82 Documentation and Information Science*. For computer systems applied to specific applications, see the associated category.

**63 Cybernetics, Artificial Intelligence and Robotics 362**

Includes feedback and control theory, information theory, machine learning, and expert systems. For related information see also *54 Man/System Technology and Life Support*.

**64 Numerical Analysis 366**

Includes iteration, differential and difference equations, and numerical approximation.

**65 Statistics and Probability 369**

Includes data sampling and smoothing; Monte Carlo method; time series and analysis; and stochastic processes.

**67 Theoretical Mathematics 371**

Includes algebra, functional analysis, geometry, topology set theory, group theory and and number theory.

# Subject Categories of the Division H. Physics

Select a category to view the collection of records cited. N.A. means no abstracts in that category.


## 70 Physics (General) 372

Includes general research topics related to mechanics, kinetics, magnetism, and electrodynamics. For specific areas of physics see *categories 71 through 77*. For related instrumentation see *35 Instrumentation and Photography;* for geophysics, astrophysics or solar physics see *46 Geophysics, 90 Astrophysics,* or *92 Solar Physics*.

## 71 Acoustics 407

Includes sound generation, transmission, and attenuation. For noise pollution see *45 Environment Pollution.* For aircraft noise see also *02 Aerodynamics* and *07 Aircraft Propulsion Propulsion and Power.*

## 72 Atomic and Molecular Physics 411

Includes atomic and molecular structure, electron properties, and atomic and molecular spectra. For elementary particle physics see *73 Nuclear Physics*.

## 73 Nuclear Physics 416

Includes nuclear particles; and reactor theory. For space radiation see *93 Space Radiation*. For atomic and molecular physics see *72 Atomic and Molecular Physics*. For elementary particle physics see *77 Physics of Elementary Particles and Fields*. For nuclear astrophysics see *90 Astrophysics*.

## 74 Optics 428

Includes light phenomena and the theory of optical devices. For lasers see *36 Lasers and Masers*.

## 75 Plasma Physics 443

Includes magnetohydrodynamics and plasma fusion. For ionospheric plasmas see *46 Geophysics.* For space plasmas see *90 Astrophysics*.

## 76 Solid-State Physics 454

Includes condensed matter physics, crystallography, and superconductivity. For related information see also *33 Electronics and Electrical Engineering* and *36 Lasers and Masers*.

## 77 Physics of Elementary Particles and Fields 488

Includes quantum mechanics; theoretical physics; and statistical mechanics. For related information see also *72 Atomic and Molecular Physics, 73 Nuclear Physics, and 25 Inorganic, Organic and Physical Chemistry.*

## Subject Categories of the Division I. Social and Information Sciences

Select a category to view the collection of records cited. N.A. means no abstracts in that category.


**80 Social and Information Sciences (General) 540**

Includes general research topics related to sociology; educational programs and curricula.

**81 Administration and Management 542**

Includes management planning and research.

**82 Documentation and Information Science 546**

Includes information management; information storage and retrieval technology; technical writing; graphic arts; and micrography. For computer documentation see *61 Computer Programming and Software*.

**83 Economics and Cost Analysis 554**

Includes cost effectiveness studies.

**84 Law, Political Science and Space Policy 554**

Includes aviation law; space law and policy; international law; international cooperation; and patent policy.


## Subject Categories of the Division J. Space Sciences

Select a category to view the collection of records cited. N.A. means no abstracts in that category.


**88 Space Sciences (General) 556**

Includes general research topics related to the natural space sciences. For specific topics in space sciences see *categories 89 through 93*.

**89 Astronomy 557**

Includes observations of celestial bodies, astronomical instruments and techniques; radio, gamma-ray, x–ray, ultraviolet, and infrared astronomy; and astrometry.

**90 Astrophysics 560**

Includes cosmology; celestial mechanics; space plasmas; and interstellar and interplanetary gases and dust.

**91 Lunar and Planetary Science and Exploration 567**

Includes planetology; selenology; meteorites; comets; and manned and unmanned planetary and lunar flights. For spacecraft design or space stations see *18 Spacecraft Design, Testing and Performance*.

## 92 Solar Physics 599

Includes solar activity, solar flares, solar radiation and sunspots. For related information see *93 Space Radiation.*

## 93 Space Radiation 600

Includes cosmic radiation; and inner and outer Earth radiation belts. For biological effects of radiation on plants and animals see *52 Aerospace Medicine*. For theory see *73 Nuclear Physics.*


# Subject Categories of the Division K. General

Select a category to view the collection of records cited. N.A. means no abstracts in that category.


## 99 General 600

Includes aeronautical, astronautical, and space science related histories, biographies, and pertinent reports too broad for categorization; histories or broad overviews of NASA programs such as Apollo, Gemini, and Mercury spacecraft, Earth Resources Technology Satellite (ERTS), and Skylab; NASA appropriations hearings.

# Document Availability Information

The mission of the NASA Scientific and Technical (STI) Program Office is to quickly, efficiently, and cost-effectively provide the NASA community with desktop access to STI produced by NASA and the world's aerospace industry and academia. In addition, we will provide the aerospace industry, academia, and the taxpayer access to the intellectual scientific and technical output and achievements of NASA.

## Eligibility and Registration for NASA STI Products and Services

The NASA STI Program offers a wide variety of products and services to achieve its mission. Your affiliation with NASA determines the level and type of services provided by the NASA STI Program. To assure that appropriate level of services are provided, NASA STI users are requested to register at the NASA Center for AeroSpace Information (CASI). Please contact NASA CASI in one of the following ways:

| | |
|---|---|
| E-mail: | help@sti.nasa.gov |
| Fax: | 301-621-0134 |
| Phone: | 301-621-0390 |
| Mail: | ATTN: Registration Services<br>NASA Center for AeroSpace Information<br>7121 Standard Drive<br>Hanover, MD 21076-1320 |

## Limited Reproducibility

In the database citations, a note of limited reproducibility appears if there are factors affecting the reproducibility of more than 20 percent of the document. These factors include faint or broken type, color photographs, black and white photographs, foldouts, dot matrix print, or some other factor that limits the reproducibility of the document. This notation also appears on the microfiche header.

## NASA Patents and Patent Applications

Patents owned by NASA are announced in the STI Database. Printed copies of patents (which are not microfiched) are available for purchase from the U.S. Patent and Trademark Office.

When ordering patents, the U.S. Patent Number should be used, and payment must be remitted in advance, by money order or check payable to the Commissioner of Patents and Trademarks. Prepaid purchase coupons for ordering are also available from the U.S. Patent and Trademark Office.

Patents and patent applications owned by NASA are available for licensing. Requests for licensing terms and further information should be addressed to:

National Aeronautics and Space Administration
Associate General Counsel for Intellectual Property
Code GP
Washington, DC 20546-0001

## Sources for Documents

One or more sources from which a document announced in the STI Database is available to the public is ordinarily given on the last line of the citation. The most commonly indicated sources and their acronyms or abbreviations are listed below, with an Addresses of Organizations list near the back of this section. If the publication is available from a source other than those listed, the publisher and his address will be displayed on the availability line or in combination with the corporate source.

Avail: NASA CASI. Sold by the NASA Center for AeroSpace Information. Prices for hard copy (HC) and microfiche (MF) are indicated by a price code following the letters HC or MF in the citation. Current values are given in the NASA CASI Price Code Table near the end of this section.

*Note on Ordering Documents: When ordering publications from NASA CASI, use the document ID number or other report number. It is also advisable to cite the title and other bibliographic identification.*

Avail: SOD (or GPO). Sold by the Superintendent of Documents, U.S. Government Printing Office, in hard copy.

Avail: BLL (formerly NLL): British Library Lending Division, Boston Spa, Wetherby, Yorkshire, England. Photocopies available from this organization at the price shown. (If none is given, inquiry should be addressed to the BLL.)

Avail: DOE Depository Libraries. Organizations in U.S. cities and abroad that maintain collections of Department of Energy reports, usually in microfiche form, are listed in Energy Research Abstracts. Services available from the DOE and its depositories are described in a booklet, *DOE Technical Information Center—Its Functions and Services* (TID-4660), which may be obtained without charge from the DOE Technical Information Center.

Avail: ESDU. Pricing information on specific data, computer programs, and details on ESDU International topic categories can be obtained from ESDU International.

Avail: Fachinformationszentrum Karlsruhe. Gesellschaft für wissenschaftlich-technische Information mbH 76344 Eggenstein-Leopoldshafen, Germany.

Avail: HMSO. Publications of Her Majesty's Stationery Office are sold in the U.S. by Pendragon House, Inc. (PHI), Redwood City, CA. The U.S. price (including a service and mailing charge) is given, or a conversion table may be obtained from PHI.

Avail: Issuing Activity, or Corporate Author, or no indication of availability. Inquiries as to the availability of these documents should be addressed to the organization shown in the citation as the corporate author of the document.

Avail: NASA Public Document Rooms. Documents so indicated may be examined at or purchased from the National Aeronautics and Space Administration (JBD-4), Public Documents Room (Room 1H23), Washington, DC 20546-0001, or public document rooms located at NASA installations, and the NASA Pasadena Office at the Jet Propulsion Laboratory.

Avail: NTIS. Sold by the National Technical Information Service. Initially distributed microfiche under the NTIS SRIM (Selected Research in Microfiche) are available. For information concerning this service, consult the NTIS Subscription Section, Springfield, VA 22161.

Avail: Univ. Microfilms. Documents so indicated are dissertations selected from Dissertation Abstracts and are sold by University Microfilms as xerographic copy (HC) and microfilm. All requests should cite the author and the Order Number as they appear in the citation.

Avail: US Patent and Trademark Office. Sold by Commissioner of Patents and Trademarks, U.S. Patent and Trademark Office, at the standard price of $1.50 each, postage free.

Avail: (US Sales Only). These foreign documents are available to users within the United States from the National Technical Information Service (NTIS). They are available to users outside the United States through the International Nuclear Information Service (INlS) representative in their country, or by applying directly to the issuing organization.

Avail: USGS. Originals of many reports from the U.S. Geological Survey, which may contain color illustrations, or otherwise may not have the quality of illustrations preserved in the microfiche or facsimile reproduction, may be examined by the public at the libraries of the USGS field offices whose addresses are listed on the Addresses of Organizations page. The libraries may be queried concerning the availability of specific documents and the possible utilization of local copying services, such as color reproduction.

# Addresses of Organizations

British Library Lending Division
Boston Spa, Wetherby, Yorkshire
England

Commissioner of Patents and Trademarks
U.S. Patent and Trademark Office
Washington, DC 20231

Department of Energy
Technical Information Center
P.O. Box 62
Oak Ridge, TN 37830

European Space Agency–
Information Retrieval Service ESRIN
Via Galileo Galilei
00044 Frascati (Rome) Italy

ESDU International
27 Corsham Street
London
N1 6UA
England

Fachinformationszentrum Karlsruhe
Gesellschaft für wissenschaftlich–technische
Information mbH
76344 Eggenstein–Leopoldshafen, Germany

Her Majesty's Stationery Office
P.O. Box 569, S.E. 1
London, England

NASA Center for AeroSpace Information
7121 Standard Drive
Hanover, MD 21076-1320

(NASA STI Lead Center)
National Aeronautics and Space Administration
Scientific and Technical Information Program Office
Langley Research Center – MS157
Hampton, VA 23681

National Technical Information Service
5285 Port Royal Road
Springfield, VA 22161

Pendragon House, Inc.
899 Broadway Avenue
Redwood City, CA 94063

Superintendent of Documents
U.S. Government Printing Office
Washington, DC 20402

University Microfilms
A Xerox Company
300 North Zeeb Road
Ann Arbor, MI 48106

University Microfilms, Ltd.
Tylers Green
London, England

U.S. Geological Survey Library National Center
MS 950
12201 Sunrise Valley Drive
Reston, VA 22092

U.S. Geological Survey Library
2255 North Gemini Drive
Flagstaff, AZ 86001

U.S. Geological Survey
345 Middlefield Road
Menlo Park, CA 94025

U.S. Geological Survey Library
Box 25046
Denver Federal Center, MS914
Denver, CO 80225

# *NASA CASI Price Tables — Effective October 1, 2001*
## *Prices are subject to change without notice*

| *Hardcopy & Microfiche Prices* | | | |
|---|---|---|---|
| *Code* | *NASA* | *U.S.** | *International** |
| A01 | $9.50 | $9.50 | $19.00 |
| A02 | $13.50 | $14.50 | $29.00 |
| A03 | $24.50 | $27.50 | $55.00 |
| A04 | $27.00 | $30.50 | $61.00 |
| A05 | $28.50 | $32.50 | $65.00 |
| A06 | $31.00 | $35.50 | $71.00 |
| A07 | $34.50 | $39.50 | $79.00 |
| A08 | $37.50 | $43.00 | $86.00 |
| A09 | $42.50 | $49.00 | $98.00 |
| A10 | $45.50 | $53.00 | $106.00 |
| A11 | $48.50 | $56.50 | $113.00 |
| A12 | $52.50 | $61.00 | $122.00 |
| A13 | $55.50 | $65.00 | $130.00 |
| A14 | $57.50 | $67.00 | $134.00 |
| A15 | $59.50 | $69.50 | $139.00 |
| A16 | $61.50 | $72.00 | $144.00 |
| A17 | $63.50 | $74.50 | $149.00 |
| A18 | $67.00 | $78.50 | $157.00 |
| A19 | $69.00 | $81.00 | $162.00 |
| A20 | $71.00 | $83.50 | $167.00 |
| A21 | $73.00 | $86.00 | $172.00 |
| A22 | $78.50 | $92.50 | $185.00 |
| A23 | $80.50 | $95.00 | $190.00 |
| A24 | $82.50 | $97.00 | $194.00 |
| A25 | $84.50 | $99.50 | $199.00 |
| A99 | Contact NASA CASI | | |

| *Exception Prices* | | | |
|---|---|---|---|
| *Code* | *NASA* | *U.S.** | *International** |
| E01 | $102.50 | $121.00 | $242.00 |
| E02 | $111.00 | $131.50 | $263.00 |
| E03 | $120.50 | $143.00 | $286.00 |
| E04 | $130.00 | $154.00 | $308.00 |
| E05 | $139.50 | $165.50 | $331.00 |
| E06 | $148.00 | $176.00 | $352.00 |
| E07 | $157.50 | $187.00 | $374.00 |
| E08 | $167.00 | $198.50 | $397.00 |
| E09 | $175.50 | $209.00 | $418.00 |
| E10 | $185.00 | $220.00 | $440.00 |
| E11 | $194.50 | $231.50 | $463.00 |
| E12 | $202.50 | $241.00 | $482.00 |
| E13 | $212.00 | $252.50 | $505.00 |
| E14 | $221.50 | $264.00 | $528.00 |
| E15 | $231.00 | $275.50 | $551.00 |
| E16 | $239.50 | $285.50 | $571.00 |
| E17 | $249.00 | $297.00 | $594.00 |
| E18 | $258.50 | $308.50 | $617.00 |
| E19 | $267.00 | $318.50 | $637.00 |
| E20 | $276.50 | $330.00 | $660.00 |
| E21 | $286.00 | $341.50 | $683.00 |
| E22 | $294.50 | $351.50 | $703.00 |
| E23 | $304.00 | $363.00 | $726.00 |
| E24 | $313.50 | $374.50 | $749.00 |
| E99 | Free | Free | Free |

### *NASA Prices:*
**For NASA libraries, NASA Employees & NASA contractors registered at NASA CASI.**

### *U.S. Prices:*
**For users within the U.S.**

### *International Prices:*
**For users outside the U.S. and International Embassies within the U.S.**

### *Processing*
**Standard N/A**
**(most orders are processed within three (3) business days, then shipped)**

**Rush**
**$10.00 per item**
**(orders are processed within one (1) business day, then shipped)**

### *Shipping & Handling Fees: per item*
**Standard (USPS Priority)**
**$2.00 U.S.**
**(delivered within 2-3 business days)**

**$7.00 International**
**(delivered within 4-7 business days)**

**USPS Express (U.S. only)**
**$13.00**
**(1-day delivery service to most destinations)**

**Fax (Up to 30 pages,**
**$16.50 U.S.**
**$24.00 International**

**Federal Express**
**User's Account Only _____**

## Federal Depository Library Program

In order to provide the general public with greater access to U.S. Government publications, Congress established the Federal Depository Library Program under the Government Printing Office (GPO), with 53 regional depositories responsible for permanent retention of material, inter-library loan, and reference services. At least one copy of nearly every NASA and NASA-sponsored publication, either in printed or microfiche format, is received and retained by the 53 regional depositories. A list of the Federal Regional Depository Libraries, arranged alphabetically by state, appears at the very end of this section. These libraries are not sales outlets. A local library can contact a regional depository to help locate specific reports, or direct contact may be made by an individual.

## Public Collection of NASA Documents

An extensive collection of NASA and NASA-sponsored publications is maintained by the British Library Lending Division, Boston Spa, Wetherby, Yorkshire, England for public access. The British Library Lending Division also has available many of the non-NASA publications cited in the STI Database. European requesters may purchase facsimile copy or microfiche of NASA and NASA-sponsored documents FIZ–Fachinformation Karlsruhe–Bibliographic Service, D-76344 Eggenstein-Leopoldshafen, Germany and TIB–Technische Informationsbibliothek, P.O. Box 60 80, D-30080 Hannover, Germany.

## Submitting Documents

All users of this abstract service are urged to forward reports to be considered for announcement in the STI Database. This will aid NASA in its efforts to provide the fullest possible coverage of all scientific and technical publications that might support aeronautics and space research and development. If you have prepared relevant reports (other than those you will transmit to NASA, DOD, or DOE through the usual contract- or grant-reporting channels), please send them for consideration to:

ATTN: Acquisitions Specialist
NASA Center for AeroSpace Information
7121 Standard Drive
Hanover, MD 21076-1320.

Reprints of journal articles, book chapters, and conference papers are also welcome.

You may specify a particular source to be included in a report announcement if you wish; otherwise the report will be placed on a public sale at the NASA Center for AeroSpace Information. Copyrighted publications will be announced but not distributed or sold.

# Federal Regional Depository Libraries

## ALABAMA

**AUBURN UNIV. AT MONTGOMERY LIBRARY**
Documents Dept.
7300 University Dr.
Montgomery, AL 36117–3596
(205) 244–3650 Fax: (205) 244–0678

**UNIV. OF ALABAMA**
Amelia Gayle Gorgas Library
Govt. Documents
P.O. Box 870266
Tuscaloosa, AL 35487–0266
(205) 348–6046 Fax: (205) 348–0760

## ARIZONA

**DEPT. OF LIBRARY, ARCHIVES, AND PUBLIC RECORDS**
Research Division
Third Floor, State Capitol
1700 West Washington
Phoenix, AZ 85007
(602) 542–3701 Fax: (602) 542–4400

## ARKANSAS

**ARKANSAS STATE LIBRARY**
State Library Service Section
Documents Service Section
One Capitol Mall
Little Rock, AR 72201–1014
(501) 682–2053 Fax: (501) 682–1529

## CALIFORNIA

**CALIFORNIA STATE LIBRARY**
Govt. Publications Section
P.O. Box 942837 – 914 Capitol Mall
Sacramento, CA 94337–0091
(916) 654–0069 Fax: (916) 654–0241

## COLORADO

**UNIV. OF COLORADO – BOULDER**
Libraries – Govt. Publications
Campus Box 184
Boulder, CO 80309–0184
(303) 492–8834 Fax: (303) 492–1881

**DENVER PUBLIC LIBRARY**
Govt. Publications Dept. BSG
1357 Broadway
Denver, CO 80203–2165
(303) 640–8846 Fax: (303) 640–8817

## CONNECTICUT

**CONNECTICUT STATE LIBRARY**
231 Capitol Avenue
Hartford, CT 06106
(203) 566–4971 Fax: (203) 566–3322

## FLORIDA

**UNIV. OF FLORIDA LIBRARIES**
Documents Dept.
240 Library West
Gainesville, FL 32611–2048
(904) 392–0366 Fax: (904) 392–7251

## GEORGIA

**UNIV. OF GEORGIA LIBRARIES**
Govt. Documents Dept.
Jackson Street
Athens, GA 30602–1645
(706) 542–8949 Fax: (706) 542–4144

## HAWAII

**UNIV. OF HAWAII**
Hamilton Library
Govt. Documents Collection
2550 The Mall
Honolulu, HI 96822
(808) 948–8230 Fax: (808) 956–5968

## IDAHO

**UNIV. OF IDAHO LIBRARY**
Documents Section
Rayburn Street
Moscow, ID 83844–2353
(208) 885–6344 Fax: (208) 885–6817

## ILLINOIS

**ILLINOIS STATE LIBRARY**
Federal Documents Dept.
300 South Second Street
Springfield, IL 62701–1796
(217) 782–7596 Fax: (217) 782–6437

## INDIANA

**INDIANA STATE LIBRARY**
Serials/Documents Section
140 North Senate Avenue
Indianapolis, IN 46204–2296
(317) 232–3679 Fax: (317) 232–3728

## IOWA

**UNIV. OF IOWA LIBRARIES**
Govt. Publications
Washington & Madison Streets
Iowa City, IA 52242–1166
(319) 335–5926 Fax: (319) 335–5900

## KANSAS

**UNIV. OF KANSAS**
Govt. Documents & Maps Library
6001 Malott Hall
Lawrence, KS 66045–2800
(913) 864–4660 Fax: (913) 864–3855

## KENTUCKY

**UNIV. OF KENTUCKY**
King Library South
Govt. Publications/Maps Dept.
Patterson Drive
Lexington, KY 40506–0039
(606) 257–3139 Fax: (606) 257–3139

## LOUISIANA

**LOUISIANA STATE UNIV.**
Middleton Library
Govt. Documents Dept.
Baton Rouge, LA 70803–3312
(504) 388–2570 Fax: (504) 388–6992

**LOUISIANA TECHNICAL UNIV.**
Prescott Memorial Library
Govt. Documents Dept.
Ruston, LA 71272–0046
(318) 257–4962 Fax: (318) 257–2447

## MAINE

**UNIV. OF MAINE**
Raymond H. Fogler Library
Govt. Documents Dept.
Orono, ME 04469–5729
(207) 581–1673 Fax: (207) 581–1653

## MARYLAND

**UNIV. OF MARYLAND – COLLEGE PARK**
McKeldin Library
Govt. Documents/Maps Unit
College Park, MD 20742
(301) 405–9165 Fax: (301) 314–9416

## MASSACHUSETTS

**BOSTON PUBLIC LIBRARY**
Govt. Documents
666 Boylston Street
Boston, MA 02117–0286
(617) 536–5400, ext. 226
Fax: (617) 536–7758

## MICHIGAN

**DETROIT PUBLIC LIBRARY**
5201 Woodward Avenue
Detroit, MI 48202–4093
(313) 833–1025 Fax: (313) 833–0156

**LIBRARY OF MICHIGAN**
Govt. Documents Unit
P.O. Box 30007
717 West Allegan Street
Lansing, MI 48909
(517) 373–1300 Fax: (517) 373–3381

## MINNESOTA

**UNIV. OF MINNESOTA**
Govt. Publications
409 Wilson Library
309 19th Avenue South
Minneapolis, MN 55455
(612) 624–5073 Fax: (612) 626–9353

## MISSISSIPPI

**UNIV. OF MISSISSIPPI**
J.D. Williams Library
106 Old Gym Bldg.
University, MS 38677
(601) 232–5857 Fax: (601) 232–7465

## MISSOURI

**UNIV. OF MISSOURI – COLUMBIA**
106B Ellis Library
Govt. Documents Sect.
Columbia, MO 65201–5149
(314) 882–6733 Fax: (314) 882–8044

## MONTANA

**UNIV. OF MONTANA**
Mansfield Library
Documents Division
Missoula, MT 59812–1195
(406) 243–6700 Fax: (406) 243–2060

## NEBRASKA

**UNIV. OF NEBRASKA – LINCOLN**
D.L. Love Memorial Library
Lincoln, NE 68588–0410
(402) 472–2562 Fax: (402) 472–5131

## NEVADA

**THE UNIV. OF NEVADA LIBRARIES**
Business and Govt. Information Center
Reno, NV 89557–0044
(702) 784–6579 Fax: (702) 784–1751

## NEW JERSEY

**NEWARK PUBLIC LIBRARY**
Science Div. – Public Access
P.O. Box 630
Five Washington Street
Newark, NJ 07101–7812
(201) 733–7782 Fax: (201) 733–5648

## NEW MEXICO

**UNIV. OF NEW MEXICO**
General Library
Govt. Information Dept.
Albuquerque, NM 87131–1466
(505) 277–5441 Fax: (505) 277–6019

**NEW MEXICO STATE LIBRARY**
325 Don Gaspar Avenue
Santa Fe, NM 87503
(505) 827–3824 Fax: (505) 827–3888

## NEW YORK

**NEW YORK STATE LIBRARY**
Cultural Education Center
Documents/Gift & Exchange Section
Empire State Plaza
Albany, NY 12230–0001
(518) 474–5355 Fax: (518) 474–5786

## NORTH CAROLINA

**UNIV. OF NORTH CAROLINA – CHAPEL HILL**
Walter Royal Davis Library
CB 3912, Reference Dept.
Chapel Hill, NC 27514–8890
(919) 962–1151 Fax: (919) 962–4451

## NORTH DAKOTA

**NORTH DAKOTA STATE UNIV. LIB.**
Documents
P.O. Box 5599
Fargo, ND 58105–5599
(701) 237–8886 Fax: (701) 237–7138

**UNIV. OF NORTH DAKOTA**
Chester Fritz Library
University Station
P.O. Box 9000 – Centennial and University Avenue
Grand Forks, ND 58202–9000
(701) 777–4632 Fax: (701) 777–3319

## OHIO

**STATE LIBRARY OF OHIO**
Documents Dept.
65 South Front Street
Columbus, OH 43215–4163
(614) 644–7051 Fax: (614) 752–9178

## OKLAHOMA

**OKLAHOMA DEPT. OF LIBRARIES**
U.S. Govt. Information Division
200 Northeast 18th Street
Oklahoma City, OK 73105–3298
(405) 521–2502, ext. 253
Fax: (405) 525–7804

**OKLAHOMA STATE UNIV.**
Edmon Low Library
Stillwater, OK 74078–0375
(405) 744–6546 Fax: (405) 744–5183

## OREGON

**PORTLAND STATE UNIV.**
Branford P. Millar Library
934 Southwest Harrison
Portland, OR 97207–1151
(503) 725–4123 Fax: (503) 725–4524

## PENNSYLVANIA

**STATE LIBRARY OF PENN.**
Govt. Publications Section
116 Walnut & Commonwealth Ave.
Harrisburg, PA 17105–1601
(717) 787–3752 Fax: (717) 783–2070

## SOUTH CAROLINA

**CLEMSON UNIV.**
Robert Muldrow Cooper Library
Public Documents Unit
P.O. Box 343001
Clemson, SC 29634–3001
(803) 656–5174 Fax: (803) 656–3025

**UNIV. OF SOUTH CAROLINA**
Thomas Cooper Library
Green and Sumter Streets
Columbia, SC 29208
(803) 777–4841 Fax: (803) 777–9503

## TENNESSEE

**UNIV. OF MEMPHIS LIBRARIES**
Govt. Publications Dept.
Memphis, TN 38152–0001
(901) 678–2206 Fax: (901) 678–2511

## TEXAS

**TEXAS STATE LIBRARY**
United States Documents
P.O. Box 12927 – 1201 Brazos
Austin, TX 78701–0001
(512) 463–5455 Fax: (512) 463–5436

**TEXAS TECH. UNIV. LIBRARIES**
Documents Dept.
Lubbock, TX 79409–0002
(806) 742–2282 Fax: (806) 742–1920

## UTAH

**UTAH STATE UNIV.**
Merrill Library Documents Dept.
Logan, UT 84322–3000
(801) 797–2678 Fax: (801) 797–2677

## VIRGINIA

**UNIV. OF VIRGINIA**
Alderman Library
Govt. Documents
University Ave. & McCormick Rd.
Charlottesville, VA 22903–2498
(804) 824–3133 Fax: (804) 924–4337

## WASHINGTON

**WASHINGTON STATE LIBRARY**
Govt. Publications
P.O. Box 42478
16th and Water Streets
Olympia, WA 98504–2478
(206) 753–4027 Fax: (206) 586–7575

## WEST VIRGINIA

**WEST VIRGINIA UNIV. LIBRARY**
Govt. Documents Section
P.O. Box 6069 – 1549 University Ave.
Morgantown, WV 26506–6069
(304) 293–3051 Fax: (304) 293–6638

## WISCONSIN

**ST. HIST. SOC. OF WISCONSIN LIBRARY**
Govt. Publication Section
816 State Street
Madison, WI 53706
(608) 264–6525 Fax: (608) 264–6520

**MILWAUKEE PUBLIC LIBRARY**
Documents Division
814 West Wisconsin Avenue
Milwaukee, WI 53233
(414) 286–3073 Fax: (414) 286–8074

# Typical Report Citation and Abstract

❶ **19970001126** NASA Langley Research Center, Hampton, VA USA
❷ **Water Tunnel Flow Visualization Study Through Poststall of 12 Novel Planform Shapes**
❸ Gatlin, Gregory M., NASA Langley Research Center, USA Neuhart, Dan H., Lockheed Engineering and Sciences Co., USA;
❹ Mar. 1996; 130p; In English
❺ Contract(s)/Grant(s): RTOP 505-68-70-04
❻ Report No(s): NASA-TM-4663; NAS 1.15:4663; L-17418; No Copyright; Avail: CASI; A07, Hardcopy; A02, Microfiche
❼ To determine the flow field characteristics of 12 planform geometries, a flow visualization investigation was conducted in the Langley 16- by 24-Inch Water Tunnel. Concepts studied included flat plate representations of diamond wings, twin bodies, double wings, cutout wing configurations, and serrated forebodies. The off-surface flow patterns were identified by injecting colored dyes from the model surface into the free-stream flow. These dyes generally were injected so that the localized vortical flow patterns were visualized. Photographs were obtained for angles of attack ranging from 10’ to 50’, and all investigations were conducted at a test section speed of 0.25 ft per sec. Results from the investigation indicate that the formation of strong vortices on highly swept forebodies can improve poststall lift characteristics; however, the asymmetric bursting of these vortices could produce substantial control problems. A wing cutout was found to significantly alter the position of the forebody vortex on the wing by shifting the vortex inboard. Serrated forebodies were found to effectively generate multiple vortices over the configuration. Vortices from 65’ swept forebody serrations tended to roll together, while vortices from 40’ swept serrations were more effective in generating additional lift caused by their more independent nature.
❽ Author
❾ *Water Tunnel Tests; Flow Visualization; Flow Distribution; Free Flow; Planforms; Wing Profiles; Aerodynamic Configurations*

## Key

1. Document ID Number; Corporate Source
2. Title
3. Author(s) and Affiliation(s)
4. Publication Date
5. Contract/Grant Number(s)
6. Report Number(s); Availability and Price Codes
7. Abstract
8. Abstract Author
9. Subject Terms

# SCIENTIFIC AND TECHNICAL AEROSPACE REPORTS

*A Biweekly Publication of the National Aeronautics and Space Administration*

VOLUME 39, DECEMBER 28, 2001

## 01
## AERONAUTICS (GENERAL)

*Includes general research topics related to manned and unmanned aircraft and the problems of flight within the Earth's atmosphere. Also includes manufacturing, maintenance, and repair of aircraft. For specific topics in aeronautics see categories 02 through 09. For information related to space vehicles see 12 Astronautics.*

**20010120406** University Aviation Association, Auburn, AL USA
**Collegiate Aviation Review, Volume 18, No. 1**
Carney, Thomas Q., Editor, Purdue Univ., USA; Luedtke, Jacqueline R., Editor, Utah State Univ., USA; Barker, Ballard M., Editor, Florida Inst. of Tech., USA; Bowen, Brent D., Editor, Nebraska Univ., USA; Carstenson, Larry G., Editor, University Aviation Association, USA; Chubb, Gerald P., Editor, Ohio State Univ., USA; Galloway, B. J., Editor, Ohio Univ., USA; Green, Mavis F., Editor, Illinois Univ. at Urbana-Champaign, USA; Karp, Merrill R., Editor, Arizona State Univ., USA; Lindseth, Paul D., Editor, North Dakota Univ., USA; October 2000; ISSN 1523-5955; 102p; In English; See also 20010120407 through 20010120413; Copyright; Avail: Issuing Activity

Papers published in this volume were selected from submissions that were subjected to a blind peer review process, and were presented at the 2000 Fall Education Conference of the University Aviation Association. The papers are: (1) University Aviation Education: An Integrated Model; (2) The FAA: A Tombstone Agency? Putting the Nickname to the Test; (3) The Relationship of Document and Quantitative Literacy with Learning Styles and Selected Personal Variables for Aviation University Students; (4) Memory Strategies for the Pilot; (5) A Follow-up Survey of 1985-1996 Graduates of the Aviation Management Program Bachelor of Science Degree at Southern Illinois University Carbondale; (6) Collision Avoidance at Non-towered Airports; (7) Attracting Women to Aviation Careers: What Recent Studies Reveal.
Derived from text
*Aeronautics; Conferences; Education*

**20010120414** University Aviation Association, Auburn, AL USA
**Collegiate Aviation Review, Volume 19**
Carney, Thomas Q., Editor, Purdue Univ., USA; Luedtke, Jacqueline R., Editor, Daniel Webster Coll., USA; Barker, Ballard M., Editor, Florida Inst. of Tech., USA; Bowen, Brent D., Editor, Nebraska Univ., USA; Carstenson, Larry G., Editor, Nebraska Univ., USA; Chubb, Gerald P., Editor, Ohio State Univ., USA; Galloway, B. J., Editor, Ohio Univ., USA; Green, Mavis F., Editor, Embry-Riddle Aeronautical Univ., USA; Karp, Merrill R., Editor, Arizona State Univ., USA; Lindseth, Paul D., Editor, North Dakota Univ., USA; October 2001; ISSN 1523-5955; 194p; In English; See also 20010120415 through 20010120426; Copyright; Avail: Issuing Activity

The Collegiate Aviation Review is published annually by the University Aviation Association, and is distributed to the members of the Association. Papers published in this volume were selected from submissions that were subjected to a blind peer review process, and were presented at the 2000 Fall Education Conference of the Association. The University Aviation Association is the only professional organization representing all levels of the non-engineering/technology element in collegiate aviation education. Working through its officers, trustees, committees and professional staff, the University Aviation Association plays a vital role in collegiate aviation and in the aviation industry. The University Aviation Association accomplishes its goals through several objectives. These objectives are: to encourage and promote the attainment of the highest standards in aviation education at the college level. to provide a means of developing a cadre of aviation experts who make themselves available for such activities as consultation, aviation program evaluation, speaking assignments, and other professional contributions that stimulate and develop aviation education. to furnish a national vehicle for the dissemination of intelligence relative to aviation

among institutions of higher education and governmental and industrial organizations in the aviation/aerospace field. to permit the interchange of information among institutions that offer non-engineering oriented aviation programs including business technology, transportation, and education. to actively support aviation/aerospace-oriented teacher education with particular emphasis on the presentation of educational workshops and the development of educational materials in the aviation and aerospace fields.
Author
*Aircraft Industry; Technology Assessment; Civil Aviation; Universities*

**20010123758** Nebraska Univ., Aviation Inst., Omaha, NE USA
**Aviation Institute 2001 Self Study Report for the Council on Aviation Accreditation**
Schaaf, Michaela M., Nebraska Univ., USA; Acheson, Densel K., Nebraska Univ., USA; Bowen, Brent D., Nebraska Univ., USA; Fink, Mary M., Nebraska Univ., USA; Larson, Michael K., Nebraska Univ., USA; Lehrer, Henry R., Nebraska Univ., USA; Lutte, Rebecca K., Nebraska Univ., USA; Tarry, Scott E., Nebraska Univ., USA; Vlasek, Scott E., Nebraska Univ., USA; 2001; 134p; In English
Report No.(s): UNOAI-01-3; Copyright; Avail: Issuing Activity
This report outlines the Aviation Accreditation of the University of Nebraska at Omaha. The organization and administration of the Aviation Program is discussed, including the budget of the program. The curriculum is described including institutional requirements, plan of study, degree requirements, and course sequencing and descriptions. Information about the faculty and students of the Aviation Program is provided. Finally, the program's relations with industry are discussed.
CASI
*Education; Aeronautics*

## 02
## AERODYNAMICS

*Includes aerodynamics of flight vehicles, test bodies, airframe components and combinations, wings, and control surfaces. Also includes aerodynamics of rotors, stators, fans and other elements of turbomachinery. For related information, see also 34 Fluid Mechanics and Heat Transfer.*

**20010117674** NASA Ames Research Center, Moffett Field, CA USA
**Navier-Stokes Flowfield Simulation of Boeing 747-200 as Platform for SOFIA**
Srinivasan, G.R., NASA Ames Research Center, USA; Apr. 08, 1994; 1p; In English; 33rd; AIAA Aerspace Sciences, 2-12 Jan. 1995, Reno, NV, USA; Sponsored by American Inst. of Aeronautics and Astronautics, USA
Contract(s)/Grant(s): RTOP 505-59-00; No Copyright; Avail: Issuing Activity; Abstract Only
Steady and unsteady viscous, three-dimensional flowfields are calculated using a thin layer approximation of Navier-Stokes equations in conjunction with Chimera overset grids. The finite-difference numerical scheme uses structured grids and a pentadiagonal flow solver called "OVERFLOW". The configuration of Boeing 747-200 has been chosen as one of configurations to be used as a platform for the SOFIA (Stratospheric Observatory For Infrared Astronomy). Initially, the steady flowfield of the full aircraft is calculated for the clean configuration (without a cavity to house telescope). This solution is then used to start the unsteady flowfield of a configuration containing cavity housing the observation telescope and its peripheral units. Analysis of unsteady flowfield in the cavity and its influence on the tail empennage, as well as the noise due to turbulence and optical quality of the flow are the main focus of this study. For the configuration considered here, the telescope housing cavity is located slightly downstream of the portwing. The entire flow-field is carefully constructed using 45 overset grids and consists of nearly 4 million grid points. All the computations axe done at one freestream flow condition of M(sub infinity) = 0.85, alpha = 2.5deg, and a Reynolds of Re = 1.85x10deg
Author
*Boeing 747 Aircraft; Navier-Stokes Equation; Structured Grids (Mathematics); Computational Grids*

**20010117734** NASA Ames Research Center, Moffett Field, CA USA
**Aerodynamics Characteristics of Multi-Element Airfoils at -90 Degrees Incidence**
Stremel, Paul M., NASA Ames Research Center, USA; Apr. 08, 1994; 1p; In English; AIAA Aerospace Sciences, 9-12 Jan. 1995, Reno, NV, USA; Sponsored by American Inst. of Aeronautics and Astronautics, USA
Contract(s)/Grant(s): RTOP 505-59-36; No Copyright; Avail: Issuing Activity; Abstract Only

A developed method has been applied to calculate accurately the viscous flow about airfoils normal to the free-stream flow. This method has special application to the analysis of tilt rotor aircraft in the evaluation of download. In particular, the flow about an XV-15 airfoil with and without deflected leading and trailing edge flaps at -90 degrees incidence is evaluated. The multi-element aspect of the method provides for the evaluation of slotted flap configurations which may lead to decreased drag. The method solves for turbulent flow at flight Reynolds numbers. The flow about the XV-15 airfoil with and without flap deflections has been calculated and compared with experimental data at a Reynolds number of one million. The comparison between the calculated and measured pressure distributions are very good, thereby, verifying the method. The aerodynamic evaluation of multielement airfoils will be conducted to determine airfoil/flap configurations for reduced airfoil drag. Comparisons between the calculated lift, drag and pitching moment on the airfoil and the airfoil surface pressure will also be presented.
Author
*Airfoils; Viscous Flow; Turbulent Flow; Pressure Distribution; Aerodynamic Drag; Free Flow*

**20010119438** NASA Ames Research Center, Moffett Field, CA USA
**Forced Diffusion of Trailing Vorticity from a Hovering Rotor**
McAlister, Kenneth W., NASA Ames Research Center, USA; Tung, Chee, NASA Ames Research Center, USA; Heineck, James T., NASA Ames Research Center, USA; [2001]; 1p; In English; American Helicopter Society 57th Annual Forum and Technology Display, 9-11 May 2001, Washington, DC, USA; Sponsored by American Helicopter Society, Inc., USA; No Copyright; Avail: Issuing Activity; Abstract Only

A small turbulence generating device was Attached near the tip of a hovering rotor blade In order to alter the structure of the trailing vortex. Stereo particle image velocimetry (PIV) images were used to quantify the wake behind the rotor blade during the first revolution. An analysis of the 3D-velocity field includes a method for accounting for vortex wander. The results show that a major change in the size and intensity of the trailing vortex can be achieved.
Author
*Diffusion; Particle Image Velocimetry; Rotor Blades (Turbomachinery); Vortices; Aerodynamic Stability*

**20010119591** Army Research Lab., Human Research and Engineering Directorate, Aberdeen Proving Ground, MD USA
**Navier-Stokes Computations of Finned Missiles at Supersonic Speeds**
Haroldsen, David J.; Sturek, Walter B., Sr; Sep. 2001; 15p; In English
Report No.(s): AD-A394907; ARL-RP-35; No Copyright; Avail: CASI; A03, Hardcopy; A01, Microfiche

The U.S. Army Research Laboratory (ARL) is interested in applying state-of-the-art high performance computing tools to predict the aerodynamics of Army shell at angle of attack for a wide range of Mach number from high subsonic to high supersonic. In this paper, the WIND flow solver has been used to study the aerodynamics of two missile configurations. The GridPro grid generation software has been utilized to generate the computational grids. Several aspects of interest concerning the generation of grids for use with WIND and the process of obtaining solutions is discussed. Comparisons are shown between computation and experiment for several turbulence models.
DTIC
*Missiles; Angle of Attack; Mach Number; Supersonic Flow; Navier-Stokes Equation; Missile Configurations; Aerodynamics*

**20010120097** NASA Ames Research Center, Moffett Field, CA USA
**Navier-Stokes Calculations For a Venus Composition Probe With Ablation and Wake Radiation**
Olynick, David R., NASA Ames Research Center, USA; Henline, William D., NASA Ames Research Center, USA; [1994]; 1p; In English; AIAA 29th Thermophysics Conference, 19-22 Jun. 1995, San Diego, CA, USA; Sponsored by American Inst. of Aeronautics and Astronautics, USA
Contract(s)/Grant(s): RTOP 232-01-04; No Copyright; Avail: Issuing Activity; Abstract Only

A numerical investigation is carried out to determine the magnitude of wake radiation for a proposed Venus composition probe. One of the scientific goals of the mission is to determine the atmospheric composition of Venus by examining the intensity of scattered sunlight through the wake of the vehicle during planetary entry. In the wake of the vehicle, excited particles generated in the bow shock and boundary layers absorb and emit radiation. Thus, the purpose of this study is to determine if the radiation sensor will be able to sense the incoming solar radiative flux relative to the radiative flux generated in the wake. During portions of the entry trajectory the incident surface heat flux will be high enough to produce significant ablation. Ablation products such

as CN are known to be strong radiators. Also, the ablation will be driven by strong radiation emanating from the bow shock. Thus, radiation and ablation will be coupled into the Navier-Stokes flow solutions.
Author
*Navier-Stokes Equation; Venus (Planet); Atmospheric Composition; Solar Flux; Shock Layers; Planetary Composition*

**20010120271** Norwegian Defence Research Establishment, Kjeller, Norway
**Measurements of Velocity Fields Caused by Wing Tip Vortices from Aircrafts in the Approach to Kjevik Airport** ***Malinger av Hastighetsfelter i Fly-Genererte Virvler Naer hus Under Innflyvningstraseen ved Kjevik Flyplass***
Andreassen, Oyvind, Norwegian Defence Research Establishment, Norway; Helgeland, Anders, Norwegian Defence Research Establishment, Norway; Sep. 05, 2001; 24p; In Norwegian
Contract(s)/Grant(s): FFIS/FFIBM Proj. 820/170
Report No.(s): FFI/RAPPORT-2001/04317; ISBN 82-464-0541-1; No Copyright; Avail: CASI; A03, Hardcopy; A01, Microfiche

Winds caused by aircraft generated vortices are measured close to a roof in the approach to Kjevik airport. It is reported that aircraft vortices have caused tiles to fall down from roofs. In this report measurements of wind velocities caused by aircrafts are presented. We find wind speeds up to only 5 m/s, which is small compared to wind caused by storms which are typically 15m/s. Based upon measurements, it is our impression that the influence from aircraft vortices on roofs are not strong. On the other hand, winds do no alone indicate hydrodynamical forces. The topology of the wind field might be of importance and we have no ability to assess that by a one point wind registration alone. We know that the aircraft caused vortices are strongly turbulent, as is the boundary layer close to the roofs and ground. to make a final conclusion about the vortex influences, we suggest that pressure measurements are performed at the actual roof. Then the forces can be estimated directly.
Author
*Boundary Layers; Pressure Measurement; Roofs; Velocity Distribution; Wing Tip Vortices*

**20010120490** Sandia Labs., Albuquerque, NM USA
**Free-Fall Rotation and Aerodynamic Motion of Rectangular Plates**
Bustamante, A. C.; Aug. 1968; 74p; In English
Report No.(s): AD-A395124; SC-RR-68-132; No Copyright; Avail: CASI; A04, Hardcopy; A01, Microfiche

The aerodynamic motion of rectangular plates observed in 18 free fall drop tests is analyzed and described. In most of the drops, the plates autorotated; the autorotation was independent of the plates' initial attitude. The autorotation generated a small lifting force which caused the plates to experience a gliding and spiraling motion.
DTIC
*Motion; Aerodynamics; Attitude (Inclination); Autorotation; Rectangular Plates; Free Fall*

**20010120785** NASA Ames Research Center, Moffett Field, CA USA
**Hypersonic Research Program at NASA Ames Research Center**
Green, Michael J., NASA Ames Research Center, USA; [1994]; 1p; In English; AIAA Atmospheric Flight Mechanics Conference, 1-3 Aug. 1994, Scottsdale, AZ, USA; Sponsored by American Inst. of Aeronautics and Astronautics, USA
Contract(s)/Grant(s): RTOP 505-70-00; No Copyright; Avail: CASI; A01, Hardcopy; A01, Microfiche; Abstract Only; Abstract Only

This paper will describe the Airbreathing Hypersonic Research Program at NASA Ames Research Center. A main theme will be the "From Computation Through Flight" research effort. General research areas covered will include systems analysis, aerodynamics and aerothermodynamics, propulsion, materials, and flight research. Illustrative results from each discipline will be presented. The synergism between computational and experimental research will be demonstrated by examples. All examples given will have been published in the open literature.
Author
*Research Projects; Aerothermodynamics; Air Breathing Engines; Propulsion*

**20010121531** NASA Ames Research Center, Moffett Field, CA USA
**Quiet Supersonic Wind Tunnel Development**
King, Lyndell S., NASA Ames Research Center, USA; [1994]; 1p; In English; Aerospace Ground Test Facilities and Flight Testing XXIX Short Course, 25 Apr. - 5 May 1994, Tullahoma, TN, USA; Sponsored by Tennessee Univ. Space Inst., USA
Contract(s)/Grant(s): RTOP 505-59-50; No Copyright; Avail: Issuing Activity; Abstract Only

The ability to control the extent of laminar flow on swept wings at supersonic speeds may be a critical element in developing the enabling technology for a High Speed Civil Transport (HSCT). Laminar boundary layers are less resistive to forward flight

than their turbulent counterparts, thus the farther downstream that transition from laminar to turbulent flow in the wing boundary layer is extended can be of significant economic impact. Due to the complex processes involved experimental studies of boundary layer stability and transition are needed, and these are performed in ”quiet” wind tunnels capable of simulating the low-disturbance environment of free flight. At Ames, a wind tunnel has been built to operate at flow conditions which match those of the HSCT laminar flow flight demonstration ’aircraft, the F-16XL, i.e. at a Mach number of 1.6 and a Reynolds number range of 1 to 3 million per foot. This will allow detailed studies of the attachment line and crossflow on the leading edge area of the highly swept wing. Also, use of suction as a means of control of transition due to crossflow and attachment line instabilities can be studied. Topics covered include: test operating conditions required; design requirements to efficiently make use of the existing infrastructure; development of an injector drive system using a small pilot facility; plenum chamber design; use of computational tools for tunnel and model design; and early operational results.
Author
*Laminar Flow; Swept Wings; Supersonic Speed; Laminar Boundary Layer; Supersonic Transports; Supersonic Wind Tunnels*

**20010122305** Sandia National Labs., Albuquerque, NM USA
**Verification and Validation for Laminar Hypersonic Flowfields**
Roy,; Jul. 18, 2000; 21p; In English
Report No.(s): DE2000-761061; SAND2000-1748C; No Copyright; Avail: Department of Energy Information Bridge
The accuracy of Mach 8 laminar flow solutions over a spherically-blunted cone is verified, and the various physical models are validated. Verification of the solution accuracy is demonstrated by monitoring iterative convergence, performing a comprehensive grid convergence study, comparison to benchmark inviscid results, and code-to-code comparisons. Although the numerical scheme is nominally second order accurate in space, the presence of first order accuracy at the shock discontinuity results in first order behavior for the surface pressure distributions as the grid is sufficiently refined. Alternative methods are proposed for analyzing the spatial convergence behavior and determining the order of accuracy for mixed first and second order schemes. Validation of the computational model is performed via surface pressure comparisons with high-quality experimental data. Careful attention is paid to the assumptions in the computational and experimental modeling. In particular, the thermodynamic state of the hypersonic wind tunnel nozzle is examined and arguments are made for the presence of a significant amount of thermal nonequilibrium. Bias errors in the experimental Mach number calibration are discussed which are related to the assumption of thermal equilibrium (minus 0.23%) and the averaging of probe data over the entire test section (plus 0.6%). Differences between the simulation results for surface pressure and the experimental data are found to be as large as 3.3%. These differences are well outside the experimental 20 error bounds, even after accounting for the experimental bias errors.
NTIS
*Flow Distribution; Laminar Flow; Wind Tunnel Nozzles; Proving*

**20010122391** Texas A&M Univ., College Station, TX USA
**AFOSR Workshop on Research and Applications of Active Materials and Smart Structures** ***Final Report, 1 Nov. 1999-15 Feb. 2001***
Lagoudas, Dimitris C.; Sanders, Brian; Cross, Charles; Apr. 26, 2001; 8p; In English
Contract(s)/Grant(s): F49620-00-100044
Report No.(s): AD-A395003; AFRL-SR-BL-TR-01-0504; No Copyright; Avail: CASI; A02, Hardcopy; A01, Microfiche
The purpose of this workshop was to provide an in-depth look at the progress in active materials and smart structures with an emphasis on Air Force systems. The technology of smart structures promises a large number of potential uses and performance enhancements for air vehicles and space systems. This workshop brought together researchers from academia, the national labs, and the aerospace industry with the focus of the discussion on Air Force systems. Every effort was made to make the workshop a two-way stream and expose researchers to the problems and needs of the Air Force as well as presenting state-of-the-an research related to active materials and smart structures. Topics discussed were, among others, actuator/sensor concepts, aerodynamic control using active materials, active propulsion systems, and smart space systems.
DTIC
*Aircraft; Aeronautical Engineering; Aerospace Systems*

**20010122404** Eloret Corp., Sunnyvale, CA USA
**One-Equation Turbulence Models in Aerodynamics**
Menter, F. R., Eloret Corp., USA; [1995]; 1p; In English; 33rd AIAA Aerospace Science Meeting and Exhibit, 9-12 Jan. 1995, Reno, NV, USA; Sponsored by American Inst. of Aeronautics and Astronautics, USA
Contract(s)/Grant(s): RTOP 505-59-50; No Copyright; Avail: Issuing Activity; Abstract Only

The present paper shows under which assumptions one-equation models can be derived from two-equation models. Based on that transformation a new one-equation turbulence model is derived that basically behaves like a two-equation model. The new model is compared in detail against existing models
Author
*Aerodynamics; Turbulence Models; Computational Fluid Dynamics; Computer Programs*

**20010123403** NASA Ames Research Center, Moffett Field, CA USA
**A Review of Evidence for High Life Coefficients on Propeller and Rotor Blades Under Static Thrust Conditions with Some New Experimental Results**
Talbot, Peter D., NASA Ames Research Center, USA; Meyer, Mark, Stanford Univ., USA; Branum, Lonnie, Army Aviation Systems Command, USA; [1994]; 10p; In English; AGARD Aerodynamic Conference, October 1994, Berlin, Germany; Sponsored by Advisory Group for Aerospace Research and Development, France; No Copyright; Avail: CASI; A02, Hardcopy; A01, Microfiche

Interest has increased recently in the thrust-producing capability of rotors at very high collective pitch angles. An early reference noted this behaviour in rotors and offered alternative models for section lift characteristics to explain it. The same phenomenon was coincidentally noted and used in a propeller code, resulting in very good correlation with static thrust data. The proposed paper will present experimental data demonstrating the pronounced persistence of thrust for propellers at increasing collective pitch angles. Comparisons with blade element/momentum theory will be made. These results are expected to point to the need to define (ultimately to explain) aerodynamic lift and drag behaviour in a rotating environment. Experimental measurements made by the U.S. Army Aeroflightdynamics Directorate at the Ames Research Center have shown that locally measured normal force coefficients along the span of a highly twisted rotor blade continue to increase at high values of collective pitch. In some cases these coefficients exceed expected values for the same type of airfoil tested under two dimensional conditions. to date no one to the authors' knowledge has defined the variation of C(n) with pitch for very high angles (to 45 deg) in a rotating environment and for a blade of reasonably high aspect ratio; however, total propeller thrust measurements support the idea that stalling does not occur in the same way as on a wing. This paper will present experimental data in the form of surface pressure distributions as well as flow visualization (microtufts) to explore the aerodynamic behavior of the rotating airfoil at high values of blade incidence. This paper also reviews experimental evidence and infers some high lift coefficient behavior from it. Comparisons between predicted thrust, utilizing modified airfoil characteristics and a blade element model, and measured thrust for both rotors and propellers that cover the extremes of collective pitch are shown and discussed.
Author
*Propeller Blades; Rotor Blades (Turbomachinery); Static Thrust; Pitch (Inclination); Aerodynamic Drag; Lift; Aerodynamic Coefficients*

**20010125633** NASA Langley Research Center, Hampton, VA USA
**An Analysis of Exact and Approximate Equations for the Temperature Distribution in an Insulated Thick Skin Subjected to Aerodynamic Heating**
Harris, Robert S., Jr., NASA Langley Research Center, USA; Davidson, John R., NASA Langley Research Center, USA; January 1961; 37p; In English
Report No.(s): NASA-TN-D-519; L-721; No Copyright; Avail: CASI; A03, Hardcopy; A01, Microfiche

The problem of calculating the temperature distribution in an insulated slab is investigated. Exact and approximate solutions are obtained, and the results are compared to determine the ranges of applicability of the approximations. The approximations are found to be within 5 percent of the exact solution when the ratio of the thermal capacitance of the metal to that of the insulation and the ratio of the conductance of the metal to that of the insulation are sufficiently large. The roots of the characteristic equation of the exact solution are generally applicable to the two-slab heat-transfer problem and are tabulated up to the first nine roots.
Author
*Temperature Distribution; Approximation; Slabs*

## 03
## AIR TRANSPORTATION AND SAFETY

*Includes passenger and cargo air transport operations; aircraft ground operations; flight safety and hazards; and aircraft accidents. Systems and hardware specific to ground operations of aircraft and to airport construction are covered in 09 Research and Support Facilities (Air). Air traffic control is covered in 04 Aircraft Communications and Navigation. For related information see also 16 Space Transportation and Safety; and 85 Technology Utilization and Surface Transportation.*

**20010117663** Sandia National Labs., Albuquerque, NM USA
**Fast Pragmatic Safety Decisions: Analysis of an Event Review Team of the Aviation Safety Action Partnership**
Ganter,; Dean,; Cloer,; May 01, 2000; 27p; In English
Report No.(s): DE2000-759430; SAND2000-1134; No Copyright; Avail: Department of Energy Information Bridge

Commercial aviation has become safe as a result of procedures and technologies that control well known hazards. Further safety improvements will require the identification of subtle and changing hazards in the combined realm of airspace, technology, commerce, and human behavior. The preconditions for a disaster may arise from the combined effects of a particular airport approach, air traffic control policies, and aircraft crew training. The potential may be revealed just once, in a near-miss that a highly skilled pilot is able to avert. Yet, because such discoveries are often related to human error, personnel are reluctant to come forward for fear of blame and punishment. With the Aviation Safety Action Programs (ASAP), the Federal Aviation Administration (FAA) is developing a nonpunitive collaborative approach that supplements traditional regulatory actions. An ASAP team is a triad composed of air carrier (corporate), pilot association (union), and FAA (regulatory) personnel who meet to review, discuss, and analyze event reports submitted voluntarily by flight personnel. The team is required to reach 'unanimous consensus' on the event report and the corrective actions to be taken. Our analysis suggests they do so through a hierarchy of shared values, a working buffer to exclude distractions, and sideband communications that build trust. ASAP appears to be a highly effective cultural mechanism for identifying novel and subtle hazards, and designing rapid, mutually acceptable corrective actions.
NTIS
*Aircraft Safety; Decision Making; Human Behavior; Airline Operations*

**20010119607** Little (Arthur D.), Inc., Cambridge, MA USA
**Rapid Off-Load Manifold (ROLM) Concept Exploration** ***Final Report, Sep. 1999-Sep 2000***
Hablanian, David A.; Sep. 2000; 52p; In English
Contract(s)/Grant(s): F41624-96-D-5002; Proj-1710
Report No.(s): AD-A394951; 69639-60; AFRL-HE-WP-TR-2001-0002; No Copyright; Avail: CASI; A04, Hardcopy; A01, Microfiche

The objectives of the Rapid Off-Load Manifold (ROLM) concept exploration effort were to gather requirements and to develop and analyze concepts for a new fuels manifold cart to support Air Force Forward Area Refueling Points (FARP) operations. The requirements for the ROLM cart were developed based on discussions with the ROLM Integrated Product Team (IPT), observation of demonstration testing of the existing Forward Area Manifold (FAM) cart, and by submitting and compiling the results of a questionnaire to the end users. Concepts were developed and analyzed, leading to description in the form of Computer Aided Design (CAD) drawings and the fabrication of a scale model. The projected performance and features of the ROLM cart are compared to the existing FAM cart in this report.
DTIC
*Refueling; Military Operations; Tanker Aircraft*

**20010119921** Texas Univ., Austin, TX USA
**The Aerial Fleet Refueling Problem**
Wiley, Victor; Aug. 2001; 204p; In English
Report No.(s): AD-A395243; CI01-256; No Copyright; Avail: CASI; A10, Hardcopy; A03, Microfiche

The deployment stage of the Aerial Fleet Refueling Problem (AFRP) for Air Mobility Command (AMC), Scott AFB, IL is efficiently solved using a Group Theoretic Tabu Search (GTTS). The GTTS uses the Symmetric Group on n-letters (S(n)) and applies it to this problem using the Java(TM) Object-Oriented Programming (OOP) language. The GTTS approach is sufficiently robust to be applied to other problem areas at AMC including the employment stage of the AFRP as well as the deployment and employment stages of the Airlift Problem. In the appendices, a brief description of the Java(TM) implementation of the S(n), developed as an essential part of this research, is presented.
DTIC
*Deployment; Jet Aircraft; Air to Air Refueling*

**20010120128** Air Command and Staff Coll., Maxwell AFB, AL USA

**Toward A Single, Integrated Planning & Execution System. Deployment Planning in the Expeditionary Aerospace**

Valle, Christopher R.; Apr. 2000; 52p; In English; Original contains color images

Report No.(s): AD-A394975; AU/ACSC/178/2000-04; No Copyright; Avail: CASI; A04, Hardcopy; A01, Microfiche

The Joint Operation Planning and Execution System (JOPES) is a combination of joint policies, procedures, and automated data processing (ADP) support used to plan and execute joint military operations. While JOPES defines three interrelated planning processes, circumstances of the past decade induced the Air Force to progress toward two distinct and segregated planning processes. Over time, technical and organizational disconnects had handicapped the highly structured peacetime deliberate planning process. Consequently, the Air Force planning process no longer adequately supported the dynamic environment of crisis action planning. to obtain the flexibility required to deploy personnel to small-scale contingencies and multiple rotational deployments, the Air Force developed a separate, unrelated process to perform individual rotational requirements. The inability of either system to adequately support the gradual escalation of events during the Air War Over Serbia (AWOS), and the consequent loss of situational awareness to existing Major Theater War (MTW) OPLANs, mandate a change to Air Force deployment planning and execution processes. To meet the rapid planning and execution timelines required of an Expeditionary Aerospace Force, the Air Force must take positive actions to achieve the collaborative planning and execution system envisioned as far back as the mid-1960s. This paper elaborates on three steps required to meet this goal: 1. A formal effort to redefine existing MTW sized Unit Type Codes (UTCs) to the scaleable, modular building blocks that support rotational contingencies, crisis action and deliberate planning. 2. Once resized, link UTCs together to form Force Modules representative of the contributions of aerospace power identified in Air Force Doctrine. 3. Continue ongoing efforts to develop the Deliberate Crisis Action Planning and Execution Segment(DCAPES) within the Global Command and Control System (GCCS).

DTIC

*Deployment; Management Planning; Military Operations*

**20010120408** Nebraska Univ., Omaha, NE USA

**The FAA: A Tombstone Agency? Putting the Nickname to the Test**

Lutte, Rebecca K., Nebraska Univ., USA; Bowen, Brent D., Nebraska Univ., USA; Collegiate Aviation Review; October 2000; Volume 18, No. 1, pp. 12-25; In English; See also 20010120406; Copyright; Avail: Issuing Activity

The purpose of this research was to investigate Federal Aviation Administration (FAA) activity before and after six catastrophic airline accidents to examine the alleged reactive policy-setting reputation of the FAA. Actions reviewed were regulatory, inspection, and enforcement activities. The study revealed that change in agency activity does occur following an accident. The location of the event appears to influence the direction of change. When accidents occurred within the USA, FAA activity increased following the accident. The opposite occurred for airline accidents outside the U.S. The increase in FAA activity following U.S. based events, supports the reactive, ”tombstone agency” reputation the FAA has acquired. In addition, the research revealed nine FAA activities judged by industry experts as having the ability to improve safety in the airline industry. Inspections and certificate actions are considered activities that will improve safety. Regulatory actions, fines, warning notices, and letters of correction were judged as non-safety enhancing activities. The result of this research was an increased understanding of how the FAA responds to airline accidents and the consequences of the response.

Author

*Airline Operations; Aircraft Accident Investigation; Aircraft Accidents; Policies; USA*

**20010120412** University of Central Washington, Ellensburg, WA USA

**Collision Avoidance at Nontowered Airports**

Sloan, Teresa Ann, University of Central Washington, USA; Collegiate Aviation Review; October 2000; Volume 18, No. 1, pp. 70-85; In English; See also 20010120406; Copyright; Avail: Issuing Activity

From January 1 of 1988 to December 31 of 1998 there were an average of 16.9 midair collisions and 17.7 fatalities per year involving general aviation aircraft in the USA. In February of 2000 alone there were five midair collisions. Most midair collisions occur in the traffic patterns of non-towered airports and on final approach. What can a general aviation pilot do to reduce the risk of a midair collision at a non-towered airport? What are the FAA’s and Transport Canada’s recommended procedures for traffic patterns? What alternative procedures are currently in use by pilots and are they safe? A review of the regulations, advisories, and various articles on the subject, a survey of flight instructors on the methods taught to enter such patterns, and a discussion of legal precedents and certificate actions will aid the pilot in choosing a method for pattern entry at non-towered airports.

Author

*Collision Avoidance; General Aviation Aircraft; Midair Collisions*

**20010120415** University of Eastern Michigan, Ypsilanti, MI USA

**Exploring the Viability of an Organizational Readiness Assessment for Participatory Management Programs in a Passenger Airline Carrier**

Bellamy, Al, University of Eastern Michigan, USA; Collegiate Aviation Review; October 2001; Volume 19, No. 1, pp. 10-28; In English; See also 20010120414; Copyright; Avail: Issuing Activity

This study attempted to determine the feasibility of conducting an organizational readiness assessment for a participatory management program for maintenance workers within a large passenger airline. Organizational readiness factors consisted of the motivation climate of the department, supervisory behaviors, and the employee's orientation to group problem-solving. The results of a questionnaire study among 73 line maintenance workers revealed that only the group orientation factors predicted employees' willingness to participate in group process improvement programs. However, strong and statistically significant correlations were shown among the willingness to participate variable and employee job satisfaction. The study revealed that employee group orientation moderates the relationships between the independent and criterion factors. Results also revealed that the employee's personality orientation moderates the relationships between the organizational factors and employees' willingness to participate in group process improvement programs.

Author

*Management Planning; Passenger Aircraft; Airline Operations; Group Dynamics*

**20010120426** Nebraska Univ., Omaha, NE USA

**Air Rage: A Policy Research Study**

Schaaf, Michaela M., Nebraska Univ., USA; Collegiate Aviation Review; October 2001; Volume 19, No. 1, pp. 168-186; In English; See also 20010120414; Copyright; Avail: Issuing Activity

Disruptive passengers are a growing concern to preserve the safety of crew and passengers in the air. A policy research study from 1996 to 2000 reveals a range of air rage incidents and airline policies. The various definitions are presented, as well as the scope of the problem. The caUSAl factors are critical in understanding the root of the problem and in eradicating air rage incidents. The application of the policy research methodology revealed a void in data collection and future research needs such as policy evaluation. Policy makers, collegiate aviation educators, and industry personnel will use these results to inform decision making. This article contributes to the academic literature of air rage as an emerging aviation safety concern.

Author

*Human Behavior; Civil Aviation; Policies*

**20010120477** NCI Information Systems, Inc., Fairborn, OH USA

**Passive Aircraft Status System (PASS) Preliminary Plan for Technology Development** ***Interim Report, Aug. 1999-Aug 2001***

January 2001; 38p; In English

Contract(s)/Grant(s): F41624-99-F-0007; Proj-2745

Report No.(s): AD-A394867; AFRL-HE-WP-TR-2001-0128; No Copyright; Avail: CASI; A03, Hardcopy; A01, Microfiche

The purpose of the Passive Aircraft Status System (PASS) demonstration is to exhibit the potential use of PASS in the aircraft maintenance arena. The PASS demonstration design and development is based upon data collected in the field from various field visits, platforms, and all levels of maintainers. This is the third phase of a three-phase effort and addresses the conceptual design and technologies used in the development of the PASS demonstration. This report represents the preliminary plan for technology development, which encapsulates and demonstrates the benefits of PASS in current and future maintenance processes.

DTIC

*Data Links; Data Systems; Passivity; Telecommunication*

**20010120488** General Accounting Office, Washington, DC USA

**Testimony before the Subcommittee on Aviation, Committee on Transportation and Infrastructure, House of Representatives. Aviation Security: Weaknesses in Airport Security and Options for Assigning Screening Responsibilities**

Sep. 21, 2001; 15p; In English

Report No.(s): AD-A395099; GAO-01-1165T; No Copyright; Avail: CASI; A01, Microfiche; A03, Hardcopy

A safe and secure civil aviation system is a critical component of the nations overall security, physical infrastructure, and economic foundation. Billions of dollars and a myriad of programs and policies have been devoted to achieving such a system. Although it is not fully known at this time what actually occurred or which of the weaknesses in the nations aviation security

apparatus contributed to the horrendous events of last week, it is clear that serious weaknesses exist in our aviation security system and that their impact can be far more devastating than previously imagined.
DTIC
*Airports; Airport Security; Warning Systems; Civil Aviation*

**20010122715** Nebraska Univ., Aviation Inst., Omaha, NE USA
**Small Aircraft Transportation System (SATS) Research Report**
Bowen, Brent D., Editor, Nebraska Univ., USA; Cullan, Tracey M., Editor, Nebraska Univ., USA; May 2000; 116p; In English; See also 20010122716 through 20010122727
Report No.(s): UNOAI-2000-3; Copyright; Avail: Issuing Activity

The Small Aircraft Transportation System (SATS) offers a safe travel alternative freeing people and products from today's system delays, creating access to more communities in less time. SATS will give more time to more people, satisfying a large portion of the emerging public demand for safe, higher-speed mobility and increased accessibility, while unleashing the full potential of the knowledge-based industrial expansion to more suburban, rural, and remote communities. The benefits include improved standards of living and quality of life for all in the new global economy. Nebraska has positioned itself as a leader state in pursuit of NASA's General Aviation Roadmap. The information contained in this publication describes the first year of efforts in Nebraska to implement the SATS concept. Specific goals for the second year of effort are included as well. It is hoped that this information will assist other states in developing their SATS programs and foster an arena of mutual collaboration.
Derived from text
*General Aviation Aircraft; NASA Programs; Airports; Nebraska*

**20010122716** Nebraska Univ., Omaha, NE USA
**NASA EPSCoR Nebraska Preparation Grant: Year 1. Research Cluster: Small Aircraft Transportation System/Nebraska Implementation Template (SATS-NIT)**
Bartle, John R., Nebraska Univ., USA; Bowen, Brent D., Nebraska Univ., USA; Gogos, George, Nebraska Univ., USA; Hinton, David W., Nebraska Univ., USA; Holmes, Bruce J., Nebraska Univ., USA; Lehrer, Henry R., Nebraska Univ., USA; Moussavi, Massoum, Nebraska Univ., USA; Reed, B. J., Nebraska Univ., USA; Schaaf, Michaela M., Nebraska Univ., USA; Smith, Russell L., Nebraska Univ., USA; Small Aircraft Transportation System (SATS) Research Report; May 2000, pp. 1-9; In English; See also 20010122715; Copyright; Avail: Issuing Activity

NASA, the U.S. Department of Transportation/Federal Aviation Administration, industry stakeholders, and academia have joined forces to pursue the NASA National General Aviation Roadmap leading to a Small Aircraft Transportation System (SATS). This strategic undertaking has a 25-year goal to improve air access and bring next-generation technologies to small communities. The envisioned outcome is to improve travel between remote communities and transportation centers in urban areas by utilizing the nation's 5,400 public use general aviation airports. to facilitate this initiative, SATS stakeholders must plan, coordinate, and implement a comprehensive upgrade of public infrastructure within the framework of the national air transportation system. Ultimately, SATS may permit tripling aviation system throughput capacity by tapping the under-utilized airspace and general aviation facilities. The SATS investments, which begin in FY 2001, are designed to support the national goal of doorstep-to-destination travel at four times the speed of highways for the nation's suburban, rural, and remote communities.
Author
*General Aviation Aircraft; Aircraft Industry; NASA Programs; Nebraska*

**20010122717** Nebraska Univ., Omaha, NE USA
**Small Aircraft Transportation System (SATS): White Paper. Policy Implications for Implementation of SATS at the State and Local Levels**
Bartle, John, Nebraska Univ., USA; Bowen, Brent, Nebraska Univ., USA; Deichert, Jerome, Nebraska Univ., USA; Lehrer, Henry, Nebraska Univ., USA; Krane, Dale, Nebraska Univ., USA; Reed, B. J., Nebraska Univ., USA; Smith, Russell, Nebraska Univ., USA; Small Aircraft Transportation System (SATS) Research Report; May 2000, pp. 10-19; In English, 17 Aug. 1999, Washington, DC, USA; See also 20010122715; Copyright; Avail: Issuing Activity

The National Aeronautics and Space Administration (NASA), U.S. Department of Transportation (DOT), Federal Aviation Administration (FAA), industry stakeholders, and academia have joined forces to pursue the NASA National General Aviation Roadmap leading to a Small Aircraft Transportation System (SATS). This strategic undertaking has a 25-year goal to bring the next-generation technologies to and improve travel between remote communities and transportation centers in urban areas by utilizing the nation's 5,400 public use general aviation airports. to facilitate this initiative, a comprehensive upgrade of public infrastructure must be planned, coordinated, and implemented within the framework of the national air transportation system.

Emanating from such a project of comprehensive national infrastructure change are seemingly unlimited issues of public policy, regulatory change, and financial viability (Bowen, Holmes, & Hansen, 1999). This review provides a cursory overview of the initial public policy issues. Funded by the Nebraska NASA EPSCoR Program, this study proposes to deliver research support in key public infrastructure areas in coordination with the General Aviation Program Office at the NASA Langley Research Center. The purpose for this research into areas of public policy is intended to provide a SATS implementation template for states. Toward this, focused research is in progress in the areas of systemic change and innovation, in public infrastructure, public finance, and economics for SATS planning in the states, and state and local airport planning for SATS implementation. Since this level of change is centrally focused at the state level, it is crucial to focus in the areas of state and local government. It is intended that the resulting template can be utilized by any state, with particular attention drawn to the specific differences of rural and urban areas (Bowen, Holmes, et al., 1999). Presented herein are several initial thoughts on key policy concerns raised by SATS prepared by the UNO (University of Nebraska at Omaha) team.
Author
*Air Transportation; General Aviation Aircraft; NASA Programs; Policies*

**20010122718** NASA Langley Research Center, Hampton, VA USA
**Development of a 21st Century Small Aircraft Transportation System**
Bowen, Brent D., Nebraska Univ., USA; Holmes, Bruce J., NASA Langley Research Center, USA; Hansen, Frederick, Nebraska Univ., USA; Small Aircraft Transportation System (SATS) Research Report; May 2000, pp. 20-22; In English; See also 20010122715; Copyright; Avail: Issuing Activity

The National Aeronautics and Space Administration (NASA), U.S. Department of Transportation, Federal Aviation Administration, industry stakeholders, and academia, have joined forces to pursue the NASA National General Aviation Roadmap leading to a Small Aircraft Transportation System (SATS). This strategic undertaking has a 25-year goal to bring the next-generation technologies and improve travel between remote communities and transportation centers in urban areas by utilizing the nation's 5,400 public use general aviation airports. To facilitate this initiative, a comprehensive upgrade of public infrastructure must be planned, coordinated, and implemented within the framework of the national air transportation system. The Nebraska NASA EPSCoR Program has proposed to deliver research support in key public infrastructure areas in coordination with the General Aviation Program Office at the NASA Langley Research Center. Ultimately, SATS may permit tripling aviation system throughput capacity by tapping the underutilized general aviation facilities to achieve the national goal of doorstep-to-destination travel at four times the speed of highways for the nation's suburban, rural, and remote communities.
Author
*Air Transportation; General Aviation Aircraft; NASA Programs; Research and Development*

**20010122719** Nebraska Univ., Coll. of Public Affairs and Community Service, Omaha, NE USA
**Implementing the Small Aircraft Transportation System (SATS) in Nebraska: Public Finance and Economic Issues in Planning SATS in the States**
Bartle, John R., Nebraska Univ., USA; Deichert, Jerome A., Nebraska Univ., USA; Hinton, David W., Nebraska Univ., USA; Small Aircraft Transportation System (SATS) Research Report; May 2000, pp. 23-31; In English; See also 20010122715; Copyright; Avail: Issuing Activity

Implementing SATS in Nebraska will require a number of changes, both technical and administrative. SATS will require major improvements in the infrastructure of Nebraska airports. The issue here is, how can those improvements be financed? Financing Goals Improving airport infrastructure so that it can accommodate SATS is first and most obvious goal. A second goal is to make airports financially sustainable over the long term with limited federal assistance. A third goal, closely related to the second, is to link the implementation of SATS with anticipated local economic growth. This can leverage local funds without tax increases, enhance the equity of the finance approach, improve planning of facility size, and reduce long-term per unit cost. Many of these goals are national issues, and presumably federal policy will determine how these goals are addressed. This study examines several financing options and discusses their ease of application to Nebraska's airports.
Derived from text
*Airports; Economics; Nebraska; General Aviation Aircraft*

**20010122720** Nebraska Univ., Omaha, NE USA
**The Small Aircraft Transportation System for America: A Case in Public Infrastructure Change**
Bowen, Brent D., Nebraska Univ., USA; Small Aircraft Transportation System (SATS) Research Report; May 2000, pp. 32-35; In English; World Congress on Aviation, 19-21 Oct. 1999, San Francisco, CA, USA; See also 20010122715; Copyright; Avail: Issuing Activity

The National Aeronautics and Space Administration (NASA), U.S. Department of Transportation, Federal Aviation Administration, industry stakeholders, and academia, have joined forces to pursue the NASA National General Aviation Roadmap leading to a Small Aircraft Transportation System (SATS). This strategic undertaking has a 25-year goal to bring next-generation technologies and improve travel between remote communities and transportation centers in urban areas by utilizing the nation's 5,400 public-use general aviation airports. to facilitate this initiative, a comprehensive upgrade of public infrastructure must be planned, coordinated, and implemented within the framework of the national air transportation system. The Nebraska NASA EPSCoR Program has proposed to deliver research support in key public infrastructure areas in coordination with the General Aviation Program Office at the NASA Langley Research Center. Ultimately, SATS may permit tripling aviation system throughput capacity by tapping the underutilized general aviation facilities to achieve the national goal of doorstep-to-destination travel at four times the speed of highways for the nation's suburban, rural, and remote communities.
Derived from text
*General Aviation Aircraft; NASA Programs; Air Transportation; Airports*

**20010122721** Nebraska Univ., Aviation Inst., Omaha, NE USA
**Implementing SATS in Nebraska: Airport Change, Compliance and Rural Demographics**
Lehrer, Hank, Nebraska Univ., USA; Waugh, Terry, Nebraska Univ., USA; Penney, Kent, Nebraska Dept. of Aeronautics, USA; Small Aircraft Transportation System (SATS) Research Report; May 2000, pp. 36-42; In English; See also 20010122715; Copyright; Avail: Issuing Activity

As outlined in the grant request for this sub-cluster, the approach to be used in this part of the research work encompasses goals in the short term as well as in the long term. In the short term, the development of a state-wide conceptual framework within which to develop the possible impact of the SATS airport program on the National Plan of Integrated Airport System (NPIAS) has a high priority. Major portions of this conceptual framework will be determined by stakeholders who will be affected by the implementation and evaluation of SATS in a NPIAS setting. Additionally, a need exists to justify the integration of a SATS airport approach advanced navigation and all-weather utilization) within the state airport master planning scheme. Effecting such a comprehensive change in public infrastructure will require coordination at the grassroots will require evaluation and change with state and local entities that would be identified in the developmental phase period. An additional component of this endeavor that has begun is to shape an interstate coalition of neighboring states that my realize enhanced benefits concerning SATS development as well as gain strength from such a union.
Author
*Nebraska; Rural Areas; Demography; Air Transportation*

**20010122722** Nebraska Univ., Dept. of Public Administration, Omaha, NE USA
**Financing the Airport of the Future: The Small Aircraft Transportation System**
Bartle, John R., Nebraska Univ., USA; Small Aircraft Transportation System (SATS) Research Report; May 2000, pp. 43-50; In English; National Tax Association Annual Conference, Atlanta, GA, USA; See also 20010122715; Copyright; Avail: Issuing Activity

The objective of SATS is to reduce gridlock at hubs, reduce travel times, allow for personal control over travel, and anticipate demand shifts resulting from a migration from suburbs to rural places. The technology is presently available and economical to produce SATS aircraft. The public issue centers on the airports. SATS is a federal program, and many airports in the U.S. are under the control of local governments. The scope of the objective will require thoUSAnds of airports in rural and suburban areas to modify their infrastructure and increase their investment. Researchers at the University of Nebraska at Omaha (UNO), and others at other institutions, have prepared reports surveying the relevant issues of implementing SATS. Our UNO team focused on the issues of policy implementation, economic development, management, and finance specific to Nebraska. We are finding that these issues are similar to those in other states in our region and other rural states. This paper discusses how this investment might be financed.
Derived from text
*Airports; Air Transportation; Civil Aviation; Financial Management*

**20010122723** Nebraska Univ., Dept. of Public Administration, Omaha, NE USA
**General Aviation in Nebraska: Nebraska SATS Project Background Paper No. 1**
Smith, Russell, Nebraska Univ., USA; Wachal, Jocelyn, Nebraska Univ., USA; Small Aircraft Transportation System (SATS) Research Report; May 2000, pp. 51-79; In English; See also 20010122715; Copyright; Avail: Issuing Activity

The Nebraska SATS project is a state-level component of NASA's Small Aircraft Transportation System (SATS). During the next several years the project will examine several different factors affecting SATS implementation in Nebraska. These include

economic and taxation issues, public policy issues, airport planning processes, information dissemination strategies, and systemic change factors. This background paper profiles the general aviation system in Nebraska. It is written to provide information about the ”context” within which SATS will be pursued. The primary focus is thus on describing and providing background information about the current situation. A secondary focus is on drawing general conclusions about the ability of the current system to incorporate the types of changes implied by SATS. First, some brief information on the U.S. aviation system is provided. The next two sections profile the current general aviation aircraft and pilot base. Nebraska’s system of general aviation airports is then described. Within this section of the paper, information is provided on the different types of general aviation airports in Nebraska, airport activity levels and current infrastructure. The fourth major section of the background paper looks at Nebraska’s local airport authorities. These special purpose local governments oversee the majority of the general aviation airports in the state. Among the items examined are total expenditures, capital expenditures and planning activities. Next, the paper provides background information on the Nebraska Department of Aeronautics (NDA) and recent Federal funding for general aviation in Nebraska. The final section presents summary conclusions.
Author
*General Aviation Aircraft; Nebraska; Economics; Airports*

**20010122724** Nebraska Univ., Dept. of Civil Engineering, Omaha, NE USA
**Small Aircraft Transportation System: White Paper. SATS Systems Engineering Precursor Studies/Nebraska Implementation**
Moussavi, Massoum, Nebraska Univ., USA; Small Aircraft Transportation System (SATS) Research Report; May 2000, pp. 80-81; In English; See also 20010122715; Copyright; Avail: Issuing Activity

SATS Systems Engineering Precursor Studies were initiated to support the development of the NASA-led National General Aviation Roadmap, the National Research Council (NRC) SATS Study, the Federal Aviation Administration (FAA) SATS Mission Needs Statement development, and the SATS Non Advocate Review (NAR) effort. The studies are designed to define SATS and provide a body of reference material to help determine whether a SATS development program should proceed. The University of Nebraska’s Aviation Institute is actively participating in the SATS program through its NASA Nebraska EPSCoR Preparation Grant, which began in May of 1999. The SATS Systems Engineering Precursor Studies/Nebraska Implementation cluster of this grant is supporting the on-going National SATS effort by developing a computer-based decision support system/model for SATS implementation in the State of Nebraska. The systems engineering requirements and SATS metrics for implementation in Nebraska are being identified and their inter-relationships (cause-and-effect relationships) are being investigated.
Derived from text
*General Aviation Aircraft; Systems Engineering; Nebraska; Air Transportation*

**20010122725** NASA Langley Research Center, Hampton, VA USA
**National General Aviation Roadmap for a Small Aircraft Transportation System (SATS)**
Holmes, Bruce J., NASA Langley Research Center, USA; Small Aircraft Transportation System (SATS) Research Report; May 2000, pp. 82; In English; See also 20010122715; Copyright; Avail: Issuing Activity

The National Aeronautics and Space Administration (NASA), Federal Aviation Administration, as well as state, industry, and academia partners have joined forces to pursue the NASA National General Aviation Roadmap leading to a Small Aircraft Transportation System (SATS). This long-term strategic undertaking has a goal to bring next-generation technologies and improve air access to small communities. The envisioned outcome is to improve travel between remote communities and transportation centers in urban areas by utilizing a new generation of single-pilot light planes for personal and business transportation between the nation’s 5,400 public use general aviation airports. Current NASA investments in aircraft technologies are enabling industry to bring affordable, safe, and easy-to-use features to the marketplace, including ”Highway in the Sky” glass cockpit operating capabilities, affordable crash worthy composite airframes, more efficient IFR flight training, and revolutionary engines. To facilitate this initiative, a comprehensive upgrade of public infrastructure must be planned, coordinated, and implemented within the framework of the national air transportation system. State partnerships are proposed to coordinate research support in key public infrastructure areas. Ultimately, SATS may permit more than tripling aviation system throughput capacity by tapping the under-utilized general aviation facilities to achieve the national goal of doorstep-to-destination travel at four times the speed of highways for the nation’s suburban, rural, and remote communities.
Author
*General Aviation Aircraft; NASA Programs; Rural Areas; Air Transportation*

**20010122726** NASA Langley Research Center, Hampton, VA USA
**National General Aviation Roadmap Definition for a Small Aircraft Transportation System Concept**
Holmes, Bruce J., NASA Langley Research Center, USA; Small Aircraft Transportation System (SATS) Research Report; May 2000, pp. 83-90; In English; See also 20010122715; Copyright; Avail: Issuing Activity

This paper presents trends and forces that shape 21 st century demand for higher-speed personal air transportation and outlines guidance developed by NASA in partnership with other federal and state government and industry partners, for Small Aircraft Transportation System (SATS) investment and partnership planning.
Author
*General Aviation Aircraft; Air Transportation; Airports; Economy*

**20010122727** Nebraska Univ., Aviation Inst., Omaha, NE USA
**Small Aircraft Transportation System (SATS): A Collaborative Effort Between Nebraska EPSCoR and NASA Langley Research Center**
Small Aircraft Transportation System (SATS) Research Report; May 2000, pp. 91-104; In English; See also 20010122715; Copyright; Avail: Issuing Activity

Implementing SATS in Nebraska will require a number of changes, both technical and administrative. SATS will require major improvements in the infrastructure of Nebraska airports. Improving airport infrastructure so that it can accommodate SATS is first and most obvious goal. A second goal is to make airports financially sustainable over the long term with limited federal assistance. A third goal, closely related to the second, is to link the implementation of SATS with anticipated local economic growth. This can leverage local funds without tax increases, enhance the equity of the finance approach, improve planning of facility size, and reduce long-term per unit cost. Many of these goals are national issues, and presumably federal policy will determine how these goals are addressed. This study examines several financing options and discusses their ease of application to Nebraska's airports.
Author
*Airports; Nebraska; NASA Programs; Air Transportation*

## 04
## AIRCRAFT COMMUNICATIONS AND NAVIGATION

*Includes all modes of communication with and between aircraft; air navigation systems (satellite and ground based); and air traffic control. For related information see also 06 Avionics and Aircraft Instrumentation; 17 Space Communications; Spacecraft Communications, Command and Tracking, and 32 Communications and Radar.*

**20010121544** Massachusetts Inst. of Tech., Lab. for Information and Decision Systems, USA
**Distributed and Centralized Conflict Management Under Traffic Flow Management Constraints**
Feron, Eric, Massachusetts Inst. of Tech., USA; Sep. 24, 2001; 1p; In English
Contract(s)/Grant(s): NCC2-1209; No Copyright; Avail: Issuing Activity; Abstract Only

The past year's activity has concentrated on the following two activities: (1) Refining and completing our study on the stability of interacting flows of aircraft when they have to resolve conflicts in a decentralized and sequential manner. More specifically, it was felt that some of the modeling assumptions made during previous research (such offset maneuvering models) could be improved to include more realistic models such as heading changes when analyzing interacting flow stability problems. We extended our analysis to achieve this goal. The results of this study have been submitted for presentation at the 2002 American Control Conference; (2) Examining the issues associated with delay propagation across multiple enroute sectors. This study was initiated at NASA in cooperation with Dr. Karl Bilimoria. Considering a set of adjacent sectors, this ongoing study concentrates on the effect of various traffic flow management strategies on the propagation of delays and congestion across sectors. The problem description and findings so far are reported in the attached working paper "Enroute sector buffering capacity."
Author
*Air Traffic; Management Methods*

**20010125640** Colorado Univ., Colorado Center for Astrodynamics Research, Boulder, CO USA
**GPS: A New Tool for Ocean Science *Final Report***
Komjathy, Attila, Colorado Univ., USA; Garrison, James L., NASA Goddard Space Flight Center, USA; Zavorotny, Valery, National Oceanic and Atmospheric Administration, USA; GPS World Magazine; [2001]; 8p; In English
Contract(s)/Grant(s): NAG1-1927; Copyright; Avail: Issuing Activity

In this article, we demonstrate wind retrieval (estimate its speed) from reflected signals obtained by a GPS receiver on board an aircraft to illustrate the potential of using GPS for remote-sensing applications. Before showing those results, we provide some background on radar remote sensing and discuss the theoretical model we used to interpret reflection data. This model describes the power and correlation properties of the reflected GPS signals as a function of scattering geometry and environmental parameters related to the reflecting surface.
Derived from text
*Global Positioning System; Remote Sensing; Signal Reflection; Wind Profiles; Ocean Surface*

## 05
## AIRCRAFT DESIGN, TESTING AND PERFORMANCE

*Includes all stages of design of aircraft and aircraft structures and systems. Also includes aircraft testing, performance, and evaluation, and aircraft and flight simulation technology. For related information, see also 18 Spacecraft Design, Testing and Performance and 39 Structural Mechanics. For land transportation vehicles, see 85 Technology Utilization and Surface Transportation.*

**20010119060** Missouri Univ., Columbia, MO USA
**Low-Temperature Plasma Coating for Aluminum** ***Final Report, 29 Jun. 1996-31 Mar. 2001***
Yasuda, Hirotsugu; Bierwagen, Gordon P.; Deffeyes, Joan E.; Wieliczka, David; Mar. 2001; 426p; In English; Original contains color images
Contract(s)/Grant(s): Proj-4346
Report No.(s): AD-A393077; AFRL-ML-WP-TR-2001-4104; No Copyright; Avail: CASI; A19, Hardcopy; A04, Microfiche

The primary objective of this research project was to provide an alternative corrosion protection through means of processes more environmentally benign than conventional methodologies. Hexavalent chromium (Cr+6) has historically been acknowledged to exhibit the technological forefront in collision protection of aluminum alloys. The Systems Approach Interface Engineering (SAIE) concept, adopted in this project, emphasizes the fact that the corrosion protection of a metal depends on the overall corrosion protective behavior of an entire system, including the bulk characteristics of the coatings(s) and interfacial factors. The primary methodologies used were plasma processing. The technology showed superior corrosion resistant results to traditional aircraft coating systems. This technology is applicable to aircraft piece parts.
DTIC
*Aluminum Alloys; Protective Coatings; Corrosion Prevention; Chromium*

**20010119580** Lockheed Martin Tactical Aircraft Systems, Fort Worth, TX USA
**Simulation Assessment Validation Environment (SAVE). Software User's Manual** ***Final Report, 1 Apr. 1995-30 Sep. 2000***
Cole, Paul; Bassett, Bob; Herndon, Marcia; Collins, Paul; Jacobson, Kathy; Sep. 2000; 428p; In English; Original contains color images
Contract(s)/Grant(s): F33615-95-C-5538; Proj-2025
Report No.(s): AD-A393041; JRES01046-1; AFRL-ML-WP-TR-2001-4089; No Copyright; Avail: CASI; A19, Hardcopy; A04, Microfiche

This document provides appropriate documentation for the user of the SAVE Virtual Manufacturing (VM) Environment. Two primary focus areas include use and implementation. In addition, the SAVE Final Report covers the full period of the SAVE Program, from April 1995 through September 2000, and a detailed description of the SAVE software system is documented in the SAVE Software Product End Item Report.
DTIC
*Aeronautical Engineering; Simulation*

**20010119581** Northrop Grumman Corp., Bethpage, NY USA
**Laminated Object Manufacturing-Based Design Ceramic Matrix Composites** ***Final Report, 1 Jun. 1998-25 Sep. 2000***
Mailunas, Raymond; Apr. 2001; 242p; In English; Original contains color images
Contract(s)/Grant(s): F33615-98-C-5121; Proj-8Y10
Report No.(s): AD-A393080; AFRL-ML-WP-TR-2001-4074; No Copyright; Avail: CASI; A11, Hardcopy; A03, Microfiche

Tbis report summarizes the significant accomplishments of the Laminated Object Manufacturing Based Design for Ceramic Matrix Composites Program. The overall objective of the twenty-seven month long effort was to further develop LOM based solid freeform fabrication for the rapid design and manufacture of CMC components for DoD applications. Program goals included

the development of( 1) a new LOM based design methodology for CMC (2) optimized preceramic polymer CMC material forms specific for LOM processing (3) LOM system upgrades to increase fabrication efficiencies and improve part tolerances /accuracy and (4) demonstration of the combined design methodology and materials and hardware improvements via the rapid design and LOM fabrication of a CMC prototype component. This program was funded through DARPA Contract No.F336l5-98-C-5 121 administered by the Air Force Wright Laboratory. Program participants included Northrop Grumman Corp. (Prime) Helisys Inc., and the University of Dayton Research Institute (UDRI). The technical approach included tasks in LOM based CMC design methodology development material and LOM system development and methodology demonstration. The demonstration component was an engine exhaust washed high temperature blastshield representative of structures anticipated on future military vertical short takeoff and landing (VSTOL) and low observable (LO) aircraft with shielded exhaust.
DTIC
*Computer Aided Design; Ceramic Matrix Composites; Efficiency; Prototypes; Systems Engineering*

**20010119605** Air Command and Staff Coll., Maxwell AFB, AL USA
**Counter Narcotics Missions for Unmanned Aerial Vehicles**
Snyder, Erik L.; Apr. 2000; 33p; In English; Original contains color images
Report No.(s): AD-A394937; AU/ACSC/165/2000-04; No Copyright; Avail: CASI; A03, Hardcopy; A01, Microfiche

With the ongoing draw down of US military forces and shrinking budgets, finding a more cost efficient means of accomplishing military missions is increasingly important. Current Department of Defense counter-narcotic missions operating in conjunction with U.S. Customs and the U.S. Coast Guard should consider using Unmanned Aerial Vehicles (UAVs) as adjunct to military forces or as the primary mission platform. UAVs have proven themselves as a valuable asset the military commander brings to the fight. Used effectively during military operations in Bosnia and Kosovo, UAVs were limited to intelligence and reconnaissance missions. Given the capabilities of UAVs, they can be more actively integrated into other military operations to enhance US military mission accomplishment. More specifically, UAVs should be incorporated into Intelligence, Surveillance, and Reconnaissance (ISR) roles specifically tailored to meet the challenges of the counter-narcotic mission. to support this proposition, my research will analyze current and proposed capabilities of UAVs as seen by military and industry leaders. Second, the mission of counter narcotics ISR will be examined to identify matching capabilities to the mission. Then an analysis of what specific capabilities UAVs can be incorporated into the mission of counter narcotics interdiction. Fourth, the integration of UAVs with current weapons systems to produce a synergistic effect will be analyzed. Finally, this paper will show that UAVs can be effectively integrated to enhance US Navy missions within our area of responsibility.
DTIC
*Military Operations; Pilotless Aircraft; Narcotics*

**20010119606** Air Command and Staff Coll., Maxwell AFB, AL USA
**Operational Considerations Related to Cockpit Automation and Crew Complement in the C-17**
Slatter, Steven R.; Apr. 2000; 37p; In English; Original contains color images
Report No.(s): AD-A394949; AU/ACSC/161/2000-04; No Copyright; Avail: CASI; A03, Hardcopy; A01, Microfiche

The newest airlifter in the Air Force inventory, the C-17, has a cockpit crew complement of two (pilot and copilot). This is a departure from the traditional airlift crew makeup that included additional crewmembers to handle navigation and aircraft systems. The extensive use of cockpit automation allowed this crew reduction. Major airlines, also making extensive use of cockpit automation, are finding challenges with automation in their fairly routine and mundane ops (compared with that of the military). Recent research has shown that automation can actually, rather than decreasing workload, increase cockpit workload beyond that of less automated aircraft during those periods where workload is already traditionally high. The mission of the C-17 is likely to see a less experienced crew flying low-level in a threat environment, talking to multiple controlling agencies, and trying to get into a location they’ve never seen after a 15 hour double air-refueling flight from the continental United States. These issues warrant operational consideration when employing the C-17 on some of it s most demanding missions, and are also applicable to other new or upgraded aircraft where similar cockpit/crew situations exist.
DTIC
*Commercial Aircraft; Airline Operations; Automatic Control*

**20010119611** Air Command and Staff Coll., Maxwell AFB, AL USA
**New Missions for the CV-22 ”OSPREY” in a Changing World**
Settergren, Daniel J.; Apr. 2000; 38p; In English; Original contains color images
Report No.(s): AD-A394968; AU/ACSC/157/2000-04; No Copyright; Avail: CASI; A03, Hardcopy; A01, Microfiche

The CV-22 OSPREY will become operational within the next few years. Although it is seen as a replacement for the aging, but still capable, MH-53J PAVELOW, the CV-22 improves upon the basic operating capabilities of its predecessor. The OSPREY will also be able to perform some of the same missions of the MC-130 COMBAT TALON. The CV-22 must fill the operational missions and roles currently performed by the MH-53, but it is also capable of much more. The task put forth to mission planners, tacticians, and Air Force leaders is to envision new roles and missions for the CV-22 that take advantage of its unique capabilities. After providing background information on the CV-22, the MH-53, and the MC-130, the author defines several likely threats that the military will face in the years to come. by reviewing documents such as Joint Vision 2010, Air Force 2025, and studies by the National Defense Panel and National Defense University, a common picture emerged of the threats and operating environments facing the US military in the next 10 to 15 years. Based on these scenarios the author answers the following research question: Based on likely future scenarios, are there new roles or missions that take advantage of the unique capabilities of the CV-22 beyond those already in development?
DTIC
*Vertical Takeoff Aircraft; Fighter Aircraft; Combat; Military Operations*

**20010119612** Air Command and Staff Coll., Maxwell AFB, AL USA
**Cockpit Automation and Mode Confusion: The Use of Auditory Inputs for Error Mitigation**
Spencer, Charles F., Jr; Apr. 2000; 41p; In English
Report No.(s): AD-A394969; AU/ACSC/167/2000-04; No Copyright; Avail: CASI; A03, Hardcopy; A01, Microfiche
The application of computer technology in modern cockpits has resulted in sophisticated automation that has created situations of mode confusion where the pilot is uncertain about the status or behavior of cockpit automation. Based on current levels of cockpit automation, classifications of mode confusion, and clinical knowledge concerning human cognitive and attentive processes, could an audible attention step help mitigate unrecognized mode error? The Software-Hardware-Environment-Liveware model forms a framework for the analysis of government and academic research concerning pilot automation experiences and use, cognitive models, information and decision processing, and the auditory attention channel. Pilot experiences and several aircraft accidents suggest that mode error is both common and potentially dangerous enough to warrant attempts at mitigation. Studies indicate that the monitoring requirement levied by automation lowers pilot system situational awareness without providing sufficient or proper feedback. Operators can also suffer from cognitive lockup and task channeling, which makes attention diversion difficult. An auditory input might provide an effective attention step if it demands appropriate attention, provides situation reporting, and offers problem guidance. These requirements might be fulfilled if the content is predictive, informational, localized, properly timed, and the theories of effective auditory characteristics proposed by Human Factors research are considered.
DTIC
*Cockpits; Auditory Signals; Automatic Control; Applications Programs (Computers); Feedback; Computer Systems Design*

**20010119624** NASA Ames Research Center, Moffett Field, CA USA
**Aeroelastic Considerations For Rotorcraft Primary Control with On-Blade Elevons**
Ormiston, Robert A., NASA Ames Research Center, USA; [2001]; 1p; In English; American Helicopter Society 57th Annual Forum and Technology Display, 9-11 May 2001, Washington, DC, USA; Sponsored by American Helicopter Society, Inc., USA; No Copyright; Avail: Issuing Activity; Abstract Only
Replacing the helicopter rotor swashplate and blade pitch control system with on-blade elevon control surfaces for primary flight control may significantly reduce weight and drag to improve mission performance. Simplified analyses are used to examine the basic aeroelastic characteristics of such rotor blades, including pitch and flap dynamic response, elevon reversal, and elevon control effectiveness. The profile power penalty associated with deflections of elevon control surfaces buried within the blade planform is also evaluated. Results suggest that with aeroelastic design for pitch frequencies in the neighborhood of 2/rev, reasonable elevon control effectiveness may be achieved and that, together with collective pitch indexing, the aerodynamic profile power penalty of on-blade control surface deflections may be minimized.
Author
*Aeroelasticity; Elevons; Planforms; Rotor Blades (Turbomachinery); Rotary Wing Aircraft*

**20010119918** NASA Ames Research Center, Moffett Field, CA USA
**A Comparison of the AVS-9 and the Panoramic Night Vision Goggle During Rotorcraft Hover and Landing**
Szoboszlay, Zoltan, NASA Ames Research Center, USA; Haworth, Loran, NASA Ames Research Center, USA; Simpson, Carol, NASA Ames Research Center, USA; [2001]; 1p; In English; American Helicopter Society Forum, 9-11 May 2001, Unknown; Sponsored by American Helicopter Society, Inc., USA; No Copyright; Avail: Issuing Activity; Abstract Only

The purpose of this flight test was to measure any differences in pilot-vehicle performance and pilot opinion between the use of the current generation AVS-9 Night Vision Goggle and one variant of the prototype Panoramic Night Vision Goggle (the PNV.GII). The PNVGII has more than double the horizontal field-of-view of the AVS-9, but reduced image quality. The flight path of the AH-1S helicopter was used as a measure of pilot-vehicle performance. Also recorded were subjective measures of flying qualities, physical reserves of the pilot, situational awareness, and display USAbility. Pilot comment and data indicate that the benefits of additional FOV with the PNVGIIs are to some extent negated by the reduced image quality of the PNVGIIs.
Author
*Rotary Wing Aircraft; Night Vision; Aircraft Landing; Goggles; Flight Tests; Human Factors Engineering*

**20010120155** Army Aviation Systems Command, Saint Louis, MO USA
**Rotary Wing Aircraft Crash Resistance**
May 01, 1987; 46p; In English
Report No.(s): AD-A395118; No Copyright; Avail: CASI; A03, Hardcopy; A01, Microfiche
This dicument establishes minimum crashworthiness criteria for implementation in the initial stages of aircraft system design.
Derived from text
*Rotary Wing Aircraft; Crashworthiness; Systems Engineering; Aircraft Fuel Systems*

**20010120478** Cranfield Univ., Cranfield, UK
**Session A. Damage Tolerance in Helicopters: Situation Today**
Mariani, Ugo, Cranfield Univ., UK; January 2000; 293p; In English
Contract(s)/Grant(s): N68171-00-M-5512
Report No.(s): AD-A394869; No Copyright; Avail: CASI; A13, Hardcopy; A03, Microfiche
A proper validation of the type of flaws and the method used to test flawed elements is considered essential. An example is provided detailing the evidences to validate scratches in aluminum. A survey of service data and test evidences provided information on a severe manufacturing scratch, showing that plastic deformation and notch radius at crack tip are the relevant parameters for the crack initiation. The crack growing path of a component failed in service showed negligible effects of the notch were plastic deformation had occurred, although the crack was growing very close to the scratch. Milling an U' shaped gauge in SCT specimens tested at CAL made a very sharp scratch. Considering the scratch like a crack, AK was computed for each coupon. Depending on the applied stress, specimens failed if the AK was higher than the threshold value, and they gave run out if lower.
DTIC
*Helicopters; Tolerances (Mechanics); Damage*

**20010121539** NASA Ames Research Center, Moffett Field, CA USA
**Review of Full-Scale F/A-18 Research at NASA Ames Research Center**
Olson, Lawrence E., NASA Ames Research Center, USA; [1994]; 1p; In English, 24-26 May 1994, Ottawa, Medley, Alberta, Canada, Canada
Contract(s)/Grant(s): RTOP 505-63-30; No Copyright; Avail: Issuing Activity; Abstract Only
Results of flow visualization and tail buffett studies conducted on a full-scale production F/A-18 fighter aircraft in the 80- by 120-Foot Wind Tunnel of the National Full-Scale Aerodynamic Complex are presented. Test conditions range between 20 degrees and 40 degrees angle of attack, 16 degrees and -16 degrees side-slip angle, and up to a Mach number of 0.15 (corresponding to a Reynolds number of 12.3 x 10(exp 6) based on mean aerodynamic chord). Flow visualization results include both surface and off-surface techniques that examine forebody, canopy, leading-edge extension, and wing flow fields. Unsteady pressures measured at 96 locations on the port tail fin are used to determine the effect of a removable leading-edge extension fence on tail buffet loads at high angle of attack. Analyses and comparisons include tail fin bending moment and wave velocities on the tail surface. Repeatability and scaling issues are assessed through comparison with measurements from previous full-scale tests and several small-scales tests.
Author
*F-18 Aircraft; Flow Visualization; Wind Tunnel Tests; Angle of Attack; Buffeting; Full Scale Tests*

**20010121578** Defence Science and Technology Organisation, Airframes and Engines Div., Fishermans Bend, Australia
**An Analytically Validated Highly Damped Repair for Acoustically-Induced Cracking on the F/A-18 Nacelle Skin**
Galea, S. C., Defence Science and Technology Organisation, Australia; Callinan, R. J., Defence Science and Technology Organisation, Australia; June 2001; 54p; In English; Original contains color illustrations
Report No.(s): DSTO-TR-1162; DODA-AR-011-893; Copyright; Avail: Issuing Activity

The skin of an aircraft can vibrate as a result of pressure waves caused by engine and/or aerodynamic effects. In modern fighter aircraft such as the F/A-18, overall sound pressure levels have been recorded up to 170 dB over the surface of the skin. In the F/A-18, cracking has occurred in the lower nacelle external skin, typically along the boundaries of the panel. These cracks often originate from a fastener line and grow along the boundary and then turn into the centre of the panel. In the case of the F/A-18, cracking was due to higher than expected pressure levels caused by an aerodynamic disturbance at the inlet lip. Initial design of this region was based on an overall sound pressure of 160db, which was based on initial computational fluid dynamics (CFD) work. An attempt was made to repair a panel with a boron fibre patch however this repair did not appear to significantly reduce the crack growth. The design of the repair was based on in-plane loads only. In this report the aim is to develop a patch design, based on a finite element analysis, which significantly reduces crack stress intensity factor for structures subject to intense acoustic environments. A significant reduction in stress intensity is achieved by using a highly damped patch which incorporates a uni-directional boron/epoxy repair and constrained damping layers which consists of viscoelastic material, which provides the necessary damping, and [0/90] boron/ epoxy constraining layers. Such configurations have shown that theoretical reductions in stress intensity factors of up to 10 times are achievable. This has the potential of reducing the mode I stress intensity factor (K(sub I)) to the order of K(sub I) threshold thus substantially reducing crack growth.
Author
*Numerical Analysis; Acoustics; Crack Propagation; Stress Intensity Factors; Aerodynamic Configurations; Boron-Epoxy Composites; Proving*

**20010121881** Utah State Univ., Stewart Radiance Lab., USA
**IR Field Measurements from the FISTA Aircraft; Calibration, Data Reduction, and Development of IR Signature Models** ***Final Report***
Kristl, Joseph A.; Hudson, Thomas H.; Saletnik, Donald; Goodwin, Warren E.; Wilkinson, George; Jul. 10, 1999; 26p; In English
Contract(s)/Grant(s): F19628-93-C-0183; Proj-7670
Report No.(s): AD-A394460; AFRL-VS-TR-1999-1524; No Copyright; Avail: CASI; A01, Microfiche; A03, Hardcopy
This report summarizes the work performed under contract F19628-93-C-0183 from October 1993 to December 1998. All of the field measurements performed on the ground and in aircraft are summarized, with types of data and targets described. Data sets reduced and analyzed under this contract are listed. Databasing support of infrared data is presented, along with a list of aircraft target databases assembled and delivered. Aircraft infrared signature modeling work and support is also listed. Hardware and instrument development tasks accomplished are shown.
DTIC
*Measurement; Infrared Signatures; Calibrating; Infrared Radiation*

**20010122307** Sandia National Labs., Albuquerque, NM USA
**Further Evolution of Composite Doubler Aircraft Repairs Through a Focus on Niche Applications**
Roach,; Jul. 15, 2000; 9p; In English
Report No.(s): DE2000-761052; SAND2000-1688C; No Copyright; Avail: Department of Energy Information Bridge
The number of commercial airframes exceeding twenty years of service continues to grow. A typical aircraft can experience over 2,000 fatigue cycles (cabin pressurizations) and even greater flight hours in a single year. An unavoidable by-product of aircraft use is that crack and corrosion flaws develop throughout the aircraft's skin and substructure elements. Economic barriers to the purchase of new aircraft have created an aging aircraft fleet and placed even greater demands on efficient and safe repair methods. The use of bonded composite doublers offers the airframe manufacturers and aircraft maintenance facilities a cost effective method to safety extend the lives of their aircraft. Instead of riveting multiple steel or aluminum plates to facilitate an aircraft repair, it is now possible to bond a single Boron-Epoxy composite doubler to the damaged structure. The FAA's Airworthiness Assurance Center at Sandia National Labs (AANC) is conducting a program with Boeing and Federal Express to validate and introduce composite doubler repair technology to the US commercial aircraft industry. This project focuses on repair of DC-10 structure and builds on the foundation of the successful L-1011 door corner repair that was completed by the AANC, Lockheed-Martin, and Delta Air Lines. The L-1011 composite doubler repair was installed in 1997 and has not developed any flaws in over three years of service, As a follow-on effort, this DC-1O repair program investigated design, analysis, performance (durability, flaw containment, reliability), installation, and nondestructive inspection issues. Current activities are demonstrating regular use of composite doubler repairs on commercial aircraft. The primary goal of this program is to move the technology into niche applications and to streamline the design-to-installation process. Using the data accumulated to date, the team has designed, analyzed, and developed inspection techniques for an array of composite doubler repairs with high-use fuselage skin applications. The general DC-10 repair areas which provide a high payoff to FedEx and which minimize design and installation complexities have been identified as follows: (1) gouges, dents, lightning strike, and impact skin damage, and (2) corrosion grind outs in surface

skin. This paper presents the engineering activities that have been completed in order to make this technology available for widespread commercial aircraft use.
NTIS
*Aircraft Maintenance; Aircraft Structures; Boron-Epoxy Composites; Commercial Aircraft*

**20010125012** Systems and Electronics, Inc., Elk Grove Village, IL USA
**Statistical Loads Data for Cessna 172 Aircraft Using the Aircraft Cumulative Fatigue System (ACFS)** ***Final Report***
Aug. 2001; 100p; In English
Report No.(s): PB2001-108661; DOT/FAA/AR-01/44; No Copyright; Avail: CASI; A05, Hardcopy; A02, Microfiche

The purpose of this research and development program was to manufacture a small, lightweight, low-cost recorder for loads USAge monitoring of general aviation and commuter type aircraft to support the Federal Aviation Administration (FAA) Operational Loads Monitoring Program. The scope of activities performed involved the following: (1) design, development, manufacturing and test of a low-cost Airframe Cumulative Fatigue System (ACFS), (2) installation of the ACFS into a fleet of seven Cessna 172 aircraft owned and operated by Embry-Riddle Aeronautical University, (3) conduct aircraft USAge data acquisition on seven Cessna 172 aircraft, (4) define the effectiveness of ACFS in the data acquisition effort and any required design changes required for the ACFS, and (5) provide the resultant processed data from the data acquisition effort in formats useful to the FAA. Presented in this report are the description of the ACFS, the analysis and statistical summaries of the data collected from 1000 flights representing 1168 hours of Cessna 172 aircraft operational data. The end product from the data acquisition effort includes statistical information on acceleration, speeds, altitudes, and flight duration and distance.
NTIS
*Cessna 172 Aircraft; Loads (Forces); Manufacturing; Aircraft Structures; Recorders; Aircraft Control; Attitude Control*

**20010125458** Bechtel Nevada Corp., Las Vegas, NV USA
**Geometric Correction System Capabilities, Processing, and Application**
Brewster, S. B.; Jun. 30, 1999; 10p; In English
Report No.(s): DE2001-8290; DOE/NV/11718-315; No Copyright; Avail: Department of Energy Information Bridge, Microfiche

The U.S. Department of Energy's Remote Sensing Laboratory developed the geometric correction system (GCS) as a state-of-the-art solution for removing distortions from multispectral line scanner data caused by aircraft motion. The system operates on Daedalus AADS-1268 scanner data acquired from fixed-wing and helicopter platforms. The aircraft attitude, altitude, acceleration, and location are recorded and applied to the data, thereby determining the location of the earth with respect to a given datum and projection. The GCS has yielded a positional accuracy of 0.5 meters when used with a 1-meter digital elevation model. Data at this level of accuracy are invaluable in making precise aerial estimates and as input into a geographic information system. The combination of high-spatial resolution and accurate geo-rectification makes the GCS a unique tool in identifying and locating environmental conditions, finding targets of interest, and detecting changes as they occur over time.
NTIS
*Multispectral Band Scanners; Geometric Rectification (Imagery); Remote Sensing; Airborne Equipment*

## 07
## AIRCRAFT PROPULSION AND POWER

*Includes prime propulsion systems and systems components, e.g., gas turbine engines and compressors; and onboard auxiliary power plants for aircraft. For related information see also 20 Spacecraft Propulsion and Power, 28 Propellants and Fuels, and 44 Energy Production and Conversion.*

**20010118354** NASA Ames Research Center, Moffett Field, CA USA
**Large Scale Scramjet Propulsion Testing In The Mach 8 and 16 Regime At NASA Ames Research Center**
Arnold, James O., NASA Ames Research Center, USA; Deiwert, George S., NASA Ames Research Center, USA; Covington, M. Alan, NASA Ames Research Center, USA; White, Michael E., Johns Hopkins Univ., USA; [1994]; 1p; In English; Twelfth International Symposium on Airbreathing Engines, 10-15 Sep. 1995, Melbourne, Australia; No Copyright; Avail: Issuing Activity; Abstract Only

The objective of this paper is to describe the affordable, large scale scramJet test capability for flight Mach numbers between 8 and 16 which has been developed at the NASA Ames Research Center. Details of the Direct Connect Arc Facility DCAF, which can produce combustor test conditions with fuel-on testing for 10 seconds at conditions representative of Mach 8 - 12 flight, are presented and typical test results are described. Likewise, a description of the full scale combustor test capability of the 16 inch

shock tunnel is outlined. This facility is characterized by long run times (> 5 milliseconds) for an impulse facility, and it can provide conditions representative of flight conditions from Mach 12 - 16. Typical test results for this shock tunnel are discussed as well. Future upgrades to both facilities are outlined and new uses for their capabilities are discussed.
Author
*Supersonic Combustion Ramjet Engines; Full Scale Tests; Hypersonic Speed; Combustion Chambers; Fuel Tests*

**20010120270** Oak Ridge National Lab., TN USA
**Exposure of Ceramics and Ceramic Matrix Composites in Simulated and Actual Combustor Environments**
Brentnall, W. D.; Ferber, M. K.; Keiser, J. R.; Miriyala, N.; More, K. L.; Jun. 07, 1999; 9p; In English
Report No.(s): DE2001-10537; ORNL/CP-102082; KJ-01-02-00-0; No Copyright; Avail: Department of Energy Information Bridge

A high-temperature, high-pressure, tube furnace has been used to evaluate the long term stability of different monolithic ceramic and ceramic matrix composite materials in a simulated combustor environment. All of the tests have been run at 150 psia, 1204 degrees C, and 15% steam in incremental 500 h runs. The major advantage of this system is the high sample throughput; >20 samples can be exposed in each tube at the same time under similar exposure conditions. Microstructural evaluations of the samples were conducted after each 500 h exposure to characterize the extent of surface damage, to calculate surface recession rates, and to determine degradation mechanisms for the different materials. The validity of this exposure rig for simulating real combustor environments was established by comparing materials exposed in the test rig and combustor liner materials exposed for similar times in an actual gas turbine combustor under commercial operating conditions.
NTIS
*Composite Materials; Furnaces; Gas Turbines; Combustion Chambers; Stability; Ceramic Matrix Composites*

**20010120422** University of Southern Illinois, Carbondale, IL USA
**The Future and Potential of Non-Steady Flow Devices in Advanced Propulsion Designs**
Most, Michael, University of Southern Illinois, USA; Rodriguez, Charley, University of Southern Illinois, USA; Head, Larry, University of Southern Illinois, USA; Collegiate Aviation Review; October 2001; Volume 19, No. 1, pp. 102-110; In English; See also 20010120414; Copyright; Avail: Issuing Activity

Conventional aircraft powerplants generate a propulsive force through the application of a relatively constant fluidic flow. In non-steady flow propulsion, an unevenness of fluidic pressure is developed and purposefully controlled with the objective of producing thrust. This paper reviews basic non-steady flow concepts and presents potential applications for emerging technologies.
Author
*Pulsejet Engines; Propulsion System Performance; Unsteady Aerodynamics; Pneumatics*

**20010121515** Brookhaven National Lab., Upton, NY USA
**Small oil burner concepts based on low pressure air atomization**
Butcher,; Celebi,; Wei,; Kamath,; Mar. 16, 2000; 10p; In English
Report No.(s): DE2000-755030; BNL-67227; No Copyright; Avail: Department of Energy Information Bridge

The development of several novel oil burner applications based on low pressure air atomization is described. The atomizer used is a prefilming, airblast nozzle of the type commonly used in gas turbine combustion. The air pressure used can be as low as 1,300 Pa and such pressure can be easily achieved with a fan. Advantages over conventional, pressure-atomized nozzles include ability to operate at low input rates without very small passages and much lower fuel pressure requirements. The development of three specific applications is presented. The first two are domestic heating burners covering a capacity range 10 to 26 kW. The third application presented involves the use of this burner in an oil-fired thermophotovoltaic power generator system. Here the design firing rate is 2.9 kW and the system produces 500 watts of electric power.
NTIS
*Atomizing; Burners; Oils; Gas Turbine Engines*

**20010122282** Defence Science and Technology Organisation, Airframes and Engines Div., Fishermans Bend, Australia
**Measurement of the Natural Bending Modes of Rotors in the TF30 Engine**
Shilo, Mark, Defence Science and Technology Organisation, Australia; Becker, Andrew, Defence Science and Technology Organisation, Australia; September 2001; 24p; In English
Report No.(s): DSTO-TN-0393; DODA-AR-012-009; Copyright; Avail: Issuing Activity

The natural bending modes of the high and low speed shafts from the TF30 engine were measured in order to provide an unequivocal reference for validation of 3D Finite Element models of the shafts. The shafts were assembled separately, and without blades or any engine casing structure,
Author
*Bending; Shafts (Machine Elements); Measurement*

**20010123456** Oak Ridge Y-12 Plant, TN USA
**Welding and weldability of directionally solidified single crystal nickel-base super-alloys**
Vitek, J. M.; Sep. 01, 1996; 6p; In English
Report No.(s): DE2001-11013; Y/AMT-622; No Copyright; Avail: Department of Energy Information Bridge

The objective of this CRADA project was to investigate the weldability of polycrystalline, directionally-solidified, and single-crystal, nickel-base super-alloys. These materials are used extensively in turbine engine components. The ability to weld these materials is highly desirable in that it would greatly facilitate component fabrication. Welding of these materials would also have the potential benefit of allowing for the repair of cracked or worn components. Specifically, the program had four objectives: (1) to evaluate the weldability of nickel-base super-alloys; (2) to characterize the solidification microstructure of the welds; (3) to evaluate the phase stability of the weldments during exposure to service conditions; and (4) to determine the mechanical properties of the welds. Westinghouse Electric Corporation was to supply material for the program, in both as-case and heat-treated form. This was to include commercially available as well as experimental alloys developed at Westinghouse. ORNL was to perform weldability tests on the materials using a variety of welding procedures.
NTIS
*Nickel Alloys; Gas Turbine Engines; Weldability*

## 08
## AIRCRAFT STABILITY AND CONTROL

*Includes flight dynamics, aircraft handling qualities; piloting; flight controls; and autopilots. For related information, see also 05 Aircraft Design, Testing and Performance and 06 Avionics and Aircraft Instrumentation.*

**20010122270** NASA Dryden Flight Research Center, Edwards, CA USA
**Correlation of F/A-18 Tall Buffet Results**
Meyn, Larry, NASA Ames Research Center, USA; James, Kevin, Sterling Federal Systems, Inc., USA; Geenen, Robert, NASA Dryden Flight Research Center, USA; Rizk, Yehia; [1994]; 1p; In English; 4th NASA High Alpha Conference/Workshop, 12-14 Jul. 1994, Edwards, CA, USA
Contract(s)/Grant(s): RTOP 505-59-30; No Copyright; Avail: Issuing Activity; Abstract Only

Tail Buffet measurements from the second full-scale F/A-18 wind tunnel test are presented and compared with small-scale wind tunnel measurements, recent flight test measurements, and to CFD computations. Non-dimensional power spectra for unsteady pressures at the 60%-span, 45%-chord location on the vertical tail are presented from several small-scale wind tunnel tests, from the full-scale wind tunnel tests, and from flight tests. In addition non-dimensional power spectra for unsteady fin bending moment due to integrated pressures on the vertical tail are presented from full-scale wind tunnel tests, the flight test, and from CFD. Data are presented for the F/A-18 with and without the LEX fence. The data show that the dominant frequency of the unsteady fin pressures scales with velocity and inversely with model size, as with Strouhal shedding. The CFD predictions are shown to give a reasonably close prediction of the principal buffeting frequency for the LEX fence off configuration, but they failed to predict the correct trends for the change in frequency and power for the LEX fence on configuration. The overall comparisons indicate that small-scale wind tunnel tests adequately predict frequency and power of the buffeting pressures. Practical use of CFD for predictions of tail buffet will probably require a significant increase over current computer capabilities. The full-scale wind tunnel studies of tail buffet have been completed, but analysis of the data is still in progress.
Author
*F-18 Aircraft; Wind Tunnel Tests; Buffeting; Power Spectra; Bending Moments*

## 09
## RESEARCH AND SUPPORT FACILITIES (AIR)

*Includes airports, runways, hangars, and aircraft repair and overhaul facilities; wind tunnels, water tunnels, and shock tubes; flight simulators; and aircraft engine test stands. Also includes airport ground equipment and systems. For airport ground operations see 03 Air Transportation and Safety. For astronautical facilities see 14 Ground Support Systems and Facilities (Space).*

**20010120420** University of Southern Illinois, Carbondale, IL USA
**The Need for Airport Funding**
Kaps, Robert W., University of Southern Illinois, USA; NewMyer, David A., University of Southern Illinois, USA; Lanman, Richard T., University of Southern Illinois, USA; Sigler, Jason, University of Southern Illinois, USA; Collegiate Aviation Review; October 2001; Volume 19, No. 1, pp. 71-91; In English; See also 20010120414; Copyright; Avail: Issuing Activity

As a major component of the aviation industry, airports today rely on huge amounts of capital to keep the avenues of air transportation open. The Airport and Airways Development Act of 1970 became effective in May 1970 and provided a major source of airport capital improvement funding. However, since this law was passed airport capital needs have grown well beyond the capabilities of the federal government to fund them. Airports face a different financial market than their industry contemporaries; due in part to the regulated public environment, the uniqueness of airport revenue generation and debt markets. The need for airport funding will be explained by exploring the basics of airport operating costs, capital costs and revenue generation. An investigation of capital finance strategies will bring the conclusion.
Author
*Aircraft Industry; Airports; Financial Management; Revenue*

**20010121546** NASA Ames Research Center, Moffett Field, CA USA
**Reliability-Based Design of a Safety-Critical Automation System: A Case Study**
Carroll, Carol W.; Dunn, W.; Doty, L.; Frank, M. V.; Hulet, M.; [1994]; 2p; In English; A Bridge Into the 21st Century, Unknown; No Copyright; Avail: Issuing Activity; Abstract Only

In 1986, NASA funded a project to modernize the NASA Ames Research Center Unitary Plan Wind Tunnels, including the replacement of obsolescent controls with a modern, automated distributed control system (DCS). The project effort on this system included an independent safety analysis (ISA) of the automation system. The purpose of the ISA was to evaluate the completeness of the hazard analyses which had already been performed on the Modernization Project. The ISA approach followed a tailoring of the risk assessment approach widely used on existing nuclear power plants. The tailoring of the nuclear industry oriented risk assessment approach to the automation system and its role in reliability-based design of the automation system is the subject of this paper.
Author
*Wind Tunnels; Safety; Replacing; Automatic Control*

## 12
## ASTRONAUTICS (GENERAL)

*Includes general research topics related to space flight and manned and unmanned space vehicles, platforms or objects launched into, or assembled in, outer space; and related components and equipment. Also includes manufacturing and maintenance of such vehicles or platforms. For specific topics in astronautics see categories 13 through 20. For extraterrestrial exploration, see 91 Lunar and Planetary Science and Exploration.*

**20010119230** Naval War Coll., Joint Military Operations Dept., Newport, RI USA
**The Limits of Spacepower**
McNeely, Michael T.; May 18, 2001; 25p; In English
Report No.(s): AD-A395090; No Copyright; Avail: CASI; A03, Hardcopy; A01, Microfiche

The USA military has become highly dependent on space-based assets in the critical areas of communications, intelligence, surveillance and reconnaissance (ISR), and precision navigation. This dependence, coupled with the lack of redundant capabilities, leaves the U.S. particularly vulnerable in these areas, as we risk having this capability neutralized or destroyed. The CINC or JTF commander's staff must be knowledgeable of these vulnerabilities when planning a campaign or major operation, and should build alternatives, backup capabilities and redundancies into its plans and functions, in the event these critical assets are no longer available. One alternative to space-based communications and ISR capabilities is the use of unmanned aerial vehicles (UAVs). These platforms offer a variety of similar capabilities, including wide-band communications and a variety of

intelligence-collecting sensors. Other technologies are in development to offer an alternative to the Global Positioning System (GPS). Space power, like air power before it, holds tremendous promise for conducting future military operations. We are still tapping its potential and exploring the unique ways it brings synergy to the battle. We must not be so enamored by its possibilities that we pass up sensible cost-efficient alternatives, thereby placing our warfighters at risk on the battlefields of the future.
DTIC
*Military Operations; Reconnaissance; Aerospace Systems; Telecommunication*

**20010119235** Air War Coll., Maxwell AFB, AL USA
**China in Space: Civilian and Military Developments**
Thompson, David J.; Morris, William R.; Aug. 2001; 34p; In English
Report No.(s): AD-A395066; No Copyright; Avail: CASI; A03, Hardcopy; A01, Microfiche
The purpose of this paper is to discuss how China's space program aids the government in reaching for great power status.
DTIC
*Military Technology; Chinese Space Program; Aerospace Industry; Economics*

**20010119582** Booz-Allen and Hamilton, Inc., McLean, VA USA
**Department of Defense Space Technology Guide**
Jan. 01, 2001; 78p; In English; Original contains color images
Report No.(s): AD-A393837; No Copyright; Avail: CASI; A05, Hardcopy; A01, Microfiche
In preparing this DoD Space Technology Guide (STG) , the full range of national security space-related technology activities needed or under way across the U.S. space community was surveyed. Starting with the U.S. Space Command's Long Range Plan of 1998, which implemented Joint Vision 2010 and provided the basis for Service space planning documents (such as the Air Force Space Master Plan of 2000), we reviewed the national security space-relevant portions of the Defense Science and Technology (S & T) documentation, which includes the: Basic Research Plan (BRP); Defense Technology Area Plan (DTAP); Joint Warfighting Science and Technology Plan (JWSTP); Defense Technology Objectives (DTOs) of the JWSTP and DTAP.
DTIC
*Research and Development; Technologies*

**20010119619** Aerospace Corp., El Segundo, CA USA
**COTS-Based Systems: Lessons Learned from Experiences with COTS Software Use on Space Systems**
Adams, R. J.; Eslinger, S.; Sep. 10, 2001; 23p; In English
Contract(s)/Grant(s): F04701-00-C-0009
Report No.(s): AD-A395043; TR-2001(8550)-1; SMC-TR-01-19; No Copyright; Avail: CASI; A03, Hardcopy; A01, Microfiche
The incorporation of COTS software into software-intensive systems brings promises of reduced cost and schedule, along with higher reliability and maintainability by using "proven" software. However, the reality of using COTS software can be very different! This report presents the results of a survey of USAF Space and Missile Systems Center (SMC) and National Reconnaissance Office (NRO) program experience with incorporating COTS software into their systems. Six major lessons learned derived from the survey are described, along with recommendations for improving the acquisition of COTS -based systems.
DTIC
*Commercial Off-The-Shelf Products; Software Engineering; Aerospace Systems; Computer Programs*

**20010120135** Air War Coll., Maxwell AFB, AL USA
**Bad News Borscht: US Space Gets Taken for a Ride**
Hanbey, Glenn T.; Apr. 1999; 52p; In English; Original contains color images
Report No.(s): AD-A395181; AU/AWC/115/1999-04; No Copyright; Avail: CASI; A04, Hardcopy; A01, Microfiche
This paper looks at the evolving relationships between military, civil and commercial space interests in an international context. More specifically, it examines the question of whether the USA increased dependency on the commercial space sector for critical functions has ultimately made us overly dependent on the Russian space industry. This dependence would include critical functions for our commercial, civil and defense needs.
DTIC
*Military Technology; Aerospace Environments; Aerospace Industry; Armed Forces (USA)*

**20010120152** Aerospace Corp., Lab. Operations, El Segundo, CA USA

**Examination of Suspected Delta II Second-Stage Reentry Debris**

Adams, P. M.; Kao, W. H.; Jul. 15, 2001; 25p; In English

Contract(s)/Grant(s): F04701-00-C-0009

Report No.(s): AD-A395133; TR-2001(1494)-1; SMC-TR-01-16; No Copyright; Avail: CASI; A03, Hardcopy; A01, Microfiche

A piece of suspected reentry debris was submitted to the Materials Science Department for analysis to determine whether its composition was consistent with its supposed source. The debris consisted of a black-colored woven fabric that locally had clear fused-looking areas, with entrapped bubbles, and small metallic deposits. The time and location of the recovered debris correspond with the reentry of a Delta II second stage. The second-stage fuel tank, thrust chamber, and a pressure vessel impacted at several locations in Texas, and trajectory analysis, allowing for the prevailing winds, shows that the recovered debris is probably from the reentry event. The chemical composition of the fibers (calcium alumino silicate) and appearance of the piece of debris is consistent with it being from the outer woven E-glass fabric from the Delta second-stage thrust chamber. The metallic deposits on the fabric are believed to be residue from the aluminum flange. E-glass has a 'softening' point of about 850 deg C and a 'melting' point of approximately 1200 deg C. The large number of bubbles trapped in the fused glass is also consistent with the orbital reentry scenario and assumes the material was relatively fluid and had reached a temperature above the melting point of E-glass.

DTIC

*Debris; E Glass; Delta Launch Vehicle; Trajectory Analysis; Metallic Glasses*

**20010120154** Air Force Inst. of Tech., Wright-Patterson AFB, OH USA

**Characterization of Operator-Reported Discrepancies in Unmanned On-Orbit Space Systems**

Ferris, David L.; Jun. 2001; 89p; In English

Report No.(s): AD-A395122; C101-2133; No Copyright; Avail: CASI; A05, Hardcopy; A01, Microfiche

The purpose of this research is to characterize the number and type of problems satellite operators encounter during the course of routine daily activities. In the context of this paper, a discrepancy is defined as the perception by an operator that some portion of the space system has failed to operate as designed. Discrepancies can therefore include ground system malfunctions, procedural errors, and even misdiagnosis that a problem exists, in addition to actual spacecraft anomalies. The study is designed to test the following hypotheses using a verifiable, quantitative analysis: (1) the majority of problems encountered by an operator do not involve the spacecraft at all, but are attributed to other elements of the space system; and (2) correlations exist between aspects of a space system design and the nature of problems experienced by the operations staff over the long term. to perform an applied, rather than theoretical, analysis, several representative aerospace organizations provided historical discrepancy reports for satellites currently being flown. Government civilian and military organizations participated in the study, which encompassed spacecraft from several mission areas, including remote sensing, research & development, communications, and observatories. Raw discrepancy data was collected from each organization in the form of electronic databases or hand-written logs. Data conversion consisted of selecting similar fields of interest from each database; removing references to the program, organization, or spacecraft; replacing program-specific terminology with standardized nomenclature; and merging the individual databases into one data set. Statistical analysis of the entire data set was performed to test the two hypotheses above.

DTIC

*Aerospace Systems; Data Bases; Systems Engineering; Pilotless Aircraft*

**20010123388** Lovell (Jim), TX USA

**Lost Moon: The Perilous Voyage of Apollo 13**

Lovell, Jim, Lovell (Jim), USA; Kluger, Jeffrey, Discover Magazine, USA; [1994]; In English

Report No.(s): LC-94-28052; ISBN 0-395-67029-2; Copyright; Avail: Issuing Activity

America launched seven Apollo expeditions to land on the moon. Six of the efforts succeeded outstandingly. One failed. "Lost Moon" is the story of that disaster and the incredible heroism of the three astronauts who brought their crippled vehicle back to earth. This account - written by Jim Lovell, commander of the mission, and his co-author, Jeffrey Kluger - captures the high drama of that unique event and is told in the vernacular of the men in the sky and on the ground who masterminded this triumph of heroism, intellectual brilliance and raw courage. A thrilling story of a thrilling episode in the history of space exploration.

Derived from text

*Apollo 13 Flight; Astronauts; Spacecrews*

**20010124833** Johns Hopkins Univ., Applied Physics Lab., Laurel, MD USA

**The MESSENGER Science Planning Tool**

Choo, Teck H., Johns Hopkins Univ., USA; Murchie, Scott L., Johns Hopkins Univ., USA; Jen, Julia S., Johns Hopkins Univ., USA; Mercury: Space Environment, and Surface and Interior; 2001, pp. 11-12; In English; See also 20010124826; No Copyright; Abstract Only; Available from CASI only as part of the entire parent document

The Mercury Surface, Space Environment, Geochemistry, and Ranging (MESSENGER) mission will substantially improve the knowledge of the planet Mercury. Its seven science payload elements include scannable, dual wide- and narrow-angle cameras (WAC and NAC) for color and stereo imaging; a gamma-ray and neutron spectrometer; an X-ray spectrometer; a magnetometer; a laser altimeter; a combined UV (ultraviolet) and visible-NIR (near infrared) spectrometer; an energetic particle and plasma spectrometer; and a radio science investigation. Key constraints on the acquisition of science data are: limitations on off-sun pointing of the spacecraft, required to keep it shielded from solar illumination by a sunshade; the volumes of data that can be stored on either of the 8-Gb solid-state recorders and that can be downlinked daily; and the viewing and illumination conditions resulting from MESSENGER's elliptical orbit. The goal of planning science data acquisition is to maximize the MESSENGER instruments' coverage of the planet under favorable illumination conditions and at high spatial resolution, while keeping within spacecraft pointing limits and not exceeding available data storage and downlink resources. The MESSENGER Science Planning Tool (SPT) has been developed to find the optimal solution to this problem in an automated fashion, to minimize the cost and time required for observation planning and to respond efficiently to changes in the spacecraft's predicted trajectory on-orbit. Additional information is contained in the original extended abstract.

Author

*Mercury (Planet); Space Missions; Spacecraft Equipment*

**20010124847** European Space Agency. European Space Research and Technology Center, ESTEC, Space Science Dept., Noordwijk, Netherlands

**BepiColombo: An Interdisciplinary Mission to the Planet Mercury**

Grard, R., European Space Agency. European Space Research and Technology Center, ESTEC, Netherlands; Mukai, T., Institute of Space and Astronautical Science, Japan; Workshop on Mercury: Space Environment, Surface, and Interior; 2001, pp. 34; In English; See also 20010124826; No Copyright; Abstract Only; Available from CASI only as part of the entire parent document

The questions about Mercury as a planet that form the central rationale of the BepiColombo mission include: What will be found on the uninspected hemisphere of Mercury? How did the planet evolve geologically? Why is Mercury's density so high? What is its internal structure and is there a liquid outer core? What is the origin of Mercury's magnetic field? What is the chemical composition of the surface? Is there any water ice in the polar regions? Which volatile materials compose the vestigial atmosphere (exosphere)? How does the planet's magnetic field interact with the solar wind? BepiColombo's other objectives go beyond the exploration of the planet and its environment, to take advantage of Mercury's close proximity to the Sun: Fundamental science: is Einstein's theory of gravity correct? Impact threat: what asteroids lurk on the sunward side of the Earth? A system and technology study has revealed that the best way to fulfil the scientific goals is to send two orbiters and one lander to Mercury. The Planetary Orbiter is dedicated to remote sensing, radio science and asteroid observations. The Magnetospheric Orbiter accommodates mostly the field, wave and particle instruments. The Surface Element, a lander module, makes in situ observations that serve as ground-truth references. The method for transporting the spacecraft elements to their destinations emerges from a trade-off between mission cost and launch flexibility. It combines ion propulsion, chemical propulsion and gravity assists. BepiColombo will be launched in 2009. ESA (European Space Agency) is discussing a cooperation with the Japanese Institute of Space and Astronomical Science (ISAS) which has expressed a keen interest to provide the Magnetospheric Orbiter.

Author

*Mercury (Planet); Space Missions; European Space Agency*

**20010124864** Institut de Physique du Globe, Paris, France

**An Artificial Seismic Impact Experiment on Bepi Colombo**

Lognonne, P., Institut de Physique du Globe, France; Giardini, D., Eidgenoessische Technische Hochschule, Switzerland; Langevin, Y., Institut d'Astrophysique Spatiale, France; Mizutani, H., Institute of Space and Astronautical Science, Japan; Mercury: Space Environment, and Surface and Interior; 2001, pp. 58; In English; See also 20010124826; No Copyright; Abstract Only; Available from CASI only as part of the entire parent document

The Bepi Colombo mission plans to deploy in 2012 a lander on Mercury. A seismometer is considered on the model payload. We propose to use the Solar Electrical Propulsion Module (SEPM) on each of the two spacecrafts to produce active seismic sources, in order to constrain the thickness of the crust and possibly the thickness of the mantle. Assuming the impact position and time to be known by radio-tracking, the two events are needed to achieve a unique determination of both these thicknesses

and the mean shear and bulk velocities. We propose different scenarios, where the lander is able to land up to four days in advance of the impacts, with cost in Delta V of a few tens m/s. Only a ligh beacon is needed on the SEPM to achieve these scenario, with no change in the present design of the spacecrafts. We compare the expected signals with those recorded during the Apollo missions by the impacts of the LEM (Launch Environment Monitor), taking into account the improvements of sensors in term of sensitivity and bandwidth. We conclude with the expected results and error bars in the determination of the inner structure of the planet, from crust to core. A comparison with other geophysical methods is then done.
Author
*Seismographs; Planetary Crusts; Planetary Mantles; Mercury (Planet); Space Missions; Impact Tests; Seismic Waves*

**20010125132** NASA Kennedy Space Center, Cocoa Beach, FL USA
**Technology Development for Human Exploration Beyond LEO in the New Millennium IAA-13-3 Strategies and Plans for Human Mars Missions**
Larson, William E., NASA Kennedy Space Center, USA; Lueck, Dale E., NASA Kennedy Space Center, USA; Parrish, Clyde F., NASA Kennedy Space Center, USA; Sanders, Gerald B., NASA Johnson Space Center, USA; Trevathan, Joseph R., NASA Johnson Space Center, USA; Baird, R. Scott, NASA Johnson Space Center, USA; Simon, Tom, NASA Johnson Space Center, USA; Peters, T., NASA Johnson Space Center, USA; [2001]; 15p; In English; 51st International Astronautical Federation, 1-5 Oct. 2001, Toulouse, France; No Copyright; Avail: CASI; A03, Hardcopy; A01, Microfiche

As we look forward into the new millennium, the extension of human presence beyond Low-Earth Orbit (LEO) looms large in the plans of NASA. The Agency's Strategic Plan specifically calls out the need to identify and develop technologies for 100 and 1000-day class missions beyond LEO. to meet the challenge of these extended duration missions, it is important that we learn how to utilize the indigenous resources available to us on extraterrestrial bodies. This concept, known as In-Situ Resource Utilization (ISRU) can greatly reduce the launch mass & cost of human missions while reducing the risk. These technologies may also pave the way for the commercial development of space. While no specific target beyond LEO is identified in NASA's Strategic Plan, mission architecture studies have been on-going for the Moon, Mars, Near-Earth Asteroids and Earth/Moon & Earth/Sun Libration Points. As a result of these studies, the NASA Office of Space Flight (Code M) through the Johnson and Kennedy Space Centers, is leading the effort to develop ISRU technologies and systems to meet the current and future needs of human missions beyond LEO and on to Mars. This effort also receives support from the NASA Office of Biological and Physical Research (Code U), the Office of Space Science (Code S), and the Office of Aerospace Technology (Code R). This paper will present unique developments in the area of fuel and oxidizer production, breathing air production, water production, C02 collection, separation of atmospheric gases, and gas liquefaction and storage. A technology overview will be provided for each topic along with the results achieved to date, future development plans, and the mission architectures that these technologies support.
Author
*Long Duration Space Flight; In Situ Resource Utilization; Materials Recovery*

## 14
## GROUND SUPPORT SYSTEMS AND FACILITIES (SPACE)

*Includes launch complexes, research and production facilities; ground support equipment, e.g., mobile transporters; and test chambers and simulators. Also includes extraterrestrial bases and supporting equipment. For related information see also 09 Research and Support Facilities (Air).*

**20010120103** Naval Research Lab., Washington, DC USA
**Multi-Tethered Space-Based Interferometers: Particle System Model**
Gates, Stephen S.; Sep. 14, 2001; 35p; In English
Report No.(s): AD-A395110; NRL/MR/8231-01-8579; No Copyright; Avail: CASI; A03, Hardcopy; A01, Microfiche

Dynamics models are presented for a class of space-based interferometers comprised of multiple component bodies, interconnected in various arrangements, by low-mass flexible tethers of variable length. The tethered constellations are to perform coordinated rotational scanning accompanied by baseline dimensional changes, as well as spin axis realignments and spin-up/spin-down maneuvers. The mechanical idealization is a system of N point masses interconnected by massless tethers of variable length. Both extensible and inextensible tethers are considered. Expressions for system angular and linear momenta are developed. The unrestricted nonlinear motion equations are derived via Lagranges equations. Rheonomic constraints are

introduced to allow prescribed motion of any degrees of freedom, and the associated physical forces are determined. The linearized equations of motion are obtained for the steady rotation of a system with extensible tethers of constant unstrained length. DTIC

*Angular Momentum; Equations of Motion; Interferometers; Tetherlines; Mathematical Models*

## 15
## LAUNCH VEHICLES AND LAUNCH OPERATIONS

*Includes all classes of launch vehicles, launch/space vehicle systems, and boosters; and launch operations. For related information see also 18 Spacecraft Design, Testing, and Performance; and 20 Spacecraft Propulsion and Power.*

**20010122251** Argonne National Lab., IL USA

**Dynamics sensor validation for reUSAble launch vehicle propulsion**

Herzog, J. P.; \; 14p; In English

Report No.(s): DE2001-10816; ANL/RA/CP-96510; No Copyright; Avail: Department of Energy Information Bridge, Microfiche

Expert Microsystems teamed with Argonne National Laboratory (ANL), a DOE contractor, to develop an innovative dynamics sensor validation system under a Small Business Technology Transfer (STTR) Phase I contract with NASA. The project improves launch vehicle mission safety and system dependability by enabling rapid development and cost effective maintenance of embeddable real-time software to reliably detect process-critical sensor failures. The project focused on verifying the feasibility of two innovative software methods developed by ANL to provide high fidelity sensor data validation for nuclear power generating stations, the Sequential Probability Ratio Test (SPRT) algorithm and the Multivariate State Estimation Technique (MSET) algorithm, as core elements of a commercial Dynamics Sensor Validation System (DSVS). The research verified that ANL algorithms enable highly reliable data validation for high frequency Space Shuttle Main Engine (SSME) dynamics sensors, such as accelerometers and strain gauges. Phase I culminated in production of a prototype run-time module which validates SSME flight accelerometer data with very high reliability. The resulting sensor validation development system is widely applicable to reUSAble launch vehicle (RLV) and ground support control and monitoring systems.

NTIS

*Propulsion; Failure; ReUSAble Launch Vehicles; Technology Transfer; Detection*

**20010122289** Sandia National Labs., Albuquerque, NM USA

**Environmental Testing Philosophy for a Sandia National Laboratories' Small Satellite Project: A Retrospective**

Cap,; Aug. 24, 2000; 12p; In English

Report No.(s): DE2000-761043; SAND2000-0296C; No Copyright; Avail: Department of Energy Information Bridge

Sandia has recently completed the flight certification test series for the Multi-Spectral Thermal Imaging satellite (MTI), which is a small satellite for which Sandia was the system integrator. A paper was presented at the 16th Aerospace Testing Seminar discussing plans for performing the structural dynamics certification program for that satellite. The testing philosophy was originally based on a combination of system level vibroacoustic tests and component level shock and vibration tests. However, the plans evolved to include computational analyses using both Finite Element Analysis and Statistical Energy Analysis techniques. This paper outlines the final certification process and discuss lessons learned including both things that went well and things that should/could have been done differently.

NTIS

*Certification; Dynamic Structural Analysis; Flight Tests; Artificial Satellites*

**20010125604** NASA Marshall Space Flight Center, Huntsville, AL USA

**Pressure-Driven Magnetically-Coupled Conveyance**

Robertson, Glen A., Inventor, NASA Marshall Space Flight Center, USA; Jan. 09, 2001; 8p; In English

Patent Info.: Filed 18 Dec. 1998; NASA-Case-MFS-31184-1; US-Patent-6,170,404; US-Patent-Appl-SN-216492; No Copyright; Avail: CASI; A02, Hardcopy; A01, Microfiche

This invention has the ability to provide the initial acceleration necessary for spacecraft to attain earth orbit without use of traditional rocket propellants. The invention also has the ability to provide an alternative means of ground transportation without the direct use of fossil fuel. The invention 6 utilizes a pressurized, nonmagnetic tube to accelerate and translate a piston. The piston

is magnetically coupled to a conveyance, which travels along the outside of the tube. The conveyance, in turn. can be either a spacecraft or a vehicle suitable for ground transportation.
Official Gazette of the U.S. Patent and Trademark Office
*Fossil Fuels; Rocket Propellants; Surface Vehicles; Acceleration (Physics)*

## 16
## SPACE TRANSPORTATION AND SAFETY

*Includes passenger and cargo space transportation, e.g., shuttle operations; and space rescue techniques. For related information, see also 03 Air Transportation and Safety and 15 Launch Vehicles and Launch Vehicles, and 18 Spacecraft Design, Testing and Performance. For space suits, see 54 Man/System Technology and Life Support.*

**20010122948** NASA Johnson Space Center, Houston, TX USA
**STS-108 Flight Day Highlights: Flight Day 1**
Dec. 06, 2001; In English; Videotape: 23 min. 37 sec. playing time, in color, with sound
Report No.(s): NONP-NASA-VT-2001206814; BRF-1431A; No Copyright; Avail: CASI; B02, Videotape-Beta; V02, Videotape-VHS

On this first day of the STS-108 mission, the crewmembers of Endeavour, Commander Dominic Gorie, Pilot Mark Kelly, and Mission Specialists Linda Godwin and Daniel Tani, are seen during various prelaunch activities, including the ceremonial breakfast, suitup, departing the Operations and Checkout (O&C) Building, and boarding the orbiter. The launch of Endeavour is shown. The payload bay doors open once in orbit and Pilot Kelly is seen as the solid rocket boosters ignite.
CASI
*Spacecraft Launching; Spacecrews; Crew Procedures (Preflight); Crew Procedures (Inflight); Endeavour (Orbiter)*

## 17
## SPACE COMMUNICATIONS, SPACECRAFT COMMUNICATIONS, COMMAND AND TRACKING

*Includes space systems telemetry; space communications networks; astronavigation and guidance; and spacecraft radio blackout. For related information, see also 04 Aircraft Communications and Navigation and 32 Communications and Radar.*

**20010117890** NASA Goddard Space Flight Center, Greenbelt, MD USA
**Spaceborne Global Positioning System for Spacecraft**
Dougherty, Lamar F., Inventor, NASA Goddard Space Flight Center, USA; Niles, Frederick A., Inventor, NASA Goddard Space Flight Center, USA; Wennersten, Miriam D., Inventor, NASA Goddard Space Flight Center, USA; Apr. 03, 2001; 28p; In English; Provisional application of US-Patent-Appl-SN-092491, filed 8 Jul. 1998
Patent Info.: Filed 7 Jul. 1999; NASA-Case-GSC-13991-1; US-Patent-6,211,822; US-Patent-Appl-SN-348876; US-Patent-Appl-SN-092491; No Copyright; Avail: CASI; A03, Hardcopy; A01, Microfiche

The spaceborne Global Positioning System receiver provides navigational solutions and is designed for use in low Earth orbit. The spaceborne GPS receiver can determine the orbital position of a spacecraft using any of the satellites wi thin the GPS constellation. It is a multiple processor system incorporating redundancy by using a microcontroller to handle the closure of tracking loops for acquired GPS satellites, while a separate microprocessor computes the spacecraft navigational solution and handles other tasks within the receiver. 'Me spaceborne GPS receiver can use either microcontroller or the microprocessor to close the satellite tracking loops. The use of microcontroller provides better tracking performance of acquired GPS satellites. The spaceborne GPS receiver utilizes up to seven separate GPS boards, with each board including its own set of correlators, down-converters and front-end components. The spaceborne GPS receiver also includes telemetry and time-marking circuitry. The spaceborne GPS receiver communicates with other spacecraft systems through a variety of interfaces and can be software-configured to support several different mission profiles.
Official Gazette of the U.S. Patent and Trademark Office
*Global Positioning System; Navigation Satellites; Satellite Tracking; Low Earth Orbits*

## 18
## SPACECRAFT DESIGN, TESTING AND PERFORMANCE

*Includes satellites; space platforms; space stations; spacecraft systems and components such as thermal and environmental controls; and spacecraft control and stability characteristics. For life support systems, see 54 Man/System Technology and Life Support. For related information, see also 05 Aircraft Design, Testing and Performance, 39 Structural Mechanics, and 16 Space Transportation and Safety.*

**20010124844** Johns Hopkins Univ., Applied Physics Lab., Laurel, MD USA
**The MESSENGER Scientific Payload**
Gold, Robert E., Johns Hopkins Univ., USA; McNutt, Ralph, L., Jr., Johns Hopkins Univ., USA; Santo, Andrew G., Johns Hopkins Univ., USA; Solomon, Sean C., Carnegie Institution of Washington, USA; Mercury: Space Environment, and Surface and Interior; 2001, pp. 29-30; In English; See also 20010124826; No Copyright; Abstract Only; Available from CASI only as part of the entire parent document

The Mercury, Surface, Space Environment, Geochemistry, and Ranging (MESSENGER) spacecraft will be the first to orbit the planet Mercury and the first spacecraft to visit Mercury in more than 30 years. MESSENGER will launch in March 2004 with a miniaturized set of seven instruments. Along with the spacecraft telecommunications system, these instruments will provide a comprehensive view of the structure and composition of the planet. MESSENGER will orbit Mercury for one Earth year following two flybys of Venus and two of Mercury. Mercury, the least studied of the terrestrial planets, holds the prospect for unraveling important aspects of the origin and early history of the solar system. Mercury is a challenging body to orbit, however, because of high propulsive-energy requirements and the severe thermal environment. to date, Mercury has been visited by spacecraft only during three flybys by Mariner 10 in 1974 and 1975. The MESSENGER mission has been designed on the basis of a detailed progression from the science questions to be answered, through mission design and implementation, to the instrument suite needed to obtain the necessary data. by adhering strictly to the science requirements while also pursuing aggressively miniaturization and packaging optimization so as to minimize payload mass, the instrument suite meets all mission constraints while enabling the measurements required for addressing fully the science questions that define the mission. Additional information is contained in the original extended abstract.
Author
*Mercury (Planet); Miniaturization; Mission Planning; Spacecraft Equipment; Payloads; Space Missions*

## 19
## SPACECRAFT INSTRUMENTATION AND ASTRIONICS

*Includes the design, manufacture, or use of devices for the purpose of measuring, detecting, controlling, computing, recording, or processing data related to the operation of space vehicles or platforms. For related information, see also 06 Aircraft Instrumentation and Avionics; For spaceborne instruments not integral to the vehicle itself see 35 Instrumentation and Photography; For spaceborne telescopes and other astronomical instruments see 89 Astronomy, Instrumentation and Photography; For spaceborne telescopes and other astronomical instruments see 89 Astronomy.*

**20010118257** Norwegian Defence Research Establishment, Kjeller, Norway
**Report on the ASPOC Commissioning**
Svenes, Knut, Norwegian Defence Research Establishment, Norway; Narheim, Bjorn, Norwegian Defence Research Establishment, Norway; Aug. 13, 2001; 35p; In English; Original contains color illustrations
Contract(s)/Grant(s): FFIE Proj. 768/172
Report No.(s): FFI/RAPPORT-2001/03961; ISBN 82-464-0530-6; No Copyright; Avail: CASI; A03, Hardcopy; A01, Microfiche

This report constitutes a summary of the commissioning activities for the Aspoc instrument on the Cluster-11 satellites. This work was carried out during the autumn of 2000, and the report covers the check-out activities for all the instruments. Some recommendations for future processes of this nature are also discussed.
Author
*Sun; Dynamic Characteristics; Earth (Planet); Electromagnetic Interactions*

**20010125600** NASA Dryden Flight Research Center, Edwards, CA USA
**Wind Advisory System**
Curto, Paul A., Inventor, NASA Dryden Flight Research Center, USA; Brown, Gerald E., Inventor, NASA Dryden Flight Research Center, USA; Zysko, Jan A., Inventor, NASA Dryden Flight Research Center, USA; Oct. 30, 2001; 8p; In English

Patent Info.: NASA-Case-DRC-09901-6; US-Patent-6,311,107; US-Patent-Appl-SN-606102; No Copyright; Avail: CASI; A02, Hardcopy; A01, Microfiche

The present invention is a two-part wind advisory system comprising a ground station at an airfield and an airborne unit placed inside an aircraft. The ground station monitors wind conditions (wind speed, wind direction, and wind gust) at the airfield and transmits the wind conditions and an airfield ID to the airborne unit. The airborne unit identifies the airfield by comparing the received airfield ID with airfield IDs stored in a database. The airborne unit also calculates the headwind and crosswind for each runway in both directions at the airfield using the received wind conditions and runway information stored in the database. The airborne unit then determines a recommended runway for takeoff and landing operations of the aircraft based on th~ runway having the greatest headwind value and displays the airfield ID, wind conditions, and recommended runway to the pilot. Another embodiment of the present invention includes a wireless internet based airborne unit in which the airborne unit can receive the wind conditions from the ground station over the internet.

Official Gazette of the U.S. Patent and Trademark Office

*Airports; Wind Velocity; Wind Direction; Monitors; Display Devices*

## 20
## SPACECRAFT PROPULSION AND POWER

***Includes main propulsion systems and components, e.g., rocket engines; and spacecraft auxiliary power sources. For related information, see also 07 Aircraft Propulsion and Power; 28 Propellants and Fuels; 15 Launch Vehicles and Launch Operations; and 44 Energy Production and Conversion.***

**20010122285** NASA Ames Research Center, Moffett Field, CA USA

**Simulation of SSTO Flow Environment**

Park, Chung Sik, NASA Ames Research Center, USA; Sharma, Surendra, NASA Ames Research Center, USA; [1995]; 1p; In English; 33rd Aerospace Science Meeting, 10-15 Jan. 1995, Reno, NV, USA

Contract(s)/Grant(s): RTOP 967-10-60; No Copyright; Avail: Issuing Activity; Abstract Only

To replace the aging Space Shuttle fleet, it is hoped that a reUSAble single stage to orbit (SSTO) vehicle will be developed within next decade. To optimize the heatshield mass, the detailed information of the base flow field as well as the heating rate is required. It is the main goal of current study to analyze such flow field and to scale the heat flux rate experimentally. Flow environment of the proposed SSTO vehicle will be simulated at the EAST facility of NASA Ames Research Center. A rocket model with a pressure chamber and nozzle. will be built to simulate the flow' field of SSTO. Combustible gas mixture will be ignited by means of a capacitor bank to simulate the rocket plume. The rocket engine parameters will be changed systematically, while several optical diagnosis will be used to quantify the thermophysical variables of the flow field and the heat flux rate onto the rocket.

Author

*Single Stage to Orbit Vehicles; Simulation; Heat Shielding; Flow Distribution; Heat Flux; Flux (Rate)*

**20010122934** NASA Ames Research Center, Moffett Field, CA USA

**Preliminary Studies of a Pulsed Detonation Rocket Engine**

Cambier, Jean-Luc, Eloret Corp., USA; Adelman, H. G., Rekenthaler Technology Associates Corp., USA; Menees, G. P., Rekenthaler Technology Associates Corp., USA; [1995]; 1p; In English; 31st AIAA Joint Propulsion Conference, 10-12 Jul. 1995, San Diego, CA, USA; Sponsored by American Inst. of Aeronautics and Astronautics, USA

Contract(s)/Grant(s): RTOP 307-50-42; No Copyright; Avail: Issuing Activity; Abstract Only

In the new era of space exploration, there is a strong need for more efficient, cheaper and more reliable propulsion devices. With dramatic increase in specific impulse, the overall mass of fuel to be lifted into orbit is decreased, and this leads, in turn, to much lower mass requirements at lift-off, higher payload ratios and lower launch costs. The Pulsed Detonation engine (PDE) has received much attention lately due to its unique combination of simplicity, light-weight and efficiency. Current investigations focus principally on its use as a low speed, airbreathing engine, although other applications have also been proposed. Its use as a rocket propulsion device was first proposed in 1988 by the present authors. The superior efficiency of the Pulsed Detonation Rocket Engine (PDRE) is due to the near constant volume combustion process of a detonation wave. Our preliminary estimates suggest that the PDRE is theoretically capable of achieving specific impulses as high as 720 sec, a dramatic improvement over the current 480 sec of conventional rocket engines, making it competitive with nuclear thermal rockets. In addition to this remarkable efficiency, the PDRE may eliminate the need for high pressure cryogenic turbopumps, a principal source of failures. The heat transfer rates are also much lower, eliminating the need for nozzle cooling. Overall, the engine is more reliable and has

a much lower weight. This paper will describe in detail the operation of the PDRE and calculate its performance, through numerical simulations. Engineering issues will be addressed and discussed, and the impact on mission profiles will also be presented. Finally, the performance of the PDRE using in-situ resources, such as CO and O2 from the martian atmosphere, will also be computed.
Author
*Pulse Detonation Engines; Propulsion; Specific Impulse*

**20010125613** NASA Marshall Space Flight Center, Huntsville, AL USA
**Low-Cost Gas Generator and Ignitor**
Dennis, Henry J., Jr., Inventor, NASA Marshall Space Flight Center, USA; Hissam, D. Andy, Inventor, NASA Marshall Space Flight Center, USA; Myers, W. Neill, Inventor, NASA Marshall Space Flight Center, USA; Taylor, Eric S., Inventor, NASA Marshall Space Flight Center, USA; Feb. 20, 2001; 6p; In English
Patent Info.: Filed 18 Jun. 1999; NASA-Case-MFS-31343-1; US-Patent-6,189,315; US-Patent-Appl-SN-350412; No Copyright; Avail: CASI; A02, Hardcopy; A01, Microfiche

A gas generator and ignitor assembly for powering a turbine of a turbopump assembly for a rocket engine comprises an injector and a combustion chamber. the injector having a body member including a fuel inlet and an oxidizer inlet spaced one from the other and communicating with respective radially spaced apart annular members in the body member. Three annuli communicate with the fuel inlet and two annuli communicate with the oxidizer inlet. the annuli which communicates with the oxidizer being positioned between pairs of the other annuli, The body member is enclosed by a plate having an array of bores arranged in two series with three radially spaced apart groups of circular rows in each series. The outer series has 28 groups of triplet bores while the inner series has 14 groups of triplet bores. The annuli which communicate with oxidizer feed bores of each series that are between the other bores of a triplet. the latter bores communicating with annuli that communicate with fuel. The inner and outer bores of the triplets of each series are inclined relatively to each other and to the third bore of the triplet so that fuel and oxidizer atomizes as it is sprayed into the inlet of the combustion chamber where the propellants are mixed. and burned. The burning of the propellants is effected by ignition of a plug of solid propellant fuel mounted to communicate with the interior of the combustion chamber.
Official Gazette of the U.S. Patent and Trademark Office
*Gas Generators; Ignition; Turbine Pumps; Annuli*

## 23
## CHEMISTRY AND MATERIALS (GENERAL)

*Includes general research topics related to the composition, properties, structure, and use of chemical compounds and materials as they relate to aircraft, launch vehicles, and spacecraft. For specific topics in chemistry and materials see categories 24 through 29. For astrochemistry see category 90 Astrophysics.*

**20010117651** Federal Energy Technology Center, Morgantown, WV USA
**Characteristics and Performance of Supercritical Fluid Extraction (SFE) in the Analysis of Petroleum Hydrocarbons in Soils and Sludges**
Hawthorne, S. B.; Jan. 01, 1999; 19p; In English
Report No.(s): DE2000-760133; DE-FC21-93MC30098-62; No Copyright; Avail: Department of Energy Information Bridge

This project was designed to evaluate and improve Supercritical Fluid Extraction (SFE) methods and instrumentation for the analytical-scale extraction of petroleum hydrocarbons ranging from BTEX components to PAH's and heavy crudes from soils and sludges.
NTIS
*Extraction; Hydrocarbons; Supercritical Fluids; Crude Oil*

**20010117658** Pacific Northwest National Lab., Richland, WA USA
**Organic Analysis of AW-101 and AN-107 Tank Waste**
Klinger, G. S.; Urie, M. W.; Campbell, J. A.; Clauss, S. A.; Clauss, T. W.; Aug. 14, 2000; 409p; In English
Report No.(s): DE2000-760036; PNWD-2461; BNFL-RPT-001; No Copyright; Avail: Department of Energy Information Bridge

Thirty jars of waste material from tank AW-101 and seventeen jars of waste material from tank AN-107 were received by Battelle. The contents of all jars of AW-101 were mixed to provide a single composite, as were the contents of all jars of AN-107. Each composite was homogenized and representative sub-samples extracted for organic, radiochemical, and inorganic regulatory

analyses. The representative sub-samples were analyzed for inorganic, radiochemical, and organic analyses for analytes of interest as defined in Test Plan BNFL-29953-2. This report presents the organic results.
NTIS
*Chemical Composition; Radioactive Wastes; Organic Compounds*

**20010118625** Brookhaven National Lab., Upton, NY USA
**Gamma irradiation testing of montan wax for use in waste management systems**
Soo,; Heiser,; Hart,; Sep. 08, 1996; 20p; In English
Report No.(s): DE2000-757137; BNL-67335; No Copyright; Avail: Department of Energy Information Bridge, Microfiche

A field demonstration was funded by the US Department of Energy (DOE) to quantify the potential use of montan wax as a subsurface barrier material for nuclear waste management applications. As part of that demonstration, a study was completed to address some of the characteristics of the wax. of particular interest is its resistance to chemical and structural changes that would influence its integrity as a barrier to minimize the migration of contaminants from their storage or disposal locations. Properties that were evaluated included hardness, melting point, molecular weight, and biodegradation as a function of gamma radiation dose. Based on the data obtained to date the wax is extremely resistant to radiation-induced change. Coupled with low permeability, the material shows promise as a subsurface barrier material.
NTIS
*Waxes; Radioactive Wastes; Barrier Layers; Gamma Rays; Waste Management*

**20010119200** Oak Ridge National Lab., TN USA
**Coulomb Repulsion in Miniature Ion Mobility Spectrometry**
Xu, J.; Whitten, W. B.; Ramsey, J. M.; Aug. 08, 1999; 8p; In English
Report No.(s): DE2000-751582; ORNL/CP-105777; No Copyright; Avail: Department of Energy Information Bridge, Microfiche

We have undertaken a study of ion mobility resolution in a miniature ion mobility spectrometer with a drift channel 1.7 mm in diameter and 35 mm in length. The device attained a maximum resolution of 14 in separating ions of NO, O(sub 2), and methyl iodine. The ions were generated by pulses from a frequency-quadrupled Nd:YAG laser. Broadening due to Coulomb repulsion was modeled theoretically and shown experimentally to have a major effect on the resolution of the miniature device.
NTIS
*Spectrometers; Ion Mobility Spectroscopy; Ions; Neodymium Lasers; YAG Lasers*

**20010119201** Oak Ridge National Lab., TN USA
**KeV Ion Beam Induced Surface Modification of SiC Hydrogen Sensor**
Muntele, C. I.; Ila, D.; Williams, E. K.; Poker, D. B.; Hensley, D. K.; Nov. 29, 1999; 6p; In English
Report No.(s): DE2000-751521; ORNL/CP-105629; No Copyright; Avail: Department of Energy Information Bridge, Microfiche

Silicon carbide, a wide-bandgap semiconductor, is currently used to fabricate an efficient high temperature hydrogen sensor. When a palladium coating is applied on the exposed surface of silicon carbide, the chemical reaction between palladium and hydrogen produces a detectable change in the surface chemical potential. Rather than applying a palladium film, we have implanted palladium ions into the silicon face of 6H, n-type SiC samples. The implantation energies and fluences, as well as the results obtained by monitoring the current through the sample in the presence of hydrogen are included in this paper.
NTIS
*Hydrogen; Silicon Carbides; Ion Implantation; Surface Treatment; Gas Detectors; Ion Beams; Palladium*

**20010119211** Brookhaven National Lab., Upton, NY USA
**Characterization of Mixed-Metal Oxides Using Synchrotron-Based Time-Resolved X-Ray Diffraction and X-Ray Absorption Spectroscopy**
Rodriguez, J. A.; Nov. 29, 1999; 6p; In English
Report No.(s): DE2000-751123; BNL-67067; No Copyright; Avail: Department of Energy Information Bridge

Mixed-metal oxides play a relevant role in many areas of materials science, physics, chemistry, and the electronic industry. In principle, the combination of two metals in an oxide matrix can lead to materials with novel properties and a superior performance in technological applications. In this article we illustrate the use of two synchrotron-based techniques, time-resolved x-ray diffraction (TR-XRD) and x-ray absorption near-edge spectroscopy (XANES), in the characterization of the physical and chemical properties of mixed-metal oxides. We focus on the behavior of compounds of the MeMoO4 type (Me=Fe, Co, or Ni),

which result from adding oxides of the MeO type to MoO3 and constitute an interesting group of materials due to their structural, electronic, and catalytic properties.
NTIS
*Absorption Spectroscopy; Chemical Properties; Mixed Oxides*

**20010119214** Brookhaven National Lab., Upton, NY USA
**Evaluation of Coatings and Mortars for Protection of Concrete Cooling Tower Structures from Microbiologically Influenced Corrosion in Geothermal Power Plants**
Allan, M. L.; Oct. 01, 1999; 32p; In English
Report No.(s): DE2000-751115; BNL-66980; No Copyright; Avail: Department of Energy Information Bridge

Microbiologically influenced corrosion (MIC) is a common problem that causes deterioration of concrete in cooling towers used in geothermal power plants. MIC can be attributed to a number of different types of bacteria, particularly sulphur oxidizing and nitrifying. The objective of the work reported was evaluate strategies and materials in for repair and prevention of MIC. In the first phase of research documented in this report laboratory tests were conducted to compare the suitability of six different materials for protecting concrete from Thiobacillus ferrooxidans. These were three epoxy coatings, an epoxy sealant, an epoxy-modified cement mortar and a latex-modified mortar. The concrete used as a substrate was based on Type V cement and the mix proportions were similar to those used in construction of a cooling tower basin that had experienced MIC. The materials were tested for bond strength and resistance to sulphuric acid and T. ferroxidans. An Atlas cell arrangement was used to simulate a thermal gradient and examine performance in both immersed and vapor zones. of the materials tested to date the epoxy coatings were most promising and will be subjected to tests to evaluate resistance to nitrifying and heterotrophic bacteria. Field tests to expose the coatings to cooling water are also planned. General recommendations for concrete repair and protection are discussed in this report.
NTIS
*Concretes; Cooling Systems; Epoxy Resins; Protective Coatings; Towers*

**20010119595** Materials Research Society, Warrendale, PA USA
**Symposium M Thermal Barrier Coatings -- 2000 Volume 645E**
Antelo, Maria A.; Padture, Nitin P.; Pint, Bruce; Sampath, Sanjay; Wortman, David J.; Jan. 2000; 62p; In English
Report No.(s): AD-A394914; No Copyright; Avail: CASI; A04, Hardcopy; A01, Microfiche

The proceedings for the Symposium M, Thermal Barrier Coatings-2000 is presented in this report.
DTIC
*Conferences; Thermal Control Coatings*

**20010120016** Argonne National Lab., IL USA
**Risk assessment of nonhazardous oil-field waste disposal in salt caverns**
Elcock, D.; Mar. 05, 1998; 16p; In English
Report No.(s): DE2001-10669; ANL/EA/CP-95785; No Copyright; Avail: Department of Energy Information Bridge

In 1996, Argonne National Laboratory (ANL) conducted a preliminary technical and legal evaluation of disposing of nonhazardous oil-field wastes (NOW) into salt caverns. Argonne determined that if caverns are sited and designed well, operated carefully, closed properly, and monitored routinely, they could be suitable for disposing of oil-field wastes. On the basis of these findings, Argonne subsequently conducted a preliminary evaluation of the possibility that adverse human health effects (carcinogenic and noncarcinogenic) could result from exposure to contaminants released from the NOW disposed of in domal salt caverns. Steps used in this evaluation included the following: identifying potential contaminants of concern, determining how humans could be exposed to these contaminants, assessing contaminant toxicities, estimating contaminant intakes, and calculating human cancer and noncancer risk estimates. Five postclosure cavern release scenarios were assessed. These were inadvertent cavern intrusion, failure of the cavern seal, failure of the cavern through cracks, failure of the cavern through leaky interbeds, and a partial collapse of the cavern roof. Assuming a single, generic, salt cavern and generic oil-field wastes, potential human health effects associated with constituent hazardous substances (arsenic, benzene, cadmium, and chromium) were assessed under each of these scenarios. Preliminary results provided excess cancer risk and hazard index (referring to noncancer health effects) estimates that were well within the US Environmental Protection Agency (EPA) target range for acceptable exposure risk levels. These results led to the preliminary conclusion that from a human health perspective, salt caverns can provide an acceptable disposal method for nonhazardous oil-field wastes.
NTIS
*Hazards; Oil Fields; Waste Disposal; Salt Beds; Carcinogens; Contaminants*

**20010120405** Los Alamos National Lab., NM USA

**Intrinsic Residual Stresses in Metal Films Synthesized by Energetic Particle Deposition**

Misra, A.; Nastasi, M.; Sep. 15, 2000; 20p; In English

Report No.(s): DE2000-762303; LA-UR-00-4339; No Copyright; Avail: Department of Energy Information Bridge, Microfiche

Residual stresses are intrinsic to all physical vapor deposited coatings. Bombardment with energetic particles (ions or neutrals) has a strong influence on both the sign and the magnitude of intrinsic stresses. For example, stresses can change from large tensile to large compressive with increasing particle bombardment. We develop a model for the evolution of tensile residual stress with increasing bombardment based on the hypothesis that the tensile stresses originate due to the attractive interatomic forces between the coalescing crystallite. The model predictions are shown to compare favorably with experimental results.

NTIS

*Energetic Particles; Metal Films; Residual Stress; Vapor Deposition*

**20010120543** Argonne National Lab., IL USA

**Risk Assessment of Nonhazardous Oil-Field Waste Disposal in Salt Caverns**

Elcock, D.; Mar. 10, 1998; 17p; In English

Report No.(s): DE2001-10683; ANL/EA/CP-95861; No Copyright; Avail: Department of Energy Information Bridge, Microfiche

Salt caverns can be formed in underground salt formations incidentally as a result of mining or intentionally to create underground chambers for product storage or waste disposal. For more than 50 years, salt caverns have been used to store hydrocarbon products. Recently, concerns over the costs and environmental effects of land disposal and incineration have sparked interest in using salt caverns for waste disposal. Countries using or considering using salt caverns for waste disposal include Canada (oil-production wastes), Mexico (purged sulfates from salt evaporators), Germany (contaminated soils and ashes), the UK (organic residues), and the Netherlands (brine purification wastes). In the US, industry and the regulatory community are pursuing the use of salt caverns for disposal of oil-field wastes. In 1988, the US Environmental Protection Agency (EPA) issued a regulatory determination exempting wastes generated during oil and gas exploration and production (oil-field wastes) from federal hazardous waste regulations - even though such wastes may contain hazardous constituents. At the same time, EPA urged states to tighten their oil-field waste management regulations. The resulting restrictions have generated industry interest in the use of salt caverns for potentially economical and environmentally safe oil-field waste disposal. Before the practice can be implemented commercially, however, regulators need assurance that disposing of oil-field wastes in salt caverns is technically and legally feasible and that potential health effects associated with the practice are acceptable. In 1996, Argonne National Laboratory (ANL) conducted a preliminary technical and legal evaluation of disposing of nonhazardous oil-field wastes (NOW) into salt caverns. It investigated regulatory issues; the types of oil-field wastes suitable for cavern disposal; cavern design and location considerations; and disposal operations, closure and remediation issues. It determined that if caverns are sited and designed well, operated carefully, closed properly, and monitored routinely, they could, from technical and legal perspectives, be suitable for disposing of oil-field wastes.

NTIS

*Caves; Oil Fields; Underground Storage; Waste Disposal; Waste Management*

**20010120545** Argonne National Lab., IL USA

**Specular and Diffuse X-Ray Scattering from Tungsten/Carbon Multilayers Having a High Reflectivity at 10 keV**

Macrander, A.; Sep. 10, 1998; 14p; In English

Report No.(s): DE2001-10685; ANL/XFD/CP-95865; No Copyright; Avail: Department of Energy Information Bridge, Microfiche

X-ray scattering measurements at 10 keV from multilayers having a period of 24.8 angstroms and consisting of 100 W/C bilayers are reported. Specular scans revealed first order reflectivities in the range 73.5% to 78.0% with bandpasses in the range of 1.5% to 1.7%. Total roughness (or interface grading) values deduced from fitting were in the range 2.5 to 3.0 for the last-to-grow surface of the W layers. Diffuse scattering measurements were made in a novel geometry that permitted investigation of in-plane momentum transfers up to 0.2/angstrom. This is roughly an order of magnitude larger than is possible in conventional rocking scans. A power law dependence of the diffuse scattering after integration over a 'Brillioun zone' is found. The exponent of this power law, 1.75, when interpreted using a logarithmic correlation function leads to a value of 1.0 angstrom for the correlated roughness.

NTIS

*Reflectance; X Ray Scattering; X Ray Diffraction*

**20010120787** Defence Science and Technology Organisation, Weapons Systems Div., Fishermans Bend, Australia

**Nucleophilic Nitration of Selected Aza-aromatics: Experiments and Modelling**

Lochert, Ian J., Defence Science and Technology Organisation, Australia; Dorsett, Helen E., Defence Science and Technology Organisation, Australia; July 2001; 30p; In English

Report No.(s): DSTO-TN-0389; DODA-AR-011-981; Copyright; Avail: Issuing Activity

Nitration of isoquinoline and phthalazine has been successfully demonstrated using a novel process which does not require strong acids. In this study, nitration of isoquinoline was repeated and the method applied to 1-nitroisoquinoline and the aza-aromatics quinoline, quinazoline, quinoxaline and pyridine. Nitration of only quinoline was observed, with a product yield lower than that reported for nitration of isoquinoline. For 1-nitroisoquinoline and quinoxaline, the substrates were recovered essentially unchanged. For quinazoline and pyridine, neither the substrates nor any reaction products were isolated. In no case was multiple nitration detected. Thus, while the scope of the reaction is broader than initially reported, it is clearly not a universal method for nitrating aza-aromatics. Molecular modelling calculations have identified a correlation between the acidity of the intended nitration site and the observed yield, which might be used to screen potential substrates for this nitration technique.
Author

*Acidity; Reaction Products; Quinoxalines; Nitration*

**20010120797** Argonne National Lab., IL USA

**Waste minimization in analytical chemistry through innovative sample preparation techniques**

Smith, L. L.; May 28, 1998; 14p; In English

Report No.(s): DE2001-10820; ANL/CMT-ACL/CP-96543; No Copyright; Avail: Department of Energy Information Bridge

Because toxic solvents and other hazardous materials are commonly used in analytical methods, characterization procedures result in significant and costly amount of waste. We are developing alternative analytical methods in the radiological and organic areas to reduce the volume or form of the hazardous waste produced during sample analysis. For the radiological area, we have examined high-pressure, closed-vessel microwave digestion as a way to minimize waste from sample preparation operations. Heated solutions of strong mineral acids can be avoided for sample digestion by using the microwave approach. Because reactivity increases with pressure, we examined the use of less hazardous solvents to leach selected contaminants from soil for subsequent analysis. We demonstrated the feasibility of this approach by extracting plutonium from a NET reference material using citric and tartaric acids with microwave digestion. Analytical results were comparable to traditional digestion methods, while hazardous waste was reduced by a factor often. We also evaluated the suitability of other natural acids, determined the extraction performance on a wider variety of soil types, and examined the extraction efficiency of other contaminants. For the organic area, we examined ways to minimize the wastes associated with the determination of polychlorinated biphenyls (PCBs) in environmental samples. Conventional methods for analyzing semivolatile organic compounds are labor intensive and require copious amounts of hazardous solvents. For soil and sediment samples, we have a method to analyze PCBs that is based on microscale extraction using benign solvents (e.g., water or hexane). The extraction is performed at elevated temperatures in stainless steel cells containing the sample and solvent. Gas chromatography-mass spectrometry (GC/MS) was used to quantitate the analytes in the isolated extract. More recently, we developed a method utilizing solid-phase microextraction (SPME) for natural water samples. In this SPME technique, a fused-silica fiber coated with a polymeric film is exposed to the sample, extraction is allowed to take place, and then the analytes are thermally desorbed for GC analysis. Unlike liquid-liquid extraction or solid-phase extraction, SPME consumes all of the extracted sample in the analysis, significantly reducing the required sample volume.
NTIS

*Analytical Chemistry; Hazardous Materials; Soil Sampling; Solvents; Stainless Steels; Toxicity*

**20010121504** Sandia National Labs., Albuquerque, NM USA

**Demonstration of a Prototype Real-Time Gas Sensor Designed for Robotic Deployment**

Mowry, C. D.; Tisone, G. C.; Gray, P. C.; Wagner, J. S.; Clark, B. F.; Aug. 01, 2000; 15p; In English

Report No.(s): DE2000-760740; SAND2000-1927; No Copyright; Avail: Department of Energy Information Bridge, Microfiche

A prototype, proof-of-concept infrared-based (IR) gas sensor is described and demonstrated. The sensor occupies less than 400 cubic inches and was constructed using 'off-the-shelf' components to selectively detect SF6 gas. It was designed for robotic deployment in applications such as atmospheric plume tracer studies. The optical detection scheme fulfills robotic deployment requirements of small size, rapid response, and ruggedness. Results demonstrate real-time detection (less than 1 second response) of a gas mixture containing 100 ppm of SF6. The sensor could be customized for other potential (tracer) gases that absorb IR

radiation. The sensor was not optimized in this work, however appropriate methods to improve detection limits and decrease size are discussed.
NTIS
*Gas Analysis; Gas Detectors; Sulfur Hexafluoride; Infrared Detectors*

**20010121875** Argonne National Lab., IL USA
**Transient Oxide Phases and Scale Strain in MCrAlY: A Light Scattering Study**
Renusch, D.; Jun. 03, 1998; 13p; In English
Report No.(s): DE2001-10682; ANL/MSD/CP-95860; No Copyright; Avail: Department of Energy Information Bridge

We have used Raman 'fingerprinting' to investigate the temperature dependence of the transient oxide phases in the scale formed on MCrAl and MCrAlY (M=Ni,Co) in the temperature range 300 to 1200 C. In particular, by extending our Raman spectra to include second order scattering, we are able to track the evolution of NiO in the scales. We find that the inclusion of Y, while improving scale adhesion, inhibits the formation of Co oxide. We have also exploited the strain dependence of ruby fluorescence to extract the residual strain in the oxide scale.
NTIS
*Light Scattering; Oxides; Raman Spectra; Temperature Dependence*

**20010121947** Los Alamos National Lab., NM USA
**Towards Efficient Detection and Identification of Single Biomolecules by Surface-Enhanced Raman Scattering**
Emory, S.; Jan. 01, 2000; 14p; In English
Report No.(s): DE2000-763332; LA-UR-00-467; No Copyright; Avail: Department of Energy Information Bridge, Microfiche

Advances in ultrasensitive instrumentation have allowed the detection of single fluorescent molecules in solution, on dielectric surfaces, and in low-temperature solids. However, these studies are limited by the requirement of a high fluorescence quantum yield and do not often provide sufficient spectroscopic information for identification. These problems are addressed by surface-enhanced Raman scattering (SERS) which provides highly resolved vibrational information, does not suffer from rapid photobleaching, and eliminates the need for fluorescent tagging of nonfluorescent species. Recent studies of single silver nanoparticles reveal intrinsic enhancement factors. These giant enhancement factors allow single-molecule SERS spectra to be obtained using visible or near-infrared excitation. The detection efficiency of experiments using visible excitation has thus far been relatively low. Approaches to detecting single labeled and unlabeled biomolecules and to increasing the overall detection efficiency of single-molecule SEW with visible excitation are presented.
NTIS
*Raman Spectra; Detection; Scattering*

**20010122235** North Carolina Univ., Chapel Hill, NC USA
**Final Report: Mechanistic Studies of Transitional Metal Catalyzed Alternating Copolymerization of Carbon Monoxide with Olefins, July 1, 1994-May 31, 1998**
Brookhart, M.; May 31, 1998; 5p; In English
Report No.(s): DE2001-761173; No Copyright; Avail: Department of Energy Information Bridge

The basic objectives of this program were to elucidate the fundamental mechanisms of Pd(H)- and Ni(LI)-catalyzed alternating copolymerizations of carbon monoxide with olefins and to develop and investigate new catalytic systems. Specifically, well-defined organometallic precursors that yield active catalyst systems were investigated to determine the catalyst resting state, details of the carbon-carbon bond coupling processes, the kinetics of chain growth, and the modes of chain termination and chain transfer. Proposed transient intermediates were prepared through independent low-temperature synthesis to verify their involvement in the catalytic cycle.
NTIS
*Alkenes; Carbon Monoxide; Catalysts; Copolymerization; Organometallic Compounds; Transition Metals; Polyatomic Molecules*

**20010122259** Argonne National Lab., IL USA
**On-Loom, Real-Time, Noncontact Detection of Fabric Defects by Ultrasonic Imaging**
Chien, H. T.; Sep. 08, 1998; 11p; In English
Report No.(s): DE2001-10803; ANL/ET/CP-96455; No Copyright; Avail: Department of Energy Information Bridge, Microfiche

A noncontact, on-loom ultrasonic inspection technique was developed for real-time 100% defect inspection of fabrics. A prototype was built and tested successfully on loom. The system is compact, rugged, low cost, requires minimal maintenance,

is not sensitive to fabric color and vibration, and can easily be adapted to current loom configurations. Moreover, it can detect defects in both the pick and warp directions. The system is capable of determining the size, location, and orientation of each defect. to further improve the system, air-coupled transducers with higher efficiency and sensitivity need to be developed. Advanced detection algorithms also need to be developed for better classification and categorization of defects in real-time.
NTIS
*Defects; Fabrics; Imaging Techniques; Inspection; Prototypes*

**20010122263** Argonne National Lab., IL USA
**General Kinetic-Flow Coupling Model for FCC Riser Flow Simulation**
Chang, S. L.; May 18, 1998; 9p; In English
Report No.(s): DE2001-10795; ANL/ES/CP-96406; No Copyright; Avail: Department of Energy Information Bridge, Microfiche

A computational fluid dynamic (CFD) code has been developed for fluid catalytic cracking (FCC) riser flow simulation. Depending on the application of interest, a specific kinetic model is needed for the FCC flow simulation. This paper describes a method to determine a kinetic model based on limited pilot-scale test data. The kinetic model can then be used with the CFD code as a tool to investigate optimum operating condition ranges for a specific FCC unit.
NTIS
*Computational Fluid Dynamics; Cracking (Chemical Engineering); Computerized Simulation*

**20010122361** Argonne National Lab., IL USA
**Plastic flow produced by single ion impacts on metals**
Birtcher, R. C.; Oct. 30, 1998; 19p; In English
Report No.(s): DE2001-10758; ANL/MSD/CP-96336; No Copyright; Avail: Department of Energy Information Bridge, Microfiche

Single ion impacts have been observed using in situ transmission electron microscopy and video recording with a time resolution of 33 milliseconds. Gold was irradiated at 50 K and room temperature. Single ion impacts produce holes, modify existing holes, and extrude material into the initial specimen hole and holes formed by other ion impacts. The same behavior is observed at both temperatures. At both temperatures, ion impacts result in craters and ejected material. Ion impacts produce more small craters than large ones for all ion masses, while heavier mass ions produce more and larger craters than lighter mass ions. This comparison is affected by the ion energy. As the energy of an ion is increased, the probability for deposition near the surface decreases and fewer craters are formed. For a given ion mass, crater production depends on the probability for displacement cascade production in the near surface region. Crater and holes are stable at room temperature, however, ion impacts near an existing crater may cause flow of material into the crater either reshaping or annihilating it. Holes and craters result from the explosive outflow of material from the molten zone of near-surface cascades. The outflow may take the form of molten material, a solid lid or an ejected particle. The surface is a major perturbation on displacement cascades resulting from ion impacts.
NTIS
*Gold; Ion Beams; Ion Impact; Irradiation; Plastic Flow*

**20010122373** Argonne National Lab., IL USA
**Trifluoromethylmetallate Anions as Components of Molecular Charge Transfer Salts and Superconductors**
Schlueter, J. A., Argonne National Lab., USA; Oct. 14, 1998; 64p; In English
Report No.(s): DE2001-10739; ANL/CHM/CP-96133; No Copyright; Avail: Department of Energy Information Bridge, Microfiche

Whereas polymeric and common inorganic anions frequently deprive the synthetic chemist of a chance to modify a charge transfer salt's structure through anion alterations, discrete organometallic anions provide a vast opportunity to probe the structure/property correlations of a material through rational synthetic methods. We have recently undertaken a research effort aimed at the crystallization of conducting charge transfer salts which possess modifiable, organometallic anions as the charge compensating entities. This research has been richly rewarded with the discovery of a new family of bis(ethylenedithio) tetrathiafulvalene (BEDT-TTF or ET) based molecular superconductors. Herein is presented a summary of over twenty (kappa)(ET)(sub 2)M(CF(sub 3))(sub 4)(1,1,2-trihaloethane) (M = Cu, Ag, Au) superconducting salts. Three new related salts are also reported: (ET)(sub 2) (trans-Ag(CF(sub 3)),(CN)(sub 2)), (kappa)(sub L)(BEDT-TSF)(sub 2)Ag(CF(sub 3))(sub 4)(TCE), and (kappa)(sub L)(ET)(sub 2)Ag(CF(sub 3))(sub 3)Cl(TCE).
NTIS
*Organometallic Compounds; Anions; Chemical Composition*

**20010122381** Argonne National Lab., IL USA

**Thermomechanical behavior of plasma-sprayed zirconia thermal barrier coatings**

Singh, J. P.; Apr. 01, 1998; 6p; In English

Report No.(s): DE2001-10706; ANL/ET/CP-95982; No Copyright; Avail: Department of Energy Information Bridge, Microfiche

The effect of coating porosity and thickness on the resistance to damage of yttria stabilized zirconia thermal barrier coatings in an oxidizing environment by thermal cycling was evaluated. Hardness and elastic modulus of an as-processed porous coating were lower than those of a dense coating and the porous coating failed after fewer thermal cycles. Similarly, specimen with a thicker coating failed after fewer thermal cycles than specimen with a thinner coating. The earlier failure of the porous coating is due to lower fracture toughness and enhanced oxidation of the coating/substrate interface, whereas, the earlier failure of the thick coating is due to higher thermal transient stresses that developed in the coating during thermal cycling. Generally, an increase in coating density led to initial increase in both hardness and elastic modulus with increasing thermal cycles. However, hardness and density gradually decreased as the number of thermal cycles increase because of microcracks formation and growth. Microscopic observations indicated that the formation of multiple microcracks and their subsequent growth and coalescence led to final coating failure.

NTIS

*Protective Coatings; Porosity; Thickness; Thermal Cycling Tests; Thermal Control Coatings; Thermal Stresses*

**20010122652** Sandia National Labs., Albuquerque, NM USA

**Design and Analysis of a Preconcentrator for the ChemLab**

Wong, C. C.; Flemming, J. H.; Manginell, R. P.; Kottenstette, R. J.; Frye-Mason, G. C.; Jul. 17, 2000; 10p; In English

Report No.(s): DE2000-761831; SAND2000-1872C; No Copyright; Avail: Department of Energy Information Bridge

Preconcentration is a critical analytical procedure when designing a microsystem for trace chemical detection, because it can purify a sample mixture and boost the small analyte concentration to a much higher level allowing a better analysis. This paper describes the development of a micro-fabricated planar preconcentrator for the (mu)ChemLab(trademark) at Sandia. to guide the design, an analytical model to predict the analyte transport, adsorption and resorption process in the preconcentrator has been developed. Experiments have also been conducted to analyze the adsorption and resorption process and to validate the model. This combined effort of modeling, simulation, and testing has led us to build a reliable, efficient preconcentrator with good performance.

NTIS

*Mathematical Models; Fabrication; Concentrators; Trace Elements; Chemical Analysis*

**20010122667** Los Alamos National Lab., NM USA

**Optimizing the Metalloid Content in Bulk Metallic Glasses**

Jin, O.; Schwarz, R. B.; Jan. 01, 2000; 13p; In English

Report No.(s): DE2000-763341; LA-UR-00-753; No Copyright; Avail: Department of Energy Information Bridge, Microfiche

We have studied the effect of phosphorus content on the formation and properties of bulk Pd-Cu-P and Pd-Ni-P metallic glasses. It was found that the molar volumes of the Pd-Ni-P bulk glasses plotted as a function of P content follow a straight line whereas those for the Pd-Cu-P glasses follow two straight lines of different slopes, intersecting at a critical P concentration. The transition in molar volume behavior is attributed to a change in the alloy's short-range order with increasing P content. The origin of this structural change is discussed based on x-ray photoelectron spectroscopy (XPS) measurements.

NTIS

*Metallic Glasses; Metalloids; Phosphorus*

**20010122791** Florida Univ., Gainesville, FL USA

**Final Report: Development of Laser Excited Atomic Fluorescence and Ionization Methods, May 1, 1988-December 31, 1998**

Winefordner, J. D.; Dec. 31, 1998; 34p; In English

Report No.(s): DE2001-761214; No Copyright; Avail: Department of Energy Information Bridge

Laser excited atomic fluorescence and ionization spectrometry are fundamentally the most sensitive of atomic spectroscopic methods. In principle, single atom detection can be demonstrated for both techniques. The goal of this research program is to develop these methods for practical ultra trace elemental analysis in a wide variety of matrices. This is being done through fundamental studies of atomization processes with the aim of developing optimum atom reservoirs for practical analysis, studies of laser excitation processes for fluorescence and ionization with the aim of enhancing our understanding of the dynamics of atom

and ion populations in these reservoirs and finding efficient single and multi-step excitation schemes for many elements, and studies of techniques for photon and ion detection with the aim of improved analytical performance.
NTIS
*Excitation; Ionization; Trace Elements; Atomizing; Laser Induced Fluorescence*

**20010122792** Rochester Univ., NY USA
**LLE Quarterly Report (July-September 1999) (Library for Laser Energetics)**
Jan. 07, 2000; 52p; In English
Report No.(s): DE2001-761211; DOE/SF-19460-321; No Copyright; Avail: Department of Energy Information Bridge

This volume of the LLE Review, covering the period July-September 1999, features a theoretical analysis of a process that generates mass perturbations of an imploding target driven by modulated laser illumination. The process, referred to as laser imprint, impacts the integrity of the shell during direct-drive implosions, potentially quenching target performance. In this article V. N. Goncharov, J. A. Delettrez, S. Skupsky, and R. P. J. Town present a model of the generation of mass perturbations and analyze the mass perturbation growth due to nonuniform ablation pressure. Stabilizing mechanisms of thermal conduction smoothing and mass ablation are shown to suppress the acceleration perturbation, and mass ablation is also shown to impact velocity perturbations. The model predicts that a direct-drive cryogenic NIF target will remain intact during the implosion when l-Thz SSD beam smoothing is used.
NTIS
*Implosions; Laser Ablation; Cryogenics; Conductive Heat Transfer*

**20010123065** Argonne National Lab., IL USA
**US-RERTR Advanced Fuel Development Plans: 1999**
Meyer, M. K.; Oct. 22, 1998; 11p; In English
Report No.(s): DE2001-11070; ANL/ED/CP-97520; No Copyright; Avail: Department of Energy Information Bridge, Microfiche

Twelve fuel alloys were included in the very-high-density RERTR-1 and RERTR-2 microplate irradiation experiments. Experience gained during fabrication and results from the post-irradiation examination of these fuels has allowed us to narrow the focus of our fuel development efforts in preparation for the next set of irradiation experiments. Specific technical problems in both the areas of fuel fabrication and irradiation performance remain to be addressed. Examples of these are powder fabrication, fuel phase gamma stability versus density, and fuel-matrix interaction. In order to more efficiently address metal alloy fuel performance issues, work will continue on establishing a theoretical basis for alloy stability and metal alloy dispersion fuel irradiation performance. Plans to address these fuel development issues in the coming year will be presented.
NTIS
*Uranium Alloys; Irradiation; Metal Fuels*

**20010123093** Los Alamos National Lab., NM USA
**Generalized Multi-Edge Analysis for K-Edge Densitometry**
Collins, M.; Jul. 26, 1998; 10p; In English
Report No.(s): DE2001-761712; LA-UR-98-3089; No Copyright; Avail: Department of Energy Information Bridge

In K-edge densitometry (KED), a continuous-energy x-ray beam is transmitted through a liquid sample. The actinide content of the sample can be measured through analysis of the transmitted portion of the x-ray beam. Traditional methods for KED analysis allow the simultaneous calculation of, at most, two actinide concentrations. A generalized multi-edge KED analytical method is presented, allowing up to six actinide concentrations to be calculated simultaneously. Applications of this method for hybrid KED/x-ray fluorescence (HKED) systems are discussed. Current HKED systems require the operator to know the approximate actinide content of each sample, and manually select the proper analysis mode. The new multi-edge KED technique allows rapid identification of the major actinide components in a sample, independent of actinide content. The proper HKED analysis mode can be selected automatically, without requiring sample content information from the user. Automatic HKED analysis would be especially useful in an analytical laboratory setting, where samples with truly unknown characteristics are encountered. Because this technique requires no hardware modifications, several facilities that use HKED may eventually benefit from this approach.
NTIS
*Density Measurement; X Ray Fluorescence; Numerical Analysis; Actinide Series*

**20010123141** Department of Energy, Richland, WA USA
**Data Validation Procedure for Chemical Analysis**
Price, W. H.; Oct. 10, 2000; 211p; In English
Report No.(s): DE2000-766663; BHI-01435-REV-0; No Copyright; Avail: Department of Energy Information Bridge
This document provides procedures for use by organizations tasked with validating chemical analytical data.
NTIS
*Chemical Analysis; Data Management; Proving*

**20010123209** Argonne National Lab., IL USA
**Neutron spectroscopy of high-density amorphous ice**
Kolesnikov, A. I.; Jul. 17, 1998; 11p; In English
Report No.(s): DE2001-10895; ANL/IPNS/CP-96860; No Copyright; Avail: Department of Energy Information Bridge, Microfiche
Vibrational spectra of high-density amorphous ice (hda-ice) for H(sub 2)O and D(sub 2)O samples were measured by inelastic neutron scattering. The measured spectra of hda-ice are closer to those for high-pressure phase ice-VI, but not for low-density ice-Ih. This result suggests that similar to ice-VI the structure of hda-ice should consist of two interpenetrating hydrogen-bonded networks having no hydrogen bonds between themselves.
NTIS
*Hydrogen; Spectroscopy; Neutrons; Ice; Amorphous Materials; Density (Mass/Volume)*

**20010123250** Los Alamos National Lab., NM USA
**Gallium Content in PuO(sub 2) Using Laser Induced Breakdown Spectroscopy (LIBS)**
Smith, C. A.; Martinez, M. A.; Veirs, D. K.; Aug. 29, 1999; 7p; In English
Report No.(s): DE2001-762289; LA-UR-99-2785; No Copyright; Avail: Department of Energy Information Bridge
Laser Induced Breakdown Spectroscopy (LIBS) has been applied to the semi-quantitative analysis of gallium in plutonium oxide at the Los Alamos Plutonium Facility. The oxide samples were generated by the Thermally Induced Gallium Removal (TIGR) process, a pretreatment step prior to MOX fuel processing. The TIGR process uses PuO(sub 2) containing 1 wt% gallium (nominal) as feed material. Following the TIGR process, gallium content was analyzed by LIBS and also by conventional wet chemical analysis (ICP-MS). Although the data range was insufficient to obtain an adequate calibration, general agreement between the two techniques was good. LIBS was found to have a useful analytical range of 34-400 ppm for Ga in PuO(sub 2).
NTIS
*Gallium; Laser-Induced Breakdown Spectroscopy; Quantitative Analysis; Plutonium Oxides*

**20010123417** Ames Lab., IA USA
**Analytical Chemistry at the Interface Between Materials Science and Biology**
O'Brien, J. C.; Sep. 21, 2000; 127p; In English
Report No.(s): DE2001-764626; IS-T 1904; No Copyright; Avail: Department of Energy Information Bridge
No abstract prepared.
NTIS
*Analytical Chemistry; Biology; Materials Science*

**20010123425** Carnegie-Mellon Univ., Pittsburgh, PA USA
**Final Report: Acidic Properties of Doped Aerogels, April 19, 1993-June 30, 1998**
Boyse, R.; Jun. 30, 1998; 5p; In English
Report No.(s): DE2001-763235; No Copyright; Avail: Department of Energy Information Bridge
Over this grant period we have studied extensively zirconia and alumina aerogels doped with a wide variety of dopants including silica, sulfate, phosphate, tungstate and combinations thereof. These results have deepened our understanding of the effects of dopants on acidic properties, which is the main goal of the project, and in particular led to the development of a hierarchy with which the Broensted acid strength of different samples can be meaningfully compared. We provide a more detailed description of several specific systems.
NTIS
*Acidity; Aerogels; Doped Crystals; Aluminum Oxides*

**20010123447** Institute of Paper Science and Technology, Atlanta, GA USA

**Synthesis, characterization and application of water-soluble and easily removable cationic pressure-sensitive adhesives** ***Quarterly Report***

Sep. 30, 1999; 9p; In English

Report No.(s): DE2001-761025; DOE/GO/10379-Q; No Copyright; Avail: Department of Energy Information Bridge, Microfiche

The Institute studied the adsorption of cationic pressure-sensitive adhesive (PSA) on wood fiber, and the buildup of PSA in a closed water system during paper recycling; the results are presented. Georgia Tech worked to develop an environmentally friendly polymerization process to synthesize a novel re-dispersible PSA by co-polymerizing an oil-soluble monomer (butyl acrylate) and a cationic monomer MAEPTAC; results are presented. At the University of Georgia at Athens the project focused on the synthesis of water-soluble and easily removable cationic polymer PSAs.

NTIS

*Adhesives; Recycling; Paper (Material)*

**20010123454** Argonne National Lab., IL USA

**Structural analysis of a completely amorphous Pu-238-doped zircon by neutron diffraction**

Fortner, J. A.; Dec. 16, 1998; 8p; In English

Report No.(s): DE2001-11025; ANL/CMT/CP-96768; No Copyright; Avail: Department of Energy Information Bridge

The structure of a completely amorphous zircon was determined by time-of-flight neutron diffraction at Argonnes Intense Pulsed Neutron Source (IPNS). The sample of metamict zircon (ZrSiO4),initially doped to 8.85 weight percent Pu-238, had been completely amorphized by alpha-recoil damage since its synthesis in 1981 at the Pacific Northwest National Laboratory (PNNL). The measured diffraction structure factor, S(Q), indicated a completely amorphous sample, with no signs of residual zircon microcrystallinity. The pair distribution function obtained indicated that the structure was that of an oxide glass, retaining the Si-O, Zr-O, and O-O bond lengths of crystalline zircon.

NTIS

*Zirconium; Plutonium 238; Doped Crystals*

**20010123539** Argonne National Lab., IL USA

**Lithium-endohedral C60 complexes**

Scanlon, L. G.; May 04, 1998; 7p; In English

Report No.(s): DE2001-10641; ANL/CHM/CP-95622; No Copyright; Avail: Department of Energy Information Bridge, Microfiche

High capacity, reversible, lithium intercalated carbon anodes have been prepared, 855 m.Ah/g, which exceed the capacity for stage 1 lithium intercalated carbon anodes, 372 mAh/g. Since there is very little hydrogen content in the high capacity anode, the fullerene C(sub 60) lattice is used to investigate the nature of lithium ion bonding and spacing between lithiums in endohedral lithium complexes of C(sub 60). Three lithium-endohedral complexes have been investigated using ab initio molecular orbital calculations involving 2,3 and 5 lithium. The calculated results suggest that lithium cluster formation may be important for achieving the high capacity lithium carbon anodes.

NTIS

*Complex Compounds; Rare Earth Compounds; Lithium*

**20010123551** Department of Energy, Richland, WA USA

**Coal/Polymer Coprocessing with Efficient Use of Hydrogen**

Broadbelt, L. J.; De Witt, M. J.; Mar. 20, 1997; 11p; In English

Report No.(s): DE2001-7927; DE-FG22-96PC96204-01; No Copyright; Avail: Department of Energy Information Bridge

Environmental and economical concerns over diminishing landfill space and the growing abundance of mixed plastic waste mandate development of viable strategies for recovering high-valued resources from waste polymers. Co-processing of waste polymer mixtures with coal allows for the simultaneous conversion of coal and plastics into high-valued fuels. However, there is limited information about the underlying reaction pathways, kinetics, and mechanisms controlling coal liquefaction in the presence of polymeric materials. A series of model compound experiments has been conducted, providing a starting point for unraveling the complex, underlying chemistry. Neat pyrolysis studies of model compounds of polyethylene and coal were conducted in batch reactors. Tetradecane (C(sub 14) H(sub 30)) was used as a polyethylene mimic, and 4-(naphthylmethyl)bibenzyl (NBBM) was used as a coal model compound. Reaction temperatures were 420 and 500 C, and batch reaction times ranged from 5--150 minutes. Detailed product analysis using gas chromatography and mass spectrometry enabled

the reactant conversion and product selectivities to be determined. Reaction of single components and binary mixtures allowed the kinetic coupling between feedstocks to be examined.
NTIS
*Coal Liquefaction; Hydrogen; Waste Disposal; Binary Mixtures; Polymers; Chemical Reactions*

**20010123636** Bechtel Nevada Corp., Las Vegas, NV USA
**Bechtel Nevada and Fiberchem Environmental, Inc.: Cooperative Research and Technology Development Project *Final Report***
Pollina, R. J.; Apr. 01, 1999; 36p; In English
Report No.(s): DE2000-764651; DOE/NV/11718-297; No Copyright; Avail: Department of Energy Information Bridge
This is a report summarizing work on a small project dedicated to adapting a new chemical sensing platform for the US Department of Energy and its customers. At the same time and in the spirit of technology transfer, FCI Environmental, Inc., would receive technical support in the form of expertise from the US Department of Energy to assist in developing this product. The sensor is a hybrid integrated-circuit, optical waveguide, chemical sensor that is patented by FCI Environmental, Inc., and manufactured under license by Texas Instruments, Inc. A down-hole penetrometer probe was designed for use in hot, 60 C, hydrocarbon-saturated, saline environment at a depth of 200 feet. The probe design includes three chemical sensing, hybrid integrated-circuits with chemical reference and measurement channels, a water seal, output electronics, and a removable measurement head for replacement in the field. A hand-held chemical detector prototype - containing a hybrid integrated-circuit chemical sensor with reference channel, user alarm, and level display - was designed and constructed, and a software interface developed to operate the hand-held sensor interfaced with a laboratory data acquisition system.
NTIS
*Prototypes; Chemical Analysis; Penetrometers; Sensors*

**20010123637** Bechtel Nevada Corp., Las Vegas, NV USA
**Self-Contained, Hand-held, Optical Waveguide, Chemical Sensor System**
Pollina, R. J.; Nov. 01, 1998; 9p; In English
Report No.(s): DE2000-764649; DOE/NV/11718-258; No Copyright; Avail: Department of Energy Information Bridge
A self-contained, hand-held, optical waveguide, chemical detection system has been built to detect and quantify gases and vapors. The system uses a hybrid integrated circuit (IC) containing optical waveguides coated with sensing chemistry as the optical platform. The IC with sensing chemistry is available commercially under the name Sensor-on-a-Chip. This IC is mounted in a small, uniquely designed sample chamber where the measured analyte is identified by the sensing chemistry and biochemistry. Continuous or stop-flow sampling is possible. Sensitivities in the low parts-per-million have been attained for hydrocarbons and alcohol. Analyte coverage is only limited by the sensing chemistries and biochemistries that are available.
NTIS
*Detection; Hybrid Circuits; Chemical Analysis; Gas Detectors*

**20010123649** Carnegie Institution of Washington, Washington, DC USA
**Final Report: High Pressure Synchrotron Infrared Spectroscopy, September 1, 1996-December 31, 1998**
Henley, R. J.; Dec. 31, 1998; 7p; In English
Report No.(s): DE2001-764603; No Copyright; Avail: Department of Energy Information Bridge
The goal of the project has been the construction of a versatile facility for measuring far to near-infrared spectra of natural and synthetic materials from ambient to ultrahigh pressures at variable temperatures using new synchrotrons infrared microspectroscopy techniques. The measurements address a broad range of problems in Earth and planetary science.
NTIS
*Construction; Synchrotrons; Infrared Spectra*

**20010123658** Institute of Paper Science and Technology, Atlanta, GA USA
**Control of Soluble Fouling in High Solids Black Liquor Concentrators**
Frederick, W. J.; Chen, F.; Hsieh, G.; Lien, S.; Murphy, R. W.; Mar. 31, 2000; 8p; In English
Report No.(s): DE2001-764427; DOE/GO/10387-Q; No Copyright; Avail: Department of Energy Information Bridge
For Task A. 1, some shakedown runs (both successful and unsuccessful ones) for black liquor volubility have been completed. Based on these, the experimental apparatus and operating procedures have been continually modified to attempt to overcome the persistent experimental problems associated with collecting samples of filtered black liquor at high solids. The crystallization experiments with kraft black liquor (Task B.2) are well under way. The falling film plate evaporator is now fully operational (Task

C.1), and has been tested with water. In the computational fluid dynamics model development work (Task D.2.4), a preliminary comparison of flow dynamics models to experimental results was completed, and heat transfer models with simplifying assumptions have been completed (Task D.3).
NTIS
*Concentrators; Crystallization; Fouling*

**20010123905** Virginia Univ., Dept. of Chemical Engineering, Charlottesville, VA USA
**Theoretical and Experimental Study of Mixed Solvent Electrolytes: Final Report**
Cummings, P. T.; O'Connell, J. P.; Jan. 31, 1995; 26p; In English
Report No.(s): DE2001-764042; DE-FG05-88ER13943-F; No Copyright; Avail: Department of Energy Information Bridge
The goals of the research program evolved into six areas: (1) Molecular simulation of phase equilibria in aqueous and mixed solvent electrolyte solutions; (2) Molecular simulation of solvation and structure in supercritical aqueous systems; (3) Extension of experimental database on mixed solvent electrolytes; (4) Analysis of the thermodynamic properties of mixed solvent electrolyte solutions and mixed electrolyte solutions using fluctuation solution theory; (5) Development of analytic expressions for thermodynamic properties of mixed solvent electrolyte solutions using analytically solved integral equation approximations; and (6) Fundamental modeling of mixed solvent electrolytes using numerically solved integral equation approximation theories.
NTIS
*Electrolytes; Solvents; Simulation*

**20010123926** California Univ., Lawrence Berkeley Lab., Berkeley, CA USA
**Intercomparison of simulation models for CO2 disposal in underground storage reservoirs**
Pruess, K.; Tsang, C. F.; Law, D.; Oldenburg, C.; Jan. 01, 2001; 31p; In English
Report No.(s): DE2001-775181; LBNL-47353; No Copyright; Avail: Department of Energy Information Bridge
An intercomparison study between simulation codes for terrestrial sequestration of CO(sub 2) is proposed. The objectives are, on the one hand, to focus and evaluate key processes through numerical simulation and, on the other, to explore the strengths of different codes and achieve acceptance of such codes for use in the development of geologic systems for CO(sub 2) disposal. This will be carried out through the study of a series of test problems by groups using their simulation codes. A progression from simple and uncoupled to increasingly complex and coupled problems is envisioned. The proposed study will attempt to involve interested technical groups worldwide, and will proceed through an iterative process of problem definition, solution comparison, discussion and refinement. The Internet will be used as a medium for communicating and organizing activities, and for a flexible exchange of information and documentation of results. In addition, it is planned to hold a series of workshops. The present write-up includes an initial set of eight proposed test problems and represents the first step in the process. Readers are encouraged to communicate with us at the email address above to indicate their interest and to provide suggestions and input.
NTIS
*Carbon Dioxide; Computerized Simulation; Reservoirs; Underground Storage; Mathematical Models*

**20010123958** Argonne National Lab., IL USA
**Damage Evolution and Residual Stresses in Plasma-Sprayed Zirconia Thermal Barrier Coatings**
Singh, J. P.; Feb. 03, 1999; 8p; In English
Report No.(s): DE2001-10934; ANL/ET/CP-97088; No Copyright; Avail: Department of Energy Information Bridge
Air-plasma-sprayed zirconia thermal barrier coatings were subjected to thermal cycling and residual stress evolution in thermally grown oxide scale was studied by micro- and macro-ruby fluorescence spectroscopy. The macro approach reveals that compressive stress in the oxide scale increases with increasing number of thermal cycles (and thus increasing scale thickness), reaching a value of 1.8 GPa at a scale thickness of 3-4 micrometers (80 cycles). Micro-ruby fluorescence spectroscopy indicates that protrusions of the zirconia top coat into the bond coat act as localized areas of high stress concentration, leading to damage initiation during thermal cycling.
NTIS
*Damage; Residual Stress; Stress Concentration; Thermal Control Coatings*

**20010124117** California Univ., Lawrence Berkeley Lab., Berkeley, CA USA
**Raman Spectroscopy Characterization of Amorphous Carbon Coatings for Computer Hard Disks**
Ager, J. W.; May 07, 1998; 7p; In English
Report No.(s): DE2000-767498; LBNL-41884; No Copyright; Avail: Department of Energy Information Bridge, Microfiche

Amorphous carbon films are used as protective coatings on magnetic media to protect the magnetic layer from wear and abrasion caused by the read/write head during hard disk drive start-up and operation. A key requirement in increasing the storage capacity and reliability of hard-disk drives is improving the performance of these coatings. This cooperative agreement used optical characterization techniques developed at Lawrence Berkeley National Laboratory (LBNL) to study thin-film hard disk media produced by Seagate Technology, major US hard drive manufacturer. The chief scientific goal was relating quantitatively the results of the optical characterization to the underlying chemical structure of the overcoat. In a collaboration with Seagate, LBNL, and Cambridge University, optical and electron-based characterization were used to evaluate the chemical structure of overcoats. The sp3 fraction of the sputtered amorphous carbon films was measured quantitatively for the first time and related to the optical spectroscopy results. This work and other selected aspects of the research performed under the agreement were presented at technical meetings and published in the open literature. The chief technical goal was designing manufacturing processes for the protective carbon overcoat for use in new generations of Seagate disk drives. to this end, joint research carried out under this agreement enabled Seagate to speed development of new coatings which are currently being used in the production of disk media in Seagate's disk-media manufacturing plants in Fremont, CA.
NTIS
*Amorphous Materials; Characterization; Protective Coatings; Thin Films; Magnetic Disks*

**20010125009** Sandia National Labs., Albuquerque, NM USA
**Microfabricated Gas Phase Chemical Analysis Systems**
Casalnuovo, S. A.; Frye-Mason, G. C.; Heller, E. J.; Hietala, V. M.; Kottenstette, R. J.; Aug. 02, 1999; 4p; In English
Report No.(s): DE2001-9687; SAND99-2003C; No Copyright; Avail: Department of Energy Information Bridge, Microfiche
A portable, autonomous, hand-held chemical laboratory ((mu)ChemLab(trademark)) is being developed for trace detection (ppb) of chemical warfare (CW) agents and explosives in real-world environments containing high concentrations of interfering compounds. Microfabrication is utilized to provide miniature, low-power components that are characterized by rapid, sensitive and selective response. Sensitivity and selectivity are enhanced using two parallel analysis channels, each containing the sequential connection of a front-end sample collector/concentrator, a gas chromatographic (GC) separator, and a surface acoustic wave (SAW) detector. Component design and fabrication and system performance are described.
NTIS
*Chemical Analysis; Fabrication; Gas Chromatography; Miniaturization; Vapor Phases*

**20010125090** Argonne National Lab., IL USA
**Aqueous biphasic systems for metal separations: A microcalorimetric analysis of polymer/salt interactions**
Chaiko, D. J.; Hatton, T. A.; Zaslavsky, B.; May 03, 1999; 16p; In English
Report No.(s): DE2001-11789; ANL/CMT/CP-98943; No Copyright; Avail: Department of Energy Information Bridge
Certain radionuclide ions (e.g., TcO4)(sup 16)) exhibit unusually strong affinities toward the polymer-rich phase in aqueous biphase systems generated by combinations of salt solutions with polymers such as poly(ethylene glycol) (PEG) and poly(propylene glycol) (PPG). Thus, aqueous polymer phases could potentially be used to selectively extract these ions during pretreatment of radioactive tank wastes at Hanford. to help develop a fundamental understanding of the interactions between various ions and polymers in aqueous solution, interaction enthalpies between sodium perrhenate and a random copolymer of PEG and PPG (UCON-50) were measured by microcalorimetric titration. An entropy compensation effect was observed in this system in which changes in enthalpic interactions were balanced by entropy changes such that the interaction free energy remained constant and approximately equal to zero.
NTIS
*Radioactive Isotopes; Aqueous Solutions; Solvent Extraction; Radioactive Wastes; Pretreatment*

**20010125155** Argonne National Lab., IL USA
**Comparison of the corrosion behaviors of the glass-bonded sodalite ceramic waste form and reference HLW glasses**
Ebert, W. L.; Lewis, M. A.; May 06, 1999; 11p; In English
Report No.(s): DE2001-11790; ANL/CMT/CP-98944; No Copyright; Avail: Department of Energy Information Bridge
A glass-bonded sodalite ceramic waste form is being developed for the long-term immobilization of salt wastes that are generated during spent nuclear fuel conditioning activities. A durable waste form is prepared by hot isostatic pressing (HIP) a mixture of salt-loaded zeolite powders and glass frit. A mechanistic description of the corrosion processes is being developed to support qualification of the CWF for disposal. The initial set of characterization tests included two standard tests that have been used extensively to study the corrosion behavior of high level waste (HLW) glasses: the Material Characterization Center-1

(MCC-1) Test and the Product Consistency Test (PCT). Direct comparison of the results of tests with the reference CWF and HLW glasses indicate that the corrosion behaviors of the CWF and HLW glasses are very similar.
NTIS
*Radioactive Wastes; Ceramics; Corrosion Resistance*

**20010125247** Argonne National Lab., IL USA
**Performance testing of hydrogen transport membranes at elevated temperatures and pressures**
Balachandran, U.; Cugini, A. V.; Dorris, S. E.; Fisher, E. P.; Graham, W. J.; Jun. 16, 1999; 8p; In English
Report No.(s): DE2001-11774; ANL/ET/CP-98887; No Copyright; Avail: Department of Energy Information Bridge

The development of hydrogen transport ceramic membranes offers increased opportunities for hydrogen gas separation and utilization. Commercial application of such membranes will most likely take place under conditions of elevated temperature and pressure, where industrial processes producing and or utilizing hydrogen occur, and where such membranes are theoretically expected to have the greatest permeability. Hydrogen separation membrane performance data at elevated temperature is quite limited, and data at elevated pressures is conspicuously lacking. This paper will describe the design, construction, and recent experimental results obtained from a membrane testing unit located at the U.S. Department of Energy's Federal Energy Technology Center (FETC). The membrane testing unit is capable of operating at temperatures up to 900 C and pressures up to 500 psi. Mixed-oxide ceramic ion-transport membranes, fabricated at Argonne National Laboratory (ANL), were evaluated for hydrogen permeability and characterized for surface changes and structural integrity using scanning electron microscopy/X-ray microanalysis (SEM/EDS), X-ray photoelectron spectroscopy (XPS) and atomic force microscopy (AFM), as a function of temperature, pressure, and hydrogen exposure.
NTIS
*Hydrogen; Membranes; Ceramics; Performance Tests*

**20010125394** Argonne National Lab., IL USA
**Measurement of low levels of alpha in (sup 99)Mo product solutions**
Conner, C.; Liberatore, M. W.; Sedlet, J.; Vandegrift, G. F.; Mar. 05, 1998; 12p; In English
Report No.(s): DE2001-8128; ANL/CMT/CP-94428; No Copyright; Avail: Department of Energy Information Bridge, Microfiche

The conclusions of this report are that molybdenum can effectively be separated from uranium and plutonium using TRU-Resin; and that separation of the Mo-99 from the actinides will reduce the analyst's exposure and simplify analysis for the actinide elements.
NTIS
*Molybdenum Isotopes; Alpha Particles; Radiochemical Separation*

**20010125415** Argonne National Lab., IL USA
**New developments in the application of synchrotron radiation to material science**
Sinha, S. K.; Apr. 21, 1999; 9p; In English
Report No.(s): DE2001-11764; ANL/XFD/CP-98810; No Copyright; Avail: Department of Energy Information Bridge, Microfiche

Recent developments in the application of synchrotrons radiation to materials science are discussed, using techniques which exploit the high brilliance of the newer synchrotrons sources, such as microbeam techniques and correlation spectroscopy. These include studies of environmental systems, residual stress, slow dynamics of condensed matter systems and studies of liquid surfaces and thin magnetic films.
NTIS
*Synchrotron Radiation; Nuclear Research and Test Reactors*

**20010125473** Argonne National Lab., IL USA
**One MeV Electron Irradiation of Solid Xe Nanoclusters in Al: An In-Situ HRTEM Study**
Donnelly, S. E.; Furuya, K.; Song, M.; Birtcher, R. C.; Allen, C. W.; Dec. 05, 1997; 16p; In English
Report No.(s): DE2001-8097; ANL/MSD/CP-93622; No Copyright; Avail: Department of Energy Information Bridge, Microfiche

Thin film samples of a simple embedded nanocluster system consisting of solid Xe precipitates in Al have been subjected to 1 MeV electron irradiation in a high-voltage electron microscope. High-resolution images have been recorded on videotape in order to monitor the changes to the system resulting from the passage of electrons through the film. Inspection of the video

recordings (in some cases frame-by-frame) reveals that complex, rapid processes occur under the electron beam. These include, movement of small clusters, coalescence of neighboring clusters, shape changes, the apparent melting and resolidification of the Xe, and the creation and annealing of extended defects within the Xe lattice. A tentative interpretation of some of the observations is presented in terms of the electron-induced displacement processes at the surface of the clusters.
NTIS
*Electron Irradiation; Thin Films; Xenon; Radiation Effects*

**20010125475** Argonne National Lab., IL USA
**Solvent Extraction in the Treatment of Acidic High-Level Liquid Waste: Where Do We Stand**
Horwitz, E. P.; Schulz, W. W.; Jun. 18, 1998; 32p; In English
Report No.(s): DE2001-8094; ANL/CHM/CP-93488; No Copyright; Avail: Department of Energy Information Bridge, Microfiche

During the last 15 years, a number of solvent extraction/recovery processes have been developed for the removal of the transuranic elements, SR-90 and Cs-137 from acidic high-level liquid waste. These processes are based on the use of a variety of both acidic and neutral extractants. This chapter will present an overview and analysis of the various extractants and flowsheets developed to treat acidic high-level liquid waste streams. The advantages and disadvantages of each extractant along with comparisons of the individual systems are discussed.
NTIS
*Cesium 137; Solvent Extraction; Strontium 90; Radioactive Wastes*

**20010125539** SRI International Corp., Menlo Park, CA USA
**Nuclear Energy Research Initiative (NERI) Program** ***Progress Report***
Engelhardt, G. R.; Macdonald, D. D.; Apr. 01, 2000; 8p; In English
Report No.(s): DE2001-763898; No Copyright; Avail: Department of Energy Information Bridge, Microfiche

High-speed methods for calculating concentrations and potential distributions inside pit and crevice corrosion cavities have been developed. Exchange current densities and transfer coefficients for oxygen reduction on Alloy C-22 and carbon steel for the range of temperature 25-95 degrees Celsius have been determined. The results of the comparative study showed that Alloy 22 has a unique resistance to pitting in NaCl solutions, including those at elevated temperatures (to 90 degrees Celsius).
NTIS
*Alloys; Carbon Steels; Cavities; Pitting; Corrosion Resistance; Cavitation Corrosion*

**20010125542** Los Alamos National Lab., NM USA
**Homogeneous and Biphasic Catalysis in Dense Phase Carbon Dioxide**
Tumas, W.; Feb. 01, 2000; 12p; In English
Report No.(s): DE2001-763403; LA-UR-00-1087; No Copyright; Avail: Department of Energy Information Bridge, Microfiche

We and others have found that dense phase fluids, particularly carbon dioxide, are effective solvents for a wide range of homogeneous catalytic transformations. A major focus of our recent research program at Los Alamos has been to benchmark the reactivity and selectivity of catalytic reactions in liquid and supercritical carbon dioxide relative to conventional organic solvents, as well as to develop new concepts for catalytic chemistry. We will summarize product distributions, selectivity, kinetics, temperature/pressure effects and mechanistic studies for three important classes of catalytic reactions in dense phase carbon dioxide: selective oxidation; reduction including hydroboration and asymmetric hydrogenation; and carbon-carbon bond forming reactions. We will also report on new systems that incorporate CO2-philic ligands for catalysis as well as newly developed systems which involve either CO2-soluble polymer-supported ligands or biphasic catalysis in carbon dioxide/water emulsions for enhancing reactivity and separation.
NTIS
*Catalysis; Solvents; Carbon Dioxide; Phase Transformations; Binary Systems (Materials); Supercritical Fluids*

**20010125569** Argonne National Lab., IL USA
**Stress Corrosion Cracking Behavior of Irradiated Model Austenitic Stainless Steel Alloys**
Chung, H. M.; Karlsen, T. M.; Ruther, W. E.; Shack, W. J.; Strain, R. V.; Jul. 16, 1999; 18p
Report No.(s): DE2001-11896; ANL/ET/CP-99539; No Copyright; Avail: Department of Energy Information Bridge, Microfiche

Slow-strain-rate tensile tests (SSRTs) and post-test fractographic analyses by scanning electron microscopy were conducted on 16 austenitic stainless steel (SS) alloys that were irradiated at 289 C in He. After irradiation to approximately 0.3 x 10(exp 21) n/sq cm and approximately 0.9 x 10(exp 21) n/sq cm (E is greater than 1 MeV), significant heat-to-heat variations in the degree

of intergranular and transgranular stress corrosion cracking (IGSCC and TGSCC) were observed. Following irradiation to a fluence of approximately 0.3 x 10(exp 21) n/sq cm, a high-purity laboratory heat of Type 316L SS (Si approximately 0.024 wt%) exhibited the highest susceptibility to IGSCC. The other 15 alloys exhibited negligible susceptibility to IGSCC at this low fluence. The percentage of TGSCC on the fracture surfaces of SSRT specimens of the 16 alloys at approximately 0.3 x 10(exp 21) n/sq cm (E is greater than 1 MeV) could be correlated well with N and Si concentrations; all alloys that contained less than 0.01 wt.% N and less than 1.0 wt.% Si were susceptible, whereas all alloys that contained more than 0.01 wt.% N or more than 1.0 wt.% Si were relatively resistant. High concentrations of Cr were beneficial. Alloys that contain less than 15.5 wt.% Cr exhibited greater percentages of TGSCC and IGSCC than those alloys with approximately 18 wt.% Cr, whereas an alloy that contains more than 21 wt.% Cr exhibited less susceptibility than the lower-Cr alloys under similar conditions.
NTIS
*Austenitic Stainless Steels; Fractography; Intergranular Corrosion; Irradiation; Stress Corrosion Cracking*

**20010125572** Argonne National Lab., IL USA
**Fouling Characteristics of Compact Heat Exchangers and Enhanced Tubes**
Panchal, C. B.; Rabas, T. J.; Jul. 15, 1999; 9p
Report No.(s): DE2001-11893; ANL/ES/CP-99515; No Copyright; Avail: Department of Energy Information Bridge, Microfiche

Fouling is a complex phenomenon that: (1) encompasses formation and transportation of precursors, and (2) attachment and possible removal of foulants. A basic understanding of fouling mechanisms should guide the development of effective mitigation techniques. The literature on fouling in complex flow passages of compact heat exchangers is limited; however, significant progress has been made with enhanced tubes.
NTIS
*Fouling; Heat Exchangers*

**20010125573** Argonne National Lab., IL USA
**Photorefractivity in Liquid Crystals Doped with a Soluble Conjugated Polymer**
Niemczyk, M. P.; Svec, W. A.; Wasielewski, M. R.; Wiederrecht, G. P.; Jul. 07, 1999; 10p
Report No.(s): DE2001-11891; ANL/CHM/CP-99495; No Copyright; Avail: Department of Energy Information Bridge, Microfiche

Photoconductive polymers are doped into liquid crystals to create a new mechanism for space-charge field formation in photorefractive liquid crystal composites. The composites contain poly(2,5-bis(2(prime)-ethylhexyloxy) -1,4-phenylenevinylene) (BEH-PPV) and the electron acceptor N,N(prime)-dioctyl- 1,4:5,8-naphthalenediimide, NI. Using asymmetric energy transfer (beam coupling) measurements that are diagnostic for the photorefractive effect, the direction of beam coupling as a function of grating fringe spacing inverts at a spacing of 5.5 micrometers. We show that the inversion is due to a change in the dominant mechanism for space-charge field formation. At small fringe spacings, the space-charge field is formed by ion diffusion in which the photogenerated anion is the more mobile species. At larger fringe spacings, the polarity of the space charge field inverts due to dominance of a charge transport mechanism in which photogenerated holes are the most mobile species due to hole migration along the BEH-PPV chains coupled with interchain hole hopping. Control experiments are presented, which use composites that can access only one of the two charge transport mechanisms. The results show that charge migration overlong distances leading to enhanced photorefractive effects can be obtained using conjugated polymers dissolved in liquid crystals.
NTIS
*Conjugation; Doped Crystals; Liquid Crystals; Photorefractivity; Space Charge*

**20010125591** Los Alamos National Lab., NM USA
**Uranium Isotopic Analysis with the FRAM Isotopic Analysis Code**
Vo, D. T.; Sampson, T. E.; May 01, 1999; 30p; In English
Report No.(s): DE2001-8192; LA-13580; No Copyright; Avail: Department of Energy Information Bridge, Microfiche

FRAM is the acronym for Fixed-energy Response-function Analysis with Multiple efficiency. This software was developed at Los Alamos National Laboratory originally for plutonium isotopic analysis. Later, it was adapted for uranium isotopic analysis in addition to plutonium. It is a code based on a self-calibration using several gamma-ray peaks for determining the isotopic ratios. The versatile-parameter database structure governs all facets of the data analysis. User editing of the parameter sets allows great flexibility in handling data with different isotopic distributions, interfering isotopes, and different acquisition parameters such as energy calibration and detector type.
NTIS
*Uranium Isotopes; Gamma Ray Spectra; Isotope Ratios; Functional Analysis; Computer Programs*

**20010125592** Florida State Univ., Tallahassee, FL USA
**Energy Transformation in Molecular Electronic Systems**
Kasha, M.; May 17, 1999; 6p; In English
Report No.(s): DE2001-8186; DOE/ER/60517-T1; No Copyright; Avail: Department of Energy Information Bridge, Microfiche
This laboratory has developed many new ideas and methods in the electronic spectroscopy of molecules. This report covers the contract period 1993-1995. A number of the projects were completed in 1996, and those papers are included in the report. The DOE contract was terminated at the end of 1995 owing to a reorganizational change eliminating nationally the projects under the Office of Health and Environmental Research, U. S. Department of Energy.
NTIS
*Spectroscopy; Molecules*

**20010125594** Department of Energy, Richland Operations Office, Richland, WA USA
**Sampling and Analysis Instruction for the Demolition of the Masonry Block for the 108-F Biological Laboratory**
Byrnes, M. E.; Jun. 07, 1999; 24p; In English
Report No.(s): DE2001-8150; BHI-01288-REV-0; No Copyright; Avail: Department of Energy Information Bridge, Microfiche
This sampling and analysis instruction (SAI) has been prepared to clearly define the sampling and analysis activities to be performed in support of the demolition and disposition (or disposal) of the 108-F Biological Laboratory masonry block walls.
NTIS
*Sampling; Chemical Analysis; Waste Disposal; Concretes*

## 24
## COMPOSITE MATERIALS

*Includes physical, chemical, and mechanical properties of laminates and other composite materials.*

**20010117713** Los Alamos National Lab., NM USA
**Deformation of a Beryllium-Aluminum Composite**
Carter, D. H.; Mar. 01, 2000; 156p; In English
Report No.(s): DE2000-752672; LA-13687-T; No Copyright; Avail: Department of Energy Information Bridge
The physical and mechanical properties of beryllium, especially the combination of low density and high elastic modulus, make it an attractive candidate for a structural material. Intrinsic problems exist with Be as a monolithic material, as its structural behavior is complex due to its hexagonal close-packed crystal structure. Therefore, great value may be found in investigating composites of Be, such as beryllium-aluminum. However, one needs to understand the behavior of the individual phases in a Be composite and their interaction during the sequence of elasticity, plasticity, and fracture. The approach taken in this dissertation was to monitor the elastic loading of each phase, in combination with detailed studies of the composite's mechanical behavior for strains up to 5 percent. In addition, the experiments were performed on a unique type of composite microstructure. This consisted of interpenetrating phases formed from liquid immiscibility, rather than conventional powder processing, which is limited by reactions at interfaces. The results were interpreted in terms of plasticity models and finite element calculations that describe the interaction between the phases and the local stress states established by compatibility requirements between the phases.
NTIS
*Deformation; Crystal Structure; Metal Matrix Composites*

**20010118913** Sandia National Labs., Albuquerque, NM USA
**Relationship Between Nanomechanical and Chemical Properties in Polymer Composites**
Steffan, C. E.; Liu, H.; Winter, R. M.; Cabibil, H.; Lozano, J.; Jul. 12, 2000; 6p; In English
Report No.(s): DE2000-760801; SAND2000-1625C; No Copyright; Avail: Department of Energy Information Bridge
Polymer matrix composites have seen increasing use in ever more demanding situations in aerospace (B-2 stealth bomber), automotive (leaf springs) and recreational (bicycle frames) applications. The unique advantages of polymer matrix composites, such as high specific stiffness and strength, long fatigue life, corrosion resistance and ease of fabrication into complex geometries, make them ideal candidates for such applications. It is recognized today that a key region within a polymer matrix composite is the interphase region, lying between the reinforcement and bulk polymer.
NTIS
*Chemical Properties; Polymer Matrix Composites*

**20010119538** Brookhaven National Lab., Upton, NY USA

**Theory of point-defects, non-stoichiometry, and solute additions in SmCo5+x-Sm2Co17-y and related compounds**

Welch,; Sep. 03, 1998; 7p; In English

Report No.(s): DE2001-10386; BNL-65210; KC02010300; No Copyright; Avail: Department of Energy Information Bridge, Microfiche

There is considerable interest in the possibility of producing Sm-Co-based nanocomposite magnets by rapid solidification and other far-from-equilibrium processing methods. Thermodynamic and kinetic models are quite valuable in understanding and optimizing such methods. This paper describes a method of estimation, utilizing tight-binding-based bond-order interatomic interaction potentials, of the thermodynamic properties of point defects such as vacancies, interstitials, antisite defects, and solute additions in the SmCo(sub 5+x) and Sm(sub 2)Co (sub 17)-y phases and related rare-earth-transition metal compounds. Illustrative calculations for point defects in SmCo(sub 5) will be presented. The results suggest a unified model of the thermodynamic properties of the SmCo(sub 5+x) -- Sm(sub 2) Co(sub 17(minus)y) region of the phase diagram, based on the 1-5 structure and the replacement of Sm by interacting dumbbell interstitials to form the 2-17 structure; the model is similar in nature to theories of the thermodynamics of metal hydrides.

NTIS

*Point Defects; Thermodynamic Properties; Intermetallics*

**20010119590** Denver Univ., Denver, CO USA

**Biaxial Failure Analysis of Graphite Reinforced Polyimide and Epoxy Fabric Composites** ***Final Report, 1 Jun. 1997-31 May 2001***

Kumosa, Maciej S.; Predecki, Paul K.; Benedikt, B.; Dragoi, D.; Kumosa, L.; Aug. 31, 2001; 130p; In English

Contract(s)/Grant(s): F49620-97-1-0426; Proj-3484

Report No.(s): AD-A394906; AFRL-SR-BL-TR-01-0476; No Copyright; Avail: CASI; A07, Hardcopy; A02, Microfiche

Comprehensive analyses of residual stresses in unidirectional and fabric graphite/polyimide composites were conducted in this study. In the experimental part of this research, numerous XRD measurements were made to determine residual strains and stresses in embedded Al and Ag inclusions placed in four ply 8 harness satin (8HS) woven and 6 ply unidirectional graphite/PMR-15 composites. In the modeling part of this research, the residual thermal stresses in the unidirectional and woven composites were evaluated by performing linear and visco-elastic computations. In addition, analytical approaches were used to predict the magnitudes of the residual thermal stresses in the composites as a function of temperature, time, composite architecture and external loads. The numerically and analytically determined residual stresses in the composites were subsequently compared to the residual stresses determined from the X-ray analysis in conjunction with the application of the linear elastic and visco-elastic Eshelby models for multiple ellipsoidal inclusions. The effect of external bending loads on the residual strains and stresses in the embedded particles was also experimentally and numerically investigated. A new methodology was proposed for the evaluation of interfaminar residual thermal stresses in unidirectional and woven polymer matrix composites based on XRD measurements of residual stresses in embedded crystalline inclusions in conjunction with the application of the visco-elastic Eshelby method for multiple inclusions.

DTIC

*Graphite-Epoxy Composites; Failure Analysis; Polyimides*

**20010120040** Virginia Polytechnic Inst. and State Univ., Blacksburg, VA USA

**Second International Conference on Fatigue of Composites** ***Final Report***

Reifsnider, Kenneth; Jun. 2000; 102p; In English

Report No.(s): AD-A394616; AFRL-SR-BL-TR-01-0482; No Copyright; Avail: CASI; A06, Hardcopy; A02, Microfiche

On June 4-7, 2000, the Second International Conference on Fatigue of Composites was held in Williamsburg, Virginia, USA. The first such conference was held in June 1997 in Paris, France. The present conference built on that foundation, by providing a forum for a limited number of leading reports from numerous countries around the world to present and discuss the science and technology of this subject Composite materials have 'come of age' in the applied community. Dental materials, medical prosthetics, high performance turbines, fuel cells, and many other engineering systems are critically dependent on composite materials. Most of these applications involve applied environments that change with time, and many applications involve time-variable severe environments (mechanical, chemical, and thermal). Fatigue, as a discipline, has become the study of the changes in the properties and performance of materials and material systems as a result of the application of such time-variable applied environments. It was the intent of the organizing committee that this conference, the only one of its kind, bring together

the world's best experts and convene the community of interested scientists and engineers to advance the field of Fatigue of Composite Materials.
DTIC
*Composite Materials; Research and Development; Fatigue (Materials)*

**20010120042** Army Research Lab., Human Research and Engineering Directorate, Aberdeen Proving Ground, MD USA
**Metal Matrix Composites for Ordnance Applications. NDIA Firepower Symposium Held in U. S. Army Research Laboratory, Aberdeen Proving Ground, MD on 20 Jun 2001**
Hoppel, Christopher; Beatty, John H.; Montgomery, Jonathan S.; Bender, James M.; Bogetti, Travis A.; Jun. 20, 2001; 22p; In English; Proceedings from Armaments for the Army Transformation Conference, 18-20 June 2001 sponsored by NDIA. Contains Viewgraphs Only
Report No.(s): AD-A394503; No Copyright; Avail: CASI; A03, Hardcopy; A01, Microfiche
No abstract.
Author
*Metal Matrix Composites; Ordnance*

**20010121496** Argonne National Lab., IL USA
**Development and application of NDE methods for monolithic and continuous fiber ceramic matrix composites**
Ellingson, W. A.; May 21, 1999; 15p; In English
Report No.(s): DE2001-10584; ANL/ET/CP-95453; No Copyright; Avail: Department of Energy Information Bridge, Microfiche
Monolithic structural ceramics and continuous fiber ceramic matrix composites (CMCs) are being developed for application in many thermally and chemically aggressive environments where structural reliability is paramount. We have recently developed advanced nondestructive evaluation (NDE) methods that can detect distributed 'defects' such as density gradients and machining-induced damage in monolithic materials, as well as delamination, porosity, and throughwall cracks in CMC materials. These advanced NDE methods utilize (a) high-resolution, high-sensitivity thermal imaging; (b) high-resolution X-ray imaging; (c) laser-based elastic optical scattering; (d) acoustic resonance; (e) air-coupled ultrasonic methods; and (f) high-sensitivity fluorescent penetrant technology. This paper discusses the development and application of these NDE methods relative to ceramic processing and ceramic components used in large-scale industrial gas turbines and hot gas filters for gas stream particulate cleanup.
NTIS
*Ceramic Matrix Composites; Ceramic Fibers; Nondestructive Tests*

**20010121505** Sandia National Labs., Albuquerque, NM USA
**Evaluation of Hand Lay-Up and Resin Transfer Molding in Composite Wind Turbine Blade Manufacturing**
Cairns,; Shramstad,; Jun. 01, 2000; 242p; In English
Report No.(s): DE2000-760737; SAND2000-1425; No Copyright; Avail: Department of Energy Information Bridge, Microfiche
The majority of the wind turbine blade industry currently uses low cost hand lay-up manufacturing techniques to process composite blades. While there are benefits to the hand lay-up process, drawbacks inherent to this process along with advantages of other techniques suggest that better manufacturing alternatives may be available. Resin Transfer Molding (RTM) was identified as a processing alternative and shows promise in addressing the shortcomings of hand lay-up. This report details a comparison of the RTM process to hand lay-up of composite wind turbine blade structures. Several lay-up schedules and critical turbine blade structures were chosen for comparison of their properties resulting from RTM and hand lay-up processing. The geometries investigated were flat plate, thin and thick flanged T-stiffener, I-beam, and root connection joint. It was found that the manufacturing process played an important role in laminate thickness, fiber volume, and weight for the geometries investigated. RTM was found to reduce thickness and weight and increase fiber volumes for all substructures. RTM resulted in tighter material transition radii and eliminated the need for most secondary bonding operations. These results would significantly reduce the weight of wind turbine blades. Hand lay-up was consistently slower in fabrication times for the structures investigated. A comparison of mechanical properties showed no significant differences after employing fiber volume normalization techniques to account for geometry differences resulting from varying fiber volumes. The current root specimen design does not show significant mechanical property differences according to process and exceeds all static and fatigue requirements.
NTIS
*Resin Transfer Molding; Turbine Blades; Wind Turbines; Composite Materials*

**20010121884** Argonne National Lab., IL USA
**High heat flux erosion of carbon fibre composite materials in the TEXTOR tokamak**
Hassanein, A.; Mar. 10, 1998; 21p; In English
Report No.(s): DE2001-10679; ANL/TD/CP-95856; No Copyright; Avail: Department of Energy Information Bridge

During plasma disruptions, ELMs (edge localized modes), or vertical displacement events (VDEs) high transient heat loads to the plasma facing materials can cause damage such as thermal erosion, cracking, or melting. Self shielding processes, which take place when a material surface is exposed to a high heat flux from an incident plasma, can lead to a reduction of the deposited energy. Experiments using the fast pneumatic probe of the TEXTOR tokamak were carried out to investigate these effects. The materials tested were carbon fiber reinforced materials with and without Si-addition. The probe with the material specimens was introduced into the edge plasma up to a depth of 9 cm in front of the ALT41 main limiter with a residence time of 80 ms. After the repeated exposure to the TEXTOR-plasma, the material specimens were examined by profilometry and electron microscopy to determine the damage and erosion. It was found that only a very limited zone of the probe tip of about 2.5 mm extension in radial direction showed erosion. The maximum erosion was observed at the very tip of the probe with approx. 30 (micro)m per exposure. The results of the erosion quantification are compared with the results from numerical simulations and from plasma diagnostic measurements during the exposure of the specimens.
NTIS
*Carbon; Heat Flux; Tokamak Devices; Plasmas (Physics)*

**20010122647** Los Alamos National Lab., NM USA
**Ion Irradiation Effects in the Ceramic Composite MgTiO3Er2Ti2O7**
Montaner, E. P.; Valdez, J. A.; Sickafus, K. E.; Sep. 01, 2000; 12p; In English
Report No.(s): DE2000-763042; LA-UR-00-4467; No Copyright; Avail: Department of Energy Information Bridge, Microfiche

We have developed a new ceramic-ceramic composite consisting of the mineral geikielite as a matrix phase and the mineral pyrochlore as a minor, second phase. We are investigating this material for use as a possible nuclear waste-form for the immobilization and storage of surplus actinides or high-level radioactive wastes. We performed radiation damage experiments by irradiating composite MgTiO3-Er2Ti2O7samples along with single crystals of MgTiO3 and Er2Ti2O7 (at a temperature of about 120 K) with 350 keV Xe(++) ions to ion fluences. Irradiated samples were analyzed using transmission electron microscopy (TEM) and nanoindentation techniques.
NTIS
*Ceramics; Ion Irradiation; Radiation Damage; Composite Materials*

**20010122709** California Univ., Dept. of Mechanical and Aerospace Engineering, Los Angeles, CA USA
**Intelligent Processing of Thick Composites** ***Final Report, 16 Jun. 1993 - 30 Apr. 1998***
Hahn, H. T.; Kang, M.; Lin, M.; Shin, D.; Sonmez, F.; Mar. 1999; 12p; In English
Contract(s)/Grant(s): N00014-93-1-0650
Report No.(s): AD-A395275; No Copyright; Avail: CASI; A03, Hardcopy; A01, Microfiche

Composites consolidation in various manufacturing processes has been studied from a unified point of view to develop a simulation model. As a result a master formulation is now available and can be tailored to each manufacturing process. Process simulation codes have been developed for the resin transfer molding (RTM) and %%autoclave/compression molding processes. The other key results are: (1) development of a finite element code RTMSIM to simulate resin transfer molding process; (2) development of a simple analytical model to explain the mechanisms of enhanced mold filling when high%permeability layers are used; (3) development of a rapid prototyping method for RTM based on the laminated object manufacturing process; (4) development of an intelligent thermal control system to ensure a better temperature uniformity in compression molding; (5) development of a unified process simulation model; and (5) development of a new kinetics model.
DTIC
*Composite Materials; Artificial Intelligence; Finite Element Method*

**20010122949** Pacific Northwest National Lab., Richland, WA USA
**Thermal Decomposition of Radiation-Damaged Polystyrene**
Abrefah, J.; Klinger, G. S.; Sep. 26, 2000; 35p; In English
Report No.(s): DE2000-763386; PNNL-13313; No Copyright; Avail: Department of Energy Information Bridge

The radiation-damaged polystyrene material (polycube) used in this study was synthesized by mixing a high-density polystyrene (Dylene Fines no. 100) with plutonium and uranium oxides. The polycubes were used on the Hanford Site in the 1960s for criticality studies to determine the hydrogen-to-fissile atom ratios for neutron moderation during processing of spent nuclear

fuel. Upon completion of the studies, two methods were developed to reclaim the transuranic (TRU) oxides from the polymer matrix.
NTIS
*Polystyrene; Thermal Decomposition; Radiation Damage*

**20010123094** Argonne National Lab., IL USA
**Fabrication and characterization of a porous-matrix oxide fibrous monoliths**
Polzin, B. J.; Mar. 02, 1999; 11p; In English
Report No.(s): DE2001-10961; ANL/ET/CP-97264; No Copyright; Avail: Department of Energy Information Bridge, Microfiche
We have fabricated unidirectional fibrous monoliths based on dense ZrSiO(sub 4) cells that are surrounded by a porous, weak ZrSiO(sub 4) cell boundary phase. We coextruded a duplex filament, cut it to short lengths, bundled the lengths and packed them into an extruder, and then extruded a new filament. This filament was cut and packed into a bar die to produce test specimens. After heat treatment, the specimens were tested in four-point flexure and examined by scanning electron microscopy. Load-displacement curves were linear to failure, but some evidence of toughening was observed microscopically.
NTIS
*Zirconium Oxides; Silicon Oxides; Filaments; Extruding; Fibers*

**20010123231** Argonne National Lab., IL USA
**Process to Recover Fibers from Polymer Matrix Composites**
Jody, B. J.; Daniels, E. J.; Pomykala, J. A.; Jul. 19, 2000; 8p; In English
Report No.(s): DE2000-761241; ANL/ES/CP-101526; No Copyright; Avail: Department of Energy Information Bridge
Carbon-fiber reinforced-polymer-matrix composites (PMC) are widely used by the aerospace and aircraft industries because of their high strength-to-weight ratio. Because of this virtue, the automotive industry is considering using them for automotive applications. However, the degree to which PMC materials can be recycled is of concern. We are developing a thermal treatment process for recycling the fibers in PMC materials. Batch testing at the bench scale demonstrated that carbon fibers could be successfully recovered from PMC structures. Experiments conducted on PMC materials having urethane-based, epoxy-based, and urea/phenolic-based substrates showed that fibers that are completely free of residual organic materials could be recovered efficiently and economically. Evaluation of the recovered fibers demonstrated that they are suitable for short-fiber applications. A continuous infrared treatment reactor capable of processing up to 5 kg of PMC material per hour has been designed and is expected to be ready for testing in the summer of this year. Economic analysis of the process suggests a simple payback of less than two years.
NTIS
*Polymer Matrix Composites; Carbon Fibers; Automobiles*

**20010123910** Los Alamos National Lab., NM USA
**Linking Damage Models to Quantified Experimental Meso-Scopic Damage Measurements**
Thissel, W.; Zurek, A.; Feb. 01, 2000; 6p; In English
Report No.(s): DE2001-763367; LA-UR-00-939; No Copyright; Avail: Department of Energy Information Bridge
This paper describes the techniques that we employ and are developing in capturing, measuring, and describing the evolution of dynamic damage accumulation in metals, from the first nucleation event up to final failure surface formation. These measurements are used in damage model development, verification, and validation. Ta and Cu quantification examples are given.
NTIS
*Metals; Mathematical Models; Damage Assessment; Characterization*

**20010123964** Argonne National Lab., IL USA
**Front-flash thermal imaging characterization of continuous fiber ceramic composites**
Deemer, C.; Apr. 23, 1999; 9p; In English
Report No.(s): DE2001-10924; ANL/ET/CP-97040; No Copyright; Avail: Department of Energy Information Bridge, Microfiche
Infrared thermal imaging has become increasingly popular as a nondestructive evaluation method for characterizing materials and detecting defects. One technique, which was utilized in this study, is front-flash thermal imaging. We have developed a thermal imaging system that uses this technique to characterize advanced material systems, including continuous fiber ceramic composite (CFCC) components. In a front-flash test, pulsed heat energy is applied to the surface of a sample, and decay of the surface temperature is then measured by the thermal imaging system. CFCC samples with drilled flat-bottom holes at the back surface (to serve as 'flaws') were examined. The surface-temperature/time relationship was analyzed to determine the depths of the flaws

from the front surface of the CFCC material. Experimental results on carbon/carbon and CFCC samples are presented and discussed.
NTIS
*Ceramics; Carbon-Carbon Composites; Fiber Composites; Nondestructive Tests; Infrared Inspection*

**20010125464** Argonne National Lab., IL USA
**Vibration analysis of composite disks**
Gupta, A.; Mulcahy, T. M.; Hull, J. R.; Abboud, R. G.; Nov. 18, 1997; 5p; In English
Report No.(s): DE2001-8112; ANL/ET/CP-94031; No Copyright; Avail: Department of Energy Information Bridge, Microfiche
Often, disks rotating at high speeds are fabricated from high-strength, filament-wound composites. The carbon and glass fiber bundles, or tows that makeup a filament, are often similar in different disk designs, and steady-state stress analyses are usually reported. Typically, little information is reported about the dynamic deformation and vibrations of the disk, which are important for understanding instabilities at high rotational speeds. First, experimental and FEM modal analyses are performed for a non-rotating disk to verify the FEM model. The disk is made from composite rings which are press-fit or urethane bonded onto a hub. Then, the FEM model is used to analyze the effect of prestressing and stress stiffening due to rotation at various speeds.
NTIS
*Vibration; Dynamic Structural Analysis; Rotating Disks; Composite Materials*

**20010125532** Ames Lab., IA USA
**Microstructure-Strength Relationship of a Deformation-Processed Aluminum-Magnesium Composite**
Xu, K.; Sep. 12, 2000; 59p; In English
Report No.(s): DE2001-764682; IS-T 1915; No Copyright; Avail: Department of Energy Information Bridge
Composites formed by mechanical working (i.e., rolling, swaging, or wire drawing) of two-phase ductile metal mixtures have received substantial consideration in recent years because of the unique properties they show compared to conventional materials. During mechanical deformation, the two phases deform together, causing the second minor phase to elongate, which results in a fibrous structure within the matrix. Therefore, these composites are referred to as in situ composites or Deformation-Processed Metal Matrix Composites (DMMCS). This type of composite can be fabricated in various ways. The first step to fabricate the deformation-processed composites is the production of a two-phase billet. This can be achieved by casting techniques or powder metallurgy processes. Casting methods can be used for composites if the phase equilibria of the alloy possess a two-phase equilibrium field. Powder metallurgy methods can be used for composites of elements with disparate melting points or unfavorable equilibrium phase diagrams.
NTIS
*Deformation; Metal Matrix Composites; Microstructure; Aluminum; Magnesium; Mechanical Properties*

**20010125543** Louisiana State Univ., Baton Rouge, LA USA
**International Conference (1st) on Multiscale Materials Phenomena in Harsh Environments**
Kalia, Rajiv K.; Nakano, Aiichiro; Razis, Panos; Vashishta, Priya; Voyiadjis, George; June 2000; 40p; In English, 19-24 Jun. 2000, Limassol, Cyprus; Original contains color images
Report No.(s): AD-A394818; No Copyright; Avail: CASI; A03, Hardcopy; A01, Microfiche
The conference will focus on various thermo-mechanical aspects including deformation, the influence of large strains and strain rates, creep. fatigue, and dynamic fracture in these materials. The conference will feature recent developments in ab initio electronic structure calculations, large scale molecular-dynamics simulations based on reliable interactions, finite-element methods, parallel algorithms for materials simulations, and immersive and interactive visualization environments for virtual design of materials. The proposed conference is unique in that it will combine state-of-the-art multiscale modeling with recent experimental results.
Derived from text
*Composite Materials; Creep Properties; Deformation; Electronic Structure; Finite Element Method; Molecular Dynamics; Strain Rate*

**20010125599** NASA Marshall Space Flight Center, Huntsville, AL USA
**Composite Tank**
DeLay, Thomas K., Inventor, NASA Marshall Space Flight Center, USA; Dec. 12, 2000; 4p; In English
Patent Info.: Filed 22 Dec. 1998; NASA-Case-MFS-31379-1; US-Patent-6,158,605; US-Patent-Appl-SN-218652; No Copyright; Avail: CASI; A01, Hardcopy; A01, Microfiche

A composite tank for containing liquid oxygen and the method of making the same Wherein a water-soluble mandrel having ing the desired tank configuration and a cylindrical protuberance on at least one end is fitted with an inner boss conformance, to the configuration of the mandrel and in outer boss conforming to the configuration of the inner boss, the bosses each having a tubular portion for receiving the protuberance on the mandrel and a spherical portion. The mandrel and the bosses are first coated with a nickel coating. The mandrel is then wrapped with graphite fibers wetted with an epoxy resin and this resin is cured. A layer of insulating foam is then applied to the tank and cured. The insulating foam is machined to a desired concentration and a layer of aramid fibers wetted with a second epoxy resin is wrapped around the tank. The second resin is cured and the water soluble mandrel is washed from inside the tank.
Official Gazette of the U.S. Patent and Trademark Office
*Liquid Oxygen; Tanks (Containers)*

**20010125609** NASA Langley Research Center, Hampton, VA USA
**Highlights of NASA's Role In Developing State-Of-The-Art Nondestructive Evaluation For Composites**
Madaras, Eric, NASA Langley Research Center, USA; [2001]; 11p; In English; American Helicopter Society Hampton Roads Chapter Structure Specialist Meeting, 30 Oct. - 1 Nov. 2001, Williamsburg, VA, USA; Sponsored by American Helicopter Society, Inc., USA; Copyright; Avail: Issuing Activity

Since the 1970's, when the promise of composites was being pursued for aeronautics applications, NASA has had programs that addressed the development of NDE (NonDestructive Evaluation) methods for composites. These efforts included both microscopic and macroscopic NDE. At the microscopic level, NDE investigations interrogated composites at the submicron to micron level to understand a composite's microstructure. A novel microfocus CT system was developed as well as the science underlying applications of acoustic microscopy to a composite's component material properties. On the macroscopic scale NDE techniques were'developed that advanced the capabilities to be faster and more quantitative. Techniques such as stiffness imaging, ultrasonic arrays, laser based ultrasound, advanced acoustic emission, thermography, and novel health monitoring systems were researched. Underlying these methods has been a strong modeling capability that has aided in method development.
Author
*Nondestructive Tests; Composite Materials*

## 25
## INORGANIC, ORGANIC AND PHYSICAL CHEMISTRY

*Includes the analysis, synthesis, and use inorganic and organic compounds; combustion theory; electrochemistry; and photochemistry. For related information see also 34 Fluid Dynamics and Thermodynamics, For astrochemistry see category 90 Astrophysics.*

**20010117632** Department of Energy, Aiken, SC USA
**Optimization of Cesium Removal from Hanford Envelope A Simulant with SuperLig 639 Ion Exchange Resin**
King, W. D.; Jul. 27, 2000; 35p; In English
Report No.(s): DE2000-759135; BNF-003-98-0169; No Copyright; Avail: Department of Energy Information Bridge

Hanford Radioactive Waste materials have been categorized into four envelopes labeled A through D as specified in the Tank Waste Remediation Contract between BNFL and DOE. 1 Envelopes A, B and C contain only solubilized species and are specified as Low-Activity Waste (LAW). Each envelope is defined based on compositional maximums of chemical and radioactive constituents. Envelopes A and B contain low concentrations of organic species and the primary form of technetium is pertechnetate (TcO4-). Envelope C contains higher levels of organic species and technetium which is primarily in the nonpertechnetate form (presumably complexed TcO2). Envelope D is sludge which has been separated from the supernate and is referred to as High Activity Waste. The current plant design utilizes SuperLig ion exchange resins to remove cesium and technetium (the primary radioactive constituents) from the Hanford LAW. The process is designed to produce a decontaminated waste stream and a concentrated eluate waste stream for vitrification into low and high activity glasses, respectively.
NTIS
*Ion Exchange Resins; Technetium; Cesium; Optimization; Radioactive Wastes*

**20010117668** NASA Glenn Research Center, Cleveland, OH USA
**Shapes of Nonbuoyant Round Luminous Hydrocarbon/Air Laminar Jet Diffusion Flames, Appendix H**
Lin, K.-C., Michigan Univ., USA; Faeth, G. M., Michigan Univ., USA; Sunderland, P. B., NASA Glenn Research Center, USA; Urban, D. L., NASA Glenn Research Center, USA; Yuan, Z.-G., NASA Glenn Research Center, USA; Laminar Soot Processes

(LSP); Dec. 15, 2000; ISSN 0010-2180, pp. 209-226; Repr. from Combustion and Flame (Elsevier Science, Inc.), v. 116, 1999 p 415-431; In English
Contract(s)/Grant(s): NAG3-1245; NAG3-2048; Copyright; Avail: Issuing Activity

The shapes (luminous flame boundaries) of round luminous nonbuoyant soot-containing hydrocarbon/air laminar jet diffusion flames at microgravity were found from color video images obtained on orbit in the Space Shuttle Columbia. Test conditions included ethylene- and propane-fueled flames burning in still air at an ambient temperature of 300 K ambient pressures of 35-130 kPa, initial jet diameters of 1.6 and 2.7 mm, and jet exit Reynolds numbers of 45-170. Present test times were 100-200 s and yielded steady axisymmetric flames that were close to the laminar smoke point (including flames both emitting and not emitting soot) with luminous flame lengths of 15-63 mm. The present soot-containing flames had larger luminous flame lengths than earlier ground-based observations having similar burner configurations: 40% larger than the luminous flame lengths of soot-containing low gravity flames observed using an aircraft (KC-135) facility due to reduced effects of accelerative disturbances and unsteadiness; roughly twice as large as the luminous flame lengths of soot-containing normal gravity flames due to the absence of effects of buoyant mixing and roughly twice as large as the luminous flame lengths of soot-free low gravity flames observed using drop tower facilities due to the presence of soot luminosity and possible reduced effects of unsteadiness, Simplified expressions to estimate the luminous flame boundaries of round nonbuoyant laminar jet diffusion flames were obtained from the classical analysis of Spalding; this approach provided successful correlations of flame shapes for both soot-free and soot-containing flames, except when the soot-containing flames were in the opened-tip configuration that is reached at fuel flow rates near and greater than the laminar smoke point fuel flow rate.
Author
*Shapes; Soot; Jet Flow; Diffusion Flames; Hydrocarbons; Microgravity*

**20010117669** Michigan Univ., Dept. of Aerospace Engineering, Ann Arbor, MI USA
**Soot Formation in Laminar Acetylene/Air Diffusion Flames at Atmospheric Pressure, Appendix C**
Xu, F., Michigan Univ., USA; Faeth, G. M., Michigan Univ., USA; Laminar Soot Processes (LSP); Dec. 15, 2000; ISSN 0010-2180, pp. 100-116; Repr. from Combustion and Flame(Elsevier Science, Inc.), v. 125, 2001 p 804-819; In English
Contract(s)/Grant(s): NAG3-1245; NAG3-1878; NAG3-2048; Copyright; Avail: Issuing Activity

The flame structure and soot-formation (soot nucleation and growth) properties of axisymmetric laminar coflowing jet diffusion flames were studied experimentally. Test conditions involved acetylene-nitrogen jets burning in coflowing air at atmospheric pressure. Measurements were limited to the axes of the flames and included soot concentrations, soot temperatures, soot structure, major gas species concentrations, radical species (H, OH, and O) concentrations, and gas velocities. The results show that as distance increases along the axes of the flames, detectable soot formation begins when significant H concentrations are present, and ends when acetylene concentrations become small. Species potentially associated with soot oxidation-O2, CO2, H2O, O, and OH-are present throughout the soot-formation region so that soot formation and oxidation proceed at the same time. Strong rates of soot growth compared to soot nucleation early in the soot-formation process, combined with increased rates of soot nucleation and oxidation as soot formation proceeds, causes primary soot particle diameters to reach a maximum relatively early in the soot-formation process. Aggregation of primary soot particles proceeds, however, until the final stages of soot oxidation. Present measurements of soot growth (corrected for soot oxidation) in laminar diffusion flames were consistent with earlier measurements of soot growth in laminar premixed flames and exhibited encouraging agreement with existing hydrogen-abstraction/carbon-addition (HACA) soot growth mechanisms in the literature that were developed based on measurements within laminar premixed flames. Measured primary soot particle nucleation rates in the present laminar diffusion flames also were consistent with corresponding rates measured in laminar premixed flames and yielded a crude correlation in terms of acetylene and H concentrations and the temperature.
Author
*Soot; Laminar Flow; Diffusion Flames; Acetylene*

**20010117716** Brookhaven National Lab., Upton, NY USA
**Homogeneous redox catalysis on CO2 fixation**
Fujita, E.; Feb. 03, 2000; 74p; In English
Report No.(s): DE2000-752156; BNL-67153; No Copyright; Avail: Department of Energy Information Bridge

The twin problems of global warming and diminishing finite fossil fuels resources have stimulated research into CO2 fixation and utilization. Natural photosynthetic CO2 fixation utilizes sunlight and chlorophyll as the energy source and photocatalyst to generate carbohydrates and oxygen from CO2 and H2O. Natural photosynthesis occurring over a few hundred million years has created a vast quantity of fossil fuels that currently fill our current energy needs. Unfortunately, current consumption rates are rapidly depleting our supply of fossil fuels. Even with the advent of fuel farms it is unlikely that natural photosynthesis will be

able to balance the production and use of fuels. It is therefore necessary to explore alternative routes to fuel (and chemical) production and it is likely that artificial photosynthesis will play an increasingly important role in the future.
NTIS
*Carbon Dioxide; Oxidation-Reduction Reactions; Global Warming; Fossil Fuels*

**20010117720** NASA Glenn Research Center, Cleveland, OH USA
**Structure and Soot Properties of Nonbuoyant Ethylene/Air Laminar Jet Diffusion Flames, Appendix I**
Urban, D. L., NASA Glenn Research Center, USA; Yuan, Z.-G., NASA Glenn Research Center, USA; Sunderland, P. B., NASA Glenn Research Center, USA; Linteris, G. T., NASA Johnson Space Center, USA; Voss, J. E., NASA Johnson Space Center, USA; Lin, K.-C., Michigan Univ., USA; Dai, Z., Michigan Univ., USA; Sun, K., Michigan Univ., USA; Faeth, G. M., Michigan Univ., USA; Laminar Soot Processes (LSP); Dec. 15, 2000, pp. 227-242; Repr. from AIAA Journal, v. 36, no. 8, Aug. 1998 p 1346-1360; In English
Contract(s)/Grant(s): NAG3-1245; NAG3-1878; NAG3-2048; Copyright; Avail: Issuing Activity

The structure and soot properties of round, soot-emitting, nonbuoyant, laminar jet diffusion flames are described, based on long-duration (175-230/s) experiments at microgravity carried out on orbit In the Space Shuttle Columbia. Experiments] conditions included ethylene-fueled flames burning in still air at nominal pressures of 50 and 100 kPa and an ambient temperature of 300 K with luminous Annie lengths of 49-64 mm. Measurements included luminous flame shapes using color video imaging, soot concentration (volume fraction) distributions using deconvoluted laser extinction imaging, soot temperature distributions using deconvoluted multiline emission imaging, gas temperature distributions at fuel-lean (plume) conditions using thermocouple probes, not structure distributions using thermophoretic sampling and analysis by transmission electron microscopy, and flame radiation using a radiometer. The present flames were larger, and emitted soot men readily, than comparable observed during ground-based microgravity experiments due to closer approach to steady conditions resulting from the longer test times and the reduced gravitational disturbances of the space-based experiments.
Author
*Jet Flow; Diffusion Flames; Ethylene; Soot; Microgravity*

**20010117721** Michigan Univ., Dept. of Aerospace Engineering, Ann Arbor, MI USA
**Structure of Soot Growth Region of Laminar Premixed Methane/Oxygen Flames, Appendix B**
Xu, F., Michigan Univ., USA; Faeth, G. M., Michigan Univ., USA; Laminar Soot Processes (LSP); Dec. 15, 2000; ISSN 0010-2180, pp. 88-99; Repr. from Combustion and Flame (Elsevier Science, Inc.), v. 121, 2000 p 640-650; In English
Contract(s)/Grant(s): NAG3-1245; NAG3-1878; NAG3-2048; Copyright; Avail: Issuing Activity

The structure of the soot growth region of laminar premixed methane/oxygen flames (fuel-equivalence ratios of 1.60 - 2.77) was studied both experimentally and computationally. Measurements were carried out in flames stabilized on a flat flame burner operated at standard temperature and pressure, and included velocities by laser velocimetry, soot volume fractions by laser extinction, soot temperatures by multiline emission, gas temperatures (where soot was absent) by corrected fine-wire thermocouples, major gas species concentrations by sampling and gas chromatography, and hydrogen atom concentrations by the Li/LiOH technique in conjunction with atomic absorption to find the proportion of free lithium in the flames. The measured concentrations of major gas species were in reasonably good agreement with predictions based on the detailed mechanisms of Leung and Lindstedt, and Frenklach and coworkers. The measurements also confirmed predictions of both these mechanisms that H-atom concentrations are in local thermodynamic equilibrium throughout the soot growth region even through the concentrations of major gas species are not. Thus, present findings support recent evaluations of the hydrogen-abstraction/carbon-addition (HACA) soot growth mechanism in similar flames, where the approximation that H-atom concentrations were in local thermodynamic equilibrium was adopted, based on predictions using the two mechanisms, due to the absence of direct H-atom concentration measurements.
Author
*Soot; Premixed Flames; Methane; Oxygen; Lithium; Hydrogen Atoms*

**20010117722** Michigan Univ., Dept. of Aerospace Engineering, Ann Arbor, MI USA
**Structure of Laminar Permanently Blue, Opposed-Jet Ethylene-Fueled Diffusion Flames, Appendix E**
Lin, K.-C., Michigan Univ., USA; Faeth, G. M., Michigan Univ., USA; Laminar Soot Processes (LSP); Dec. 15, 2000; ISSN 0010-2180, pp. 159-172; Repr. from Combustion and Flame (Elsevier Science, Inc.), v. 115, 1998 p 468-480; In English
Contract(s)/Grant(s): N00014-93-0321; NAG3-1245; NAG3-2048; Copyright; Avail: Issuing Activity

The structure and state relationships of laminar soot-free (permanently blue) ethylene-fueled diffusion flames at various strain rates were studied both experimentally and computationally using an opposed-jet configuration. Measurements of gas

velocities, temperatures, and compositions were carried out along the stagnation stream line. Corresponding predictions of flame structure were obtained, based on numerical simulations using several contemporary reaction mechanisms for methane oxidation. Flame conditions studied included ethylene-fueled opposed-jet diffusion flames having stoichiometric mixture fractions of 0.7 with measurements involving strain rates of 60-240/s and predictions involving strain rates of 0-1140/s at normal temperature and pressure. It was found that measured major gas species concentrations and temperature distributions were in reasonably good agreement with predictions using mechanisms due to GRI-Mech and Peters and that effects of preferential diffusion significantly influence flame structure even when reactant mass diffusivities are similar. Oxygen leakage to fuel-rich conditions and carbon monoxide leakage to fuel-lean conditions both increased as strain rates increased. Furthermore, increased strain rates caused increased fuel concentrations near the flame sheet, decreased peak gas temperatures, and decreased concentrations of carbon dioxide and water vapor throughout the flames. State relationships for major gas species and gas temperatures were found to exist over a broad range of strain rates, providing potential for significant computational simplifications for modeling purposes in some instances.
Author
*Laminar Flow; Jet Flow; Diffusion Flames; Ethylene; Gas Temperature; Gas Composition*

**20010117737** Georgia Univ., Athens, GA USA
**Relativistic and Correlation Effects in CuH, AgH and AuH: Comparison of Various Relativistic Methods**
Collins, Charlene L., Georgia Univ., USA; Dyall, Kenneth G., NASA Ames Research Center, USA; Schaefer, Henry F., III, Georgia Univ., USA; Jun. 10, 1994; 2p; In English; Submitted to the Journal of Chemical Physics
Contract(s)/Grant(s): RTOP 232-01-04; No Copyright; Avail: Issuing Activity; Abstract Only

The effects of relativity on the bond lengths, dissociation energies, and harmonic vibrational frequencies of the 1Epsilon(+) electronic ground states of the group IB hydrides CuH, AgH and AuH have been evaluated with a variety of ab initio methods. These properties were investigated with moderately-sized basis sets at the self-consistent field Hartree Fock (SCF HF) level and with second-order Moller-Plesset (MP2) perturbation theory for electron correlation. Comparisons were made between all-electron results using the nonrelativistic Hamiltonian, perturbation theory (PT) at first-order with only the one-electron non-fine structure terms of the Breit-Pauli Hamiltonian, the spin-free Douglas-Kroll (DK) transformed Dirac Hamiltonian and the untransformed Dirac Hamiltonian, and results using two sets of relativistic effective core potentials (RECPs). The expected trends of bond length decrease, dissociation energy increase and harmonic frequency increase with both relativity and correlation are found. Both sets of RECPs are shown to give good results, if accompanied by a reasonable basis set. The DK method is demonstrated to be an inexpensive, reliable approximation to the DHF method.
Author
*Hydrides; Copper; Gold; Silver; Relativistic Effects; Dissociation; Electron States; Perturbation Theory; Hartree Approximation*

**20010117739** NASA Ames Research Center, Compuitational Chemistry Branch, Moffett Field, CA USA
**The Low-Lying Electronic States of Mg2(+)**
Ricca, Alessandra, NASA Ames Research Center, USA; Bauschlicher, Charles W., Jr., NASA Ames Research Center, USA; Apr. 22, 1994; 1p; In English; T be published in Chemical Physical Letters
Contract(s)/Grant(s): RTOP 323-02-04; No Copyright; Avail: Issuing Activity; Abstract Only

The low-lying doublet and quartet states of Mg+ have been studied using a multireference configuration interaction approach. The effect of inner-shell correlation has been included using the core-polarization potential method. The computed spectroscopic constants, lifetimes, and oscillator strengths should help resolve the difference between the recent experiments and previous theoretical calculations.
Author
*Magnesium; Configuration Interaction; Electron States*

**20010117864** Michigan Univ., Dept. of Aerospace Engineering, Ann Arbor, MI USA
**State Relationships of Laminar Permanently-Blue Opposed-Jet Hydrocarbon-Fueled Diffusion Flames, Appendix G**
Lin, K.-C., Michigan Univ., USA; Faeth, G. M., Michigan Univ., USA; Laminar Soot Processes (LSP); Dec. 15, 2000, pp. 181-208; Repr. from Environ. Comb. Tech. (Overseas Publishers Association), v. 1 p 53-79; In English
Contract(s)/Grant(s): N00014-93-0321; NAG3-1245; NAG3-2048; Copyright; Avail: Issuing Activity

The structure and state relationships of laminar soot-free (permanently-blue) diffusion flames at various strain rates were studied experimentally using an opposed-jet configuration, motivated by the importance of soot-free hydrocarbon-fueled diffusion flames for many practical applications. Measurements of gas velocities, temperatures and compositions were carried out along the stagnation stream line. Flame conditions studied included propylene- and 1,3-butadiene-fueled opposed-jet

diffusion flames having a stoichiometric mixture fractions of 0.7 and strain rates of 60-240/s at normal temperature and pressure. It was found that oxygen leakage to fuel-rich conditions and carbon monoxide leakage to fuel-lean conditions both increased as strain rates increased. Furthermore, increased strain rates caused increased fuel concentrations near the flame sheet decreased peak gas temperatures, and decreased concentrations of carbon dioxide and water vapor throughout the flames. State relationships for major gas species and gas temperatures for these flames were found to exist over broad ranges of strain rates. In addition, current measurements, as well as previous measurements and predictions of ethylene-fueled permanently-blue diffusion flames, all having a stoichiometric mixture fraction of 0.7, were combined to establish generalized state relationships for permanently-blue diffusion flames for this stoichiometric mixture fraction. The combined measurements and predictions support relatively universal generalized state relationships for N2, CO2, H2O and fuel over a broad range of strain rates and fuel types. State relationships for O2 in the fuel-rich region, and for CO in the fuel-lean region, however, are functions of strain rate and fuel type. State relationships for H2 and temperature exhibit less universality, mainly due to the increased experimental uncertainties for these variables. The existence of state relationships for soot-free hydrocarbon-fueled diffusion flames provides potential for significant computational simplifications for modeling purposes in many instances, allowing for effects of finite-rate chemistry while avoiding time-consuming computations of Arrhenius expressions.
Author
*Diffusion Flames; Jet Flow; Laminar Flow; Hydrocarbons; Strain Rate*

**20010117871** Federal Energy Technology Center, Morgantown, WV USA
**Organic-Contaminant Destruction Unit Eco Logic Process Gas Phase Chemical Reduction**
Jun. 17, 1998; 106p; In English
Report No.(s): DE2000-759873; DE-AR21-96MC33091-03; No Copyright; Avail: Department of Energy Information Bridge

This report describes the Eco Logic Process and discusses the procedures and results of a pilot-scale treatability study on explosives in shell casings. The study was conducted as part of a contract which was awarded to Science Applications International Corporation (SAIC) and Eco Logic by the Department of Energy's Federal Energy Technology Center (FETC) in Morgantown, West Virginia to conduct treatability studies on complex hazardous wastes, energetic and low level mixed wastes. The US Army currently decontaminates spent shell casings using a bailout or high pressure wash process that removes a large amount of the propellant from the casing but not enough to allow recycle of the entire casing intact; the US Army currently projects the use of a metal parts furnace to completely decontaminate the shell casings. Use of the Eco Logic Process to decontaminate the shell casings would allow the shell casing to be reused intact. In addition to explosives commonly used by the Army such as TNT and Composition B, ARDEC personnel also were interested in the decontamination of shell casings with a residual of the propellant Yellow D which is a common energetic in artillery shell casings used by the Navy. A series of treatability tests on neat samples of explosive as well as shell casings containing each explosive were performed between June 9 and June 20, 1997 at the US Army's Edgewood Research Development, Engineering Center (ERDEC) toxic test chamber facility located at Aberdeen Proving Ground, Maryland, including a 2 gram neat sample of TNT and 10 gram samples of TNT, composition B and Yellow D to determine optimal treatment conditions for each explosive followed by two tests on washed shell casings containing trace amounts of TNT and a total of six tests, two each on shell casings lined with 10 grams of TNT, composition B and Yellow D.
NTIS
*Decontamination; Destruction; Waste Management; Explosives*

**20010118266** California Univ., Lawrence Berkeley Lab., Berkeley, CA USA
**Ultrafast infrared studies of chemical reaction dynamics in room-temperature liquids**
Yang, H.; Nov. 01, 1999; 160p; In English
Report No.(s): DE2000-760337; LBNL-44634; No Copyright; Avail: Department of Energy Information Bridge, Microfiche

Femtosecond infrared spectroscopy provides sufficient spectral and temporal resolution to support a detailed investigation of the early events of a photochemical reaction. Previously unreported transient species that arise as intermediates during the course of a reaction may have lifetimes that are too short for conventional characterization. For these species, quantum-mechanical (density functional theoretical and 'ab initio') electronic structure calculations provide invaluable insight into chemical properties including molecular structure and energetic. With the combination of experimental and theoretical results, it is possible to assemble a comprehensive picture of the reaction dynamics of a system that is intricately influenced by the surrounding solvent molecules.
NTIS
*Reaction Kinetics; Photochemical Reactions*

**20010118528** Brookhaven National Lab., Upton, NY USA

**Advanced dielectric continuum models of solvation, their connection to microscopic solvent models, and application to electron transfer reactions**

Rostov,; Basilevsky,; Newton,; Jun. 22, 2000; 20p; In English

Report No.(s): DE2000-759012; BNL-66707; No Copyright; Avail: Department of Energy Information Bridge

Some recent advances in dielectric continuum models for static and dynamic aspects of molecular solvation are discussed, and connections with molecular-level solvent models are noted. The traditional Born-Onsager-Kirkwood (BKO) model is compared to a more flexible model (the so-called frequency-resolved cavity model (FRCM)) which assigns distinct inner and outer solute cavities in accommodating, respectively, the inertialess (optical) and inertial solvent response. Sample calculations of solvent reorganization energy ((lambda)(sub s)) are presented for various thermal and optical electron transfer (ET) processes, based on self-consistent reaction field models using molecular orbital (MO) or configuration interaction (CI) solvent wave functions.

NTIS

*Dielectrics; Electron Transfer; Continuum Modeling*

**20010118529** Brookhaven National Lab., Upton, NY USA

**Chemistry of SO2 on model metal and oxide catalysts: Photoemission and XANES studies**

Rodriguez,; Jirsak,; Chaturvedi,; Hrbek,; Freitag,; Jul. 09, 2000; 6p; In English

Report No.(s): DE2000-759011; BNL-66705; No Copyright; Avail: Department of Energy Information Bridge

High-resolution synchrotron based photoemission and x-ray absorption spectroscopy have been used to study the interaction of SO2 with a series of metals and oxides. The chemistry of SO2 on metal surfaces is rich. At low coverages, the molecule fully decomposes into atomic S and O. At large coverages, the formation of SO3 and SO4 takes place. The following sequence was found for the reactivity of the metals towards SO2: Pt (approx) Rh < Ru < Mo << Zn, Sn, Cs. Alloying can be useful for reducing the chemical affinity of a metal for SO2 and controlling S poisoning. Pd atoms bonded to Rh and Pt atoms bonded to Sn interact weakly with SO2. In general, SO2 mainly reacts with the O centers of metal oxides. SO4 is formed on CeO2 and SO3 on ZnO. On these systems there is no decomposition of SO2. Dissociation of the molecule is observed after introducing a large amount of Ce(sup 3+) sites in ceria, or after depositing Cu or alkali metals on the oxide surfaces. These promote the catalytic activity of the oxides during the destruction of SO2.

NTIS

*Absorption Spectroscopy; Catalytic Activity; Dissociation; X Ray Spectroscopy; Sulfur Dioxides*

**20010118914** Illinois Univ., Urbana-Champaign, IL USA

**Electrohydraulic Valve-trains for Direct Injection Compression Ignition Careless Engine Operations** ***Final Report***

Tsao, T. C.; Tai, C.; Stubbs, A.; Hanson, A.; Apr. 25, 2000; 37p; In English

Report No.(s): DE2000-760873; No Copyright; Avail: Department of Energy Information Bridge

Most existing variable-timing systems, which perform a camshaft phase shift or a switch to another cam lobe profile, offer measurable improvements at some engine operating points. A microprocessor controlled careless valvetrain, which continuously adjusts the parameters of valve motion with changing operating conditions, offers much more flexibility and potential benefits as they allow more complete optimization of engine events over the entire operating speed range. However, such devices can be complex, bulky, and relatively expensive, so their applications tend to be limited. The goal of this project is to investigate the technical challenges, and develop the enabling valve design and control capability for the careless operation of small compression ignition direct injection (CIDI) engines. In this project the feasibility of such type of valvetrain has been investigated. The operation of the system to fire a single cylinder in a careless 2.0 liter 4 cylinder S1 engine has been demonstrated with wide opened throttle. Groundwork on analytical modeling and initial experimental testing has been conducted to address some of the known critical issues and discover new technical challenges for the electrohydraulic valvetrain. This report presents the results obtained from this Phase I investigation.

NTIS

*Ignition Systems; Fuel Injection; Diesel Engines*

**20010118932** Sandia National Labs., Albuquerque, NM USA

**Fundamental Efficiency Limitations for Low Electron Energy Cathololuminescence**

Seager, C. H.; Tallant, D. R.; Aug. 01, 2000; 6p; In English

Report No.(s): DE2000-761851; SAND2000-1992C; No Copyright; Avail: Department of Energy Information Bridge

The design of field emission displays is severely constrained by the universally poor cathodoluminescence (CL) efficiency of most phosphors at low excitation energies. As part of the effort to understand this phenomenon, the authors have measured the time decay of spectrally-resolved, pulsed CL and photoluminescence (PL) in several phosphors activated by rare earth and transition metal impurities, including Y(sub 2)O(sub 3):Eu, Y(sub 2)SiO(sub 5):Tb, and Zn(sub 2)SiO(sub 4):Mn. Activator concentrations ranged from (approximately)0.25 to 10%. The CL decay curves are always non-linear on a log(CL)-linear(time) plot--i.e. they deviate from first order decay kinetics. These deviations are always more pronounced at short times and larger activator concentrations and are largest at low beam energies where the decay rates are noticeably faster. PL decay is always slower than that seen for CL, but these differences disappear after most of the excited species have decayed. They have also measured the dependence of steady state CL efficiency on beam energy. They find that larger activator concentrations accelerate the drop in CL efficiency seen at low beam energies. These effects are largest for the activators which interact more strongly with the host lattice. While activator-activator interactions are known to limit PL and CL efficiency in most phosphors, the present data suggest that a more insidious version of this mechanism is partly responsible for poor CL efficiency at low beam energies. This enhanced concentration quenching is due to the interaction of nearby excited activators. These interactions can lead to non-radiative activator decay, hence lower steady state CL efficiency. Excited state clustering, which may be caused by the large energy loss rate of low energy primary electrons, appears to enhance these interactions. In support of this idea, they find that PL decays obtained at high laser pulse energies resemble the non-linear decays seen in the CL data.
NTIS
*Cathodoluminescence; Electron Energy; Excitation; Pulsed Lasers; Transition Metals*

**20010119138** Sandia National Labs., Albuquerque, NM USA
**Development of New Hybrid Organic-Inorganic Materials for Hydrogen Separation Membranes at Sandia National Laboratories**
Loy, D. A.; Jul. 14, 2000; 8p; In English
Report No.(s): DE2000-761835; SAND2000-1888C; No Copyright; Avail: Department of Energy Information Bridge
We have been developing a new class of hybrid organic-inorganic materials as candidates for hydrogen separation membranes. This type of material shows significant promise for use in membranes due to good thermal and chemical stability, and ease of processing into defect-free thin films. These polysilsesquioxanes are easily prepared from the hydrolysis and condensation of organotrialkoxysilane monomers with reactive organic functionalities, such as maleimide and methacryloxypropyl groups, that are stable to sol-gel conditions but can be 'cured' thermally or chemically as a membrane. Introducing highly dispersed catalysts into these materials was realized through the pre-coordination of palladium to a silane monomer before the polymerization. Finally, a new route to inorganic membranes from polysilsesquioxanes with thermally cleavable organic substituents was investigated. This new method circumvents some of the difficulties associated with sol-gel fabrication of silica membranes by using well-defined, processible precursors.
NTIS
*Fabrication; Hydrogen; Membranes; Organic Materials; Polymerization*

**20010119226** Michigan Univ., Dept. of Aerospace Engineering, Ann Arbor, MI USA
**Structure of Laminar Permanently Blue, Opposed-Jet Ethylene-Fueled Diffusion Flames**
Lin, K.-C., Michigan Univ., USA; Faeth, G. M., Michigan Univ., USA; Laminar Soot Processes (LSP); Dec. 15, 2000; ISSN 0010-2180, pp. 75-87; Repr. from Combustion and Flame (Elsevier Science, Inc.), v. 115, 1998 p 468-480; In English
Contract(s)/Grant(s): N00014-93-0321; NAG3-1245; NAG3-2048; Copyright; Avail: Issuing Activity
The structure and state relationships of laminar soot-free (permanently blue) ethylene-fueled diffusion flames at various strain rates were studied both experimentally and computationally using an opposed-jet configuration. Measurements of gas velocities, temperatures, and compositions were carried out along the stagnation stream line. Corresponding predictions of flame structure were obtained, based on numerical simulations using several contemporary reaction mechanisms for methane oxidation. Flame conditions studied included ethylene-fueled opposed-jet diffusion flames having stoichiometric mixture fractions of 0.7 with measurements involving strain rates of 60-240/s and predictions involving strain rates of 0-1140/s at normal temperature and pressure. It was found that measured major gas species concentrations and temperature distributions were in reasonably good agreement with predictions using mechanisms due to GRI-Mech and Peters and that effects of preferential diffusion significantly influence flame structure even when reactant mass diffusivities are similar. Oxygen leakage to fuel-rich conditions and carbon monoxide leakage to fuel-lean conditions both increased as strain rates increased. Furthermore, increased strain rates caused increased fuel concentrations near the flame sheet, decreased peak gas temperatures, and decreased concentrations of carbon dioxide and water vapor throughout the flames. State relationships for major gas species and gas temperatures were found to exist

over a broad range of strain rates, providing potential for significant computational simplifications for modeling purposes in some instances.
Author
*Laminar Flow; Jet Flow; Diffusion Flames; Ethylene; Gas Temperature; Gas Composition; Velocity Measurement*

**20010119233** Air Force Inst. of Tech., Wright-Patterson AFB, OH USA
**Novel Quaso-Phase-Matched Devices in Periodically Pole Lithium Niobate**
Russell, Stephen M.; May 2001; 108p; In English; Original contains color images
Report No.(s): AD-A395068; No Copyright; Avail: CASI; A06, Hardcopy; A02, Microfiche

The ability to engineer novel quasi-phase-matched (QPM) structures in bulk periodically poled ferroelectric crystals has led to the development of a wide variety of innovative QPM devices. Lithium niobate has been the material of choice in many of these devices due to its large nonlinear coefficient (d33 ^ 27 pm/V), low cost, and wide availability. However, its large coercive field (^ 2 1 kV/mm) has limited fabrication of periodically poled lithium niobate (PPLN) samples to a maximum thickness of 1 mm. This crystal aperture limitation combined with the low damage fluence of lithium niobate has restricted pulsed PPLN systems to low energy operation. In this thesis, we circumvent these limitations through innovative QPM grating designs and pumping schemes. In this work we report the design, fabrication, and demonstration of three novel PPLN devices. The first device generated broadband mid-infrared radiation by using highly elliptical beams to pump PPLN crystals with a fan-out grating design. The signal and idler beams were spatially and angelarly chirped while covering spectral bands as large as 3900/cu cm. The endfaces of the crystals were polished plane-parallel to force the system to operate in a monolithic optical parametric oscillator configuration. The second device used stacks of segmented multi-grating PPLN crystals to produce large signal energies with excellent beam quality. Signal energies as high as 33 mJ were generated in uncoated lithium niobate. In pursuit of the design for this system, we also explored several other unique QPM structures. The final device reported in this thesis is a widely tunable two-frequency injection-seeded optical parametric generator (OPG) . In this two-stage system the output from the first stage was filtered to generate two narrow spectral lines. These lines were then used to seed the OPG process in the second stage.
DTIC
*Crystals; Lithium Niobates; Ferroelectricity; Parametric Amplifiers*

**20010119240** Air Force Inst. of Tech., Wright-Patterson AFB, OH USA
**Study in Calcium Carbonate Crystal Formation at the Air/Water Interface in the Presence of a Magnetic Field**
Paschke, Timothy M.; Sep. 17, 2001; 14p; In English
Report No.(s): AD-A395048; No Copyright; Avail: CASI; A03, Hardcopy; A01, Microfiche

Calcium carbonate aggregates as calcite on the surface of a Ca(OH)2 solution exposed to air. We grew these crystals on solution of initial concentration 0.30 mg/L. Our studies show static magnetic field to have no effect on the fractal dimension of these crystals. Fields up to 10 kG parallel to the interface, 2 kG perpendicular to the interface, as well as high gradient were examined. For all conditions fractal dimension was DF = 1.61 t 0.05.
DTIC
*Calcium Carbonates; Air Water Interactions; Crystals; Magnetostatic Fields*

**20010119550** Lawrence Livermore National Lab., Livermore, CA USA
**Distribution of Soluble and Precipitated Iron and Chromium Products Generated by Anodic Dissolution of 316L Stainless Steel and Alloy C-22** ***Final Report***
Estill, J.; Farmer, J.; Gordon, S.; King, K.; Logotetta, L.; Aug. 11, 1999; 17p; In English
Report No.(s): DE2001-10450; UCRL-ID-135289; No Copyright; Avail: Department of Energy Information Bridge

At near neutral pH and at applied potentials above the threshold potential for localized breakdown of the passive film, virtually all of the dissolved chromium appeared to be in the hexavalent oxidation state (Cr(VI)). In acidic environments, such as crevice solutions formed during the crevice corrosion of 316L and C-22 samples in 4 M NaCl, virtually all of the dissolved chromium appeared to be in the trivalent oxidation state (Cr(III)). These general observations appear to be consistent with the Pourbaix diagram for chromium. At high pH and high anodic polarization (pH approximately 8 and 800 mV vs. SHE), the predominate species is believed to be the soluble chromate anion (CrO4(2-)). At the same pH, but lower polarization (pH approximately 8 and 0 mV vs. SHE), the predominate species are believed to be precipitates such as trivalent Cr(OH)3 (center-dot) n(H2O) and hexavalent Cr2O3. In acidified environments such as those found in crevices (pH less than 3), soluble Cr(3+) is expected to form over a wide range of potential extending from 400 mV vs. SHE to approximately 1200 mV vs. SHE. Again, this is consistent with the observations from the creviced samples. In earlier studies by the principal investigator, it has been found that low-level chromium contamination in ground water is usually in the hexavalent oxidation state. In general, dissolved iron measured during

the crevice experiments appears to be Fe(II) in acidic media and Fe(III) in near-neutral and alkaline solutions. In the case of cyclic polarization measurements, the dissolved iron measured at the end of some cyclic polarization measurements with C-22 appeared to be in the Fe(III) state. This is probably due to the high electrochemical potential at which these species were generated during the potential scan. Note that the reversal potential was approximately 1200 mV vs. Ag/AgCl during these scans. These results are also consistent with the corresponding Pourbaix diagrams. For example, in acidic media (pH 0 to 1), Fe(+2) would be expected to form at relatively low potential, with conversion to Fe(+3) at high applied potential (greater than about 700 mV vs. SHE). In neutral to alkaline pH, precipitates of Fe(OH)2, Fe(OH)3, Fe2O3, or F3O4) would be expected, with some hydrolyzed species of Fe(+3) possible.
NTIS
*Chromium; Iron; pH; Alloys; Stainless Steels*

**20010119577** Argonne National Lab., IL USA
**Ordering in classical Coulombic systems**
Schiffer, J. P.; Jan. 22, 1998; 10p; In English
Report No.(s): DE2001-10583; ANL/PHY/CP-95452; No Copyright; Avail: Department of Energy Information Bridge, Microfiche

The author discusses the properties of classical Coulombic matter at low temperatures. It has been well known for some time that infinite Coulombic matter will crystallize in body-centered cubic form when the quantity (Lambda) (the dimensionless ratio of the average two-particle Coulomb energy to the kinetic energy per particle) is larger than (approximately) 175. But the systems of such particles that have been produced in the laboratory in ion traps, or ion beams, are finite with surfaces defined by the boundary conditions that have to be satisfied. This results in ion clouds with sharply defined curved surfaces, and interior structures that show up as a set of concentric layers that are parallel to the outer surface. The ordering does not appear to be cubic, but the charges on each shell exhibit a 'hexatic' pattern of equilateral triangles that is the characteristic of liquid crystals. The curvature of the surfaces prevents the structures on successive shells from interlocking in any simple fashion. This class of structures was first found in simulations and later in experiments.
NTIS
*Kinetic Energy; Coulomb Potential; Crystallization*

**20010119617** Air Force Research Lab., Munitions Directorate, Eglin AFB, FL USA
**Energetic Materials Pyrometry** ***Final Report, Oct. 1996-Oct 1998***
Hopkins, Mark F.; Derniak, Eustace L.; Garcia, John P.; Oct. 1999; 190p; In English; Prepared in cooperation with the University of Arizona, Optical Sciences Center, Tucson, AZ
Contract(s)/Grant(s): Proj-2502
Report No.(s): AD-A395036; AFRL-MN-EG-TR-2001-7066; No Copyright; Avail: CASI; A09, Hardcopy; A02, Microfiche

In this research, a remotely located, high-speed, infrared (IR) camera is used to obtain detailed measurements of the passive radiation from an object in an energetic environment. This radiation information is used to determine both the emissivity and the temperature of the surface of an object. However, before the temperature or emissivity was determined, the functional form of the emissivity was assumed to be an Mth degree polynomial with respect to wavelength dependence. Using a commercial Fourier transform spectrometer, this functional form was verified to accuracy's on the order of 0.1%, to be a polynomial of the second degree. With the advent of large (greater than 128 X 128 pixels), high-speed, IR detector arrays, it has now become possible to realize IR imaging spectrometers that have very high spatial resolution. The IR spectrometer system developed in this research utilized a large detector array to allow multiple spectral images to be formed simultaneously on the image plane, with the information from each spectral image being concurrently collected. In conjunction with the correct emissivity model, this imaging IR spectrometer can determine the temperature of the surface of an object within an energetic environment to within +/- 5 degrees Celsius. These experimentally verified temperature/emissivity maps can then be integrated into the newly developed computer models. This additional information will result in more accurate computer codes for modeling the energetic environment. In turn, this will allow the weapon designer to optimize weapon performance with respect to different materials, geometries and kinetics.
DTIC
*Energetic Particles; Computerized Simulation; Temperature Measurement; Emissivity; Imaging Spectrometers*

**20010119928** Wyoming Univ., Dept. of Chemistry, Laramie, WY USA
**DEPSCoR98: Tandem TGA/MS Studies of Single Propellants** ***Final Report, Apr. 1998-May 2001***
Bohle, David S.; May 2001; 12p; In English
Contract(s)/Grant(s): F49620-98-1-0461; Proj-3484
Report No.(s): AD-A395219; AFRL-SR-BL-TR-01-0513; No Copyright; Avail: CASI; A03, Hardcopy; A01, Microfiche

To prepare new economical HEDM derivatives from the condensation reactions of nitric oxide with organic substrates. Once prepared these derivatives were tested for energy content, thermal stability, and product output upon decomposition. The outcome of these experiments were then used to assess which cations, and conditions, are the best to metathesize with the heavy/dense alkali metals initially isolated. We now have an excellent understanding of what the main products will be from these reactions, and the optimal conditions for their formation. This has proven to be a surprisingly variable reaction, and a variety of products can form from the addition of NO to a given substrate, but the determining variables are the base employed, substrate/base ratio, and the temperature. Nitric oxide pressure is also a likely variable as well, indeed many of the products we have characterized are new because we used ca. 3 atm of NO pressure, whereas prior researchers typically use only 1 atm. These compounds are now being tested at Thiokol for propellant characteristics after having undergone safety tests beforehand.
DTIC
*Composite Materials; Propellants; Thermogravimetry; Nitric Oxide; Mass Spectroscopy*

**20010120023** Argonne National Lab., IL USA
**Recent Advances in the Development of Extraction Chromatographic Materials for the Isolation of Radionuclides from Biological and Environmental Samples**
Dietz, M. L.; Nov. 30, 1998; 9p; In English
Report No.(s): DE2001-10654; ANL/CHM/CP-95681; No Copyright; Avail: Department of Energy Information Bridge
The determination of low levels of radionuclides in environmental and biological samples is often hampered by the complex and variable nature of the samples. One approach to circumventing this problem is to incorporate into the analytical scheme a separation and preconcentration step by which the species of interest can be isolated from the major constituents of the sample. Extraction chromatography (EXC), a form of liquid chromatography in which the stationary phase comprises an extractant or a solution of an extractant in an appropriate diluent coated onto an inert support, provides a simple and efficient means of performing a wide variety of metal ion separations. Recent advances in extractant design, in particular the development of extractants capable of metal ion recognition or of strong complex formation even in acidic media, have substantially improved the utility of the method. For the preconcentration of actinides, for example, an EXC resin consisting of a liquid diphosphonic acid supported on a polymeric substrate has been shown to exhibit extraordinarily strong retention of these elements from acidic chloride media. This resin, together with other related materials, can provide the basis of a number of efficient and flexible schemes for the separation and preconcentration of radionuclides form a variety of samples for subsequent determination.
NTIS
*Isolation; Liquid Chromatography; Radioactive Isotopes*

**20010120024** Argonne National Lab., IL USA
**Solvent Extraction Separation of Trivalent Lanthanide and Actinide Ions Using an Aqueous Aminomethane diphosphonic Acid**
Jensen, M. P.; Oct. 14, 1998; 9p; In English
Report No.(s): DE2001-10653; ANL/CHM/CP-95678; No Copyright; Avail: Department of Energy Information Bridge
The possibility of separating the trivalent lanthanides, represented by EU(3+), and actinides, represented by Cf(3+), using HDEHP in toluene and an aqueous phase containing N-piperidinomethane- 1,1-diphosphotic acid, PMDPA, has been investigated.This modified aqueous phase offers potential advantages over the diethylenetriamine pentaacetic acid based TALSPEAK process because of the improved complexation properties of PMDPA in acidic solutions, and the ability to decompose PMDPA before disposal. Extraction experiments were conducted at 25 C in 2 M NaClO4 between -log (H(+)) 1 and 2. The studies enabled us to derive the aqueous phase speciation, the stability constants of the aqueous complexes, and the Cf/Eu separation factors. Despite the presence of an amino group in PMDPA that should favor the retention of the actinides in the aqueous phase, the Cf/Eu separation factors are near unity under the conditions studied.
NTIS
*Decomposition; Solvent Extraction; Actinide Series*

**20010120025** Argonne National Lab., IL USA
**Co-Adsorption Studies of Hydrogen with Nitrogen in Zeolites**
Eckert, J.; Feb. 17, 1998; 9p; In English
Report No.(s): DE2001-10652; ANL/IPNS/CP-95674; No Copyright; Avail: Department of Energy Information Bridge

The use of co-adsorption studies of N2 with H2 makes it possible to obtain information about adsorption of N2 by monitoring changes in the rotational spectrum of the co-adsorbed H2 molecules. We present such results on N2/H2 in Na-13X.
NTIS
*Adsorption; Hydrogen; Nitrogen*

**20010120026** Argonne National Lab., IL USA
**Adsorption Sites in Zeolites A and X Probed by Competitive Adsorption of H2 with N2 or O2: Implications for N2/O2 Separation**
Eckert, J.; Aug. 31, 1998; 9p; In English
Report No.(s): DE2001-10651; ANL/IPNS/CP-95673; No Copyright; Avail: Department of Energy Information Bridge
We determine details of the adsorption of O2 or N2 in Na(+) and Li(+) exchanged zeolites by way of their effect on coadsorbed H2 molecules using inelastic neutron scattering (INS) techniques. Adsorption site occupancies are deduced with the aid of Monte Carlo simulations. The expected stronger binding of N2 (compared with O2) in LiX is evident in coadsorption spectra of N2 or O2 with H2.
NTIS
*Adsorption; Hydrogen; Inelastic Scattering; Nitrogen; Oxygen*

**20010120027** Argonne National Lab., IL USA
**Status of Cross-Section Data for Gas Production from Vanadium and Al-26 from Silicon Carbide in a D-T Fusion Reactor**
Gomes, I. C.; Aug. 11, 1998; 10p; In English
Report No.(s): DE2001-10650; ANL/TD/CP-95667; No Copyright; Avail: Department of Energy Information Bridge
Current designs of fusion-reactor systems seek to use radiation-resistant, low-activation materials that support long service lifetimes and minimize radioactive-waste problems after decommissioning. Reliable assessment of fusion materials performance requires accurate neutron-reaction cross sections and radioactive-decay constants. The problem areas usually involve cross sections since decay parameters tend to be better known. The present study was motivated by two specific questions: (1) Why are the V-51(n,np) Ti-50 cross section values in the ENDF/B-VI library so large (a gas production issue); (2) How well known are the cross sections associated with producing 7.4 x 10(exp 5) y Al-26 in silicon carbide by the process Si-28(n,np+d) Al-27(n,2n) Al-26 (a long-lived radioactivity issue). The energy range 14-15 MeV of the D-T fusion neutrons is emphasized. Cross-section error bars are needed so that uncertainties in the gas and radioactivity generated over the lifetime of a reactor can be estimated. We address this issue by comparing values obtained from prominent evaluated cross-section libraries. Small differences between independent evaluations indicate that a physical quantity is well known while the opposite signals a problem. Hydrogen from V-51(n,p)Ti-51 and helium from V-51(n,(alpha))Sc-48 are also important sources of gas in vanadium, so they too were examined. We conclude that V-51(n,p)Ti-51 is adequately known but V-51(n,np+d)Ti-50 is not. The status for helium generation data is quite good. Due to recent experimental work, Al-27(n,2n)Al-26 seems to be fairly well known. However, the situation for Si-28(n,np+d)Al-27 remains unsatisfactory.
NTIS
*Aluminum Isotopes; Neutron Cross Sections; Silicon Carbides; Fusion Reactors; Reactor Design*

**20010120030** Argonne National Lab., IL USA
**Surface Area and Chemical Reactivity Characteristics of Uranium Metal Corrosion Products**
Totemeier, T. C.; Feb. 17, 1998; 14p; In English
Report No.(s): DE2001-10646; ANL/ED/CP-95647; No Copyright; Avail: Department of Energy Information Bridge
The results of an initial characterization of hydride-containing corrosion products from uranium metal Zero Power Physics Reactor (ZPPR) fuel plates are presented. Sorption analyses using the Brunauer-Emmett-Teller (BET) method with a Kr adsorbate were performed to measure the specific areas of corrosion product samples. The specific surface areas of the corrosion products varied from 0.66 to 1.01 sq m/g. The reactivity of the products in Ar-9%O(2) and Ar-20%O2 were measured at temperatures between 35 C and 150 C using a thermo-gravimetric analyzer. Ignition of the products occurred at temperatures of 150 C and above. The oxidation rates below ignition were comparable to rates observed for uranium metal.
NTIS
*Corrosion; Reactivity; Uranium; Zero Power Reactors*

**20010120032** Argonne National Lab., IL USA

**Interactions of Multiphase Hydrodynamics, Droplet Evaporation, and Chemical Kinetics in FCC Riser Reactors**

Chang, S. L.; Feb. 17, 1998; 12p; In English

Report No.(s): DE2001-10644; ANL/ES/CP-95641; No Copyright; Avail: Department of Energy Information Bridge

A computational fluid dynamics (CFD) computer code, ICRKFLO, has been developed for flow simulation of fluid catalytic cracking (FCC) riser reactors, which convert crude oil into gasoline and other valuable products. The FCC flow, especially in the entry region, is a three-phase reacting flow including hot catalyst particles, inert lift gas, and feed oil droplets. The impact of the hydrodynamics processes of heat transfer, droplet evaporation, and mixing on the chemical kinetics or riser performance can be significant. ICRKFLO was used to evaluate the impact of these processes on the performance of an advanced FCC unit. The code solves for major flow properties of all three phases in an FCC riser, with models governing the transport of catalyst particles and feed oil droplet, the vaporization of the feed oil droplets, the cracking of the oil vapor, and the formation and deposition of coke on particles. First, the code was validated against available test data of a pilot-scale FCC unit. Then, flow calculations for the FCC unit were performed. Computational results indicate that the heat transfer and droplet vaporization processes have a significant impact on the performance of a pilot-scale FCC unit. The impact is expected to be even greater on commercial scale units.

NTIS

*Computational Fluid Dynamics; Computer Programs; Cracking (Chemical Engineering); Drops (Liquids); Flow Characteristics; Risers*

**20010120036** Argonne National Lab., IL USA

**Oxidation kinetics of reaction products formed in uranium metal corrosion**

Totemeier, T. C.; Apr. 22, 1998; 11p; In English

Report No.(s): DE2001-10623; ANL/ED/CP-95535; No Copyright; Avail: Department of Energy Information Bridge, Microfiche

The oxidation behavior of uranium metal ZPPR fuel corrosion products in environments of Ar-4%O2 and Ar-20%O2 were studied using thermo-gravimetric analysis (TGA). These tests were performed to extend earlier work in this area specifically, to assess plate-to-plate variations in corrosion product properties and the effect of oxygen concentration on oxidation behavior. The corrosion products from two relatively severely corroded plates were similar, while the products from a relatively intact plate were not reactive. Oxygen concentration strongly affected the burning rate of reactive products, but had little effect on low-temperature oxidation rates.

NTIS

*Fuel Corrosion; Reaction Kinetics; Uranium*

**20010120074** Argonne National Lab., IL USA

**Electronic structure studies of the interaction of water with a Cu (100) surface**

Zapol, P.; Naleway, C. A.; Deutsch, P. W.; Curtiss, L. A.; Aug. 11, 2000; 13p; In English

Report No.(s): DE2000-761266; ANL/CHM/CP-102583; No Copyright; Avail: Department of Energy Information Bridge

The results of a density functional study of the chemisorption of water on a Cu(100) surface are presented. Both atomic cluster and periodic supercell models of the surface were used in the investigation. From the cluster studies a single water molecule is bound by about 0.6 eV to the surface and is in an on-top site. The addition of a second water molecule in a site adjacent to the first.

NTIS

*Electronic Structure; Water; Copper; Surface Reactions; Chemisorption*

**20010120088** Sandia National Labs., Albuquerque, NM USA

**Causes of Color in Minerals and Gemstones**

Hlava, P. F.; Jun. 07, 2000; 5p; In English

Report No.(s): DE2000-760776; SAND2000-1441C; No Copyright; Avail: Department of Energy Information Bridge

The colors that one sees when looking at a mineral or gemstone are due to the response of that persons eye to the energies of the light, the emission spectrum of the illumination, and, most importantly, physical phenomena in the material that cause some colors to be absorbed while others are undisturbed or enhanced. It is beyond the scope of this talk to do more than touch on the physiology of the eye that allows us to see colors. Likewise, we will not dwell on the emission spectra of various light sources.

Rather, we will concentrate on the various ways in which materials, especially minerals and their heights of perfection - gemstones, produce color from white light.
NTIS
*Color; Light Emission; Physical Factors; Minerals*

**20010120093** Argonne National Lab., IL USA
**In-situ imaging of charge carriers in an electrochemical cell**
Gerald, R. E.; Jan. 30, 1998; 12p; In English
Report No.(s): DE2001-10617; ANL/CMT/CP-95511; No Copyright; Avail: Department of Energy Information Bridge, Microfiche

A toroid cavity nuclear magnetic resonance (NMR) detector capable of quantitatively recording radial concentration profiles, diffusion constants, displacements of charge carriers, and radial profiles of spin-lattice relaxation time constants was employed to investigate the charge/discharge cycle of a solid-state electrochemical cell. One-dimensional radial concentration profiles (1D-images) of ions solvated in a polyethylene oxide matrix were recorded by F-19 and Li-7 NMR for several cells. A sequence of F-19 NMR images, recorded at different stages of cell polarization, revealed the evolution of a region of the polymer depleted of charge carriers. From these images it is possible to extract the transference number for the Li+ ion. Spatially localized diffusion coefficients and spin-lattice relaxation time constants can be measured simultaneously for the ions in the polymer electrolyte by a spin-labeling method that employs the radial B(sub 1)-field gradient of the toroid cavity. A spatial resolution of 7 (micro)m near the working electrode was achieved with a gradient strength of 800 gauss/cm. With this apparatus, it is also possible to investigate novel intercalation anode materials for lithium ion storage. These materials are coated onto the working electrode in a thin film. The penetration depth of lithium cations in these films can be imaged at different times in the charge/discharge cycle of the battery.
NTIS
*Charge Carriers; Electrochemical Cells; Cavity Resonators; Toroids*

**20010120112** Clark-Atlanta Univ., GA USA
**Study of the Sub- and Supercritical Behavior of Fuel Droplets** ***Final Report, 3 Jan. 1998-31 May 2001***
Yeboah, Yaw D.; Aug. 31, 2001; 57p; In English
Contract(s)/Grant(s): F49620-98-1-0373; Proj-2308
Report No.(s): AD-A395049; AFRL-SR-BL-TR-01-0509; No Copyright; Avail: CASI; A04, Hardcopy; A01, Microfiche

A study of the droplet gasification and combustion characteristics of hydrocarbon fuel droplets was conducted at sub- and supercritical. The experimental setup provided quiescent and convective environments under supercritical pressure and temperature conditions. The droplet combustion experiment hardware consisted of: a liquid pressurizing and transfer system; a high pressure and temperature combustion chamber; a droplet formation, deployment and ignition system; and a high speed CCD imaging system. The gasification and combustion characteristics of droplets of several hydrocarbons under quiescent environments were studied. Specifically, the mass emission rates and combustion characteristics of 1.5-mm-diameter suspended droplets of a series of hydrocarbons ranging from hexane (C6) to tetradecane (Cl4) were measured at sub- and supercritical pressures and temperatures using the high-speed image system. The images of droplet gasification and combustion revealed interesting phenomena and provided better understanding of the droplet behavior in sub- and supercritical pressure and temperature environments.
DTIC
*Drops (Liquids); Hydrocarbon Fuels; Supercritical Pressures; Combustion Physics*

**20010120120** Calspan Field Services, Inc., AEDC Div., Arnold AFS, TN USA
**Ozone Flow Tagging Scheme for Air Inlet Testing** ***Final Report, 6 Sep. 1996-31 Dec. 1999***
Debarber, Peter A.; Dec. 1999; 18p; In English; Original contains color images
Contract(s)/Grant(s): F40600-96-C-0002
Report No.(s): AD-A395004; No Copyright; Avail: CASI; A03, Hardcopy; A01, Microfiche

Two separately tunable, narrowband excimer lasers were used to photo-dissociate O2. The O-atom photoproducts rapidly react with ambient O2 to form O3, and thus marked a volume of air with a line of ozone. After a fixed time delay, a second laser measured progress of the tagged volume of air by photodissociating ozone, and monitoring the vibrationally excited O2 photoproduct by planar laser induced fluorescence (PLIF). The spatial displacement of the tagged line was used to measure the

velocity in a time-of-flight fashion. Because of ozone's rapid formation (approx. 20 microsecs) and long chemical lifetime (approx. 2 s), a broad range of velocity measurements are possible.
DTIC
*Flow; Ozone; Air Intakes; Velocity Measurement; Flow Characteristics; Air Flow*

**20010120121** Emory Univ., Dept. of Chemistry, Atlanta, GA USA
**Theoretical Studies of Gas Phase Elementary Reactions** ***Final Report, 15 Feb. 1998-14 Feb 2001***
Morokuma, Keiji; Aug. 17, 2001; 19p; In English
Contract(s)/Grant(s): F49620-93-1-0063; Proj-2303
Report No.(s): AD-A395002; AFRL-SR-BL-TR-01-0520; No Copyright; Avail: CASI; A03, Hardcopy; A01, Microfiche
This final technical report begins with the objective, followed by detailed reports on new accomplishments and new findings obtained in the project. They are presented in six sections: (A) Potential Energy Surfaces of Ion-Molecule Reactions, (B) Potential Energy Surfaces of Ions, (C) Potential Energy Surfaces for Photochemical Reactions and Nonadiabatic Processes, (D) Potential Energy Surfaces of Open-Shell Molecules, (E) Dynamics and Kinetics in the Ground Electronic State, and (F) Potential Energy Surfaces for the Dynamics of Chemical Laser Systems. The Publication List and Interactions/Transactions conclude the report.
DTIC
*Phase Transformations; Gases; Chemical Reactions; Numerical Analysis; Vapor Phases*

**20010120122** Materials Research Society, Warrendale, PA USA
**Materials Research Society Symposium Proceedings Volume 635. Anisotropic Nanoparticles - Synthesis, Characterization and Applications**
Lyon, L. A.; Stranick, Stephan J.; Keating, Christine D.; Searson, Peter C.; Nov. 2000; 212p; In English; Pres: Symposium, 27-29 Nov 2000, Boston, MA. For individual articles, see
Report No.(s): AD-A395000; No Copyright; Avail: CASI; A10, Hardcopy; A03, Microfiche
This volume contains a series of papers originally presented at Symposium C, "Anisotropic Nanoparticles Synthesis, Characterization and Applications," at the 2000 MRS Fall Meeting in Boston, Massachusetts. In addition to support from the Materials Research Society, this symposium was co-sponsored by NIST, NSF-DMR, and ONR, with corporate support from SurroMed, Inc. and Digital Instruments. The purpose of this symposium was to review the broad multidisciplinary activities in this rapidly growing area. The properties of nanoscale materials are derived from the additional dimensional and compositional degrees of freedom that arise when the physical dimensions of the system are smaller than a characteristic length scale of interest. Anisotropic particles can exhibit novel and enhanced properties compared to isotropic spherical particles. This symposium focused on all aspects of anisotropy on the nanoscale, including anisotropy resulting from shape (e.g. rods, nanowires, biomolecules), juxtaposition of different materials (e.g. nanoparticle heterodimers), compositional heterogeneity (e.g. core-shell particles, multi layer nanowires) or the intrinsic directionality of a probe (e.g. electromagnetism). in addition to the synthesis of new anisotropic materials, the ability to address individual nanostructures (e.g. electrically, magnetically, or optically) is important for technological applications such as nanoelectronics and biomedical engineering.
DTIC
*Anisotropy; Nanotechnology; Synthesis (Chemistry)*

**20010120265** Argonne National Lab., IL USA
**Synergistic effects in the extraction of metal ions by mixtures of dialkylphosphoric acids and substituted crown ethers**
Chiarizia, R.; Dec. 03, 1998; 9p; In English
Report No.(s): DE2001-10655; ANL/CHM/CP-95682; No Copyright; Avail: Department of Energy Information Bridge
The extraction of alkaline earth cations from weakly acidic solutions by three dialkylphosphoric acids and various isomers of dicyclohexano-18-crown-6, both alone and in combination in toluene solutions, has been examined to determine the effect of both the crown ether stereochemistry and the structure of the organophilic anion on the magnitude of the synergistic effects. The synergistic effects have been found to differ considerably among the crown ether isomers and to vary with the extent of alkyl chain branching in the dialkylphosphoric acid. Attempts to correlate the synergistic effects with ligand strain energies from molecular mechanics calculations are described.
NTIS
*Chain Reactions (Chemistry); Ethers; Stereochemistry; Alkaline Earth Metals; Cations; Alkyl Compounds; Ion Extraction*

**20010120266** Argonne National Lab., IL USA

**Imaging diffusion with non-uniform B(sub 1) gradients**

Woelk, K.; Jan. 30, 1998; 12p; In English

Report No.(s): DE2001-10616; ANL/CMT/CP-95510; No Copyright; Avail: Department of Energy Information Bridge, Microfiche

Rotating-frame imaging with the mathematically well-defined, non-constant magnetic field gradient of toroid cavity detectors represents a new technique to evaluate diffusion in solids, fluids or mixed-phase systems. While conventional NMR methods to measure diffusion utilize constant magnetic field gradients and, therefore, constant k-space wave numbers across the sample volume, the hyperbolic B(sub 1) fields of toroid cavity detectors exhibit large ranges of wave numbers radially distributed around the central conductor. As a consequence, signal amplitudes decay depending on the radial distance from the center axis of the torus. Applying a numerical finite-difference procedure to solve partial differential transport equations makes it possible not only to determine diffusion in toroid detectors to a high precision but also to include and accurately reproduce transport phenomena at or through singularities, such as phase transitions, membranes or impermeable boundaries.

NTIS

*Diffusion; Magnetic Fields; Imaging Techniques*

**20010120485** Illinois Univ. at Urbana-Champaign, IL USA

**Sixth Conference on Molecular Reaction Dynamics in Condensed Matter** ***Final Report, 1 Jul. 2000 - 30 Jun. 2001***

Dlott, Dana D.; Jun. 2001; 8p; In English; Sixth Symposium on Molecular Reaction Dynamics in Condensed Matter, held in Laguna Beach, CA, on 28 Feb-3 Mar 2001

Contract(s)/Grant(s): F49620-00-1-0332; AF Proj. 2303

Report No.(s): AD-A395019; AFRL-SR-BL-TR-01-0519; No Copyright; Avail: CASI; A02, Hardcopy; A01, Microfiche

The Sixth Conference on Molecular Reaction Dynamics in Condensed Matter was held Feb. 28 - Mar 3 at the Hotel La Casa del Camino in Laguna Beach, CA, sponsored by AFOSR and UC Irvine, and organized by D. Dlott and A. Apkarian. There were 39 attendees, including professors, graduate students, postdoctoral fellows, technical staff members from national laboratories and a representative from AFOSR. 34 talks were presented. There were 21 invited talks (50 minutes with discussion) and 9 contributed talks (25 minutes with discussion). Lively discussion continued until the wee hours. The conference website is: http://dlottgroup.scs.uiuc.edu/moldyn/. Symposia on the following topics were presented: (1) New frontiers; (2) Multidimensional spectroscopy; (3) Condensed phase dynamics; (4) Chemical reaction dynamics; and (5) Confined molecules: clusters and droplets.

DTIC

*Condensed Matter Physics; Conferences; Molecular Dynamics; Quantum Chemistry*

**20010120491** Arizona State Univ., Tempe, AZ USA

**Thermal Analysis and Potentiostatic Instruments for Relaxor Ferroelectric Research** ***Final Report, 1 Apr. 2000 - 31 Mar. 2001***

Petuskey, William; Aug. 30, 2001; 7p; In English

Contract(s)/Grant(s): F49620-00-1-0234

Report No.(s): AD-A395127; AFRL-SR-BL-TR-01-0495; No Copyright; Avail: CASI; A02, Hardcopy; A01, Microfiche

The funds provided by this grant were used to purchase a thermo-analytical balance, with additional thermal analytical capabilities, and a general purpose potentiostat/galvanostat in support of ongoing research on the thermochemistry of ferroelectric relaxors of ceramic system of PbO-MgO-Nb2O5-TiO2. This research is being carried out at Arizona State University, funded by a primary grant awarded by the AFOSR (ISSA-99-0013, entitled 'Grain Growth in Relaxer Ferroelectrics'). The equipment includes a high vacuum system capable of maintaining better than 10-8 bar pressure in the measuring chamber. Early trials indicate that the equipment will provide the needed accuracy for the required measurements. An auxiliary differential thermal analyzer (DTA) was constructed out of individually purchased parts and combined with existing equipment. This will enable testing of new compositions prior to their introduction into the thermal analyzer and allow for a survey of general reaction behavior of the samples. In addition, this procedure was used as a precaution to identify situations of excessive corrosion that might damage the main instrument. A potentiostat/galvanostat was purchased with two purposes in mind. One was to develop a method of analyzing lead content in liquid metal probes embedded in lead oxide samples. This method is being attempted to provide thermochemical data that would corroborate the information obtained from the gravimetric experiments. The second purpose of this equipment

was to be used in the development of microchemical cells designed to control the lead oxide vapor pressure to which ferroelectric relaxor materials are exposed during synthesis.
DTIC
*Thermal Analysis; Ferroelectricity; Pressure Measurement; Ferroelectric Materials; Thermochemistry*

**20010120535** Argonne National Lab., IL USA
**Survey of high voltage electron microscopy worldwide in 1998**
Allen, C. W.; Mar. 05, 1998; 5p; In English
Report No.(s): DE2001-10672; ANL/MSD/CP-95793; No Copyright; Avail: Department of Energy Information Bridge

High voltage TEMs (transmission electron microscope) were introduced commercially thirty years ago, with the installations of 500 kV Hitachi instruments at the Universities of Nagoya and Tokyo. Since that time 53 commercial instruments, having maximum accelerating potentials of 0.5-3.5 MV, will have been delivered by the end of 1998. Table 1 summarizes the sites and some information regarding those HVEMS (high voltage electron microscope) which are available in 1998. This corrects, updates and expands an earlier report of this sort. There have been three commercial HVEM manufacturers: AEI (UK), Hitachi and JEOL (Japan). The proportion of the total number of HVEMS produced by each manufacturer is similar to that reflected in Table 1: AEI and Kratos/AEI, Hitachi and JEOL. The term Kratos/AEI refers to instruments delivered after the takeover of AEI by Grates in the late 1970s. In Table 1 only maximum accelerating potentials are listed, which is generally also the design value for which the resolution for imaging was optimized. It is important to realize that in many applications, especially those studying irradiation effects, much lower voltages may be employed somewhat routinely to minimize atom displacements by the incident electron beam during analysis. These minimum values range from 100 kV for the AEI and Kratos/AEI instruments to typically 400 kV for the current generation of atomic resolution instruments, the latter being well above the thresholds for displacement in light elements such as Al and Si and for displacement of anions in many ceramic materials such as the high Tc superconductors, for example. An additional potential problem is electron-induced sputtering and differential sputtering (unequal sputtering rates in multicomponent materials), especially when accurate elemental microanalysis is being attempted. These same issues may arise for intermediate voltage TEMs as well, of course.
NTIS
*Transmission Electron Microscopy; Electric Potential; Commerce*

**20010120536** Argonne National Lab., IL USA
**Motion and structure of water adsorbed in type-A zeolites**
Trouw, F. R.; Mar. 05, 1998; 9p; In English
Report No.(s): DE2001-10673; ANL/IPNS/CP-95797; No Copyright; Avail: Department of Energy Information Bridge

The motion of water adsorbed in Type-A zeolites has been measured using quasi-elastic and inelastic neutron spectroscopy. Changes in the charge-compensating cation has a dramatic effect on the low frequency vibrational spectrum, which has a well defined low frequency feature for sodium and lithium but no such peak is present for the case of potassium and calcium. At 297K the low frequency feature is still visible, while there is also quasielastic broadening of the elastic line due to diffusion of the water protons. These measurements are interpreted in the light of the results from computer simulations of these materials.
NTIS
*Water; Zeolites; Surface Properties; Sorption*

**20010120538** Argonne National Lab., IL USA
**Novel sulfonate containing ET based synmetals**
Wang, H. H.; Jul. 31, 1998; 6p; In English
Report No.(s): DE2001-10675; ANL/CHM/CP-95835; No Copyright; Avail: Department of Energy Information Bridge

Electrocrystallization of ET in the presence of aromatic and aliphatic sulfonate anions has led to many new ET salts. These new ET based sulfonate complexes are characterized with use of x-ray diffraction, four-probe conductivity measurements, ESR (Electron Spin Resonance) and Raman spectroscopes. A new (kappa)(4x4) donor packing motif was observed in (ET)(sub 2)(C(sub 6)H(sub 5)CH(sub 2)SO(sub 3))H(sub 2)O. Strong hydrogen bonding between the sulfonate anion S-O and the donor ethylene C-H provides the driving force for the ET salt formation. Many of these new sulfonate salts are highly conductive with some remaining metallic to (approximately)4 K.
NTIS
*Electrochemistry; Ethylene; Sulfonates*

**20010120539** Argonne National Lab., IL USA

**Time-resolved infrared absorption studies of the dynamics of radical reactions**

MacDonald, R. G.; Mar. 06, 1998; 5p; In English

Report No.(s): DE2001-10676; ANL/CHM/CP-95839; No Copyright; Avail: Department of Energy Information Bridge

There is very little information available about the dynamics of radical + radical interactions. These processes are important in combustion being chain termination steps as well as generating new molecular species. to study these processes, a new experimental apparatus has been constructed to investigate radical-radical dynamics. The first radical or atomic species is produced with a known concentration in a microwave discharge flow system. The second is produced by pulsed laser photolysis of a suitable photolyte. The time dependence of individual rovibrational states of the product is followed by absorption of a continuous infrared laser. This approach will allow the reaction of interest to be differentiated from other radical reactions occurring simultaneously. The experimental approach is highly versatile, being able to detect a number of molecular species of particular interest to combustion processes such as water, methane, acetylene etc. at the state specific level. State specific infrared absorption coefficients of radicals can be measured in situ allowing for the determination of the absolute concentrations and hence branching ratios for reactions having multiple reaction pathways.

NTIS

*Reaction Kinetics; Radicals; Time Dependence; Absorptivity; Combustion; Combustion Physics*

**20010120556** Argonne National Lab., IL USA

**Experiments on explosive interactions between zirconium-containing melt and water (ZREX)**

Cho, D. H., Argonne National Lab., USA; Apr. 10, 1998; 19p; In English

Report No.(s): DE2001-10732; ANL/RE/CP-96080; No Copyright; Avail: Department of Energy Information Bridge, Microfiche

The results of two series of experiments on explosive interactions between zirconium-containing melt and water are described. The first series of experiments involved dropping 1-kg batches of zirconium-zirconium dioxide mixture melt into a column of water while the second series employed 1.2-kg batches of zirconium-stainless steel mixture melt. Explosions took place only in those tests which were externally triggered. While the extent of zirconium oxidation in the triggered experiments was quite large, the explosion energies estimated from the experimental measurements were found to be small compared to the combined thermal and chemical energy available.

NTIS

*Explosives; Zirconium; Chemical Explosions*

**20010120836** Massachusetts Inst. of Tech., Dept. of Nuclear Engineering, Cambridge, MA USA

**Using Nuclear Magnetic Resonance and the Dipolar Field to Study Structural Properties of Two-Phase Liquid Systems**

Brown, Scott M.; Sep. 2001; 92p; In English

Report No.(s): AD-A395312; No Copyright; Avail: CASI; A05, Hardcopy; A01, Microfiche

Nuclear Magnetic Resonance (NMR) is a convenient and noninvasive means for studying the internal structure of diamagnetic substances. The extraction of length scale information in liquid NMR spectroscopy is largely limited to sizes below the diffusion length (^ 50 microns). Breaking translational symmetry using the nuclear dipolar field imparts a scale dependence, and provides a means of measuring length scales above this limit. The use of the dipolar field in liquid NMR to make structural measurements is a relatively novel concept in the field, and previous techniques have been largely limited to test cases. This thesis examines the extraction of length-scale information from a relatively complex two-phase liquid system, specifically a poly-disperse oil/water emulsion. Theory is developed and then compared to experimental results, with good agreement. Simple scaling laws are identified which provide a simple means of using the technique for length scale measurements. The thesis then focuses on developing the theory and feasibility of using the developed dipolar NMR technique to study flowing systems, in order to extract average length scale and interfacial properties, including interfacial velocity and interfacial area.

DTIC

*Nuclear Magnetic Resonance; Dipoles; Two Phase Flow; Complex Systems; Liquid Phases*

**20010121492** NASA Ames Research Center, Moffett Field, CA USA

**Vapor Phase Catalytic Ammonia Reduction**

Flynn, Michael T., NASA Ames Research Center, USA; [1994]; 1p; In English; 24th International Conference on Environmental Systems, 20-23 Jun. 1994, Friedrichshafen, Germany

Contract(s)/Grant(s): RTOP 199-61-62; No Copyright; Avail: Issuing Activity; Abstract Only

This paper discusses the development of a Vapor Phase Catalytic Ammonia Reduction (VPCAR) teststand and the results of an experimental program designed to evaluate the potential of the technology as a water purification process. In the

experimental program the technology is evaluated based upon product water purity, water recovery rate, and power consumption. The experimental work demonstrates that the technology produces high purity product water and attains high water recovery rates at a relatively high specific power consumption. The experimental program was conducted in 3 phases. In phase I an Igepon(TM) soap and water mixture was used to evaluate the performance of an innovative Wiped-Film Rotating-Disk evaporator and associated demister. In phase II a phenol-water solution was used to evaluate the performance of the high temperature catalytic oxidation reactor. In phase III a urine analog was used to evaluate the performance of the combined distillation/oxidation functions of the processor.
Author
*Vapor Phases; Ammonia; Water Reclamation; Water Quality; Energy Consumption; Test Stands*

**20010121572** Sandia National Labs., Albuquerque, NM USA
**Conservation of Momentum and Tensile Instability in Particle Methods**
Swegle,; May 01, 2000; 22p; In English
Report No.(s): DE2000-759439; SAND2000-1223; No Copyright; Avail: Department of Energy Information Bridge, Microfiche
This paper considers conservation of momentum and tensile instability in transient dynamic particle methods. Local particle methods are defined as representing a continuous body with particles which discretize the body. The particles carry the field variables and are used for interpolation purposes. They also are discrete chunks of matter which must have mass and volume which in sum represent the total mass and volume of the body. In particle methods, a function is approximated by summing data-weighted shape functions over the particles, Conservation of momentum is considered from the standpoint of Newtons third law, and the conditions which the shape functions must satisfy in order to conserve momentum are derived. The tensile instability is considered from the standpoint of the strength of interaction between particles, and the concept of area vectors which define the surfaces on which the stresses act is introduced. The local nature of the approximation is shown to produce area vectors and forces which decrease as the distance between particles increases. This situation is shown to be similar to other particle systems, such as gravitational systems of particles or molecular dynamics. The instability is shown to be the expected behavior of the physical system represented by the discretization scheme. Finally, these concepts are applied to a specific example, that of moving least squares.
NTIS
*Molecular Dynamics; Stability; Tensile Properties; Conservation Laws; Statistical Analysis*

**20010121880** North Carolina Univ., Dept. of Chemistry, Chapel Hill, NC USA
**Laser Initiated Decomposition in Aerosol Fuels: A Method for Probing the Early Stages of Ignition and Detonation**
Miller, Roger E.; Baer, Tomas; September 2001; 6p; In English
Contract(s)/Grant(s): F49620-00-1-0191
Report No.(s): AD-A394953; AFRL-SR-BL-TR-01-0517; No Copyright; Avail: CASI; A02, Hardcopy; A01, Microfiche
The DURIP grant has been used to purchase two new infra-red laser systems that have been used to initiate combustion of energetic aerosol particles. One is a CO2 laser capable of delivering up to 1.5 J of pulsed power, while the other is an OPO laser pumped by an existing Nd:YAG laser to provide tunable radiation in the 2.7 to 3.3 micrometers range. These lasers have been used to help unravel the decomposition of base catalyzed nitromethane, CH3NO2. The first four steps in its decomposition have been confirmed by the first positive experimental identification of seven intermediates including CH2NO2(-), R2NH2(+) , NO2(-), RNH3(+), and NH4(+). In addition, a controversial reaction step was confirmed by isotopic labeling studies. The mechanism for the base catalyzed nitromethane decomposition is now established. The study of aerosol particles has been advanced by the development of methods to create coated particles and to carry out depth profiling using variable power IR laser heating. The ability to create particles with heterogeneously mixed core and outer layer, coupled with the tunability of the OPO infra-red laser has made it possible to ignite a particle from either the core or from the outside. Finally, a method employing a ”chemical thermometer” has been developed to monitor the temperature of a rapidly combusting particle. The thermometer is the dissociation of glycerol ions, which produces parent and two daughter ions whose intensities depend strongly on the ion vibrational energy.
DTIC
*Fuels; Ignition; Detonation; Carbon Dioxide Lasers; Energetic Particles*

**20010121885** Argonne National Lab., IL USA
**X-ray absorption spectroscopy studies of electrochemically deposited thin oxide films**
Balasubramanian, M.; Jun. 02, 1998; 10p; In English
Report No.(s): DE2001-10828; ANL/CMT/CP-96578; No Copyright; Avail: Department of Energy Information Bridge

We have utilized in situ X-ray Absorption Fine Structure Spectroscopy to investigate the structure and composition of thin oxide films of nickel and iron that have been prepared by electrodeposition on a graphite substrate from aqueous solutions. The films are generally disordered. Structural information has been obtained from the analysis of the data. We also present initial findings on the local structure of heavy metal ions, e.g. SR and Ce, incorporated into the electrodeposited nickel oxide films. Our results are of importance in a number of technological applications, among them, batteries, fuel cells, electrochromic and ferroelectric materials, corrosion protection, as well as environmental speciation and remediation.
NTIS
*Electrochromism; Fine Structure; Metal Ions; Thin Films; X Ray Absorption; Heavy Metals*

**20010121950** Oak Ridge National Lab., TN USA
**Hydrofluoric Acid Corrosion Testing on Unplated and Electroless Gold-Plated Samples**
Osborne, P. E.; Icenhour, A. S.; Del Cul, G. D.; Aug. 01, 2000; 22p; In English
Report No.(s): DE2000-763206; ORNL/TM-2000/137; No Copyright; Avail: Department of Energy Information Bridge, Microfiche

The Molten Salt Reactor Experiment (MSRE) remediation requires that almost 40 kg of uranium hexafluoride (UF6) be converted to uranium oxide (UO). In the process of this conversion, six moles of hydrofluoric acid (HP) are produced for each mole of UF6 converted.
NTIS
*Corrosion Tests; Hydrofluoric Acid; Gold Coatings*

**20010122225** Argonne National Lab., IL USA
**Comparison of a semi-analytic and a CFD model uranium combustion to experimental data**
Clarksean, R.; Apr. 01, 1998; 16p; In English
Report No.(s): DE2001-10713; ANL/TD/CP-96012; No Copyright; Avail: Department of Energy Information Bridge, Microfiche

Two numerical models were developed and compared for the analysis of uranium combustion and ignition in a furnace. Both a semi-analytical solution and a computational fluid dynamics (CFD) numerical solution were obtained. Prediction of uranium oxidation rates is important for fuel storage applications, fuel processing, and the development of spent fuel metal waste forms. The semi-analytical model was based on heat transfer correlations, a semi-analytical model of flow over a flat surface, and simple radiative heat transfer from the material surface. The CFD model numerically determined the flowfield over the object of interest, calculated the heat and mass transfer to the material of interest, and calculated the radiative heat exchange of the material with the furnace. The semi-analytical model is much less detailed than the CFD model, but yields reasonable results and assists in understanding the physical process. Short computation times allowed the analyst to study numerous scenarios. The CFD model had significantly longer run times, was found to have some physical limitations that were not easily modified, but was better able to yield details of the heat and mass transfer and flow field once code limitations were overcome.
NTIS
*Combustion; Ignition; Uranium; Numerical Analysis; Furnaces*

**20010122246** Argonne National Lab., IL USA
**Performance-based, cost- and time-effective PCB analytical methodology**
Alvarado, J. S.; Jun. 11, 1998; 13p; In English
Report No.(s): DE2001-10837; ANL/ER/CP-96618; No Copyright; Avail: Department of Energy Information Bridge

Laboratory applications for the analysis of PCBs (polychlorinated biphenyls) in environmental matrices such as soil/sediment/sludge and oil/waste oil were evaluated for potential reduction in waste, source reduction, and alternative techniques for final determination. As a consequence, new procedures were studied for solvent substitution, miniaturization of extraction and cleanups, minimization of reagent consumption, reduction of cost per analysis, and reduction of time. These new procedures provide adequate data that meet all the performance requirements for the determination of PCBs. Use of the new procedures reduced costs for all sample preparation techniques. Time and cost were also reduced by combining the new sample preparation procedures with the power of fast gas chromatography. Separation of Aroclor 1254 was achieved in less than 6 min by using DB-1 and SPB-608 columns. With the greatly shortened run times, reproducibility can be tested quickly and consequently with low cost. With performance-based methodology, the applications presented here can be applied now, without waiting for regulatory approval.
NTIS
*Polychlorinated Biphenyls; Waste Management*

**20010122252** Argonne National Lab., IL USA

**Solution exchange corrosion testing with the glass-zeolite ceramic waste form in demineralized water at 90 C**

Simpson, L. J.; May 19, 1998; 11p; In English

Report No.(s): DE2001-10812; ANL/CMT/CP-96491; No Copyright; Avail: Department of Energy Information Bridge, Microfiche

A ceramic waste form of glass-bonded zeolite is being developed for the long-term disposition of fission products and transuranic elements in wastes from the U.S. Department of Energy's spent nuclear fuel conditioning activities. Solution exchange corrosion tests were performed on the ceramic waste form and its potential base constituents of glass, zeolite 5A, and sodalite as part of an effort to qualify the ceramic waste form for acceptance into the Civilian Radioactive Waste Management System. Solution exchange tests were performed at 90 C by replacing 80 to 90% of the leachate with fresh demineralized water after set time intervals. The results from these tests provide information about corrosion mechanisms and the ability of the ceramic waste form and its constituent materials to retain waste components. The results from solution exchange tests indicate that radionuclides will be preferentially retained in the zeolites without the glass matrix and in the ceramic waste form, with respect to cations like Li, K, and Na. Release results have been compared for simulated waste from candidate ceramic waste forms with zeolite 5A and its constituent materials to determine the corrosion behavior of each component.

NTIS

*Ceramics; Corrosion Resistance; Glass; Waste Management*

**20010122254** Argonne National Lab., IL USA

**Using synthetic model systems to understand charge separation and spin dynamics in photosynthetic reaction centers**

Wasielewski, M. R.; Aug. 27, 1998; 10p; In English

Report No.(s): DE2001-10810; ANL/CHM/CP-96489; No Copyright; Avail: Department of Energy Information Bridge, Microfiche

Our current work in modeling reaction center dynamics has resulted in the observation of each major spin-dependent photochemical pathway that is observed in reaction centers. The development of new, simpler model systems has permitted us to probe deeply into the mechanistic issues that drive these dynamics. Based on these results we have returned to biomimetic chlorophyll-based electron donors to mimic these dynamics. Future studies will focus on the details of electronic structure and energetic of both the donor-acceptor molecules and their surrounding environment that dictate the mechanistic pathways and result in efficient photosynthetic charge separation.

NTIS

*Spin Dynamics; Photochemical Reactions*

**20010122258** Argonne National Lab., IL USA

**Progress in Metal Ion Separation and Preconcentration: An Overview**

Bond, A. H.; May 19, 1998; 14p; In English

Report No.(s): DE2001-10804; ANL/CHM/CP-96464; No Copyright; Avail: Department of Energy Information Bridge, Microfiche

A brief historical perspective covering the most mature chemically-based metal ion separation methods is presented, as is a summary of the recommendations made in the 1987 National Research Council (NRC) report entitled 'Separation and Purification: Critical Needs and Opportunities'. A review of Progress in Metal Ion Separation and Preconcentration shows that advances are occurring in each area of need cited by the NRC. Following an explanation of the objectives and general organization of this book, the contents of each chapter are briefly summarized and some future research opportunities in metal ion separations are presented.

NTIS

*Histories; Metal Ions; Progress*

**20010122367** Argonne National Lab., IL USA

**Corrosion performance of structural alloys in oxygen/sulfur/chlorine-containing environments**

Natesan, K., Argonne National Lab., USA; Jun. 22, 1998; 12p; In English

Report No.(s): DE2001-10747; ANL/ET/CP-96200; No Copyright; Avail: Department of Energy Information Bridge, Microfiche

Component reliability and long-term trouble-free performance of structural materials are essential in power-generating processes that utilize coal as a feedstock. The combustion environments encompass a wide range of oxygen partial pressures, from excess-air conditions in conventional systems to air-deficient conditions in low-NO(sub x) systems. Apart from the environmental aspects of the effluent from coal combustion, one concern from the systems standpoint is the aggressiveness of the combustion

environment toward boiler structural components such as waterwall tubes and steam superheaters. The corrosion tests in this program address the individual and combined effects of oxygen, sulfur, and chlorine on the corrosion response of several ASME-coded and noncoded boiler materials exposed to air-deficient and excess-air combustion conditions. Data in this paper address the corrosion behavior of structural materials such as Type 347 stainless steel, Alloys 800, 825, 625, 214, and Hastelloy X when exposed at 650 C to excess-air combustion conditions with and without HCl. Thermodynamic calculations were made to evaluate the gas chemistries formed from coal combustion. The results of such calculations, coupled with oxygen/sulfur/chlorine thermochemical diagrams, were used to select the gas environments for the laboratory test program. Results are presented for weight change, thickness loss, microstructural characteristics of corrosion products, mechanical integrity and cracking of scales, and the mechanistic understanding gained on the role of sulfur and chlorine in the corrosion process.
NTIS
*Corrosion Prevention; Corrosion Resistance; Alloys; Corrosion Tests; Boilers*

**20010122368** Argonne National Lab., IL USA
**Corrosion performance of iron aluminides in single- and multioxidant environments**
Natesan, K., Argonne National Lab., USA; Jun. 22, 1998; 13p; In English
Report No.(s): DE2001-10746; ANL/ET/CP-096199; No Copyright; Avail: Department of Energy Information Bridge, Microfiche

Iron aluminide intermetallics are being developed for use as structural materials and/or as cladding for conventional engineering alloys. In addition to their strength advantages, these materials exhibit excellent resistance to corrosion in single- and multioxidant environments at elevated temperatures through the formation of slow-growing, adherent alumina scales. Even though these intermetallics develop protective oxide scales in single-oxidant environments, the simultaneous presence of several reactants in the environment (typical of practical systems) can lead to development of oxide scales that are nonprotective and that undergo breakaway corrosion, or to nonoxide scales that are detrimental to the performance of the underlying alloy. This paper describes the corrosion performance of Fe-Al intermetallics in environments that contain sulfur, carbon, chlorine, and oxygen and that are typical of fossil energy systems. Emphasis is on mechanisms of scale development and breakdown, performance envelopes for long-term USAge of these materials, and approaches to modifying the surfaces of engineering alloys by cladding or coating them with intermetallics to improve their corrosion resistance.
NTIS
*Intermetallics; Iron Aluminides; Oxidation; Oxidation Resistance*

**20010122376** Oak Ridge National Lab., TN USA
**Gas Release During Saltwell Pumping: Interpretation of Operational Data**
Huckaby, J. L.; Peurrung, L. M.; Gauglitz, P. A.; Sep. 16, 1999; 58p; In English
Report No.(s): DE2001-10723; PNNL-13029; No Copyright; Avail: Department of Energy Information Bridge, Microfiche

The Hanford Site has 149 single-shell tanks (SSTs) containing radioactive waste that is a complex mix of radioactive and chemical products. of these, 67 are known or suspected to have leaked liquid into the surrounding soil, while 82 are considered sound (Hanlon 1999). to minimize the amount of material that potentially could leak into the surrounding soil, all of the SSTs are scheduled to have drainable liquid removed and to be designated as interim stabilized. Of the SSTs, 119 have been declared stabilized, and only 30 require further processing (Hanlon 1999). Many of the tanks have been declared stabilized administratively, with only 45 tanks having had drainable liquid removed. The pending consent decree between the Washington State Department of Ecology and the Office of River Protection. (U.S. District Court Eastern District of Washington, 1999) sets a milestone to complete interim stabilization by September 2004. While process equipment exists for removing drainable liquid, and its operation is well known from previous pumping campaigns, a number of safety issues associated with the release and potential ignition of flammable gases within the tanks needs to be addressed. The safety concerns associated with flammable gases stem from the observation that some of the waste in the SSTs generates and retains hazardous quantities of flammable gases, including hydrogen, nitrous oxide, and ammonia. of the 30 SSTs remaining to be declared interim stabilized, 29 need to have drainable liquid removed by saltwell pumping (waste in tank 241-C-106 will be removed by sluicing), and 16 of these are on the Flammable Gas Watch List (FGWL) (Hopkins 1995; Hanlon 1999). Most of these tanks are in Facility Group 2 (Noorani 1997); that is, it is believed that tank operations may induce the release of significant quantities of flammable gas, but gas release does not occur spontaneously. In particular, saltwell pumping to remove the interstitial liquid from SSTs is expected to cause the release of much of the retained gas, both insoluble (principally hydrogen) and soluble (principally ammonia), posing a number of safety concerns (Peurrung et al. 1997; Meader 1996).
NTIS
*Pumping; Chemicals; Radioactive Wastes; Flammable Gases*

**20010122388** Ames Lab., IA USA

**Research and Development Report in Chemistry, Engineering, Metallurgy and Physics** ***Annual Report, Jul. 1961 - Jun. 1962***

Jun. 1962; 339p; In English

Contract(s)/Grant(s): W-7405-eng-82

Report No.(s): AD-A395244; No Copyright; Avail: CASI; A15, Hardcopy; A03, Microfiche

This annual summary report for Ames Laboratory at the Iowa State University of Science and Technology, Ames, Iowa describes research and development in the areas of chemistry, engineering, metallurgy and physics.

DTIC

*Laboratories; Research Management; Research and Development; Technologies*

**20010122402** NASA Ames Research Center, Moffett Field, CA USA

**Electronic spectroscopy of diatomic molecules**

Partridge, Harry, NASA Ames Research Center, USA; Langhoff, Stephen R., NASA Ames Research Center, USA; Bauschlicher, Charles W., Jr., NASA Ames Research Center, USA; [1994]; 1p; In English

Contract(s)/Grant(s): RTOP 232-01-04; No Copyright; Avail: Issuing Activity; Abstract Only

This article provides an overview of the principal computational approaches and their accuracy for the study of electronic spectroscopy of diatomic molecules. We include a number of examples from our work that illustrate the range of application. We show how full configuration interaction benchmark calculations were instrumental in improving the understanding of the computational requirements for obtaining accurate results for diatomic spectroscopy. With this understanding it is now possible to compute radiative lifetimes accurate to within 10% for systems involving first- and second-row atoms. We consider the determination of the infrared vibrational transition probabilities for the ground states of SiO and NO, based on a globally accurate dipole moment function. We show how we were able to assign the a(sup ”5)II state of CO as the upper state in the recently observed emission bands of CO in an Ar matrix. We next discuss the assignment of the photoelectron detachment spectra of NO and the alkali oxide negative ions. We then present several examples illustrating the state-of-the-art in determining radiative lifetimes for valence-valence and valence-Rydberg transitions. We next compare the molecular spectroscopy of the valence isoelectronic B2, Al2, and AlB molecules. The final examples consider systems involving transition metal atoms, which illustrate the difficulty in describing states with different numbers of d electrons.

Author

*Electron Spectroscopy; Diatomic Molecules; Numerical Analysis*

**20010122403** NASA Ames Research Center, Moffett Field, CA USA

**Advanced Automation for Ion Trap Mass Spectrometry-New Opportunities for Real-Time Autonomous Analysis**

Palmer, Peter T., NASA Ames Research Center, USA; Wong, C. M., NASA Ames Research Center, USA; Salmonson, J. D., NASA Ames Research Center, USA; Yost, R. A., Florida Univ., USA; Griffin, T. P., Florida Univ., USA; Yates, N. A., Virginia Univ., USA; [1994]; 1p; In English; Conference on Computer Applications in Analytical Spectroscopy, 14-18 Jun. 1994, Snowbird, UT, USA

Contract(s)/Grant(s): RTOP 506-71-41; No Copyright; Avail: Issuing Activity; Abstract Only

The utility of MS/MS for both target compound analysis and the structure elucidation of unknowns has been described in a number of references. A broader acceptance of this technique has not yet been realized as it requires large, complex, and costly instrumentation which has not been competitive with more conventional techniques. Recent advancements in ion trap mass spectrometry promise to change this situation. Although the ion trap’s small size, sensitivity, and ability to perform multiple stages of mass spectrometry have made it eminently suitable for on-line, real-time monitoring applications, advance automation techniques are required to make these capabilities more accessible to non-experts. Towards this end we have developed custom software for the design and implementation of MS/MS experiments. This software allows the user to take full advantage of the ion trap’s versatility with respect to ionization techniques, scan proxies, and ion accumulation/ejection methods. Additionally, expert system software has been developed for autonomous target compound analysis. This software has been linked to ion trap control software and a commercial data system to bring all of the steps in the analysis cycle under control of the expert system. These software development efforts and their utilization for a number of trace analysis applications will be described.

Author

*Automatic Control; Mass Spectroscopy; Analytical Chemistry; Software Engineering; Ion Traps (Instrumentation)*

**20010122655** Department of Energy, Aiken, SC USA
**On-Line/At-Line Technetium Monitor Using Scintillating Ion Exchange Resins for the Savannah River Site**
Wach, S. T.; Aug. 30, 2000; 22p; In English
Report No.(s): DE2000-761642; BNF-003-98-0130; No Copyright; Avail: Department of Energy Information Bridge

The results of this study indicate that the combination of extraction chromatography and on-line flow-cell scintillation counting can exceed a Tc-99 detection limit of 0.005 Ci/mL in the presence of SR-90, Cs-137, and Pu-239 in less than an 18 minute analysis time.

NTIS
*Ion Exchange Resins; Rivers; Technetium Isotopes; Extraction; Chromatography; Scintillation*

**20010122662** New Orleans Univ., LA USA
**Electronic and nuclear factors in intramolecular charge and excitation transfer.** ***Final Report, Oct. 1992 - Jun. 1995***
Piotrowiak, P.; Jun. 01, 1995; 30p; In English
Report No.(s): DE2000-764562; DOE/ER/14310-1-VOL-1; No Copyright; Avail: Department of Energy Information Bridge, Microfiche

In this report we describe the October 1992 through June 1995 progress our Department of Energy supported projects gathered under the broad title 'Electronic and Nuclear Factors in Intramolecular Charge and Excitation Transfer'. As the title indicates, our work is devoted to developing a better understanding of the fundamental factors controlling the rate and efficiency of photoinduced electron and electronic energy transfer processes. The two topics of special focus are: (1) the electrolyte effects in intramolecular electron transfer (2) the role of the MO, as well as vibrational mode, symmetry in determining the donor-acceptor electronic coupling.

NTIS
*Excitation; Electron Transfer; Molecules*

**20010122712** Pennsylvania State Univ., Dept. of Mechanical and Nuclear Engineering, University Park, PA USA
**Measurement of Radicals and Visualization of Flame Propagation in Propellant Combustion** ***Final Report, 1 Mar. 1999 - 31 May 2001***
Thynell, Stefan T.; Litzinger, Thomas A.; May 2001; 7p; In English
Contract(s)/Grant(s): DAAD19-99-1-0027
Report No.(s): AD-A395281; ARO-39468.1-EG-RIP; No Copyright; Avail: CASI; A02, Hardcopy; A01, Microfiche

This report describes instrumentation acquired as part of the DoD-DUR!P program. The major pieces of equipment purchased were components that upgraded an existing triple quadrupole spectrometer to a molecular beam sampling capability, a high-speed film camera, and components for a data acquisition system. These components are now being utilized in studies on the interaction between a high-temperature, high-pressure plasma and a solid propellant. The plasma is being generated by a capacitive discharge that lasts about 300 micros, depending upon ambient pressure, capillary size, and capillary material as the temporal variation of resistance of the plasma has a controlling influence on the behavior of the RLC circuit. The molecular beam sampling capability allows the identification and possibly quantification of radicals present in the plasma due to decomposition of capillary material and solid propellant, as well as reactions between species present in the plasma and decomposition products of the propellant. The high-speed film camera has been used to capture the evolution of the plasma to reveal the complex structure of the underexpanded supersonic jet.

DTIC
*Molecular Beams; Propellants; Combustion; Spectrometers; Plasmas (Physics); Propellant Combustion; Supersonic Jet Flow*

**20010122788** Rutgers - The State Univ., New Brunswick, NJ USA
**Cellulase: A Key Enzyme for Fermentation Feedstocks. Final report, Proposed Experimentation and Revised Budget**
Eveleigh, D. E.; Macmillan, J. D.; Jan. 24, 2000; 8p; In English
Report No.(s): DE2001-761224; DOE/ER/13794-1-VOL-1; No Copyright; Avail: Department of Energy Information Bridge

Biomass can be fermented to a range of useful products. For efficiency a well characterized and effective cellulase is necessary to gain fermentable sugars from cellulosics (forest by-products and agricultural wastes and municipal refuse). Microbial cellulase systems are comprised of multiple components namely, endoglucanase (EG), cellobiohydrolase (CBH), and beta-glucosidase, which act synergistically. However, their mechanism of interaction in the hydrolysis of crystalline cellulose is poorly understood.

NTIS
*Biomass; Cellulose; Enzymes; Fermentation; Agriculture*

**20010122789** State Univ. of New York, Binghamton, NY USA

**Photochemistry of Intermolecular C-H Bond Activation Reactions**

Lees, A. J.; Jun. 01, 2000; 27p; In English

Report No.(s): DE2001-761218; No Copyright; Avail: Department of Energy Information Bridge

The major goal of this project has been to gain photophysical and photochemical insight as to why transition-metal organometallic systems facilitate intermolecular C-H bond activation reactions with various hydrocarbon substrates. The emphasis of the research has been to determine the details of the solution photochemistry involved in C-H activation via quantitative measurements of these processes.

NTIS

*Hydrocarbons; Photochemical Reactions; Intermolecular Forces; Organometallic Compounds*

**20010122794** Rutgers - The State Univ., Piscataway, NJ USA

**Structure and Reactivity of Model Thin Film Catalysts. Performance report, February 16, 1990-February 15, 1993**

Madey, T. E.; Aug. 03, 1992; 14p; In English

Report No.(s): DE2001-761196; DOE/ER/13985-4; DOE/ER/13985-1-VOL-1; No Copyright; Avail: Department of Energy Information Bridge

The overall theme of this project is to characterize the structure and reactivity of model bimetallic catalysts, ie, ultrathin films of one metal deposited onto single crystal surfaces of a second metal. The focus is on atomically rough substrates that are morphologically unstable in the presence of a monolayer film, i.e.,the surfaces may become microscopically faceted upon annealing.

NTIS

*Crystal Surfaces; Thin Films; Catalysts; Bimetals; Mathematical Models; Reactivity*

**20010122820** Los Alamos National Lab., NM USA

**Uranium hydride initiation kinetics: Effects of oxide thickness**

Teter, D. F.; Hanrahan, R. J.; Wetteland, C. J.; Sep. 01, 2000; 8p; In English

Report No.(s): DE2000-763931; LA-UR-00-4514; No Copyright; Avail: Department of Energy Information Bridge

The kinetics of hydride formation in uranium have been extensively studied. However, the initiation or nucleation kinetics on oxidized specimens have not been specifically measured as a function of oxide thickness. Since the first qualitative observations of the initiation of hydrides in uranium by Owen and Scudmore in 1966, steps are usually taken to minimize the oxide film thickness so that the reaction kinetics being measured are for the hydrogen gas/uranium metal system. Specimens are mechanically abraded or pre-hydrided to remove most of the oxide before exposing to hydrogen gas.

NTIS

*Chemical Reactions; Nucleation; Reaction Kinetics; Uranium Compounds*

**20010122929** Sandia National Labs., Albuquerque, NM USA

**Examination of the Mesoscopic Scale Response of Shock Compressed Heterogeneous Materials Using a Line-Imaging Velocity Interferometer**

Trott, W. M.; Castaneda, J. N.; OHare, J. J.; Knudson, M. D.; Chhabildas, L. C.; Sep. 26, 2000; 10p; In English

Report No.(s): DE2000-764032; SAND2000-1208C; No Copyright; Avail: Department of Energy Information Bridge

In order to provide detailed response data for validation of three dimensional (3-D) numerical simulations of heterogeneous materials subjected to impact loading, an optically recording velocity interferometer system (ORVIS) has been adapted to a line-imaging instrument capable of generating precise mesoscopic scale measurements of spatially resolved velocity variations during dynamic deformation. While the use of this diagnostic has been demonstrated on several different classes of heterogeneous materials, studies have focused on pressed granular sugar as a stimulant material for the widely used explosive HMX (cyclotetramethylentetranitramine). Tests on this material address mesoscopic scale thermomechanical effects in the absence of complications due to rapid reactions. For low-density (65 percent theoretical maximum density) pressings of sugar, material response has been investigated as a function of both impact velocity and changes in particle size distribution. The amplitude and frequency of observed transverse and longitudinal wave structures are generally consistent with the highly structured mesoscopic response seen in the 3-D simulations. In parallel with instrumental developments, several approaches for detailed analysis of the spatially resolved velocity-time data are being evaluated. The utility of Fast Fourier Transform (FFT) filtering for reduction of certain types of ORVIS image data has been demonstrated.

NTIS

*Mechanical Properties; Heterogeneity; Transverse Waves; Sugars; Impact Loads*

**20010122936** NASA Ames Research Center, Moffett Field, CA USA

**Intermediates in the Formation of Aromatics in Hydrocarbon Combustion**

Walch, Stephen P., NASA Ames Research Center, USA; [1994]; 1p; In English; 1994 Gordon Conference on Atomic and Molecular Interactions, 3-8 Jul. 1994, New London, NH, USA

Contract(s)/Grant(s): NAS2-14031; NCC2-478; RTOP 537-02-20; No Copyright; Avail: Issuing Activity; Abstract Only

The formation of the first benzene ring is believed to be the rate limiting step in soot formation. Two different mechanisms have been proposed for formation of cyclic C6 species. The first involves the reaction of two acetylenes to give CH2CHCCH (vinyl acetylene), the loss of a H to give CHCHCCH (n-C41-13) or CH2CCCH (iso-C4H3), and addition of another acetylene to n-C4H3, followed by ring closure to give phenyl radical. Miller and Melius argue that only n-C4H3 leads to phenyl radical and since iso-C4H3 is more stable than n-C4H3 this mechanism is unlikely. An alternative mechanism proposed by them is formation of benzene from the dimerization of two CH2CCH (propargyl) radicals (formed by the reaction of singlet methylene with C2H2). We report reaction pathways and accurate energetics (from CASSCF/internally contracted CI calculations) for the reactions of CH(pi-2) and CH2-1 with acetylene, the reaction of vinylidene with acetylene, and the reaction of n-C4H3 and iso-C4H3 with acetylene. These calculations identify two new reactive intermediates CHCHCH ( a A"-2 ground state in Cs symmetry; spin coupling is a doublet from three singly occupied orbitals) and CHCCH (B-3 ground state in C2 symmetry) from the reaction of CH with acetylene. These species dimerize with no barrier to form benzene and para-benzyne, respectively. CHCCH is proposed as a reactive intermediate which can add to benzene to give higher polynuclear aromatic hydrocarbons or fullerenes. The addition of a C3H2 unit releases two C-C bond energies and thus the resulting addition product contains sufficient energy to break several CH bonds leading to a reduction in the H to C ratio as the cluster size increases. It is found that iso-C4H3 adds to acetylene to initially give a fulvene radical but that this species rearranges to phenyl radical. Thus, the reaction of acetylene with iso-C4H3 does lead to phenyl radical and the cyclization pathway may also contribute to formation of the initial benzene ring.

Author

*Benzene; Hydrocarbon Combustion; Soot; Reaction Kinetics*

**20010123043** Brookhaven National Lab., Upton, NY USA

**Momentum Dependence of pi-pi(asterik) Excitations of Benzene Rings in Condensed Phases**

Hayahsi,; Watanabe,; Udagawa,; Kao,; Aug. 08, 2000; 14p; In English

Report No.(s): DE2000-767155; BNL-67620; KC0204011; No Copyright; Avail: Department of Energy Information Bridge

The action of radiation on molecular liquids is of crucial importance in many fields, e.g., radiation chemistry and radiation biology. In principle, the interaction between radiation and matter can be fully described by the so-called loss function. The loss function is simply the imaginary part of the inverse dielectric function.

NTIS

*Excitation; Liquids; Momentum; Particle Interactions*

**20010123044** Brookhaven National Lab., Upton, NY USA

**Isotope Methods in Homogeneous Catalysis**

Bullock,; Bender,; Dec. 01, 2000; 62p; In English

Report No.(s): DE2000-767154; BNL-67609; KC030201; No Copyright; Avail: Department of Energy Information Bridge

The use of isotope labels has had a fundamentally important role in the determination of mechanisms of homogeneously catalyzed reactions. Mechanistic data is valuable since it can assist in the design and rational improvement of homogeneous catalysts. There are several ways to use isotopes in mechanistic chemistry. Isotopes can be introduced into controlled experiments and followed where they go or don't go; in this way, Libby, Calvin, Taube and others used isotopes to elucidate mechanistic pathways for very different, yet important chemistries. Another important isotope method is the study of kinetic isotope effects (KIEs) and equilibrium isotope effect (EIEs). Here the mere observation of where a label winds up is no longer enough - what matters is how much slower (or faster) a labeled molecule reacts than the unlabeled material. The most careti studies essentially involve the measurement of isotope fractionation between a reference ground state and the transition state. Thus kinetic isotope effects provide unique data unavailable from other methods, since information about the transition state of a reaction is obtained. Because getting an experimental glimpse of transition states is really tantamount to understanding catalysis, kinetic isotope effects are very powerful.

NTIS

*Catalysis; Isotope Effect; Isotopes; Isotopic Labeling*

**20010123064** Argonne National Lab., IL USA

**X-ray absorption near-edge spectroscopy of plutonium solid species**

Kropf, A. J.; Oct. 22, 1998; 17p; In English

Report No.(s): DE2001-11073; ANL/CMT/CP-97542; No Copyright; Avail: Department of Energy Information Bridge, Microfiche

We present XANES at the L(sub III) edge for four plutonium solid phases: Pu(III)F3, Pu(IV)O2, NaPu(V)O2CO3, and Ba3Pu(VI)O6. These correspond to the four important oxidation states in the process chemistry and environmental chemistry of plutonium. by a fitting method that uses an arc tangent function and gaussian curves, it was possible to reproducibly determine the edge energy and distinguish among the four oxidation states. These data demonstrate a 1.85 (+/-) 0.20 eV shift per oxidation state.

NTIS

*Plutonium; Absorption Spectroscopy; X Ray Absorption; Environmental Chemistry*

**20010123136** Brookhaven National Lab., Upton, NY USA

**Electrocatalysis on surfaces modified by metal monolayers deposited at underpotentials**

Adzic, R.; Dec. 01, 2000; 46p; In English

Report No.(s): DE2000-767095; BNL-67616; KC030202; No Copyright; Avail: Department of Energy Information Bridge

The remarkable catalytic properties of electrode surfaces modified by monolayer amounts of metal adatoms obtained by underpotential deposition (UPD) have been the subject of a large number of studies during the last couple of decades. This interest stems from the possibility of implementing strictly surface modifications of electrocatalysts in an elegant, well-controlled way, and these bi-metallic surfaces can serve as models for the design of new catalysts. In addition, some of these systems may have potential for practical applications. The UPD of metals, which in general involves the deposition of up to a monolayer of metal on a foreign substrate at potentials positive to the reversible thermodynamic potential, facilitates this type of surface modification, which can be performed repeatedly by potential control. Recent studies of these surfaces and their catalytic properties by new in situ surface structure sensitive techniques have greatly improved the understanding of these systems.

NTIS

*Electrocatalysts; Electrodes; Catalysis; Surface Treatment; Surface Properties*

**20010123404** Oak Ridge National Lab., TN USA

**Perfluoro(Methylcyclohexane) Tracer Tagging Test and Demonstration**

Sigman, M. E.; Wise, M. B.; Guerin, M. R.; McCoig, T. M.; Fraser, J. A.; Jun. 01, 2000; 34p; In English

Report No.(s): DE2001-769299; C/ORNL99-0562; No Copyright; Avail: Department of Energy Information Bridge

On February 14 and 15, 2000, a demonstration of current perfluorocarbon tagging technology and the future potential of these methods was held at Oak Ridge National Laboratory (ORNL). The demonstration consisted of a brief technical discussion followed by a laboratory demonstration. The laboratory demonstrations included the detection of letters, parcels, briefcases and lockers containing perfluorocarbon-tagged papers. Discrimination between tagged and non-tagged items and between three perfluorocarbon tags was demonstrated along with the detection of perfluorocarbon in a background of non-fluorinated volatile organic solvent. All demonstrations involved real-time detection using a direct sampling ion trap mass spectrometer. The technical results obtained at ORNL during and in preparation for the demonstration are presented in Appendix 1 to assist Tracer Detection Technology Corp. in further evaluating their position on development and marketing of perfluorocarbon tracer technology.

NTIS

*Mass Spectrometers; Organic Compounds; Marking; Perfluoro Compounds; Detection; Solvents*

**20010123407** Colorado State Univ., Fort Collins, CO USA

**eFinal Report: Nanomaterials in Secondary Battery Research and Development, July 1, 1995-September 14, 1999**

Martin, C. R.; Jan. 31, 2000; 7p

Report No.(s): DE2001-765142; No Copyright; Avail: Department of Energy Information Bridge

We have been exploring the rate capabilities of nanostructured Li-ion battery electrodes. These nanostructured electrodes are prepared via the template method, a general procedure used to prepare nanomaterials pioneered in the principal investigator's laboratory. The nanostructured electrodes consist of nanofibers or tubules of the electrode material that protrude from a current-collector surface like the bristles of a brush. These nanostructured electrodes show dramatically improved rate capabilities relative to conventional electrode designs.

NTIS

*Electric Batteries; Electrodes; Nanostructure (Characteristics)*

**20010123408** Utah Univ., Salt Lake City, UT USA

**Atomic force microscopy for the study of specially prepared surfaces including transferred Langmuir-Blodgett layers. Final report**

Miller, J. D.; Jun. 02, 1999; 10p; In English

Report No.(s): DE2001-765118; No Copyright; Avail: Department of Energy Information Bridge

During the past four years a major number of surface science research programs in the Department of Metallurgical Engineering at the University of Utah have involved the use of the Atomic Force Microscope (AFM) and the Langmuir-Blodgett (LB) film balance procured with financial assistance from DOE (Department of Energy) under grant number DE-FG03-96ER76049. These instruments have been used for research in the areas of nonsulfide flotation chemistry, mineral processing, waste paper de-inking, water treatment, treatment of contaminated soil, coal preparation, and plastics recycling. In addition, the AFM and LB film balance have been of great help to university researchers in other departments at the University of Utah and elsewhere, as well as researchers from industry.

NTIS

*Atomic Force Microscopy; Surface Layers; Langmuir-Blodgett Films*

**20010123448** Los Alamos National Lab., NM USA

**Some Observations on the Structure of TATB**

Phillips, D. S.; Schwarz, R. B.; Skidmore, C. B.; Hiskey, M. A.; Son, S. F.; Jun. 28, 1999; 7p; In English

Report No.(s): DE2001-761024; LA-UR-99-3397; No Copyright; Avail: Department of Energy Information Bridge, Microfiche

The recent discovery of second-harmonic light generation (SHG) from 1,3,5-triamino- 2,4,6-trinitrobenzene (TATB) has renewed interest in both the crystallography and the identification of defect structures in this material. The accepted crystal structure is triclinic but centrosymmetric (P-1); SHG is not expected from materials of this symmetry. A wide variety of syntheses have been shown to produce SHG-positive materials, including an emulsion technique, two different recrystallization methods, and a variety of combined reaction - precipitation processes. In addition, two standard commercial powders have shown the property after annealing in the 300 C range. We have examined the structures of several of these powders using polarized light microscopy (PLM), scanning electron microscopy (SEM), and powder X-ray diffraction (XRD). We find that SHG-positive materials typically contain crystals both more transparent and more strongly faceted (i.e. more perfect) than weak-SHG ones and that the positive samples show stronger texture in their powder diffraction patterns. These results are compared with predictions from Cady's structure.

NTIS

*TATB; X Ray Diffraction; Crystallography; Harmonic Generations*

**20010123455** Argonne National Lab., IL USA

**Flash photolysis-shock tube studies**

Michael, J. V.; Mar. 05, 1998; 7p; In English

Report No.(s): DE2001-11024; ANL/CHM/CP-95779; No Copyright; Avail: Department of Energy Information Bridge, Microfiche

Following earlier investigations on the dissociation rates of halogen containing molecules, we studied the thermal decompositions of CHCl3 and CF3Br. In addition, we measured the branching ratio and rate constants for the thermal decomposition of H2CO. We studied three bimolecular rate processes: H + H2CC0, CF3 + H2, and H + CF3H. Decomposition studies in reflected shock waves on three reactions were completed using atomic resonance absorption spectroscopic (ARAS) detection and/or the laser schlieren density gradient (LS) method.

NTIS

*Photolysis; Halogens; Hydrocarbons; Flash Lamps; Shock Tubes*

**20010123465** Argonne National Lab., IL USA

**Transuranic separation using organophophorus extractants adsorbed onto superparamagnetic carriers**

Nunez, L.; Oct. 07, 1998; 17p; In English

Report No.(s): DE2001-10987; ANL/CMT/CP-97378; No Copyright; Avail: Department of Energy Information Bridge, Microfiche

Polymeric coated ferromagnetic carriers with an absorbed layer of octyl(phenyl) -N,N-diisobutylcarba moylmethylphosphine oxide (CMPO) diluted by tributyl phosphate (TBP) are being evaluated for application in the separation and the recovery of low concentrations of americium, plutonium, and uranium from nuclear waste solutions. Due to their chemical nature, these extractants selectively complex americium and plutonium contaminants onto the particles and the complexed

particles can be recovered from the solution using a magnet. Physical and chemical characterization of the extractant-absorbed particles were performed by gamma and liquid scintillation counting, scanning electron microscopic (SEM) micrograph, and other physical measurements. Plutonium, americium,and uranium separations have been performed at various HNO3 and HCl concentrations. Parameters were studied to determine the limitations and capacity of the process. The status of the chemistry and application of the process to Department of Energy (DOE) remediation efforts for actinide decontamination are discussed.
NTIS
*Radioactive Wastes; Solvent Extraction; Decontamination*

**20010123540** Argonne National Lab., IL USA
**Influence of corannulene's curved carbon lattice (C20H10) on lithium intercalation**
Scanlon, L. G.; Jun. 08, 1998; 9p; In English
Report No.(s): DE2001-10640; ANL/CHM/CP-95621; No Copyright; Avail: Department of Energy Information Bridge, Microfiche

Ab initio molecular orbital calculations have been used to investigate the influence of corannulene's curved carbon lattice (C(sub 20)H(sub 10)) on lithium intercalation. This has been approximated by investigating the reaction of lithium atoms with either the corannulene molecule directly or with a sandwich structure formed from two corannulene molecules. In the first case, one corannulene molecule, three, six and seven lithiums have been used to form Li(sub 3)(C(sub 20)H(sub 10)), Li(sub 6)(C(sub 20)H(sub 10)) and Li(sub 7)(C(sub 20)H(sub 10)). The last complex has a lithium to carbon ratio of 1:2.86 indicative of a high capacity lithium carbon anode versus the 1:6 ratio found in stage 1 lithium intercalated graphite. The change in Gibbs energy for formation of Li(sub 3)(C(sub 20)H(sub 10)) with a multiplicity of 4 (3 unpaired electrons) is -4.75 kcal/mole. However, when a multiplicity of 2 is used (1 unpaired electron), the change in Gibbs energy is -8.49 kcal/mole. The change in Gibbs energy for formation of Li(sub 6)(C(sub 20)H(sub 10)) and Li(sub 7)(C(sub 20)H(sub 10)) (multiplicity of 2) are -26.48 and -26.47 kcal/mole, respectively. In all the lithium corannulene complexes described, each complex has a molecular orbital composed only of lithium orbitals, indicative of lithium cluster formation. However, in the formation of Li(sub 3)(C(sub 20)H(sub 10)) with three lithium atoms intercalated between two corannulene carbon lattices, there are no molecular orbitals indicative of lithium cluster formation. The multiplicity for this chemical system is 4 and the corannulene lattices are stacked one over the other like saucers. The corannulene carbon lattices are separated by approximately 4.5 (angstrom). The separations between lithiums are 3.13, 3.60 and 3.79 (angstrom). These results are in contrast to those found in the Li(sub 3)C(sub 60) endohedral complex with a multiplicity of 4. In this complex there is a molecular orbital composed only of lithium orbitals. The calculated results in this investigation suggest that the carbon lattice stacking configuration is important for lithium cluster formation. For Li(sub 6)(C(sub 20)H(sub 10)), a transition state intermediate complex has been found through the geometry optimization process. Optimization of this structure results in a complex which is 13.42 kcal/mole more stable. These preliminary results indicate that the energy of activation for the removal of one lithium from this complex is on the order of 13.42 kcal/mole or 0.58 eV.
NTIS
*Carbon; Lithium Compounds; Chemical Composition; Molecular Orbitals; Sandwich Structures*

**20010123543** Argonne National Lab., IL USA
**Ab initio and density functional studies of hydrocarbon adsorption in zeolites**
Curtiss, L. A.; Aug. 21, 1998; 9p; In English
Report No.(s): DE2001-10635; ANL/CHM/CP-95597; No Copyright; Avail: Department of Energy Information Bridge, Microfiche

The adsorption energies of methane and ethane in zeolites are investigated with ab initio molecular orbital theory and density functional theory. In this work we have used zeolite cluster models containing two, three, and five tetrahedral (Si, Al) atoms and have found equilibrium structures for complexes of methane, ethane, and propane with an acid site. If a large enough cluster is used and correlation effects are included via perturbation theory, the calculated adsorption energy for ethane is about 5 kcal/mol compared with the experimental value of 7.5 kcal/mol. The B3LYP density functional method gives a much smaller binding of (approximately)1 kcal/mol for ethane. The reason for the failure of density fictional theory is unclear.
NTIS
*Adsorption; Ethane; Hydrocarbons; Methane; Zeolites*

**20010123619** Institute of Gas Technology, Des Plaines, IL USA
**Development of METHANE de-NOX reburning process** ***Quarterly Report, 1 Oct. - 31, 1999***
Dec. 31, 1999; 9p; In English
Report No.(s): DE2001-760510; DOE/GO/10418-Q; No Copyright; Avail: Department of Energy Information Bridge, Microfiche

The use of biomass and wood waste solids and sludges as fuel is often hampered by their low heating values and the presence of bound nitrogen that result in inefficient combustion and high NOx emission. Cofiring supplemental fuel through auxiliary burners helps with improving the combustion effectiveness and NOx reduction, but the benefits are limited to the fractional heat input of the auxiliary fuel. Demonstration tests have shown over 60% reduction in NOx, CO and VOC emissions, and a 2% increase in boiler thermal efficiency using only 8 to 13% natural gas.
NTIS
*Wood; Biomass; Fuels; Sludge*

**20010123651** Indiana Univ., Bloomington, IN USA
**Neutron Polarizers Based on Polarized 3He**
Snow, W. M.; Feb. 01, 2000; 10p; In English
Report No.(s): DE2001-764599; No Copyright; Avail: Department of Energy Information Bridge
With the support of a 1996 grant from the Office of Energy Research (DE-FG0296ER45587), we have developed and tested neutron spin-filters based on the large spin dependence of the cross section for neutron capture by He-3.
NTIS
*Helium Isotopes; Neutrons; Polarizers*

**20010123750** Argonne National Lab., IL USA
**Bethe surface of liquid water**
Dingfelder, M.; Oct. 14, 1998; 14p; In English
Report No.(s): DE2001-11038; ANL/PHY/CP-97429; No Copyright; Avail: Department of Energy Information Bridge
The Bethe surface of liquid water, earlier calculated using a semi-empirical model, is compared with recent available data from IXS-experiments (inelastic X-ray scattering; Compton scattering of high energy photons) in liquid water. No alarming discrepancy is found on a global view of the Bethe surface. The extrapolation to the optical limit (viz., at zero momentum transfer) is shown and the reliability of these data is discussed in detail.
NTIS
*Liquid Surfaces; Water*

**20010123754** Argonne National Lab., IL USA
**First-principles study of pi-bonded (100) planar defects in diamond**
Zapol, P.; Dec. 16, 1998; 9p; In English
Report No.(s): DE2001-11033; ANL/CHM/CP-96910; No Copyright; Avail: Department of Energy Information Bridge, Microfiche
A periodic density functional study of the high-energy (pi)-bonded (100) stacking fault in diamond that can serve as a prototype of a twist grain boundary has been carried out. Information on formation energies, geometries and the electronic structure has been obtained. A single point electronic structure calculation of a (Sigma)5 twist grain boundary based on the geometry taken from a molecular dynamics simulation has also been performed.
NTIS
*Diamonds; Electronic Structure; Crystal Defects*

**20010123909** Los Alamos National Lab., NM USA
**Thermodynamic Model for the Hysteresis in Metal-Hydrogen Systems**
Schwarz, R. B.; Khachaturyan, A. G.; Feb. 01, 2000; 21p; In English
Report No.(s): DE2001-763368; LA-UR-00-953; No Copyright; Avail: Department of Energy Information Bridge
A phenomenon common to most metal-hydrogen systems is the presence of hysteresis in their cyclic absorption/resorption characteristics. Because hysteresis on a reversible transformation is indicative of a dissipative mechanism, early models attributed the hysteresis to the plastic deformation needed to accommodate the volume change upon hydride formation. A friction model, however, cannot explain the reproducibility of the hysteresis over thoUSAnd of cycles. We propose that the hysteresis is an intrinsic thermodynamic phenomenon caused by the coherency strains between the parent metal phase and the transformed hydride phase. In this paper, we summarize the salient features of the model and explain its relevance to known metal-hydrogen systems.
NTIS
*Hysteresis; Thermodynamics; Mathematical Models; Metal Hydrides*

**20010123911** Los Alamos National Lab., NM USA

**Stability of Pyrochlore Oxides**

Minervini, L.; Grimes, R.; Sickafus, K.; Feb. 01, 2000; 10p; In English

Report No.(s): DE2001-763366; LA-UR-00-935; No Copyright; Avail: Department of Energy Information Bridge

A Contour plot of the disorder reaction energies across a wide variety of A(sub 2)B(sub 2)O(sub 7) pyrochlore oxides has been produced using atomistic simulation calculations based on energy minimization techniques. Cations studied range from LU(sup 3+) to La(sup 3+) on the A site and Ti(sup 4+) to Ce(sup 4+) on the B site. The results relate the experimentally observed stability range of the pyrochlore structure to A and B cation size and disorder. Disorder enthalpies decrease dramatically with increasing B cation size while the rate of increase with A cation size depends markedly on the particular B cation. The association of anion Frenkel and cation antisite disorders is found to be of importance.

NTIS

*Cations; Contours; Enthalpy; Molecular Structure*

**20010123914** Energy and Environmental Analysis, Inc., Durham, NC USA

**Conceptual and Calculation Model for Gas Formation from Impure Calcined Plutonium Oxides**

Lyman, J.; Eller, P.; Feb. 01, 2000; 7p; In English

Report No.(s): DE2001-763361; LA-UR-00-865; No Copyright; Avail: Department of Energy Information Bridge

Safe transport and storage of pure and impure plutonium oxides requires an understanding of processes that may generate or consume gases in a confined storage vessel. We have formulated conceptual and calculational models for gas formation from calcined materials. The conceptual model for impure calcined plutonium oxides is based on the data collected to date and the anticipated post-calcination behavior of the plutonium oxide and of the dominant impurities known to be present. by its very nature, a conceptual model does not purport to lay to rest all technical aspects of an issue. Instead, a conceptual model provides an intellectual framework for evaluating a broad range of data and for posing relevant hypotheses that can be tested through additional work. The conceptual model is thereby improved as additional data is acquired. The conceptual model assumes that plutonium in calcined impure oxides exists predominantly as plutonium dioxide. Dominant impurity phases are assumed to be chloride salts, binary and complex oxides of transition metals, and alkaline earth oxides.

NTIS

*Plutonium Oxides; Radioactive Wastes; Containment; Mathematical Models; Materials Handling; Confinement*

**20010124069** Florida Univ., Dept. of Chemical Engineering, Gainesville, FL USA

**Development of viscometers for kraft black liquor. Final report, phases I, II, IIA, and III**

Fricke, A. K.; Crisalle, O. D.; Nov. 01, 1999; 173p; In English

Report No.(s): DE2001-763247; DOE/GO/10564-F; No Copyright; Avail: Department of Energy Information Bridge

This report documents the results of performance evaluations and final recommendations for several prototype sensors designed for use as on-line viscometers for black liquor application. More specifically, the report addresses all the goals established for Phase I through Phase III of the US Department of Energy Cooperative Agreement entitled Development of Viscometers for Kraft Black Liquor (DE-FC02-93CF11 O564). The motivation for this study is to fulfill the need for an extensive evaluation of instruments for measuring the viscosity of black liquor. The viscosity of the black liquor has a significant effect on the effectiveness of all the major operations used to process the liquor through a series of evaporators and concentrators, storage tanks, and its ultimate firing in the recovery boiler. In spite of its relevance, the viscosity is not routinely measured on-line in most pulping mills. Instrument manufacturers encounter a major economic barrier when developing viscometers for black liquor applications because of the relatively high risk that the costs of testing and design may not be recoverable if the new market fails to provide a large and exclusive customer base. The development process involves significant technical barriers given that the sensors must work in hostile environment characterized by high temperatures, corrosive liquids and gases, and the presence of suspended solids. Furthermore, the viscosity is a sensitive function of temperature and solids content.

NTIS

*Liquids; Economics; Manufacturing; Viscometers*

**20010124085** Federal Energy Technology Center, Morgantown, WV USA

**Preparation and characterization of composite membrane for high temperature gas separation**

Ilias, S.; King, F. G.; Mar. 26, 1998; 53p; In English

Report No.(s): DE2001-775210; DE-FG22-93MT93008-17; No Copyright; Avail: Department of Energy Information Bridge

A new class of perm-selective inorganic membrane was developed by electroless deposition of palladium thin-film on a microporous (alpha)-alumina ceramic substrate ((phi)39 mm x 2 mm thickness, nominal pore size 150 nm and open porosity

(approx) 42%). The new membrane was characterized by Scanning Electron Micrography (SEM), Energy Dispersive X-ray Analysis (EDX) and conducting permeability experiments with hydrogen, helium, argon and carbon dioxide at temperatures from 473 K to 673 K and feed pressures from 136 kPa to 274 kPa. The results indicate that the membrane has both high permeability and selectivity for hydrogen. The hydrogen transport through the Pd-composite membrane closely followed Sievert's law. A theoretical model is presented to describe the performance of a single-stage permeation process. The model uses a unified mathematical formulation and calculation methods for two flow patterns (cocurrent and countercurrent) with two permeable components and a nonpermeable fraction in the feed and a sweep stream in the permeate. The countercurrent flow pattern is always better than the cocurrent flow pattern with respect to stage cut and membrane area. The effect of flow configuration decreases with increasing membrane selectivity or with decreasing permeate/feed ratio.
NTIS
*Ceramics; High Temperature Gases; Palladium; Photomicrography; Thin Films; Aluminum Oxides; Mathematical Models*

**20010124130** Oak Ridge National Lab., TN USA
**Analysis of Hydrogen Generation and Accumulation in U-233 Tube Vaults**
Ally, M. R.; Willis, K. J.; Sep. 01, 1999; 136p; In English
Report No.(s): DE2001-769370; ORNL/TM-1999/188; No Copyright; Avail: Department of Energy Information Bridge

The purpose of the (sup 233)U Safe Storage Program is to enhance the safe storage of (sup 233)U-bearing materials. This report describes the work done at the Oak Ridge National Laboratory's Radiochemical Development Facility (RDF) to address questions related to possible hydrogen generation and accumulation in (sup 233)U tube vaults. The objective of this effort was to verify assumptions in the mathematical model used to estimate the hydrogen content of the gaseous atmosphere that possibly could occur inside the tube vaults in Building 3019 and to evaluate proposed measures for mitigating any hydrogen concerns. A mathematical model was developed using conservative assumptions to evaluate possible hydrogen generation and accumulation in the tube vaults. The model concluded that an equilibrium concentration would be established below the lower flammability limit (LFL) of 4.1% hydrogen. The major assumptions used in the model that were validated are as follows: (1) The shield plug does not form a seal with the tube vault wall, thus allowing the hydrogen gas to diffuse past the shield plug to the upper section of the tube vault. (2) The tube vault end-cap leaks sufficiently to allow air to be drawn into the tube vault by the off-gas system, thereby purging hydrogen from the upper section of the tube vault. (3) Any hydrogen gas generated completely mixes with the other gases present in the lower section of the tube vault and does not stratify beneath the shield plug. (4) The diffusion coefficient determined from the literature for constant diffusion of hydrogen in air is valid. The coefficient is corrected for temperatures from 0 to 25 C. Another assumption used in the model, that hydrogen generated by radiolytic decomposition of hydrogen-bearing materials (e.g., moisture and plastic) leaks from the cans under steady-state condition, as opposed to a sudden release resulting from rupture of the can(s), was beyond the scope of this investigation. Several parameters from the original model were recalculated based on the above conclusions. Using the temperature-corrected diffusion coefficient in item 4, the worst-case equilibrium concentration that would be expected based on the theoretical well is 1.3% hydrogen. Based on complete mixing of hydrogen (item 3), rather than hydrogen collecting and concentrating below the shield plug as assumed in the model, the time after loss of off-gas service for the hydrogen concentration to reach the LFL from the equilibrium concentration of 1.3% is estimated to be 18 days. The time for the hydrogen concentration to reach 50% of the LFL was estimated to be 4.6 days.
NTIS
*Leakage; Uranium 233; Mathematical Models; Storage Tanks; Hydrogen Production; Safety*

**20010125017** Oak Ridge National Lab., TN USA
**Ion-Beam-Induced Defects and Defect Interactions in Perovskite-Structure Titanates**
Boatner, L. A.; Jiang, W.; Meldrum, A.; Thevuthasan, S.; Weber, W. J.; Aug. 23, 1999; 13p; In English
Report No.(s): DE2001-11335; ORNL/CP-104443; No Copyright; Avail: Department of Energy Information Bridge

Ion-beam irradiation of perovskite structures results in the production and accumulation of defects. Below a critical temperature, irradiation also leads to a crystalline-to-amorphous transformation. The critical temperature for amorphization under 800 keV Kr(sup +) ion irradiation is 425,440 and 550 K for SRTiO3, CaTiO3 and BaTiO3, respectively. The results of ion-channeling studies on SRTiO3 irradiated with 1.0 MeV Au(sup 2+) ions suggest that the crystalline-to-amorphous transformation is dominated by the accumulation and interaction of irradiation-induced defects. In SiTiO(sub 3) irradiated with He(sup +) and O(sup +) ions at 180 K, isochronal annealing studies indicate that there is significant recovery of defects on both the oxygen and cation sublattices between 200 and 400 K. These results suggest that defect recovery processes may control the kinetics of amorphization. A fit of the direct-impact/defect-stimulated model to the data for SRTiO3 suggests that the kinetics of amorphization are controlled by both a nearly athermal irradiation-assisted recovery process with an activation energy of 0.1 plus or minus 0.05 eV and a thermal defect recovery process with an activation energy of 0.6 plus or minus 0.1 eV. In SRTi0(sub 3)

implanted with 40 keV H(sup +) to 5.0 x 10(exp 16) and 1.0 x 10(exp 17) ions/square cm, annealing at 470 K increases the backscattering yield from SR and Ti and is mostly likely due to the coalescence of H2 into bubble nuclei. Annealing at 570 K and higher results in the formation of blisters or large cleaved areas.
NTIS
*Ion Irradiation; Ion Beams; Perovskites; Defects*

**20010125022** Argonne National Lab., IL USA
**Analysis of technology options to reduce the fuel consumption of idling trucks**
Stodolsky, F.; Gaines, L.; Vyas, A.; Aug. 22, 2000; 40p; In English
Report No.(s): DE2000-764207; ANL/ESD-43; No Copyright; Avail: Department of Energy Information Bridge

Long-haul trucks idling overnight consume more than 838 million gallons (20 million barrels) of fuel annually. Idling also emits pollutants. Truck drivers idle their engines primarily to (1) heat or cool the cab and/or sleeper, (2) keep the fuel warm in winter, and (3) keep the engine warm in the winter so that the engine is easier to start. Alternatives to overnight idling could save much of this fuel, reduce emissions, and cut operating costs. Several fuel-efficient alternatives to idling are available to provide heating and cooling: (1) direct-fired heater for cab/sleeper heating, with or without storage cooling; (2) auxiliary power units; and (3) truck stop electrification. Many of these technologies have drawbacks that limit market acceptance. Options that supply electricity are economically viable for trucks that are idled for 1,000--3,000 or more hours a year, while heater units could be used across the board. Payback times for fleets, which would receive quantity discounts on the prices, would be somewhat shorter.
NTIS
*Fuel Consumption; Trucks; Technology Assessment; Internal Combustion Engines*

**20010125031** Thomas Jefferson National Accelerator Facility, Newport News, VA USA
**Measurement of Deuteron Tensor Polarization in Elastic Electron Scattering**
Gustafsson, K. K.; Nov. 01, 2000; 230p; In English
Report No.(s): DE2000-767960; JLAB-R-00-002; DOE/ER/40150-1772; PP00-078; No Copyright; Avail: Department of Energy Information Bridge, Microfiche

No abstract prepared.
NTIS
*Deuterons; Elastic Scattering; Tensors*

**20010125064** Argonne National Lab., IL USA
**TEM investigation of a ceramic waste form for immobilization of process salts generated during electrometallurgical treatment of spent nuclear fuel**
Esh, D. W.; Frank, S. M.; Goff, K. M.; Johnson, S. G.; Moschetti, T. L.; May 06, 1999; 10p; In English
Report No.(s): DE2001-11766; ANL/ED/CP-98816; No Copyright; Avail: Department of Energy Information Bridge

Transmission electron microscopy (TEM) examination is presented of the microstructure of a ceramic waste form developed at Argonne National Lab - West for immobilization of actinides and fission products present in an electrorefiner salt. The material is produced by occluding the salt in zeolite granules, followed by hot isostatic pressing of the occluded zeolite in a mixture with a borosilicate glass. The paper presents results from a cold surrogate ceramic waste form, as well as Pu-239 and Pu-238 loaded samples.
NTIS
*Ceramics; Microstructure; Wastes; Waste Treatment; Spent Fuels*

**20010125141** Deacon Research, CA USA
**Chemical Composition and Flow Velocity as a Function of Operating Conditions for an Arc Jet Heater**
Bamford, Douglas J., Deacon Research, USA; Romanovsky, Alexander, Deacon Research, USA; [1994]; 1p; In English; AIAA 29th Thermophysics Conference, June 1995, San Diego, CA, USA; Sponsored by American Inst. of Aeronautics and Astronautics, USA
Contract(s)/Grant(s): NAS2-13879; RTOP 232-01-04; No Copyright; Avail: Issuing Activity; Abstract Only

We have used laser-induced fluorescence (LIF) to carry out a detailed, systematic survey of the properties of the free stream of the 20 Megawatt Aerodynamic Heating Facility at NASA/Ames Research Center. In both air and nitrogen flows we have measured the atomic nitrogen absolute number density and flow velocity at each operating condition. In air flows we have also measured the atomic oxygen absolute number density and rotational/translational temperature at each operating condition. These results have been used to provide, for the first time, a direct, nonintrusive measurement of the enthalpy on the centerline of the

flow. In addition, the observed arc jet properties can be used to test and improve computer simulations of the arc jet flow which include detailed chemical rate processes (especially nitrogen atom recombination) taking place during the supersonic expansion. Author

*Air Flow; Chemical Composition; Computerized Simulation; Flow Velocity; Jet Flow; Aerodynamic Heating*

**20010125386** Argonne National Lab., IL USA

**In-situ laser Raman scattering and far infrared spectroscopy studies of corrosion-passivation phenomena in metals**

Melendres, C. A.; Jun. 28, 1999; 17p; In English

Report No.(s): DE2001-11865; ANL/CMT/CP-99356; No Copyright; Avail: Department of Energy Information Bridge, Microfiche

Vibrational spectroscopic and electrochemical techniques are among the most useful tools for the elucidation of corrosion-passivation phenomena in metals. The former can provide information on the structure and composition of corrosion films 'in situ' in aqueous solution environments, while thermodynamic and kinetic information may be obtained using electrochemical techniques. In this paper, we demonstrate the application of Laser Raman Scattering (LRS) and Synchrotrons Far Infrared Reflectance Spectroscopy (SFIRS), coupled with electrochemical methods, for the determination of the structure and composition of surface films on nickel and copper in aqueous solution environment. The corrosion film on nickel has been found to consist of NiO and Ni(OH)(sub 2) in the passive region of potential and NiOOH in the transpassive region. The film on copper consists of Cu(sub 2)O, CUO and Cu(OH)(sub 2). We also show for the first time that SFIRS can be used to obtain information on the adsorption of ions on a metal surface with sub-monolayer sensitivity. Adsorption of Cl(sup (minus)), Br(sup (minus)), SO(sup (minus)2), and PO(sub 4)(sup (minus)3) was found to occur at gold electrodes in perchloric acid solution. We also observed that when two different ions are present in solution, the more strongly adsorbed ion determined the corrosion behavior of the metal.

NTIS

*Corrosion; Far Infrared Radiation; Infrared Spectroscopy; Metal Surfaces; Raman Spectroscopy; Synchrotrons*

**20010125414** Argonne National Lab., IL USA

**Overview of resid characterization by mass spectrometry and small angle scattering techniques**

Hunt, J. E.; Winans, R. E.; Jul. 14, 1999; 6p; In English

Report No.(s): DE2001-11791; ANL/CHM/CP-98951; No Copyright; Avail: Department of Energy Information Bridge

The purpose of this presentation is to discuss what is known about the molecular structures found in petroleum resid from mass spectrometry and small angle neutron and X-ray scattering methods. The question about molecular size distributions and the occurrence of aggregation in the asphaltene fraction will be examined. Our understanding of this problem has evolved with the application of new analytical methods. Also, correlations with results from other approaches will be discussed. In addition, the issue of the nature of the heteroatom-containing molecules will be examined and the challenges that remain in this area.

NTIS

*Molecular Structure; Crude Oil; Scattering*

**20010125426** Argonne National Lab., IL USA

**Thermal-hydraulic development a small, simplified, proliferation-resistant reactor**

Farmer, M. T.; Hill, D. J.; Sienicki, J. J.; Spencer, B. W.; Wade, D. C.; Jul. 02, 1999; 29p; In English

Report No.(s): DE2001-11745; ANL/RE/CP-98725; No Copyright; Avail: Department of Energy Information Bridge, Microfiche

This paper addresses thermal-hydraulics related criteria and preliminary concepts for a small (300 MWt), proliferation-resistant, liquid-metal-cooled reactor system. A main objective is to assess what extent of simplification is achievable in the concepts with the primary purpose of regaining economic competitiveness. The approach investigated features lead-bismuth eutectic (LBE) and a low power density core for ultra-long core lifetime (goal 15 years) with cartridge core replacement at end of life. This potentially introduces extensive simplifications resulting in capital cost and operating cost savings including: 1) compact, modular, pool-type configuration for factory fabrication, 2) 100+% natural circulation heat transport with the possibility of eliminating the main coolant pumps, 3) steam generator modules immersed directly in the primary coolant pool for elimination of the intermediate heat transport system, and 4) elimination of on-site fuel handling and storage provisions including rotating plug. Stage 1 natural circulation model and results are presented. Results suggest that 100+% natural circulation heat transport is readily achievable using LBE coolant and the long-life cartridge core approach; moreover, it is achievable in a compact pool configuration considerably smaller than PRISM A (for overland transportability) and with peak cladding temperature within the existing database range for ferritic steel with oxide layer surface passivation. Stage 2 analysis follows

iteration with core designers. Other thermal hydraulic investigations are underway addressing passive, auxiliary heat removal by air cooling of the reactor vessel and the effects of steam generator tube rupture.
NTIS
*Thermodynamics; Thermohydraulics; Liquid Metal Cooled Reactors; Systems Engineering; Cost Effectiveness; Reactor Design*

**20010125434** Argonne National Lab., IL USA
**W, F, and I: Three Quantities Basic to Radiation Physics**
Inokuti, M.; Nov. 11, 1998; 35p; In English; Doke Symposium, 29 March 1998, Tokyo, Japan
Contract(s)/Grant(s): W-31109-ENG-38
Report No.(s): DE2001-11101; ANL/PHY/CP-97653; No Copyright; Avail: Department of Energy Information Bridge, Microfiche

The W value is an index of the mean number of ions produced in a gas subjected to ionizing radiation. Formally, it is defined as the radiation energy absorbed (usually expressed in units of eV) 'per ion pair of either sign produced', or, in a simpler language, 'per electron liberated'. The basic knowledge up to 1961 is eloquently articulated in a classic essay by Platzman (1), which Professor Doke loves to cite. The theme of Platzman was to explain from the point of view of basic physics the magnitude and characteristics of the ratio W/I, where I is the (first) ionization threshold energy. In summary, major characteristics are as follows. (1) The W value for a given gas depends weakly on the properties of the radiation such as the mass and charge of particles or initial energies (provided they are sufficiently high). This makes the ionization measurement useful as a method of dosimetry, viz., the determination of the absorbed energy. (2) The ratio W/I is always greater than unity because a part of the absorbed energy must be used in nonionizing events such as discrete excitation or molecular dissociation into neutral fragments and also in producing subexcitation electrons, viz., electrons with kinetic energies too low to cause electronic excitation or ionization (2). (3) The ratio W/I is 1.7-1.8 for rare gases, and 2.1-2.6 for gases of common molecules (depending on the electronic structure, going from 'hard' to 'soft'). Calculation of the W value is possible from three approaches: (i) the energy balance of Platzman, heuristic for general understanding and appropriate for an estimate; (ii) the Fowler equation (3) for the direct evaluation of the mean number of ions produced; and (iii) the method of Spencer and Fano (4) through the degradation spectra (or the track length distributions) of charged particles, most importantly of electrons, present in the medium. The Fowler method is good for obtaining the mean number of ions or excited states resulting from the incidence of particles of relatively low energies, while the Spencer-Fano method is good for the incidence of high-energy particles.
NTIS
*Ionizing Radiation; Atomic Physics*

**20010125457** Lawrence Livermore National Lab., Livermore, CA USA
**Scrounge-atron: a phased approach to the advanced hydrotest facility utilizing proton radiography**
Alford, O. J.; Barnes, P. D.; Chargin, A. K.; Dekin, W. D.; Hartouni, E. P.; Mar. 01, 1999; 5p; In English
Report No.(s): DE2001-8316; UCRL-JC-133131; DP0102015; No Copyright; Avail: Department of Energy Information Bridge, Microfiche

The Department of Energy has initiated its Stockpile Stewardship and Management Program (SSMP) to provide a single, integrated technical program for maintaining the continued safety and reliability of the nation's nuclear weapons stockpile in the absence of nuclear testing. Consistent with the SSMP, the Advanced Hydrotest Facility (AHF) has been conceived to provide improved radiographic imaging with multiple axes and multiple time frames. The AHF would be used to better understand the evolution of nuclear weapon primary implosion shape under normal and accident scenarios. There are three fundamental technologies currently under consideration for use on the AHF. These include linear induction acceleration, inductive-adder pulsed-power technology (both technologies using high current electron beams to produce an intense X-ray beam) and high-energy proton accelerators to produce a proton beam. The Scrounge-atron (a proton synchrotron) was conceived to be a relatively low cost demonstration of the viability of the third technology using bursts of energetic protons, magnetic lenses, and particle detectors to produce the radiographic image. In order for the Scrounge-atron to provide information useful for the AHF technology decision, the accelerator would have to be built as quickly and as economically as possible. These conditions can be met by scrounging parts from decommissioned accelerators across the country, especially the Main Ring at Fermilab. The Scrounge-atron is designed to meet the baseline parameters for single axis proton radiography: a 20 GeV proton beam of ten pulses, 10(sup 11) protons each, spaced 250 ns apart.
NTIS
*Radiography; Synchrotrons; Protons; Nuclear Weapons; Research Facilities*

**20010125495** Argonne National Lab., IL USA

**Imprinting artificial magnetic structures**

Lohstroh, W.; Sep. 25, 1998; 17p; In English

Report No.(s): DE2001-10840; ANL/MSD/CP-96642; No Copyright; Avail: Department of Energy Information Bridge

Recently we created La/Fe multilayers with a helical magnetic structure imprinted from the conditions of growth rather than by the magnetic interactions between layers. Each sublayer was 30(angstrom) thick, and during deposition the sample was rotated in an external field of 3 Oe., a field strong enough to magnetize the Fe layer being deposited but not sufficient to perturb the magnetization of the Fe layers already grown. As a result, adjacent Fe layers formed a helical structure with a chirality and periodicity determined by the rotational direction and speed of the substrate and the rate of deposition. Following this discovery, an extensive set of experiments (mainly using Kerr effect magnetometry and polarized neutron reflectivity) was undertaken to ascertain the stability of imprinted magnetic structures, and to understand the onset of magnetization during growth. La/Fe imprinted helical magnetic structures (of different La and Fe thicknesses) were found to be stable in time and to be permanently erased only by magnetic fields larger than 90 Oe.

NTIS

*Magnetization; Deposition; Lanthanum; Iron; Magnetic Field Configurations; Substrates*

**20010125510** Sandia National Labs., Albuquerque, NM USA

**Using Microelectrodes to Determine the Availability and Behavior of Pit Initiation Sites in Aluminum**

Wall, F. D.; Martinez, M. A.; Nov. 21, 2000; 12p; In English

Report No.(s): DE2001-767987; SAND2000-2895C; No Copyright; Avail: Department of Energy Information Bridge, Microfiche

A repetitive polarization experiment was developed which allows measurement of multiple pitting potentials from a single experiment. Automated data analysis is used to extract potentials relating to metastable and stable pit initiation. A multi-electrode sample was used to evaluate the dependence between subsequent pits in aluminum. It was found that the events have little or no dependence on prior sample history. The repetitive polarization experiment was used to evaluate the effect of sample size and purity on pit initiation in aluminum. Pitting potentials increased for decreasing sample size. No clear potential was observed for 99% and 99.99% purity inclusions was not found to control pitting behavior.

NTIS

*Aluminum; Electrodes; Pitting*

**20010125511** Sandia National Labs., Albuquerque, NM USA

**Effect of Chlorine Implantation on the Pitting Behavior of Aluminum**

Wall, F. D.; Barbour, J. C.; Sullivan, J. P.; Missert, N. A.; Bunker, B. C.; Nov. 21, 2000; 12p; In English

Report No.(s): DE2001-767986; SAND2000-2894C; No Copyright; Avail: Department of Energy Information Bridge, Microfiche

Using plasma-beam techniques, an engineered on Al thin film substrates. Electrochemical Al oxide has been placed testing indicates that this structure has a low susceptibility to pitting corrosion making it an ideal control on which to study the impact of intentionally introduced defects. Results from potentiodynamic polarization experiments and chemical etching indicate that this engineered oxide is extremely robust compared to air-formed oxides. Subsequent ion beam implantation was used to introduce Cl into the deposited oxide. Minimal impact on both electrical and ionic conductivity of the oxide was observed for Cl concentrations of approximately 0.4%. Approximately an order of magnitude higher Cl concentration is expected in an oxide formed after HNO3 etching to the peak of the Cl implant distribution. This oxide had an elevated ionic conductivity and enhanced susceptibility to pit initiation.

NTIS

*Aluminum Oxides; Implantation; Pitting*

**20010125520** Arizona Univ., Tucson, AZ USA

**Final Report: Theoretical Studies on Radiation-Induced Transformations in Nucleic Acid Bases, May 1, 1993-April 30, 1996**

Adamowicz, L.; Apr. 30, 1996; 12p; In English

Report No.(s): DE2001-765172; No Copyright; Avail: Department of Energy Information Bridge

In the proposal we identified several elemental molecular properties related to the effects observed in genetic material exposed to ionizing irradiation, and we studied them by means of the ab-initio quantum chemistry. The chemistry of irradiation is complex and biological consequences are significant. This includes cell death, mutations, carcinogenic transformations, etc.

In the proposal we theoretically modeled several elemental processes related to the radiolysis of components of the nucleic acids, i.e., the pyrimidine nucleobases cytosine, uracine and thymine. Based on the state-of-the-art ab-initio calculations, we obtained information on the structural and spectroscopic properties of transition intermediate reactants.
NTIS
*Irradiation; Nucleic Acids; Quantum Chemistry; Genetics; Radiolysis*

**20010125525** Department of Energy, Washington, DC USA
**Catalytic Membrane Program**
Liu, P. K. T.; Jan. 31, 2000; 6p; In English
Report No.(s): DE2001-764722; DOE/GO/10561-Q; No Copyright; Avail: Department of Energy Information Bridge
This is a summary of the following activities: (1) CO2 membrane material development; (2) use of USC protocol for M and P low cost ceramic substrate; (3) thermal and hydrothermal stability test; (4) alternative carbon membrane development; (5) economic analysis; (6) field test preparation; and (7) presentation.
NTIS
*Catalysts; Carbon Dioxide; Membranes; Field Tests*

**20010125530** Ames Lab., IA USA
**Novel Applications of the Methyltrioxorhenium/Hydrogen Peroxide Catalytic System**
Stankovic, S.; Sep. 12, 2000; 75p; In English
Report No.(s): DE2001-764687; IS-T 1895; No Copyright; Avail: Department of Energy Information Bridge
In the presence of catalytic amounts of MTO, methyltrioxorhenium, methyl trimethylsilyl ketene acetals are oxidized with urea hydrogen peroxide to afford cx-hydroxy and a-siloxy esters. On treatment with potassium fluoride, the cc-hydroxy esters are obtained in high yields.
NTIS
*Acetals; Hydrogen Peroxide; Ketenes; Ureas; Catalytic Activity*

**20010125562** Argonne National Lab., IL USA
**Structural and Magnetic Properties of UCo(sub 1/3)T(sub 2/3)Al Solid Solutions (T = Ru, Pt, Rh)**
Andreev, A. V.; Bordallo, H. N.; Chang, S.; Nakotte, H.; Schultz, A. J.; Aug. 06, 1999; 10p; In English
Report No.(s): DE2001-11912; ANL/IPNS/CP-99682; No Copyright; Avail: Department of Energy Information Bridge, Microfiche
We report on neutron diffraction studies of UCo(1/3)T(2/3)Al (T = Ru, Pt, Rh). All three solid solutions form in the hexagonal ZrNiAl structure. The Ru-containing compound is found to be chemically ordered, while the Pt-containing compound is nearly disordered and the Rh-containing compound is purely disordered. All three compounds exhibit long-range magnetic order with rather small U moments.
NTIS
*Magnetic Properties; Neutron Diffraction; Solid Solutions*

**20010125567** Argonne National Lab., IL USA
**Surface and Interface Modification Science and Technology**
Park, J. H.; Jul. 19, 1999; 12p; In English
Report No.(s): DE2001-11898; ANL/ET/CP-99592; No Copyright; Avail: Department of Energy Information Bridge, Microfiche
Surface modification of solids is of scientific and technological interest due to its significant benefits in a wide variety of applications. Various coatings applications such as corrosion protection and electrical insulators and conductors are required for proper engineering design based on geometrical relationships between interfaces and on thermodynamic/kinetic considerations for the development of surface modifications. This paper will explore three basic examples: the proton conductor BaCeO3, high-temperature protective coatings, and epitaxial relationships between interfaces.
NTIS
*Protective Coatings; Surface Properties*

**20010125595** Argonne National Lab., IL USA
**Structure and electrochemical potential simulation for the cathode material Li(1+x)V(3)O(8)**
Benedek, R.; Thackeray, M. M.; Yang, L. H.; Dec. 05, 1997; 9p; In English
Report No.(s): DE2001-8137; ANL/CMT/CP-94702; No Copyright; Avail: Department of Energy Information Bridge, Microfiche

The structure and electrochemical potential of monoclinic Li(sub 1+x)V3O8 were calculated within the local-density-functional-theory framework by use of plane-wave-pseudopotential methods. Special attention was given to the compositions 1+x=1.2 and 1+x=4, for which x-ray diffraction structure refinements are available. The calculated low-energy configuration for 1+x=4 is consistent with the three Li sites identified in x-ray diffraction measurements and predicts the position of the unobserved Li. The location of the tetrahedrally coordinated Li in the calculated low-energy configuration for 1+x=1.5 is consistent with the structure measured by x-ray diffraction for Li(sub 1.2)V3O8. Calculations were also performed for the two monoclinic phases at intermediate Li compositions, for which no structural information is available. Calculations at these compositions are based on hypothetical Li configurations suggested by the ordering of vacancy energies for Li4V3O8 and tetrahedral site energies in Li(sub 1.5)V3O8. The internal energy curves for the two phases cross near 1+x=3. Predicted electrochemical potential curves agree well with experiment.
NTIS
*Electrochemistry; Cathodes; Lithium Oxides; Crystal Structure*

**20010125597** Lawrence Livermore National Lab., Livermore, CA USA
**Analysis of heat transfer during quenching of a gear blank**
Aceves, S. M.; Sahai, V.; Mar. 01, 1999; 32p; In English
Report No.(s): DE2001-8406; UCRL-JC-133520; DP0301010; No Copyright; Avail: Department of Energy Information Bridge, Microfiche

This paper presents experimental and numerical results for the quench of a gear blank in agitated and stagnant oil. Heat transfer within the gear blank is analyzed with a whole domain-optimizer technique inverse solution method, to calculate the time history at every point in the gear blank. The development of this procedure represents the first stage in an overall analysis of the quench process that will later include material phase transformations and deformation. The paper presents ten variations in setting up the inverse problem, to analyze which combination of independent variables and decision variables results in the best match between experimental and numerical results. The results indicate that dividing the boundary of the gear blank into four zones and assigning a fixed heat transfer coefficient or heat flux to each zone yields an average RMS (root mean square) error (average difference between experimental and numerical results) of the order of 40 K. This error can be reduced by either increasing the number of zones, by reducing the number of thermocouples being matched, or by allowing the heat transfer or heat flux to vary within the zones. of these possibilities, variation of heat transfer within the zones gives the best improvement in the quality of the match for the amount of extra effort required to run the problem.
NTIS
*Boundary Element Method; Quenching (Cooling); Thermal Analysis; Regions*

**20010125622** Argonne National Lab., IL USA
**Computational,Electrochemical and Li-7 NMR Studies of Lithiated Disordered Carbons Electrodes in Lithium Ion Cells**
Sandi, G.; Gerald, R.; Scanlon, L. G.; Carrado, K. A.; Winans, R. E.; Jan. 07, 1998; 9p; In English
Report No.(s): DE2001-8100; ANL/CHM/CP-93688; No Copyright; Avail: Department of Energy Information Bridge, Microfiche

Disordered carbons that deliver high reversible capacity in electrochemical cells have been synthesized by using inorganic clays as templates to control the pore size and the surface area. The capacities obtained were much higher than those calculated if the resultant carbon had a graphitic-like structure. Computational chemistry was used to investigate the nature of lithium bonding in a carbon lattice unlike graphite. The lithium intercalated fullerene Li(n)-C60 was used as a model for our (non-graphitic) disordered carbon lattice. A dilithium-C60 system with a charge and multiplicity of (0,1) and a trilithium-C60 system with a charge and multiplicity of (0,4) were investigated. The spatial distribution of lithium ions in an electrochemical cell containing this novel disordered carbon material was investigated in situ by Li-7 NMR using an electrochemical cell that was incorporated into a toroid cavity nuclear magnetic resonance (NMR) imager. The concentration of solvated Li(+) ions in the carbon anode appears to be larger than in the bulk electrolyte, is substantially lower near the copper/carbon interface, and does not change with cell charging.
NTIS
*Carbon; Lithium; Metal Ions; Order-Disorder Transformations; Spatial Distribution; Electrochemistry*

**20010125625** General Electric Co., Schenectady, NY USA
**Measurement of the Fundamental Parameters for the Film-Rupture/Oxidation Mechanism**
Attanasio, S. A.; Fish, J. S.; Morton, D. S.; Rosecrans, P. M.; Was, G. S.; Apr. 23, 1999; 12p
Report No.(s): DE2001-8233; KAPL-P-000215; No Copyright; Avail: Department of Energy Information Bridge, Microfiche

Identification of the mechanism responsible for primary water stress corrosion cracking (PWSCC) in nickel-base alloys is a controversial topic. Numerous mechanisms, including the film-rupture/oxidation (i.e., slip-oxidation or slip-dissolution) mechanism, have been proposed to explain PWSCC. According to this mechanism, the observed sensitivity of PWSCC to material and environmental factors may be explained by the combined effects of repassivation kinetics, oxide rupture strain, and crack tip strain rate (which includes creep). Previous research has shown that increasing the Cr content of Ni-9%Fe-Cr from 16 to 30 wt% strongly decreases PWSCC susceptibility. Consequently, measurements of these three fundamental parameters (repassivation, oxide rupture, and creep) were performed as a function of Cr content, and SCC crack growth rates were predicted on the basis of the resulting data. This paper illustrates that considering these three parameters concurrently may contribute to the understanding of Cr effects on PWSCC of Ni-base alloys. However, it is not clear whether the film-rupture/oxidation mechanism can adequately predict the observed crack growth rates for Alloy 600 at 338 C.
NTIS
*Nickel Alloys; Stress Corrosion Cracking; Passivity; Rupturing; Oxidation*

**20010125626** Argonne National Lab., IL USA
**Trace, isotopic analysis of micron-sized grains: Mo, Zr analysis of stardust (SiC and graphite grains)**
Pellin, M. J.; Nicolussi, G. K.; Feb. 19, 1998; 13p; In English
Report No.(s): DE2001-8139; ANL/CHM/CP-94712; No Copyright; Avail: Department of Energy Information Bridge, Microfiche

Secondary Neutral Mass Spectrometry using resonant laser ionization can provide for both high useful yields and high discrimination while maintaining high lateral and depth resolutions. An example of the power of the method is measurement of the isotopic composition of Mo and Zr in 1-5 micrometers presolar SiC and graphite grains isolated from the Murchison CM2 meteorite for the first time. These grains have survived the formation of the Solar System and isotopic analysis reveals a record of the stellar nucleosynthesis present during their formation. Mo and Zr, though present at less than 10 ppm in some grains, are particularly useful in that among their isotopes are members that can only be formed by distinct nucleosynthetic processes known as s-, p-, and r-process. Successful isotopic analysis of these elements requires both high selectivity (since these are trace elements) and high efficiency (since the total number of atoms available are limited). Resonant Ionization Spectroscopy is particularly useful and flexible in this application. While the sensitivity of this t.edmique has often been reported in the past, we focus hereon the very low noise properties of the technique. We further demonstrate the efficacy of noise removal by two complimentary methods. First we use the resonant nature of the signal to subtract background signal. Second we demonstrate that by choosing the appropriate resonance scheme background can often be dramatically reduced.
NTIS
*Isotope Effect; Murchison Meteorite; Trace Elements*

## 26
## METALS AND METALLIC MATERIALS

*Includes physical, chemical, and mechanical properties of metals and metallic materials; and metallurgy.*

**20010118522** Brookhaven National Lab., Upton, NY USA
**Rapidly-Solidified Permanent Magnet Materials: Factors Affecting Quenchability and Magnetic Properties in Nd2Fe14B**
Lewis,; Kramer,; McCallum,; Branagan,; Nov. 02, 1999; 22p; In English
Report No.(s): DE2000-759021; BNL-66785; No Copyright; Avail: Department of Energy Information Bridge

Insight into the solidification behavior of Nd(sub 2)Fe(sub 14)B-based materials processed by rapid solidification techniques has been obtained by a systematic experimental study of the Curie temperatures of selected phases found in these materials. Nd(sub 2)Fe(sub 14)B-based materials fabricated by two disparate rapid solidification techniques, inert gas atomization (IGA) and melt-spinning, has been studied. The compositions of the starting materials have been altered with additions of the refractory elements Ti and C which are known to alter the solidification behavior of these materials. Special emphasis has been placed on trying to understand the effect of alloying additions upon the nature of the quenched glass, the distribution of the elemental additions within the Nd(sub 2)Fe(sub 14)B lattice and the evolution of the elemental partitioning with quench rate and annealing condition. The experimental Curie temperature data obtained using thermal analysis methods from the particles produced by gas-atomization is consistent with both an ejection of quenched-in refractory species from the crystalline Nd(sub 2)Fe(sub 14)B lattice and with increased crystallographic order as particle size, and hence grain size, increases. Magnetic ac susceptibility measurements performed on nominally-amorphous Nd(sub 2)Fe(sub 14)B ribbons produced by melt-spinning indicate a decrease

of the Curie temperature with increasing quench rate, a result that may be attributed either to the degree of Ti/C retention in the glass or to the degree of disorder in the glass, independent of Ti/C retention.
NTIS
*Neodymium Compounds; Iron Compounds; Boron Compounds; Quenching (Cooling); Magnetic Properties*

**20010118523** Brookhaven National Lab., Upton, NY USA
**Influence of nanoengineered Cu defects on aluminum pitting initiation**
Wall,; Son,; Missert,; Barbour,; Martinez,; Nov. 01, 1999; 12p; In English
Report No.(s): DE2000-759020; BNL-66784; No Copyright; Avail: Department of Energy Information Bridge

Nanoengineering technologies have been used to generate well defined arrays of pure Cu islands within an Al thin film matrix in order to examine the impact of noble particle defects on the initiation of metastable pitting. The Cu particles form local galvanic cells with the surrounding Al matrix and drive metastable corrosion. Electrical isolation of the Cu particles from the Al occurs due to selective Al dissolution and appears to correlate to cessation of metastable events. Distributions of parameters related to the electrochemical signature of an event suggests that size and spacing of particles do not impact the signatures of individual events. However, event frequency data indicate that the propensity for a structure to induce localized events is linked to Cu island diameter and separation.
NTIS
*Aluminum; Pitting; Defects; Nanotechnology*

**20010118541** Brookhaven National Lab., Upton, NY USA
**Measurements of the properties of beryllium foil**
Zhao,; Wang,; Mar. 31, 2000; 21p; In English
Report No.(s): DE2000-757135; BNL-67337; No Copyright; Avail: Department of Energy Information Bridge, Microfiche

The electrical conductivity of beryllium at radio frequency (800 MHz) and liquid nitrogen temperature were investigated and measured. This summary addresses a collection of beryllium properties in the literature, an analysis of the anomalous skin effect, the test model, the experimental setup and improvements, MAFIA simulations, the measurement results and data analyses. The final results show that the conductivity of beryllium is not as good as indicated by the handbook, yet very close to copper at liquid nitrogen temperature.
NTIS
*Beryllium; Electrical Resistivity; Data Processing; Metal Foils; Electrical Measurement*

**20010118927** Sandia National Labs., Albuquerque, NM USA
**Fatigue Damage Accumulation in 63Sn-37Pb Solder Alloy**
Wei, Y.; Chow, C. L.; Neilsen, M. K.; Fang, H. E.; Jul. 27, 2000; 8p; In English
Report No.(s): DE2000-761833; SAND2000-1887C; No Copyright; Avail: Department of Energy Information Bridge

This paper presents the application of a TMF damage model to assess reliability of a typical 63Sn-37Pb solder joint material. The damage model is introduced to quantify the fatigue damage accumulation in the solder alloy taking into account the presence of micro-defects as they initiate, coalesce, grow, and coarsen under TMF loading. The effect of damage on solder behavior is captured with a coupled viscoplastic damage constitutive model. The proposed model is applied to calculate the hysteresis loops of solder under applied strain rates 10(-3)/s, 10(-4)/s and 10(-5)/s at temperature 80 C. The model is also able to characterize the cyclic softening of solder that has been observed experimentally under fatigue loading. Based on the concept of equivalent damage accumulation, a failure criterion is proposed for the determination of fatigue life. It is shown that mechanical behavior and fatigue life of 63Sn-37Pb solder alloy can be satisfactorily predicted.
NTIS
*Fatigue (Materials); Mechanical Properties; Tin Alloys; Lead Alloys; Mathematical Models*

**20010118928** Sandia National Labs., Albuquerque, NM USA
**Damage Mechanics Based Fatigue Life Prediction for 63Sn-37Pb Solder Materials**
Wei, Y.; Chow, C. L.; Neilsen, M. K.; Fang, H. E.; Jul. 27, 2000; 10p; In English
Report No.(s): DE2000-761834; SAND2000-1886C; No Copyright; Avail: Department of Energy Information Bridge

This paper presents a method of TMF analysis based on the theory of damage mechanics to examine the fatigue damage accumulation in 63 Sn-37Pb solder. The method is developed by extending a viscoplastic damage model proposed earlier by the authors (Wei, et al 1999, 2000). A computer simulation is carried out to calculate hysteresis loops at three different strain ranges. The damage-coupled fatigue damage model is applied to predict the cyclic softening behavior of the material and the prediction

is found to agree well with the experiment. With a proposed failure criterion based on the concept of damage accumulation, the TMF model is also found to predict successfully the fatigue life of 63 Sn-37Pb solder.
NTIS
*Tin Alloys; Lead Alloys; Mathematical Models; Fatigue Life; Computerized Simulation*

**20010118933** Sandia National Labs., Albuquerque, NM USA
**Porosity in Stainless Steel LENS Powders and Deposits**
SUSAn, D. F.; Puskar, J. D.; Brooks, J. A.; Robino, C. V.; Aug. 01, 2000; 10p; In English
Report No.(s): DE2000-761852; SAND2000-1993C; No Copyright; Avail: Department of Energy Information Bridge

Laser Engineered Net Shaping (LENS) utilizes a laser beam to melt fine powders to produce three-dimensional engineering structures line by line and layer by layer. When building these structures, defects including lack-of-fusion (LOF) at interlayer boundaries and intralayer porosity are sometimes observed. LOF defects can be minimized by adjusting processing parameters, but the sources of intralayer porosity are less apparent. In this paper, the amount and-size distributions of 17-4PH and 304L powders and pores within the powder were characterized in parallel with the intralayer porosity in LENS deposits fabricated from the same materials. Intralayer porosity increased with increased powder porosity but was not well correlated with deposition parameters. The results demonstrate the importance of careful characterization and specification of starting powders on the quality of the final LENS deposits.
NTIS
*Porosity; Powder (Particles); Stainless Steels; Deposits; Laser Beams*

**20010119053** Oak Ridge National Lab., TN USA
**Recent Development of Metallic Materials**
Liu, C. T.; Nieh, T. G.; Jul. 02, 1999; 4p; In English
Report No.(s): DE2001-10473; ORNL/CP-103351; KC-02-01-05-0; No Copyright; Avail: Department of Energy Information Bridge, Microfiche

Metallic materials play a vital role in the development of advanced engineering systems for industrial applications. In this paper, the recent development of two metallic alloy families will be briefly reviewed: (1) ordered intermetallics, and (2) bulk metallic glasses. Ordered intermetallic alloys based on aluminides and silicides possess many promising properties for structural use at elevated temperatures in hostile environments. This is because these alloys have excellent oxidation and corrosion resistance, high temperature strength, and relatively low material density. Bulk metallic glasses containing multiple alloying elements constitute a new and exciting class of metallic materials with attractive mechanical, chemical, and magnetic properties for structural and functional use. Recent development indicates that bulk metallic glasses with high glass forming ability can be readily produced by conventional melting and casting techniques.
NTIS
*Alloying; Casting; Oxidation Resistance; Functionals; Metallic Glasses*

**20010119422** Brookhaven National Lab., Upton, NY USA
**Dependence of Total Hemispherical Emissivity of Inconel-718 on Surface Oxidation and Temperature**
Greene, G. A.; Sep. 01, 1999; 30p; In English
Report No.(s): DE2000-750781; BNL-52579; No Copyright; Avail: Department of Energy Information Bridge

Total hemispherical emissivities were measured for Inconel-718 as a function of sample temperature. Measurements were made with both unoxidized and oxidized samples. The oxidation temperatures were 1000 C, 1100 C, and 1142 C and the oxidation times were 15, 30, and 60 minutes. The oxidized samples showed a significant increase in emissivity over the unoxidized one which was in an as received condition. No apparent pattern was observed in the change of emissivity as a function of oxidation time at a given oxidation temperature. In some cases, emissivity measurements made with increasing temperature were greater than those made with descending temperature. One possible explanation for this is the spalling of the oxide layer as the sample area changed (contracted) with descending sample temperature.
NTIS
*Emissivity; Inconel (Trademark); Oxidation*

**20010119568** Department of Energy, Richland Operations Office, Richland, WA USA
**Final Report for Interim Stabilization of 116-KE-4 and 116-KW-3 Contamination Areas**
Mahood, R. O.; Aug. 20, 1999; 18p; In English
Report No.(s): DE2001-10504; BHI-01290-REV-0; No Copyright; Avail: Department of Energy Information Bridge, Microfiche

The 116-KE-4 and 116-KW-3 sites, which are also known as 107-KE and 107-KW, are located in the 100-K Area of the Hanford Site. Each site included five contamination areas (CA). This report discusses the interim stabilization of the 10 CAs. The work consisted primarily of earth moving. Cutting the steel pipelines and scrap and disposal of the material at the Environmental Restoration Disposal Facility was necessary to complete interim stabilization.
NTIS
*Pipelines; Scrap; Radioactive Wastes; Waste Disposal*

**20010119602** Lehigh Univ., Materials Research Center, Bethlehem, PA USA
**Grain Boundary Chemistry and Creep Resistance of Alumina** ***Final Report, 1 Sep. 1999-31Mar. 2110***
Harmer, Martin P.; Chan, Helen M.; Rickman, Jeffrey M.; Mar. 2001; 123p; In English
Contract(s)/Grant(s): F49620-98-1-0117
Report No.(s): AD-A394927; No Copyright; Avail: CASI; A06, Hardcopy; A02, Microfiche
The Lehigh group has pioneered work on the role of segregating rare earth dopants on the grain boundary structure and tensile creep behavior of alumina. In an attempt to clarify the exact mechanism that controls creep behavior of the doped aluminas, various advanced characterization techniques have been applied including: secondary ion mass spectrometry (SIMS), scanning transmission electron microscopy (STEM), orientation image microscopy (OIM), x-ray absorption studies which include x-ray absorption near edge structure (XANES) and extended x-ray absorption fine structure (EXAFS), and atomistic computer simulation and studies of the creep kinetics. Combined use of high resolution STEM and EXAFS allowed the determination of the dopant grain boundary segregation behavior and the atomic structural environment around the grain boundary segregated dopant ions.
DTIC
*Aluminum Oxides; Creep Strength; Tensile Creep; Grain Boundaries; Creep Properties*

**20010119987** Argonne National Lab., IL USA
**Effects of LWR coolant environments on fatigue lives of austenitic stainless steels**
Chopra, O. K.; Jan. 13, 1998; 14p; In English
Report No.(s): DE2001-10546; ANL/ET/CP-95218; No Copyright; Avail: Department of Energy Information Bridge
Fatigue tests have been conducted on Types 304 and 316NG stainless steels to evaluate the effects of various material and loading variables, e.g., steel type, strain rate, dissolved oxygen (DO) in water, and strain range, on the fatigue lives of these steels. The results confirm significant decreases in fatigue life in water. Unlike the situation with ferritic steels, environmental effects on Types 304 and 316NG stainless steel are more pronounced in low-DO than in high-DO water. Experimental results have been compared with estimates of fatigue life based on a statistical model. The formation and growth of fatigue cracks in air and water environments are discussed.
NTIS
*Austenitic Stainless Steels; Coolants; Ferrous Metals; Pressure Vessels; Environment Effects*

**20010119996** Department of Energy, Operations Office, Richland, WA USA
**Interim Stabilization of 116-KE-4 and 116-KW-3 Effluent Pipeline Contamination Areas** ***Final Report***
Mahood, R. O.; Aug. 20, 1999; 53p; In English
Report No.(s): DE2001-10505; BHI-01295-Rev-0; No Copyright; Avail: Department of Energy Information Bridge
The 116-KE-4 and 116-KW-3 sites, also known as 107-KE and 107-KW,are located in the 100-K Area of the Hanford Site. A trench in a contamination area (CA) at the 116-KE-4 site contained 255 m (837 ft) of 1.8-m (6-ft)-diameter steel effluent pipeline. This report describes the cutting of the steel pipelines and scrap and disposal of the material at the Environmental Restoration Disposal Facility. After the steel pipelines, scrap metal, and debris were removed, interim stabilization of the CAsat 116-KE-4 and 116-KW-3 was completed by covering the CAs with clean-fill and downposting to underground radioactive material areas.
NTIS
*Pipelines; Radioactive Materials; Stabilization; Steels; Scrap*

**20010120004** Sandia National Labs., Albuquerque, NM USA
**Determination of Solid-State Sulfidation Mechanisms in Ion-Implanted Copper**
Barbour,; Braithwaite,; Wright,; Sep. 19, 2000; 17p; In English
Report No.(s): DE2000-763115; SAND2000-2302C; No Copyright; Avail: Department of Energy Information Bridge, Microfiche

Global Nuclear Materials Management (GNMM) is a concept that envisions a dynamic and transparent framework to assure that all nuclear materials in the world - whether in civilian or military programs - are being used legitimately, safely, and security. The concept of such a system built on national and international programs has gained increasing attention and acceptance over the last year. Senior officials and scientists in the USA and key international organizations have acknowledged the urgent need to transparently ensure this responsible management of nuclear materials worldwide, from cradle to grave. They have recognized that to meet this need, all states possessing nuclear materials, whatever their policy towards nuclear power and nuclear weapons may be, must help build and subscribe to a system of effective, durable, and consistent minimum standards for nuclear materials management.
NTIS
*Solid State; Sulfidation; Ion Implantation; Copper*

**20010120015** Argonne National Lab., IL USA
**Kinetics of high temperature oxidation of copper foils: A quantitative in situ QEXAFS investigation**
Hilbrandt, N.; Mar. 05, 1998; 4p; In English
Report No.(s): DE2001-10670; ANL/CHM/CP-95788; No Copyright; Avail: Department of Energy Information Bridge
Based on previous results (1) further details of the oxidation of copper foil 2 Cu + O(sub 2) (r-arrow) 2 CuO were resolved using high quality, high temperature Cu(sub 2)O and CuO standards for Cu-K XAFS and Cu-K PCA (2) analysis. These were prepared from copper foils using the same experimental techniques as for the oxidation under study. As the reaction can be divided into a step-wise oxidation mechanism: 2 Cu + 0.5 O(sub 2) (r-arrow)Cu(sub 2)O; Cu(sub 2)O + 0.5 O(sub 2) (r-arrow) 2 CuO, we attempted to check whether the formation of CuO is kinetically inhibited (delayed) or whether it takes place simultaneously to the formation of Cu(sub 2)O. to achieve an optimal time resolution the QEXAFS technique (3) was applied. This investigation was completed by X Ray Diffraction (XRD) and Scanning Electron Microscopy (SEM) investigations on samples quenched within the oxidation period.
NTIS
*Copper Oxides; High Temperature; Metal Foils; Oxidation; Reaction Kinetics; Quantitative Analysis*

**20010120019** Argonne National Lab., IL USA
**Fracture and creep of an Al2O3-SiC(whisker-)TiC(particle) composite**
DeArellano-Lopez, A. R.; Feb. 25, 1998; 20p; In English
Report No.(s): DE2001-10659; ANL/ET/CP-95765; No Copyright; Avail: Department of Energy Information Bridge
High-temperature fracture strength and compressive creep of an electrodischarge-machinable composite, Al(sub 2)O(sub 3)-30.9 vol.% SiC whiskers-23 vol.% TiC particles have been studied to 1200 C and 1450 C, respectively, in inert atmosphere. Microstructures of fractured and deformed specimens were examined by scanning and transmission electron microscopy. Fast fracture occurred at T (le) 1200 C. Steady-state creep was achieved for T > 1350 C at stresses < 80 MPa, with the rate-controlling mechanism being partially unaccommodated grain-boundary sliding, with a stress exponent of (approx)1 and an activation energy of (approx)470 kJ/mol.
NTIS
*Aluminum Oxides; Creep Properties; Fracture Strength; Composite Materials; Silicon Carbides*

**20010120061** Sandia National Labs., Albuquerque, NM USA
**Constitutive Model Development for Predicting Thermal Mechanical Fatigue Deformation in Solder Interconnects**
Vianco,; Neilsen,; Fossum,; Burchett,; Sep. 18, 2000; 12p; In English
Report No.(s): DE2000-763110; SAND2000-2290C; No Copyright; Avail: Department of Energy Information Bridge, Microfiche
A unified creep-plasticity (UCP) model was developed to describe the deformation of 97In-3Ag (wt. percent) solder for the purpose of predicting thermal mechanical fatigue in electronic interconnects. The UCP model uses a hyperbolic sine function of effective stress in its kinetic equation for the inelastic strain rate.
NTIS
*Solders; Deformation; Thermal Fatigue*

**20010120081** Sandia National Labs., Albuquerque, NM USA
**Determiniation of Thermal Conductivity of 304 Stainless Steel Using Parameter Estimation Techniques**
Blackwell, B. F.; Gill, W.; Dowding, K. J.; Voth, T. E.; Jun. 27, 2000; 10p; In English
Report No.(s): DE2000-760791; SAND2000-1563C; No Copyright; Avail: Department of Energy Information Bridge

Sensitivity coefficients were analyzed in order to guide the design of an experiment to estimate the thermal conductivity of 304 stainless steel. The uncertainty on the temperature measurements was estimated by several means and its impact on the estimated conductivity is discussed. The estimated thermal conductivity of 304 stainless steel is consistent with results from other sources. Sensitivity coefficients were analyzed in order to guide the design of an experiment to estimate the thermal conductivity of 304 stainless steel. The uncertainty on the temperature measurements was estimated by several means and its impact on the estimated conductivity is discussed. The estimated thermal conductivity of 304 stainless steel is consistent with results from other sources.

NTIS

*Stainless Steels; Thermal Conductivity; Parameter Identification*

**20010120541** Argonne National Lab., IL USA

**Refracted X-ray Fluorescence (RXF) applied to the study of thermally grown oxide scales on Fe-Cr-Ni-(RE) alloys**

Koshelev, I.; Jun. 03, 1998; 15p; In English

Report No.(s): DE2001-10678; ANL/MSD/CP-95845; No Copyright; Avail: Department of Energy Information Bridge

Refracted X-Ray Fluorescence (RXF) is applied to the study of the thermally grown scales on Fe25Cr20Ni(RE) alloys. The evolution of chromia scales is investigated for alloys containing reactive elements (RE) Y and Zr as well as the corresponding RE-free alloy. For these alloys, scale compositions, scale thicknesses and growth rates are measured and information about concentration depth profiles is obtained.

NTIS

*Reactivity; Oxides; X Ray Fluorescence; Alloys*

**20010120558** Argonne National Lab., IL USA

**Magnetic Anisotropy and its Microstructural Origin in Epitaxially Grown SmCo Thin Films**

Benaissa, M., Argonne National Lab., USA; Apr. 15, 1998; 6p; In English

Report No.(s): DE2001-10734; ANL/MSD/CP-96112; No Copyright; Avail: Department of Energy Information Bridge, Microfiche

Microstructural features and magnetic behavior of epitaxially grown SmCo thin films with very high in-plane anisotropy are presented. Transmission electron microscopy was used to characterize the microstructure while magnetic measurements were performed using dc and SQUID magnetometers. Two substrate orientations were studied, i.e., MgO(100)/Cr(100)/SmCo(11(bar 2)0) and MgO(110)/Cr(211)/SmCo(1(bar 1)00). In the former, the SmCo(11(bar 2)0) film shows a bicrystalline microstructure, whereas in the latter, a uniaxial one is observed. Both microstructure consist of grains with a mixture of SmCo(sub 3) , Sm(sub 2)Co(sub 7) and SmCo(sub 3) polytypoids. A deviation from the c-axes was observed in the in-plane anisotropy of the SmCo(11(bar 2)0) thin film. A strong exchange interaction between the grains would, in principle, explain the observed deviation. On the other hand, both SmCo(11(bar 2)0) and (1(bar 1)00) thin films show very high coercivity values with pinning-type characteristics. Possible coercivity mechanisms related to intergranular exchange interactions and local variation in magnetocrystalline anisotropy constants are discussed.

NTIS

*Samarium Compounds; Cobalt Alloys; Anisotropy; Microstructure; Magnetic Properties*

**20010120846** Johns Hopkins Univ., Dept. of Mechanical Engineering, Baltimore, MD USA

**Experimental Determination of Dislocation Core Structures by HRTEM** ***Final Report, 4 Apr. - 31 Jul. 2001***

Hemker, Kevin J.; Chen, Mingwei; Jul. 2001; 8p; In English

Contract(s)/Grant(s): F49620-98-1-0208

Report No.(s): AD-A395178; AFRL-SR-BL-TR-01-0508; No Copyright; Avail: CASI; A02, Hardcopy; A01, Microfiche

The overarching scientific goal of this study is to use state-of-the-art TEM techniques to experimentally characterize dislocation core structures in metals and alloys at the atomic scale. The past year has involved the culmination of efforts on intermetallic alloys and pure fcc metals and the development of new techniques for the study of bcc metals and alloys. Our work on (Ni, Fe)3 Ge indicated that changes in mechanical behavior associated with Fe additions are related to variations in dislocation core geometry and its effect on dislocation mobility. These findings have both motivated and been found to be in agreement with first principles based calculations of dislocation core structures in these alloys. In a related study, our weak-beam TEM and HREM experimental observations of dislocation core structures in fcc gold and iridium have been shown to be in excellent agreement with theoretical predictions for these metals. More recent efforts have focused on developing the techniques for characterizing dislocation core structures in bcc metals. Direct HREM observations of dislocation cores and the derivation of localized electron

structure data from electron energy loss spectra (EELS) measurements are long term goals, and preliminary steps toward these challenging tasks are underway.
DTIC
*Atomic Energy Levels; Metals; Body Centered Cubic Lattices; Electron Energy; Energy Dissipation*

**20010121495** Argonne National Lab., IL USA
**Phase formation in Zr/Fe multilayers during Kr ion irradiation**
Motta, A. T.; Jan. 29, 1998; 9p; In English
Report No.(s): DE2001-10587; ANL/MSD/CP-95489; No Copyright; Avail: Department of Energy Information Bridge, Microfiche

A detailed study has been conducted of the effect of Kr ion irradiation on phase formation in Zr-Fe metallic multilayers, using the Intermediate Voltage Electron Microscope (IVEM) at Argonne National Laboratory. Metallic multilayers were prepared with different overall compositions (near 50-50 and Fe-rich), and with different wavelengths (repetition thicknesses). These samples were irradiated with 300 keV Kr ions at various temperatures to investigate the final products, as well as the kinetics of phase formation. For the shorter wavelength samples, the final product was in all cases an amorphous Zr-Fe phase, in combination with Fe, while specially for the larger wavelength samples, in the Fe-rich samples the intermetallic compounds ZrFe(sub 2) and Zr(sub 3)Fe were formed in addition to the amorphous phase. The dose to full reaction decreases with temperature, and with wavelength in a manner consistent with a diffusion-controlled reaction.
NTIS
*Zirconium Alloys; Ion Irradiation*

**20010121528** Brookhaven National Lab., Upton, NY USA
**Resonant x-ray scattering from the surface of a dilute liquid Hg-Au alloy**
Dimasi, E.; Nov. 29, 1999; 6p; In English
Report No.(s): DE2000-752148; BNL-67125; No Copyright; Avail: Department of Energy Information Bridge

Surfaces play an important role in nucleating bulk phases in solid alloys, and because of the reduced atomic coordination, surface often exhibit structure and phase behavior distinct from that of the bulk. Liquid metal alloys can be expected to exhibit an even richer variety of surface phases: since the particles are not constrained to lattice sites, the composition at the surface can vary dramatically from that of the bulk. With the application of surface sensitive x-ray scattering techniques to the liquid metal-vapor interface, a number of liquid metal alloys have in fact been shown to exhibit interesting structural phenomena, such as surface segregation and microscopic precursors to wetting, that previously could be only theoretically predicted or indirectly inferred from experiment.
NTIS
*Gold Alloys; Mercury Alloys; X Ray Diffraction; Liquid Alloys*

**20010121536** NASA Ames Research Center, Moffett Field, CA USA
**Ab Initio Calculations Applied to Problems in Metal Ion Chemistry**
Bauschlicher, Charles W., Jr., NASA Ames Research Center, USA; Langhoff, Stephen R., NASA Ames Research Center, USA; Partridge, Harry, NASA Ames Research Center, USA; [1994]; 1p; In English; Third Symposium on Reactions Between Hydrocarbons and Metal Atoms, 30 May - 1Jun. 1994, Oslo, Norway
Contract(s)/Grant(s): RTOP 232-01-04; No Copyright; Avail: Issuing Activity; Abstract Only

Electronic structure calculations can provide accurate spectroscopic data (such as molecular structures) vibrational frequencies, binding energies, etc.) that have been very useful in explaining trends in experimental data and in identifying incorrect experimental measurements. In addition, ab initio calculations. have given considerable insight into the many interactions that make the chemistry of transition metal systems so diverse. In this review we focus on cases where calculations and experiment have been used to solve interesting chemical problems involving metal ions. The examples include cases where theory was used to differentiate between disparate experimental values and cases where theory was used to explain unexpected experimental results.
Author
*Metal Ions; Electronic Structure; Transition Metals*

**20010122230** Argonne National Lab., IL USA

**Structural and magnetic studies of fcc Fe films with self-organized lateral modulation on striped Cu(110)-O(2x1) substrates**

Li, D.; Sep. 21, 1998; 15p; In English

Report No.(s): DE2001-10830; ANL/MSD/CP-96581; No Copyright; Avail: Department of Energy Information Bridge

Fcc Fe wedges of 0-12 monolayer (ML) were grown by means of molecular beam epitaxy onto a novel substrate: flat Cu(110) with an oxygen-induced, long-range ordered striped phase, and studied in-situ with medium energy electron diffraction (MEED) and the surface magneto-optical Kerr effect (SMOKE). In contrast to Fe growth on either clean or oxygen-saturated Cu(110), the films on the striped substrates retain a layer-by-layer growth mode up to 6-7 ML and are fcc at least up to 12 ML. In addition, satellite peaks were observed on both sides of the MEED (0,0) streak, indicating a long-range-ordered lateral modulation of the Fe surface. We postulate that the Fe films grow conformally onto the original striped substrate. SMOKE studies show that these fcc Fe wedges are ferromagnetic with an easy axis along the original stripes for Fe thickness 4ML and a remnant magnetization that increases linearly with thickness beyond 4 ML.

NTIS

*Magnetic Materials; Substrates; Molecular Beam Epitaxy*

**20010122249** Argonne National Lab., IL USA

**Effect of low dose-rate irradiation on the microstructure of 304 stainless steel**

Cole, J. I.; Dec. 02, 1998; 9p; In English

Report No.(s): DE2001-10831; ANL/ED/CP-96583; No Copyright; Avail: Department of Energy Information Bridge

Changes in mechanical and corrosion properties caused by the development of radiation-induced microstructure have relevance to the aging and lifetime extension of light water reactors (LWR's). However, much of the current data related to microstructural development in irradiated metals are generated from studies carried out at much higher dose-rates than encountered in LWR's. An opportunity exists to study the influence of low dose-rate irradiation on microstructural development for a variety of structural and surveillance materials extracted from the experimental breeder reactor EBR-II. In this study, irradiated 304 stainless steel hexagonal 'hex' duct material is examined in order to compare microstructure in the dose-rate range of 10(exp -7)-10(exp -9) dpakec. The samples, taken from the reflector locations in EBR-II, experienced a total dose between 10 and 12 dpa at a temperature of (approximately)375 C. Transmission electron microscopy (TEM) results reveal that there is a moderate dose-rate effect on microstructural development for samples irradiated in the range of 2 x 10(exp -8) to 4 x 10(exp -8) dpa/sec, however a substantial dose rate-effect exists between dose-rates of 2 x 10(exp -8) and 1 x 10(exp -9) dpa/sec Transmission electron microscopy (TEM) results will detail the development of the microstructure in terms of radiation-induced cavities, dislocations, and precipitates.

NTIS

*Radiation Dosage; Microstructure; Stainless Steels; Radiation Effects*

**20010122256** Argonne National Lab., IL USA

**Surface alloying of silicon into aluminum substrate**

Xu, Z.; Oct. 28, 1998; 11p; In English

Report No.(s): DE2001-10806; ANL/TD/CP-96466; No Copyright; Avail: Department of Energy Information Bridge, Microfiche

Aluminum alloys that are easily castable tend to have lower silicon content and hence lower wear resistance. The use of laser surface alloying to improve the surface wear resistance of 319 and 320 aluminum alloys was examined. A silicon layer was painted onto the surface to be treated. A high power pulsed Nd:YAG laser with fiberoptic beam delivery was used to carry out the laser surface treatment to enhance the silicon content. Process parameters were varied to minimize the surface roughness from overlap of the laser beam treatment. The surface-alloyed layer was characterized and the silicon content was determined.

NTIS

*Alloying; Silicon; Surface Treatment; Aluminum Alloys*

**20010122257** Argonne National Lab., IL USA

**Laser beam welding of AZ31B-H24 magnesium alloy**

Leong, K. H.; Sep. 29, 1998; 11p; In English

Report No.(s): DE2001-10805; ANL/TD/CP-96465; No Copyright; Avail: Department of Energy Information Bridge, Microfiche

The laser beam weldability of AZ31B magnesium alloy was examined with high power CW CO2 and pulsed Nd:YAG lasers. The low viscosity and surface tension of the melt pool make magnesium more difficult to weld than steel. Welding parameters necessary to obtain good welds were determined for both CW CO2 and pulsed Nd:YAG lasers. The weldability of the magnesium alloy was significantly better with the Nd:YAG laser. The cause of this improvement was attributed to the higher absorption of the Nd:YAG beam. A lower threshold beam irradiance was required for welding, and a more stable weldpool was obtained.
NTIS
*Carbon Dioxide Lasers; YAG Lasers; Neodymium Lasers; Magnesium Alloys; Welding*

**20010122262** Argonne National Lab., IL USA
**Tensile Impact Properties of Vanadium-Base Alloys Irradiated at Less Than 430 C**
Chung, H. M.; May 18, 1998; 11p; In English
Report No.(s): DE2001-10796; ANL/ET/CP-96420; No Copyright; Avail: Department of Energy Information Bridge, Microfiche
Tensile and impact properties were investigated at 430 C on V-Cr-Ti, V-Ti-Si, and V-Ti alloys after irradiation to approximately 2-46 dpa at 205-430 C in lithium or helium in the Fast Flux Test Facility (FFTF), High Flux Isotope Reactor (HFIR), Experimental Breeder Reactor II (EBR-II), and Advanced Test Reactor (ATR). A 500-kg heat of V-4Cr-4Ti exhibited high ductile-brittle transition temperature and minimal uniform elongation as a result of irradiation-induced loss of work-hardening capability. Work-hardening capabilities of 30- and 100-kg heats of V-4Cr-4Ti varied significantly with irradiation conditions, although the 30-kg heat exhibited excellent impact properties after irradiation at approximately 390-430 C. The origin of the significant variations in the work-hardening capability of V-4Cr-4Ti is not understood, although fabrication variables, annealing history, and contamination from the irradiation environment are believed to play important roles. A 15-kg heat of V-3Ti-1Si exhibited good work-hardening capability and excellent impact properties after irradiation at approximately 390-430 C. Helium atoms, either charged dynamically or produced via transmutation of boron in the alloys, promote work-hardening capability in V-4Cr-4Ti and V-3Ti-1Si.
NTIS
*Ductile-Brittle Transition; Irradiation; Tensile Properties; Titanium Alloys; Vanadium Alloys; Work Hardening*

**20010122292** Defence Science and Technology Organisation, Airframes and Engines Div., Fishermans Bend, Australia
**An Experimental Study of the Relationship Between Electrical Conductivity and Early Fatigue Damage in A12024**
Rajic, N., Defence Science and Technology Organisation, Australia; Burke, S. K., Defence Science and Technology Organisation, Australia; Galea, S. C., Defence Science and Technology Organisation, Australia; July 2001; 20p; In English; Original contains color illustrations
Report No.(s): DSTO-TN-0387; DODA-AR-011-963; Copyright; Avail: Issuing Activity
An experimental study is described that explores the feasibility of detecting fatigue damage at the pre-macrocrack stage on the basis of electrical conductivity measurements made with a commercial eddy current instrument. Tests on dog-bone specimens fabricated from A12024-T4 showed no significant change in conductivity with exposure to sustained cyclic loading. These results point to a low prospect for success in using conventional eddy-current methods to measure electrical conductivity for the routine detection of pre-macrocrack fatigue damage in A12024.
Author
*Electrical Resistivity; Crack Propagation; Alloys; Cyclic Loads*

**20010122295** Defence Science and Technology Organisation, Airframes and Engines Div., Fishermans Bend, Australia
**Thermographic Assessment of the Heat Dissipation Associated with Fatigue Crack Growth in Mild Steel**
Rajic, N., Defence Science and Technology Organisation, Australia; August 2001; 32p; In English; Original contains color illustrations
Report No.(s): DSTO-TR-1190; DODA-AR-011-962; Copyright; Avail: Issuing Activity
This report examines the feasibility of predicting rates of crack growth in mild steel based on an evaluation of the crack tip dissipated energy. A numerical scheme is developed to provide a basis for the computation of dissipated power from measurements of temperature acquired using remote infrared detection. An experimental study is then described where measurements of crack-growth rate in mild-steel coupons exposed to constant amplitude cyclic loading are related to calculations of power dissipation. A simple linear relationship is indicated, with testing also providing some evidence of geometry independence, a key finding with regard to the possible use of dissipated energy as a fatigue characterisation parameter. However,

further testing involving a more complex loading sequence led to a noticeable change in relationship indicating that the heat dissipation rate is unlikely to offer a simple basis for the prediction of crack growth rate under all loading conditions.
Author
*Feasibility Analysis; Crack Propagation; Steels; Numerical Analysis; Computation*

**20010122303** Argonne National Lab., IL USA
**Environmental Effects on Fatigue Crack Initiation in Piping and Pressure Vessel Steels**
Chopra, O. K.; Aug. 02, 2000; 15p; In English
Report No.(s): DE2000-761238; ANL/ET/CP-101179; No Copyright; Avail: Department of Energy Information Bridge

The ASME Boiler and Pressure Vessel Code provides rules for the construction of nuclear power plant components. An appendix of the Code specifies fatigue design curves for structural materials. However, the effects of light water reactor (LWR) coolant environments are not explicitly addressed by the Code design curves. Test data illustrate potentially significant effects of LWR environments on the fatigue resistance of carbon and low-alloy steels and austenitic stainless steels. This paper summarizes the work performed at Argonne National Laboratory on the fatigue of piping and pressure vessel steels LWR coolant environments. The existing fatigue S-N data have been evaluated to establish the effects of various material and loading variables, such as steel type, strain range, strain rate, temperature, and dissolved-oxygen level in water, on the fatigue lives of these steels. Statistical models are presented for estimating the fatigue S-N curves for carbon and low-alloy steels and austenitic stainless steels as a function of materials, loading, and environmental variables. Methods for incorporating environmental effects in the ASME Code fatigue evaluations are discussed. Differences between the methods and their impact on the design fatigue curves are also discussed.
NTIS
*Crack Initiation; Fatigue (Materials); Light Water Reactors*

**20010122359** Argonne National Lab., IL USA
**Microstructural examination of irradiated V-(4-5%)Cr-(4-5%)Ti**
Gelles, D. S.; May 04, 1998; 14p; In English
Report No.(s): DE2001-10761; ANL/ET/CP-96361; No Copyright; Avail: Department of Energy Information Bridge, Microfiche

Microstructural examination results are reported for two heats of V-(4-5%) Cr-(4-5%)Ti irradiated in the EBR-II X530 experiment to 4.5 dpa at (approximately)400 C to provide an understanding of the microstructural evolution that may be associated with degradation of mechanical properties. Fine precipitates were observed in high density intermixed with small defect clusters for all conditions examined following the irradiation. The irradiation-induced precipitation does not appear to be affected by preirradiation heat treatment at 950-1125 C. There was no evidence for a significant density of large (diameter >10 nm) dislocation loops or network dislocations. Analytical investigations successfully demonstrated that the precipitates were enriched in titanium, depleted in vanadium and contained no nitrogen. These results are discussed in terms of future alloy development options.
NTIS
*Vanadium Alloys; Chromium Alloys; Titanium Alloys; Irradiation; Microstructure*

**20010122379** Argonne National Lab., IL USA
**Microstructure of V-4Cr-4Ti alloy after low-temperature irradiation by ions and neutrons**
Gazda, J.; Apr. 01, 1998; 8p; In English
Report No.(s): DE2001-10714; ANL/ET/CP-96042; No Copyright; Avail: Department of Energy Information Bridge, Microfiche

Recent interest in the application of a V-4Cr-4Ti alloy in the ITER prompted an investigation of the effects of low-to-moderate temperature irradiation (less than 420 C) on the alloy's mechanical properties. Two sets of experiments were conducted. The effects of fast neutron irradiation to (approx-equal)4 dpa at 390 C were investigated in the X530 experiment in the EBR-II reactor. Irradiation with single (4.5-MeV Ni(sup 2)) and dual ion beams (350-keV He(sup +) simultaneously with 4.5-MeV Ni(sup 2)) complemented this study. TEM observations showed the formation of a high density of point-defect clusters and dislocation loops (less than nm diameter) distributed uniformly in both types of specimens. Mechanical property testing of neutron irradiated material showed embrittlement of the alloy. The deformed microstructure were examined by TEM to determine the causes of embrittlement and revealed dislocation channels propagating through the undeformed matrix. The channels are the sole slip paths and they cause early onset of necking and loss of work-hardening. Based on a review of the available literature, suggestions are made for further research of slip localization in V-4Cr-4Ti alloys.
NTIS
*Chromium Alloys; Titanium Alloys; Irradiation; Mechanical Properties; Microstructure*

**20010122479** Argonne National Lab., IL USA

**Mechanical Properties and Microstructural Characteristics of Laser and Electron-Beam Welds in V-4Cr-4Ti**

Chung, H. M.; May 18, 1998; 11p; In English

Report No.(s): DE2001-10797; ANL/ET/CP-96421; No Copyright; Avail: Department of Energy Information Bridge, Microfiche

Mechanical properties and microstructural characteristics of laser and electron-beam welds of a 500-kg heat of V4Cr4Ti were investigated in as-welded condition and after postwelding heat treatment by impact testing, microhardness measurement, optical microscopy, X-ray diffraction, and transmission electron microscopy (TEM). Ductile-brittle transition temperatures of the laser and electron-beam welds were significantly higher than that of the base metal. However, excellent impact properties could be restored in both types of welds by postwelding annealing at 1000 C for one hour in vacuum. Analysis by TEM revealed that annealed weld zones were characterized by extensive networks of fine V(C,O,N) precipitates, which clean away O, C, and N interstitial from the grain matrices. This process is accompanied by simultaneous annealing-out of the dense dislocations present in the weld zone. This finding could be useful in identifying an optimal welding procedure by controlling and adjusting the cooling rate of the weld zone by an innovative method to maximize the precipitation of V(C,O,N).

NTIS

*Heat Treatment; Mechanical Properties; Microstructure; Vanadium Alloys*

**20010123062** Argonne National Lab., IL USA

**Development and compatibility of magnesium matrix fuel plates clad with 6061 aluminum alloy**

Wiencek, T. C.; Oct. 22, 1998; 15p; In English

Report No.(s): DE2001-11078; ANL/ET/CP-97559; No Copyright; Avail: Department of Energy Information Bridge, Microfiche

Aluminum (Al) is a commonly used matrix for research reactor fuel plates. It has been found that a reaction between the fuel and the aluminum matrix may reduce or increase the irradiation stability of the fuel. to further understand the contribution of the reaction to the irradiation stability, experiments to develop a non-reacting matrix were performed. The work focused on magnesium (Mg), which is an excellent non-reacting matrix candidate and has a neutron absorption coefficient similar to Al. to avoid the formation of a liquid Al/Mg phase, improvements were made to the roll bonding process to achieve acceptable bonding at 415 C. After these methods were developed, fuel plates were produced with two fuels, uranium (U)-2 w/o molybdenum (Mo) and U-10-w/o Mo with two matrices, Al and Mg. A reaction between the magnesium and the 6061 Al cladding was discovered to take place during the processing at 415 C. to minimize the amount of reaction, methods were successfully developed to roll bond the fuel plates at 275 C. No reaction zone was observed in fuel plates processed at 275 C. Using this method, fuel plates with a Mg matrix are planned to be fabricated and included in the next irradiation matrix for the RERTR high density fuel development program.

NTIS

*Aluminum Alloys; Fuels; Irradiation; Magnesium; Nuclear Reactors*

**20010123211** Argonne National Lab., IL USA

**Synthesis and casting of a lithium-bismuth compound for an ion-replacement electrorefiner**

McDeavitt, S. M.; Nov. 23, 1998; 6p; In English

Report No.(s): DE2001-10893; ANL/CMT/CP-96844; No Copyright; Avail: Department of Energy Information Bridge, Microfiche

The intermetallic compound Li(sub 3)Bi played an integral part in the demonstration of an ion replacement electrorefining method developed at Argonne National Laboratory. The Li(sub 3)Bi compound was generated in a tilt-pour casting furnace using high-purity lithium and bismuth metals as the initial charge. At first, small-scale ((approximately) 20 g) experiments were conducted to determine the materials synthesis parameters. In the end, four larger-scale castings (500 g to 1250 g) were completed in a tantalum crucible. The metals were heated slowly to melt the charge, and the formation reaction proceeded vigorously above the melting point of bismuth ((approximately) 270 C). For the large-scale melts, the furnace power was temporarily turned off at this point. After several minutes, the tantalum crucible stopped glowing, and the furnace power was turned on. The temperature was then increased to (approximately) 1200 C to melt and homogenize the compound, and liquid Li(sub 3)Bi was cast into cold stainless steel molds. Approximately 3.7 kg of Li(sub 3)Bi was generated by this method.

NTIS

*Casting; Lithium Compounds; Bismuth Compounds*

**20010123223** Sandia National Labs., Albuquerque, NM USA

**Uncertainty Estimation in the Determination of Thermal Conductivity of 304 Stainless Steel**

Blackwell, B. F.; Gill, W.; Dowding, K. J.; Easterling, R. G.; Sep. 27, 2000; 12p; In English

Report No.(s): DE2000-764054; SAND2000-2379C; No Copyright; Avail: Department of Energy Information Bridge

The thermal conductivity of 304 stainless steel has been estimated from transient temperature measurements and knowing the volumetric heat capacity. Sensitivity coefficients were used to guide the design of this experiment as well as to estimate the confidence interval in the estimated thermal conductivity. The uncertainly on the temperature measurements was estimated by several means, and its impact on the estimated conductivity is discussed. The estimated thermal conductivity of 304 stainless steel is consistent with results from other sources.

NTIS

*Stainless Steels; Thermal Conductivity*

**20010123224** Sandia National Labs., Albuquerque, NM USA

**Equation of State Measurements of Materials Using a Three-Stage Gun to Impact Velocities of 11km/s**

Reinhart, W. D.; Chhabildas, L. C.; Carroll, D. E.; Thornhill, T. G.; Winfree, N. A.; Sep. 26, 2000; 15p; In English

Report No.(s): DE2000-764037; SAND2000-2370C; No Copyright; Avail: Department of Energy Information Bridge

Understanding high pressure behavior of homogeneous as well as heterogeneous materials is necessary in order to address the physical processes associated with hypervelocity impact events related to space science applications including orbital debris impact and impact lethality. At very high impact velocities, material properties will be subjugated to phase-changes, such as melting and vaporization. These phase states cannot be obtained through conventional gun technology. These processes need to be represented accurately in hydrodynamic codes to allow credible computational analysis of impact events resulting from hypervelocity impact. In this paper, techniques that are being developed and implemented to obtain the needed shock loading parameters (Hugoniot states) for material characterization studies, namely shock velocity and particle velocity, will be described at impact velocities up to 11 km/s. What is new in this report is that these techniques are being implemented for use at engagement velocities never before attained utilizing two-stage light-gas gun technology.

NTIS

*Light Gas Guns; Mechanical Properties; Impact Tests; Hypervelocity Impact; Equations of State*

**20010123261** Brookhaven National Lab., Upton, NY USA

**Phonon precursors of martensitic transformations**

Shapiro, S. M.; Aug. 17, 2000; 2p; In English

Report No.(s): DE2000-767293; BNL-67659; No Copyright; Avail: Department of Energy Information Bridge

All shape memory materials (SMM) undergo a Martensitic transformation and many, but not all, exhibit anomalies in their phonon dispersion curves in the high temperature Austentic phase. These anomalies are precursors to the transformation since the atomic displacements associated with the anomalous phonon are nearly identical to that necessary to transform the material from the Austentic to Martensitic phase.

NTIS

*Phonons; Martensitic Transformation; Shape Memory Alloys*

**20010123405** Oak Ridge National Lab., TN USA

**Effect of Surface Condition and Heat Treatment on Corrosion of Type 316L Stainless Steel in a Mercury Thermal Convection Loop**

Pawel, S. J.; DiStefano, J. R.; Manneschmidt, E. T.; Jul. 01, 2000; 46p; In English

Report No.(s): DE2001-769298; ORNL/TM-2000/195; No Copyright; Avail: Department of Energy Information Bridge

Two thermal convection loops (TCLs) fabricated from 316L stainless steel and containing mercury and a variety of 316L coupons representing variable surface conditions and heat treatments have been operated continuously for 2000 hours. Surface conditions included surface ground, polished, gold-coated, chemically etched, bombarded with Fe to simulate radiation damage, and oxidized. Heat treatments included solution treated, welded, and sensitized. In addition, a nitrogen doped 316L material, termed 316LN, was also examined in the solution treated condition. Duplicate TCLs were operated in this experiment, both were operated with a 305 C peak temperature, a 65 C temperature gradient, and mercury velocity of 1.2 m/min, but only one included a 36 h soak in Hg at 310 C just prior to operation to encourage wetting. Results indicate that the soak in Hg at 310 C had no lasting effect on wetting or compatibility with Hg. Further, based on examination of post-test wetting and coupon weight loss, only the

gold-coated surfaces revealed significant interaction with Hg. In areas wetted significantly by Hg, the extreme surface of the stainless steel (ca 10 micrometers) was depleted in Ni and Cr compared to the bulk composition.
NTIS
*Stainless Steels; Corrosion; Surface Treatment*

**20010123419** Pennsylvania Univ., Philadelphia, PA USA
**Final Report: Hardening and Strain Localization in Single and Polycrystalline Materials Under Cyclic and Monotonic Deformation, January 11, 1985-July 31, 1997**
Laird, C.; Bassani, J. L.; Mar. 03, 2000; 7p; In English
Report No.(s): DE2001-764611; No Copyright; Avail: Department of Energy Information Bridge

The subject program on substructure evolution initially focused on strain localization produced by fatigue cycling and especially how such localization affects the cyclic response of polycrystalline pure metal. The latter stages have dealt with strain localization in the heavy monotonic deformation of alloys, which eventually produces forms of localized deformation that include coarse slip bands (CSBs), which are aligned to slip planes and macroscopic shear bands (MSBs), which are not aligned to slip planes. These forms of strain localization are important in that they limit the USAble ductility of the material in forming processes.
NTIS
*Deformation; Edge Dislocations; Substructures; Alloys*

**20010123429** Los Alamos National Lab., NM USA
**Simulator for Copper Ore Leaching**
Travis, B.; May 14, 1999; 19p; In English
Report No.(s): DE2001-763213; LA-UR-98-3705; No Copyright; Avail: Department of Energy Information Bridge, Microfiche

This is the final report of a one-year, Laboratory Directed Research and Development (LDRD) project at Los Alamos National Laboratory (LANL). Copper is a strategic metal and the nation needs a secure supply both for industrial use and military needs. However, demand is growing worldwide and is outstripping the ability of the mining industry to keep up. Improved recovery methods are critically needed to maintain the balance of supply and demand. The goal of any process design should be to increase the amount of copper recovered, control movement of acid and other environmentally harmful chemicals, and reduce energy requirements. to achieve these ends, several improvements in current technology are required, the most important of which is a better understanding of, and the ability to quantify, how fluids move through heterogeneous materials in a complex chemical environment. The goal of this project is create a new modeling capability that couples hydrology with copper leaching chemistry. Once the model has been verified and validated, we can apply the model to specific problems associated with heap leaching (flow channeling due to non-uniformities in heap structure, precipitation/dissolution reactions, and bacterial action), to understand the causes of inefficiencies, and to design better recovery systems. We also intend to work with representatives of the copper mining industry to write a coordinated plan for further model development and application that will provide economic benefits to the industry and the nation.
NTIS
*Copper; Leaching; Mining; Optimization; Production Engineering*

**20010123438** Los Alamos National Lab., NM USA
**Sensitivity of Simulated Anisotropy to Initial Texture Definitions**
Necker, C. T.; Tome, C. N.; Jean-Prost, F.; Korzekwa, D. A.; Aug. 01, 1999; 10p; In English
Report No.(s): DE2001-761119; LA-UR-99-2724; No Copyright; Avail: Department of Energy Information Bridge, Microfiche

Free compression tests were performed on 0.040 inch thick 5754 aluminum sheet stock producing a slight in-plane anisotropy. A visco-plastic self-consistent (VPSC) deformation modeling code was used to model the mechanical properties and resultant deformation textures. Calculations using a discretized description of the initial texture simulated the deformation texture very closely. Simulation of the mechanical properties were also captured nicely with one exception. The direction of simulated in-plane anisotropy was reversed from the experimental results. Simulation of the impact of various texture components on the anisotropy indicted that the shift of texture toward stronger brass, (l-brace)110(r-brace), and Goss, (l-brace)110(r-brace) components led to the reversal of anisotropy. The simulated deformation texture was more intense than the experimental texture in the brass and Goss positions. This result suggests that the more intense simulated texture components may be responsible for the reversal of an isotropy.
NTIS
*Aluminum; Mechanical Properties; Compression Tests*

**20010123467** Argonne National Lab., IL USA

**Experimental and calculated swelling behavior of U-10 wt.% Mo under low irradiation temperatures**

Rest, J.; Sep. 29, 1998; 16p; In English

Report No.(s): DE2001-10983; ANL/ET/CP-97352; No Copyright; Avail: Department of Energy Information Bridge, Microfiche

SEM micrographs of U-10 wt.% Mo irradiated at low temperature in the ATR to about 40 at. % burnup show the presence of cavities. We have used a rate-theory-based model to investigate the nucleation and growth of cavities during low-temperature irradiation of uranium-molybdenum alloys in the presence of irradiation-induced interstitial-loop formation and growth. In addition, the evolution of forest dislocations was calculated based on dislocation loop growth and simultaneous climb and glide of unfaded loops. Consolidation of the dislocation structure takes into account capture of interstitial dislocation loops and annihilation of adjacent dislocations, as well as loss to grain boundaries. A di-interstitial is assumed to be the nucleus of a dislocation loop. Cavities are nucleated when two gas atoms come together in the presence of at least one vacancy. Cavity growth occurs by the influx of gas atoms and/or vacancies. In turn, the free interstitial concentration, and thus (due to recombination) the free-vacancy concentration, depends on the dislocation density. Bias-driven growth of cavities can lead to substantial swelling of the alloy (void swelling). However, our calculations indicate that the swelling mechanism in the U-10 wt.% Mo alloy at low irradiation temperatures is fission gas driven. The calculations also indicate that the observed bubbles must be associated with a sub-grain structure. Calculated swelling and bubble-size-distribution are compared with irradiation data.

NTIS

*Nucleation; Cavities; Irradiation; Uranium Alloys; Molybdenum Alloys*

**20010123538** Argonne National Lab., IL USA

**Ab initio Monte Carlo investigation of small lithium clusters**

Srinivas, S.; Jun. 16, 1999; 23p; In English

Report No.(s): DE2001-10902; ANL/CHM/CP-96914; No Copyright; Avail: Department of Energy Information Bridge, Microfiche

Structural and thermal properties of small lithium clusters are studied using ab initio-based Monte Carlo simulations. The ab initio scheme uses a Hartree-Fock/density functional treatment of the electronic structure combined with a jump-walking Monte Carlo sampling of nuclear configurations. Structural forms of Li(sub 8) and Li(sub 9)(sup +) clusters are obtained and their thermal properties analyzed in terms of probability distributions of the cluster potential energy, average potential energy and configurational heat capacity all considered as a function of the cluster temperature. Details of the gradual evolution with temperature of the structural forms sampled are examined. Temperatures characterizing the onset of structural changes and isomer coexistence are identified for both clusters.

NTIS

*Electronic Structure; Lithium; Thermodynamic Properties; Metal Clusters; Hartree Approximation; Monte Carlo Method*

**20010123724** Lawrence Livermore National Lab., Livermore, CA USA

**Advances in crosswell electromagnetics steel cased boreholes**

Harben, P. E.; Kirkendall, B. A.; Lewis, J. P.; Mar. 01, 1999; 6p; In English

Report No.(s): DE2001-11324; UCRL-JC-133853; AC1005000; No Copyright; Avail: Department of Energy Information Bridge

The Crosswell electromagnetic (EM) induction technique ideally measures the resistivity distribution between boreholes which may often be cased with carbon steel. Quantification of the effect of such steel casing on the induced field is the most significant limitation of the technique. Recent data acquired at a site in Richmond, California quantify the effect of steel casing on induction measurements and demonstrate this effect to be separable. This unique site contains adjacent steel and plastic wells in which frequency soundings demonstrate low spectrum (1.0 - 50 Hz) measurements an effective means of isolating the casing response from, the formation response. It is also shown that the steel casing effect on the induction coil is highly localized, and limited to less than 0.30 meters above and below the coil.

NTIS

*Magnetic Induction; Electromagnetism; Electrical Resistivity*

**20010123725** Oak Ridge National Lab., TN USA

**Oxide Dispersion Strengthened Fe3Al-Based Alloy Tubes: Application Specific Development for the Power Generation Industry**

Kad, B. K.; Jul. 01, 1999; 29p; In English

Report No.(s): DE2001-11315; ORNL/SUB/97-SY009/1; No Copyright; Avail: Department of Energy Information Bridge

A detailed and comprehensive research and development methodology is being prescribed to produce Oxide Dispersion Strengthened (ODS)-Fe3Al thin walled tubes, using powder extrusion methodologies, for eventual use at operating temperatures of up to 1100 C in the power generation industry. A particular in service application anomaly of Fe3Al-based alloys is that the environmental resistance is maintained up to 1200 C, well beyond where such alloys retain sufficient mechanical strength. Grain boundary creep processes at such high temperatures are anticipated to be the dominant failure mechanism.
NTIS
*Oxide Dispersion Strengthening; Alloys*

**20010123739** Argonne National Lab., IL USA
**Dynamic inert metal anode**
Hryn, J. N.; Nov. 09, 1998; 8p; In English
Report No.(s): DE2001-11093; ANL/ES/CP-97631; No Copyright; Avail: Department of Energy Information Bridge, Microfiche

A new concept for a stable anode for aluminum electrowinning is described. The anode consists of a cup-shaped metal alloy container filled with a molten salt that contains dissolved aluminum. The metal alloy can be any of a number of alloys, but it must contain aluminum as a secondary alloying metal. A possible alloy composition is copper with 5 to 15 weight percent aluminum. In the presence of oxygen, aluminum on the metal anode's exterior surface forms a continuous alumina film that is thick enough to protect the anode from chemical attack by cryolite during electrolysis and thin enough to maintain electrical conductivity. However, the alumina film is soluble in cryolite, so it must be regenerated in situ. Film regeneration is achieved by the transport of aluminum metal from the anode's molten salt interior through the metal wall to the anode's exterior surface, where the transported aluminum oxidizes to alumina in the presence of evolving oxygen to maintain the protective alumina film. Periodic addition of aluminum metal to the anode's interior keeps the aluminum activity in the molten salt at the desired level. This concept for an inert anode is viable as long as the amount of aluminum produced at the cathode greatly exceeds the amount of aluminum required to maintain the anode's protective film.
NTIS
*Electrowinning; Aluminum; Anodes*

**20010123745** Argonne National Lab., IL USA
**In-situ transmission electron microscopy study of ion-irradiated copper: comparison of the temperature dependence of cascade collapse in FCC- and BCC- metals, e**
Daulton, T. L.; Oct. 23, 1998; 32p; In English
Report No.(s): DE2001-11084; ANL/MSD/CP-97587; No Copyright; Avail: Department of Energy Information Bridge, Microfiche

The kinetics which drive cascade formation and subsequent collapse into point-defect clusters is investigated by analyzing the microstructure produced in situ by low fluence 100 keV Kr ion irradiations of fcc-Cu over a wide temperature range (18-873 K). The yield of collapsed point-defect clusters is demonstrated unequivocally to be temperature dependent, remaining approximately constant up to lattice temperatures of 573 K and then abruptly decreasing with increasing temperature. This drop in yield is not caused by defect loss during or following ion irradiation. This temperature dependence can be explained by a thermal spike effect. These in-situ yield measurements are compared to previous ex-situ yield measurements in fcc-Ni and bcc-Mo.
NTIS
*Copper; Transmission Electron Microscopy; In Situ Measurement; Kinetics; Body Centered Cubic Lattices; Face Centered Cubic Lattices*

**20010123917** Virginia Univ., Dept. of Materials Science and Engineering, Charlottesville, VA USA
**Microstructural evolution in elastically stressed systems. Final report**
Johnson, W. C.; Sep. 14, 1997; 6p; In English
Report No.(s): DE2001-763350; DE-FG05-93ER45507-F; No Copyright; Avail: Department of Energy Information Bridge

The results, which have been compared to numerical simulations and found to be in very good agreement, predict that deviations in composition on the order of several atomic percent (measured with respect to equilibrium compositions) are possible at the interface. Interfacial compositions are strongly time dependent and are also influenced by the stress state.
NTIS
*Microstructure; Stresses; Elastic Properties*

**20010124067** Los Alamos National Lab., NM USA

**Material Physics of Deformation of AA5182 Under Hot Rolling Conditions**

Stout, M. G.; Beaudoin, A. J.; Feb. 01, 2000; 6p; In English

Report No.(s): DE2001-763398; LA-UR-00-1031; No Copyright; Avail: Department of Energy Information Bridge

The forming process of hot rolling not only has obvious commercial importance but also is scientifically challenging to understand. Accurate characterization is difficult as material physics affecting plastic deformation change on the same time scale as that of the process itself. Recovery and recrystallization provide examples: the development of an annealed state may occur between rolling passes, with subsequent impact on upcoming rolling passes. We have used the constitutive response of the metal in interrupted loading experiments to ascertain whether recrystallization or recovery is an active mechanism as a function of deformation history, complimenting a study of Wells, et al.

NTIS

*Plastic Deformation; Steels; Hot Working; Metal Working; Mechanical Properties*

**20010124092** Oak Ridge National Lab., TN USA

**Oxidation of Mo-41Re at Low Oxygen Pressures: 2000 Status Report**

DiStefano, J. R.; Chitwood, L. D.; Oct. 01, 2000; 32p; In English

Report No.(s): DE2001-769320; ORNL/TM-2000/291; No Copyright; Avail: Department of Energy Information Bridge

Rhenium generally improves the properties of molybdenum, and, therefore, there is interest in use of Mo-Re alloys in space system applications. Both Mo and Re have relatively low solubilities for oxygen but readily form oxide scales when exposed to oxidizing environments above approx. 350 C. Studies are being conducted on Mo-41Re to determine the rate of oxidation, type of scale formation, and effects on mechanical properties as a function of temperature and partial pressure of oxygen. Thus far, weight gains associated with formation of MoO(sub 2) have been found for Po(sub 2) less than 10(sup 13) Pa (torr) in vacuum, and weight losses associated with evaporation of MoO(sub 3) above 10(sup -3) Pa. However, no significant changes in tensile properties were measured.

NTIS

*Molybdenum; Mechanical Properties; Rhenium; Technology Utilization*

**20010124095** Argonne National Lab., IL USA

**Effect of low dose rate irradiation on the swelling of 12% cold-worked 316 stainless steel**

Allen, T. R.; Mar. 02, 1999; 17p; In English

Report No.(s): DE2001-10981; ANL/ED/CP-97347; No Copyright; Avail: Department of Energy Information Bridge, Microfiche

In pressurized water reactors (PWRs), stainless steel components are irradiated at temperatures that may reach 400 C due to gamma heating. If large amounts of swelling (>10%) occur in these reactor internals, significant swelling related embrittlement may occur. Although fast reactor studies indicate that swelling should be insignificant at PWR temperatures, the low dose rate conditions experienced by PWR components may possibly lead to significant swelling. to address these issues, JNC and ANL have collaborated to analyze swelling in 316 stainless steel, irradiated in the EBR-II reactor at temperatures from 376-444 C, at dose rates between 4.9 x 10(exp -8) and 5.8 x 10(exp -7) dpa/s, and to doses of 56 dpa. For these irradiation conditions, the swelling decreases markedly at temperatures less than approximately 386 C, with the extrapolated swelling at 100 dpa being around 3%. For temperatures greater than 386 C, the swelling extrapolated to 100 dpa is around 9%. For a factor of two difference in dose rate, no statistically significant effect of dose rate on swelling was seen. For the range of dose rates analyzed, the swelling measurements do not support significant (>10%) swelling of 316 stainless steel in PWRs.

NTIS

*Pressurized Water Reactors; Swelling; Stainless Steels*

**20010124129** Argonne National Lab., IL USA

**Fabrication of a simple materials system for study of Hg in a stainless steel**

Allen, C. W.; Jan. 04, 1999; 12p; In English

Report No.(s): DE2001-11032; ANL/MSD/CP-96891; No Copyright; Avail: Department of Energy Information Bridge

The Spallation Neutron Source (SNS), currently under construction at Oak Ridge National Laboratory, is expected to employ a Hg target encased in a stainless steel. Little is known about the metallurgical behavior of this materials engineering system, which will occur in a service environment involving elevated temperatures and intense radiation. Under normal equilibrium conditions, however, Hg is known to be insoluble in and non-reactive with solid Fe and Cr but to form one or more intermetallics with Ni. Hg has been implanted into alloy 304L. For implantations at 400 and 500 C to a fluence of 3 x 10(exp 16) cm(sup -2) sub-micron

sized precipitates of Hg are formed, as judged, for example, from their solidification behavior on cooling during TEM observation. The formation of such a system of microtargets and possible studies employing them as in situ TEM specimens are discussed, which can provide useful empirical information in conjunction with SNS target development.
NTIS
*Mercury (Metal); Stainless Steels; Fabrication*

**20010124135** Reilly (Robert) and Associates, Northfield, IL USA
**Making of Steel Strapping and Strip. Semi-Annual Report for Period Ending April 30, 2000**
Reilly, R. D.; Jul. 22, 2000; 7p; In English
Report No.(s): DE2001-763387; DOE/GO/10412-S; No Copyright; Avail: Department of Energy Information Bridge

The direction for the heat treating method has been established with input from the work to date on the Northwestern contract for the project entitled 'Effects of Steel Composition and Quench Rate on Microstructure and Mechanical Properties of Strapping'. The conclusion has been accepted by ourselves and Northwestern that our direction to heat treat to a Martensitic microstructure will give us optimum physical properties in the final product. The attached comparison from the American Society of Metals 'Handbook of Quenchants and Quenching Technology' clearly shows the superiority of this end objective (Quenched and Tempered) as compared to 'Normalized and Tempered' structures. Present industry practice produces a 'Normalized' or a close compromise to this structure which is obtained by Quenching in Lead. It is not possible to prevent some lead adherence to products produced in this manner and the industry has been searching for new methods to avoid this environmental hazard which is present not only in the production process but in the product as well. It is appropriate to review our production methodology at this time in order to reconfirm the steps taken which have been previously designated by those knowledgeable in the field to be proven in former steel conversion practice.
NTIS
*Microstructure; Quenching (Cooling); Martensite; Metal Strips; Heat Treatment; Metals*

**20010125010** Sandia National Labs., Albuquerque, NM USA
**Stressed Heat Affected Zone Simulations of AerMet 100 Alloy**
Puskar, J. D.; Smith, M. F.; Aug. 03, 1999; 11p; In English
Report No.(s): DE2001-9688; SAND99-2004C; No Copyright; Avail: Department of Energy Information Bridge, Microfiche

AerMet 100 is a high strength, high fracture toughness alloy designed for use in aerospace applications. In previous work the welding behavior of this alloy has been evaluated, and it has been shown that a softened region in the heat-affected zone (HAZ) is a principal feature of the weld zone. A model for this softening, based on classical theories of precipitate coarsening and isothermal softening data, was developed and found to provide a reasonable description for weld thermal cycle simulation (Gleeble) experiments. Recent work has shown, however, that softening in real welds is not always well predicted by this model, so that additional effects, which are not captured in conventional Gleeble thermal cycle simulations must be addressed. In particular, the stresses associated with real weld HAZ's may modify the softening kinetics. In the current work, Gleeble simulations in both stress-free and stressed conditions have been conducted and the kinetics compared. The accuracy of the thermal model predictions have also been considered regarding their impact on estimated hardness values.
NTIS
*Heat Affected Zone; Thermal Simulation; Welding; Alloys; Aerospace Engineering*

**20010125029** Department of Energy, Idaho Operations Office, Idaho Falls, ID USA
**Improved Life of Die Casting Dies of H13 Steel by Attaining Improved Mechanical Properties and Distortion Control During Heat Treatment**
Wallace, J. F.; Schwam, D.; Oct. 01, 1998; 255p; In English
Report No.(s): DE2001-750976; DOE/ID/13320-3; No Copyright; Avail: Department of Energy Information Bridge, Microfiche

The ultimate goal of this project is to increase die casting die life by using fast enough quenching rates to obtain good toughness and fatigue resistance in premium grade H-13 steel dies. The main tasks of the project were to compile a database on physical and mechanical properties of H-13; conduct gas quenching experiments to determine cooling rates of dies in difference vacuum furnaces; measure the as-quenched distortion of dies and the residual stresses; generate finite element analysis models to predict cooling rates, distortion, and residual stress of gas quenched dies; and establish rules and create PC-based expert system for prediction of cooling rates, distortion, and residual stress in vacuum/gas quenched H-13 dies. Cooling curves during gas quenching of H-13 blocks and die shapes have been measured under a variety of gas pressure. Dimensional changes caused by the gas quenching processes have been determined by accurate mapping of all surfaces with coordinate measuring machines before and after the quench. Residual stresses were determined by the ASTM E837 hole-drilling strain gage method. to facilitate

the computer modeling work, a comprehensive database of H-13 mechanical and physical properties has been compiled. Finite element analysis of the heat treated shapes has been conducted using the TRAST/ABAQUS codes. There is a good fit between the predicted and measured distortion contours. However, the magnitude of the predicted distortion and residual stresses does not match well the measured values. Further fine tuning of the model is required before it can be used to predict distortion and residual stress in a quantitative manner. This last step is a prerequisite to generating rules for a reliable expert system.
NTIS
*Casting; Cooling; Distortion; Fracture Strength; Residual Stress*

**20010125242** Argonne National Lab., IL USA
**Diffuse x-ray scattering from short-period W/C multilayers at in-plane momentum transfers 0.10-0.17 angstrom(sup -1)**
Headrick, R. L.; Liu, C. L.; Macrander, A. T.; Apr. 20, 1999; 14p; In English
Report No.(s): DE2001-11768; ANL/XFD/CP-98830; No Copyright; Avail: Department of Energy Information Bridge

X-ray scattering measurements at 10 keV from multilayers having a period of 24.8 (angstrom) and consisting of 100 W/C bilayers are reported. Specular scans revealed first-order reflectivities in the range 73.5% to 78.0% with bandpasses in the range of 1.5% to 1.7%. Total roughness (or interface grading) values deduced from fitting to the specular data only were in the range 2.5 to 3.0 (angstrom) for the last-to-grow surface of the W layers. Diffuse scattering measurements were made in a geometry that permitted investigation of in-plane momentum transfers up to 0.17 (angstrom)(sup (minus)1). This is roughly an order of magnitude larger than is possible in conventional rocking scans. Reasonable fitting results were obtained for an in-plane correlation function that has a Fourier transform proportional to exp(-vq(sub y)(sup 2)(vert-bar)z(sub i)-z(sub j)(vert-bar)), where z(sub i)-z(sub j) is the average separation between the i(sup th) and j(sup th) interfaces and q(sub y) is the in-plane momentum transfer.
NTIS
*X Ray Scattering; Momentum Transfer*

**20010125244** Argonne National Lab., IL USA
**Corrosion performance of structural alloys**
Natesan, K.; Jul. 15, 1999; 14p; In English
Report No.(s): DE2001-11770; ANL/ET/CP-98866; No Copyright; Avail: Department of Energy Information Bridge

Component reliability and long-term trouble-free performance of structural materials are essential in power-generating and gasification processes that utilize coal as a feedstock. During combustion and conversion of coal, the environments encompass a wide range of oxygen partial pressures, from excess-air conditions in conventional boilers to air-deficient conditions in 10W-NO(sub x) and gasification systems. Apart from the environmental aspects of the effluent from coal combustion and conversion, one concern from the systems standpoint is the aggressiveness of the gaseous/deposit environment toward structural components such as waterwall tubes, steam superheaters, syngas coolers, and hot-gas filters. The corrosion tests in the program described in this paper address the individual and combined effects of oxygen, sulfur, and chlorine on the corrosion response of several ASME-coded and noncoded structural alloys that were exposed to air-deficient and excess-air environments typical of coal-combustion and gasification processes. Data in this paper address the effects of preoxidation on the subsequent corrosion performance of structural materials such as 9Cr-1Mo ferritic steel, Type 347 austenitic stainless steel, Alloys 800, 825, 625, 214, Hastelloy X, and iron aluminide when exposed at 650 C to various mixed-gas environments with and without HCI. Results are presented for scaling kinetics, microstructural characteristics of corrosion products, detailed evaluations of near-surface regions of the exposed specimens, gains in our mechanistic understanding of the roles of S and Cl in the corrosion process, and the effect of preoxidation on subsequent corrosion.
NTIS
*Component Reliability; Corrosion Tests; Oxygen; Sulfur; Chlorine; Alloys*

**20010125392** Argonne National Lab., IL USA
**Correlation between swelling and radiation-induced segregation in iron-chromium-nickel alloys**
Allen, T. R.; Busby, J. T.; Kenik, E. A.; Was, G. S.; Mar. 05, 1998; 22p; In English
Report No.(s): DE2001-8133; ANL/ED/CP-94626; No Copyright; Avail: Department of Energy Information Bridge, Microfiche

The magnitudes of both void swelling and radiation-induced segregation (RIS) in iron-chromium-nickel alloys are dependent on bulk alloy composition. Because the diffusivity of nickel via the vacancy flux is slow relative to chromium, nickel enriches and chromium depletes at void surfaces during irradiation. This local composition change reduces the subsequent vacancy flux to the void, thereby reducing void swelling. In this work, the resistance to swelling from major element segregation is estimated using diffusivities derived from grain boundary segregation measurements in irradiated iron-chromium-nickel alloys. The

resistance to void swelling in iron- and nickel-base alloys correlates with the segregation and both are functions of bulk alloy composition. Alloys that display the greatest amount of nickel enrichment and chromium depletion are found to be most resistant to void swelling, as predicted. Additionally, swelling is shown to be greater in alloys in which the RIS profiles are slow to develop.
NTIS
*Radiation Effects; Iron Alloys; Nickel Alloys; Chromium Alloys*

**20010125393** Argonne National Lab., IL USA
**Modeling the effect of irradiation and post-irradiation annealing on grain boundary composition in austenitic Fe-Cr-Ni alloys**
Allen, T.; Busby, J. T.; Kenik, E. A.; Was, G. S.; Mar. 05, 1998; 8p; In English
Report No.(s): DE2001-8132; ANL/ED/CP-94624; No Copyright; Avail: Department of Energy Information Bridge, Microfiche
Many irradiation effects in Fe-Cr-Ni alloys such as radiation-induced segregation, radiation-enhanced diffusion, and void swelling are known to vary with bulk alloy composition. The development of microstructural and microchemical changes during irradiation and during post-irradiation annealing is determined by the rate of diffusion of point defects and alloying elements. To accurately predict the changes in grain boundary chemistry due to radiation-induced segregation and post-irradiation annealing, the composition dependence of diffusion parameters, such as the migration energy, must be known. A model has been developed which calculates migration diffusivity. The advantages of this calculational method are that a single set of input parameters can be used for a wide range of bulk alloy compositions, and the effects of local order can easily be incorporated into the calculations. A description of the model is presented, and model calculations are compared to segregation measurements from seven different iron-chromium-nickel alloys, irradiated with protons to doses from 0.1 to 3.0 dpa at temperatures between 200 C and 600 C. Results show that segregation trends can be modeled using a single set of input parameters with the difference between model calculation and measurement being less than 5 at%, but usually less than 2 at%. Additionally, model predictions are compared to grain boundary composition measurements of neutron irradiated 304 stainless steel following annealing. For the limited annealing data available, model calculations correctly predict the magnitude and time scale for recovery of the grain boundary composition.
NTIS
*Irradiation; Annealing; Alloys; Diffusivity*

**20010125396** Argonne National Lab., IL USA
**Irradiation creep of vanadium-base alloys**
Tsai, H.; Matsui, H.; Billone, M. C.; Strain, R. V.; Smith, D. L.; May 18, 1998; 15p; In English
Report No.(s): DE2001-8118; ANL/ET/CP-94176; No Copyright; Avail: Department of Energy Information Bridge, Microfiche
A study of irradiation creep in vanadium-base alloys is underway with experiments in the Advanced Test Reactor (ATR) and the High Flux Isotope Reactor (HFIR) in the US. Test specimens are thin-wall sealed tubes with internal pressure loading. The results from the initial ATR irradiation at low temperature (200-300 C) to a neutron damage level of 4.7 dpa show creep rates ranging from (approx)0 to 1.2 x 10(sup - 5)/dpa/MPa for a 500-kg heat of V-4Cr-4Ti alloy. These rates were generally lower than reported from a previous experiment in BR-10. Because both the attained neutron damage levels and the creep strains were low in the present study, however, these creep rates should be regarded as only preliminary. Substantially more testing is required before a data base on irradiation creep of vanadium alloys can be developed and used with confidence.
NTIS
*Irradiation; Creep Properties; Vanadium Alloys*

**20010125397** Argonne National Lab., IL USA
**Environmentally assisted cracking of LWR materials**
Chopra, O. K.; Chung, H. M.; Kassner, T. F.; Park, J. H.; Shack, W. J.; Dec. 05, 1997; 23p; In English
Report No.(s): DE2001-8116; ANL/ET/CP-94125; No Copyright; Avail: Department of Energy Information Bridge, Microfiche
The effect of dissolved oxygen level on fatigue life of austenitic stainless steels is discussed and the results of a detailed study of the effect of the environment on the growth of cracks during fatigue initiation are presented. Initial test results are given for specimens irradiated in the Halden reactor. Impurities introduced by shielded metal arc welding that may affect susceptibility to stress corrosion cracking are described. Results of calculations of residual stresses in core shroud weldments are summarized. Crack growth rates of high-nickel alloys under cyclic loading with R ratios from 0.2-0.95 in water that contains a wide range of dissolved oxygen and hydrogen concentrations at 289 and 320 C are summarized.
NTIS
*Crack Propagation; Austenitic Stainless Steels; Fatigue Life; Dissolved Gases*

**20010125398** Argonne National Lab., IL USA

**Nondestructive evaluation and characterization of damage and repair to continuous-fiber ceramic composite panels**

Sun, J. G.; Petrak, D. R.; Pillai, T. A. K.; Deemer, C.; Ellingson, W. A.; Apr. 01, 1998; 10p; In English

Report No.(s): DE2001-8115; ANL/ET/CP-94120; No Copyright; Avail: Department of Energy Information Bridge, Microfiche

Continuous fiber ceramic matrix composites are currently being developed for a variety of high-temperature applications. Because of the high costs of making these components, minor damage incurred during manufacturing or operation must be rewired in order to extend the life of the components. In this study, five ceramic-grade Nicalon(trademark) fiber/SiNC-matrix composite panels were intentionally damaged with a pendulum-type impactor during an impact test. The damaged panels were then repaired at Dow Corning Corporation. Three nondestructive evaluation (NDE) methods were used to study the characteristics of the panels after the damage and again after the panels were repaired. The NDE methods were X-ray radiography, infrared thermal imaging, and air-coupled ultrasound. The results showed that the impact test induced various types of damage in the panels. The NDE data that were obtained by the three NDE methods were correlated with each other.

NTIS

*Nondestructive Tests; Ceramic Matrix Composites; Damage*

**20010125451** Lawrence Livermore National Lab., Livermore, CA USA

**Simulation of void growth in tantalum at high-strain rate**

Belak, J.; Dec. 08, 1998; 7p; In English

Report No.(s): DE2001-8351; UCRL-JC-132650; DP0101031; No Copyright; Avail: Department of Energy Information Bridge, Microfiche

The dynamic fracture (spallation) of ductile metals is known to initiate through the nucleation and growth of microscopic voids. Here, we apply atomistic molecular dynamics modeling to the early growth of nanoscale (2 nm radius) voids in face centered cubic metals using embedded atom potential models. The voids grow through anisotropic dislocation nucleation and emission into a cuboidal shape in agreement with experiment. The mechanism of this nucleation process is presented. The resulting viscous growth exponent at late times is about three times larger than expected from experiment for microscale voids, suggesting either a length scale dependence or a inadequacy of the molecular dynamics model such as the perfect crystal surrounding the void.

NTIS

*Voids; Fracture Mechanics; Tantalum; Strain Rate; Models*

**20010125469** Argonne National Lab., IL USA

**Stress-induced amorphization at moving crack tips in NiTi**

Okamoto, P. R.; Heuer, J.; Lam, N. Q.; Ohnuki, S.; Matsukawa, Y.; Jan. 29, 1998; 9p; In English

Report No.(s): DE2001-8104; ANL/MSD/CP-93805; No Copyright; Avail: Department of Energy Information Bridge, Microfiche

In situ fracture studies on thin-film NiTi intermetallic compounds have been carried out in the high-voltage electron microscope at Argonne National Laboratory. Local stress-induced amorphization of regions directly in front of moving crack tips has been observed under tensile loading conditions. The stress-induced amorphization at crack tips exhibits a temperature dependence similar to that of ion-induced amorphization of NiTi. The upper limiting temperature for stress-induced amorphization is the same as that for ion-induced amorphization of crystalline NiTi and for amorphous phase formation during ion-beam mixing of Ni and Ti multilayer specimens. This upper limiting temperature of 600K is also the lowest temperature at which stress-induced amorphous phase crystallizes during isothermal annealing. This isothermal crystallization temperature is nearly 200K less than the kinetic crystallization temperature during heating of unrelaxed NiTi glasses formed by rapid quenching or vapor phase deposition.

NTIS

*Intermetallics; Fracture Strength; Thin Films; Crack Tips*

**20010125470** Argonne National Lab., IL USA

**Transmission Electron Microscopy Study of Cascade Collapse in Copper During In-Situ Ion-Irradiation at Elevated Temperatures**

Daulton, T. L.; Kirk, M. A.; Rehn, L. E.; Jan. 29, 1998; 9p; In English

Report No.(s): DE2001-8102; ANL/MSD/CP-93693; No Copyright; Avail: Department of Energy Information Bridge, Microfiche

The basic mechanisms driving the collapse of point defects produced in collision cascades are investigated by transmission electron microscope (TEM) characterization of defect microstructure produced in face centered cubic-Cu irradiated with low-fluences of heavy (100 keV Kr) ions at elevated temperature (23-600 C). Areal defect yields are determined from direct TEM observation of the total defect production integrated over the duration of the in-situ ion-irradiation. They are unequivocally demonstrated to decrease with increasing lattice temperature. This decrease in defect yield indicates a proportional decrease in the probability of collapse of cascade regions into defects of size where visible contrast is produced in a TEM.
NTIS
*Collapse; Copper; Face Centered Cubic Lattices; Microstructure; Point Defects*

**20010125471** Argonne National Lab., IL USA
**In-Situ Observation of Atomic Self-Organization Processes in Xe Nanocrystals Embedded in Al**
Mitsuishi, K.; Song, M.; Furuya, K.; Birtcher, R. C.; Allen, C. W.; Mar. 10, 1998; 10p; In English
Report No.(s): DE2001-8101; ANL/MSD/CP-93692; No Copyright; Avail: Department of Energy Information Bridge, Microfiche

Self-organization processes in Xe nanocrystals embedded in Al are observed with in-situ high-resolution electron microscopy. Under electron irradiation, stacking fault type defects are produced in Xe nanocrystals. The defects recover in a layer by layer manner. Detailed analysis of the video reveals that the displacement of Xe atoms in the stacking fault was rather small for the Xe atoms at boundary between Xe and Al, suggesting the possibility of the stacking fault in Xe precipitate originating inside of precipitate, not at the Al/Xe interface.
NTIS
*Nanocrystals; Xenon; Crystal Defects*

**20010125494** Argonne National Lab., IL USA
**Finite element modeling of the effect of interface anomalies on thermal stresses in alumina scales**
Wright, J. K.; Jun. 10, 1998; 15p; In English
Report No.(s): DE2001-10841; ANL/MSD/CP-96647; No Copyright; Avail: Department of Energy Information Bridge

The scales that grow from oxidation often develop a convoluted morphology or interface pores. High thermal stresses can develop locally and are potentially detrimental to the scale or interface integrity. Finite element simulations are used to examine residual thermal stresses and strains that result when these deviations from a flat interface have formed, and the resulting geometry is subsequently cooled to room temperature. A variety of geometries will be considered for alumina scales on a FeCrAl substrate.
NTIS
*Thermal Stresses; Aluminum Oxides; Oxidation; Finite Element Method; Mathematical Models; Scale (Corrosion)*

**20010125534** Los Alamos National Lab., NM USA
**Interpretation of Experiments and Modeling of Internal Strains in Beryllium Using a Polycrystal Model**
Tome, C.; Daymond, M.; Bourke, M.; Mar. 01, 2000; 11p; In English
Report No.(s): DE2001-764000; LA-UR-00-1153; No Copyright; Avail: Department of Energy Information Bridge, Microfiche

The elastic and plastic anisotropy of Be have been examined during a uniaxial compression test, by in-situ monitoring in a pulsed neutron beam. Comparisons between the measured hkil strains and the predictions from an elasto-plastic self consistent (EPSC) model are made. Agreement is qualitatively correct for most planes in the elasto-plastic regime. Possible mechanisms responsible for the quantitative discrepancies between model and experiment are discussed.
NTIS
*Beryllium; Polycrystals; Strain Rate*

**20010125566** Argonne National Lab., IL USA
**Electrochemical Studies of Mg-Doped LirTi5O12 Anodes**
Chen, C. H.; Jansen, A. N.; Vaughey, J.; Jul. 19, 1999; 4p; In English
Report No.(s): DE2001-11899; ANL/CMT/CP-99598; No Copyright; Avail: Department of Energy Information Bridge, Microfiche

Commercial lithium-ion batteries use carbon as the material of choice for the anode. However, because lithiated carbon has a voltage very close to the potential of metallic lithium, there are concerns about the safety of fully-charged carbon electrodes. The safety issue can be addressed by using a material that intercalates lithium at a higher voltage. A promising material is the lithium-titanium-oxide spinel material Li4Ti5O12 which can accommodate three Li+ ions per formula unit (corresponding to 175 mAh/g) in a two-phase reaction at approximately 1.5 V versus lithium. One of the drawbacks of this system is that the end-member

Li4Ti5O12 is electronically insulating, which limits electron transfer at the electrode surface. by doping this material with magnesium, Li(4-x)Mg(x)Ti5O12, we introduced mixed-valent Ti(4+)/Ti(3+) into the stoichiometric spinel structure and thereby increased the electronic conductivity by several orders of magnitude without sacrificing electrochemical performance. In this presentation we will provide data on the extent of the solid solution in Li(4-x)Mg(x)Ti5O12, the variation of electronic conductivity as a function of dopant concentration and the rate capability of the doped material.
NTIS
*Anodes; Carbon; Lithium Batteries; Lithium Oxides; Electrochemistry*

**20010125575** Argonne National Lab., IL USA
**Decomposition Mechanism in Supercooled Liquid Alloys**
Johnson, W. L.; Loffler, J. F.; Thiyagarajan, P.; Jul. 12, 1999; 16p; In English
Report No.(s): DE2001-11887; ANL/IPNS/CP-99464; No Copyright; Avail: Department of Energy Information Bridge, Microfiche

The authors performed small-angle neutron scattering experiments on the bulk amorphous alloy Zr(41.2)Ti(13.8)Cu(12.5)Ni(10)Be(22.5) (Vit1(reg-sign)) and on further alloys, where the ZrTi and CuBe content have been changed, following the tie-line in the direction of Zr(46.8)Ti(8.2)Cu(7.5)Ni(10)Be(27.5) (Vit4(reg-sign)). The Small Angle Neutron Scattering (SANS) data of the samples, preannealed at temperatures between 330 C and 390 C, show interference peaks giving evidence for spatially correlated arrangements of inhomogeneities. The Q values of the interference peaks, Q(sub max), decrease with increasing annealing temperature T(sub a) and, at a given annealing temperature, with composition following the tie-line from Vit1 to Vit4. They find that, in two distinguished regimes, the data follow a relation 1/L(exp 2) proportional to T(sub a) as predicted by Cahn's theory (L = 2(pi)/Q(sub max) is the wavelength of the decomposition), with a crossover at the glass transition temperature T(sub g) = 350 C. The authors explain the crossover by different diffusion mechanisms below and above T(sub g).
NTIS
*Zirconium Alloys; Amorphous Materials; Decomposition; Glass Transition Temperature; Liquid Alloys; Neutron Scattering*

**20010125588** General Electric Co., Schenectady, NY USA
**Finite Element Evaluation of Residual Stress in a Thread Form Generated by a Cold-Rolling Process**
Martin, J. A.; Feb. 26, 1999; 11p; In English
Report No.(s): DE2001-8218; KAPL-P-000120; No Copyright; Avail: Department of Energy Information Bridge, Microfiche

This paper presents a finite element evaluation of residual stress in a thread form generated by a cold rolling process. Included in this evaluation are a mesh development study, methodology sensitivity studies, and the effects of applied loads on the stress in a rolled thread root. A finite element analysis of the thread forming process using implicit modeling methodology, incremental large deformation, elastic-plastic material properties, and adaptive meshing techniques was performed. Results of the study indicate the axial component of the residual stress in the thread root of the fastener is highly compressive. Results also indicate that a rolled threaded fastener loaded to an average tensile stress equal to yield through the cross-section will retain compressive stresses in the thread root. This compressive stress state will be advantageous when evaluating fasteners for fatigue and environmental concerns.
NTIS
*Threads; Metal Working; Cold Rolling; Finite Element Method; Residual Stress; Fasteners*

**20010125596** Argonne National Lab., IL USA
**Critical Current Densities in Bi-2223 Sinter Forgings**
Balachandran, U.; Fisher, B. L.; Goretta, K. C.; Harris, N. C.; Murayama, N.; Jul. 23, 1999; 9p; In English
Report No.(s): DE2001-11904; ANL/ET/CP-99641; No Copyright; Avail: Department of Energy Information Bridge, Microfiche

(Bi,Pb)2SR2Ca2Cu3Ox (Bi-2223) bars, prepared by sinter forging, exhibited good phase purity and strong textures with the c axes of the Bi-2223 grains parallel to the forging direction. The initial zero-field critical current density (J(sub c)) of the bars was 10(exp 3) A/sq cm, but because the forged bars were uncoated, this value decreased with repeated thermal cycling. J(sub c) as a function of applied magnetic field magnitude and direction roughly followed the dependencies exhibited by Ag-sheathed Bi-2223 tapes, but the forged bars were more strongly dependent on field strength and less strongly dependent on field angle.
NTIS
*Critical Current; Current Density; Magnetic Field Configurations; Sintering; Bismuth Oxides; Bars*

**20010125630** Bettis Atomic Power Lab., West Mifflin, PA USA

**Mean Stress and Environmental Effects on Fatigue in Type 304 Stainless Steel**

Kandra, J. T.; Leax, T. R.; Wire, G. L.; Apr. 01, 1999; 19p; In English

Report No.(s): DE2001-8000; B-T-3262; No Copyright; Avail: Department of Energy Information Bridge, Microfiche

Fatigue life tests were performed in air on Type 304 stainless steel (304 SS) to establish the effect of mean stress under both load control and strain control. An apparent reduction of up to 26% in strain-amplitude occurred in the low and intermediate cycle regime (10(exp 8) cycles) for a mean stress of 138 Mpa. A quantitative description of mean stress effects using the Smith-Watson-Topper equivalent strain parameter was developed, which incorporates mean stress through the maximum stress. This description provided a tighter fit to the data, and allowed separation of mean stress and cold work effects. With this separation, the effect of mean stress was reduced to 12% decrease in strain amplitude at 138 Mpa. The stress-life curve apparently increased with increasing mean stress, due to the significant work hardening that occurred in tests with high mean stresses, especially under load control. Tests were performed on double-edge notched specimens of 304 SS in air and low oxygen water at 288 C. The elastically calculated increase in the notch tip stress accounted within 10% for the fatigue life reductions for a K(sub t) = 4.8 notch, but was 38% conservative for a K(sub t) = 8.8 notch. Fatigue crack initiation lives (defined as an 0.127 mm crack) in low oxygen water at 288 C were reduced by a factor of four to eight on cycles over those in air. Crack growth occurred throughout most of the fatigue initiation life. The increase in crack growth rate of 304 SS in water appears to be large enough to explain the reduced 'initiation' life in this environment.

NTIS

*Crack Propagation; Environment Effects; Fatigue Life; Metal Fatigue; Stainless Steels*

**20010125642** Argonne National Lab., IL USA

**Thermal imaging and air-coupled ultrasound characterization of a continuous-fiber ceramic composite panels**

Sun, J. G.; Easler, T. E.; Szweda, A.; Pillai, T. A. K.; Deemer, C.; Apr. 01, 1998; 10p; In English

Report No.(s): DE2001-8114; ANL/ET/CP-94119; No Copyright; Avail: Department of Energy Information Bridge, Microfiche

SYLRAMIC(trademark) continuous fiber ceramic-matrix composites (Nicalon(trademark) fiber/SiNC matrix) were fabricated by Dow Corning Corporation with the polymer-impregnation and pyrolysis (PIP) process. The composite microstructure and its uniformity, and the completeness of infiltration during processing were studied as a function of number of PIP cycles. Two nondestructive evaluation (NDE) methods, i.e., infrared thermal imaging and air-coupled ultrasound (UT), were used to investigate flat composite panels of two thicknesses and various sizes. The thermal imaging method provided two-dimensional (2D) images of through-thickness thermal diffusivity distributions, and the air-coupled UT method provided 2D images of through-thickness ultrasonic transmission of the panel components. Results from both types of NDEs were compared at various PIP cycles during fabrication of the composites. A delaminated region was clearly detected and its progressive repair was monitored during processing. The NDE data were also correlated to results obtained from destructive characterization.

NTIS

*Thermal Mapping; Ultrasonics; Ceramic Matrix Composites; Microstructure; Infiltration*

## 27
## NONMETALLIC MATERIALS

*Includes physical, chemical, and mechanical properties of plastics, elastomers, lubricants, polymers, textiles, adhesives, and ceramic materials. For composite materials see 24 Composite Materials.*

**20010118263** Oak Ridge National Lab., TN USA

**Hydroxylapatite Otologic Implants**

McMillan, A. D.; Lauf, R. J.; Beale, B.; Johnson, R.; Jan. 01, 2000; 14p; In English

Report No.(s): DE2000-760360; C/ORNL97-0459; No Copyright; Avail: Department of Energy Information Bridge, Microfiche

A Cooperative Research and Development Agreement (CRADA) between Lockheed Martin Energy Research Corporation (LMER) and Smith and Nephew Richards Inc. of Bartlett, TN, was initiated in March 1997. The original completion date for the Agreement was March 25, 1998. The purpose of this work is to develop and commercialize net shape forming methods for directly creating dense hydroxylapatite (HA) ceramic otologic implants. The project includes three tasks: (1) modification of existing gelcasting formulations to accommodate HA slurries; (2) demonstration of gelcasting to fabricate green HA ceramic components of a size and shape appropriate to otologic implants: and (3) sintering and evaluation of the HA components.

NTIS

*Ceramics; Shapes; Sintering*

**20010118264** Oak Ridge National Lab., TN USA
**Rapid Prototyping of Ceramics**
Nunn, S. D.; Conway, B.; Jan. 01, 2000; 10p; In English
Report No.(s): DE2000-760358; C/ORNL97-0488; No Copyright; Avail: Department of Energy Information Bridge, Microfiche

This Cooperative Research and Development Agreement (CRADA) between Lockheed Martin: Energy Research Corporation (Contractor) and Performance Research (Participant) was initiated to fabricate high performance automotive components of ceramic materials. A further purpose of a the CRADA was to investigate the use of solid free-form fabrication methods (rapid prototyping) to produce these components. There was excellent cooperation between the partners and good progress was being made, however, cancellation of half of the project funds at ORNL ended work on the CRADA before all of the planned tasks could be completed.

NTIS
*Ceramics; Fabrication*

**20010118533** Brookhaven National Lab., Upton, NY USA
**Use of Recycled Polymers for Encapsulation of Radioactive, Hazardous and Mixed Wastes**
Lagerraaen,; Kalb,; Nov. 01, 1997; 30p; In English
Report No.(s): DE2000-759000; BNL-66575; No Copyright; Avail: Department of Energy Information Bridge, Microfiche

Polyethylene encapsulation is a waste treatment technology developed at Brookhaven National Laboratory using thermoplastic polymers to safely and effectively solidify hazardous, radioactive and mixed wastes for disposal. Over 13 years of development and demonstration with surrogate wastes as well as actual waste streams on both bench and full scale have shown this to be a viable and robust technology with wide application. Process development efforts have previously focused on the use of virgin polymer feedstocks. In order to potentially improve process economics and serve to lessen the municipal waste burden, recycled polymers were investigated for use as encapsulating agents. Recycled plastics included low-density polyethylene, linear low-density polyethylene, high-density polyethylene and polypropylene, and were used as a direct substitute for or blended together with virgin resin. Impacts on processing and final waste form performance were examined.

NTIS
*Encapsulating; Radioactive Wastes; Resins; Waste Treatment*

**20010119055** Edgewood Chemical Biological Center, Aberdeen Proving Ground, MD USA
**Investigation of Polyurethane Adhesives for Use in the Apache Aviator NBC Protective Mask** ***Final Report, Sep. 2000-Feb. 2001***
Young, Gerald P.; Ciborowski, Steven; May, David; Oswald, Lawrence; Gross, Steven; Aug. 2001; 21p; In English
Contract(s)/Grant(s): Proj-62262255200
Report No.(s): AD-A394894; ECBC-TR-174; No Copyright; Avail: CASI; A03, Hardcopy; A01, Microfiche

Polyurethane adhesives are currently used in Apache aviator masks to secure polycarbonate lenses to a bromobutyl-natural rubber face piece. An alternative polyurethane adhesive packaged in a pre-measured assembly was investigated to determine its suitability for mask remanufacturing operations. Seventy-five prototype assemblies were prepared with the standard and alternative adhesive. The composite assemblies were then destructively tested on an Instron machine, in tension, to compare rupture strength of the polycarbonate-adhesive-rubber joint as a function of curing regime and surface preparation. Rupture load measurements indicate the alternative adhesive investigated is adequate for securing lenses within the aviator mask. Stress applied at joint failure ranged from 146 to 343 pounds per square inch. Prototypes cured at 63 degrees Celsius are approximately 38% stronger than ambient cured specimens.

DTIC
*Polycarbonates; Adhesives; Masks; Protective Clothing*

**20010119193** Oak Ridge National Lab., TN USA
**Micromechanical Constitutive Model of Progressive Crushing in Random Carbon Fiber Polymer Matrix Composites**
Lee, H. K.; Simunovic, S.; Sep. 01, 1999; 63p; In English
Report No.(s): DE2000-754359; ORNL/TM-1999/158; No Copyright; Avail: Department of Energy Information Bridge

A micromechanical damage constitutive model is presented to predict the overall elastoplastic behavior and damage evolution in random carbon fiber polymer matrix composites (RFPCs). to estimate the overall elastoplastic damage responses, an effective yield criterion is derived based on the ensemble-volume averaging process and first-order effects of eigenstrains due to the existence of spheroidal (prolate) fibers. The proposed effective yield criterion, to ether with the assumed overall associative plastic flow rule and hardening law, constitutes the analytical foundation for the estimation of effective elastoplastic behavior of

ductile matrix composites. First, an effective elastoplastic constitutive dama e model for aligned fiber-reinforced composites is proposed. A micromechanical damage constitutive model for RFPCs is then developed. The average process over all orientations upon overning constitutive field equations and overall yield function for aligned fiber-reinforced composites i s performed to obtain the constitutive relations and effective yield function of RFPCs. The discrete numerical integration algorithms and the continuum tangent operator are also presented to implement the proposed damage constitutive model. The damage constitutive model forms the basis for the progressive crushing in composite structures under impact loading.
NTIS
*Carbon Fibers; Crushing; Mathematical Models; Micromechanics; Polymer Matrix Composites*

**20010119236** Iowa State Univ. of Science and Technology, Dept. of Materials Science and Engineering, Ames, IA USA
**New Protonated and Anhydrous Chalcogenide Glasses**
Karthikeyan, Annamalai; Martindale, Chad A.; Martin, Steve W.; Sep. 25, 2001; 3p; In English; Original contains color images; Presented at the Godrdon Research Conference, Bristol, RI
Contract(s)/Grant(s): N00014-99-1-0538
Report No.(s): AD-A395060; No Copyright; Avail: CASI; A01, Hardcopy; A01, Microfiche

While hydrated electrolytes exhibit high proton conductivities, their use is limited by significant methanol cross-over, mechanical stability and temperatures below 100 deg C. These limitations can be overcome by synthesizing anhydrous proton conducting materials. In this direction we are investigating the development of anhydrous proton conductors. Protonated (and anhydrous) chalcogenide glass and glass-ceramic materials have been prepared for the first time. These materials open a new choice for the development of fast proton conducting (FPC) electrolytes intended for electrochemical applications, fuel cells in particular. These FPC materials, with proper addition of dopants, are expected to have high proton motion and better thermal stability than polymeric electrolytes. The protonated materials were prepared in three steps. First B2S3 glass was prepared from the elements. A B2S3 melt was bubbled with H2S(g) and thioboric acid crystals (HBS2) were obtained. Finally, HBS2 was used as a precursor for the preparation of different glass and glass-ceramic materials, of varying compositions, by adding (i) B2S3/GeS2.
DTIC
*Chalcogenides; Glass; Protons; Electrolytes; Electrochemical Cells*

**20010119545** Oak Ridge National Lab., TN USA
**Superplastic Deformation and Viscous Flow in an Zr-Based Metallic Glass at 410 C**
Liu, C. T.; Mukai, T.; Nieh, T. G.; Wadsworth, J.; Wang, J. G.; Dec. 01, 1998; 6p; In English
Report No.(s): DE2001-10430; ORNL/CP-102733; KC-02-01-05-0; No Copyright; Avail: Department of Energy Information Bridge

The thermal properties of an amorphous alloy (composition in at %: Zr(l0)Al(5)Ti(l7.9)Cu(14.6)Ni), and particularly the glass transition and crystallization temperature as a function of heating rate, were characterized using Differential Scanning Calorimetry (DSC). X-ray diffraction analyses and Transmission Electron Microscopy were also conducted on samples heat-treated at different temperatures for comparison with the DSC results. Superplasticity in the alloy was studied at 410 C, a temperature within the supercooled liquid region. Both single strain rate and strain rate cycling tests in tension were carried out to investigate the deformation behavior of the alloy in the supercooled liquid region. The experimental results indicated that the alloy did not behave like a Newtonian fluid.
NTIS
*Deformation; Metallic Glasses; Thermodynamic Properties; Viscous Flow; Thermal Analysis*

**20010119557** Oak Ridge National Lab., TN USA
**Effects of Damage on Hydrogen-Implant-Induced Thin-Film Separation from Bulk Silicon Carbide**
Gregory, R. B.; Holland, O. W.; Thomas, D. K.; Wetteroth, T. A.; Wilson, S. R.; Apr. 05, 1999; 7p; In English
Report No.(s): DE2001-10469; ORNL/CP-104376; KC-02-02-05-0; No Copyright; Avail: Department of Energy Information Bridge, Microfiche

Exfoliation of Sic by hydrogen implantation and subsequent annealing forms the basis for a thin-film separation process which, when combined with hydrophilic wafer bonding, can be exploited to produce silicon-carbide-on-insulator, SiCOI. Sic thin films produced by this process exhibit unacceptably high resistivity because defects generated by the implant neutralize electrical carriers. Separation occurs because of chemical interaction of hydrogen with dangling bonds within microvoids created by the implant, and physical stresses due to gas-pressure effects during post-implant anneal. Experimental results show that exfoliation of Sic is dependent upon the concentration of implanted hydrogen, but the damage generated by the implant approaches a point

when exfoliation is, in fact, retarded. This is attributed to excessive damage at the projected range of the implant which inhibits physical processes of implant-induced cleaving. Damage is controlled independently of hydrogen dosage by elevating the temperature of the SiC during implant in order to promote dynamic annealing. The resulting decrease in damage is thought to promote growth of micro-cracks which form a continuous cleave. Channeled H(sup +) implantation enhances the cleaving process while simultaneously minimizing residual damage within the separated film. It is shown that high-temperature irradiation and channeling each reduces the hydrogen fluence required to affect separation of a thin film and results in a lower concentration of defects. This increases the potential for producing SiCOI which is sufficiently free of defects and, thus, more easily electrically activated.
NTIS
*Annealing; Hydrogen; Silicon Carbides; Thin Films*

**20010119608** Defence Science and Technology Organisation, Aeronautical and Maritime Research Lab., Melbourne Australia
**Bond Durability of Grit-Blast and Silane Treated Metallic Adherends Bonded With Room Temperature Curing Adhesives**
Rider, Andrew; Jul. 2001; 61p; In English; Original contains color images
Report No.(s): AD-A394952; DSTO-TR-1187; DODA-AR-011-949; No Copyright; Avail: CASI; A04, Hardcopy; A01, Microfiche

The ”Australian Silane Treatment” has been successfully used for bonded repairs carried out at RAAF Airbases for a number of years. This surface treatment has provided a reliable and non-toxic alternative to surface pre-treatments recommended in Structural Repair Manuals (SRM) for metallic adhesive bonded repairs. Generally, however, the silane treatment has only been applied in bonded repairs involving the use of high temperature curing structural adhesives. The purpose of the study detailed in this report was to examine the feasibility of extending the application of the silane pre-treatment to metallic repairs involving the use of room temperature or paste adhesive systems employed in a range of airbase repairs. Wedge style durability tests were conducted for a range of metallic adherends and room temperature curing adhesives. The durability performance of the grit-blast and epoxy silane metallic adherend pre-treatment was compared with standard pre-treatments recommended in a range of SRMs. Generally, the data indicated that the grit-blast and silane pre-treatment offered either improved or similar performance to the SRM alternative pre-treatments on the basis of results from wedge style durability tests conducted at 50 deg C and 100% relative humidity.
DTIC
*Silanes; Adhesives; Adhesive Bonding; Surface Treatment*

**20010119620** Florida Univ., Dept. of Chemistry and Physics, Gainesville, FL USA
**Controlled Redox and Electrical Properties in Polyheterocycles** ***Progress Report, 1 Sep. 2000-31 Aug. 2001***
Reynolds, John R.; Sep. 20, 2001; 22p; In English
Contract(s)/Grant(s): F49620-00-1-0047
Report No.(s): AD-A395045; 2; No Copyright; Avail: CASI; A03, Hardcopy; A01, Microfiche

Electrochromic and conducting polymers may prove especially important for a number of Air Force applications including chameleon coatings, informational displays, IR and microwave attenuation, dialed tint windows, and gap sealants. We are developing conjugated, redox active, and conducting polymers with controllable electronic band gaps that range from 1.1 eV to 4.0 eV, thus spanning from the NIR, through the entire visible spectrum, and into the UV. We have developed a reproducible method by which electrochromic coloration efficiencies (CE) can be measured accurately for polymer films. We have investigated the use of BF3 ethyl etherate as an alterative media for the electrochemical synthesis of highly electroactive polymer films and shown it to be applicable to preparing high quality polythiophene and donor-acceptor polymers which can be n-type doped. Electrochromic devices (ECD’s) with especially high color contrasts between bleached and colored states have been developed. We have broadened the visible absorption in polymer ECD’s while retaining the high contrast by having two cathodically coloring polymers with different Lambda(sub max) values deposited as a bilayer on a single electrode. Functionalized 3,4-propylenedioxythiophene polymers have been developed as soluble conducting polymers for blending into elastomeric hosts and as solution processable high contrast electrochromic polymers. We have prepared multi-color electrochromic and red emitting polymers through the synthesis of soluble low band gap polymers containing conjugated donor and acceptor units.
DTIC
*Electrical Properties; High Polymers; Oxidation-Reduction Reactions; Electrochromism; Electrochemical Synthesis*

**20010119919** Minnesota Univ., Minneapolis, MN USA

**Design, Modeling and Computation of Active Thin Films** ***Final Report, 1 Jun. 1998-31 May 2001***

Luskin, Mitchell; James, Richard; Sep. 24, 2001; 7p; In English

Contract(s)/Grant(s): DAAG55-98-1-0335

Report No.(s): AD-A395247; ARO-P-37259-1-MA; No Copyright; Avail: CASI; A02, Hardcopy; A01, Microfiche

A new theory and numerical methods for the mechanical behavior of thin films were developed. The theory was applied to shape memory and ferromagnetic shape memory materials. This suggested several new designs for microactuators. One of these, a microvalve, was numerically simulated. It showed a reversible motion induced by temperature change and a nearly square hysteresis loop (valve opening vs. temperature). In addition, the deformation and transformation of a thin film by indentation and the disappearance of the indentation by heating and reverse phase transformation were numerically simulated.

DTIC

*Microinstrumentation; Actuators; Numerical Analysis; Simulation*

**20010119955** NASA Kennedy Space Center, Cocoa Beach, FL USA

**Electrostatic Charging of Polymers by Particle Impact at Low Pressures**

Calle, Carlos I., NASA Kennedy Space Center, USA; Mantovani, J. G., Florida Inst. of Tech., USA; Buhler, C. R., Swales Aerospace, USA; Hogue, M. D., NASA Kennedy Space Center, USA; Nowicki, A. W., DYNACS Engineering Co., Inc., USA; Groop, E. E., NASA Kennedy Space Center, USA; [2001]; 4p; In English; 4th International Conference on Applied Electrostatics, October 2001, Dalian, China

Contract(s)/Grant(s): DEN10-27900; No Copyright; Avail: CASI; A01, Hardcopy; A01, Microfiche

Studies of the electrostatic interaction between micrometer-sized particles and polymer surfaces are of great interest to NASA's planetary exploration program. The unmanned landing missions to Mars planned for this decade as well as the possible manned missions that might take place during the second decade of this century require a better understanding of the electrostatic response of the materials used in landing crafts and equipment when exposed to wind-blown dust or to surface dust and sand particles. We report on preliminary experiments designed to measure the electrostatic charge developed on five polymer surfaces as they are impacted simultaneously by Mars simulant particles less than 5 micrometers in diameter moving at 20 m/s. Experiments were performed in a CO2 atmosphere at 10 mbars of pressure using a particle delivery method that propels the particles with contact. Experiments were also performed in dry air at atmospheric pressures using a pressurized particle delivery system. The five polymer surfaces, commonly used in space applications, were chosen so that they span the triboelectric series. Author

*Electrostatic Charge; Electrometers; Friction Factor; Impact Loads*

**20010119984** Argonne National Lab., IL USA

**Mechanical properties of Ce(0.9)Gd(0.1)O(2-x) and Ce(0.9)Gd(0.1)O(2-x) + Al2O3 composites**

Routbort, J. L.; Jan. 12, 1998; 11p; In English

Report No.(s): DE2001-10551; ANL/ET/CP-95258; No Copyright; Avail: Department of Energy Information Bridge

The room-temperature elastic moduli, fracture strength, and fracture toughness of dense, fine-grained, pure Ce(sub 0.9)Gd(sub 0.1)O(sub 1.95) and composites containing 1.3 and 9.1 wt. % Al(sub 2)O(sub 3) were investigated. Addition of 9.1 wt.% Al(sub 2)O(sub 3) to Ce(sub 0.9)Gd(sub 0.1)O(sub 1.95) changed the fracture mode from intergranular to transgranular and increased room-temperature fracture strength from 65 to 125 MPa and fracture toughness from 1.3 to 1.6 MPam(sup 1/2). In addition, steady-state compressive creep was measured for Ce(sub 0.9)Gd(sub 0.1)O(sub 1.95) and the Ce(sub 0.9)Gd(sub 0.1)O(sub 2(minus)x) + 9.1 wt.% Al(sub 2)O(sub 3) composite. The stress exponent (approx)1.3 and the activation energy (approx)480 kJ/mole for Ce(sub 0.9)Gd(sub 0.1)O(sub 1.95) suggested diffusional flow controlled by the cations. There was no difference in creep rate between Ce(sub 0.9)Gd(sub 0.1)O(sub 2(minus)x) and the composite.

NTIS

*Activation Energy; Ceramics; Mechanical Properties; Cerium Oxides*

**20010119986** Argonne National Lab., IL USA

**Low-temperature MOCVD growth of oriented PbZrxTi1-xO3 thin films on Si substrates**

Chen, N.; May 08, 1998; 11p; In English

Report No.(s): DE2001-10548; ANL/ET/CP-95225; No Copyright; Avail: Department of Energy Information Bridge

Polycrystalline Pb(Zr(sub 0.6)Ti(sub 0.4))O(sub 3) (PZT) thin films, 3000-6000 A thick, have been grown by metal-organic chemical vapor deposition (MOCVD) on (111)Pt/Ti/SiO(sub 2)/Si substrates at temperatures as low as 450-525 C. Random and (111)-oriented, or occasionally (100)-oriented, PZT films can be deposited directly on (111)Pt/Ti/SiO(sub 2)/Si. In addition,

highly (100)-oriented films can be deposited consistently by using 150-250 A thick (100)-oriented PbTiO(sub 3) (PT) or TiO(sub 2) as a template. Films were characterized by X-ray diffraction, electron microscopy, and electrical measurements. The as-grown (100)-oriented films on (111)Pt/TiSiO(sub 2)/Si substrates exhibited dielectric constants ((var epsilon)(sub r)) of up to 600, remnant polarization (P(sub r)) of 40 (micro)C/cm(sup 2), coercive field of 55 kV/cm, and breakdown field of 2-6 x 10(sub 7) V/m.
NTIS
*Breakdown; Metalorganic Chemical Vapor Deposition; Thin Films; Polycrystals; Dielectrics*

**20010119988** Argonne National Lab., IL USA
**Development of mixed-conducting ceramic membranes for hydrogen separation**
Guan, J.; May 18, 1998; 15p; In English
Report No.(s): DE2001-10545; ANL/ET/CP-95197; No Copyright; Avail: Department of Energy Information Bridge
SRCeO(sub 3)-based and BaCeO(sub 3)-based proton conductors have been prepared and their transport properties have been investigated by impedance spectroscopy in conjunction with open circuit voltage and water vapor evolution measurements. BaCe(sub 0.8)Y(sub 0.2)O(sub 3-(delta)) exhibits the highest conductivity in a hydrogen-containing atmosphere; however, its electronic conductivity is not adequate for hydrogen separation in a nongalvanic mode. In an effort to enhance ambipolar conductivity and improve interfacial catalytic properties, BaCe(sub 0.8)Y(sub 0.2)O(sub 3-(delta)) cermets have been fabricated into membranes. The effects of ambipolar conductivity, membrane thickness, and interfacial resistance on permeation rates have been investigated. In particular, the significance of interfacial resistance is emphasized.
NTIS
*Ceramics; Hydrogen; Membranes*

**20010119990** Argonne National Lab., IL USA
**Characterization and durability testing of a glass-bonded ceramic waste form**
Johnson, S. G.; May 18, 1998; 11p; In English
Report No.(s): DE2001-10543; ANL/ED/CP-95195; No Copyright; Avail: Department of Energy Information Bridge
Argonne National Laboratory is developing a glass bonded ceramic waste form for encapsulating the fission products and transuranics from the conditioning of metallic reactor fuel. This waste form is currently being scaled to the multi-kilogram size for encapsulation of actual high level waste. This paper will present characterization and durability testing of the ceramic waste form. An emphasis on results from application of glass durability tests such as the Product Consistency Test and characterization methods such as X-ray diffraction and scanning electron microscopy. The information presented is based on a suite of tests utilized for assessing product quality during scale-up and parametric testing.
NTIS
*Ceramics; Glass; Radioactive Wastes; Durability; Performance Tests; Encapsulating*

**20010119991** Argonne National Lab., IL USA
**Examination of subaerially altered basaltic glass with TEM and EELS**
Luo, J. S.; Jun. 17, 1998; 11p; In English
Report No.(s): DE2001-10542; ANL/CMT/CP-95167; No Copyright; Avail: Department of Energy Information Bridge
We have examined the weathered surfaces of 720 year old Hawaiian basalt glasses that were recovered from a subaerial environment with high-resolution transmission electron microscopy (TEM) and energy filtered imaging and electron energy loss spectroscopy (EELS) techniques. Whereas the alteration products (palagonite) were physically detached from the underlying glass in most samples, a gel-like amorphous layer was observed adjacent to the glass in a few samples. To our knowledge, this is the first time a gel layer has been observed on weathered basalt. This is significant because analogous gel layers have been observed on nuclear waste glasses reacted in laboratory tests, and this demonstrates an important similarity in the mechanisms of the weathering of basalt and the corrosion of waste glasses.
NTIS
*Glass; Corrosion; Basalt; Imaging Techniques; Amorphous Materials*

**20010120035** Argonne National Lab., IL USA
**Ceramic breeder materials: status and needs**
Johnson, C. E.; Feb. 02, 1998; 18p; In English
Report No.(s): DE2001-10626; ANL/CMT/CP-95540; No Copyright; Avail: Department of Energy Information Bridge, Microfiche

The tritium breeding blanket is one of the most important components of a fusion reactor because it directly involves both energy extraction and tritium production, both of which are critical to fusion power. Because of their overall desirable properties, lithium-containing ceramic solids are recognized as attractive tritium breeding materials for fusion reactor blankets. Indeed, their inherent thermal stability and chemical inertness are significant safety advantages. In numerous in-pile experiments, these materials have performed well, showing good thermal stability and good tritium release characteristics. Tritium release is particularly facile when an argon or helium purge gas containing hydrogen, typically at levels of about 0.1%, is used. However, the addition of hydrogen to the purge gas imposes a penalty when it comes to recovery of the tritium produced in the blanket. In particular, a large amount of hydrogen in the purge gas will necessitate a large multiple-stage tritium purification unit, which could translate into higher costs. Optimizing tritium release while minimizing the amount of hydrogen necessary in the purge gas requires a deeper understanding of the tritium release process, especially the interactions of hydrogen with the surface of the lithium ceramic. This paper reviews the status of ceramic breeder research and highlights several issues and data needs.
NTIS
*Ceramics; Tritium; Blankets (Fusion Reactors)*

**20010120123** Oklahoma Univ., Dept. of Chemistry, Norman, OK USA
**Liquid Crystals and Ordered Polymers for Infrared and Microwave Applications** ***Final Report, 1 Jun. 1998-3 May 2001***
Fung, Bing M.; May 2001; 9p; In English
Contract(s)/Grant(s): F49620-98-1-0453; Proj-3484
Report No.(s): AD-A394995; AFRL-SR-BL-TR-01-0516; No Copyright; Avail: CASI; A02, Hardcopy; A01, Microfiche
(1) A large number of new liquid crystals were synthesized for possible applications in advanced electro-optic devices operating in infrared and microwave ranges. These compounds contain an electron-donating group and an electron-accepting group separated by a conjugated mesogenic core. The 'push-pull' structure imparts a large longitudinal dipole moment on the molecule, resulting in very large dielectric anisotropy and significant birefringence extending to the infrared region. The electro-optic properties of several of these compounds dissolved in room-temperature nematic solvents have been measured. (2) Macroscopically oriented epoxy thermosets were formed by polymerizing liquid crystalline diepoxides with an aromatic diamine. They show increased mechanical strength over unoriented samples, and possess optical anisotropy. (3) Two short projects not originally planned were also carried out. The first was the production of super-strong cellulose aerogels, and the second was an NMR study of a polymer-dispersed liquid crystal (PDLC) system.
DTIC
*Polymers; Liquid Crystals; Electro-Optics; Synthesis (Chemistry); Crystallinity*

**20010120838** California Univ., Davis, CA USA
**Field Activated Combustion Synthesis of Ceramic and Composite Materials** ***Final Report, 1 May 1998-30 Jun. 2001***
Munir, Z. A.; Jul. 01, 2001; 16p; In English
Contract(s)/Grant(s): DAAG-55-98-1-0081
Report No.(s): AD-A395298; 94-6036494-W; ARO-37538.1-MS; No Copyright; Avail: CASI; A03, Hardcopy; A01, Microfiche
The thrust of the work completed is an investigation on the effect of an electric field on the synthesis and densification of complex materials. Experimental investigations were made on the field effect in the synthesis of: (a) solid solution precursors for nanoscale modulated composites, (b) a high temperature ceramic with relatively high fracture toughness, (c) macro-alloyed high temperature silicides, and (d) hard material of boride composites with highly oriented precipitates. Modeling studies on the effect of the electric field (current) on synthesis reactions were also made. In addition, an important new direction in the completed work was the investigation of the simultaneous synthesis and densification of nanometric materials. The latter work has led to the issuance of a U.S. Patent and a pending application for an International Patent. The work was facilitated by the use of the Spark Plasma Synthesis (SPS) apparatus, the only one of its kind in the U.S..
DTIC
*Composite Materials; Electrical Properties; Ceramics; Combustion Synthesis*

**20010121493** Pacific Northwest National Lab., Richland, WA USA
**Evaluation of the Long-Term Performance of Titanate Ceramics for Immobilization of Excess Weapons Plutonium: Results from Pressurized Unsaturated Flow and Single Pass Flow-Through Testing**
McGrail, B. P.; Schaef, H. T.; Icenhower, J. P.; Martin, P. F.; Orr, R. D.; Sep. 13, 1999; 46p; In English
Report No.(s): DE2001-10594; PNNL-12240; No Copyright; Avail: Department of Energy Information Bridge, Microfiche
This report summarizes our findings from pressurized unsaturated flow (PUF) and single-pass flow-through (SPFT) experiments to date. Results from the PUF test of a Pu-bearing ceramic with enclosing surrogate high-level waste glass show that

the glass reacts rapidly to alteration products. Glass reaction causes variations in the solution pH in contact with the ceramic materials. We also document variable concentrations of Pu in solution, primarily in colloidal form, which appear to be related to secular variations in solution composition. The apparent dissolution rate of the ceramic waste form, based on Ba concentrations in the effluent, is estimated at (le) 10(sup (minus)5) g/(m(sup 2) (center dot) d). Pu-bearing colloids were recovered in the size range of 0.2 to 2 (micro)m, but it is not clear that such entities would be transported in a system that is not advective-flow dominated. Results from SPFT experiments give information on the corrosion resistance of two surrogate Pu-ceramics (Ce-pyrochlore and Ce-zirconolite) at 90 C over a pH range of 2 to 12. The two ceramics were doped with minor quantities ((approximately)0.1 mass%) of MoO(sub 3), so that concentrations of Mo in the effluent solution could be used to monitor the reaction behavior of the materials. The data obtained thus far from experiments with durations up to 150 d do not conclusively prove that the solid-aqueous solution systems have reached steady-state conditions. Therefore, the dissolution mechanism cannot be determined. Apparent dissolution rates of the two ceramic materials based on Ce, Gd, and Mo concentrations in the effluent solutions from the SPFT are nearly identical and vary between 1.1 to 8.5 x 10(sup (minus)4) g/(m(sup 2) (center dot) d). In addition, the data reveal a slightly amphoteric dissolution behavior, with a minimum apparent rate at pH = 7 to 8, over the pH range examined. Results from two related ceramic samples suggest that radiation damage can have a measurable effect on the dissolution of titanium-based ceramics. The rare earth pyrochlores, Gd(sub 2)Ti(sub 2)O(sub 7) and Lu(sub 2)Ti(sub 2)O(sub 7), are being studied as part of the DOE (Department of Energy) Environmental Management Science Program, and the results are germane to this study. The corrosion resistances of both heavy-ion bombarded and pristine (non-bombarded) specimens are being examined with the SPFT test. Initial data indicate that the dissolution rate may increase by a factor of 3 times or more when these materials become amorphous from radiation damage.
NTIS
*Ceramics; Titanates; Plutonium; Radioactive Wastes*

**20010121879** Iowa State Univ. of Science and Technology, Dept. of Materials Science and Engineering, Ames, IA USA
**A New Method to Prepare Polycrystalline Meta-Thioboric Acid, (HBS2)3**
Karthikeyan, Annamalai; Martindale, Chad A.; Martin, Steve W.; Sep. 25, 2001; 6p; In English
Contract(s)/Grant(s): N00014-99-1-0538
Report No.(s): AD-A395192; No Copyright; Avail: CASI; A02, Hardcopy; A01, Microfiche

Thioacids (ex: thioboric acid) are important precursors in exploring new chalcogenide ceramic and glassy materials. We report here a new facile method to prepare crystalline meta-thioboric acid (c-(HBS2)3). c-(HBS2)3 was prepared by reacting H2S with B2S3, in the vapor phase and the product was obtained as a vapor condensate. The technique is fairly simple and quick compared to the time consuming and wet routes of thiolysis of boron tribromide. The reaction takes place at much lower temperatures and in the vapor phase, thus achieving higher purity.
DTIC
*Polycrystals; Ceramics; Boric Acids; Hydrogen Sulfide; Chalcogenides; Chemical Reactions*

**20010122234** Lawrence Livermore National Lab., Livermore, CA USA
**Modeling high-pressure and high-temperature phase changes in bulk carbon**
Glosi, J. N.; Ree, F. H.; Jul. 01, 1999; 6p; In English
Report No.(s): DE2001-10150; UCRL-JC-132849; No Copyright; Avail: Department of Energy Information Bridge, Microfiche

The phase diagram of carbon is not experimentally well known at high pressure and/or high temperature. We have determined the phase diagram of carbon by means of Monte Carlo and molecular dynamics simulations methods using the Brenner bond order potential. The melting line of diamond was found to have a positive slope with the graphite-diamond-liquid triple point in agreement with an estimated value based on experiment. The present calculation predicts a first-order phase transition in liquid carbon terminated by a critical point and by a triple point on the graphite melting line. The low-density liquid is predominantly sp bonded with little sp(sup 3) character. The high-density liquid is mostly sp(sup 3) bonded with little sp character.
NTIS
*Carbon; Phase Diagrams; Monte Carlo Method; Molecular Dynamics*

**20010122355** Argonne National Lab., IL USA
**Photorefractivity in Polymer-Stabilized Liquid Crystals Films**
Wasielewski, M. R.; May 08, 1998; 4p; In English
Report No.(s): DE2001-10775; ANL/CHM/CP-96402; No Copyright; Avail: Department of Energy Information Bridge, Microfiche

We have shown that polymer-stabilized liquid crystals (PSLCs) are capable of forming photorefractive gratings that operate in the thick grating regime. Polymer stabilization alters the charge transport and trapping characteristics of LCs, resulting in longer lived gratings, while maintaining the advantages of high orientational birefringence within LCs. Furthermore, very low applied electric fields (800 V/cm) and low optical intensities (100 mW/sq cm) are required to create large photorefractive effects in these materials. It is expected that optimization of the redox potentials of the chromophores within the PSLCs will continue to improve the performance of these materials.
NTIS
*Liquid Crystals; Photorefractivity; Optimization; Gratings (Spectra)*

**20010122356** Argonne National Lab., IL USA
**Development of Nondestructive Evaluation Methods for Structural Ceramics**
Ellingson, W. A.; Aug. 19, 1998; 12p; In English
Report No.(s): DE2001-10774; ANL/ET/CP-96399; No Copyright; Avail: Department of Energy Information Bridge, Microfiche

During the past year, the focus of our work on nondestructive evaluation (NDE) methods was on the development and application of these methods to technologies such as ceramic matrix composite (CMC) hot-gas filters, CMC high-temperature heat exchangers, and CMC ceramic/ceramic joining. Such technologies are critical to the 'Vision 21 Energy-Plex Fleet' of modular, high-efficiency, low-emission power systems. Specifically, our NDE work has continued toward faster, higher sensitivity, volumetric X-ray computed tomographic imaging with new amorphous silicon detectors to detect and measure axial and radial density variations in hot-gas filters and heat exchangers; explored the potential use of high-speed focal-plane-array infrared imaging technology to detect delaminations and variations in the thermal properties of SiC/SiC heat exchangers; and explored various NDE methods to characterize CMC joints in cooperation with various industrial partners. Work this year also addressed support of Southern Companies Services, Inc., Power Systems Development Facility, where NDE is needed to assess the condition of hot-gas candle filters. This paper presents the results of these efforts.
NTIS
*Ceramic Matrix Composites; Imaging Techniques; Infrared Imagery; Nondestructive Tests*

**20010122371** Argonne National Lab., IL USA
**Trend of neutron-scattering studies of hard materials**
Loong, C. K., Argonne National Lab., USA; Apr. 17, 1998; 10p; In English
Report No.(s): DE2001-10743; ANL/IPNS/CP-96195; No Copyright; Avail: Department of Energy Information Bridge, Microfiche

Future high-tech applications will undoubtedly demand materials for carrying out complex tasks under stringent or adverse conditions. One of the important goals in materials design is to be able to introduce specific desirable properties in the components at an early stage during fabrication and to predict the performance of the final product. This approach requires a database of atomic-level structures and response of a variety of key materials and sophisticated algorithms for large-scale computations. Slow (cold to epithermal) neutrons probe the organization and dynamic response of atomic nuclei and electrons in a substance (bulk and low-dimensional) thereby providing a valuable means for a microscopic interpretation of materials properties. For decades neutron technologists and instrument scientists have striven to improve the neutron sources and instrumentation for condensed-matter research. In this International Workshop of the JHT Projects and the N-Arena, I wish to comment on the trend of instrument development, using some recent studies of hard materials as an example. The requirement for high strength at high temperatures has led to intense studies of nitride- and carbide-based ceramics. Additional incentives include the lower density, lower thermal expansion, and better corrosion and oxidation resistance of ceramics as compared to metals. However, the current strength and reliability of nitride and carbide ceramics are not sufficient to replace the metallic counterparts such as heat engine components. The knowledge of atomic short-to-long 1 range ordering, the microstructure of the crystalline grains and intergranular phases as well as the dynamic response of atoms to applied force and temperature fields is an important prerequisite for the realization of wide-spread high-temperature applications of ceramics. The goal of neutron-scattering methodology is to provide the best means for high-resolution characterization of these properties over a wide range of length and time scales (0.1-1000 nm and 10(sup (minus)8)-10(sup (minus)13) sec. Obviously, many different kinds of instruments have to be developed in parallel with the advancement of neutron sources.
NTIS
*Neutron Scattering; Ceramics; Mechanical Properties; Neutron Diffraction*

**20010122714** Dayton Univ., Structural Integrity Div., OH USA

**Fracture Behavior of a Si3N4-BN Fibrous Monolith Ceramic** ***Final Report, 1 Oct. 1999 - 1 Apr. 2001***

Pierce, J. L.; Zawada, L. P.; Staehler, J. M.; Apr. 2001; 204p; In English; Original contains color images; Prepared in collaboration with Systran, Inc., 2146 Linden Ave., Dayton, OH

Contract(s)/Grant(s): AF Proj. 2302

Report No.(s): AD-A395288; AFRL-ML-WP-TR-2001-4102; No Copyright; Avail: CASI; A10, Hardcopy; A03, Microfiche

The two different microstructures of Si3N4-BN fibrous monolith ceramic material were compared to each other and to monolithic Si3N4 in order to evaluate the fracture behavior and effect of cell size on the mechanical performance of the material. The room temperature behavior was evaluated through fast-fracture tensile testing of straight-sided, dogbone, and modified single-edge notched specimens with various notch lengths. Load-unload and cyclic fracture tests were performed along with several non-destructive evaluation (NDE) techniques including x-ray radiography, thermography, ultrasonic c-scanning, and acoustic emission to determine critical stages of damage evolution in each. The Si3N4-BN materials tested showed non-catastrophic fracture behavior compared to the monolithic Si3N4 in tension and demonstrated to be insensitive to stress concentrations imparted by the notches. The influence of individual cell size on the fracture behavior of the FM materials was not evident as the cell bundles formed by the processing technique, not the individual cells, were the dominate microstructural feature. Cell bundle size in the materials tested was shown to influence the behavior as the displacements, extent of damage, and fracture energies were higher with larger cell bundles.

DTIC

*Silicon Nitrides; Cyclic Loads; Acoustic Emission; Fracture Mechanics*

**20010122823** Los Alamos National Lab., NM USA

**Cement waste-form development for PuF4 residues at the Rocky Flats Environmental Technology Site**

Smith, C. A.; Veazey, G.; Nakoaka, R. K.; Sep. 01, 2000; 11p; In English

Report No.(s): DE2000-763925; LA-UR-00-4531; No Copyright; Avail: Department of Energy Information Bridge

This report describes the development of a waste form to stabilize Plutonium Tetrafluoride-based residue solids at the Rocky Flats Environmental Technology Site (WETS). The residue solids stream is composed of a spectrum from almost all PuF4 to almost all NaF. The work focused on the performance evaluation of several Portland cement/water/residues formulations. Performance standards were chosen to address the Waste Isolation Pilot Plant-Waste Acceptance Criteria (WIPP-WAC), Environmental Protection Agency Resource Conservation and Recovery Act (EPMRCRA), Transuranic Package Transporter Safety Analysis Report for Packaging (TRUPAC II SARP), and Safeguards Termination Limit (STL).

NTIS

*Cements; Environment Protection; Radioactive Wastes; Waste Disposal; Packaging*

**20010122893** Argonne National Lab., IL USA

**Development of oxide fibrous monolith systems**

Goretta, K. C.; Mar. 02, 1999; 15p; In English

Report No.(s): DE2001-10962; ANL/ET/CP-97265; No Copyright; Avail: Department of Energy Information Bridge, Microfiche

Fibrous monolithic ceramics generally have a cellular structure that consists of a strong cell surrounded by a weaker boundary phase. Fibrous monoliths (FMs) are produced from powders by conventional ceramic fabrication techniques, such as extrusion. When properly engineered, they exhibit fail gracefully . Several compositions of ceramics and cermets have been processed successfully in fibrous monolithic form. The most thoroughly investigated fibrous monolith consists of Si(sub 3)N(sub 4) cells and a BN cell-boundary phase. Through appropriate selection of initial powders and extrusion and hot-pressing parameters, very tough final products have been produced. The resultant high toughness is due primarily to delamination during fracture along textured platelike BN grains. The primary objectives of our program are to develop: (1) Oxide-based FMs, including new systems with improved properties; (2) FMs that can be pressureless sintered rather than hot-pressed; (3) Techniques for continuous extrusion of FM filaments, including solid freeform fabrication (SFF) for net-shape fabrication of FMs; (4) Predictive micromechanical models for FM design and performance; and (5) Ties with industrial producers and users of FMs.

NTIS

*Ceramics; Cermets; Ceramic Fibers; Fabrication*

**20010122946** Argonne National Lab., IL USA

**Demonstration of packaging of Fernald Silo I waste in chemically bonded phosphate ceramic**

Wagh, A. S.; Jan. 27, 1999; 11p; In English

Report No.(s): DE2001-11049; ANL/ET/CP-97467; No Copyright; Avail: Department of Energy Information Bridge, Microfiche

This paper summarizes our experience in bench-scale packaging of Fernald Silo I waste in chemically bonded phosphate ceramics. The waste was received from the Fernald Environmental Management Project (FEMP), and its treatability was studied in our laboratory. This waste contained As(sup 5+), Ba, Cr(sup 6+), Ni, Pb, Se(sup 4+), and Zn as the hazardous contaminants. In addition, the total specific activity of all the radioactive isotopes in the waste was 3.85 (micro)Ci/g, of which that of radium alone was 0.477 (micro)Ci/g. This indicated that radon (a daughter product of the radium) in the waste could present a serious handling problem during this study. For this reason, the waste was handled and stored in a flowing-air glovebox. We made waste form samples with an actual waste loading of 66.05 wt. and subjected them to the Environmental Protection Agency (EPA) Toxicity Characteristic Leaching Procedure (TCLP). The results showed excellent stabilization of all contaminants. Actual levels detected in the leachate were well below the EPAs most stringent Universal Treatment Standards and in almost all cases were one order of magnitude below this limit. Radioactivity in the leachate was also very low. Alpha activity was 25 (+/-) 2.5 pCi/mL, while beta activity was 9.81 (+/-) 0.98 pCi/mL. This very low activity was attributed to the efficient stabilization of radium as insoluble radium phosphate in the waste form, thus prohibiting its leaching. This study indicates that the chemically bonded phosphate ceramic process may be a very suitable way to package Silo I waste for transportation and storage or disposal.
NTIS
*Ceramics; Packaging; Waste Disposal*

**20010123031** Brookhaven National Lab., Upton, NY USA
**Recent work on renormalization group for the colored glass condensate**
McLerran,; Apr. 06, 2000; 5p; In English
Report No.(s): DE2000-767193; BNL-67799; No Copyright; Avail: Department of Energy Information Bridge
In this brief report, I summarize the recent work which I have been doing with E. Iancu and A. Leonidov tcl get explicit formulae for the renormalization group equations which describe the Colored Glass Condensate.
NTIS
*Glass; Renormalization Group Methods; Condensates*

**20010123052** Brookhaven National Lab., Upton, NY USA
**Effect of Radiation on Spinel Ceramics for Permanent Containers for Nuclear Waste Transportation and Storage**
Adams, J.; Cowgill, M.; Moskowitz, P.; Rokhvarger, A.; Apr. 30, 2000; 9p; In English
Report No.(s): DE2000-767142; BNL-67518; No Copyright; Avail: Department of Energy Information Bridge
NUCON Systems, Inc., NY (Nucon) has proposed an alternative waste management technology and developed ceramic material formulations from inexpensive spinel (MgAlzOd) refractory powder (no inorganic additives) in order to fabricate ceramic containers for the transportation and permanent storage of nuclear waste. Nucon has contracted with the Brookhaven National Laboratory (BNL) Department of Advanced Technology (DAT) to develop a test methodology and provide evaluation of the effects of radiation on these materials. The Gamma Irradiation Facility (GIF) of BNL was used to irradiate samples. The radiation resistance of three spinel compositions (B1, B2, and C2) and two physical forms (slip cast bars and extruded rods) were tested. The spinel compositions differ only in particle and crystal size distributions and suppliers. Compressive strengths of unirradiated baseline samples were compared to those of samples irradiated to total gamma doses of 1x10(exp 8), 5x10(exp 8), and 1x10(exp 9) rad. Other physical evaluations included water absorption, bulk and geometric density, apparent specific gravity, and apparent porosity. This presentation discusses the first results of the application of the BNL-Nucon's test methodology. The paper is a continuation of the series of presentations on the 'ceramic container' project made at the Waste Management Technology Section of the American Ceramic Society Annual Meetings of 1995, 1998, and 1999.
NTIS
*Ceramics; Radiation Effects; Radioactive Wastes; Spinel; Waste Management*

**20010123130** Brookhaven National Lab., Upton, NY USA
**Thermoplastic Encapsulation Treatability Study of Fernald Silo 1 and Silo 3 Wastes**
Lageraaen, P. R.; Adams, J. W.; Milian, L. W.; Kalb, P. D.; May 01, 1998; 54p; In English
Report No.(s): DE2000-767121; BNL-52594; No Copyright; Avail: Department of Energy Information Bridge
Treatability studies for polyethylene and sulfur polymer microencapsulation of Fernald Silo 1 and Silo 3 wastes were conducted at Brookhaven National Laboratory (BNL). The treatability work, which included optimal formulation development and processibility testing, was performed to determine the applicability of these solidification technologies for the Fernald Silo mixed wastes. A surrogate was used during formulation development for the Silo 1 waste. Processing results in conjunction with leach testing of waste forms to measure waste form performance were used to establish the most effective thermoplastic/waste composition. A series of waste form specimens were cast from the surrogate and mixed waste encapsulated product with both

polyethylene and sulfur polymer for more comprehensive testing at the University of Cincinnati. This data will be compared with treatability results from alternative solidification and stabilization methods such as cementation and phosphate-bonded ceramics, to evaluate treatment options for Fernald Silo wastes. Based on the treatability results, polyethylene and sulfur polymer microencapsulation can successfully process Silo wastes. Considering waste form leach performance using the Universal Treatment Standard limits, based on testing conducted at BNL, polyethylene and sulfur polymer are both viable treatment methods for Silo 3 waste. For Silo 1 waste, polyethylene microencapsulation is recommended due to the high lead concentration in the waste.
NTIS
*Encapsulating; Polyethylenes; Sulfur Compounds*

**20010123131** Brookhaven National Lab., Upton, NY USA
**Low temperature glasses for hanford tank wastes**
Cao, H.; Adams, J. W.; Kalb, P. D.; Sep. 30, 1995; 19p; In English
Report No.(s): DE2000-767120; BNL-52595; No Copyright; Avail: Department of Energy Information Bridge

TWRS (Tank Waste Remediation System) wastes contain certain chemical components which, either because of their limited solubility or volatilization at high temperatures, present problems for conventional vitrification technologies. The current task completed by BNL (Brookhaven National Laboratory) concerns the use of low temperature glasses for tank waste remediation. A literature review of existing technologies highlighted lead-iron-phosphate glasses, with melt temperatures of around 900 C, as a significant improvement over existing borosilicate formulations. However, concerns over leachability of the high lead levels in the glass matrix has kindled interest in the development of lead-free phosphate glasses. As part of this current task, crucible studies were performed to scope the potential of advanced phosphate glasses. Based on pioneer work on iron-aluminum-phosphate and tin-phosphate glasses, new formulations were investigated, modified with cations to enhance chemical durability and reduce melt temperatures. Dissolution of matrix metals using a standard leach test, the Product Characterization Test (PCT), was the basis used to evaluate the new glasses. Cursory results indicate that low-temperature glasses can indeed be prepared with melt temperatures between 450 and 900 C. Durability of these glasses and composites compares favorably with lead-iron-phosphate glasses, and is an improvement over reference borosilicate formulations. The capacity to incorporate high percentages of sodium was demonstrated, however much waste-specific work will be required to further qualify and quantify treatability of tank waste components.
NTIS
*Radioactive Wastes; Glass*

**20010123138** Brookhaven National Lab., Upton, NY USA
**Effect of radiation on spinel ceramics for permanent containers for nuclear waste transportation and storage**
Adams, J.; Cowgill, M.; Moskowitz, P.; Rokhvarger, A.; Apr. 30, 2000; 9p; In English
Report No.(s): DE2000-767085; BNL-67518; No Copyright; Avail: Department of Energy Information Bridge

NUCON Systems, Inc., NY (Nucon) has proposed an alternative waste management technology and developed ceramic material formulations from inexpensive spinel (MgAlzOd) refractory powder (no inorganic additives) in order to fabricate ceramic containers for the transportation and permanent storage of nuclear waste. Nucon has contracted with the Brookhaven National Laboratory (BNL) Department of Advanced Technology (DAT) to develop a test methodology and provide evaluation of the effects of radiation on these materials. The Gamma Irradiation Facility (GIF) of BNL was used to irradiate samples. The radiation resistance of three spinel compositions (B1, B2, and C2) and two physical forms (slip cast bars and extruded rods) were tested. The spinel compositions differ only in particle and crystal size distributions and suppliers. Compressive strengths of unirradiated baseline samples were compared to those of samples irradiated to total gamma doses of 1x108, 5x108, and 1x109 rad. Other physical evaluations included water absorption, bulk and geometric density, apparent specific gravity, and apparent porosity. This presentation discusses the first results of the application of the BNL- Nucon's test methodology. The paper is a continuation of the series of presentations on the 'ceramic container' project made at the Waste Management Technology Section of the American Ceramic Society Annual Meetings of 1995, 1998, and 1999.
NTIS
*Ceramics; Radioactive Wastes; Spinel; Containment*

**20010123399** Argonne National Lab., IL USA
**Mechanical and Electrical Properties of ZnO/Ag Nanocomposites**
Hayashi, Y.; Aug. 27, 1998; 13p; In English
Report No.(s): DE2001-10942; ANL/ET/CP-97181; No Copyright; Avail: Department of Energy Information Bridge

Effects of Ag particle dispersions on microstructural development and some properties were investigated for ZnO/Ag nanocomposites. They were fabricated by Pulse Electric Current Sintering (PECS) Process to achieve finer and densified microstructure. ZnO/Ag nanocomposites with novel microstructure which were prepared by a reduction process using Ag2O fine powders were compared with microcomposites prepared by mixing of Ag and ZnO powders. Scanning electron microscopic observation indicated that fine Ag particles were homogeneously dispersed within the ZnO matrix grains and at the grain boundaries for ZnO/Ag nanocomposites prepared by the reduction process using Ag2O fine powder. Hardness and fracture toughness increased with increasing the Ag volume fraction. Linear resistivity was decreased with increasing Ag volume fraction. However, the mechanical and electrical properties appeared to the significantly different for composites prepared by two different powder processes.
NTIS
*Mechanical Properties; Microstructure; Powder (Particles); Nanocomposites; Electrical Properties; Zinc Oxides*

**20010123400** Argonne National Lab., IL USA
**Phonon Densities of States and Related Thermodynamic Properties of High Temperature Ceramics**
Loong, C. K.; Aug. 28, 1998; 27p; In English
Report No.(s): DE2001-10941; ANL/IPNS/CP-97166; No Copyright; Avail: Department of Energy Information Bridge
Structural components and semiconductor devices based on silicon nitride, aluminum nitride, and gallium nitride are expected to function more reliably at elevated temperatures and at higher levels of performance because of the strong atomic bonding in these materials. The degree of covalency, lattice specific heat, and thermal conductivity are important design factors for the realization of advanced applications. We have determined the phonon densities of states of these ceramics by the method of neutron scattering. The results provide a microscopic interpretation of the mechanical and thermal properties. Moreover, experimental data of the static, structures, and dynamic excitations of atoms are essential to the validation of interparticle potentials employed for molecular-dynamics simulations of high-temperature properties of multi-component ceramic systems. We present an overview of neutron-scattering investigations of the atomic organization, phonon excitations, as well as calculations of related thermodynamic properties of Si3N4, (beta)-sialon, AlN and GaN. The results are compared with those of the oxide analogs such as SiO2 and Al2O3.
NTIS
*Atomic Excitations; Ceramics; High Temperature; Mechanical Properties; Phonons; Semiconductor Devices; Thermodynamic Properties; Silicon Nitrides*

**20010123464** Argonne National Lab., IL USA
**Thermodynamic and nonstoichiometric behavior of the GdBa2Cu3Ox system**
Tetenbaum, M.; Sep. 29, 1998; 12p; In English
Report No.(s): DE2001-10988; ANL/CMT/CP-97381; No Copyright; Avail: Department of Energy Information Bridge, Microfiche
Electromotive force (EMF) measurements of oxygen fugacities as a function of stoichiometry have been made on the GdBa2Cu3O(sub x) system in the temperature range (approximately)400-600 C by means of an oxygen titration technique with an yttria-stabilized zirconia electrolyte. Equations for the variation of oxygen partial pressure with composition and temperature have been derived from our EMF measurements. The shape of the 400 C isotherms as a function of oxygen stoichiometry for the Gd and Nd cuprate systems suggests the presence of miscibility gaps at values of x that are higher than those in the YBa2Cu3O(sub x) system. For a given oxygen stoichiometry, oxygen partial pressures above Gd-123 and Nd-123 cuprate systems are higher (above x = 6.5) than that for the Y-123 system. A thermodynamic assessment and intercomparison of our partial pressure measurements with the results of related measurements will be presented.
NTIS
*Electromotive Forces; Gadolinium; Yttria-Stabilized Zirconia; Thermodynamic Properties*

**20010123727** Lawrence Livermore National Lab., Livermore, CA USA
**Maldi analysis of estane degradation**
Haining, J.; Kober, E. M.; LeMay, J. D.; Mays, J.; Nonidez, W.; Mar. 26, 1999; 7p; In English
Report No.(s): DE2001-11312; UCRL-JC-133769; No Copyright; Avail: Department of Energy Information Bridge
SEUMALDI has been successfully used to accurately measure the MW of hydrolysis degradation products from Estane 5703. Reasonable structure assignments have been made to the degradation products and several observations reported. Most of the low MW degradation peaks have been identified as ester hydrolysis fragments. The data suggest that the polyester macrodiol may be

shorter than the (approximately)2000 amu reported by the manufacturer. Experiments are ongoing to determine if hydrolysis occurs within the material's applied environment.
NTIS
*Degradation; Hydrolysis*

**20010123735** Argonne National Lab., IL USA
**Development of a ceramic waste form for high-level waste disposal**
Esh, D. W.; Nov. 30, 1998; 10p; In English
Report No.(s): DE2001-11116; ANL/NT/CP-97702; No Copyright; Avail: Department of Energy Information Bridge, Microfiche

A ceramic waste form is being developed by Argonne National Laboratory (ANL) as part of the demonstration of the electrometallurgical treatment of spent nuclear fuel. The halide, alkaline earth, alkali, transuranic, and rare earth fission products are stabilized in zeolite which is combined with glass and processed in a hot isostatic press (HIP) to form a ceramic composite. The mineral sodalite is formed in the HIP from the zeolite precursor. The process, from starting materials to final product, is relatively simple. An overview of the processing operations is given. The metrics that have been developed to measure the success or completion of processing operations are developed and discussed. The impact of variability in processing metrics on the durability of the final product is presented.
NTIS
*Ceramics; Waste Disposal; Zeolites; Sodalite*

**20010123954** Argonne National Lab., IL USA
**Neutron Scattering Studies of Industry-Relevant Materials: Connecting Microscopic Behavior to Applied Properties**
Loong, C. K.; Jan. 04, 1999; 22p; In English
Report No.(s): DE2001-10940; ANL/IPNS/CP-97165; No Copyright; Avail: Department of Energy Information Bridge

Certain systems of oxides, nitrides, and carbides have been recognized as the basic components of advanced materials for applications as engineering and electronic ceramics, catalysts, sensors, etc., under extreme environments. An understanding of the basic atomic and electronic properties of these systems will benefit enormously the industrial development, of new materials featuring tailored properties. We present an overview of neutron-scattering studies of the crystal phases, microstructure, phonon, and magnetic excitations of key materials including rare-earth phosphates, phosphate glasses, nanostructured metal oxides, as well as silicon nitride and silicon carbide ceramics. A close collaboration among neutron-scattering experimentation, molecular-dynamics simulation and material synthesis is emphasized.
NTIS
*Carbides; Molecular Dynamics; Neutron Scattering; Nitrides; Oxides; Microstructure*

**20010123955** Argonne National Lab., IL USA
**High-Temperature Compressive Deformation of Si3N4/BN Fibrous Monoliths**
Routbort, J. L.; Feb. 04, 1999; 10p; In English
Report No.(s): DE2001-10938; ANL/ET/CP-97126; No Copyright; Avail: Department of Energy Information Bridge

Fibrous monolithic Si3N4/BN (approximately 85 vol. Si3N4/15 vol. BN) and monolithic Si3N4 ceramics were compressed at a nearly constant strain rate (var-epsilon) at 1200-1400 C in N2. The var-epsilon range was approximately 1x10(exp -6) to 5x10(exp -6)/s; the stress (sigma) range was 37-202 MPa. The Si3N4 and the unidirectional fibrous monoliths that were oriented with the long axis of the Si3N4 cells parallel to the compression direction exhibited plasticity at 1300 and 1400 C, with var-epsilon proportional to sigma. A 0/90 degree cross-ply Si3N4/BN laminate also exhibited significant plasticity, but it was weaker than the above-mentioned ceramics. The unidirectional fibrous monoliths that were compressed perpendicular to the cell direction fractured at approximately 50 MPa in all tests. A +/- 45 degree laminate tested at 1300 C fractured at a stress of approximately 40 MPa. Low fracture stress correlated with shear through BN layers.
NTIS
*Ceramics; Deformation; Laminates; Silicon Nitrides; Boron Nitrides*

**20010125161** Argonne National Lab., IL USA
**Scale up issues involved with the ceramic waste form: Ceramic-container interactions and ceramic cracking quantification**
Bateman, K. J.; DiSanto, T.; Goff, K. M.; Johnson, S. G.; OHolleran, T.; May 03, 1999; 11p; In English
Report No.(s): DE2001-11778; ANL/NT/CP-98912; No Copyright; Avail: Department of Energy Information Bridge

Argonne National Laboratory is developing a process for the conditioning of spent nuclear fuel to prepare the material for final disposal. Two waste streams will result from the treatment process, a stainless steel based form and a ceramic based form. The ceramic waste form will be enclosed in a stainless steel container. In order to assess the performance of the ceramic waste form in a repository two factors must be examined, the surface area increases caused by waste form cracking and any ceramic/canister interactions that may release toxic material. The results indicate that the surface area increases are less than the High Level Waste glass and any toxic releases are below regulatory limits.
NTIS
*Spent Fuels; Waste Disposal*

**20010125241** Argonne National Lab., IL USA
**Surface analysis of rubbers and plastics using secondary neutral mass spectrometry**
Pellin, M. J.; Savina, M. R.; Aug. 23, 1999; 23p; In English
Report No.(s): DE2001-11765; ANL/CHM/CP-98812; No Copyright; Avail: Department of Energy Information Bridge
Rubber and plastics are complex mixtures of long-chain polymers, smaller organic additives used as plasticizers, mildicides, fungicides, colorants, etc., and inorganic additives such as carbon and silica. Surface analysis of such materials is at once difficult and important. The difficulty lies in the need to identify specific carbon molecules on a very similar organic surface. The importance arises from the dramatic effect that the distribution and concentration of additives have on the physical properties of polymeric materials. Recently we have had some success in applying laser desorption post-ionization mass spectrometry in measuring the surface concentration and distribution of both additives and the polymer molecules themselves. The key has been to use the photoionization properties of the analyte of interest to augment mass spectrometric information.
NTIS
*Plastics; Rubber; Surface Properties*

**20010125403** Argonne National Lab., IL USA
**Round-robin testing of a standard material for acceptance testing of low-activity radioactive waste products**
Ebert, W. L.; May 13, 1999; 11p; In English
Report No.(s): DE2001-11805; ANL/CMT/CP-99016; No Copyright; Avail: Department of Energy Information Bridge
A round robin test program was conducted with a glass that was developed for use as a standard test material for acceptance testing of low-activity waste glasses made with Hanford tank wastes. The program was conducted to measure the between-laboratory reproducibility of composition analysis and durability test results. Participants were free to select the methods used to analyze the glass composition. The durability tests closely followed the Product Consistency Test (PCT) Method A, except that tests were conducted at both 40 and 90 C, and parallel tests with a reference glass were not required. Samples that had been crushed, sieved, and washed to remove fines were provided to participants for tests and analyses. The results are presented in this paper. While the results are still being analyzed, the reproducibility of both the composition and PCTs results compare favorably with the results of round robins conducted with other glasses.
NTIS
*Radioactive Wastes; Glass*

**20010125404** Argonne National Lab., IL USA
**Development of NDE methods for hot gas filters**
Deemer, C.; Ellingson, W. A.; Koehl, E. R.; Lee, H.; Spohnholtz, T.; Jul. 21, 1999; 13p; In English
Report No.(s): DE2001-11804; ANL/ET/CP-99007; No Copyright; Avail: Department of Energy Information Bridge
Ceramic hot gas candle filters are currently under development for hot gas particulate cleanup in advanced coal-based power systems. The ceramic materials for these filters include nonoxide monolithic, nonoxide-fiber-reinforced composites, and nonoxide reticulated foam. A concern is the lack of reliable data on which to base decisions for reusing or replacing hot gas filters during plant shutdowns. The work in this project is aimed at developing nondestructive evaluation (FIDE) technology to allow detection, and determination of extent, of life-limiting characteristics such as thermal fatigue, oxidation, damage from ash bridging such as localized cracking, damage from local burning, and elongation at elevated temperature. Although in-situ NDE methods are desirable in order to avoid disassembly of the candle filter vessels, the current vessel designs, the presence of filter cakes and possible ash bridging, and the state of NDE technology prevent this. Candle filter producers use a variety of NDE methods to ensure as-produced quality. While impact acoustic resonance offers initial promise for examining new as-produced filters and for detecting damage in some monolithic filters when removed from service, it presents difficulties in data interpretation, it lacks localization capability, and its applicability to composites has yet to be demonstrated. Additional NDE technologies being developed and evaluated in this program and whose applicability to both monolithics and composites has been

demonstrated include (1) full-scale thermal imaging for analyzing thermal property variations; (2) fret, high-spatial-resolution X-ray imaging for detecting density variations and dimensional changes; (3) air-coupled ultrasonic methods for determining through-thickness compositional variations; and (4) acoustic emission technology with mechanical loading for detecting localized bulk damage. New and exposed clay-bonded SiC filters and CVI-SiC composite filters have been tested with these additional NDE methods.
NTIS
*Nondestructive Tests; Ceramics; High Temperature Gases*

**20010125409** Argonne National Lab., IL USA
**High-dielectric-constant ferroelectric thin film and bulk ceramic capacitors for power electronics**
Auciello, O. H.; Baldo, P.; Baumann, P.; Erck, R. A.; Giumarra, J.; Aug. 10, 1999; 9p; In English
Report No.(s): DE2001-11797; ANL/ET/CP-98991; No Copyright; Avail: Department of Energy Information Bridge

Significant effort is presently focused on reducing the size and weight of power electronic modules. to achieve these goals in high-power capacitors, alternative materials and fabrication processes are needed. Thin film (greater than 0.5 micrometers) and bulk capacitors that use perovskite-based ferroelectric dielectrics are promising alternative technologies. Ferroelectrics possess high dielectric constants, thus offering substantial increases in volumetric capacitance. In thin film form, these materials display low loss and high breakdown strength. The unique properties of some of these materials, such as a nonlinear dielectric response or a high energy-storage capacity accompanying a phase change, can be exploited for power electronic capacitors. Prototype capacitors of two such materials, (Ba,SR)TiO3 and PbZrO3, have been fabricated in both thin film and bulk ceramic form. The influence of fabrication conditions on dielectric properties has been studied. Initial studies have demonstrated the viability of perovskite ferroelectrics for next-generation capacitor components.
NTIS
*Ceramics; Thin Films; Dielectric Properties; Capacitors*

**20010125472** Argonne National Lab., IL USA
**Phase Stability of the Mixed-Conducting SR-Fe-Co-O System**
Ma, B.; Balachandran, U.; Hodges, J. P.; Jorgensen, J. D.; Miller, D. J.; Dec. 12, 1997; 9p; In English
Report No.(s): DE2001-8099; ANL/ET/CP-93672; No Copyright; Avail: Department of Energy Information Bridge, Microfiche

Mixed-conducting ceramic oxides have potential uses in high-temperature electrochemical applications such as solid oxide fuel cells, batteries, sensors, and oxygen-permeable membranes. The SR-Fe-Co-O system combines high electronic/ionic conductivity with appreciable oxygen permeability at elevated temperatures. Dense ceramic membranes made of this material can be used to separate high-purity oxygen from air without the need for external electrical circuitry, or to partially oxidize methane to produce syngas. Samples of SR2Fe(3-x)Co(x)O(y) (with x = 0, 0.6, 1.0, and 1.4) were prepared by solid-state reaction method in atmospheres with various oxygen partial pressures (pO2) and were characterized by X-ray diffraction, scanning electron microscopy, and electrical conductivity testing. Phase components of the sample are dependent on cobalt concentration and pO2. Electrical conductivity increases with increasing temperature and cobalt content in the material.
NTIS
*Ceramics; Oxides; Stability*

**20010125492** Argonne National Lab., IL USA
**Development of mixed-conducting ceramics for gas separation applications**
Balachandran, U.; Dec. 02, 1998; 9p; In English
Report No.(s): DE2001-10845; ANL/ET/CP-96660; No Copyright; Avail: Department of Energy Information Bridge

Mixed-conducting oxides are used in many applications, including fuel cells, gas separation membranes, sensors, and electrocatalysis. This paper describes mixed-conducting ceramic membranes that are being developed to selectively remove oxygen and hydrogen from gas streams in a nongalvanic mode of operation (i.e., with no electrodes or external power supply). Because of its high combined electronic/ionic conductivity and significant oxygen permeability, the mixed-conducting SR-Fe-Co oxide (SFC) has been developed for high-purity oxygen separation and/or partial oxidation of methane to synthesis gas, i.e., syngas, a mixture of carbon monoxide and hydrogen. The electronic and ionic conductivities of SFC were found to be comparable in magnitude and are presented as a function of temperature. The oxygen flux through dense SFC tubes during separation of oxygen from air is compared with the oxygen flux during methane conversion. Unlike SFC, in which the ionic and electronic conductivities are nearly equivalent, BaCe(sub 0.80)Y(sub 0.20)O(sub 3) (BCY) exhibits protonic conductivity that is significantly higher than its electronic conductivity. To enhance the electronic conductivity and increase hydrogen permeation, metal powder was combined with the BCY to form a cermet membrane. Nongalvanic permeation of hydrogen through the cermet

membrane was demonstrated and characterized as a function of membrane thickness. A sintering aid was developed to avoid interconnected porosity in and improve the mechanical properties of the cermet membrane.
NTIS
*Ion Exchange Membrane Electrolytes; Mixed Oxides; Fractionation; Fuel Cells; Cermets*

**20010125512** Sandia National Labs., Albuquerque, NM USA
**Uncertainty Analysis of Decomposing Polyurethane Foam**
Hobbs, M. L.; Romero, V. J.; Nov. 15, 2000; 11p; In English
Report No.(s): DE2001-767887; SAND2000-2862C; No Copyright; Avail: Department of Energy Information Bridge, Microfiche

Sensitivity/uncertainty analyses are necessary to determine where to allocate resources for improved predictions in support of our nation's nuclear safety mission. Yet, sensitivity/uncertainty analyses are not commonly performed on complex combustion models because the calculations are time consuming, CPU intensive, nontrivial exercises that can lead to deceptive results. To illustrate these ideas, a variety of sensitivity/uncertainty analyses were used to determine the uncertainty associated with thermal decomposition of polyurethane foam exposed to high radiative flux boundary conditions. The polyurethane used in this study is a rigid closed-cell foam used as an encapsulant. Related polyurethane binders such as Estane are used in many energetic materials of interest to the JANNAF community.
NTIS
*Polyurethane Foam; Sensitivity Analysis; Thermal Decomposition*

**20010125515** Sandia National Labs., Albuquerque, NM USA
**Fracture Behavior of Double-Ion-Exchanged Glass**
Beauchamp, E. K.; Oct. 27, 2000; 21p; In English
Report No.(s): DE2001-767222; SAND2000-2770C; No Copyright; Avail: Department of Energy Information Bridge, Microfiche

Mechanical strength measurements have been made on double ion-exchanged disc samples to determine reliability and dependence on stressing rate. The sodium aluminosilicate glass had been exchanged for 24 hours in KNO3 at 500 C and then for 30 minutes at 400 C in a 30/70 mix of sodium nitrate and potassium nitrate to produce a stress profile with a compressive stress peak below the surface. Very narrow ranges in failure stress values were observed in all tests with Weibull moduli as high as 61. The results suggest an insensitivity to the initial flaw size. Failure stress showed an anomalous slight increase with decreasing stressing rate. Fractographic examination revealed that the failure process involved a sequential activation of successively less severe flaws as the applied load increased. Fracture propagation from these flaws produced an array of shallow cracks on the surface loaded in tension. Ultimately, failure resulted from propagation of a very small flaw (dimensions of about one micrometer).
NTIS
*Crack Propagation; Defects; Failure; Fracture Mechanics; Ion Exchanging*

**20010125571** Argonne National Lab., IL USA
**XAF/XANES Studies of Plutonium-Loaded Sodalite/Glass Composite Waste Forms**
Aase, S. B.; Kropf, A. J.; Lewis, M. A.; Reed, D. T.; Richmann, M. K.; Jul. 14, 1999; 11p
Report No.(s): DE2001-11894; ANL/CMT/CP-99518; No Copyright; Avail: Department of Energy Information Bridge, Microfiche

A sodalite/glass ceramic waste form has been developed to immobilize highly radioactive nuclear wastes in chloride form, as part of an electrochemical cleanup process. Simulated waste forms have been fabricated which contain plutonium and are representative of the salt from the electrometallurgical process to recover uranium from spent nuclear fuel. X-ray absorption fine structure spectroscopy (XAFS) and x-ray absorption near-edge spectroscopy (XANES) studies were performed to determine the location, oxidation state and form of the plutonium within these waste forms. Plutonium, in the non-fission-element case, was found to segregate as plutonium(IV) oxide with a crystallite size of at least 20 nm. With fission elements present, the crystallite size was about 2 nm. No plutonium was observed within the sodalite or glass in the waste form.
NTIS
*Absorption Spectroscopy; Plutonium; Radioactive Wastes; Waste Management*

## 28
## PROPELLANTS AND FUELS

*Includes rocket propellants, igniters and oxidizers; their storage and handling procedures; and aircraft fuels. For nuclear fuels see 73 Nuclear Physics. For related information see also 07 Aircraft Propulsion and Power, 20 Spacecraft Propulsion and Power, and 44 Energy Production and Conversion.*

**20010117637** Brookhaven National Lab., Upton, NY USA
**Landfill Gas Conversion to LNG and LCO2** ***Final Report, Mar. 1998 - Feb. 1999***
Cook,; Neyman,; Siwajek,; Brown,; Van Hauwaert,; Feb. 25, 1998; 102p; In English
Report No.(s): DE2000-758999; BN--66525; No Copyright; Avail: Department of Energy Information Bridge, Microfiche

Process designs and economics were developed to produce liquified natural gas (LNG) and liquid carbon dioxide (CO2) from landfill gas (LFG) using the Acrion CO2 wash process. The patented Acrion CO2 wash process uses liquid CO2 to absorb contaminants from the LFG. The process steps are compression, drying, CO2 wash contaminant removal and CO2 recovery, residual CO(sub 2) removal, and methane liquefaction. Three flowsheets were developed using different residual CO2 removal schemes. These included physical solvent absorption (methanol), membranes, and molecular sieves. The capital and operating costs of the flowsheets were very similar. The LNG production cost was around ten cents per gallon. In parallel with process flowsheet development, the business aspects of an eventual commercial project have been explored. The process was found to have significant potential commercial application. The business plan effort investigated the economics of LNG transportation, fueling, vehicle conversion, and markets. The commercial value of liquid CO2 was also investigated. This Phase 1 work, March 1998 through February 1999, was funded under Brookhaven National laboratory contract 725089 under the research program entitled 'Liquefied Natural Gas as a Heavy Vehicle Fuel.' The Phase 2 effort will develop flowsheets for the following: (1) CO2 and pipeline gas production, with the pipeline methane being liquefied at a peak shaving site; (2) sewage digester gas as an alternate feedstock to LFG; and (3) the use of mixed refrigerants for process cooling. Phase 2 will also study the modification of Acrion's process demonstration unit for the production of LNG and a market site for LNG production.
NTIS
*Carbon Dioxide; Liquefied Natural Gas; Methane; Contaminants*

**20010117638** Brookhaven National Lab., Upton, NY USA
**Seaport Liquid Natural Gas Study**
Cook,; Feb. 01, 1999; 140p; In English
Report No.(s): DE2000-758997; BNL-66527; No Copyright; Avail: Department of Energy Information Bridge, Microfiche

The Seaport liquid natural gas (LNG) study has attempted to evaluate the potential for using LNG in a variety of heavy-duty vehicle and equipment applications at the ports of Los Angeles and Oakland. Specifically, this analysis has focused on the handling and transport of containerized cargo to, from and within these two facilities. In terms of containerized cargo throughput, Los Angeles and Oakland are the second and sixth busiest ports in the US, respectively, and together handle nearly 4.5 million TEUs per year. At present, the landside handling and transportation of containerized cargo is heavily dependent on diesel-powered, heavy-duty vehicles and equipment, the utilization of which contributes significantly to the overall emissions impact of port-related activities. Emissions from diesel units have been the subject of increasing scrutiny and regulatory action, particularly in California. In the past two years alone, particulate matter from diesel exhaust has been listed as a toxic air contaminant by CAM, and major lawsuits have been filed against several of California's largest supermarket chains, alleging violation of Proposition 65 statutes in connection with diesel emissions from their distribution facilities. CARE3 has also indicated that it may take further regulatory action relating to the TAC listing. In spite of these developments and the very large diesel emissions associated with port operations, there has been little AFV penetration in these applications. Nearly all port operators interviewed by CALSTART expressed an awareness of the issues surrounding diesel use; however, none appeared to be taking proactive steps to address them. Furthermore, while a less controversial issue than emissions, the dominance of diesel fuel use in heavy-duty vehicles contributes to a continued reliance on imported fuels. The increasing concern regarding diesel use, and the concurrent lack of alternative fuel use and vigorous emissions reduction activity at the Ports provide both the backdrop and the impetus for this study.
NTIS
*Combustion Products; Exhaust Emission; Exhaust Gases; Liquefied Natural Gas; Materials Handling*

**20010117652** Federal Energy Technology Center, Morgantown, WV USA
**Natural Gas Hydrates Storage Project**
Rogers, R. E.; Jun. 01, 1999; 57p; In English
Report No.(s): DE2000-760130; DE-AC26-97FT33203-01; No Copyright; Avail: Department of Energy Information Bridge

Since economical and environmental conditions could be positively affected by greater use of natural gas, especially for peak-loading events of power plants, the feasibility of overcoming a major impediment of safe, above-ground storage in heavily populated areas was sought in this work. Principal deterrent to utilizing natural gas to its fullest is the difficulty of on-site storage; principal incentive to utilizing natural gas to its fullest is its clean-burning quality and its relatively low cost.
NTIS
*Hydrates; Natural Gas; Storage*

**20010117715** Bechtel Nevada Corp., Las Vegas, NV USA
**Closure Report for Building 650 Leachfield Corrective Action Unit 94: Nevada Test Site, Nevada**
Parsons, S. M.; Oct. 01, 1998; 386p; In English
Report No.(s): DE2000-752360; DOE/NV/11718-256; No Copyright; Avail: Department of Energy Information Bridge

This report addresses the closure of Corrective Action Unit (CAU) 461, Joint Test Assembly (JTA) Sites identified in Appendix III of the Federal Facility Agreement and Consent Order (FFACO). Closure was completed following the approved Streamlined Approach for Environmental Restoration Work Plan. The site is located at the Tonopah Test Range in south central Nevada. CAU 461 consists of three Corrective Action Sites (CASS): CAS Number (No.) TTR-001 (1987 W79 JTA), CAS No. TA-52-003-0960 (Depleted Uranium Artillery Round No. 2), and CAS No. TA-52- 002-TAML (DU Impact Site). The 1987 W79 JTA was believed to be the impact site of a failed artillery round test package containing DU and high explosives (HE). Based on review of historical documentation two potential sites were identified. The two sites were designated as DU Round 1A and lB. DU Artillery Round No. 2 was a detonated, buried W79 20-centimeter (cm) (8-inch) diameter DU artillery round located under two witness bars. The DU Impact Site is an area 55 meters (m) by 50 meters (m) (180 feet by 160 feet) of disturbed ground containing metal fragments and DU impacted soil from a failed weapons test. Historical documentation and fragment examination suggest that during the 1960s, a 150-cm (60-in) diameter weapons test unit incurred parachute failure, impacted, and released DU.
NTIS
*Nevada; Test Ranges; Closing*

**20010117869** Brookhaven National Lab., Upton, NY USA
**Liquid Natural Gas (LND): An Alternative Fuel from Landfill Gas (LFG) and Wastewater Digester Gas**
Vandor,; Mar. 01, 1999; 70p; In English
Report No.(s): DE2000-758998; BNL-66526; No Copyright; Avail: Department of Energy Information Bridge, Microfiche

This Research and Development Subcontract sought to find economic, technical, and policy links between methane recovery at landfill and wastewater treatment sites in New York and Maryland, and ways to use that methane as an alternative fuel - compressed natural gas (CNG) or liquid natural gas (LNG) - in centrally fueled Alternative Fueled Vehicles (AFVs).
NTIS
*Compressed Gas; Liquefied Natural Gas; Waste Water*

**20010117870** Brookhaven National Lab., Upton, NY USA
**Development of Atom-Economical Catalytic Pathways for Conversions of Syngas to Energy Liquids**
Mahajan,; Wegrzyn,; Lee,; Gurevich,; Mar. 01, 1999; 6p; In English
Report No.(s): DE2000-759005; BNL-66589; No Copyright; Avail: Department of Energy Information Bridge, Microfiche

The subject of catalytic syngas conversions to fuels and chemicals is well studied. But globally, the recent focus is on development of technologies that offer an economical route to desired products. Economical transport of natural gas from remote locations and within clathrate hydrates is of continuing interest at Brookhaven National Laboratory (BNL). Under this project, a Liquid Phase Low Temperature (LPLT) concept is being applied to attain highly efficient transformations of natural-gas derived syngas to specific products. Furthermore, a more precise term 'Atom Economy' has been recently introduced by Trost to describe development of highly efficient homogeneously catalyzed synthesis of organic molecules. The term 'Atom Economy' is defined as maximizing the number of atoms of all raw materials that end up in the product with any other reactant required on in catalytic amount. For application to methane transformations that may involve one or more steps, atom economy of each of these steps is critical. The authors, therefore, consider atom-economy synonymous with overall energy efficiency of a process. This paper describes potential liquid products from catalytic syngas conversions, i.e., gas to liquids (GTL) technologies and process considerations that are necessary for economical transport of natural gas. As such, the present study defines an atom-economical standard to directly compare competing GTL technologies.
NTIS
*Catalysis; Gas Transport; Clathrates*

**20010118503** Bio-Process Innovations, Inc., West Lafayette, IN USA

**Pilot Plant Scale Reactor/Separator for Ethanol from Cellulosics. ERIP/DOE Quarterly Reports 7, 8** ***Final Report***

Cale, M. C.; Moelhman, M.; Sep. 30, 1999; 9p; In English

Report No.(s): DE2000-760707; No Copyright; Avail: Department of Energy Information Bridge, Microfiche

The objective of this project was to develop and demonstrate a continuous low energy process for the conversion of cellulosics to ethanol. BPI's process involves a proprietary low temperature pretreatment step which allows recycle of the pretreatment chemicals and recovery of a lignin stream. The pretreated biomass is then converted to glucans and xylans enzymatically and these sugars simultaneously fermented to ethanol (SSF) in BPI's Continuous Stirred Reactor Separator (CSRS). The CSRS is a multi stage bio-reactor where the glucans are first converted to ethanol using a high temperature tolerant yeast stran, followed by xylan SSF on the lower stages using a second xylose fermenting yeast strain. Ethanol is simultaneously removed from the bio-reactor stages, speeding the fermentation, and allowing the complete utilization of the biomass.

NTIS

*Biomass; Ethyl Alcohol; Fermentation*

**20010118532** Brookhaven National Lab., Upton, NY USA

**Atom-Economical Pathways to Methanol Fuel Cell from Biomass**

Mahajan,; Wegrzyn,; Mar. 01, 1999; 6p; In English

Report No.(s): DE2000-759004; BNL-66590; No Copyright; Avail: Department of Energy Information Bridge, Microfiche

An economical production of alcohol fuels from biomass, a feedstock low in carbon and high in water content, is of interest. At Brookhaven National Laboratory (BNL), a Liquid Phase Low Temperature (LPLT) concept is under development to improve the economics by maximizing the conversion of energy carrier atoms (C, H) into energy liquids (fuel). So far, the LPLT concept has been successfully applied to obtain highly efficient methanol synthesis. This synthesis was achieved with specifically designed soluble catalysts, at temperatures of 150 C. A subsequent study at BNL yielded a water-gas-shift (WGS) catalyst for the production of hydrogen from a feedstock of carbon monoxide and H2O at temperatures of 120 C. With these LPLT technologies as a background, this paper extends the discussion of the LPLT concept to include methanol decomposition into 3 moles of H2 per mole of methanol. The implication of these technologies for the atom-economical pathways to methanol fuel cell from biomass is discussed.

NTIS

*Biomass; Fuel Cells; Methyl Alcohol*

**20010119050** Oak Ridge National Lab., TN USA

**Bamboo: An Overlooked Biomass Resource**

Scurlock, J. M. O.; Feb. 01, 2000; 34p; In English

Report No.(s): DE2000-754363; ORNL/TM-1999/264; No Copyright; Avail: Department of Energy Information Bridge

Bamboo is the common term applied to a broad group (1250 species) of large woody grasses, ranging from 10 cm to 40 m in height. Already in everyday use by about 2.5 billion people, mostly for fiber and food within Asia, bamboo may have potential as a bioenergy or fiber crop for niche markets, although some reports of its high productivity seem to be exaggerated. Literature on bamboo productivity is scarce, with most reports coming from various parts of Asia. There is little evidence overall that bamboo is significantly more productive than many other candidate bioenergy crops, but it shares a number of desirable fuel characteristics with certain other bioenergy feedstocks, such as low ash content and alkali index. Its heating value is lower than many woody biomass feedstocks but higher than most agricultural residues, grasses and straws. Although non-fuel applications of bamboo biomass may be actually more profitable than energy recovery, there may also be potential for co-productio n of bioenergy together with other bamboo processing. A significant drawback is the difficulty of selective breeding, given the lack of knowledge of flowering physiology. Further research is also required on propagation techniques, establishment and stand management, and mechanized harvesting needs to be developed.

NTIS

*Biomass; Agriculture; Energy Technology; Grasses*

**20010119430** National Renewable Energy Lab., Golden, CO USA

**Life Cycle Assessment of a Biomass Gasification Combined-Cycle Power System**

Mann, M. K.; Spath, P. L.; Dec. 01, 1997; 161p; In English

Report No.(s): DE2000-567454; NREL/TP-430-23076; DE98002709; No Copyright; Avail: Department of Energy Information Bridge

The potential environmental benefits from biomass power are numerous. However, biomass power may also have some negative effects on the environment. Although the environmental benefits and drawbacks of biomass power have been debated for some time, the total significance has not been assessed. This study serves to answer some of the questions most often raised in regard to biomass power: What are the net CO2 emissions? What is the energy balance of the integrated system? Which substances are emitted at the highest rates? What parts of the system are responsible for these emissions? to provide answers to these questions, a life cycle assessment (LCA) of a hypothetical biomass power plant located in the Midwest USA was performed. LCA is an analytical tool for quantifying the emissions, resource consumption, and energy use, collectively known as environmental stressors, that are associated with converting a raw material to a final product. Performed in conjunction with a technoeconomic feasibility study, the total economic and environmental benefits and drawbacks of a process can be quantified. This study complements a technoeconomic analysis of the same process, reported in Craig and Mann and updated here. The process studied is based on the concept of power generation in a biomass integrated gasification combined cycle (BIGCC) plant. Broadly speaking, the overall system consists of biomass production, its transportation to the power plant, electricity generation, and any upstream processes required for system operation. The biomass is assumed to be supplied to the plant as wood chips from a biomass plantation, which would produce energy crops in a manner similar to the way food and fiber crops are produced today. Transportation of the biomass and other materials is by both rail and truck. The IGCC plant is sized at 113 MW, and integrates an indirectly-heated gasifier with an industrial gas turbine and steam cycle.
NTIS
*Biomass; Energy Budgets; Gasification; Life (Durability)*

**20010119434** Oak Ridge National Lab., TN USA
**HTS Magnets for Advanced Magnetoplasma Space Propulsion Applications**
Carte, M. D.; Squire, F. R.; Chang-Diaz, J. P.; Schwenterly, S. W.; Jul. 12, 1999; 9p; In English
Report No.(s): DE2000-15057; ORNL/CP-105116; No Copyright; Avail: Department of Energy Information Bridge, Microfiche
Plasma rockets are being considered for both Earth-orbit and interplanetary missions because their extremely high exhaust velocity and ability to modulate thrust allow very efficient use of propellant mass. In such rockets, a hydrogen or helium plasma is RF-heated and confined by axial magnetic fields produced by coils around the plasma chamber. High-temperature superconducting (HTS) coils cooled by the propellant are desirable to increase the energy efficiency of the system. We describe a set of prototype HTS coils that are being considered for the VASIMR (Variable Specific Impulse Magnetoplasma Rocket) thruster proposed for testing on the Radiation Technology Demonstration (RTD) satellite. Since this satellite will be launched by the Space Shuttle, for safety reasons liquid helium will be used as propellant and coolant. The coils must be designed to operate in the space environment at field levels of 1 T. This generates a unique set of requirements. Details of the overall winding geometry and current density, as well as the challenging thermal control aspects associated with a compact, minimum weight design will be discussed.
NTIS
*High Temperature Superconductors; Propulsion; Prototypes*

**20010119560** Pacific Northwest National Lab., Richland, WA USA
**Energy R and D in the Netherlands**
Luiten, E. E. M.; Dooley, J. J.; Blok, K.; Sep. 07, 1999; 44p; In English
Report No.(s): DE2001-10486; PNNL-12177; No Copyright; Avail: Department of Energy Information Bridge, Microfiche
This report documents trends in R and D and in particular (public) energy R and D in the Netherlands. Besides quantitative information on R and D and energy R and D, the report gives an impression of changes in science and technology policy, energy policy and changes in energy research priorities (both organizational and financial). In the Netherlands, 2.09% of GDP (or $6.7 billion) was invested in R and D activities in 1995. The private sector financed 46% of all R and D in that year. A small but significant fraction (9.3%) of the research performed in the Netherlands is financed by foreign public and private sector entities. Energy R and D has been identified by the national Strategic Foresight Activity as an important area of R and D for government support in the future. This is due in part to the overall decline in public support for energy R and D that occurred from 1985 to 1995. However, recent concern over climate change and energy policy has resulted in increased budgets for energy R and D. Recent policy documents (e.g., the Memorandum on Energy R and D in April 1998) and initiatives (e.g., a recent university energy R and D program; intensification of climate policy, partly in R and D) indicate the growing interest in addressing the issue of climate change partly through energy R and D. The Dutch government believes that the liberalization of the energy market in the Netherlands justifies an active role for the government to guarantee the longer-term transformation to a sustainable energy system. In terms of climate policy, the expanded and more efficient use of natural gas is seen as a suitable transition option towards a sustainable energy system. However, energy efficiency (and in particular energy efficiency in the industrial sector) and the

introduction of renewable technologies (solar energy, wind energy and biomass) are generally favored for the long term. Recently, additional funding was allocated for research on industrial 'breakthrough' technologies, photovoltaic energy, and biomass research. Best available data suggest that the private sector's energy R and D investments are on par with and quite close to the level of the government's energy R and D budgets. Renewable energy R and D, nuclear fission and fusion are predominantly financed by the public sector. However, energy efficiency receives the largest share of the total governmental energy RD and D budget (about 40%). The majority of the private sector's energy R and D investments are devoted to energy efficiency. Private sector investments also exceed those of the government in the area of power storage technologies.
NTIS
*Research and Development; Netherlands; Biomass; Energy Policy; Energy Technology; Energy Conservation; Climate Change*

**20010119567** Department of Energy, Richland Operations Office, Richland, WA USA
**Sampling and Analysis Instruction for the 384 Day Tank**
Smith, D. S.; Aug. 20, 1999; 21p; In English
Report No.(s): DE2001-10503; BHI-01280-REV-1; No Copyright; Avail: Department of Energy Information Bridge, Microfiche
The 384 Day Tanks were used to store diesel fuel and Bunker C for the 384 Powerhouse in the 300 Area of the Hanford Site in Richland, Washington. The tanks are located near the center of the300 Area, to the north of the 384 Building. This instruction defines the sampling and analysis activities to be performed in support of the decommissioning of the 384 Day Tanks. The purpose of the sampling is to determine whether a release from the tanks has occurred and the extent of the contamination, if any.
NTIS
*Storage Tanks; Diesel Fuels; Decommissioning; Leakage*

**20010119992** Argonne National Lab., IL USA
**Determinants of alternative fuel vehicle choice in the continental USA**
Tompkins, M.; Dec. 18, 1997; 31p; In English
Report No.(s): DE2001-10541; ANL/ES/CP-95147; No Copyright; Avail: Department of Energy Information Bridge
This paper describes the ongoing investigation into the determinants of alternative fuel vehicle choice. A stated preference vehicle choice survey was conducted for the 47 of the continental U.S. states, excluding California. The national survey is based on and is an extension of previous studies on alternative fuel vehicle choice for the State of California conducted by the University of California's Institute of Transportation Studies (UC ITS). Researchers at UC ITS have used the stated-preference national survey to produce a series of estimates for new vehicle choice models. Three of these models are presented in this paper. The first two of the models were estimated using only the data from the national survey. The third model presented in this paper pools information from the national and California surveys to estimate a true national model for new vehicle choice.
NTIS
*Fuels; Transportation; Substitutes*

**20010120017** Argonne National Lab., IL USA
**Studies of the thermodynamics of extraction F-elements**
Nash, K. L.; Dec. 07, 1998; 9p; In English
Report No.(s): DE2001-10668; ANL/CHM/CP-95777; No Copyright; Avail: Department of Energy Information Bridge
Though they were discovered in the 18th century, practical applications of individual lanthanides were not possible until the development of first ion exchange and later solvent extraction techniques. Today, solvent extraction using lipophilic organophosphorus complexants is the principal separation technique applied for lanthanide production by hydrometallurgy. Separations chemistry (coprecipitation, ion exchange, and solvent extraction) also was central to both the discovery of the individual actinides and to the preparation of samples of sufficient purity to allow elucidation of their chemical/physical properties. Solvent extraction, in the form of the PUREX process, has become the single most important separations process in actinide technology. In this report, the basic thermodynamics of extraction of actinide and lanthanide metal ions is discussed.
NTIS
*Solvent Extraction; Fluorides; Hydrometallurgy; Thermodynamics; Rare Earth Elements; Physical Chemistry*

**20010120051** Brookhaven National Lab., Upton, NY USA
**Carbon dioxide fixation**
Fujita, E.; Jan. 12, 2000; 34p; In English
Report No.(s): DE2000-752960; BNL-67078; No Copyright; Avail: Department of Energy Information Bridge

Solar carbon dioxide fixation offers the possibility of a renewable source of chemicals and fuels in the future. Its realization rests on future advances in the efficiency of solar energy collection and development of suitable catalysts for CO(sub 2) conversion. Recent achievements in the efficiency of solar energy conversion and in catalysis suggest that this approach holds a great deal of promise for contributing to future needs for fuels and chemicals.
NTIS
*Carbon Dioxide; High Energy Fuels*

**20010120067** Los Alamos National Lab., NM USA
**Effects of Humidity and Other Variables on the Strength of PBX 9501**
Browning, R. Y.; Meyer, T.; Sep. 15, 2000; 8p; In English
Report No.(s): DE2000-762301; LA-UR-00-4301; No Copyright; Avail: Department of Energy Information Bridge, Microfiche

Pellets of PBX 9501 were first dried for three months to remove residual moisture, then stored in different humidity levels for 41 days while monitoring the moisture uptake by measuring the change in mass of the pellets. Several reference pellets were left in the dry environment, and one sample that had been conditioned to a high moisture content was changed back to a dry environment. A standard compression test was done on these pellets to determine the efforts of the moisture content on the mechanical properties. The load deflection behavior did not change character, but the peak stress decreased noticeably with increasing moisture content. Results from earlier tests on other variables are reviewed, and recommendations for improving surveillance testing techniques are presented.
NTIS
*Humidity; Mechanical Properties; Moisture Content; Explosives*

**20010120268** Massachusetts Inst. of Tech., Dept. of Chemistry, Cambridge, MA USA
**Optical Supramolecules for Chemical and Physical Sensing** ***Final Report, 1 Feb. 1998-30 Nov. 2000***
Nocera, Daniel G.; Nov. 2000; 19p; In English
Contract(s)/Grant(s): F49620-98-1-0203; Proj-2303
Report No.(s): AD-A395213; AFRL-SR-BL-TR-01-0512; No Copyright; Avail: CASI; A03, Hardcopy; A01, Microfiche

Proposal F49620-98-1-0203 addresses the diverse chemical and physical sensing needs of the USA Air Force. All the techniques developed in this program are based on monitoring a bright luminescence from a molecule or supramolecule reporter site. by controlling the rates for energy flow within the supra/molecular architecture, the intensity and lifetime of the luminescence may be adjusted to address chemosensing and physical sensing applications of interest to the Air Force. Sub-projects within F49620-98-1-0203 included he development of an optical chemosensor for the detection of polyaromatic signatures of JP4, and the development of new optical diagnostic techniques to measure vorticity and pressure over aerodynamic surfaces.
DTIC
*Optical Measurement; Luminescence; Jet Engine Fuels*

**20010120404** Sandia National Labs., Albuquerque, NM USA
**Relative Evaluation of the Independent Volume Measures of Caverns**
Munson, D. E.; Aug. 01, 2000; 79p; In English
Report No.(s): DE2000-761960; SAND2000-2041; No Copyright; Avail: Department of Energy Information Bridge, Microfiche

Throughout the construction and operation of the caverns of the Strategic Petroleum Reserve (SPR), three types of cavern volume measurements have been maintained. These are: (1) the calculated solution volume determined during initial construction by solution mining and any subsequent solutioning during oil transfers; (2) the calculated sonar volume determined through sonar surveys of the cavern dimensions; and (3) the direct metering of oil to determine the volume of the cavern occupied by the oil. The objective of this study is to compare these measurements to each other and determine, if possible, the uncertainties associated with a given type of measurement. Over time, each type of measurement has acquired a customary, or an industry accepted, stated uncertainty. This uncertainty is not necessarily the result of a technical analysis. Ultimately there is one definitive quantity, the oil volume measure by the oil custody transfer meters, taken by all parties to the transfer as the correct ledger amount and for which the SPR Project is accountable. However, subsequent transfers within a site may not be with meters of the same accuracy. In this study, a very simple theory of the perfect relationship is used to evaluate the correlation (deviation) of the various measures. This theory permits separation of uncertainty and bias. Each of the four SPR sites are examined, first with comparisons between the calculated solution volumes and the sonar volumes determined during construction, then with comparisons of the oil inventories and the sonar volumes obtained either by surveying through brine prior to oil filling or through the oil directly.
NTIS
*Caves; Underground Storage; Crude Oil; Volume*

**20010120537** Argonne National Lab., IL USA

**Characterizing and modeling subarea-level energy transactions**

Kavicky, J. A.; Mar. 05, 1998; 7p; In English

Report No.(s): DE2001-10674; ANL/DIS/CP-95814; No Copyright; Avail: Department of Energy Information Bridge

This paper describes the application of an electrical network characterization method to an optimization model that is designed to simulate subarea-level energy transactions. The network characterization method determines subarea clusters of system buses that electrically respond to perturbations in a very similar manner. The method produces a reduced number of transmission constraints and preserves parallel path representations. The least-cost, linear programming (LP) formulation takes advantage of data reduction techniques to simplify model transmission constraints, while supporting parallel path system characteristics and energy tagging of subarea transactions. An overview of the proposed method describes the problem domain and key model features. The paper then presents two model applications that illustrate generator siting and line overload screening analyses.

NTIS

*Optimization; Electric Power Transmission*

**20010120555** Argonne National Lab., IL USA

**Lifecycle-analysis for heavy vehicles**

Gaines, L., Argonne National Lab., USA; Apr. 16, 1998; 20p; In English

Report No.(s): DE2001-10731; ANL/ES/CP-96075; No Copyright; Avail: Department of Energy Information Bridge, Microfiche

Various alternative fuels and improved engine and vehicle systems have been proposed in order to reduce emissions and energy use associated with heavy vehicles (predominantly trucks). For example, oil companies have proposed improved methods for converting natural gas to zero-aromatics, zero-sulfur diesel fuel via the Fischer-Tropsch process. Major heavy-duty diesel engine companies are working on ways to simultaneously reduce particulate-matter and NOX emissions. The trend in heavy vehicles is toward use of lightweight materials, tires with lower rolling resistance, and treatments to reduce aerodynamic drag. In this paper, we compare the Mecycle energy use and emissions from trucks using selected alternatives, such as Fisher-Tropsch diesel fuel and advanced fuel-efficient engines. We consider heavy-duty, Class 8 tractor-semitrailer combinations for this analysis. The total life cycle includes production and recycling of the vehicle itself, extraction, processing, and transportation of the fuel itself, and vehicle operation and maintenance. Energy use is considered in toto, as well as those portions that are imported, domestic, and renewable. Emissions of interest include greenhouse gases and criteria pollutants. Argonne's Greenhouse Gases, Regulated Emissions, and Energy Use in Transportation (GREET) model is used to generate per-vehicle fuel cycle impacts. Energy use and emissions for materials manufacturing and vehicle disposal are estimated by means of materials information from Argonne studies. We conclude that there are trade-offs among impacts. For example, the lowest fossil energy use does not necessarily result in lowest total energy use, and lower tailpipe emissions may not necessarily result in lower lifecycle emissions of all criteria pollutants.

NTIS

*Diesel Engines; Trucks; Energy Conservation; Life Cycle Costs; Fuel Consumption*

**20010120795** Argonne National Lab., IL USA

**Analytical performance of direct-hydrogen-fueled Polymer Electrolyte Fuel Cell (PEFC) systems for transportation applications**

Doss, E. D.; Jun. 02, 1998; 10p; In English

Report No.(s): DE2001-10822; ANL/TD/CP-97554; No Copyright; Avail: Department of Energy Information Bridge

The performance of a stand-alone polymer electrolyte fuel cell (PEFC) system directly fueled by hydrogen has been evaluated for transportation vehicles. The study was carried out using a systems analysis code and a vehicle analysis code. The systems code includes models for the various PEFC components and is applicable for steady-state and transient situations. At the design point the system efficiency is above 50% for a 50-kW system. The efficiency improves under partial load and approaches 60% at 40% load, as the fuel cell operating point moves to lower current densities on the V-I polarization curve. At much lower loads, the system efficiency drops because of the deterioration in the performance of the compressor, expander, and eventually the fuel cell. The system performance suffers at lower temperatures, as the V-I characteristic curve for the fuel cell shifts downward because of the increased ohmic losses. The results of the transient analysis indicate that the hydrogen-fueled PEFC system can start rather rapidly, within seconds from ambient conditions. However, the warm-up time constant to reach the design operating temperatures is about 180 s. It is important during this period for the coolant to bypass the system radiator until the coolant temperature approaches the design temperature for the fuel cell. The systems analysis code has been applied to two mid-size vehicles: the near-term Ford AIV Sable and the future P2000 vehicle. The results of this study show that the PEFC system in these vehicles

can respond well to the demands of the FUDS and Highway driving cycles, with both warm and cold starting conditions. The results also show that the fuel-cell AIV Sable vehicle has impressive gains in fuel economy over that of the internal combustion engine vehicle. However, this vehicle will not be able to meet the PNGV goal of 80 mpg. On the other hand, the P2000 vehicle approaches this goal with variable efficiency of the compressor and expander. It is expected to exceed that goal by a big margin, if the efficiency of the compressor and expander can be maintained constant (at 0.8) over the power range of the fuel cell system.
NTIS
*Electrolytic Cells; Polymers; Internal Combustion Engines; System Effectiveness; Fuel Cells*

**20010121506** Sandia National Labs., Albuquerque, NM USA
**CaveMan Version 3.0: A Software System for SPR Cavern Pressure Analysis**
Ballard, S.; Ehgartner, B. L.; Jul. 01, 2000; 162p; In English
Report No.(s): DE2000-759468; SAND2000-1751; No Copyright; Avail: Department of Energy Information Bridge, Microfiche

The U.S. Department of Energy Strategic Petroleum Reserve currently has approximately 500 million barrels of crude oil stored in 62 caverns solution-mined in salt domes along the Gulf Coast of Louisiana and Texas. One of the challenges of operating these caverns is ensuring that none of the fluids in the caverns are leaking into the environment. The current approach is to test the mechanical integrity of all the wells entering each cavern approximately once every five years. An alternative approach to detecting cavern leaks is to monitor the cavern pressure, since leaking fluid would act to reduce cavern pressure. Leak detection by pressure monitoring is complicated by other factors that influence cavern pressure, the most important of which are thermal expansion and contraction of the fluids in the cavern as they come into thermal equilibrium with the host salt, and cavern volume reduction due to salt creep. Cavern pressure is also influenced by cavern enlargement resulting from salt dissolution following introduction of raw water or unsaturated brine into the cavern. However, this effect only lasts for a month or two following a fluid injection. In order to implement a cavern pressure monitoring program, a software program called CaveMan has been developed. It includes thermal, creep and salt dissolution models and is able to predict the cavern pressurization rate based on the operational history of the cavern. Many of the numerous thermal and mechanical parameters in the model have been optimized to produce the best match between the historical data and the model predictions. Future measurements of cavern pressure are compared to the model predictions, and significant differences in cavern pressure set program flags that notify cavern operators of a potential problem. Measured cavern pressures that are significantly less than those predicted by the model may indicate the existence of a leak.
NTIS
*Thermodynamic Equilibrium; Applications Programs (Computers); Domes (Geology); Salt Beds; Crude Oil*

**20010121512** Minnesota Valley Alfalfa Producers, Granite Falls, MN USA
**Minnesota Agri-Power Project *Quarterly Report, Apr. - Jun. 1999***
Wilbur, D.; Jul. 20, 1999; 15p; In English
Report No.(s): DE2000-759445; DOE/GO/10147-Q; No Copyright; Avail: Department of Energy Information Bridge, Microfiche

Feedstock processing and system improvements continue. Work continues on the design and cost estimate for the first new alfalfa processing plant. Accurate operating cost estimates have been developed into a financial model for analysis of various operating practices. The simultaneous production of alfalfa leaf meal and other products has continued to operate as allowed by market conditions. Work continued in an effort to reduce the tramp particulate emissions at the Prism facility to fully meet the MPCA requirements. Emissions' monitoring as required by the MPCA was completed. Results indicate emission levels below alfalfa industry norms. Work also continued to improve the Standard Operating Procedures. Monitoring of the physical quality of all products continued. This work is being done without DOE support.
NTIS
*Alfalfa; Agriculture; Industrial Plants; Manufacturing*

**20010121871** Oak Ridge National Lab., TN USA
**Mechanical Design of Steel Tubing for Use in Black Liquor Recovery Boilers**
Taljat, B.; Zacharaia, T.; Wang, X.; Kesier, J.; Swindeman, R.; May 26, 1999; 5p; In English
Report No.(s): DE2000-754817; ORNL/P99-104688; No Copyright; Avail: Department of Energy Information Bridge

Finite element models were developed for thermal-mechanical analysis of black liquor recovery boiler floor tubes. Residual stresses in boiler floors due to various manufacturing processes were analyzed. The modeling results were verified by X-ray and neutron diffraction measurements at room temperature on as-manufactured tubes as well as tubes after service. The established finite element models were then used to evaluate stress conditions during boiler operation. Using these finite element models, a

parametric response surface study was performed to investigate the influence of material properties of the clad layer on stresses in the floor tubes during various boiler operating conditions, which yielded a generalized solution of stresses in the composite tube floors. The results of the study are useful for identifying the mechanisms of cracking experienced by recovery boilers. Based on the results of the response surface study, a recommendation was made for more suitable materials in terms of the analyzed mechanical properties. Alternative materials and manufacturing processes are being considered to improve the resistance to cracking and the in-service life of composite tubes. to avoid numerous FE stress-strain analyses of composite tubes made of different material combinations, a response surface study was performed that considered two essential mechanical properties of the clad material - coefficient of thermal expansion and yield stress - as independent variables. The response surface study provided a generalized solution of stresses in the floor in terms of the two selected parameters.
NTIS
*Finite Element Method; Thermal Analysis; Thermal Expansion; Boilers; Steels; Pipes (Tubes)*

**20010121876** Sandia National Labs., Albuquerque, NM USA
**Accurate Velocity Measurements of the Two-Stage Light-Gas Gun Projectile**
Thornhill,; Reinhart,; Konrad,; Chhabildas,; Sep. 14, 2000; 14p; In English
Report No.(s): DE2000-763101; SAND2000-2268C; No Copyright; Avail: Department of Energy Information Bridge, Microfiche

An Optical Beam Reflectance (O13R) technique for measuring projectile velocities has been implemented on Sandia National Laboratories' two-stage light gas gun. This is an adaptation of a technique developed in the late 1970s to measure projectile velocities for Equation of State (EOS) studies. The OBR system allows for projectile velocity measurements in the barrel extension section of the Shock Thermodynamics Applied Research (STAR) facility two-stage gas gun. The use of this system has enhanced EOS experiments and impact planarity on the gun by allowing projectile/target impacts to occur while the tail of the projectile is still located in the barrel extension. Three probe (114 mm spacing) velocity measurements have a calculated accuracy of 0.2 percent. A shot comparing velocity measurements using the OBR, and Magnetic Velocity Induction System2 (MAVIS), show agreement within error bounds. This paper summarizes the OBR system hardware, application, and error analysis. Also presented are results from shots ranging in projectile velocities to 7.0 km/s using two to five probes per measurement. Impact planarity measurements for EOS investigations resulting from adaptation of this new test methodology will also be discussed.
NTIS
*Projectiles; Velocity; Guns; Error Analysis*

**20010121952** Los Alamos National Lab., NM USA
**Fuel composition effects on fuel processor dynamics**
Borup, R. L.; Inbody, M. A.; Sep. 22, 2000; 5p; In English
Report No.(s): DE2000-763155; LA-UR-00-4459; No Copyright; Avail: Department of Energy Information Bridge, Microfiche

This report describes our progress in examining fuel effects on hydrogen generation technology research for the specific purpose of hydrogen production for protonexchange- membrane (PEM) fuel cells. The goal of this research is to explore the effects of various fuels, fuel constituents and fuel impurities on the performance of on-board hydrogen generation devices and consequently on the overall performance of a PEM fuel cell system utilizing a hydrocarbon fuel.
NTIS
*Fuels; Hydrogen Production*

**20010121954** National Renewable Energy Lab., Golden, CO USA
**Alternative Fuel News: Official Publication of the Clean Cities Network and the Alternative Fuels Data Center, Volume 4**
Ficker, C.; Sep. 08, 2000; 12p; In English
Report No.(s): DE2000-764500; NREL/BR-540-28052; No Copyright; Avail: Department of Energy Information Bridge, Microfiche

This issue of Alternative Fuel News discusses Executive Order 13149 which is designed to not only increase the use of alternative fuel by federal agencies but also to increase the use of fuel efficient vehicles in the federal fleet. Also highlighted is the 6th National Clean Cities Conference and Expo held in San Diego, May 7-10, 2000, which attracted nearly 1,000 people for three action-packed days of alternative fuel activities. The work to develop a market for alternative fuels is more important than ever.
NTIS
*Fuels; Alternatives; Conferences*

**20010121975** Sandia National Labs., Albuquerque, NM USA

**Relative Evaluation of Storage Cavern Volume Measurements**

Munson, D. E.; Myers, R. E.; Aug. 30, 2000; 22p; In English

Report No.(s): DE2000-761888; SAND2000-2180C; No Copyright; Avail: Department of Energy Information Bridge, Microfiche

Over the course of the construction and operation of the Strategic Petroleum Reserve (SPR) crude oil storage caverns, three types of measurements of the cavern volumes have been maintained: calculated solution volumes based on dissolution of salt by raw water, calculated sonar volumes based on the sonar surveys of the cavern dimensions, and cavern volumes occupied by metered oil inventories. Because these are frequently made almost concurrently, the measures are of the same, but unknown, cavern volume and it is possible to make a comparative evaluation of the volumes. In this way it may be possible to understand and determine the uncertainties involved in these measures. A very simple theory shows that any measure can contain a bias produced by a systematic error and a scatter produced by a random error. by equating volumes determined by different measurement types it is possible to distinguish biases from random scatter. As a result a comparative evaluation of solution volumes against sonar volumes suggests that a bias of a few percent exists, and this bias seems to depend upon the specific survey company. Because the bias can be removed from the raw results, the remaining random uncertainty data can be analyzed statistically. The random scatter, which is a sum of the scatter of the sonic survey and the solutioning process is very nearly a normal distribution and has a standard deviation of 5.78 %, which appears to be reasonable. This statistical uncertainty suggests a +/- 2 % uncertainty in the sonar measurements and a +/- 3 % uncertainty in the solutioning data. These two values are less than the +/- 59 % that is customarily associated with these two measures by the survey companies and construction contractors. Evaluation of the equivalent sonar volumes when compared to the oil inventories also show bias and scatter. When analyzed statistically, the random uncertainty in the equivalent sonar volumes compared to the oil inventory also gives essentially a normal distribution with a standard deviation of 1.69 %. These results suggest that the deduced +/- 2 % scatter in the sonar survey dominates the uncertainty, with the very small oil inventory uncertainty governed by the highly accurate oil custody transfer meter.

NTIS

*Underground Storage; Underground Structures; Reserves; Surveys*

**20010122286** National Renewable Energy Lab., Golden, CO USA

**DOE Bioethanol Pilot Plant: A Tool for Commercialization**

Brown, H.; Aug. 31, 2000; 4p; In English

Report No.(s): DE2000-764520; NREL/BR-580-28397; DOE/GO-102000-1114; No Copyright; Avail: Department of Energy Information Bridge, Microfiche

With funding from the DOE National Biofuels Program, NREL has constructed a fermentation pilot plant facility. The plant was explicitly designed to assist industry and outside researchers develop commercial bioprocessing technology. Companies that are exploring biofuels technologies can utilize the facilities and expertise of NREL through a variety of flexible business-venture arrangements.

NTIS

*Commercialization; Bioprocessing; Ethyl Alcohol*

**20010122290** Bechtel Nevada Corp., Las Vegas, NV USA

**Streamlined Approach for Environmental Restoration Closure Report for Corrective Action Unit 461: Joint Test Assembly Sites Tonopah Test Range, Nevada**

Smith, J. L.; Sep. 01, 1999; 330p; In English

Report No.(s): DE2000-752098; DOE/NV-566; DOE/NV/11718-369; No Copyright; Avail: Department of Energy Information Bridge

This report addresses the closure of Corrective Action Unit (CAU) 461, Joint Test Assembly (JTA) Sites identified in Appendix III of the Federal Facility Agreement and Consent Order (FFACO). Closure was completed following the approved Streamlined Approach for Environmental Restoration Work Plan. The site is located at the Tonopah Test Range in south central Nevada. CAU 461 consists of three Corrective Action Sites (CASS): CAS Number (No.) TTR-001 (1987 W79 JTA), CAS No. TA-52-003-0960 (Depleted Uranium (DU) Artillery Round No. 2), and CAS No. TA-52- 002-TAML (DU Impact Site). The 1987 W79 JTA was believed to be the impact site of a failed artillery round test package containing DU and high explosives (HE). Based on review of historical documentation two potential sites were identified. The two sites were designated as DU Round 1A and lB. DU Artillery Round No. 2 was a detonated, buried W79 20-centimeter (cm) (8-inch) diameter DU artillery round located under two witness bars. The DU Impact Site is an area 55 meters (m) by 50 meters (m) (180 feet by 160 feet) of disturbed ground

containing metal fragments and DU impacted soil from a failed weapons test. Historical documentation and fragment examination suggest that during the 1960s, a 150-cm (60-in) diameter weapons test unit incurred parachute failure, impacted, and released DU.
NTIS
*Nevada; Test Ranges; Closing; Environment Effects*

**20010122366** Argonne National Lab., IL USA
**Hydrogen production and carbon dioxide recovery from KRW oxygen-blown gasification**
Doctor, R. D., Argonne National Lab., USA; Oct. 22, 1998; 9p; In English
Report No.(s): DE2001-10748; ANL/ES/CP-96203; No Copyright; Avail: Department of Energy Information Bridge, Microfiche

An oxygen-blown KRW integrated gasification combined-cycle plant producing hydrogen, electricity, and supercritical-CO(sub 2), was studied in a full-energy cycle analysis extending from the cord mine to the final destination of the gaseous product streams. A location in the mid-western US was chosen 160-km from Old Ben No.26 mine which ships 3,866 tonnes/day of Illinois No.6 coal by diesel locomotive. Three parallel gasifier trains, each capable of providing 42% of the plant's 413.5 MW nominal capacity use a combined total of 3,488 tonnes/day of 1/4 inch prepared coal. The plant produces a net 52 MW of power and 3.71 x 10(sup 6) nm(sup 3)/day of 99.999% purity hydrogen which is sent 100 km by pipeline at 34 bars. The plant also produces 3.18 x 10(sup 6) nm(sup 3)3/day of supercritical CO(sub 2) at 143 bars, which is sequestered in enhanced oil recovery operations 500 km away. A CO(sub 2) emission rate of 1 kgCO(sub 2)/kWh was assumed for power purchases outside the fence of the IGCC plant.
NTIS
*Gasification; Gas Recovery; Hydrogen Production; Carbon Dioxide*

**20010122653** Idaho National Engineering and Environmental Lab., Idaho Falls, ID USA
**Safety Issues with Hydrogen as a Vehicle Fuel**
Cadwallader, L. C.; Herring, J. S.; Sep. 01, 1999; 78p; In English
Report No.(s): DE2000-761801; INEEL/EXT-99-00522; No Copyright; Avail: Department of Energy Information Bridge

This report is an initial effort to identify and evaluate safety issues associated with the use of hydrogen as a vehicle fuel in automobiles. Several forms of hydrogen have been considered: gas, liquid, slush, and hydrides. The safety issues have been discussed, beginning with properties of hydrogen and the phenomenology of hydrogen combustion. Safety-related operating experiences with hydrogen vehicles have been summarized to identify concerns that must be addressed in future design activities and to support probabilistic risk assessment. Also, applicable codes, standards, and regulations pertaining to hydrogen USAge and refueling have been identified and are briefly discussed. This report serves as a safety foundation for any future hydrogen safety work, such as a safety analysis or a probabilistic risk assessment.
NTIS
*Automobiles; Combustion; Hydrogen Fuels; Safety Factors*

**20010122669** Los Alamos National Lab., NM USA
**Review of Emerging Technologies for Sustainable Use of Coal for Power Generation**
Lackner,; Ziock,; Jan. 01, 2000; 13p; In English
Report No.(s): DE2000-763338; LA-UR-00-748; No Copyright; Avail: Department of Energy Information Bridge, Microfiche

Concerns about climate change and environmental consequences of increased levels of atmospheric CO2 will require the power generation industry to reduce CO2 emissions from current levels. Unfortunately, for reductions to have the desired effect they will have to be large. While the schedule of the Kyoto Protocol may appear daunting, in the long term mere compliance with the protocol will hardly change the rate of increase of atmospheric CO2. There are, however, technical, economical, and practical choices that will allow the industry to meet the requirements of the protocol and ultimately stop the increase in atmospheric CO2 without eliminating coal from the fuel mix. In this paper, we present a review of current and emerging technologies for CO2 sequestration. We provide a summary of the underlying scientific principles and discuss the practical and economic aspects of sequestration technologies, which will allow continuing use of global coal resources with minimum or no impact on CO2 levels in the atmosphere.
NTIS
*Atmospheric Composition; Carbon Dioxide; Carbon Dioxide Concentration; Coal*

**20010122904** Federal Energy Technology Center, Morgantown, WV USA

**Advanced Solids NMR Studies of Coal Structure and Chemistry**

Zilm, K. W.; Sep. 01, 1998; 18p; In English

Report No.(s): DE2000-766406; DE-FG22-95PC95227-06; No Copyright; Avail: Department of Energy Information Bridge, Microfiche

This report covers the progress made on the title project for the final project period and summarizes the completion of the grant. The study of coal chemical structure is a vital component of research efforts to develop better chemical utilization of coals, and for furthering our basic understanding of coal geochemistry. In this grant we are addressing several structural questions pertaining to coals with advances in state of the art solids Nuclear Magnetic Resonance (NMR) methods. The final activities of the grant focused on moving the analytical methods developed over the duration of the grant from the low field instrumentation used to newly acquired very high field NMR instrumentation. The project accomplishments and output are summarized.

NTIS

*Chemical Composition; Coal; Geochemistry; Nuclear Magnetic Resonance*

**20010122910** National Renewable Energy Lab., Golden, CO USA

**Determining the Cost of Producing Ethanol from Corn Starch and Lignocellulosic Feedstocks**

McAloon, A.; Taylor, F.; Yee, W.; Ibsen, K.; Wooley, R.; Oct. 25, 2000; 44p; In English

Report No.(s): DE2000-766198; NREL/TP-580-28893; No Copyright; Avail: Department of Energy Information Bridge, Microfiche

The mature corn-to-ethanol industry has many similarities to the emerging lignocellulose-to-ethanol industry. It is certainly possible that some of the early practitioners of this new technology will be the current corn ethanol producers. In order to begin to explore synergies between the two industries, a joint project between two agencies responsible for aiding these technologies in the Federal government was established. This joint project of the USDA-ARS and DOE/NREL looked at the two processes on a similar process design and engineering basis, and will eventually explore ways to combine them. This report describes the comparison of the processes, each producing 25 million annual gallons of fuel ethanol. This paper attempts to compare the two processes as mature technologies, which requires assuming that the technology improvements needed to make the lignocellulosic process commercializable are achieved, and enough plants have been built to make the design well-understood. Assumptions about yield and design improvements possible from continued research were made for the emerging lignocellulose process. In order to compare the lignocellulose-to-ethanol process with the commercial corn-to-ethanol costs, it was assumed that the lignocellulose plant was an Nth generation plant, built after the industry had been sufficiently established to eliminate first-of-a-kind costs. This places the lignocellulose plant costs on a similar level with the current, established corn ethanol industry, whose costs are well known. The resulting costs of producing 25 million annual gallons of fuel ethanol from each process were determined. The figure shows the production cost breakdown for each process. The largest cost contributor in the corn starch process is the feedstock; for the lignocellulosic process it is the capital cost, which is represented by depreciation cost on an annual basis.

NTIS

*Corn; Costs; Ethyl Alcohol; Product Development; Production Costs*

**20010122944** National Renewable Energy Lab., Golden, CO USA

**Biomass Cofiring: A Renewable Alternative for Utilities (Fact sheet)**

Craig, K.; Aug. 30, 1999; 2p; In English

Report No.(s): DE2000-766452; NREL/FS-570-27048; DOE/GO-10099-914; No Copyright; Avail: Department of Energy Information Bridge

Cofiring refers to the practice of introducing biomass as a partial substitute fuel in high-efficiency coal boilers. This is the nearest term low-cost option for the efficient conversion of biomass to electricity. Cofiring has been practiced, tested, and evaluated for a variety of boiler technologies.

NTIS

*Biomass; Boilers; Fuel Production*

**20010123216** Federal Energy Technology Center, Morgantown, WV USA

**Comprehensive investigation of the liberation characteristics of pyrite and other mineral matter from coal**

King, R. P.; Schneider, C. L.; Jul. 31, 1998; 8p; In English

Report No.(s): DE2000-765655; DE-FG22-95PC95220-06; No Copyright; Avail: Department of Energy Information Bridge, Microfiche

The objective of this project is the development of methods for the measurement, prediction and modeling of the liberation characteristics of mineral matter and pyrite from coal, and to implement these findings in viable computer-simulation systems for coal cleaning plants. The central thrust of the project will be based on using the Andrews-Mika diagram as a convenient and experimentally verifiable model for the liberation characteristics of the constituents of coal during comminution. In order to establish the Andrews-Mika diagram, it is necessary to develop efficient techniques for density fractionation and for the measurement of the liberation spectrum in products obtained from the comminution of narrow composition fractions of coal. Dense-liquid techniques are used to produce fractionated samples, and image-analysis techniques, using linear-intercept analysis, are used to measure the liberation spectrum. The prediction of the liberation of mineral matter and pyrite from coal after comminution is based on a linear stochastic model for the description of the mineralogical texture and the random fracture pattern associated with the comminution process. Stereological correction of the distribution of linear grades is required for both the measurement and prediction of the true distribution of volumetric grades in the particle population.
NTIS
*Coal; Pyrites*

**20010123221** Federal Energy Technology Center, Morgantown, WV USA
**USGS Toxic Substances from Coal Combustion: Forms of Occurrence Analysis**
Kolker, A.; Mroczkowski, S. J.; Palmer, C. A.; Finkelman, R. B.; Apr. 01, 1999; 15p; In English
Report No.(s): DE2000-765150; DE-AI22-95PC95145-06; No Copyright; Avail: Department of Energy Information Bridge, Microfiche

Detailed information on trace-element modes of occurrence in coal is essential to understanding and predicting trace-element transformations taking place during coal combustion. The USGS has developed quantitative and semi-quantitative methods for determining the mode of occurrence of trace elements in coal. This information is needed to generate predictive models for trace-element behavior, the ultimate goal of DOE contract DE-AC22-95PC95101 Toxic Substances From Coal Combustion--A Comprehensive Assessment; awarded to PSI, Inc. USGS activities in support of this contract have a direct bearing on the predictive equations being developed as the primary product of the PSI program.
NTIS
*Coal; Combustion Products*

**20010123222** National Renewable Energy Lab., Golden, CO USA
**Biofuels: Ethanol - Separating Fact from Fiction**
McDonald, D.; May 10, 2000; 4p; In English
Report No.(s): DE2000-765141; NREL/BR-580-24401; DOE/GO-10099-736; No Copyright; Avail: Department of Energy Information Bridge, Microfiche

This fact sheet presents documented information that dispels some of the myths that people have developed about ethanol. Once the facts are revealed, it becomes clear that using and producing ethanol for transportation is good for the country's economy, environment, and energy future.
NTIS
*Ethyl Alcohol; Transportation*

**20010123412** Johns Hopkins Univ., Applied Physics Lab., Laurel, MD USA
**Final report for the Advanced Natural Gas Vehicle Project**
Wozniak, J.; Feb. 16, 1999; 28p; In English
Report No.(s): DE2001-765105; JHU/APL TL-99-054; No Copyright; Avail: Department of Energy Information Bridge

The project objective was to develop the technologies necessary to prototype a dedicated compressed natural gas (CNG) powered, mid-size automobile with operational capabilities comparable to gasoline automobiles. A system approach was used to design and develop the engine, gas storage system and vehicle packaging. The 2.4-liter DOHC (double overhead cam) engine was optimized for natural gas operation with high-compression pistons, hardened exhaust valves, a methane-specific catalytic converter and multi-point gaseous injection. The chassis was repackaging to increase space for fuel storage with a custom-designed, cast-aluminum, semi-trailing arm rear suspension system, a revised flat trunk sheet-metal floorpan and by equipping the car with run-flat tires. An Integrated Storage system (ISS) was developed using all-composite, small-diameter cylinders encapsulated within a high-strength fiberglass shell with impact-absorbing foam. The prototypes achieved the target

goals of a city/highway driving range of 300 miles, ample trunk capacity, gasoline vehicle performance and ultra low exhaust emissions.
NTIS
*Fuel Systems; Automobiles; Natural Gas; Internal Combustion Engines; Prototypes*

**20010123413** Utah Univ., Salt Lake City, UT USA
**Final Report: Optimization of Chemical Process Heater and Combustion Systems, September 1, 1996-August 31, 1999**
Smith, P.; Aug. 31, 1999; 59p; In English
Report No.(s): DE2001-765104; No Copyright; Avail: Department of Energy Information Bridge
The optimization of ethylene furnace operations using cfd (computational fluid dynamics)-based simulations has been addressed. The optimization problems have been cast into various formulations: the Multidisciplinary feasible (MDF) approach, the All-At-Once (AAO) approach and the Individual discipline feasible (IDF) approach. These approaches mainly differ in their handling of the state equations as constraints, and hence some of the formulations place restrictions on the methods used to solve the state equations.
NTIS
*Combustion; Furnaces; Optimization; Computational Fluid Dynamics; Heating Equipment*

**20010123422** Desert Research Inst., Reno, NV USA
**Integrated renewable hydrogen/utility systems. Final report, phase I**
Jan. 01, 2000; 66p; In English
Report No.(s): DE2001-763244; DOE/GO/10342-F; No Copyright; Avail: Department of Energy Information Bridge
The Desert Research Institute (DRI) has completed Phase 1 of a Department of Energy contract to employ hydrogen as an energy storage medium for remote, renewable utility applications. The goal of this two-phase project is to bring about technologies to accelerate the use of clean, renewable energy worldwide in an economically feasible and technically viable way. The goal is being met through the development of design and analysis tools, assembly of a test system, and ultimately, installation of a fill prototype system in Phase 2 of the project. This approach takes advantage of hydrogen's ability to store large amounts of intermittent energy in a dispatchable and cost effective way The design and control system tools developed from this project will provide the basis for smart control technology critical for future distributed power systems. The test and fill prototype systems will serve as pathfinders for using hydrogen as a utility energy storage medium. The expected location of the prototype system is Kotzebue, Alaska, a village with a remote yet growing wind farm as well as realistic loads and environmental conditions.
NTIS
*Energy Storage; Hydrogen; Prototypes; Systems Engineering; Renewable Energy*

**20010123431** Combustion Resources, LLC, Provo, UT USA
**Clean production of coke from waste carbonaceous fines** ***Quarterly Report, Jul. - Sep. 1999***
Eatough, C. N.; Oct. 01, 1999; 8p; In English
Report No.(s): DE2001-763186; DOE/GO/10395-Q; No Copyright; Avail: Department of Energy Information Bridge, Microfiche
During the previous reporting period, adequate supplies of coke breeze, petroleum coke fines, and coal fines to perform the required testing were identified and acquired. Coke breeze was obtained from the coking operations at Geneva Steel in Provo, Utah. Petroleum coke was acquired from the Chevron USA refinery in North Salt Lake City, Utah. Coal fines were received from Covol Technologies, Inc. of Lehi, Utah. Each of these feedstock materials was analyzed for proximate and ultimate analyses.
NTIS
*Waste Utilization; Coke; Production Engineering*

**20010123440** Loragen Transportation Electronics, San Luis Obispo, CA USA
**Indirect sensing technique for diesel fuel quantity control** ***Final Report***
MacCarley, C. A.; May 25, 1999; 59p; In English
Report No.(s): DE2001-761086; L-DOE-1-0559; No Copyright; Avail: Department of Energy Information Bridge, Microfiche
Related Inventions Program, for the development and commercialization of a method for improved diesel engine fuel quantity control with the objective of reducing exhaust smoke under full-load conditions. The proposed method involves advanced sensing, signal processing, and adaptive feedback control techniques. This report describes the accomplishments and results of this project. While originally conceived as a method suitable for OEM implementation only, modifications were made to utilize the technology in a retrofit system, applicable to existing diesel-powered vehicles. This required the development of an additional

sensor and improved adaptive control algorithms, and verification testing on naturally aspirated and turbocharged diesel engines. The result of this work is a low-cost microprocessor-based control system that can be retrofitted to a wide range of diesel engines to prevent visible partilculate emissions and poor efficiency caused by full-load overfueling. The system is designated the Electronic Diesel Smoke Reduction System (EDSRS). Dynamometer emission tests have confirmed the effectiveness of the system at maintaining exhaust smoke at 5/40 maximum capacity for all speeds. At the present state of development, a commercial prototype system is beginning in-service testing on diesel vehicles having a range of displacements from 1.8 L (naturally aspirated) to 7.3 L (turbocharged).
NTIS
*Diesel Fuels; Exhaust Emission; Exhaust Gases; Diesel Engines; Control Systems Design*

**20010123449** Brelsford Engineering, Inc., Bozeman, MT USA
**BEI hydrolysis process and reactor system refined engineering proto-type. BEI pilot-plant improvement and operations demonstrations**
Brelsford, D. L.; Oct. 01, 1999; 6p; In English
Report No.(s): DE2001-761020; DOE/GO/10322-Q; USDOE/EE/10322; No Copyright; Avail: Department of Energy Information Bridge, Microfiche

This BEI project involves BEI-HP and RS's applications toward potential commercial validity demonstrations for dilute-acid corn-fiber cellulose-hydrolysis processing with an aim toward fuel ethanol production.
NTIS
*Ethyl Alcohol; Fuel Production; Pilot Plants; Systems Engineering*

**20010123534** Argonne National Lab., IL USA
**Engineering assessment of CO2 recovery, transport, and utilization**
Doctor, R. D.; Oct. 09, 1998; 10p; In English
Report No.(s): DE2001-10910; ANL/ES/CP-96980; No Copyright; Avail: Department of Energy Information Bridge, Microfiche

The need to establish benchmarks for available power-generating cycles having reduced atmospheric emissions of CO(sub 2) served as the basis for this study. Innovative process technologies need this benchmark so they can be appreciated in their proper perspective. An oxygen-blown KRW (Kellogg-Rust-Westinghouse) coal-gasification plant producing hydrogen, electricity, and supercritical-CO(sub 2), was studied in a full-energy cycle analysis extending from the coal mine to the final destination of the gaseous product streams. A location in the mid-western US 100 mi from Old Ben No. 26 mine was chosen. Three parallel gasifier trains, each capable of providing 42% of the plant's 413.5 MW nominal capacity use 3,845 tons/day of Illinois No. 6 coal from this mine. The plant produces a net 52 MW of power and 131 MMscf/day of 99.999% purity hydrogen which is sent 62 mi by pipeline at 34 bars. The plant also produces 112 MMscf/day of supercritical-CO(sub 2) at 143 bars, which is sequestered in enhanced oil recovery operations 310 mi away.
NTIS
*Hydrogen; Coal Derived Gases; Coal; Coal Gasification; Energy Conversion Efficiency*

**20010123617** Hawaiian Commercial and Sugar Co., Puunene, HI USA
**Closed-loop biomass co-firing9** ***Quarterly Report, Oct. - Dec. 1999***
Jakeway, L.; Nakahata, M.; Jan. 01, 2000; 49p; In English
Report No.(s): DE2001-760523; DOE/GO/10479-Q; No Copyright; Avail: Department of Energy Information Bridge, Microfiche

Tasks included the following: analyze data from small plot harvests; large-scale planting of high-fiber cane variety; pilot-scale testing of fuel blends; procuring harvest equipment; perform harvest and co-firing trials for full-scale demonstration.
NTIS
*Biomass; Feedback Control*

**20010123623** National Renewable Energy Lab., Golden, CO USA
**Bioethanol - the Climate-Cool Fuel: Biofuels For the Global Environment Fact Sheet**
Nov. 17, 1997; 2p; In English
Report No.(s): DE2000-767385; NREL/FS-420-23761; DOE/GO-10097-515; No Copyright; Avail: Department of Energy Information Bridge, Microfiche

Bioethanol is alcohol fuel made from cellulosic biomass-renewable resources such as trees, grasses, much of the material in municipal solid waste, and forestry and agricultural residues. Compared to the fossil fuels it will displace, bioethanol contributes little or no net CO2 to the earth's atmosphere.
NTIS
*Alcohols; Environment Protection; Fuels*

**20010123627** National Renewable Energy Lab., Golden, CO USA
**Next Generation Natural Gas Vehicle (NGNGV) Program Brochure**
Elling, J.; Oct. 26, 2000; 6p; In English
Report No.(s): DE2000-767315; NREL/BR-540-29162; DOE/GO-102000-1137; No Copyright; Avail: Department of Energy Information Bridge, Microfiche

The Department of Energy's Office of Transportation Technologies is initiating the Next Generation Natural Gas Vehicle (NGNGV) Program to develop commercially viable medium- and heavy-duty natural gas vehicles. These new vehicles will incorporate advanced alternative fuel vehicle technologies that were developed by DOE and others.
NTIS
*Natural Gas; Transportation*

**20010123652** Auburn Univ., AL USA
**Enhancement of Dilute-Acid Total-Hydrolysis Process**
Lee, Y. Y.; Apr. 20, 2000; 22p; In English
Report No.(s): DE2001-764595; DOE/GO/10475-Q; No Copyright; Avail: Department of Energy Information Bridge

In order to assess the current situation of the kinetic investigation in our project, we have given further thought on this issue and performed detailed analysis of literature information. Some of these efforts are summarized here. The principal molecular mechanism of acid hydrolysis, which was confirmed by model and tracer studies, is outlined. Acid hydrolysis, leading finally to a fission of glycosidic bonds, proceeds in three steps. The reaction starts with a proton of catalyzing acid interacting rapidly with the glycosidic oxygen linking two sugar units, forming a so-called conjugate acid. The next step is the cleavage of the C-O bond and breakdown the conjugate acid to the cyclic carbonium ion, which adopts a half-chair conformation. After a rapid addition of formation of the intermediate carbonium in the middle of the polysaccharide water, free sugar and proton is liberated. The ion then takes place more rapidly at the end than chain.
NTIS
*Augmentation; Hydrolysis; Procedures*

**20010123959** Argonne National Lab., IL USA
**Numerical Study of Short Residence Time FCC Riser Flows with a New Flow/Kinetics Modeling Technique**
Chang, S. L.; Aug. 25, 1998; 11p; In English
Report No.(s): DE2001-10933; ANL/ES/CP-97070; No Copyright; Avail: Department of Energy Information Bridge

Fluid Catalytic Cracking (FCC) technology is the most important process used by the refinery industry to convert crude oil to valuable lighter products such as gasoline. New and modified processes are constantly developed by refinery companies to improve their global competitiveness and meet more stringent environmental regulations. Short residence time FCC riser reactor is one of the advanced processes that the refining industry is actively pursuing because it can improve the yield selectivity and efficiency of an FCC unit. However, as the residence time becomes shorter, the impact of the mixing between catalyst and feed oil at the feed injection region on the product yield becomes more significant. Currently, most FCC computer models used by the refineries perform sophisticated kinetic calculations on simplified flow field and can not be used to evaluate the impact of fluid mixing on the performance of an FCC unit. Argonne National Laboratory (AFL) is developing a computational fluid dynamic (CFD) code ICRKFLO for FCC riser flow modeling. The code, employing hybrid hydrodynamic-chemical kinetic coupling techniques, is used to investigate the effect of operating and design conditions on the product yields of FCC riser reactors. Numerical calculations were made using the code to examine the impacts of the operating and design conditions on the product yields. The controlling parameters under investigation include the residence time, reaction temperature, and catalyst/oil ratio. This paper describes the CFD code, presents computation results, and discusses the effects of operating conditions on the performance of short residence time FCC riser reactors.
NTIS
*Computational Fluid Dynamics; Computerized Simulation; Cracking (Chemical Engineering); Kinetics; Refining; Risers*

**20010123960** Argonne National Lab., IL USA

**Numerical Iinvestigation of the Scale-Up Effects on Flow, Heat Transfer, and Kinetics Processes of FCC Units**

Chang, S. L.; Aug. 25, 1998; 12p; In English

Report No.(s): DE2001-10932; ANL/ES/CP-97069; No Copyright; Avail: Department of Energy Information Bridge

Fluid Catalytic Cracking (FCC) technology is the most important process used by the refinery industry to convert crude oil to valuable lighter products such as gasoline. Process development is generally very time consuming especially when a small pilot unit is being scaled-up to a large commercial unit because of the lack of information to aide in the design of scaled-up units. Such information can now be obtained by analysis based on the pilot scale measurements and computer simulation that includes controlling physics of the FCC system. A computational fluid dynamic (CFD) code, ICRKFLO, has been developed at Argonne National Laboratory (ANL) and has been successfully applied to the simulation of catalytic petroleum cracking risers. It employs hybrid hydrodynamic-chemical kinetic coupling techniques, enabling the analysis of an FCC unit with complex chemical reaction sets containing tens or hundreds of subspecies. The code has been continuously validated based on pilot-scale experimental data. It is now being used to investigate the effects of scaled-up FCC units. Among FCC operating conditions, the feed injection conditions are found to have a strong impact on the product yields of scaled-up FCC units. The feed injection conditions appear to affect flow and heat transfer patterns and the interaction of hydrodynamics and cracking kinetics causes the product yields to change accordingly.

NTIS

*Computational Fluid Dynamics; Computerized Simulation; Cracking (Chemical Engineering); Heat Transfer; Kinetics*

**20010124134** Lawrence Livermore National Lab., Livermore, CA USA

**Modeling of non-ideal aluminized explosives**

Fried, L. E.; Howard, W. M.; Souers, P. C.; Jun. 01, 1999; 6p; In English

Report No.(s): DE2001-11326; UCRL-JC-132717; No Copyright; Avail: Department of Energy Information Bridge

We have implemented a Wood-Kirkwood kinetic detonation model based on multi-species equations of state and multiple reaction rate laws. Finite rate laws are used for the slowest chemical reactions, while other reactions are given infinite rates and are kept in constant thermodynamic equilibrium. Within the context of WK theory, we study the chemical interaction between Al and HMX detonation products in non-ideal explosives. We develop a kinetic rate law for the combustion of Al in a condensed detonation that depends on the pressure and the detonation product gases. We use a Murnaghan form for the equation of state of the solid and liquid Al and Al(sub 2)O(sub 3). We find that we can replicate experimental detonation velocities for HMX/Al composites to within a few percent for a wide range of aluminum content. We discuss the uncertainties in our model and the implications of our results on the modeling of other non-ideal explosives.

NTIS

*Detonation; Reaction Kinetics; Explosives*

**20010125008** Sandia National Labs., Albuquerque, NM USA

**Miniaturized Explosive Preconcentrator for Use in a Man-Portable Field Detection System**

Hannum, D. W.; Linker, K. L.; Parmeter, J. E.; Rhykerd, C. L.; Varley, N. R.; Aug. 02, 1999; 10p; In English

Report No.(s): DE2001-9686; SAND99-2000C; No Copyright; Avail: Department of Energy Information Bridge, Microfiche

We discuss the design and testing of a miniaturized explosives preconcentrator that can be used to enhance the capabilities of man-portable field detection systems, such as those based on ion mobility spectrometry (IMS). The preconcentrator is a smaller version of a similar device that was developed recently at Sandia National Laboratories for use in a trace detection portal that screens personnel for explosives. Like its predecessor, this preconcentrator is basically a filtering device that allows a small amount of explosive residue in a large incoming airflow to be concentrated into a much smaller air volume via adsorption and resorption, prior to delivery into a chemical detector. We discuss laboratory testing of this preconcentrator interfaced to a commercially available IMS-based detection system, with emphasis on the explosives 2,4,6-trinitrotoluene (TNT) and cyclotrimethylenetrinitramine (RDX). The issues investigated include optimization of the preconcentrator volume and inlet airflow, the use of different types of adsorbing surfaces within the preconcentrator, Wd preconcentrator efficiency and concentration factor. We discuss potential field applications of the preconcentrator, as well as avenues for further investigations and improvements.

NTIS

*Detection; Explosives; Miniaturization; RDX; Trinitrotoluene*

**20010125030** Federal Energy Technology Center, Morgantown, WV USA
**Development of a Coal Quality Expert TM: A DOE Assessment**
Oct. 31, 2000; 19p; In English
Report No.(s): DE2000-768100; DOE/NETL-2001/1133; No Copyright; Avail: Department of Energy Information Bridge, Microfiche

This document serves as the US Department of Energy (DOE) post project assessment of the Clean Coal Technology (CCT) Round 1 project Development of a Coal Quality Expert. In 1990, CQ Inc., then a subsidiary of the Electric Power Research Institute (EPRI), and Combustion Engineering (now ABB Combustion Engineering, Inc.) executed a cooperative agreement with DOE. Both contractors became co-prime contractors for the project; project management and administrative duties were delegated to CQ Inc. Project participants included several contractors and utilities. The total project cost was $21.7 million, of which 50% was provided by DOE.
NTIS
*Agreements; Contractors; Project Management; Quality Control*

**20010125066** Argonne National Lab., IL USA
**Time resolved small angle x-ray scattering reactivity studies on coals, asphaltenes, and polymers**
Seifert, S.; Thiyagarajan, P.; Winans, R. E.; Jul. 02, 1999; 8p; In English
Report No.(s): DE2001-11781; ANL/CHM/CP-98917; No Copyright; Avail: Department of Energy Information Bridge

The objective of this study is to examine changes in the structures of coals, asphaltenes, and polymers in situ with small angle X-ray scattering (SAXS) during thermal treatments. We have built a SAXS instrument at the Basic Energy Sciences Synchrotrons Radiation Center at the Advanced Photon Source that allows us to obtain scattering data on very small samples and in the millisecond time domain. The Argonne Premium Coal samples, petroleum derived asphaltenes, and polymers with functionality to model fossil fuels were used in this study. The information that can be derived from these experiments includes: changes in fractal dimensionality, surface topology, and size and type of porosity. The information is correlated with other methods on the same samples.
NTIS
*Photons; Fossil Fuels; Crude Oil; X Ray Scattering*

**20010125098** California Energy Commission, Sacramento, CA USA
**Transportation Technology Status Report: (1) Alternative Fuel Vehicles; (2) Automotive Fuel Economy. Staff Report**
December 1997; 110p; In English
Report No.(s): PB2001-108320; P500-97-013; No Copyright; Avail: CASI; A06, Hardcopy; A02, Microfiche

Transportation remains a vital component of California's economy and affects the quality of life for many individuals. The current system, however, also creates challenges and problems. The state can play an important role in identifying options to help maximize the benefits currently enjoyed from transportation, and also reduce its adverse impacts. For example, the transportation sector contributes large amounts of air pollutants in California. Tailpipe and evaporative emissions contribute to the formation of ozone. Tailpipe emissions also add to carbon dioxide emissions from fossil fuel combustion. Through dependence on one fuel the state economy is vulnerable to petroleum price increases which pose an energy security risk. Reducing this risk can be achieved by developing alternative fuel vehicle technologies that offer choices for the driving public.
NTIS
*Automobile Fuels; Transportation; California; Energy Conservation; Clean Energy; Clean Fuels*

**20010125106** National Defence Research Establishment, Dept. of Weapons and Protection, Stockholm, Sweden
**Evaluation of an Explosive Detector Device called MO-2M** ***Utvaerdering av Explosivaemnesdetektorn MO-2M***
Sarholm, L.; Persson, B.; October 1999; ISSN 1104-9154; 24p; In Swedish
Report No.(s): PB2001-108122; FOA-R-99-01235-310-SE; No Copyright; Avail: CASI; A03, Hardcopy; A01, Microfiche

A handheld explosives detector called MO-2M and marketed by ChemSpace, s.r.o Czech Republic, has been evaluated by FOA(Swedish Defense Research Establishment) on behalf of FHTC. The MO-2M detector is built on a new generation of highly sensitive Ion Mobility Spectroscopy (IMS), increasing the sensitivity to 0.01 ppb for explosives. The results from the tests with MO-2M have been compared with equal tests carried out by the National Laboratory of Forensic Science, analyzed with a detector called EGIS using Gas Chromotography/Chemiluminescence technology.
NTIS
*Explosives; Indicating Instruments; Detection*

**20010125176** National Renewable Energy Lab., Golden, CO USA
**Biomass Power and State Renewable Energy Policies Under Electric Industry Restructuring**
Porter, K.; Wiser, R.; Oct. 09, 2000; 12p; In English
Report No.(s): DE2000-765094; NREL/CP-620-28747; No Copyright; Avail: Department of Energy Information Bridge

The paper discusses policies that foster renewable energy as enacted by states in response to utility restructuring. In particular, it discusses the role of biomass in these policies.

NTIS
*Biomass; Renewable Energy; Electric Power Plants; Policies*

**20010125178** National Renewable Energy Lab., Golden, CO USA
**Bioethanol: Moving into the Marketplace**
Sheehan, J.; Sep. 28, 2000; 4p; In English
Report No.(s): DE2000-765087; NREL/BR-580-28828; DOE/GO-102000-1109; No Copyright; Avail: Department of Energy Information Bridge

In the last ten years advances in biotechnology have reduced the cost of bioethanol by almost 25%. The Department of Energy bioethanol program targets process improvements intended to allow bioethanol to compete with gasoline in the marketplace. Researchers are utilizing biomass feedstock for bioethanol conversion. The bioethanol conversion technology depends on hydrolysis and fermentation. to maximize biomass fermentation, biotechnology researchers have produced new strains of yeast and bacteria.

NTIS
*Biomass; Biomass Energy Production; Biotechnology; Ethyl Alcohol*

**20010125402** Argonne National Lab., IL USA
**Thermal management concepts for higher efficiency heavy vehicles**
Wambsganss, M. W.; May 19, 1999; 14p; In English
Report No.(s): DE2001-11808; ANL/ET/CP-99033; No Copyright; Avail: Department of Energy Information Bridge

Thermal management is a cross-cutting technology that directly or indirectly affects engine performance, fuel economy, safety and reliability, aerodynamics, driver/passenger comfort, materials selection, emissions, maintenance, and component life. This review paper provides an assessment of thermal management for large trucks, particularly as it impacts these features. Observations arrived at from a review of the state of the art for thermal management for over-the-road trucks are highlighted and commented on. Trends in the large truck industry, pertinent engine truck design and performance objectives, and the implications of these relative to thermal management, are presented. Finally, new thermal management concepts for high efficiency vehicles are described.

NTIS
*Temperature Control; Trucks; Thermodynamic Efficiency*

**20010125411** Argonne National Lab., IL USA
**Fuel-flexible partial oxidation reforming of hydrocarbons for automotive applications**
Ahmed, S.; Carter, J. D.; Kopasz, J. P.; Krumpelt, M.; Wilkenhoener, R.; Jun. 07, 1999; 9p; In English
Report No.(s): DE2001-11794; ANL/CMT/CP-98970; No Copyright; Avail: Department of Energy Information Bridge

Micro-reactor tests indicate that our partial oxidation catalyst is fuel-flexible and can reform conventional (gasoline and diesel) and alternative (ethanol, methanol, natural gas) fuels to hydrogen rich product gases with high hydrogen selectivity. Alcohols are reformed at lower temperatures (less than 600 C) while alkanes and unsaturated hydrocarbons require slightly higher temperatures. Cyclic hydrocarbons and aromatics have also been reformed at relatively low temperatures, however, a different mechanism appears to be responsible for their reforming. Complex fuels like gasoline and diesel, which are mixtures of a broad range of hydrocarbons, require temperatures of greater than 700 C for maximum hydrogen production.

NTIS
*Automobiles; Fuels; Oxidation; Hydrocarbons*

**20010125412** Argonne National Lab., IL USA
**Partial oxidation fuel reforming for automotive power systems**
Ahmed, S.; Chalk, S.; Krumpelt, M.; Kumar, R.; Milliken, J.; Sep. 07, 1999; 7p; In English
Report No.(s): DE2001-11793; ANL/CMT/CP-98964; No Copyright; Avail: Department of Energy Information Bridge

For widespread use of fuel cells to power automobiles in the near future, it is necessary to convert gasoline or other transportation fuels to hydrogen on-board the vehicle. Partial oxidation reforming is particularly suited to this application as it eliminates the need for heat exchange at high temperatures. Such reformers offer rapid start and good dynamic performance. Lowering the temperature of the partial oxidation process, which requires the development of a suitable catalyst, can increase the reforming efficiency. Catalytic partial oxidation (or autothermal) reformers and non-catalytic partial oxidation reformers developed by various organizations are presently undergoing testing and demonstration. This paper summarizes the process chemistries as well as recent test data from several different reformers operating on gasoline, methanol, and other fuels.
NTIS
*Automobiles; Fuel Cells; Hydrogen; Oxidation*

**20010125456** Lawrence Livermore National Lab., Livermore, CA USA
**Modeling thermally driven energetic response of high explosives in ALE3D**
Aro, C.; McCallen, R. C.; Neely, R.; Nichols, A. L.; Sharp, R.; Oct. 01, 1998; 12p; In English
Report No.(s): DE2001-8317; UCRL-JC-133140; DP0101031; No Copyright; Avail: Department of Energy Information Bridge, Microfiche

The authors have improved their ability to model the response of energetic materials to thermal stimuli and the processes involved in the energetic response. Traditionally, the analyses of energetic materials have involved coupled thermal transport/chemical reaction codes. This provides only a reasonable estimate of the time and location of ensuing rapid reaction. To predict the violence of the reaction, the mechanical motion must be included in the wide range of time scales associated with the thermal hazard. The ALE3D code has been modified to assess the hazards associated with heating energetic materials in weapons by coupling to thermal transport model and chemistry models. They have developed an implicit time step option to efficiently and accurately compute the hours of heating to reaction of the energetic material. Since, on these longer time scales, materials can be expected to have significant motion, it is even more important to provide high-order advection for all components, including the chemical species. They show two examples of coupled thermal/mechanical/chemical models of energetic materials in thermal environments.
NTIS
*Explosives; Chemical Reactions; Thermal Simulation; Computerized Simulation*

**20010125481** Federal Energy Technology Center, Morgantown, WV USA
**Advanced Power Systems: Ash Behavior in Power Systems. Includes the Semiannual Report for the Period January 01, 1998 - June 30, 1998**
Sep. 01, 1998; 94p; In English
Report No.(s): DE2001-7952; DE-FC21-93MC30097-37; No Copyright; Avail: Department of Energy Information Bridge, Microfiche

The overall goal of this initiative is to develop fundamental knowledge of ash behavior in power systems for the purpose of increasing power production efficiency, reducing operation and maintenance costs, and reducing greenhouse gas emissions into the atmosphere. The specific objectives of this initiative focus primarily on ash behavior related to advanced power systems and include the following: Determine the current status of the fundamental ash interactions and deposition formation mechanisms as already reported through previous or ongoing projects at the EERC or in the literature; Determine sintering mechanisms for temperatures and particle compositions that are less well known and remain for the most part undetermined; Identify the relationship between the temperature of critical viscosity (T(sub cv)) as measured in a viscometer and the crystallization occurring in the melt; Perform a literature search on the use of heated-stage microscopy (HSM) for examining in situ ash-sintering phenomena and then validate the use of HSM in the determination of viscosity in spherical ash particles; Ascertain the formation and stability of specific mineral or amorphous phases in deposits typical of advanced power systems; and Evaluate corrosion for alloys being used in supercritical combustion systems.
NTIS
*Ashes; Corrosion Tests; Dynamic Characteristics*

**20010125483** Federal Energy Technology Center, Morgantown, WV USA

**Reducing Power Production Costs by Utilizing Petroleum Coke**

Sep. 01, 1998; 11p; In English

Report No.(s): DE2001-7943; DE-FC21-93MC30098-55; No Copyright; Avail: Department of Energy Information Bridge, Microfiche

A Powder River Basin subbituminous coal from the North Antelope mine and a petroleum shot coke were received from Northern States Power Company (NSP) for testing the effects of parent fuel properties on coal-coke blend grindability and evaluating the utility of petroleum coke blending as a strategy for improving electrostatic precipitator (ESP) particulate collection efficiency. Petroleum cokes are generally harder than coals, as indicated by Hardgrove grindability tests. Therefore, the weaker coal component may concentrate in the finer size fractions during the pulverizing of coal-coke blends. The possibility of a coal-coke size fractionation effect is being investigated because it may adversely affect combustion performance. Although the blending of petroleum coke with coal may adversely affect combustion performance, it may enhance ESP particulate collection efficiency. Petroleum cokes contain much higher concentrations of V relative to coals. Consequently, coke blending can significantly increase the V content of fly ash resulting from coal-coke combustion. Pentavalent vanadium oxide (V2O5) is a known catalyst for transforming gaseous sulfur dioxide (SO3(g)) to gaseous sulfur trioxide (SO3(g)). The presence of SO3(g) strongly affects fly ash resistivity and, thus, ESP performance.

NTIS

*Coal; Coke; Crude Oil; Electrostatic Precipitators; Mixtures*

**20010125484** Federal Energy Technology Center, Morgantown, WV USA

**Hydrodynamic Models for Slurry Bubble Column Reactors - Final Technical Report Also Includes the Quarterly Technical Report for the Period 01/01/1997 - 03/31/1997**

Gidaspow, D.; Aug. 15, 1997; 88p; In English

Report No.(s): DE2001-7939; DE-FG22-94PC94208-12; No Copyright; Avail: Department of Energy Information Bridge, Microfiche

The objective of this study is to develop a predictive experimentally verified computational fluid dynamic (CFD) three phase model. It predicts the gas, liquid, and solid hold-ups (volume fractions) and flow patterns in the industrially important bubble-coalesced (churn-turbulent) regime. The input into the model can be either particulate viscosities as measured with a Brookfield viscometer or effective restitution coefficient for particles. A combination of x-ray and gamma-ray densitometers was used to measure solid and liquid volume fractions. There is a fair agreement between the theory and the experiment. A CCD camera was used to measure instantaneous particle velocities. There is a good agreement between the computed time average velocities and the measurements. There is an excellent agreement between the viscosity of 800 micrometers glass beads obtained from measurement of granular temperature (random kinetic energy of particles) and the measurement using a Brookfield viscometer. A relation between particle Reynolds stresses and granular temperature was found for developed flow. Such measurement and computations gave a restitution coefficient for a methanol catalyst to be about 0.9. A transient, two-dimensional hydrodynamic model for production of methanol from syn-gas in an Air Products/DOE LaPorte slurry bubble column reactor was developed. The model predicts downflow of catalyst at the walls and oscillatory particle and gas flow at the center, with a frequency of about 0.7 Hertz. The computed temperature variation in the rector with heat exchangers was only about 5 K, indicating good thermal management. The computed slurry height, the gas holdup and the rate of methanol production agree with LaPorte's reported data. Unlike the previous models in the literature, this model computes the gas and the particle holdups and the particle rheology. The only adjustable parameter in the model is the effective particle restitution coefficient.

NTIS

*Bubbles; Catalysts; Computational Fluid Dynamics; Flow Distribution; Reynolds Stress; Slurries; Hydrodynamics*

**20010125485** Federal Energy Technology Center, Morgantown, WV USA

**Silicon Carbide Joining: Final Topical Report**

Oct. 01, 1998; 6p; In English

Report No.(s): DE2001-7938; DE-FC21-93MC30097-41; No Copyright; Avail: Department of Energy Information Bridge, Microfiche

Future energy systems will be required to fire lower-grade fuels and meet higher energy conversion efficiencies than today's systems. The steam cycle used at present is limited to a maximum temperature of 550 C because above that, the stainless steel tubes deform and corrode excessively. to boost efficiency significantly, much higher working fluid temperatures are required. Although high-temperature alloys will suffice for the construction of these components in the near term, the greatest efficiency increases can be reached only with the use of advanced structural ceramics such as silicon carbide (SiC). However, SiC does not

melt, but instead sublimes at temperatures over 2000 C. Therefore, it is not possible to join pieces of it through welding, and most brazing compounds have much lower melting points, so the joints lose strength at temperatures much lower than the maximum use temperature of the SiC. Since larger objects such as heat exchangers cannot be easily created from smaller ceramic pieces, the size of the SiC structures that can presently be manufactured are limited by the size of the sintering furnaces (approximately 10 feet for sintered alpha SiC). In addition, repair of the objects will require the use of field-joining techniques. Some success has been had by causing silicon and carbon to react at 1400-1500 C to form SiC in a joint, but these joints contain continuous channels of unreacted silicon, which cause the joints to corrode and creep excessively at temperatures below 1260 C. The objective of this work conducted at the Energy Environmental Research Center (EERC) is to develop a patentable technique for joining large SiC structures in the field. The key to developing a successful technique will be the use of reactive joining compounds to lower the joining temperature without leaving continuous channels of unreacted compounds that can weaken the joint at temperatures below 1260 C or serve as conduits for transport of corrodents. In addition, the method of heating the joint to cause the reaction bonding must be applicable to structures that are large in two dimensions, which precludes the use of furnaces for heating the samples. Special efforts will be made in this project to transfer the developed technologies to the materials industry via licensing agreements through the EERC Foundation.
NTIS
*Energy Conversion; Energy Technology; Heat Resistant Alloys; Silicon Carbides; Joints (Junctions)*

**20010125498** National Renewable Energy Lab., Golden, CO USA
**Using LNG as a Fuel in Heavy-Duty Tractors**
Aug. 09, 1999; 28p; In English
Report No.(s): DE2001-10183; NREL/SR-540-24146; No Copyright; Avail: Department of Energy Information Bridge

Recognizing the lack of operational data on alternative fuel heavy-truck trucks, NREL (National Renewable Energy Laboratory) contracted with the Trucking Research Institute (TRI) in 1994 to obtain a cooperative agreement with Liquid Carbonic. The purpose of this agreement was to (1) purchase and operate liquid natural gas (LNG)-powered heavy duty tractor trailers with prototype Detroit Diesel Corporation (DDC) Series 60 natural gas (S60G) engines in over-the-road commercial service applications; and (2) collect and provide operational data to DDC to facilitate the on-road prototype development of the engine and to NREL for the Alternative Fuels Data Center. The vehicles operated from August 1994 through April of 1997 and led to a commercially available, emissions-certified S60G in 1998. This report briefly documents the engine development, the operational characteristics of LNG, and the lessons learned during the project.
NTIS
*Trucks; Clean Fuels; Liquefied Natural Gas; Automobile Fuels*

**20010125499** Oak Ridge National Lab., TN USA
**Chemical Conversion of TNT: Production of 2,4,6-Trinitrobenzoic Acid**
Asrat'ev, A. A.; Marchukov, V. A.; Suschev, V. G.; Aleksandrov, A. V.; Semenov, V. V.; Aug. 01, 2000; 27p; In English
Report No.(s): DE2001-769293; ORNL/TM-2000/117; No Copyright; Avail: Department of Energy Information Bridge, Microfiche

Oxidation of 2,4,6-trinitrotoluene (TNT) by aqueous nitric acid at high temperature and pressure gives 2,4,6-trinitrobenzoic acid (TNBA) and other valuable products, such as 1,3,5-trinitrobenzene (TNB). Optimization of the kinetics proved to be critical for the selective oxidation of the methyl group. High yield of a desired product can be obtained only under a narrow range of conditions. Thus, the best yield (70 to 75%) of TNBA was achieved at a 35 to 45% conversion of TNT (80% nitric acid, 194 C, 20 min), whereas the decarboxylation product (TNB) was the major component of the reaction mixture after a 50-min reaction. Subsequent separation of TNBA was achieved by selective extraction with aqueous bicarbonate. Practical technology development steps for a continuous mode of operation leading to the chief products are also discussed. This technology can use commercial raw trotyl and trotyl from discharged ammunition as the starting material. The latter could be of particular importance for the conversion program aimed at the utilization of ammunition supplies.
NTIS
*Trinitrotoluene; Explosives*

**20010125501** Oak Ridge National Lab., TN USA
**Costs of Producing Biomass from Riparian Buffer Strips**
Turhollow, A.; Jul. 01, 2000; 72p; In English
Report No.(s): DE2001-769246; ORNL/TM-1999/146; No Copyright; Avail: Department of Energy Information Bridge, Microfiche

Nutrient runoff from poultry litter applied to agricultural fields in the Delmarva Peninsula contributes to high nutrient loadings in Chesapeake Bay. One potential means of ameliorating this problem is the use of riparian buffer strips. Riparian buffer strips intercept overland flows of water, sediments, nutrients, and pollutants; and ground water flows of nutrients and pollutants. Costs are estimated for three biomass systems grown on buffer strips: willow planted at a density of 15,300 trees/ha (6200 trees/acre); poplar planted at a density of 1345 trees/ha (545 trees/acre); and switchgrass. These costs are estimated for five different scenarios: (1) total economic costs, where everything is costed (cash costs, noncash costs (e.g., depreciation), land rent, labor; (2) costs with Conservation Reserve Program (CRP) payments (which pays 50% of establishment costs and an annual land rent); (3) costs with enhanced CRP payments (which pays 95% of establishment costs and an annual payment of approximately 170% of land rent for trees and 150% of land rent for grasses); (4) costs when buffer strips are required, but harvest of biomass is not required costs borne by biomass are for yield enhancing activities (e.g., fertilization), harvest, and transport; and (5) costs when buffer strips are required, and harvest of biomass is required to remove nutrients (costs borne by biomass are for yield enhancing activities and transport). CRP regulations would have to change to allow harvest.
NTIS
*Biomass; Costs; Grasses; Environment Protection*

**20010125526** Cornell Univ., Ithaca, NY USA
**Microbial ecology of thermophilic anaerobic digestion. Final report**
Zinder, S. H.; Apr. 15, 2000; 8p; In English
Report No.(s): DE2001-764721; No Copyright; Avail: Department of Energy Information Bridge
This grant supported research on methanogenic archaea. The two major areas that were supported were conversion of acetic acid to methane and nitrogen fixation by Methanosarcina. Among the achievements of this research were the isolation of novel methanogenic cultures, elucidation of the pathways from acetate to methane, description of a specific DNA-binding complex in nitrogen fixing methanogens, and demonstration of an alternative nitrogenase in Methanosarcina.
NTIS
*Ecology; Microbiology; Thermophiles; Anaerobes; Methane*

**20010125528** Department of Energy, Washington, DC USA
**Anaerobic Pump**
Mar. 31, 2000; 9p; In English
Report No.(s): DE2001-764713; DOE/GO/10300-Q; No Copyright; Avail: Department of Energy Information Bridge
This is a combined quarterly report which reflects the project progress and performance during the six (6) month project extension period, November 1999 through March 2000. The project time extension period was requested by Dr. Schimel, TMC, and granted by DOE on Nov. 15, 1999. The current project status is the first Steady State for both prototypes has been completed and the next steady state loading has begun. A more detailed analysis of this Anaerobic Pump (AP) and conventional digester (CD) data sets is given in Dr. Boone's quarterly progress report attached in Appendix A. A task-wise summary of the work completed during the last 6 months is presented in Section 2.
NTIS
*Prototypes; Anaerobes; Pumps*

**20010125605** NASA Glenn Research Center, Cleveland, OH USA
**Reduced Toxicity Fuel Satellite Propulsion System Including Axial Thruster and ACS Thruster Combination**
Schneider, Steven J., Inventor, NASA Glenn Research Center, USA; Nov. 06, 2001; 30p; In English; Division of US-Patent-Appl-SN-291883, filed 14 Apr. 1999
Patent Info.: Filed 17 Apr. 2001; NASA-Case-LEW-16636-5; US-Patent-6,311,477; US-Patent-Appl-SN-837820; US-Patent-Appl-SN-291883; No Copyright; Avail: CASI; A03, Hardcopy; A01, Microfiche
A reduced toxicity fuel satellite propulsion system including a reduced toxicity propellant supply for consumption in an axial class thruster and an ACS class thruster. The system includes suitable valves and conduits for supplying the reduced toxicity propellant to the ACS decomposing element of an ACS thruster. The ACS decomposing element is operative to decompose the reduced toxicity propellant into hot propulsive gases. In addition the system includes suitable valves and conduits for supplying the reduced toxicity propellant to an axial decomposing element of the axial thruster. The axial decomposing element is operative to decompose the reduced toxicity propellant into hot gases. The system further includes suitable valves and conduits for supplying

a second propellant to a combustion chamber of the axial thruster, whereby the hot gases and the second propellant auto-ignite and begin the combustion process for producing thrust.
Official Gazette of the U.S. Patent and Trademark Office
*Combustion Chambers; Decomposition; Ignition; Propellant Combustion; Propellant Consumption; Reaction Kinetics; Toxicity*

**20010125647** Argonne National Lab., IL USA
**Future prospects for compression ignition fuel in California: fuel-related implications of possible pathways to mitigation of public health threats**
Eberhardt, J. J.; Rote, D. M.; Saricks, C. L.; Stodolsky, F.; Apr. 08, 1999; 18p; In English
Report No.(s): DE2001-11752; ANL/ES/CP-98738; No Copyright; Avail: Department of Energy Information Bridge, Microfiche

This paper documents methods and results of an investigation of the options for and year 2010 consequences of possible new limitations on the use of diesel fuel in California, USA. California's Air Resources Board (CARB) will undertake a risk management process to determine steps necessary to protect the health and safety of the public from carcinogenic species resident on diesel combustion exhaust particles. Environmental activist groups continue to call for the elimination of diesel fuel in California and other populous states. It is the declared intention of CARB not to ban or restrict diesel fuel, per se, at this time. Thus, two 'mid-course' strategies now appear feasible: 1) Increased penetration of natural gas, LPG (liquefied petroleum gas), and possibly lower alcohols into the transportation fuels market, to the extent that some Cl applications would revert to spark-ignition (SI) engines. 2) New specifications requiring diesel fuel reformulation based on more detailed investigation of exhaust products of individual diesel fuel constituents.
NTIS
*Air Pollution; Diesel Fuels; Public Health*

## 29
## SPACE PROCESSING

*Includes space-based development of materials, compounds, and processes for research or commercial application. Also includes the development of materials and compounds in simulated reduced-gravity environments. For legal aspects of space commercialization see 84 Law, Political Science and Space Policy.*

**20010123401** RECOM Technologies, Inc., Moffett Field, CA USA
**Results From The First Interactive Scientific Expert System In Space**
Groleau, Nicolas, RECOM Technologies, Inc., USA; Frainier, Richard J., RECOM Technologies, Inc., USA; [1994]; 1p; In English; American Society for Gravitational and Space Biology, 20-22 Oct. 1994, San Francisco, CA, USA; Sponsored by American Society for Gravitational and Space Biology, USA
Contract(s)/Grant(s): RTOP 233-02-07; No Copyright; Avail: Issuing Activity; Abstract Only

We describe recent work on automation and support of science experiments on the Space Shuttle. PI-in-a-Box, the first interactive expert system for scientific support, was flown onboard STS-58 in October 1993. It was designed to help astronauts perform better science in space by providing expert-level advice in real-time. The system provides help with 'technician' tasks such as data acquisition, data quality monitoring, and diagnostic, troubleshooting and repair. The system also performs 'expert' reasoning on the scientific model and experiment steps scheduling. It can make scheduling recommendations based on hardware status, time available, and agreement between predictions and flight data. The system was successfully deployed and used throughout the mission. Most of the 'technician' skills of the system were used with success. The scientific model study performed correctly, but we believe the results were not exploited by the astronauts because of Spacelab operational pressures. Also, portions of the system were designed around rigid schedule constraints that were essentially relaxed during the mission. This version was tailored to a specific vestibular experiment known as the 'rotating dome'. We are currently expanding our effort in various scientific (other life and microgravity sciences experiments) and technological directions (integrated telescience, astronaut science advisor, and autonomous control).
Author
*Autonomy; Data Acquisition; Expert Systems; Maintenance; Real Time Operation; Scheduling; Spacecraft Equipment*

## 31
## ENGINEERING (GENERAL)

*Includes general research topics to engineering and applied physics, and particular areas of vacuum technology, industrial engineering, cryogenics, and fire prevention. For specific topics in engineering see categories 32 through 39.*

**20010117665** Sandia National Labs., Albuquerque, NM USA
**STAMMT-R Solute Transport and Multirate Mass Transfer in Radial Coordinates**
Haggerty, R.; Fleming, S. W.; McKenna, S. A.; Jul. 01, 2000; 71p; In English
Report No.(s): DE2000-759366; SAND99-0164; No Copyright; Avail: Department of Energy Information Bridge

STAMMT-R is a FORTRAN 77 code that solves the advective-dispersive and rate-limited mass transfer equations for solute transport in groundwater in radial coordinates. STAMMT-R is unique in that rate-limited mass transfer can be modeled as heterogeneous at the pore-scale. Heterogeneous rate-limited mass transfer is diffusion concurrently into and out of a distribution of immobile zones, which may include matrix blocks of varying sizes or geologic materials with differing diffision characteristics. NTIS

*Applications Programs (Computers); Mass Transfer; Computer Programming; Solutes*

**20010118278** Micronic, Inc., Miami, FL USA
**Electronic Refrigerant Leak Detector**
Talamas, E.; Sep. 27, 1999; 7p; In English
Report No.(s): DE2000-760124; No Copyright; Avail: Department of Energy Information Bridge

The project was comprised of three main tasks: (1) develop, design, and fabricate 20 sensors; (2) develop, design, and fabricate five test instruments; and (3) testing and data analysis.
NTIS

*Fabrication; Leakage; Refrigerants; Performance Tests*

**20010119599** Texas A&M Univ., Dept. of Aerospace Engineering, College Station, TX USA
**Active Materials Characterization Laboratory** ***Final Report, 1 May 1999-28 Feb. 2001***
Lagoudas, Dimitris C.; Jan. 2001; 4p; In English
Contract(s)/Grant(s): F49620-99-1-0257
Report No.(s): AD-A394918; No Copyright; Avail: CASI; A01, Hardcopy; A01, Microfiche

The Active Materials Laboratory has recently acquired upgraded and new equipment made possible by the AFOSR in the form of a research grant as a part of the Defense University Research Instrumentation Program. These purchases have aided the laboratory in achieving its goals of improving the current testing and analysis capabilities as well as contributing to the ability of creating a Remotely Observable Active Materials (ROAM) Laboratory. The ROAM Laboratory has been established to expand the knowledge base of active materials in general through cooperative learning and education from applicable experiments. A variety of equipment has been purchased by means of the DURIP research grant including: (1) a Differential Scanning Calorimeter (DSC); (2) a tension/torsion test frame; (3) upgraded control and data acquisition capabilities of existing MTS servo-hydraulic tensile load frames; (4) widefield metallograph; (5) in-situ low force load apparatus for observation with the widefield metallograph; and (6) a quantitative metallographic analysis system. A brief description of each of the equipment listed as well as its integration into the ROAM Lab will be given in the following section.
DTIC

*Laboratory Equipment; Quantitative Analysis; Calorimeters; Metallography*

**20010119999** National Renewable Energy Lab., Golden, CO USA
**Renewable Energy Technologies for Designing and Constructing Low-Energy Commercial Buildings**
Hayter, S. J.; Jenior, M. M.; Judkoff, R.; Ketcham, M. S.; Torcellini, P. A.; Jul. 27, 1998; 10p; In English
Report No.(s): DE2001-10344; NREL/CP-550-24818; No Copyright; Avail: Department of Energy Information Bridge, Microfiche

The Thermal Test Facility (TTF) at the National Renewable Energy Laboratory (NREL) in Golden, Colorado, was designed and constructed using a whole-building energy design approach. This approach treats a building as a single unit, not as a shell containing many separate systems. It relies on the use of energy simulation tools for optimization throughout the design process, and requires the involvement and commitment of the architect, engineer, and owner. It can produce a building that requires substantially less energy than a building designed and constructed with conventional means. TTF operating costs are 63% less than those of a code-compliant basecase building. These savings were achieved by implementing an approach that optimized

passive solar technologies and integrated energy-efficient building systems. Passive solar technologies include daylighting, high-efficiency lighting systems, engineered overhangs, direct solar gains for heating, thermal mass building materials, managed glazing, and a good thermal envelope. The energy-efficient heating, ventilating, and air-conditioning (HVAC) system, designed to work with the building's passive solar technologies, includes ventilation air preheat, ceiling fans, indirect/direct evaporative cooling, and an automatic control system. This paper focuses on the design features of the TTF and the results of tests conducted on the TTF since its completion in 1996. These results demonstrate the success of the whole-building approach.
NTIS
*Design; Buildings; Energy Technology; Space Heating (Buildings); Renewable Energy; Automatic Control*

**20010120001** Sandia National Labs., Albuquerque, NM USA
**Swing-Free Cranes via Input Shaping of Operator Commands**
Groom, K. N.; Parker, G. G.; Robinett, R. D.; Leban, F.; Aug. 25, 1999; 7p; In English
Report No.(s): DE2001-10340; SAND99-2185C; No Copyright; Avail: Department of Energy Information Bridge, Microfiche
This paper presents an open-loop control method for suppressing payload oscillation or swing caused by operator commanded maneuvers in rotary boom cranes and the method is experimentally verified on a one-sixteenth scale model of a Hagglunds shipboard crane. The crane configuration consists of a payload mass that swings like a spherical pendulum on the end of a lift-line which is attached to a boom capable of hub rotation (slewing) and elevation (luffing). Positioning of the payload is accomplished through the hub and boom angles and the load-line length. Since the configuration of the crane affects the excitation and response of the payload, the swing control scheme must account for the varying geometry of the system. Adaptive forward path command filters are employed to remove components of the command signal which induce payload swing.
NTIS
*Payload Control; Cranes; Loads (Forces); Adaptive Filters*

**20010120058** NASA Ames Research Center, Moffett Field, CA USA
**Helium Dilution Cryocooler for Space Applications**
Roach, Pat, NASA Ames Research Center, USA; Feb. 26, 2001; 1p; In English; Original contains color illustrations
Contract(s)/Grant(s): RTOP 629-60-01; No Copyright; Avail: Issuing Activity; Abstract Only
NASA's New Millenium Program Space Technology presents the Helium Dilution Cryocooler for Space Applications. The topics include: 1) Capability; 2) Applications; and 3) Advantages. This paper is in viewgraph form.
CASI
*Aerospace Engineering; Cryogenic Cooling; Helium; Technology Utilization*

**20010120086** Sandia National Labs., Albuquerque, NM USA
**Robocasting and Mechanical Testing of Aqueous Silicon Nitride Slurries**
He, G. P.; Hirschfeld, D. A.; Cesarano, J.; Stuecker, J. N.; Jun. 12, 2000; 10p; In English
Report No.(s): DE2000-760781; SAND2000-1493C; No Copyright; Avail: Department of Energy Information Bridge
Aqueous slurries of silicon nitride were freeform fabricated using a novel technique termed robocasting. The process utilizes high solids loading slurries of 52%, by volume, which is within 10% of maximum consolidated density, while using no binder and less than 2%, by weight, organics in the form of polyelectrolyte dispersants. The combined effects of polyelectrolyte, pH, and solids loading were optimized to produce slurries with a shear thinning rheology suitable for the robocasting process. Through the layer-wise process, silicon nitride ceramic parts were fabricated without molds and subsequently fired to greater than 99% theoretical density. Four point bend testing yielded an average strength of 737 MPa using ASTM standard C-1161.
NTIS
*Slurries; Silicon Nitrides; Fabrication*

**20010120130** Purdue Univ., Research Foundation, West Lafayette, IN USA
**Scanning Probe Microscope** ***Final Report, 1 Apr. 1999-31 Mar. 2001***
Melloch, Michael R.; Mar. 31, 2001; 5p; In English
Contract(s)/Grant(s): F49620-99-1-0187; Proj-3484
Report No.(s): AD-A394926; AFRL-SR-BL-TR-01-0466; No Copyright; Avail: CASI; A01, Microfiche; A01, Hardcopy
This DURIP allowed us to purchase a Digital Instruments Dimension 3100 Atomic Force Microscope (AFM), which is a versatile tool that can serve dual functions, both as an AFM and a scanning-tunneling microscope (STM) . The AFM and the STM are separated units and are mounted on two different stages both of which minimize external noise and vibration. Within the purview of each of these units lie several modes of imaging. As an AFM, imaging is done in two modes namely the tapping mode

and the contact mode. These modes have the capability of resolving step heights of a few angstroms and have a be done in several ways depending upon the kind of atoms that one is imaging.
DTIC
*Imaging Techniques; Scanning Electron Microscopy; Electron Microscopes*

**20010120468** NASA Ames Research Center, Moffett Field, CA USA
**Steady Secondary Momentum and Enthalpy Streaming in the Pulse Tube Refrigerator**
Lee, J. M., NASA Ames Research Center, USA; Kittel, P., NASA Ames Research Center, USA; Timmerhaus, K. D., Colorado Univ., USA; Radebaugh, R., National Inst. of Standards and Technology, USA; [1994]; 1p; In English; International Cryocooler Conference, 28-30 Jun. 1994, Vail, CO, USA
Contract(s)/Grant(s): RTOP 233-02-05-03; No Copyright; Avail: Issuing Activity; Abstract Only

Our study investigates the steady secondary streaming that occurs in the pulse tube refrigerator through application of the conservation laws and support by flow visualization experiments. A series expansion of the mass, momentum and energy conservation laws for an axisymmetric system yields a set of linear differential equations. The series solution is expanded in the small parameter epsilon = 1/Str where Str is the Strouhal number. The O(1) basic flow problem is solved for the case of a compressible ideal gas oscillating within a cylindrical tube. The phase and amplitude of the boundary conditions on axial velocity are treated as independent parameters. The basic solution for the gas domain is solved for the case of temperature and heat flux coupling to the tube wall. The temperature coupled solution shows how the Fourier number of the tube wall affects the gas temperature, phase angle, and time-averaged enthalpy flow. The basic solution is also examined for the time-averaged Reynolds stresses which are shown to be the driving force that produces steady secondary momentum streaming. Calculated solutions to the steady momentum streaming are shown to be in qualitative agreement with flow visualization experiments.
Author
*Enthalpy; Boundary Conditions; Cylindrical Bodies; Tube Heat Exchangers; Refrigerators*

**20010120471** Stanford Univ., Stanford, CA USA
**DURIP 00 Test Equipment for a W-Band Microwave Source**
Siemann,; January 2000; 4p; In English
Contract(s)/Grant(s): F49620-00-1-0264
Report No.(s): AD-A394556; AFRL-SR-BL-TR-01-0489; No Copyright; Avail: CASI; A01, Hardcopy; A01, Microfiche

The funds from this equipment grant were used to purchase the following: one (1) Agilent Technologies Millimeter Wave Vector Network Analyzer ($130,882), assorted Millitech Inc. millimeter wave waveguide componEnts ($2,676), and assorted Newport Corp. positioning stages and optical componants ($53,254). The unexpended balance of $13,188 is being returned to the government. All of the above equipment is being directly applied to accelerate research progress on the 94 GHz 'klystrino' concept being studied under the FY99 Vacuum Electronics MURI.
DTIC
*Microwaves; Positioning; Waveguides*

**20010120496** General Accounting Office, Washington, DC USA
**National Laboratories: Better Performance Reporting Could Aid Oversight of Laboratory-Directed R and D Program. Report to Congressional Requesters**
Sep. 2001; 22p; In English
Report No.(s): AD-A395162; GAO-01-927; No Copyright; Avail: CASI; A03, Hardcopy; A01, Microfiche

In fiscal year 1992, the Department of Energy (DOE) created the Laboratory Directed Research and Development (LDRD) program, which formalized a long-standing policy of allowing its multi-program national laboratories discretion to conduct self-initiated, independent research and development (R&D). DOE requires that LDRD work must focus on the advanced study of scientific or technical problems, experiments directed toward proving a scientific principle, or early analysis of experimental facilities or devices.
DTIC
*Research Facilities; Research and Development; Laboratories*

**20010120546** Argonne National Lab., IL USA

**Equipment Design Guidelines for Remote Hot Cell Operations**

Wahlquist, D. R.; Jul. 10, 1998; 11p; In English

Report No.(s): DE2001-10686; ANL/ED/CP-95878; No Copyright; Avail: Department of Energy Information Bridge, Microfiche

Hot cells provide a unique and challenging environment for designing remotely operated equipment. A typical hot cell is an isolated room used to protect operators from highly contaminated and radioactive equipment. Hot cells usually have thick reinforced concrete walls and leaded glass windows. Operations within the hot cell are accomplished using master-slave manipulators and overhead crane or electro-mechanical manipulator systems. The inability to perform hands-on operation and maintenance in hot cells requires special design considerations. Some of these design considerations include operational interfaces, radiation, accessibility, replaceability/interchangeability, decontamination, atmospheric conditions, functionality, operator fatigue, and ease of use. This paper will discuss guidelines for designing hot cell remotely operated equipment that has been used successfully at Argonne National Laboratory. General topics in this paper will include master-slave manipulator types and limitations, overhead handling systems, viewing limitations, types and sizes of typical fasteners, hot cell compatible materials, mockup testing, guide features for mating parts, modularity, labeling, electrical fasteners, and lifting fixtures.

NTIS

*Manipulators; Design Analysis; Remote Control; Radiation Protection*

**20010120796** Argonne National Lab., IL USA

**Recovery characteristics of high damping elastomers used in seismic isolation bearings**

Kulak, R. F.; Jun. 02, 1998; 10p; In English

Report No.(s): DE2001-10821; ANL/RE/CP-96553; No Copyright; Avail: Department of Energy Information Bridge

The protection of nuclear and civil structures from the destructive effects of earthquakes has been the focus of intense research and development throughout the world. Seismic isolation is an effective means for reducing and even eliminating the devastating consequences of earthquakes on people, equipment and structures. Engineers have developed many devices for implementing the seismic isolation strategy and the most effective and economical ones have been identified through the test of time. One of these devices is the laminated elastomeric isolation bearing. The behavior of high damping elastomer bearings during several recent earthquakes has shown that they are a viable device for mitigating the effects of earthquakes. In this paper, results are presented from recent tests on two different elastomers. The first is a highly filled, high modulus, high damping elastomer and the second is a highly-filled, low modulus, high damping elastomer. The stiffness recovery characteristics of the high modulus elastomer subjected to beyond design basis strains and the results of seven years of aging on the low modulus elastomer are presented.

NTIS

*Earthquakes; Elastomers; Isolation; Nuclear Structure*

**20010121499** Sandia National Labs., Albuquerque, NM USA

**Simulations of a Furnace Brazing Process Using Tera-Scale Computing**

Hosking, F. M.; Gianoulakis, S. E.; Aug. 14, 2000; 8p; In English

Report No.(s): DE2000-760768; SAND2000-0840C; No Copyright; Avail: Department of Energy Information Bridge, Microfiche

Thermal responses in a production brazing furnace can be very difficult to predict or measure due to changing loading and heating conditions. An efficient approach to determining acceptable furnace brazing cycles is to apply computational models that can solve these potentially complex thermal problems. Recent developments in massively parallel computing have facilitated finer-scale temporal and spatial thermal analyses. Sandia National Laboratories has conducted terascale simulations to thermally characterize a production brazing process. The model accounts for thermal radiation and conduction as the principal heat transfer drivers in the batch-style hydrogen furnace. Computed peak temperatures are within one to two percent of the programmed and measured values. Thermal responses in the work zone are particularly sensitive to the thermal enclosure, defined by the furnace's heating elements. A two percent change in the radiation enclosure can yield up to an eight percent change in the peak brazing temperature. Computational data are less sensitive to differences in the inputted materials thermal properties than changes to the thermal enclosure. Examples of how the thermal model can be used to determine optimal loading and heating conditions for production brazing are discussed.

NTIS

*Brazing; Furnaces; Mathematical Models; Thermal Analysis*

**20010121508** Sandia National Labs., Albuquerque, NM USA

**Summary of Thermal Testing of the Furnace Characterization Unit (FCU) for the Coast Guard** ***Final Report***

Nakos, J. T.; Pantuso, J. G.; Bentz, J. H.; Jun. 01, 2000; 162p; In English

Report No.(s): DE2000-759456; SAND2000-1534; No Copyright; Avail: Department of Energy Information Bridge, Microfiche

This report summarizes the results of a series of calibration experiments performed on The Furnace Characterization Unit (FCU). The FCU was developed for the Coast Guard by Hughes and Associates and Ktech Corp. This device will be used to characterize furnaces used to determine the thermal response of marine bulkheads in fires. Hughes/Ktech contracted with Sandia National Laboratories to provide the thermal environment required to simulate afire. A series of eight (8) experiments (3 'check tests' and 5 calibration tests) using two different temperature environments - a 'stair step' profile and a logarithmic profile were performed. Results of the Sandia installed instrumentation is presented. Data from the FCU instrumentation installed by Ktech is presented in a separate report due to its large volume. An uncertainty analysis of the Sandia thermocouple measurements is provided.

NTIS

*Furnaces; Thermal Environments; Defense Program; High Temperature Tests*

**20010122661** National Renewable Energy Lab., Golden, CO USA

**Impact of Vehicle Air-Conditioning on Fuel Economy, Tailpipe Emissions, and Electric Vehicle Range: Preprint**

Farrington, R.; Rugh, J.; Sep. 22, 2000; 12p; In English

Report No.(s): DE2000-764573; NREL/CP-540-28960; No Copyright; Avail: Department of Energy Information Bridge, Microfiche

Vehicle air-conditioning can significantly impact fuel economy and tailpipe emissions of conventional and hybrid electric vehicles and reduce electric vehicle range. In addition, a new US emissions procedure, called the Supplemental Federal Test Procedure, has provided the motivation for reducing the size of vehicle air-conditioning systems in the US. The SFTP will measure tailpipe emissions with the air-conditioning system operating. Current air-conditioning systems can reduce the fuel economy of high fuel-economy vehicles by about 50% and reduce the fuel economy of today's mid-sized vehicles by more than 20% while increasing NOx by nearly 80% and CO by 70%.

NTIS

*Air Conditioning; Air Conditioning Equipment; Electric Motor Vehicles*

**20010122824** Stanford Linear Accelerator Center, Menlo Park, CA USA

**Calculations on Cylindrical Metal Vacuum Chambers in Pulsed Magnetic Fields**

Oct. 08, 1964; 9p; In English

Report No.(s): DE2000-763863; SLAC-TN-63-46; No Copyright; Avail: Department of Energy Information Bridge

It has been suggested that metallic vacuum chambers might be suitable for pulsed magnets operating at audio frequencies, with pulse widths nominally 1/360 sec. In the present note calculations are given for a simple model of such a system, in order to estimate the effects of field attenuation and eddy current losses. The results of the calculation may be summarized briefly as follows, where the results apply to a cylindrical chamber of non-maeyletic stainless steel, 3.0 cm in inside diameter and 0.15 in wall thickness: (1) With steady-state harmonic excitation, the field in the interior is reduced by a factor of (approximately) 1.03 at 2,000 cps compared to dc; (2) With transient operation, the exponential decay time is about 0.021 millisecond; (3) With square-wave excitation, at 200 gauss and 180 pps, the power dissipation in the stainless steel is about 24 watts/foot, or about a factor of 20 less if half-sine-wave pulses are used instead of square pulses. These results seem encouraging enough to warrant experimental investigation of this type of vacuum chamber for pulsed steering.

NTIS

*Vacuum Systems; Magnetic Fields; Cylindrical Chambers; Vacuum Chambers*

**20010123096** National Renewable Energy Lab., Golden, CO USA

**New Building Approach Saves Energy and Cost: Building America Project Summary Fact Sheet**

Hendron, B.; Oct. 26, 2000; 2p; In English

Report No.(s): DE2000-767307; NREL/FS-550-28476; No Copyright; Avail: Department of Energy Information Bridge

Houses built by Pulte Homes as part of the U.S. Department of Energy's Building America program in Tucson, Arizona, save money for the home owners by reducing electric air-conditioning costs and gas-heating costs with little or no additional investment.

NTIS

*Energy Conservation; Residential Energy*

**20010123437** Vortec Corp., Collegeville, PA USA
**Method for producing glass fiber** ***Quarterly Report, Apr. - Jun. 1999***
Simpson, J. C.; Jul. 01, 1999; 26p; In English
Report No.(s): DE2001-763175; VOR98/QTR/63200; DOE/GO/10319-Q; No Copyright; Avail: Department of Energy Information Bridge, Microfiche

The following technical progress report summarizes the work performed over the period of April 1999 to June 1999 on the project 'Method for Producing Glass Fiber.' The following sections review the progress made on the individual tasks. The final section describes the work planned for the next quarter, July 1999 to September 1999.
NTIS
*Production Engineering; Glass Fibers*

**20010123446** Virginia Polytechnic Inst. and State Univ., Blacksburg, VA USA
**Final Technical Status Report as of January 2000 (Virginia Polytechnic Institute and State University)**
Jan. 12, 2000; 22p; In English
Report No.(s): DE2001-761027; No Copyright; Avail: Department of Energy Information Bridge, Microfiche

This project was completed in January 1996 after a panel of four Licensing Executive Society members met in Boston (December 1995) to discuss the requirements for, incentive of and barriers to licensing horn independent inventors and small businesses. Three team members from Mohawk Research Corporation reviewed and analyzed the discussion notes to reach a series of recommendations which are contained in a report which was submitted in February under separate cover. This completes this project.
NTIS
*Licensing; Commerce*

**20010125015** Lawrence Livermore National Lab., Livermore, CA USA
**Determination of blowout pressures during electron beam welding**
Sunwoo, A.; Apr. 01, 1999; 7p; In English
Report No.(s): DE2001-11328; UCRL-JC-133546; No Copyright; Avail: Department of Energy Information Bridge

During electron beam (EB) welding of developmental units, weld blowouts occurred. It is well documented that the presence of moisture causes the weld blowout. The detrimental effects of water vapor on the weld are experimentally proven. The availability of water vapor in the melt increases the onset and severity of blowout and porosity. Because water vapor is insoluble in the molten metal, it will consequently form either bubbles or boil. On the other hand, hydrogen will react with other impurities present in the melt to form insoluble gas bubbles, which most likely will be entrapped in the fusion zone as porosity. This study attempts to answer the question of what is the critical weld blowout pressure, and to compare the experimental results to the estimated pressure values, so that validated calculations could be extended to other weld configurations.
NTIS
*Electron Beam Welding; Blowouts*

**20010125113** Budapest Univ. of Technology and Economics, Budapest, Hungary
**Periodica Polytechnica Electrical Engineering, Volume 43, No. 4, 1999** ***Annual Report***
Selenyi, E.; 1999; 86p; In English
Report No.(s): PB2001-107357; No Copyright; Avail: CASI; A05, Hardcopy; A01, Microfiche

This document includes information on the following topics: Intelligent Stereo Vision System; Improved Stratified Control for Hexapod Robots and Object Manipulation with Finger Relocation; Genetic Algorithms-Based Fuzzy Logic Systems for Dynamic Modeling of Robots; Design and Evaluation Environment for Collision-free Motion Planning of Cooperating Redundant Robots; Object Manipulation with Dextrous Robotic Hand Using Simulated Annealing; Stable Object Grasping with Dextrous Hand in Three-Dimension; and Modeling, Flatness and Simulation of a Class of Cranes.
NTIS
*Mechanical Engineering; Electrical Engineering*

**20010125114** Budapest Univ. of Technology and Economics, Budapest, Hungary
**Periodica Polytechnica Mechanical Engineering, Volume 43, No. 2, 1999** ***Annual Report***
Radonyi, L.; 1999; 170p; In English
Report No.(s): PB2001-107353; No Copyright; Avail: CASI; A08, Hardcopy; A02, Microfiche

Partial Contents: Robot Motion Realization using LabVIEW; Geometrical Errors of Parallel Robots; New PC (personal computer) and Labview Based Robot Control System; and Constant Kinetic Energy Robot Trajectory Planning.
NTIS
*Robots; Mechanical Engineering; Hungary*

**20010125171** California Univ., Lawrence Berkeley Lab., Berkeley, CA USA
**Advanced Lighting Program Development** ***Final Report***
Rubinstein, F.; Johnson, S.; Feb. 01, 1998; 30p; In English
Report No.(s): DE2000-765125; LBNL-41679; No Copyright; Avail: Department of Energy Information Bridge

The report presents a long-range plan for a broad-based, coordinated research, development and market transformation program for reducing the lighting energy intensities in commercial and residential buildings in California without compromising lighting quality. An effective program to advance lighting energy efficiency in California must be based on an understanding that lighting is a mature field and the lighting industry has developed many specialized products that meet a wide variety of light needs for different building types. Above all else, the lighting field is diverse and there are applications for a wide range of lighting products, systems, and strategies. Given the range of existing lighting solutions, an effective energy efficient lighting research portfolio must be broad-based and diverse to match the diversity of the lighting market itself. The belief that there is one solution--a magic bullet, such as a better lamp, for example-that will propel lighting efficiency across all uses to new heights is, in the authors; opinion, an illusion. A multi-path program is the only effective means to raising lighting efficiency across all lighting applications in all building types. This report presents a list of 27 lighting technologies and concepts (key activities) that could form the basis of a coordinated research and market transformation plan for significantly reducing lighting energy intensities in California buildings. The total 27 key activities into seven broad classes as follows: Light sources; Ballasts; Luminaires; Lighting Controls; Lighting Systems in Buildings; Human Factors and Education. Each of the above technology classes is discussed in terms of background, key activities, and the energy savings potential for the state. The report concludes that there are many possibilities for targeted research, development, and market transformation activities across all sectors of the building lighting industry. A concerted investment by the state to foster efficiency improvements in lighting systems in commercial and residential buildings would have a major positive impact on energy use and environmental quality in California.
NTIS
*Illuminating; California; Energy Conservation*

**20010125237** Oak Ridge National Lab., TN USA
**Multilayer Thermionic Refrigeration**
Mahan, G. D.; Aug. 30, 1999; 6p; In English
Report No.(s): DE2001-11470; ORNL/CP-104507; No Copyright; Avail: Department of Energy Information Bridge

A review is presented of our program to construct an efficient solid state refrigerator based on thermionic emission of electrons over periodic barriers in the solid. The experimental program is to construct a simple device with one barrier layer using a three layers: metal-semiconductor-metal. The theoretical program is doing calculations to determine: (1) the optimal layer thickness, and (2) the thermal conductivity.
NTIS
*Refrigerators; Solid State; Thermionic Emission; Electrons*

**20010125519** Rocky Research Corp., Boulder City, NV USA
**Final Report: Absorption Chiller Corrosion Protection, September 1, 1999-March 31, 1999**
Chandler, T.; Mar. 31, 1999; 41p; In English
Report No.(s): DE2001-765178; No Copyright; Avail: Department of Energy Information Bridge

Corrosion control methods are needed by chiller manufacturers for the introduction of new designs of high-efficiency triple-effect and direct-fired double-effect LiBr machines using high temperature stages. For lithium bromide systems corrosion inhibitors are lacking what adequately protect mild steels, while use of exotic alloys is cost-prohibitive. The purpose of the research effort is to identify cost-effective materials to be used in combination with new inhibitors to control corrosion in high-efficiency triple-effect absorption chillers.
NTIS
*Absorption Cooling; Corrosion Prevention; Steels; Cooling*

## 32
## COMMUNICATIONS AND RADAR

*Includes radar; radio, wire, and optical communications; land and global communications; communications theory. For related information see also 04 Aircraft Communications and Navigation; and 17 Space Communications, Spacecraft Communications, Command and Tracking; for search and rescue see 03 Air Transportation and Safety, and 16 Space Transportation and Safety.*

**20010117853** Los Alamos National Lab., NM USA

**Application of Electrical and Calorimetric Methods to the A.C. Loss Characterization of Cable Conductors**

Coletta, C.; Gherardi, L.; Gomory, F.; Cereda, E.; Ottoboni, V.; Sep. 13, 1998; 7p; In English

Report No.(s): DE2000-760125; LA-UR-98-4108; No Copyright; Avail: Department of Energy Information Bridge

Due to the higher currents (and therefore higher losses) compared to individual wires and tapes, the ac loss characterization of HTS cable conductors carrying transport current can be performed using calorimetric as well as electrical methods. We discuss the main features of two calorimetric methods, one based on temperature profile determination, and one, more recently developed, based on nitrogen boil-off rate, and of the electrical method, substantially derived from that already established for tapes, based on voltage measurement by a Lock-In amplifier. Advantages and limits of each approach are analyzed and compared. Tests have been carried out with the three methods on samples 1 to 1.5 m long cut from a Bi-2223 cable conductor prototype fabricated by Pirelli in a longer length. Results obtained from measurements covering a wide range of currents are compared and thoroughly discussed.

NTIS

*Heat Measurement; Conductors; Losses; Temperature Profiles*

**20010118507** Norwegian Defence Research Establishment, Kjeller, Norway

**Digital Calibration of Radar Measurements with Unsynchronized Transmitter and Receiver** ***Digitalt Kalibrerte Radarmalinger Med Usynkronisert Sender og Mottaker***

Olsen, Karl Erik, Norwegian Defence Research Establishment, Norway; Johnsrud, Steiner, Norwegian Defence Research Establishment, Norway; Oct. 02, 2001; 50p; In Norwegian; Original contains color illustrations

Contract(s)/Grant(s): FFIE Proj. 726/170

Report No.(s): FFI/RAPPORT-2001/04614; ISBN 82-464-0545-4; No Copyright; Avail: CASI; A03, Hardcopy; A01, Microfiche

The report describes a signal processing algorithm used on radar data collected from a unsynchronized radar system. The algorithm makes corrections for the missing synchronization between transmitter and receiver, and has the capability to separate targets in range and velocity. Results from collected radar data are presented.

Author

*Signal Processing; Algorithms; Correction; Radar Data*

**20010119232** Army Command and General Staff Coll., Fort Leavenworth, KS USA

**Command and Control Systems: Outlooks for a Digitized Future**

McCaffery, Michael R.; Jun. 01, 2001; 289p; In English

Report No.(s): AD-A395081; No Copyright; Avail: CASI; A13, Hardcopy; A03, Microfiche

This thesis is designed to do two things. First, this study examines the evolution of command and control (C2) systems through history. Second, this study examines the Army's current Force XXI digitization initiative. The first part develops the research areas; the second applies them to Force XXI. History reveals that C2 systems evolve when three areas are evolved holistically: organizations, procedures, and communications. The subject areas are the basis for a comparison of Force XXI with commercial and academic trends where increased information technology (IT) is involved. In the first subject area: organizations, commercial firms have adapted to leverage technology by moving from hierarchies to flat and networked organizational structures Force XXI proposes a 'flattened organization to achieve efficiencies through information technology. In procedures, the Army and commercial organizations face similar challenges: micromanagement and information overload. In the Army, most C2 procedures stem from the Military Decision-Making Process. Commerce uses similar procedures to address the two challenges and achieve greater effectiveness. In communications, commercial firms insist on interoperability, flexibility, upgrade-ability, and portability. Commonly used technologies such as the Internet and Microsoft Windows/Office usually drive the baseline of compatibility. Force XXI implements a number of systems which perform similar functions.

DTIC

*Command and Control; Digital Techniques; Information Systems; Armed Forces (USA)*

**20010119433** Oak Ridge National Lab., TN USA

**Cryogenic System for a High Temperature Superconducting Power Transmission Cable**

Demko, J. A.; Gouge, M. J.; Hughey, R. L.; Lue, J. W.; Martin, R.; Jul. 12, 1999; 9p; In English

Report No.(s): DE2000-15058; ORNL/CP-105072; No Copyright; Avail: Department of Energy Information Bridge, Microfiche

High-temperature superconducting (HTS) cable systems for power transmission are under development that will use pressurized liquid nitrogen to provide cooling of the cable and termination hardware. Southwire Company and Oak Ridge National Laboratory have been operating a prototype HTS cable system that contains many of the typical components needed for a commercial power transmission application. It is being used to conduct research in the development of components and systems for eventual commercial deployment. The cryogenic system was built by Air Products and Chemicals, Allentown, Pennsylvania, and can circulate up to 0.35 kg/s of liquid nitrogen at temperatures as low as 67 K at pressures of 1 to 10 bars. Sufficient cooling is provided for testing a 5 m-long HTS transmission cable system that includes the terminations required for room temperature electrical connections. Testing of the 5 m HTS transmission cable has been conducted at the design conditions of 1250 A and 7.5 kV line to ground. This paper contains a description of the essential features of the HTS cable cryogenic system and performance results obtained during operation of the system. The salient features of the operation that are important in large commercial HTS cable applications will be discussed.

NTIS

*Cryogenics; High Temperature Superconductors; Superconducting Power Transmission*

**20010119616** Air Force Research Lab., Human Effectiveness Directorate, Wright-Patterson AFB, OH USA

**The Intelligibility of Multiple Talkers Separated Spatially in Noise** ***Final Report, Dec. 1987-Sep. 1993***

Ericson, Mark A.; McKinley, Richard L.; May 2001; 28p; In English

Contract(s)/Grant(s): Proj-7231

Report No.(s): AD-A395035; AFRL-HE-WP-SR-2001-0009; No Copyright; Avail: CASI; A03, Hardcopy; A01, Microfiche

Speech communication are seldom isolated auditory events in quiet environments. Frequently, the desired speech signal is confounded with other speech signals and noises. Real-world environments often degrade the intelligibility of the desired speech signal. In this book chapter (Binaural and Spatial Hearing in Real and Virtual Environments, Lawrence Erlbaum Associates, Mahwah NJ, publishers, 1997), the literature on the speech intelligibility of competing messages and the masking of speech is reviewed. The literature on the detection of speech is included to describe factors that can affect speech intelligibility. Following the review, several experiments are presented in which the effects of various conflicting signals on speech communications are measured. Virtual audio over headphones is used to investigate the effects of directional separation of talkers, the quantity and gender of talkers, the degree of masker interaural correlation, masking level, and selective attention. The results are discussed and compared with the previous literature.

DTIC

*Binaural Hearing; Intelligibility; Talking; Noise (Sound)*

**20010120043** NASA Goddard Space Flight Center, Greenbelt, MD USA

**Automatic Weather Station (AWS) Lidar**

Rall, Jonathan A. R., NASA Goddard Space Flight Center, USA; Campbell, James, NASA Goddard Space Flight Center, USA; Abshire, James B., NASA Goddard Space Flight Center, USA; Spinhirne, James D., NASA Goddard Space Flight Center, USA; [2001]; 3p; In English; International Geoscience and Remote Sensing Symposium, 9-13 Jul. 2001, Sydney, Australia; No Copyright; Avail: CASI; A01, Hardcopy; A01, Microfiche

A ground based, autonomous, low power atmospheric lidar instrument is being developed at NASA Goddard Space Flight Center. We report on the design and anticipated performance of the proposed instrument and show data from two prototype lidar instruments previously deployed to Antarctica.

Author

*Automatic Weather Stations; Optical Radar; Prototypes; Deployment*

**20010120124** Naval Research Lab., Washington, DC USA

**Ultra-Near Field Facility for RCS Research**

Medgyesi-Mitschang, L. N.; Moore, P. G.; Smith, D. L.; Lambrakos, S. G.; Aug. 31, 2001; 104p; In English

Report No.(s): AD-A394988; NRL/MR/5050--01-8565; No Copyright; Avail: CASI; A06, Hardcopy; A02, Microfiche

This investigation demonstrated, experimentally and theoretically, the application of near field and ultra-near field techniques in the microwave region to characterize the scattering and radiation phenomena near targets and in the reactive region of antenna. The Ultra-Near Field Facility research facility was designed and built at NRL for this purpose. Requisite sensors and associated

processing software for measuring the ultra-near fields from bistatically illuminated targets as well as antenna systems were developed and tested. The present phase of the program focused principally on the investigation of the ultra-near field scattering from planar structures. Important features of EM phenomena associated with ship stacks/masts can be analyzed by studying the scattering from classes of planar structures. This motivated the present approach. to gain deeper insight into the scattering mechanisms and to characterize the fields in the proximity of such surfaces, extensive computer simulations were also carried out. In the modeling, it was assumed that the surfaces were two dimensional (2-D) permitting the effect of vertical and horizontal polarization to be studied independently. The numerical simulations were based on a method of moments formulation for bodies of translation (BOTs). These constitute a general class of 2-D surfaces. They are extensively treated in the literature and thus provide a robust departure point for this effort. The propagated and evanescent fields in the proximity of these surfaces were delineated using frequency wave-vector (Omega-Kappa) transformations of the calculated and measured fields. The effect of surface discontinuities on the propagating and evanescent field structure was examined. Preliminary investigations were also carried out for selected finite quasi-periodic arrays and models provided by NSWCCD.
DTIC
*Electromagnetic Radiation; Radar Cross Sections; Computerized Simulation; Experimentation; Near Fields; Microwave Frequencies; Scattering*

**20010120147** Air War Coll., Maxwell AFB, AL USA
**Military Dependence on Commercial Satellite Communications Systems -Strength or Vulnerability**
Hook, Jack A., Jr.; Apr. 1999; 58p; In English
Report No.(s): AD-A395141; AU/AWC/128/1999-04; No Copyright; Avail: CASI; A04, Hardcopy; A01, Microfiche
The military's growing dependence on commercial satellite communications systems will become a strength or vulnerability based on how well the right balance is achieved between commercial and military systems. Determining that balance is a function of clearly understanding both DoD's requirements and the vulnerabilities and risks associated with the use of, and dependence on, commercial systems.
DTIC
*Vulnerability; Satellite Communication; Military Operations; Telecommunication*

**20010120840** Naval Air Warfare Center, Weapons Div., China Lake, CA USA
**Radar Scattering Center Localization by Subspace Fitting** ***Interim Report, Oct. 1999-Apr. 2001***
Borden, Brett; Aug. 2001; 19p; In English
Contract(s)/Grant(s): N00014-01-WR-20168; N00014-00-WR-20063
Report No.(s): AD-A395293; NAWCWPNS-TP-8502; No Copyright; Avail: CASI; A03, Hardcopy; A01, Microfiche
The application of radar data to the problem of noncooperative target recognition (NCTR) usually begins by estimating the position and strength of the significant scattering centers from the bright spot locations of a radar image (e.g., high range resolution (HRR) or inverse synthetic aperture radar (ISAR)). In practical situations, these images are usually contaminated by noise and can be of very low quality resolution-factors that confound the scattering center localization process and can preclude NCTR by radar means. We describe a simple method, based on subspace fitting techniques, that can be applied to the position and strength estimation problem in this environment. The scheme is robust against noise corruption and allows for super-resolved estimates of all (or some) of the scatterers. Examples based on synthetic data are presented.
DTIC
*Synthetic Aperture Radar; Radar Data; Radar Scattering; Target Recognition*

**20010121948** Sandia National Labs., Albuquerque, NM USA
**Using Vector Spherical Harmonics to Compute Antenna Mutual Impedance from Measured or Computed Fields**
Brock,; Sep. 06, 2000; 67p; In English
Report No.(s): DE2000-763320; SAND2000-2217; No Copyright; Avail: Department of Energy Information Bridge, Microfiche
The mutual impedance is described in terms of a physical observable called the reaction, introduced by Rumsey. The reaction theorem is related to the reciprocity theorem derived by Lorentz, and an understanding of the reciprocity theorem is helpful for understanding the reaction concept. In the following, the Lorentz reciprocity theorem is derived and examined in some detail. In order to understand better the generality and applicability of the theorem, it is derived in a very general form. The medium in which the elements are embedded is assumed linear and time-invariant, but not homogeneous or even isotropic. The validity of the theorem does place constraints on the medium, and these constraints will be stated. After the discussion of the reciprocity theorem, an expression for the mutual impedance in terms of the reaction quantity is written. The reaction is a term contained in the mathematical statement of the reciprocity theorem, and thus the discussion of the reciprocity theorem is very relevant to

understanding the mutual impedance. Once the expression for mutual impedance is written, the fields can be expanded in vector spherical harmonics, and the mutual impedance is ultimately written in terms of the expansion coefficients. This process is somewhat tedious and is described in detail. Although the final result may appear unwieldy, it is straightforward to program a computer to perform the computation. The first advantage, of course, is the avoidance of the need to integrate a wildly oscillating integrand that is slow to converge. The second advantage is that mutual impedance can be computed for many sets of element positions, using a single measurement or computation of the fields around an element.
NTIS
*Impedance; Reciprocity Theorem; Spherical Harmonics*

**20010121959** California Univ., Lawrence Berkeley Lab., Berkeley, CA USA
**Experiences with TCP/IP over an ATM OC12 WAN**
Nitzan, R. L.; Tierney, B. L.; Dec. 23, 1999; 12p; In English
Report No.(s): DE2000-764365; LBNL-44765; No Copyright; Avail: Department of Energy Information Bridge, Microfiche

This paper discusses the performance testing experiences of a 622.08 Mbps OC12 link. The link will be used for large bulk data transfer, and as such, of interest are both the ATM level throughput rates and end-to-end TCP/IP throughput rates. Tests were done to evaluate the ATM switches, the IP routers, the end hosts, as well as the underlying ATM service provided by the carrier. A low level of cell loss, (resulting in less than .01% packet loss), decreased the TCP throughput rate considerably when one TCP flow was trying to use the entire OC12 bandwidth. Identifying and correcting cell loss in the network proved to be extremely difficult. TCP Selective Acknowledgement (SACK) improved performance dramatically, and the maximum throughput rate increased from 300 Mbps to 400 Mbps. The effects of TCP slow start on performance at OC12 rates are also examined, and found to be insignificant for very large file transfers (e.g., for a 10 GB file). Finally, a history of TCP performance over high-speed networks is presented.
NTIS
*Performance Tests; Computer Systems Performance; Data Transmission*

**20010122310** Sandia National Labs., Albuquerque, NM USA
**Miniature, High-Resolution Laser Radar Operating at Video Rates**
Smithpeter,; Nellums,; Lebien,; Studor,; Jun. 26, 2000; 10p; In English
Report No.(s): DE2000-761044; SAND2000-1548C; No Copyright; Avail: Department of Energy Information Bridge

The authors are developing a laser radar to meet the needs of NASA for a 5-lb, 150 cubic inch image sensor with a pixel range accuracy of 0.1-inch. NASA applications include structural dynamics measurements, navigation guidance in rendezvous and proximity operations, and space vehicle inspection. The sensor is based on the scannerless range imager architecture developed at Sandia. This architecture modulates laser floodlight illumination and a focal plane receiver to phase encode the laser time of flight (TOF) for each pixel. They believe this approach has significant advantages over architectures directly measuring TOF including high data rate, reduced detector bandwidth, and conventional FPA detection. A limitation of the phase detection technique is its periodic nature, which provides relative range information over a finite ambiguity interval. To extend the operating interval while maintaining a given range resolution, a LADAR sensor using dual modulation frequencies has been developed. This sensor also extends the relative range information to absolute range by calibrating a gating function on the receiver to the TOF. The modulation frequency values can be scaled to meet the resolution and range interval requirements of different applications. Results from the miniature NASA sensor illustrate the advantages of the dual-frequency operation and the ability to provide the range images of 640 by 480 pixels at 30 frames per second.
NTIS
*Lasers; Optical Radar; Laser Beams; Design Analysis*

**20010122392** Academy of Sciences (Russia), Inst. for Laser Physics, Saint Petersburg, Russia
**Generation of High Power Microwave Radiation with the Aid of High Explosive** ***Final Report***
Mintsev, V., Academy of Sciences (Russia), Russia; January 1995; 95p; In Russian
Contract(s)/Grant(s): F61708-94-W-0777
Report No.(s): AD-A394997; SPC-94-4101; No Copyright; Avail: CASI; A05, Hardcopy; A01, Microfiche

The present paper looks into the Magnetic Flux Compressors (MFC) from the point of view of their integration with high power microwave sources. First of all the typical constructions and principals of there operations will be considered. After that

the possibilities of production of video impulse will be discussed and MFC as a pulsed power system for feeding relativistic microwave generators will be described.
DTIC
*Microwave Equipment; Compressors; Magnetic Flux*

**20010122393** Academy of Sciences (Russia), Inst. for Laser Physics, Saint Petersburg, Russia
**Magnetic Flux Compressors with Flux Trapping** ***Final Report***
Mintsev, V., Academy of Sciences (Russia), Russia; January 1995; 40p; In English
Contract(s)/Grant(s): F61708-94-W-0777
Report No.(s): AD-A394996; SPC-94-4101; No Copyright; Avail: CASI; A03, Hardcopy; A01, Microfiche

The present paper looks into the Magnetic Flux Compressors (MFC) from the point of view of their integration with high power microwave sources. First of all the typical constructions and principals of there operations will be considered. After that the possibilities of production of video impulse will be discussed and MFC as a pulsed power system for feeding relativistic microwave generators will be described.
DTIC
*Microwave Equipment; Compressors; Magnetic Flux*

**20010122664** California Univ., Lawrence Berkeley Lab., Berkeley, CA USA
**Network-Aware Distributed Storage Cache for Data Intensive Environments**
Tierney, B. L.; Lee, J. R.; Johnston, W. E.; Crowley, B.; Holding, M.; Dec. 23, 1999; 9p; In English
Report No.(s): DE2000-764335; LBNL-42896; No Copyright; Avail: Department of Energy Information Bridge, Microfiche

Modern scientific computing involves organizing, moving, visualizing, and analyzing massive amounts of data at multiple sites around the world. The technologies, the middleware services, and the architectures that are used to build useful high-speed, wide area distributed systems, constitute the field of data intensive computing. In this paper the authors describe an architecture for data intensive applications where they use a high-speed distributed data cache as a common element for all of the sources and sinks of data. This cache-based approach provides standard interfaces to a large, application-oriented, distributed, on-line, transient storage system. They describe their implementation of this cache, how they have made it network aware, and how they do dynamic load balancing based on the current network conditions. They also show large increases in application throughput by access to knowledge of the network conditions.
NTIS
*Architecture (Computers); Data Transmission; On-Line Systems*

**20010122665** California Univ., Lawrence Berkeley Lab., Berkeley, CA USA
**NetLogger Methodology for High Performance Distributed Systems Performance Analysis**
Tierney, B.; Johnston, W.; Crowley, B.; Hoo, G.; Brooks, C.; Dec. 23, 1999; 8p; In English
Report No.(s): DE2000-764331; LBNL-42611; No Copyright; Avail: Department of Energy Information Bridge, Microfiche

The authors describe a methodology that enables the real-time diagnosis of performance problems in complex high-performance distributed systems. The methodology includes tools for generating precision event logs that can be used to provide detailed end-to-end application and system level monitoring; a Java agent-based system for managing the large amount of logging data; and tools for visualizing the log data and real-time state of the distributed system. The authors developed these tools for analyzing a high-performance distributed system centered around the transfer of large amounts of data at high speeds from a distributed storage server to a remote visualization client. However, this methodology should be generally applicable to any distributed system. This methodology, called NetLogger, has proven invaluable for diagnosing problems in networks and in distributed systems code. This approach is novel in that it combines network, host, and application-level monitoring, providing a complete view of the entire system.
NTIS
*End-to-End Data Systems; Data Base Management Systems; Diagnosis; Reliability Analysis*

**20010122797** Argonne National Lab., IL USA
**AC losses in Bi-2223 tapes and in the 1-kA transmission line model**
Fisher, L. M.; Sep. 04, 1998; 6p; In English
Report No.(s): DE2001-10707; ANL/ET/CP-96000; No Copyright; Avail: Department of Energy Information Bridge, Microfiche

We present here results of our study of the 5-m-long AC transmission tine model with 1 kA current capability at 77 K. Primary attention was paid to the current characteristics and AC losses in individual tapes and in the core of the cable. The losses were

measured as a function of AC magnetic field amplitude in various orientations of magnetic field with respect to the plane of the tape and filaments. Hysteresis losses were. close to the losses in the AC regime, meaning that eddy current losses in tapes may be neglected when compared with hysteresis losses. We designed and constructed a 5-m-long model of the AC transmission line using multi filamentary Bi-2223 tapes. The current core of the model contains 120 tapes for the forward line and 120 tapes for the backward line. The AC losses in the current core were substantially greater than those seen in the individual tapes. The reason for this is related to a complex magnetic field distribution inside the current core.
NTIS
*Transmission Lines; Magnetic Field Configurations; Alternating Current*

**20010123060** North Carolina Univ., Charlotte, NC USA
**A Novel Principle for Data Processing from Hand-Held Ground Penetrating Radars** ***Final Report, 1 Jul. 1998-30 Jun. 2001***
Klibanov, Michael V.; Lucas, Thomas R.; Jun. 26, 2001; 35p; In English
Contract(s)/Grant(s): DAAG55-98-1-0401
Report No.(s): AD-A395289; ARO-38897.8-C1-LMD; No Copyright; Avail: CASI; A03, Hardcopy; A01, Microfiche
The goal of this project was to develop a new algorithm of inverse problems to image locations and electrical properties of land mines using GPR data. These parameters, in turn, might be used on a next stage as an input for the classification procedure. Such a method has been developed and tested on models. Accurate images of mine-like targets are demonstrated. Comparison with the best competing algorithm in the field favors the algorithm of this project. The main innovation, as compared with conventional algorithms is the differential rather than conventional integral form of the resulting system. This enables one to obtain solutions in a much shorter time, as compared with the conventional techniques.
DTIC
*Electrical Properties; Classifications; Algorithms*

**20010123443** Wisconsin Univ., Madison, WI USA
**Collaboration on Modeling of Ion Bernstein Wave Antenna Array and Coupling to Plasma on Tokamak Fusion Text Reactor** ***Final Report***
Intrator, T.; Jun. 01, 2000; 8p; In English
Report No.(s): DE2001-761048; No Copyright; Avail: Department of Energy Information Bridge, Microfiche
This proposal was peer reviewed and funded as a Collaboration on ”Low Phase Speed Radio Frequency Current Drive Experiments at the Tokamak Fusion Test Reactor” The original plans we had were to carry out the collaboration proposal by including a post doctoral scientist stationed at PPPL. In response to a 60+% funding cut, all expenses were radically pruned. The post doctoral position was eliminated, and the Principal Investigator (T. Intrator) carried out the brunt of the collaboration. Visits to TFTR enabled T. Intrator to set up access to the TFTR computing network, database, and get familiar with the new antennas that were being installed in TFTR during an up to air. One unfortunate result of the budget squeeze that TFTR felt for its last year of operation was that the experiments that we specifically got funded to perform were not granted run time on TFTR., On the other hand we carried out some modeling of the electric field structure around the four strap direct launch Ion Bernstein Wave (IBW) antenna that was operated on TFTR. This turned out to be a useful exercise and shed some light on the operational characteristics of the IBW antenna and its coupling to the plasma. Because of this turn of events, the project was renamed ’Modeling of Ion Bernstein Wave Antenna Array and Coupling to Plasma on Tokamak Fusion Test Reactor’.
NTIS
*Antenna Arrays; Tokamak Devices; Plasma Control; Fusion Reactors*

**20010123912** Los Alamos National Lab., NM USA
**Scheduling with Global Information in Distributed Systems**
Petrini, F.; Feng, W.; Feb. 01, 2000; 7p; In English
Report No.(s): DE2001-763364; LA-UR-00-894; No Copyright; Avail: Department of Energy Information Bridge
Buffered coscheduling is a distributed scheduling methodology for time-sharing communicating processes in a distributed system, e.g., PC (personal computer) clusters. The principle mechanisms involved in this methodology are communication buffering and strobing. With communication buffering, communication generated by each processor is buffered and performed at the end of regular intervals (or time slices) to amortize communication and scheduling overhead. This regular communication structure is then leveraged by introducing a strobing mechanism which performs a total exchange of information at the end of each time slice. Thus, a distributed system can rely on this global information to more efficiently schedule communicating processes rather than rely on isolated or implicit information gathered from local events between processors. In this paper we describe how buffered coscheduling is implemented in the context of our SMART simulator. We then present peformance measurements for

two synthetic workloads and demonstrate the effectiveness of buffered coscheduling under different computational granularities, context-switch times, and time-slice granularities.
NTIS
*Interprocessor Communication; Scheduling; Simulators; Parallel Processing (Computers); Distributed Processing*

**20010124084** Sandia National Labs., Albuquerque, NM USA
**Agent Communications using Distributed Metaobjects**
Goldsmith, S. Y.; Spires, S. V.; Jun. 10, 1999; 11p; In English
Report No.(s): DE2001-7894; SAND99-1500C; No Copyright; Avail: Department of Energy Information Bridge

There are currently two proposed standards for agent communication languages, namely, KQML (Finin, Lobrou, and Mayfield 1994) and the FIPA ACL. Neither standard has yet achieved primacy, and neither has been evaluated extensively in an open environment such as the Internet. It seems prudent therefore to design a general-purpose agent communications facility for new agent architectures that is flexible yet provides an architecture that accepts many different specializations. In this paper we exhibit the salient features of an agent communications architecture based on distributed metaobjects. This architecture captures design commitments at a metaobject level, leaving the base-level design and implementation up to the agent developer. The scope of the metamodel is broad enough to accommodate many different communication protocols, interaction protocols, and knowledge sharing regimes through extensions to the metaobject framework. We conclude that with a powerful distributed object substrate that supports metaobject communications, a general framework can be developed that will effectively enable different approaches to agent communications in the same agent system. We have implemented a KQML-based communications protocol and have several special-purpose interaction protocols under development.
NTIS
*Architecture (Computers); Protocol (Computers); Communication Networks; Mathematical Models; Object-Oriented Programming*

**20010124109** NASA Ames Research Center, Moffett Field, CA USA
**Communication Research in Aviation and Space Operations: Symptoms and Strategies of Crew Coordination**
Kanki, Barbara G., NASA Ames Research Center, USA; [1994]; 1p; In English; International Aerospace Congress, 15-19 Aug. 1994, Moscow, Russia
Contract(s)/Grant(s): RTOP 190-06-12; No Copyright; Avail: Issuing Activity; Abstract Only

The day-to-day operators of today's aerospace systems work under increasing pressures to accomplish more with less. They work in operational systems which are complex, technology-based, and high-risk; in which incidents and accidents have far-reaching and costly consequences. For these and other reasons, there is concern that the safety net formerly built upon redundant systems and abundant resources may become overburdened. Although we know that human ingenuity can overcome incredible odds, human nature can also fail in unpredictable ways. Over the last 20 years, a large percentage of aviation accidents and incidents have been attributed to human errors rather than hardware or environmental factors alone. A class of errors have been identified which are not due to a lack of individual, technical competencies. Rather, they are due to the failure of teams to utilize readily available resources or information in a timely fashion. These insights began a training revolution in the aviation industry called Cockpit Resource Management, which later became known as Crew Resource Management (CRM) as its concepts and applications extended to teams beyond the flightdeck. Then, as now, communication has been a cornerstone in CRM training since crew coordination and resource management largely resides within information transfer processes--both within flightcrews, and between flightcrews and the ground operations teams that support them. The research I will describe takes its roots in CRM history as we began to study communication processes in order to discover symptoms of crew coordination problems, as well as strategies of effective crew management. On the one hand, communication is often the means or the tool by which team members manage their resources, solve problems, maintain situational awareness and procedural discipline. Conversely, it is the lack of planning and resource management, loss of vigilance and situational awareness, and non-standard communications that are implicated in accidents and incidents. NASA/Ames Crew Factors researchers have been developing a model of effective crew coordination in order to understand the sources of performance breakdowns, and to develop effective solutions and interventions. Because communication is a primary mechanism by which information is received and transmitted, and because it is observable behavior, we focus on these group processes in order to identify patterns of communication that distinguish effective from less effective crew performance. Since a prime objective is to develop training recommendations for enhancing communication skills, we interpret our findings in the context of relevant task and environmental conditions, role and procedural constraints, and the normal real-time parameters of flight operations. Another research objective is to consider how communication and coordination can be enhanced through design. For example, flight deck and hardware design as well as procedural and software design may greatly influence the efficiency with which crews communicate and coordinate their work. In addition, teams and tasks may be

designed, organized, and trained so that team interactions with each other are based upon appropriately shared knowledge, procedures and situation awareness. In short, we are interested in enhancing communication practices through (1) the training of specific communication skills, and (2) the design of equipment, tasks, procedures, and teams that optimize smooth, unambiguous communication processes. Two examples of communication research will be described; one in aviation and one in space operations. The first example is a high-fidelity full mission simulation study which investigates the affect of flightdeck automation on crew coordination and communication (contrasting crew performance in the DC-9 vs. MD88). Additional information is contained in the original extended abstract.
Author
*Flight Crews; Communication; Data Transmission; Education; Coordination*

**20010125065** National Defence Research Establishment, Div. of Command and Control Warfare, Linkoeping, Sweden
**Simulations Environments for Totally Mobile Radio Networks** ***Simuleringsmiljoe foer helt mobila radionaet***
Joensson, C., National Defence Research Establishment, Sweden; Sterner, U., National Defence Research Establishment, Sweden; December 1999; ISSN 1104-9154; 22p; In Swedish
Report No.(s): PB2001-108206; FOA-R-99-01370-504-SE; No Copyright; Avail: CASI; A03, Hardcopy; A01, Microfiche

In the development of military command and control systems and supporting communication systems, there is a need of assessment and evaluation of tactical communication networks. Above all, their influence on the command and control ability. The impact of different techniques, methods or components need to be assessed in new contexts. It is also essential to be able to, under controlled conditions, evaluate tactical communication systems' ability to support tactical courses of events. Specifically, with such a competence the whole picture of the problem is the focus, not the technical details. to be able to do this, we suggest that an ability to assess and evaluate communications systems is established. A recognized simulations tool to support such an ability necessary. We briefly describe the alternatives we have found interesting: OPNET, GloMoSim ns-2, and COMNET-III.
NTIS
*Mobile Communication Systems; Communication Networks; Computerized Simulation*

**20010125101** National Defence Research Establishment, Div. of Sensor Technology, Linkoeping, Sweden
**Signal Processing in Radar Imaging Applications** ***qSignalbehandlingsmetoder foer Radaravbildingar***
Akermark, H., National Defence Research Establishment, Sweden; June 2000; ISSN 1104-9154; 51p; In Swedish
Report No.(s): PB2001-108208; FOA-R-00-01564-408-SE; No Copyright; Avail: CASI; A04, Hardcopy; A01, Microfiche

Target recognition is a key component in tomorrow's sensor systems. For battlefield awareness and remotely piloted vehicles, the ability to identify targets of interest is crucial, and the long range and all-weather capability of radar systems give such sensors a unique position. During the last decades, target recognition research has focused on radar imaging, where scattered data is transformed to provide target specific properties. In this report, the transformation is presented in some detail, in particular three of its more important aspects: motion compensation, the effects of complex and irregular target motion and scattering from dispersive structures. These areas are all major hurdles on the way to deployable sensor systems, and techniques for mitigating their effects have been developed. Even though several of the techniques give good results in some cases, more research is needed.
NTIS
*Target Recognition; Signal Processing; Radar Imagery; Radar Detection; Military Technology*

**20010125102** National Defence Research Establishment, Div. of Sensor Technology, Linkoeping, Sweden
**Analysis of the Coupling of Target Motion to Radar Imaging** ***Analys av Malroerelsers Kopping till Radaravibildningar***
Akermark, H., National Defence Research Establishment, Sweden; June 2000; ISSN 1104-9154; 41p; In Swedish
Report No.(s): PB2001-108207; FOA-R-00-01579-408-SE; No Copyright; Avail: CASI; A03, Hardcopy; A01, Microfiche

Target recognition is one of the most important challenges for tomorrow's military sensor systems. The long range and all-weather capabilities of radar systems stress the importance of radar based research for this application. Radar imaging methods, in our case of aircraft targets, have developed as one of the main tools towards operative systems. So far, these methods have not reached the required imaging performance, mainly due to the coupling between resolution and target motion. In this report, an analysis of the large scale tactical motion and the small scale technical motion of performed, with consideration to radar imaging and target recognition. The technical target motion is studied with motion data from Saab Aerospace AB. An important conclusion is that, often, we will not be able to generate two-dimensional radar images, except with limited resolution. This shows the importance of studying other waveforms that are less dependent of target motion, and also to study target glint for one-dimensional imaging.
NTIS
*Target Recognition; Radar Detection*

**20010125103** National Defence Research Establishment, Div. of Sensor Technology, Linkoeping, Sweden

**Effects of Target Shape and Reflection on Laser Radar Cross Sections**

Steinvall, O.; September 1999; 29p; In English

Report No.(s): PB2001-108148; FOA-R-99-01201-408-612-SE; No Copyright; Avail: CASI; A03, Hardcopy; A01, Microfiche

We have derived expressions for the cross sections of some basic objects like cones, paraboloides and cylinders and used some convenient approximations for the target angular reflection from diffuse and specular targets. The laser radar cross section and the detailed pulse stretching vs. the shape of the target and the BRDF (bidirectional reflectance distribution function) angular dependence have been evaluated. The results are of interest for many laser radar applications like ranging, 3-D (three dimensional) imaging/modeling, tracking, antisensor laser and target recognition.

NTIS

*Optical Radar; Target Recognition; Display Devices*

**20010125104** National Defence Research Establishment, Dept. of Command and Control Warfare Technology, Linkoeping, Sweden

**Military Aspects of Satellites Integrated into Mobile Data Communications Networks** ***Militaera Aspekter pae Satelliter Integrerade i Mobila Datakommunikationsnaet***

Ekblad, U.; October 1999; 41p; In Swedish

Report No.(s): PB2001-108147; FOA-R-99-01228-5040-SE; Copyright; Avail: National Technical Information Service (NTIS)

Satellites and terrestrial communication networks complement each other. Satellites also fulfil military needs that terrestrial networks cannot satisfy. There are reasons for studying whether satellites ought to be integrated into a Swedish military terrestrial mobile data communication network. The report describes mainly the possibilities and advantages with satellites integrated into terrestrial mobile data communication networks, but also problems, shortcomings, and disadvantages are treated. In the beginning of a conflict, satellites can be used for setting up other systems fast and easy. The great flexibility characterizing satellite communications will be of great advantage in the fragmented battlefield where satellites with advantage can be used for connecting 'islands.'

NTIS

*Military Operations; Communication Satellites*

**20010125109** General Accounting Office, Washington, DC USA

**Defense Spectrum Management. More Analysis Needed to Support Spectrum Use Decisions for the 1755-1850 MHz Band**

August 2001; 64p; In English

Report No.(s): PB2001-107937; GAO-01-795; No Copyright; Avail: CASI; A04, Hardcopy; A01, Microfiche

The use of commercial mobile wireless communications, such as personal communications services and cell phones, has been escalating worldwide over the radio frequency spectrum. This spectrum is a scarce and finite resource, which serves ever increasing and competing public and private uses. The federal government has supported commercial services by making spectrum available as these services developed over the years. Some representatives of the commercial mobile radio service industry claim additional spectrum is needed to support advanced communications systems, called third generation systems. Other members of the industry question the need for, or feasibility of providing, large amounts of additional spectrum to meet industry requirements. These members point to the need for increased efficiency in the use of spectrum through new technologies. Third generation systems are being developed to provide mobile voice, high-speed data, and Internet capabilities and are expected to contribute significantly to the economic well-being of the USA. Because of the importance of this issue to private and public interests in the USA, you asked us to assess DOD's (Department of Defense) study of the 1755 to 1850 MHz band and determine whether the study provides a sound basis for decisions about the reallocation of this spectrum. As part of this assessment, we reviewed and analyzed an industry consortium report that reached different conclusions on space operations than the DOD study. We also reviewed a separate ongoing Air Force analysis that has similar conclusions on space operations to the DOD study. We did not review the Department of Commerce or the Federal Communications Commission (FCC) report or each agency's process to identify and select additional spectrum for third generation wireless systems.

NTIS

*Carrier Frequencies; Radio Frequencies; Wireless Communication; Access Control; Regulations; Decision Making*

**20010125111** Helsinki Univ. of Technology, Electromagnetics Lab., Espoo, Finland

**Conditions for the Parameter Dyadics of Lossy Bi-Anisotropic Media**

Lindell, I. V.; October 2000; 16p; In English

Report No.(s): PB2001-107371; ISBN 951-22-5228-7; Copyright; Avail: National Technical Information Service (NTIS)

Conditions for the parameter dyadics are derived for bi-anisotropic media to be lossy (power absorbing). The conditions, which can be expressed easily in terms of the 6 x 6 matrix of four parameter dyadics as being Hermitian and negative definite, are brought to the level of individual parameter dyadics as four separate dyadic conditions. The theory is applied to three particular medium classes: bi-isotropic media, uniaxial bi-anisotropic media and gyrotropic bi-anisotropic media as a set of inequalities for the scalar parameters. The conditions are needed for judging the physical realizability of parameter values of new composite media.

NTIS

*Electromagnetic Radiation; Dyadics; Lossy Media*

**20010125168** California Univ., Lawrence Berkeley Lab., Berkeley, CA USA

**Using Multicast in the Global Communications Infrastructure for Group Communication**

Agarwal, D. A.; Jul. 30, 1999; 7p; In English; 21st; 21st Seismic Research Symposium: Technologies for Monitoring the Comprehensive Nuclear-Test-Ban Treaty, 21-24 Sep. 1999, Las Vegas, NV, USA

Report No.(s): DE2000-767536; LBNL-44096; No Copyright; Avail: Department of Energy Information Bridge, Microfiche

International Monitoring System (IMS) stations and the International Data Centre (IDC) of the Preparatory Commission for the Comprehensive Nuclear-Test-Ban Treaty Organization generate data and products that must be transmitted to one or more receivers. The application protocols used to transmit the IMS data and IDC products will be CD-x and IMS-x and the World Wide Web (WWW). These protocols use existing Internet applications and Internet protocols to send their data. The primary Internet applications in use are electronic mail (e-mail) and the file transfer protocol (ftp). The primary Internet communication protocol in use is the Transmission Control Protocol (TCP), which provides reliable delivery to the receiver. These Internet applications and protocol provide unicast (point-to-point) communication. A message sent using unicast has a single recipient; any message intended for more than one recipient must be sent to each recipient individually. In the current design, the IDC and the National Data Centres (NDC's) provide data forwarding to the appropriate receivers. The overhead associated with using unicast to transmit messages to multiple receivers either directly or through a forwarder increases linearly with the number of receivers. In addition, using a forwarding site introduces possible delays and possible points of failure in the path to the receivers. Reliable multicast provides communication services similar to TCP but for a group of receivers. The reliable multicast protocol provides group membership services and message delivery ordering. If an IMS station were to send its data using reliable multicast instead of unicast, only sites that are members of the multicast group would receive the data at approximately the same time. This might provide an efficient means of disseminating station data or IDC data products to all receivers and eliminate or greatly reduce the need for data forwarding. Several commercial and research reliable multicast protocols exist for the Internet. Each of these protocols is designed to serve a specific community of users and applications. The author has undertaken a study to determine if reliable multicasting is appropriate for use in the Global Communication Infrastructure (GCI).

NTIS

*Internets; Messages; Point to Point Communication; Protocol (Computers); Receivers*

**20010125455** Lawrence Livermore National Lab., Livermore, CA USA

**Design of a TEM waveguide for ultra-wideband applications**

Pao, H. Y.; Poggio, A.; Jan. 01, 1999; 6p; In English

Report No.(s): DE2001-8319; UCRL-JC-132764; No Copyright; Avail: Department of Energy Information Bridge, Microfiche

Impulse launching and receiving antennas are required for ultra-wideband applications involving high-fidelity transmitting and sensing of impulse electromagnetic fields. Due to their dispersive characteristics conventional wideband antennas, such as log-periodic arrays, spiral antennas, and ridged horn type antennas, perform poorly as high-fidelity antennas for wideband impulsive waveforms. However, a TEM (Transmission Electron Microscope) horn forms a natural structure for low-dispersion launching and receiving of ultra-wideband impulses.

NTIS

*Waveguides; Transmission Electron Microscopy; Broadband; Electromagnetic Fields; Transmission*

## 33
## ELECTRONICS AND ELECTRICAL ENGINEERING

*Includes development, performance, and maintainability of electrical/electronic devices and components; related test equipment. and microelectronics and integrated circuitry. For related information see also 60 Computer Operations and Hardware; and 76 Solid-State Physics. For communications equipment and devices see 32 Communications and Radar.*

**20010118262** Oak Ridge National Lab., TN USA
**Gelcasting Polycrystalline Alumina**
Janney, M. A.; Zuk, K. J.; Wei, G. C.; Jan. 01, 2000; 16p; In English
Report No.(s): DE2000-760507; C/ORNL95-0389; ORNL/C95-0389; No Copyright; Avail: Department of Energy Information Bridge, Microfiche

OSRAM SYLVANIA INC. is a major U.S. manufacturer of high-intensity lighting. Among its products is the Lumalux TM line of high-pressure sodium vapor arc lamps, which are used for industrial, highway, and street lighting. The key to the performance of these lamps is the polycrystalline alumina (PCA) tube that is used to contain the plasma that is formed in the electric arc. That plasma consists of ionized sodium, mercury, and xenon vapors. The key attributes of the PCA tubes are their transparency ((approximately)97% total transmittance in the visible), their refractoriness (inner wall temperature can reach l2OO C), and their chemical resistance (sodium and mercury vapor are extremely corrosive). The current efficiency of the lamps is very high, up to 100 initial lumens per watt. (Compare incandescent lamps 10-20 lumens per watt, fluorescent lamps 25-90 lumens per watt.)
NTIS
*Efficiency; Electric Arcs; Arc Lamps; Sodium Vapor*

**20010118912** Sandia National Labs., Albuquerque, NM USA
**Overview of High Reliability Transformer Encapsulation Materials**
Arris, H. W.; Jul. 12, 2000; 7p; In English
Report No.(s): DE2000-760800; SAND2000-1624C; No Copyright; Avail: Department of Energy Information Bridge

Sandia National Laboratories (SNL) has been encapsulating electronic components for over 40 years. Several formulations have been in use and tested for 30 years. A prime objective in using formulations that have not changed lies in gaining a better understanding of the encapsulant long term aging and comparability characteristics. We have developed several formulations that are tailored to withstand a variety of environments. In some instances commercially available formulations have been used. Depending on the formulation and the component requirements, the encapsulant are used to attenuate or mitigate shock, provide improved mechanical properties, or improve electrical properties. Formulations that we have developed include epoxies, urethanes, and silicones. Filler materials such as Mica, Glass Micro Balloons (GMB), and Al2O3 may also be incorporated into these formulations. The intent of this paper is to present an overview of encapsulation formulations that have been utilized for magnetic and transformer component applications.
NTIS
*Encapsulating; Transformers; Aging (Materials); Equipment Specifications*

**20010119589** PixelVision, Inc., Beaverton, OR USA
**Advances in Pixelvision, Inc. Back-Illuminated CCD Imaging Technologies for Low Light Level Imaging Applications**
Williams, George M.; Janesick, James R.; Dosluoglu, Taner; Reinheimer, Alice; Jul. 1997; 23p; In English
Report No.(s): AD-A394905; No Copyright; Avail: CASI; A03, Hardcopy; A01, Microfiche

With the goal of optimizing high resolution, low noise, back-illuminated CCD night vision imaging performance within the context of commercial manufacturability and cost effectiveness, PixelVision, Inc., in partnership with Scientific Imaging Technologies, Inc. (SITe) has undertaken, using its commercial Sandbox(TM) CCD processing service, a series of experimental design, performance optimization, and manufacturability efforts that has resulted in greater than 160 independent CCD designs. These low light level imagers have been demonstrated superior to conventional image intensified approaches for a broad range of night vision applications. This paper describes a systems level approach by the authors to globally enhance all of the performance parameters of back-illuminated CCD technologies with the goal of manufacturing high yielding, cost effective imagers optimized for night vision applications. We group the CCD performance parameters (which for low light level imaging must be simultaneously optimized) into four primary CCD operations: (1) Charge Generation (e.g. QE), (2) Charge Collection (e.g. MTF), (3) Charge Transfer (e.g. CTE), and (4) Charge Detection (e.g. Read Noise). to demonstrate the process used to optimize these four CCD operations for night vision applications, this paper contains CCD transfer Curve data for two PixelVision,

Inc. Sandbox(TM) CCD devices. CCD transfer Curves, a formal methodology of CCD test and optimization, is the only demonstrated method of characterizing all of the performance characteristics of a CCD in a single, context independent data set. DTIC

*Image Processing; Night Vision; Charge Coupled Devices*

**20010119926** FMC Corp., Ground Systems Div., Santa Clara, CA USA

**Electric Drive Study. Volume 2**

Rodler, Waldo E., Jr.; Shafer, Kenneth W.; Dec. 1987; 296p; In English

Contract(s)/Grant(s): DAAE07-84-C-R017

Report No.(s): AD-A395233; No Copyright; Avail: CASI; A13, Hardcopy; A03, Microfiche

This report details the approach and results of a survey of motors, solid-state controls, alternator/generators, and servo components which were potential candidates for the advanced electric drive study. In addition, solid-state components and various materials such as advanced magnetics were included in the survey.

Derived from text

*Electric Motors; Servomechanisms; Magnetic Materials*

**20010119958** NASA Goddard Space Flight Center, Greenbelt, MD USA

**Wavelength Division Multiplexing Scheme for Radio-Frequency Single Electron Transistors**

Stevenson, Thomas R., NASA Goddard Space Flight Center, USA; Pellerano, F. A., NASA Goddard Space Flight Center, USA; Stahle, C. M., NASA Goddard Space Flight Center, USA; Aidala, K., Yale Univ., USA; Schoelkopf, R. J., Yale Univ., USA; [2001]; 4p; In English; 9th International Conference on Low Temperature Detectors, 23-27 Jul. 2001, Madison, WI, USA; No Copyright; Avail: CASI; A01, Hardcopy; A01, Microfiche

We describe work on a wavelength division multiplexing scheme for radio-frequency single electron transistors. We use a network of resonant impedance matching circuits to direct applied rf carrier waves to different transistors depending on carrier frequency. Using discrete components, we made a two-channel demonstration of this concept and successfully reconstructed input signals with small levels of cross coupling. A lithographic version of the rf circuits had measured parameters in agreement with electromagnetic modeling, with reduced cross capacitance and inductance, and should allow 20 to 50 channels to be multiplexed. Author

*Wavelength Division Multiplexing; Radio Frequencies; Transistors; Electron Transfer*

**20010120033** Argonne National Lab., IL USA

**Design of a gate-turn-off (GTO) switch for pulsed power application**

Despe, O.; Jul. 10, 1998; 5p; In English

Report No.(s): DE2001-10628; ANL/ASD/CP-95550; No Copyright; Avail: Department of Energy Information Bridge, Microfiche

A Gate-Turn-Off (GTO) thyristor switch and its gate drive circuit have been developed as a replacement for the thyratron switch used in the positron converter solenoid lens power supply at the Advanced Photon Source (APS) to deliver a current pulse of 6000 A at 60-Hz repetition rate. This paper discusses the characteristics of the GTOs under consideration, the gate drive circuit, and some test results.

NTIS

*Thyristors; Switches*

**20010120062** Sandia National Labs., Albuquerque, NM USA

**Effects of Alternating Bias Irradiation on Defects in MOS Devices**

Felix,; Fleetwood,; Riewe,; Winokur,; Sep. 14, 2000; 4p; In English

Report No.(s): DE2000-763107; SAND2000-2276C; No Copyright; Avail: Department of Energy Information Bridge, Microfiche

A comprehensive model of MOS radiation response must apply to switched and alternating bias exposure as well as static bias irradiation. Previous work has shown that defect buildup and annealing during alternating and switched bias irradiation is often qualitatively different than at steady-state bias. For example, changing the bias from positive to zero or negative values and delivering an additional dose of radiation can lead a significant reduction in net oxide-trap charge due to radiation-induced charge neutralization. Moreover, enhanced interface trap buildup has been observed under some alternating bias conditions. These effects

have been characterized at a phenomenological level, but the underlying defect buildup and annealing processes are not well understood.
NTIS
*Irradiation; Transistors; Defects*

**20010120068** Sandia National Labs., Albuquerque, NM USA
**Failure Analysis of MEMS Using Thermally-Induced Voltage Alteration**
Walraven,; Cole,; Tangyunyong,; Sep. 12, 2000; 11p; In English
Report No.(s): DE2000-762125; SAND2000-2259C; No Copyright; Avail: Department of Energy Information Bridge, Microfiche

Electrical shorting in micro-electro-mechanical systems (MEMS) is a significant production and manufacturing concern. We present a new approach to localizing shorted MEMS devices using Thermally-Induced Voltage Alteration (TIVA). In TIVA, the shorted, thermally isolated MEMS device is very sensitive to thermal stimulus. The site of the MEMS short will respond as a thermocouple when heated. by monitoring the potential across the shorted MEMS device as a laser scans across the sample, an image showing the location of the thermocouple (short site) can be generated. The TIVA signal for thermally isolated MEMS devices is much higher than that observed for conventional IC interconnections. This results from the larger temperature gradients generated during laser scanning due to little or no substrate heat sinking. The capability to quickly localize shorted MEMS structures is demonstrated by several examples. Thermal modeling of heat distributions is presented and is consistent with the experimental results.
NTIS
*Failure Analysis; Microelectromechanical Systems; Voltage Regulators*

**20010120069** Brookhaven National Lab., Upton, NY USA
**Modeling of Transient Ionizing Radiation Effects in Bipolar Devices at High Dose-Rates**
Fjeldly,; Deng,; Shur,; Hjalmarson,; Muyshondt,; Sep. 12, 2000; 11p; In English
Report No.(s): DE2000-762114; SAND2000-2252C; No Copyright; Avail: Department of Energy Information Bridge, Microfiche

We have developed a dynamic model for photoelectric effect in bipolar devices exposed to a wide range of ionizing radiation intensities. We represent the stationary and dynamic photocurrents by current sources in parallel with each p-n-junction. These sources include the prompt photocurrent of the depletion regions, and the delayed response associated with the build-up and discharge of excess charge carriers in the quasi-neutral regions adjacent to the junctions. The latter are described in terms of dynamic delay times for each q-n region, which can be represented by RC equivalent delay circuits. The model has been implemented in the circuit simulator AIMSpice, and has been verified by numerical simulations.
NTIS
*Dynamic Models; Electric Current; Photoelectric Effect; Radiation Effects*

**20010120083** Sandia National Labs., Albuquerque, NM USA
**Electrical and Fluidic Packaging of Surface Micromachined Electro-Microfluidic Devices**
Galambos, P. C.; Benavides, G. L.; Jun. 26, 2000; 10p; In English
Report No.(s): DE2000-760788; SAND2000-1547C; No Copyright; Avail: Department of Energy Information Bridge

Microfluidic devices have applications in chemical analysis, biomedical devices and ink-jets. An integrated microfluidic system incorporates electrical signals on-chip. Such electro-microfluidic devices require fluidic and electrical connection to larger packages. Therefore electrical and fluidic packaging of electro-microfluidic devices is key to the development of integrated microfluidic systems. Packaging is more challenging for surface micromachined devices than for larger bulk micromachined devices. However, because surface micromachining allows incorporation of electrical traces during microfluidic channel fabrication, a monolithic device results. A new architecture for packaging surface micromachined electro-microfluidic devices is presented. This architecture relies on two scales of packaging to bring fluid to the device scale (picoliters) from the macroscale (microliters). The architecture emulates and utilizes electronics packaging technology. The larger package consists of a circuit board with embedded fluidic channels and standard fluidic connectors. The embedded channels connect to the smaller package, an Electro-Microfluidic Dual-Inline-Package (EMDIP) that takes fluid to the microfluidic integrated circuit (MIC). The fluidic connection is made to the back of the MIC through Bosch(sup 2) etched holes that take fluid to surface micromachined channels on the front of the MIC. Electrical connection is made to bond pads on the front of the MIC.
NTIS
*Micromachining; Packaging; Circuits*

**20010120084** Sandia National Labs., Albuquerque, NM USA

**Longevity Improvement of Optically Activated, High Gain GaAs Photoconductive Semiconductor Switches**

Mar, A.; Loubriel, G. M.; Zutavern, F. J.; O'Malley, M. W.; Helgeson, W. E.; Jun. 22, 2000; 6p; In English

Report No.(s): DE2000-760787; SAND2000-1545C; No Copyright; Avail: Department of Energy Information Bridge

The longevity of high gain GaAs photoconductive semiconductor switches (PCSS) has been extended to over 100 million pulses. This was achieved by improving the ohmic contacts through the incorporation of a doped layer that is very effective in the suppression of filament formation, alleviating current crowding. Damage-free operation is now possible at much higher current levels than before. The inherent damage-free current capacity of the bulk GaAs itself depends on the thickness of the doped layers and is at least 10OA for a dopant diffusion depth of 4 microns. The contact metal has a different damage mechanism and the threshold for damage (approximately 40A) is not further improved beyond a dopant diffusion depth of about 2 microns. In a diffusion-doped contact switch, the switching performance is not degraded at the onset of contact metal erosion, unlike a switch with conventional contacts. For fireset applications operating at 1kV/lkA levels and higher, doped contacts have not yet resulted in improved longevity. We employ multi-filament operation and InPb solder/Au ribbon wirebonding to demonstrate greater than 100 shot lifetime at 1kV/1kA.

NTIS

*Semiconductors (Materials); Switches; Photoconductivity*

**20010120087** Sandia National Labs., Albuquerque, NM USA

**GaN Electronics For High Power, High Temperature Applications**

Pearton, S. J.; Ren, F.; Zhang, A. P.; Dang, G.; Cao, X. A.; Jun. 12, 2000; 10p; In English

Report No.(s): DE2000-760777; SAND2000-1467C; No Copyright; Avail: Department of Energy Information Bridge

A brief review is given of recent progress in fabrication of high voltage GaN and AlGaN rectifiers. GaN/AlGaN heterojunction bipolar transistors and GaN metal-oxide semiconductor field effect transistors. Improvements in epitaxial layer quality and in fabrication techniques have led to significant advances in device performance.

NTIS

*Field Effect Transistors; Gallium Nitrides; Aluminum Nitrides; Bipolar Transistors; Metal Oxide Semiconductors*

**20010120105** Stanford Univ., Board of Trustees, Stanford, CA USA

**Non Traditional Transport Processes in Tunneling and Proximity Junctions** ***Final Report, 15 Dec. 1995-30 Sep. 2000***

Beasley, M. R.; Sep. 2001; 8p; In English

Contract(s)/Grant(s): N00014-96-1-0258

Report No.(s): AD-A395108; No Copyright; Avail: CASI; A02, Hardcopy; A01, Microfiche

Several project aimed at dealing with fundamental limitations in the present superconducting electronics technology based on Josephson junctions were carried out. The need for high resistance superconductor/normal metal/ superconductor Josephson junctions was reiterated and some constraints on the more favorable technology were established. A phenomenological theory of Josephson coupling in high Tc superconductor/normal metal/superconductor junctions was developed. The practical considerations to develop a new concept for memory storage in superconducting electronics based on the superconductor/ ferromagnet proximity effect were pursued.

DTIC

*Josephson Junctions; Ferromagnetism; High Temperature Superconductors; Electron Tunneling; Phenomenology*

**20010120142** Air Command and Staff Coll., Maxwell AFB, AL USA

**Integrating Commercial Electronic Equipment to Improve Military Capabilities**

Bohler, Jeffrey A.; Apr. 1999; 35p; In English; Original contains color images

Report No.(s): AD-A395153; AU/ACSC/012/1999-04; No Copyright; Avail: CASI; A03, Hardcopy; A01, Microfiche

There is a new information revolution brewing. Hand held electronic devices are invading the home and the workplace. As capabilities increase, the cost of commercially available personal electronic devices continues to decline dramatically. These devices include Personal Data Assistants (PDAs), Cellular Phones, Pagers, GPS receivers, and Digital imaging equipment. The military should plan for the integration and use of these devices to enhance effectiveness of operations. by designing open architecture systems that are upgrade capable, the military can take advantage of emerging technologies. There are issues to be considered: integration, reliability, training, security and invasion of privacy.

DTIC

*Electronic Equipment; Imaging Techniques; Military Technology; Design Analysis*

**20010120263** Arizona Univ., Optical Sciences Center, Tucson, AZ USA

**In Situ High Sensitivity Brillouin Light Scattering Spectrometer for MBE-Grown Thin Films** ***Final Report, 1 Apr. 1999 - 31 Mar. 2001***

Falco, Charles M.; Keavney, David J.; Aug. 2001; 3p; In English

Contract(s)/Grant(s): F49620-99-1-0147; Proj-3484

Report No.(s): AD-A395007; AFRL-SR-BL-TR-01-0495; No Copyright; Avail: CASI; A01, Hardcopy; A01, Microfiche

This instrumentation project involved the purchase of a high-resolution six-pass tandem Fabry Perot interferometer, a 200 nW frequency-doubled Nd:YAG laser, a custom-designed UHV chamber, a cryogenic sample manipulator, and associated vacuum hardware for interfacing this chamber with the MBE system. Therefore, we have completed all of the design, purchasing, and construction of the equipment needed to complete this project and add the BLS capability on our existing AFM/STM MBE system.

DTIC

*Light Scattering; Thin Films; Molecular Beam Epitaxy; Instruments*

**20010120470** Auburn Univ., AL USA

**The Reactive Bridge: A Novel Solid-State Low Energy Initiator**

Baginski, Thomas A., Auburn Univ., USA; Apr. 16, 2001; 28p; In English; 45th Annual Fuze Conference, 16-18 Apr. 2001, Arlington, VA, USA; Original contains color images

Report No.(s): AD-A394509; No Copyright; Avail: CASI; A01, Microfiche; A03, Hardcopy

This report concerns the reactive bridge, a solid-state low energy initiator.

DTIC

*Solid State; Reactivity*

**20010120492** Pennsylvania State Univ., Materials Research Lab., University Park, PA USA

**Electron Backscatter Diffraction (EBSD) System for Crystallographic Imaging in a SEM** ***Final Report, 1 Apr. 2000 - 31 Mar. 2001***

Messing, Gary L.; Aug. 28, 2001; 3p; In English

Contract(s)/Grant(s): F49620-00-1-0231

Report No.(s): AD-A395128; AFRL-SR-BL-TR-01-0474; No Copyright; Avail: CASI; A01, Hardcopy; A01, Microfiche

The Electron Backscatter Diffraction (EBSD) System was purchased and installed. Training is currently ongoing and the technique is being used to probe a variety of research problems including work support by our AFOSR/DARPA ferroelectric project. Imaging using EBSD is a relatively new, powerful, and elegant characterization technique for measuring micro- to mesostructural crystallography. As part of a SEM system, EBSD involves indexing the Kikuchi patterns formed by electrons backscattered from the sample. Through computer automation, the electron beam is slowly rastered over the sample as the pattern from each spot is analyzed. The result is an image of the microstructure based on crystallographic orientation. It should be noted that this capability has only been commercialized since 1993. EBSD provides sample resolution fine enough to crystallographically index individual grains, while offering a field of view large enough and data processing fast enough to provide statistically significant measurements of texture on either a localized or global basis. This coupling of fine resolution and relatively wide field of view makes it possible to analyze textures in virtually any type of sample from semiconductors, piezoelectrics, geological rocks, etc.

DTIC

*Electron Diffraction; Crystallography; Semiconductors (Materials); Backscattering*

**20010120534** Argonne National Lab., IL USA

**Enhanced adhesion buffer layer for deep x-ray lithography using hard x-rays**

DeCarlo, F.; Aug. 28, 1998; 20p; In English

Report No.(s): DE2001-10614; ANL/XFD/CP-95506; No Copyright; Avail: Department of Energy Information Bridge, Microfiche

The first step in the fabrication of microstructure using deep x-ray lithography (DXRL) is the irradiation of an x-ray sensitive resist like polymethylmethacrylate (PMMA) by hard x-rays. At the Advanced Photon Source, a dedicated beamline allows the proper exposure of very thick (several mm) resists. to fabricate electroformed metal microstructure with heights of several mm, a PMMA sheet is glued onto a metallic plating base. An important requirement is that the PMMA layer must adhere well to the plating base. The adhesion is greatly reduced by the penetration of even a small fraction of hard x-rays through the mask absorber

into the substrate. In this work we will show a novel technique to improve the adhesion of PMMA onto high-Z substrates for DXRL. Results of the improved adhesion are shown for different exposure/substrate conditions.
NTIS
*Adhesion; Substrates; Lithography; X Rays; Polymethyl Methacrylate; Electroforming; Barrier Layers*

**20010120837** Lehigh Univ., Bethlehem, PA USA
**Low Temperature Polysilicon Thin Film Transistors in Advanced Display Technologies** ***Final Report, May 1996-Jul. 2000***
Hatalis, Miliadis K.; Sep. 2000; 125p; In English
Contract(s)/Grant(s): F33615-96-1-1939
Report No.(s): AD-A395301; AFRL-HE-WP-TR-2000-0172; No Copyright; Avail: CASI; A06, Hardcopy; A02, Microfiche

In this final project report, we detail the work completed in developing a polysilicon thin film transistor (TFT) technology that was successfully applied in fabricating a working VGA Active Matrix Organic Light Emitting Diode (AMOLED) display prototype. Using the high throughput, low cost method of Rapid Thermal Processing (RTP), we achieved glass compatible crystallization temperatures of polysilicon. We identify that RTP results in superior TFT performance uniformity, which is critical for fabrication of AMOLEDs. We successfully developed and integrated novel microelectronic processes and techniques while fabricating AMOLED displays, culminating in the demonstration of a VGA AMOLED prototype display operated at a brightness of 101 nits. Using our high throughput, low cost process polysilicon TFT technology, we fabricated display driver circuits, including low temperature shift registers that run at clock frequencies as high as 20 MHz. Finally, several processing issues that were investigated in order to improve the performance of AMOLED displays are described. This includes work on low temperature silicides for TFTs, a novel hillock-free aluminum metallization, and the ability of this aluminum metallization to form ohmic contacts to indium tin oxide.
DTIC
*Low Temperature; Silicon Polymers; Thin Films; Transistors*

**20010121527** Brookhaven National Lab., Upton, NY USA
**Oxygen deficiency and vacancy formation in lSCO/PLZT/lSCO capacitors**
Friessnegg, T.; Nov. 29, 1999; 5p; In English
Report No.(s): DE2000-752149; BNL-67118; No Copyright; Avail: Department of Energy Information Bridge

The potential applications of ferroelectric thin films in the fabrication of non-volatile memory devices have drawn a lot of attention to the perovskite oxide materials. Current efforts are directed towards integration with standard silicon device technology. Long term reliability issues such as fatigue, imprint and aging are important aspects in the realization of these devices.
NTIS
*Capacitors; Ferroelectricity; Computer Storage Devices; Perovskites; Hypoxia*

**20010121878** Sandia National Labs., Albuquerque, NM USA
**Optical Sensing of Microsystem Motion and Performance**
Holswade, S. C.; Dickey, F. M.; Jul. 05, 2000; 15p; In English
Report No.(s): DE2000-760762; SAND2000-0575C; No Copyright; Avail: Department of Energy Information Bridge, Microfiche

Microsystems involve several fabrication technologies, but share the common trait of dimensions and motions measured in microns. Small feature sizes and deflections make the detection of microdevice motion particularly difficult. The rapid operating frequencies of many microactuators compound the detection problem. Effective feedback, control, and performance measurement of microactuators thus become problematic. These measurements are particularly important, however, due to the developmental nature of many microsystem technologies. Wear, lifetime issues, and optimized drive signals, for example, are poorly understood for many actuation devices. As microactuators move out of the development stage, and begin to perform work on external assemblies and environments, the various load conditions will also come into account. Since microactuators involve small masses and inertias, effective driving of external loads may require feedback-based control of the microdevice. Optical sensing technologies offer solutions to these problems of sensor motion, microactuator analysis during the development process, and integrated feedback for microactuators driving external loads. Optical methods also lend themselves to the effectively one-dimensional nature of many microsystem motions, limiting the required signal analysis to practical levels that support real-time measurement and control. This paper describes several optical techniques for sensing motion, performance, and feedback data, some of which can be integrated with the microsystems themselves. For microactuators, experimental results

indicate that real-time performance measurements are particularly revealing for understanding device motion and response. For microsensors, experimental results are also presented for interpreting motion using external and integrated optical techniques.
NTIS
*Microelectronics; Optical Equipment; Microinstrumentation; Micromechanics; Microelectromechanical Systems*

**20010121956** National Renewable Energy Lab., Golden, CO USA
**Motor Challenge Turning Point, November 1998**
Nov. 19, 1998; 8p; In English
Report No.(s): DE2000-764480; NREL/BR-330-24898; DOE/GO-10098-586; No Copyright; Avail: Department of Energy Information Bridge, Microfiche

The November 1998 of Turning Point highlights the US Industrial Electric Motor Systems Market Opportunities Assessment Report--the first of its kind in 20 years. Sponsored by DOE's Motor Challenge Program, the comprehensive assessment describes motor-system use in the industrial sector. This issue also introduces the latest version of MotorMaster+ motor management software- MotorMaster+ 3.0, and includes a case study on a fan system optimization project that yielded significant energy and cost savings for a Louisiana-Pacific plant.
NTIS
*Electric Motors; Market Research*

**20010122276** Sandia National Labs., Albuquerque, NM USA
**Aluminum-Free P-n-P InGaAsN Double Heterojunction Bipolar Transistors**
Chang, P. C.; Li, N. Y.; Baca, A. G.; Monier, C.; Laroche, J. R.; Aug. 01, 2000; 8p; In English
Report No.(s): DE2000-761866; SAND2000-2038C; No Copyright; Avail: Department of Energy Information Bridge, Microfiche

The authors have demonstrated an aluminum-free P-n-P GaAs/InGaAsN/GaAs double heterojunction bipolar transistor (DHBT). The device has a low turn-on voltage (V(sub ON)) that is 0.27 V lower than in a comparable P-n-P AlGaAs/GaAs HBT. The device shows near-ideal DC characteristics with a current gain ((beta)) greater than 45. The high-speed performance of the device are comparable to a similar P-n-P AlGaAs/GaAs HBT, with f(sub T) and f(sub MAX) values of 12 GHz and 10 GHz, respectively. This device is very suitable for low-power complementary HBT circuit applications, while the aluminum-free emitter structure eliminates issues typically associated with AlGaAs.
NTIS
*Heterojunction Devices; Semiconductors (Materials); Bipolar Transistors*

**20010122306** Sandia National Labs., Albuquerque, NM USA
**Rapid Prototyping of Patterned Multifunctional Nanostructures**
Fan, F.; Lu, Y.; Lopez, G. P.; Brinker, C. J.; Jul. 18, 2000; 8p; In English
Report No.(s): DE2000-761058; SAND2000-1747C; No Copyright; Avail: Department of Energy Information Bridge

The ability to engineer ordered arrays of objects on multiple length scales has potential for applications such as microelectronics, sensors, wave guides, and photonic lattices with tunable band gaps. Since the invention of surfactant templated mesoporous sieves in 1992, great progress has been made in controlling different mesophases in the form of powders, particles, fibers, and films. to date, although there have been several reports of patterned mesostructures, materials prepared have been limited to metal oxides with no specific functionality. For many of the envisioned applications of hierarchical materials in micro-systems, sensors, waveguides, photonics, and electronics, it is necessary to define both form and function on several length scales. In addition, the patterning strategies utilized so far require hours or even days for completion. Such slow processes are inherently difficult to implement in commercial environments. The authors present a series of new methods of producing patterns within seconds. Combining sol-gel chemistry, Evaporation-Induced Self-Assembly (EISA), and rapid prototyping techniques like pen lithography, ink-jet printing, and dip-coating on micro-contact printed substrates, they form hierarchically organized silica structures that exhibit order and function on multiple scales: on the molecular scale, functional organic moieties are positioned on pore surfaces, on the mesoscale, mono-sized pores are organized into one-, two-, or three-dimensional networks, providing size-selective accessibility from the gas or liquid phase, and on the macroscale, two-dimensional arrays and fluidic or photonic systems may be defined. These rapid patterning techniques establish for the first time a link between computer-aided design and rapid processing of self-assembled nanostructures.
NTIS
*Nanostructures (Devices); Rapid Prototyping; Computer Aided Design; Microelectronics*

**20010122389** Texas Univ., Microelectronics Research Center, Austin, TX USA

**Packaging Enhanced Optoelectronic Interconnects for Data Communications: High-performance Unidirectional Electrooptic Modulator Based on Polymeric Highly Multi-Mode Waveguides** ***Final Report, 1 Mar. 1999 - 29 Feb. 2000***

Chen, Ray T.; Sun, Degui; Lu, Xuejun; Taboada, John M.; Dubinovsky, Michael; Feb. 2000; 52p; In English

Contract(s)/Grant(s): F49620-99-1-0168; AF Proj. 3484

Report No.(s): AD-A395211; AFRL-SR-BL-TR-01-0522; No Copyright; Avail: CASI; A04, Hardcopy; A01, Microfiche

A unidirectional electro-optic modulator based on polymeric highly multi-mode waveguides was constructed using the standard VLSI techniques. A high unidirectional coupling efficiency of 100% was achieved. A high modulation depth of 99% was also experimentally achieved at 633nm wavelength. The modulator was packaging enhanced by vertically configuring the guiding multi-mode waveguide and the dumping planar waveguide. The device packing density improved by a factor of two. Based on the same configuration, a packaging enhanced polarization-insensitive thermo-optic was also built. The switch operating at wavelengths of 632.8nm and 1.3 micrometers has been demonstrated experimentally with extinction ratios of 21dB and 22dB, respectively. Such devices have an intrinsic wide optical bandwidth due to the large dynamic range of the phase-matching condition implied by the multi-mode waveguides. These devices can be used in optoelectronic interconnects for data communications.

DTIC

*Electro-Optics; Modulators; Data Transmission; Phase Matching*

**20010122643** Sandia National Labs., Albuquerque, NM USA

**Investigation of Body-Tie Effects on Ion Beam Induced Charge Collection in Silicon-On-Insulator FETs Using the Sandia Nuclear Microprobe**

Walsh,; Dodd,; Shaneyfelt,; Schwank,; Sep. 19, 2000; 21p; In English

Report No.(s): DE2000-763118; SAND2000-2310C; No Copyright; Avail: Department of Energy Information Bridge, Microfiche

Silicon-on-insulator (S01) technology exhibits three main advantages over bulk silicon technology for use in radiation environments. (1) SOI devices are immune to latchup, (2)the volume of the sensitive region (body) and hence total charge collection per transient irradiation is much reduced in SOI devices and (3) the insulating layer blocks charge collection from the substrate (i.e., no fimneling effect). This effectively raises the single event upset threshold for the SOI device. However, despite their small active volume SOI devices are still vulnerable to single event effects (SEE). Inherent in the SOI transistor design is a parasitic npn bipolar junction transistor (BJT), where the source-body-drain acts as an emitter-base-collector BJT. An ion strike to a floating (not referenced to a specific potential) body can create a condition called snapback, where excess minority carriers in the drain-body junction forward bias the sourcebody junction, causing the parasitic BJT to turn on and inject current into the drain. Tying the body to the source limits the emitter-base current and reduces the sensitivity of the device to single ion strikes. Unfortunately, the body-tie loses effectiveness with distance due to resistivity, and in regions far enough from the tie the BJT is still in effect. Using the Sandia nuclear microprobe we have created charge collection maps of SOI FETs which have different body-tie designs. Comparisons of the experiment to DAVINCI simulations are also presented. Effects of body-ties and operating voltage on snap-back thresholds are also presented and predictions of performance in radiation environments made for the different designs.

NTIS

*Irradiation; Field Effect Transistors; SOI (Semiconductors)*

**20010122648** Sandia National Labs., Albuquerque, NM USA

**Characteristics of Novel InGaAsN Double Heterojunction Bipolar Transistors**

Li, N. Y.; Chang, P. C.; Baca, A. G.; Laroche, J. R.; Ren, F.; Aug. 01, 2000; 15p; In English

Report No.(s): DE2000-761865; SAND2000-2037C; No Copyright; Avail: Department of Energy Information Bridge, Microfiche

The authors demonstrate, for the first time, both functional Pnp AlGaAs/InGaAsN/GaAs (Pnp InGaAsN) and Npn InGaP/InGaAsN/GaAs (Npn InGaAsN) double heterojunction bipolar transistors (DHBTs) using a 1.2 eV In(sub 0.03)Ga(sub 0.97)As(sub 0.99)N(sub 0.01) as the base layer for low-power electronic applications. The Pnp InGaAsN DHBT has a peak current gain ((beta)) of 25 and a low turn-on voltage (V(sub ON)) of 0.79 V. This low V(sub ON) is (approximately) 0.25 V lower than in a comparable Pnp AlGaAs/GaAs HBT. For the Npn InGaAsN DHBT, it has a low V(sub ON) of 0.81 V, which is 0.13 V lower than in an InGaP/GaAs HBT. A peak (beta) of 7 with nearly ideal I-V characteristics has been demonstrated. Since GaAs is used as the collector of both Npn and Pnp InGaAsN DHBTs, the emitter-collector breakdown voltage (BV(sub CEO)) are 10 and 12 V, respectively, consistent with the BV(sub CEO) of Npn InGaP/GaAs and Pnp AlGaAs/GaAs HBTs of comparable

collector thickness and doping level. All these results demonstrate the potential of InGaAsN DHBTs as an alternative for application in low-power electronics.
NTIS
*Bipolar Transistors; Heterojunction Devices; Indium Compounds; Gallium Compounds; Semiconductors (Materials); Characterization*

**20010122880** Argonne National Lab., IL USA
**Nanofluid technology: current status and future research**
Choi, S. U. S.; Oct. 20, 1998; 26p; In English
Report No.(s): DE2001-11048; ANL/ET/CP-97466; No Copyright; Avail: Department of Energy Information Bridge, Microfiche
Downscaling or miniaturization has been a recent major trend in modern science and technology. Engineers now fabricate microscale devices such as microchannel heat exchangers, and micropumps that are the size of dust specks. Further major advances would be obtained if the coolant flowing in the microchannels were to contain nanoscale particles to enhance heat transfer. Nanofluid technology will thus be an emerging and exciting technology of the 21st century. This paper gives a brief history of the Advanced Fluids Program at Argonne National Laboratory (ANL), discusses the concept of nanofluids, and provides an overview of the R and D program at ANL on the production, property characterization, and performance of nanofluids. It also describes examples of potential applications and benefits of nanofluids. Finally, future research on the fundamentals and applications of nanofluids is addressed.
NTIS
*Coolants; Heat Transfer; Microchannels*

**20010122911** Fermi National Accelerator Lab., Batavia, IL USA
**Light Source Unit for Hybrid Photodiode Calibration**
Freeman, J.; Los, S.; Ronzhim, A.; Oct. 31, 2000; 15p; In English
Report No.(s): DE2000-766197; FERMILAB-TM-2127; No Copyright; Avail: Department of Energy Information Bridge, Microfiche
The hybrid photodiode (HPD(1)) will be used for the CMS HCAL readout. The light source was designed and built to check the functionality of the readout. The technical parameters of the unit are presented.
NTIS
*Calibrating; Light Sources; Photodiodes*

**20010123036** Brookhaven National Lab., Upton, NY USA
**Power compression of low-frequency rf by means of a thyratron**
Zhao,; Sep. 20, 2000; 9p; In English
Report No.(s): DE2000-767181; BNL-67709; No Copyright; Avail: Department of Energy Information Bridge
To generate brief pulses of RF (radio frequency) of low frequency and very high power, the author proposes a novel system of power compression. A tetrode of modest capacity fills a storage RF cavity of very high Q. A switch then diverts the energy into the load cavity. to switch the power, a thyratron should be suitable for frequencies up to perhaps -200 MHz. Some thyratrons are capable of a closed-circuit current of about 10 kA and an open-circuit voltage of about 100 kV. With a commercial thyratron the system may deliver a pulse of power of tens even hundreds of megawatts. Presented here are the principles of operation of such a system, a schematic engineering layout and a proposed circuit diagram, including the firing circuit. Theoretically, there is no limitation on the power compression ratio.
NTIS
*Thyratrons; Compression Ratio; Systems Engineering; Radio Frequencies*

**20010123219** Princeton Univ., Plasma Physics Lab., NJ USA
**Control of the Electric Field Profile in the Hall Thruster**
Fruchtman, A.; Fisch, N. J.; Raitses, Y.; Oct. 05, 2000; 29p; In English
Report No.(s): DE2000-765155; PPPL-3494; No Copyright; Avail: Department of Energy Information Bridge, Microfiche
Control of the electric field profile in the Hall Thruster through the positioning of an additional electrode along the channel is shown theoretically to enhance the efficiency. The reduction of the potential drop near the anode by use of the additional electrode increases the plasma density there, through the increase of the electron and ion transit times, causing the ionization in the vicinity of the anode to increase. The resulting separation of the ionization and acceleration regions increases the propellant and energy utilizations. An abrupt sonic transition is forced to occur at the axial location of the additional electrode, accompanied

by the generation of a large (theoretically infinite) electric field. This ability to generate a large electric field at a specific location along the channel, in addition to the ability to specify the electric potential there, allows one further control of the electric field profile in the thruster. In particular, when the electron temperature is high, a large abrupt voltage drop is induced at the vicinity of the additional electrode, a voltage drop that can comprise a significant part of the applied voltage.
NTIS
*Electric Fields; Hall Thrusters; Electrodes*

**20010123220** Princeton Univ., Plasma Physics Lab., NJ USA
**Variational Principle for Optimal Accelerated Neutralized Flow**
Fruchtman, A.; Fisch, N. J.; Sep. 01, 2000; 14p; In English
Report No.(s): DE2000-765154; PPPL-3493; No Copyright; Avail: Department of Energy Information Bridge, Microfiche

Minimizing the energy deposited in the electron current in neutralized flows, such as in the Hall thruster, is examined. Modifying the electron current along the channel by inserting emitting electrodes, can enhance the efficiency. By employing variational methods, an optimal electron current distribution is found. The efficiency enhancement due to this effect, however, is shown to be small.
NTIS
*Electrons; Variational Principles*

**20010123259** Brookhaven National Lab., Upton, NY USA
**Front-End Electronics for Imaging Detectors**
De Geronimo, G.; O'Connor, G.; Radeka, V.; Yu, B.; Jul. 01, 2000; 8p; In English
Report No.(s): DE2000-767295; BNL-67700; No Copyright; Avail: Department of Energy Information Bridge

A key criterion for an imaging detector is the ability to perform 'quantum limited imaging', that is, to distinguish the signal charge due to a single quantum from any noise generated in the detector and/or the readout system. In addition to obtaining image intensity distribution as a function of position by quantum counting or charge integration, energy and timing measurements on every particle or photon may be performed. While a detailed optimization of an electronic readout may be different for each of the great variety of imaging detectors and their applications, all detectors, with very few exceptions, are capacitive sources of charge. The signal charge is produced either directly by ionization, or indirectly by scintillation and photo-detection.
NTIS
*Electronic Equipment; Detection; Imaging Techniques*

**20010123421** Los Alamos National Lab., NM USA
**Designing a Micro-Mechanical Transistor**
Mainieri, R.; Jun. 03, 1999; 9p; In English
Report No.(s): DE2001-763245; LA-UR-99-2676; No Copyright; Avail: Department of Energy Information Bridge

This is the final report of a three-year, Laboratory-Directed Research and Development (LDRD) project at the Los Alamos National Laboratory (LANL). Micro-mechanical electronic systems are chips with moving parts. They are fabricated with the same techniques that are used to manufacture electronic chips, sharing their low cost. Micro-mechanical chips can also contain electronic components. by combining mechanical parts with electronic parts it becomes possible to process signal mechanically. to achieve designs comparable to those obtained with electronic components it is necessary to have a mechanical device that can change its behavior in response to a small input - a mechanical transistor. The work proposed will develop the design tools for these complex-shaped resonant structures using the geometrical ray technique. To overcome the limitations of geometrical ray chaos, the dynamics of the rays will be studied using the methods developed for the study of nonlinear dynamical systems. This leads to numerical methods that execute well in parallel computer architectures, using a limited amount of memory and no inter-process communication.
NTIS
*Design Analysis; Transistors; Chips (Electronics); Fabrication; Microelectromechanical Systems*

**20010123442** Advanced Energy Systems, Inc., USA
**Inexpensive, High-Performance, Electron Gun** ***Final Report***
Bluem, H. P.; May 30, 2000; 12p; In English
Report No.(s): DE2001-761060; DOE/HEP/82723-1; No Copyright; Avail: Department of Energy Information Bridge, Microfiche

Although high performance photocathode guns find widespread application, their expense and complexity places them beyond the resources of many facilities and makes them unsuitable for commercial applications. A robust photocathode with a quantum efficiency greater than one percent that does not require an ultra-high vacuum environment would permit a major reduction in photo-cathode gun system complexity and cost by significantly reducing the drive laser power. This in turn will enable greatly expanded application of high performance photocathode technology. The focus of this research was a high quantum efficiency cathode which would also exhibit sufficient robustness to allow use in a system suitable for commercial applications.
NTIS
*Electron Guns; Low Cost; Quantum Efficiency*

**20010123622** California Univ., Lawrence Berkeley Lab., Berkeley, CA USA
**Amorphous Diamond Flat Panel Displays: Final Report of ER-LTR CRADA project with SI Diamond Technology**
Ager, J. W.; May 08, 1998; 7p; In English
Report No.(s): DE2000-767497; LBNL-41883; No Copyright; Avail: Department of Energy Information Bridge, Microfiche

The objective of this project was to determine why diamond-based films are unusually efficient electron emitters (field emission cathodes) at room temperature. Efficient cathodes based on diamond are being developed by SI Diamond Technology (SIDT) as components for bright, sunlight-readable, flat panel displays. When the project started, it was known that only a small fraction of the cathode area is active in electron emission and that the emission sites themselves are sub-micron in size. The critical challenge of this project was to develop new microcharacterization methods capable of examining known emission sites. The research team used a combination of cathode emission imaging (developed at SIDT), micro-Raman spectroscopy (LBNL), and electron microscopy and spectroscopy (National Center for Electron Microscopy, LBNL) to examine the properties of known emission sites. The most significant accomplishment of the project was the development at LBNL of a very high resolution scanning probe that, for the first time, measured simultaneously the topography and electrical characteristics of single emission sites. The increased understanding of the emission mechanism helped SIDT to develop a new cathode material, 'nano-diamond' which they have incorporated into their Field Emission Picture Element (FEPix) product. SIDT is developing large-format flat panel displays based on these picture elements that will be brighter and more efficient than existing outdoor displays such as Jumbotrons. The energy saving that will be realized if field emission displays are introduced commercially is in line with the energy conservation mission of DOE. The unique characterization tools developed in this project (particularly the new scanning microscopy method) are being used in ongoing BES-funded basic research.
NTIS
*Amorphous Materials; Diamond Films; Field Emission; Flat Panel Displays; Topography*

**20010123925** Los Alamos National Lab., NM USA
**Characterization of Epitaxial Growth of Semiconducting Rhenium 'Disilicide' Films**
Misra, A.; Verdier, M.; Mitchell, T. E.; Mahan, J. E.; Jan. 01, 2000; 9p; In English
Report No.(s): DE2001-763325; LA-UR-00-321; No Copyright; Avail: Department of Energy Information Bridge

We have characterized, through transmission electron microscopy (TEM), the ReSi(sub 2-x) thin films grown by reactive deposition on (001) Si. ReSi(sub 2.x) thin films exhibit a distorted body-centered tetragonal MoSi(sub 2)-type structure, and have excellent epitaxy on (001) Si since the face diagonal of the Si unit cell is equal to the c lattice parameter of silicide. The Si-deficient composition in the 'disilicide' may be accommodated by collapse and shear of missing Si planes to form planar faults. Kirkendall voids are also observed at the film-substrate interface. The engineering of the defect and interface structures of these complex, non-stoichiometric silicides for optimized optoelectronic properties are discussed.
NTIS
*Semiconducting Films; Thin Films; Epitaxy; Rhenium Compounds*

**20010124075** NASA Goddard Space Flight Center, Greenbelt, MD USA
**Multiplexing of Radio-Frequency Single Electron Transistors**
Stevenson, Thomas R., NASA Goddard Space Flight Center, USA; Pellerano, F. A., NASA Goddard Space Flight Center, USA; Stahle, C. M., NASA Goddard Space Flight Center, USA; Aidala, K., Yale Univ., USA; Schoelkopf, R. J., Yale Univ., USA; [2001]; 6p; In English; No Copyright; Avail: CASI; A02, Hardcopy; A01, Microfiche

We present results on wavelength division multiplexing of radio-frequency single electron transistors. We use a network of resonant impedance matching circuits to direct applied rf carrier waves to different transistors depending on carrier frequency. A two-channel demonstration of this concept using discrete components successfully reconstructed input signals with small levels

of cross coupling. A lithographic version of the rf circuits had measured parameters in agreement with electromagnetic modeling, with reduced cross capacitance and inductance, and should allow 20 to 50 channels to be multiplexed.
Author
*Wavelength Division Multiplexing; Transistors; Radio Frequencies; Carrier Frequencies; Electron Acceleration*

**20010124133** Sandia National Labs., Albuquerque, NM USA
**Predicted Pulsed-Power/Flash-Lamp Performance of the NIF Main Amplifier**
Fulkerson, E. S.; Hammond, J.; Harjes, H. C.; Moore, W. B. S.; Smith, D. L.; Jun. 22, 1999; 6p; In English
Report No.(s): DE2001-7922; SAND99-1560C; No Copyright; Avail: Department of Energy Information Bridge

The laser glass for the National Ignition Facility (NIF) Main Amplifier system is pumped by a system of 192 pulsed power/flash lamp assemblies. Each of these 192 assemblies consists of a 1.6 MJ (nominal) capacitor bank working with a Pre-Ionization/Lamp Check (PILC) pulser to drive an array of 40 flash lamps. This paper describes the predicted performance of these Power Conditioning System (PCS) modules in concert with flashlamp assemblies in NIF. Each flashlamp assembly consists of 20 parallel sets of lamps in series pairs. The sensitivity of system performance to various design parameters of the PILC pulser and the main capacitor bank is described. Results of circuit models are compared to sub-scale flashlamp tests and to measurements taken in tests of a PCS module driving a flashlamp assembly in the First Article NIF Test Module facility at Sandia National Laboratories. Also included are predictions from a physics-based, semi-empirical amplifier gain code.
NTIS
*Design Analysis; Ignition; Pulse Generators; Amplifiers; Luminaires; Performance Prediction*

**20010124863** European Space Agency. European Space Research and Technology Center, ESTEC, Space Science Dept., Noordwijk, Netherlands
**Electric Field Double Probe Antenna for the BepiColombo/MMO Satellite**
Laakso, H., European Space Agency. European Space Research and Technology Center, ESTEC, Netherlands; Grard, R., European Space Agency. European Space Research and Technology Center, ESTEC, Netherlands; Johlander, B., European Space Agency. European Space Research and Technology Center, ESTEC, Netherlands; Klinge, D., European Space Agency. European Space Research and Technology Center, ESTEC, Netherlands; Lebreton, J.-P., European Space Agency. European Space Research and Technology Center, ESTEC, Netherlands; Mercury: Space Environment, and Surface and Interior; 2001, pp. 57; In English; See also 20010124826; No Copyright; Abstract Only; Available from CASI only as part of the entire parent document

The Space Science Department of the European Space Agency has been developing double probe antennas for 30 years. The first antennas were successfully operated on the GEOS (Geodynamic Experimental Ocean Satellite)-1, -2 and ISEE (International Sun Earth Explorers)-1 satellites in 1977-1982. The proved concept was also used for the NASA Polar satellite, launched in 1996. However, it was quickly found on Polar that this type of antenna can be unstable in certain occasions. Based upon detailed studies, a new design was approved for the four Cluster satellites, launched in summer 2000. Now after one year of measurements, we know that the new sensor design is providing us with electric field observations of unprecedented quality. Therefore we are proposing to use the same proven technique on the BepiColombo/MMO (Mission Management Organization) satellite. Instrumentation: Electric field measurements are made with a double probe antenna that consists of a pair of electric probes that are placed on the tips of two opposing booms. On a spinning satellite the booms are made of a thin wire and can be quite long, of several tens of meters, in order to have the sensors in a lownoise environment. In addition, the high-quality quasistatic electric field measurements require that the preamplifiers are located close to the sensors, outside the main electronics compartment placed inside the satellite. This will be a challenge for a Mercury mission as the environment is very hot. Based upon an initial thermal analysis, however, we have been able to design a pre-amplifier box that can provide a pleasant environment for the instrument electronics. Scientific Objectives: The main variables monitored with a double probe antenna are the two-dimensional electric fields in the spin plane and the spacecraft potential where the latter is proportional to the electron density. These measurements are of fundamental importance when the structure and dynamics of the Mercury plasma environment is studied. With such observations, one can investigate the problems related to acceleration of charged particles, plasma drifts and flows, plasma waves, and variations of the plasma density. These are important issues as we will attempt to understand the Mercury plasma environment and how it respond to the solar wind variations.
Author
*Electric Fields; Space Probes; Satellite Antennas; Measuring Instruments; Mercury (Planet)*

**20010125003** Sandia National Labs., Albuquerque, NM USA

**Focused Ion Beam Induced Effects on MOS Transistor Parameters**

Abramo, M. T.; Antoniou, N.; Campbell, A. N.; Fleetwood, D. M.; Hembree, C. E.; Jul. 28, 1999; 11p; In English

Report No.(s): DE2001-9677; SAND99-1977C; No Copyright; Avail: Department of Energy Information Bridge, Microfiche

We report on recent studies of the effects of 50 keV focused ion beam (FIB) exposure on MOS transistors. We demonstrate that the changes in value of transistor parameters (such as threshold voltage, V(sub t)) are essentially the same for exposure to a Ga+ ion beam at 30 and 50 keV under the same exposure conditions. We characterize the effects of FIB exposure on test transistors fabricated in both 0.5 (micro)m and 0.225 (micro)m technologies from two different vendors. We report on the effectiveness of overlying metal layers in screening MOS transistors from FIB-induced damage and examine the importance of ion dose rate and the physical dimensions of the exposed area.

NTIS

*Ion Beams; Transistors; Metal Oxide Semiconductors; Fabrication; Metal Ions*

**20010125006** Sandia National Labs., Albuquerque, NM USA

**Research Opportunities in Crystalline Silicon Photovoltaics for the 21st Century**

Atwater, H. A.; Ciszek, T.; Feldman, L. C.; Gee, J.; Rohatgi, A.; Jul. 28, 1999; 16p; In English

Report No.(s): DE2001-9682; SAND99-1995C; No Copyright; Avail: Department of Energy Information Bridge, Microfiche

Crystalline silicon continues to be the dominant semiconductor material used for terrestrial photovoltaics. This paper discusses the scientific issues associated with silicon photovoltaics processing, and cell design that may yield cell and module performance improvements that are both evolutionary and revolutionary in nature. We first survey critical issues in 'thick' crystalline silicon photovoltaics, including novel separations processes for impurity removal, impurity and defect fundamentals, interface passivation, the role of hydrogen. Second, we outline emerging opportunities for creation of a very different 'thin-layer' silicon cell structure, including the scientific issues and engineering challenges associated with thin-layer silicon processing and cell design.

NTIS

*Crystallinity; Semiconductors (Materials); Silicon; Photovoltaic Cells*

**20010125240** Brookhaven National Lab., Upton, NY USA

**Monolithic preamplifier-shaper for measurement loss and transition radiation**

Kandasamy,; Nov. 08, 1999; 7p; In English

Report No.(s): DE2001-11473; BNL-66629; KA0404; No Copyright; Avail: Department of Energy Information Bridge

A custom monolithic circuit has been developed for the Time Expansion Chamber (TEC) of the PHENIX detector at the Relativistic Heavy Ion Collider (RHIC) at Brookhaven National Laboratory (BNL). This detector identifies particles by sampling their ionization energy loss (dE/dx) over a 3 cm drift space and by detecting associated transition radiation (TR) photons. The requirement of being simultaneously sensitive to dE/dx and TR events requires a dual-gain system. We have developed a compact solution featuring an octal preamplifier/shaper (P/S) IC with a split gain stage. The circuit, fabricated in 1.2 (micro)m CMOS process, incorporates a trans-impedance preamplifier and a 70 ns unipolar CR-RC(sup 4) shaper with ion tail compensation and active DC offset cancellation. Digitally selectable gain, peaking time, and tail cancellation as well as channel-by-channel charge injection and disable can be configured in the system via a 3-wire interface. The 3.5 x 5 square mm die is packaged in a fine-pitch 64-pin PQFP. Equivalent input noise is less than 1500 rms electrons at a power dissipation of 30 mW per channel. On a sample of 2400 chips, the DC offset was 2.3 +/- 3 mV rms without trimming. A chamber-mounted TEC-PS Printed Circuit Board (PCB) houses four PIS chips, on-board calibration circuit, and 64 analog differential line drivers which transmit the shaped pulses to crate-mounted flash ADCs. 7 m apart An RS-422 link provides digital configuration downloading and read back, and supplies the calibration strobe. The 24.6 cm x 9.5 cm board dissipates 8.5 W.

NTIS

*Preamplifiers; Radiation Detectors*

**20010125440** Argonne National Lab., IL USA

**In-situ observation of xenon nanocrystals in aluminum under electron and ion irradiation in transmission electron microscope**

Furuya, K.; Nov. 11, 1998; 5p; In English; 14th; 14th International Congress on Electron Microscopy, 31 Aug. - 4 Sep. 1998, Cancun, Mexico

Contract(s)/Grant(s): W-31109-ENG-38

Report No.(s): DE2001-11095; ANL/MSD/CP-97636; No Copyright; Avail: Department of Energy Information Bridge, Microfiche

In-situ ion irradiation in the transmission electron microscope (TEM) is one of the unique techniques to investigate the structural evolution of materials induced by particle bombardments. In spite of many efforts to get clear results from in-situ ion irradiation, the results were sometimes unclear because of physical and technical problems associated with TEM and ion beam hardwares. This paper describes a newly developed ion beam interface with an ultra-high voltage TEM (HVTEM) for in-situ observation of ion implantation of metals and alloys in atomic scale.
NTIS
*Xenon; Nanocrystals; Ion Irradiation; Electron Irradiation*

**20010125497** Sandia National Labs., Albuquerque, NM USA
**Very Low-Power Consumption Analog Pulse Processing ASIC for Semiconductor Radiation Detectors**
Wessendorf, K. O.; Lund, J. C.; Brunett, B. A.; Laguna, G. R.; Clements, J. W.; Aug. 23, 1999; 8p; In English
Report No.(s): DE2001-10184; SAND99-2170C; No Copyright; Avail: Department of Energy Information Bridge

We describe a very-low power consumption circuit for processing the pulses from a semiconductor radiation detector. The circuit was designed for use with a cadmium zinc telluride (CZT) detector for unattended monitoring of stored nuclear materials. The device is intended to be battery powered and operate at low duty-cycles over a long period of time. This system will provide adequate performance for medium resolution gamma-ray pulse-height spectroscopy applications. The circuit incorporates the functions of a charge sensitive preamplifier, shaping amplifier, and peak sample and hold circuit. An application specific integrated circuit (ASIC) version of the design has been designed, built and tested. With the exception of the input field effect transistor (FET), the circuit is constructed using bipolar components. In this paper the design philosophy and measured performance characteristics of the circuit are described.
NTIS
*Semiconductors (Materials); Radiation Detectors; Equipment Specifications*

**20010125514** Sandia National Labs., Albuquerque, NM USA
**Application of TIVA in Design Debug**
Kolachina, S.; Taylor, B.; Wills, K. S.; Cole, E. I.; Nov. 15, 2000; 7p; In English
Report No.(s): DE2001-767881; SAND2000-2854C; No Copyright; Avail: Department of Energy Information Bridge, Microfiche

Thermally-Induced Voltage Alteration (TIVA) is a relatively new technique for locating electrical defects in integrated circuits. In this paper a novel application of TIVA, locating design anomalies, is described. A newly designed integrated circuit with high and inconsistent I(sub DDQ) currents was initially diagnosed with limited success using various failsite isolation techniques. The TIVA technique was successful in accurately locating design anomalies. Results from TIVA identified a spurious ring oscillator in the design. Design modifications carried out using a focused ion beam (FIB) verified the accuracy of the results from TIVA. This study clearly extends the use of TIVA beyond that of locating electrical defects and anomalies and into the realm of design debug.
NTIS
*Anomalies; Checkout; Defects; Integrated Circuits*

**20010125527** Northeastern Univ., Boston, MA USA
**Diffraction tomography for multi-monostatic ground penetrating radar imaging. Final project report**
Devaney, A. J.; Deming, R.; Jan. 01, 1997; 30p; In English
Report No.(s): DE2001-764717; No Copyright; Avail: Department of Energy Information Bridge

The current report summarizes much of the work reported a paper entitled Inverse Problems which is the major contribution of the work performed in this grant. In particular, a generalized diffraction tomographic (DT) algorithm is derived for subsurface imaging from multi frequency multi-monostatic ground penetrating radar (GPR) data. The algorithm is based on the Born approximation for vector electromagnetic scattering and incorporates realistic near field models for the receiving and transmitting antennas. The forward scattering model is inverted analytically using the regularized pseudo inverse operator to yield an algorithm for imaging the underground region based on scattered field measurements at a set of receiving antennas. Whereas the usual inversion algorithms of DT require a lossless background medium and ideal point sources and receivers, the algorithm described here allows an attenuating background and arbitrary transmitting and receiving antennas. The algorithm places no restrictions on the radar frequency, and can thus include shallow imaging applications where the wavelengths are on the same order as the depth

of buried objects of interest. Versions of the algorithm are given for both the 3 dimensional and the 2.5 dimensional cases. Results are given of computer simulations designed to test the algorithm.
NTIS
*Algorithms; Diffraction; Ground Penetrating Radar; Imaging Techniques; Tomography; Computerized Simulation*

**20010125601** NASA Marshall Space Flight Center, Huntsville, AL USA
**Power Divider for Harmonically Rich Waveforms**
Sims, William Herbert, III, Inventor, NASA Marshall Space Flight Center, USA; Nov. 20, 2001; 12p; In English
Patent Info.: Filed 29 Oct. 1998; NASA-Case-MFS-31186-1; US-Patent-6,320,478; US-Patent-Appl-SN-182553; No Copyright; Avail: CASI; A03, Hardcopy; A01, Microfiche

A power divider divides an RF signal into two output signals having a phase difference of 180 deg. or a multiple thereof. When the RF signal is a square wave or another harmonically rich signal. the phases of the fundamental and the harmonics have the proper relationship. The divider can be implemented in the form of microstrips on a board, with one of the output microstrips having several bends to provide a different electrical length from the other.
Official Gazette of the U.S. Patent and Trademark Office
*Radio Frequencies; Dividers*

**20010125614** Argonne National Lab., IL USA
**Simplified analytic formula for magneto-optical Kerr effects in ultrathin magnetic films**
You, C. Y.; Jun. 10, 1998; 14p; In English
Report No.(s): DE2001-10842; ANL/MSD/CP-96648; No Copyright; Avail: Department of Energy Information Bridge

Expressions are presented for various magneto-optical Kerr effects in the ultrathin film limit with arbitrary magnetization direction by considering the multiple reflections within an optically thin film. The Kerr effect of p- and s-polarization consists of products of two factors: the prefactor, dependent only on the optical parameters of the system, and the main factor of the polar Kerr effect for normal incidence in the ultrathin limit.
NTIS
*Magneto-Optics; Thin Films; Kerr Magnetooptical Effect*

## 34
## FLUID MECHANICS AND THERMODYNAMICS

*Includes fluid dynamics and kinematics and all forms of heat transfer; boundary layer flow; hydrodynamics; hydraulics; fluidics; mass transfer and ablation cooling. For related information see also 02 Aerodynamics.*

**20010118506** Thermoscience Inst., Moffett Field, CA USA
**Axisymmetric Time-Dependent Computations of Expansion Tube Flow**
Wilson, Gregory J., Thermoscience Inst., USA; [1994]; 1p; In English; 33rd Aerospace Science Meeting, 9-12 Jan. 1995, Reno, NV, USA
Contract(s)/Grant(s): RTOP 505-70-91; No Copyright; Avail: Issuing Activity; Abstract Only

The goal of this work is to add insight about the flow within expansion tubes by using computational fluid dynamics. This is accomplished by comparing the results of axisymmetric numerical simulations with finite-rate chemistry to data from the HYPULSE expansion tube facility which was previously the NASA Langley expansion tube. The numerical simulations begin at the opening of the primary diaphragm and compute the flow throughout the whole facility and, thus, are able to follow and assess the effect of many of the flow features created during operation of the facility. One particular issue that will be investigated is the effect of boundary layer formation in the acceleration tube on the test gas volume and test gas conditions. Both laminar and turbulent boundary layers will be implemented. The effect of momentary shock reflection off the secondary diaphragm will also be investigated. There is concern that such a reflection will stagnate the test gas and create high levels of dissociated molecules. This is particularly important in propulsion experiments where a freestream composition different from flight conditions may influence ignition and burning data. Several different models of diaphragm rupture will be implemented in order to help understand the importance of this issue.
Author
*Tubes; Computational Fluid Dynamics; Free Flow; Laminar Boundary Layer*

**20010118543** NASA Langley Research Center, Hampton, VA USA

**Turbulence Modeling Effects on the Prediction of Equilibrium States of Buoyant Shear Flows**

Zhao, C. Y., Hong Kong Polytechnic, Hong Kong; So, R. M. C., Hong Kong Polytechnic, Hong Kong; Gatski, T. B., NASA Langley Research Center, USA; Theoretical Computational Fluid Dynamics; [2001]; Volume 14, pp. 399-422; In English

Contract(s)/Grant(s): Y-W18; PolyU5154/99E; No Copyright; Avail: CASI; A03, Hardcopy; A01, Microfiche

The effects of turbulence modeling on the prediction of equilibrium states of turbulent buoyant shear flows were investigated. The velocity field models used include a two-equation closure, a Reynolds-stress closure assuming two different pressure-strain models and three different dissipation rate tensor models. As for the thermal field closure models, two different pressure-scrambling models and nine different temperature variance dissipation rate, Epsilon(0) equations were considered. The emphasis of this paper is focused on the effects of the Epsilon(0)-equation, of the dissipation rate models, of the pressure-strain models and of the pressure-scrambling models on the prediction of the approach to equilibrium turbulence. Equilibrium turbulence is defined by the time rate (if change of the scaled Reynolds stress anisotropic tensor and heat flux vector becoming zero. These conditions lead to the equilibrium state parameters. Calculations show that the Epsilon(0)-equation has a significant effect on the prediction of the approach to equilibrium turbulence. For a particular Epsilon(0)-equation, all velocity closure models considered give an equilibrium state if anisotropic dissipation is accounted for in one form or another in the dissipation rate tensor or in the Epsilon(0)-equation. It is further found that the models considered for the pressure-strain tensor and the pressure-scrambling vector have little or no effect on the prediction of the approach to equilibrium turbulence.

Author

*Turbulence Models; Buoyancy; Shear Flow; Energy Dissipation; Computational Fluid Dynamics*

**20010119199** Oak Ridge National Lab., TN USA

**Semi-Empirical Excess Pressure Equation for CO(sub 2)-H(sub 2)O fluids at 400 C, 0--400 MPa**

Blencoe, J. G.; Anovitz, L. M.; Singh, J.; Sep. 12, 1999; 8p; In English

Report No.(s): DE2000-751601; ORNL/CP-105949; No Copyright; Avail: Department of Energy Information Bridge, Microfiche

Highly accurate and precise density data for CO(sub 2)-H(sub 2)O mixtures at 400 C 10-400 MPa, were used to develop a modified, B-truncated virial equation for excess pressure (P(sup ex)). This function and empirical equations of state for H(sub 2)O and CO(sub 2) accurately represent the experimentally determined densities, and interpolate smoothly between data points. Integrating the P(sub ex) expression with respect to molar volume yields an equation for excess Helmholtz free energy, which can be used to calculate other excess properties of interest. The P(sup ex) modeling method has important advantages over more conventional, alternative approaches.

NTIS

*Equations of State; Free Energy; Density (Mass/Volume); Virial Coefficients*

**20010119239** Scripps Institution of Oceanography, Marine LIFE Research Group, La Jolla, CA USA

**Turbulence Processes in the Stable Marine Atmospheric Boundary Layer** ***Annual Report, 30 Nov. 2000-30 Sep. 2001***

Dorman, Clive E.; Brooks, Ian M.; Jan. 2000; 5p; In English

Contract(s)/Grant(s): N00014-01-1-0258

Report No.(s): AD-A395050; No Copyright; Avail: CASI; A01, Hardcopy; A01, Microfiche

The long-term goals of this study are to improve our understanding of turbulence processes within the stable marine atmospheric boundary layer in spatially heterogeneous coastal environments with the aim of improving numerical representation of such environments.

DTIC

*Atmospheric Boundary Layer; Turbulence; Wind (Meteorology); Coastal Water*

**20010119432** Oak Ridge National Lab., TN USA

**Hydrodynamics of Gas-Liquid Counterflow Through Corrugated Parallel Plates**

de Almeida, V. F.; Nov. 05, 1999; 4p; In English

Report No.(s): DE2000-15059; ORNL/CP-105498; No Copyright; Avail: Department of Energy Information Bridge, Microfiche

Structured packings utilized in today's distillation packed towers consist of stacked units of many vertically oriented parallel corrugated plates. The V-shaped corrugations are oriented at a fixed angle with respect to the vertical direction, and the corrugation angle in adjacent plates are oriented in reverse direction. Points of contact at the crests of the corrugations between adjacent plates form an unconsolidated porous medium with known topology. Modern structured packings have been gaining acceptance in several separation processes, particularly distillation where gas/vapor and liquid flow countercurrently through the packing. In

addition, structured packings have been credited with relatively low pressure drop, high efficiency, low holdup,and higher capacity; the packing also can be made corrosion resistive.
NTIS
*Corrugated Plates; Counterflow; Hydrodynamics; Parallel Plates*

**20010119562** Atomic Energy Commission, Idaho Operations Office, Idaho Falls, ID USA
**Two-Phase Mass Flow Measurement Using Noise Analysis**
Blotter, J.; Stephens, A. G.; Keller, J. G.; Evans, R. P.; May 01, 1999; 6p; In English
Report No.(s): DE2001-10489; INEEL/CON-99-00524; No Copyright; Avail: Department of Energy Information Bridge, Microfiche

The purpose of this work is to develop a low cost, non-intrusive, mass flow measurement sensor for two-phase flow conditions in geothermal applications. The emphasis of the work to date has been on a device that will monitor two-phase flow in the above-ground piping systems. The flashing brines have the potential for excessive scaling and corrosion of exposed surfaces, which can reduce the effectiveness of any measurement device. A major objective in the work has been the development of an instrument that is less susceptible to the scaling and corrosion effects. The focus of the project efforts has been on transducer noise analysis, a technology initiated at the INEEL. A transducer sensing a process condition will have, in addition to its usual signal, various noise components superimposed upon the primary signal that can be related to flow. Investigators have proposed that this technique be applied to steam and liquid water flow mixtures where the signal from an accelerometer mounted on an external pipe surface is evaluated to determine flow rate.
NTIS
*Brines; Corrosion; Flow Velocity; Flow Measurement; Water*

**20010119584** Deutsches Zentrum fuer Luft- und Raumfahrt e.V., Goettingen, Germany
**GAMM 2000 Annual Meeting, Minisymposia, Short Communications in Mathematics and Mechanics, Section 9-25, University of Gottingen, Germany, April 2-7, 2000 -Volume 81 - Supplement 3**
Meier, Gerd E.; Apr. 2000; 362p; In English
Contract(s)/Grant(s): F61775-00-W-F017
Report No.(s): AD-A394877; CSP-00-5017-SUPPL-3; No Copyright; Avail: CASI; A16, Hardcopy; A03, Microfiche

This is the final Conference Proceedings for GAMM 2000, held 2-7 April 2000 at the University of Goettingen. This is an interdisciplinary conference in Fluid Mechanics and Numerics in general and include topics such as Aspects of Vortex Dynamics; Controlling Chaos; Multi-scale Theory; Flow Control and optimization; Gas Dynamic; Aerothermodynamic; Turbulence; and others.
DTIC
*Conferences; Fluid Mechanics*

**20010119604** Army Research Lab., Human Research and Engineering Directorate, Aberdeen Proving Ground, MD USA
**A Numerical Investigation of Supersonic Flow Around Aft Bodies** ***Final Report, Jun. 1990-Jul. 2000***
Catalano, George D.; Sturek, Walter B.; Sep. 2001; 24p; In English
Report No.(s): AD-A394929; ARL-RP-32; No Copyright; Avail: CASI; A03, Hardcopy; A01, Microfiche

A numerical investigation has been made for supersonic flow past a cylindrical aft body with and without base bleed and a cylindrical boat tail. Comparison was made to available experimental data. The effect of grid cell density and turbulence models were examined. The calculation of the base flow region was much more highly dependent on grid density that was the forebody or outer flow field Agreement between the numerical and experimental results improved with the inclusion of the base bleed.
DTIC
*Turbulent Flow; Compressible Flow; Supersonic Flow; Afterbodies*

**20010119614** California Univ., Lawrence Radiation Lab., Berkeley, CA USA
**Necessary Conditions for Similar Solutions of Problems of Turbulent-Gas Dynamics**
Croweley, Barbara K.; Jan. 31, 1967; 29p; In English
Report No.(s): AD-A395022; UCRL-50211; No Copyright; Avail: CASI; A03, Hardcopy; A01, Microfiche

The quasi-one-dimensional conservation equations with friction, heat, and mass sources are considered. Necessary conditions for similar solutions of these equations are mathematically derived, and these conditions are verified by sample computer calculations.
DTIC
*Conservation Equations; Gas Dynamics; Problem Solving; Turbulence*

**20010119959** NASA Ames Research Center, Moffett Field, CA USA
**Effects of Heat Release on a Two-Dimensional Reacting Shear Layer**
Moser, Robert, NASA Ames Research Center, USA; Higuera, F., Center for Turbulence Research, USA; [1994]; 1p; In English; Forty Seventh Meeting of the American Physical Society, Division of Fluid Dynamics, 20-22 Nov. 1994, Atlanta, GA, USA; Sponsored by American Physiological Society, USA
Contract(s)/Grant(s): RTOP 505-59-50; No Copyright; Avail: Issuing Activity; Abstract Only

The diffusion controlled binary reaction between initially segregated reactants in a two-dimensional low Mach number mixing layers is studied via numerical simulation. The stoichiometric ratio of the reactants is chosen to be much larger than one, as is typical of hydrocarbon flames in air. This results is a flame that is offset from the main vortical region of the mixing layer. In agreement with experimental observations, the flame remains surprisingly uncontorted during the flow evolution and is not entrained into the mixing layer. The effect of the heat release of the flame on the evolution of the mixing layer is thus similar to the effect of a difference in free-stream density between the two sides of the layer. The resulting baroclinic torque inhibits the familiar rolup and pairing of mixing layer vortices common in constant density flows. This also contributes to the layers inability to entrain the flame. The increase in viscosity caused by the heating of the flame reduces the effective Reynolds number of the flow. But, contrary to what has commonly been suggested, this is not the major reason for the inhibition of the usual large-scale mixing layer structures.
Author
*Mixing Layers (Fluids); Binary Mixtures; Chemical Reactions; Free Flow; Heat Transfer*

**20010120095** NASA Ames Research Center, Moffett Field, CA USA
**Heating Analysis of the Lockheed Lifting Body**
Palmer, Grant, NASA Ames Research Center, USA; Henline, Bill, NASA Ames Research Center, USA; Olynick, Dave, NASA Ames Research Center, USA; [1994]; 1p; In English; 29th AIAA Thermophysics Conference, 19-22 Jun. 1995, San Diego, CA, USA; Sponsored by American Inst. of Aeronautics and Astronautics, USA
Contract(s)/Grant(s): RTOP 527-10-01; No Copyright; Avail: Issuing Activity; Abstract Only

Computational fluid dynamic (CFD) analysis is performed on the Lockheed Lifting Body Single-Stage-to-Orbit vehicle to determine the heat transfer to the vehicle during its descent trajectory. Seven species, chemical nonequilibriurn computations using the GASP code will be completed at several trajectory points to assess the thermal protection requirements of the vehicle. Sophisticated surface boundary conditions including in-depth conduction, catalycity, and a variable temperature wall have been incorporated into the flow solver.
Author
*Computational Fluid Dynamics; Heat Transfer; Thermal Protection; Boundary Conditions*

**20010120125** Army Research Lab., Human Research and Engineering Directorate, Aberdeen Proving Ground, MD USA
**Computational Fluid Dynamics Modeling of a 40-mm Grenade with and Without Jet Flow** ***Final Report, Feb. 1999-Mar. 2001***
Sahu, Jubaraj; Heavey, Karen R.; Sep. 2001; 38p; In English; Original contains color images
Contract(s)/Grant(s): Proj-1L162618AH80
Report No.(s): AD-A394984; ARL-TR-2572; No Copyright; Avail: CASI; A03, Hardcopy; A01, Microfiche

This report describes a computational study undertaken to consider the aerodynamic effect of small tiny jets as a means to provide the control authority needed to maneuver a projectile at low subsonic speeds. Scalable Navier-Stokes computational techniques have been used to obtain numerical solutions for the jet-interaction flow field for a projectile at subsonic speeds. Computed results have been obtained at low subsonic speeds at 0 deg and 4 deg angle of attack. Both steady and unsteady jets have been considered. For comparison purposes, a jet-off case was also computed. Qualitative flow field features show the interaction of jets with the free stream flow. Numerical results show the effect of the jet locations and sizes on the flow field and surface pressures, and hence on the aerodynamic coefficients. Unsteady jet results have been obtained for a two-dimensional (2-D) jet flow and compared with experimental data for validation. Some results obtained with an unsteady jet for the subsonic projectile

are included. These numerical results are being assessed to determine if small tiny jets can be used to provide the control authority needed for maneuvering munitions in lieu of canards and fins.
DTIC
*Computational Fluid Dynamics; Mathematical Models; Aerodynamic Coefficients; Numerical Analysis*

**20010120126** Army Research Lab., Human Research and Engineering Directorate, Aberdeen Proving Ground, MD USA
**On the Aerodynamic Heating of a KE Pentrator - Conductive Material Heating and Thermal Gradients Prior to Transient Impact Loading** ***Final Report, Oct. 2000-May 2001***
Bjerke, Todd W.; Sep. 2001; 30p; In English
Contract(s)/Grant(s): 1L1601102AH42
Report No.(s): AD-A394983; ARL-TR-2574; No Copyright; Avail: CASI; A03, Hardcopy; A01, Microfiche

The temperature increase in the main body portion of a kinetic energy penetrator flying at sea level with a speed of 1,500 m/s was calculated using an analytical conduction analysis with a convective boundary condition. The penetrator was modeled as a smooth cylinder of uniform diameter and material properties. The results from a previously published computational fluid dynamics simulation were used to provide the convective heat transfer coefficient and the temperature of the gas flowing over the surface of the penetrator. A separation of variables solution was used for the parabolic time-dependent conduction equation. The derived solution along with material properties for tungsten and depleted uranium were used to obtain the temperature increase profile through the radius of the penetrator as a function of flight time Both materials showed significant heating within 3 5 of flight. The tungsten penetrator exhibited nearly uniform heating across the radius, whereas heating of the depleted uranium penetrator was confined to the outermost region of the cylinder due to its low coefficient of thermal conductivity.
DTIC
*Penetration; Kinetic Energy; Aerodynamic Heating; Heat Transfer Coefficients; Convective Heat Transfer*

**20010120129** Wright State Univ., Dept. of Mechanical and Materials Engineering, Dayton, OH USA
**Computational Mechanics Approach for Multidisciplinary Nonlinear Sensitivity Analysis** ***Final Report, 1 Mar. 1998-30 Nov. 2000***
Grandhi, Ramana V.; Jan. 2000; 6p; In English
Contract(s)/Grant(s): F49620-98-1-0354
Report No.(s): AD-A394973; AFRL-SR-BL-TR-01-0503; No Copyright; Avail: CASI; A02, Hardcopy; A01, Microfiche

Efficient and accurate prediction of nonlinear airloads is necessary for designing the aircraft in the transonic regime. The flow in the transonic regime is a mixture of subsonic and supersonic flow with embedded shocks. The governing transonic aerodynamic equations are highly nonlinear and are computationally expensive to solve. The aerodynamic nonlinearities have a significant impact on the aeroelastic quantities and on the resulting designs. Hence they have to be taken into account. Full fledged euler or Navier-Stokes solution methods cannot be used in the preliminary design due to the enormous cost involved.
DTIC
*Aerodynamics; Computer Programming; Aerodynamic Loads*

**20010120479** Deutsches Zentrum fuer Luft- und Raumfahrt e.V., Goettingen, Germany
**GAMM 2000 Annual Meeting, Volume 81**
Meier, Gerd E., Deutsches Zentrum fuer Luft- und Raumfahrt e.V., Germany; April 2000; 164p; In English; GAMM 2000 Annual Meeting, 2-7 Apr. 2000, Gottingen, German Democratic Republic
Contract(s)/Grant(s): F61775-00-W-F017
Report No.(s): AD-A394875; CSP-00-5017-SUPPL-1; No Copyright; Avail: CASI; A08, Hardcopy; A02, Microfiche

This is the final Conference Proceedings for GAMM 2000, held 2-7 April 2000 at the University of Goettingen. This is an interdisciplinary conference in Fluid Mechanics and Numerics in general and include topics such as Aspects of Vortex Dynamics; Controlling Chaos; Multi-scale Theory; Flow Control and optimization; Gas Dynamic; Aerothermodynamic; Turbulence; and others.
DTIC
*Fluid Mechanics; Turbulence; Aerothermodynamics*

**20010120493** Johns Hopkins Univ., Dept. of Mechanical Engineering, Baltimore, MD USA
**Instrumentation to Support PIV and HPIV Measurements in an Axial Turbomachine Flow Visualization Facility** ***Final Report, Apr. 2000 - Mar. 2001***
Katz, Joseph; Meneveau, Charles; Jun. 09, 2001; 24p; In English; Original contains color images

Contract(s)/Grant(s): F49620-00-1-0199
Report No.(s): AD-A395130; AFRL-SR-BL-TR-01-0485; No Copyright; Avail: CASI; A03, Hardcopy; A01, Microfiche

This DURIP grant has provided instrumentation that supports an AFOSR sponsored program. The objective of this program is to measure the unsteady flow in axial turbomachines and use the data to address turbulence and flow modeling issues that are specific to such complex environments. The motivation is to examine turbulence and unsteady flow phenomena at three levels of modeling: passage-averaged, steady RANS, unsteady RANS, and subgrid scale stress modeling for LES. The report describes in detail our unique two-stage axial-turbomachine flow visualization facility, specifying the instruments purchased under the resent grant and how they fit into the system. This facility contains fluid (concentrated solution of NaI in water with an optical index of refraction that matches that of the acrylic blades of the second stage. Consequently, it allows unobstructed view on an entire stage including the rotor, stator and the gas between blade rows. Two and three dimensional velocity measurement can be performed using 2-D Particle Image Velocimetry, planar 3-D measurements using stereo-IV and full 3-D HPIV. The report also describes current 2-D PIV measurements and presents sample data. With available access to any desired plane, these measurements provide data on rotor-stator interactions, the effects of wakes on downstream blades, tip leakage flows and hub vortices and their interactions with neighboring blades, unsteady separation, particularly off-design conditions, etc.
DTIC
*Turbomachinery; Turbulence Models; Axial Flow; Flow Visualization*

**20010120494** New Mexico Univ., Dept. of Mechanical Engineering, Albuquerque, NM USA
**PIV Diagnostics for Flow Control Applications** ***Final Report, Apr. 2000 - Apr. 2001***
Vorobieff, Peter; Truman, C. R.; Jul. 31, 2001; 5p; In English
Contract(s)/Grant(s): F49620-00-1-0186
Report No.(s): AD-A395131; AFRL-SR-BL-TR-01-0468; No Copyright; Avail: CASI; A01, Hardcopy; A01, Microfiche

We have developed a flexible instrumentation system for quantitative velocity-field measurement in a variety of experiments. The system integrates lasers, digital cameras, and a translation stage for PIV (particle image velocimetry) diagnostics. Several flows have already been investigated: the onset of vortex shedding in a water tow tank, development of a far wake in a water tow tank, Kelvin-Helmholtz instability in a wind tunnel, and a flow from a long crack in a pipe. Among the most important new results obtained with the experimental equipment provided by this grant is the following. We have determined the Reynolds number (i.e., critical velocity) at which the second wake (a regular pattern emerging in the far wake of a bluff body) is destroyed by turbulence.
DTIC
*Particle Image Velocimetry; Flow Characteristics; Velocity Distribution; Diagnosis*

**20010120839** General Electric Co., Cincinnati, OH USA
**Data Book Physical Properties and Flow Characteristics of Air**
Hobbs, J. L.; Lapides, M. E.; Mar. 1956; 62p; In English
Contract(s)/Grant(s): AF 33(600)-38062; AT (11-1)-171
Report No.(s): AD-A395296; APEX-527; No Copyright; Avail: CASI; A04, Hardcopy; A01, Microfiche

This report presents data on the physical properties and flow characteristics of air. These data have been compiled from several different sources outside the Department and from charts prepared within the Department. The report was prepared as a data book to be used as an aid in calculations.
DTIC
*Charts; Flow Characteristics; Air Flow*

**20010120842** Woods Hole Oceanographic Inst., MA USA
**Spatial Variability of Bottom Turbulence Over a Linear Sand Ridge Mooring Deployment and AUTOSUB AUV Survey Cruise Report**
Voulgaris, George; Trowbridge, John H.; Terray, Eugene; Aug. 2001; 45p; In English
Contract(s)/Grant(s): N00014-01-1-0255
Report No.(s): AD-A395286; WHOI-2001-09; No Copyright; Avail: CASI; A03, Hardcopy; A01, Microfiche

Two successful AUTOSUB deployments were carried out during August 1999 as part of the AUTOSUB Thematic Program project titled ”Spatial Variability of Bottom Turbulence over a Linear Sand Ridge”, funded by the Natural Environment Research Council (NERC), U.K. The AUTOSUB Autonomous Underwater Vehicle (AUV) was deployed and used to survey flow patterns at a location near the Broken Bank, southern North Sea, U.K. The AUV was equipped with acoustic flow and turbulence sensors and its surveys aimed at mapping the spatial variation of flow and turbulence near the bed and over topographic features. Three instrumented bottom mounted frames were also deployed, around the AUV survey area, for a period of approximately 5 days.

The purpose of this array was to gather information on the temporal variability of the flow and turbulence near the seabed and to identify the important terms that drive circulation around the bank. Additional data were gathered including CTD casts, seabed samples and acoustic images of the seabed (side-scan sonar). The purpose of this data collection was to help identify the flow patterns around ridges and to understand the mechanisms controlling the maintenance and evolution of such features. This report describes the operations carried out by researchers from the University of South Carolina, Woods Hole Oceanographic Institution, Southampton Centre and the AUTOSUB Team on the R.V. RRS Challenger during the period 17 - 28th August 1999.
DTIC
*Turbulence; Ocean Bottom; Spatial Distribution; Variability*

**20010121541** NASA Ames Research Center, Moffett Field, CA USA
**Numerical Generation of Asymmetric Flows about Slender Bodies of Revolution at Extreme Incidence**
Murman, Scott M., MCAT Inst., USA; Schiff, Lewis B., NASA Ames Research Center, USA; [1994]; 1p; In English; AIAA 33rd Aerospace Sciences Meeting and Exhibit, 9-12 Jan. 1995, Reno, NV, USA; Sponsored by American Inst. of Aeronautics and Astronautics, USA
Contract(s)/Grant(s): RTOP 505-68-00; No Copyright; Avail: Issuing Activity; Abstract Only

It is well known that slender bodies of revolution will develop an asymmetric, unsteady flow pattern in experimental tests, if the angle of incidence to the oncoming stream is above a critical value. It has been suggested that the origin of these asymmetric flows may stem from geometric imperfections of the model being tested, or from disturbances in the oncoming stream. In numerical simulations, it is possible to generate bodies of revolution which are perfectly symmetric about their longitudinal axis, and to impose uniform flow conditions which are free from disturbances. The current work presents numerical simulations of the flow about an ogive-cylinder configuration at 40 and 60 degree angle of incidence. These simulations. were performed using numerical algorithms which are also symmetric about the lateral plane of the cylinder body. The flowfields at 40 degree angle of attack were seen to remain symmetric to the round-off accuracy of the computer. At 60 degree angle of attack, a lateral force coefficient developed of O(1) which progressed to an alternate vortex shedding in time. The nature of this lateral force generation and vortex shedding was dependent on the choice of numerical algorithm. The origin of the asymmetries observed in the 60 degree angle of attack computations were traced to round-off errors in the implicit block-matrix inverter. A means of inverting the implicit operator matrices, which maintains the symmetry of the overall numerical algorithm was implemented.
Author
*Unsteady Flow; Computerized Simulation; Bodies of Revolution; Angle of Attack; Slender Bodies*

**20010122272** NASA Ames Research Center, Moffett Field, CA USA
**Progress In Incompressible Pump Flow Calculations**
Kiris, Cetin, MCAT Inst., USA; Kwak, Dochan, NASA Ames Research Center, USA; [1994]; 1p; In English; Workshop for CFD Applications in Rocket Propulsion, 19-21 Apr. 1994, Huntsville, AL, USA
Contract(s)/Grant(s): RTOP 505-59-53; No Copyright; Avail: Issuing Activity; Abstract Only

Steady and unsteady flows for propulsion systems are efficiently simulated by solving the incompressible Navier-Stokes equations. The solution method is based on the pseudo compressibility approach and uses an implicit-upwind differencing scheme together with the Gauss-Seidel line relaxation method. Current computations use one equation Baldwin-Barth turbulence model which is derived from a simplified form of the standard kappa - epsilon model equations. The resulting computer code is applied to the flow analysis inside an advanced rocket pump impeller in steadily rotating reference frames. Numerical results are compared with experimental measurements. The effects of exit and shroud cavities with the leak-age flow are investigated. Time-accurate incompressible Navier-Stokes formulation with the overlapped grid scheme capability was evaluated by using MIT flapping foil experiment. The grid dependency, turbulence model effects, and the effect of order of differencing were investigated. Numerical results were compared against experimental data. The resulting procedure were applied to unsteady flapping foil calculations. Two upstream NACA 0025 foils perform high frequency synchronized motion and generate unsteady flow conditions to the downstream larger stationary foil. Comparison between unsteady experimental data and numerical results from two different moving boundary procedures will be presented.
Author
*Computerized Simulation; Compressibility; Boundaries; Computational Grids; Incompressible Flow; Mathematical Models; Propulsion System Configurations; Unsteady Flow*

**20010122275** Purdue Univ., School of Mechanical Engineering, West Lafayette, IN USA

**Performance of Straight-Fin and Microchannel Heat Exchangers in Steady and Periodic Flows** ***Final Report, May 1999 - May 2001***

Alexander, Aaron; Mongeau, Luc; Braun, James E.; Oct. 08, 2001; 54p; In English

Contract(s)/Grant(s): N00014-99-1-0642

Report No.(s): AD-A395249; HL2001-18; No Copyright; Avail: CASI; A04, Hardcopy; A01, Microfiche

The performance of straight-fin and microchannel heat exchangers was investigated in steady and periodic flows. Steady flow measurements were performed using an open test section wind tunnel. Periodic flow measurements were performed using a thermoacoustic cooler prototype. Detailed temperature measurements were made for varying operating conditions using thermocouple arrays. The results suggest that nondimensional heat transfer coefficients based on stack end temperatures calculated from steady flow data may be applicable to predict the thermal performance in a periodic flow, provided the root-mean-square local particle velocity is used as the velocity scale. The accuracy of rms-based steady flow correlations may be comparable or in some cases better than that of linearized boundary layer models frequently used in thermoacoustics.

DTIC

*Heat Exchangers; Thermoacoustic Effects; Flow Measurement; Temperature Effects; Test Chambers*

**20010122293** University of Central Florida, Mechanical, Materials, and Aerospace Engineering, Orlando, FL USA

**Investigation of Conjugate Heat Transfer in Turbine Blades and Vanes** ***Final Report***

Kassab, A. J., University of Central Florida, USA; Kapat, J. S., University of Central Florida, USA; [2001]; 31p; In English

Contract(s)/Grant(s): NAG3-2311; NRA-99-GRC-2; No Copyright; Avail: CASI; A03, Hardcopy; A01, Microfiche

We report on work carried out to develop a 3-D coupled Finite Volume/BEM-based temperature forward/flux back (TFFB) coupling algorithm to solve the conjugate heat transfer (CHT) which arises naturally in analysis of systems exposed to a convective environment. Here, heat conduction within a structure is coupled to heat transfer to the external fluid which is convecting heat into or out of the solid structure. There are two basic approaches to solving coupled fluid structural systems. The first is a direct coupling where the solution of the different fields is solved simultaneously in one large set of equations. The second approach is a loose coupling strategy where each set of field equations is solved to provide boundary conditions for the other. The equations are solved in turn until an iterated convergence criterion is met at the fluid-solid interface. The loose coupling strategy is particularly attractive when coupling auxiliary field equations to computational fluid dynamics codes. We adopt the latter method in which the BEM is used to solve heat conduction inside a structure which is exposed to a convective field which in turn is resolved by solving the NASA Glenn compressible Navier-Stokes finite volume code Glenn-HT. The BEM code features constant and bi-linear discontinuous elements and an ILU-preconditioned GMRES iterative solver for the resulting non-symmetric algebraic set arising in the conduction solution. Interface of flux and temperature is enforced at the solid/fluid interface, and a radial-basis function scheme is used to interpolated information between the CFD and BEM surface grids. Additionally, relaxation is implemented in passing the fluxes from the conduction solution to the fluid solution. Results from a simple test example are reported.

Author

*Conductive Heat Transfer; Finite Volume Method; Turbine Blades; Vanes; Computational Fluid Dynamics; Mathematical Models*

**20010122399** Deutsches Zentrum fuer Luft- und Raumfahrt e.V., Goettingen, Germany

**GAMM 2000 Annual Meeting: Minisymposia, Short Communications in Mathematics and Mechanics, Volume 81**

Meier, Gerd E., Deutsches Zentrum fuer Luft- und Raumfahrt e.V., Germany; April 2000; 277p; In English; GAMM 2000 Annual Meeting: Minisymposia, Short Communications in Mathematics and Mechanics, Section 1-8, 2-7 Apr. 2000, Gottingen, Germany

Contract(s)/Grant(s): F61775-00-W-F017

Report No.(s): AD-A394876; CSP-00-5017-VOL-81-SUPPL-2; No Copyright; Avail: CASI; A13, Hardcopy; A03, Microfiche

This is the final Conference Proceedings for GAMM 2000, held 2-7 April 2000 at the University of Goettingen. This is an interdisciplinary conference in Fluid Mechanics and Numerics in general and include topics such as Aspects of Vortex Dynamics; Controlling Chaos; Multi-scale Theory; Flow Control and optimization; Gas Dynamic; Aerothermodynamic; Turbulence; and others.

DTIC

*Fluid Mechanics; Aerothermodynamics; Turbulence*

**20010122400** Defence Science and Technology Organisation, Sirframes and Engines Div., Fishermans Bend, Australia
**Review of Vortex Methods for Simulation of Vortex Breakdown**
Levinski, Oleg, Defence Science and Technology Organisation, Australia; September 2001; 36p; In English
Report No.(s): DSTO-TR-1211; DODA-AR-012-021; Copyright; Avail: Issuing Activity

The aim of this work is to identify current developments in the field of vortex breakdown modelling in order to initiate the development of a numerical model for the simulation of F/A-18 empennage buffet. Some attempts at using vortex models for prediction of vortex breakdown were found in the open literature. Their advantages and shortcomings are discussed, allowing the evaluation of their feasibility for the computation of LEX vortex burst. It was concluded that vortex methods are able to simulate an onset of breakdown in simple vortical flows. However, their predictive abilities require further improvement to provide accurate modelling of the temporal and spatial characteristics of the unsteady pressure field past a burst LEX vortex.
Author
*Vortex Breakdown; Simulation; Models; Buffeting*

**20010122649** Sandia National Labs., Albuquerque, NM USA
**Massively Parallel Direct Simulation of Multiphase Flow**
Cook, B. K.; Preece, D. S.; Williams, J. R.; Aug. 10, 2000; 4p; In English
Report No.(s): DE2000-761863; SAND2000-2035C; No Copyright; Avail: Department of Energy Information Bridge, Microfiche

The authors' understanding of multiphase physics and the associated predictive capability for multi-phase systems are severely limited by current continuum modeling methods and experimental approaches. This research will deliver an unprecedented modeling capability to directly simulate three-dimensional multi-phase systems at the particle-scale. The model solves the fully coupled equations of motion governing the fluid phase and the individual particles comprising the solid phase using a newly discovered, highly efficient coupled numerical method based on the discrete-element method and the Lattice-Boltzmann method. A massively parallel implementation will enable the solution of large, physically realistic systems.
NTIS
*Multiphase Flow; Parallel Processing (Computers)*

**20010122827** Pacific Northwest National Lab., Richland, WA USA
**Review of Upscaling Methods for Describing Unsaturated Flow**
Wood, B. D.; Sep. 26, 2000; 29p; In English
Report No.(s): DE2000-763385; PNNL-13325; No Copyright; Avail: Department of Energy Information Bridge

The representation of small-scale features can be a challenge when attempting to model unsaturated flow in large domains. Upscaling methods offer the possibility of reducing the amount of resolution required to adequately simulate such a problem. In this report, the various upscaling techniques that are discussed in the literature are reviewed. The following upscaling methods have been identified from the literature: (1) stochastic methods; (2) renormalization methods; and (3) volume averaging and homogenization methods; in addition, a final technique, full resolution numerical modeling, is also discussed. Each of these techniques has its advantages and disadvantages. The trade-off is a reduction in accuracy in favor of a method that is easier to employ. For practical applications, the most reasonable approach appears to be one in which any of the upscaling methods identified above maybe suitable for upscaling in regions where the variations in the parameter fields are small. For regions where the subsurface structure is more complex, only the homogenization and volume averaging methods are probably suitable. With the continual increases in computational capacity, fill-resolution numerical modeling may in many instances provide a tractable means of solving the flow problem in unsaturated systems.
NTIS
*Mathematical Models; Scaling Laws; Stochastic Processes; Normalizing (Statistics)*

**20010122932** NASA Ames Research Center, Moffett Field, CA USA
**The NASA Ames Hypersonic Combustor-Model Inlet CFD Simulations and Experimental Comparisons**
Venkatapathy, E., NASA Ames Research Center, USA; Tokarcik-Polsky, S., NASA Ames Research Center, USA; Deiwert, G. S., NASA Ames Research Center, USA; [1995]; 1p; In English; 6th International AIAA Aerospace Plane and Hypersonic Technologies Conference, 10-14 Apr. 1995, Chatanooga, TN, USA
Contract(s)/Grant(s): RTOP 505-70-62; No Copyright; Avail: Issuing Activity; Abstract Only

Computations have been performed on a three-dimensional inlet associated with the NASA Ames combustor model for the hypersonic propulsion experiment in the 16-inch shock tunnel. The 3-dimensional inlet was designed to have the combustor inlet flow nearly two-dimensional and of sufficient mass flow necessary for combustion. The 16-inch shock tunnel experiment is a short

duration test with test time of the order of milliseconds. The flow through the inlet is in chemical non-equilibrium. Two test entries have been completed and limited experimental results for the inlet region of the combustor-model are available. A number of CFD simulations, with various levels of simplifications such as 2-D simulations, 3-D simulations with and without chemical reactions, simulations with and without turbulent conditions, etc., have been performed. These simulations have helped determine the model inlet flow characteristics and the important factors that affect the combustor inlet flow and the sensitivity of the flow field to these simplifications. In the proposed paper, CFD modeling of the hypersonic inlet, results from the simulations and comparison with available experimental results will be presented.
Author
*Hypersonic Flight; Combustion Chambers; Computational Fluid Dynamics; Simulation; Shock Tunnels; Inlet Flow*

**20010122939** Computer Sciences Corp., Moffett Field, CA USA
**Parallel Preconditioning for CFD Problems on the CM-5**
Simon, Horst D., Computer Sciences Corp., USA; Kremenetsky, Mark D., Thinking Machines Corp., USA; Richardson, John, Thinking Machines Corp., USA; [1994]; 1p; In English; International Workshop on Solution Techniques for Large-Scale CFD Problems, 26-28 Sep. 1994, Montreal, Quebec, Canada
Contract(s)/Grant(s): NAS2-12961; RTOP 536-01-11; No Copyright; Avail: Issuing Activity; Abstract Only

Up to today, preconditioning methods on massively parallel systems have faced a major difficulty. The most successful preconditioning methods in terms of accelerating the convergence of the iterative solver such as incomplete LU factorizations are notoriously difficult to implement on parallel machines for two reasons: (1) the actual computation of the preconditioner is not very floating-point intensive, but requires a large amount of unstructured communication, and (2) the application of the preconditioning matrix in the iteration phase (i.e. triangular solves) are difficult to parallelize because of the recursive nature of the computation. Here we present a new approach to preconditioning for very large, sparse, unsymmetric, linear systems, which avoids both difficulties. We explicitly compute an approximate inverse to our original matrix. This new preconditioning matrix can be applied most efficiently for iterative methods on massively parallel machines, since the preconditioning phase involves only a matrix-vector multiplication, with possibly a dense matrix. Furthermore the actual computation of the preconditioning matrix has natural parallelism. For a problem of size n, the preconditioning matrix can be computed by solving n independent small least squares problems. The algorithm and its implementation on the Connection Machine CM-5 are discussed in detail and supported by extensive timings obtained from real problem data.
Author
*Parallel Processing (Computers); Massively Parallel Processors; Linear Systems; Algorithms; Matrices (Mathematics); Computational Fluid Dynamics*

**20010123423** FAS Engineering, Inc., Glendale, CA USA
**Two-phase reaction turbine**
Fabris, G.; Oct. 01, 1999; 59p; In English
Report No.(s): DE2001-763242; No Copyright; Avail: Department of Energy Information Bridge

We have updated our familiarity with relevant literature of direct and indirect importance for success of this project. These included not only fluid dynamics of two-phase flashing flows but also of number of other practical hardware oriented subjects.
NTIS
*Turbine Engines; Two Phase Flow; Energy Technology*

**20010123424** Los Alamos National Lab., NM USA
**Self-Consistent Multiscale Theory of Internal Wave, Mean-Flow Interactions**
Holm, D. D.; Aceves, A.; Allen, J. S.; Alber, M.; Camassa, R.; Jun. 03, 1999; 16p; In English
Report No.(s): DE2001-763237; LA-UR-99-2674; No Copyright; Avail: Department of Energy Information Bridge

This is the final report of a three-year, Laboratory Directed Research and Development (LDRD) project at Los Alamos National Laboratory (LANL). The research reported here produced new effective ways to solve multiscale problems in nonlinear fluid dynamics, such as turbulent flow and global ocean circulation. This was accomplished by first developing new methods for averaging over random or rapidly varying phases in nonlinear systems at multiple scales. We then used these methods to derive new equations for analyzing the mean behavior of fluctuation processes coupled self consistently to nonlinear fluid dynamics. This project extends a technology base relevant to a variety of multiscale problems in fluid dynamics of interest to the Laboratory and applies this technology to those problems. The project's theoretical and mathematical developments also help advance our

understanding of the scientific principles underlying the control of complex behavior in fluid dynamical systems with strong spatial and temporal internal variability.
NTIS
*Internal Waves; Nonlinear Systems; Oceanography; Mathematical Models; Ocean Dynamics*

**20010123439** Dartmouth Coll., Hanover, NH USA
**Two-Phase Potential Flow *Final Report***
Wallis, G. B.; Jun. 11, 1999; 7p; In English
Report No.(s): DE2001-761114; No Copyright; Avail: Department of Energy Information Bridge, Microfiche
The objective of this work was to devise essentially exact solutions to a set of well-defined basic problems of inviscid fluid flow with particulate inclusions. This would help to establish a sound basis for fundamental theoretical developments in the field of two-phase flow. The results of this effort have ranged from basic theorems and the formulation of conservation laws for two-phase mixtures, to detailed predictions for specific geometrical patterns and experimental confirmation of these results.
NTIS
*Particulates; Inviscid Flow; Two Phase Flow*

**20010123728** Lawrence Livermore National Lab., Livermore, CA USA
**Coupling various methods for convection-diffusion problems with applications to flows in porous media**
Lazrov, R. D.; Pasciak, J. E.; Vassilevski, P. S.; May 06, 1999; 50p; In English
Report No.(s): DE2001-11310; UCRL-JC-134160; Rept-97-ERD-114; No Copyright; Avail: Department of Energy Information Bridge
No abstract prepared.
NTIS
*Porosity; Porous Materials*

**20010123763** Lawrence Livermore National Lab., Livermore, CA USA
**Exploiting the power of DSM and SMP clusters for parallel CFD**
Anderson, S. E.; Cohen, R. H.; Curtis, B. C.; Dannevik, W. P.; Dimits, A. M.; Mar. 15, 1999; 18p; In English
Report No.(s): DE2001-11325; UCRL-JC-133693; No Copyright; Avail: Department of Energy Information Bridge
The new generation of powerful DSM and SMP cluster computers enables simulations of fluid dynamics at sufficient resolution to compute the complex nonlinear interactions of small-scale turbulent motions with a large-scale driving flow. With a new programming model of hierarchical shared memory multitasking, it is possible to exploit these new systems without disrupting the flow of small and medium-sized jobs that makes their existence possible.
NTIS
*Computational Fluid Dynamics; Simulation; Computers*

**20010123927** Argonne National Lab., IL USA
**Investigation of Particle/Gas Flow Characteristics in Pipelines**
Golchert, B. M.; Jul. 14, 1999; 9p; In English
Report No.(s): DE2001-10931; ANL/ES/CP-97068; No Copyright; Avail: Department of Energy Information Bridge
Gas-solid flows occur frequently in many industrial processes and systems, such as in pulverized coal transport pipelines and portions of fluid catalytic cracking (FCC) risers. Many of these systems have been modeled and optimized over the years by engineering know-how, which has been derived from the operating experience with the unit. However, it is being recognized that a more detailed, analytic tool is necessary to improve the efficiency of these systems due to heightened industrial competitiveness. In addition to this competition, increasingly stringent environmental regulations force the industry to improve their systems to comply with these regulations. In part, these two conditions explain the recent interest in computational fluid dynamics (CFD) applied to industrial systems. A successfully validated CFD simulation can provide detailed information on an industrial flow system based on a limited amount of experimental data. Once a CFD code has been properly validated, it may then be used to suggest optimal operating conditions. Given the wide range of information provided by a CFD code, the term optimal; may refer to optimal material output, optimal energy efficiency, minimal (optimal) pollutant emission, or optimal lowest operating cost, for example. This versatility has been recently recognized by a number of industries (for example, refinery, chemical, aluminum, and glass), all of which have identified CFD as a critical field for advancement of their technology. The ultimate goal of applying CFD to the modeling of an industrial system is to produce meaningful data that may be used by the company to improve plant performance. The amount of useable data partially depends on how the system is numerically modeled. Any physical system may

be modeled by a Eulerian or Lagrangian approach (or a mixture of the two for multi-phase systems). Most of the recent work in modeling gas-solid flows is based on a Lagrangian model for the solid phase. While this approach models the physics of the system on a microscopic level very well, it is often difficult to extract engineering system information from a Lagrangian formulation. This thought has been re-confirmed in a recent paper. Therefore, a Eulerian approach was used in this code to model all phases of the system. After validation of the code, it was seen that the Eulerian approach provided information needed to improve a coal transfer system.
NTIS
*Computational Fluid Dynamics; Flow Characteristics; Gas Flow; Pipelines; Solids Flow; Two Phase Flow*

**20010124064** NASA Ames Research Center, Moffett Field, CA USA
**A Navier-Strokes Chimera Code on the Connection Machine CM-5: Design and Performance**
Jespersen, Dennis C., NASA Ames Research Center, USA; Levit, Creon, NASA Ames Research Center, USA; [1994]; 1p; In English; 2nd Overset Composite Grid and Solution Technology Symposium, 25-28 Oct. 1994, Fort Walton Beach, FL, USA
Contract(s)/Grant(s): RTOP 505-59-53; No Copyright; Avail: Issuing Activity; Abstract Only

We have implemented a three-dimensional compressible Navier-Stokes code on the Connection Machine CM-5. The code is set up for implicit time-stepping on single or multiple structured grids. For multiple grids and geometrically complex problems, we follow the 'chimera' approach, where flow data on one zone is interpolated onto another in the region of overlap. We will describe our design philosophy and give some timing results for the current code. A parallel machine like the CM-5 is well-suited for finite-difference methods on structured grids. The regular pattern of connections of a structured mesh maps well onto the architecture of the machine. So the first design choice, finite differences on a structured mesh, is natural. We use centered differences in space, with added artificial dissipation terms. When numerically solving the Navier-Stokes equations, there are liable to be some mesh cells near a solid body that are small in at least one direction. This mesh cell geometry can impose a very severe CFL (Courant-Friedrichs-Lewy) condition on the time step for explicit time-stepping methods. Thus, though explicit time-stepping is well-suited to the architecture of the machine, we have adopted implicit time-stepping. We have further taken the approximate factorization approach. This creates the need to solve large banded linear systems and creates the first possible barrier to an efficient algorithm. to overcome this first possible barrier we have considered two options. The first is just to solve the banded linear systems with data spread over the whole machine, using whatever fast method is available. This option is adequate for solving scalar tridiagonal systems, but for scalar pentadiagonal or block tridiagonal systems it is somewhat slower than desired. The second option is to 'transpose' the flow and geometry variables as part of the time-stepping process: Start with x-lines of data in-processor. Form explicit terms in x, then transpose so y-lines of data are in-processor. Form explicit terms in y, then transpose so z-lines are in processor. Form explicit terms in z, then solve linear systems in the z-direction. Transpose to the y-direction, then solve linear systems in the y-direction. Finally transpose to the x direction and solve linear systems in the x-direction. This strategy avoids inter-processor communication when differencing and solving linear systems, but requires a large amount of communication when doing the transposes. The transpose method is more efficient than the non-transpose strategy when dealing with scalar pentadiagonal or block tridiagonal systems. For handling geometrically complex problems the chimera strategy was adopted. For multiple zone cases we compute on each zone sequentially (using the whole parallel machine), then send the chimera interpolation data to a distributed data structure (array) laid out over the whole machine. This information transfer implies an irregular communication pattern, and is the second possible barrier to an efficient algorithm. We have implemented these ideas on the CM-5 using CMF (Connection Machine FORTRAN), a data parallel language which combines elements of FORTRAN 90 and certain extensions, and which bears a strong similarity to High Performance FORTRAN. We make use of the Connection Machine Scientific Software Library (CMSSL) for the linear solver and array transpose operations.
Author
*Connection Machine; Linear Systems; Navier-Stokes Equation; Computational Fluid Dynamics; Finite Difference Theory*

**20010124070** Sterling Software, Inc., Moffett Field, CA USA
**Interactive Visualization of Computational Fluid Dynamics using Mosaic**
Clucas, Jean, Sterling Software, Inc., USA; Watson, Velvin, NASA Ames Research Center, USA; [1994]; 10p; In English; 2nd International World Wide Web Conference, 17-20 Oct. 1994, Chicago, IL, USA
Contract(s)/Grant(s): NAS2-13210; RTOP 536-01-11; No Copyright; Avail: CASI; A02, Hardcopy; A01, Microfiche

The Web provides new Methods for accessing Information world-wide, but the current text-and-pictures approach neither utilizes all the Web's possibilities not provides for its limitations. While the inclusion of pictures and animations in a paper communicates more effectively than text alone, It Is essentially an extension of the concept of "publication." Also, as use of the Web increases putting images and animations online will quickly load even the "Information Superhighway." We need to find forms of communication that take advantage of the special nature of the Web. This paper presents one approach: the use of the

Internet and the Mosaic interface for data sharing and collaborative analysis. We will describe (and In the presentation, demonstrate) our approach: using FAST (Flow Analysis Software Toolkit), a scientific visualization package, as a data viewer and interactive tool called from MOSAIC. Our intent is to stimulate the development of other tools that utilize the unique nature of electronic communication.
Author
*Computational Fluid Dynamics; Scientific Visualization; Software Development Tools; Flow Visualization*

**20010124140** Los Alamos National Lab., NM USA
**Particles and Patterns in Cellular Automata**
Jen, E.; Das, R.; Beasley, C. E.; Jun. 03, 1999; 11p; In English
Report No.(s): DE2001-763243; LA-UR-99-2675; No Copyright; Avail: Department of Energy Information Bridge

This is the final report of a three-year, Laboratory Directed Research and Development (LDRD) project at Los Alamos National Laboratory (LANL). Our objective has been to develop tools for studying particle interactions in a class of dynamical systems characterized by discreteness, determinism, local interaction, and an inherently parallel form of evolution. These systems can be described by cellular automata (CA) and the behavior we studied has improved our understanding of the nature of patterns generated by CAs, their ability to perform global computations, and their relationship to continuous dynamical systems. We have also developed a rule-table mathematics that enables one to custom-design CA rule tables to generate patterns of specified types, or to perform specified computational tasks.
NTIS
*Automata Theory; Particle Interactions; Pattern Recognition; Dynamical Systems*

**20010125139** NASA Ames Research Center, Moffett Field, CA USA
**Rapid Distortion Theory for Compressible Homogeneous Turbulence Under Isotropic Mean Strain**
Blaisdell, G. A., Purdue Univ., USA; Coleman, G. N., California Univ., USA; Mansour, N. N., NASA Ames Research Center, USA; [1994]; 1p; In English; Second Symposium on Transitional and Turbulent Compressible Flows 1996 Joint ASME/SME Fluid Engineering Conference, 13-18 Aug. 1995, Hilton Head, SC, USA; Sponsored by American Society of Mechanical Engineers, USA
Contract(s)/Grant(s): RTOP 505-59-50; No Copyright; Avail: Issuing Activity; Abstract Only

The case of isotropic compressible turbulence subjected to rapid isotropic compression is studied using inviscid rapid distortion theory and direct numerical simulation. An exact solution to the rapid distortion problem is given, and results are compared to those of direct numerical simulation. Implications for modelling turbulent flows are discussed.
Author
*Direct Numerical Simulation; Mathematical Models; Homogeneous Turbulence; Compressible Flow; Distortion*

**20010125145** Federal Energy Technology Center, Morgantown, WV USA
**Rheological Properties of Defense Waste processing Facility Melter Feeds**
Mao, F.; Ebadian, M. A.; Oct. 20, 1998; 41p; In English
Report No.(s): DE2001-968; DE-FG21-95EW55094-24; No Copyright; Avail: Department of Energy Information Bridge, Microfiche

In the present investigation, viscosity measurements have been carried out for two types of simulated Defense waste slurries, a Savannah River slurry and a Hanford slurry. The measurements were conducted in two experimental options. A rotational viscometer was used to measure viscosity under well-defined temperature and pH value operating conditions. The solids concentration used for this option was lower than 15 wt.%. Both the slurries have been investigated using this experimental option. The Savannah River slurry has also been investigated in a pipeline flow system, which measured the pressure drop as the slurry flowed through the pipe. The slurry's viscosity can be extracted from the pressure drop information. These investigations have been performed in relatively wide parameter ranges. The solids concentration of the slurry tested in the pipeline system was as high as 25 wt.%. The slurry pH in both experimental options covered a range of 4 to 13.5. The highest operating temperature was 66 C for the rotational viscometer and 55 C for the pipeline system. In FY97, the experiments for the Hanford slurry in the pipeline system will be performed.
NTIS
*Pipelines; Rheology; Slurries; Viscometers; Radioactive Wastes*

**20010125152** MCAT Inst., Mountain View, CA USA

**CFD Optimization on Network-Based Parallel Computer System**

Cheung, Samson H., MCAT Inst., USA; [1994]; 1p; In English; 10th AIAA Computing in Aerospace Meeting, 12-18 Mar. 1994, San Antonio, TX, USA; Sponsored by American Inst. of Aeronautics and Astronautics, USA

Contract(s)/Grant(s): RTOP 509-10-00; No Copyright; Avail: Issuing Activity; Abstract Only

Combining multiple engineering workstations into a network-based heterogeneous parallel computer allows application of aerodynamic optimization with advance computational fluid dynamics codes, which is computationally expensive in mainframe supercomputer. This paper introduces a nonlinear quasi-Newton optimizer designed for this network-based heterogeneous parallel computer on a software called Parallel Virtual Machine. This paper will introduce the methodology behind coupling a Parabolized Navier-Stokes flow solver to the nonlinear optimizer. This parallel optimization package has been applied to reduce the wave drag of a body of revolution and a wing/body configuration with results of 5% to 6% drag reduction.

Author

*Computational Fluid Dynamics; Parallel Computers; Optimization; Software Engineering; Aerodynamic Configurations*

**20010125480** Bettis Atomic Power Lab., West Mifflin, PA USA

**Interfacial Friction in Gas-Liquid Annular Flow: Analogies to Full and Transition Roughness**

Bauer, R. C.; Beus, S. G.; Fore, L. B.; Mar. 01, 1999; 24p; In English

Report No.(s): DE2001-8003; B-T-3258; No Copyright; Avail: Department of Energy Information Bridge, Microfiche

New film thickness and pressure gradient data were obtained in a 5.08 by 101.6 mm duct for nitrogen and water in annular flow. Pressures of 3.4 and 17 atm and temperatures of 38 and 93 C were used to vary the gas density and liquid viscosity. These data are used to compute interfacial shear stresses and interfacial friction factors for comparison with several accepted literature correlations. These comparisons are reasonable for small values of the relative film thickness. However, the new data cover conditions not approached by the data used to construct those correlations. by combining the current data with the results of two other comprehensive modern experimental studies, a new correlation for the interfacial friction factor has been developed. This correlation adds elements of transition roughness to Wallis' fully-rough analogy to better predict interfacial friction factors over a wide range of gas Reynolds numbers and liquid film thicknesses.

NTIS

*Analogies; Correlation; Film Thickness; Fluid Films; Friction Factor; Pressure Gradients*

**20010125489** Argonne National Lab., IL USA

**Heat-shield Design for Glovebox Applications**

Frigo, A. A.; Jul. 10, 1998; 20p; In English; 1998 Annual Conference and Exposition of the American Glovebox Society, 13-15 Jul. 1998, Orlando, FL, USA

Contract(s)/Grant(s): W-31109-ENG-38

Report No.(s): DE2001-10869; ANL/CMT/CP-96761; No Copyright; Avail: Department of Energy Information Bridge, Microfiche

Heat shields can often be used in place of insulation materials as an effective means of insulating glovebox furnace vessels. If used properly, shields can accomplish two important objectives: thermal insulation of the vessel to maintain a desired process temperature and protection of the glovebox, equipment, and user. A heat-shield assembly can be described as an arrangement of thin, properly-spaced, metal sheets that reduce radiation heat transfer. The main problem encountered in the design of a heat shield assembly is choosing the number of shields. In determining the heat transfer characteristics of a heat-shield assembly, a number of factors must be taken into consideration. The glovebox or outside environment, material properties, geometry, and operating temperature all have varying effects on the expected results. A simple method, for planar-horizontal and cylindrical-vertical shields, allowing the approximation of the outermost shield temperature, the practical number of shields, and the net heat-transfer rate will be presented. Methods used in the fabrication of heat-shield assemblies will also be discussed.

NTIS

*Heat Shielding; Furnaces*

## 35
## INSTRUMENTATION AND PHOTOGRAPHY

*Includes remote sensors; measuring instruments and gauges; detectors; cameras and photographic supplies; and holography. For aerial photography see 43 Earth Resources and Remote Sensing. For related information see also 06 Avionics and Aircraft Instrumentation; and 19 Spacecraft Instrumentation.*

**20010117633** Brookhaven National Lab., Upton, NY USA
**Neutron algorithm verification testing**
Cowgill,; Mosby,; Jul. 19, 2000; 9p; In English
Report No.(s): DE2000-759052; BNL-67165; No Copyright; Avail: Department of Energy Information Bridge

Active well coincidence counter assays have been performed on uranium metal highly enriched in (sup 235)U. The data obtained in the present program, together with highly enriched uranium (HEU) metal data obtained in other programs, have been analyzed using two approaches, the standard approach and an alternative approach developed at BNL. Analysis of the data with the standard approach revealed that the form of the relationship between the measured reals and the (sup 235)U mass varied, being sometimes linear and sometimes a second-order polynomial. In contrast, application of the BNL algorithm, which takes into consideration the totals, consistently yielded linear relationships between the totals-corrected reals and the (sup 235)U mass. The constants in these linear relationships varied with geometric configuration and level of enrichment. This indicates that, when the BNL algorithm is used, calibration curves can be established with fewer data points and with more certainty than if a standard algorithm is used. However, this potential advantage has only been established for assays of HEU metal. In addition, the method is sensitive to the stability of natural background in the measurement facility.
NTIS
*Algorithms; Neutrons; Uranium Isotopes; Intermetallics*

**20010119555** Department of Energy, Nevada Operations Office, Las Vegas, NV USA
**Vapor Phase Detection Using Chemi-Resistor Sensor Arrays**
Lewis, N. S.; Feb. 17, 1999; 7p; In English
Report No.(s): DE2001-10465; No Copyright; Avail: Department of Energy Information Bridge, Microfiche

This paper focuses on two main areas: understanding sensor response times so as to obtain improved time response in the field when needed for vapor tracking and classification, and improved theoretical understanding of the sensor response properties that generate the pattern on the array in response to a given analyte.
NTIS
*Measuring Instruments; Vapor Phases; Detection*

**20010119579** Army Research Lab., Sensors Directorate, Adelphi, MD USA
**Dual-Band Imaging of Military Targets Using a QWIP Focal Plane Array**
Goldberg, A.; Fischer, T.; Kennerly, S.; Wang, S.; Sundaram, M.; Jan. 2001; 21p; In English; Original contains color images; Prepared in collaboration with Sanders, Lockheed Martin, Nashua, NH and Lockheed Martin Electronics and Missiles, Orlando, FL
Report No.(s): AD-A392953; No Copyright; Avail: CASI; A03, Hardcopy; A01, Microfiche

We present dual-band infrared image data collected as part of the Multidomain Smart Sensors effort at the U. S. Army Research Laboratory (ARL). The goal of this effort is to produce large-format, staring focal plane arrays (FPAs) that are able to see the battlefield in both the 3 to 5-micrometer (mid-wave infrared or MWIR) and 8 to l2-micrometer (long-wave infrared or LWIR) atmospheric transmission windows. The data was collected under laboratory and field test conditions using a simultaneously integrating, pixel-registered, 256 x 256, dual-band focal plane array produced by Lockheed Martin using quantum-well infrared photodetector (QWIP) technology. The dual-band FPA was installed in a camera that was taken in the field to gather image data on military targets. The pixel-registered dual-band FPA is well suited for the application of image fusion algorithms. We also applied some of these image fusion techniques to the imagery to enhance the visibility of targets.
DTIC
*Quantum Wells; Focal Plane Devices; Photometers*

**20010119929** Stanford Univ., Information Systems Lab., Stanford, CA USA
**Multivariable Control, Simulation, Optimization, and Signal Processing for the Microlithographic Process** ***Final Report, 15 Sep. 1995-30 Jun. 2001***
Kailath, Thomas; Jun. 2001; 25p; In English

Contract(s)/Grant(s): F49620-95-1-0525
Report No.(s): AD-A395210; AFRL-SR-BL-TR-01-0527; No Copyright; Avail: CASI; A03, Hardcopy; A01, Microfiche

The objective of this Multidisciplinary University Research Initiative (MURI) program is to apply multivariable control, simulation, optimization and signal processing techniques to the microlithography sequence.

DTIC

*Signal Processing; Simulation; Multivariate Statistical Analysis; Photolithography*

**20010119948** Sandia National Labs., Albuquerque, NM USA

**Nuclear Emission Microscopies**

Doyle,; Walsh,; Renfrow,; Vizkelethy,; Schenkel,; Sep. 19, 2000; 19p; In English

Report No.(s): DE2000-763114; SAND2000-2301C; No Copyright; Avail: Department of Energy Information Bridge, Microfiche

Alternatives to traditional nuclear microprobe analysis emerged two years ago with the invention of Ion-Electron Emission Microscopy (IEEM). With Nuclear Emission Microscopy the ion beam is only partially focused so as to fill the field of view of a special emission particle microscope system fitted with a single particle Position Sensitive Detector (PSD). When a single ion strikes the sample, the emitted secondaries (e.g. electrons, photons, ions, ...) are projected at great magnification onto this PSD where position signals are generated. These X and Y signals are then put into coincidence with the IBA signal(s) made by this same ion in a fashion completely analogous to traditional NMA. In this paper, an update will be given on the state of Nuclear Emission Microcopies, which currently includes IEEM and High Charged Ion- Secondary Ion Mass Spectroscopy (HCI-SIMS). In addition, a new type of full-field nuclear imaging is proposed: Ion-Photon Emission Microscopy or IPEM.

NTIS

*Ion Microscopes; Ion Emission; Electrons*

**20010120005** Sandia National Labs., Albuquerque, NM USA

**Luminescent Layers for Ion-Photon Emission Microscopy**

Yang,; Doyle,; Rossi,; Nigam,; Bousnani,; Sep. 18, 2000; 17p; In English

Report No.(s): DE2000-763112; SAND2000-2292C; No Copyright; Avail: Department of Energy Information Bridge, Microfiche

Ion Beam Induced Luminescence (IBIL) combined with Ion Beam Induced Charge Collection (IBICC) is applied in a quantitative study of the IBIL generation yield and detection efficiency for several plastic phosphor materials. The main purpose of this study is to search for strongly luminescent materials that can be used to easily coat samples to be studied with Ion Photon Emission Microscopy (IPEM). A special focus is given to plastic scintillation materials because thin films are easily prepared, and such films have already been used for single event triggering. The emission yield was found to be low for typical Bicron plastic phosphors (only about 70 photons/ion/micron). The total collection, transmission and photon detection efficiency of the optical microscope used in this study was determined to be only about 0.00003. For thin film plastic phosphors about 20 microns thick, the detection efficiency was only 0.04 photons/ion. This means that using these plastics, IPEM would need to be performed with about 20 more beam fluence to obtain data, such as IBICC, similar to a standard scanned nuclear microprobe. Improvements are discussed.

NTIS

*Ion Emission; Photons; Microscopy*

**20010120144** Air Force Inst. of Tech., Wright-Patterson AFB, OH USA

**Design, Construction and Evaluation of the CSU Optical Fog Detector**

Emert, ScottE.; Jun. 12, 2001; 146p; In English

Report No.(s): AD-A395148; C101-257; No Copyright; Avail: CASI; A07, Hardcopy; A02, Microfiche

The goal of this project was to develop an inexpensive cloud/fog detector that could be used to automate sampling equipment at remote (unmanned) cloud/fog research sites. A secondary objective was to test the ability of this sensor to measure/track trends in fog/cloud liquid water content (LWC). This characteristic is important because LWC is a significant indicator of a cloud's ability to process aerosols and gases and changes in LWC often correspond to changes in fog/cloud solute concentration. The following actions were taken to help realize these objectives. An evaluation of the use of commercially available optical components for fog detection has been performed. The research reinforced the need to have an inexpensive cloud/fog detector that could be used

to automate sampling equipment at remote (unmanned) cloud/fog research sites. No such instrument is currently available commercially.
DTIC
*Fog; Optical Equipment; Detectors; Clouds (Meteorology); Design Analysis*

**20010120486** Army Research Lab., Survivability/Lethality Analysis Directorate, White Sands Missile Range, NM USA
**Search and Target Acquisition: Single Line of Sight Versus Wide Baseline Stereo** ***Final Report***
Watkins, Wendell R.; Sep. 2001; 76p; In English; Original contains color images
Report No.(s): AD-A395020; ARL-TR-831; No Copyright; Avail: CASI; A05, Hardcopy; A01, Microfiche

The purpose of this paper is to present the results of two observer experiments for comparison of the use of wide baseline stereo vision (biocular viewing of two line of sight (LOS) images) and mono vision (biocular viewing of single LOS images) for performing search and target-acquisition tasks. To quantify the advantage of using wide baseline stereo vision, a joint field test was conducted in Soesterberg, The Netherlands in September 1998. A multiple baseline imagery database was obtained with personnel wearing forest camouflage uniforms arrayed at two rural terrain sites. The weather condition for site 1 was clear to partly cloudy and site 2 was overcast with light rain. The preliminary analysis of the site 1 database indicated that wide baseline stereo could be used to improve search and target acquisition but that the baseline was too wide for many of the closer targets at that site. The database from site 2 was then analyzed through observer testing with single LOS and wide baseline stereo displays. The results indicate that stereo vision can be effectively used to reduce false alarm detection rates. Additionally, guidelines for optimum stereo display were obtained that could be used to improve positive target detection.
DTIC
*Line of Sight; Target Acquisition; Stereoscopic Vision; Visual Perception; Weather*

**20010121514** Sandia National Labs., Albuquerque, NM USA
**Uncertainty Analysis of an Accelerometer DAQ System**
Nakos, J. T.; May 01, 2000; 72p; In English
Report No.(s): DE2000-759438; SAND2000-1152; No Copyright; Avail: Department of Energy Information Bridge, Microfiche

An uncertainty analysis was performed on two very similar piezoresistive (PR) accelerometer type data acquisition (DAQ) systems typical of those in the 'Shock Lab' in Building 860, Area I, and the 'Mechanical Shock Lab' or 'Actuator,' Building 6570, in Tech Area III. Components included in the analysis were Endevco Model 7270A PR-type accelerometers (most often used), connecting cables, Dynamics Model 7600A and 8000 signal conditioner/amplifiers, DSP digitizers, and IBM compatible PC systems. The analysis was performed assuming the data have been validated and issues, such as faulty transducers, cables, and other 'major' potential problems, have been resolved. This analysis can be easily modified for other PR type transducers. Results from the analysis show that, excluding systematic uncertainties caused by accelerometer mounting methods, the uncertainty of the entire DAQ system used in typical accelerometer measurements is about plus or minus 5 per cent (95 per cent confidence) or plus or minus 8 per cent (99 per cent confidence). Most of that uncertainty is because of the Endevco accelerometer little of the uncertainty is because of the remainder of the DAQ system.
NTIS
*Accelerometers; Data Acquisition; Systems Engineering; Statistical Analysis*

**20010122666** Sandia National Labs., Albuquerque, NM USA
**Applications for Infrared Imaging Equipment in Photovoltaic Cell, Module, and System Testing**
King,; Kratochvil,; Quintana,; McMahon,; Sep. 25, 2000; 6p; In English
Report No.(s): DE2000-763342; SAND2000-2342C; No Copyright; Avail: Department of Energy Information Bridge, Microfiche

Anomalous temperature distributions are often an indication of atypical behavior in a device under investigation. Portable infrared (IR) imaging systems (cameras) now provide a convenient method for measuring both absolute and relative temperature distributions on small and large components with a high degree of temperature and spatial resolution. This diagnostic tool can be applied during the development, production, monitoring, and repair of photovoltaic cells, modules, and systems. Planar objects with nearly uniform material composition are ideally suited for analysis using IR imaging. This paper illustrates investigations of localized shunting in cells, resistive solder bonds in field aged modules, module bypass diode functionality, reverse-bias (hot spot) heating in modules, temperature distributions in flat-plate and concentrator modules, batteries during charging, and electronic component temperature in power processing equipment.
NTIS
*Imaging Techniques; Infrared Imagery; Modules; Photovoltaic Cells; Temperature Distribution*

**20010122825** Stanford Linear Accelerator Center, Menlo Park, CA USA

**Analysis of Laser Tracker and Total Station Surveys**

LeCocq, C. M.; Jul. 12, 2000; 21p; In English

Report No.(s): DE2000-763823; SLAC-TN-00-1; No Copyright; Avail: Department of Energy Information Bridge

The SMX 4500 laser tracker has proven itself to be a beneficial addition to SLAC's (Stanford Linear Accelerator Center) set of alignment tools. Through actual field surveys and laboratory testing, a question regarding some unknown scale factor appearing after adjusting the combined tracker and total station results arose. Through a simple line survey and instrument analysis and then progressing through more and more rigorous network adjustments, the authors deduced that the apparent scale problem was in fact more likely attributed to wrong offset values introduced into the adjustment by mixing TC2002 total station data with the laser tracker measurements. A recalibration procedure of all of SLAC's total station prisms was designed and analyzed.

NTIS

*Lasers; Alignment; Linear Accelerators*

**20010122950** Los Alamos National Lab., NM USA

**Streak Camera Enhanced Quadrupole Scan Technique**

Gierman, S. M.; Feb. 01, 2000; 19p; In English

Report No.(s): DE2000-763356; LA-UR-00-810; No Copyright; Avail: Department of Energy Information Bridge

A streak camera is used in combination with the quadruple scan technique to characterize the temporal dependence of the trace-space distribution of a bunched electron beam. The quadruple scan procedure is used to determine the ellipse that represents the beam on the two-dimensional trace space (the xx plane), and the streak camera diagnostic shows how electrons in axial slices at different locations within a single, average bunch contribute to the trace-space distribution and emittance of the full bunch. For purposes of analysis, the 15-20 ps FWHM electron bunch is partitioned into seven contiguous 4-ps slices. The quadruple scans are performed over a range of focusing strengths in the solenoid lens that is wrapped around the photocathode cell of an 1l-cell 1300 MHz rf photoinjector. The radial focusing of the solenoid is intended to reverse a space-charge-driven emittance blow-up that occurs in the low-energy end of the photoinjector and that is correlated with the axially nonuniform transverse space-charge field. In the parameter space investigated in this experiment, the solenoid does not appear to perform that function. Simulations of the experiment with the particle code PARMELA indicate that by keeping the transverse dimension of the beam small, the focusing does circumvent an rf-driven emittance growth, but otherwise does little to reverse the emittance blow-up that occurs in the first few cells.

NTIS

*Electron Beams; Electron Bunching; Emittance; Scanners; Solenoids; Temporal Distribution*

**20010122951** Fermi National Accelerator Lab., Batavia, IL USA

**Beam test results for the BTeV silicon pixel detector**

Chiodini, G.; Appel, J. A.; Sep. 28, 2000; 2p; In English

Report No.(s): DE2000-764083; FERMILAB-CONF-00/227-E; No Copyright; Avail: Department of Energy Information Bridge

The authors report the results of the BTeV silicon pixel detector tests carried out in the MTest beam at Fermilab in 1999-2000. The pixel detector spatial resolution has been studied as a function of track inclination, sensor bias, and readout threshold.

NTIS

*Performance Tests; Particle Beams*

**20010124077** NASA Goddard Space Flight Center, Greenbelt, MD USA

**Multi-Sensor Registration of Earth Remotely Sensed Imagery**

LeMoigne, Jacqueline, NASA Goddard Space Flight Center, USA; Cole-Rhodes, Arlene, Morgan State Univ., USA; Eastman, Roger, Loyola Coll., USA; Johnson, Kisha, Morgan State Univ., USA; Morisette, Jeffrey, Science Systems and Applications, Inc., USA; Netanyahu, Nathan S., Bar-Ilan Univ., Israel; Stone, Harold S., NASA Goddard Space Flight Center, USA; Zavorin, Ilya, NASA Goddard Space Flight Center, USA; [2001]; 9p; In English

Contract(s)/Grant(s): NAS2-37143; No Copyright; Avail: CASI; A02, Hardcopy; A01, Microfiche

Assuming that approximate registration is given within a few pixels by a systematic correction system, we develop automatic image registration methods for multi-sensor data with the goal of achieving sub-pixel accuracy. Automatic image registration is usually defined by three steps; feature extraction, feature matching, and data resampling or fusion. Our previous work focused on image correlation methods based on the use of different features. In this paper, we study different feature matching techniques and present five algorithms where the features are either original gray levels or wavelet-like features, and the feature matching is based on gradient descent optimization, statistical robust matching, and mutual information. These algorithms are tested and

compared on several multi-sensor datasets covering one of the EOS Core Sites, the Konza Prairie in Kansas, from four different sensors: IKONOS (4m), LANDSAT-7/ETM+ (30m), MODIS (500m), and SeaWIFS (1000m).
Author
*Image Correlators; Image Processing; Imaging Spectrometers; Imagery; Pattern Recognition; Remote Sensing; Wavelet Analysis*

**20010124840** Paris-Sud Univ., Inst. d'Astrophysique Spatiale, Orsay, France
**IMS: The Infrared Mapping Spectrometer of the BepiColombo Mission**
Erard, S., Paris-Sud Univ., France; Mercury: Space Environment, and Surface and Interior; 2001, pp. 23-24; In English; See also 20010124826; No Copyright; Abstract Only; Available from CASI only as part of the entire parent document

The IR (infrared) Spectrometer on board BepiColombo's MPO (Mercury Planetary Orbiter) aims at investigating the 0.8-2.8 micron range, where the absorption bands of major rock-forming minerals are found. Spatial resolution values on the order of 100 m are needed for regolith mixing studies (approximately 200 - 300 m mixing scale), while moderate spectral resolution only is required (approximately 20-40 nm spectral sampling).
Author
*Absorption Spectra; Infrared Spectrometers; Mercury (Planet); Mineral Exploration; Remote Sensing; Spacecraft Equipment*

**20010124845** Rutherford Appleton Lab., Space Science and Technology Dept., Chilton, UK
**CIXS: An X-Ray Spectrometer for ESA's BepiColombo Mission to Mercury**
Grande, M., Rutherford Appleton Lab., UK; Dunkin, S. K., Rutherford Appleton Lab., UK; Kellett, B. J., Rutherford Appleton Lab., UK; Mercury: Space Environment, and Surface and Interior; 2001, pp. 31-32; In English; See also 20010124826; No Copyright; Abstract Only; Available from CASI only as part of the entire parent document

Mercury can be considered as an 'end-member' of the terrestrial planets in our Solar System - it is the closest planet to the Sun, it is the smallest and has the highest uncompressed density. It remains mostly unexplored apart from three flybys by Mariner 10 in 1974 and 1975. Understanding the composition of Mercury is a key to our understanding of the process of the formation and evolution of the Solar System BepiColombo, ESA's (European Space Agency) Cornerstone mission to Mercury, will conduct an extensive investigation of the planet using two orbiters and a lander. This paper outlines a possible X-ray spectrometer that would be ideally suited to the BepiColombo mission, and highlights some of the outstanding science that can be achieved with such an instrument. Additional information is contained in the original extended abstract.
Author
*European Space Agency; Mercury (Planet); Space Missions; X Ray Spectrometers; Spacecraft Equipment*

**20010124852** Johns Hopkins Univ., Applied Physics Lab., Laurel, MD USA
**Overview of the MESSENGER Mercury Dual Imaging System**
Hawkins, S. E., III, Johns Hopkins Univ., USA; Boldt, J. D., Johns Hopkins Univ., USA; Darlington, E. H., Johns Hopkins Univ., USA; Grey, M. P., Johns Hopkins Univ., USA; Kardian, C. J., Jr., Johns Hopkins Univ., USA; Murchie, S. L., Johns Hopkins Univ., USA; Peacock, K., Johns Hopkins Univ., USA; Schaefer, E. D., Johns Hopkins Univ., USA; Williams, B. D., Johns Hopkins Univ., USA; Mercury: Space Environment, and Surface and Interior; 2001, pp. 42-43; In English; See also 20010124826; No Copyright; Abstract Only; Available from CASI only as part of the entire parent document

The Mercury Dual Imaging System (MDIS) is part of the science payload to be flown on the NASA Discovery mission MESSENGER. MDIS is comprised of wide- and narrow-angle cameras sensitive to visible wavelengths. The Mercury Surface, Space Environment, Geochemistry, and Ranging (MESSENGER) spacecraft will be launched in the spring of 2004 aboard a Delta 2925H-9.5 rocket. MESSENGER will arrive at Mercury in the spring of 2009 to begin its year-long mission to study the planet. Prior to Mercury orbit insertion, the two Mercury fly-bys will provide imaging opportunities in addition to those during the mission orbital phase. Mission goals are to produce a global monochrome map at 250-m average resolution or better and a color map at 2-km average resolution or better. The success of MESSENGER is strongly tied to developing a capable and robust spacecraft and science payload with minimal mass. Mercury's eccentric orbit poses a challenge to the design of the spacecraft, with the intensity of the solar radiation varying from about 4.6-10.6 times the total irradiance falling on the Earth. Because of this severe thermal environment, a sunshade protects the spacecraft from direct solar illumination, but strongly constrains its range of pointing. to compensate for this limited pointing capability, the dual cameras of MDIS are mounted on either side of a rotating platform, pivoted about a common axis as shown in Fig. 1. The two cameras will be co-aligned to within the pointing accuracy of the spacecraft of 0.1 degrees. The pivot platform design enables the instrument to acquire optical navigation (OpNav) images and star field calibrations, and greatly increases opportunities to image key features with minimal impact on spacecraft pointing.

The nominal scan range of the platform is -40 degrees in the sunward direction to +50 degrees planetward. Additional information is contained in the original extended abstract.
Author
*Cameras; Imaging Techniques; Mercury (Planet); Mercury Surface; Spacecraft Equipment; Space Missions*

**20010124867** Colorado Univ., Lab. for Atmospheric and Space Physics, Boulder, CO USA
**The Mercury Atmospheric and Surface Composition Spectrometer (MASCS) for the MErcury: Surface, Space ENvironment, GEochemistry, Ranging (MESSENGER) Mission**
McClintock, William E., Colorado Univ., USA; Holsclaw, Gregory M., Colorado Univ., USA; Mercury: Space Environment, and Surface and Interior; 2001, pp. 62; In English; See also 20010124826; No Copyright; Abstract Only; Available from CASI only as part of the entire parent document

MASCS (Mercury Atmospheric and Surface Composition Spectrometer) is one of seven science instruments aboard the MESSENGER spacecraft, which will orbit Mercury beginning in 2009. It consists of a small Cassegrain telescope that simultaneously feeds a scanning grating Ultraviolet-Visible Spectrometer (UVVS) and a fixed grating Visible-Infrared Spectrograph (VIRS). The UVVS will measure the composition and structure of Mercury's exosphere, study its neutral and coronal gas, and search for and measure ionized atmospheric species. These measurements will contribute to our understanding of the processes that generate and maintain the atmosphere, the connection between surface and atmospheric composition, the transport of volatile materials on and near Mercury, and the nature of the bright radar-reflective materials at its poles. The VIRS will measure surface reflectance from 0.3 to 1.4 micrometers with a spatial resolution approximately 5 km. This wavelength range contains spectral signatures of Fe(++), Ca Silicates, TiO2 and FeO. These measurements will be combined with multispectral images obtained with the Mercury Dual Imaging System and elemental composition measurements from the MESSENGER Gamma Ray and X-Ray Spectrometers to determine composition and study the effects of space weathering on the surface. In this presentation we describe the capabilities of the MASCS, its measurement and science objectives, and how those objectives help to answer the key science questions that define the MESSENGER Mission.
Author
*Atmospheric Composition; Mercury Atmosphere; Mercury (Planet); Space Missions; Spacecraft Instruments; Spectrometers; Planetary Composition; Infrared Astronomy; Ultraviolet Astronomy*

**20010124872** Deutsche Forschungsanstalt fuer Luft- und Raumfahrt, Inst. of Space Sensor Technology and Planetary Exploration, Berlin, Germany
**A Combined Stereo Camera/Laser Altimeter Experiment Package for the BepiColombo Polar Orbiter**
Oberst, J., Deutsche Forschungsanstalt fuer Luft- und Raumfahrt, Germany; Wagner, R., Deutsche Forschungsanstalt fuer Luft- und Raumfahrt, Germany; Hoffmann, H., Deutsche Forschungsanstalt fuer Luft- und Raumfahrt, Germany; Jaumann, R., Deutsche Forschungsanstalt fuer Luft- und Raumfahrt, Germany; Neukum, G., Deutsche Forschungsanstalt fuer Luft- und Raumfahrt, Germany; Mercury: Space Environment, and Surface and Interior; 2001, pp. 70-71; In English; See also 20010124826; No Copyright; Abstract Only; Available from CASI only as part of the entire parent document

BepiColombo, a mission to Mercury initiated by the European Space Agency (ESA), is scheduled for launch near the beginning of the next decade. Our team proposes to contribute an instrument package to the Mercury Polar Orbiter (MPO) which combines a camera and a laser altimeter. The camera portion of the instrument, inherited from the HRSC (High Resolution Stereo Camera) on Mars Express, is a multiple line scanner, operated in the pushbroom mode. The scanner is proposed to have nine line sensors, 5128 pixels each, oriented perpendicular to the spacecraft's motion. Three of the sensors are pointed forward, nadir, and backward, respectively, to collect stereo data. Other sensors are designed to obtain image data at multiple phase angles, or in color. From a periapsis height of 400 km, the camera, operating at a scan rate of approximately 300 Hz, will obtain a ground pixel size of 10 m. The laser will operate at e.g. 1 Hz, its clock being precisely synchronized with the scanner. The science goals of the instrument are in the general reconnaissance as well as geoscientific studies of the planet. Observations of the libration of Mercury are among the foremost goals of BepiColombo, for which our instrument is uniquely suited. Owing to the slow rotation rate of the planet, image data from adjacent orbits will have good overlap (greater than 50%) near the equator, which is essential for the tracking of Mercury's librations. The typical data analysis will include the automatic extraction of large numbers (estimated at greater than 25,000 per orbit) of triple-tiepoints between the stereo images using digital image matching techniques. These tiepoints, in combination with the range measurements by the laser allow us to accurately model the orbit and attitude of the spacecraft, surface topography, as well as rotation of the planet. For the analysis, the synchroneous operation of the laser and the camera is essential, as this will allow us to directly obtain the image line/sample coordinates of all laser surface reflection points (greater than 5000 per orbit) and include them in the analysis. We simulated data acquisition and analysis for triple stereo image swaths of 30 minutes near pericenter and generated a set of 100 triple-tiepoints (in practice this number will be much larger, see

above). The camera parameters described above and the nominal parameters of the spacecraft's polar orbit were adopted. The results of our model suggest that one can determine the orientation of Mercury's rotational axis within less than 1 degree after one orbit. Our current model assumes that unbiased inertial spacecraft trajectory data are given and suffer from random errors only. Additional information is contained in the original extended abstract.
Author
*Laser Altimeters; Librational Motion; Mercury (Planet); Scanners; Stereophotography; Space Missions; Spacecraft Instruments*

**20010124873** Consiglio Nazionale delle Ricerche, Inst. Fisica Spazio Interplanetario, Rome, Italy
**Scientific Merits and Technical Aspects of a Thermal/Energetic Neutral Particle Detector on Board the ESA BepiColombo Mission**
Orsini, S., Consiglio Nazionale delle Ricerche, Italy; DeAngelis, E., Consiglio Nazionale delle Ricerche, Italy; DiLellis, A. M., AMDL, Italy; Barabash, S., Swedish Inst. of Space Physics, Sweden; Daglis, I. A., National Observatory of Athens, Greece; Delcourt, D., Centre National de la Recherche Scientifique, France; Kallio, E., Finnish Meteorological Inst., Finland; Killen, R., Southwest Research Inst., USA; Livi, S., Johns Hopkins Univ., USA; Milillo, A., Consiglio Nazionale delle Ricerche, Italy; Mercury: Space Environment, and Surface and Interior; 2001, pp. 72; In English; See also 20010124826; No Copyright; Abstract Only; Available from CASI only as part of the entire parent document

The Neutral Particle/ENA (energetic neutral atom) Detectors on board the ESA (European Space Agency) BepiColombo mission to Mercury has the purpose to investigate the Hermean exospheric composition, the interaction of the solar wind between both the magnetospheric plasma and the planet surface. by applying unfolding techniques, with this instrument we can detect the thermal particles of the exosphere and energetic neutral atoms generated via charge-exchange or sputtering processes. In particular it will be possible: (a) to obtain in-situ measurements of the exospheric composition and density; (b) to investigate the surface composition of the planet and the global exospheric characteristics, by analyzing the massive sputtered particles; (c) to study the exospheric dynamical evolution through ENA remote sensing; (d) to image the magnetospheric plasma flow patterns and the variations occurring during disturbed periods by observing the short time fluctuations of the ENA signal, thus providing crucial global information necessary for the interpretation of simultaneous in situ ion measurements. In the present paper, some details of the scientific merits and technical aspects of this instrument are briefly presented and discussed.
Author
*Energetic Particles; Mercury (Planet); Neutral Atoms; Neutral Particles; Space Missions; Mercury Atmosphere; Atmospheric Composition*

**20010124888** NASA Goddard Space Flight Center, Greenbelt, MD USA
**The X-Ray Spectrometer for Mercury MESSENGER**
Starr, R. D., Catholic Univ. of America, USA; Ho, G. C., Johns Hopkins Univ., USA; Schlemm, C., Johns Hopkins Univ., USA; Gold, R. E., Johns Hopkins Univ., USA; Goldsten, J. O., Johns Hopkins Univ., USA; Boynton, W. V., Arizona Univ., USA; Trombka, J. I., NASA Goddard Space Flight Center, USA; Mercury: Space Environment, and Surface and Interior; 2001, pp. 102-103; In English; See also 20010124826; No Copyright; Abstract Only; Available from CASI only as part of the entire parent document

Mercury is the closest planet to the Sun and because it is so close, it is difficult to study from Earth-based observatories. Its proximity to the Sun has also limited the number of spacecraft to visit this tiny planet to just one, Mariner 10, which flew by Mercury twice in 1974 and once in 1975. Mariner 10 provided a wealth of new information about Mercury, yet much still remains unknown about Mercury's geologic history and the processes that led to its formation. The origin of Mercury's metal-rich composition is just one area of investigation awaiting more and improved data to sort between competing hypotheses. Mercury plays an important role in comparative planetology, and many of the processes that were important during its formation are relevant to the Earth's early history. MESSENGER (Mercury Surface, Space Environment, Geochemistry, and Ranging) is a Discovery mission that has been designed to fly by and orbit Mercury. It will launch in March 2004, flyby Mercury in 2007 and 2008 and enter an elliptical orbit in April 2009. During the one-year orbital phase, a suite of instruments on board the MESSENGER spacecraft will study the exosphere, magnetosphere, surface, and interior of Mercury. One of these instruments will be an X-Ray Spectrometer (XRS) that will measure surface elemental abundances. Remote X-ray spectroscopy has been accomplished before on the Apollo 15 and 16 missions, and more recently on NEAR Shoemaker. The MESSENGER XRS will measure characteristic X-ray emissions induced in the surface of Mercury by the incident solar flux. The Ka lines for the elements Mg, Al, Si, S, Ca, Ti, and Fe will be detected with spatial resolution on the order of 40 km when counting statistics are not a limiting factor. These measurements can be used to obtain quantitative information on elemental composition.
Author
*Mercury (Planet); Mercury Surface; X Ray Spectroscopy; Space Missions; Spacecraft Instruments; X Ray Astronomy*

**20010125020** Argonne National Lab., IL USA

**Irradiation of Nd-Fe-B permanent magnets with APS bending magnet x-rays and (sup 60)Co (gamma)-rays**

Alderman, J.; Job, P. K.; Puhl, J.; Sep. 08, 2000; 27p; In English

Report No.(s): DE2000-764212; LS-288; No Copyright; Avail: Department of Energy Information Bridge

The Advanced Photon Source (APS), as well as other third-generation synchrotron light sources, uses permanent magnets in the insertion devices to produce x-rays for scientific research. When placed in a high-energy storage ring, these permanent magnets are subjected to irradiation from synchrotron radiation, high-energy bremsstrahlung, and bremsstrahlung-produced photoneutrons. Previous investigations have exhibited varying degrees of degradation in the intensity of magnetization of these magnets due to irradiation from electron beams, (sup 60)Co (gamma)rays, and high-energy neutrons. The APS specifically uses Nd-Fe-B permanent magnets in their insertion devices. Although no detectable radiation-induced demagnetization has been observed in the APS insertion devices so far, partial demagnetization has been observed in at least one insertion device at the European Synchrotron Radiation Facility (ESRF), where Nd-Fe-B permanent magnets are also used.

NTIS

*Permanent Magnets; Photons; Iron; Neodymium; Boron; Cobalt 60; Irradiation; Synchrotron Radiation*

**20010125140** Colorado Univ., Cooperative Inst. for Research in the Environmental Sciences, Boulder, CO USA

**Design and Calibration of Autonomous Coherent Doppler Lidar for Space Missions** ***Final Report, 1 Dec. 1998 - 30 Nov. 2001***

Frehlich, Rod G., Colorado Univ., USA; [2001]; 2p; In English

Contract(s)/Grant(s): NAG8-1551; No Copyright; Avail: CASI; A01, Hardcopy; A01, Microfiche

Developed a new algorithm for the simulation of three dimensional homogeneous turbulent velocity fields. For typical atmospheric conditions it is impossible to produce a simulated velocity field that simultaneously satisfy a given spatial correlation and the corresponding spatial spectrum because of spectral aliasing. The new algorithms produce a turbulent velocity field which has accurate spatial correlations which is required for performance predictions from space-based systems. Developed a new algorithm for extracting the spatial statistics of the atmospheric velocity field using coherent Doppler lidar. The performance of the algorithm was compared with past methods and the new algorithm produces useful results for space-based data, which was not possible before. Developed new methods for verification of the errors in ground-based and space-based Doppler lidar wind measurements. These new methods do not require independent in situ data. This is an important issue for the verification of space-based Doppler lidar measurements of the global wind field. The performance of the new algorithm was compared with past results for both space-based and ground-based operation. The new algorithm has the best performance and is the only algorithm that performed satisfactory for spacebased operation. The performance of coherent Doppler lidar for a space missions with various scanning geometries was determined using computer simulation which contained the effects of random instrumental velocity errors, wind shear, wind variability along the range-gate and from shot-to-shot, and random variations in atmospheric aerosol backscatter over the measurement volume. The bias in the velocity estimates was small and the accuracy in the is typically less than 0.5 m/s for high signal conditions. For a large number of shot per velocity estimate, the threshold signal level for acceptable estimates is proportional to the number of shots to the minus one half power. This agrees with previous results determined for ground-based measurements. The use of multi-element optical detectors for autonomous operation of coherent Doppler lidar was shown to be a very promising technique. Optimal detector geometries were determined by computer simulation of performance: for ground-based testing with a fixed calibration target and for space-based operation using the random surface returns. The effects of refractive turbulence on ground-based calibration of coherent Doppler lidar was determined by computer simulations and compared with theoretical predictions. New techniques were required to correctly predict performance for the focused beam geometry commonly used for verification of space-based operation. An improved velocity estimator was evaluated for space-based applications were signal shot measurements are used to produce vector wind measurements. This permits more accurate measurements when the signal level is not known a priori or not available from multiple shot measurements. The average Doppler lidar signal spectrum including the effects of velocity turbulence was derived and calculated. This permits new estimation algorithms for turbulence based on spectral estimates. In situ atmospheric measurements were conducted and analyzed using an instrumented kite-platform. This work helps provide the required in situ data for verification of Doppler lidar velocity statistics. Author

*Autonomy; Doppler Radar; Space Missions; Algorithms; Computerized Simulation; Calibrating; Remote Sensing*

**20010125616** NASA Marshall Space Flight Center, Huntsville, AL USA

**System and Method for Determining Rate of Rotation Using Brushless DC Motor**

Howard, David E., Inventor, NASA Marshall Space Flight Center, USA; Smith, Dennis A., Inventor, NASA Marshall Space Flight Center, USA; Nov. 07, 2000; 6p; In English

Patent Info.: Filed 27 Jul. 1998; NASA-Case-MFS-31143-1; US-Patent-6,144,198; US-Patent-Appl-SN-128634; No Copyright; Avail: CASI; A02, Hardcopy; A01, Microfiche

A system and method are provided for measuring rate of rotation. A brushless DC motor is rotated and produces a back electromagnetic force (emf) on each winding thereof. Each winding's back-emf is squared. The squared outputs associated with each winding are combined, with the square root being taken of such combination, to produce a DC output proportional only to the rate of rotation of the motor's shaft.

Official Gazette of the U.S. Patent and Trademark Office

*Shafts (Machine Elements); Speed Indicators*

**20010125617** NASA Langley Research Center, Hampton, VA USA

**Cryogenic, Absolute, High Pressure Sensor**

Chapman, John J., Inventor, NASA Langley Research Center, USA; Shams. Qamar A., Inventor, NASA Langley Research Center, USA; Powers, William T., Inventor, NASA Langley Research Center, USA; Jun. 05, 2001; 8p; In English; Continuation of abandoned US-Patent-Appl-SN-681245, filed 22 Jul. 1996

Patent Info.: Filed 10 Dec. 1996; NASA-Case-LAR-15280-2-SB; US-Patent-6,240,785; US-Patent-Appl-SN-778065; US-Patent-Appl-SN-681245; No Copyright; Avail: CASI; A02, Hardcopy; A01, Microfiche

A pressure sensor is provided for cryogenic, high pressure applications. A highly doped silicon piezoresistive pressure sensor is bonded to a silicon substrate in an absolute pressure sensing configuration. The absolute pressure sensor is bonded to an aluminum nitride substrate. Aluminum nitride has appropriate coefficient of thermal expansion for use with highly doped silicon at cryogenic temperatures. A group of sensors, either two sensors on two substrates or four sensors on a single substrate are packaged in a pressure vessel.

Official Gazette of the U.S. Patent and Trademark Office

*Cryogenic Temperature; Detection; High Pressure; Pressure Sensors*

**20010125619** NASA Langley Research Center, Hampton, VA USA

**Thickness Measurement Device for Ice, or Ice Mixed with Water or Other Liquid**

Weinstein, Leonard M., Inventor, NASA Langley Research Center, USA; May 29, 2001; 11p; In English; Continuation-in-part of abandoned US-Patent-Appl-SN-060590, filed 15 Apr. 1998, which is a continuation-in-part of US-Patent-Appl-SN-619779, filed 20 Mar. 1996

Patent Info.: Filed 4 Apr. 2000; NASA-Case-LAR-16093-1; US-Patent-6,239,601; US-Patent-Appl-SN-545860; US-Patent-Appl-SN-060590; US-Patent-Appl-SN-619779; No Copyright; Avail: CASI; A03, Hardcopy; A01, Microfiche

A Device and Method are provide for determining the thickness of a layer of solid ice, a mixture of ice and water, or a mixture of ice arid other liquid, accumulated on the outer surface of an object. First and second total impedance sensors are operated at first and second frequencies. Corresponding first and second AC total impedance measuring circuits are coupled to The first and second sensors to produce output voltages based on the total impedance changes sensed by the sensors. A processor is coupled to the first and second measuring circuits to generate an output value using the measured output voltages. The output value s indicative of the thickness of the ice or ice and water mixture, or ice and other liquid.

Official Gazette of the U.S. Patent and Trademark Office

*Alternating Current; Ice; Thickness; Depth Measurement*

## 36
## LASERS AND MASERS

*Includes lasing theory, laser pumping techniques, maser amplifiers, laser materials, and the assessment of laser and maser outputs. For cases where the application of the laser or maser is emphasized see also the specific category where the application is treated. For related information see also 76 Solid-State Physics.*

**20010118508** Norwegian Defence Research Establishment, Kjeller, Norway

**Thermal Effects in End-Pumped Solid State Lasers: Influence on Resonator Stability, Beam Quality, and Output Power**

Stenersen, Knut, Norwegian Defence Research Establishment, Norway; Lippert, Espen, Norwegian Defence Research Establishment, Norway; Rustad, Gunnar, Norwegian Defence Research Establishment, Norway; Arisholm, Gunnar, Norwegian Defence Research Establishment, Norway; Jul. 30, 2001; 38p; In English

Contract(s)/Grant(s): FFIE Proj. 792/115

Report No.(s): FFI/RAPPORT-2001/03865; ISBN 82-464-0531-4; No Copyright; Avail: CASI; A03, Hardcopy; A01, Microfiche

A theoretical analysis is given of the magnitudes of thermal effects in end-pumped high-power solid state lasers, and their influence on the laser output characteristics, particularly the beam quality and conversion efficiency. The theory of thermal lensing and stress-induced birefringence found in laser textbooks for the case of top-hat pump- and resonator modes, is extended to cover the more general case of Gaussian modes. Analytic expressions for these cases are derived. Expressions are also derived for the reduction of the birefringence loss, which can be achieved by inserting a quarter- wave plate between the laser rod and the laser end mirror. An analysis is given of the tolerance of laser resonators to thermal lensing, providing guide lines for the choice of resonator parameters in order to ensure sufficient resonator stability margins. Finally, a few examples are given of the results of rigorous numerical simulations of an end-pumped ND:YAG laser. It is found that the analytic theory provides fairly good guide lines concerning the choice of resonator parameters in many cases, but there are also cases where the numerical simulations provide quite surprising results. In particular, it is found that good performance can be obtained even if the thermal focal length on the laser rod axis is substantially shorter than the limit for a stable resonator. For optimal choices of resonator parameters and pump beam diameter, it is found that a 50 W pump beam at 808 mn can be converted to more than 20 W output at 1064 nm, with a beam quality of M(sup 2) less than 2.
Author
*Numerical Analysis; Magnitude; Temperature Effects; Solid State; Losses; Laser Outputs; High Power Lasers*

**20010118908** Sandia National Labs., Albuquerque, NM USA
**Alternative Form of Laser Beam Characterization**
Knorovsky, G. A.; MacCallum, D. O.; Jun. 30, 2000; 9p; In English
Report No.(s): DE2000-760792; SAND2000-1574C; No Copyright; Avail: Department of Energy Information Bridge

Careful characterization of laser beams used in materials processing such as welding and drilling is necessary to obtain robust, reproducible processes and products. Recently, equipment and techniques have become available which make it possible to rapidly and conveniently characterize the size, shape, mode structure, beam quality (Mz), and intensity of a laser beam (incident power/unit area) as a function of distance along the beam path. This facilitates obtaining a desired focused spot size and also locating its position. However, for a given position along the beam axis, these devices typically measure where the beam intensity level has been reduced to I/ez of maximum intensity at that position to determine the beam size. While giving an intuitive indication of the beam shape since the maximum intensity of the beam varies greatly, the contour so determined is not an iso-contour of any parameter related to the beam intensity or power. In this work we shall discuss an alternative beam shape formulation where the same measured information is plotted as contour intervals of intensity.
NTIS
*Drilling; Laser Beams*

**20010119585** Defense Science Board, Washington, DC USA
**Defense Science Board Task Force on High Energy Laser Weapon Systems Applications *Final Report***
Welch, Larry D.; Latham, Donald C.; Jun. 2001; 213p; In English
Report No.(s): AD-A394880; No Copyright; Avail: CASI; A10, Hardcopy; A03, Microfiche

This is the final report of the DSB Task Force on High Energy Laser (HEL) Weapon System Applications. The Task Force was tasked to review and evaluate recent and on-going programs in HEL applications, examine recent supporting technology advancements and their applications, and determine what remains to be done to ”weaponize” these systems in applicable combat theater environments. They were asked to make recommendations on the need for additional DoD research efforts, strategic and tactical impact of HEL systems on future military operations, and capabilities of the U.S. defense industrial base to support development of HEL systems. In this report, the Task Force states that high power lasers have the potential to change future military operations in dramatic ways. The USA is in a position to exploit current high energy laser technology to take advantage of speed-of-flight engagement, precisely controlled effects, deep magazines, low cost per shot, and reduced logistics footprint.
Derived from text
*Laser Weapons; High Power Lasers; USA; Defense Program*

**20010120037** Hughes Research Labs., Malibu, CA USA
**Kilowatt Yb:YAG Laser Illuminator**
Sumida, David S.; Bruesselbach, Hans; Reeder, Robin; Byren, Robert W.; Mar. 01, 1997; 5p; In English
Report No.(s): AD-A394868; No Copyright; Avail: CASI; A01, Hardcopy; A01, Microfiche

We report 0.6 kW quasi-cw output power for our diode- side-pumped Yb:YAG power oscillator. This 2-mm diameter rod pump cavity is the smallest of three pump cavities slated for use in a multi-kilowatt Yb:YAG illuminator master-oscillator

power-amplifier (MOPA) source. In preliminary results, we have also obtained 225 W cw average output power using alternative cw pump diode arrays. Latest performance data and on-going MOPA development will be described.
DTIC
*YAG Lasers; Oscillators; Continuous Radiation; Illuminators*

**20010120480** Academy of Sciences (Russia), Inst. for Laser Physics, Saint Petersburg, Russia
**Laser Optics 2000: Solid State Lasers. Volume 4350**
Ustugov, Vladimir I., Academy of Sciences (Russia), Russia; Sep. 14, 2001; 213p; In English
Report No.(s): AD-A394954; CSP-00-5049; No Copyright; Avail: CASI; A10, Hardcopy; A03, Microfiche
The Final Proceedings for the Tenth Conference on Laser Optics, held 26-30 June 2000 in St. Petersburg, Russia. This is an interdisciplinary conference. Topics include generation of ultrashort light pulses, application of nonlinear correction techniques in adaptive optics and lasers, advanced methods of beam control and pointing; diode-pumped solid state lasers; high average power gas and solid-state lasers; and lasers in medicine and medical applications.
DTIC
*Solid State Lasers; Beams (Radiation); Correction*

**20010120481** Academy of Sciences (Russia), Inst. for Laser Physics, Saint Petersburg, Russia
**Laser Optics 2000: High-Power Gas Lasers, Volume 4351**
Danilov, Oleg B., Editor, Academy of Sciences (Russia), Russia; Sep. 14, 2001; 194p; In English; Laser Optics 2000: High-Power Gas Lasers, 26-20 Jun. 2000, Saint Petersburg, Russia
Report No.(s): AD-A394955; CSP-00-5049-VOL-4351; No Copyright; Avail: CASI; A09, Hardcopy; A03, Microfiche
The Final Proceedings for the Tenth Conference on Laser Optics, held 26-30 June 2000 in St. Petersburg, Russia. This is an interdisciplinary conference. Topics include generation of ultrashort light pulses, application of nonlinear correction techniques in adaptive optics and lasers, advanced methods of beam control and pointing; diode-pumped solid state lasers; high average power gas and solid-state lasers; and lasers in medicine and medical applications.
DTIC
*Solid State Lasers; Optics; Gas Lasers; High Power Lasers; Beams (Radiation)*

**20010120482** Academy of Sciences (Russia), Inst. for Laser Physics, Saint Petersburg, Russia
**Laser Optics 2000: Ultrafast Optics and Superstrong Laser Fields, Volume 4352**
Yashin, Vladimir E., Academy of Sciences (Russia), Russia; Andreev, Alexander A., Academy of Sciences (Russia), Russia; Sep. 14, 2001; 278p; In English; Laser Optics 2000: Ultrafast Optics and Superstrong Laser Fields, 26-30 Jun. 2000, Saint Petersburg, Russia
Report No.(s): AD-A394956; CSP-00-5049-VOL-4352; No Copyright; Avail: CASI; A13, Hardcopy; A03, Microfiche
The Final Proceedings for the Tenth Conference on Laser Optics, held 26-30 June 2000 in St. Petersburg, Russia. This is an interdisciplinary conference. Topics include generation of ultrashort light pulses, application of nonlinear correction techniques in adaptive optics and lasers, advanced methods of beam control and pointing; diode-pumped solid state lasers; high average power gas and solid-state lasers; and lasers in medicine and medical applications.
DTIC
*Solid State Lasers; Optics; Beams (Radiation); Laser Outputs*

**20010120841** Michigan Univ., Solid-state Electronics Lab., Ann Arbor, MI USA
**Integrated Transmitters and Long-Wavelength VCSELs** ***Annual Report, 1 Oct. 2000-30 Sep. 2001***
Bhattacharya, Pallab; Oct. 11, 2001; 9p; In English
Contract(s)/Grant(s): N00014-96-1-0024
Report No.(s): AD-A395292; No Copyright; Avail: CASI; A02, Hardcopy; A01, Microfiche
The objective of this program is to develop InP-based monolithically integrated transmitters, including internal (current) and external modulation. The basic issues involved in such integration and operation of the individual devices will be explored both theoretically and experimentally. Thus, intrinsic and extrinsic factors that limit internal and external modulation, propagation and scattering of light in guided structures and through mirrors, and circuits, materials and lithography issues to develop high-frequency (less than 30 GHz) transmitters will be explored. Integrated chips with driver circuits and guided wave elements will be developed and tested. At the same time we are also developing novel top- and edge-emitting microcavity laser structures in which zero or very low threshold currents are expected due to phonon confinement. Preliminary results, both theoretical and

experimental, are very encouraging, and we envisage that these low threshold, high frequency devices will be extremely useful for chip-to-chip and array-based optical interconnects.
DTIC
*Solid State Lasers; Lasers; Cavities; Emitters; Optical Interconnects*

**20010121554** Georgia Univ., Dept. of Chemistry, Athens, GA USA
**Pulsed Infrared Laser System to Study Metal Ion Solvation** ***Final Report, 31 Mar. 2000 - 30 Mar. 2001***
Duncan, Michael A.; Sep. 2001; 9p; In English
Contract(s)/Grant(s): F49620-00-1-0188; AF Proj. 3484
Report No.(s): AD-A395168; AFRL-SR-BL-TR-01-0518; No Copyright; Avail: CASI; A02, Hardcopy; A01, Microfiche

A new Nd:YAG laser was purchased using AFOSR-DURIP funds and this laser was incorporated into a new infrared laser spectroscopy system based on emerging OPO/OPA technology. This laser is now employed in the study of the IR spectroscopy of size-selected metal ion complexes. Initial results have been obtained for Mg(+) and Fe(+) ions in complexes with CO2 and in mixed CO2/Ar complexes. The initial results are quite promising, and they suggest that this IR spectroscopy methodology will become a general way to determine the structures of clusters and to investigate their growth dynamics.
DTIC
*YAG Lasers; Infrared Spectroscopy; Laser Spectroscopy; Infrared Lasers; Carbon Dioxide*

**20010122397** Academy of Sciences (Russia), Inst. for Laser Physics, Saint Petersburg, Russia
**Laser Optics 2000: Semiconductor Lasers and Optical Communication, Volume 4354**
Gurevich, Serguei A., Academy of Sciences (Russia), Russia; Rosanov, Nikolay N., Academy of Sciences (Russia), Russia; Sep. 14, 2001; 212p; In English; Laser Optics 2000: Semiconductor Lasers and Optical Communication, 26-30 Jun. 2000, Saint Petersburg, Russia
Report No.(s): AD-A394958; CSP-00-5049; No Copyright; Avail: CASI; A10, Hardcopy; A03, Microfiche

The Final Proceedings for the Tenth Conference on Laser Optics, held 26-30 June 2000 in St. Petersburg, Russia. This is an interdisciplinary conference. Topics include generation of ultrashort light pulses, application of nonlinear correction techniques in adaptive optics and lasers, advanced methods of beam control and pointing; diode-pumped solid state lasers; high average power gas and solid-state lasers; and lasers in medicine and medical applications.
DTIC
*Solid State Lasers; Semiconductor Lasers; Beams (Radiation); Optical Communication*

**20010122398** Academy of Sciences (Russia), Inst. for Laser Physics, Saint Petersburg, Russia
**Laser Optics 2000: Control of Laser Beam Characteristics and Nonlinear Methods for Wavefront Control, Volume 4353**
Sherstobitov, Vladimir E., Editor, Academy of Sciences (Russia), Russia; Soms, Leonid N., Editor, Academy of Sciences (Russia), Russia; Sep. 14, 2001; 365p; In English; Laser Optics 2000: Control of Laser Beam Characteristics and Nonlinear Methods for Wavefront Control, 26-30 Jun. 2000, Saint Petersburg, Russia
Report No.(s): AD-A394957; CSP-00-5049-Vol-4353; No Copyright; Avail: CASI; A16, Hardcopy; A03, Microfiche

The Final Proceedings for the Tenth Conference on Laser Optics, held 26-30 June 2000 in St. Petersburg, Russia. This is an interdisciplinary conference. Topics include generation of ultrashort light pulses, application of nonlinear correction techniques in adaptive optics and lasers, advanced methods of beam control and pointing; diode-pumped solid state lasers; high average power gas and solid-state lasers; and lasers in medicine and medical applications.
DTIC
*Optics; Laser Beams; Beams (Radiation); Wave Fronts*

**20010122478** Argonne National Lab., IL USA
**Laser beam welding of any metal**
Leong, K. H.; Oct. 01, 1998; 11p; In English
Report No.(s): DE2001-10807; ANL/TD/CP-96467; No Copyright; Avail: Department of Energy Information Bridge, Microfiche

The effect of a metal's thermophysical properties on its weldability are examined. The thermal conductivity, melting point, absorptivity and thermal diffusivity of the metal and the laser beam focused diameter and welding speed influence the minimum beam irradiance required for melting and welding. Beam diameter, surface tension and viscosity of the molten metal affect weld pool stability and weld quality. Lower surface tension and viscosity increases weld pool instability. With larger beam diameters causing wider welds, dropout also increases. Effects of focused beam diameter and joint fitup on weldability are also examined.

Small beam diameters are sensitive to beam coupling problems in relation to fitup precision in addition to beam alignment to the seam. Welding parameters for mitigating weld pool instability and increasing weld quality are derived from the above considerations. Guidelines are presented for the tailoring of welding parameters to achieve good welds. Weldability problems can also be anticipated from the properties of a metal.
NTIS
*Laser Welding; Metals; Thermophysical Properties*

**20010123210** Argonne National Lab., IL USA
**Performance of the small-angle diffractometer, SAND at IPNS**
Thiyagarajan, P.; Jul. 17, 1998; 17p; In English
Report No.(s): DE2001-10894; ANL/IPNS/CP-96859; No Copyright; Avail: Department of Energy Information Bridge, Microfiche

The time-of-flight small-angle diffractometer (SAND) has been serving the scientific user community since 1996. One notable feature of SAND is its capability to measure the scattered intensity in a wide Q (4(pi)sin(theta)/(lambda), where 2(theta) is the scattering angle and (lambda) is the wavelength of the neutrons) range of 0.0035 to 0.5 (angstrom)(sup (minus)1) in a single measurement. The optical alignment system makes it easy to set up the instrument and the sample. The cryogenically cooled MgO filter reduces the fast neutrons over two orders of magnitude, while still transmitting over 70% of the cold neutrons. A drum chopper running at 15 Hz suppresses the delayed neutron background. SAND has a variety of ancillary equipment to control the sample environment. In this paper we describe the features of the SAND instrument, compare its data on a few standard samples with those measured at well established centers in the world, and display two scientific examples which take advantage of measuring data in a wide Q-range in a single measurement. With a new set of tight collimators the Q(sub min) can be lowered to 0.002 (angstrom)(sup (minus)1) and the presently installed high-angle bank of detectors will extend the Q(sub max) to 2 (angstrom)(sup (minus)1).
NTIS
*Alignment; Cold Neutrons; Collimators; Diffractometers; Synchrotrons*

**20010123898** Argonne National Lab., IL USA
**Laser ablation of concrete**
Savina, M.; Oct. 05, 1998; 10p; In English
Report No.(s): DE2001-10992; ANL/CHM/CP-97403; No Copyright; Avail: Department of Energy Information Bridge, Microfiche

Laser ablation is effective both as an analytical tool and as a means of removing surface coatings. The elemental composition of surfaces can be determined by either mass spectrometry or atomic emission spectroscopy of the atomized effluent. Paint can be removed from aircraft without damage to the underlying aluminum substrate, and environmentally damaged buildings and sculptures can be restored by ablating away deposited grime. A recent application of laser ablation is the removal of radioactive contaminants from the surface and near-surface regions of concrete. We present the results of ablation tests on concrete samples using a high power pulsed Nd:YAG laser with fiber optic beam delivery. The laser-surface interaction was studied on various model systems consisting of Type I Portland cement with varying amounts of either fine silica or sand in an effort to understand the effect of substrate composition on ablation rates and mechanisms. A sample of non-contaminated concrete from a nuclear power plant was also studied. In addition, cement and concrete samples were doped with non-radioactive isotopes of elements representative of cooling waterspills, such as cesium and strontium, and analyzed by laser-resorption mass spectrometry to determine the contamination pathways. These samples were also ablated at high power to determine the efficiency with which surface contaminants are removed and captured. The results show that the neat cement matrix melts and vaporizes when little or no sand or aggregate is present. Surface flows of liquid material are readily apparent on the ablated surface and the captured aerosol takes the form of glassy beads up to a few tens of microns in diameter. The presence of sand and aggregate particles causes the material to disaggregate on ablation, with intact particles on the millimeter size scale leaving the surface. Laser resorption mass spectrometric analysis showed that cesium and potassium have similar chemical environments in the matrix, as do strontium and calcium.
NTIS
*Laser Ablation; Radioactive Contaminants; Concretes; Decontamination*

**20010124086** California Univ., Lawrence Berkeley Lab., Berkeley, CA USA
**Possible experiment at LEUTL to characterize surface roughness Wakefield effects**
Biedron, S. G.; Dattoli, G.; Fawley, W. M.; Freund, H. P.; Huang, Z.; Jan. 10, 2001; 6p; In English
Report No.(s): DE2001-775179; LBNL-47331; No Copyright; Avail: Department of Energy Information Bridge

Wakefield effects due to internal vacuum chamber roughness may increase the electron beam energy spread and so have become an immediate concern for future x-ray free-electron laser (FEL) project developments such as the SLAC Linac Coherent Light Source (LCLS) and the DESY TESLA x-ray FEL. We describe a possible experiment to characterize the effects of surface roughness on an FEL driven by self-amplified spontaneous emission (SASE) operation. Although the specific system described is not completely identical to the above-proposed projects, much useful scaling information could be obtained and applied to shorter wavelength systems.

NTIS
*Free Electron Lasers; Spontaneous Emission; Surface Roughness; Coherent Light; Electron Beams*

**20010125105** National Defence Research Establishment, Div. of Sensor Technology, Linkoeping, Sweden
**Multifunction Laser Radar *Final Report***
Karlsson, C.; Olsson, F.; Letalick, D.; December 1999; 22p; In English
Report No.(s): PB2001-108134; FOA-R-99-01301-408-SE; No Copyright; Avail: CASI; A03, Hardcopy; A01, Microfiche

In this paper, the design and performance of a simple 1.55 micron CW (continuous wave), FMCW (frequency modulated continuous wave) CLR (clear sky outgoing long-wave radiation)-system with an output power of 1W is presented. A polarization-independent fibrer optic circulator is used as the transmit/receive-switch in the system, which allows for a very simple and small system with no polarization-maintaining components and fibers. The demonstration proved that the performance of the multifunction laser radar system was near the theoretical upper limit. Furthermore, it also proved the applicability to some interesting military applications. Especially whispering rangefinding on diffuse targets up to 3 km was demonstrated. The system is capable of performing wind measurements even in very clear atmospheric conditions. The military use of coherent laser radar systems includes, e.g., whispering ranging of targets, vibrometry for target characterization, wind measurement for weapon correction, etc..

NTIS
*Optical Radar; Wind Velocity; Measuring Instruments*

**20010125635** NASA Langley Research Center, Hampton, VA USA
**Method of Controlling Lasing Wavelength(s)**
Barnes, Norman P., Inventor, NASA Langley Research Center, USA; Murray, Keith E., Inventor, NASA Langley Research Center, USA; Hutcheson, Ralph L., Inventor, NASA Langley Research Center, USA; Oct. 31, 2000; 9p; In English
Patent Info.: Filed 13 May 1998; NASA-Case-LAR-15564-1-SB; US-Patent-6,141,368; US-Patent-Appl-SN-078410; No Copyright; Avail: CASI; A02, Hardcopy; A01, Microfiche

A method is provided to control the lasing wavelength of a laser material without changing or adjusting the mechanical components of a laser device, The rate at which the laser material is pumped with the pumping energy is controlled so that lasing occurs at one or more lasing wavelengths based on the rate. The lasing wavelengths are determined by transition lifetimes and/or energy transfer rates.

Official Gazette of the U.S. Patent and Trademark Office
*Lasing; Laser Materials; Wavelengths*

## 37
## MECHANICAL ENGINEERING

*Includes mechanical devices and equipment; machine elements and processes. For cases where the application of a device or the host vehicle is emphasized see also the specific category where the application or vehicle is treated. For robotics see 63 Cybernetics, Artificial Intelligence, and Robotics; and 54 Man/System Technology and Life Support.*

**20010117662** Sandia National Labs., Albuquerque, NM USA
**Materials Issues for Micromachines Development: ASCI Program Plan**
Fang,; Battaile,; Benavides,; Ensz,; Buchheit,; May 01, 2000; 36p; In English
Report No.(s): DE2000-759431; SAND2000-1308; No Copyright; Avail: Department of Energy Information Bridge

This report summarizes materials issues associated with advanced micromachines development at Sandia. The intent of this report is to provide a perspective on the scope of the issues and suggest future technical directions, with a focus on computational materials science. Materials issues in surface micromachining (SMM), Lithographic-Galvan oformung-Abformung (LIGA: lithography, electrodeposition, and molding), and meso-machining technologies were identified. Each individual issue was assessed in four categories: degree of basic understanding; amount of existing experimental data capability of existing models; and, based on the perspective of component developers, the importance of the issue to be resolved. Three broad requirements for micromachines emerged from this process. They are: (1) tribological behavior, including stiction, friction, wear, and the use of surface treatments to control these, (2) mechanical behavior at microscale, including elasticity, plasticity, and the effect of microstructural features on mechanical strength, and (3) degradation of tribological and mechanical properties in normal (including aging), abnormal and hostile environments. Resolving all the identified critical issues requires a significant cooperative and complementary effort between computational and experimental programs. The breadth of this work is greater than any single program is likely to support. This report should serve as a guide to plan micromachines development at Sandia.
NTIS
*Mechanical Properties; Microelectromechanical Systems; Tribology; Elastic Properties*

**20010117709** National Renewable Energy Lab., Golden, CO USA
**Exploring Low Emission Lubricants for Diesel Engines**
Perez, J. M.; Jul. 06, 2000; 388p; In English
Report No.(s): DE2000-758768; NREL/SR-570-28521; No Copyright; Avail: Department of Energy Information Bridge, Microfiche

A workshop to explore the technological issues involved with the removal of sulfur from lubricants and the development of low emission diesel engine oils was held in Scottsdale, Arizona, January 30 through February 1, 2000. It presented an overview of the current technology by means of panel discussions and technical presentations from industry, government, and academia.
NTIS
*Diesel Engines; Lubricants; Removal*

**20010118258** Department of Energy, Washington, DC USA
**CFCC applications for diesel engine valve guides. DOE Continuous Fiber Ceramic Composite Program. Phase II A/B. Final report**
Twait, D.; Long, M.; Apr. 14, 1999; 61p
Report No.(s): DE2000-761919; DOE/CE/41002-F; No Copyright; Avail: Department of Energy Information Bridge, Microfiche

The driving forces for diesel and alternative fuel technology are reliability, durability, efficiency, and emission regulations. The self-lubricating exhaust valve guides technology was expected to increase the reliability and durability of advanced, fuel efficient diesel engines and diesel engines which use low emission fuels. For this reason, the objective of this program was to develop a self-lubricating carbon fiber/ silicon nitride composite exhaust valve guide for diesel engines. The program was divided into three phases - Phase I - Exploratory Development, Phase II - Process Engineering and Component Development, and Phase III - Pilot Scale Process Development. The results of Phase I were presented in a final report. This report summarizes the results of Phase II. Phase II consisted of three major tasks: Process Optimization for Manufacturing, Component Fabrication and Testing, and Component Evaluation.
NTIS
*Ceramics; Diesel Engines; Valves*

**20010118916** Brookhaven National Lab., Upton, NY USA
**Error reduction in duct leakage testing through data cross-checks**
Andrews, J. W.; Dec. 31, 1998; 20p; In English
Report No.(s): DE2000-760980; BNL-66147; No Copyright; Avail: Department of Energy Information Bridge

One way to reduce uncertainty in scientific measurement is to devise a protocol in which more quantities are measured than are absolutely required, so that the result is over constrained. This report develops a method for so combining data from two different tests for air leakage in residential duct systems. An algorithm, which depends on the uncertainty estimates for the measured quantities, optimizes the use of the excess data. In many cases it can significantly reduce the error bar on at least one of the two measured duct leakage rates (supply or return), and it provides a rational method of reconciling any conflicting results from the two leakage tests.
NTIS
*Ducts; Algorithms; Leakage; Performance Prediction; Reliability Analysis; Accuracy*

**20010119530** Lawrence Livermore National Lab., Livermore, CA USA

**Exhaust energy recovery for control of a homogenous charge compression ignition engine**

Martinez-Frias, J. M.; Aceves, S. M.; Flowers, D.; Smith, J. R.; Dibble, R.; Apr. 03, 2000; 30p; In English

Report No.(s): DE2000-756835; UCRL-JC-138377; No Copyright; Avail: Department of Energy Information Bridge

This work investigates a purely thermal control system for HCCI (homogenous charge compression ignition) engines, where thermal energy from exhaust gas recirculation (EGR) and compression work in the supercharger are either recycled or rejected as needed. HCCI engine operation is analyzed with a detailed chemical kinetics code, HCT (Hydrodynamics, Chemistry and Transport), which has been extensively modified for application to engines. HCT is linked to an optimizer that determines the operating conditions that result in maximum brake thermal efficiency, while meeting the restrictions of low NOx and peak cylinder pressure. The results show the values of the operating conditions that yield optimum efficiency as a function of torque for a constant engine speed (1800 rpm). For zero torque (idle), the optimizer determines operating conditions that result in minimum fuel consumption. The optimizer is also used for determining the maximum torque that can be obtained within the operating restrictions of NOx and peak cylinder pressure. The results show that a thermally controlled HCCI engine can successfully operate over a wide range of conditions at high efficiency and low emissions.

NTIS

*Internal Combustion Engines; Thermal Energy; Exhaust Gases; Thermodynamic Efficiency*

**20010119572** Argonne National Lab., IL USA

**Vibratory response of a precision double-multi-layer monochromator positioning system using a generic modeling program with experimental verification**

Barraza, J.; Jul. 29, 1998; 8p; In English

Report No.(s): DE2001-10573; ANL/XFD/CP-95384; No Copyright; Avail: Department of Energy Information Bridge, Microfiche

A generic vibratory response-modeling program has been developed as a tool for designing high-precision optical positioning systems. The systems are modeled as rigid-body structures connected by linear non-rigid elements such as complex actuators and bearings. The full dynamic properties of each non-rigid element are determined experimentally or theoretically, then integrated into the program as inertial and stiffness matrices. Thus, it is possible to have a suite of standardized structural elements for modeling many different positioning systems that use standardized components. This paper will present the application of this program to a double-multi-layer monochromator positioning system that utilizes standardized components. Calculated results are compared to experimental modal analysis results.

NTIS

*Monochromators; Positioning; Computerized Simulation; Vibration Effects*

**20010119981** Argonne National Lab., IL USA

**Identification of root cause and abatement of vibration of monochromator**

Jendrzejczyk, J. A.; Jan. 13, 1998; 15p; In English

Report No.(s): DE2001-10559; ANL/ET/CP-95325; No Copyright; Avail: Department of Energy Information Bridge

Silicon crystal mirrors are used to reflect high-intensity X-ray beams. A large amount of heat is generated in each mirror. to minimize the effect of thermal expansion on the crystal mirrors, heat is removed by pumping liquid gallium (with a boiling point of 29.8 C) through passages in the crystal mirrors. During system operation, mirror motion should be kept to an acceptable level to avoid performance degradation. There are many potential sources of excitation to the crystal assembly; one such source is the flowing gallium. Two series of tests were performed earlier for a near-prototypical gallium cooling system. This paper describes a series of tests to measure the general vibration response characteristics of critical components in the monochromator system that contains the mirrors. The main objective of this work is to identify the root cause of vibration and to recommend general guidelines for abatement of vibration. This is achieved by performing many tests to understand the response characteristics under various conditions, by analysis of the response data, and by use of some theoretical considerations.

NTIS

*Liquid Metals; Cooling Systems; Mirrors; Silicon; Beams (Radiation)*

**20010120146** Air Force Inst. of Tech., Wright-Patterson AFB, OH USA

**Issues in the Design, Modeling, and Manufacture of Multiple Joint Solder Self-Assembled Micro-Electro-Mechanical Systems (MEMS)**

Kladitis, Paul E.; Aug. 06, 2001; 332p; In English

Report No.(s): AD-A395144; No Copyright; Avail: CASI; A15, Hardcopy; A03, Microfiche

Using the surface tension of molten solder to assemble micro-sized structures or micro-electro-mechanical systems (MEMS), otherwise known as ”solder self-assembly” is a recent development. Complex three-dimensional assemblies, previously not realizable, can now be realized using surface micromachined MEMS and solder assembly. Not only can complex or non-complex assemblies be realized using solder self-assembly, but realized by adopting means already established commercially for mass production. This work is the first in the world to quantify or address the known entirety of major issues that go into realizing multiple joint solder self-assembled polysilicon surface micromachined MEMS. An assembly process for multiple joint solder self-assembled MEMS is developed with a yield of 94.3%. Chemical, temperature, and timing issues are detailed for the assembly process. Guidelines on the proper design of hinges, solder pads, and connecting structures for multiple joint solder self- assembled MEMS are developed. 259 two joint test structures were designed, assembled, and measured. An assembly model of series connected n-solder joint, microstructures is developed. The experimental results are compared to the model predictions.
DTIC
*Microelectromechanical Systems; Microstructure; Silicon Polymers; Solders; Mathematical Models; Self Assembly*

**20010120484** Liquid Drive Corp., Holly, MI USA
**Variable Speed Fan Drive Assembly** ***Final Report***
Ressler, H. E.; Aug. 13, 1962; 21p; In English
Contract(s)/Grant(s): DA-20-018-ORD-23658
Report No.(s): AD-A395012; No Copyright; Avail: CASI; A01, Microfiche; A03, Hardcopy

This report covers designing, building and testing of a variable speed fan drive. Speed control automatic from 0 to approximately 4900 rpm governed by engine coolant temperature. Unit includes a fail safe device which operates the fan at maximum speed in the event of a control failure. Unit also includes a deepwater fording switch to reduce fan speed when engine compartment is flooded. Direction of rotation is counter-clockwise viewed from output end. Tests performed on unit included a functional check on speed modulation, declutching, fail safe devices and deep water fording switch operation. All these tests were performed using a 1765 rpm electric motor. A high speed test of approximately 4800 rpm was also made to assure satisfactory operation at elevated speed. Results obtained from above tests indicate that fan drive will perform satisfactorily, but final evaluation is best obtained by operating under actual engine conditions.
DTIC
*Mechanical Drives; Speed Control; Electric Motors*

**20010122288** Sandia National Labs., Albuquerque, NM USA
**Heat-Pipe Wick Characterization**
Jones, J. L.; Aug. 15, 2000; 11p; In English
Report No.(s): DE2000-761870; SAND2000-2067C; No Copyright; Avail: Department of Energy Information Bridge, Microfiche

The development of liquid metal heat-pipes for use in solar powered Stirling engines has led to an in-depth analysis of heat-pipe wick properties. To model the flow of liquid sodium through the wick its two-phase permeability measurement is of interest. The permeability will be measured by constructing a test cell made up of a wick sample sintered to a manifold. Measuring the volumetric flow rate through the wick will allow for a determination of the wick’s permeability as a function of pressure. Currently, simple estimates of permeability as a function of vapor fraction of a porous media are being used as a model to calculate the two-phase permeability. The above mentioned experiment will be used to test the existing formulas validity. The plan is to make use of a known procedure for testing permeability and apply those techniques to a felt-metal wick. The results will be used to verify and/or modify the two-phase permeability estimates. With the increasing desire to replace directly illuminated engines with the much more efficient heat-pipe apparatus it is inherently clear that the usefulness of known wick properties will make wick permeability design a simpler process.
NTIS
*Stirling Engines; Heat Pipes; Wicks; Liquid Metals*

**20010122369** Argonne National Lab., IL USA
**Transient analysis of a flywheel battery containment during a full rotor burst event**
Hsieh, B. J., Argonne National Lab., USA; Apr. 17, 1998; 8p; In English
Report No.(s): DE2001-10745; ANL/RE/CP-96198; No Copyright; Avail: Department of Energy Information Bridge, Microfiche

Flywheels are being developed for use in an Advanced Locomotive Propulsion System (ALPS) targeted for use in high speed passenger rail service. The ALPS combines high performance, high speed gas turbines, motor/generators and flywheels to provide a light-weight, fuel-efficient power system. Such a system is necessary to avoid the high cost of railway electrification, as is

currently done for high speed rail service (greater than 100mph) since diesels are too heavy. The light-weight flywheel rotors are made from multilayered composite materials, and are operated at extremely high energy levels. Metal containment structures have been designed to enclose the rotors and provide encapsulation of the rotor during postulated failure events. One such event is a burst mode failure of the rotor in which the composite rim is assumed to burst into debris that impacts against the containment. This paper presents a finite element simulation of the transient structural response of a subscale metal flywheel containment structure to a rotor burst event.
NTIS
*Finite Element Method; Flywheels; Computerized Simulation; Composite Materials; Structural Analysis; Transient Response*

**20010124080** Oak Ridge National Lab., TN USA
**Comparing Maintenance Costs of Geothermal Heat Pump Systems with other HVAC Systems in Lincoln Public Schools: Repair, Service, and Corrective Actions**
Martin, M. A.; Durfee, D. J.; Hughes, P. J.; Jun. 19, 1999; 15p; In English
Report No.(s): DE2001-7918; ORNL/CP-103345; EB 40 02 00 0; No Copyright; Avail: Department of Energy Information Bridge
The Lincoln Public School District, in Lincoln, Nebraska, recently installed vertical-bore geothermal heat pump systems in four, new, elementary schools. Because the district has consistent maintenance records and procedures, it was possible to study repair, service and corrective maintenance requests for 20 schools in the district. Each school studied provides cooling to over 70% of its total floor area and uses one of the following heating and cooling systems: vertical-bore geothermal heat pumps (GHPs), air-cooled chiller with gas-fired hot water boiler (ACUGHWB), water-cooled chiller with gas-fired hot water boiler (WCCYGHWB), or water-cooled chiller with gas-fired steam boiler (WCUGSB). Preventative maintenance and capital renewal activities were not included in the available database. GHP schools reported average total costs at 2.13 cents/ft(sup 2)-yr, followed by ACC/GHWB schools at 2.88 cents/ft(sup 2)-yr, WCC/GSB schools at 3.73 cents/ft(sup 2)-yr, and WCC/GHWB schools at 6.07 cents/ft(sup 2)-yr. Because of tax-exemptions on material purchases, a reliance on in-house labor, and the absence of preventative maintenance records in the database, these costs are lower than those reported in previous studies. A strong relationship (R(sup 2)=O.52) was found between costs examined and cooling system age: the newer the cooling equipment, the less it costs to maintain.
NTIS
*Heat Pumps; Maintenance; Schools; Space Heating (Buildings); Economic Analysis; Geothermal Technology*

**20010124093** Oak Ridge National Lab., TN USA
**Heavy Vehicle Propulsion System Materials Program Semiannual Progress Report for October 1999 through March 2000**
Johnson, D. R.; Aug. 01, 2000; 126p; In English
Report No.(s): DE2001-769300; ORNL/TM-2000/233; No Copyright; Avail: Department of Energy Information Bridge
There are two objectives for this project. The first is to evaluate the cost effectiveness and maturity of various Smart Materials Technologies, which are under consideration for diesel engine applications, such as fuel injection systems. The second is to develop Smart Materials, to be incorporated into working actuators and sensors.
NTIS
*Diesel Engines; Propulsion System Configurations; Smart Materials*

**20010125589** Air-Conditioning and Refrigeration Technology Inst., Inc., Arlington, VA USA
**Elastohydrodynamic Lubrication with Polyolester Lubricants and HFC Refrigerants, Final Report, Volume 1**
Gunsel, S.; Pozebanchuk, M.; Apr. 01, 1999; 234p; In English
Report No.(s): DE2001-8212; DOE/CE/23810-102-VOL-1; No Copyright; Avail: Department of Energy Information Bridge, Microfiche
The objective of this study was to investigate the film formation properties of refrigeration lubricants using the ultrathin film elastohydrodynamic (EHD) interferometry technique and to study the effects of refrigerants on film formation. Film thickness measurements were conducted as a function of lubricant viscosity, speed, temperature, and refrigerant concentration. Based on the EHD film thickness data, effective pressure-viscosity coefficients were calculated for the test fluids at different temperatures and the effects of refrigerants on pressure-viscosity properties were investigated.
NTIS
*Lubrication; Refrigerants; Elastohydrodynamics; Film Thickness*

**20010125606** NASA Marshall Space Flight Center, Huntsville, AL USA

**Apparatus and Method for Generating Thrust Using a Two Dimensional, Asymmetrical Capacitor Module**

Campbell, Jonathan W., Inventor, NASA Marshall Space Flight Center, USA; Nov. 13, 2001; 7p; In English

Patent Info.: Filed 8 Mar. 2000; NASA-Case-MFS-31419-1; US-Patent-6,317,310; US-Patent-Appl-SN-520817; No Copyright; Avail: CASI; A02, Hardcopy; A01, Microfiche

A capacitor module system is provided for creating a thrust force. The system includes a capacitor module provided with a first conductive element having a cylindrical geometry. The first conductive element can be a hollow cylinder or a solid cylinder. The capacitor module also includes a second conductive element axially spaced from the first conductive element and of smaller axial extent. The second conductive element can be a flat disk, a dome, or a conductive tip at the end of a dielectric rod. A dielectric element is disposed between the first conductive element and the second conductive element. The system also includes a high voltage source having first and second terminals connected respectively to the first and second conductive elements. The high voltage source applies a high voltage to the conductive elements of sufficient value to create a thrust force on the module inducing movement thereof.

Official Gazette of the U.S. Patent and Trademark Office

*Asymmetry; Thrust; Cylindrical Bodies*

**20010125615** NASA Marshall Space Flight Center, Huntsville, AL USA

**Orbital Friction Stir Weld System**

Ding, R. Jeffrey, Inventor, NASA Marshall Space Flight Center, USA; Carter, Robert W., Inventor, NASA Marshall Space Flight Center, USA; Jul. 10, 2001; 10p; In English

Patent Info.: Filed 18 Dec. 1998; NASA-Case-MFS-31269-1; US-Patent-6,269,052; US-Patent-Appl-SN-216484; No Copyright; Avail: CASI; A02, Hardcopy; A01, Microfiche

This invention is an apparatus for joining the ends of two cylindrical (i.e., pipe-shaped) sections together with a friction stir weld. The apparatus holds the two cylindrical sections together and provides back-side weld support as it makes a friction stir weld around the circumference of the joined ends.

Official Gazette of the U.S. Patent and Trademark Office

*Cylindrical Bodies; Friction; Welding Machines*

**20010125618** NASA Marshall Space Flight Center, Huntsville, AL USA

**Resealable Roller Clutch**

Myers, W. Neill, Inventor, NASA Marshall Space Flight Center, USA; Oct. 24, 2000; 10p; In English

Patent Info.: Filed 9 Dec. 1998; NASA-Case-MFS-31258; US-Patent-6,135,255; US-Patent-Appl-SN-207710; No Copyright; Avail: CASI; A02, Hardcopy; A01, Microfiche

A clutch that connects a first rotating member to a second rotating member in a manner that allows directional rotation between the two members in an engaged mode and free rotation between the members in a disengaged mode. The novelty of this invention ties in the combination of directional rotation (i.e., rotation in one direction) capability with free rotation (i.e.. rotation in both directions) capability in a single device.

Official Gazette of the U.S. Patent and Trademark Office

*Clutches; Rollers*

**20010125629** NASA Marshall Space Flight Center, Huntsville, AL USA

**Friction Stir Weld System for Welding and Weld Repair**

Ding, R. Jeffrey, Inventor, NASA Marshall Space Flight Center, USA; Romine, Peter L., Inventor, NASA Marshall Space Flight Center, USA; Oelgoetz, Peter A., Inventor, NASA Marshall Space Flight Center, USA; Jan. 16, 2001; 6p; In English; Provisional application of US-Patent-Appl-SN-111418, filed 8 Dec. 1998

Patent Info.: Filed 8 Dec. 1999; NASA-Case-MFS-30125-1; US-Patent-6,173,880; US-Patent-Appl-SN-459388; US-Patent-Appl-SN-111418; No Copyright; Avail: CASI; A02, Hardcopy; A01, Microfiche

A friction stir weld system for welding and weld repair has a base foundation unit connected to a hydraulically controlled elevation platform and a hydraulically adjustable pin tool. The base foundation unit may be fixably connected to a horizontal surface or may be connected to a mobile support in order to provide mobility to the friction stir welding system. The elevation platform may be utilized to raise and lower the adjustable pin tool about a particular axis. Additional components which may be necessary for the friction stir welding process include back plate tooling, fixturing and/or a roller mechanism.

Author

*Friction Welding; Hydraulic Control*

## 38
## QUALITY ASSURANCE AND RELIABILITY

*Includes approaches to, and methods for reliability analysis and control, inspection, maintainability, and standardization.*

**20010117654** Los Alamos National Lab., NM USA
**Digital Spall Radiograph Analysis System**
Harris, C. L.; Jan. 01, 1990; 23p; In English
Report No.(s): DE2000-760076; LA-SUB-00-56; No Copyright; Avail: Department of Energy Information Bridge

This report describes progress on work to develop a cost effective, rapid response system for measuring momentum and kinetic energy of the Armor/Anti-Armor (As) system at for the Advanced Technology Assessment Center (ATAC) Los Alamos National Laboratory. The system will exploit data contained in two sets of simultaneous co-planar flash radiographs taken along the center line of anticipated span motion. Data contained in each set (which is proportional to the mass and z-number of the span material intersected by the exposing x-ray at each point) is digitized and used to construct a three dimensional model (called the reconstructed span image) that approximates the original span cloud. From the model the mass of span fragments is computed. The two sets of radiographs, separated in time, represent the span configuration at two instants of time. Span fragments from the first instant are matched with those from the second instant to determine velocity. Evaluation of the fidelity of candidate reconstruction algorithms is the highest priority task in this development program for the obvious reason that the efficacy of the projected span analysis system depends upon the fidelity of the reconstruction techniques.
NTIS
*Digital Systems; Radiography; Data Acquisition*

**20010117664** Sandia National Labs., Albuquerque, NM USA
**Sandia Heat Flux Gauge Thermal Response and Uncertainty Models**
Blanchat,; Humphries,; Gill,; May 01, 2000; 46p; In English
Report No.(s): DE2000-759428; SAND2000-1111; No Copyright; Avail: Department of Energy Information Bridge

The Sandia Heat Flux Gauge (HFG) was developed as a rugged, cost-effective technique for performing steady state heat flux measurements in the pool fire environment. The technique involves reducing the time-temperature history of a thin metal plate to an incident heat flux via a dynamic thermal model, even though the gauge is intended for use at steady state. In this report, the construction of the gauge is reviewed. The thermal model that describes the dynamic response of the gauge to the fire environment is then advanced and it is shown how the heat flux is determined from the temperature readings. This response model is based on first principles, with no empirically adjusted constants. A validation experiment is presented where the gauge was exposed to a step input of radiant heat flux. Comparison of the incident flux, determined from the thermal response model, with the known flux input shows that the gauge exhibits an noticeable time lag. The uncertainty of the measurement is analyzed, and an uncertainty model is put forth using the data obtained from the experiment. The uncertainty model contains contributions from seventeen separate sources loosely categorized as being either from uncontrolled variability, missing physics, or simplifying assumptions. As part of the missing physics, an empirical constant is found that compensates for the gauge time lag. Because this compensation is incorporated into the uncertainty model instead of the response model, this information can be used to advantage in analyzing pool fire data by causing large uncertainties in non-steady state situations. A short general discussion on the uncertainty of the instrument is presented along with some suggested design changes that would facilitate the determination and reduction of the measurement uncertainty.
NTIS
*Mathematical Models; Measuring Instruments; Heat Flux; Steady State*

**20010119418** Oak Ridge National Lab., TN USA
**Application of Phosphor Thermometry to a Galvanneal Temperature Measurement System**
Beshears, D. L.; Allison, S. W.; Andrews, W. H.; Cates, M. R.; Grann, E. B.; Jun. 01, 1999; 18p; In English
Report No.(s): DE2000-750981; ORNL/TM-1999/129; No Copyright; Avail: Department of Energy Information Bridge

The Galvanneal Temperature Measurement System (GTMS) was developed for the American Iron and Steel Institute by the Oak Ridge National Laboratory through a partnership with the National Steel Midwest Division in Portage, Indiana. The GTMS provides crucial on-line thermal process control information during the manufacturing of galvanneal steel. The system has been used with the induction furnaces to measure temperatures ranging from 840 to 1292 F with an accuracy of better than +/- 9 F. The

GTMS provides accurate, reliable temperature information thus ensuring a high quality product, reducing waste, and saving energy. The production of uniform, high-quality galvanneal steel is only possible through strict temperature control.
NTIS
*Steels; Temperature Control; Temperature Measurement*

**20010120002** Oak Ridge National Lab., TN USA
**Modeling Manufacturing Processes to Mitigate Technological Risk**
Allgood, G. O.; Manges, W. W.; Oct. 24, 1999; 6p; In English
Report No.(s): DE2001-10191; ORNL/CP-104233; No Copyright; Avail: Department of Energy Information Bridge, Microfiche

An economic model is a tool for determining the justifiable cost of new sensors and subsystems with respect to value and operation. This process balances the R and D costs against the expense of maintaining current operations and allows for a method to calculate economic indices of performance that can be used as control points in deciding whether to continue development or suspend actions. The model can also be used as an integral part of an overall control loop utilizing real-time process data from the sensor groups to make production decisions (stop production and repair machine, continue and warn of anticipated problems, queue for repairs, etc.). This model has been successfully used and deployed in the CAFE Project. The economic model was one of seven (see Fig. 1) elements critical in developing an investment strategy. It has been successfully used in guiding the R and D activities on the CAFE Project, suspending activities on three new sensor technologies, and continuing development o f two others. The model has also been used to justify the development of a new prognostic approach for diagnosing machine health using COTS equipment and a new algorithmic approach. maintaining current operations and allows for a method to calculate economic indices of performance that can be used as control points in deciding whether to continue development or suspend actions. The model can also be used as an integral part of an overall control loop utilizing real-time process data from the sensor groups to make production decisions (stop production and repair machine, continue and warn of anticipated problems, queue for repairs, etc.).
NTIS
*Manufacturing; Data Processing; Algorithms*

**20010120003** Lawrence Livermore National Lab., Livermore, CA USA
**Signal analysis approach to ultrasonic evaluation of diffusion bond quality**
Chinn, D.; Thomas, G.; Jun. 08, 1999; 8p; In English
Report No.(s): DE2001-10147; UCRL-JC-132803; No Copyright; Avail: Department of Energy Information Bridge, Microfiche

Solid state bonds like the diffusion bond are attractive techniques for joining dissimilar materials since they are not prone to the defects that occur with fusion welding. Ultrasonic methods can detect the presence of totally unbonded regions but have difficulty sensing poor bonded areas where the substrates are in intimate contact. Standard ultrasonic imaging is based on amplitude changes in the signal reflected from the bond interface. Unfortunately amplitude alone is not sensitive to bond quality. We demonstrated that there is additional information in the ultrasonic signal that correlates with bond quality. In our approach we interrogated a set of dissimilar diffusion bonded samples with broad band ultrasonic signals. The signals were digitally processed and the characteristics of the signals that corresponded to bond quality were determined. These characteristics or features were processed with pattern recognition algorithms to produce predictions of bond quality. The predicted bond quality was then compared with the destructive measurement to assess the classification capability of the ultrasonic technique.
NTIS
*Bonding; Ultrasonics; Diffusion Welding*

**20010121510** Sandia National Labs., Albuquerque, NM USA
**High Shock, High Frequency Characteristics of a Mechanical Isolator for a Piezoresistive Accelerometer, the ENDEVCO 7270AM6(asterik)**
Bateman, V. I.; Brown, F. A.; Nusser, M. A.; Jul. 01, 2000; 90p; In English
Report No.(s): DE2000-759454; SAND2000-1528; No Copyright; Avail: Department of Energy Information Bridge, Microfiche

A mechanical isolator has been developed for a piezoresistive accelerometer. The purpose of the isolator is to mitigate high frequency shocks before they reach the accelerometer because the high frequency shocks may cause the accelerometer to resonate. Since the accelerometer is undamped, it often breaks when it resonates. The mechanical isolator was developed in response to impact test requirements for a variety of structures at Sandia National Laboratories (SNL). An Extended Technical Assistance Program (ETAP) with the accelerometer manufacturer has resulted in a commercial mechanically isolated accelerometer that is available to the general public, the ENDEVCO 7270AM6(asterick), for three shock acceleration ranges of 6,000 g, 20,000 g, and 60,000 g. The in-axis response shown in this report has acceptable frequency domain performance from DC to 10 kHz and 10(XO)over a temperature range of (minus)65 F to +185 F. Comparisons with other isolated accelerometers show that the

ENDEVCO 7270AM6 has ten times the bandwidth of any other commercial isolator. ENDEVCO 7270AM6 cross-axis response is shown in this report.
NTIS
*Accelerometers; High Frequencies; Isolators; Piezoelectricity; Mechanical Devices*

**20010123547** Argonne National Lab., IL USA
**Results from an iron-proportional tube calorimeter prototype**
Schoessow, P.; Feb. 03, 1998; 10p; In English
Report No.(s): DE2001-10630; ANL-HEP-CP-98-02; No Copyright; Avail: Department of Energy Information Bridge, Microfiche

We have studied the energy resolution of a prototype gas tracking calorimeter in a test beam at Fermilab as part of the detector development program for the MINOS long baseline neutrino oscillation experiment. The calorimeter consisted of 25 layers of 1.5 inch thick steel plates interleaved with planes of aluminum proportional tubes. The tube cells are square, with 0.9 cm edges and open tops. Cathode strips were used for read out transverse to the wire cells. The tubes operated with a nonflammable gas mixture of 88% CO(sub 2), 9.5% isobutane and 2.5% argon which gave an operating range of >500 V (limited by the electronics). We read out the wire signals on the tubes and in some configurations the cathode stripe as well. We studied positrons, pions and muons over a momentum range of 2.5-30 GeV/c and achieved energy resolutions of about 40%/(radical)E for EM and 71%/(radical)E for hadronic showers.
NTIS
*Iron; Calorimeters; Showers; Counters*

**20010123620** Harvest Energy Technology, Sun Valley, CA USA
**Laser ultrasonic furnace tube coke monitor** ***Quarterly Report, 1 May - 1 Aug. 1999***
Aug. 15, 1999; 13p; In English
Report No.(s): DE2001-760366; No Copyright; Avail: Department of Energy Information Bridge, Microfiche

The overall aim of the project is to demonstrate the performance and practical use of a probe for measuring the thickness of coke deposits located within the high-temperature tubes of a thermal cracking furnace. The objective of work during this period was to enhance the sensitivity and signal-to-noise ratio of the probe measurement. Testing identified that the primary source of signal noise was traced to imperfections in the sacrificial stand-off, which was formed using a casting procedure. Laminations, voids, and impurities contained in the casting result in attenuation and dispersion of the ultrasonic signal. This report describes the work performed to optimize the signal conductance of the sacrificial stand-off.
NTIS
*Coke; Furnaces; Monitors*

**20010123908** Los Alamos National Lab., NM USA
**Determining Performance with Limited Testing when Reliability and Confidence are Mandated**
Dolin, R. M.; Treml, C. A.; Feb. 01, 2000; 13p; In English
Report No.(s): DE2001-763371; LA-UR-00-1005; No Copyright; Avail: Department of Energy Information Bridge

In an environment of increased cost, regulation, and accountability the ability to do unlimited testing to verify the performance parameters of a product are diminishing. At the same time liability and maintenance concerns are requiring that clearly established operating conditions be defined. Because of this, product developers often encounter situations where reliability, and the confidence in that reliability, are mandated but only a limited number of tests can be performed to validate these mandated conditions. A methodology is presented for establishing performance parameters in these situations. The methodology is based on Bayesian Hypothesis Testing theory. It is shown how an iterative hypothesis can be defined, Within the Bayesian framework equations are derived for computing a necessary prior, determining the minimum number of tests needing to be performed, establishing how many failures can be observed for a given number of tests, and inferring an overall reliability distribution.
NTIS
*Confidence; Reliability; Bayes Theorem; Failure Analysis; Performance Tests*

**20010125028** National Defence Research Establishment, Avd. foer Vapen och Skydd, Tumba, Sweden
**Torsional Hopkinson- a Method for Fast Torsional Loads** ***Vrid-Hopkinson: En Metod foer Snabba Skjuvbelastningar***
Eriksson, J.; Pettersson, A.; Nilsson, M.; Skoglund, P.; December 2000; ISSN 1104-9154; 60p; In Swedish
Report No.(s): PB2001-107272; FOA-R-00-01775-310-SE; No Copyright; Avail: CASI; A04, Hardcopy; A01, Microfiche

This report describes the principle for a torsional Hopkinson bar, which is a method for testing material behavior under fast shear loads. The mechanical construction, data measuring system and data processing are described in some detail. The apparatus allows shear strain rates up to 5000s-1. The equipment, which is unique for Sweden and possible also the Nordic countries, has mainly been used for investigating metallic materials but composites have also been tested.
NTIS
*Stress-Strain Relationships; Mechanical Properties; Shear Stress; Metals*

**20010125441** Lawrence Livermore National Lab., Livermore, CA USA
**MIR wall surveyor**
Lehman, S. K.; Aug. 01, 1998; 60p; In English
Report No.(s): DE2001-8424; UCRL-ID-131932; No Copyright; Avail: Department of Energy Information Bridge, Microfiche
This report addresses the problem of determining the layer thickness of a wall probed with a monostatic, hand-held implementation of Lawrence Livermore National Laboratory's Micropower Impulse Radar (MIR). Our goal is to locate the layers of the wall, and measure its overall thickness. The physical constraints require the device to be held fixed or swept rapidly over the wall. Thus an insufficient amount of backscattered data are collected to use diffraction tomographic techniques to form images. The problem is therefore one of determining the wall layers from a set of time series reflection data. We develop two channel signal processing algorithms to determine the location of the layers of a wall, using as inputs the time series returned from the wall and the incident pulse. We study the problem using a finite difference time domain (FDTD) computer code to simulate the electromagnetic propagation within and scattering from a wall probed with five pulses. We use the results to develop and test signal processing procedures for locating the individual layers. We study two classes of algorithms: a deconvolution approach to determine a layered impulse response, and a correlation approach. After testing the algorithms on the FDTD results, we down-select to a suitable method.
NTIS
*Walls; Measuring Instruments; Radar Measurement; Finite Difference Time Domain Method; Thickness; Radio Probing*

**20010125585** Argonne National Lab., IL USA
**Damage characterization of a Si3N4-BN fibrous monolith using NDE techniques**
Deemer, C. M.; Ellingson, W. A.; Finch, J. L.; Staehler, J. M.; Sun, J. G.; Jun. 29, 1999; 13p; In English
Report No.(s): DE2001-11855; ANL/ET/CP-99319; No Copyright; Avail: Department of Energy Information Bridge, Microfiche
A variety of nondestructive evaluation techniques were utilized to document the damage characteristics of a Si(sub 3)N(sub 4)-BN fibrous monolith. The techniques included X-ray radiography, infrared thermography, ultrasonic C-scanning, and acoustic emission detection. The focus of this paper is the nondestructive evaluation results from a modified single-edge notched tensile specimen inspected before and after testing. of the techniques performed, the thermography and ultrasonic methods were the most successful at identifying the predominant types of damage incurred in the fibrous monolith material. Polished cross-sections of the specimen revealed that hairline cracks had developed along inter and intra-laminar BN cell bundle boundaries. Neither type of crack could be identified from the X-ray radiograph. The delaminated zones were matched with results from the thermography and C-scans. The acoustic emissions correlated well with changes in the load-displacement data and provided source locations consistent with the thermal and C-scan images.
NTIS
*Damage; Nondestructive Tests; Silicon Nitrides; Boron Nitrides; Thermography; Ultrasonic Scanners; Fibers*

## 39
## STRUCTURAL MECHANICS

*Includes structural element design, analysis and testing; dynamic responses of structures; weight analysis; fatigue and other structural properties; and mechanical and thermal stresses in structure. For applications see 05 Aircraft Design, Testing and Performance and 18 Spacecraft Design, Testing and Performance.*

**20010120072** Sandia National Labs., Albuquerque, NM USA
**Segmented Aluminum Honeycomb Characteristics in T-Direction, Dynamic Crush Environments**
Bateman, B. I.; Brown, F. A.; Nusser, M. A.; Swanson, L. H.; Aug. 23, 2000; 71p; In English
Report No.(s): DE2000-761967; SAND2000-2109; No Copyright; Avail: Department of Energy Information Bridge, Microfiche
Thirteen segmented aluminum honeycomb samples (5 inches in diameter and 1.5 inches in height) have been crushed in an experimental configuration that uses a drop table impact machine. The 38.0 pcf bulk density samples are a unique segmented

geometry that allows the samples to be crushed while maintaining a constant cross-sectional area. A crush weight of 175 lb was used to determine the rate sensitivity of the honeycomb's highest strength orientation, T-direction, in a dynamic environment of approximately 50 fps impact velocity. Experiments were conducted for two honeycomb manufacturers and at two temperatures, ambient and 165 F. Independent measurements of the crush force were made with a custom load cell and a force derived from acceleration measurements on the drop table using the Sum of Weighted Accelerations Technique with a Calibrated Force (SWAT-CAL). Normalized stress-strain curves for all thirteen experiments are included and have excellent repeatability. These data are strictly valid for material characteristics in the T orientation because the cross-sectional area of the honeycomb did not change during the crush. The dynamic crush data have a consistent increase in crush strength of (approximately) 7-19% as compared to quasi-static data and suggest that dynamic performance may be inferred from static tests. An uncertainty analysis estimates the error in these data is +/- 11%.
NTIS
*Honeycomb Structures; Segments; Stress-Strain Relationships*

**20010120115** NASA Langley Research Center, Langley Research Center, Hampton, VA USA
**Matrix Analysis of Longitudinal and Torsional Vibrations in Nonuniform Multibranch Beams**
Wingate, Robert T.; Feb. 1967; 51p; In English
Report No.(s): AD-A395013; NASA-TN-D-3844; No Copyright; Avail: CASI; A04, Hardcopy; A01, Microfiche

Since longitudinal modes and frequencies provide basic data for dynamic analyses of arbitrary beam-like structures and since closed-form solutions for the modes are generally not feasible to obtain, an approximate method is developed for computing the natural frequencies and the corresponding mode shapes for a variable-section, unconstrained multibranch beam. A lumped mass analogy employing influence coefficients is used to represent the beam. The simultaneous equations of motion for the lumped mass system are derived in matrix form and algebraically manipulated to yield a classical eigenvalue equation solvable by standard procedures. The orthogonality relationship of the natural modes is derived and used to form the basis of an orthogonal sweeping process for determination of modes above the fundamental. Numerical examples including an application to a solid-fuel launch system are presented. Also, a detailed discussion is devoted to the theoretical verifications of the approximate modes and frequencies.
DTIC
*Torsion; Beams (Supports); Torsional Vibration; Matrices (Mathematics); Longitudinal Stability*

**20010120119** NASA Langley Research Center, Langley Research Center, Hampton, VA USA
**Study of Dynamic Response to Impact Loadings of Acceleration Sensors Having Various Mounting Characteristics**
McCarty, John L.; Pearson, Jerome; May 1967; 53p; In English
Report No.(s): AD-A395005; NASA-TN-D-3973; No Copyright; Avail: CASI; A04, Hardcopy; A01, Microfiche

An analytical investigation was performed to study the dynamic response to impact loadings of acceleration sensors having various mounting characteristics. Analytically represented impacting bodies were subjected to input force pulses of half-sine, triangular, quarter -sine, and rectangular shapes, approximating typical target impact acceleration signatures. Studies were made with an analog computer of the acceleration time histories measured by acceleration sensors of different mass which are coupled to the impacting body by a mounting system having various combinations of damping and spring stiffness. Boundaries for the system parameters were established that defined conditions for which the accelerometer assembly and its coupling have a negligible effect on the accelerations experienced by the impacting body. These boundaries define ranges of the parameters of the two-degree-of-freedom system for which the impact response characteristics can be evaluated from a single-degree-of-freedom analysis. Ekirther, with a knowledge of these parameters and the impact velocity, the shape and the magnitude of specific input pulses applied to the impacting body can be defined from characteristics of the acceleration-time-history response of an acceleration sensor mounted to that body.
DTIC
*Accelerometers; Dynamic Response; Impact Acceleration*

**20010120469** Academy of Sciences of the Ukraine, Inst. of Materials Science Problems, Kiev, Ukraine
**Deformation Mechanisms and Destruction of New Perspective Materials: Actual Problems of Strength**
Jul. 03, 2001; 356p; In English; 37th International Seminar, 2-5 Jul. 2001, Kieve, Ukraine
Contract(s)/Grant(s): F61775-01-WF029
Report No.(s): AD-A394452; EOARD-CSP-01-5029; No Copyright; Avail: CASI; A03, Microfiche; A16, Hardcopy

The Final Proceedings for Deformation mechanisms and destruction of new perspective materials: Actual Problems of Strength, 2 July 2001 - 5 July 2001. Deformation and destruction mechanisms of new advanced materials: (1) ceramics; (2)

nanocrystals; (3) amorphous metal alloys; (4) quasicrystals; (5) gradient and layered materials; (6) memory shape materials; (7) sintered materials; and (8) high specific strength materials.
DTIC
*Mechanical Properties; Deformation; Destruction; Alloys*

**20010121498** Sandia National Labs., Albuquerque, NM USA
**Recent Advances in High-Pressure Equation-of-State Capabilities**
Asay, J. R.; Hall, C. A.; Knudson, M. D.; Jul. 24, 2000; 13p; In English
Report No.(s): DE2000-760769; SAND2000-0849C; No Copyright; Avail: Department of Energy Information Bridge, Microfiche

For many scientific and programmatic applications, it is necessary to determine the shock compression response of materials to several tens of Mbar. In addition, a complete EOS (equation of state) is often needed in these applications, which requires that shock data be supplemented with other information, such as temperature measurements or by EOS data off the principal Hugoniot. Recent developments in the use of fast pulsed power techniques for EOS studies have been useful in achieving these goals. In particular, the Z accelerator at Sandia National Laboratories, which develops over 20 million amperes of current in 100-200 ns, can be used to produce microM-Mbar shock pressures and to obtain continuous compression data to pressures exceeding 1 Mbar. With this technique, isentropic compression data have been obtained on several materials to pressures of several hundred kbar. The technique has also been used to launch ultra-high velocity flyer plates to a maximum velocity of 14 km/s, which can be used to produce impact pressures of several Mbar in low impedance materials and over 10 Mbar in high impedance materials. The paper will review developments in both of these areas.
NTIS
*Shock Loads; Compression Loads; Equations of State*

**20010122671** Los Alamos National Lab., NM USA
**Validation of Structural Dynamics Models at Los Alamos National Laboratory**
Doebling, S. W.; Hemez, F. M.; Jan. 01, 2000; 18p; In English
Report No.(s): DE2000-763335; LA-UR-00-725; No Copyright; Avail: Department of Energy Information Bridge, Microfiche

This publication proposes a discussion of the general problem of validating numerical models for nonlinear, transient dynamics. The predictive quality of a numerical model is generally assessed by comparing the computed response to test data. If the correlation is not satisfactory, an inverse problem must be formulated and solved to identify the sources of discrepancy between test and analysis data. Some of the most recent work summarized in this publication has focused on developing test-analysis correlation and inverse problem solving capabilities for nonlinear vibrations. Among the difficulties encountered, we cite the necessity to satisfy continuity of the response when several finite element optimization are successively carried out and the need to propagate variability throughout the optimization of the model's parameters. After a brief discussion of the formulation of inverse problems for nonlinear dynamics, the general principles which, we believe, should guide future developments of inverse problem solving are discussed. In particular, it is proposed to replace the resolution of an inverse problem with multiple forward, stochastic problems. The issue of defining an adequate metrics for test-analysis correlation is also addressed. Our approach is illustrated using data from a nonlinear vibration testbed and an impact experiment both conducted at Los Alamos National Laboratory in support of the advanced strategic computing initiative and our code validation and verification program.
NTIS
*Dynamic Structural Analysis; Mathematical Models; Nonlinearity*

**20010123063** Argonne National Lab., IL USA
**Dynamic modulus estimation and structural vibration analysis**
Gupta, A.; Nov. 18, 1998; 10p; In English
Report No.(s): DE2001-11074; ANL/ET/CP-97550; No Copyright; Avail: Department of Energy Information Bridge, Microfiche

Often the dynamic elastic modulus of a material with frequency dependent properties is difficult to estimate. These uncertainties are compounded in any structural vibration analysis using the material properties. Here, different experimental techniques are used to estimate the properties of a particular elastomeric material over a broad frequency range. Once the properties are determined, various structures incorporating the elastomer are analyzed by an interactive finite element method to

determine natural frequencies and mode shapes. Then, the finite element results are correlated with results obtained by experimental modal analysis.
NTIS
*Elastomers; Frequency Ranges; Dynamic Modulus of Elasticity*

**20010123458** Lawrence Livermore National Lab., Livermore, CA USA
**Implementation of rotary inertia effect on the free vibration response of beams**
Nukala, P. K.; Jun. 01, 1999; 10p; In English
Report No.(s): DE2001-11000; UCRL-ID-134510; No Copyright; Avail: Department of Energy Information Bridge, Microfiche
No abstract prepared.
NTIS
*Beams (Radiation); Free Vibration*

**20010123459** Lawrence Livermore National Lab., Livermore, CA USA
**Implementation of modal combination rules for response spectrum analysis using GEMINI**
Nukala, P. K.; Jun. 01, 1999; 30p; In English
Report No.(s): DE2001-10999; UCRL-ID-134511; No Copyright; Avail: Department of Energy Information Bridge, Microfiche
One of the widely used methodologies for describing the behavior of a structural system subjected to seismic excitation is response spectrum modal dynamic analysis. Several modal combination rules are proposed in the literature to combine the responses of individual modes in a response spectrum dynamic analysis. In particular, these modal combination rules are used to estimate the representative maximum value of a particular response of interest for design purposes. Furthermore, these combination rules also provide guidelines for combining the representative maximum values of the response obtained for each of the three orthogonal spatial components of an earthquake. This report mainly focuses on the implementation of different modal combination rules into GEMINI (I).
NTIS
*Earthquakes; Spectrum Analysis; Structural Analysis*

## 42
## GEOSCIENCES (GENERAL)

*Includes general research topics related to the Earth sciences, and the specific areas of petrology, mineralogy, and general geology. For other specific topics in geosciences see categories 41 through 48.*

**20010117657** Sandia National Labs., Albuquerque, NM USA
**Effective-Porosity and Dual-Porosity Approaches to Solute Transport in Fractured Tuff of the Saturated Zone at Yucca Mountain: Implications for Repository Performance Assessment**
Arnold, B. W.; Zhang, H.; Parsons, A. M.; Aug. 03, 2000; 19p; In English
Report No.(s): DE2000-760044; SAND99-1598C; No Copyright; Avail: Department of Energy Information Bridge
The effective-porosity approach and the dual-porosity approach are examined as two alternative conceptual models of radionuclide migration in fractured media of the saturated zone at Yucca Mountain. Numerical simulations of one-dimensional radionuclide transport are performed for the domain relevant to repository performance assessment using the two alternative conceptual approaches. The dual-porosity solute transport modeling produces similar results to the effective-porosity model for fracture spacing of less than approximately 1 m and greater than about 200 m, corresponding to values of effective porosity equal to the matrix porosity and the fracture porosity, respectively. For intermediate values of fracture spacing, the dual-porosity approach results in concentration breakthrough curves that differ significantly from the effective porosity approach and are characterized by earlier first arrival, greater apparent dispersion, and lower concentrations at later times. The effective-porosity approach, as implemented in recent performance assessment analyses of saturated zone transport at Yucca Mountain, is conservative compared to the dual-porosity approach from the perspective of both radionuclide concentrations and generally for travel times.
NTIS
*Fracturing; Porosity; Radioactive Isotopes*

**20010117661** Sandia National Labs., Albuquerque, NM USA

**Fast Grid Search Algorithm for Seismic Source Location**

Aldridge, D. F.; Jul. 01, 2000; 30p; In English

Report No.(s): DE2000-759476; SAND2000-1765; No Copyright; Avail: Department of Energy Information Bridge

The spatial and temporal origin of a seismic energy source are estimated with a first grid search technique. This approach has greater likelihood of finding the global minimum of the arrival time misfit function compared with conventional linearized iterative methods. Assumption of a homogeneous and isotropic seismic velocity model allows for extremely rapid computation of predicted arrival times, but probably limits application of the method to certain geologic environments and/or recording geometries. Contour plots of the arrival time misfit function in the vicinity of the global minimum are extremely useful for quantizing the uncertainty of an estimated hypocenter solution and analyzing the resolving power of a given recording configuration. In particular, simultaneous inversion of both P-wave and S-wave arrival times appears to yield a superior solution in the sense of being more precisely localized in space and time. Future research with this algorithm may involve investigating the utility of nonuniform residual weighting schemes, incorporating linear and/or layered velocity models into the calculation of predicted arrival times, and applying it toward rational design of microseismic monitoring networks.

NTIS

*Algorithms; Microseisms; Spatial Distribution; Temporal Distribution*

**20010118268** California Univ., Lawrence Berkeley Lab., Berkeley, CA USA

**Coupled thermohydromechanical analysis of a heater test in unsaturated clay and fractured rock at Kamaishi Mine**

Rutqvist, J.; Noorishad, J.; Tsang, C. F.; Aug. 01, 1999; 112p; In English

Report No.(s): DE2000-760335; LBNL-44203; No Copyright; Avail: Department of Energy Information Bridge, Microfiche

The recent interest in coupled thermohydromechanical (THM) processes associated with geological disposal of spent nuclear fuel, and in particular the issue of resaturation of a clay buffer around a waste canister, has encouraged major development of the finite element computer program ROCMAS in the past three years. The main objective is to develop a tool for analysis of THM processes in practical field scale, including fractured rock masses and detailed behavior of the near-field, nonisothermal and unsaturated system composed of rock fractures and clay buffer. In this report, the ROCMAS code is presented and applied for modeling of coupled THM processes in small laboratory samples of bentonite clay as well as a large in situ THM experiment in fractured rocks, at Kamaishi Mine, Japan.

NTIS

*Clays; Fractures (Materials); Spent Fuels; Finite Element Method; Applications Programs (Computers)*

**20010118270** California Univ., Lawrence Berkeley Lab., Berkeley, CA USA

**Parallel implementation of the TOUGH2 software package for large scale multiphase fluid and heat flow simulations**

Elmroth, E.; Ding, C. H. Q.; Wu, Y. S.; Pruess, K.; May 01, 1999; 13p; In English

Report No.(s): DE2000-760323; LBNL-43385; No Copyright; Avail: Department of Energy Information Bridge, Microfiche

Groundwater flow related problems touch many important areas in todays society, such as nuclear waste isolation, environmental remediation, geothermal reservoir engineering. Because of the complexity of geometry, composition, multiphase, and especially long time scales involved, numerical simulation play vital roles in the solutions of these problems. This contribution describes the ongoing development of a parallel version of the widely used TOUGH2 software package for numerical simulation of flow and transport in porous and fractured media. The contribution includes our experiences from the software development, descriptions of algorithms and methods developed, and a presentation of the current status of the software, including parallel performance results on Cray T3E-900.

NTIS

*Heat Transfer; Multiphase Flow; Ground Water; Software Engineering*

**20010118279** Implo Treat Systems, Nogal, NM USA

**Wellbottom Fluid Implosion System to Stimulate Existing Well Flow: Semi-Annual Report for the Period August-October 1999**

Brieger, E. F.; Nov. 01, 1999; 14p; In English

Report No.(s): DE2000-760114; DOE/GO/10446-S; DOE/10446-1; No Copyright; Avail: Department of Energy Information Bridge

This is a semi-annual report of the Wellbottom Fluid Implosion System to Stimulate Existing Well Flow reporting for the period August - October 1999.
NTIS
*Implosions; Wells*

**20010118924** Geological Survey, Reston, VA USA
**Geologic evaluation of the Oasis Valley Basin, Nye County, Nevada**
Fridrich, C. J.; Minor, S. A.; Mankinen, E. A.; Jan. 13, 2000; 57p; In English
Report No.(s): DE2000-761029; USGS-OFR-99-533-A; No Copyright; Avail: Department of Energy Information Bridge
This report documents the results of a geologic study of the area between the underground-nuclear-explosion testing areas on Pahute Mesa, in the northwesternmost part of the Nevada Test Site, and the springs in Oasis Valley, to the west of the Test Site. The new field data described in this report are also presented in a geologic map that is a companion product and that covers nine 7.5-minute quadrangles centered on Thirsty Canyon SW, the quadrangle in which most of the Oasis Valley springs are located. At the beginning of this study, published detailed maps were available for three of the nine quadrangles of the study area: namely Thirsty Canyon; Beatty; and Thirsty Canyon SE. Maps of the last two of these quadrangles, however, required extensive updating owing to recent advances in understanding of the regional structure and stratigraphy. The new map data are integrated in this report with new geophysical data for the Oasis Valley area, include gravity, aeromagnetic, and paleomagnetic data.
NTIS
*Stratigraphy; Nevada; Geological Surveys; Underground Explosions; Nuclear Explosions*

**20010118925** Geological Survey, Reston, VA USA
**Geologic map of the Oasis Valley Basin and vicinity, Nye County, Nevada**
Fridrich, C. J.; Minor, S. A.; Ryder, P. L.; Slate, J. L.; Jan. 13, 2000; 47p; In English
Report No.(s): DE2000-761035; USGS-OFR-99-533-B; No Copyright; Avail: Department of Energy Information Bridge
This map and accompanying cross sections present an updated synthesis of the geologic framework of the Oasis Valley area, a major groundwater discharge site located about 15 km west of the Nevada Test Site. Most of the data presented in this compilation is new geologic map data, as discussed below. In addition, the cross sections incorporate new geophysical data that have become available in the last three years. Geophysical data are used to estimate the thickness of the Tertiary volcanic and sedimentary rocks on the cross sections, and to identify major concealed structures. Large contiguous parts of the map area are covered either by alluvium or by volcanic units deposited after development of the major structures present at the depth of the water table and below. Hence, geophysical data provide critical constraints on our geologic interpretations. A companion paper by Fridrich and others and the above-cited reports by Hildenbrand and others and Mankinen and others provide explanations of the interpretations that are presented graphically on this map. This map covers nine 7.5-minute quadrangles in Nye County, Nevada, centered on the Thirsty Canyon SW quadrangle, and is a compilation of one published quadrangle map and eight new quadrangle maps, two of which have been previously released. The cross sections that accompany this map were drawn to a depth of about 5 km below land surface at the request of hydrologists who are modeling the Death Valley groundwater system.
NTIS
*Nevada; Valleys; Geological Surveys; Hydrology; Ground Water; Maps*

**20010119540** Bonneville Power Administration, Portland, OR USA
**Design and Analysis of Salmonid Tagging Studies in the Columbia Basin, Volume 3, A New Model for Estimating Survival Probabilities and Residualization from a Release-Recapture Study of Fall Chinook Salmon (Oncorhynchus tschawytscha)Smolts in the Snake River**
Lowther, A. B.; Skalski, J.; Sep. 01, 1997; 29p; In English
Report No.(s): DE2001-10414; DOE/BP-02341-6; No Copyright; Avail: Department of Energy Information Bridge, Microfiche
Standard release-recapture analysis using Cormack-Jolly-Seber (CJS) models to estimate survival probabilities between hydroelectric facilities for Snake River fall chinook salmon (Oncorhynchus tschawytscha) ignore the possibility of individual fish residualizing and completing their migration in the year following tagging.
NTIS
*Survival; Columbia River Basin (ID-OR-WA); Fishes; Marking*

**20010119541** Bonneville Power Administration, Portland, OR USA
**Design and Analysis of Salmonid Tagging Studies in the Columbia Basin; Volume X; Instructional Guide to Using Program Capthist to Create Surph Files for Survival Analysis Using Ptagis Data Files**
Skalski, J.; Westhagen, P.; Dec. 01, 1997; 24p; In English
Report No.(s): DE2001-10415; DOE/BP-02341-4; No Copyright; Avail: Department of Energy Information Bridge
Project 89-107, Epidemiological Survival Methods, was developed to provide statistical guidance on the design and analysis of PIT-tag survival studies to the Northwest fisheries community.
NTIS
*Epidemiology; Marking; Survival*

**20010119542** Bonneville Power Administration, Portland, OR USA
**Grande Ronde Basin Fish Habitat Enhancement Project** ***Annual Report, 1998***
McGowan, V. R.; Powell, R. M.; May 01, 1999; 65p; In English
Report No.(s): DE2001-10417; DOE/BP-16114-1; No Copyright; Avail: Department of Energy Information Bridge
The primary goal of 'The Grande Ronde Basin Fish Habitat Improvement Project' is to access, create, improve, protect, and restore reparian and in-stream habitats for anadromous salmonids, thereby maximizing opportunities for natural fish production within the basin.
NTIS
*Augmentation; Fishes; Habitats*

**20010119995** Department of Energy, Aiken, SC USA
**SRS Geology/Hydrogeology Environmental Information Document**
Denham, M. E.; Aug. 31, 1999; 218p; In English
Report No.(s): DE2001-10526; WSRC-TR-95-0046; No Copyright; Avail: Department of Energy Information Bridge
The purpose of the Savannah River Site Geology and Hydrogeology Environmental Information Document (EID) is to provide geologic and hydrogeologic information to serve as a baseline to evaluate potential environmental impacts. This EID is based on a summary of knowledge accumulated from research conducted at the Savannah River Site (SRS) and surrounding areas.
NTIS
*Geology; Hydrology; Rivers; Grasslands*

**20010120064** Sandia National Labs., Albuquerque, NM USA
**Multiphase Flow and Cavern Abandonment in Salt**
Ehgartner,; Tidwell,; Sep. 14, 2000; 15p; In English
Report No.(s): DE2000-763099; SAND2000-1495C; No Copyright; Avail: Department of Energy Information Bridge, Microfiche
Although the depositional environment of salt is generally wet, many salt deposits (particularly domal salts) contain interstitial gas. It is hypothesized that the long-term state of an initially liquid filled cavern in gassy salt will be gas filled. With the interest in using caverns for waste disposal, the long-term state of a cavern must be known. This raises such questions as: Under what conditions will gas migrate into a salt cavern and alternatively, under what conditions will liquids imbibe into the salt. Over what time scales do these processes operate and what is the equilibrium state of a salt cavern. To answer these questions, an understanding of the processes governing two-phase flow in salt is needed. Here, we consider the long-term performance of salt caverns by way of a survey of pertinent literature followed by a brief review of first principles. to support these efforts a suite of simple laboratory experiments were conducted. These were investigated with the aid of light transmission imaging, which allowed direct visualization of the flow of brine through thin slabs of salt.
NTIS
*Multiphase Flow; Mineral Deposits; Caves*

**20010120071** Department of Energy, Savannah River Site, Aiken, SC USA
**Basement Surface Faulting and Topography for Savannah River Site and Vicinity**
Cumbest, R. J.; Dec. 17, 1998; 48p; In English
Report No.(s): DE2000-762016; WSRC-TR-98-00346; No Copyright; Avail: Department of Energy Information Bridge, Microfiche

This report integrates the data from more than 60 basement borings and over 100 miles of seismic reflection profiling acquired on the Savannah River Site to map the topography of the basement (unweathered rock) surface and faulting recorded on this surface.
NTIS
*Rivers; Rocks; Topography; Geological Faults*

**20010120531** Bechtel Nevada Corp., Las Vegas, NV USA
**Lithology and Stratigraphy of Holes Drilled in LANL-Use Areas of the Nevada Test Site**
Prothro, L. B.; Drellack, S. L.; Allen, B. M.; Jul. 01, 1999; 152p; In English
Report No.(s): DE2001-10609; DOE/NV/11718-254; No Copyright; Avail: Department of Energy Information Bridge, Microfiche

Geologic data for ten holes drilled in areas used by Los Alamos National Laboratory at the Nevada Test Site are presented in this report. The holes include emplacement holes, instrumentation holes, and Underground Test Area wells drilled during calendar years 1991 through 1995. For each hole a stratigraphic log, a detailed lithologic log, and one or two geologic cross sections are presented, along with a supplemental data sheet containing information about the drilling operations, geology, or references. For three of the holes, graphic data summary sheets with geologic and geophysical data are provided as plates.
NTIS
*Lithology; Stratigraphy; Sites; Nevada*

**20010121494** Bonneville Power Administration, Portland, OR USA
**Effects of Alder Mine on the water, sediments, and benthic macroinvertebrates of Alder Creek *Annual Report***
Edmonds, R.; Peplow, D.; May 28, 1999; 98p; In English
Report No.(s): DE2001-10590; DOE/BP-09396-1; No Copyright; Avail: Department of Energy Information Bridge, Microfiche

The Alder Mine, an abandoned gold, silver, copper, and zinc mine in Okanogan County, Washington, produces heavy metal-laden effluent that affects the quality of water in a tributary of the Methow River. The annual mass loading of heavy metals from two audits at the Alder Mine was estimated to exceed 11,000 kg per year. In this study, water samples from stations along Alder Creek were assayed for heavy metals by ICP-AES (inductively coupled plasma - atomic emission spectrometry) and were found to exceed Washington State's acute freshwater criteria for cadmium (Cd), copper (Cu), selenium (Se), and zinc (Zn).
NTIS
*Water Pollution; Tributaries; Sediments; Streams; Effluents; Fresh Water*

**20010121560** NASA Ames Research Center, Moffett Field, CA USA
**Amorphous to Amorphous Form Transitions of Water Ice and Astrophysical Implications**
Jenniskens, Peter, NASA Ames Research Center, USA; Blake, David F., NASA Ames Research Center, USA; Jan. 01, 1994; 1p; In English; International Conference on Dust, Molecules, and Backgrounds: From Lab to Space, 12-15 Sep. 1994, Capri, Italy
Contract(s)/Grant(s): RTOP 185-52-12-06; No Copyright; Avail: CASI; A01, Hardcopy; A01, Microfiche

We have combined Selected Area Electron Diffraction (SAED) and cryogenic techniques in an instrumental configuration that allows observing the structure of vapor deposited ice as it evolves during warmup. The ice is deposited in-situ inside an Hitachi H-500 H transmission electron microscope at a base pressure of 1-5 x 10(exp -7) torr on a thin amorphous carbon substrate at 15K or 86K and warmed up at a rate of 1-2 K/min. We find a progression of amorphous forms and well defined amorphous to amorphous transitions. Apart from the well known low-density form of ice, we confirm the presence of a high-density form and find a third amorphous form that coexists with cubic ice. We will report too on the amorphous to crystalline transition and the implications of these results for radical diffusion and gas retention observed in laboratory analog studies of interstellar and cometary ices.
Author
*Vapor Deposition; Ice; Electron Diffraction; Crystallinity; Amorphous Materials*

**20010121966** Pacific Northwest National Lab., Richland, WA USA
**Third Quarter Hanford Seismic Report for Fiscal Year 2000**
Hartshorn, D. C.; Reidel, S. P.; Rohay, A. C.; Sep. 01, 2000; 38p; In English
Report No.(s): DE2000-761358; PNNL-11557-15; No Copyright; Avail: Department of Energy Information Bridge

Hanford Seismic Monitoring provides an uninterrupted collection of high-quality raw and processed seismic data from the Hanford Seismic Network (HSN) for the U.S. Department of Energy and its con-tractors. Hanford Seismic Monitoring also locates and identifies sources of seismic activity and monitors changes in the historical pattern of seismic activity at the Hanford Site.

The data are compiled, archived, and published for use by the Hanford Site for waste management, Natural Phenomena Hazards assessments, and engineering design and construction. In addition, the seismic monitoring organization works with the Hanford Site Emergency Services Organization to provide assistance in the event of a significant earthquake on the Hanford Site. The HSN and the Eastern Washington Regional Network (E WRN) consist of 42 individual sensor sites and 15 radio relay sites maintained by the Hanford Seismic Monitoring staff. The HSN uses 21 sites and the EWRN uses 36 sites; both networks share 16 sites. The networks have 46 combined data channels because Gable Butte and Frenchman Hills East are three-component sites. The reconfiguration of the telemetry and recording systems was completed during the first quarter. All leased telephone lines have been eliminated and radio telemetry is now used exclusively. For the HSN, there were 818 triggers on two parallel detection and recording systems during the third quarter of fiscal year (FY) 2000. Thirteen seismic events were located by the Hanford Seismic Network within the reporting region of 46-47(degree) N latitude and 119-120(degree) W longitude; 7 were earthquakes in the Columbia River Basalt Group, 1 was an earthquake in the pre-basalt sediments, and 5 were earthquakes in the crystalline basement. Three earthquakes occurred in known swarm areas, and 10 earthquakes were random occurrences. No earthquakes triggered the Hanford Strong Motion Accelerometers during the third quarter of FY 2000.
NTIS
*Earthquakes; Seismology; Radio Telemetry; Accelerometers; Sediments*

**20010122644** Sandia National Labs., Albuquerque, NM USA
**Determination of Rock Mass Modulus Using the Plate Loading Method in Ambient and Thermally Perturbed Environments at Yucca Mountain, Nevada**
George,; Riggins,; Finley,; Aug. 03, 2000; 7p; In English
Report No.(s): DE2000-763097; SAND98-1858C; No Copyright; Avail: Department of Energy Information Bridge, Microfiche
The welded tuffs of Yucca Mountain are being considered by the United States Department of Energy (DOE) as potential host media for the storage of high level waste (HLW). As part of the Site Characterization efforts for the Yucca Mountain Project (YMP), a mechanically excavated Exploratory Studies Facility (ESF) was completed in 1997. A Thermal Testing Facility (TTF), subsequently constructed off the main drift of the ESF, includes the Single Heater Test block and the Drift Scale Test (DST).
NTIS
*Characterization; Igneous Rocks; Petrology; Rocks*

**20010122645** Department of Energy, National Petroleum Technology Office, Tulsa, OK USA
**Methodology to Integrate Magnetic Resonance and Acoustic Measurements for Reservoir Characterization**
Parra, J. O.; Hackert, C. L.; Ni, Q.; Collier, H. A.; Sep. 22, 2000; 125p; In English
Report No.(s): DE2000-763085; DOE/BC/15203-1; No Copyright; Avail: Department of Energy Information Bridge, Microfiche
This report contains eight sections. Some individual subsections contain lists of references as well as figures and conclusions when appropriate. The first section includes the introduction and summary of the first-year project efforts. The next section describes the results of the project tasks: (1) implementation of theoretical relations between effect dispersion and the stochastic medium; (2) imaging analyses using core and well log data; (3) construction of dispersion and attenuation models at the core and borehole scales in poroelastic media; (4) petrophysics and a catalog of core and well log data from Siberia Ridge field; (5) acoustic/geotechnical measurements and CT imaging of core samples from Florida carbonates; and (6) development of an algorithm to predict pore size distribution from NMR core data. The last section includes a summary of accomplishments, technology transfer activities and follow-on work for Phase 2.
NTIS
*Acoustic Measurement; Characterization; Magnetic Resonance*

**20010122658** Bechtel Nevada Corp., Las Vegas, NV USA
**Recompletion Report for Well UE-10j**
Townsend, M. J.; May 01, 2000; 122p; In English
Report No.(s): DE2000-764640; DOE/NV/11718-414; No Copyright; Avail: Department of Energy Information Bridge, Microfiche
Existing Well UE-10j was deepened and recompleted for the U.S. Department of Energy, Nevada Operations Office in support of the Nevada Environmental Restoration Project at the Nevada Test Site, Nye County, Nevada. The well was originally drilled to a total depth of 725.4 meters in 1965 for use as a hydrologic test hole in the northern portion of Yucca Flat in Area 8 of the Nevada Test Site. The well is located up-gradient of the Yucca Flat underground test area and penetrates deep into the Paleozoic rocks that form the lower carbonate aquifer of the NTS and surrounding areas. The original 24.4-centimeter-diameter borehole was drilled to a depth of 725.4 meters and left uncompleted. Water-level measurements were made periodically by the

U.S. Geological Survey, but access to the water table was lost between 1979 and 1981 due to hole sloughing. In 1993, the hole was opened to 44.5 centimeters and cased off to a depth of 670.0 meters. The hole diameter was then decreased to 31.1 centimeters for drilling to a total depth of 796.4 meters. The depth to water in the open borehole was measured at 658.7 meters on March 18, 1993.
NTIS
*Aquifers; Wells; Drilling; Geological Surveys; Nevada*

**20010122659** Bechtel Nevada Corp., Las Vegas, NV USA
**Completion Report for Well ER-EC-4**
Townsend, M. J.; Sep. 01, 2000; 122p; In English
Report No.(s): DE2000-764634; DOE/NV/11718-397; No Copyright; Avail: Department of Energy Information Bridge, Microfiche

Well ER-EC-4 was drilled for the US Department of Energy, Nevada Operations Office in support of the Nevada Environmental Restoration Project at the Nevada Test Site, Nye County, Nevada. This well was drilled in the summer of 1999 as part of the U.S Department of Energy's hydrogeologic investigation well program in the Western Pahute Mesa - Oasis Valley region just west of the Test Site. A 44.5-centimeter surface hole was drilled and cased off to a depth of 263.7 meters below the surface. The hole diameter was then decreased to 31.1 centimeters for drilling to a total depth of 1,062.8 meters. One completion string with three isolated slotted intervals was installed in the well. A preliminary composite, static, water level was measured at the depth of 228.3 meters, two months after installation of the completion string. Detailed lithologic descriptions with preliminary stratigraphic assignments are included in the report. These are based on composite drill cuttings collected every 3 meters, and 35 sidewall samples taken at various depths below 286.5 meters, supplemented by geophysical log data. Detailed chemical and mineralogical studies of rock samples are in progress. The well was collared in basalt and penetrated Tertiary-age lava and tuff of the Thirsty Canyon Group, the Volcanics of Fortymile Canyon, and the Timber Mountain Group. The preliminary geologic interpretation of data from this well helps pinpoint the location of the western margin of the Timber Mountain caldera complex in the southern Nevada volcanic field.
NTIS
*Wells; Nevada; Drilling*

**20010122826** Oak Ridge National Lab., TN USA
**Bioenergy Watershed Restoration in Regions of the West: What are the Environmental/Community Issues?**
Graham, R. L.; Huff, D. D.; Kaufmann, M. R.; Shepperd, W. D.; Sheehan, J.; Jul. 01, 1999; 10p; In English
Report No.(s): DE2000-763391; ORNL/CP-108384; No Copyright; Avail: Department of Energy Information Bridge

Throughout the western mountainous regions, wildfire risks are elevated due to both fire suppression activities which have changed the forest structure making it more susceptible to stand-killing fires and the expansion of human structures (houses, light commercial) into these same forests. by providing a market for currently noncommercial but flammable materials (small trees, tops, and branches), new and existing bioenergy industries could be a key factor in reducing the regional forest fuel loads. Although bioenergy would appear to be an ideal answer to the problem in many ways, the situation is complicated and numerous issues need resolution. A public fearful of logging in these regions needs assurance that harvesting for bioenergy is an environmentally and socially responsible solution to the current fuel build up in these forests. This is especially important given that biomass harvesting cannot pay its own way under current energy market conditions and would have to be supported in some fashion.
NTIS
*Fires; Forests; Restoration; Watersheds; Environment Protection*

**20010122835** Department of Energy, Savannah River Site, Aiken, SC USA
**Electromagnetic Borehole Flowmeter Testing in R-Area**
Flach, G. P.; Oct. 12, 2000; 96p; In English
Report No.(s): DE2000-765407; WSRC-TR-2000-00170; No Copyright; Avail: Department of Energy Information Bridge, Microfiche

Six constant-rate, multiple-well aquifer tests were recently conducted in R-area to provide site-specific in situ hydraulic parameters for assessing groundwater flow and contaminant transport models of R-Reactor Seepage Basins (RRSB) plume migration and RRSB remedial alternatives. The pumping tests were performed in the Upper Three Runs and Gordon aquifers between December 1999 and February 2000. The tests provide reliable estimates of horizontal conductivity averaged over aquifer thickness, and a relatively large horizontal zone of influence. to complement these results, Electromagnetic Borehole Flowmeter

(EBF) testing was subsequently performed to determine the vertical variation of horizontal conductivity for RPC-2PR, RPC-3PW, RPT-2PW, RPT-3PW, RPT-4PW and RPT-30PZ. The EBF data generally indicate significant aquifer heterogeneity over the tested screen intervals. The vertical variation of groundwater flow in or out of the well screen under ambient conditions was also measured. These data have implications for contaminant monitoring.
NTIS
*Flowmeters; Ground Water; Mathematical Models; Contaminants; Fluid Flow*

**20010122916** Department of Energy, National Petroleum Technology Office, Tulsa, OK USA
**Advanced Characterization of Fractured Reservoirs in Carbonate Rocks: The Michigan Basin**
Wood, J. R.; Harrison, W. B.; Oct. 24, 2000; 73p; In English
Report No.(s): DE2000-765659; DOE/BC/15100-1; No Copyright; Avail: Department of Energy Information Bridge, Microfiche
The main objective of this project is for a university-industry consortium to develop a comprehensive model for fracture carbonate reservoirs based on the 'data cube' concept using the Michigan Basin as a prototype. This project combined traditional historical data with 2D and 3D seismic data as well as data from modern logging tools in a novel way to produce a new methodology for characterizing fractured reservoirs in carbonate rocks. Advanced visualization software was used to fuse the data and to image it on a variety of scales, ranging from basin-scale to well-scales.
NTIS
*Reservoirs; Structural Basins; Carbonates; Rocks*

**20010123028** Oak Ridge Y-12 Plant, TN USA
**Groundwater Protection Program Calendar Year 1999 Evaluation of Groundwater Quality Data for the Chestnut Ridge Hydrogeologic Regime at the U.S. Department of Energy Y-12 Plant, Oak Ridge, Tennessee**
Sep. 01, 2000; 53p; In English
Report No.(s): DE2000-767250; Y/SUB/00-MVM64V/3; No Copyright; Avail: Department of Energy Information Bridge
This report presents an evaluation of the water quality monitoring data obtained by the Y-12 Plant Groundwater Protection Program (GWPP) in the Chestnut Ridge Hydrogeologic Regime (Chestnut Ridge Regime) during calendar year (CY) 1999. Groundwater and surface water monitoring is performed in the Chestnut Regime at several hazardous and nonhazardous waste management facilities associated with the U.S. Department of Energy (DOE) Oak Ridge Y-12 Plant. Applicable provisions of DOE Order 5400.1A -General Environmental Protection Program - require evaluation of available monitoring data with regard to: (1) groundwater quality in areas that are, or could be, affected by Y-12 Plant operations, (2) the quality of surface water and groundwater where contaminants are most likely to migrate beyond the DOE Oak Ridge Reservation (ORR) property line, and (3) long-term trends in groundwater quality at the Y-12 Plant.
NTIS
*Ground Water; Water Quality; Environment Protection; Hazardous Wastes; Surface Water*

**20010123029** Oak Ridge Y-12 Plant, TN USA
**Groundwater Protection Program Calendar Year 1999 Evaluation of Groundwater and Surface Water Quality Data for the Bear Creek Hydrogeologic Regime at the U.S. Department of Energy Y-12 Plant, Oak Ridge, Tennessee**
Sep. 01, 2000; 97p; In English
Report No.(s): DE2000-767248; Y/SUB/00-MVM64V/4; No Copyright; Avail: Department of Energy Information Bridge
This report presents an evaluation of the water quality monitoring data obtained by the Y-12 Plant Groundwater Protection Program (GWPP) in the Bear Creek Hydrogeologic Regime (Bear Creek Regime) during calendar year (CY) 1999. The Bear Creek Regime contains many confirmed and potential sources of groundwater and surface water contamination associated with the U.S. Department of Energy (DOE) Oak Ridge Y-12 Plant. Applicable provisions of DOE Order 5400.1A - General Environmental Protection Program - require evaluation of groundwater and surface water quality near the Y-12 Plant to: (1) gauge groundwater quality in areas that are, or could be, affected by plant operations, (2) determine the quality of surface water and groundwater where contaminants are most likely to migrate beyond the DOE Oak Ridge Reservation (ORR) property line, and (3) identify and characterize long-term trends in groundwater quality.
NTIS
*Ground Water; Environment Protection; Contamination; Surface Water*

**20010123047** Brookhaven National Lab., Upton, NY USA

**Micro X-Ray Fluorescence Tomography on Single Sediment Particles from New York/New Jersey Harbor**

Vekemans, B.; Vincze, L.; Szaloki, I.; Van Grieken, R.; Adams, F.; Jun. 18, 2000; 11p; In English

Report No.(s): DE2000-767150; BNL-67287; No Copyright; Avail: Department of Energy Information Bridge

Since routine dredging of the New York/New Jersey Harbor is required to allow access to modern deep-craft commercial shipping, large quantities of sediments must be removed from the harbor bottoms and subsequently dealt with. These sediments consist of a mixture of fine sand and silt, with some natural organic material. Toxic contaminants are ubiquitous, however. Next to organic contaminants (pesticides, industrial solvents, polychlorinated biphenyls, dioxins, furans, polycyclic aromatic hydrocarbons), the sediments contain low concentrations of heavy metals (including Ag, Cd, Cr, Pb, Sb, Se, Tl, Be, As, Hg, and Zn).

NTIS

*Contaminants; Sediments; Tomography; Water Pollution*

**20010123406** Oak Ridge National Lab., TN USA

**Genetic Modification of Short Rotation Poplar Biomass Feedstock for Efficient Conversion to Ethanol**

Dinus, R. J.; Jun. 01, 2000; 83p; In English

Report No.(s): DE2001-769297; ORNL/SUB/99-4500007253/1; No Copyright; Avail: Department of Energy Information Bridge

Poplar breeders in the USA have focused on raising adaptability, growth rates, and pest/stress resistance. Significant increases have been achieved via classical selection and breeding along with intensified cultural practices. Efficiencies have also been gained in harvesting and handling. Considering the aforementioned improvements in productivity, the time seems optimal for choosing feedstock qualities to modify and for undertaking the necessary research and development. Indeed, shortened rotations resulting from past research mean that opportunities for modifying feedstock qualities can be exploited more easily. Many poplars are propagated clonally, thereby permitting rapid, inexpensive propagation of valuable variants. Thus, poplars seem an ideal venue for testing and applying techniques to improve feedstock quality, e.g., reduced lignin content.

NTIS

*Biomass; Trees (Plants); Agriculture*

**20010123435** Georgia Univ., Athens, GA USA

**Effects of fertilization and competition control on carbon and nutrient allocation and physiology in loblolly pine plantation *Quarterly Report, Jul. - Sep. 1999***

Hendrick, R.; Will, R.; Teskey, R.; Borders, B.; Bailey, R.; Oct. 01, 1999; 29p; In English

Report No.(s): DE2001-763182; DOE/GO/10363-Q; No Copyright; Avail: Department of Energy Information Bridge, Microfiche

All of our plots have been established, all monitoring equipment has been installed, and we are making good progress on our field and laboratory measurements. Analysis is proceeding on relevant datasets.

NTIS

*Conifers; Agriculture*

**20010123444** Florida Univ., Gainesville, FL USA

**Diagnosis and correction of soil nutrient limitations in intensively managed Southern pine forests *Quarterly Report, Jul. - Sep. 1999***

Comerford, N. B.; Oct. 01, 1999; 5p; In English

Report No.(s): DE2001-761037; DOE/GO/10415; DOE/ED/10415-3; No Copyright; Avail: Department of Energy Information Bridge, Microfiche

The development of model coding for the project has continued. The features added during the past 3 months are: Changing soil water content with time based on a external data set; Flexibility in defining root growth during the defined time based on an external data set; Incorporation of mineralization for each time step based on an external data set.

NTIS

*Forests; Soils; Models*

**20010123624** Department of Energy, Richland Operations Office, Richland, WA USA
**Chinese Gold Miners of the Mid-Columbia Region. Phase II and Phase III**
Sharpe, J. J.; Sep. 29, 2000; 54p; In English
Report No.(s): DE2000-767361; BHI-01421-REV-0; No Copyright; Avail: Department of Energy Information Bridge, Microfiche

This report contains Phase 2, data collection, and Phase 3, evaluation guidelines for the Chinese Gold Miners of the Mid-Columbia Region, specifically the Hanford Reach.

NTIS
*Data Acquisition; Gold; Mining*

**20010123638** Bechtel Nevada Corp., Las Vegas, NV USA
**Atmospheric Correction Algorithm for Hyperspectral Imagery**
Pollina, R. J.; Sep. 01, 1999; 9p; In English
Report No.(s): DE2000-764643; DOE/NV/11718-367; No Copyright; Avail: Department of Energy Information Bridge

In December 1997, the US Department of Energy (DOE) established a Center of Excellence (Hyperspectral-Multispectral Algorithm Research Center, HyMARC) for promoting the research and development of algorithms to exploit spectral imagery. This center is located at the DOE Remote Sensing Laboratory in Las Vegas, Nevada, and is operated for the DOE by Bechtel Nevada. This paper presents the results to date of a research project begun at the center during 1998 to investigate the correction of hyperspectral data for atmospheric aerosols. Results of a project conducted by the Rochester Institute of Technology to define, implement, and test procedures for absolute calibration and correction of hyperspectral data to absolute units of high spectral resolution imagery will be presented. Hybrid techniques for atmospheric correction using image or spectral scene data coupled through radiative propagation models will be specifically addressed. Results of this effort to analyze HYDICE sensor data will be included. Preliminary results based on studying the performance of standard routines, such as Atmospheric Pre-corrected Differential Absorption and Nonlinear Least Squares Spectral Fit, in retrieving reflectance spectra show overall reflectance retrieval errors of approximately one to two reflectance units in the 0.4- to 2.5-micron-wavelength region (outside of the absorption features). These results are based on HYDICE sensor data collected from the Southern Great Plains Atmospheric Radiation Measurement site during overflights conducted in July of 1997. Results of an upgrade made in the model-based atmospheric correction techniques, which take advantage of updates made to the moderate resolution atmospheric transmittance model (MODTRAN 4.0) software, will also be presented. Data will be shown to demonstrate how the reflectance retrieval in the shorter wavelengths of the blue-green region will be improved because of enhanced modeling of multiple scattering effects.

NTIS
*Algorithms; Atmospheric Correction; Atmospheric Models; Calibrating; Correction*

**20010123642** TRW Environmental Services, Las Vegas, NV USA
**Preliminary paper: Development of the Reference Design Description for a geologic repository**
Daniel, R. B.; Rindskopf, M. S.; Nov. 20, 1997; 7p; In English
Report No.(s): DE2000-757283; TPM 647; No Copyright; Avail: Department of Energy Information Bridge, Microfiche

This report describes the current Reference Design Description (RDD) design expectations for a potential geologic repository that could be located at Yucca Mountain in Nevada.

NTIS
*Radioactive Wastes; Systems Engineering; Underground Storage*

**20010123755** Argonne National Lab., IL USA
**Modeling of dry deposition over regional scales with use of satellite data**
Xu, Y.; Oct. 12, 1998; 7p; In English
Report No.(s): DE2001-11031; ANL/ER/CP-96890; No Copyright; Avail: Department of Energy Information Bridge, Microfiche

Dry deposition, an essential component in the atmospheric budget of many trace chemicals, can deliver a major portion of the chemicals deposited at sensitive receptors at the surface of the Earth. Dry deposition in atmospheric numerical models is often described with modules that provide estimates of the deposition velocity V(sub d), which is the downward flux divided by concentration at a specified height. A fairly common practice in dry deposition modules is to describe surface conditions that affect dry deposition in terms of broad land use and seasonal categories. This practice can lead to unrealistic values for V(sub d), however, when vegetative conditions for one land use category vary considerably within the domain, when abrupt changes in surface conditions are imposed by a change in seasonal category, or when environmental conditions change vegetative properties within one season. to improve this situation, surface spectral reflectance sensed by environmental satellites can be used to provide

more realistic depictions of the spatial and temporal variations in surface conditions. Such an approach is explored here, by extending of methods described by Gao (1995) and Gao and Wesely (1995), in conjunction with a previously developed dry deposition module (Wesely, 1989). In addition, because simulations of biogenic emissions usually rely on an adequate description of many of the surface conditions that affect dry deposition, we examine a method of using a single source of satellite data with modules for both biogenic emission rates and dry deposition velocities. The Biogenic Emissions Inventory System (BEIS) version 2.2, which is a version similar to the model described by Geron et al., is used. Results are presented for ozone V(sub d), isoprene emission rates, and emission rates of other monoterpenes in the eastern half of the US and nearby areas for selected periods during 1989.
NTIS
*Atmospheric Chemistry; Deposition; Atmospheric Models*

**20010123916** Sandia National Labs., Albuquerque, NM USA
**Computer and Centrifuge Modeling of Decoupled Explosions in Civilian Tunnels**
Preece, D. S.; Weatherby, J. R.; Blanchat, T. K.; Davie, N. T.; Calderone, J. J.; Sep. 21, 2000; 24p; In English
Report No.(s): DE2001-763352; SAND2000-2361C; No Copyright; Avail: Department of Energy Information Bridge

Geotechnical structures such as underground bunkers, tunnels, and building foundations are subjected to stress fields produced by the gravity load on the structure and/or any overlying strata. These stress fields may be reproduced on a scaled model of the structure by proportionally increasing the gravity field through the use of a centrifuge. This technology can then be used to assess the vulnerability of various geotechnical structures to explosive loading. Applications of this technology include assessing the effectiveness of earth penetrating weapons, evaluating the vulnerability of various structures, counter-terrorism, and model validation. This document describes the development of expertise in scale model explosive testing on geotechnical structures using Sandia's large scale centrifuge facility. This study focused on buried structures such as hardened storage bunkers or tunnels. Data from this study was used to evaluate the predictive capabilities of existing hydrocodes and structural dynamics codes developed at Sandia National Laboratories (such as Pronto/SPH, Pronto/CTH, and ALEGRA).
NTIS
*Underground Structures; Computerized Simulation; Centrifuges; Stress Distribution*

**20010125013** Geological Survey, Reston, VA USA
**Quality-Assurance Plan for District Ground-Water Activities of the U.S. Geological Survey** ***Final Report***
Brunett, J. O.; Barber, N. L.; Burns, A. W.; Fogelman, R. P.; Gillies, D. C.; 1997; 20p; In English
Report No.(s): PB2001-108674; USGS/OFR-97-11; No Copyright; Avail: CASI; A03, Hardcopy; A01, Microfiche

As the Nations principal earth-science information agency, the U.S. Geological Survey (USGS) is depended upon to collect data of the highest quality. This document provides the framework for collecting, analyzing and reporting ground-water data that are quality assured and quality controlled.
NTIS
*Geological Surveys; Ground Water; Quality Control; Data Acquisition*

**20010125024** Argonne National Lab., IL USA
**Atmospheric Radiation Measurement Program facilities newsletter, September 2000**
Sisterson, D. L.; Holdridge, D. J.; Sep. 19, 2000; 2p; In English
Report No.(s): DE2000-764205; ANL/ER/NL-00-09; No Copyright; Avail: Department of Energy Information Bridge

This is the third water vapor IOP and it will focus on the lower portions of the atmosphere. Again, scientists will work to achieve absolute calibrations of water vapor instrumentation. For this purpose, several instruments will be deployed, and measurements will be compared. Instruments to be used include radiosondes, Raman lidar, chilled-mirror hygrometers, surface meteorological observation station (SMOS) towers, a variety of microwave radiometers, and global positioning systems (GPS). The current experiment has two goals. The first is to characterize the accuracy of the water vapor measurements, especially the daily operational observations being made around the clock in the lower levels of the atmosphere at the CART site. The second goal is to develop techniques for improving the accuracy of these observations in order to obtain the best possible water vapor measurements under a wide range of atmospheric conditions.
NTIS
*Atmospheric Radiation; Radiation Measurement; Meteorological Instruments; Water Vapor; Meteorological Parameters*

**20010125100** Geological Survey, Water Resources Div., Montgomery, AL USA

**Water Resources Data for Alabama Water Year 2000** ***Annual Report, 1 Oct. 1999 - 30 Sep. 2000***

Pearman, J. L.; Stricklin, V. E.; Psinakis, W. L.; July 2001; 730p; In English

Report No.(s): PB2001-108236; USGS/WDR/AL-00/1; No Copyright; Avail: CASI; A99, Hardcopy; A06, Microfiche

Water resources data for the 2000 water year for Alabama consist of records of stage, discharge, and water quality of streams; stages and contents of lakes and reservoirs; and water levels in wells. This report includes record on both surface and ground water in the State. Specifically, it contains: (1) discharge records for 130 streamflow-gaging stations, for 41 partial-record or miscellaneous streamflow stations; (2) stage and content records for 14 lakes and reservoirs and stage at 40 stations; (3) water-quality records for 18 streamflow-gaging stations, for 61 ungaged streamsites, and for two precipitation stations; (4) water temperature and specific conductance at 14 surface-water stations; (5) dissolved oxygen at 11 stations; (6) sediment data at 50 stations; (7) chemical analyses of bed material at six stations; (8) water-level records for three recording observation wells; and (9) water-quality records for 52 ground-water stations. Also included are lists of active and discontinued continuous-record surface-water-quality stations, and partial-record and miscellaneous surface-water-quality stations. These data represent that part of the National Water Data System operated by the U.S. Geological Survey and cooperating Federal, State, and local agencies in Alabama.

NTIS

*Alabama; Surface Water; Ground Water; Hydrology; Water Quality; Water Resources*

**20010125107** Geological Survey, Water Resources Div., Troy, NY USA

**Water Resources Data for New York, Water Year 2000. Volume 1. Eastern New York, Excluding Long Island** ***Annual Report, 1 Oct. 1999 - 30 Sep. 2000***

2001; 538p; In English

Report No.(s): PB2001-108018; USGS-WDR-NY-00-1; No Copyright; Avail: CASI; A23, Hardcopy; A04, Microfiche

Water resources data for the 2000 water year for New York consists of records of stage, discharge, and water quality of streams; stage, contents, and water quality of lakes and reservoirs; and ground-water levels. This volume contains records for water discharge at 139 gaging stations; stage only at 10 gaging stations; stage and contents at four gaging stations, and 18 other lakes and reservoirs; water quality at 32 gaging stations; and water levels at five observation wells. Also included are data for 34 crest-stage partial-record stations. Locations of all these sites are shown on figure 8. Additional water data were collected at various sites not involved in the systematic data-collection program, and are published as miscellaneous measurements and analyses. These data together with the data in volumes 2 and 3 represent that part of the National Water Data System operated by the U.S. Geological Survey in cooperation with State, Municipal, and Federal agencies in New York.

NTIS

*New York; Surface Water; Ground Water; Hydrology; Water Resources*

**20010125229** Department of Energy, Aiken, SC USA

**Geotechnical Seismic Assessment Report for Defense Waste Processing Facility**

McHood, M.; Oct. 04, 2000; 54p; In English

Report No.(s): DE2000-765049; WSRC-TR-95-00072; No Copyright; Avail: Department of Energy Information Bridge

High level waste facilities at the Savannah River Site include several major structures that must meet seismic requirements, including the Defense Waste Processing Facility. Numerous geotechnical and geological investigations have been performed to characterize the in-situ static and dynamic properties of the soil sediments. These investigations have led to conclusions concerning the stability of foundation soils in terms of liquefaction potential and structure settlement. This report reviews past work that addresses seismic soil stability and presents the results of more recent analyses incorporating updated seismic criteria.

NTIS

*Dynamic Characteristics; Geotechnical Engineering; Sediments; Soils; Radioactive Wastes; Waste Treatment*

**20010125453** Lawrence Livermore National Lab., Livermore, CA USA

**Ultrasonic characterization of synthetic soils for application to near surface geophysics**

Berge, P.; Bonner, B. P.; Boro, C.; Hardy, E.; Ruddle, C.; Nov. 11, 1999; 11p; In English

Report No.(s): DE2001-8323; UCRL-JC-132889; EW45100000; No Copyright; Avail: Department of Energy Information Bridge, Microfiche

Effective seismic interrogation of the near subsurface requires that measured parameters, such as compressional and shear velocities and attenuation, be related to important soil properties. Porosity, composition (clay content), and fluid content and identification are of particular interest. The ultrasonic (100-500 kHz) pulse transmission technique was used to collect data for

highly attenuating materials appropriate to the vadose zone. Up to several meters of overburden was simulated by applying low uniaxial stress of 0.1 Mpa to the sample. The approach has been to make baseline measurements for pure quartz sand, because the elastic properties are relatively well known except at the lowest pressures. Second phases are then added to modify the sample microstructure and ultrasonic measurements are made to characterize the effect of the admixed second phase. Samples are fabricated from Ottawa sand mixed with a swelling clay (Wyoming bentonite), and with a common organic soil amendment, peat. Compressional (P) velocities are low, ranging from 169 to 360 m/s for the mixtures at low stress. Shear (S) velocities are about half of the compressional velocity, but show different sensitivity to microstructure. Adding clay increases the shear amplitude dramatically with respect to P, and also changes the sensitivity of the velocities to load. These experiments demonstrate that P and S velocities are sensitive to the amount and type of admixed second phase, even at low concentrations. Other properties of the transmitted signals which include the ratio of S and P amplitudes, velocity gradient with depth, and the frequency content of transmitted pulses, provide additional information are not now used in near-surface surveys.
NTIS
*Soils; Characterization; Geophysics; Admixtures; Mechanical Properties; Ultrasonic Tests*

**20010125479** Oak Ridge Y-12 Plant, TN USA
**Geophysical Surveys of a Known Karst Feature, Oak Ridge Y-12 Plant, Oak Ridge, Tennessee**
Doll, W. E.; Nyquist, J. E.; Carpenter, P. J.; Kaufmann, R. D.; Carr, B. J.; Dec. 01, 1998; 16p; In English
Report No.(s): DE2001-8046; Y/TS-1736; No Copyright; Avail: Department of Energy Information Bridge, Microfiche
Geophysical data were acquired at a site on the Oak Ridge Reservation, Tennessee to determine the characteristics of a mud-filled void and to evaluate the effectiveness of a suite of geophysical methods at the site. Methods that were used included microgravity, electrical resistivity, and seismic refraction. Both microgravity and resistivity were able to detect the void as well as overlying structural features. The seismic data provide bedrock depth control for the other two methods, and show other effects that are caused by the void.
NTIS
*Electrical Resistivity; Geophysics; Surveys*

**20010125529** Illinois Univ. at Urbana-Champaign, Urbana, IL USA
**Investigation of groundwater flow paths through combined inversion of strontium isotope ratios and hydraulic head data. Final report**
Johnson, T. M.; Dec. 04, 1999; 31p; In English
Report No.(s): DE2001-764712; No Copyright; Avail: Department of Energy Information Bridge
Strontium (SR) isotope and other geochemical data were collected for groundwater samples from the Snake River Plain aquifer in the vicinity of the Idaho National Engineering and Environmental Laboratory (INEEL). These geochemical data provide strong evidence for slow and fast groundwater flow zones that had not been previously characterized. The geochemical data were combined with existing hydraulic head data in groundwater flow and transport models. These models enable quantitative extraction of flow information from the data (i.e., inversion of the data). This new approach and the implications for INEEL environmental activities will be reported in two journal articles. One submitted recently and a second in preparation.
NTIS
*Geochemistry; Ground Water; Isotope Ratios; Strontium Isotopes; Hydrology Models; Hydraulics*

**20010125538** Lehigh Univ., Bethlehem, PA USA
**Surface and solution-interface geochemistry of lead sulfide and lead selenide minerals** ***Final Report, 1 May 1998***
Moses, C. O.; Ilton, E. S.; May 01, 1998; 13p; In English
Report No.(s): DE2001-763926; No Copyright; Avail: Department of Energy Information Bridge, Microfiche
This project was an investigation into the aqueous reactivity of sulfide minerals and their selenide analogs (endmember and solid-solution compositions). The specific goal was a comprehensive and integrated understanding of reactivity based on fundamental high-vacuum surface chemistry and the rates of aqueous exchange and dissolution reactions. The focus was on PbS (galena) and PbSe (clausthalite).
NTIS
*Geochemistry; Lead Selenides; Lead Sulfides*

**20010125541** Los Alamos National Lab., NM USA

**Critique of Dual Continuum Formulations of Multicomponent Reactive Transport in Fractured Porous Media**

Lichtner, P. C.; Feb. 01, 2000; 30p; In English

Report No.(s): DE2001-763406; LA-UR-00-1097; No Copyright; Avail: Department of Energy Information Bridge, Microfiche

Subsurface flow processes may take place at many different scales. The different scales refer to rock pore structure, micro-fractures, distinct fracture networks ranging from small to large fracture spacing, and even faults. Presently, there is no satisfactory methodology for describing quantitatively flow and reactive transport in multi-scale media. Approaches commonly applied to model fractured systems include single continuum models (SCM), equivalent continuum models (ECM), discrete fracture models (DFM), and various forms of dual continuum models (DCM). The SCM describes flow in the fracture network only and is valid in the absence of fracture-matrix interaction. The ECM, on the other hand, requires pervasive interaction between fracture and matrix and is based on averaging their properties. The ECM is characterized by equal fracture and matrix solute concentrations, but generally different mineral concentrations. The DFM is perhaps the most rigorous, but would require inordinate computational resources for a highly fractured rock mass. The DCM represents a fractured porous medium as two interacting continua with one continuum corresponding to the fracture network and the other the matrix. A coupling term provides mass transfer between the two continua. Values for mineral and solute concentrations and other properties such as liquid saturation state may be assigned individually to fracture and matrix. Two forms of the DCM are considered characterized by connected and disconnected matrix blocks. The former is referred to as the DCCM (dual continuum connected matrix) model and the latter as the DCDM (dual continuum disconnected matrix) model. In contrast to the DCCM model in which concentration gradients in the matrix are allowed only parallel to the fracture, the DFM provides for matrix concentration gradients perpendicular to the fracture. The DFM and DCCM models can agree with each other only in the case where both reduce to the ECM. The DCCM model exhibits the incorrect behavior as the matrix block size increases, resulting in reduced coupling between fracture and matrix continua. The DCDM model allows for matrix gradients within individual matrix blocks in which the symmetry of the surrounding fracture geometry is preserved. However, the DCDM model breaks down for simultaneous heat and mass transport and cannot account for significant changes in porosity and permeability caused by chemical reactions.

NTIS

*Multiphase Flow; Porous Materials; Fractures (Materials); Fluid Flow; Rocks; Continuum Modeling*

**20010125593** Lawrence Livermore National Lab., Livermore, CA USA

**Comparing geophysical measurements to theoretical estimates for soil mixtures at low pressures**

Wildenschild, D.; Berge, P. A.; Berryman, K. G.; Bonner, B. P.; Roberts, J. J.; Jan. 15, 1999; 10p; In English

Report No.(s): DE2001-8169; UCRL-JC-132893; EW45100000; No Copyright; Avail: Department of Energy Information Bridge, Microfiche

The authors obtained good estimates of measured velocities of sand-peat samples at low pressures by using a theoretical method, the self-consistent theory of Berryman, using sand and porous peat to represent the microstructure of the mixture. They were unable to obtain useful estimates with several other theoretical approaches, because the properties of the quartz, air and peat components of the samples vary over several orders of magnitude. Methods that are useful for consolidated rock cannot be applied directly to unconsolidated materials. Instead, careful consideration of microstructure is necessary to adapt the methods successfully. Future work includes comparison of the measured velocity values to additional theoretical estimates, investigation of Vp/Vs ratios and wave amplitudes, as well as modeling of dry and saturated sand-clay mixtures. The results suggest that field data can be interpreted by comparing laboratory measurements of soil velocities to theoretical estimates of velocities in order to establish a systematic method for predicting velocities for a full range of sand-organic material mixtures at various pressures. Once the theoretical relationship is obtained, it can be used to estimate the soil composition at various depths from field measurements of seismic velocities. Additional refining of the method for relating velocities to soil characteristics is useful for development inversion algorithms.

NTIS

*Geophysics; Soils; Low Pressure; Microstructure*

## 43
## EARTH RESOURCES AND REMOTE SENSING

*Includes remote sensing of earth features, phenomena and resources by aircraft, balloon, rocket, and spacecraft; analysis or remote sensing data and imagery; development of remote sensing products; photogrammetry; and aerial photographs. For instrumentation see 35 Instrumentation and Photography.*

**20010117647** NASA Langley Research Center, Hampton, VA USA
**Direct Comparisons of Radiances Measured by Independent Contemporary ERB Instruments**
Haeffelin, Martial, Virginia Polytechnic Inst. and State Univ., USA; Wielicki, Bruce, NASA Langley Research Center, USA; Priestley, Kory, NASA Langley Research Center, USA; Duvel, Jean Philippe, Laboratoire de Meteorologie Dynamique, France; Viollier, Michel, Laboratoire de Meteorologie Dynamique, France; [2001]; 3p; In English
Contract(s)/Grant(s): NAG1-2106; No Copyright; Avail: CASI; A01, Hardcopy; A01, Microfiche

Comparisons of radiance measurements from overlapping independent Earth and cloud radiation budget (ERB) missions are an important contribution to the validation process of the these missions and are essential to the construction of a consistent long-term record of ERB observations. Measurements from the CERES instrument on TRMM are compared to ScaRaB on Resurs (Jan-Mar 1999) and CERES on Terra (Mar-Apr 2000).
Author
*Atmospheric Radiation; Radiance; Comparison; Radiation Measurement*

**20010117868** Instituto Nacional de Pesquisas Espacias, Sao Jose dos Campos, Brazil
**Shade Fraction Image In The Characterization and Mapping of Babacu (Attalea speciosa Mart. ex Spreng.) In Forest Areas *Imagem Fracao Sombra na Caracterizacao e Mapeamento de Babacu (Attalea speciosa Mart ex Spreng.) em Areas de Floresta***
Thales, Marcelo Cordeiro, Instituto Nacional de Pesquisas Espacias, Brazil; 2001; 144p; In Portuguese; Original contains color illustrations
Report No.(s): INPE-8382-TDI/772; No Copyright; Avail: CASI; A07, Hardcopy; A02, Microfiche

The babacu palm (Attalea speciosa, Mart. ex Spreng.) occurs in several Brazilian states, inserted in several vegetation units (or vegetation associations). High densities of the species are found in neotropical forest ecosystems and is a consequence of human interference or natural disturbances. Youngs palms in deforested areas survive cutting and burnings, dominating the secondary forest progressively. After abandonment, the regeneration of those areas happens slowly and their biomass stagnates in a smaller value than the original forest biomass, with consequent implications in the biogeochemical cycle (carbon budget). LANDSAT-TM images are useful in the monitoring of land use and land cover of Amazonia and the areas with the presence of babacu are characterized by dark patches as a result of shade due to the architecture and morphology of the canopy. Digital videography and aerial photography, used as ground truth, in association with techniques of image processing, such as analysis of spectral mixture, segmentation and classification, were used to characterize the areas of babacu dominance. The density of babacu cover was related with radiometric values of the images to generate an equation to be used to derive a map of the different densities of babacu cover. As a result it was verified that as the babacu cover increased, the values of digital number and apparent reflectance decreased, particularly in the near infrared band (TM-4), while the values of the shade fraction image increased. This fact is demonstrated through the significant relationship, at the 5% level, using either linear or exponential relationship between the values of density of babacu cover, estimated through the videography, and of shade fraction image. These relationships served as a basis for slicing the shade fraction image using both models of regression (linear and exponential), that were compared with the results of the classification of the segmented images. The best results were obtained using the sliced image through the exponential regression model and the classification of segmented image with thresholds 5 and 15 of similarity and area, respectively, and classified with threshold of acceptance of 99%, which presented value of Kappa equal the 0,45.
Author
*Vegetation; Brazil; Biogeochemistry; Land Use; Amazon Region (South America); Dominance; Ecosystems*

**20010119957** NASA Goddard Space Flight Center, Greenbelt, MD USA
**Validation of MODIS Aerosol Optical Depth Retrieval Over Land**
Chu, D. A., Science Systems and Applications, Inc., USA; Kaufman, Y. J., NASA Goddard Space Flight Center, USA; Ichoku, C., Science Systems and Applications, Inc., USA; Remer, L. A., NASA Goddard Space Flight Center, USA; Tanre, D., Centre National de la Recherche Scientifique, France; Holben, B. N., NASA Goddard Space Flight Center, USA; [2001]; 16p; In English; Original contains color illustrations; No Copyright; Avail: CASI; A03, Hardcopy; A01, Microfiche

Aerosol optical depths are derived operationally for the first time over land in the visible wavelengths by MODIS (Moderate Resolution Imaging Spectroradiometer) onboard the EOSTerra spacecraft. More than 300 Sun photometer data points from more than 30 AERONET (Aerosol Robotic Network) sites globally were used in validating the aerosol optical depths obtained during July - September 2000. Excellent agreement is found with retrieval errors within (Delta)tau=+/- 0.05 +/- 0.20 tau, as predicted, over (partially) vegetated surfaces, consistent with pre-launch theoretical analysis and aircraft field experiments. In coastal and semi-arid regions larger errors are caused predominantly by the uncertainty in evaluating the surface reflectance. The excellent fit was achieved despite the ongoing improvements in instrument characterization and calibration. This results show that MODIS-derived aerosol optical depths can be used quantitatively in many applications with cautions for residual clouds, snow/ice, and water contamination.
Author
*Aerosols; Optical Thickness; Photometers; Spectral Reflectance; Spectroradiometers*

**20010120096** Virginia Polytechnic Inst. and State Univ., Dept. of Mechanical Engineering, Blacksburg, VA USA
**Evaluation and Improvement of Earth Radiation Budget Data Sets** ***Final Report, 1 Oct. 2000 - 30 Sep. 2001***
Haeffelin, Martial P. A., Virginia Polytechnic Inst. and State Univ., USA; [2001]; 3p; In English
Contract(s)/Grant(s): NAG1-2106; No Copyright; Avail: CASI; A01, Hardcopy; A01, Microfiche

The tasks performed during this grant are as follows: (1) Advanced scan patterns for enhanced spatial and angular sampling of ground targets; (2) Inter-calibration of polar orbiter in low Earth orbits (LEO) and geostationary (GEO) broadband radiance measurements; (3) Synergism between CERES on TRMM and Terra; (4) Improved surface solar irradiance measurements; (5) SW flux observations from Ultra Long Duration Balloons at 35 km altitude; (6) Nighttime cloud property retrieval algorithm; (7) Retrievals of overlapped and mixed-phase clouds.
Derived from text
*Earth Radiation Budget; Earth Radiation Budget Experiment*

**20010122735** Jet Propulsion Lab., California Inst. of Tech., Pasadena, CA USA
**Imaging Radar in the Mojave Desert-Death Valley Region**
Farr, Tom G., Jet Propulsion Lab., California Inst. of Tech., USA; Field Trip and Workshop on the Martian Highlands and Mojave Desert Analogs; 2001, pp. 19-20; In English; See also 20010122728; No Copyright; Avail: CASI; A01, Hardcopy; A01, Microfiche

The Mojave Desert-Death Valley region has had a long history as a test bed for remote sensing techniques. Along with visible-near infrared and thermal IR sensors, imaging radars have flown and orbited over the area since the 1970's, yielding new insights into the geologic applications of these technologies. More recently, radar interferometry has been used to derive digital topographic maps of the area, supplementing the USGS 7.5' digital quadrangles currently available for nearly the entire area. As for their shorter-wavelength brethren, imaging radars were tested early in their civilian history in the Mojave Desert-Death Valley region because it contains a variety of surface types in a small area without the confounding effects of vegetation. The earliest imaging radars to be flown over the region included military tests of short-wavelength (3 cm) X-band sensors. Later, the Jet Propulsion Laboratory began its development of imaging radars with an airborne sensor, followed by the Seasat orbital radar in 1978. These systems were L-band (25 cm). Following Seasat, JPL embarked upon a series of Space Shuttle Imaging Radars: SIRA (1981), SIR-B (1984), and SIR-C (1994). The most recent in the series was the most capable radar sensor flown in space and acquired large numbers of data swaths in a variety of test areas around the world. The Mojave Desert-Death Valley region was one of those test areas, and was covered very well with 3 wavelengths, multiple polarizations, and at multiple angles. At the same time, the JPL aircraft radar program continued improving and collecting data over the Mojave Desert Death Valley region. Now called AIRSAR, the system includes 3 bands (P-band, 67 cm; L-band, 25 cm; C-band, 5 cm). Each band can collect all possible polarizations in a mode called polarimetry. In addition, AIRSAR can be operated in the TOPSAR mode wherein 2 antennas collect data interferometrically, yielding a digital elevation model (DEM). Both L-band and C-band can be operated in this way, with horizontal resolution of about 5 m and vertical errors less than 2 m. The findings and developments of these earlier investigations are discussed.
Author
*Imaging Radar; Death Valley (CA); Mojave Desert (CA); Remote Sensing; Imaging Techniques*

**20010122748** Tennessee Univ., Dept. of Geological Sciences, Knoxville, TN USA
**Remote Sensing of Evaporite Minerals in Badwater Basin, Death Valley, at Varying Spatial Scales and in Different Spectral Regions**
Moersch, J. E., Tennessee Univ., USA; Farmer, J., Arizona State Univ., USA; Baldridge, A., Arizona State Univ., USA; Field Trip

and Workshop on the Martian Highlands and Mojave Desert Analogs; 2001, pp. 45-46; In English; See also 20010122728; No Copyright; Avail: CASI; A01, Hardcopy; A01, Microfiche

A key concept behind the overall architecture of NASA's Mars Surveyor Program is that remote sensing observations made from orbit will be used to guide the selection of landing sites for subsequent missions to the surface. An important component of the orbital phase of this strategy is mineralogical mapping of the surface with infrared spectrometers and imaging systems. Currently, the Mars Global Surveyor Thermal Emission Spectrometer (TES) is spectrally mapping Mars in the 6-50 micrometer region at a spatial resolution of 3 km. Starting later this year, the Thermal Emission Imaging System (THEMIS) aboard the Mars 2001 Odyssey orbiter will image the entire surface of the planet in eight broad bands in the 6.5-14.5 micrometer region at a spatial resolution of 100 m. In 2003, ESA plans to launch the OMEGA instrument on Mars Express, which will map the planet in the visible and near infrared regions from an elliptical orbit at spatial resolutions of up to 100 m. Currently, NASA is selecting a visible and near-infrared mapping spectrometer for an orbiter that will launch in 2005. This instrument will likely map at a constant spatial resolution of at least 50 m. From an astrobiological perspective, the utility of these spectral datasets will be in locating potential paleohabitats for martian life, via the detection of minerals that form in the presence of liquid water. Deposits of evaporite minerals in putative martian paleolake basins are a particularly attractive target to look for because of the areal extent of these features, the strong spectral features of these minerals, and the characteristic sequences in which they appear along the margin of a basin. Despite considerable geomorphic evidence indicating the presence of ancient lake basins on Mars, to date no evaporite deposits have been reported from the TES experiment. But is this to be expected, given the limited spatial resolution of TES data? Might we still hope to find such deposits in upcoming experiments? One way to address this question is to use existing datasets from terrestrial analog sites to attempt to determine spatial and spectral thresholds of detectability for these minerals in a natural setting Author

*Remote Sensing; Death Valley (CA); Spatial Resolution; Spectral Bands; Mineral Deposits; Structural Basins; Sedimentary Rocks*

**20010123061** Army Construction Engineering Research Lab., Army Engineer Research and Development Center, Champaign, IL USA

**Underground Storage Tank Location and Mapping of Former Landfills by Electromagnetic Surveys for the Delaware National Guard *Final Report***

Nielsen, Paul H., Army Construction Engineering Research Lab., USA; August 2001; 46p; In English; Original contains color images

Report No.(s): AD-A395231; ERDC/CERL-TR-01-57; No Copyright; Avail: CASI; A03, Hardcopy; A01, Microfiche

The Delaware Army National Guard tasked the U.S. Army Engineer Research and Development Center (ERDC), Construction Engineering Research Laboratory (CERL) to provide electromagnetic surveys to identify possible subsurface metallic features at various locations at the New Castle Rifle Range, New Castle, DE and at the Bethany Beach, Delaware National Guard Training Base. Surveys were conducted using multi-frequency electromagnetic profilers to induce eddy currents and measure the resultant secondary fields, giving an average conductivity value for the affected search volume. Images were generated from the data using commercial spread-sheet and mapping software. This report presents the results of the electromagnetic surveys conducted to locate subsurface metallic features at the two sites.

DTIC

*Electromagnetic Radiation; Storage Tanks; Landfills; Underground Storage*

**20010123258** Wisconsin Univ., Madison, WI USA

**Final Report: High Spectral Resolution Atmospheric Emitted Radiance Studies with the ARM UAV**

Revercomb, H. E.; Dec. 31, 1999; 34p; In English

Report No.(s): DE2001-761175; No Copyright; Avail: Department of Energy Information Bridge

The active participation in the Atmospheric Radiation Measurement (ARM) Unmanned Airborne Vehicle (UAV) science team that was anticipated in the grant proposal was indefinitely delayed after the first year due to a programmatic decision to exclude the high spectral resolution observations from the existing ARM UAV program. However, this report shows that substantial progress toward the science objectives of this grant have made with the help of separate funding from NASA and other agencies. In the four year grant period (including time extensions), a new high spectral resolution instrument has been flown and has successfully demonstrated the ability to obtain measurements of the type needed in the conduct of this grant. In the near term, the third water vapor intensive observing period (WVIOP-3) in October 2000 will provide an opportunity to bring the high spectral resolution observations of upwelling radiance into the ARM program to complement the downwelling radiance observations from

the existing ARM AERI instruments. We look forward to a time when the ARM-UAV program is able to extend its scope to include the capability for making these high spectral resolution measurements from a UAV platform.
NTIS
*Emittance; Radiation Measurement; Spectral Resolution; Pilotless Aircraft; Atmospheric Radiation*

**20010123451** Argonne National Lab., IL USA
**Diurnal evapotranspiration estimates in the Walnut River Watershed**
Song, J.; Oct. 05, 1998; 7p; In English
Report No.(s): DE2001-11030; ANL/ER/CP-96888; No Copyright; Avail: Department of Energy Information Bridge, Microfiche

Evapotranspiration is an essential component of the surface hydrological balance, but obtaining accurate estimates of the water vapor flux over large terrestrial areas can be difficult because of the substantial temporal and spatial variability in surface moisture conditions that can occur. This variability is often very large in the Great Plains and other portions of the Mississippi River Basin. Nevertheless, variations in soil moisture content, groundwater levels, and runoff in streams and rivers cannot be fully assessed without some knowledge of evapotranspiration rates. Here, observations made at the Walnut River Watershed (WRW), which is near Wichita, Kansas, and has an area of approximately 5000 km(sup 2), are used to improve and test a modeling system that estimates long-term evapotranspiration with use of satellite remote sensing data with limited surface measurements. The techniques may be applied to much larger areas. As is shown in Fig. 1, the WRW is located in the Red River Basin and is enclosed by the southern Great Plains Clouds and Radiation Testbed (CART) of the US Department of Energys Atmospheric Radiation Measurement (ARM) program. The functional relationships involving the satellite data, surface parameters, and associated subgrid-scale fluxes are modeled in this study by the parameterization of subgrid-scale surface (PASS) fluxes scheme, which is used in a modified and improved form (PASS2). The advantage of this modeling system is that it can make effective use of satellite remote sensing data and can be run for large areas for which flux data do not exist and surface meteorological data are available from only a limited number of ground stations. In this study, the normalized difference vegetation index (NDVI) or simple ratio (SR) and surface brightness temperature at each pixel for the WRW were derived from advanced very high resolution radiometers data collected by a ground station at Argonne National Laboratory from the National Oceanic and Atmospheric Administrations NOAA-12 and NOAA-14 satellites. The satellite data were subjected to atmospheric corrections for three intensive observation days of the 1997 Cooperative Atmosphere-Surface Exchange Study (CASES-97) experiment, which was conducted in cooperation with the Argonne Boundary Layer Experiments (ABLE) effort and the ARM Program.
NTIS
*Remote Sensing; Evapotranspiration; Kansas; Surface Temperature; Normalized Difference Vegetation Index*

**20010124074** NASA Goddard Space Flight Center, Greenbelt, MD USA
**The Potential of Using LANDSAT 7 Data for the Classification of Sea Ice Surface Conditions During Summer**
Markus, Thorsten, NASA Goddard Space Flight Center, USA; Cavalieri, Donald J., NASA Goddard Space Flight Center, USA; Ivanoff, Alvaro, Raytheon Information Technology and Scientific Services, USA; [2001]; 19p; In English; No Copyright; Avail: CASI; A03, Hardcopy; A01, Microfiche

During spring and summer, the Surface of the Arctic sea ice cover undergoes rapid changes that greatly affect the surface albedo and significantly impact the further decay of the sea ice. These changes are primarily the development of a wet snow cover and the development of melt ponds. As melt pond diameters generally do not exceed a couple of meters, the spatial resolutions of sensors like AVHRR and MODIS are too coarse for their identification. LANDSAT 7, on the other hand, has a spatial resolution of 30 m (15 m for the pan-chromatic band). The different wavelengths (bands) from blue to near-infrared offer the potential to distinguish among different surface conditions. LANDSAT 7 data for the Baffin Bay region for June 2000 have been analyzed. The analysis shows that different surface conditions, such as wet snow and meltponded areas, have different signatures in the individual LANDSAT bands. Consistent with in-situ albedo measurements, melt ponds show up as blueish whereas dry and wet ice have a white to gray appearance in the LANDSAT true-color image. These spectral differences enable the distinction of melt ponds. The melt pond fraction for the scene studied in this paper was 37%.
Author
*Ponds; Melting; Sea Ice; LANDSAT 7; Satellite Imagery; Remote Sensing*

**20010124076** NASA Goddard Space Flight Center, Greenbelt, MD USA

**Enhancement of Tropical Land Cover Mapping with Wavelet-Based Fusion and Unsupervised Clustering of SAR and LANDSAT Image Data**

LeMoigne, Jacqueline, NASA Goddard Space Flight Center, USA; Laporte, Nadine, Maryland Univ., USA; Netanyahuy, Nathan S., Bar-Ilan Univ., Israel; [2001]; 9p; In English

Contract(s)/Grant(s): NRA-99-OES-06; NAS2-37143; No Copyright; Avail: CASI; A02, Hardcopy; A01, Microfiche

The characterization and the mapping of land cover/land use of forest areas, such as the Central African rainforest, is a very complex task. This complexity is mainly due to the extent of such areas and, as a consequence, to the lack of full and continuous cloud-free coverage of those large regions by one single remote sensing instrument, In order to provide improved vegetation maps of Central Africa and to develop forest monitoring techniques for applications at the local and regional scales, we propose to utilize multi-sensor remote sensing observations coupled with in-situ data. Fusion and clustering of multi-sensor data are the first steps towards the development of such a forest monitoring system. In this paper, we will describe some preliminary experiments involving the fusion of SAR and LANDSAT image data of the Lope Reserve in Gabon. Similarly to previous fusion studies, our fusion method is wavelet-based. The fusion provides a new image data set which contains more detailed texture features and preserves the large homogeneous regions that are observed by the Thematic Mapper sensor. The fusion step is followed by unsupervised clustering and provides a vegetation map of the area.

Author

*Imagery; In Situ Measurement; Mapping; Remote Sensing; Satellite Imagery; Thematic Mappers (LANDSAT); Wavelet Analysis*

**20010124078** NASA Langley Research Center, Hampton, VA USA

**Towards GPS Surface Reflection Remote Sensing of Sea Ice Conditions**

Komjathy, A., Colorado Univ., USA; Maslanik, J. A., Colorado Univ., USA; Zavorotny, V. U., Colorado Univ., USA; Axelrad, P., Colorado Univ., USA; Katzberg, S. J., NASA Langley Research Center, USA; [2000]; 10p; In English; 6th International Conference on Remote Sensing for Marine and Coastal Environments, 1-3 May 2000, Charleston, SC, USA

Contract(s)/Grant(s): NAG1-1927; No Copyright; Avail: CASI; A02, Hardcopy; A01, Microfiche

This paper describes the research to extend the application of Global Positioning System (GPS) signal reflections, received by airborne instruments, to cryospheric remote sensing. The characteristics of the GPS signals and equipment afford the possibility of new measurements not possible with existing radar and passive microwave systems. In particular, the GPS receiving systems are small and light-weight, and as such are particularly well suited to be deployed on small aircraft or satellite platforms with minimal impact. Our preliminary models and experimental results indicate that reflected GPS signals have potential to provide information on the presence and condition of sea and fresh-water ice as well as the freeze/thaw state of frozen ground. In this paper we show results from aircraft experiments over the ice pack near Barrow, Alaska suggesting correlation between forward scattered GPS returns and RADARSAT backscattered signals.

Author

*Global Positioning System; Remote Sensing; Sea Ice; Cryogenic Equipment*

**20010124894** Northwestern Univ., Dept. of Geological Sciences, Evanston, IL USA

**Quality Assessment of Mariner 10 Digital Elevation Models**

Wilkison, S. L., Northwestern Univ., USA; Robinson, M. S., Northwestern Univ., USA; Watters, T. R., National Air and Space Museum, USA; Cook, A. C., National Air and Space Museum, USA; Mercury: Space Environment, and Surface and Interior; 2001, pp. 113-114; In English; See also 20010124826; No Copyright; Abstract Only; Available from CASI only as part of the entire parent document

New camera positions and orientation data were used to create a new map of Mariner 10 stereo coverage. The automated digital stereo analysis provides continuous topographic data with 1-2 km spatial resolution and 0.5 to 2 km vertical resolution. Wilkison et al. reported an analysis of crater topography using this stereo data, examining the depth to diameter ratio (d/D) for immature and mature complex craters within a DEM (digital elevation model) of the Discovery Quadrangle. The d/D results agree with those of Pike for mature complex craters. However, the d/D results for immature complex craters diverged from that of Pike. Crater depth shallows as the immature complex craters approached the pixel size of the stereo matching box, or 'patch', which was typically 5 to 12 pixels (in radius), with image resolution of 1-2 km. We hypothesized that the patch size used in matching the stereo images created a smoothing effect of the topography within the DEM. to determine how the patch size was affecting the topography of the DEM, we performed a series of simple tests. These tests allow us to realistically place bounds on the accuracy and precision of the Mariner 10 DEMs. Additional information is contained in the original extended abstract.

Author

*Image Resolution; Mariner 10 Space Probe; Spatial Resolution; Elevation; Stereophotography; Planetary Mapping*

## 44
## ENERGY PRODUCTION AND CONVERSION

*Includes specific energy conversion systems, e.g., fuel cells; and solar, geothermal, windpower, and waterwave conversion systems; energy storage; and traditional power generators. For technologies related to nuclear energy production see 73 Nuclear Physics. For related information see also 07 Aircraft Propulsion and Power; 20 Spacecraft Propulsion and Power, and 28 Propellants and Fuels.*

**20010117650** Pacific Northwest National Lab., Richland, WA USA
**Hanford Site Near-Facility Environmental Monitoring Data Report for Calendar Year 1998**
Perkins, C. J.; Markes, B. M.; McKinney, S. D.; Mitchell, R. M.; Roos, R. C.; Aug. 16, 2000; 227p; In English
Report No.(s): DE2000-760134; PNNL-12088-VOL-2; No Copyright; Avail: Department of Energy Information Bridge

This document summarizes the results of the Waste Management Federal Services, Inc., Northwest Operations Near-Facility Environmental Monitoring program for 1998 in the 100, 200/600, and 300/400 Areas of the Hanford Site, in south-central Washington State. Surveillance activities included sampling and analyses of ambient air, surface water, groundwater, soil, sediments, and biota. Also, external radiation measurements and radiological surveys were taken at waste disposal sites, radiologically controlled areas, and roads. These activities were conducted to assess and control the effects of nuclear facilities and waste sites on the local environment.
NTIS
*Environmental Monitoring; Surveillance; Air Sampling; Water Sampling*

**20010117659** Sandia National Labs., Albuquerque, NM USA
**Development and Testing of an Approach to Anti-Islanding in Utility-Interconnected Photovoltaic Systems**
Stevens, J. W.; Bonn, R. H.; Ginn, J. W.; Gonzalez, S.; Kern, G.; Aug. 01, 2000; 63p; In English
Report No.(s): DE2000-759506; SAND2000-1939; No Copyright; Avail: Department of Energy Information Bridge

This report documents the development of an inverter control method that detects and avoids islanding in utility-interconnected photovoltaic installations. This method is applicable to single and multiple inverters connected to a single utility distribution line. The anti-islanding approach is described and its performance is demonstrated on both a theoretical basis and with results from tests conducted at Sandia National Laboratories and Ascension Technology, a division of Applied Power Corporation. It has been demonstrated that this approach is effective for single and multiple photovoltaic inverter installations for the special case where the inverter contains a version of anti-islanding software compatible with IEEE Std 929-2000.The report also describes the anti-islanding technique so that it can be incorporated into photovoltaic systems lacking this feature. A test procedure that ascertains whether an anti-islanding capability exists in a PV inverter is also presented.
NTIS
*Inverters; Performance Tests*

**20010117714** National Renewable Energy Lab., Golden, CO USA
**Energy Conservation Team *Annual Report, FY 1999***
Oct. 19, 1999; 76p; In English
Report No.(s): DE2000-752662; NREL/TP-540-27223; No Copyright; Avail: Department of Energy Information Bridge

This report highlights progress achieved during FY 1999 under the Light-duty Fuels Utilization R and D Program. The program is comprised of two elements: the Advanced Petroleum-Based APB Fuels Program which focused on developing and testing advanced fuels for use with compression-ignition direct-injection (CIDI) engines and fuel cells and the Alternative Fuels Program which focused on Natural gas and natural gas derived fuels. The report contains 17 summaries of industry and National Laboratory projects. Fuel efficient vehicles with very low emissions are essential to meet the challenges of climate change, energy security, and improved air quality. The authors anticipate cooperative efforts with the auto and energy industries to develop new and innovative technologies that will be used to make advanced transportation vehicles that are fuel efficient, clean, and safe.
NTIS
*Fuels; Energy Conservation; Energy Policy*

**20010117865** Atomic Energy Commission, Idaho Operations Office, Idaho Falls, ID USA
**Energy Efficient Aluminum Production: Pilot-Scale Cell Tests *Final Report***
Christini, R. A.; Dec. 30, 1999; 38p; In English
Report No.(s): DE2000-758726; DOE/ID/13219; No Copyright; Avail: Department of Energy Information Bridge, Microfiche

A cermet anode that produces oxygen and a cathode material that is wetted by aluminum can provide a dimensionally stable inter-electrode distance in the Hall-Heroult cell. This can be used to greatly improve the energy and/or productivity efficiencies.

The concept, which was developed and tested, uses a system of vertically interleaved anodes and cathodes. The major advantage of this concept is the significant increase in electrochemical surface area compared to a horizontal orientation of anode and cathode that is presently used in the Hall-Heroult process. This creates an additional advantage for energy reduction of 1.3 kWh/lb or a 20% productivity improvement. The voltages obtained in an optimized cell test met the energy objectives of the project for at least two weeks. An acceptable current efficiency was never proven, however, during either pilot scale or bench scale tests with the vertical plate configuration. This must be done before a vertical cell can be considered viable. Anode corrosion rate must be reduced by at least a factor of three in order to produce commercial purity aluminum. It is recommended that extensive theoretical and bench scale investigations be done to improve anode materials and to demonstrate acceptable current efficiencies in a vertical plate cell before pilot scale work is continued.
NTIS
*Anodes; Cathodes; Electrolytic Cells; Cermets; Electrochemical Cells*

**20010118521** Brookhaven National Lab., Upton, NY USA
**Photovoltaics and the Evironment 1998: Report on the Workshop Photovoltaics and the Environment 1999**
Fthenakis,; Zweibel,; Moskowitz,; Feb. 01, 1999; 276p; In English; Photovoltaics and the Evironment 1998, 1998, Unknown
Report No.(s): DE2000-759023; BNL-52557; No Copyright; Avail: Department of Energy Information Bridge
The objective of the workshop 'Photovoltaics and the Environment' was to bring together PV manufacturers and industry analysts to define EH and S issues related to the large-scale commercialization of PV technologies.
NTIS
*Technology Utilization; Photovoltaic Conversion; Industries*

**20010118540** Brookhaven National Lab., Upton, NY USA
**Brookhaven national laboratory environmental monitoring plan**
Daum,; Dorsch,; Fry,; Green,; Lee,; Sep. 22, 1999; 232p; In English
Report No.(s): DE2000-757141; BNL-52584; No Copyright; Avail: Department of Energy Information Bridge, Microfiche
Triennial update that describes the BNL Environmental Monitoring Program for all media (air, surface water, ground water, etc.) in accordance with DOE ORDER 5400.5
NTIS
*Environmental Monitoring; Ground Water; Air Quality*

**20010119191** Atomic Energy Commission, Idaho Falls, ID USA
**Stress and Permeability Heterogeneity within the Dixie Valley Geothermal Reservoir: Recent Results from Well 82-5**
Hickman, S. H.; Zoback, M. D.; Barton, C. A.; Benoit, R.; Svitek, J.; Dec. 01, 1999; 14p; In English
Report No.(s): DE2000-754683; DOE/ID/13762; No Copyright; Avail: Department of Energy Information Bridge
We collected borehole televiewer, temperature and flowmeter logs and conducted a hydraulic fracturing test in a well (82-5) that penetrated the SFZ within the known boundaries of the geothermal field but which failed to encounter significant permeability. Although stuck drill pipe prevented direct access to the SFZ, borehole breakouts and cooling cracks indicated a (approximately) 90 degree rotation in the azimuth of the least horizontal principal stress (Shmin) in well 82-5 at about 2.7 km depth. This rotation, together with the low (Shmin) magnitude measured at 2.5 km depth in well 82-5, is most readily explained through the occurrences of one or more normal faulting earthquakes in the hanging wall of the SFZ in the northern part of the reservoir. The orientation of (Shmin) below 2.7 km (i.e., (approximately) 20 to 50 m above the top of the SFZ) is such that both the overall SFZ and natural fractures directly above the SFZ are optimally oriented for normal faulting failure. If these fracture and stress orient ations persist into the SFZ itself, then the existence of a local stress relief zone (i.e., anormalously high (Shmin) magnitude) is the most likely explanation for the very low fault zone permeability encountered in well 82-5.
NTIS
*Boreholes; Heterogeneity; Permeability; Reservoirs; Geothermal Resources; Stress Distribution*

**20010119195** National Renewable Energy Lab., Golden, CO USA
**Building integrated PV for commercial and institutional structures, a sourcebook for architects**
Eiffert, P.; Kiss, G.; Feb. 14, 2000; 92p; In English
Report No.(s): DE2000-753782; NREL/BK-520-25272; No Copyright; Avail: Department of Energy Information Bridge
This sourcebook on building-integrated photovoltaics (BIPV) is intended for architects and designers interested in learning more about today's sustainable solar buildings. The booklet includes 16 design briefs describing actual structures; they illustrate how electricity-generating BIPV products (such as special roofing systems, vertical-wall systems, skylights, and awnings, all of

which contain PV cells, modules, and films) can be integrated successfully into many different kinds of buildings. It also contains basic information about BIPV technologies, an overview of US product development activities and development programs, descriptions of major software design tools, and a bibliography.
NTIS
*Buildings; Photovoltaic Conversion; Software Engineering; Space Heating (Buildings)*

**20010119216** Brookhaven National Lab., Upton, NY USA
**Potential Impact on National Energy Use and Carbon Emissions of an Energy Management Course**
Krajewski, R. F.; Sep. 01, 1999; 44p; In English
Report No.(s): DE2000-751110; BNL-66885; No Copyright; Avail: Department of Energy Information Bridge
This report reviews a draft training program planned for the International Union of Operating Engineers and uses it as a general model in terms of its possible goals. Using information contained within the energy evaluation and reporting structure of the US government and the buildings industry, an approach is formed for evaluating of this training program as it is applied to commercial buildings. This approach uses the estimated impact such a training program would have on energy use and carbon emissions if it were to be applied on a broad or national basis. Additional information regarding approaches commercial sector site energy evaluations is provided.
NTIS
*Commercial Energy; Energy Policy; Emission; Management Systems*

**20010119546** National Renewable Energy Lab., Golden, CO USA
**Thermophotovoltaic Cell Temperature Measurement Issues**
Emery, K.; Moriarty, T.; Nov. 13, 1998; 13p; In English
Report No.(s): DE2001-10431; NREL/CP-520-25619; No Copyright; Avail: Department of Energy Information Bridge
The power produced by photovoltaic devices changes with temperature, ranging from 0.1% to nearly 1% per degree Celsius depending on the structure. The temperature across the surface of TPV cells will vary depending on the amount of absorbed power. Thus the temperature over a region of a wafer where there is no cell will be different from a region of the wafer containing a cell with an antireflection coating and back surface reflector. Vacuum hold-downs or back surface probes may result in local hot spots. Bonding a cell to a heat sink may not be practical in a research environment, and a temperature gradient between the heat sink and space-charge region will still exist. Procedures for determining the current versus voltage (I-V) characteristics at a given temperature are discussed. For continuous illumination measurement systems, the temperature of the heat sink or backside of the device can be directly measured. The temperature can also be inferred by placing the sample at a known temperature in the dark, and monitoring the open-circuit voltage (Voc) as a high-speed shutter is opened. The maximum Voc from this method corresponds to the temperature in the dark and the plate temperature can then be lowered until this maximum Voc is reached. The temperature can also be indirectly determined from the dark I-V characteristics, assuming negligible series resistance in the ideal case that the voltage in the dark at a given current and temperature corresponds to the Voc and short circuit voltage (Isc) at that temperature. A high-intensity flash simulator will produce negligible cell heating during the flash and therefore the cell temperature may be easily set before the flash.
NTIS
*Open Circuit Voltage; Photovoltaic Cells; Temperature Gradients; Temperature Measurement*

**20010119603** Air Command and Staff Coll., Maxwell AFB, AL USA
**Solar Power Constellations Implications for the USA Air Force**
Ramos, Kim; Apr. 2000; 39p; In English
Report No.(s): AD-A394928; AU/ACSC/146/2000-04; No Copyright; Avail: CASI; A03, Hardcopy; A01, Microfiche
As the world population increases and natural resources used to produce energy decrease, alternative methods to produce sustainable, environmental cost effective energy are required. One proposed solution to the problem is solar power satellites. Solar power satellites are satellites, which collect the energy of the sun, convert it onto a beam, and beam that energy to a receiving antenna. The receiving antenna converts the beam into electricity and feeds the electricity into a power grid. The receiving antenna may be located on another satellite, or on Earth. Presented here are several solar power satellite proposals, architectures, incremental technology demonstrations and predictions as to when they will become commercially viable. Given the previous information, this paper analyzes the implications for the Air Force in relation to doctrine and future plans. The research method consisted of a search of scientific journals, published symposium papers, and research reports. The search focused on the current research on solar power satellites, and Air Force programs, which have power issues. Based on the research, the Air Force should plan to capitalize on the advantages of solar power satellite constellations. Solar power satellites can assist with implementing

various plans (i.e., long endurance unmanned aerial vehicles, space-based radar, lasers, and small satellites), complying with public law, and reducing the logistics tail associated with an expeditionary force.
DTIC
*Solar Energy; Satellite Antennas; Solar Power Satellites; Satellite Constellations*

**20010119997** National Renewable Energy Lab., Golden, CO USA
**New Concepts for High-Intensity PV Modules for Use with Dish Concentrator Systems**
Coutts, T. J.; Duda, A.; Kurtz, S. R.; Ward, J. S.; Oct. 06, 1998; 10p; In English
Report No.(s): DE2001-10361; NREL/CP-520-25552; No Copyright; Avail: Department of Energy Information Bridge, Microfiche

In this paper we report on our efforts to fabricate monolithically interconnected modules (MIMS) from GaAs device structures. The small size of the component cells comprising the MIM allows for operation at very high flux densities. This relaxes the requirement for a small spot-size to be generated by the optics. The devices are grown on semi-insulating substrates, allowing the incorporation of an extremely efficient back surface reflector (BSR). This BSR is an effective tool for thermal management of the array. The possibility of using this device configuration in conjunction with the large dish concentrators developed by the solar thermal community is examined. The advantages of using multijunction devices for this application is also discussed.
NTIS
*Concentrators; Solar Cells; Temperature Control; Gallium Arsenides; Flux Density*

**20010119998** National Renewable Energy Lab., Golden, CO USA
**Validation of a Model for a Two-Bladed Flexible Rotor System: Progress to Date**
Kelley, N. D.; Osgood, R. M.; Wright, A. D.; Nov. 19, 1998; 17p; In English
Report No.(s): DE2001-10349; NREL/CP-500-25514; No Copyright; Avail: Department of Energy Information Bridge, Microfiche

At the National Renewable Energy Laboratory, we tested a very flexible wind turbine. This machine, the Cannon Wind Eagle turbine, exhibited an ability to significantly reduce the rotor flap-wise bending moments through a unique combination of a flexible rotor and hub design. In parallel to this testing effort, we developed analytical models of this machine using our simulation codes. The goal of this work was to validate the analytical models of this machine by comparing analytical predictions to measured results from the real machine. We first describe briefly the simulation codes used in this study. We then describe the wind turbine we analyzed. We then describe analytical model validation progress for this flexible rotor and show preliminary validation results. Finally, we make conclusions and state our plans for future studies.
NTIS
*Rotors; Wind Turbines; Prediction Analysis Techniques; Mathematical Models; Renewable Energy*

**20010120034** Argonne National Lab., IL USA
**Layered carbon lattices and their influence on the nature of lithium bonding in lithium intercalated carbon anodes**
Scanlon, L. G.; May 27, 1998; 21p; In English
Report No.(s): DE2001-10627; ANL/CHM/CP-95548; No Copyright; Avail: Department of Energy Information Bridge, Microfiche

Ab initio molecular orbital calculations have been used to investigate the nature of lithium bonding in stage 1 lithium intercalated carbon anodes. This has been approximated by using layered carbon lattices such as coronene, (C(sub 24)H(sub 12)),anthracene, and anthracene substituted with boron. With two coronene carbon lattices forming a sandwich structure and intercalated with either 2, 3, 4 or 6 six lithiums, it has been found that the predominant mode of bonding for the lithium is at the carbon edge sites as opposed to bonding at interior carbon hexagon sites. Formation of all structures is thermodynamically allowed except for the two lithium case in which there is repulsion between the lattices. The optimized structure with six lithiums gives a reasonable approximation for the stage 1 lithium intercalated carbon anode. In this case the lithium to carbon ratio is 1:8 versus 1:6 occurring in the stage 1 graphite. The coronene lattices are eclipsed with a separation of 4.03 (angstrom). However, there is a slight ruffling of the lattice. Separation between adjacent lithiums is either 3.32 (angstrom) or 2.98 (angstrom). Even though the separation between lithiums is very small, composition of the molecular orbitals suggests that there is no lithium cluster formation. The highest occupied molecular orbitals are composed of a combination of lithium and carbon orbitals. In contrast, in the C(sub 60) fullerene lattice with three and five lithiums intercalated, there are molecular orbitals composed only of lithiums, indicative of cluster formation. For anthracene and boron substituted anthracene, lithium bonding takes place within the carbon hexagon sites. The separation between lithiums in a sandwich type structure with two anthracenes in the eclipsed conformation is 5.36 (angstrom). The effect of boron in a carbon lattice has been evaluated by comparing the difference in behavior of a single

anthracene lattice reacting with a dilithium cluster as compared to a 1, 4, 5, 8-tetraboroanthracene lattice. The effect of boron substitution is to increases lattice flexibility by allowing the lattice to twist and lithium to bond at adjacent hexagon sites. The thermodynamic feasibility of the reaction between the dilithium cluster and the boron substituted anthracene lattice is enhanced.
NTIS
*Anodes; Lithium; Molecular Orbitals; Organic Compounds*

**20010120041** Army Research Lab., Human Research and Engineering Directorate, Aberdeen Proving Ground, MD USA
**Storage Reliability of Reserve Batteries**
Swank, Jeff; Goldberg, Allan; Apr. 17, 2001; 18p; In English; Original contains color images; Proceedings from The 45th Annual Fuze Conference, 16-18 April 2001 Sponsored by NDIA, The original document contains color images
Report No.(s): AD-A394523; No Copyright; Avail: CASI; A03, Hardcopy; A01, Microfiche

This report concerns the storage reliability of reserve batteries. Items developed for munitions have a 20 yr. shelf life requirement over a wide temperature range. Developers need to prove storage reliability. Actual documentation is preferred. Science can be difficult, time-consuming and costly.
DTIC
*Storage Batteries; Storage Stability; Electric Batteries*

**20010120108** Corps of Engineers, Engineer Reseach and Development Center, Champaign, IL USA
**Site Evaluation for Application of Fuel Cell Technology: U.S. Coast Guard Air Station Cape Cod, MA** ***Final Report***
Binder, Michael J.; Holcomb, Franklin H.; Taylor, William R.; Torrey, J. M.; Westerman, John F.; Jul. 01, 2001; 46p; In English
Report No.(s): AD-A395097; ERDC/CERL-TR-01-56; No Copyright; Avail: CASI; A03, Hardcopy; A01, Microfiche

Fuel cells are an environmentally clean, quiet, and a highly efficient method for generating electricity and heat from natural gas and other fuels. Researchers at the U.S. Army Engineer Research and Development Center (ERDC), Construction Engineering Research Laboratory (CERL) have actively participated in the development and application of advanced fuel cell technology since fiscal year 1993 (FY93). CERL selected and evaluated application sites, supervised the design and installation of fuel cells, actively monitored the operation and maintenance of fuel cells, and compiled 'lessons learned' for feedback to manufacturers of commercially available fuel cell power plants and their thermal interfaces installed at Department of Defense (DoD) locations. This report presents an overview of the information collected at the U.S. Coast Guard Academy, New London, CT, along with a conceptual fuel cell installation layout and description of potential benefits the technology can provide at that location.
DTIC
*Defense Program; Fuel Cell Power Plants; Natural Gas*

**20010120113** Corps of Engineers, Engineer Research and Development Center, Champaign, IL USA
**Site Evaluation for Application of Fuel Cell Technology, Edwards Air Force Base, CA** ***Final Report***
Binder, Michael J.; Holcomb, Franklin H.; Taylor, WIlliam R.; Aug. 01, 2001; 29p; In English
Contract(s)/Grant(s): DACA-80-94-D-0020
Report No.(s): AD-A395031; ERDC/CERL-TR-01-60; No Copyright; Avail: CASI; A03, Hardcopy; A01, Microfiche

Fuel cells are an environmentally clean, quiet, and a highly efficient method for generating electricity and heat from natural gas and other fuels. Researchers at the U.S. Army Engineer Research and Development Center (ERDC), Construction Engineering Research Laboratory (CERL) have actively participated in the development and application of advanced fuel cell technology since fiscal year 1993 (FY93), and have selected and evaluated application sites, supervised the design and installation of fuel cells, actively monitored the operation and maintenance of fuel cells, and compiled 'lessons learned' for feedback to manufacturers for 29 of 30 commercially available fuel cell power plants and their thermal interfaces installed at Department of Defense (DoD) locations. This report presents an overview of the information collected at Edwards Air Force Base, CA, along with a conceptual fuel cell installation layout and description of potential benefits the technology can provide at that location. Similar summaries of the site evaluation surveys for the remaining sites where CERL has managed and continues to monitor fuel cell installation and operation are available in the companion volumes to this report.
DTIC
*Defense Program; Fuel Cells; Energy Technology*

**20010120114** Corps of Engineers, Engineer Research and Development Center, Champaign, IL USA

**Site Evaluation for Application of Fuel Cell Technology, U.S. Coast Guard Academy, New London, CT**

Holcomb, Franklin H.; Binder, Michael J.; Taylor, WIlliam R.; Torrey, J. M.; Westerman, John F.; Jul. 01, 2001; 55p; In English

Report No.(s): AD-A395029; ERDC/CERL-TR-01-55; No Copyright; Avail: CASI; A04, Hardcopy; A01, Microfiche

Fuel cells are an environmentally clean, quiet, and a highly efficient method for generating electricity and heat from natural gas and other fuels. Researchers at the U.S. Army Engineer Research and Development Center (ERDC), Construction Engineering Research Laboratory (CERL) have actively participated in the development and application of advanced fuel cell technology since fiscal year 1993 (FY93). CERL selected and evaluated application sites, supervised the design and installation of fuel cells, actively monitored the operation and maintenance of fuel cells, and compiled lessons learned" for feedback to manufacturers of commercially available fuel cell power plants and their thermal interfaces installed at Department of Defense (DoD) locations. This report presents an overview of the information collected at the U.S. Coast Guard Academy, New London, CT, along with a conceptual fuel cell installation layout and description of potential benefits the technology can provide at that location.

DTIC

*Defense Program; Energy Technology; Fuel Cells*

**20010120117** Georgia Inst. of Tech., School of Mechanical Engineering, Atlanta, GA USA

**Investigating the Integration of a Solid Oxide Fuel Cell and a Gas Turbine System with Coal Gasification Technologies**

Plummer, Dawson A.; Sep. 2001; 62p; In English

Report No.(s): AD-A395009; No Copyright; Avail: CASI; A04, Hardcopy; A01, Microfiche

Solid oxide fuel cell (SOFC) technology incorporates electrochemical reactions that generate electricity and high quality heat. The coupling of this technology with gas turbine bottoming cycles, to form hybrid power systems, leads to high efficiency levels. The purpose of this study is to conceptually integrate the hybrid power system with existing and imminent coal gasification technologies. The gasification technologies include the Kellogg Brown Root (KBR) Transport Reactor and entrained coal gasification. Parametric studies will be performed wherein pertinent fuel cell stack process settings such as operation voltage, inverse equivalence ratio and fuel utilization will be varied. Power output, system efficiency and costs will be the dependent variables of interest. Coal gasification data and a proven SOFC model will be used to test the theoretical integration. Feasibility and economic comparisons between the new integrated system and existing conventional systems will also be made.

DTIC

*Gas Turbines; Coal Gasification; Solid Oxide Fuel Cells*

**20010120551** Argonne National Lab., IL USA

**Design, integration, and trade-off analyses of gasoline-fueled polymer electrolyte fuel cell systems for transportation**

Kumar, R., Argonne National Lab., USA; Sep. 14, 1998; 7p; In English

Report No.(s): DE2001-10726; ANL/CMT/CP-96053; No Copyright; Avail: Department of Energy Information Bridge, Microfiche

Prototype fuel-cell-powered vehicles have recently been demonstrated in Japan, Europe, and North America. Conceptual designs and simulations of fuel-cell-powered vehicles have also been published. Many of these simulations include detailed vehicle performance models, but they use relatively simplistic fuel-cell power system models. We have developed a comprehensive model of a polymer electrolyte fuel cell (PEFC) power system for automotive propulsion. This system simulation has been used to design and analyze fuel-cell systems and vehicles with gasoline (or other hydrocarbons) as the on-board fuel. The major objective of this analysis is to examine the influence of design parameters on system efficiency and performance, and component sizes.

NTIS

*Electrolytic Cells; Fuel Cells; Systems Simulation; Propulsion System Performance; Propulsive Efficiency*

**20010120552** Argonne National Lab., IL USA

**MCFC component development at ANL**

Bloom, I., Argonne National Lab., USA; Sep. 15, 1998; 7p; In English

Report No.(s): DE2001-10727; ANL/CMT/CP-96055; No Copyright; Avail: Department of Energy Information Bridge, Microfiche

Argonne National Laboratory is developing advanced cathode and electrolyte components for the molten carbonate fuel cell (MCFC). Working in support of the MCFC developers, the goal of this effort is to extend the life of the MCFC cell and to improve its performance.
NTIS
*Molten Carbonate Fuel Cells; Electrolytes; Cathodes*

**20010120553** Argonne National Lab., IL USA
**Removal of CO from reformate for PEFC application**
Lee, S. H. D.; Sep. 14, 1998; 7p; In English
Report No.(s): DE2001-10728; ANL/CMT/CP-96056; No Copyright; Avail: Department of Energy Information Bridge, Microfiche

Polymer electrolyte fuel cells (PEFCs) are being actively developed worldwide for transportation applications. The fuel gas generated from reforming hydrocarbon fuels contains small amounts of CO (0.5-1 vol%), even after the water-gas shift reaction. Carbon monoxide is preferentially adsorbed on the platinum electrocatalyst in the PEFC, thus blocking the access of H(sub 2) to the surface of the catalyst and resulting in the degradation of the cell performance. Therefore, the CO concentration in the PBFC reformate must be reduced to a tolerable level of (le) 100 ppm (1). Catalytic preferential oxidation (2), anode air bleed (3), or a combination of the two can be used to reduce CO to trace levels, but their use in a dynamically varying system is problematic. We are developing a sorption process based on the reversible complex-forming and dissociation reactions of CO with Cu(I). These reactions are well documented in patent and literature.
NTIS
*Electrolytic Cells; Fuel Cells; Hydrocarbons; Carbon Monoxide; Hydrocarbon Fuels*

**20010121507** Sandia National Labs., Albuquerque, NM USA
**Energy Storage Concepts for a Restructured Electric Utility Industry**
Iannucci, J.; Schoenung, S.; Jul. 01, 2000; 57p; In English
Report No.(s): DE2000-759466; SAND2000-1550; No Copyright; Avail: Department of Energy Information Bridge, Microfiche

The electric utility industry in the USA is being restructured and is now evolving from a regulated monopoly to a partially competitive, partially regulated group of electricity providers. This report outlines a wide range of innovative ways in which energy storage could be advantageously used in all aspects of this electric supply system of the future, including customer-sited storage. Nine scenarios that consider the use of storage in the restructured utility industry are described. From these scenarios, four themes for guiding the economic and technical application of energy storage are presented.
NTIS
*Utilities; Electric Energy Storage; Electricity; Economic Impact*

**20010121513** Colorado State Univ., Fort Collins, CO USA
**High throughput manufacturing of high efficiency solar cells**
Dec. 31, 1999; 6p; In English
Report No.(s): DE2000-759440; DOE/GO/10305-Q; No Copyright; Avail: Department of Energy Information Bridge, Microfiche

This is our sixth quarterly report for the ERIP project 709, High Throughput Manufacturing of High Efficiency Solar Cells. Monthly reports are submitted via electronic mail to our invention coordinator, Rolf Butters. The project officially started on May 30, 1998, with a one year extension granted in March 1999. During the past three months we have been progressing on the following activities listed below. We have been following the tasks outlined in our Statement of Work (SOW), section D-3 tasks 1-6. The schedule given in our Statement of Work is for a project duration of one year with the machine building (tasks 1-4) expected to be completed in the first nine months and the testing and optimization of the system (tasks 5-6) to be completed in the last three months. The technical progress on the design and assembly phase is completed. However, tasks 4-6 are being completed in this, the second year of the project.
NTIS
*Manufacturing; Solar Cells; Systems Engineering; Performance Tests*

**20010121953** Sandia National Labs., Albuquerque, NM USA
**Dewarless Logging Too: 1st Generation**
Henfling,; Normann,; Aug. 01, 2000; 23p; In English
Report No.(s): DE2000-763144; SAND2000-1680; No Copyright; Avail: Department of Energy Information Bridge, Microfiche

This report focuses on Sandia National Laboratories' effort to create high-temperature logging tools for geothermal applications without the need for heat shielding. One of the mechanisms for failure in conventional downhole tools is temperature. They can only survive a limited number of hours in high temperature environments. For the first time since the evolution of integrated circuits, components are now commercially available that are qualified to 225 C with many continuing to work up to 300 C. These components are primarily based on Silicon-On-Insulator (SOI) technology. Sandia has developed and tested a simple data logger based on this technology that operates up to 300 C with a few limiting components operating to only 250 C without thermal protection. An actual well log to 240 C without shielding is discussed. The first prototype high-temperature tool measures pressure and temperature using a wire-line for power and communication. The tool is based around the HT83C51 microcontroller. A brief discussion of the background and status of the High Temperature Instrumentation program at Sandia, objectives, data logger development, and future project plans are given.
NTIS
*SOI (Semiconductors); Data Processing Equipment; High Temperature Environments; Thermal Protection*

**20010121960** California Univ., Lawrence Berkeley Lab., Berkeley, CA USA
**Redox shuttle additives for overcharge protection in lithium batteries**
Richardson, T. J.; Ross, P. N.; Nov. 11, 1999; 8p; In English
Report No.(s): DE2000-764356; LBNL-44503; No Copyright; Avail: Department of Energy Information Bridge, Microfiche
Seven new redox shuttle additives with shuttle current onset potentials above 4.2 V vs Li/Li+ are reported, along with diffusion coefficients for the neutral additives. The dependence of the limiting shuttle current on the respective diffusion coefficients of the oxidized and reduced forms of an additive is clarified. Overcharge protection in liquid electrolyte Li/LiMn2O4 cells is demonstrated.
NTIS
*Lithium Batteries; Battery Chargers; Oxidation-Reduction Reactions*

**20010121962** American Wind Energy Association, Washington, DC USA
**Windpower 2000. technical progress report, final**
Keelen, L.; Aug. 07, 2000; 23p; In English
Report No.(s): DE2000-761580; No Copyright; Avail: Department of Energy Information Bridge
No abstract prepared.
NTIS
*Windpower Utilization; Energy Technology; Reports*

**20010122218** National Renewable Energy Lab., Golden, CO USA
**Arizona Consumer's Guide to Buying a Solar Electric System**
Starrs, T.; Wenger, H.; Sep. 11, 2000; 20p; In English
Report No.(s): DE2000-764572; NREL/BR-520-28901; No Copyright; Avail: Department of Energy Information Bridge, Microfiche
Consumers in Arizona are showing increased interest in solar electric systems for their homes and businesses. This booklet provides basic information about buying a PV system. Photovoltaic (PV) systems are reliable, pollution free, and use a renewable source of energy-the sun. A PV system can be a substantial investment and careful planning will help ensure that you make the right decisions.
NTIS
*Arizona; Photovoltaic Conversion; Renewable Energy*

**20010122243** Argonne National Lab., IL USA
**Stabilization of insertion electrodes for lithium batteries**
Thackeray, M. M.; Sep. 03, 1998; 23p; In English
Report No.(s): DE2001-10951; ANL/CMT/CP-97217; No Copyright; Avail: Department of Energy Information Bridge, Microfiche
This paper discusses the techniques that are being employed to stabilize LiMn(sub 2)O(sub 4) spinel and composite Li(sub x)MnO(sub 2) positive electrodes. The critical role that spinel domains play in stabilizing these electrodes for operation at both 4 V and 3 V is highlighted. The concept of using an intermetallic electrode MM(prime) where M is an active alloying element and M(prime) is an inactive element (or elements) is proposed as an alternative negative electrode (to carbon) for lithium-ion cells. An analogy to metal oxide insertion electrodes, such as MnO(sub 2), in which Mn is the electrochemically active ion and O is

the inactive ion, is made. Performance data are given for the copper-tin electrode system, which includes the intermetallic phases eta-Cu(sub 6)Sn(sub 5) and Li(sub 2)CuSn.
NTIS
*Lithium Batteries; Intermetallics; Electrodes; Stabilization*

**20010122245** Argonne National Lab., IL USA
**Resistivity of bipolar plate materials at the cathode interface in molten carbonate fuel cells**
Kaun, T. D.; Nov. 18, 1998; 15p; In English
Report No.(s): DE2001-10838; ANL/CMT/CP-96628; No Copyright; Avail: Department of Energy Information Bridge
Measurements of oxide scale resistivity for prospective bipolar plate materials in the molten carbonate fuel cell (MCFC) are coupled with observations of microstructural/compositional change over time. This work searches for a compromise to the high corrosion rate of Type 316L and the high oxide scale resistance of Type 310S. We tested a group of materials having chromium content ranging from 16 to 31 wt%, including Nitronic 50 and NKK, a Ni-Cr-Fe alloy. Chromium content was found to be the primary determinant of oxide scale composition. In the MCFC cathode compartment, stainless steels generally formed a duplex structure with an inner Cr-rich layer and an outer, Fe-rich layer. The composition of the inner Cr-rich layer was related to the base alloy and had a controlling effect on scale resistivity. Oxide scale resistivity was measured for two electrolyte compositions: Li/K and Li/Na carbonates. Changes in the physical/mechanical properties (spallation/cracking) in the oxide scale of Type 316L provided an understanding of its resistivity fluctuations over time.
NTIS
*Molten Carbonate Fuel Cells; Oxidation Resistance*

**20010122277** Sandia National Labs., Albuquerque, NM USA
**Testing to Support Improvements to PV Components and Systems**
Thomas, H.; Kroposki, B.; Witt, C.; Bower, W. I.; Bonn, R. H.; Jul. 15, 2000; 6p; In English
Report No.(s): DE2000-761054; SAND2000-1689C; No Copyright; Avail: Department of Energy Information Bridge
The National Photovoltaic (PV) Program is sponsored by the US Department of Energy and includes a PV Manufacturing Research and Development (R and D) project conducted with industry. This project includes advancements in PV components to improve reliability, reduce costs, and develop integrated PV systems. Participants submit prototypes, pre-production hardware products, and examples of the resulting final products for a range of tests conducted at several national laboratories, independent testing laboratories, and recognized listing agencies. The purpose of this testing is to use the results to assist industry in determining a product's performance and reliability, and to identify areas for potential improvement. This paper briefly describes the PV Manufacturing R and D project, participants in the area of PV systems, balance of systems, and components, and several examples of the different types of product and performance testing used to support and confirm product performance.
NTIS
*Manufacturing; Performance Tests; Photovoltaic Cells*

**20010122308** Sandia National Labs., Albuquerque, NM USA
**Progress in Photovoltaic Components and Systems**
Thomas,; Kroposki,; Witt,; Bower,; Jul. 15, 2000; 6p; In English
Report No.(s): DE2000-761050; SAND2000-1686C; No Copyright; Avail: Department of Energy Information Bridge
The Photovoltaic Manufacturing Research and Development project is a government/industry partnership between the US Department of Energy and members of the US photovoltaic (TV) industry. The purpose of the project is to work with industry to improve manufacturing processes, reduce manufacturing costs, and improve the performance of PV products. This project is conducted through phased solicitations with industry participants selected through a competitive evaluation process. Starting in 1995, the two most recent solicitations include manufacturing improvements for balance-of-system (BOS) components, energy storage, and PV system design improvements. This paper surveys the work accomplished since that time, as well as BOS work currently in progress in the PV Manufacturing research and development project to identify areas of continued interest and product trends. Industry participants continue to work to improve inverters and to expand the features and capabilities of this key component. The industry also continues to advance fully integrated systems that meet standards for performance and safety. All participants included manufacturing improvements to reduce costs and improve reliability. Accomplishments of the project's participants are summarized to illustrate the product and manufacturing trends.
NTIS
*Photovoltaic Cells; Design Analysis; Manufacturing*

**20010122372** Argonne National Lab., IL USA

**Assessment of carbon reduction technology opportunities in the petroleum refining industry**

Petrick, M., Argonne National Lab., USA; Sep. 14, 1998; 9p; In English

Report No.(s): DE2001-10741; ANL/ES/CP-96168; No Copyright; Avail: Department of Energy Information Bridge, Microfiche

The refining industry is a major source of CO(sub 2) emissions in the industrial sector and therefore in the future can expect to face increasing pressures to reduce emission levels. The energy used in refining is impacted by market dictates, crude quality, and environmental regulations. While the industry is technologically advanced and relatively efficient opportunities nevertheless exist to reduce energy USAge and CO(sub 2) emissions. The opportunities will vary from refinery to refinery and will necessarily have to be economically viable and compatible with each refiner's strategic plans. Recognizing the many factors involved, a target of 15-20% reduction in CO(sub 2) emissions from the refining sector does not appear to be unreasonable, assuming a favorable investment climate.

NTIS

*Exhaust Emission; Exhaust Gases; Technology Assessment; Carbon Monoxide; Pollution Control*

**20010122641** Sandia National Labs., Albuquerque, NM USA

**Investigation of Factors Influencing the Accuracy of Pyrheliometer Calibrations**

Thacher, P. D.; Boyson, W. E.; King, D. L.; Sep. 21, 2000; 6p; In English

Report No.(s): DE2000-763139; SAND2000-2322C; No Copyright; Avail: Department of Energy Information Bridge, Microfiche

The accuracy of solar cells calibrated as primary reference cells is directly dependent on the accuracy of the pyrheliometer used to measure the direct beam solar irradiance on the cell. Pyrheliometers are also used in measuring performance of concentrating photovoltaic modules. In order to reduce errors in photovoltaic performance measurements, we have investigated the calibration uncertainties for pyrheliometers from two manufacturers. Our calibration comparisons are relative to an absolute cavity radiometer traceable to the World Radiometric Reference. This paper quantifies the effects of aging, temperature, time-rate-of-change of temperature, wind, solar spectral shifts, linearity, window transmission, and solar tracking on pyrheliometer calibrations. Uncertainty remaining after accounting for these factors is 0.8 percent at the 2-sigma level.

NTIS

*Pyroheliometers; Calibrating; Solar Cells; Energy Conversion Efficiency*

**20010122663** National Renewable Energy Lab., Golden, CO USA

**NREL PV Working with Industry, V. 27, Third Quarter 2000**

Poole, L.; Nahan, R.; Sep. 12, 2000; 12p; In English

Report No.(s): DE2000-764540; NREL/BR-520-28491; No Copyright; Avail: Department of Energy Information Bridge, Microfiche

NREL PV Working With Industry is a quarterly newsletter devoted to the research, development, and deployment performed by NREL staff in concert with their industry and university partners. The third quarter, contains articles on several important PV-related conferences held in the prior three months: the REAP/HBCU Conference and the IPS-2000 Photochemistry Conference. The issue also contains a preview article of the PV Specialists conference held in Alaska in September. The editorialist is John Benner, PV Specialist Conference Program Chairman.

NTIS

*Photovoltaic Conversion; Conferences*

**20010122670** Sandia National Labs., Albuquerque, NM USA

**PV Hybrid VRLA Battery Test Results from a Telecommunications Site**

Hund,; Stevens,; Sep. 25, 2000; 6p; In English

Report No.(s): DE2000-763337; SAND2000-2340C; No Copyright; Avail: Department of Energy Information Bridge, Microfiche

A new valve regulated lead-acid (VRLA) gel motive power battery and photovoltaic (PV) system power center have been tested in the laboratory and at a PV hybrid telecommunication site. The power center provides battery charge control, system remote communications, and data acquisition at the field test site. Extensive laboratory and field-test data were used to improve battery performance by optimizing, regulation voltages, finish-charge, and system design. After 1.5-years of service, battery and

charge controller performance have met all performance requirements for the remote communications site at Sandia National Laboratories.
NTIS
*Electric Batteries; Photovoltaic Conversion; Performance Tests*

**20010122886** Argonne National Lab., IL USA
**Update on cavern disposal of NORM-contaminated oil field wastes**
Veil, J. A.; Sep. 22, 1998; 16p; In English
Report No.(s): DE2001-10973; ANL/EA/CP-97318; No Copyright; Avail: Department of Energy Information Bridge, Microfiche

Some types of oil and gas production and processing wastes contain naturally occurring radioactive material (NORM). If NORM is present at concentrations above regulatory levels in oil field waste, the waste requires special disposal practices. The existing disposal options for wastes containing NORM are limited and costly. Argonne National Laboratory has previously evaluated the feasibility, legality, risk and economics of disposing of nonhazardous oil field wastes, other than NORM waste, in salt caverns. Cavern disposal of nonhazardous oil field waste, other than NORM waste, is occurring at four Texas facilities, in several Canadian facilities, and reportedly in Europe. This paper evaluates the legality, technical feasibility, economics, and human health risk of disposing of NORM-contaminated oil field wastes in salt caverns as well. Cavern disposal of NORM waste is technically feasible and poses a very low human health risk. From a legal perspective, a review of federal regulations and regulations from several states indicated that there are no outright prohibitions against NORM disposal in salt caverns or other Class II wells, except for Louisiana which prohibits disposal of radioactive wastes or other radioactive materials in salt domes. Currently, however, only Texas and New Mexico are working on disposal cavern regulations, and no states have issued permits to allow cavern disposal of NORM waste. On the basis of the costs currently charged for cavern disposal of nonhazardous oil field waste (NOW), NORM waste disposal in caverns is likely to be cost competitive with existing NORM waste disposal methods when regulatory agencies approve the practice.
NTIS
*Oil Fields; Radioactive Wastes; Waste Disposal*

**20010122895** Argonne National Lab., IL USA
**Supporting R and D of industrial fuel cell developers**
Krumpelt, M.; Sep. 11, 1998; 13p; In English
Report No.(s): DE2001-10959; ANL/CMT/CP-97261; No Copyright; Avail: Department of Energy Information Bridge, Microfiche

Argonne National Laboratory is supporting the industrial developers of molten carbonate fuel cells (MCFCs) and tubular solid oxide fuel cells (SOFCs). The results suggest that a lithium concentration level of 65-75 mols in the LiNa electrolyte will improve cell performance. They have made inroads in understanding the interfacial resistance of bipolar plate materials, and they have reduced the air electrode overpotential in OSFCs by adding dopants.
NTIS
*Lithium; Molten Carbonate Fuel Cells; Solid Oxide Fuel Cells*

**20010122898** Argonne National Lab., IL USA
**Impurity characterization of solar wind collectors for the genesis discovery mission by resonance ionization mass spectrometry**
Calaway, W. F.; Feb. 01, 1999; 9p; In English
Report No.(s): DE2001-10901; ANL/CHM/CP-96909; No Copyright; Avail: Department of Energy Information Bridge, Microfiche

NASA's Genesis Discovery Mission is designed to collect solar matter and return it to earth for analysis. The mission consists of launching a spacecraft that carries high purity collector materials, inserting the spacecraft into a halo orbit about the L1 sun-earth libration point, exposing the collectors to the solar wind for two years, and then returning the collectors to earth. The collectors will then be made available for analysis by various methods to determine the elemental and isotopic abundance of the solar wind. In preparation for this mission, potential collector materials are being characterized to determine baseline impurity levels and to assess detection limits for various analysis techniques. As part of the effort, potential solar wind collector materials have been analyzed using resonance ionization mass spectrometry (RIMS). RIMS is a particularly sensitivity variation of secondary neutral mass spectrometry that employs resonantly enhanced multiphoton ionization (REMPI) to selectively post-ionize an element of interest, and thus discriminates between low levels of that element and the bulk material. The high sensitivity and selectivity of

RIMS allow detection of very low concentrations while consuming only small amounts of sample. Thus, RIMS is well suited for detection of many heavy elements in the solar wind, since metals heavier than Fe are expected to range in concentrations from 1 ppm to 0.2 ppt. In addition, RIMS will be able to determine concentration profiles as a function of depth for these implanted solar wind elements effectively separating them from terrestrial contaminants. RIMS analyses to determine Ti concentrations in Si and Ge samples have been measured. Results indicate that the detection limit for RIMS analysis of Ti is below 100 ppt for 10(sup 6) averages. Background analyses of the mass spectra indicate that detection limits for heavier elements will be similar. Furthermore, detection limits near 1 ppt are possible with higher repetition rate lasers where it will be possible to increase signal averaging to 10(sup 8) laser shots.
NTIS
*Solar Wind; Accumulators; Genesis Mission; Materials Selection; Composition (Property); Impurities*

**20010122900** IT Corp., Las Vegas, NV USA
**Corrective Action Investigation Plan for Corrective Action Unit 490: Station 44 Burn Area, Tonopah Test Range, Nevada (with Record of Technical Change No. 1)**
Jun. 09, 2000; 111p; In English
Report No.(s): DE2000-766540; DOE/NV-613; No Copyright; Avail: Department of Energy Information Bridge

This Corrective Action Investigation Plan (CAIP) contains the US Department of Energy, Nevada Operations Office's approach to collect the data necessary to evaluate corrective action alternatives appropriate for the closure of Corrective Action Unit (CAU) 490 under the Federal Facility Agreement and Consent Order. Corrective Active Unit 490 consists of four Corrective Action Sites (CASs): 03-56-001-03BA, Fire Training Area (FTA); RG-56-001-RGBA, Station 44 Burn Area; 03-58-001-03FN, Sandia Service Yard; and 09-54-001-09L2, Gun Propellant Burn Area. These CASs are located at the Tonopah Test Range near Areas 3 and 9. Historically, the FTA was used for training exercises where tires and wood were ignited with diesel fuel. Records indicate that water and carbon dioxide were the only extinguishing agents used during these training exercises. The Station 44 Burn Area was used for fire training exercises and consisted of two wooden structures. The two burn areas (ignition of tires, wood, and wooden structures with diesel fuel and water) were limited to the building footprints (10 ft by 10 ft each). The Sandia Service Yard was used for storage (i.e., wood, tires, metal, electronic and office equipment, construction debris, and drums of oil/grease) from approximately 1979 to 1993. The Gun Propellant Burn Area was used from the 1960s to 1980s to burn excess artillery gun propellant, solid-fuel rocket motors, black powder, and deteriorated explosives; additionally, the area was used for the disposal of experimental explosive items. Based on site history, the focus of the field 21investigation activities will be to: (1) determine the presence of contaminants of potential concern (COPCs) at each CAS, (2) determine if any COPCs exceed field-screening levels and/or preliminary action levels, and (3) determine the nature and extent of contamination with enough certainty to support selection of corrective action alternatives for each CAS. The scope of this CAIP is to resolve the question of whether or not potentially hazardous wastes were generated at three of the four CASs within CAU 490, and whether or not potentially hazardous and radioactive wastes were generated at the fourth CAS in CAU 490 (CAS 09-54-001-09L2). Suspected CAS-specific COPCs include volatile organic compounds, semivolatile organic compounds, total petroleum hydrocarbons, polychlorinated biphenyls, pesticides, explosives, and uranium and plutonium isotopes. The results of this field investigation will support a defensible evaluation of corrective action alternatives in the corrective action decision document.
NTIS
*Alternatives; Hazardous Wastes; Volatile Organic Compounds; Fires*

**20010122902** National Renewable Energy Lab., Golden, CO USA
**Biomass Cofiring: A Renewable Alternative for Utilities**
Craig, K.; Aug. 30, 1999; 1p; In English
Report No.(s): DE2000-766454; NREL/FS-570-27049; DOE/GO-10099-915; No Copyright; Avail: Department of Energy Information Bridge

One biopower initiative is to develop small modular biopower systems. This one-page fact sheet gives some specifics about the initiative.
NTIS
*Biomass; Utilities*

**20010122903** National Renewable Energy Lab., Golden, CO USA
**Technologies Recently Available for Licensing - 1999**
Brown, H.; Touryan, K.; Sep. 07, 1999; 2p; In English
Report No.(s): DE2000-766451; NREL/FS-720-26915; No Copyright; Avail: Department of Energy Information Bridge

An NREL Technology Transfer fact sheet describing four technologies that are available for licensing: steel weld weakness detection, cadmium telluride solar cell enhancement, HOMER model for choosing optimal electrical systems for remote areas, and inner-flame matrix burner.
NTIS
*Cadmium Tellurides; Solar Cells; Technology Transfer*

**20010122915** General Electric Co., Hanford Atomic Products Operation, Richland, WA USA
**Facilities and Office Services Environmental Control Plan**
Galbreath, C. J.; Sep. 28, 2000; 17p; In English
Report No.(s): DE2000-765682; BHI-01423-REV-0; No Copyright; Avail: Department of Energy Information Bridge, Microfiche

This environmental control plan (ECP) is for the Bechtel Hanford, Inc. (BHI) Facilities and Office Services (F and OS) organization that serves all of the Environmental Restoration Contractor's (ERC) projects that support environmental restoration cleanup at the Hanford Site. F and OS supports the cleanup mission at the Hanford Site by providing the following services: Office space allocations; Office move coordination; Furniture allocations; Facility maintenance; Janitorial services; Pest control; Coordination of infrastructure and utility services; New facility development; 100-N Water Plant oversight.
NTIS
*Reservoirs; Environmental Control; Environmental Cleanup*

**20010123215** Argonne National Lab., IL USA
**Advanced cell technology for high performance Li-Al/FeS2 secondary batteries**
Henriksen, G. L.; Jul. 10, 1998; 17p; In English
Report No.(s): DE2001-10886; ANL/CMT/CP-96824; No Copyright; Avail: Department of Energy Information Bridge, Microfiche

In early 1993, Argonne National Laboratory (ANL) initiated a major R (research) and D (development) effort to develop bipolar Li-Al/LiCL-LiBr-KBr/FeS(sub 2) batteries for electric vehicles, targeting the USABC Long-Term Goals. Significant advancements were achieved in the areas of (i) chemical purity, (ii) electrode and electrolyte additives, and (iii) peripheral seals. It was determined that key chemical constituents contained undesirable impurities. ANL developed new chemical processes for preparing Li(sub 2)S, FeS, and CoS(sub 2) that were 98.5% pure. We evaluated a large variety of electrode and electrolyte additives for reducing cell area specific impedance (ASI). Candidate positive electrode additives offered increased electronic conductivity, enhanced reaction kinetics, and/or improved porous electrode morphology. CoS(sub 2), CuFeS(sub 2), MgO, and graphite (fibers) were identified as the most beneficial impedance-reducing positive electrode additives. Although electronically conductive carbon and graphite additives produced measurable ASI reductions in the negative electrode, they degraded its structural integrity and were deemed impractical. LiI and LiF were identified as beneficial electrolyte additives, that enhance positive electrode kinetics. ANL refined its baseline metal/ceramic peripheral seal and increased its strength by a factor of three (achieving a safety factor 10). In parallel, ANL developed a high-strength advanced metal/ceramic seal that offers appreciable cost reductions.
NTIS
*Carbon; Electric Batteries; Electrodes; Electric Motor Vehicles*

**20010123396** Argonne National Lab., IL USA
**Development of a High-Power Lithium-Ion Battery**
Jansen, A. N.; Sep. 02, 1998; 16p; In English
Report No.(s): DE2001-10947; ANL/CMT/CP-97206; No Copyright; Avail: Department of Energy Information Bridge

Safety is a key concern for a high-power energy storage system such as will be required in a hybrid vehicle. Present lithium-ion technology, which uses a carbon/graphite negative electrode, lacks inherent safety for two main reasons: (1) carbon/graphite intercalates lithium at near lithium potential, and (2) there is no end-of-charge indicator in the voltage profile that can signal the onset of catastrophic oxygen evolution from the cathode (LiCoO2). Our approach to solving these safety/life problems is to replace the graphite/carbon negative electrode with an electrode that exhibits stronger two-phase behavior further away from lithium potential, such as Li4Ti5O12. Cycle-life and pulse-power capability data are presented in accordance with the Partnership for a New Generation of Vehicles (PNGV) test procedures, as well as a full-scale design based on a spreadsheet model.
NTIS
*Lithium Batteries; Electrodes; Lithium; Metal Ions*

**20010123397** Argonne National Lab., IL USA

**Copper-Tin Anodes for Rechargeable Lithium Batteries: An Example of the Matrix Effect in an Intermetallic System**

Kepler, K. D.; Sep. 02, 1998; 18p; In English

Report No.(s): DE2001-10945; ANL/CMT/CP-97204; No Copyright; Avail: Department of Energy Information Bridge

Lithium batteries are typically constructed from a lithium cobalt oxide cathode and a carbon anode. We have investigated intermetallic anode materials based on tin, which can provide a high capacity at a slightly higher voltage (400 mV) than metallic lithium and thus reduce the safety concerns associated with the carbon anode. In particular, we have investigated the copper-tin system at around the composition Cu6Sn5 and have determined the effect on cycling and capacity of electrodes with various ratios of copper to tin. Anode compositions that are slightly copper rich (Cu6Sn4) were found to exhibit greater utilization of the tin than those with the stoichiometric bronze ratio (Cu6Sn5) or those having a slight excess of tin (Cu6Sn5). The differences in electrochemical behavior are explained in terms of an inert matrix model.

NTIS

*Anodes; Copper; Intermetallics; Tin; Lithium Batteries*

**20010123409** International Solar Electric Technology, Inglewood, CA USA

**Large area low cost processing for CIS photovoltaics. Final technical report**

Basol, B.; Norsworthy, G.; Leidholm, C.; Halani, A.; Roe, R.; Jul. 22, 1999; 22p; In English

Report No.(s): DE2001-765116; No Copyright; Avail: Department of Energy Information Bridge

An ink coating method was developed for CIS (copper indium diselenide) absorber deposition. The technique involves four processing steps: (1) preparation of a Cu-In alloy powder, (2) preparation of an ink using this powder, (3) deposition of the ink on a substrate in the form of a precursor layer, and (4) selenization to convert the Cu-In precursor into a fused CIS film. Absorbers grown by this low-cost, large-area method were used in the fabrication of 10.5% efficient solar cells.

NTIS

*Thin Films; Solar Cells; Copper Indium Selenides; Inks; Deposition*

**20010123415** Wisconsin Univ., Madison, WI USA

**Research on solar processes. Project final report**

Oct. 01, 1999; 10p; In English

Report No.(s): DE2001-764764; DOE/GO/10152-F; No Copyright; Avail: Department of Energy Information Bridge

The University of Wisconsin (UW) Solar Energy Laboratory (SEL) has been supported by the US Department of Energy through the Golden Field office. The contract was moved to National Renewable Energy Laboratory (NREL) for the period of May 26, 1999 through May 25, 2000. The majority of the projects were to be completed after the end of the DoE (Department of Energy) contract period (December 1999) since continued DoE funding was anticipated. Although the DoE funding has continued, it is now monitored through NREL. This report summarizes work to date. Two MS (Master of Science) theses will be submitted to NREL in December 1999 as part of the current contract. Copies will also be sent to DoE. The SEL has addressed a number of issues with the developments to TRNSYS (Transient System Simulation) in anticipation of release of version 15. The two major developments have been a complete overhaul of the IISiBat graphical user interface and the addition. The Center for the Scientific Study of Buildings (CSTB) in Sophia Antipolis, France has completely rewritten IISiBat as a native Windows program, replacing the current version written in LISP. LISP, while it allows programs to run on both Windows and UNIX platforms cannot make use of many of the standard Windows programming tools. Consequently the current IISiBat version (2.0) feels rather clumsy to use. Other additions to IISiBat include the ability to create multi-layered system diagrams, and the ability to automatically generate HTML (hypertext markup language) based documentation for new Types that the user has developed and wishes to add to the standard TRNSYS library.

NTIS

*Solar Energy; Simulation; Renewable Energy*

**20010123416** Ascension Technology, Inc., Lincoln Center, MA USA

**Ballast-mounted PV arrays: Phase 2 final report**

Kern, E. C.; Mar. 01, 2000; 30p; In English

Report No.(s): DE2001-764761; DOE/GO/10257-F; No Copyright; Avail: Department of Energy Information Bridge

The expansive flat rooftops of industrial and commercial buildings across America offer the largest, most secure, and potentially least-cost real estate opportunity to install massive amounts of solar photovoltaic (PV) generation in the building sector. Unfortunately, mechanical penetration of roofing membranes is very expensive and perceived by building owners and operators to increase the likelihood of leaking. In response Ascension Technology has pioneered the development of low-cost

ballasted approaches for mounting PV arrays. Recently, however, we have experienced our first two instances in which strong winds have moved our arrays on rooftops and heightened our interest, and the PV industries need to develop zero-penetration mounting techniques that are more secure, yet remain low in cost. In this PV BONUS project, Ascension Technology and its partners addressed wind loading on solar panels and the suitability of using frictional forces between ballast trays and roofing materials to resist PV arrays sliding on rooftops. The primary goal of the project is to capture the potential cost savings made possible by ballast-mounting by showing under what conditions it can satisfy wind loading concerns. A secondary goal is to address a more geographically constrained concern regarding withstanding seismic forces.
NTIS
*Photovoltaic Cells; Roofs; Industrial Areas; Anchors (Fasteners); Ballast (Mass)*

**20010123420** Pennsylvania Univ., Philadelphia, PA USA
**Structure and Dynamics in Low-Dimensional Guest-Host Systems**
Fischer, J. E.; May 01, 2000; 12p; In English
Report No.(s): DE2001-764604; No Copyright; Avail: Department of Energy Information Bridge
This is the final report of the fourth of four three year grants of the same title. The program evolved from an earlier Department of Energy grant on graphite intercalation compounds. Since its inception eight years ago, the focus evolved continuously from conjugated polymers to fullerenes, disordered carbons for Li-ion battery applications, and most recently carbon nanotubes, with side excursion back to GIC's to exploit a recent advance in synthesis of a potentially exciting new phase. The unifying themes are the versatility of carbon in forming novel solids, and the flexibility of intercalation chemistry to provide new materials with potentially useful properties.
NTIS
*Electric Batteries; Flexibility; Graphite; Intercalation*

**20010123445** Synertech Systems Corp., Syracuse, NY USA
**Fundamental study of black liquor gasification kinetics using a pressurized entrained-flow reactor (PEFR)** ***Quarterly Report, July - September 1999***
Oct. 29, 1999; 4p; In English
Report No.(s): DE2001-761036; No Copyright; Avail: Department of Energy Information Bridge, Microfiche
The goal of the program is to identify the optimal operating window for black liquor gasification. The goals during this year are to prepare the PEFR for operation, conduct a series of preliminary screening tests to bracket BLG operating conditions, and develop a process model that can guide identification of the optimal operating window.
NTIS
*Gasification; Kinetics*

**20010123463** Argonne National Lab., IL USA
**LiMn(sub 2-x)Cu(sub x)O(sub 4) spinels (0.1 (le) x (le) 0.5): A new class of 5 V cathode materials for Li batteries. I. electrochemical, structural and spectroscopic studies**
Ein-Eli, Y.; Oct. 05, 1998; 40p; In English
Report No.(s): DE2001-10990; ANL/CMT/CP-97391; No Copyright; Avail: Department of Energy Information Bridge, Microfiche
A series of electroactive spinel compounds, LiMn(sub 2 - x)Cu(sub x)O4 (0.1 (le) x (le) 0.5) has been studied by crystallographic, spectroscopic and electrochemical methods and by electron-microscopy. These LiMn(sub 2 - x)Cu(sub x)O4 spinels are nearly identical in structure to cubic LiMn2O4 and successfully undergo reversible Li intercalation. The electrochemical data show a remarkable reversible electrochemical process at 4.9 V which is attributed to the oxidation of Cu(sup 2+) to Cu(sub 3+). The inclusion of Cu in the spinel structure enhances the electrochemical stability of these materials upon cycling. The initial capacity of LiMn(sub 2 - x)Cu(sub x)O4 spinels decreases with increasing x from 130mAh/g in LiMn2O4 (x=0) to 70 mAh/g in;LiMn(sub 1.5)Cu(sub 0.5)O(sub 4); (x=0.5). The data also show slight shifts to higher voltage for the delithiation reaction that normally occurs at 4.1 V in standard Li(sub 1 - x)Mn2O4 electrodes (1 (ge) x (ge) 0) corresponding to the oxidation of Mn(sup 3+) to Mn(sup 4+). Although the powder X-ray diffraction pattern of; LiMn(sub 1.5)Cu(sub 0.5)O(sub 4); shows a single-phase spinel product, neutron diffraction data show a small, but significant quantity of an impurity phase, the composition and structure of which could not be identified. X-ray absorption spectroscopy was used to gather information about the oxidation states of the manganese and copper ions. The composition of the spinel component in the LiMn(sub 1.5)Cu(sub 0.5)O(sub 4) was determined from X-ray diffraction and XANES data to be Li(sub 1.01)Mn(sub 1.67)Cu(sub 0.32)O(sub 4) suggesting, to a best approximation, that the impurity in the sample was a lithium-copper-oxide phase. The substitution of

manganese by copper enhances the reactivity of the spinel structure towards hydrogen; the compounds are more easily reduced at moderate temperature ((approximately) 200 C) than LiMn2O4.
NTIS
*Spinel; Composition (Property); Cathodic Coatings*

**20010123618** Institute of Paper Science and Technology, Atlanta, GA USA
**Study of soluble scale fouling control in high solids black liquor concentrators. Progress report, quarter 5 (October 1, 1999-December 31, 1999)** ***Quarterly Report, 1 Oct. - 31 Dec. 1999***
Frederick, W. J.; Chen, F.; Hsieh, G.; Lien, S.; Murphy, R. W.; Jan. 01, 2000; 7p; In English
Report No.(s): DE2001-760516; DOE/GO/10387-Q; No Copyright; Avail: Department of Energy Information Bridge, Microfiche

During this quarter, work has finally resumed on the black liquor solubility experiments, but no new data have been generated. The crystallization experiments with inorganic model solutions have been completed, and crystallization experiments with kraft black liquor have been started. The Annular Test Cell apparatus is now fully operational, while construction of the falling film evaporator pilot plant is nearly complete. Startup of this unit is planned for late in Quarter 6. In the CFD model development work, the relaxation of simplifying assumptions in the falling film model have been completed, and expressions were developed to estimate film velocity/film Reynolds number relations. Also, thin film data taken for a range of conventional fluids were compared to predictions using selected methods, and attempts were initiated to extrapolate to approximate black liquor evaporator conditions.
NTIS
*Fouling; Pilot Plants*

**20010123621** Department of Energy, Nevada Operations Office, Las Vegas, NV USA
**Project Execution Plan, Waste Management Division, Nevada Operations Office, U.S. Department of Energy, April 2000**
Apr. 01, 2000; 44p; In English
Report No.(s): DE2001-756489; DOE/NV-612; No Copyright; Avail: Department of Energy Information Bridge, Microfiche

This plan addresses project activities encompassed by the U.S. Department of Energy/Nevada Operations Office Waste Management Division and conforms to the requirements contained in the 'Life Cycle Asset Management' U.S. Department of Energy Order O430.1A; the Joint Program Office Policy on Project Management in Support of DOE Order O430.1, and the Project Execution and Engineering Management Planning Guide. The plan also reflects the milestone philosophies of the Federal Facility Agreement and Consent Order, as agreed to by the state of Nevada; and traditional project management philosophies such as the development of life cycle costs, schedules, and work scope; identification of roles and responsibilities; and baseline management and controls.
NTIS
*Nevada; Waste Management*

**20010123629** National Renewable Energy Lab., Golden, CO USA
**Field Verification Program for Small Wind Turbines, No. 1, October 2000** ***Quarterly Report, 2nd Quarter***
Tu, P.; Forsyth, T.; Nov. 02, 2000; 7p; In English
Report No.(s): DE2000-767310; NREL/TP-500-28946; No Copyright; Avail: Department of Energy Information Bridge, Microfiche

The Field Verification Program for Small Wind Turbines quarterly report provides industry members with a description of the program, its mission, and purpose. It also provides a vehicle for participants to report performance data, activities, and issues during quarterly test periods.
NTIS
*Wind Turbines; Performance*

**20010123640** Lawrence Livermore National Lab., Livermore, CA USA
**Colloidal spray deposition technique for the processing of thin film solid oxide fuel cells**
Pham, A. Q.; Lee, T. H.; Glass, R. S.; Aug. 31, 1999; 9p; In English
Report No.(s): DE2000-757342; UCRL-JC-135760; No Copyright; Avail: Department of Energy Information Bridge, Microfiche

An improved version of the colloidal deposition technique is described. Using an ultrasonic atomizer to gently lay down the colloidal solution on a heated substrate, high quality thin films of various materials were prepared.
NTIS
*Solid Oxide Fuel Cells; Thin Films*

**20010123653** Pepco, Inc., Snyderville, UT USA
**Develop Improved Battery Charger (Turbo-Z Battery Charging System). Final Report**
Sep. 01, 1999; 57p; In English
Report No.(s): DE2001-764594; No Copyright; Avail: Department of Energy Information Bridge
The output of this project was a flexible control board. The control board can be used to control a variety of rapid battery chargers. The control module will reduce development cost of rapid battery charging hardware. In addition, PEPCO's proprietary battery charging software have been pre-programmed into the control microprocessor. This product is being applied to the proprietary capacitive charging system now under development.
NTIS
*Battery Chargers; Control Boards; Systems Engineering*

**20010123654** Materials Research Group, Inc., Wheat Ridge, CO USA
**Manufacturable CuIn(Ga)Se2-Based Solar Cells via Development of Co-Sputtered CuInSe2 Absorber Layers**
Eisgruber, I.; Mar. 20, 1999; 44p; In English
Report No.(s): DE2001-764593; No Copyright; Avail: Department of Energy Information Bridge
Yield and reproducibility remain issues in CuIn(Ga)Se2 (CIGS) photovoltaic module fabrication. While small-area cells (1 sq cm) over 18% efficient have been reported, the best large-area manufactured devices (1 sq ft) are 11% efficient with about 60% yield. If improvements in large-area manufacturing can accomplish 15% efficiency and 90% yield, the result is a doubling in throughput leading to a reduction in cost per watt of over 50%. The challenge now facing the photovoltaics industry is to bring the efficiencies of small-area cells and large-area industrial modules closer together and to raise manufacturing yields.
NTIS
*Copper Selenides; Efficiency; Photovoltaic Conversion; Solar Cells*

**20010123655** Endless Energy Corp., New Gloucester, ME USA
**Maine Coast Winds**
Lee, H. C.; Boice, M.; Mar. 31, 2000; 7p; In English
Report No.(s): DE2001-764433; No Copyright; Avail: Department of Energy Information Bridge
The Maine Coast Wind Project is intended to verify the performance of the AOC 15/50 turbine under coastal conditions. A secondary goal is to create a model for commercially competitive wind power installations at small, distributed sites. to date, the first of two installations is progressing very well, with sites for the second installation being reviewed.
NTIS
*Coasts; Windpower Utilization; Installing*

**20010123656** Windward Engineering, LLC, Salt Lake City, UT USA
**DOE Field Verification Program for Small Wind Turbines**
Hansen, A. C.; Davis, D. A.; Apr. 26, 2000; 13p; In English
Report No.(s): DE2001-764430; No Copyright; Avail: Department of Energy Information Bridge
During the second quarter of this project the Whisper 900 turbine in Spanish Fork Utah, and the second turbine at the NREL/NWTC were both brought online with complete data acquisition systems operational. Since monitoring of the turbine in Spanish Fork began, it has operated with 99.3% availability. The downtime was all related to testing operations, not faults in the turbine system.
NTIS
*Data Acquisition; Ground Truth; Wind Turbines*

**20010123657** Hawaiian Commercial and Sugar Co., Puunene, HI USA
**Closed Loop Biomass Co-Firing. Quarterly Technical Progress Report for the Period January-March 2000**
Jakeway, L.; Nakahata, M.; Apr. 01, 2000; 15p; In English
Report No.(s): DE2001-764428; DOE/GO/10479-Q; No Copyright; Avail: Department of Energy Information Bridge

Subagreements were finalized between HC&S Co. and University of California - Davis and the University of Hawaii to perform work required in the pilot-scale and full-scale demonstration tasks. The seed plot that contains the high-fiber cane variety is showing good growth. A visit was made by Dr. Ralph Overend this quarter to be apprised of project progress. Preliminary testing was performed with the 'Cuba' mill at HC&S that will be used to prepare biomass samples for the pilot-scale testing. Solid fuel feeder calibration tests were performed for one of the boilers at the Puunene factory for bagasse and coal fuel.
NTIS
*Fuel Tests; Biomass; Feedback Control*

**20010123730** Department of Energy, Richland, WA USA
**384 Day Tanks Site Assessment Report**
Smith, D. S.; Aug. 20, 1999; 65p; In English
Report No.(s): DE2001-11284; BHI-01296-Rev-0; No Copyright; Avail: Department of Energy Information Bridge
This report documents the site conditions, sampling results,and final conclusions regarding the site assessment of the 384 DayTanks associated with the 384 Fuel Bunker (also known as the 366Fuel Bunker), located in the 300 Area of the Hanford Site. The 384Fuel Bunker and 384 Day Tanks were originally used to supply fuel for the 384 Powerhouse boilers.
NTIS
*Storage Tanks; Diesel Fuels*

**20010123919** Sandia National Labs., Albuquerque, NM USA
**Plasma-Texturization for Multicrystalline Silicon Solar Cells**
Ruby, D. S.; Zaidi, S. H.; Narayanan, S.; Sep. 25, 2000; 6p; In English
Report No.(s): DE2001-763327; SAND2000-2338C; No Copyright; Avail: Department of Energy Information Bridge
Multicrystaliine Si (mc-Si) cells have not benefited from the cost-effective wet-chemical texturing processes that reduce front surface reflectance on single-crystal wafers. We developed a maskless plasma texturing technique for mc-Si cells using Reactive Ion Etching (RIE) that results in much higher cell performance than that of standard untextured cells. Elimination of plasma damage has been achieved while reducing front reflectance to extremely low levels. Internal quantum efficiencies higher than those on planar and wet-textured cells have been obtained, boosting cell currents and efficiencies by up to 110/0 on monocrystalline Si and 2.5% on Multicrystalline Si cells.
NTIS
*Silicon Oxides; Solar Cells; Polycrystals; Surface Treatment*

**20010123921** AWS Scientific, Inc., Albany, NY USA
**NY/NJ Distributed Wind Power Field Verification Project. Quarterly Report for the 2nd Quarter 2000**
Jul. 01, 2000; 6p; In English
Report No.(s): DE2001-763306; No Copyright; Avail: Department of Energy Information Bridge
During the 2ndQuarter, AWS successfully executed an Agreement for Professional and Technical Services with Liberty Science Center, the host for the Jersey City, NJ installation. The Agreement officially commits host organization cost sharing for the project and describes the specific responsibilities of each party. Also by the end of June, AWS had reached verbal agreement on contract language with the Town of Babylon, L.I., NY's attorney, but the agreement was still unsigned as of the end of the reporting period. Work continues with all of the host organizations to prepare for the host site installations. Several project meetings were held during the quarter, including site visits to the Town of Babylon on April 11 and June 19, and a site visit to Quail Hill Farm on May 10. A presentation on the project was made on April 11 to Town of Babylon officials (including the Town's Department of Environmental Conservation, Environmental Conservation Committee and Attorney's Office), as well as representatives of the Long Island Power Authority and New York State Energy Research and Development Authority, to provide the various parties with an overview of the project and to assign responsibility for individual tasks. Current plans call for installation of the foundation at the Webster site in mid-July, with foundation installation at Liberty Science Center to follow immediately upon approval from the NJ Department of Environmental Protection (DEP) to proceed with the project.
NTIS
*Renewable Energy; Windpower Utilization*

**20010123922** Endless Energy Corp., New Gloucester, ME USA
**Maine Coast Winds. Quarterly Technical Progress Report for the period April-June 2000**
Lee, H. C.; Boice, M.; Jul. 01, 2000; 13p; In English
Report No.(s): DE2001-763290; No Copyright; Avail: Department of Energy Information Bridge

The Maine Coast Wind Project is intended to verify the performance of the AOC (Atlantic Orient Corporation) 15/50 turbine under coastal conditions. A secondary goal is to create a model for commercially competitive wind power installations at small, distributed sites. Endless Energy Corporation (EEC) has made considerable progress in tie first - installation, and is currently in discussion with a party for the second turbine.
NTIS
*Windpower Utilization; Wind (Meteorology)*

**20010124066** Argonne National Lab., IL USA
**Beta-FeOOH: A New Positive Electrode Material for Lithium Secondary Batteries**
Amine, K.; Sep. 11, 1998; 16p; In English
Report No.(s): DE2001-10946; ANL/CMT/CP-97205; No Copyright; Avail: Department of Energy Information Bridge
Beta-iron oxy-hydroxide, which exhibits a (2x2) tunnel-type structure-similar to that of alpha-MnO2, was found to intercalate reversibly lithium in the tunnels. This material exhibits a potential slightly higher than 2 V with a capacity of 275 mAh/g and very good cyclic reversibility. X-ray Photoelectron Spectroscopy (XPS) investigation of discharged material showed that iron is reduced to the divalent state, and the lithium incorporated in the tunnels was purely ionic. This explains the good reversibility of this electrode material.
NTIS
*Electrodes; Hydroxides; Lithium Batteries*

**20010124068** Sandia National Labs., Albuquerque, NM USA
**Diagnostic Analysis of Silicon Photovoltaic Modules after 20-Year Field Exposure**
Quintana, M. A.; King, D. L.; Hosking, F. M.; Kratochvil, J. A.; Johnson, R. W.; Sep. 25, 2000; 6p; In English
Report No.(s): DE2001-763330; SAND2000-2339C; No Copyright; Avail: Department of Energy Information Bridge
The objective of this study was to investigate the technology used by Spectrolab Inc. to manufacture photovoltaic modules that have provided twenty years of reliable service at Natural Bridges National Monument in southeastern Utah. A field survey, system performance tests, and a series of module and materials tests have confirmed the durability of the modules in the array. The combination of manufacturing processes, materials, and quality controls used by Spectrolab resulted in modules that have maintained a performance level close to the original specifications for twenty years. Specific contributors to the durability of the modules included polyvinyl-butyral (PVB) encapsulant, expanded metal interconnects, silicon oxide antireflective coating, and excellent solder/substrate solderability.
NTIS
*Performance Tests; Solar Cells; Evaluation*

**20010124091** Oak Ridge National Lab., TN USA
**Carbon Dioxide Information Analysis Center, Fiscal Year 1999 Annual Report**
Cushman, R. M.; Boden, T. A.; Hook, L. A.; Jones, S. B.; Kaiser, D. P.; Mar. 01, 2000; 41p; In English
Report No.(s): DE2001-769321; ORNL/CDIAC-126; No Copyright; Avail: Department of Energy Information Bridge
Fiscal Year 1999 was a busy and productive one for the Carbon Dioxide Information Analysis Center (CDIAC) at Oak Ridge National Laboratory (ORNL). This report summarizes quite a few new and updated data and information products, and the 'What's Coming in FY 2000' section describes our plans for the first fiscal year in the third millennium (or the final fiscal year of the second millennium, depending on how you feel about this issue).
NTIS
*Carbon Dioxide; Information Resources Management*

**20010124100** Argonne National Lab., IL USA
**First-Principles Calculation of Atomic Structure and Electrochemical Potential of Li(1+x)V3O8**
Benedek, R.; Aug. 27, 1998; 15p; In English
Report No.(s): DE2001-10950; ANL/CMT/CP-97216; No Copyright; Avail: Department of Energy Information Bridge
Interest in the gamma-bronze, Li(1+x)V3O(g), as a possible electrode material in rechargeable Li batteries has stimulated several experimental studies on this system. Detailed interpretation of the electrochemical and physical-property measurements is complicated by uncertainties regarding the structural arrangement of Li atoms as a function of x and by a phase transition between two monoclinic structures (gamma(sub a), gamma(sub b)) during intercalation. to elucidate the atomic structures and the phase transition, first-principles calculations are performed with the local-density-functional-theory (LDFT) planewave pseudopotential method for both gamma(sub a) and gamma(sub b), as a function of lithiation. Calculations for the compositions

1+x = 1.5 and 1+x = 4 confirm that the Li configuration determined in the existing x-ray diffraction structure refinements (at 1+x = 1.2 and 1+x = 4 respectively), coincide with the predicted low-energy configurations. Structure predictions were made at intermediate compositions, for which no experimental structure measurement is available. The order in which the tetrahedrally coordinated Li sites are filled at equilibrium as a function of x in gamma(sub a), was predicted. Calculated electrochemical potentials as a function of composition agree well with experimental data.
NTIS
*Atomic Structure; Bronzes; Electrodes; Electrochemistry*

**20010124101** Argonne National Lab., IL USA
**Structural and Electrochemical Analysis of Layered Compounds from Li2MnO3**
Johnson, C. S.; Sep. 02, 1998; 18p; In English
Report No.(s): DE2001-10949; ANL/CMT/CP-97208; No Copyright; Avail: Department of Energy Information Bridge

Layered lithium-manganese-oxide electrodes with the general formula Li(2-x)MnO(3-x/2), and structural analogs in which some of the manganese has been substituted by Zr or Al have been prepared and characterized by structural and electrochemical methods. Although the discharge capacity for electrode compositions that contained Zr or Al fades at a slower rate in lithium cells than an unsubstituted compound, Li(2-x)MnO(3-x/2), these materials deliver lower capacities (approximately 90 mAh/g after 20 cycles) than Li(2-x)MnO(3-x/2) when cycled between 3.8 and 2.0 V at a C/8-C/10 rate. Under humid conditions or in contact with carbon, Li(2-x)MnO(3-x/2) compounds transform slowly to gamma-MnO2 on standing at room temperature, whereas the Zr- and Al-substituted materials appear to be more resistant to the conversion to gamma-MnO2.
NTIS
*Analytical Chemistry; Electrochemistry; Electrodes*

**20010124131** Argonne National Lab., IL USA
**Novel applications exploiting the thermal properties of nanostructured materials**
Eastman, J. A.; Nov. 20, 1998; 11p; In English
Report No.(s): DE2001-11042; ANL/MSD/CP-97456; No Copyright; Avail: Department of Energy Information Bridge

A new class of heat transfer fluids, termed nanofluids, has been developed by suspending nanocrystalline particles in liquids. Due to the orders-of-magnitude larger thermal conductivities of solids compared to those of liquids such as water, significantly enhanced thermal properties are obtained with nanofluids. The use of nanofluids could impact many industrial sectors, including transportation, energy supply and production, electronics, textiles, and paper production by, for example, decreasing pumping power needs or reducing heat exchanger sizes. In contrast to the enhancement in effective thermal transport rates that is obtained when nanoparticles are suspended in fluids, nanocrystalline coatings are expected to exhibit reduced thermal conductivities compared to coarse-grained coatings. Reduced thermal conductivities are predicted to arise because of a reduction in the mean free path of phonons due to presence of grain boundaries. This behavior, combined with improved mechanical properties, makes nanostructured zirconia coatings excellent candidates for future applications as thermal barriers.
NTIS
*Working Fluids; Thermodynamic Properties*

**20010124132** Los Alamos National Lab., NM USA
**Modeling and Analysis of the Ranchero Coaxial Explosive Pulse Power Generator System**
Atchison, W. L.; Goforth, J. H.; Lindemuth, I. R.; Reinovsky, R. E.; Jun. 28, 1999; 24p; In English
Report No.(s): DE2001-761017; LA-UR-99-3380; No Copyright; Avail: Department of Energy Information Bridge, Microfiche

A key element in the design of a coaxial generator system is the simplicity of the geometry. The clean cylindrical geometry allows us a reasonable chance at modeling RANCHERO performance using our 1D and 2D MHD modeling codes. The results of numerical simulations have been compare to several tests of the RANCHERO system in a variety of configurations. Recent comparisons of 1D calculations with the REOT-2 data have been extremely good and suggest that the generator is behaving in a very 1D like nature until reaching 90-95% of peak current. Differences between calculated current and measured performance during the last 3 mm (out of 70 mm) of flux compression may be a consequence of either the EOS for SF6, 2D effects, or both. This study will examine the existing models and attempt to provide a robust integrated model which can then be used to drive design studies, pre- and post-shot analysis, and predict performance parameters for slight variations of the base design of RANCHE RO.
NTIS
*Pulse Generators; Magnetohydrodynamics; Performance Prediction*

**20010124137** Argonne National Lab., IL USA
**Lithium Insertion into Hollandite-Type TiO2**
Noailles, L. D.; Sep. 02, 1998; 18p; In English
Report No.(s): DE2001-10948; ANL/CMT/CP-97207; No Copyright; Avail: Department of Energy Information Bridge

Hollandite-type TiO2 compounds, isostructural with alpha-MnO2, have been investigated as insertion electrodes for lithium batteries. Parent materials of K(x)Ti8O16 (0x2) were treated with concentrated acid to yield TiO2 products that were essentially free of potassium. Lithium can be inserted into the (2x2) tunnels of the TiO2 structure chemically (with n-butyllithium) and electrochemically to an approximate composition Li(0.5)TiO2. The lithium ions can be easily removed from the lithiated structure by chemical reaction with bromine; cyclic voltammetry indicates that high voltages are required to remove the lithium by electrochemical methods. The poor electrochemical behavior of hollandite-TiO2 contrasts strongly with alpha-MnO2 electrodes. The superior properties of alpha-Mn2 electrodes are attributed to the presence of oxygen ions, either as H2O or Li2O, in the (2x2) channels; lithia-stabilized electrodes, (0.15)Li2O (center-dot)-MnO2, show good cycling behavior and a rechargeable capacity of approximately 180 mAh/g.
NTIS
*Electrodes; Lithium; Manganese Oxides; Titanium Oxides; Metal Ions*

**20010125007** Sandia National Labs., Albuquerque, NM USA
**Modeling a Dry Etch Process for Large-Area Devices**
Buss, R. J.; Hebner, G. A.; Ruby, D. S.; Yang, P.; Jul. 28, 1999; 6p; In English
Report No.(s): DE2001-9683; SAND99-1996C; No Copyright; Avail: Department of Energy Information Bridge, Microfiche

There has been considerable interest in developing dry processes which can effectively replace wet processing in the manufacture of large area photovoltaic devices. Environmental and health issues are a driver for this activity because wet processes generally increase worker exposure to toxic and hazardous chemicals and generate large volumes of liquid hazardous waste. Our work has been directed toward improving the performance of screen-printed solar cells while using plasma processing to reduce hazardous chemical USAge.
NTIS
*Drying; Plasmas (Physics); Photovoltaic Cells; Models; Manufacturing*

**20010125023** Argonne National Lab., IL USA
**Evaluation of electric vehicle production and operating costs**
Cuenca, R. M.; Gaines, L. L.; Vyas, A. D.; May 23, 2000; 102p; In English
Report No.(s): DE2000-764206; ANL/ESD-41; No Copyright; Avail: Department of Energy Information Bridge

This report presents an analysis of the initial cost of electric vehicles (EVs). The manufacturing and retail cost structure of mature conventional vehicles produced at high volume is analyzed first, and the contributions by various cost categories to vehicle price are estimated. The costs are then allocated to such vehicle component groups as body, chassis, and powertrain. The similarities and differences among various component systems are reviewed. In electric vehicles, an electric drive replaces the conventional powertrain, and a battery pack replaces the fuel system. Three types of traction motors are reviewed, and their cost in high-volume production is analyzed. Various components of the motor and controller package are analyzed, and their representative costs are summarized. Four types of EV batteries are reviewed, and their costs are presented. Various alternatives for the low-, medium-, and high-volume production of EVs are evaluated, and some sample costs are presented. A methodology that estimates initial and operating costs on the basis of this analysis is presented. The methodology also estimates the average lifetime cost of owning and operating an electric vehicle.
NTIS
*Operating Costs; Manufacturing; Electric Motor Vehicles; Cost Estimates*

**20010125067** National Renewable Energy Lab., Golden, CO USA
**Market Assessment of Residential Grid-Tied PV Systems in Colorado: Executive Summary**
Farhar, B.; Coburn, T.; Sep. 13, 2000; 18p; In English
Report No.(s): DE2000-765089; NREL/TP-550-28872; No Copyright; Avail: Department of Energy Information Bridge

This is the Executive Summary of a report that presents research done in response to a decision by the Colorado Governor's Office of Energy Conservation and Management (OEC) and Colorado utility companies to consider making residential grid-tied photovoltaic (PV) systems available in Colorado. The idea was to locate homeowners willing to pay the costs of grid-tied PV (GPV) systems without batteries--$8,000 or $12,000 for a 2- or 3-kilowatt (kW) system, respectively, in 1996. These costs represented two-thirds of the actual installed cost of $6 per watt at that time and assumed the remainder would be subsidized. The

National Renewable Energy Laboratory (NREL) and OEC partnered to conduct a market assessment for GPV technology in Colorado. The study encompassed both qualitative and quantitative phases. The market assessment concluded that a market for residential GPV systems exists in Colorado today. That market is substantial enough for companies to successfully market PV systems to Colorado homeowners. These homeowners appear ready to learn more, inform themselves, and actively purchase GPV systems. The present situation is highly advantageous to Colorado's institutions - primarily its state government and its utility companies, and also its homebuilders - if they are ready to move forward on GPV technology.
NTIS
*Colorado; Energy Conservation; Market Research; Photovoltaic Conversion*

**20010125092** Sandia National Labs., Albuquerque, NM USA
**InSitu X-Ray Diffraction Studies on Lithium-Ion Battery Cathodes**
Doughty, D. H.; Ingersoll, D.; Rodriguez, M. A.; Jul. 13, 1999; 12p; In English
Report No.(s): DE2001-9008; SAND99-1767C; No Copyright; Avail: Department of Energy Information Bridge, Microfiche

In this paper numerical simulations of Mach 10 air flow over a hollow cylinder flare are presented in comparison with recent experimental results. The numerical study is performed using a Direct Simulation Monte Carlo code and the experimental results were obtained in the ONERA R5Ch wind tunnel. The flow phenomena involved include shock wave boundary layer interaction in hypersonic laminar flow. An analysis of the requirements on the grid resolution, number of particle simulators and run time is performed. Measured and calculated surface properties including pressure and heat transfer are compared.
NTIS
*Cathodes; Computerized Simulation; Metal Ions; X Ray Diffraction; Hypersonic Wind Tunnels; Lithium*

**20010125093** Sandia National Labs., Albuquerque, NM USA
**InSitu X-Ray Diffraction Studies on Lithium-Ion Battery Cathodes**
Doughty, D. H.; Ingersoll, D.; Rodriguez, M. A.; Jul. 13, 1999; 8p; In English
Report No.(s): DE2001-9006; SAND99-1767C; No Copyright; Avail: Department of Energy Information Bridge, Microfiche

LiNi(sub 0.8)Co(sub 0.2)O(sub 2) and LiNiO(sub 2) have been characterized in-situ XRD. LiNi(sub 0.8)Co(sub 0.2)O(sub 2) does not undergo a monoclinic phase transformation but remains a hexagonal lattice throughout the entire charging cycle. It is hypothesized that Co-doping may help stabilize the hexagonal structure.
NTIS
*Cathodes; X Ray Diffraction; Nickel; Lithium Batteries; Crystal Structure*

**20010125172** National Renewable Energy Lab., Golden, CO USA
**Solar Buildings: Transpired Air Collectors**
Nov. 24, 1998; 2p; In English
Report No.(s): DE2000-765101; NREL/FS-550-24499; DOE/GO-10098-558; No Copyright; Avail: Department of Energy Information Bridge

Transpired air collectors preheat building ventilation air by using the building's ventilation fan to draw fresh air through the system. The intake air is heated as it passes through the perforated absorber plate and up the plenum between the absorber and the south wall of the building. Reduced heating costs will pay for the systems in 3 - 12 years.
NTIS
*Air Flow; Solar Collectors; Solar Heating*

**20010125173** National Renewable Energy Lab., Golden, CO USA
**SunLab: Advancing Concentrating Solar Power Technology**
Nov. 24, 1998; 2p; In English
Report No.(s): DE2000-765100; NREL/FS-550-24647; DOE/GO-10098-565; No Copyright; Avail: Department of Energy Information Bridge

Concentrating solar power (CSP) technologies, including parabolic troughs, power towers, and dish/engines, have the potential to provide the world with tens of thoUSAnds of megawatts of clean, renewable, cost-competitive power.
NTIS
*Solar Thermal Electric Power Plants; Parabolic Reflectors*

**20010125174** National Renewable Energy Lab., Golden, CO USA
**SolMaT: The Solar Thermal Manufacturing Technology Initiative**
Crawford, D.; Nov. 24, 1998; 2p; In English
Report No.(s): DE2000-765099; NREL/FS-550-24648; DOE/GO-10098-566; No Copyright; Avail: Department of Energy Information Bridge

SolMaT works with manufacturers to lower the cost of manufacturing components for concentrating solar power systems.
NTIS
*Manufacturing; Solar Thermal Electric Power Plants*

**20010125175** National Renewable Energy Lab., Golden, CO USA
**SunLab: Concentrating Solar Power Program Overview**
Nov. 24, 1998; 4p; In English
Report No.(s): DE2000-765098; NREL/FS-550-24649; DOE/GO-10098-567; No Copyright; Avail: Department of Energy Information Bridge

DOE's Concentrating Solar Power (CSP) program is collaborating with its partners in the private sector to develop two new solar technologies -- power towers and dish/engines -- to meet the huge commercial potential for solar power. Concentrating solar power plants produce electric power by first converting the sun's energy into heat, and then to electricity in a conventional generator.
NTIS
*Electric Power Plants; Solar Energy Conversion*

**20010125226** National Renewable Energy Lab., Golden, CO USA
**Post-Lamination Manufacturing Process Automation for Photovoltaic Modules** ***Annual Report, 15 Jun. 1999 - 14 Jul. 2000***
Nowlan, M. J.; Murach, J. M.; Sutherland, S. F.; Lewis, E. R.; Hogan, S. J.; Sep. 29, 2000; 42p; In English
Report No.(s): DE2000-765085; NREL/SR-520-28789; No Copyright; Avail: Department of Energy Information Bridge

Spire is addressing the PVMaT project goals of photovoltaic (PV) module cost reduction and improved module manufacturing process technology. New cost-effective automation processes are being developed for post-lamination PV module assembly, where post-lamination is defined as the processes after the solar cells are encapsulated. These processes apply to both crystalline and thin-film solar cell modules. Four main process areas are being addressed: (1) Module buffer storage and handling between steps; (2) Module edge trimming, edge sealing, and framing; (3) Junction-box installation; and (4) Testing for module performance, electrical isolation, and ground-path continuity.
NTIS
*Cost Reduction; Crystallinity; Laminates; Photovoltaic Cells*

**20010125227** National Renewable Energy Lab., Golden, CO USA
**Apollo(R) Thin Film Process Development,** ***May 1999 - Apr. 2000***
Cunningham, D. W.; Skinner, D. E.; Sep. 17, 2000; 36p; In English
Report No.(s): DE2000-765084; NREL/SR-520-28710; No Copyright; Avail: Department of Energy Information Bridge

In this report, the results are presented and discussed from the following areas: CdS and CdTe optimization. In this section, semiconductor properties, optical properties, and device optimization are discussed. Crystallographic characteristics were determined under collaborative work with the Institute of Energy Conversion, (University of Delaware) and NREL. In addition to this, module performance results are presented to illustrate the efficiency improvements gained as a result of this research. In the Reliability and testing section, both indoor stress testing and outdoor long term test systems are described. Detailed design, set up and initial results are presented. In the Health, Safety and Environment section are described the handling of waste treatment systems at the Fairfield plant, reclaimed cadmium metal recycling and closed loop/zero discharge studies.
NTIS
*Cadmium Tellurides; Crystallography; Optical Properties; Thin Films; Crystal Structure; Cadmium Sulfides*

**20010125228** National Renewable Energy Lab., Golden, CO USA
**Survey of Thermal Storage for Parabolic Trough Power Plants,** ***13 Sep. 1999 - 12 Jun. 2000***
Sep. 29, 2000; 61p; In English
Report No.(s): DE2000-765081; NREL/SR-550-27925; No Copyright; Avail: Department of Energy Information Bridge

The purpose of this report is to identify and selectively review previous work done on the evaluation and use of thermal energy storage systems applied to parabolic trough power plants. Appropriate storage concepts and technical options are first discussed, followed by a review of previous work.
NTIS
*Heat Storage; Parabolic Reflectors; Surveys*

**20010125410** Argonne National Lab., IL USA
**Towards standardizing the measurement of electrochemical properties of solid state electrolytes in lithium batteries**
Dees, D. W.; Henriksen, G. L.; May 06, 1999; 5p; In English
Report No.(s): DE2001-11796; ANL/CMT/CP-98987; No Copyright; Avail: Department of Energy Information Bridge

The purpose of this paper is to stimulate thought and discussion in the technical community on standardization of the experimental determination of the pertinent electrochemical properties of solid electrolytes in lithium batteries. This standardization is needed for comparison and modeling of solid electrolytes in a practical lithium battery. The appropriate electrochemical properties include transport, thermodynamic, and physical parameters that generally depend on concentration and temperature. While it is beyond the scope of this work to put forward definitive measurement techniques for all types of solid electrolytes, it is hoped that comparisons between various techniques to examine a dissolved binary lithium salt in a dry polymer solvent will lead to improved understanding and methodology for examining solid electrolytes.
NTIS
*Electrochemistry; Solid Electrolytes; Lithium Batteries; Standardization*

**20010125478** Argonne National Lab., IL USA
**Small Angle Neutron Scattering Analysis of Novel Carbons for Lithium Secondary Batteries**
Sandi, G.; Thiyagarajan, P.; Winans, R.; Carrado, K.; Jan. 14, 1998; 8p; In English
Report No.(s): DE2001-8091; ANL/CHM/CP-93252; No Copyright; Avail: Department of Energy Information Bridge, Microfiche

Small angle neutron scattering analyses of carbonaceous materials used as anodes in lithium ion cells have been performed. The carbons have been synthesized using pillared clays (PILCs) as inorganic templates. Pillared clays are layered silicates whose sheets have been permanently propped open by sets of thermally stable molecular props. The calcined PILC was loaded with five different organic precursors and heated at 700 C under nitrogen. When the inorganic pillars were removed by acid treatment, carbon sheets are produced with holes. The fitting of the data in the high q region suggested that the carbon sheets have voids with radii ranging from 4 to 8 angstroms. Similar radii were obtained for the PILC and PILC/organic precursor, which suggests that the carbon was well distributed in the clay prior to pyrolysis.
NTIS
*Carbon; Carbonaceous Materials; Clays; Neutron Scattering*

**20010125486** Federal Energy Technology Center, Morgantown, WV USA
**Riverton Dome Gas Exploration and Stimulation Technology Demonstration, Wind River Basin, Wyoming**
Aug. 28, 1998; 4p; In English
Report No.(s): DE2001-7937; DE-FC26-97FT34181-03; No Copyright; Avail: Department of Energy Information Bridge, Microfiche

This project will provide a full demonstration of an entirely new package of exploration technologies that will result in the discovery and development of significant new gas reserves now trapped in unconventional low-permeability reservoirs. This demonstration includes the field application of these technologies, prospect definition and well siting, and a test of this new strategy through wildcat drilling. In addition this project includes a demonstration of a new stimulation technology that will improve completion success in these unconventional low permeability reservoirs which are sensitive to drilling and completion damage. The work includes two test wells to be drilled by Snyder Oil Company on the Shoshone/Arapahoe Tribal Lands in the Wind River Basin. This basin is a foreland basin whose petroleum systems include Paleozoic and Cretaceous source beds and reservoirs which were buried, folded by Laramide compressional folding, and subsequently uplifted asymmetrically. The anomalous pressure boundary is also asymmetric, following differential uplift trends.
NTIS
*Reservoirs; Drilling; Natural Gas Exploration*

**20010125500** Oak Ridge National Lab., TN USA

**Transportation Energy Data Book, Edition 20**

Davis, S. C.; Oct. 01, 2000; 354p; In English

Report No.(s): DE2001-769291; ORNL-6959; No Copyright; Avail: Department of Energy Information Bridge, Microfiche

The Transportation Energy Data Book: Edition 20 is a statistical compendium prepared and published by Oak Ridge National Laboratory (ORNL) under contract with the Office of Transportation Technologies in the Department of Energy (DOE). Designed for use as a desk-top reference, the data book represents an assembly and display of statistics and information that characterize transportation activity, and presents data on other factors that influence transportation energy use. The purpose of this document is to present relevant statistical data in the form of tables and graphs. The latest editions of the Data Book are available to a larger audience via the Internet (www-cta.ornl.gov/data/tedb.htm). This edition of the Data Book has 12 chapters which focus on various aspects of the transportation industry. Chapter 1 focuses on petroleum; Chapter 2-energy; Chapter 3-greenhouse gas emissions; Chapter 4-criteria pollutant emissions; Chapter 5-transportation and the economy; Chapter 6-highway vehicles; Chapter 7-light vehicles; Chapter 8-heavy vehicles; Chapter 9-alternative fuel vehicles; Chapter 10-fleet vehicles; Chapter 11-household vehicles; and Chapter 12-nonhighway modes. The sources used represent the latest available data. There are also three appendices which include detailed source information for some tables, measures of conversion, and the definition of Census divisions and regions. A glossary of terms and a title index are also included for the readers convenience.

NTIS

*Transportation; Transportation Energy; Statistical Analysis*

**20010125524** Siyeh Development Corp., Browning, MT USA

**Field verification program for small wind turbines. Supplemental power for the town of Browning waste-water treatment facility. Quarterly report for the period October 1999-December 1999**

Wilde, M. H.; Jan. 01, 2000; 30p; In English

Report No.(s): DE2001-764724; DOE/GO/10459-Q; No Copyright; Avail: Department of Energy Information Bridge

The agreement between the USDOE (DOE) and Siyeh Development Corporation (Siyeh) of Browning, MT, is under The Field Verification Program For Small Wind Turbines and is titled Supplemental Power for the Town of Browning Wastewater Treatment Facility. A team of organizations was assembled as project partners and contributors in this endeavor. Included in that number are: Siyeh, the Town of Browning, MT (Browning), Bergey Windpower (Bergey), the Indian Health Service (IHS) and the Blackfeet Indian Housing Authority (BIHA).

NTIS

*Wind Turbines; Waste Water; Water Treatment*

**20010125540** Hawaiian Commercial and Sugar Co., Puunene, HI USA

**Closed-Loop Biomass Co-Firing *Quarterly Report, Apr. - Jun. 2000***

Jakeway, L.; Nakahata, M.; Jul. 01, 2000; 16p; In English

Report No.(s): DE2001-763410; DOE/GO/10479-Q; No Copyright; Avail: Department of Energy Information Bridge, Microfiche

This document is divided in three parts: (1) Effort was focused on completing preparation of biomass and coal fuels for the pilot scale tests to be performed at Sandia National Laboratory in Livermore, CA; (2) Planting configurations were finalized for the large-scale demonstration. Specifications of the drip tubing to accommodate for row lengths and field slope were determined; (3) Another solid fuel feeder calibration test was performed for one of the feeders on Boiler 2 at the Puunene factory using bagasse as the solid fuel.

NTIS

*Biomass; Coal; Calibrating*

**20010125561** Argonne National Lab., IL USA

**Liquid Fuel Reformer Development**

Ahmed, S.; Krumpelt, M.; Pereira, C.; Wilkenhoener, R.; Jul. 30, 1999; 11p; In English

Report No.(s): DE2001-11914; ANL/CMT/CP-99684; No Copyright; Avail: Department of Energy Information Bridge, Microfiche

At Argonne National Laboratory we are developing a process to convert hydrocarbon fuels to a clean hydrogen feed for a fuel cell. The process incorporates a partial oxidation/steam reforming catalyst that can process hydrocarbon feeds at lower temperatures than existing commercial catalysts. We have tested the catalyst with three diesel-type fuels: hexadecane, low-sulfur diesel fuel, and a regular diesel fuel. We achieved complete conversion of the feed to products. Hexadecane yielded products

containing 60% hydrogen on a dry, nitrogen-free basis at 800 C. For the two diesel fuels, higher temperatures, 850 C, were required to approach similar levels of hydrogen in the product stream. At 800 C, hydrogen yield of the low sulfur diesel was 32%, while that of the regular diesel was 52%. Residual products in both cases included CO, CO2, ethane, ethylene, and methane.
NTIS
*Catalysts; Diesel Fuels; Hydrocarbon Fuels; Hydrogen Fuels*

**20010125565** Argonne National Lab., IL USA
**Intermetallic Insertion Anodes for Lithium Batteries**
Johnson, C. S.; Kahaian, A. J.; Kepler, K. D.; Scott, M.; Thackerary, M. M.; Jul. 19, 1999; 4p; In English
Report No.(s): DE2001-11900; ANL/CMT/CP-99599; No Copyright; Avail: Department of Energy Information Bridge, Microfiche

Intermetallic alloys have been investigated for many years as anode materials for lithium batteries and, more recently, as alternative electrodes to carbon, because of several intrinsic advantages including high capacity and safety. Some of the most studied alloys utilize tin as the active component because of its high theoretical capacity (996 mAh/g) and its slightly higher operating voltage (is less than 400 mV) compared to metallic lithium. to date, the use of binary lithium alloys as anodes has been limited to the select number of main group elements (e.g., Sn) that can be lithiated at an appropriate voltage with acceptable kinetics. A major disadvantage of binary Li(x)M alloy systems is that major phase changes occur during the electrochemical cycling of lithium. Severe volume expansion and contraction of the metal matrix, which limit the cycle life of the lithium cell, normally accompany these phase changes. The. most successful approach to overcoming this limitation has been the use of intermetallic alloys MM(prime) consisting of two or more metals, at least one of which is an 'active' alloying element (M) and the other an 'inactive' (M(prime)) element. During the reaction with lithium, such a system breaks up into regions of Li(x)M and inactive M(prime). In our work, we have extended the concept of intermetallic electrodes to include topotactic reactions in which the intermetallic compound provides a host structure for lithium.
NTIS
*Anodes; Binary Alloys; Electrodes; Intermetallics; Lithium Batteries*

**20010125568** Argonne National Lab., IL USA
**Commercial Viability of Hybrid Vehicles: Best Household Use and Cross National Considerations**
Santini, D. J.; Vyas, A. D.; Jul. 16, 1999; 13p; In English
Report No.(s): DE2001-11897; ANL/ES/CP-99558; No Copyright; Avail: Department of Energy Information Bridge, Microfiche

Japanese automakers have introduced hybrid passenger cars in Japan and will soon do so in the US. In this paper, we report how we used early computer simulation model results to compare the commercial viability of a hypothetical near-term (next decade) hybrid mid-size passenger car configuration under varying fuel price and driving patterns. The fuel prices and driving patterns evaluated are designed to span likely values for major OECD nations. Two types of models are used. One allows the 'design' of a hybrid to a specified set of performance requirements and the prediction of fuel economy under a number of possible driving patterns (called driving cycles). Another provides an estimate of the incremental cost of the hybrid in comparison to a comparably performing conventional vehicle. In this paper, the models are applied to predict the NPV cost of conventional gasoline-fueled vehicles vs. parallel hybrid vehicles. The parallel hybrids are assumed to: (1) be produced at high volume; (2) use nickel metal hydride battery packs; and (3) have high-strength steel bodies. The conventional vehicle also is assumed to have a high-strength steel body. The simulated vehicles are held constant in many respects, including 0-60 time, engine type, aerodynamic drag coefficient, tire rolling resistance, and frontal area. The hybrids analyzed use the minimum size battery pack and motor to meet specified 0-60 times. A key characteristic affecting commercial viability is noted and quantified: that hybrids achieve the most pronounced fuel economy increase (best use) in slow, average-speed, stop-and-go driving, but when households consistently drive these vehicles under these conditions, they tend to travel fewer miles than average vehicles. We find that hours driven is a more valuable measure than miles. Estimates are developed concerning hours of use of household vehicles versus driving cycle, and the pattern of minimum NPV incremental cost (or benefit) of selecting the hybrid over the conventional vehicle at various fuel prices is illustrated. These results are based on data from various OECD motions on fuel price, annual miles of travel per vehicle, and driving cycles assumed to be applicable in those nations. Scatter in results plotted as a function of average speed, related to details of driving cycles and the vehicles selected for analysis, is discussed.
NTIS
*Computerized Simulation; Electric Batteries; Gasoline; Automobiles*

**20010125590** Los Alamos National Lab., NM USA

**Field Trip Guide to Serpentinite, Silica-Carbonate Alteration, and Related Hydrothermal Activity in the Clear Lake Region, California**

Goff, F.; Guthrie, G.; Jun. 01, 1999; 34p; In English

Report No.(s): DE2001-8204; LA-13607-MS; No Copyright; Avail: Department of Energy Information Bridge, Microfiche

This guide is designed to familiarize scientists with the geology, structure, alteration, and fluids typical of California serpentinites for purposes of carbon dioxide sequestration. Goff et al and Goff and Lackner describe the geology and geochemistry of some of the serpentinites from this area. Mechanisms of silica-carbonate alteration were outlined by Barnes et al. Donnelly-Nolan et al most recently reviewed relations between regional hydrothermal alteration and Quarternary volcanic activity. Stanley et al summarized geophysical characteristics of the region.

NTIS

*Hydrothermal Systems; California; Silicon Dioxide; Carbonates; Serpentine*

**20010125602** Argonne National Lab., IL USA

**Hybrid Options for Light-Duty Vehicles**

An, F.; Stodofsky, F.; Santini, D.; Jul. 19, 1999; 13p; In English

Report No.(s): DE2001-11903; ANL/ES/CP-99638; No Copyright; Avail: Department of Energy Information Bridge, Microfiche

Hybrid electric vehicles (HEVs) offer great promise in improving fuel economy. In this paper, we analyze why, how, and by how much vehicle hybridization can reduce energy consumption and improve fuel economy. Our analysis focuses on efficiency gains associated solely with vehicle hybridization. We do not consider such other measures as vehicle weight reduction or air- and tire-resistance reduction, because such measures would also benefit conventional technology vehicles. The analysis starts with understanding the energy inefficiencies of light-duty vehicles associated with different operation modes in US and Japanese urban and highway driving cycles, with the corresponding energy-saving potentials. The potential for fuel economy gains due to vehicle hybridization can be estimated almost exclusively on the basis of three elements: the reducibility of engine idling operation, the recoverability of braking energy losses, and the capability of improving engine load profiles to gain efficiency associated with specific HEV configurations and control strategies. Specifically, we evaluate the energy efficiencies and fuel economies of a baseline MY97 Corolla-like conventional vehicle (CV), a hypothetical Corolla-based minimal hybrid vehicle (MHV), and a MY98 Prius-like full hybrid vehicle (FHV). We then estimate energy benefits of both MHVs and FHVs over CVs on a performance-equivalent basis. We conclude that the energy benefits of hybridization vary not only with test cycles, but also with performance requirements. The hybrid benefits are greater for 'Corolla (high) performance-equivalent' vehicles than for 'Prius (low) performance-equivalent' vehicles. An increasing acceleration requirement would result in larger fuel economy benefits from vehicle hybridization.

NTIS

*Power Efficiency; Electric Motor Vehicles; Energy Consumption*

**20010125621** Sandia National Labs., Albuquerque, NM USA

**Parametric Models for Estimating Wind Turbine Fatigue Loads for Design**

Manuel, L.; Veers, P. S.; Winterstein, S. R.; Nov. 21, 2000; 14p; In English

Report No.(s): DE2001-767985; SAND2000-2893C; No Copyright; Avail: Department of Energy Information Bridge, Microfiche

International standards for wind turbine certification depend on finding long-term fatigue load distributions that are conservative with respect to the state of knowledge for a given system. Statistical models of loads for fatigue application are described and demonstrated using flap and edge blade-bending data from a commercial turbine in complex terrain. Distributions of rainflow-counted range data for each ten-minute segment are characterized by parameters related to their first three statistical moments (mean, coefficient of variation, and skewness). Quadratic Weibull distribution functions based on these three moments are shown to match the measured load distributions if the non-damaging low-amplitude ranges are first eliminated. The moments are mapped to the wind conditions with a two-dimensional regression over ten-minute average wind speed and turbulence intensity. With this mapping, the short-term distribution of ranges is known for any combination of average wind speed and turbulence intensity. The long-term distribution of ranges is determined by integrating over the annual distribution of input conditions. First we study long-term loads derived by integration over wind speed distribution alone, using standard-specified turbulence levels. Next we perform this integration over both wind speed and turbulence distribution for the example site. Results are compared between standard-driven and site-driven load estimates. Finally, using statistics based on the regression of the

statistical moments over the input conditions, the uncertainty (due to the limited data set) in the long-term load distribution is represented by 95 angstroms confidence bounds on predicted loads.
NTIS
*Estimating; Loads (Forces); Mathematical Models; Turbulence; Wind Turbines*

## 45
## ENVIRONMENT POLLUTION

*Includes atmospheric, water, soil, noise, and thermal pollution.*

**20010117646** Instituto Nacional de Pesquisas Espacias, Sao Jose dos Campos, Brazil
**Evaluation of Contaminants Produced In Biomass Burning Sites and Transported to Regions Without Burning** ***Avaliacao de Contaminantes Produzidos em Locais de Queimadas e Transportados para Regioes Onde Nao se Queima***
Aires, Claudia Boian, Instituto Nacional de Pesquisas Espacias, Brazil; 2001; 108p; In Portuguese
Report No.(s): INPE-8433-TDI/775; No Copyright; Avail: CASI; A06, Hardcopy; A02, Microfiche

In the Brazilian continent there is a great opposition between source regions of biomass burning (Brazil Central) and no source regions like, for example, south region. Air mass trajectories calculus on troposphere (between 0 and 4 km) show the existence of an ”air mass corridor circulation” between source regions and no source. The aim of this work is to realize measures of trace gases in this ”air mass corridor circulation” and to use the measures of carbon monoxide concentrations, to quantify the influence of biomass burning realized in Brazil Central (savannah areas) over regions of low index of biomass burning. It was realized two campaigns with Bandeirante/INPE aircraft in the years 1999 and 2000, where it was measured carbon monoxide, ozone and carbon dioxide. With these campaigns we had excellent results and with carbon monoxide measurements, it was possible in two campaigns the identification of CO concentrations gradient between source regions and no source. We developed a model to estimated the transport term and to quantity the influence of biomass burning realized in Brazil Central over regions of low index of biomass burning. The methodology developed was efficient and it was possible the identification of high percentages of CO (maximum value of 25% first campaign and 11% in the second campaign) due transport in no source regions and percentages of approximately 59% in regions near to great sources.
Author
*Contaminants; Biomass Burning; Brazil; Air Masses*

**20010118269** California Univ., Lawrence Berkeley Lab., Berkeley, CA USA
**Additionality of emissions reductions from clean development mechanism projects: issues and options for project-level assessments**
Meyers, S.; Jul. 01, 1999; 16p; In English
Report No.(s): DE2000-760331; LBNL-43704; No Copyright; Avail: Department of Energy Information Bridge, Microfiche

The Clean Development Mechanism (CDM), provided for in the Kyoto Protocol, is designed to encourage project activities in developing countries that result in greenhouse gas (GHG) emissions reductions. to receive credit, emissions reductions should be additional to what would occur in the absence of the CDM. Establishing a workable way to judge whether reductions are additional to what would happen otherwise is a vexing challenge. The problems with project-level assessment in the AIJ phase have led to interest in simpler approaches for determining project additionality and baselines. Because a project-level approach takes each case separately, however, it affords greater opportunity than alternative approaches to ensure that emissions reductions are likely additional. This paper considers improvements to a project-level approach that could reduce the problems that have arisen in the past.
NTIS
*Exhaust Emission; Pollution Control*

**20010119437** Oak Ridge National Lab., TN USA
**Review of Subcritical Source-Driven Noise Analysis Measurements**
Valentine, T. E.; Nov. 01, 1999; 65p; In English
Report No.(s): DE2000-15041; ORNL/TM-1999/288; No Copyright; Avail: Department of Energy Information Bridge, Microfiche

Subcritical source-driven noise measurements are simultaneous Rossia and randomly pulsed neutron measurements that provide measured quantities that can be related to the subcritical neutron multiplication factor. In fact, subcritical source-driven noise measurements should be performed in lieu of Rossia measurements because of the additional information that is obtained

from noise measurements such as the spectral ratio and the coherence functions. The basic understanding of source-driven noise analysis measurements can be developed from a point reactor kinetics model to demonstrate how the measured quantities relate to the subcritical neutron multiplication factor.
NTIS
*Neutrons; Noise Measurement*

**20010119532** Fermi National Accelerator Lab., Batavia, IL USA
**Production and release of airborne radionuclides due to the operations of NuMI**
Boehnlein, D. J.; Cossairt, J. D.; Aug. 26, 1999; 26p; In English
Report No.(s): DE2001-10362; FERMILAB-TM-2089; No Copyright; Avail: Department of Energy Information Bridge, Microfiche

The operation of the NuMI beamline will result in the production of significant quantities of airborne radionuclides due to the large proton beam intensities to be delivered to this facility. In this report we predict the production of airborne radionuclides and their release to the environment during NuMI operations. An estimate is provided of the maximum dose equivalent that might be delivered by this pathway to a hypothetical individual continuously present at the Fermilab site boundary. Likewise, the dose equivalent rate due to exposure to activated air within the NuMI target station enclosure is estimated. It is concluded that the airborne radioactivity produced in the course of NuMI operations will be in compliance with applicable Federal and State regulations.
NTIS
*Air Pollution; Dosage; Neutrino Beams; Pollution Transport*

**20010119548** Lawrence Livermore National Lab., Livermore, CA USA
**Model for Simulating Airflow and Pollutant Dispersion Around Buildings**
Chan, S. T.; Lee, R. L.; Feb. 24, 1999; 12p; In English
Report No.(s): DE2001-10440; UCRL-JC-132242; No Copyright; Avail: Department of Energy Information Bridge

A three-dimensional numerical mode1 for simulating airflow and pollutant dispersion around buildings is described. The model is based on an innovative finite element approach and fully implicit time integration techniques. Linear and nonlinear eddy viscosity/diffusivity submodels are provided for turbulence parameterization. Model predictions for the flow-field and dispersion patterns around a surface-mounted cube are compared with measured data from laboratory experiments.
NTIS
*Air Flow; Buildings; Eddy Viscosity; Flow Distribution; Contaminants*

**20010120050** Brookhaven National Lab., Upton, NY USA
**Survey of noise suppression systems for engine generator sets**
Krishna, C. R.; Oct. 01, 1999; 33p; In English
Report No.(s): DE2000-752962; BNL-67163; No Copyright; Avail: Department of Energy Information Bridge

The U.S. Army Communications & Electronics Command (CECOM) Research Development & Engineering (RD&E) is developing a new standard family of medium-sized mobile power systems. Noise reduction from the levels in current such equipment is required to meet the specifications. Brookhaven National Laboratory (BNL) was tasked to assess the status of noise suppression technologies to achieve this. The report summarizes the results of a preliminary market survey of noise suppression technologies and a background review of diesel engine noise. Recommendations are made for a design strategy and for some specific steps to be followed.
NTIS
*Diesel Engines; Noise Reduction; Electric Generators; Surveys*

**20010120099** Norwegian Defence Research Establishment, Kjeller, Norway
**Risk Assessment of Marine Pollution** ***Risikovurdering av Sjoforurensninger***
Voie, Oyvind, Norwegian Defence Research Establishment, Norway; Storstenvik, Anders, Norwegian Defence Research Establishment, Norway; Jun. 15, 2001; 76p; In Norwegian
Contract(s)/Grant(s): FFIBM Proj. 813/138.2
Report No.(s): FFI/RAPPORT-2001/04130; ISBN 82-464-0536-5; No Copyright; Avail: CASI; A05, Hardcopy; A01, Microfiche

A risk assessment guideline has been developed for marine or freshwater pollution. Generic criteria for ”worst case” situations have been calculated for sediment, water and biota. For situations other than ”worst case” a risk calculator may be used to generate site specific acceptance criteria.
Author
*Risk; Water Pollution; Toxicology; Marine Biology*

**20010120101** Air Force Inst. of Tech., Wright-Patterson AFB, OH USA
**A History of Visibility Protection: The Struggle Against Complexity**
McCarthy, John F.; Aug. 31, 2001; 107p; In English
Report No.(s): AD-A395115; No Copyright; Avail: CASI; A06, Hardcopy; A02, Microfiche

Many national parks and wilderness areas, particularly those in the Southwestern USA, are known for their unique and beautiful scenery. Millions of people visit these areas each year to view their spectacular scenic vistas. In 1977, Congress made the protection of visibility in these areas a national priority. Part II of this article provides an overview of the history and purpose of visibility regulation, and Part III describes the scientific basis for such regulation. Part IV discusses the early years of visibility protection; Part V evaluates visibility protection in the 199Os; and Part VI discusses EPA’s recent efforts at dealing with the visibility problem.
DTIC
*Visibility; Air Pollution; Parks*

**20010121524** Brookhaven National Lab., Upton, NY USA
**Carbon dioxide (reduction)**
Fujita, A.; Jan. 12, 2000; 10p; In English
Report No.(s): DE2000-752152; BNL-67077; No Copyright; Avail: Department of Energy Information Bridge

The twin problems of global warming, caused by an increase in atmospheric carbon dioxide (CO2) concentrations, and limited fossil fuel resources have stimulated research in the utilization of CO2. These problems would be partially alleviated by the development of artificial photochemical systems that could economically fix CO2 into fuels or useful chemicals. During the past one and a half decades, intensive efforts have been directed toward the photochemical production of carbon monoxide (CO) and formic acid (HCOOH) from CO2. These systems have several common elements: they all contain photosensitizers (such as metalloporphyrins, ruthenium or rhenium complexes with bipyridine), electron mediators or catalysts, and sacrificial electron donors (such as tertiary amines or ascorbic acid). Recent progress along these lines has resulted in advances in our understanding of the interaction of CO2 molecules with metal complexes, and the factors controlling the efficient storage of solar energy in the form of reduced carbon compounds.
NTIS
*Carbon Dioxide; Air Pollution; Fuel Production*

**20010121532** RECOM Technologies, Inc., Moffett Field, CA USA
**A Knowledge-Based Representation Scheme for Environmental Science Models**
Keller, Richard M., RECOM Technologies, Inc., USA; Dungan, Jennifer L., Johnson Controls, Inc., USA; [1994]; 1p; In English; AIAA 1994 Workshop on AI Technologies for Environmental Applications, 30-31 Jul. 1994, Seattle, WA, USA; Sponsored by American Inst. of Aeronautics and Astronautics, USA
Contract(s)/Grant(s): RTOP 233-01-02; No Copyright; Avail: Issuing Activity; Abstract Only

One of the primary methods available for studying environmental phenomena is the construction and analysis of computational models. We have been studying how artificial intelligence techniques can be applied to assist in the development and use of environmental science models within the context of NASA-sponsored activities. We have identified several high-utility areas as potential targets for research and development: model development; data visualization, analysis, and interpretation; model publishing and reuse, training and education; and framing, posing, and answering questions. Central to progress on any of the above areas is a representation for environmental models that contains a great deal more information than is present in a traditional software implementation. In particular, a traditional software implementation is devoid of any semantic information that connects the code with the environmental context that forms the background for the modeling activity. Before we can build AI systems to assist in model development and USAge, we must develop a representation for environmental models that adequately describes a model’s semantics and explicitly represents the relationship between the code and the modeling task at hand. We have developed one such representation in conjunction with our work on the SIGMA (Scientists’ Intelligent Graphical

Modeling Assistant) environment. The key feature of the representation is that it provides a semantic grounding for the symbols in a set of modeling equations by linking those symbols to an explicit representation of the underlying environmental scenario. Author

*Environment Models; Artificial Intelligence; Knowledge Based Systems*

**20010121571** Defence Science and Technology Organisation, Combatant Protection and Nutrition Branch, Fishermans Bend, Australia

**Background Bioaerosols and Aerosols at Two Sites in Northern Australia: Preliminary Measurements**

Tilley, R. Ian, Defence Science and Technology Organisation, Australia; Ho, Jim, Defence Science and Technology Organisation, Australia; Eamus, Derek, Defence Science and Technology Organisation, Australia; August 2001; 18p; In English

Report No.(s): DSTO-TR-1203; DODA-AR-012-008; Copyright; Avail: Issuing Activity

The biological aerosol content of the air has been measured at Darwin and RAAF Base Tindal in the Northern Territory of Australia. The number of culturable bacteria and fungal spores together with organic material caught in a spore trap are reported. The total airborne particulate matter in the size range 0.5 to 30 microns was also measured at Tindal in October 1998 and April 1999. The ability of an aerodynamic particle sizer to act as an early warning device for the presence of biological warfare agents in this environment is discussed. It was concluded that such a device could only be successfully used as a trigger in the event of a military release of a biological agent in an environment with a well characterized aerosol background.

Author

*Aerosols; Bacteria; Particles; Spores; Size Distribution*

**20010121949** Pacific Northwest National Lab., Richland, WA USA

**Groundwater Sampling and Analysis Plan for the 100-BC-5 Operable Unit**

Sweeney, M. D.; Sep. 25, 2000; 16p; In English

Report No.(s): DE2000-763207; PNNL-13326; No Copyright; Avail: Department of Energy Information Bridge, Microfiche

The purpose of this plan is to describe groundwater sampling and analysis for the Comprehensive Environmental Response, Compensation, and Liability Act (CERCLA) in the 1OO-BC-5Operable Unit. The plan describes the well network constituents analyzed, sampling protocol, and reporting and quality assurance requirements. Sampling and analysis requirements for this Operable Unit are specified in the change control form to the Federal Facility Agreement and Consent Order (Appendix A). The 100-BC-5 Operable Unit is the groundwater/surface water operable unit associated with past nuclear reactor operations in the 100-B,C Area of the U.S. Department of Energys (DOEs) Hanford Site. The operable unit includes the groundwater below the source operable units (100-BC- 1 through -4) plus the adjacent groundwater, surface water, sediments and aquatic biota impacted by 100-B,C Area operations (DOE/RL-90-08).

NTIS

*Ground Water; Water Sampling; Chemical Analysis*

**20010122250** Argonne National Lab., IL USA

**Fluid transfer concentration of airborne radioxenon to enhance monitoring capabilities**

Russ, W. R.; May 27, 1998; 13p; In English

Report No.(s): DE2001-10818; ANL/RA/CP-96529; No Copyright; Avail: Department of Energy Information Bridge, Microfiche

To facilitate airborne radioxenon monitoring, a xenon concentration method with potential advantages over current technology in simplicity, size, and cost has been developed. The concentration technique is based on the preferential absorption of heavy noble gases (krypton, xenon, and radon) by certain organic fluids. to implement this concentration technique, a radioxenon monitoring system requires three integrated sub-systems: (1) an absorption sub-system; (2) a degassing sub-system; and (3) a radiation detection sub-system. This study is focused on the characterization and optimization of the first two sub-systems. Measurements using a small prototype absorption tower have indicated a xenon removal factor of approximately 50% and the specific concentration at saturation of certain organic fluids to be about 2.5 times the specific concentration in the sampled air. Various techniques for degassing have been investigated, including heating, purging, agitation and vacuum. Ultrasonic agitation of a thin film in a strong vacuum has been shown to be an effective means of degassing the transfer fluid continuously. Various schemes for integrating all of the sub-systems are considered. Combining the small prototype absorption and degassing sub-systems should result in a transfer efficiency of about 33% and a single stage concentration factor of about 6.7.

NTIS

*Xenon; Radiation Detectors*

**20010122280** NASA Ames Research Center, Moffett Field, CA USA

**Direct Monitoring of Trace Atmospheric Species via Ion Trap Mass Spectrometry**

Palmer, P. T., NASA Ames Research Center, USA; Pearson, Richard, NASA Ames Research Center, USA; Saimonson, Jay D., NASA Ames Research Center, USA; Wong, Carla M., NASA Ames Research Center, USA; [1994]; 1p; In English; ASMS Conference on Mass Spectrometry and Applied Topics, 29 May - 3 Jun. 1994, Chicago, IL, USA

Contract(s)/Grant(s): RTOP 506-71-41; No Copyright; Avail: Issuing Activity; Abstract Only

There is an ever-increasing emphasis on the part of government agencies, academia, and industry on enhancing our understanding of atmospheric processes and assessing the impact of human activities on these processes. While issues such as the ozone hole and rising levels of greenhouse gases have received major attention. relatively little is known about the types, concentrations, sources, and sinks of hydrocarbons in the troposphere and stratosphere. Such information would be of tremendous utility in assessing the roles of various anthropogenic and biogenic processes on global carbon cycles. An ion trap mass spectrometer has been developed for monitoring trace levels of hydrocarbons in the atmosphere on NASA's DC-8 "flying laboratory". This aircraft is used to provide measurements in support of a number of "Mission to Planet Earth" activities and tropospheric chemistry experiments. In past missions, specific compounds have been monitored via highly specialized instrumentation, fast GO, or collection of whole air samples for subsequent ground-based analysis. The ion trap has several features. including small size. excellent sensitivity, and broad applicability, which make it highly atttrat:ive for atmospheric monitoring. The design of this instrument, its air sampling interface. and the various complications associated with aircraft-deployment will be described. Data showing the sensitivity of the instrument for detecting hydrocarbons at mixing ratios below one part-per-billion, and the use of MS/MS for direct, on-line, real-time monitoring will be presented.

Author

*Atmospheric Chemistry; Trace Elements; Environmental Monitoring; Ion Traps (Instrumentation); Mass Spectrometers; Hydrocarbons; Air Sampling*

**20010122287** Pacific Northwest National Lab., Richland, WA USA

**Groundwater Sampling and Analysis Plan for the 100-FR-3 Operable Unit**

Sweeney, M. D.; Sep. 25, 2000; 16p; In English

Report No.(s): DE2000-763205; PNNL-13327; No Copyright; Avail: Department of Energy Information Bridge, Microfiche

The purpose of this plan is to describe groundwater sampling and analysis for the Comprehensive Environmental Response, Compensation, and Liability Act (CERCLA) in the 100-FR-3Operable Unit. The plan describes the well network constituents analyzed, sampling protocol, and reporting and quality assurance requirements. Sampling and analysis requirements for this operable unit are specified in the change control form to the Federal Facility Agreement and Consent Order (Appendix A). The 100-FR-3 Operable Unit is the groundwater/surface water operable unit associated with past nuclear reactor operations in the 100-FArea of the U.S. Department of Energys (DOEs) Hanford Site. The operable unit includes the groundwater below the source operable units (100-FR-1 and 100-FR-2) plus the adjacent groundwater, surface water, sediments, and aquatic biota impacted by 100-FArea operations DOE/RL-93-82.

NTIS

*Ground Water; Water Sampling; Chemical Analysis*

**20010122297** NASA Ames Research Center, Moffett Field, CA USA

**Physical and Radiative Properties of Arctic Atmospheric Aerosols**

Pueschel, R. F., NASA Ames Research Center, USA; Kinne, S. A., NASA Ames Research Center, USA; [1994]; 1p; In English

Contract(s)/Grant(s): RTOP 464-14-16-10; No Copyright; Avail: Issuing Activity; Abstract Only

Atmospheric aerosols sampled in the Arctic basin by impactors have been analyzed for the total aerosol and its black carbon fraction. The mass of black carbon aerosol in the lower troposphere is one percent (1 g black carbon in 100 g total aerosol), reduced to one part in 10(exp 4) in the stratosphere. The aerosol single scatter albedos vary between 1.0 in the stratosphere, currently dominated by high light scattering due to Pinatubo volcanic aerosol, and 0.94 in the lower troposphere. The aerosol has the potential to regionally warm the earth-atmosphere system because of the high surface albedo of snow-covered surfaces in the Arctic.

Author

*Arctic Regions; Aerosols; Carbon; Light Scattering*

**20010122377** Argonne National Lab., IL USA
**Methods to reduce CO2 release to the atmosphere**
Jody, B. J.; Apr. 10, 1998; 8p; In English
Report No.(s): DE2001-10717; ANL/ES/CP-96052; No Copyright; Avail: Department of Energy Information Bridge, Microfiche

The U.S. anthropogenic emission of CO(sub 2) is over 5.5 billion tons a year. Over 1/3 of it is emitted by power plants, and 90% of all power plant emissions is released by coal fired units. Figure 1 shows the amount of coal used and the amount of electricity generated from coal over a several year period. Burning one lb of coal produces about 2.1 lbs of CO(sub 2) and about 1 kWh of electricity, or a 1000 MW coal-fired plant emits over 1000 tons of CO(sub 2) per hour. Therefore, power plants are good candidates for reducing CO(sub 2) emissions. Emissions can be reduced by conserving energy, fuel and oxidant treatment prior to combustion, using fuels with higher H/C ratios, and by capturing the CO(sub 2).

NTIS
*Air Pollution; Electricity; Carbon Dioxide; Coal*

**20010122803** California Univ., Lawrence Berkeley Lab., Berkeley, CA USA
**Dual alkali approaches for the capture and separation of CO(sub 2)**
Huang, H. P.; Shi, Y.; Li, W.; Chang, S. G.; Apr. 04, 2000; 22p; In English
Report No.(s): DE2001-775133; LBNL-45858; No Copyright; Avail: Department of Energy Information Bridge

The Solvay process utilizes two alkalis in sequential order to convert CO(sub 2) to sodium carbonate for commercial use. The ability to transform CO(sub 2) into sodium carbonate cost-effectively would be a breakthrough in CO(sub 2) sequestration by providing benign long-term storage of CO(sub 2). However, the Solvay process was not designed for CO(sub 2) sequestration and is not practical for use in the sequestration of CO(sub 2) from fossil fuel power plants. This paper investigates methods to modify the process in order to make it effective for the control of power plant CO(sub 2) emissions. The new modified process, called the Dual Alkali Approach, attempts to replace either or both bases, ammonia and lime, in the Solvay process with other compounds to make CO(sub 2) capture and separation efficient. Ammonia was replaced with different amines in aqueous solutions of salts and it was found that bicarbonate precipitation did occur. A method to regenerate the amine in the second step has not been implemented. However, the second step in Solvay Process has been implemented without using lime, namely, ammonia has been regenerated from an ammonium chloride solution using activated carbon. The HCl adsorbed in the activated carbon was removed by water to regenerate the activated carbon.

NTIS
*Alkalies; Carbon Dioxide; Ammonia; Hydrochloric Acid; Fossil Fuels*

**20010122822** Los Alamos National Lab., NM USA
**Accelerated Monte Carlo for particle dispersion**
Fitzgerald, M.; Picard, R.; Sep. 01, 2000; 18p; In English
Report No.(s): DE2000-763927; LA-UR-00-4528; No Copyright; Avail: Department of Energy Information Bridge

We discuss adaptive importance sampling for individual steps in Markov chains. Such chains arise in many simulation problems, such as related to airborne particle dispersion. Through use of experimental design for simulation runs and regression methods for analysis of the output, import ante sampling transit ion kernels are defined which substantially improve convergence times.

NTIS
*Air Pollution; Monte Carlo Method; Particle Diffusion; Markov Chains*

**20010123090** Argonne National Lab., IL USA
**Argonne National Laboratory - West's approach to filter characterization**
Miller, T. A.; Feb. 10, 1999; 14p; In English
Report No.(s): DE2001-10972; ANL/NT/CP-97317; No Copyright; Avail: Department of Energy Information Bridge, Microfiche

Like other DOE facilities, ANL-W uses a variety of nuclear grade, industrial grade, or furnace-type particulate filters to control airborne radioactivity and hazardous contaminants in radiological containment structures or processes. As designed, these filters entrain and ultimately concentrate contaminants in the media. Toxic metal contaminants include cadmium, chromium, lead; and mercury present in sufficient concentrations to exhibit the hazardous waste characteristic of toxicity as defined in 40 CFR 261.24. Radionuclide contaminants deposited in the media may at times accumulate in sufficient quantity to classify the filter as transuranic or remote-handled waste. Upon their removal from the ventilation system, these particulate filters become wastes, which must be characterized to determine their hazardous and radioactive classifications. A well defined filter characterization

process is essential for the proper/consistent waste characterization and minimization and for maintaining personnel radiological exposures as-low-as-reasonably-achievable (ALARA) (1,2). ANL-W has developed an approach to filter sampling and characterization to meet these needs. The ANL-W filter sampling and characterization process is designed to ensure representative sampling and/or process knowledge is utilized in characterizing the filters. The data obtained through sampling and/or process knowledge is used to show compliance with the Resource Conservation and Recovery Act (3) and Treatment/Storage/Disposal Facility Waste Acceptance Criteria. The ANL-W filter characterization involves the collection of process information, filter handling and sampling, sample analysis, data management filter characterization, and waste handling. Each element of the process is streamlined to ensure proper characterization while minimizing radiological exposure to maintenance workers, samplers, laboratory personnel, and waste handlers.
NTIS
*Air Filters; Hazardous Wastes; Radioactive Contaminants; Radioactive Wastes; Waste Management; Research Facilities*

**20010123091** Argonne National Lab., IL USA
**Options and cost for disposal of NORM waste**
Veil, J. A.; Oct. 22, 1998; 16p
Report No.(s): DE2001-11076; ANL/EA/CP-97554; No Copyright; Avail: Department of Energy Information Bridge, Microfiche

Oil field waste containing naturally occurring radioactive material (NORM) is presently disposed of both on the lease site and at off-site commercial disposal facilities. The majority of NORM waste is disposed of through underground injection, most of which presently takes place at a commercial injection facility located in eastern Texas. Several companies offer the service of coming to an operator's site, grinding the NORM waste into a fine particle size, slurrying the waste, and injecting it into the operator's own disposal well. One company is developing a process whereby the radionuclides are dissolved out of the NORM wastes, leaving a nonhazardous oil field waste and a contaminated liquid stream that is injected into the operator's own injection well. Smaller quantities of NORM are disposed of through burial in landfills, encapsulation inside the casing of wells that are being plugged and abandoned, or land spreading. It is difficult to quantify the total cost for disposing of NORM waste. The cost components that must be considered, in addition to the cost of the operation, include analytical costs, transportation costs, container decontamination costs, permitting costs, and long-term liability costs. Current NORM waste disposal costs range from $15/bbl to $420/bbl.
NTIS
*Oil Fields; Radioactive Materials; Waste Disposal*

**20010123132** Brookhaven National Lab., Upton, NY USA
**Particles of difference. Conference on Air Quality II**
Schwartz, S. E.; Sep. 21, 2000; 20p; In English
Report No.(s): DE2000-767113; BNL-67468; KP1201030; No Copyright; Avail: Department of Energy Information Bridge

It is no longer appropriate, if it ever was, to think of atmospheric aerosols as homogeneous spheres of uniform composition and size. Within the USA, and even more globally, not only the mass loading but also the composition, morphology, and size distribution of atmospheric aerosols are highly variable, as a function of location, and at a given location as a function of time. Particles of a given aerodynamic size may differ from one another, and even within individual particles material may be inhomogeneously distributed, as for example, carbon spherules imbedded in much larger sulfate particles. Some of the particulate matter is primary, that is, introduced into the atmosphere directly as particles, such as carbon particles in diesel exhaust. Some is secondary, that is, formed in the atmosphere by gas-to-particle conversion. Much of the material is inorganic, mainly sulfates and nitrates resulting mainly from energy-related emissions. Some of the material is carbonaceous, in part primary, in part secondary, and of this material some is anthropogenic and some biogenic. While the heterogeneity of atmospheric aerosols complicates the problem of understanding their loading and distribution, it may well be the key to its solution. by detailed examination of the materials comprising aerosols it is possible to infer the sources of these materials. It may be possible as well to identify specific health impairing agents. The heterogeneity of aerosol particles is thus the key to identifying their sources, to understanding the processes that govern their loading and properties, and to devising control strategies that are both effective and efficient. Future research must therefore take cognizance of differences among aerosol particles and use these differences to advantage.
NTIS
*Aerosols; Particulates*

**20010123402** Johns Hopkins Univ., Atmospheric and Ionospheric Remote Sensing Group, Laurel, MD USA
**Photolysis Rate Coefficient Calculations in Support of SOLVE Campaign** ***Final Report***
Lloyd, Steven A., Johns Hopkins Univ., USA; Swartz, William H., Johns Hopkins Univ., USA; Nov. 20, 2001; 10p; In English
Contract(s)/Grant(s): NAG1-2270; No Copyright; Avail: CASI; A02, Hardcopy; A01, Microfiche

The objectives for this SOLVE project were 3-fold. First, we sought to calculate a complete set of photolysis rate coefficients (j-values) for the campaign along the ER-2 and DC-8 flight tracks. En route to this goal, it would be necessary to develop a comprehensive set of input geophysical conditions (e.g., ozone profiles), derived from various climatological, aircraft, and remotely sensed datasets, in order to model the radiative transfer of the atmosphere accurately. These j-values would then need validation by comparison with flux-derived j-value measurements. The second objective was to analyze chemistry along back trajectories using the NASA/Goddard chemistry trajectory model initialized with measurements of trace atmospheric constituents. This modeling effort would provide insight into the completeness of current measurements and the chemistry of Arctic wintertime ozone loss. Finally, we sought to coordinate stellar occultation measurements of ozone (and thus ozone loss) during SOLVE using the Midcourse Space Experiment(MSX)/Ultraviolet and Visible Imagers and Spectrographic Imagers (UVISI) satellite instrument. Such measurements would determine ozone loss during the Arctic polar night and represent the first significant science application of space-based stellar occultation in the Earth's atmosphere.
Author
*Photolysis; Satellite Instruments; Earth Atmosphere; Remote Sensing; Climatology; Ozone Depletion*

**20010123430** Photonic Sensor Systems, Inc., Atlanta, GA USA
**Sensor System to Monitor Ammonia** ***Final Report***
Edwards, J. G.; Oct. 01, 1999; 18p; In English
Report No.(s): DE2001-763210; DOE/GO/10005-F; No Copyright; Avail: Department of Energy Information Bridge, Microfiche

This final technical report summarizes the results of a project to develop a prototype integrated optic ammonia NHJ sensor for agricultural and industrial applications. The majority of the support for this project was provided by the Department of Energy (DOE) through Cooperative Agreement DE-FC36-94GO1OOO5. The sensor is based on a planar integrated optic wave guide interferometer developed at the Georgia Tech Research Institute (GTRI). The feasibility of using this technology for detecting ammonia was first demonstrated at GTRI with assistance from DOE through Cooperative Agreement DE-FC02-891D12905. This project is a continuation of that work. The overall goal is to develop a gas-phase ammonia sensor suitable for: 1: monitoring gaseous nitrogen transfer from agricultural crop lands and 2: facilitating the use of ammonia in a variety of industrial applications such as ammonia production and large scale refrigeration. The specific objective of this phase of the project was to fabricate a prototype ammonia sensor and evaluate its accuracy and reliability in real-world settings. Four major tasks were planned: design and fabrication, testing and characterization, evaluation, and reporting.
NTIS
*Ammonia; Remote Sensing; Design Analysis*

**20010123436** Los Alamos National Lab., NM USA
**Emergency Responders' 'Rules-of-Thumb' for Air Toxics Release in Urban Environments**
Brown, M. J.; Jun. 08, 1999; 25p; In English
Report No.(s): DE2001-763179; LA-UR-98-4539; No Copyright; Avail: Department of Energy Information Bridge, Microfiche

For an outdoor plume release, closing the windows and doors and staying inside may be initially safer than remaining indoors. Due to infiltration (e.g., leaks, ventilation) there may come a time when it is actually safer to be outdoors rather than indoors. Emergency response decision makers responsible for public announcements should be aware that safe zones may change from inside buildings to outside buildings during the course of an event. Simple dispersion models exist to approximate both outdoor and indoor concentrations as a function of time. Unfortunately, the ventilation of buildings is case dependent, so that strict guidelines for when to go outside may be difficult to derive. (e.g., nitrogen oxides, carbon monoxide, ozone, particulate, volatile organic compounds). Although the sources are typically not representative of short-time plume releases, the results from these studies can be used to help interpret indoor vs. outdoor relationships. Results should be viewed with caution, however, as indoor sources of air pollution (e.g., CO from stoves, VOC'S (voltile organic compounds) from carpets and paints) can confuse comparisons. Several studies indicate that pollutant levels indoors follow the general trends outdoors.
NTIS
*Air Pollution; Public Health; Urban Planning*

**20010123462** Argonne National Lab., IL USA

**Regional emissions of air pollutants in China**

Streets, D. G.; Oct. 05, 1998; 17p; In English

Report No.(s): DE2001-10991; ANL/DIS/CP-97401; No Copyright; Avail: Department of Energy Information Bridge, Microfiche

As part of the China-MAP program, sponsored by the US National Aeronautics and Space Administration, regional inventories of air pollutants emitted in China are being characterized, in order that the atmospheric chemistry over China can be more fully understood and the resulting ambient concentrations in Chinese cities and the deposition levels to Chinese ecosystems be determined with better confidence. In addition, the contributions of greenhouse gases from China and of acidic aerosols that counteract global warming are being quantified. This paper presents preliminary estimates of the emissions of some of the major air pollutants in China: sulfur dioxide (SO2), nitrogen oxides (NO(sub x)), carbon monoxide (CO), and black carbon (C). Emissions are estimated for each of the 27 regions of China included in the RAINS-Asia simulation model and are subsequently distributed to a 1(degree) x 1(degree) grid using appropriate disaggregation factors. Emissions from all sectors of the Chinese economy are considered, including the combustion of biofuels in rural homes. Emissions from larger power plants are calculated individually and allocated to the grid accordingly. Data for the period 1990-1995 are being developed, as well as projections for the future under alternative assumptions about economic growth and environmental control.

NTIS

*Air Quality; Atmospheric Chemistry; Air Pollution; China*

**20010123549** Federal Energy Technology Center, Morgantown, WV USA

**Engineering development of coal-fired high-performance power systems**

Oct. 01, 1998; 27p; In English

Report No.(s): DE2001-7931; DE-AC22-95PC95143-12; No Copyright; Avail: Department of Energy Information Bridge

A High Performance Power System (HIPPS) is being developed. This system is a coal-fired, combined cycle plant with indirect heating of gas turbine air. Foster Wheeler Development Corporation and a team consisting of Foster Wheeler Energy Corporation, Bechtel Corporation, University of Tennessee Space Institute and Westinghouse Electric Corporation are developing this system. In Phase 1 of the project, a conceptual design of a commercial plant was developed. Technical and economic analyses indicated that the plant would meet the goals of the project which include a 47 percent efficiency (HHV) and a 10 percent lower cost of electricity than an equivalent size PC plant. The concept uses a pyrolyzation process to convert coal into fuel gas and char. The char is fired in a High Temperature Advanced Furnace (HITAF). The HITAF is a pulverized fuel-fired boiler/air heater where steam is generated and gas turbine air is indirectly heated. The fuel gas generated in the pyrolyzer is then used to heat the gas turbine air further before it enters the gas turbine. The project is currently in Phase 2, which includes engineering analysis, laboratory testing and pilot plant testing. Research and development is being done on the HIPPS systems that are not commercial or being developed on other projects. Pilot plant testing of the pyrolyzer subsystem and the char combustion subsystem are being done separately, and after each experimental program has been completed, a larger scale pyrolyzer will be tested at the Power Systems Development Facility (PSDF) in Wilsonville, AL. The facility is equipped with a gas turbine and a topping combustor, and as such, will provide an opportunity to evaluate integrated pyrolyzer and turbine operation. This report addresses the areas of technical progress for this quarter. In order to prepare the CETF for the HIPPS char combustion test program, the following three subsystems were designed during this quarter: (1) Flue Gas Recycle System; (2) Pulverized Coal Feed System; and (3) Limestone Feed System The flue gas recycle system is added to simulate the performance of a commercial char burner fired with gas turbine exhaust. Since synthetically made char will be used for the tests at the CETF, the limestone injection system was added to produce a char more representative of that from an actual pyrolyzer. The pulverized coal system is included to provide a supplemental support fuel if a stable flame can not be maintained with char firing only.

NTIS

*Coal; Combustion Chambers; Pilot Plants; Regeneration (Engineering); Flue Gases; Recycling*

**20010123550** Federal Energy Technology Center, Morgantown, WV USA

**Novel process for removal and recovery of vapor-phase mercury**

Oct. 20, 1998; 5p; In English

Report No.(s): DE2001-7928; DE-AC22-95PC95257-34; No Copyright; Avail: Department of Energy Information Bridge

The purpose of this project is to investigate the application of a sorbent-based process for removing and recovering mercury in the flue gas of coal-fired power plants. The process is based on the sorption of mercury by noble metals and the regeneration of the sorbent by thermal means, recovering the desorbed mercury for recycling. ADA Technologies holds a patent on this process (US 5,409,522) and has tested it under conditions typical of municipal waste incinerators. In this process, the noble metal sorbent

is regenerated thermally, and the mercury is recovered for commercial recycle. Consequently, ADA has adopted the name 'Mercu-RE' to describe its process. ADA has been testing its process under conditions typical of coal-fired power plants where the mercury concentration is low (below 10 (micro)g/m(sup 3)) and little pressure drop can be tolerated. Methods of accommodating the Mercu-RE process to the circumstances and conditions of coal-fired power plants comprise the core of the program.
NTIS
*Flue Gases; Vapor Phases; Power Plants; Recycling; Mercury (Metal)*

**20010123626** Federal Energy Technology Center, Morgantown, WV USA
**Novel Process for Removal and Recovery of Vapor-Phase Mercury**
Jan. 21, 2000; 6p; In English
Report No.(s): DE2000-767332; DE-AC22-95PC95257-39; No Copyright; Avail: Department of Energy Information Bridge, Microfiche

The purpose of this project is to investigate the application of a sorbent-based process for removing and recovering mercury in the flue gas of coal-fired power plants. The process is based on the sorption of mercury by noble metals and the regeneration of the sorbent by thermal means, recovering the desorbed mercury for recycling. ADA Technologies holds a patent on this process (US 5,409,522) and has tested it under conditions typical of municipal waste incinerators. In this process, the noble metal sorbent is thermally regenerated, and the mercury is recovered for commercial recycle or disposal. ADA has adopted the name 'Mercu-RE' to describe its process.
NTIS
*Sorption; Vapor Phases; Mercury (Metal); Removal*

**20010123635** Bechtel Nevada Corp., Las Vegas, NV USA
**National Emission Standards for Hazardous Air Pollutants, Calendar Year 1999**
Grossman, R. F.; Jun. 01, 2000; 58p; In English
Report No.(s): DE2000-764941; DOE/NV/11718-442; No Copyright; Avail: Department of Energy Information Bridge

The Nevada Test Site (NTS) is operated by the US Department of Energy's Nevada Operations Office (DOE/NV) as the site for nuclear weapons testing, now limited to readiness activities and experiments in support of the national Stockpile Stewardship Management Program. It is located in Nye County, Nevada, with the southeast corner about 105 km (65 mi) northwest of Las Vegas, Nevada. The NTS covers about 3,561 sq km (1,375 sq mi), an area larger than Rhode Island. Its size is about 46 to 56 km (28 to 35 mi) east to west and from 64 to 88 km (40 to 55 mi) north to south. The NTS is surrounded, except on the south side, by public exclusion areas (Nellis Air Force Range (NAFR)) that provide another 24 to 104 km (15 to 65 mi) between the NTS and public lands. The NTS is characterized by desert valley and Great Basin mountain topography, with a climate, flora, and fauna typical of the southwest deserts. Population density within 150 km (93 mi) of the NTS is only about 0.2 persons per square kilometer, excluding the Las Vegas area. Restricted access, low population density in the surrounding area, and extended wind transport times are advantageous factors for the activities conducted at the NTS. Surface waters are scarce on the NTS and there is great depth to slow-moving groundwater.
NTIS
*Air Pollution; Deserts; Exhaust Emission; Pollution Control; Standards*

**20010123650** National Science Foundation, Arlington, VA USA
**Atmospheric Chemistry Colloquium for Emerging Senior Scientists, 1997**
Wine, P. H.; Nov. 23, 1998; 41p; In English
Report No.(s): DE2001-764601; DOE/ER/62484-F; No Copyright; Avail: Department of Energy Information Bridge

The Department of Energy's Atmospheric Chemistry Program is providing partial funding for the Atmospheric Chemistry Colloquium for Emerging Senior Scientists (ACCESS) and FY 1997 Gordon Research Conference in Atmospheric Chemistry.
NTIS
*Atmospheric Chemistry; Conferences*

**20010123751** Argonne National Lab., IL USA
**Emission estimates for air pollution transport models**
Streets, D. G.; Oct. 09, 1998; 14p; In English
Report No.(s): DE2001-11036; ANL/DIS/CP-97412; No Copyright; Avail: Department of Energy Information Bridge

The results of studies of energy consumption and emission inventories in Asia are discussed. These data primarily reflect emissions from fuel combustion (both biofuels and fossil fuels) and were collected to determine emissions of acid-deposition precursors (SO2) and NO(sub x)) and greenhouse gases (CO2, CO, CH4, and NMHC) appropriate to RAINS-Asia regions. Current work is focusing on black carbon (soot), volatile organic compounds, and ammonia.
NTIS
*Air Pollution; Energy Consumption; Fuel Combustion; Pollution Transport; Acid Rain*

**20010123923** Argonne National Lab., IL USA
**Regional-scale influences on urban air quality: A field study in Phoenix, Arizona**
Gaffney, J. S.; Oct. 12, 1998; 9p; In English
Report No.(s): DE2001-11028; ANL/ER/CP-96886; No Copyright; Avail: Department of Energy Information Bridge, Microfiche

Regional air quality can play an important role in determining whether urban ozone or PM-2.5 standards are exceeded. Background levels of nitrogen oxide species (NO(sub x)) and their interactions with natural organics can generate secondary aerosol products via formation of nitric acid and its subsequent reaction with ammonia to form ammonium nitrate. Natural organics and reactive anthropogenic organic compounds, particularly aromatic species and monoterpenes, can also lead to the formation of secondary organic aerosols, contributing to the formation of PM-2.5. Long-range transport and chemical transformation of hydrocarbons and NO(sub x) via both photochemical reactions and nighttime chemistry can yield significant regional levels of ozone and other oxidants, such as peroxyacyl nitrates (R-C=O-O-O-NO2); PANs). The PANs are key species in determining the apparent age of an air parcel. The most common member of the family is peroxyacetyl nitrate (R=CH3-; PAN), which typically accounts for more than 85% of the PANs found in an urban or rural site. The PANs are in equilibrium with NO2. Peroxyacyl radicals (R-C=O-O-O) are typically produced by the photooxidation reactions of organics, particularly those of aldehyde oxidation products with OH radical during the daytime (photochemically active) periods. Proposed mechanisms for nighttime formation of PANs include abstraction reactions of nitrate radical (NO3) and the initiation of OH chemistry by olefin-ozone reactions.
NTIS
*Air Quality; Atmospheric Chemistry; Arizona; Aerosols*

**20010124073** NASA Goddard Space Flight Center, Greenbelt, MD USA
**Importance of the Annual Cycles of SST and Solar Irradiance for Circulation and Rainfall: A Climate Model Simulation Study**
Sud, Yogesh C., NASA Goddard Space Flight Center, USA; Lau, William K. M., NASA Goddard Space Flight Center, USA; Walker, G. K., General Sciences Corp., USA; Mehta, V. M., Maryland Univ., USA; [2001]; 30p; In English; No Copyright; Avail: CASI; A03, Hardcopy; A01, Microfiche

Annual cycle of climate and precipitation is related to annual cycle of sunshine and sea-surface temperatures. Understanding its behavior is important for the welfare of humans worldwide. For example, failure of Asian monsoons can cause widespread famine and grave economic disaster in the subtropical regions. For centuries meteorologists have struggled to understand the importance of the summer sunshine and associated heating and the annual cycle of sea-surface temperatures (SSTs) on rainfall in the subtropics. Because the solar income is pretty steady from year to year, while SSTs depict large interannual variability as consequence of the variability of ocean dynamics, the influence of SSTs on the monsoons are better understood through observational and modeling studies whereas the relationship of annual rainfall to sunshine remains elusive. However, using NASA's state of the art climate model(s) that can generate realistic climate in a computer simulation, one can answer such questions. We asked the question: if there was no annual cycle of the sunshine (and its associated land-heating) or the SST and its associated influence on global circulation, what will happen to the annual cycle of monsoon rains? by comparing the simulation of a 4-year integration of a baseline Control case with two parallel anomaly experiments: 1) with annual mean solar and 2) with annual mean sea-surface temperatures, we were able to draw the following conclusions: (1) Tropical convergence zone and rainfall which moves with the Sun into the northern and southern hemispheres, specifically over the Indian, African, South American and Australian regions, is strongly modulated by the annual cycles of SSTs as well as solar forcings. The influence of the annual cycle of solar heating over land, however, is much stronger than the corresponding SST influence for almost all regions, particularly the subtropics; (2) The seasonal circulation patterns over the vast land-masses of the Northern Hemisphere at mid and high latitudes also get strongly influenced by the annual cycles of solar heating. The SST influence is largely limited to the oceanic regions of these latitudes; (3) The annual mode of precipitation over Amazonia has an equatorial regime revealing a maxima in the month of March associated with SST, and another maxima in the month of January associated with the solar annual cycles, respectively. The baseline simulation, which has both annual cycles, depicts both annual modes and its rainfall is virtually equal to the sum of those two modes; (4) Rainfall over Sahelian-Africa is significantly reduced (increased) in simulations lacking

(invoking) solar irradiation with (without) the annual cycle. In fact, the dominant influence of solar irradiation emerges in almost all monsoonal-land regions: India, Southeast Asia, as well as Australia. The only exception is the Continental USA, where solar annual cycle shows only a relatively minor influence on the annual mode of rainfall.
Author
*Annual Variations; Sea Surface Temperature; Solar Radiation; Atmospheric Circulation; Rain; Climate Models; Sunlight*

**20010124079** Federal Energy Technology Center, Morgantown, WV USA
**In situ infrared study of catalytic decomposition of NO**
AlmUSAiteer, K.; Krishnamurthy, R.; Chuang, S. S. C.; Aug. 18, 1998; 28p; In English
Report No.(s): DE2001-7924; DE-FG22-95PC95224-06; No Copyright; Avail: Department of Energy Information Bridge

The growing concerns for the environment and increasingly stringent standards for NO emission have presented a major challenge to control NO emissions from electric utility plants and automobiles. Catalytic decomposition of NO is the most attractive approach for the control of NO emission for its simplicity. Successful development of an effective catalyst for NO decomposition will greatly decrease the equipment and operation cost of NO control. Due to lack of understanding of the mechanism of NO decomposition, efforts on the search of an effective catalyst have been unsuccessful. Scientific development of an effective catalyst requires fundamental understanding of the nature of active site, the rate-limiting step, and an approach to prolong the life of the catalyst. Research is proposed to study the reactivity of adsorbates for the direct NO decomposition and to investigate the feasibility of two novel approaches for improving catalyst activity and resistance to sintering. The first approach is the use of silanation to stabilize metal crystallites and supports for Cu-ZSM-5 and promoted Pt catalysts; the second is utilization of oxygen spillover and desorption to enhance NO decomposition activity. An innovative infrared reactor system will be used to observe and determine the dynamic behavior and the reactivity of adsorbates during NO decomposition, oxygen spillover, and silanation. A series of experiments including X-ray diffraction, temperature programmed desorption, temperature programmed reaction, X-ray photoelectron spectroscopy will be used to characterized the catalysts. The information obtained from this study will provide a scientific basis for developing an effective catalyst for the NO decomposition under practical flue gas conditions.
NTIS
*Catalysts; Decomposition; Infrared Radiation; Nitrous Oxides; Exhaust Emission; Flue Gases*

**20010125000** Pacific Northwest National Lab., Richland, WA USA
**Project W420 Air Sampler Probe Placement Qualification Tests for Four 6-Inch Diameter Stacks: 296-A-25, 296-B-28, 296-S-22, and 296-T-18**
Maughan, A. D.; Glissmeyer, J. A.; Sep. 30, 1998; 74p; In English
Report No.(s): DE2001-941; PNNL-12016; No Copyright; Avail: Department of Energy Information Bridge, Microfiche

The W420 project covers the upgrading of effluent monitoring systems at six ventilation exhaust stacks in tank-farm facilities at the U.S. Department of Energy's Hanford Site. The discharge stacks of five of the six systems will be completely replaced. Four of these (296-A-25, 296-B-28, 296-S-22, and 296-T-18) will be of the same size, 6-inches in diameter and about 12-ft high. This report documents tests that were conducted to verify that these four stacks meet the applicable regulatory criteria regarding the placement of the air sampling probe. These criteria ensure that the contaminants in the stack are well mixed with the airflow at the location of the probe such that the extracted sample represents the whole. There are also criteria addressing the transport of the sample to the collection device. These are not covered in this report, but will need to be addressed later. These tests were conducted by Pacific Northwest National Laboratory on a full-scale model of the 6-inch stick. The sequence of tests addresses the acceptability of the flow angle relative to the probe and the uniformity of air velocity and gaseous and particle tracers in the cross section of the stack. All tests were successful, and all acceptance criteria were met.
NTIS
*Air Sampling; Performance Tests; Stacks; Monitors*

**20010125001** Federal Energy Technology Center, Morgantown, WV USA
**Technology Assessment of Dust Suppression Techniques applied During Structural Demolition**
Boudreaux, J. F.; Ebadian, M. A.; Dua, S. K.; Aug. 06, 1997; 25p; In English
Report No.(s): DE2001-955; DE-FG21-95EW55094-18; No Copyright; Avail: Department of Energy Information Bridge, Microfiche

Hanford, Fernald, Savannah River, and other sites are currently reviewing technologies that can be implemented to demolish buildings in a cost-effective manner. In order to demolish a structure and, at the same time, minimize the amount of dust generated by a given technology, an evaluation must be conducted to choose the most appropriate dust suppression technology. Thus, the purpose of this research, which was conducted by the Hemispheric Center for Environmental Technology (HCET) at Florida

International University (FIU), was to perform an experimental study of dust aerosol abatement (dust suppression) methods as applied to nuclear D and D. This experimental study specifically targeted the problem of dust suppression during demolition. The resulting data were used in the development of mathematical correlations that can be applied to structural demolition. In the Fiscal Year 1996 (FY96), the effectiveness of different dust suppressing agents was investigated for different types of concrete blocks. Initial tests were conducted in a broad particle size range. In Fiscal Year 1997 (FY97), additional tests were performed in the size range in which most of the particles were detected. Since particle distribution is an important parameter for predicting deposition in various compartments of the human respiratory tract, various tests were aimed at determining the particle size distribution of the airborne dust particles. The effectiveness of dust suppressing agents for particles of various size was studied. Instead of conducting experiments on various types of blocks, it was thought prudent to carry out additional tests on blocks of the same type. Several refinements were also incorporated in the test procedures and data acquisition system used in FY96.
NTIS
*Aerosols; Dust; Technology Assessment; Buildings*

**20010125019** California Univ., Lawrence Berkeley Lab., Berkeley, CA USA
**Estimating the greenhouse gas benefits of forestry projects: A Costa Rican Case Study**
Busch, C.; Sathaye, J.; Arturo, G.; Azofeifa, S.; Sep. 01, 2000; 117p; In English
Report No.(s): DE2000-764328; LBNL-42289; No Copyright; Avail: Department of Energy Information Bridge

If the Clean Development Mechanism proposed under the Kyoto Protocol is to serve as an effective means for combating global climate change, it will depend upon reliable estimates of greenhouse gas benefits. This paper sketches the theoretical basis for estimating the greenhouse gas benefits of forestry projects and suggests lessons learned based on a case study of Costa Rica's Protected Areas Project, which is a 500,000 hectare effort to reduce deforestation and enhance reforestation. The Protected Areas Project in many senses advances the state of the art for Clean Development Mechanism-type forestry projects, as does the third-party verification work of SGS International Certification Services on the project. Nonetheless, sensitivity analysis shows that carbon benefit estimates for the project vary widely based on the imputed deforestation rate in the baseline scenario, e.g. the deforestation rate expected if the project were not implemented. This, along with a newly available national dataset that confirms other research showing a slower rate of deforestation in Costa Rica, suggests that the use of the 1979--1992 forest cover data originally as the basis for estimating carbon savings should be reconsidered. When the newly available data is substituted, carbon savings amount to 8.9 Mt (million tones) of carbon, down from the original estimate of 15.7 Mt. The primary general conclusion is that project developers should give more attention to the forecasting land use and land cover change scenarios underlying estimates of greenhouse gas benefits.
NTIS
*Climatology; Costa Rica; Estimating; Forest Management; Greenhouse Effect*

**20010125096** California Energy Commission, Sacramento, CA USA
**Global Climate Change (1997): Greenhouse Gas Emissions Reduction Strategies for California, Volume 2**
January 1998; 180p; In English; Original contains color illustrations
Report No.(s): PB2001-108342; P500-98-001V2; No Copyright; Avail: CASI; A09, Hardcopy; A02, Microfiche

Over the past 20 years, the potential for human-made emissions of greenhouse gases to damage the earth's atmosphere has become an issue of increasing concern to scientific communities and leaders of the world's industrialized nations. For billions of years, naturally-occurring greenhouse gases, primarily carbon dioxide (CO2), methane (CH4), nitrous oxide (N2O), tropospheric (lower atmosphere) ozone (O3), and water vapor have maintained the balance of the earth's atmosphere, stabilizing temperatures in a range that allows life as we know it to exist. Now, in the last days of the 20th Century, evidence is growing that anthropogenic sources of these gases have the potential to substantially alter that balance, and global climate patterns, posing significant economic and environmental risks to all nations. In December, 1995, the United Nations' Intergovernmental Panel on Climate Change, which includes over 2,500 scientists, issued its report stating that 'the balance of evidence suggests a discernible human influence on global climate.'
NTIS
*Environment Effects; Air Pollution; Climate Change; California; Greenhouse Effect; Global Warming; Energy Policy*

**20010125097** California Energy Commission, Sacramento, CA USA
**Global Climate Change, 1997: Greenhouse Gas Emissions Reduction Strategies for California, Volume 1, v**
January 1998; 26p; In English
Report No.(s): PB2001-108341; P500-98-001V1; No Copyright; Avail: CASI; A03, Hardcopy; A01, Microfiche

California has led the nation in adopting far-reaching policies to improve energy efficiency, reduce energy costs, and mitigate the adverse impacts on the environment of energy production and use. As well as reducing energy use as a matter of sound economic and environmental policy, the state has substantially reduced emissions that contribute to global climate change, including carbon dioxide and methane. Major state policies have included creating energy-efficient buildings and requiring energy-saving appliances; developing energy-efficient industrial processes; promoting lower-emission alternatives to gasoline and diesel fuel; substantial switching to cleaner natural gas to generate electricity; and researching, developing and commercializing renewable energy resources. Although some of California's lower energy use is the result of a milder climate and less energy-intensive industries than many other states, it is partly because of these energy policies that California's carbon dioxide (CO2) emissions are about 40 percent less, per capita, than the national average.
NTIS
*Environment Pollution; Clean Energy; Clean Fuels; California; Energy Conversion Efficiency; Renewable Energy; Exhaust Gases*

**20010125099** California Energy Commission, Sacramento, CA USA
**Air Quality Emission Offsets: Constraints and Opportunities for Power Plant Development Projects**
August 1997; 42p; In English
Report No.(s): PB2001-108318; P700-97-002; No Copyright; Avail: CASI; A03, Hardcopy; A01, Microfiche
This report provides information to decision makers and interested parties on the air quality constraints to and opportunities for developing new power plants in California. It is based on a description of air districts' ambient air quality standards attainment status, offset requirements, offset strategies allowed, and offset costs and availability. Air quality issues (particularly offsets availability) are often very complex when considered during the review of a power plant licensing case. This report hopefully provides the information needed to resolve some of these issues in advance of licensing cases.
NTIS
*Air Pollution; Emission; Electric Power Plants; California; Regulations*

**20010125147** NASA Ames Research Center, Moffett Field, CA USA
**Biomass Burning Emissions in the Cerrado of Brazil Computed with Remote Sensing Data and GIS**
Guild, Liane S., NASA Ames Research Center, USA; Brass, James A., NASA Ames Research Center, USA; Chatfield, Robert B., NASA Ames Research Center, USA; Hlavka, Christine A., NASA Ames Research Center, USA; Riggan, Philip J., San Francisco State Univ., USA; Setzer, Alberto, Instituto Nacional de Pesquisas Espacias, Brazil; Pereira, Joao A. Raposo, Instituto Brasileiro do Meio Ambiente e dos Recursos Naturais Renovaveis, Brazil; [1994]; 1p; In English; International Symposium on Resource and Environmental Monitoring, 26-30 Sep. 1994, Rio de Janeiro, Brazil
Contract(s)/Grant(s): RTOP 579-43-03-10; No Copyright; Avail: Issuing Activity; Abstract Only
Biomass burnin is a common force in much of the developing tropical world where it has wide-ranging environmental impacts. Fire is a component of tropical deforestation and is 0 p often used to clear broad expanses of land for shifting agriculture and cattle ranching. Frequent burning in the tropical savannas is a distinct problem from that of primary forest. In Brazil, most of the burning occurs in the cerrado which occupies approximately 1,800,000 km2, primarily on the great plateau in central Brazil. Wildland and agricultural fires are dramatic sources of regional air pollution in central Brazil. Biomass burning is an important source of a large number of trace gases including greenhouse gases and other chemically active species. Knowledge of trace gas emissions from biomass burning in Brazil is limited by a number of factors, most notably relative emission factors for gases from specific fire types/fuels and accurate estimates of temporal and spatial distribution and extent of fire activity. Estimates of trace gas emissions during September 1992 will be presented that incorporates a digital map of vegetation classes, pyrogenic emission factors calculated from ground and aircraft missions, and Instituto Nacional de Pesquisas Espaciais (INPE) fire products derived from Advanced Very High Resolution Radiometer (AVHRR) data. The regional emissions calculated from National Oceanographic and Atmospheric Administration (NOAA) AVHRR estimates of fire activity will provide an independent estimate for comparison with results obtained by the National Aeronautics and Space Administration (NASA) Transport and Atmospheric Chemistry Near the Equator - Atlantic (TRACE-A) experiments.
Author
*Atmospheric Chemistry; Biomass Burning; Brazil; Remote Sensing; Oceanography; Exhaust Emission*

**20010125150** NASA Ames Research Center, Moffett Field, CA USA

## Simulating Local and Intercontinental Pollutant Effects of Biomass Burning: Integration of Several Remotely Sensed Datasets

Chatfield, Robert B., NASA Ames Research Center, USA; Vastano, John A., NASA Ames Research Center, USA; Guild, Liane, NASA Ames Research Center, USA; Hlavka, Christine, NASA Ames Research Center, USA; Brass, James A., NASA Ames Research Center, USA; [1994]; 2p; In English; ECORIO 1994, Unknown

Contract(s)/Grant(s): RTOP 579-43-03-10; No Copyright; Avail: Issuing Activity; Abstract Only

Burning to clear land for crops and to destroy pests is an integral and largely unavoidable part of tropical agriculture. It is easy to note but difficult to quantify using remote sensing. This report describes our efforts to integrate remotely sensed data into our computer model of tropical chemical trace-gas emissions, weather, and reaction chemistry (using the MM5 mesoscale model and our own Global-Regional Atmospheric Chemistry Simulator). The effects of burning over the continents of Africa and South America have been noticed in observations from several satellites. Smoke plumes hundreds of kilometers long may be seen individually, or may merge into a large smoke pall over thoUSAnds of kilometers of these continents. These features are related to intense pollution in the much more confined regions with heavy burning. These emissions also translocate nitrogen thoUSAnds of kilometers in the tropical ecosystems, with large fixed-nitrogen losses balanced partially by locally intense fertilization downwind, where nitric acid is rained out. At a much larger scale, various satellite measurements have indicated the escape of carbon monoxide and ozone into large filaments which extend across the Tropical and Southern Atlantic Ocean. Our work relates the source emissions, estimated in part from remote sensing, in part from conventional surface reports, to the concentrations of these gases over these intercontinental regions. We will mention work in progress to use meteorological satellite data (AVHRR, GOES, and Meteosat) to estimate the surface temperature and extent and height of clouds, and explain why these uses are so important in our computer simulations of global biogeochemistry. We will compare our simulations and interpretation of remote observations to the international cooperation involving Brazil, South Africa, and the USA in the TRACE-A (Transport and Atmospheric Chemistry near the Equator - Atlantic) and SAFARI (Southern Africa Fire Atmosphere Research Initiative) and remote-sensing /aircraft/ecosystem observational campaigns.

Author

*Biogeochemistry; Computerized Simulation; Remote Sensing; Exhaust Gases; Ecosystems; Biomass Burning*

**20010125151** NASA Ames Research Center, Moffett Field, CA USA

## Low Ozone in the Marine Boundary Layer of the Tropical Pacific Ocean

Singh, Hanwant B., NASA Ames Research Center, USA; Gregory, G. L., NASA Langley Research Center, USA; Andesrson, B., NASA Langley Research Center, USA; Browell, E., NASA Langley Research Center, USA; Sachse, G. W., NASA Langley Research Center, USA; Davis, D. D., Georgia Inst. of Tech., USA; Crawford, J., Georgia Inst. of Tech., USA; Bradshaw, J. D., Georgia Inst. of Tech., USA; Talbot, R., New Hampshire Univ., USA; Blake, D. R., California Univ., USA; [1994]; 2p; In English

Contract(s)/Grant(s): RTOP 464-54-01-10; No Copyright; Avail: Issuing Activity; Abstract Only

Aircraft measurements of ozone, its key precursors, and a variety of chemical tracers were made in the troposphere of the western and central Pacific in October 1991. These data are presented and analyzed to examine the occurrence of low ozone concentrations in the remote marine boundary layer of the tropical and equatorial Pacific Ocean. The data from these flights out of Guam, covering an area extending from the equator to 20 N and from south of the Philippines to Hawaii, show average O3 concentrations as low as 8-9 ppb (ppb=10(exp-9)v/v) at altitudes of 0.3-0.5 km in the boundary layer. Individual measurements as low as 2-5 ppb were recorded. Low O3 concentrations do not always persist in space and time. High O3, generally associated with the transport of upper tropospheric air, was also encountered in the boundary layer. In practically all cases, O3 increased to values as large as 25-30 ppb within 2 km above the boundary layer top. Steady state model computations are used to suggest that these low O3 concentrations are a result of net photochemical O3 destruction in a low NO environment, sea-surface deposition, and extremely low net entrainment rates (1-2 mm per second) from the free troposphere. Day/night measurements of ethane, propane, gaseous and aerosol Cl suggest that daytime (morning) Cl atom concentrations in the vicinity of 10(exp 5) molecules per cubic centimeter may be present in the marine boundary layer. This Cl atom abundance can be rationalized only if sea salt aerosols can release free chlorine (Cl2) to the gas phase in the presence of sun light (and possibly O3). These Cl atom concentrations, however, are still insufficient and Cl (or Br) chemistry is not likely to be an important cause of the observed low O3.

Author

*Ocean Surface; Ozone; Pacific Ocean; Photochemical Reactions; Boundary Layers*

**20010125442** Lawrence Livermore National Lab., Livermore, CA USA

**Large-eddy simulation of the stable boundary layer and implications for transport and dispersion**

Cederwall, R. T.; Street, R. L.; Feb. 01, 1999; 11p; In English

Report No.(s): DE2001-8416; UCRL-JC-133362; No Copyright; Avail: Department of Energy Information Bridge, Microfiche

Large-eddy simulation (LES) of the evolving stable boundary layer (SBL) provides unique data sets for assessing the effects of stable stratification on transport and dispersion. The simulations include the initial development of the convective boundary layer (CBL) in the afternoon, followed by the development of an SBL after sunset with a strong, surface-based temperature inversion. The structure of the turbulence is modified significantly by negative buoyancy associated with the temperature inversion. The magnitude of velocity variances is reduced by an order of magnitude compared to that in the CBL, and the vertical velocity variance is damped further as the static stability preferentially damps vertical motions. The advanced subgrid-scale turbulence model allows simulation of intermittently enhanced periods of turbulence in the SBL that are often observed. During these turbulent episodes, mixing is increased within the SBL. Air pollution models that account only for the long-term mean structure of the SBL do not include the effects of these episodes. In contrast, our LES results imply that material released near the surface and mixed to higher elevations would be transported by stronger winds and in different directions, due to the vertical shear of horizontal wind speed and direction. Material released at altitude in the SBL will tend to be mixed downward toward the surface during these turbulent episodes in a fumigation-like scenario at night.

NTIS

*Air Pollution; Boundary Layers; Large Eddy Simulation; Atmospheric Models*

**20010125487** Federal Energy Technology Center, Morgantown, WV USA

**Second Generation Advanced Reburning for High Efficiency NOx Control**

Oct. 30, 1998; 30p; In English

Report No.(s): DE2001-7934; DE-AC22-95PC95251-12; No Copyright; Avail: Department of Energy Information Bridge, Microfiche

This project is designed to develop a family of novel NO(x) control technologies, called Second Generation Advanced Reburning which has the potential to achieve 90+% NO(x) control in coal fired boilers at a significantly lower cost than SCR. The fourth reporting period in Phase 2 (July 1 - September 30, 1998) included experimental activities at pilot scale and combined chemistry-mixing modeling on gas reburning. The pilot scale tests reported in previous Quarterly Reports QR-2 and QR-3 were continued. The objective was to simulate furnace conditions at the Greenidge boiler No. 6 owned and operated by NYSEG and to improve the process performance. The tests were conducted in EER's Boiler Simulator Facility (BSF). During the reporting period, measurements of CO and ammonia emissions were conducted for reburn and SNCR conditions, as well as tests on the effect of sodium on NO(x) control efficiency. Exhaust levels of CO remained below 100 ppm in all tests. Prospective process conditions for the full-scale facility have been identified that can provide over 80% NO(x) reduction while maintaining ammonia slip below 4 ppm. Addition of sodium resulted in NO(x) control improvement of about 7-10 percentage points. The objective of modeling work was to further understand the influence of the mixing process on gas reburning and to identify factors that can increase the effectiveness of NO reduction. Modeling results demonstrated that the main features of gas reburning could be described using a detailed chemical mechanism with one-dimensional representation of mixing.

NTIS

*Ammonia; Boilers; Nitrogen Oxides; Sodium*

**20010125523** California Univ., Davis, CA USA

**Final Report: Plant Nitrogen Budgets Under Elevated Carbon Dioxide Levels: Regulations by Nitrogen Absorption and Assimilation, September 1, 1995-August 31, 1999**

Bloom, A.; Aug. 31, 1999; 9p; In English

Report No.(s): DE2001-765144; No Copyright; Avail: Department of Energy Information Bridge

To monitor short-term responses of plants to elevated carbon dioxide, we developed a system that simultaneously monitors shoot exchange of CO2O2, and H2O and root exchange of CO2O2 pH, NH4, and NO3. This is the only system in the world with these capabilities.

NTIS

*Carbon Dioxide; Plants (Botany); Nitrogenation; Assimilation*

**20010125570** Argonne National Lab., IL USA

**Role of Rare-Earth Dopants in Nanophase Zirconia Catalysts for Automotive Emission Control**

Loong, C. K.; Ozawa, M.; Jul. 16, 1999; 22p

Report No.(s): DE2001-11895; ANL/IPNS/CP-99536; No Copyright; Avail: Department of Energy Information Bridge, Microfiche

Rare earth (RE) modification of automotive catalysts (e.g., ZrO2) for exhaust gas treatment results in outstanding improvement of the structural stability, catalytic functions, and resistance to sintering at high temperatures. Owing to the low redox potential of nonstoichiometric CeO2, oxygen release and intake associated with the conversion between the 3+ and 4+ oxidation states of the Ce ions in Ce-doped ZrO2 provide the oxygen storage capacity that is essentially to effective catalytic functions under dynamic air-to-fuel ratio cycling. Doping tripositive RE ions such as La and Nd in ZrO2, on the other hand, introduces oxygen vacancies that affect the electronic and ionic conductivity. These effects, in conjunction with the nanostructure and surface reactivity of the fine powders, present a challenging problem in the development of better ZrO2-containing three-way catalysts. We have carried out in-situ small-to-wide angle neutron diffraction at high temperatures and under controlled atmospheres to study the structural phase transitions, sintering behavior, and Ce3+ to Ce4+ redox process. We found substantial effects due to RE doping on the nature of aggregation of nanoparticles, defect formation, crystal phase transformation, and metal-support interaction in ZrO2 catalysts for automotive emission control.

NTIS

*Catalysts; Doped Crystals; Exhaust Emission; Oxygen; Rare Earth Elements; Structural Stability; Zirconium Oxides*

**20010125641** NASA Ames Research Center, Moffett Field, CA USA

**Pinatubo Aerosol Evolution: Using Composite Data Sets to Build the Global- to Micro-Scale Picture and Assess Consistency of Different Measurements**

Russell, Philip B., NASA Ames Research Center, USA; Pueschel, R. F., NASA Ames Research Center, USA; Livingston, J. M., SRI International Corp., USA; Bergstrom, R., Bay Area Environmental Research Inst., USA; Hamill, P., San Jose State Univ., USA; [1994]; 1p; In English; American Geophysical Union Western Pacific Geophysics Meeting, 25-29 Jul. 1994, Honduras; Sponsored by American Geophysical Union, USA

Contract(s)/Grant(s): RTOP 665-45-10; No Copyright; Avail: Issuing Activity; Abstract Only

This paper brings together experimental evidence required to build realistic models of the global evolution of physical, chemical, and optical properties of the aerosol resulting from the 1991 Pinatubo volcanic eruption. Such models are needed to compute the effects of the aerosol on atmospheric chemistry, dynamics, radiation, and temperature. Whereas there is now a large and crowing body of post-Pinatubo measurements by a variety of techniques, some results are in conflict, and a self-consistent, unified picture is needed, along with an assessment of remaining uncertainties. This paper examines, data from photometers, radiometers, impactors, optical counter/sizers, and lidars operated on the ground, aircraft, balloons, and spacecraft. Example data sources include: (1) Tracking sunphotometers and lidars at Mauna Loa Observatory (MLO) and on the DC-8. (2) Particle spectrometers and wire impactors on the ER-2 and DC-8. (3) Dustsondes (particle counter/sizers on balloons). and (3) SAGE II, SAM II, AVHRR, CLAES, and ISAMS sensors on a variety of satellites. We assess the mutual consistency of these disparate data sets and recommend 'consensus' properties and uncertainties in the process of developing a composite data set. Recommended properties include the spatial and temporal evolution of particle chemical composition, shape, wavelength-and temperature-dependent refractive index, size distribution, and optical depth spectra. Supporting references are cited and representative data shown.

Author

*Aerosols; Atmospheric Chemistry; Chemical Composition; Size Distribution*

## 46
## GEOPHYSICS

*Includes earth structure and dynamics, aeronomy; upper and lower atmosphere studies; ionospheric and magnetospheric physics; and geomagnetism. For related information see 47 Meteorology and Climatology; and 93 Space Radiation.*

**20010117725** Virginia Polytechnic Inst. and State Univ., Dept. of Mechanical Engineering, Blacksburg, VA USA

**Dynamic Electrothermal Model of a Sputtered Thermopile Thermal Radiation Detector for Earth Radiation Budget Applications**

Weckmann, Stephanie, Virginia Polytechnic Inst. and State Univ., USA; Aug. 28, 1997; 117p; In English; Original contains color illustrations

Contract(s)/Grant(s): NCC1-243; NAS1-96059; No Copyright; Avail: CASI; A06, Hardcopy; A02, Microfiche

The Clouds and the Earth's Radiant Energy System (CERES) is a program sponsored by the National Aeronautics and Space Administration (NASA) aimed at evaluating the global energy balance. Current scanning radiometers used for CERES consist of thin-film thermistor bolometers viewing the Earth through a Cassegrain telescope. The Thermal Radiation Group, a laboratory in the Department of Mechanical Engineering at Virginia Polytechnic Institute and State University, is currently studying a new sensor concept to replace the current bolometer: a thermopile thermal radiation detector. This next-generation detector would consist of a thermal sensor array made of thermocouple junction pairs, or thermopiles. The objective of the current research is to perform a thermal analysis of the thermopile. Numerical thermal models are particularly suited to solve problems for which temperature is the dominant mechanism of the operation of the device (through the thermoelectric effect), as well as for complex geometries composed of numerous different materials. Feasibility and design specifications are studied by developing a dynamic electrothermal model of the thermopile using the finite element method. A commercial finite element-modeling package, ALGOR, is used.

Author

*Thermopiles; Thermal Radiation; Radiation Detectors; Earth Radiation Budget; Thermal Analysis; Finite Element Method*

**20010119234** Air Force Inst. of Tech., Wright-Patterson AFB, OH USA

**The Impact of Thermally Forced, Nonperiodic Internal Gravity Waves on Convective Development**

Weekley, Daniel L.; Sep. 20, 2001; 80p; In English

Report No.(s): AD-A395067; C101-130; No Copyright; Avail: CASI; A05, Hardcopy; A01, Microfiche

The thermal forcing in the upper troposphere resulting from deep convection produces internal gravity-wave like disturbances called buoyancy bores. Although they propagate in a manner similar to gravity waves, their structure in time and space is nonperiodic; they travel as a pulse, propagating radially in all directions from the source of thermal forcing. The passage of these bores through the troposphere causes vertical displacements throughout the column in which they occupy. The actual displacements depend upon the vertical structure, or mode, of the bore. Some bores cause local subsidence, while other bores are characterized low-level ascent and upper-level subsidence. Based upon idealized simulations, theories about the contribution of bores to the suppression or enhancement of convection differ. One holds that bores are capable of suppressing convection away from a mesoscale convective system (MCS) while another holds that low-level convergence is supported by bores near an MCS. This paper investigates buoyancy bore behavior in a mesoscale model simulation using initial and boundary conditions from an actual convective outbreak in the central plains of the USA. Despite low-level forcing produced by colliding outflow boundaries on this day, convection failed to initiate between two MCSs due to mid- to upper-level subsidence. Through manipulation of the convective parameterization scheme within the model, the initiation and suppression of convective heating regions is explicitly controlled. This technique of manual convective initiation allows for a better isolation of the specific sources of thermal forcing. Once the behavioral characteristics of buoyancy bores are ascertained, an analysis of buoyancy bore behavior during the simulated convective outbreak is conducted. The bores suspected of enhancing low-level convergence near MCSs never manifest themselves in the simulations.

DTIC

*Convective Heat Transfer; Gravity Waves; Mesoscale Phenomena; Mathematical Models; Wind Profiles*

**20010119924** Aerospace Corp., Lab. Operations, El Segundo, CA USA

**Comparison of MODTRAN and FASCODE for Selection of a Cirrus Cloud Detection Band Near the 1.38-micrometers Water Absorption Window**

Mazuk, S.; Lynch, D. K.; Aug. 30, 2001; 18p; In English; Original contains color images

Contract(s)/Grant(s): 404701-00-C-0009

Report No.(s): AD-A395238; TR-2001(8570)-13V; SMC-TR-01-20; No Copyright; Avail: CASI; A03, Hardcopy; A01, Microfiche

We compared the results of the MODTRAN and FASCODE models over the 1.375-urn cirrus detection channel from MODIS. The comparison of the band average transmission yields values that are significantly different between the two models. We find that MODTRAN' 5 spectral resolution is not high enough to completely model the spectral structure in this band; therefore, FASCODE should be used wherever possible.

DTIC

*Spectra; Atmospheric Models; Cirrus Clouds; Detection*

**20010119960** Norwegian Defence Research Establishment, Kjeller, Norway

**HF NVIS Communication: High Latitude Channel Characteristics** ***HF NVIS Kommunikasjon: Kanalkarakteristikk pa HoyeBreddegrader***

Jodalen, Vivianne, Norwegian Defence Research Establishment, Norway; Aug. 22, 2001; 38p; In Norwegian; Original contains color illustrations

Contract(s)/Grant(s): FFIE Proj. 742/110

Report No.(s): FFI/RAPPORT-2001/04168; ISBN 82-464-0538-1; No Copyright; Avail: CASI; A03, Hardcopy; A01, Microfiche

The HF DAMSON (Doppler and Multipath SOunding Network) was operated on two NVIS (Near Vertical Incidence Skywave) paths in northern Scandinavia during two measurement campaigns in October 1999 and March 2000, respectively. Channel measurements on the two paths Harstad-Abisko (90 km) and Harstad-Kiruna (190 km) have been analyzed in terms of signal-to-noise ratios, signal strength, Doppler and delay spread. These channel parameters can seriously affect the performance of communications. High latitude channel characteristics versus time of day, frequency and geomagnetic conditions are described in the report and the two paths are compared. Also, the variability of one particular frequency is addressed.

Author

*High Frequencies; Communication Networks; Multipath Transmission*

**20010122405** Defence Science and Technology Organisation, Maritime Operations Div., Fishermans Bend, Australia

**Methods of Obtaining Soil Strength Data for Modelling Vehicle Trafficability on Beaches**

Mulhearn, P. J., Defence Science and Technology Organisation, Australia; September 2001; 22p; In English

Report No.(s): DSTO-GD-0299; DODA-AR-012-010; Copyright; Avail: Issuing Activity

Estimates of vehicle mobility or trafficability over beaches are useful for the planning of amphibious operations. If the bearing capacity of a beach is too small, then beach matting, which is heavy and bulky, needs to be transported. If the bearing capacity is large enough then the matting can be left behind, saving space and time. Bearing capacity also effects the speed at which vehicles can transit the beach. A widely used model for predicting mobility is the NATO Reference Mobility Model, version II, (NRMM II). The most critical parameter for mobility forecasts in this and similar models is sediment strength as determined by the cone index, CI, which is the resistance to penetration by soil of a standard shaped cone in pounds per square inch. The methods of obtaining CI are reviewed in this report. The best way is to use a cone penetrometer directly, but there are other less direct methods available and these are discussed.

Author

*Beaches; Mathematical Models; Soil Science; Amphibious Vehicles*

**20010122733** Planetary Society, Pasadena, CA USA

**Mojave Desert Stream Beds Resembling Martian Channels**

Burke, J. D., Planetary Society, USA; Field Trip and Workshop on the Martian Highlands and Mojave Desert Analogs; 2001, pp. 15; In English; See also 20010122728; No Copyright; Abstract Only; Available from CASI only as part of the entire parent document

In 1970, while investigating lunar robotic roving missions, members of the JPL rover team flew over parts of the Mojave desert looking for test sites. We observed some sinuous channels quite unlike the braided arroyos normally found on alluvial fans. Investigating these channels on the ground, we found that they occur only where a stream emerges from a canyon into a region of deep windblown sand. The peculiar stream beds have steep sides, may contain inner meandering channels, taper away to nothing at their lower ends with no evidence of a delta or debris deposit , and are thus clearly the result of erosion and deposition processes different from those acting on normal Mojave Desert alluvium. In many respects they resemble lunar sinuous rilles, except that the lunar rilles (e.g., Schroeter's Valley) extend to much larger sizes. Now that similar features have been seen on Mars, it is worthwhile to reexamine the Mojave rilles as a martian analog. The best examples of these channels are found on the Twenty-nine Palms US Marine Corps Base, northwest of the main base area. Others can be seen southeast of Interstate Highway 15 between Barstow and Baker.

Author

*Mojave Desert (CA); Streams; Beds (Geology); Erosion; Wind Effects*

**20010122738** Case Western Reserve Univ., Dept. of Geological Sciences, Cleveland, OH USA

**The Ferrar Dolerite: An Antarctic Analog for Martian Basaltic Lithologies and Weathering Processes**

Harvey, R. P., Case Western Reserve Univ., USA; Field Trip and Workshop on the Martian Highlands and Mojave Desert Analogs; 2001, pp. 25-26; In English; See also 20010122728; No Copyright; Avail: CASI; A01, Hardcopy; A01, Microfiche

The Ferrar Dolerite is one of the most prominent rocks of East Antarctica, forming well-exposed cliffs along the length of the Transantarctic Mountains. The Ferrar serves as an excellent analog for martian igneous lithologies on a number of scales, from planetary (global concepts of its origin) to the outcrop and hand specimen (cm-scale weathering features) to the microscopic (thin-section scale petrologic similarities to martian meteorites).
Author
*Antarctic Regions; Cliffs; Lithology; Mars Surface; Weathering*

**20010122741** Eoetvoes LORANd Univ., Dept. of Physical Geography, Budapest, Hungary
**Double Craters and Crater Modification**
Kereszturi, A., Eoetvoes LORANd Univ., Hungary; Field Trip and Workshop on the Martian Highlands and Mojave Desert Analogs; 2001, pp. 31-32; In English; See also 20010122728; No Copyright; Avail: CASI; A01, Hardcopy; A01, Microfiche

Connected double craters can be divided into two groups: (1) the two crater formed by the simultaneous impact of two bodies; (2) one crater postdates the other. In the first cases we can find nearly straight wall between the two craters (or no wall at the small craters), in the second cases the younger crater rim postdates the older crater. On Mars we can find several great double craters without straight walls or postdating rims. In this case some process eroded away the straight wall or the rim part where the two craters connected. The presence of the erosion/deposition process is suggested by the smooth sedimentary infill too. Because the surface erosion processes greatly varied during the evolution of Mars, we can expect different ratio for the erosion of connected double craters in different times. Based on their diameter distribution it is possible to analyze this tendency.
Author
*Mars Craters; Erosion; Deposition*

**20010122745** Jet Propulsion Lab., California Inst. of Tech., Pasadena, CA USA
**Australian Red Dune Sand: A Potential Martian Regolith Analog**
Kuhlman, K. R., Jet Propulsion Lab., California Inst. of Tech., USA; Marshall, J., Search for Extraterrestrial Intelligence Inst., USA; Evans, N. D., Oak Ridge National Lab., USA; Luttge, A., Rice Univ., USA; Field Trip and Workshop on the Martian Highlands and Mojave Desert Analogs; 2001, pp. 39-40; In English; See also 20010122728
Contract(s)/Grant(s): DE-AC05-00OR-22725; DE-AC05-76OR-00033; No Copyright; Avail: CASI; A01, Hardcopy; A01, Microfiche

To demonstrate the potential scientific and technical merits of in situ microscopy on Mars, we analyzed a possible Martian regolith analog - an acolian red dune sand from the central Australian desert (near Mt. Olga). This sand was chosen for its ubiquitous red coating and the desert environment in which is it found. Grains of this sand were analyzed using a variety of microanalytical techniques. A database of detailed studies of such terrestrial analogs would assist the study of geological and astrobiological specimens in future missions to Mars. Potential instrument concepts for in situ deployment on Mars include local electrode atom probe nanoanalysis (LEAP), vertical scanning white light interferometry (VSWLI), scanning electron microscopies, energy dispersive x-ray microanalysis (EDX), atomic force microscopy (AFM) and X-ray diffraction (XRD). While in situ deployment of these techniques is many years away, ground-based studies using these analytical techniques extend our understanding of the data obtained from instruments to be flown in the near future.
Author
*Australia; Sands; Mars Surface; Regolith; Interferometry; Scanning Electron Microscopy; Microanalysis; X Ray Diffraction*

**20010122746** Jet Propulsion Lab., California Inst. of Tech., Pasadena, CA USA
**Ventifact Formation in the Mojave Desert: Field Analogs for Martian Processes**
Laity, J. E., California State Univ., USA; Bridges, N. T., Jet Propulsion Lab., California Inst. of Tech., USA; Boyle, T. K., California State Univ., USA; Field Trip and Workshop on the Martian Highlands and Mojave Desert Analogs; 2001, pp. 41-42; In English; See also 20010122728; No Copyright; Avail: CASI; A01, Hardcopy; A01, Microfiche

Two field studies in the Mojave Desert, California, shed light on processes of ventifact formation. The field sites are located on a ridge at Little Cowhole Mountain, which lies approximately 12 km south of Baker, and on an unnamed ridge situated along the northern boundary of the Mojave River Sink (Rasor Road site). The rocks at Little Cowhole Mountain are a blue-grey marble/dolomite, whereas those at Rasor Road are Miocene volcanic rocks (basalt). At both sites the abrasive agent is a fine-grained aeolian sand which was probably derived largely from the Mojave River. There are minimal modem inputs of sand to either site: abrasion occurs as a result of unique climatic and topographic conditions which allow pre-existing sand to be recycled from one aspect of the ridge to the other. Climatic conditions are well suited for ventifact formation. Owing, to the dry climate (marked by low average relative humidity, infrequent dew, and low annual rainfall), rates of chemical weathering are low. Where resurfacing of the rocks by sand abrasion proceeds at a rate greater than weathering, the ventifacts are considered ”active.”

Active ventifacts are found atop and straddling the ridge crests, in the zone of maximum wind velocity and sediment supply. Inactive ventifacts occur where modem weathering Processes exceed abrasion rates; principally on the basal two-thirds of the hillslope, where wind velocity and sediment supply are lower. At intermediate locations between the slope base and crest, ventifacts are either active or inactive, depending on local conditions. The presence of relict ventifacts at the study sites, as well as elsewhere in the eastern Mojave Desert, suggests that the conditions for venti fact formation must have been more intense and extensive in the past. Together, the studies illustrate that the processes that interact to form ventifacts are highly complex, and must be studied at many scales. Small-scale effects, such as local topography, plant cover, or even the spatial distribution of boulders, strongly influence the formation of each individual ventifact. Mesoscale effects (hillslope form, total availability of sediment, seasonality of winds, etc.) determine the distribution of overall erosional energy and the location of active and relict forms.
Author
*Mojave Desert (CA); Sands; Wind Effects; Topography; Wind (Meteorology); Wind Velocity; Abrasion*

**20010122753** National Air and Space Museum, CEPS, Washington, DC USA
**Aeolian and Pluvial Features in the Eastern Mojave Desert as Potential Analogs for Features on Mars**
Zimbelman, J. R., National Air and Space Museum, USA; Field Trip and Workshop on the Martian Highlands and Mojave Desert Analogs; 2001, pp. 55-56; In English; See also 20010122728; No Copyright; Avail: CASI; A01, Hardcopy; A01, Microfiche

The semi-arid environment of the eastern Mojave Desert has allowed aeolian processes to play a significant role in the Pleistocene and Holocene history of the region. This abstract summarizes some of the observations derived from over twenty years of field work in the eastern Mojave Desert and surroundings, focusing on aeolian features that should be analogs to features seen in MOC images of Mars.
Author
*Mojave Desert (CA); Mars Surface; Wind (Meteorology); Wind Effects; Mars Photographs*

**20010124107** NASA Ames Research Center, Moffett Field, CA USA
**Use of Molecular Fossils for the Interpretation of Paleoenvironments on Early Earth: The Synthesis of Lipid Biomarkers by Methane-Oxidizing Bacteria**
Jahnke, Linda L., NASA Ames Research Center, USA; Summons, Roger E., NASA Ames Research Center, USA; [1994]; 1p; In English; Gordon Research Conference on Origin of Life, 22-26 Aug. 1994, Newport, RI, USA; Sponsored by Gordon Research Conferences, Inc., USA
Contract(s)/Grant(s): RTOP 185-52-32; No Copyright; Avail: Issuing Activity; Abstract Only

Over the course of Earth's history, the most important biological influence has come from the evolution of oxygenic photosynthesis and the development of an oxygen-rich biosphere. Although the availability of free oxygen had profound effects on subsequent biological and planetary evolution, clear paleobiological evidence of the timing of this transition is lacking. Recent technical advances in the microanalysis of organic matter has made it possible to detect residual molecules (biomarkers) in proterozoic (2.5 to 0.6 billion years) sedimentary rock characteristic of specific groups of microorganisms. When coupled with the carbon isotopic fractionations characteristic of biological systems and the new field of compound specific isotope analysis, biomarkers could prove to be a powerful tool for decoding ancient biochemistry from the geological record. We have been studying the carbon isotope fractionations associated with the synthesis of organic biomarker molecules in several types of methane-oxidizing bacteria that should have been key to carbon cycling in paleoenvironments after the evolution of oxygenic photosynthesis.
Author
*Oxygen; Biological Evolution; Methane; Oxidation; Photosynthesis; Precambrian Period; Planetary Evolution; Paleontology; Biogeochemistry; Archaebacteria; Paleobiology*

**20010124843** NASA Goddard Space Flight Center, Greenbelt, MD USA
**Magnetosphere-Regolith/Exosphere Coupling: Differences and Similarities to the Earth Magnetosphere-Ionosphere Coupling**
Gjerleov, J. W., NASA Goddard Space Flight Center, USA; Slavin, J. A., NASA Goddard Space Flight Center, USA; Mercury: Space Environment, and Surface and Interior; 2001, pp. 28; In English; See also 20010124826; No Copyright; Abstract Only; Available from CASI only as part of the entire parent document

Of the three Mercury passes made by Mariner 10, the first and third went through the Mercury magnetosphere. The third encounter which occurred during northward IMF (interplanetary magnetic field) showed quiet time magnetic fields. In contrast the third encounter observed clear substorm signatures including dipolarization, field-aligned currents (FACs) and injection of energetic electrons at geosynchronous orbit. However, the determined cross-tail potential drop and the assumed height integrated

conductance indicate that the FAC should be 2-50 times weaker than observed. We address this inconsistency and the fundamental problem of FAC closure whether this takes place in the regolith or in the exosphere. The current state of knowledge of the magnetosphere-exosphere/regolith coupling is addressed and similarities and differences to the Earth magnetosphere-ionosphere coupling are discussed.
Author
*Mariner 10 Space Probe; Mercury (Planet); Regolith; Planetary Magnetospheres; Exosphere*

**20010124981** NASA Goddard Space Flight Center, Greenbelt, MD USA
**Response to Comment on "Does the Earth Have an Adaptive Infrared IRIS?"**
Bell, Thomas L., NASA Goddard Space Flight Center, USA; Chou, Ming-Dah, NASA Goddard Space Flight Center, USA; Lindzen, Richard S., Massachusetts Inst. of Tech., USA; Hou, Arthur Y., NASA Goddard Space Flight Center, USA; [2001]; 1p; In English; No Copyright; Avail: Issuing Activity; Abstract Only

Harrison's (2001) Comment on the Methodology in Lindzen et al (2001) has prompted re-examination of several aspects of study. Probably the most significant disagreement in our conclusions is due to our different approaches to minimizing the influence of long-time-scale variations in the variables A and T on the results. Given the strength of the annual cycle and the 20-month period covered by the data, we believe that removing monthly means is a better approach to minimizing the long-time-scale behavior of the data than removal of the linear trend, which might actually add spurious long- time- scale variability into the modified data. We have also indicated how our statistical methods of establishing statistical significance differ. More definitive conclusions may only possible after more data have been analyzed, but we feel that our results are robust enough to encourage further study of this phenomenon.
Author
*Statistical Analysis; Infrared Radiation; Infrared Imagery*

**20010125138** Colorado Univ., ITRF Working Group, Boulder, CO USA
**The Terrestrial Reference Frame and the Dynamic Earth**
Altamimi, Zuheir, Colorado Univ., USA; Angermann, Detlef, Colorado Univ., USA; Argus, Don, Colorado Univ., USA; Blewitt, Geoff, Colorado Univ., USA; Boucher, Claude, Colorado Univ., USA; Chao, Ben, Colorado Univ., USA; Drewes, Hermann, Colorado Univ., USA; Eanes, Richards, Colorado Univ., USA; Feissel, Martine, Colorado Univ., USA; Ferland, Remi, Colorado Univ., USA; EOS, Transactions; Jun. 19, 2001; ISSN 0096-3941; Volume 82, No. 25, pp. 273, 278-279; In English; Copyright; Avail: Issuing Activity

One of the main tasks of modern geodesy- the science of measuring and mapping the Earth's surface-is to define and maintain this global terrestrial reference frame. How well the reference frame can be realized has important implications for our ability to study both regional and global properties of the Earth, including post-glacial rebound, sea-level change, plate tectonics, regional subsidence and loading, plate boundary deformation, and Earth orientation excitation. Two coordinate frames are commonly used: a rotating system fixed to the Earth's surface (terrestrial; used for most practical applications) and an essentially inertial system fixed to the stars (celestial; where dynamical equations of motion can be solved). The celestial reference frame was historically specified by the equator, ecliptic, and pole of rotation of the Earth and was realized by the two-dimensional coordinates of a large number of stars. The present-day International Celestial Reference Frame (ICRF) is defined by the coordinates of a much smaller set of essentially stationary quasars whose positions are far better known.
Derived from text
*Geodesy; Earth Surface; Earth Orientation; Plates (Tectonics); Celestial Reference Systems*

**20010125144** Colorado Univ., Dept. of Aerospace Engineering, Boulder, CO USA
**Measuring Postglacial Rebound with GPS and Absolute Gravity**
Larson, Kristine M., Colorado Univ., USA; vanDam, Tonie, European Center for Geodynamics and Seismology, Luxembourg; Geophysical Research Letters; Dec. 01, 2000; ISSN 0094-8276; Volume 27, No. 23, pp. 3925-3928; In English
Contract(s)/Grant(s): NAG5-6147
Report No.(s): Paper-2000GL011946; Copyright; Avail: Issuing Activity

We compare vertical rates of deformation derived from continuous Global Positioning System (GPS) observations and episodic measurements of absolute gravity. We concentrate on four sites in a region of North America experiencing postglacial rebound. The rates of uplift from gravity and GPS agree within one standard deviation for all sites. The GPS vertical deformation rates are significantly more precise than the gravity rates, primarily because of the denser temporal spacing provided by continuous

GPS tracking. We conclude that continuous GPS observations are more cost efficient and provide more precise estimates of vertical deformation rates than campaign style gravity observations where systematic errors are difficult to quantify.
Author
*Deformation; Global Positioning System; Gravitation; North America; Earth Crust*

**20010125646** NASA Goddard Space Flight Center, Greenbelt, MD USA
**Earth-Atmospheric Coupling During Strong Earthquakes by Analyzing MODIS Data**
Ouzounov, Dimitar, NASA Goddard Space Flight Center, USA; Williams, Robin G., NASA Goddard Space Flight Center, USA; Freund, Friedemann, NASA Ames Research Center, USA; [2001]; 1p; In English; International Association of Geomagnetism and Aeronomy (IAGA) and International Association of Seismology and Physics of the Earth's Interior Meeting (IASPEI), 20-31 Aug. 2001, Hanoi, Viet Nam; Sponsored by International Association of Geomagnetism and Aeronomy, Unknown; No Copyright; Avail: Issuing Activity; Abstract Only

Interactions between the Earth and the atmosphere during major earthquakes (M greater than 5) are the subject of this investigation. Recently a mechanism has been proposed predicting the build-up of positive ground potentials prior to strong earthquake activity. Connected phenomena include: transient conductivity of rocks, injection of currents, possibly also electromagnetic emission and light emission from high points at the surface of the Earth. to understand this process we analyze vertical atmospheric profiles, land surface and brightness (temperature) data, using the Moderate Resolution Imaging Spectroradiometer (MODIS) onboard NASA's Terra satellite launched in December 1999. MODIS covers the entire Earth every 1-2 days in 36 wavelength bands (20 visible and 16 infrared) at different spatial resolutions (250 m, 500 m, and 1 km). Using MODIS data we look for correlations between the atmospheric dynamics and solid Earth processes for the January 2001 strong earthquakes in San Salvador and India. As part of the build-up of positive grounds potential, an IR luminescence is predicted to occur in the 8-12 micrometer band. We use the MODIS data to differentiate between true "thermal" signals and IR luminescence. Indeed, on the basis of a temporal and spatial distribution analysis, a thermal anomaly pattern is found that appears to be related to the seismic activity. Aerosol content and atmospheric instability parameters also change when ground charges build up causing ion emission and leading to a thin aerosol layer over land. We analyze the aerosol content, atmospheric pressure, moisture profile and lifted index. Anomalous trends have been identified in few days prior to the main shocks. The significance of this observation should be explored further using other data sets.
Author
*Air Land Interactions; Earthquakes; Imaging Spectrometers; Atmospheric Physics; Land Surface Temperature; Brightness Temperature*

## 47
## METEOROLOGY AND CLIMATOLOGY

*Includes weather observation forecasting and modification*

**20010117644** NASA Goddard Space Flight Center, Greenbelt, MD USA
**Geometrical Effects on the Electromagnetic Radiation from Lightning Return Strokes**
Willett, J. C., Air Force Research Lab., USA; Smith, D. A., Los Alamos National Lab., USA; LeVine, D. M., NASA Goddard Space Flight Center, USA; [2001]; 2p; In English; International Workshop on Physics of Lightning, August 2001, Nagoya, Japan; No Copyright; Avail: CASI; A01, Hardcopy; A01, Microfiche

The morphological difference between the electromagnetic radiation-field waveforms of "first" and "subsequent" return strokes in cloud-to-ground lightning flashes is well known and can be used to identify the formation of new channels to ground. This difference is generally believed due to the existence of branches on first-stroke channels, whereas subsequent strokes re-illuminate only the main channel of a previous stroke; but experimental evidence for this hypothesis is relatively weak. It has been argued for the influence of channel geometry on the fine structure of radiation from subsequent return strokes by comparing the field-change waveforms recorded at the same station from strokes within the same flash and between different flashes of both natural and triggered lightning. The present paper introduces new evidence for both of these hypotheses from a comparison of waveforms between sensors in different directions from the same stroke.
Author
*Electromagnetic Radiation; Lightning; Thermodynamic Cycles; Waveforms*

**20010117648** Los Alamos National Lab., NM USA

**Forward-in-Time Differencing for Fluids: Nonhydrostatic Modeling of Rotating Stratified Flow on a Mountainous Sphere**

Smolarkiewicz, P. K.; Grubisic, V.; Margolin, L. G.; Mar. 31, 1999; 10p; In English

Report No.(s): DE2000-760144; LA-UR-98-4385; No Copyright; Avail: Department of Energy Information Bridge

Traditionally, numerical models for simulating planetary scale weather and climate employ the hydrostatic primitive equations - an abbreviated form of Navier-Stokes equations that neglect vertical accelerations and use simplified inertial forces. Although there is no evidence so far that including nonhydrostatic effects in global models has any physical significance for large scale solutions, there is an apparent trend in the community toward restoring Navier-Stokes equations (or at least their less constrained forms) in global models of atmospheres and oceans. The primary motivation for this is that the state-of-the-art computers already admit resolutions where local nonhydrostatic effects become noticeable. Other advantages include the convenience of local mesh refinement; better overall accuracy; insubstantial computational overhead relative to hydrostatic models; universality and therefore convenience of maintaining a single large code; as well as conceptual simplicity and mathematical elegance - features important for education. The few existing nonhydrostatic global models differ in analytic formulation and numerical design, reflecting their different purposes and origins. Much of our present research improves the design of a high-performance numerical model for simulating the flows of moist (and precipitating), rotating, stratified fluids past a specified time-dependent irregular lower boundary. This model is representative of a class of nonhydrostatic atmospheric codes employing the an elastic equations of motion in a terrain-following curvilinear framework, and contains parallel implementations of semi-Lagrangian and Eulerian approximations selectable by the user. The model has been employed in a variety of applications; the quality of results suggest that modern nonoscillatory forward-in-time (NFT) methods are superior to the more traditional centered-in-time-and-space schemes, in terms of accuracy, computational efficiency, flexibility, and robustness.

NTIS

*Grid Generation (Mathematics); Mathematical Models; Navier-Stokes Equation; Rotating Fluids; Stratified Flow*

**20010117666** Federal Energy Technology Center, Morgantown, WV USA

**Holocene cyclicity in western North Dakota: Climate change interpreted from fluctuations in alluvial sedimentation**

Hartman, J. H.; Beck, D. L.; Kuehn, D. D.; Reid, J. R.; Reiten, J.; Jul. 01, 1999; 194p; In English

Contract(s)/Grant(s): DE-FC21-93MC-30098

Report No.(s): DE2000-759251; No Copyright; Avail: Department of Energy Information Bridge

This project undertook a close examination of the relationship between Holocene alluvial sedimentation and climatic variation. Although various techniques have been employed to interpret climate during postglacial times, the few studies in semiarid badlands terrains have focused on a general understanding of the broadscale climatic history. This project interpreted finer sedimentary patterns to recognize and interpret climatic variations that may occur as short-period cycles. Such interpretations provide a new approach to examining climatic variability in the past, reflecting periods of extended dry and moist conditions, and will result in the development of a more rigorous basis for interpreting human interactions with both their physical and biotic surroundings.

NTIS

*Holocene Epoch; Arid Lands; Climatology; Topography; Sedimentary Rocks*

**20010117667** Brookhaven National Lab., Upton, NY USA

**GMS-5 IR and Visible Imagery for November 1996-February 1997 from the Arm External Data center**

Barr-Kumarakulasinghe, S. A.; Mar. 23, 1998; 4p; In English

Report No.(s): DE2000-752957; BNL-66877; No Copyright; Avail: Department of Energy Information Bridge

The El-Nino Southern Oscillation (ENSO) and Madden Julian Oscillations (MJO) are strongly influenced by radiative and other associated cloud processes in the Tropical Western Pacific (TWP). ENSO and MJO events in turn are important to global climate. The Geostationary Meteorological Satellites (GMS) capture the cloud and radiative processes by providing approximately hourly images of the TWP. Use of the satellite data by the research community is facilitated when the data is processed and made available in convenient data formats and media. Motivated by the success of the GMS-4 infrared (IR) satellite imagery CD-ROM produced by the Meteorological Research Institute (MRI) (1994), the Atmospheric Radiation Measurement Program's External Data Center (ARM-XDC) has produced a complementary data set on a CD-ROM covering the period from November 1996 to February 1997.

NTIS

*Madden-Julian Oscillation; Southern Oscillation; Satellite Imagery; Meteorological Satellites; Atmospheric Chemistry*

**20010117710** Brookhaven National Lab., Upton, NY USA

**Catalog of ARM external data**

Tichler, J. L.; Mar. 23, 1998; 6p; In English

Report No.(s): DE2000-752955; BNL-66879; No Copyright; Avail: Department of Energy Information Bridge

The term 'external data' refers to data generated outside the Atmospheric Radiation Measurement (ARM) program that augments the ARM data. Data sets designated as ARM 'external data' are collected by the ARM External Data Center (XDC). They are usually converted to either netCDF or HDF. These data are distributed by the ARM Archive and to the ARM experiment Center. External data is managed in a fashion similar to ARM data. The only exception is that for certain external data sets, the provider has specified that these only be distributed to members of the ARM Science Team and not be made available to the general scientific community. The decisions on what external data sets are acquired is made by the ARM Program Office, with input provided by the ARM Science Team.

NTIS

*Atmospheric Radiation; Radiation Measurement; Data Management*

**20010117711** Brookhaven National Lab., Upton, NY USA

**Frequency interactions to explain Madden Julian oscillations and intra seasonal oscillations**

Barr-Kumarakulasinghe, S. A.; Mar. 23, 1998; 4p; In English

Report No.(s): DE2000-752954; BNL-66880; No Copyright; Avail: Department of Energy Information Bridge

Deep convective activity as seen by outgoing longwave radiation (OLR) (less than 180 wm(-2)) is shown to occur at 20 to 60 periods in a more coherent manner during the boreal winters of El-Nino Southern Oscillation (ENSO) warm events. The coherent pattern is seen in the spectra of the TWP equatorial region closer to the date line. The frequency interaction of gravity waves, emanating from diurnal or 5- to 6-day convective activity is hypothesized to be the cause of the Madden Julian Oscillation (MJO) global wind pressure oscillations.

NTIS

*Pressure Oscillations; Southern Oscillation; Annual Variations; Convection*

**20010117712** Brookhaven National Lab., Upton, NY USA

**Metadata systems for ARM, SGP and NSA sites**

Doty, K. J.; Jan. 10, 1999; 2p; In English

Report No.(s): DE2000-752953; BNL-66881; No Copyright; Avail: Department of Energy Information Bridge

The Atmospheric Radiation Measurement (ARM) Program, funded by the Environmental Sciences Division of the U.S. Department of Energy (DOE), is a major global change research program whose focus is to better understand the influences of human activity on the earths climate. The ARM program has set up instruments at three primary measuring sites around the world. These sites are the Southern Great Plains (SGP) of the USA, the Tropical Western Pacific (TWP) and the North Slope of Alaska (NSA). The sites were selected to provide opportunities to observe a wide range of climatologically important meteorological conditions. Scientists will be able to use the parametric data gathered at these sites to study the effects and interactions of sunlight, energy transfer, and clouds on climate.

NTIS

*Meteorology; Atmospheric Radiation; Radiation Measurement; Data Management*

**20010117723** NASA Ames Research Center, Moffett Field, CA USA

**Impact of Uncertainties and Errors in Converting NWS Radiosonde Hygristor Resistances to Relative Humidity**

Westphal, Douglas L., NASA Ames Research Center, USA; [1994]; 1p; In English; AGU Chapman Conference on Water Vapor in the Climate System, 25-28 Oct. 1994, Jekyll Island, GA, USA; Sponsored by American Geophysical Union, USA

Contract(s)/Grant(s): RTOP 460-47-00-10; No Copyright; Avail: Issuing Activity; Abstract Only

A set of 2,600 6-second, National Weather Service soundings from NASA's FIRE-II Cirrus field experiment are used to illustrate previously known errors and new potential errors in the VIZ and SDD ) brand relative humidity (RH) sensors and the MicroART processing software. The entire spectrum of RH is potentially affected by at least one of these errors. (These errors occur before being converted to dew point temperature.) Corrections to the errors are discussed. Examples are given of the effect that these errors and biases may have on numerical weather prediction and radiative transfer. The figure shows the OLR calculated for the corrected and uncorrected soundings using an 18-band radiative transfer code. The OLR differences are sufficiently large to warrant consideration when validating line-by-line radiation calculations that use radiosonde data to specify the atmospheric state, or when validating satellite retrievals. in addition, a comparison of observations of RH during FIRE-II derived from GOES

satellite, raman lidar, MAPS analyses, NCAR CLASS sondes, and the NWS sondes reveals disagreement in the RH distribution and underlines our lack of an understanding of the climatology of water vapor.
Author
*Error Analysis; Numerical Weather Forecasting; Radiosondes; Atmospheric Moisture; Water Vapor*

**20010118274** California Univ., Lawrence Berkeley Lab., Berkeley, CA USA
**Impact of climate change on the conduct of evaluation: The establishment of new evaluation guidelines**
Vine, E.; Sathaye, J.; May 01, 1999; 15p; In English
Report No.(s): DE2000-760300; LBNL-42990; No Copyright; Avail: Department of Energy Information Bridge, Microfiche
In this paper, we present an overview of guidelines recently developed for the monitoring, evaluation, reporting, verification and certification (MERVC) of energy-efficiency projects for climate change mitigation on behalf of the U.S. Environmental Protection Agency (EPA). These guidelines address several key issues, including methods for estimating gross and net energy savings and greenhouse gas (GHG) emission reductions.
NTIS
*Climate Change; Environment Protection; Energy Conservation*

**20010118513** Virginia Polytechnic Inst. and State Univ., Dept. of Mechanical Engineering, Blacksburg, VA USA
**Satellite Imagery Analysis for Nighttime Temperature Inversion Clouds**
Kawamoto, K., Virginia Polytechnic Inst. and State Univ., USA; Minnis, P., Virginia Polytechnic Inst. and State Univ., USA; Arduini, R., Virginia Polytechnic Inst. and State Univ., USA; Smith, W., Jr., Virginia Polytechnic Inst. and State Univ., USA; [2001]; 10p; In English
Contract(s)/Grant(s): NAG1-2106; No Copyright; Avail: CASI; A02, Hardcopy; A01, Microfiche
Clouds play important roles in the climate system. Their optical and microphysical properties, which largely determine their radiative property, need to be investigated. Among several measurement means, satellite remote sensing seems to be the most promising. Since most of the cloud algorithms proposed so far are daytime use which utilizes solar radiation, Minnis et al. (1998) developed a nighttime use one using 3.7-, 11 - and 12-microns channels. Their algorithm, however, has a drawback that is not able to treat temperature inversion cases. We update their algorithm, incorporating new parameterization by Arduini et al. (1999) which is valid for temperature inversion cases. This updated algorithm has been applied to GOES satellite data and reasonable retrieval results were obtained.
Author
*Satellite Imagery; Data Retrieval; Solar Radiation; Temperature Inversions; Clouds (Meteorology)*

**20010118907** NASA Langley Research Center, Hampton, VA USA
**Satellite Calibration and Verification of Remotely Sensed Cloud and Radiation Properties Using ARM UAV Data *Final Report, 28 Feb. 1995 - 28 Feb. 1998***
Minnis, Patrick, NASA Langley Research Center, USA; Charlock, Thomas P., NASA Langley Research Center, USA; Sep. 23, 1998; 8p; In English
Contract(s)/Grant(s): DE-IA02-95ER-61992
Report No.(s): DE2000-760145; DOE/ER61992-F; No Copyright; Avail: CASI; A02, Hardcopy; A01, Microfiche
The work proposed under this agreement was designed to validate and improve remote sensing of cloud and radiation properties in the atmosphere for climate studies with special emphasis on the use of satellites for monitoring these parameters to further the goals of the Atmospheric Radiation Measurement (ARM) Program.
NTIS
*Radiation Measurement; Remote Sensing; Satellite Observation; Monitors*

**20010119922** North Carolina State Univ., Raleigh, NC USA
**The Mesoscale Evolution of Explosive Cyclogenesis: A Numerical Study of the March 1993 Storm of the Century**
Pfeiffer, Karl D.; Sep. 17, 2001; 227p; In English
Report No.(s): AD-A395242; No Copyright; Avail: CASI; A11, Hardcopy; A03, Microfiche
The early, overwater cyclogenesis of the March 12-14 1993 Storm of the Century (SOC93) is investigated using mesoscale simulation datasets. Numerical results indicate that the convective available potential energy for initial development; ;is supplied by a mid-level cold pool that develops in western Texas through evaporative cooling and convective overturning in the elevated mixed layer (EML). The EML and mountain-plains solenoid (MPS) endemic to the Mexican plateau interact with a

terrain-induced low-level moist flow to sustain shallow convection in this layer; the resulting cold pool propagates to the Texas Gulf Coast early on 12 March.
DTIC
*Meteorology; Cyclogenesis; Cyclones; Mesoscale Phenomena*

**20010120053** Brookhaven National Lab., Upton, NY USA
**Surface characterization data for the arm cart sites**
Cialella, A. T.; Mar. 23, 1998; 8p; In English
Report No.(s): DE2000-752958; BNL-66876; No Copyright; Avail: Department of Energy Information Bridge

The External Data Center (XDC), located at Brookhaven National Laboratory, is responsible for providing data to the Atmospheric Radiation Measurement (ARM) Program that is generated outside of the program and covers the Cloud and Radiation Testbed (CART) areas. One division of external data is surface characterization data. These data are maintained in a Geographic Information Systems (GIS) and provide visual geographic data about the ARM CART sites. The XDC has been collecting these data since the early 1990s. This paper details the new acquisitions for the 1997-1998 fiscal year.
NTIS
*Atmospheric Radiation; Clouds (Meteorology); Radiation Measurement; Climatology*

**20010120104** Air Force Inst. of Tech., Wright-Patterson AFB, OH USA
**Analysis of the 1998 Southeast Monsoon and the Diurnal Rainfall Cycle in the South China Sea (SCS)**
McLeod, Raymond S.; Jun. 13, 2001; 76p; In English; Original contains color images
Report No.(s): AD-A395109; No Copyright; Avail: CASI; A05, Hardcopy; A01, Microfiche

The onset and maintenance of the Southeast Asian monsoon (SEAM) has far-reaching implications for global circulation as well as and the local welfare of a substantial portion of the world's population residing in Southeast Asia. Significant delay or premature onset can lead to extreme famine or flood, respectively. Before accurate prediction of the strength or weakness of any given monsoon, one must understand the fundamental structure and significant events that lead to the onset and how the monsoon maintains itself. Analysis of data from the 1998 South China Sea Monsoon Experiment (SCSMEX) has revealed fundamental structures and influences associated with the summer monsoon over this region. Comparison of SCSMEX data with independent data such as the Tropical Rainfall Measuring Mission (TRMM) has confirmed diurnal variations in rainfall over this region.
DTIC
*China; Diurnal Variations; Monsoons; Rain; Seas; Meteorological Parameters*

**20010120133** Colorado State Univ., Fort Collins, CO USA
**Vegetation Impacts on Maximum and Minimum Temperatures in Northeast Colorado**
Hanamean, James R., Jr.; Sep. 20, 2001; 78p; In English; Original contains color images
Report No.(s): AD-A395190; No Copyright; Avail: CASI; A05, Hardcopy; A01, Microfiche

The impact of vegetation on the microclimate has not been adequately considered in the analysis of temperature forecasting and modeling. Vegetation has transpirational and evaporational influences in the area it inhabits, affecting the surface energy budget. The presence of vegetation, as compared to bare soil, modulates the diurnal temperature cycle. During the day, transpiring vegetation partitions a greater portion of the incoming solar energy into latent heat, decreasing the maximum temperature. At night, the vegetated area radiates energy and allows condensation, increasing the minimum temperatures via latent heat release. A daily 850-700 mb layer mean temperature, computed from the National Center for Environmental Prediction-National Center for Atmospheric Research (NCEP-NCAR) reanalysis, and satellite-derived greenness values, as defined by NDVI (Normalized Difference Vegetation Index), were correlated with surface maximum and minimum temperatures at six sites in Northeast Colorado for the years 1989-98. These sites encompass a wide array of environments, from irrigated-urban to short grass prairie. The explained variance (r-squared value) of surface maximum and minimum temperature by only the 850-700 mb layer mean temperature was subtracted from the corresponding explained variance by the 850-700 mb layer mean temperature and NDVI values. The subtraction shows that by including NDVI values in the analysis, the r-squared values, and thus the degree of explanation of the surface temperatures, increase by a mean of 6 percent for the maxima and 8 percent for the minima over the period March through October.
DTIC
*Atmospheric Temperature; Vegetation; Weather Forecasting; Colorado; Microclimatology*

**20010120145** Air Force Inst. of Tech., Wright-Patterson AFB, OH USA

**Variability of Tropical Cyclone Wind-Pressure Relationships**

Vilpors, Steven E.; Jan. 2001; 127p; In English

Report No.(s): AD-A395145; C101-259; No Copyright; Avail: CASI; A07, Hardcopy; A02, Microfiche

The variability of maximum sustained wind versus minimum sea level pressure (MSLP) in tropical cyclones is investigated using North Atlantic (1959-1999) and western North (NW) Pacific (1959-1999) best track data. A comparison is made of intensity estimates determined from aircraft reconnaissance, Dvorak (1975,1984) satellite analysis, and Global Positioning System (GPS) drop windsonde data. A review and comparison is made of past research on the variable relationship between maximum sustained wind versus MSLP in tropical cyclones (TCs). It is shown that the current analysis techniques are not reliable for assessing the large variability of maximum sustained wind versus MSLP for many cyclones of atypical structure.

DTIC

*Cyclones; Variability; Wind Pressure; Tropical Storms; Wind (Meteorology)*

**20010120151** Oregon State Univ., Corvallis, OR USA

**Spatial Variations of the Wave, Stress and Wind Fields in the Shoaling Zone** ***Final Report, 2 Jan. 1997-21 Jan 2001***

Mahrt, Larry; Sep. 17, 2001; 39p; In English

Contract(s)/Grant(s): N000149710279

Report No.(s): AD-A395135; No Copyright; Avail: CASI; A03, Hardcopy; A01, Microfiche

We have used fast response atmospheric measurements from a small low-flying research aircraft, a tower at the end of a pier and offshore buoys to study air-sea interaction in the coastal zone. The research aircraft also measures the wave field using three downward pointing lasers. Our analysis of this data indicates that the influence of shoaling waves is significant but less important than originally thought. Nonetheless, computer models of air-sea interaction fail to properly account for the important influence of the surface wave state. Atmospheric flow of warm air over a colder sea surface can lead to complete collapse of the atmospheric turbulence and sea state. This collapse is not presently simulated in boundary layer models.

DTIC

*Wind (Meteorology); Computerized Simulation; Spatial Distribution; Research Aircraft; Surface Waves; Meteorological Parameters*

**20010120559** Argonne National Lab., IL USA

**Procedure for the Automatic Estimation of Mixed Layer Height**

Coulter, R. L., Argonne National Lab., USA; Apr. 15, 1998; 7p; In English

Report No.(s): DE2001-10735; ANL/ER/CP-96114; No Copyright; Avail: Department of Energy Information Bridge, Microfiche

The daytime mixed layer results from mechanical and thermal turbulence processes driven by differences in air-surface temperature and moisture. As such, the height of the mixed layer (z(sub i)) is a measure of the effectiveness of energy transfer from the sun to the earth's surface and, in turn, to the lower atmosphere (Stun, 1989). Maximum daytime values for z(sub i) in the region of the Southern Great Plains (SGP) Cloud and Radiation Testbed (CART) vary from less than 100 m in cloudy, moist, calm, stable conditions to nearly 3 km in clear, dry, unstable conditions. The principal characteristic of the mixed layer is that scalar quantities such as moisture and temperature are mixed throughout. Thus, z(sub i) becomes one of the principal scaling parameters used to describe the structure of the lower planetary boundary layer. Normally, a stable layer (a potential temperature inversion) at the top of the mixed layer interfaces between processes in the lower atmosphere and in the free atmosphere above. The strength of this inversion limits the rate of growth of z(sub i) with time and the vertical transfer of energy and moisture. When and if z(sub i) reaches the condensation level, clouds can form; hence, cloud base height (particularly for fair-weather cumulus clouds) often coincides with z(sub i) later in the day. Although the concept of the mixed layer height is straightforward, its measurement can be relatively difficult, or at least awkward. The most reliable method is an analysis of potential temperature and mixing ratio profiles retrieved from balloon ascents. (The potential temperature changes from constant to increasing with height; the mixing ratio changes from constant to decreasing with height.) Often however, the profiles of temperature and moisture are ambiguous, with multiple inversions or none at all. In addition these profiles supply only a snapshot of the atmospheric structure that may well be unrepresentative of the average, either in time or space. In some instances, the term 'well mixed' should not be applied to the lower atmosphere at all; during and after precipitation, for instance, the changes in surface and lower atmospheric conditions cause large ambiguities. This paper describes an automatic estimation method using radar profiler data and discusses a one-year climatology of z(sub i) over the SGP CART site.

NTIS

*Mixing Height; Atmospheric Circulation; Temperature Inversions; Atmospheric Boundary Layer; Mixing Layers (Fluids); Planetary Boundary Layer; Mixing Ratios*

**20010121549** NASA Ames Research Center, Moffett Field, CA USA

**Cloud-Aerosol Interactions in Tropical Storms**

Puesschel, R. F., NASA Ames Research Center, USA; Ferry, G. V., NASA Ames Research Center, USA; Allen, D. A., NASA Ames Research Center, USA; Howard, S. D., NASA Ames Research Center, USA; Hallett, J., Desert Research Inst., USA; Hudson, J., Desert Research Inst., USA; Arnott, P., Desert Research Inst., USA; Foster, T. C., California Polytechnic State Univ., USA; Livingston, J. M., SRI International Corp., USA; [1994]; 2p; In English; Fourth Aerosol Conference, 29 Aug. - 2 Sep. 1994, Los Angeles, CA, USA

Contract(s)/Grant(s): RTOP 460-22-81-10; No Copyright; Avail: Issuing Activity; Abstract Only

During the Coupled Ocean-Atmosphere Response Experiment (COARE) of the Tropical Ocean and the Global Atmosphere (TOGA) program we measured cloud and aerosol particles aboard the NASA DC-8 over the warm pool of the western Pacific. Instruments on the aircraft included a condensation nuclei counter, optical particle counters, two-dimensional shadow probes and an ice crystal replicator. The size range covered by these instruments was from =0.01 micron to 6.4 mm diameter; particle shapes were determined for particles of sizes D greater than 1 micron.

Derived from text

*Aerosols; Air Water Interactions; Radiation Counters; Size Distribution; Tropical Storms*

**20010121951** Massachusetts Univ., Amherst, MA USA

**Development of a UAV-Mounted 95 GHz Radar System to Conduct Scientific Studies of Clouds** ***Final Report***

McIntosh, R. E.; May 16, 2000; 31p; In English

Report No.(s): DE2000-763174; No Copyright; Avail: Department of Energy Information Bridge, Microfiche

This report describes the development and testing of the Compact Millimeter-Wave Radar (CMR). CMR is a solid-state W-band radar designed for integration on the Department of Engergy's (DOEs) Atmospheric Radiation Measurement (ARM) Unmanned Aerial Vehicle (UAV) platforms. One of the primary scientific objectives of the DOE ARM-UAV program was to investigate the role of clouds in the Earths atmospheric radiation balance. W-band radars have the ability to profile a wide variety of clouds, including ones with high optical extinction. The DOE ARM-UAV program funded UMass to investigate whether the size, weight and power consumption of typical airborne W-band radars could be reduce to meet the constraints imposed by the UAV payload capacity, and based on the results of this study, funded UMass to build the CMR. In the sections to follow, the design and development of the CMR will be described, results from comparisons between CMR and the UMass Cloud Profiling Radar System (CPRS) presented and upgrades that will enhance the sensitivity of CMR by 20 dB discussed.

NTIS

*Clouds (Meteorology); Millimeter Waves; Radar; Atmospheric Radiation*

**20010122247** Argonne National Lab., IL USA

**Argonne Boundary Layer Experiments Facility: Using minisodars to complement a wind profiler network**

Coulter, R. L.; Jun. 05, 1998; 7p; In English

Report No.(s): DE2001-10835; ANL/ER/CP-96605; No Copyright; Avail: Department of Energy Information Bridge

The Argonne Boundary Layer Experiments (ABLE) facility, located in south central Kansas, east of Wichita, is devoted primarily to investigations of and within the planetary boundary layer (PBL), including the dynamics of the mixed layer during both day and night; effects of varying land use and land form; the interactive role of precipitation, runoff, and soil moisture; storm development; and energy budgets on scales of 10 to 100 km. Located entirely within the Walnut River watershed, ABLE provides intense measurements within the northeast quadrant (Fig. 1) of the Southern Great Plains (SGP) Cloud and Radiation Testbed (CART) of the Atmospheric Radiation Measurement (ARM) Program (Stokes and Schwarz, 1994). by combining the continuous measurements of ABLE with ancillary continuous measurements of, for example, the ARM and the Global Energy Water cycle Experiment (GEWEX) (Kinster and Shukla, 1990) programs, ABLE provides a platform within which shorter, more intensive studies, such as those conducted by the Cooperative Atmosphere-Surface Exchange Studies (CASES) Program, can realize the full benefit of a wide variety of atmospheric measurements on many scales; this allows the study of hypothesized features of PBL development and dynamics, including frontal dynamics, nocturnal boundary development and breakdown, urban heat island effects, precipitation enhancement, and modification of the surface energy budget partitioning.

NTIS

*Sodar; Boundary Layers; Remote Sensing*

**20010122386** Colorado State Univ., Fort Collins, CO USA

**A Statistical Frequency Analysis of Lightning Producing Storms During STEPS 2000**

Cabosky, Steven R.; Jan. 2001; 104p; In English; Original contains color images

Report No.(s): AD-A395252; CI01-260; No Copyright; Avail: CASI; A06, Hardcopy; A02, Microfiche

Most cloud-to-ground (CG) lightning lowers negative charge to ground, but roughly 10% of flashes are reversed and transfer positive charge to ground. A small number of storms produce predominately (greater than 50%) positive CG lightning, and recent studies have associated the occurrence of tornadoes, hail, and microbursts with these ”positive” storms. Much of this work has been centered on case studies. The use of case studies, however, is limited; the nature of case selection is subjective and possibly susceptible to researcher bias. This research presents a new method for addressing how a thunderstorm ”looks” from a statistical perspective, and is based on information readily available to researchers and operational forecasters alike. A statistical analysis of High Plains thunderstorms during the summer of 2000 was conducted as part of the Severe Thunderstorm Electrification and Precipitation Study (STEPS). WSR-88D NEXRAD and National Lightning Detection Network (NLDN) data sets were used to produce statistical radar reflectivity distributions based on cloud-to-ground (CG) lightning flash densities.
DTIC
*Thunderstorms; Cloud-to-Ground Discharges; Electrification*

**20010122654** Department of Meteorology, Kampala, Uganda
**Republic of Uganda: Assessment of vulnerability to climate change as well as adaptation and mitigation options. Final technical report. (USA Country Studies Programme)**
Mar. 31, 1999; 84p; In English
Report No.(s): DE2000-761651; DOE/PO-FINAL; No Copyright; Avail: Department of Energy Information Bridge
Uganda spans almost 236,000 km(sup 2) of which about 15.3 percent is open water, 2 percent swamps and 26.2 percent forest. Uganda’s population is about 20 million. There are in most areas of Uganda quite well marked wet and dry seasons. The rain seasons in most parts of the country begin shortly after the hottest time of the year and are related, with a short time lag, to the main air current, both on the surface and in the upper atmosphere. On the surface these currents are generally known as the Southeast and Northeast Monsoons and these winds tend to move with the sun. Uganda (particularly the western districts) also receives rain from a westerly airstream coming from the directions of the Congo. Climate is considered as one of the major resources and rainfed agriculture is the mainstay of the economy accounting for about 50 percent GDP as of 1996 and over 95 percent of the merchandise exports and therefore the growth of the agricultural sector greatly determines the performance of the economy. It provides employment for about 80 percent of population and is the economic base for much of the manufacturing and service industries. Negative climate change would therefore adversely affect the economy. National Policies must therefore be evolved to tackle the problem of global warning associated witn greenhouse gas emissions.
NTIS
*Climate Change; Uganda; Agriculture; Economics; Marshlands*

**20010122906** Argonne National Lab., IL USA
**Global Environmental Management: A Historical Perspective**
Taylor, J.; Oct. 24, 2000; 28p; In English
Report No.(s): DE2000-766358; ANL/CGC-004-0900; No Copyright; Avail: Department of Energy Information Bridge, Microfiche
Our understanding of the Earth system has been developing rapidly over the past few decades in response to major global environmental problems such as the depletion of the ozone layer and the impact of global climate change. Our desire to understand the Earth system is partly driven by the need to manage the human impacts. In the case of human-induced global climate change, mathematical models have been instrumental in defining the existence of the potential for global warming. We can study the evolution of our understanding in global climate change over the past 200 years and critically assess how our changing understanding of the earth system has influenced our management decisions.
NTIS
*Climate Change; Climatology; Mathematical Models; Global Warming*

**20010123452** Argonne National Lab., IL USA
**Convergence estimates over the ABLE region during CASES-97 obtained from radar wind profiler and sodar data**
Coulter, R. L.; Sep. 29, 1998; 7p; In English
Report No.(s): DE2001-11029; ANL/ER/CP-96887; No Copyright; Avail: Department of Energy Information Bridge
Values of w calculated from the divergence of minisodar (MS) and radar wind profiler (RWP) horizontal wind profiles were found to agree quite well for an equilateral triangle of measurement sites located at the Argonne Boundary Layer Experiments (ABLE) facility. Values of w averaged over the daytime within the mixed layer were on the order of 0.5 cm/s. Correcting for height differences of 60-100 m among the three measurement sites separated by 63 km was helpful, particularly during windy conditions.

A regular output of daily or even hourly values from this network is possible. Upgrades to the ox RWP now being implemented will improve the near-surface radar estimates.
NTIS
*Sodar; Atmospheric Circulation; Meteorological Radar; Wind Profiles*

**20010125025** Argonne National Lab., IL USA
**Atmospheric Radiation Measurement Program facilities newsletter, August 2000**
Sisterson, D. L.; Aug. 30, 2000; 2p; In English
Report No.(s): DE2000-764204; ANL/ER/NL-00-08; No Copyright; Avail: Department of Energy Information Bridge

The primary objective of this USDA program is to provide information to the agricultural community about the geographic and temporal climatology of UV-B radiation. Scientists also use the data to determine changes in stratospheric ozone levels, cloud cover, and aerosols as they pertain to UV-B radiation and to improve the understanding of factors that control transmission of UV-B radiation. Advances have been made in areas of agriculture, human health effects, ecosystem studies, and atmospheric science. ARM Program personnel are excited about being a part of such a worthwhile effort.
NTIS
*Agriculture; Atmospheric Radiation; Climatology; Meteorology; Radiation Measurement; Ecosystems*

**20010125108** National Weather Service, Climate Prediction Center, Camp Springs, MD USA
**Proceedings of the Annual Climate Diagnostics and Prediction Workshop (25th)**
October 2000; 380p; In English; Proceedings of the Annual Climate Diagnostics and Prediction Workshop (25th), 23-27 Oct. 2000, Palisades, NY, USA
Report No.(s): PB2001-108013; No Copyright; Avail: CASI; A17, Hardcopy; A03, Microfiche

This document contains information on the following subjects: Review and Assessment of Recent Climate Anomalies; Diagnosis and Prediction of Links Between Climate Variability and Extreme Events; Diagnosis and Prediction of Global-Scale Modes of Variability; Experimental Long-Lead Prediction on Monthly, Seasonal and Interannual Time Scales; Experimental Long-Lead Prediction on Monthly, Seasonal and Interannual Scales; Climate Applications; Land Processes and Seasonal Predictability; Land Processes and Seasonal Predictability and Diagnosis and Prediction of Regional Monsoon Characteristics; and Diagnosis and Prediction of Regional Monsoon Characteristics.
NTIS
*Conferences; Climatology; Weather Forecasting*

**20010125136** NASA Ames Research Center, Moffett Field, CA USA
**Photochemical Explanation for Sprites**
Borucki, W. J., NASA Ames Research Center, USA; [1994]; 1p; In English; 1994 American Geophysical Union Meeting, 5-9 Dec. 1994, San Francisco, CA, USA; Sponsored by American Geophysical Union, USA
Contract(s)/Grant(s): RTOP 186-06-01-04; No Copyright; Avail: Issuing Activity; Abstract Only

Lightning-induced discharges occurring well above clouds showing vigorous lightning activity have recently been observed from high flying aircraft and the space shuttle. The nature of, and mechanisms that produce, these ”sprites” are unknown. A numerical model has been constructed to investigate the possibility that ultraviolet light emitted by the hot discharge columns at the cloud top penetrate to sufficiently high altitudes that atomic and molecular species present at those altitudes are excited and then produce the visible light by fluorescence. calculations show that at altitudes above the clouds, strong absorption by oxygen and ozone removes most of radiation at photoreactive wavelengths with the exception of a narrow band at 200 nm. Further calculations are being performed to identify the species responsible for the radiation.
Author
*Mathematical Models; Photochemical Reactions; Sprites (Atmospheric Physics); Ultraviolet Radiation*

**20010125419** Argonne National Lab., IL USA
**Comparison of NEXRAD WSR-88D rain estimates with gauge measurements for high and low reflectivity gradient precipitation events**
Jendrowski, P.; Kelly, D. S.; Klazura, G. E.; Thomale, J. M.; Apr. 14, 1999; 11p; In English
Report No.(s): DE2001-11754; ANL/ER/CP-98756; No Copyright; Avail: Department of Energy Information Bridge, Microfiche

Rain gauge measurements were compared with radar-estimated storm total precipitation for 43 rain events that occurred at ten locations. Gauge-to-radar ratios (G/R) were computed for each case. The G/R ratio is strongly related to precipitation type, with the mean G/R slightly less than 1.00 for high-reflectivity gradient cases and greater than 2.00 (factor of 2 radar

underestimation) for low-reflectivity gradient cases. both precipitation types indicated radar underestimate at the nearest ranges. However, the high-reflectivity gradient cases indicated radar overestimation at further ranges, while the low-reflectivity gradient cases indicated significant radar underestimation at all ranges. Occurrences of radar overestimates may have been related to high reflectivity returns from melting ice, bright-band effects in stratiform systems and hail from convective systems. Bright-band effects probably were responsible for improving the radar underestimates in the second range interval (50-99.9 km) for the low-reflectivity gradient cases. Other possibilities for radar overestimates are anomalous propagation (AP) of the radar beam. Smith, et al. concluded that bright band and AP lead to systematic overestimate of rainfall at intermediate ranges.
NTIS
*Precipitation (Meteorology); Radar Detection; Rain Gages; Meteorological Radar*

**20010125482** Lawrence Livermore National Lab., Livermore, CA USA
**Comparisons of Cloud Cover and Cloud Fractions using Remote-Sensing Retrievals**
Krueger, S. K.; Rodriguez, D.; May 18, 1999; 22p; In English
Report No.(s): DE2001-7949; UCRL-ID-134280; No Copyright; Avail: Department of Energy Information Bridge, Microfiche

The Department of Energy's Atmospheric Radiation Measurement (ARM) Program employs both upward- and downward-looking remote-sensing instruments to measure the horizontal and vertical distributions of clouds across its Southern Great Plains (SGP) site. No single instrument is capable of completely determining these distributions over the scales of interest to ARM's Single Column Modeling (SCM) and Instantaneous Radiative Flux (IRF) groups; these groups embody the primary strategies through which ARM expects to achieve its objectives of developing and testing cloud formation. Collectively, however, the data from ARM's cloud-detecting instruments offer the potential for such a three-dimensional characterization. Data intercomparisons, like the ones illustrated here, are steps in this direction. Specifically, they are valuable because they help: provide a measure of uncertainty in ARM's measurement capabilities, calibrate retrieval methods and refine algorithms and concepts. In the process, we are forced to think of meaningful ways in which measurements from different instruments can be compared and, perhaps, combined. While the ultimate goal of this particular effort is to develop the ability to accurately characterize cloud fields in three dimensions over time at the SGP site, along the way we will address such questions as which source, or combination of cloud data sources, offers a best estimate product and how can cloud observations be used to evaluate the representation of clouds in numerical models. Examples of some initial comparisons, involving satellite, millimeter cloud radar, whole sky imager and ceilometer data, are provided herein.
NTIS
*Cloud Cover; Clouds (Meteorology); Radiation Measurement; Remote Sensing*

**20010125535** Clark-Atlanta Univ., GA USA
**Mobile Meteorological Observation System** ***Final Report***
Grams, G. W.; Jun. 23, 1999; 18p; In English
Report No.(s): DE2001-763994; DOE/ER/79219-1-VOL-1; No Copyright; Avail: Department of Energy Information Bridge, Microfiche

With this grant from the Department of Energy's University Research Instrumentation Program Clark Atlanta University (CAU) has developed a Mobile Meteorological Observation System designed to facilitate research in the area of urban meteorology. The system includes an instrumented motorized laboratory based on a 25-foot motor coach with built-in generators to provide the platform for operating equipment at remote sites or while traveling on a highway to obtain measurements of temperature, pressure, humidity and aerosol size distributions (particle concentration in 32 size ranges) at the surface. On-board computers record and display data in real time. A monostatic phased-array Doppler acoustic radar (sodar) is mounted on the roof of the vehicle to provide real-time profiles of wind speed and direction, vertical motion, turbulence and thermal structure to determine mixing depths for atmospheric boundary-layer studies. A two-wavelength pulsed Nd:YAG laser radar (lidar) system mounted inside the vehicle is installed to provide real-time vertical profiles of aerosol backscattering, molecular density, and water vapor concentration. A trailer-mounted telescoping 100-foot 'crank up' tower with standard micrometeorological instruments can be towed to any site and used to provide data on turbulent fluxes of heat, momentum, and humidity at fixed locations. The system has been used to provide atmospheric data in a boundary layer research project. It has also been an integral part of the activity associated with the development of the Earth System Science (ESS) program at CAU. ESS is a comprehensive academic, research, and community outreach program with its primary objective to expose a large segment of the University's faculty and students to the multidisciplinary nature of ESS while simultaneously increasing the numbers of minority students pursuing academic and professional careers in that area. The mobile laboratory is currently being used on a variety of projects including laboratory

experiences for ESS courses, atmospheric boundary layer research observations, and various ESS outreach activities. The presence of the mobile facility developed under this grant has resulted in significant benefits to our Earth System Science program.
NTIS
*Meteorology; Earth Sciences; Meteorological Instruments*

## 48
## OCEANOGRAPHY

*Includes the physical, chemical and biological aspects of oceans and seas; ocean dynamics, and marine resources. For related information see also 43 Earth Resources and Remote Sensing.*

**20010118259** Miami Univ., FL USA
**Development and Evaluation of a Global Version of the Miami Isopycnic-Coordinate Ocean Model. Final report**
Bleck, R.; Rooth, C. G. H.; Okeefe, S.; Nov. 01, 1997; 4p; In English
Report No.(s): DE2000-760706; No Copyright; Avail: Department of Energy Information Bridge, Microfiche

The objective of this project was to test the ability of the Miami Isopycnic-Coordinate Ocean Model (MICOM) to simulate the global ocean circulation, setting the stage for the model's incorporation into coupled global climate models. An existing basin-scale model will be expanded to global domain; suitable atmospheric forcing fields, including precipitation and river runoff, will be selected; the modeling of ayssal flow will be improved by incorporating compressibility and particularly thermobaric effects; a sea-ice model will be added; parameterization options will be explored for subgrid-scale deep convection; parallel coarse- and fine-mesh simulations will be carried out to investigate the impact of grid resolution; the sensitivity of the model's solution to magnitude of vertical (diapycnal) exchange coefficient will be studied; and long-term trends in meridional heat transport and water-mass properties in model solutions will be documented and interpreted.
NTIS
*Climate Models; Ocean Models; Ocean Currents; Ocean Dynamics*

**20010118277** Princeton Univ., Plasma Physics Lab., NJ USA
**The Dynamics of Northeastern Forests in Changing Climate** ***Final Report, 4 Apr. 1994 - 31 Mar. 1998***
Pacala, S. W.; Mar. 31, 1998; 8p; In English
Report No.(s): DE2000-760249; No Copyright; Avail: Department of Energy Information Bridge, Microfiche

This project is the second of two awards from PER for a six-year project. The purpose, as stated in the original proposal, was to discover the scaling rules that translate leaf-level and individual-level processes into community- and ecosystem-level dynamics. The first three years of work were devoted to gathering empirical data for a new individual based model of the dynamics of a forest in northwestern Connecticut. Specifically, we developed empirical submodels predicting the growth, survivorship, dispersal and recruitment of individuals throughout the life cycle for the nine dominant tree species in the region. These submodels contained only light as a resource, because our analyses could not detect the significance of water or nitrogen over the range of sites examined, despite extensive sampling.
NTIS
*Climate Change; Forests; Predictions*

**20010119609** Scripps Institution of Oceanography, La Jolla, CA USA
**Sea Surface Micro-Structure: Relation to Air-Sea Fluxes, Bubble Transport and Electromagnetic Wave Radiation** ***Interim Report, Jun.-Aug. 2001***
Cox, Charles; Aug. 2001; 2p; In English
Contract(s)/Grant(s): N00014-99-1-0191
Report No.(s): AD-A394961; UCSD-99-1166; No Copyright; Avail: CASI; A01, Hardcopy; A01, Microfiche

Emphasis in the period since April has been on observations and analysis of thermal structures associated with microturbulence and air/sea thermal processes at the sea surface. our method of observation is based on an imaging infrared camera that we have adapted to use from a small boat. The camera responds to radiation in the three to five micrometer wavelength range. This is a useful range because the intensity of black body radiation from the water surface in this range is highly sensitive to the temperature of the source. Typically temperature variations of a few hundredths of a degree are detectable. The camera is mounted on a boom extending forward from the bow of the boat about 1 meter above the water. Our first observations at sea were not satisfactory because sky radiation reflected from the wavy water surface obscured the water temperature signal. This difficulty has been removed by surrounding the camera with an aluminum plate shield that acts like a parasol to make an infrared shadow

on the sea surface. With this apparatus in operation we have observed the microturbulent structures associated with evaporative cooling of the sea surface. The surface structures show warm pools typically a few centimeters in size, surrounded by narrow lines of cool water. Our interpretation is that the warm pools are broad areas of ascending water and the cool lines are descending. The overall shapes of these structures vary from drawn out figures resembling micro Langmuir cells to more nearly isotropic shapes. The change from isotropic to anisotropic shapes occurs rapidly and so far as we can observe, without relation to driving forces such as waves.
DTIC
*Electromagnetic Radiation; Capillary Waves; Seas; Surface Water; Bubbles*

**20010119927** Arizona Univ., Dept. of Mathematics, Tucson, AZ USA
**Modelling Swell, High Frequency Spreading and Wave Breaking** ***Annual Report, 1 Oct. 2000-30 Sepm 2001***
Zakharov, V. E.; Sep. 2001; 4p; In English
Contract(s)/Grant(s): N00014-98-1-0070
Report No.(s): AD-A395221; No Copyright; Avail: CASI; A01, Hardcopy; A01, Microfiche

In 2001, we: (1) (in collaboration with A.Pushkarev) improved and enhanced the Resio-Tracy code for the numerical solution of the Hasselmann's equation; (2) we elaborated (in collaboration with A.Dyachenko and O.Vasyliev) a new version of the exact Euler equation (Dyachenko's equations) for 2-dim potential flow of a fluid with free surface. A new version based on combination of Hamiltonian formalism and conformal mapping, makes possible an efficient use of the Fourier code; (3) we elaborated another code for solution of the MMT model and fulfilled the vast numerical and analytical study of this system. We found that the deviation from the weak-turbulent results can be explained by influence of the coherent structure (quasisolitons and collapses), which is inavoidable in the MMT model. We offered a modification of the MMT model, which demonstrate "restoring" of the weak-turbulent scenario.
DTIC
*Water Waves; Sea Floor Spreading; Gravitational Waves*

**20010121503** Sandia National Labs., Albuquerque, NM USA
**Emplacement of Mercury Wastes in the Sediments of the Deep-Ocean**
Gomez, L. S.; Jul. 20, 2000; 8p; In English
Report No.(s): DE2000-760764; SAND2000-0616C; No Copyright; Avail: Department of Energy Information Bridge, Microfiche

The primary goal of the U.S. Subseabed Disposal Project (SDP) was to assess the technical and environmental feasibility of disposing of high-level nuclear wastes in deep-sea sediments. Subseabed disposal, like other geological disposal options, was a multibarrier concept that studied the feasibility of burial of solidified and packaged high-level nuclear waste or spent nuclear fuel in high-integrity canisters, tens of meters within the stable geologic formations of the deep-ocean floor. These deep-ocean floor geologic formations are some of the most stable and predictable on earth. In the subseabed concept the multiple barriers of the waste form, the canister, the clay sediments, and the ocean waters were predicted to delay migration of radionuclides until they decayed to innocuous levels. The SDP was comprised of the following task groups: Site Assessment, Engineering Studies, Near Field, Sediment Barrier, Physical Oceanography, Biological Oceanography, Radiological Assessment, and Legal and Institutional. The SDP research team developed biosphere transport models to predict the oceanic transport of radionuclides. Researchers also developed the capability to determine and evaluate the risks associated both with normal disposal operations and with potential accidents. Safety assessments contributed to evaluation of the feasibility of the subseabed concept and helped focus required work to answer the feasibility questions. Even though the SDP models were developed to predict the transport of radionuclides, they can be used to predict the biosphere transport of non-radioactive environmental pollutants, such as mercury products and other toxic metals. Many of these pollutants cannot be destroyed or broken down through treatment or environmental degradation, and through physical, chemical, or biological processes will ultimately be deposited in the oceans.
NTIS
*Sediments; Waste Disposal; Radioactive Wastes; Ocean Bottom; Feasibility*

**20010121519** Brookhaven National Lab., Upton, NY USA
**Instability of tropical western Pacific warm pool during the boreal winter and spring**
Barr-Kumarakulasinghe,; Mar. 23, 1998; 6p; In English
Report No.(s): DE2000-755023; BNL-66878; KP120103; No Copyright; Avail: Department of Energy Information Bridge

A source of instability in the western Pacific warm pool is shown to be due to sea surface elevation variations caused by changes in the zonal sea-surface temperature (SST) gradient and the changes in the Pacific Ocean basin length in relation to the

warm pool latitudinal location. The variation of the sea-surface elevation is measured by using the thermocline depth response calculated from a two-layer ocean. The warm pool is shown to be barely at equilibrium during the boreal late winter and early spring by comparing the measured thermocline at 110(degree)W, 0(degree)E with the calculated thermocline depth. Based on this analysis, a failure or reversal of the climatological zonal winds are apparently not a necessary precursor for the instability of the warm pool and initiation of a warm event. A warm event can be initiated by an increase in the size of the warm pool and/or an increase in zonal SST differences during the boreal/winter spring. This mechanism could be an alternate mechanism for El-Nino Southern Oscillation (ENSO) dynamics to that postulated by Bjeknes (1969).
NTIS
*Climatology; Annual Variations; Stability; Sea Surface Temperature*

**20010121521** Brookhaven National Lab., Upton, NY USA
**Maintaining access to America's intermodal ports/technologies for decontamination of dredged sediment: New York/New Jersey harbor**
Stern,; Jones,; Donato,; Pauling,; Sontag,; May 01, 1998; 32p; In English
Report No.(s): DE2000-754974; BNL-65254; No Copyright; Avail: Department of Energy Information Bridge

One of the greatest drivers for maintaining access to America's Intermodal ports and related infrastructure redevelopment efforts over the next several years will be the control and treatment of contaminated sediments dredged from the nation's waterways. More than 306 million cubic meters (m(sup 3)) (400 million cubic yards (cy)) of sediments are dredged annually from US waterways, and each year close to 46 million m(sup 3) (60 million cy) of this material is disposed of in the ocean (EPA 842-F-96-003). The need to protect the environment against undesirable effects from sediment dredging and disposal practices is gaining increased attention from the public and governmental agencies. Meeting this need is a challenging task not only from the standpoint of solving formidable scientific and engineering problems, but also, and more importantly, from the need to implement complex collaborations among the many different parties concerned with the problem. Some 40 years ago, C.P. Snow pointed out the problems involved in communicating between the two cultures of the sciences and the humanities (Snow, 1993). Today, it is necessary to extend Snow's concept to a multicultural realm with groups that include governmental, industrial, environmental, academic, and the general public communicating in different languages based on widely different fundamental assumptions. The handling of contaminated sediments in the Port of New York/New Jersey (Port) exemplifies this problem. This paper describes a multicultural team that has formed as the result of a Congressional mandate for the development of procedures suitable for the decontamination of sediments in the Port under the Water Resources Development Act (WRDA) of 1992 (Section 405C) and 1996 (Section 226).
NTIS
*Pollution Control; Sediments; Water; Contamination*

**20010121551** NASA Goddard Space Flight Center, Greenbelt, MD USA
**Bathymetric Effects on a Tropical Cyclone Wave Field at Landfall**
Wright, C. W., NASA Goddard Space Flight Center, USA; Walsh, E. J., NASA Goddard Space Flight Center, USA; Vandemark, D., NASA Goddard Space Flight Center, USA; Krabill, W. B., NASA Goddard Space Flight Center, USA; Garcia, A. W., Army Engineer Research and Development Center, USA; Houston, S. H., National Oceanic and Atmospheric Administration, USA; Powell, M. D., National Oceanic and Atmospheric Administration, USA; Black, P. G., National Oceanic and Atmospheric Administration, USA; Marks, F. D., National Oceanic and Atmospheric Administration, USA; [2001]; 1p; In English; IGARSS 2001, 9-13 Jul. 2001, Sydney, Australia; No Copyright; Avail: Issuing Activity; Abstract Only

On 26 August 1998, the NASA Scanning Radar Altimeter (SRA) flew aboard one of the WP-3D hurricane research aircraft to document the sea surface directional wave spectrum in the region between Charleston, SC and Cape Hatteras, NC, as Bonnie, a large Category 3 hurricane, was making landfall near Wilmington, NC. Two days earlier, the SRA had documented the wave field spatial variation in open water when Hurricane Bonnie was 400 km east of Abaco Island, Bahamas. Bonnie was similar in size during the two flights, but the maximum speed in the NOAA Hurricane Research Division surface wind analysis was 15% lower prior to landfall (39 m/s) than it had been in the open ocean (46 m/s). This was compensated for by its faster movement prior to landfall (9.5 m/s) than when it was encountered in the open ocean (5 m/s). The slower movement matched the group velocity of waves of 65 m length, so waves at the peak of the spectrum outdistanced the storm as soon as they were generated. The higher translation speed prior to landfall matched the group velocity of waves of 230 m length, significantly increasing the effective fetch and duration of waves near the peak of the spectrum which propagated in the direction of the storm track. The open ocean wave height variation indicated that Hurricane Bonnie would have produced waves of 11 m significant wave height on the shore northeast of Wilmington had it not been for the continental shelf. The bathymetry distributed the steepening and breaking process

across the shelf so that the wavelength and wave height were reduced gradually as the shore was approached. The wave height 5 km from shore was about 4 m.
Author
*Bathymeters; Cyclones; Water Waves; Tropical Storms; Surface Waves*

**20010122224** Los Alamos National Lab., NM USA
**Biogeochemistry in the Global Parallel Ocean Program: Connections with Climate-Relevant Trace Gases**
Chu, S.; Elliott, S.; Sep. 19, 2000; 20p; In English
Report No.(s): DE2000-762845; LA-UR-00-4418; No Copyright; Avail: Department of Energy Information Bridge, Microfiche
No abstract prepared.
NTIS
*Atmospheric Composition; Biogeochemistry; Oceans; Trace Elements*

**20010122800** California Univ., Lawrence Berkeley Lab., Berkeley, CA USA
**Autonomous observing strategies for the ocean carbon cycle**
Bishop, J. K.; Davis, R. E.; Jul. 26, 2000; 6p; In English
Report No.(s): DE2001-775154; LBNL-46860; No Copyright; Avail: Department of Energy Information Bridge
Understanding the exchanges of carbon between the atmosphere and ocean and the fate of carbon delivered to the deep sea is fundamental to the evaluation of ocean carbon sequestration options. An additional key requirement is that sequestration must be verifiable and that environmental effects be monitored and minimized. These needs can be addressed by carbon system observations made from low-cost autonomous ocean-profiling floats and gliders. We have developed a prototype ocean carbon system profiler based on the Sounding Oceanographic Lagrangian Observer (SOLO; Davis et al., 1999). The SOLO/ carbon profiler will measure the two biomass components of the carbon system and their relationship to physical variables, such as upper ocean stratification and mixing. The autonomous observations within the upper 1500 m will be made on daily time scales for periods of months to seasons and will be carried out in biologically dynamic locations in the world's oceans that are difficult to access with ships (due to weather) or observe using remote sensing satellites (due to cloud cover). Such an observational capability not only will serve an important role in carbon sequestration research but will provide key observations of the global ocean's natural carbon cycle.
NTIS
*Autonomy; Oceanography; Remote Sensing; Carbon Cycle; Clouds (Meteorology)*

**20010123252** Delaware Univ., Newark, DE USA
**How to Measure Dissolved Organic Matter in Seawater. NSF Final Project Report**
Sharp, J. H.; Jul. 15, 1994; 7p; In English
Report No.(s): DE2001-761724; OCE-9200970-NSF; No Copyright; Avail: Department of Energy Information Bridge
Summary of Completed Project: Reliable measurement of the content of dissolved organic carbon in seawater has been difficult in the past and broad community achievement of this capability is the primary goal of this research project. The difficulty in the analysis was due to problems with oxidation of organic matter to carbon dioxide and measurement of the resultant carbon dioxide. In both cases, the determination of complete oxidation and correction for instrument or reagent blanks were interpreted in different fashions in various laboratories. This project was able to build on the methods development efforts of a number of investigators and then provide guidelines for many other analysts with protocols and uniform blank and samples for comparison. Broad community involvement and preliminary good agreement is the result. The project is continuing so that more thorough comparison of about 75-100 laboratories can be completed.
NTIS
*Dissolved Organic Matter; Organic Materials; Sea Water; Measuring Instruments*

**20010123257** Ohio State Univ., Columbus, OH USA
**Regulation of Photosynthetic Carbon Fixation on the Ocean Margins**
Paul, J. H.; Tabita, F. R.; Nov. 24, 1997; 8p; In English
Report No.(s): DE2001-761177; No Copyright; Avail: Department of Energy Information Bridge
The overall goal of the project is to understand the regulation of photosynthetic carbon fixation on the ocean margins.
NTIS
*Carbon; Oceanography; Photosynthesis; Regulations; Continental Shelves*

**20010124072** NASA Goddard Space Flight Center, Greenbelt, MD USA

**Comparison of DMSP SSM/I and LANDSAT 7 ETM+ Sea Ice Concentrations During Summer Melt**

Cavalieri, Donald J., NASA Goddard Space Flight Center, USA; Markus, Thorsten, NASA Goddard Space Flight Center, USA; Ivanoff, Alvaro, Science Systems and Applications, Inc., USA; [2001]; 22p; In English; No Copyright; Avail: CASI; A03, Hardcopy; A01, Microfiche

As part of NASA's EOS Aqua sea ice validation program for the Advanced Microwave Scanning Radiometer (AMSR-E), LANDSAT 7 Enhanced Thematic Mapper (ETM+) images were acquired to develop a sea ice concentration data set with which to validate AMSR-E sea ice concentration retrievals. The standard AMSR-E Arctic sea ice concentration product will be obtained with the enhanced NASA Team (NT2) algorithm. The goal of this study is to assess the accuracy to which the NT2 algorithm, using DMSP Special Sensor Microwave Imager radiances, retrieves sea ice concentrations under summer melt conditions. Melt ponds are currently the largest source of error in the determination of Arctic sea ice concentrations with satellite passive microwave sensors. to accomplish this goal, LANDSAT 7 ETM+ images of Baffin Bay were acquired under clear sky conditions on the 26th and 27th of June 2000 and used to generate high-resolution sea ice concentration maps with which to compare the NT2 retrievals. Based on a linear regression analysis of 116 25-km samples, we find that overall the NT2 retrievals agree well with the LANDSAT concentrations. The regression analysis yields a correlation coefficient of 0.98. In areas of high melt ponding, the NT2 retrievals underestimate the sea ice concentrations by about 12% compared to the LANDSAT values.

Author

*Sea Ice; Microwave Imagery; Satellite Instruments; Remote Sensing; Errors; Correlation Coefficients*

**20010125536** Federation of American Societies for Experimental Biology, Bethesda, MD USA

**Export and Molecular Level Characterization of Dissolved and Particulate Organic Matter from the Mid-Atlantic Bight *Final Report***

Repeta, D. J.; Eglinton, T. I.; Chen, R. F.; Feb. 01, 2000; 10p; In English

Report No.(s): DE2001-763993; DOE/ER61528; DOE/OR759,KP0202,KP120203; No Copyright; Avail: Department of Energy Information Bridge, Microfiche

As part of the OMP (Organic Matter Particulate) field program, Dr. Repeta served as chief scientist on two whole shelf cruises to survey the MAB (Mid-Atlantic Bight), one in late winter/spring (February/March 1996) and one in summer (July/August, 1996). Our field program surveyed the shelf under two very different biogeochemical regimes. In the late winter/spring, river discharge and primary productivity are maximal. The water column is well mixed, relatively fresh, and has high standing stocks of nutrients and biomass. In summer, both primary production and river discharge decrease. A strong pycnocline develops that restricts the freshwater inputs to a very shallow surface layer, and isolates surface water from colder deep water (cold pool). Our objective was to inventory dissolved and particulate forms of carbon (and to the extent possible, nitrogen) in order to establish spatial gradients and seasonal patterns of elemental distribution and flux on a much wider area of the shelf than accounted for by the moored array. We proposed to use geochemical tracers that integrate over longer spatial and temporal scales to supplement C cycling studies conducted by the benthic, water column processes and moored array teams of OMP.

NTIS

*Particulates; Organic Materials*

## 51
## LIFE SCIENCES (GENERAL)

*Includes general research topics related to plant and animal biology (non-human); ecology; microbiology; and also the origin, development, structure, and maintenance, of animals and plants in space and related environmental conditions. For specific topics in life sciences see categories 52 through 55.*

**20010119224** NASA Ames Research Center, Moffett Field, CA USA

**How Cyanobacterial Distributions Reveal Flow and Irradiance Conditions of Photosynthetic Biofilm Formation**

Prufert-Bebout, Lee, NASA Ames Research Center, USA; [2001]; 1p; In English; National Astrobiology Institute Meeting, 9-12 Apr. 2001, Washington, DC, USA; Sponsored by National Astrobiology Inst., USA

Contract(s)/Grant(s): RTOP 344-50-92-02; No Copyright; Avail: Issuing Activity; Abstract Only

Microbial life on Earth is enormously abundant at sediment-water interfaces. The fossil record in fact contains abundant evidence of the preservation of life on such surfaces. It is therefore critical to our interpretation of early Earth history, and potentially to history of life on other planets, to be able to recognize life forms at these interfaces. On Earth this life often occurs as organized structures of microbes and their extracellular exudates known as biofilms. When such biofilms occur in areas

receiving sunlight photosynthetic biofilms are the dominant form in natural ecosystems due to selective advantage inherent in their ability to utilize solar energy. Cyanobacteria are the dominant phototrophic microbes in most modern and ancient photosynthetic biofilms, microbial mats and stromatolites. Due to their long (3.5 billion year) evolutionary history, this group has extensively diversified resulting in an enormous array of morphologies and physiological abilities. This enormous diversity and specialization results in very specific selection for a particular cyanobacterium in each available photosynthetic niche. Furthermore these organisms can alter their spatial orientation, cell morphology, pigmentation and associations with heterotrophic organisms in order to fine tune their optimization to a given micro-niche. These adaptations can be detected, and if adequate knowledge of the interaction between environmental conditions and organism response is available, the detectable organism response can be used to infer the environmental conditions causing that response. This presentation will detail two specific examples which illustrate this point, Light and water are essential to photosynthesis in cyanobacteria and these organisms have specific detectable behavioural responses to these parameters. We will present cyanobacterial responses to quantified flow and irradiance to demonstrate the interpretative power of distribution and orientation information. This study presents new results, but many such examples are already found in the literature.
Author
*Bacteria; Biofilms; Irradiance; Photosynthesis; Ecosystems*

**20010119225** NASA Ames Research Center, Moffett Field, CA USA
**Biogeochemical Processes in Microbial Ecosystems**
DesMarais, David J., NASA Ames Research Center, USA; [2001]; 1p; In English; National Astrobiology Institute Meeting, 10-12 Apr. 2001, Washington, DC, USA; Sponsored by National Astrobiology Inst., USA
Contract(s)/Grant(s): RTOP 344-50-92-02; No Copyright; Avail: Issuing Activity; Abstract Only

The hierarchical organization of microbial ecosystems determines process rates that shape Earth's environment, create the biomarker sedimentary and atmospheric signatures of life and define the stage upon which major evolutionary events occurred. In order to understand how microorganisms have shaped the global environment of Earth and potentially, other worlds, we must develop an experimental paradigm that links biogeochemical processes with ever-changing temporal and spatial distributions of microbial population, and their metabolic properties. Photosynthetic microbial mats offer an opportunity to define holistic functionality at the millimeter scale. At the same time, their Biogeochemistry contributes to environmental processes on a planetary scale. These mats are possibly direct descendents of the most ancient biological communities; communities in which oxygenic photosynthesis might have been invented. Mats provide one of the best natural systems to study how microbial populations associate to control dynamic biogeochemical gradients. These are self-sustaining, complete ecosystems in which light energy absorbed over a diel (24 hour) cycle drives the synthesis of spatially-organized, diverse biomass. Tightly-coupled microorganisms in the mat have specialized metabolisms that catalyze transformations of carbon, nitrogen. sulfur, and a host of other elements.
Author
*Biogeochemistry; Ecosystems; Microorganisms; Populations; Biomass*

**20010119528** NASA Ames Research Center, Moffett Field, CA USA
**The Effects of Long-Term Feeding of Rodent Food Bars on Lipid Peroxidation and Antioxidant Enzyme Levels In Fisher Rats**
Ramirez, Joel, Lockheed Martin Corp., USA; Zirkle-Yoshida, M., Foothill-De Anza Community Coll., USA; Piert, S., Lockheed Martin Corp., USA; Barrett, J., Adecco, USA; Yul, D., Lockheed Martin Corp., USA; Dalton, B., NASA Ames Research Center, USA; Girten, B., NASA Ames Research Center, USA; [2001]; 1p; In English
Contract(s)/Grant(s): NAS2-14263; No Copyright; Avail: Issuing Activity; Abstract Only

A specialized rodent food bar diet has been developed and utilized successfully for short-duration shuttle missions. Recent tests conducted in preparation for experiments aboard the International Space Station (ISS) indicated that long-term food bar feeding for three months induced hyperlipidemia in rats. This study examined oxidative stress status in livers of these same animals. Spectrophotometric analysis of 79 Fischer rat livers (40 female and 39 male) for lipid peroxidation (LPO) and superoxide dismutase (SOD) was conducted using Bioxytech LPO-587(TM) assay kit and SOD-525(Tm) assay kit, respectively. The treatment groups consisted of 20 male CHOW and 19 male FOOD BAR rats and 20 female CHOW and 20 female FOOD BAR rats. Statistical analysis to compare differences between groups was performed by standard analysis of variance procedures. The male FOOD BAR group LPO mean (3.6 +/- 0.2 mmol/g) was significantly (p less than or equal to 0.05) greater than that of the male CHOW group (2.1 +/-0.1 mmol/g). Moreover the female FOOD BAR group LPO mean (2.9 +/-0.1 mmol/g) was also significantly greater than the female CHOW group mean (2.2 +/-0.1 mmol/g). The mean values for SOD in both male and female groups showed no significant differences between CHOW and FOOD BAR groups. These results show that LPO levels were

significantly higher in both the male and female FOOD BAR groups compared to CHOW groups and that there was no concomitant increase in SOD levels across the group. In addition, males showed a greater difference than females in terms of LPO levels. These findings suggest a need for further investigation into the use of the current food bar formulation for long-term experiments such as those planned for the ISS.
Author
*Antioxidants; Assaying; Enzymes; Lipids; Rodents*

**20010119592** Medicine and Dentistry Univ. of New Jersey, The Cancer Inst. of New Jersey, Camden, NJ USA
**TGFbeta Type I Receptor Kinase Inhibitors - A Novel Treatment for Breast Cancer** ***Annual Report, 1 Jun. 2000-31 Mar. 2001***
Reiss, Michael; Apr. 2001; 8p; In English
Contract(s)/Grant(s): DAMD17-00-1-0510
Report No.(s): AD-A394908; No Copyright; Avail: CASI; A02, Hardcopy; A01, Microfiche

Transforming Growth Factor-Bs (TGFBeta)are polypeptides that are constitutively secreted and activated by many breast carcinomas. They contribute to the tumor's ability to invade and metastasize, to induce angiogenesis and to escape from immune destruction. These circumstances raise the question whether blocking the effects of tumor-derived TGFBeta on normal tissue (stroma, bloodvessels and immune cells) could be developed as a novel approach to the treatment of breast cancer. We propose to block TGFBeta action by developing small molecules that inhibit the type I TGFBeta receptor kinase, which is the key molecule that initiates and mediates TGFBeta signaling. We plan to develop a cell free ELISA-type assay for high-throughput screening for selective inhibitors of TBR-I kinase activity by using an antibody that specifically detects the phosphorylated form of its substrate, Smad2. Combinatorial libraries of small molecules will then be screened for potent and highly selective for the TBR-I kinase. These will then be tested against normal cells in vitro using a number of different assays for TGFBeta's biological effects. Promising compounds will then be tested for their antitumor activity against highly metastatic, -angiogenic and immunogenic varieties of transplantable breast cancers in mice.
DTIC
*Mammary Glands; Cancer; Polypeptides; Tumors*

**20010119593** International Trauma, Anesthesia and Critical Care Society, Baltimore, MD USA
**Wolf Creek VI Conference on Cardiopulmonary Resuscitation** ***Final Report***
Weil, Max; Sep. 2001; 18p; In English
Contract(s)/Grant(s): DAMD17-01-1-0749
Report No.(s): AD-A394910; No Copyright; Avail: CASI; A03, Hardcopy; A01, Microfiche

The Sixth Wolf-Creek Conference was held at the Ritz Carlton Hotel in Rancho Mirage from June 4, 2001 to June 7, 2001. Approximately 70 internationally renown experts on Cardiopulmonary Resuscitation attended the Conference and presented their most recent research findings. Four Army Medical officers attended and observed the Conference. The experts specifically focused on issues of optimizing waveforms and emergencies for defibrillation, mechanical options for improving blood flow during cardiac arrest, more optimal vasopressor interventions during CPR, myocardial and cerebral preservation during CPR, and outcome measurements. The proceedings of the Conference will be published in a Supplement of the Journal of Critical Care Medicine.
DTIC
*Resuscitation; Conferences; Medical Services*

**20010119596** Georgetown Univ., Washington, DC USA
**IGF Regulation of Cell Adhesion in Breast Cancer** ***Annual Report, 1 Jul. 1999-30 Jun. 2000***
DaCosta, Stacey; Jul. 2000; 13p; In English
Contract(s)/Grant(s): DAMD17-97-1-7061
Report No.(s): AD-A394915; No Copyright; Avail: CASI; A03, Hardcopy; A01, Microfiche

Studies with gene knockout mice have demonstrated M6P/IGF2R is an inhibitor of IGF2-dependent embryonic growth. Tumor-associated M6P/IGF2R mutations that disrupt IGF2 binding have been described suggesting that the IGF2 antagonist action of M6P/IGF2R may also play a role suppressing tumorigenesis. To investigate the role of M6P/IGF2R as an IGF2 antagonist in breast cancer, M6P/ IGF2R was overexpressed in IGF2-sensitive MCF7 cells. Recombinant IGF1 - and IGF2-dependent proliferation was compared between control transfected cells, cells constitutively overexpressing wildtype M6P/IGF2R and cells overexpressing an IGF2-binding or an M6P-binding defective mutant. Despite 5- to 10-fold overexpression of wildtype M6P/IGF2R, IGF2-dependent growth in either monolayer or in suspension culture was unaffected. to confirm this

unanticipated negative result, MCF7 cell clones engineered to overexpress wildtype M6P/IGF2R under the control of a doxycycline inducible promoter were utilized. Ten- to 15-fold induction of M6P/IGF2R expression with doxycycline resulted in no change of growth rate for cells in the presence of IGF2 when compared with control cells. It has previously been demonstrated that affinity of IGF2 for M6P/IGF2R suppresses autocrine IGF2 activity (Ellis, M. J. C. et a!., Mol Endo 10:286-297, 1996). These data therefore suggests that M6P/IGF2R may operate to inhibit autocrine IGF2 within the secretory pathway but not efficiently suppress the action of IGF2 after it has been released from the cell.
DTIC
*Cancer; Genetic Engineering; Mammary Glands*

**20010119597** Michigan State Univ., East Lansing, MI USA
**Role of Era Splicing Variants in Regulation of Ap-1 Directed Gene Transcription in Breast Cancer Cells** ***Annual Report***
Bollig, Aliccia B.; Miksicek, Richard J.; Jun. 2001; 57p; In English
Contract(s)/Grant(s): DAMD17-99-1-9293
Report No.(s): AD-A394916; No Copyright; Avail: CASI; A04, Hardcopy; A01, Microfiche

This report presents results from functional analysis of estrogen receptor-alpha (ERa) mRNA splicing variants and offers insight into the nature of their transcriptional activity. Efforts to establish a cellular transactivating role for ERa mRNA splicing variants have identified three genes, which do not contain consensus EREs in their promoters, that are regulated by one or both of the isoforms, ERAE3 and ERAE5. Expression of a reporter gene driven by the chicken ovalbumin promoter is induced by ERAE5 in cells treated with PMA, and by ERAE3 and wt ERa with E2 and PMA cotreatment. A short region of the collagenase promoter (-73 to +63 relative to the transcription start site) containing an AP-1 motif is activated by ERAE5 and E2-liganded ERAE3 in the presence of PMA. The human IGF-1 promoter is constitutively induced by ERAE5 but is not regulated by wt ERa or ERAE3. Overexpression of c-jun enhanced receptor activities on both the ovalbumin and collagenase prbmoters. It is likely that the regulation of these noncanonical promoters by wt ERa and ERa splicing variants involves protein-protein interactions with co-regulatory proteins and upstream factors that in turn act through their cognate DNA-response elements (e.g., c-jun and c-fos). in vitro binding studies show that wt ERa directly binds c-jun and c-fos; also, ERAE3, ERAE5 and wt ERa bind the steroid receptor corepressor SMRT.
DTIC
*Genes; Mammary Glands; Cancer*

**20010119598** Georgetown Univ., Washington, DC USA
**Beta Catenin-Regulated Genes in Breast Cancer** ***Final Report, 1 Aug. 1997-31 Jul. 2000***
Feltes, Carolyn; Nov. 2000; 18p; In English; Original contains color images
Contract(s)/Grant(s): DAMD17-97-1-7164
Report No.(s): AD-A394917; No Copyright; Avail: CASI; A03, Hardcopy; A01, Microfiche

This study investigates the role of cadherin-11 in the progression of breast cancer from a less invasive, more differentiated phenotype to a more invasive, less differentiated phenotype. The cadherins are transmembrane proteins that have been shown in many previous studies to be involved in cancer progression. Cadherin-11, in particular, is expressed preferentially in breast cancers exhibiting a more invasive, less differentiated phenotype. Results of this study indicate that cadherin-11 expression in MDA-MB 231 breast cancer cells is significantly regulated by Beta-catenin signaling at both the protein and RNA levels. Beta-catenin, a signaling molecule in the wnt-1 pathway, affects transcriptional regulation of gene expression in both colon and breast cancer, including the expression of c-inyc and cyclin D. In addition, the function of cadherin-11 has been examined by stable transfection of cadherin 11 intact and/ or variant into two well-differentiated breast cancer cell lines. We have found that cadherin 11 confers a specific phenotype to normally well-differentiated epithelial cells, including increased invasion. In conclusion, examination of both the regulation and function of cadherin-11 expression may offer clues about the nature of breast cancer progression, especially the processes of invasion and metastasis.
DTIC
*Genes; Gene Expression; Cancer; Proteins*

**20010119618** RAND Corp., Santa Monica, CA USA
**Updating the Classification System for the Medicare Inpatient Rehabilitation Prospective Payment System**
Carter, Grace M.; Relies, Daniel A.; Ridgeway, Gregory K.; Feb. 2001; 76p; In English
Report No.(s): AD-A395041; RAND/DRU-2491-HCFA; No Copyright; Avail: CASI; A05, Hardcopy; A01, Microfiche

In the Balanced Budget Act of 1997, Congress mandated that the Health Care Financing Administration (HCFA) implement a Prospective Payment System (PPS) for inpatient rehabilitation. RAND contracted with HCFA to carry out the research, and

recruited a Technical Expert Panel (TEP) to advise on issues related to the design and development of such a PPS. The TEP convened in May 2000 to review our Interim Report. A key topic discussed there was the construction of Function Related Groups (FRGs), which will be the basis of the payment classification system. This report follows up the TEP suggestions, both formal and informal, for further research into FRGs. In the interim report, we used CART to obtain candidate FRGs. The TEP asked for a broader context within which to view the results. Specifically, the TEP wanted us to (1) Explore alternative model forms. Develop models to compete with CART in terms of having strong predictive performance. (2) Consider indices of function in addition to the cognitive and motor scores. Payment formulas based on these measures might offer better estimates of cost. (3) Evaluate out-of-sample performance of the models. An important element of a payment system is whether payment formulas developed from data in one year apply in future years. In this report, we describe the steps we have taken to update FRGs on newer data while incorporating the above suggestions.
DTIC
*Clinical Medicine; Public Health; Financial Management*

**20010119623** NASA Ames Research Center, Moffett Field, CA USA
**Models of Protocellular Structure, Function and Evolution**
New, Michael H., NASA Ames Research Center, USA; Pohorille, Andrew, NASA Ames Research Center, USA; Szostak, Jack W., Massachusetts General Hospital, USA; Keefe, Tony, Massachusetts General Hospital, USA; Lanyi, Janos K., California Univ., USA; [2001]; 1p; In English; National Astrobiology Institute Meeting, 9-12 Apr. 2001, Washington, DC, USA; Sponsored by National Astrobiology Inst., USA
Contract(s)/Grant(s): RTOP 344-38-00-04; No Copyright; Avail: Issuing Activity; Abstract Only

In the absence of any record of protocells, the most direct way to test our understanding, of the origin of cellular life is to construct laboratory models that capture important features of protocellular systems. Such efforts are currently underway in a collaborative project between NASA-Ames, Harvard Medical School and University of California. They are accompanied by computational studies aimed at explaining self-organization of simple molecules into ordered structures. The centerpiece of this project is a method for the in vitro evolution of protein enzymes toward arbitrary catalytic targets. A similar approach has already been developed for nucleic acids in which a small number of functional molecules are selected from a large, random population of candidates. The selected molecules are next vastly multiplied using the polymerase chain reaction.
Derived from text
*Protobiology; Enzymes; Genetics; Models*

**20010120038** Promed Trading S.A., Miami, FL USA
**Evaluation of Drug and Vaccine Candidates in the Human Malaria/Aotus Monkey Model** ***Final Report, 1 May 1995-30 Sep. 2001***
Obaldia, Nicanor; Oct. 2001; 21p; In English
Contract(s)/Grant(s): DAMD17-96-C-6051
Report No.(s): AD-A394686; No Copyright; Avail: CASI; A03, Hardcopy; A01, Microfiche

This report presents data: On the evaluation of antimalarial drugs. Experimental drugs GJ-287 (WR282650; BP20546) and GJ-QZ (WR282651; BP20537) were non toxic when given to Aotus orally at 20 mg/kg for three consecutive days and only transient changes on blood leukograms and liver enzyme ALT were detected. These drugs were not effective alone or in combination with Chloroquine when Aotus monkeys infected with Plasm odium falciparum FVO strain were treated for three consecutive days. Significant differences on Lymphocytes and Granulocytes counts were found between male and female Aotus when hematological and renal chemistry values of feral laboratory adapted Aotus monkeys were determined.
DTIC
*Infectious Diseases; Drugs; Vaccines*

**20010120039** Brooke Army Medical Center, Fort Sam Houston, TX USA
**Teledermatology** ***Final Report, 15 Apr. 1999-31 Dec. 1999***
Pak, Hon; David-Bajar, Kathleen; Smith-Cruz, Lisa L.; Jan. 2000; 15p; In English
Report No.(s): AD-A394663; No Copyright; Avail: CASI; A03, Hardcopy; A01, Microfiche

Teledermatology provides better access to care for the patient, a short turn around time for replies from the dermatologist and a savings of time, costs and resources by eliminating the need to send the patient to the dermatologist.
DTIC
*Dermatology; Costs*

**20010120137** Geological Survey, Reston, VA USA

**Extended Abstracts from BioGeo99: Applications of Geospatial Technology to Biological Sciences**

Handley, Lawrence R.; D'Erchia, Frank J.; Charron, Tammy M.; Dec. 2000; 55p; In English

Report No.(s): AD-A395174; USGS/BRD/ITR-2000-0008; No Copyright; Avail: CASI; A04, Hardcopy; A01, Microfiche

On November 2-4, 1999, the U.S. Geological Survey held BioGeo99 to provide a forum in which USGS scientists, other agencies, universities, and the private sector could meet to share information in the area of applying geospatial technologies to the biological sciences. The format for the symposium included guest speakers, panel discussions, plenary sessions, oral and poster presentations, and workshops on a wide range of topics, including the use and application of Global Positioning System (GPS), aquatic and terrestrial telemetry, national classification systems, remote sensing, metadata, and other geospatial technologies used in biological science applications. After the meeting abstracts were extended by the presenters to more fully explain what was presented and detail how geospatial technologies enhance scientific research, management of biological resources, and partnerships between government and private industry.

DTIC

*Conferences; Geological Surveys; Abstracts; Remote Sensing; Biology*

**20010120141** Air Force Inst. of Tech., Wright-Patterson AFB, OH USA

**The Effects of Ovine Interferon-Tau Treatment on Theiler's Virus-Induced Demyelination in Female SJL/J Mice**

Traweek, Kasandra T.; Aug. 2001; 251p; In English; Original contains color images

Report No.(s): AD-A395154; No Copyright; Avail: CASI; A12, Hardcopy; A03, Microfiche

Theiler's murine encephalomyelitis virus (TMEV) is a picornavirus that is used as an animal model for the study of multiple sclerosis (MS). One of the current therapies for MS involves the administration of a type I interferon, IFN-beta. The administration of IFN-beta can result in unfavored, psychological side-effects including clinical depression. A second type I interferon, ovine IFN-tau, has previously been found to be less cytotoxic than IFN-beta. This study focuses on the effects of IFN-tau on SJL/J mice at o months, 2 months, and 4 months post-infection with TMEV strain BeAn. Through neurological exams and histological analysis of the CNS, we report that IFN-tau administration significantly reversed the neurological abnormalities induced by TMEV infection when given at 4 months post-infection. Histologically, treatment at 4 months post-infection resulted in a significant decrease in lesion occurrence in the ventral and dorsal funiculi of the spinal cord. Inflammation and - demyelination were both reduced as measured via percent area effected in hemotoxylin + eosin stained and myelin oligodendrocyte glycoprotein-specific immunostained spinal cord sections embedded in paraffin. No effect was detected with treatment at 2 months post-infection.

DTIC

*Central Nervous System; Neurology; Spinal Cord; Viruses; Interferon; Animals*

**20010120143** Cornell Univ., School of Applied and Engineering Physics, Ithaca, NY USA

**Patterning Lipid Bilayers on Microfabricated Metal Electrodes**

Orth, Reid N.; Hafez, Ismail; Kmeoka, Jun; Lindau, Manfred; Craighead, Harold G.; Sep. 17, 2001; 14p; In English

Report No.(s): AD-A395150; No Copyright; Avail: CASI; A03, Hardcopy; A01, Microfiche

Lipid molecules were immobilized on surface of photolithographically patterned chromium and titanium. Large unilamellar lipid vesicles were found to bind on the native oxide surface of patterned support metals. Metal evaporation and resist liftoff techniques were used to pattern metal an a hydrophobic polymer surface. Lipids bound on solid substrates provide a biological interface for current measuring electrodes to detect bound cell or biomaterial. This patterning technique provides means to specifically bind lipids and conjugated biomaterials (polyethylene glycol (PEG), biotin, fluorescence dyes, and DNA oligomers) to the electrode surface. This technique may be applied to patterning biomaterial on metal inside thermally bonded microfluidic channels, to form titanium coated biomedical implants, and to create robust lipid-conjugated electrodes for biosensor applications.

DTIC

*Bioinstrumentation; Electrodes; Lipids; Metal Surfaces; Molecules*

**20010120148** Army Research Inst. of Environmental Medicine, Natick, MA USA

**Women at Altitude: Effect of Menstrual-Cycle Phase on Acute Mountain Sickness During Deployment to High Altitude Terrain**

Rock, Paul B.; Muza, Stephen R.; Fulco, Charles S.; Braun, Barry; Zamudio, Stacy; Oct. 2001; 45p; In English

Report No.(s): AD-A395140; USARIEM-T-01/18; No Copyright; Avail: CASI; A03, Hardcopy; A01, Microfiche

The physiologic responses to the cyclic fluctuations in ovarian steroid hormones associated with the menstrual cycle in women are well known to affect certain disease states and could alter responses to environmental stressors. Rapid deployment

to high mountain terrain induces acute mountain sickness (AMS), which can be an important source of performance decrements and Disease and Non-Battle Injury loss of personnel in military units. to determine the effect of menstrual cycle phase on the occurrence of AMS, symptoms were assessed in 39 women aged 18 to 33 years with normal menstrual cycles who were expose to 4300 m altitude continuously on the summit of Pikes Peak, CO for 12 days or in a hypobaric chamber for 60 hours during the early follicular (follicular phase group) or luteal phase (luteal phase group) of their menstrual cycle. The clinical course of AMS in these women was similar to that reported previously in men. Overall, more than 60% of the women in this study experienced AMS during the first 24 hours of altitude exposure. There were no statistically significant differences between symptom scores of the follicular and luteal phase groups. However, the prevalence of AMS was slightly lower in the luteal phase compared to follicular phase volunteers. We conclude that effects of menstrual cycle phase are too small to be of practical significance for most women involved in military operations or civilian recreational pursuits at altitudes up to 4300 m.
DTIC
*Altitude Sickness; Deployment; Mountains; Physiological Responses; Terrain; Military Operations*

**20010120150** Air Command and Staff Coll., Maxwell AFB, AL USA
**The Impact of Pregnancy on U.S. Army Readiness**
Bucher, Merideth A.; Apr. 1999; 37p; In English
Report No.(s): AD-A395136; AU/ACSC/016/1999-04; No Copyright; Avail: CASI; A03, Hardcopy; A01, Microfiche

The impact of pregnancy on U.S. Army readiness came to the forefront following the Persian Gulf War and the large-scale deployment of military servicewomen. Some deploying units reported that non-deployable rates for pregnancy among women were as much as 30% of those assigned. Numerous studies were conducted to determine the impact of pregnancy on Army readiness and different conclusions were drawn. From a tactical perspective the numbers of non-deployable for pregnancy are more than 16% in support units with a high concentration of female soldiers. Pregnancy in these units has a great impact on readiness, as well as the experience of the pregnant soldier. The Army should evaluate for implementation a one-year comprehensive Maternity Leave of Absence program that takes place during the time the soldier is non-deployable for pregnancy. A volunteer from the Reserve Component force will fill the pregnant soldiers vacancy as a deployable replacement, while gaining valuable active duty training at the same time. The MLA program would benefit the Army by integrating Reserve Component forces and by limiting the time lost from the pregnant soldiers active duty service obligation.
DTIC
*Pregnancy; Armed Forces (USA); Warfare*

**20010120530** Bechtel Nevada Corp., Las Vegas, NV USA
**Plant-Stress Measurements Using Laser-Induced Fluorescence Excitation: Poland Experiment**
Capelle, G.; Jones, S.; May 01, 1999; 16p; In English
Report No.(s): DE2001-10608; DOE/NV/11718-351; No Copyright; Avail: Department of Energy Information Bridge, Microfiche

Bechtel Nevada's Special Technologies Laboratory (STL) has been involved in remote sensing for many years, and in April 1995 STL began to study the use of active remote sensing for detecting plant stress. This work was motivated by the need to detect subsurface contamination, with the supposition that this could be accomplished by remote measurement of optical signatures from the overgrowing vegetation. The project has been a cooperative DOE (Department of Energy)/Disney effort, in which basic optical signature measurements (primarily fluorescence) were done at the Disney greenhouse facilities at Epcot Center in Florida, using instrumentation developed by STL on DOE funding. The primary instrument is a LIFI (laser induced fluorescence imaging) system, which had originally been developed for detection of surface uranium contamination at DOE sites. to deal specifically with the plant stress measurements, a LIFS (laser-induced fluorescence spectroscopy) system was built that utilizes the same laser, but captures the complete fluorescence spectrum from blue to red wavelengths. This system had continued to evolve, and the version in existence in September 1997 was sent to Poland, accompanied by two people from STL, for the purpose of making the measurements described in this report.
NTIS
*Laser Induced Fluorescence; Lasers; Plant Stress; Spectroscopy*

**20010120788** NASA Ames Research Center, Moffett Field, CA USA
**Composition of Hydrothermal Vent Microbial Communities as Revealed by Analyses of Signature Lipids, Stable Carbon Isotopes and Aquificales Cultures**
Jahnke, Linda L., NASA Ames Research Center, USA; Edger, Wolfgang, Regensburg Univ., Germany; Huber, Robert, Regensburg Univ., Germany; Hinrichs, Kai-Uwe, Woods Hole Oceanographic Inst., USA; Hayes, John M., Woods Hole

Oceanographic Inst., USA; DesMarais, David J., NASA Ames Research Center, USA; Cady, Sherry, Portland State Univ., USA; Hope, Janet M., Australian Geological Survey Organisation, Canberra, Australia; Summons, Roger E., Australian Geological Survey Organisation, Canberra, Australia; Feb. 28, 2001; 32p; In English; Sponsored in part by the Fonds der Chemischen Industrie (to KOS)

Contract(s)/Grant(s): RTOP 344-38-32-01; No Copyright; Avail: CASI; A03, Hardcopy; A01, Microfiche

Extremely thermophilic microbial communities associated with the siliceous vent walls and outflow channel of Octopus Spring, Yellowstone National Park, have been examined for lipid biomarkers and carbon isotopic signatures. These data were compared with that obtained from representatives of three Aquificales genera. Thermocrinis ruber. "Thermocrinis sp. HI", Hydrogenobacter thermophilus TK-6, Aquifex pyrophilus and Aquifex aeolicus all contained phospholipids composed not only of the usual ester-linked fatty acids, but also ether-linked alkyls. The fatty acids of all cultured organisms were dominated by a very distinct pattern of n-C-20:1 and cy-C-21 compounds. The alkyl glycerol ethers were present primarily as CIS() monoethers with the expection of the Aquifex spp. in which dialkyl glycerol ethers with a boarder carbon-number distribution were also present. These Aquificales biomarker lipids were the major constituents in the lipid extracts of the Octopus Spring microbial samples. Two natural samples, a microbial biofilm growing in association with deposition of amorphous silica on the vent walls at 92 C, and the well-known 'pink-streamers community' (PSC), siliceous filaments of a microbial consortia growing in the upper outflow channel at 87 C were analyzed. Both the biofilm and PSC samples contained mono and dialkyl glycerol ethers with a prevalence of C-18 and C-20 alkyls. Phospholipid fatty acids were comprised of both the characteristic Aquificales n-C-20:1 and cy-C-21, and in addition, a series of iso-branched fatty acids from i-C-15:0 to i-C-21:0, With i-C-17:0 dominant in the PSC and i-C-19:0 in the biofilm, suggesting the presence of two major bacterial groups. Bacteriohopanepolyols were absent and the minute quantities of archaeol detected showed that Archaea were only minor constituents. Carbon isotopic compositions of the PSC yielded information about community structure and likely physiology. Biomass was C-13-depleted (10.9%) relative to available CO2 from the source water inorganic carbon pool with lipids further depleted by 6.3% relative to biomass The C-20-21 Aquificales fatty acids of the PSC were somewhat heavier than the iso-branched fatty acids. The carbon isotopic signatures of lipid biomarkers were also explored using a pure culture, T ruber, previously isolated from the PSC. Cells grown on C02 with O2 and both H2 and thiosulfate as electron donors were only slightly depleted (3.3%) relative to the C-source while cells grown on formate with O2 showed a major discrimination (19.7%), possibly the result of a metabolic branch point involving the assimilation of C-formate to biomass and the dissimilation to CO2 associated with energy production. T. ruber lipids were slightly heavier than biomass (+1.3%) whether cells were grown using CO2 or formate. Fatty acids from CO2 grown T. ruber cells were a so slightly heavier (average +2.1%) than biomass. The relatively depleted PSC C-20-21 fatty acids suggest that any associated Thermocrinis biomass would also be similarly depleted and much too light to be explained by growth on CO2. The C-fractionations determined with the pure culture suggest that growth of Thermocrinis in the PSC is more likely to occur on formate, presumably generated by geothermal activity. This study points to the value of the analysis of the structural and isotopic composition of lipid blomarkers both in pure culture studies, and in establishing community structure and physiology, as a complement to genomic profiles of microbial diversity. This is especially so when the members of the microbial community are novel and difficult to cultivate in the laboratory.

Author

*Microorganisms; Carbon Isotopes; Lipids; Thermophiles; Biofilms; Composition (Property)*

**20010121533** NASA Ames Research Center, Moffett Field, CA USA

## Engineering Strategies for the Design of Plant Nutrient Delivery Systems for Use in Space: Approaches to Countering Microbiological Contamination

Gonzales, A. A., NASA Ames Research Center, USA; Schuerger, A. C., Walt Disney World Co., USA; Mitchell, R., Harvard Univ., USA; [1994]; 1p; In English; Committee on Space Research Meeting, 10-21 Jul. 1994, Hamburg, Germany; Sponsored by Committee on Space Research, Unknown

Contract(s)/Grant(s): RTOP 199-61-12; No Copyright; Avail: Issuing Activity; Abstract Only

Microbiological contamination of crops within space-based crop growth research chambers has been postulated as a potentially significant problem. Microbial infestations; fouling of Nutrient Delivery System (NDS) fluid loops; and the formation of biofilms, have been suggested as the most obvious and important manifestations of the problem. Strict sanitation and quarantine procedures will reduce, but not eliminate, microbial species introduced into plant growing systems in space habitats. Microorganisms transported into space will most likely occur as contaminants on spacecraft components, equipment, the crew, and plant-propagative materials. Illustrations of the potential magnitude of the microbiological contamination issue will be drawn from the literature and from documentation of laboratory and commercial field experience. Engineering strategies for limiting contamination and for the development of countermeasures will be described. Microbiological control technologies and NDS hardware will be discussed. Configurations appropriate for microgravity research facilities, as well as anticipated bio-regenerative

life support system implementations, will be explored. An efficiently designed NDS, capable of adequately meeting the environmental needs of crop plants in space, is considered to be critical in both the research and operational domains. Recommended experiments, tests and technology developments, structured to allow the development of prudent engineering solutions, will also be presented.
Author
*Microorganisms; Plant Diseases; Contaminants; Biofilms; Countermeasures; Phytotrons*

**20010121537** NASA Ames Research Center, Moffett Field, CA USA
**Effects of Cage Type and NASA Rodent Food Bar in Male Sprague-Dawley Rats**
Lau, Angela, Lockheed Martin Corp., USA; Ramirez, J., Lockheed Martin Corp., USA; Pruitt, S., Lockheed Martin Corp., USA; Melson, E., Lockheed Martin Corp., USA; Zirkle-Yoshida, M., Foothill-De Anza Community Coll., USA; Girten, B., NASA Ames Research Center, USA; Apseloff, G., Ohio State Univ., USA; [2001]; 1p; In English
Contract(s)/Grant(s): NAS2-14263; No Copyright; Avail: Issuing Activity; Abstract Only

Early prototype caging for the rodent Advanced Animal Habitat (P-AAH) for the International Space Station (ISS) is currently being tested. In this five week study, effects of the wire-bottom P-AAH cages and specialized NASA rodent food bars (FB) were compared to standard vivarium cages (VIV) with corn-cob, litter-filled bottoms, and standard Purina rat chow (CH). Ninety-six male Sprague-Dawley rats were divided into four treatment groups (24 rats/treatment): Group 1) VIV+CH, Group 2) P-AAH+CH, Group 3) VIV+FB, and Group 4) P-AAH+FB. Each VIV and P-AAH cage housed three and six rats, respectively. After five weeks of treatment rats were weighed, euthanized, and blood samples were collected. Weights of liver (LIV), kidney (KID), brain (BRN), epididymal fat (EPI), and perirenal fat (PERI) were also measured. Statistical analysis to compare differences between groups was performed by standard analysis of variance procedures (ANOVA) with a significance level of pLO.05. Results indicated P-AAH housed rats had significantly lower body weights (BW), LIV weights, and LIV/BW than VIV housed rats. FB fed rats had significantly lower blood urea nitrogen (BUN) levels and LIV/BW than CH fed rats. In addition, FB fed rats had significantly higher cholesterol (CHOL) levels, EPI/BW, PERI/BW, and total fat (EPI+PERI)/BW than CH fed rats. The P-AAH+FB group had significantly lower EPI, BRN, and total fat than VIV+FB rats. VIV+FB rats had significantly higher BRN, EPI, PERI, and total fat than VIV+CH rats. Triglycerides (TG), KID, KID/BW, and BRN/BW were not significantly different among treatment groups. These findings provide valuable information regarding cage design and food bar suitability for long-term use on the ISS.
Author
*Habitats; Diets; International Space Station; Statistical Analysis; Analysis of Variance; Cholesterol; Ureas; Nitrogen*

**20010121550** Bionetics Corp., Moffett Field, CA USA
**Pressure Control System Design for a Closed Crop Growth Chamber**
Tsai, K., Bionetics Corp., USA; Blackwell, C., Bionetics Corp., USA; [1994]; 1p; In English; 24th International Conference on Environmental Systems, 20-23 Jun. 1994, Friedrichshafen, Germany
Contract(s)/Grant(s): RTOP 106-20-07; No Copyright; Avail: Issuing Activity; Abstract Only

The Controlled Ecological Life Support System (CELSS) is an area of active research at NASA. CELSS is a plant-based bioregenerative life support system for long term manned space flights where resupply is costly or impractical. The plants in a CELSS will function to convert the carbon dioxide (exhaled by the crew) into oxygen, purify non-potable water into potable quality water, and provide food for the crew. Prior to implementing a CELSS life support system, one must have knowledge on growing plants in a closed chamber under low gravity. This information will come from research to be conducted on the CELSS Test Facility that will operate on the Space Station Freedom. Currently a ground-based CELSS Test Facility is being built at NASA Ames Research Center. It is called the EDU (Engineering Development Unit). This system will allow researchers to identify issues that may cause difficulties in the development of the CELSS Test Facility and aid in the development of new needed technologies. The EDU consists of a 1 m2 crop growth chamber that is surrounded by a containment enclosure. The containment enclosure isolates the system so there is very little mass and thermal exchange with the ambient. The leakage rate is on the order of 1 % of the enclosure's volume per day (with 0.2S psi pressure difference). The thermal leakage is less than 0.5% of the electrical power supplied to the system per degree Celsius difference from the surrounding. The pressure in the containment enclosure is regulated at 62.5 Pa below the ambient by an active controller. The goal is to maintain this set point for a variety of conditions, such as a range of operating temperatures, heat load variations that occur when the lights are turned on and off, and fluctuations in ambient pressure. In addition certain transition tracking performance is required. This paper illustrates the application of some advanced systems control methods to the task of synthesizing the EDU's pressure control system.
Author
*Closed Ecological Systems; Control Systems Design; Product Development; Pressure Regulators; Ground Tests; Crop Growth*

**20010121558** NASA Ames Research Center, Moffett Field, CA USA

**Bone, Calcium and Spaceflight: A Living Systems Experiment Relating Animals and Plants the Effects of Calcium on Plant Growth and Development**

Reiss-Bubenheim, Debra, NASA Ames Research Center, USA; Navarro, B. J., NASA Ames Research Center, USA; [1994]; 1p; In English; Hydroponic Society of America Annual Meeting, 13-18 Apr. 1994, Akron, OH, USA; Sponsored by Hydroponic Society of America, USA

Contract(s)/Grant(s): RTOP 106-30-02; No Copyright; Avail: Issuing Activity; Abstract Only

This educational outreach activity provided students with information about ARC's role in conducting life sciences research in space. Students were introduced to the scientific method while conducting a plant experiment that was correlated to the flight animal experiment. Students made daily observations, collected data and reported on their findings. This classroom experiment providing a hands-on learning opportunity about terrestrial and space biology in which exposed the students to new fields of study for future endeavors.

Author

*Bones; Calcium; Space Flight; Life Sciences; Education*

**20010122268** TGS Technology, Inc., Moffett Field, CA USA

**Subsurface Intertidal Microbes: A Cryptic Source of Organic Carbon For Beach Ecosystems**

Rothschild, Lynn J., TGS Technology, Inc., USA; Giver, Lorraine J., TGS Technology, Inc., USA; [1994]; 2p; In English; A Bridge Into the 21st Century, Unknown; Sponsored by ACW, USA; No Copyright; Avail: Issuing Activity; Abstract Only

Some freshwater, marine or hotspring beaches have no visible source of primary production, yet beneath the surface is an interstitial photosynthetic microbial community. to assess the significance of this source of organic carbon, we measured in situ carbon fixation rates in an intertidal marine beach through a diurnal cycle. Gross fixation for a transect (99 x 1 m) perpendicular to the shore was approx. 4041 mg C fixed/ day, or approx. 41 mg C fixed/ sq m day. In contrast, an adjacent well-established cyanobacterial (Lyngbya) mat was approx. 12 x as productive (approx. 490 mg C fixed/sq m day). Thus, subsurface sand mats may be an overlooked, yet important, endogenous source of organic carbon for intertidal ecosystems, as well as a sink in the global carbon cycle.

Author

*Carbon Cycle; Ecosystems; Fresh Water; Interstitials; Microorganisms*

**20010122360** Argonne National Lab., IL USA

**EPR detection of light-generated nuclear coherences in photosynthetic reaction centers**

Bechtold, M.; May 04, 1998; 4p; In English

Report No.(s): DE2001-10760; AN/CHM/CP-96349; No Copyright; Avail: Department of Energy Information Bridge, Microfiche

In this study we first discuss a pulsed EPR (electron powder ribbon) experiment designed to establish the mechanism of coherence generation. The pulse sequence employed, flash-t-((pi)/2)(sub x)-(tau), consists of a short laser pulse at time zero, followed by a variable period t. At the end of this period a non-ideal ((pi)/2) microwave pulse is applied. The resulting free-induction decay at fixed detection time (tau) is then monitored as a function of successively incremented values of t. For P(sub 700)(sup +) A(sub 1)(sup (minus)) in deuterated and (sup 15)N-substituted PSI preparations, the transverse magnetization shows an oscillatory dependence on the delay between the laser and the microwave pulse. Apparently, there are fast initial oscillations which disappear 250 ns after the laser pulse. In addition, slow persisting oscillations with frequencies of a few MHz can be observed. Basically, these slow oscillations represent nuclear coherences initiated by the laser pulse.

NTIS

*Nuclear Reactions; Deuterium Compounds; Pulsed Lasers; Coherent Radiation*

**20010122706** Army Medical Research Inst. of Chemical Defense, Aberdeen Proving Ground, MD USA

**Time-Course Effects of GA, GB, GD, GF and VX on Spinal Cord Cholinesterase and Acetylcholine Levels in Six Discrete Areas of the Rat Brain**

Benton, Bernard J.; McDonough, John H.; Koviak, Thomas A.; Shih, Tsung-Ming A.; Jan. 2001; 28p; In English; Original contains color images

Contract(s)/Grant(s): Proj-TC3

Report No.(s): AD-A395264; USAMRICD-TR-01-01; No Copyright; Avail: CASI; A03, Hardcopy; A01, Microfiche

The time-course changes of spinal cord cholinesterase (ChE) and acetylcholine (ACh) levels in six discrete regions of the rat brain were studied and compared. Rats were injected subcutaneously with a 0.9 LD50 dose of GA, GE, GD, GF or VX. They

were observed for symptoms of intoxication and head-focused microwave irradiated at 10 time points ranging from 5 minutes to 24 hours after compound administration. Brain tissue samples were homogenized and ACh analyzed using a high pressure liquid chromatographic (HPLC) method. Spinal cords were analyzed at each time point for degree of ChE inhibition. Results indicate that all five compounds produced observable signs of intoxication within 10 minutes after injection. Each compound inhibits ChE, resulting in increased levels of ACh within 10 minutes after administration, and the cortical and hippocampal areas were most sensitive to the effects of these compounds. Observable signs of intoxication, depression of spinal ChE activity and elevation of brain levels of ACh were similar for all of the compounds.
DTIC
*Brain; Cholinesterase; Spinal Cord; Acetyl Compounds*

**20010122708** Massachusetts Inst. of Tech., Cambridge, MA USA
**Electroporation of Bacteria and Yeast: An Experimental Study of Molecular Transport** ***Final Report, 15 Oct. 1990-31 Aug. 1994***
Weaver, James; Aug. 31, 1994; 4p; In English
Contract(s)/Grant(s): DAAL03-90-G-0218
Report No.(s): AD-A395274; ARO-28361.2-LS; No Copyright; Avail: CASI; A01, Hardcopy; A01, Microfiche
This reseaech involves a basic study of electroporation with an emphasis on molecular transport across cell membranes. We have explored a new mechanism for drug delivery, the use of electroporation to move molecules into, across and out of tissues. Electroporation of human skin may provide the basis for greatly enhanced transdermal drug delivery, and for non-invasive ”sensing” of biochemicals within the body. Another advance is a new general method for rapidly determinmg the clonal growth of individual cells. For more details, see attached.
DTIC
*Medical Science; Cytology; Cell Membranes (Biology)*

**20010122935** National Space Biomedical Research Inst., Houston, TX USA
**National Space Biomedical Research Institute** ***Annual Report, 1 Oct. 2000 - 30 Sep. 2001***
Sep. 30, 2001; 667p; In English
Contract(s)/Grant(s): NCC9-58; No Copyright; Avail: CASI; A99, Hardcopy; A06, Microfiche
This report outlines National Space Biomedical Research Institute (NSBRI) activities during FY 2001, the fourth year of the NSBRI’s programs. It is prepared in accordance with Cooperative Agreement NCC 9-58 between NASA’s Lyndon B. Johnson Space Center and Baylor College of Medicine (NSBRI).
Author
*Aerospace Medicine; Biomedical Data; Medical Science*

**20010122940** NASA Ames Research Center, Moffett Field, CA USA
**Effects of Spaceflight and Hindlimb Suspension on the Posture and Gait of Rats**
Fox, R. A., San Jose State Univ., USA; Corcoran, M., NASA Ames Research Center, USA; Daunton, N. G., NASA Ames Research Center, USA; Morey-Holton, E., NASA Ames Research Center, USA; [1994]; 4p; In English; 12th International Symposium on Posture and Gait, Unknown
Contract(s)/Grant(s): RTOP 199-16-12-01; No Copyright; Avail: CASI; A01, Hardcopy; A01, Microfiche
Instability of posture and gait in astronauts following spaceflight (SF) is thought to result from muscle atrophy and from changes in sensory-motor integration in the CNS (central nervous system) that occur during adaptation to microgravity (micro-G). Individuals are thought to have developed, during SF, adaptive changes for the processing of proprioceptive, vestibular and visual sensory inputs with reduced weighting of gravity-based signals and increased weighting of visual and tactile cues. This sensory-motor rearrangement in the CNS apparently occurs to optimize neuromuscular system function for effective movement and postural control in micro-G. However, these adaptive changes are inappropriate for the 1 g environment and lead to disruptions in posture and gait on return to Earth. Few reports are available on the effects of SF on the motor behavior of animals. Rats studied following 18.5 - 19.5 days of SF in the COSMOS program were described as being ..’inert, apathetic, slow’.. and generally unstable. The hindlimbs of these rats were ..’thrust out from the body with fingers pulled apart and the shin unnaturally pronated’. On the 6th postflight day motor behavior was described as similar to that observed in preflight observations. Improved understanding of the mechanisms leading to these changes can be obtained in animal models through detailed analysis of neural

and molecular mechanisms related to gait. to begin this process the posture and gait of rats were examined following exposure to either SF or hindlimb suspension (HLS), and during recovery from these conditions.
Derived from text
*Astronauts; Hindlimb Suspension; Microgravity; Posture; Rats; Sensorimotor Performance; Space Flight; Bioastronautics; Gravitational Effects*

**20010125389** NASA Ames Research Center, Moffett Field, CA USA
**Effects of Increased CO2 Level on the Well-Being, Growth and Renal Function of Rats**
Lang, C., Bionetics Corp., USA; Bonner, R., Bionetics Corp., USA; Vasques, M., NASA Ames Research Center, USA; Baer, L., Bionetics Corp., USA; Fung, P., NASA Ames Research Center, USA; Steele, M., Martin Marietta Services, Inc., USA; Wade, C., NASA Ames Research Center, USA; [1994]; 1p; In English; American Society for Gravitational and Space Biology Meeting, 19-22 Oct. 1994, San Francisco, CA, USA; Sponsored by American Society for Gravitational and Space Biology, USA
Contract(s)/Grant(s): RTOP 199-08-12; No Copyright; Avail: Issuing Activity; Abstract Only

On the Space Shuttle the mean CO2 levels have been 0.3% which is ten times normal air, while there have been extended periods with mean levels of 0.7% and peak concentrations of 2%. On the Space Station the projected mean concentration of CO2 is 0.7% and not to exceed 1.0%. to ensure that high level of CO2 does not compromise the integrity of the science on the Space Station, the effects of chronic exposure to high levels of CO2 were investigated. Following 7 days of cage adaptation animals exposed to 2% CO2 for 30 days were compared to control (ambient air) animals and the effects on the well-being, growth and renal function analyzed. Ten male rats per group were placed in individual metabolic cages which allowed monitoring of daily food and water consumption, as well as feces and urine to be collected. Cages were placed in a plexiglass chamber with internal environment controlled by a computer in conjunction with gas sensors. The elevated CO2 was held constant at 2.0 +/- 0.03% and the O2 at 20.9 +/- 0.15%. Body weight and food and water intake were measured daily for the first ten days of exposure and then every three to four days for the remaining three weeks. Urine was measured for pH, CO2 (as an indicator for bicarbonate) and ammonia (as an indicator for ammonium). During 2% CO2 exposure, animal growth, weight, food and water consumption were within normal ranges suggesting that their well-being was not affected. Urine pH decreased from 7.12 to 6.77 over the first 6 days of exposure and increased the following 24 days returning to pre-exposure levels. Urine NH4+ increased 68% the first 6 days then dropped to and remained at 29% higher than pre-exposure level. Urine bicarbonate concentration did not change the first 6 days, but significantly increased by day 30. These results of chronic exposure to 2% C02 are consistent with renal compensation for respiratory acidosis which may impact science conducted on the Space Shuttle or the Space Station if CO2 levels reach 2%.
Author
*Carbon Dioxide; Rats; Adaptation; Hypercapnia; Metabolism*

**20010125390** NASA Ames Research Center, Moffett Field, CA USA
**Aqueous Phase Non Enzymatic Chemistry of Cyanide, Formaldehyde and RNH2**
Lerner, Narcinda R., NASA Ames Research Center, USA; [1994]; 1p; In English; Gordon Research Conference on Origin of Life, 22-26 Aug. 1994, Newport, RI, USA; Sponsored by Gordon Research Conferences, Inc., USA
Contract(s)/Grant(s): RTOP 152-13-60; No Copyright; Avail: Issuing Activity; Abstract Only

It is postulated that amino acids were produced on the early earth from dilute aqueous solution of cyanide, carbonyls and ammonia (the Strecker synthesis RNH2 + R”R””C=O + KCN yields H-N(R)-C(R”)(R””)-CO2H. We have studied the products obtained from dilute aqueous solutions of cyanide, formaldehyde (R”=R””=H), ammonia (R=H) and amino acids. Solutions in the pH range from 8 to 10. at room temperature and at reactant concentrations from 0.001 M to 0.3 M have been studied. With R= H product yields were low (less than 3%). Only with R”=R””=H and R represented by the following: CH2CO2H (glycine); CH(CH3)CO2H (alanine); CH(CH2CH3)CO2H (a-amino n=butyric acids); C(CH3)2(CO2H) (a-aminoisobutyric acid); CH(CH(CH3)2)CO2H (valine); and CH(CH2CO2H)CO2H (aspartic acid), were product yields high (greater than 10%). The yields of glycine were larger with R not equal to H. The prebiotic implications of these findings will be discussed.
Author
*Alanine; Formaldehyde; Cyanides*

**20010125544** Society for In Vitro Biology, Largo, MD USA

**2000 World Congress on In Vitro Biology** ***Final Report***

Harbell, John, Society for In Vitro Biology, USA; INVITRO: Cellular & Developmental Biology; September 2001; Volume 36, No. 3, Pt. 2; 158p; In English; Proceedings of World Congress on In Vitro Biology, Jun. 2000, San Diego, CA, USA

Contract(s)/Grant(s): DAM017-00-1-0590

Report No.(s): AD-A394419; No Copyright; Avail: CASI; A08, Hardcopy; A02, Microfiche

No abstract.

Author

*In Vitro Methods and Tests; Biology*

**20010125643** NASA Ames Research Center, Moffett Field, CA USA

**Gravity and the Adaptation of Form and Function in Lower Vertebrates**

Lillywhite, Harvey B., NASA Ames Research Center, USA; [1994]; 1p; In English; XIV Federative International Congress of Anatomy, 24-30 Jul. 1994, Lisboa, Portugal

Contract(s)/Grant(s): RTOP 199-14-12-04; No Copyright; Avail: Issuing Activity; Abstract Only

Comparative data emphasizing lower vertebrates will be used to justify the following generalized conclusions or expectations: 1) Gravitational stress produces adaptive increases in arterial pressure. 2) Gravitational stress produces adaptive reorganization of anatomy. 3) Natural selection favors small body size in high G-stress environments. 4) Gravitational stress produces low-compliant perivascular tissues (morphological antigravity suit). 5) Gradients or regional zonation of vascular characters evolve along the length of elongate vertebrates living in high G-stress environments. Presentation of information will include new data gathered by the author and Dr. Alan Hargens while the author was a NRC Senior Research Associate at NASA Ames Research Center. While there is no published abstract provided at the meeting, a symposium manuscript will be published in a special volume of Journal of Experimental Zoology.

Author

*Antigravity; Cardiovascular System; Elongation; Morphology; Vertebrates*

**20010125644** NASA Ames Research Center, Moffett Field, CA USA

**Tolerance of Snakes to Hypergravity**

Lillywhite, H. B., NASA Ames Research Center, USA; Ballard, R. E., NASA Ames Research Center, USA; Hargens, A. R., NASA Ames Research Center, USA; [1994]; 1p; In English; American Society for Gravitational and Space Biology Meeting, 19-22 Oct. 1994, San Francisco, CA, USA; Sponsored by American Society for Gravitational and Space Biology, USA

Contract(s)/Grant(s): RTOP 199-14-12-04; No Copyright; Avail: Issuing Activity; Abstract Only

Sensitivity of carotid blood flow to +Gz (head-to-tail) acceleration was studied in six species of snakes hypothesized to show varied adaptive cardiovascular responses to gravity. Blood flow in the proximal carotid artery was measured in 15 snakes before, during and following stepwise increments of +0.25Gz force produced on a 2.4 m diameter centrifuge. During centrifugation each snake was confined to a straight position within an individually- fitted acrylic tube with the head facing the center of rotation. We measured the centrifugal force at the tail of the snake in order to quantify the maximum intensity of force gradient promoting antero-posterior pooling of blood. Tolerance to increased gravity was quantified as the acceleration force at which carotid blood flow ceased. This parameter varied according to the gravitational adaptation of species defined by their ecology and behavior. At the extremes, carotid blood flow decreased in response to increasing gravity and approached zero near +1Gz in aquatic and ground-dwelling species, whereas in climbing species carotid flow was maintained at forces in excess of +2Gz. Surprisingly, tolerant (arboreal) species withstood hypergravic forces of +2 to +3 G. for periods up to 1 h without cessation of carotid blood flow or apparent loss of consciousness. Data suggest that relatively tight skin of the tolerant species provides a natural antigravity suit which is of prime importance in counteracting Gz stress on blood circulation.

Author

*Adaptation; Antigravity; Blood Circulation; Cardiovascular System; Heart Function; Physiological Responses; Snakes*

**20010125645** NASA Ames Research Center, Moffett Field, CA USA

**Measurement of Effective Canopy Temperature: The Missing Link to Modeling Transpiration in Controlled Environments**

Monje, O. A., Utah State Univ., USA; McCormack, Ann, NASA Ames Research Center, USA; Bugbee, Bruce, Utah State Univ., USA; [1994]; 1p; In English; 10th American Society for Gravitational and Space Biology Meeting, 20-22 Oct. 1994, San Francisco, CA, USA; Sponsored by American Society for Gravitational and Space Biology, USA

Contract(s)/Grant(s): RTOP 199-61-62; No Copyright; Avail: Issuing Activity; Abstract Only

The objectives were to apply energy balance principles to plant canopies, and to determine which parameters are essential for predicting plant canopy transpiration (E) in controlled environments. Transpiration was accurately measured in a gas-exchange system. Absorbed radiation (R(sub abs)) by the canopy was measured with a net radiometer and calculated from short and long-wave radiation components. Average canopy foliar temperature T(sub L) can be measured with an infrared radiometer, but since T(sub L) is seldom uniform, a weighed average measurement of T(sub L) must be made. The effective canopy temperature T(sub C) is that temperature that balances the energy flux between absorbed radiation and latent heat L(sub E) and sensible heat (H) fluxes. TC should exactly equal air temperature T(sub A) when L(sub E) equals R(sub abs). When unnecessary thermal radiation from the lighting system is removed by a water filter, the magnitude of L(sub E) from transpiration approaches Rabs and T(sub C) is close to T(sub A). Unlike field models, we included the energy used in photosynthesis and found that up to 10% of Rabs was used in photosynthesis. We calculated aerodynamic conductance for H from measurements of wind speed and canopy height using the wind profile equation. Canopy aerodynamic conductance ranged from.03 to.04 m/s for wind speeds from.6 to 1 m/s; thus a 0.1 C canopy to air temperature difference results in a sensible heat flux of about 4 W/sq m, which is only 1% of R(sub abs). We examined the ability of wide angle infrared transducers to accurately integrate T(sub L) from the top to the bottom of the canopy. We measured evaporation from the hydroponic media to be approximately 1 micro mol/sq m s or 10% of R(sub abs). This result indicates that separating evaporation from transpiration is more important than exact measurement of canopy temperature.

Author

*Canopies (Vegetation); Controlled Atmospheres; Hydroponics; Latent Heat*

## 52
## AEROSPACE MEDICINE

*Includes the biological and physiological effects of atmospheric and space flight (weightlessness, space radiation, acceleration, and altitude stress) on the human being; and the prevention of adverse effects on those environments. For psychological and behavioral effects of aerospace environments see 53 Behavioral Science. For the effects of space on animals and plants see 51 Life Sciences.*

**20010117724** NASA Ames Research Center, Moffett Field, CA USA

**Fluid Redistribution and Heart Rate in Humans During Whole-Body Tilting, G(z) Centrifugation, and Lower Body Negative Pressure**

Watenpaugh, D. E., NASA Ames Research Center, USA; Breit, G. A., NASA Ames Research Center, USA; Ballard, R. E., NASA Ames Research Center, USA; Murthy, G., NASA Ames Research Center, USA; Hargens, A. R., NASA Ames Research Center, USA; [1994]; 1p; In English; American Society for Gravitational and Space Biology Meeting, 19-22 Oct. 1994, San Francisco, CA, USA; Sponsored by American Society for Gravitational and Space Biology, USA

Contract(s)/Grant(s): RTOP 199-14-12-04; No Copyright; Avail: Issuing Activity; Abstract Only

Gravity creates blood pressure gradients which redistribute body fluids towards the feet. Positive G(z) centrifugation and lower body negative pressure (LBNP) have been proposed to simulate these and other effects of gravity during long-term existence in microgravity. We hypothesized that the magnitude of upper-to-lower body fluid redistribution would increase according to the following order: short-arm centrifugation (SAC), long-arm centrifugation (LAC), head-up tilt (HUT), and LBNP. to test this hypothesis, we employed strain gauge plethysmography of the neck, thigh and calf during HUT and supine SAC and LAC up to lG(z) at the feet, and during supine LBNP to 100 mm Hg. Supine 100 mm Hg LBNP generates footward force and produces transmural blood pressures in the foot approximately equal to 1 G(z) (90 deg) HUT. Heart rate was measured via cardiotachometry. Control measurements were made while supine. SAC and LAC elicited similar increases in thigh volume at 1 G(z) (2.3 +/- 0.4 and 2.1 +/- 0.1%, respectively; mean +/- se, n greater than or equal to 7). At 100 mm Hg LBNP, thigh volume increased (3.4 +/- 0.3%) significantly more than during l G(z) centrifugation (p less than 0.05). Surprisingly, due to a paradoxical 0.6% reduction of thigh volume between 0.8 and 1.0 G(z) HUT, thigh volume was increased only 0.6 +/- 0.3% at 1 G(z) HUT. The calf demonstrated similar, although less definitive, responses to the various gravitational stimuli. Neck volume tended to decrease less during HUT than during the other stimuli. Heart rate increased similarly during HUT (18 +/- 2 beats/min) and LAC (12 +/- 2 beats/min), and exhibited still greater elevation during LBNP (29 +/- 4 beats/min), yet did not increase during SAC. These results suggest upright posture activates mechanisms that counteract footward fluid redistribution which are not activated during supine applications of simulated gravity. LAC more closely approximated effects of normal gravity (HUT) than LBNP. Therefore, when considering LBNP to simulate gravity, these findings support efforts to reduce the cardiovascular stress imposed by LBNP, while preserving the gravity-like force generated by LBNP.

Author

*Body Fluids; Heart Rate; Gravitational Effects; Centrifuging; Lower Body Negative Pressure; Microgravity*

**20010117727** NASA Ames Research Center, Moffett Field, CA USA

**Computational Approaches to Vestibular Research**

Ross, Muriel D., NASA Ames Research Center, USA; Apr. 04, 1994; 1p; In English; American Academy of Otolaryngology-Head and Neck Surgery Foundation, 18-21 Sep. 1994, USA; Sponsored by American Academy of Otolaryngology-Head and Neck Surgery Foundation

Contract(s)/Grant(s): RTOP 199-16-12-14; No Copyright; Avail: Issuing Activity; Abstract Only

The Biocomputation Center at NASA Ames Research Center is dedicated to a union between computational, experimental and theoretical approaches to the study of neuroscience and of life sciences in general. The current emphasis is on computer reconstruction and visualization of vestibular macular architecture in three-dimensions (3-D), and on mathematical modeling and computer simulation of neural activity in the functioning system. Our methods are being used to interpret the influence of spaceflight on mammalian vestibular maculas in a model system, that of the adult Sprague-Dawley rat. More than twenty 3-D reconstructions of type I and type II hair cells and their afferents have been completed by digitization of contours traced from serial sections photographed in a transmission electron microscope. This labor-intensive method has now been replace d by a semiautomated method developed in the Biocomputation Center in which conventional photography is eliminated. All viewing, storage and manipulation of original data is done using Silicon Graphics workstations. Recent improvements to the software include a new mesh generation method for connecting contours. This method will permit the investigator to describe any surface, regardless of complexity, including highly branched structures such as are routinely found in neurons. This same mesh can be used for 3-D, finite volume simulation of synapse activation and voltage spread on neuronal surfaces visualized via the reconstruction process. These simulations help the investigator interpret the relationship between neuroarchitecture and physiology, and are of assistance in determining which experiments will best test theoretical interpretations. Data are also used to develop abstract, 3-D models that dynamically display neuronal activity ongoing in the system. Finally, the same data can be used to visualize the neural tissue in a virtual environment. Our exhibit will depict capabilities of our computational approaches and some of our findings from their application. For example, our research has demonstrated that maculas of adult mammals retain the property of synaptic plasticity. Ribbon synapses increase numerically and undergo changes in type and distribution (pis less than 0.0001) in type II hair cells after exposure to microgravity for as few as nine days. The finding of macular synaptic plasticity is pertinent to the clinic, and may help explain some. balance disorders in humans. The software used in our investigations will be demonstrated for those interested in applying it in their own research.

Author

*Vestibular Tests; Mammals; Rats; Cells (Biology); Spaceborne Experiments*

**20010117730** NASA Ames Research Center, Moffett Field, CA USA

**Heart Rate Variability During Early Adaptation to Space**

Toscano, W. B., California Univ., USA; Cowings, P. S., NASA Ames Research Center, USA; [1994]; 1p; In English; Fifth International Symposium on the Autonomic Nervous System, 21-23 Oct. 1994, Rochester, MN, USA; Sponsored by American Autonomic Society, USA

Contract(s)/Grant(s): RTOP 199-70-12-14; No Copyright; Avail: Issuing Activity; Abstract Only

A recent report hypothesized that episodes of space motion sickness (SMS) were reliably associated with low frequency oscillations (less than 0.03 to less than 0.01 Hz) in heart rate variability. This paper archives a large data set for review of investigators in this field which may facilitate the evaluation of this hypothesis. Continuous recording of Electro-cardiography (ECG) and other measures were made for 6 to 12 hours per day (waking hours) of six Shuttle crewmembers for the first 3 mission days of two separate Shuttle flights. Spectral analyses of heart rate variability during approximately 200 hours of inflight is presented. In addition, nearly 200 hours of data collected on these same individuals during ground tests prior to the mission are presented. The Purpose of this Publication is to document the incidence of low frequency oscillations of heart rate in 4 people exposed to microgravity over a period of five days. In addition, this report contains spectral analyses of heart rate data collected on these same individuals during ground-based mission simulations. by archiving these data in this manner, it is our intention to make this information available to other investigators interested in studying this phenomena.

Author

*Heart Rate; Motion Sickness; Microgravity; Electrocardiography; Aerospace Medicine*

**20010117736** NASA Ames Research Center, Moffett Field, CA USA

**Bone, Calcium and Spaceflight: A Living Systems Experiment Relating Animals and Plants the Effects of Calcium on Plant Growth and Development**

Reiss-Bubenheim, D., NASA Ames Research Center, USA; Navarro, B.J., NASA Ames Research Center, USA; Morey-Holton, E., NASA Ames Research Center, USA; Jun. 30, 1994; 1p; In English; American Society for Space and Gravitational Biology,

19-22 Oct. 1994, San Francisco, CA, USA; Sponsored by American Society for Gravitational and Space Biology, USA
Contract(s)/Grant(s): RTOP 106-30-02; No Copyright; Avail: Issuing Activity; Abstract Only

This NASA-sponsored educational outreach activity provided local students with information about Ames Research Center's (ARC) role in conducting life sciences research in space. Students were introduced to the scientific method while conducting a plant experiment that correlated with the Spacelab Life Sciences-2 (SLS-2) flight animal experiment of Dr. Emily Morey-Holton entitled "Bone, Calcium and Spaceflight". Students made daily observations, collected data and reported on their findings. Students also had the opportunity to witness the STS-58 landing at Edwards Air Force Base in southern California and attended a briefing given by the Payload Commander, Dr. Rhea Seddon at ARC last month. This classroom experiment providing a hands-on learning opportunity about terrestrial and space biology and, hopefully, introduced the students to new fields of study for future endeavors.

Author

*Bones; Calcium; Space Transportation System; Life Sciences; Spacelab; Exobiology*

**20010119600** Army Research Inst. of Environmental Medicine, Natick, MA USA

**Thermal Comfort and Thermal Sensation During Exposure to Hot, Hot-Humid and Thermoneutral Environments**

Kolka, Margaret A.; Kesick, Christina M.; Levine, Leslie; McBride, Sharon A.; Stephenson, Lou A.; Jan. 1998; 30p; In English
Report No.(s): AD-A394922; USARIEM-TR-T-01/17; No Copyright; Avail: CASI; A03, Hardcopy; A01, Microfiche

It was hypothesized that high skin wettedness and elevated skin temperature would negatively affect psychophysical performance. Twelve volunteers participated in a four-hour experiment in each environmental condition Condition 1 (COND 1): T(sub a) = 28 deg C, 50% rh; Condition 2 (COND 2): T(sub a) = 36 deg C, 50% rh; and Condition 3 (COND 3): T(sub a) = 36 deg C, 75% rh. T(sub c) was significantly higher in COND 2 (37.2 +/- 0.3 deg C) and COND 3 (37.3 +/- 0.3 deg C) compared to COND 1 (36.8 +/- 0.2 deg C) during the four-hour experiments (p is less than 0.05). Mean skin temperature was lower in COND 1 (32.4 +/- 0.12 deg C), than COND 2 (35.3 +/- 0.10 deg C) and COND 3 (35.6 +/- 0.13 deg C, p is less than 0.05). Mean heat flow was higher in COND 1 (57 +/- 2 W), than COND 2(6 +/- 2 W) and COND 3 (11 +/- 5 W, p is less than 0.05). The thermal comfort and thermal sensation assessments reflected the physiological responses. The subjective index of thermal discomfort effectively discriminated among the environments. The ESQ subjective heat index scores were higher for COND 2 and COND 3 compared to COND 1 (p is less than 0.05). These subjective responses tracked skin wettedness. Skin wettedness averaged over the entire body surface was related to thermal comfort (R2 = 0.94). This research provided evidence that skin wettedness predicted thermal comfort effectively in all environments tested. The subjective assessment of thermal comfort discriminated between all environments and the heat index derived from the USARIEM Environmental Symptoms Questionnaire discriminated between the neutral and the two hot environments. Unfortunately, several indices derived from the Environmental Symptoms Questionnaire had limited utility to discriminate among significantly different environments.

DTIC

*Thermal Comfort; Skin Temperature (Biology); Physiological Responses*

**20010119920** Defence and Civil Inst. of Environmental Medicine, Downsview, Ontario Canada

**Airsickness Desensitisation for the Canadian Forces - A Recommendation**

Cheung, Bob; Jul. 2001; 32p; In English
Report No.(s): AD-A395245; DCIEM-TR-2001-110; No Copyright; Avail: CASI; A03, Hardcopy; A01, Microfiche

Airsickness is associated with other forms of motion sickness. It is a common occurrence among aircrew trainees; the problem is most acute in the early stages of training. The identification of an alternative to pharmacological treatment of airsickness for individuals regularly exposed to provocative environments while carrying out skilled or potentially hazardous tasks, is an important issue. Airsickness desensitisation has been proposed and employed by various nations as the program of choice for prevention of airsickness during early training. With the newly acquired trainers (Harvard II and the Hawk) in the Canadian Forces (CF), it is important at this time to re-evaluate the CF airsickness desensitisation program at 15 Wing. The purpose of this recommendation is to provide a scientific update on habituation to nauseogenic motion stimuli, to clarify a number of misconceptions and to provide a recommendation on an improved airsickness desensitisation program based on current valid scientific information. A number of vestibular screening tests on oculomotor and postural function that could be achieved with relative ease are proposed as part of the initial assessment for potential pathological predisposition to airsickness. It is also recommended that the current biofeedback and relaxation therapy be deleted. Ground based desensitisation should be reduced to a 2-3 week period of twice daily exposure to Coriolis stimuli of progressively increasing intensity. This is followed immediately by 10-15 hours of exposure in which incremental habituation to the more complex and provocative maneuvers are carried out.

Quantitative evaluation of the subject's progress for both ground based and in flight desensitisation is recommended. An alternative ground based desensitisation procedure using the human centrifuge is proposed.
DTIC
*Motion Sickness; Flight Training; Flight Crews; Pharmacology*

**20010120157** NASA Ames Research Center, Moffett Field, CA USA
**Quantification of Cyclic Ground Reaction Force Histories During Daily Activity in Humans**
Breit, G. A., NASA Ames Research Center, USA; Whalen, R. T., NASA Ames Research Center, USA; [1994]; 2p; In English; IC Davis Biomedical Engineering Symposium, 13-May 1994, Davis, CA, USA
Contract(s)/Grant(s): RTOP 199-26-12-34; No Copyright; Avail: CASI; A01, Hardcopy; A01, Microfiche

Theoretical models and experimental studies of bone remodeling suggest that bone density and structure are influenced by local cyclic skeletal tissue stress and strain histories. Estimation of long-term loading histories in humans is usually achieved by assessment of physical activity level by questionnaires, logbooks, and pedometers, since the majority of lower limb cyclic loading occurs during walking and running. These methods provide some indication of the mechanical loading history, but fail to consider the true magnitude of the lower limb skeletal forces generated by various daily activities. These techniques cannot account for individual gait characteristics, gait speed, and unpredictable high loading events that may influence bone mass significantly. We have developed portable instrumentation to measure and record the vertical component of the ground reaction force (GRFz) during normal daily activity. This equipment allows long-term quantitative monitoring of musculoskeletal loads, which in conjunction with bone mineral density assessments, promises to elucidate the relationship between skeletal stresses and bone remodeling.
Author
*Cyclic Loads; Mathematical Models; Musculoskeletal System; Human Beings; Bone Mineral Content*

**20010120467** NASA Ames Research Center, Moffett Field, CA USA
**A Study of Parameters Affecting Fibroblast Morphology in Response to an Applied Mechanical Force**
Grymes, Rosalind A., NASA Ames Research Center, USA; Sawyer, Christine, Bionetics Corp., USA; [1994]; 1p; In English; Mechanotransduction and the Regulation of Growth and Differentiation, 5-8 Oct. 1994, Sarasota, FL, USA; Sponsored by American Physical Society, USA
Contract(s)/Grant(s): RTOP 199-40-22; No Copyright; Avail: Issuing Activity; Abstract Only

A precisely controlled stretch/relaxation regimen (20% elongation at 6.6 cycles/min) was applied to normal human fetal, neonatal and aged dermal fibroblasts cultured on flexible membranes. Culture conditions included poly (NH2) or collagen type I coated substrate membranes; control cultures were grown on the same pliable material in the absence of applied stretch. Direct observation and immunofluorescence analyses revealed a progressive change in cell body orientation limited to the stretched dermal fibroblast cultures. Monolayers gradually (over 4 days) acquired a symmetric, radial distribution equivalent to the biaxial array of the applied force. At high seeding density, alignment was inhibited in the fetal cell cultures. This cell strain required collagen type I coating for optimal attachment to the flexible membrane, preferring growth in three-dimensional cell 'balls' on the poly(NH2) coated substrate. Neonatal cells also required the collagen type I coating, but both neonatal and aged dermal fibroblasts aligned efficiently at all seeding densities examined. The randomly oriented neonatal cells on the unstretched control membranes spontaneously detached at confluence, as a single cell sheet. Their aligned counterparts did not detach until the applied stretch stimulus was removed. Low concentrations of cytochalasin D (62.5 ng/ml) disrupted the stretch-related alignment response. Rhodamine phalloidin staining visualized fewer actin stress fibers in stretched, aligned cells than in controls. Both intercellular interactions and cytoskeletal integrity mediate the response to mechanical strain. Normal rabbit corneal stroma fibroblasts (NRC) were also analyzed, and failed to orient under these conditions. This cell type may require a different regimen, or a longer time period, to demonstrate alignment behavior. Supported by NASA Space Biology RTOP 199-40-22 and the NASA-ARC Director's Discretionary Fund.
Author
*Amino Radical; Coatings; Cornea; Culture Techniques; Exobiology; Fibroblasts; Membranes; Skin (Anatomy)*

**20010120784** NASA Ames Research Center, Moffett Field, CA USA
**A Perceptual Repetition Blindness Effect**
Hochhaus, Larry, Oklahoma State Univ., USA; Johnston, James C., NASA Ames Research Center, USA; [1994]; 1p; In English; Psychonomic Society 35th Annual Meeting, 11-13 Nov. 1994, Saint Louis, MO, USA
Contract(s)/Grant(s): RTOP 505-64-13; No Copyright; Avail: Issuing Activity; Abstract Only

Before concluding Repetition Blindness is a perceptual phenomenon, alternative explanations based on memory retrieval problems and report bias must be rejected. Memory problems were minimized by requiring a judgment about only a single briefly displayed field. Bias and sensitivity effects were empirically measured with an ROC-curve analysis method based on confidence ratings. Results from five experiments support the hypothesis that Repetition Blindness can be a perceptual phenomenon.
Author
*Blindness; Hypotheses; Retention (Psychology)*

**20010121574** NASA Ames Research Center, Moffett Field, CA USA
**Impaired Compensation for Salt-Induced Urinary Calcium Loss in a Space Flight Model**
Navidi, Meena, NASA Ames Research Center, USA; Harper, J. S., Houston Univ., USA; Evans, J., Houston Univ., USA; Fung, P., Houston Univ., USA; Wolinsky, I., Houston Univ., USA; Arnaud, S. B., NASA Ames Research Center, USA; [1994]; 1p; In English; 1994 Meeting of the American Sociaty of Bone and Mineral Research, 9-13 Sep. 1994, Kansas City, MO, USA; Sponsored by American Society of Bone and Mineral Research, USA
Contract(s)/Grant(s): RTOP 199-26-12-02; No Copyright; Avail: Issuing Activity; Abstract Only

The loss of urinary calcium (UCa) induced by high sodium (HiNa) diets is compensated for by an increase in net intestinal Ca absorption (abs.). To determine the capacity of the intestine to absorb Ca in a space flight model in which the formation of 1,25-dihydroxyvitamin D (1,25-D) is suppressed, we induced Ca loss with HiNa diets (8%) and restricted dietary Ca (0.2%). In 200 g rats with hind limbs unloaded by tail suspension (S), we examined intestinal Ca abs. by direct measurement in the duodenum (everted gut sac or S/M), vitamin D receptors (VDR) and Ca balance. We also measured serum ionized calcium (ICa), pH, parathyroid hormone (PTH) and 1,25D. PTH was related to ICa (r = -0.44, p is less than 0.02), pH (r = -0.47, p is less than 0.02) and %Ca abs. (r = -0.40, p is less than 0.05). 1,25-D was related to %Ca abs. (r = 0.60, p is less than 0.001) but not VDR or S/M. Effects of the model were lower serum 1,25-D (110 +/- 59 vs. 199 +/- 80 pg/ml, p is less than 0.005), %Ca abs. (83 +/- 6.9 vs. 93 +/- 3.2, p is less than 0.03) and Ca balance (27 +/- 0.2 vs. 30 +/- 0.3 mg/d, p is less than 0.001) in S than controls (C). The HiNa diet increased UCa excretion from 2 to 13% of dietary Ca. Responses to HiNa diets, compared to normal Na, revealed no differences in 1,25-D, Ca abs. or VDR. Ca balances were lower in HiNa (27 +/- 0.3 vs. 30 +/- 0.4 mg/d, p is less than 0.001) in spite of higher Ca intakes. The failure of S rats fed HiNa diets to increase Ca abs. in response to Na-induced Ca loss appears to be related to suppressed 1,25-D in the space flight model, the cause of which remains obscure.
Author
*Urine; Calcium; Sodium; Diets; Intestines; Space Environment Simulation*

**20010122802** California Univ., Lawrence Berkeley Lab., Berkeley, CA USA
**Medical applications of nuclear physics and heavy-ion beams**
Alonso, J. R.; Aug. 01, 2000; 19p; In English
Report No.(s): DE2001-775138; LBNL-46036; No Copyright; Avail: Department of Energy Information Bridge

Isotopes and accelerators, hallmarks of nuclear physics, are finding increasingly sophisticated and effective applications in the medical field. Diagnostic and therapeutic uses of radioisotopes are now a $10B/yr business worldwide, with over 10 million procedures and patient studies performed every year. This paper will discuss the use of isotopes for these applications. In addition, beams of protons and heavy ions are being more and more widely used clinically for treatment of malignancies. to be discussed here as well will be the rationale and techniques associated with charged-particle therapy, and the progress in implementation and optimization of these technologies for clinical use.
NTIS
*Heavy Ions; Ion Beams; Nuclear Physics; Radioactive Isotopes; Nuclear Medicine*

**20010122937** NASA Ames Research Center, Moffett Field, CA USA
**Effect of intermittent standing and walking on physiological changes induced by head-down bed rest**
Vernikos, J., NASA Ames Research Center, USA; Ludwig, D. A., North Carolina Univ., USA; Ertl, A. C., Vanderbilt Univ. Hospital, USA; Wade, C. E., NASA Ames Research Center, USA; Keil, L., NASA Ames Research Center, USA; OHara, D., NASA Ames Research Center, USA; [1994]; 1p; In English
Contract(s)/Grant(s): RTOP 199-14-12-11; No Copyright; Avail: Issuing Activity; Abstract Only

Continuous exposure to gravity may not be necessary to prevent compromised physiological function resulting from exposure to microgravity. However, minimum gravity (G) exposure requirements, effectiveness of passive Gz versus activity in a G field, and optimal G stimulus amplitude, duration, and frequency are unknown. to partially address these questions, a 4-day, 6 degree head-down bed rest (HDBR) study (one ambulatory control day, 4 full HDBR days, one recovery day) was conducted. Nine males, 30-50 yr, were subjected to four different +1 Gz (head-foot) exposure protocols (periodic standing or controlled

walking for 2 or 4 h/day in 15 min doses), plus a continuous HDBR (0 Gz) control. Standing 4 h completely prevented and standing 2 h partially prevented post-HDBR orthostatic intolerance. Both walking conditions (2 h and 4 h) attenuated the decrease in peak VO2 and prevented the increased urinary Ca2+ excretion associated with HDBR. Both 4 h conditions (standing and walking) attenuated plasma volume loss during HDBR. It was concluded that various physiological systems benefit differentially from passive +1 Gz or activity in +1 Gz and the duration (2 h vs. 4 h) of the stimulus may be an important moderating factor.
Author
*Physiological Effects; Head Down Tilt; Bed Rest; Microgravity; Walking*

**20010124103** NASA Ames Research Center, Moffett Field, CA USA
**Mechanism of Headward Fluid Shift During Exposure to Microgravity**
Hargens, Alan R., NASA Ames Research Center, USA; Parazynski, Scott E., NASA Johnson Space Center, USA; Watenpaugh, Donald E., NASA Ames Research Center, USA; Aratow, Michael, NASA Ames Research Center, USA; Murthy, Gita, NASA Ames Research Center, USA; Kawai, Yasuaki, Tottori Univ., Japan; [1994]; 1p; In English; 2nd International Congress of Pathophysiology, 19-24 Nov. 1994, Kyoto, Japan
Contract(s)/Grant(s): RTOP 199-14-12-04; RTOP 199-26-12-38; No Copyright; Avail: Issuing Activity; Abstract Only

A prominent feature of early cardiovascular adaptation to the microgravity of space flight is a shift of blood and tissue fluid from the lower body to the upper body. Symptoms of this fluid shift include facial edema, nasal congestion, and headache. Normally on Earth, the human body is exposed to hydrostatic (gravitational) blood pressure gradients during upright posture. In this posture, mean arterial pressures at head, heart, and foot levels are approximately 70, 100, and 200 mm Hg, respectively. Theoretically, all hydrostatic pressures within arteries and veins are lost during exposure to microgravity so that mean arterial pressure in all regions of the body is uniform and approximately equal to that at heart level (100 mm Hg). Acute studies of 60 head-down tilt (simulated microgravity on Earth) indicate that facial edema is caused by: 1) elevation of capillary blood pressure from 28 to 34 mm Hg, 2) reduction of blood colloid osmotic pressure 22 to 18 mm Hg, and 3) 50% increase of blood perfusion in tissues of the head. Furthermore, as compared to microvasculature in the feet, microvessels of the head have a low capacity to constrict and diminish local perfusion. Elevation of blood and tissue fluid pressures/flow in the head may also explain the higher headward bone density associated with long-term head-down tilt. These mechanistic studies of head-down tilt, along with a better understanding of the relative stresses involved with upright posture and lower body negative pressure, have facilitated development of physiologic countermeasures to maintain astronaut health during microgravity. Presently no exercise hardware is available to provide a blood pressure gradient from head to feet in space. However, recent studies in our laboratory suggest that treadmill exercise within lower body negative pressure provides equivalent or greater physiologic stress as compared to similar upright exercise on Earth.
Author
*Arteries; Astronauts; Blood Pressure; Lower Body Negative Pressure; Heart; Human Body; Hydrostatic Pressure; Hypokinesia; Microgravity; Posture; Pressure Gradients; Veins; Bioastronautics; Aerospace Medicine; Weightlessness Simulation*

**20010124106** NASA Ames Research Center, Moffett Field, CA USA
**Head-Down Suspension Alters Stress-Responsiveness and Feedback Efficacy of 9a-Fludrocortisone in Rats**
Horsley, C. J., NASA Ames Research Center, USA; Evans, J., NASA Ames Research Center, USA; Scribner, K. A., NASA Ames Research Center, USA; Keil, L. C., NASA Ames Research Center, USA; Dallman, M. F., NASA Ames Research Center, USA; [1994]; 1p; In English; First World Congress on Stress, Sep-Oct. 1994, Bethesda, MD, USA
Contract(s)/Grant(s): RTOP 199-18-12-09; No Copyright; Avail: Issuing Activity; Abstract Only

9a-Fludrocortisone (9aFF) has been used to decrease orthostatic hypotension in astronauts whorl they return to earth after space flight. An earth-based model for weightlessness in space is head-down posture in man and rats. In these studies male rats were suspended head-down or not for 7 days and treated 14 and 2 hours prior to ether stress in the AM with 9aFF (20 micrograms i.u.) at -14 and -2 h or at -2 h with steroid and at -14 h with oil; controls were treated 2x with oil. Rats were decapitated 10 min after ether and ACTH and corticosterone (B) were measured. Both ACTH and B responses were greater in suspended than control rats under all three steroid conditions, and the percentage inhibition of ACTH by 9aFF was similar. Basal activity in the HPA over the 7 d suspension period was probably not elevated since adrenal and thymus weights did not differ in the ambulatory and head down groups. We conclude that headdown suspension facilitates acute stress-induced activity in the HPA axis, but that HPA axis sensitivity to corticosteroid feedback does not change.
Author
*Adrenocorticotropin (ACTH); Astronauts; Corticosteroids; Hypotension; Weightlessness; Bioastronautics; Head Down Tilt*

**20010125146** NASA Ames Research Center, Moffett Field, CA USA

**Peripheral Microvascular Responses to Whole-Body Tilting, G(z) Centrifugation, and Lower Body Negative Pressure Stresses in Humans**

Breit, G. A., NASA Ames Research Center, USA; Watenpaugh, D. E., NASA Ames Research Center, USA; Buckley, T. M., NASA Ames Research Center, USA; Ballard, R. E., NASA Ames Research Center, USA; Murthy, G., NASA Ames Research Center, USA; Hargens, A. R., NASA Ames Research Center, USA; [1994]; 1p; In English; American Society for Gravitational and Space Biology Meeting, 19-22 Oct. 1994, San Francisco, CA, USA; Sponsored by American Society for Gravitational and Space Biology, USA

Contract(s)/Grant(s): RTOP 199-14-12-04; No Copyright; Avail: Issuing Activity; Abstract Only

The response of the cutaneous microcirculation to orthostatic stress varies along the length of the body due to the interaction of central controls with regional responses to local blood pressure. We hypothesize that artificial orthostatic stresses such as Gz centrifugation and LBNP differ from whole-body tilting in terms of the distribution of microvascular blood flow. Cutaneous microvascular flows were measured by laser Doppler flowmetry at the neck, thigh, and leg of 15 normal subjects. Volunteers underwent stepwise head-up tilt (HUT) and short- and long-arm centrifugation protocols from supine control (0 Gz) to 0.2, 0.4, 0.6, 0.8, 1.0, 0.8, 0.6, 0.4, 0.2, and 0 Gz at the feet, for 30-s periods with 10-s transitions between levels. The same subjects underwent a corresponding supine LBNP protocol, up to 100 mmHg (in 20 mmHg increments) and back to zero pressure, which produced transmural pressure across blood vessels in the foot approximately equal to the HUT protocol. In general, application of all orthostatic stresses produced significant flow reductions in the lower body (p less than 0.05) and inconsistent changes in the neck. At low levels of each stress (0.4 Gz, 40 mmHg), LBNP generated the greatest relative reduction in flow in the lower body (-66.9+/-5.7%, thigh; -60.6 +/-5.7%, leg, mean +/- SE). HUT caused a less severe flow reduction than LBNP at the thigh and leg (-39.9 +/- 8.1% and -55.9+/-4.8%), while the effects induced by both forms of centrifugation were the least profound. Higher levels of each stress generally resulted in similar responses. These responses exhibit a consistent relationship to hypothesized changes in local microvascular transmural pressure, suggesting that myogenic and veno-arteriolar reflexes play a significant role in determining microvascular perfusion during orthostatic stress.

Author

*Lower Body Negative Pressure; Microgravity; Aerospace Medicine; Human Beings; Cardiovascular System*

**20010125153** NASA Ames Research Center, Moffett Field, CA USA

**Effects of Autonomic Conditioning on Motion Sickness Tolerance**

Cowings, P. S., NASA Ames Research Center, USA; Toscano, W. B., California Univ., USA; [1994]; 1p; In English; Fifth International Symposium on the Autonomic Nervous System, 21-23 Oct. 1994, Rochester, MN, USA; Sponsored by American Autonomic Society, USA

Contract(s)/Grant(s): RTOP 199-70-12-14; No Copyright; Avail: Issuing Activity; Abstract Only

This paper presents case-studies of 9 shuttle crewmembers (prime and alternates) and one U.S. Navy F-18 pilot, as they participated in all preflight training and testing activities in support of a life sciences flight experiment aboard Spacelab-J, and Spacelab-3. The primary objective of the flight experiment was to determine if Autogenic-feedback training (AFT), a physiological self-regulation training technique would be an effective treatment for motion sickness and space motion sickness in these crewmembers. Additional objectives of this study involved the examining human Physiological- responses to motion sickness on Earth and in space, as well as developing predictive criteria for susceptibility to space motion sickness based on ground-based data. Comparisons of these crewmembers are made to a larger set of subjects from previous experiments (treatment and test-only controls subjects). This paper describes all preflight methods, results and proposed changes for future tests.

Author

*Aerospace Medicine; Motion Sickness; Automatic Control; Spacelab; Human Tolerances*

**20010125154** NASA Ames Research Center, Moffett Field, CA USA

**A Potential Treatment for Post-Flight Orthostatic Intolerance in Aero-Space Crews: Autogenic-Feedback Training**

Cowings, P. S., NASA Ames Research Center, USA; Toscano, W. B., California Univ., USA; Miller, N. E., Yale Univ., USA; Pickering, T. G., Cornell Univ., USA; Shapiro, D., California Univ., USA; [1994]; 1p; In English; Fifth International Symposium on the Autonomic Nervous System, 21-23 Oct. 1994, Rochester, MN, USA; Sponsored by American Autonomic Society, USA

Contract(s)/Grant(s): RTOP 199-70-12-14; No Copyright; Avail: Issuing Activity; Abstract Only

Postflight orthostatic intolerance has been identified as a serious biomedical problem associated with long duration exposure to microgravity in space. High priority has been given to the development of countermeasures for this disorder which are both effective and practical. A considerable body of clinical research has demonstrated that people can be taught to increase their own blood pressure voluntarily and that this is an effective treatment for chronic Orthostatic intolerance in paralyzed patients. The

present pilot study was designed to examine the feasibility of adding training in control of blood pressure to an existing preflight training program designed to facilitate astronaut adaptation to microgravity. Using in operant conditioning procedure, Autogenic-Feedback Training (AFT), three men and two women participated in four to nine (15-30 training sessions). At the end of training ranged between 20 and 50 mm Hg under both supine and 450 head-up tilt conditions. These findings suggest that AFT may be a useful alternative treatment or supplement to existing approaches for preventing postflight Orthostatic intolerance. Further, the use of operant conditioning methods for training cardiovascular responses may contribute to the general understanding of the mechanisms of orthostatic intolerance.
Author
*Clinical Medicine; Spacecrews; Orthostatic Tolerance; Physiological Responses; Cardiovascular System*

**20010125388** NASA Ames Research Center, Moffett Field, CA USA
**Interaction of Mechanical Load with Growth Hormone (GH) and Insulin-Like Growth Factor I (IGF-I) on Slow-Twitch Skeletal Muscle and Bone**
Linderman, Jon K., NASA Ames Research Center, USA; Gosselink, Kristin L., NASA Ames Research Center, USA; Wang, Tommy J., NASA Ames Research Center, USA; Mukku, Venkat R., Genetech, Inc., USA; Grindeland, Richard E., NASA Ames Research Center, USA; [1994]; 1p; In English; American Society for Gravitational and Space Biology Meeting, 19-22 Oct. 1994, San Francisco, CA, USA; Sponsored by American Society for Gravitational and Space Biology, USA
Contract(s)/Grant(s): RTOP 199-70-12-14; No Copyright; Avail: Issuing Activity; Abstract Only

Exogenous humoral growth factors, combined with increased mechanical loading, reportedly induce hypertrophy of fast-, but not slow-twitch skeletal muscles, and have little effect in attenuating atrophy of slow-twitch muscle associated with exposure to microgravity in animals with intact neuroendocrine systems. These observations suggest that anabolic adjuvants and muscle tension do not interact to stimulate growth or maintenance of slow-twitch skeletal muscle. The purpose of the present study was to determine whether a chronic increase in mechanical loading (synergistic ablation) or hindlimb unweighting (hindlimb suspension) interact with exogenous GH and IGF-I (Genentech, So San Francisco, CA) in the slow-twitch soleus muscles of female rats (approx. 250 g). Bilateral ablation of the plantaris and gastrocnemius muscles induced 38% and 40% increases in the absolute (mg/pair) and relative (mg/100 g body weight) weights of the soleus, respectively (p less than or = 0.05), in ambulatory rats. GH and IGF-I interacted with chronic loading to increase absolute soleus mass an additional 20% (p less than or = 0.05), and mixed and myofibrillar protein contents an additional 12% and 7%, respectively (NS). In contrast, hindlimb suspension (HLS) resulted in 20% and 18% decreases in the absolute and relative weights of the soleus, respectively (p less than or = 0.05); GH and IGF-I did not spare loss of soleus mass or protein content in HLS rats. HLS decreased tibial plate thickness approx. 11% (p less than or = 0.05), but not weights of the tibia or femus. GH and IGF-I increased tibial plate thickness approx. 30% (p less than or = 0.05), in ambulatory and HLS rats, and increased femur and tibial weights 12% (p less than or = 0.05) and 8% (NS), respectively, in ambulatory rats, but had no effect in HLS rats. Results of the present investigation suggest that GH and IGF-I can stimulate hypertrophy of slow-twitch skeletal muscle when chronically overloaded, but can also stimulate growth of hindlimb bones in the absence of mechanical load.
Author
*Loads (Forces); Atrophy; Body Weight; Endocrine Systems; Microgravity; Musculoskeletal System*

## 53
## BEHAVIORAL SCIENCES

*Includes psychological factors; individual and group behavior; crew training and evaluation; and psychiatric research.*

**20010117726** NASA Ames Research Center, Moffett Field, CA USA
**Psychophysiology of Humans in Space**
Cowings, P.S., NASA Ames Research Center, USA; Jan. 14, 1994; 1p; In English; Goddard Space Flight Center Engineering Colloquium, 24 Jan. 1994, Greenbelt, MD, USA; Sponsored by NASA Goddard Space Flight Center, USA
Contract(s)/Grant(s): RTOP 199-70-12-14; No Copyright; Avail: Issuing Activity; Abstract Only

Psychophysiological methods can provide aerospace medicine investigators with a unique perspective on the diagnosis and treatment of biomedical problems of humans in space. As psychophysiologists, we measure physiological responses to environmental stressors as a means of assessing and modifying their effects on behavior and performance. In the course of an 20-year research program. we have determined that this approach can be used to: (1) objectively identify physiological correlates of discomfort, malaise and performance; and (2) correct autonomic nervous system (ANS) disturbance and thereby increase tolerance to environmental stressors without the need for pharmacological intervention. The research presented will describe the

application of psychophysiological methods for studying human adaptation to space and developing behavioral medicine techniques for facilitating this adaptation as well a readaptation to Earth. The goal of this work is to enhance the safety, comfort and operational efficiency of passengers and crew during spaceflight.
Author
*Psychophysiology; Physiological Responses; Autonomic Nervous System; Human Tolerances; Aerospace Medicine*

**20010120413** Arizona State Univ., East Mesa, AZ USA
**Attracting Women to Aviation Careers: What Recent Studies Reveal**
Turney, Mary Ann, Arizona State Univ., USA; Collegiate Aviation Review; October 2000; Volume 18, No. 1, pp. 86-92; In English; See also 20010120406; Copyright; Avail: Issuing Activity

The percentage of women attracted to careers in aviation remains surprisingly low despite efforts by the industry to increase its talent pool by encouraging women to participate. This paper presents a review of literature relevant to the question of why the numbers of women choosing careers in aviation have not increased in the past two decades, and why even those who demonstrate an initial interest in the field eventually look for career satisfaction in other fields.
Author
*Females; Aircraft Industry; Occupation*

**20010120416** Embry-Riddle Aeronautical Univ., USA
**Teaching the Pilots of the New Millennium: Adult Cooperative Education in Aviation Education**
Clark, Joseph F., III, Embry-Riddle Aeronautical Univ., USA; Collegiate Aviation Review; October 2001; Volume 19, No. 1, pp. 29-40; In English; See also 20010120414; Copyright; Avail: Issuing Activity

Aviation is a very dynamic field that requires great dedication on the part of those who choose professional flying for their careers. Students must acquire a great amount of knowledge to include technical data, procedural information, social skills and more. There is much for the potential aviator to learn; sometimes it seems overwhelming to the initiate. One means of learning this vast amount of information involves the technique of cooperative education. The mixing of adult educational techniques and cooperative learning may be particularly useful in aviation. Using cooperative education in acquiring the required knowledge can teach them discipline and social skills required in surviving today's active aviation environment. The challenge then, becomes one for the college-level aviation instructor. This paper addresses techniques for teaching potential pilots the fundamentals required for the job based on adult and cooperative educational techniques.
Author
*Aircraft Pilots; Education; Civil Aviation*

**20010120417** Purdue Univ., IN USA
**The Transfer of Flight Training Procedures from an Advanced Airline Flight Simulator to the Classroom**
Fanjoy, Richard O., Purdue Univ., USA; Young, John P., Purdue Univ., USA; Collegiate Aviation Review; October 2001; Volume 19, No. 1, pp. 41-48; In English; See also 20010120414; Copyright; Avail: Issuing Activity

The current shortfall of aviation professionals has led employers to hire low-time, less experienced aviators to fill cockpit positions. Accordingly, the improved effectiveness and capacity of flight training programs has become a national priority. Collegiate aviation programs, in particular, are faced with resource constraints that mandate optimum use of available flight training devices. This paper suggests the use of off-the-shelf video teleconferencing technology to transmit certain aspects of flight training, such as systems operations and normal procedures, between the classroom and an advanced flight simulator or training device. Instruction that is normally limited to two or three students can now be given to a much larger audience and yet remain interactive. Limited sampling of student performance following flight simulator video teleconferencing sessions reflects the promise of this medium as a useful complement to other aviation training methodologies. This paper is not meant to be a formal research paper, but rather an overview of an innovative teaching technology that could lead to further study.
Author
*Education; Flight Simulators; Flight Training; Airline Operations*

**20010120419** Sky Views, LLC, USA
**The Learning Styles of College Aviation Students**
Kanske, Craig A., Sky Views, LLC, USA; Brewster, L. Tom, Oklahoma State Univ., USA; Collegiate Aviation Review; October 2001; Volume 19, No. 1, pp. 62-70; In English; See also 20010120414; Copyright; Avail: Issuing Activity

This study investigated the learning styles of collegiate aviation students. The results of this investigation were compared to the learning styles of qualified pilots in the USA Air Force, as identified in a previous study. Using the Kolb Learning Style

Inventory, the objectives were to identify the learning styles of collegiate aviation students, determine if there was a difference in learning style among the grade levels of the college students, and to note the similarities and/or differences in learning styles between the collegiate aviation students and the USA Air Force pilots. The demographic survey used in the previous study was tailored to reflect the disparity of experiences between college students and active pilots in the USA Air Force. The population for this study consisted of students enrolled in the aviation programs at Oklahoma State University-Stillwater campus, Oklahoma State University-Tulsa campus, and Southeastern Oklahoma State University on the Durant campus and at Tinker Air Force Base. Using the results of this study to identify a preferred learning style among college aviation students can provide information about the students' cognitive mapping. This mapping can be used as a tool so that courses can be more effectively designed. Modifications to this main theme can then be made for those students who have different learning styles. An ideal learning style, due to the predictive nature of Kolb's learning Style Inventory, can also identify aviation students as a discrete group from other degree programs on campus.
Author
*Civil Aviation; Statistical Analysis; Universities*

**20010120421** Arizona State Univ., AZ USA
**Retaining Women in Collegiate Aviation by Implementing Learning Style Considerations**
Karp, Merrill R., Arizona State Univ., USA; Turney, Mary Ann, Arizona State Univ., USA; Niemczyk, Mary, Arizona State Univ., USA; Green, Mavis F., Embry-Riddle Aeronautical Univ., USA; Sitler, Ruth L., Kent State Univ., USA; Bishop, James, Bryant Coll., USA; Collegiate Aviation Review; October 2001; Volume 19, No. 1, pp. 92-101; In English; See also 20010120414; Copyright; Avail: Issuing Activity

Women are clearly underrepresented in aviation. Research must be accomplished to determine which factors influence women, once they have indicated a serious interest in an aviation career, to stay in collegiate aviation programs or to leave. Addressing the issue of women's retention in aviation is one way to help address the growing commercial pilot shortage, while moving toward gender equity in this critical, national industry. Projected shortages in the commercial pilot population, coupled with the low representation of women in career pilot positions, suggest that aviation education and training institutions should re-examine the structure and organization of the aviation knowledge transfer process. Classroom enhancements could improve education methods to make them more efficient from the perspectives of increased knowledge retention, improved application to broader subjects, and reduced loss to attrition of viable pilot candidates to enter the commercial pilot workforce. This study examines how aviation education can best serve the aviation student's learning style needs. The study looks at learning style theory, from the viewpoint of the wide diversity of aviation learners who are dominantly visual, auditory, or hands-on, tactile, or kinesthetic learners, and how women's learning styles are pivotal to their success and retention in collegiate aviation. by exploring how people learn best, and then providing those learners with the tools to maximize their dominant learning styles, the next generation of pilots, both women and men, should be better prepared to enter the aviation industry and help reduce the projected commercial pilot shortages.
Author
*Aircraft Industry; Education; Females; Civil Aviation*

**20010120423** New Orleans Univ., LA USA
**Using the Job Characteristics Model to Measure the Motivating Potential of Flightdeck Positions**
Patti, Anthony L., New Orleans Univ., USA; Flouris, Triant G., Auburn Univ., USA; Collegiate Aviation Review; October 2001; Volume 19, No. 1, pp. 111-120; In English; See also 20010120414; Copyright; Avail: Issuing Activity

This paper explores the potential of using the Job Characteristics Model (JCM) for analyzing flightdeck positions. The JCM has been successfully used to study a variety of job designs and the effects prescribed treatments have on the job designs. This paper presents an overview of the job characteristics model, discusses the model's critical psychological states and shows how the Job Diagnostic Survey (JDS) can be used to measure the motivating potential of flightdeck positions. The results from our analysis and the model itself will be useful in the design of individualized LOFT (Line Oriented Flight Training) and CRM (Crew Resource Management) LOFT programs. Additionally, the JCM can be used to study the effects of automation, operation type (passenger vs. cargo), tenure as a pilot, and tenure in type on pilot motivation. From a longitudinal perspective, current data collection can serve as baseline measures for studying the aggregate, long-term effects of flightdeck job design changes.
Author
*Flight Training; Workloads (Psychophysiology); Autonomy; Human Factors Engineering*

**20010121557** NASA Ames Research Center, Moffett Field, CA USA

**Fatigue Factors in Regional Airline Operations**

Rosekind, Mark R., NASA Ames Research Center, USA; Weldon, Keri J., San Jose State Univ., USA; Co, Elizabeth L., San Jose State Univ., USA; Miller, Donna L., Sterling Software, Inc., USA; Gregory, Kevin B., Sterling Software, Inc., USA; Smith, Roy M., San Jose State Univ., USA; Johnson, Julie M., San Jose State Univ., USA; Gander, Philippa H., San Jose State Univ., USA; Lebacqz, J. Victor, NASA Ames Research Center, USA; [1994]; 1p; In English; Sponsored by National Transportation Safety Board, USA

Contract(s)/Grant(s): RTOP 505-64-53; No Copyright; Avail: Issuing Activity; Abstract Only

This paper describes human sleep and circadian physiology regarding their role as contributors to fatigue engendered by flight operations. The demands of regional airline operations are then examined for potential areas where these physiological factors will be affected. Finally, approaches to systematically investigate these issues scientifically will be described.

Author

*Fatigue (Biology); Circadian Rhythms; Sleep*

**20010122271** NASA Ames Research Center, Moffett Field, CA USA

**Is Linear Displacement Information Or Angular Displacement Information Used During The Adaptation of Pointing Responses to An Optically Shifted Image?**

Bautista, Abigail B., NASA Ames Research Center, USA; [1994]; 1p; In English; Canadian Society of Psychomotor Learning and Sports Psychology Meeting, 27-30 Oct. 1994, Hamilton, Ontario, Canada; Sponsored by Canadian Society of Psychomotor Learning and Sports Psychology, Canada

Contract(s)/Grant(s): RTOP 199-16-12-08; No Copyright; Avail: Issuing Activity; Abstract Only

Twenty-four observers looked through a pair of 20 diopter wedge prisms and pointed to an image of a target which was displaced vertically from eye level by 6 cm at a distance of 30 cm. Observers pointed 40 times, using only their right hand, and received error-corrective feedback upon termination of each pointing response (terminal visual feedback). At three testing distances, 20, 30, and 40 cm, ten pre-exposure and ten post-exposure pointing responses were recorded for each hand as observers reached to a mirror-viewed target located at eye level. The difference between pre- and post-exposure pointing response (adaptive shift) was compared for both Exposed and Unexposed hands across all three testing distances. The data were assessed according to the results predicted by two alternative models for processing spatial-information: one using angular displacement information and another using linear displacement information. The angular model of spatial mapping best predicted the observer's pointing response for the Exposed hand. Although the angular adaptive shift did not change significantly as a function of distance (F(2,44) = 1.12, n.s.), the linear adaptive shift increased significantly over the three testing distances 02 44) = 4.90 p less than 0.01).

Author

*Linear Polarization; Displacement; Targets; Wedges*

**20010122933** NASA Ames Research Center, Moffett Field, CA USA

**Effects of Perceptual Augmentation of Visual Displays: Dissociation of Performance and Situational Awareness**

Shively, R. Jay, Army Aviation and Missile Command, USA; Goodman, Allen D., San Jose State Univ., USA; [1994]; 1p; In English; 38th Annual Human Factors and Ergonomics Society, 24-28 Oct. 1994, Nashville, TN, USA

Contract(s)/Grant(s): RTOP 537-08-21; No Copyright; Avail: Issuing Activity; Abstract Only

It is intuitive that good performance is associated with, if not caused by, good situational awareness. There are, however, some situations in which these two concepts diverge. There are some trivial examples that have been identified, such as auto-pilots. However, it is also possible that these concepts diverge in a much more subtle manner. This research is focused on investigating those more subtle situations. Specifically, this research addresses the effects of perceptual display enhancement based upon Ecological Task Analysis (ETA) on performance and situational awareness. A perceptually augmented display was designed based upon ETA. Globally, performance advantages were found for the group with the enhanced display. Further, the findings demonstrate a dissociation of sub-task performance and operators' knowledge of the system subtask. The mechanisms involved in this dissociation are related to the characteristics of the display augmentation that led to the increased performance. The level of processing, and presence of feedback seem to play an important mediating role. These findings have important implications for both designers and researchers.

Author

*Situational Awareness; Human Performance; Display Devices*

**20010125133** NASA Ames Research Center, Moffett Field, CA USA

**Directions of Moving Plaids is Biased by Asymmetric Viewing Windows**

Beutter, B. R., NASA Ames Research Center, USA; Mulligan, J. B., NASA Ames Research Center, USA; Stone, L. S., NASA Ames Research Center, USA; [1994]; 1p; In English; 24th Annual Meeting of the Society for Neuroscience, 13-18 Nov. 1994, Miami Beach, FL, USA; Sponsored by Society for Neuroscience, USA

Contract(s)/Grant(s): NCC2-307; RTOP 199-16-12-37; RTOP 199-14-12-04; No Copyright; Avail: Issuing Activity; Abstract Only

Directionally selective V1 neurons are tuned to particular spatio-temporal frequencies and respond to local 1-D edge motion. At least some MT neurons however appear to respond to the actual velocity of moving 2D patterns. to better understand how the 1D local motion information available from VI is integrated to derive a 2D velocity signal we investigated human perception of moving plaids, 2-D patterns composed of the sum of two 1-D sinusoidal gratings of different orientations. We measured the effect of the shape of the viewing window on the perceived direction of plaid motion. The plaids were spatially windowed by 2-D Gaussians with unequal standard deviations (sigma 1, sigma 2). Four observers indicated perceived direction by adjusting a pointer. Direction errors were measured as a function of the difference between window orientation and true plaid direction (DELTA THETA) for several grating spatial frequencies (SF = 0.3, 0.6, 1.2 c/d) and window aspect ratios (AR = sigma 1/sigma 2 = 1, 1.4, 2, 4). Observers showed systematic errors in perceived direction (approx. 15 for AR = 4 and SF = 0.6 c/d) that peaked at DELTA THETA approx. 40. The errors increased for increasing aspect ratio and decreased for increasing spatial frequencies (or number of cycles). These results show that despite the unambiguous motion of the plaids, under these conditions human misperceive the motion. These data constrain models of motion integration from V1 to MT and, in particular, are inconsistent with algorithms that use either the Intersection of Constraints rule or cross correlation to compute the perceived direction of motion. Author

*Neurons; Sine Waves; Algorithms; Asymmetry*

## 54
## MAN/SYSTEM TECHNOLOGY AND LIFE SUPPORT

*Includes human factors engineering; bionics, man-machine, life support, space suits and protective clothing. For related information see also 16 Space Transportation and 52 Aerospace Medicine..*

**20010118902** Brookhaven National Lab., Upton, NY USA

**Human factors guidance for control room evaluation**

Ohara,; Brown,; Stubler,; Higgins,; Wachtel,; Jul. 30, 2000; 6p; In English

Report No.(s): DE2000-755033; BNL-NUREG-67215; No Copyright; Avail: Department of Energy Information Bridge

The Human-System Interface Design Review Guideline (NUREG-0700, Revision 1) was developed by the US Nuclear Regulatory Commission (NRC) to provide human factors guidance as a basis for the review of advanced human-system interface technologies. The guidance consists of three components: design review procedures, human factors engineering guidelines, and a software application to provide design review support called the 'Design Review Guideline.' Since it was published in June 1996, Rev. 1 to NUREG-0700 has been used successfully by NRC staff, contractors and nuclear industry organizations, as well as by interested organizations outside the nuclear industry. The NRC has committed to the periodic update and improvement of the guidance to ensure that it remains a state-of-the-art design evaluation tool in the face of emerging and rapidly changing technology. This paper addresses the current research to update of NUREG-0700 based on the substantial work that has taken place since the publication of Revision 1.

NTIS

*Human Factors Engineering; Man Machine Systems; Control Systems Design; Nuclear Power Plants*

**20010120020** Argonne National Lab., IL USA

**Impact of mental representational systems on design interface**

Brown-VanHoozer, S. A.; Feb. 25, 1998; 8p; In English

Report No.(s): DE2001-10658; ANL/ED/CP-95726; No Copyright; Avail: Department of Energy Information Bridge

The purpose of the studies conducted at Argonne National Laboratory is to understand the impact mental representational systems have in identifying how user comfort parameters influence how information is to best be presented. By understanding how each individual perceives information based on the three representational systems (visual, auditory and kinesthetic modalities), it has been found that a different approach must be taken in the design of interfaces resulting in an outcome that is

much more effective and representative of the users mental model. This paper will present current findings and future theories to be explored.
NTIS
*Human Factors Engineering; Auditory Perception; Mental Performance; Vision*

**20010120107** Air Force Research Lab., Human Effectiveness Directorate, Wright-Patterson AFB, OH USA
**The Effects of Prototype Helicopter Seat Cushion Concepts on Human Body Vibration Response** ***Final Report, Nov. 1992-Sep. 1998***
Smith, Suzanne D.; Sep. 1998; 17p; In English
Contract(s)/Grant(s): Proj-7184
Report No.(s): AD-A395100; AFRL-HE-WP-SR-2001-0011; No Copyright; Avail: CASI; A03, Hardcopy; A01, Microfiche

The driving-point impedance and transmissibility techniques were used to evaluate the effects of military helicopter seat cushions on human body vibration response. Small females (5th percentile or less for body weight) and large males (95th percentile or greater) were exposed to vibration in the frequency range of 3 to 21 Hz at 0.59 m/s2 rms. Transmissibilities were calculated between the acceleration measured at selected anatomical sites, including the chest, head, spine (C7), and thigh, and the input at the seat. Seating configurations included the rigid seat, a current inventory seat cushion, and a prototype cushion with an inflatable thigh support in both the deflated and inflated positions. Rigid mass tests showed that the single resonance frequency and associated magnitude peaks were significantly lower for the two prototypes. The most dramatic effects in the humans were observed in the magnitudes of the peak head and spine transmissibilities located between 4 and 6 Hz with the use of the prototype cushions. Both the deflated and inflated cushions significantly increased the peak head and spine transmissibilities in the females, while decreasing or attenuating the transmissibilities in the males as compared to the rigid seat and the current inventory cushion.
DTIC
*Human Body; Military Helicopters; Human Factors Engineering; Seats; Resonant Frequencies*

**20010120489** Air Force Research Lab., Human Effectiveness Directorate, Wright-Patterson AFB, OH USA
**The Effects of Head Orientation on Head/Helmet Vibration Response** ***Final Report, Oct. 1983 - Sep. 1998***
Smith, Suzanne D.; May 2001; 16p; In English
Contract(s)/Grant(s): AF Proj. 7184
Report No.(s): AD-A395112; AFRL-HE-WP-SR-2001-0010; No Copyright; Avail: CASI; A03, Hardcopy; A01, Microfiche

Involuntary head/helmet motion due to vibration can compromise the effective use of helmet-mounted cueing systems. Extreme off-axis head/helmet orientations are also expected during tactical maneuvers where aircraft vibration occurs. The effects of head/helmet orientation on head/helmet low frequency vibration response were investigated. Subjects were exposed to an experimental F-15 vibration signal and to sinusoidal frequencies in the range of 3 to 10 Hz. Head and helmet rms accelerations, power spectral densities, and transmissibilities were evaluated. The results showed that head/helmet orientation had minimal effect on the frequency location of the peak responses, which primarily occurred between 4 and 7 Hz for both types of exposures. However, significant increases in the peak helmet pitch responses were observed for head/helmet orientations not aligned with the vertical input axis at the seat. For these off-axis orientations, both exposures showed responses, which tended to be higher at most frequencies below 10 Hz. These head/helmet response characteristics can provide important criteria for developing hardware damping mechanisms and/or software algorithms, which minimize the effects of head/helmet motions on tracking performance and cueing system stability.
DTIC
*Vibration; Helmet Mounted Displays; Systems Engineering; Helmets*

**20010120911** NASA Ames Research Center, Moffett Field, CA USA
**A Lab-Scale CELSS**
Flynn, Mark E., Bionetics Corp., USA; Finn, Cory K., NASA Ames Research Center, USA; Srinivasan, Venkatesh, Bionetics Corp., USA; Sun, Sidney, NASA Ames Research Center, USA; [1994]; 1p; In English; 24th International Conference on Environmental Systems, 20-23 Jun. 1994, Friedrichshafen, Germany
Contract(s)/Grant(s): RTOP 199-61-12; No Copyright; Avail: Issuing Activity; Abstract Only

It has been shown that prohibitive resupply costs for extended-duration manned space flight missions will demand that a high degree of recycling and in situ food production be implemented. A prime candidate for in situ food production is the growth of higher level plants. Research in the area of plant physiology is currently underway at many institutions. This research is aimed at the characterization and optimization of gas exchange, transpiration and food production of higher plants in order to support human life in space. However, there are a number of unresolved issues involved in making plant chambers an integral part of a

closed life support system. For example, issues pertaining to the integration of tightly coupled, non-linear systems with small buffer volumes will need to be better understood in order to ensure successful long term operation of a Controlled Ecological Life Support System (CELSS). The Advanced Life Support Division at NASA Ames Research Center has embarked on a program to explore some of these issues and demonstrate the feasibility of the CELSS concept. The primary goal of the Laboratory Scale CELSS Project is to develop a fully-functioning integrated CELSS on a laboratory scale in order to provide insight, knowledge and experience applicable to the design of human-rated CELSS facilities. Phase I of this program involves the integration of a plant chamber with a solid waste processor. This paper will describe the requirements, design and some experimental results from Phase I of the Laboratory Scale CELSS Program.
Author
*Closed Ecological Systems; Plants (Botany); Long Duration Space Flight; Gas Exchange*

**20010121491** NASA Ames Research Center, Moffett Field, CA USA
**Enhanced/Synthetic Vision Systems for Advanced Flight Decks**
Kaiser, Mary K., NASA Ames Research Center, USA; Jenkins, James, NASA, USA; [1994]; 1p; In English; Society for Information Display/International Symposium, Seminar and Exhibition, 12-17 Jun. 1994, San Jose, CA, USA; Sponsored by Society for Information Display, USA
Contract(s)/Grant(s): RTOP 528-04-11; No Copyright; Avail: Issuing Activity; Abstract Only

One of the most challenging arenas for enhanced and synthetic vision systems is the flight deck. Here, pilots must perform active and supervisory control behaviors based on imagery generated in real time or transduced from imaging sensors. Although enhanced and synthetic vision technologies have been used in military vehicles for more than two decades, they have only recently been considered for civilian transport aircraft. In this paper we discuss the human performance issues still to be resolved for these systems, and consider the special constraints that must be considered for their use in the transport domain.
Author
*Enhanced Vision; Civil Aviation; Human Performance*

**20010121534** NASA Ames Research Center, Moffett Field, CA USA
**Adsorption and Desorption of Carbon Dioxide and Water Mixtures on Synthetic Hydrophobic Carbonaceous Adsorbents**
Finn, John E., NASA Ames Research Center, USA; [1994]; 1p; In English; AICHE Annual Meeting, 13-18 Nov. 1994, San Francisco, CA, USA; Sponsored by American Inst. of Chemical Engineers, USA
Contract(s)/Grant(s): RTOP 199-61-62; No Copyright; Avail: Issuing Activity; Abstract Only

Several synthetic carbonaceous adsorbents produced through pyrolysis of polymeric materials are available commercially. Some appear to have advantages over activated carbon for certain adsorption applications. In particular, they can have tailored hydrophobicities that are significantly greater than that of activated carbon, while moderately high surfaces areas are retained. These sorbents are being investigated for possible use in removing trace contaminants and excess carbon dioxide from air in closed habitats, plant growth chambers, and other applications involving purification of humid gas streams. We have analyzed the characteristics of a few of these adsorbents through adsorption and desorption experiments and standard characterization techniques. This paper presents pure and multicomponent adsorption data collected for carbon dioxide and water on two synthetic carbonaceous adsorbents having different hydrophobicities and capillary condensation characteristics. The observations are interpreted through consideration of the pore structure and surface chemistry of the solids and interactions between adsorbed carbon dioxide, water, and the solvent gas.
Author
*Adsorption; Desorption; Carbon Dioxide; Adsorbents; Water*

**20010122283** NASA Ames Research Center, Moffett Field, CA USA
**What to Do Until the Money Runs Out: A Refinement Framework for Cognitive Engineering in the Real World**
Shafto, Michael G., NASA Ames Research Center, USA; Remington, Roger W., NASA Ames Research Center, USA; Trimble, Jay W., Jet Propulsion Lab., California Inst. of Tech., USA; [1994]; 2p; In English; 16th Annual Conference of the Cognitive Science Society, 13-16 Aug. 1994, Atlanta, GA, USA
Contract(s)/Grant(s): RTOP 505-64-53; No Copyright; Avail: Issuing Activity; Abstract Only

A case study is presented to illustrate some of the problems of applying cognitive science to complex human-machine systems. Disregard for facts about human cognition often undermines the safety, reliability, and cost-effectiveness of complex systems. Yet single-point methods (for example, better user-interface design), whether rooted in computer science or in experimental psychology, fall far short of addressing systems-level problems in a timely way using realistic resources. A model-based methodology is proposed for organizing and prioritizing the cognitive engineering effort, focusing appropriate

expertise on major problems first, then moving to more sophisticated refinements if time and resources permit. This case study is based on a collaborative effort between the Human Factors Division at NASA-Ames and the Spaceborne Imaging Radar SIR-C/X-Band Synthetic Aperture Radar (SIR-C/X-SAR) Project at the Jet Propulsion Laboratory (JPL), California institute of Technology. The first SIR-C/X-SAR Shuttle mission flew successfully in April, 1994. A series of such missions is planned to provide radar data to study Earth's ecosystems, climatic and geological processes, hydrologic cycle, and ocean circulation. In addition to JPL and NASA personnel, the SIR-C/X-SAR operations team included Scientists and engineers from the German and Italian space agencies.
Author
*Human Factors Engineering; Ecosystems; Cognition; Knowledge Bases (Artificial Intelligence)*

**20010122291** Defence Science and Technology Organisation, Combatant Protection and Nutrition Branch, Fishermans Bend, Australia
**Physiological Burden of the S10 Respirator**
Scanlan, S., Defence Science and Technology Organisation, Australia; Roberts, W., Defence Science and Technology Organisation, Australia; June 2001; 32p; In English; Original contains color illustrations
Report No.(s): DSTO-TN-0380; DODA-AR-011-916; Copyright; Avail: Issuing Activity

It is well accepted that wearing a respirator increases the physiological load imposed on the user. However, there is little quantitative evidence of the impact of respiratory protection on thermal strain imposed on the user as a function of the total individual protective ensemble (IPE). This pilot study aims to use the novel technique of Thermal Imaging (TI) to assess the heat status of the face and thermal strain associated with wearing the S10 respirator. The physiological (rectal and tympanic temperatures, heart rate), psychophysical (thermal sensation and discomfort, perceived exertion) and thermal effects (thermal imaging) of the S10 respirator were measured in four healthy males (31 +/- 4.5 yrs). Each subject completed two 45 min trials consisting of acclimation (10 min), treadmill walking (30 min) and rest (5 min) in a hot environment (30 C dry bulb and 60% relative humidity), while wearing the UK MK IV overgarment with the S10 respirator (MASK) and without (CON). Generally, there was no additional thermal strain while wearing the S10 respirator. However, subjects reported thermal discomfort of the face as being significantly (p less than 0.05) more uncomfortable after 30 mins of exercise compared to being unmasked. In conclusion, the mask partially inhibited evaporative cooling of the face giving the user the perception of being more heat stressed than when unmasked, which was not matched by the recorded physiological strain. It is recommended that the design of the respirator require no significant alteration to reduce any perceived thermal load.
Author
*Body Temperature; Evaporative Cooling; Masks; Physical Exercise; Protective Clothing; Respirators; Temperature Effects*

**20010122710** Space and Naval Warfare Systems Center, San Diego, CA USA
**Monitoring Moment-to-Moment Operator Workload Using Task Load and System-State Information**
Van Orden, K. F.; Jun. 2001; 21p; In English
Report No.(s): AD-A395277; SSC/SD-TR-1864; No Copyright; Avail: CASI; A03, Hardcopy; A01, Microfiche

Assessing and understanding operator workload is an important factor for consideration during the development of new systems. It may also be important to understand fluctuations in workload within operational systems in order to efficiently apply automated processes and provide assistance at critical times. This paper describes how a simple workload measure obtained every 2 to 3 minutes during the evaluation of a prototype command and control console can be used to develop an operator's workload profile as a function of other system parameters, such as track density on the tactical plot, and task loading.
DTIC
*Command and Control; Workloads (Psychophysiology); Human Factors Engineering*

**20010125463** Los Alamos National Lab., NM USA
**Demonstration Integrated Knowledge-Based System for Estimating Human Error Probabilities**
Auflick, J. L.; Apr. 21, 1999; 6p; In English
Report No.(s): DE2001-8234; LA-UR-98-3935; No Copyright; Avail: Department of Energy Information Bridge, Microfiche

Human Reliability Analysis (HRA) is currently comprised of at least 40 different methods that are used to analyze, predict, and evaluate human performance in probabilistic terms. Systematic HRAs allow analysts to examine human-machine relationships, identify error-likely situations, and provide estimates of relative frequencies for human errors on critical tasks, highlighting the most beneficial areas for system improvements. Unfortunately, each of HRA's methods has a different philosophical approach, thereby producing estimates of human error probabilities (HEPs) that are a better or worse match to the error likely situation of interest. Poor selection of methodology, or the improper application of techniques can produce invalid

HEP estimates, where that erroneous estimation of potential human failure could have potentially severe consequences in terms of the estimated occurrence of injury, death, and/or property damage.
NTIS
*Probability Theory; Performance Prediction; Human Performance; Reliability Analysis*

## 59
## MATHEMATICAL AND COMPUTER SCIENCES (GENERAL)

*Includes general topics and overviews related to mathematics and computer science. For specific topics in these areas see categories 60 through 67.*

**20010118909** Sandia National Labs., Albuquerque, NM USA
**Nested Acceleration Algorithm for Self-Adjoint Angular Flux Boltzmann-CSD Equation**
Liscum-Powell, J.; Prinja, A. K.; Morel, J. E.; Lorence, L. J.; Jun. 30, 2000; 7p; In English
Report No.(s): DE2000-760793; SAND2000-1578C; No Copyright; Avail: Department of Energy Information Bridge

The second-order, self-adjoint angular flux (SAAF) equation, modified to include continuous slowing down (CSD), was recently used for coupled electron-photon transport. Results using the standard discrete ordinates approach with linear continuous (LC) spatial finite elements, diamond difference (DD) in energy and DSA source iteration acceleration, generally compared very favorably against the first-order form of the transport equation.
NTIS
*Algorithms; Particle Acceleration*

**20010119551** Oak Ridge National Lab., TN USA
**Epistemology and Rosen's Modeling Relation**
Dress, W. B.; Nov. 07, 1999; 12p; In English
Report No.(s): DE2001-10460; ORNL/CP-103754; No Copyright; Avail: Department of Energy Information Bridge, Microfiche

Rosens modeling relation is embedded in Popper's three worlds to provide an heuristic tool for model building and a guide for thinking about complex systems. The utility of this construct is demonstrated by suggesting a solution to the problem of pseudo science and a resolution of the famous Bohr-Einstein debates. A theory of bizarre systems is presented by an analogy with entangled particles of quantum mechanics. This theory underscores the poverty of present-day computational systems (e.g., computers) for creating complex and bizarre entities by distinguishing between mechanism and organism.
NTIS
*Quantum Mechanics; Complex Systems*

**20010119949** Sandia National Labs., Albuquerque, NM USA
**Methods for Multisweep Automation**
Shepherd,; Mitchell,; Knupp,; White,; Sep. 14, 2000; 13p; In English
Report No.(s): DE2000-763103; SAND2000-2273C; No Copyright; Avail: Department of Energy Information Bridge, Microfiche

Sweeping has become the workhorse algorithm for creating conforming hexahedral meshes of complex models. This paper describes progress on the automatic, robust generation of MultiSwept meshes in CUBIT. MultiSweeping extends the class of volumes that may be swept to include those with multiple source and multiple target surfaces. While not yet perfect, CUBIT's MultiSweeping has recently become more reliable, and been extended to assemblies of volumes. Sweep Forging automates the process of making a volume (multi) sweepable: Sweep Verification takes the given source and target surfaces, and automatically classifies curve and vertex types so that sweep layers are well formed and progress from sources to targets.
NTIS
*Algorithms; Computational Grids*

**20010121973** Los Alamos National Lab., NM USA
**Expression Template Aware Lambda Function**
Smith, S. A.; Striegnitz, J.; Sep. 19, 2000; 16p; In English
Report No.(s): DE2000-762847; LA-UR-00-4402; No Copyright; Avail: Department of Energy Information Bridge, Microfiche

The authors show how the paradigms of lambda functions and expression templates fit together in order to provide a means to increase the expressiveness of existing STL algorithms. They demonstrate how the expression templates approach could be

extended in order to work with built-in types. to be portable, their solution is based on the Portable Expression Template Engine (PETE), which is a framework that enables the development of expression template aware classes.
NTIS
*Templates; Computer Programming; Algorithms*

**20010122309** Sandia National Labs., Albuquerque, NM USA
**FETI-DP: An Efficient, Scalable and Unified Dual-Primal FETI Method**
Lesoinne,; Pierson,; Jul. 07, 2000; 10p; In English
Report No.(s): DE2000-761045; SAND2000-1597C; No Copyright; Avail: Department of Energy Information Bridge

The Finite Element Tearing and Interconnecting (FETI) algorithms are numerically scalable iterative domain decomposition methods. These methods are well documented for solving equations arising from the Finite Element discretization of second or fourth order elasticity problems. The one level FETI method equipped with the Dirichlet preconditioned was shown to be numerically scalable for second order elasticity problems while the two level FETI method was designed to be numerically scalable for fourth order elasticity problems. The second level coarse grid is an enriched version of the original one level FETI method with coarse grid. The coarse problem is enriched by enforcing transverse displacements to be continuous at the corner points. This coarse problem grows linearly with the number of subdomains. Current implementations use a direct solution method to solve this coarse problem. However, the current implementation gives rise to a full matrix system. This full matrix can lead to increased storage requirements especially if working within a distributed memory environment. Also, the factorization and subsequent forward/backward substitutions of the second level coarse problem becomes the dominant factor in solving the global problem as the number of subdomains becomes large (N(sub s); 1,000). The authors introduce an alternative formulation of the two level coarse problem that leads to a sparse system better suited for a direct method. Then they show extensions to the alternate formulation that allow optional admissible constraints to be added to improve convergence. Lastly, they report on the numerical performance, parallel efficiency, memory requirements, and overall CPU time as compared to the classical two level FETI on some large scale fourth order elasticity problems.
NTIS
*Algorithms; Finite Element Method*

**20010122374** Argonne National Lab., IL USA
**Sparse superlinearly convergent SQP with applications to two-dimensional shape optimization**
Anitescu, M., Argonne National Lab., USA; Apr. 15, 1998; 15p; In English
Report No.(s): DE2001-10738; ANL/MCS/CP-96123; No Copyright; Avail: Department of Energy Information Bridge, Microfiche

Discretization of optimal shape design problems leads to very large nonlinear optimization problems. For attaining maximum computational efficiency, a sequential quadratic programming (SQP) algorithm should achieve superlinear convergence while preserving sparsity and convexity of the resulting quadratic programs. Most classical SQP approaches violate at least one of the requirements. We show that, for a very large class of optimization problems, one can design SQP algorithms that satisfy all these three requirements. The improvements in computational efficiency are demonstrated for a cam design problem.
NTIS
*Quadratic Programming; Shape Optimization; Nonlinearity; Cams*

**20010122657** Bechtel Nevada, Los Alamos, NM USA
**Enhancing Hyperspectral Data Throughput Utilizing Wavelet-Based Fingerprints**
Ginsberg, I. W.; Sep. 01, 1999; 11p; In English
Report No.(s): DE2000-764641; DOE/NV/11718-366; No Copyright; Avail: Department of Energy Information Bridge, Microfiche

Multiresolutional decompositions known as spectral fingerprints are often used to extract spectral features from multispectral/hyperspectral data. In this study, the authors investigate the use of wavelet-based algorithms for generating spectral fingerprints. The wavelet-based algorithms are compared to the currently used method, traditional convolution with first-derivative Gaussian filters. The comparison analyses consists of two parts: (a) the computational expense of the new method is compared with the computational costs of the current method and (b) the outputs of the wavelet-based methods are compared with those of the current method to determine any practical differences in the resulting spectral fingerprints. The results show that the wavelet-based algorithms can greatly reduce the computational expense of generating spectral fingerprints, while practically no differences exist in the resulting fingerprints. The analysis is conducted on a database of hyperspectral signatures, namely,

Hyperspectral Digital Image Collection Experiment (HYDICE) signatures. The reduction in computational expense is by a factor of about 30, and the average Euclidean distance between resulting fingerprints is on the order of 0.02.
NTIS
*Wavelet Analysis; Algorithms; Signatures; Pattern Recognition*

**20010123227** Los Alamos National Lab., NM USA
**4D Reconstructions from Low-Count Spect Data Using Deformable Models with Smooth Interior Intensity Variations**
Cunningham, G. S.; Lehovich, A.; Jan. 01, 2000; 14p; In English
Report No.(s): DE2000-763349; LA-UR-00-796; No Copyright; Avail: Department of Energy Information Bridge

The Bayes Inference Engine (BIE) has been used to perform a 4D reconstruction of a first-pass radiotracer bolus distribution inside a CardioWest Total Artificial Heart, imaged with the University of Arizona's FastSPECT system. The BIE estimates parameter values that define the 3D model of the radiotracer distribution at each of 41 times spanning about two seconds. The 3D models have two components: a closed surface, composed of hi-quadratic Bezier triangular surface patches, that defines the interface between the part of the blood pool that contains radiotracer and the part that contains no radiotracer, and smooth voxel-to-voxel variations in intensity within the closed surface. Ideally, the surface estimates the ventricular wall location where the bolus is infused throughout the part of the blood pool contained by the right ventricle. The voxel-to-voxel variations are needed to model an inhomogeneously-mixed bolus. Maximum a posterior (MAP) estimates of the Bezier control points and voxel values are obtained for each time frame. We show new reconstructions using the Bezier surface models, and discuss estimates of ventricular volume as a function of time, ejection fraction, and wall motion. The computation time for our reconstruction process, which directly estimates complex 3D model parameters from the raw data, is performed in a time that is competitive with more traditional voxel-based methods (e.g., ML-EM).
NTIS
*Estimates; Heart; Three Dimensional Models*

**20010123411** California Univ., Berkeley, CA USA
**Final Report: Adaptive Numerical Algorithms for Partial Differential Equations, May 1, 1994-April 30, 1998**
Colella, P.; Mar. 14, 2000; 11p; In English
Report No.(s): DE2001-765106; No Copyright; Avail: Department of Energy Information Bridge

The goal of the work performed under this grant has been to develop high-quality tools for simulating complex systems that are represented by solutions to partial differential equations. Examples include the simulation of combustion devices and of various kinds of manufacturing processes. Such systems are characterized by the presence of multiple physical processes, of complex geometries, and of multiple length and time scales. to this end, we developed a number of new methods that are required to simulate a variety of complex systems. These include methods for decomposing problems with multiple time scales, accurate and robust finite difference discretizations, methods for adaptively concentrating computational effort where it is most needed, and general flexible methods for representing complex geometries.
NTIS
*Algorithms; Partial Differential Equations; Complex Systems*

**20010123414** Utah Univ., Salt Lake City, UT USA
**Final Report: Symposium on Adaptive Methods for Partial Differential Equations**
Pernice, M.; Johnson, C. R.; Smith, P. J.; Fogelson, A.; Dec. 08, 1998; 34p; In English
Report No.(s): DE2001-765103; No Copyright; Avail: Department of Energy Information Bridge

Complex physical phenomena often include features that span a wide range of spatial and temporal scales. Accurate simulation of such phenomena can be difficult to obtain, and computations that are under-resolved can even exhibit spurious features. While it is possible to resolve small scale features by increasing the number of grid points, global grid refinement can quickly lead to problems that are intractable, even on the largest available computing facilities. These constraints are particularly severe for three dimensional problems that involve complex physics. One way to achieve the needed resolution is to refine the computational mesh locally, in only those regions where enhanced resolution is required. Adaptive solution methods concentrate computational effort in regions where it is most needed. These methods have been successfully applied to a wide variety of problems in computational science and engineering. Adaptive methods can be difficult to implement, prompting the development of tools and environments to facilitate their use. to ensure that the results of their efforts are useful, algorithm and tool developers must maintain close communication with application specialists. Conversely it remains difficult for application specialists who

are unfamiliar with the methods to evaluate the trade-offs between the benefits of enhanced local resolution and the effort needed to implement an adaptive solution method.
NTIS
*Partial Differential Equations; Complex Systems; Computational Grids; Three Dimensional Models*

**20010123426** Los Alamos National Lab., NM USA
**Elliptic Solvers for Adaptive Mesh Refinement Grids**
Quinlan, D. J.; Dendy, J. E.; Shapira, Y.; Jun. 03, 1999; 14p; In English
Report No.(s): DE2001-763231; LA-UR-99-2673; No Copyright; Avail: Department of Energy Information Bridge

We are developing multigrid methods that will efficiently solve elliptic problems with anisotropic and discontinuous coefficients on adaptive grids. The final product will be a library that provides for the simplified solution of such problems. This library will directly benefit the efforts of other Laboratory groups. The focus of this work is research on serial and parallel elliptic algorithms and the inclusion of our black-box multigrid techniques into this new setting. The approach applies the Los Alamos object-oriented class libraries that greatly simplify the development of serial and parallel adaptive mesh refinement applications. In the final year of this LDRD, we focused on putting the software together; in particular we completed the final AMR++ library, we wrote tutorials and manuals, and we built example applications. We implemented the Fast Adaptive Composite Grid method as the principal elliptic solver. We presented results at the Overset Grid Conference and other more AMR specific conferences. We worked on optimization of serial and parallel performance and published several papers on the details of this work. Performance remains an important issue and is the subject of continuing research work.
NTIS
*Algorithms; Grid Generation (Mathematics); Multigrid Methods; Optimization; Parallel Processing (Computers)*

**20010123907** Los Alamos National Lab., NM USA
**Bridging the Gap between Speech Production and Speech Recognition**
Hogden, J. E.; Valdez, P. F.; Feb. 01, 2000; 7p; In English
Report No.(s): DE2001-763401; LA-UR-00-1084; No Copyright; Avail: Department of Energy Information Bridge

Although stochastic models of speech signals (e.g. hidden Markov models (HMM), trigrams, etc.) have lead to impressive improvements in speech recognition accuracy, it has been noted that these models have little relationship to speech production and their recognition performance on some important tasks is far from perfect. However, there have been recent attempts to bridge the gap between speech production and speech recognition using models that are stochastic and yet make more reasonable assumptions about the mechanisms underlying speech production. One of theses models, Multiple Observable, Maximum Likelihood Continuity Mapping (MO-MALCOM) is described in this paper. There are theoretical and experimental reasons to believe that MO-MALCOM learns an insertable stochastic mapping between articulator positions and speech acoustics. Furthermore, MO-MALCOM can be combined with standard speech recognition algorithms to create a speech recognition model based on a stochastic production model. Results of using MO-MALCOM speech recognition on data derived from the switchboard corpus will be discussed. A nice feature of HMMs is that maximum likelihood techniques allow the model parameters to be automatically determined from training data. The automatic parameter estimation, and the stochastic nature of the HMMs are presumably the features that allow them to cope with the amazing amount of variability in speech.
NTIS
*Speech Recognition; Speech; Mathematical Models; Markov Processes; Signal Processing*

**20010123915** Los Alamos National Lab., NM USA
**General Predictive Performance Model for Wavefront Algorithms on Clusters of SMPS**
Hoisie, A.; Lubeck, O.; Jan. 01, 2000; 18p; In English
Report No.(s): DE2001-763353; LA-UR-00-308; No Copyright; Avail: Department of Energy Information Bridge

We have recently been studying the performance of wavefront algorithms implemented using message passing on two-dimensional logical processor arrays. Wavefront algorithms are ubiquitous in parallel computing, since they represent a means of enabling parallelism in computations that contain recurrences. Our particular interest in wavefront algorithms derives from their use in discrete ordinates neutral particle transport computations, but other important uses are well known. The basis of wavefront parallelism is the data dependence graph in which the nodes may represent either physical grid points or logical processors. In the later case, a computation progresses as a wave front 'scans' through a processor grid with pairs of processors sending and receiving boundary data required in order to update a portion of the physical mesh. Those processors within each wavefront, i.e., those on a diagonal, are algorithmically independent. Intuitively, then, the nominal benefit of wavefront parallelism is related to the (continuously-changing) length of a diagonal. However, additional concurrency can be achieved by

'blocking' the computation, resulting in more wavefront 'sweeps' using smaller computational subgrids. This reduces processor idle time that accumulates as processors await their turn to compute, but requires that processors communicate more often.
NTIS
*Algorithms; Wave Fronts; Prediction Analysis Techniques; Parallel Processing (Computers)*

**20010123918** Los Alamos National Lab., NM USA
**Parallel Image Processing with Autowaves: Segmentation and Edge Extraction**
Skourikhine, A. N.; Jan. 01, 2000; 10p; In English
Report No.(s): DE2001-763331; LA-UR-00-422; No Copyright; Avail: Department of Energy Information Bridge

Biologically inspired image processing algorithms like pulse-coupled neural networks find many applications in image preprocessing such as segmentation and edge extraction. The two highly parallel methods of edge extraction from gray-scale images using pulse-coupled neural network are presented. The approach of both methods is based on phenomenon of autowaves, whose properties enable efficient parallel image processing.
NTIS
*Image Processing; Algorithms; Edge Detection*

**20010125094** Sandia National Labs., Albuquerque, NM USA
**Visual Debugging of Visualization Software: A Case Study for Particle Systems**
Angel, E.; Crossno, P.; Jul. 12, 1999; 7p; In English
Report No.(s): DE2001-9004; SAND99-1763C; No Copyright; Avail: Department of Energy Information Bridge, Microfiche

Visualization systems are complex dynamic software systems. Debugging such systems is difficult using conventional debuggers because the programmer must try to imagine the three-dimensional geometry based on a list of positions and attributes. In addition, the programmer must be able to mentally animate changes in those positions and attributes to grasp dynamic behaviors within the algorithm. In this paper we shall show that representing geometry, attributes, and relationships graphically permits visual pattern recognition skills to be applied to the debugging problem. The particular application is a particle system used for isosurface extraction from volumetric data. Coloring particles based on individual attributes is especially helpful when these colorings are viewed as animations over successive iterations in the program. Although we describe a particular application, the types of tools that we discuss can be applied to a variety of problems.
NTIS
*Algorithms; Program Verification (Computers); Computer Vision; Applications Programs (Computers)*

**20010125167** California Univ., Lawrence Berkeley Lab., Berkeley, CA USA
**Higher-Order Embedded Boundary Method for Time-Dependent Simulation of Hyperbolic Conservation Laws**
Modiano, D.; Colella, P.; Mar. 01, 2000; 17p; ASME 2000 Fluids Engineering Division Summer Meeting, 11-15 Jun. 2000, Boston, MA, USA
Report No.(s): DE2000-767572; LBNL-45239; No Copyright; Avail: Department of Energy Information Bridge, Microfiche

We present a new method for time-dependent simulation of hyperbolic conservation laws using a background Cartesian grid with an embedded boundary to represent geometry. The uxes are produced at the centers of the regular grid cell faces by a Godunov method. Since the accuracy of the ux divergence depends on the uxes consistently centered at the centroids of the irregular faces, we linearly interpolate the uxes from the regular face centers to the irregular face centroids. We compare to an exact solution the propagation of a planar wave in a straight-walled channel inclined 30 degrees to the grid. The inconsistent ux method converges at well below first order in the irregular cells, and at about first order in the full domain. The present method, with consistent uxes, converges at between first and second order in the irregular cells, and at second order in the full domain.
NTIS
*Conservation Laws; Time Dependence; Computerized Simulation*

**20010125477** Argonne National Lab., IL USA
**Reverse Engineering: Algebraic Boundary Representations to Constructive Solid Geometry**
Buchele, S. F.; Ellingson, W. A.; Dec. 17, 1997; 14p; In English
Report No.(s): DE2001-8092; ANL/ET/CP-93260; No Copyright; Avail: Department of Energy Information Bridge, Microfiche

Recent advances in reverse engineering have focused on recovering a boundary representation (b-rep) of an object, often for integration with rapid prototyping. This boundary representation may be a three-dimensional point cloud, a triangulation of points, or piecewise algebraic or parametric surfaces. This paper presents work in progress to develop an algorithm to extend the current state of the art in reverse engineering of mechanical parts. This algorithm will take algebraic surface representations as input and

will produce a constructive solid geometry (CSG) description that uses solid primitives such as rectangular block, pyramid, sphere, cylinder, and cone. The proposed algorithm will automatically generate a CSG solid model of a part given its algebraic b-rep, thus allowing direct input into a computer aided design (CAD) system and subsequent CSG model generation.
NTIS
*Algebra; Algorithms; Boundaries*

**20010125634** Oak Ridge Y-12 Plant, TN USA
**X-Ray Computed Tomography on a Cellular Polysiloxane under Compression**
Smith, R. A.; Paulus, M. J.; Branning, J. M.; Phillips, P. J.; Dec. 08, 2000; 30p; In English
Report No.(s): DE2001-769294; Y/DZ-2284; No Copyright; Avail: Department of Energy Information Bridge, Microfiche

X-ray tomographic images were collected for polydimethylsiloxane (PDMS) foam material under various levels of compression. The goal was to implement a systematic analysis method of correlating some aspect of these images to the cell morphology in order to enhance understanding of the material characteristics. X-ray attenuation of the cellular PDMS was clearly observed to increase with the specimen density as the foam material was mechanically compressed. The stochastic data derived from the digital images was used to calculate macroscopic mechanical properties at each foam compression.
NTIS
*Foams; Mechanical Properties; Methyl Polysiloxanes; Tomography*

## 60
## COMPUTER OPERATIONS AND HARDWARE

*Includes hardware for computer graphics, firmware and data processing. For components see 33 Electronics and Electrical Engineering. For computer vision see 63 Cybernetics, Artificial Intelligence and Robotics.*

**20010123634** Princeton Univ., Plasma Physics Lab., NJ USA
**Orbitmpi Documentation**
Lowe, L. L.; Oct. 05, 2000; 13p; In English
Report No.(s): DE2000-764942; PPPL-3489; No Copyright; Avail: Department of Energy Information Bridge

Orbitmpi is a parallelized version of Roscoe White's Orbit code. The code has been parallelized using MPI, which makes it portable to many types of machines. The guidelines used for the parallelization were to increase code performance with minimal changes to the code's original structure. This document gives a general description of how the parallel sections of the code run. It discusses the changes made to the original code and comments on the general procedure for future additions to Orbitmpi, as well as describing the effects of a parallelized random number generator on the code's output. Finally, the scaling results from Hecate and from Puffin are presented. Hecate is a 64-processor Origin 2000 machine, with MIPS R12000 processors and 16GB of memory, and Puffin is a PC cluster with nine dual-processor 450 MHz Pentium III (18 processors max.), with 100 Mbits ethernet communication.
NTIS
*Parallel Processing (Computers); Computer Programs; Revisions*

**20010123906** Los Alamos National Lab., NM USA
**Radiation Characterization, and SEU Mitigation, of the Virtex FPGA for Spcce-Based Reconfigurable Computing**
Fuller, E.; Caffrey, M.; Sep. 01, 2000; 11p; In English
Report No.(s): DE2001-764027; LA-UR-00-3345-REV-7/20; No Copyright; Avail: Department of Energy Information Bridge

Orbital remote sensing instruments and systems benefit from high performance, adaptable computing systems. Field programmable SRAM-based gate arrays (FPGAs) are usually the chosen platform for real-time reconfigurable computing. This technology is driven by the commercial sector, so devices intended for the space environment must be adapted from commercial product. Total ionizing dose, heavy ion and proton characterization have been performed on Virtex FPGAs fabricated on epitaxial silicon to evaluate the on-orbit radiation performance expected for this technology. The dominant risk is Single Event Upset (SEU), so upset detection and mitigation schemes have also been tested to validate the improvement in the device upset sensitivity and the system consequence of upsets.
NTIS
*Single Event Upsets; Field-Programmable Gate Arrays; Radiation Effects; Ionizing Radiation*

**20010125490** Argonne National Lab., IL USA
**Application experiences with the Globus toolkit**
Brunett, S.; Jun. 09, 1998; 12p; In English
Report No.(s): DE2001-10847; ANL/MCS/CP-96664; No Copyright; Avail: Department of Energy Information Bridge

The Globus grid toolkit is a collection of software components designed to support the development of applications for high-performance distributed computing environments, or 'computational grids'. The Globus toolkit is an implementation of a 'bag of services' architecture, which provides application and tool developers not with a monolithic system but rather with a set of stand-alone services. Each Globus component provides a basic service, such as authentication, resource allocation, information, communication, fault detection, and remote data access. Different applications and tools can combine these services in different ways to construct 'grid-enabled' systems. The Globus toolkit has been used to construct the Globus Ubiquitous Supercomputing Testbed, or GUSTO: a large-scale testbed spanning 20 sites and included over 4000 compute nodes for a total compute power of over 2 TFLOPS. Over the past six months, we and others have used this testbed to conduct a variety of application experiments, including multi-user collaborative environments (tele-immersion), computational steering, distributed supercomputing, and high throughput computing. The goal of this paper is to review what has been learned from these experiments regarding the effectiveness of the toolkit approach. to this end, we describe two of the application experiments in detail, noting what worked well and what worked less well. The two applications are a distributed supercomputing application, SF-Express, in which multiple supercomputers are harnessed to perform large distributed interactive simulations; and a tele-immersion application, CAVERNsoft, in which the focus is on connecting multiple people to a distributed simulated world.
NTIS
*Architecture (Computers); Software Development Tools; Distributed Processing*

## 61
## COMPUTER PROGRAMMING AND SOFTWARE

*Includes software engineering, computer programs, routines, algorithms, and specific applications, e.g., CAD/CAM. For computer software applied to specific applications, see also the associated category.*

**20010117728** Computer Sciences Corp., Moffett Field, CA USA
**Virtual Environments in Scientific Visualization**
Bryson, Steve, Computer Sciences Corp., USA; Cooper, D. M., NASA Ames Research Center, USA; [1994]; 1p; In English; GRAPHICON 1994, 19-24 Sep. 1994, Nizhni Novgorod, Tokyo, Winchester, Russia, Japan, Netherlands, UK, Singapore
Contract(s)/Grant(s): RTOP 536-01-11; No Copyright; Avail: Issuing Activity; Abstract Only

Virtual environment technology is a new way of approaching the interface between computers and humans. Emphasizing display and user control that conforms to the user's natural ways of perceiving and thinking about space, virtual environment technologies enhance the ability to perceive and interact with computer generated graphic information. This enhancement potentially has a major effect on the field of scientific visualization. Current examples of this technology include the Virtual Windtunnel being developed at NASA Ames Research Center. Other major institutions such as the National Center for Supercomputing Applications and SRI International are also exploring this technology. This talk will be describe several implementations of virtual environments for use in scientific visualization. Examples include the visualization of unsteady fluid flows (the virtual windtunnel), the visualization of geodesics in curved spacetime, surface manipulation, and examples developed at various laboratories.
Author
*Scientific Visualization; Virtual Reality; Human-Computer Interface*

**20010117729** NASA Ames Research Center, Moffett Field, CA USA
**High Performance Computing at NASA**
Bailey, David H., NASA Ames Research Center, USA; [1994]; 1p; In English; IBM High Performance Users Forum, 27 Sep. 1994, Tokyo, Japan; Sponsored by International Business Machines Corp., USA
Contract(s)/Grant(s): RTOP 536-01-11; No Copyright; Avail: Issuing Activity; Abstract Only

The speaker will give an overview of high performance computing in the U.S. in general and within NASA in particular, including a description of the recently signed NASA-IBM cooperative agreement. The latest performance figures of various parallel systems on the NAS Parallel Benchmarks will be presented. The speaker was one of the authors of the NAS (National Aerospace Standards) Parallel Benchmarks, which are now widely cited in the industry as a measure of sustained performance on realistic high-end scientific applications. It will be shown that significant progress has been made by the highly parallel

supercomputer industry during the past year or so, with several new systems, based on high-performance RISC processors, that now deliver superior performance per dollar compared to conventional supercomputers. Various pitfalls in reporting performance will be discussed. The speaker will then conclude by assessing the general state of the high performance computing field.
Author
*Supercomputers; Aerospace Systems*

**20010118504** NASA Ames Research Center, Moffett Field, CA USA
**A FORTRAN-90 Based Multiprecision System**
Bailey, David H., NASA Ames Research Center, USA; [1994]; 1p; In English
Contract(s)/Grant(s): RTOP 536-01-11
Report No.(s): RNR-94-013; No Copyright; Avail: Issuing Activity; Abstract Only

The author has developed a new version of his FORTRAN multiprecision computation system that is based on the FORTRAN-90 language. With this new approach, a translator program is not required - translation of FORTRAN code for multiprecision is accomplished by merely utilizing advanced features of FORTRAN-90, such as derived data types and operator extensions. This approach results in more reliable translation and also permits programmers of multiprecision applications to utilize the full power of the FORTRAN-90 language. Three multiprecision datatypes are supported in this system: multiprecision integer. real and complex. All the usual FORTRAN conventions for mixed mode operations are supported, and many of the FORTRAN intrinsics, such as SIN, EXP and MOD, are supported with multiprecision arguments. This paper also briefly describes an interesting application of this software, wherein new number-theoretic identities have been discovered by means of multiprecision computations.
Author
*Applications Programs (Computers); FORTRAN; Computation*

**20010118512** NASA Ames Research Center, Moffett Field, CA USA
**Survey of Volumetric Grid Generators**
Woo, Alex, NASA Ames Research Center, USA; Volakis, John, Michigan Univ., USA; Hulbert, Greg, Michigan Univ., USA; Case, Jeff, NASA Langley Research Center, USA; [1994]; 3p; In English
Contract(s)/Grant(s): RTOP 505-59-70; No Copyright; Avail: Issuing Activity; Abstract Only

This document is the result of an Internet Survey of Volumetric grid generators. As such we have included information from only the responses which were sent to us. After the initial publication and posting of this survey, we would encourage authors and users of grid generators to send further information. Here is the initial query posted to SIGGRID@nas and the USENET group sci.physics.computational.fluid-dynamics. Date: Sun, 30 Jan 94 11:37:52 -0800 From: woo (Alex Woo x6010 227-6 rm 315) Subject: Info Sought for Survey of Grid Generators I am collecting information and reviews of both government sponsored and commercial mesh generators for large scientific calculations, both block structured and unstructured. If you send me a review of a mesh generator, please indicate its availability and cost. If you are a commercial concern with information on a product, please also include references for possible reviewers. Please email to woo@ra-next.arc.nasa.gov. I will post a summary and probably write a short note for the IEEE Antennas and Propagation Magazine. Alex Woo, MS 227-6 woo@ames.arc.nasa.gov NASA Ames Research Center NASAMAIL ACWOO Moffett Field, CA 94035-1000 SPANET 24582::W00 (415) 604-6010 (FAX) 604-4357 fhplabs,decwrl,uunet)!ames!woo Disclaimer: These are not official statements of NASA or EMCC. We did not include all the submitted text here. Instead we have created a database entry in the freely available and widely used BIBTeX format which has an Uniform Resource Locator (URL) field pointing to more details. The BIBTeX database is modeled after those available from the BIBNET project at University of Utah.
Author
*Computational Grids; Group Dynamics; Computer Networks; Data Bases*

**20010118518** Brookhaven National Lab., Upton, NY USA
**Problem descriptions for the decision support software demonstration**
Sullivan,; Armstrong,; Osleeb,; Sep. 14, 1998; 36p; In English
Report No.(s): DE2000-759027; BNL-67000; No Copyright; Avail: Department of Energy Information Bridge

This demonstration is focused on evaluating the utility of decision support software in addressing environmental problems. Three endpoints have been selected for evaluation: (1) Visualization; (2) Sample Optimization; and (3) Cost/Benefit Analysis. The definitions for these three areas in this program are listed.
NTIS
*Decision Making; Computer Programs*

**20010118910** Sandia National Labs., Albuquerque, NM USA

**Application of a Virtual Private Network to the Finnish Remote Environmental Monitoring System**

Smartt, H. A.; Jul. 10, 2000; 10p; In English

Report No.(s): DE2000-760798; SAND2000-1601C; No Copyright; Avail: Department of Energy Information Bridge

One of the primary concerns of employing remote monitoring technologies for IAEA safeguards applications is the high cost of data transmission. Transmitting data over the Internet has been shown often to be less expensive than other data transmission methods. However, data security using the Internet has never been adequately demonstrated. The Virtual Private Network (VPN) has emerged as a solution to this problem. A field demonstration has been implemented to evaluate the use of Virtual Private Networks (via the Internet) as a means for data transmission. Evaluation points include security, reliability, and cost. The existing Finnish Remote Environmental Monitoring System, located at the STUK facility in Helsinki, Finland, is serving as the field demonstration system. Sandia National Laboratories established a Virtual Private Network between STUK Headquarters in Helsinki, Finland, and IAEA Headquarters in Vienna, Austria. Data from the existing STUK Remote Monitoring System can be viewed at the IAEA via this network.

NTIS

*Environmental Quality; Environmental Monitoring; Data Transmission; Computer Information Security*

**20010119021** Argonne National Lab., IL USA

**Automatic differentiation for message-passing parallel programs**

Hovland, P.; Jan. 27, 1998; 10p; In English

Report No.(s): DE2001-10572; ANL/MCS-P703-0198; No Copyright; Avail: Department of Energy Information Bridge, Microfiche

Many applications require the derivatives of functions defined by computer programs. Automatic differentiation (AD) is a means of developing code to compute the derivatives of complicated functions accurately and efficiently, without the difficulties associated with developing correct code by hand. We discuss some of the issues involved in developing automatic differentiation tools for parallel programming environments.

NTIS

*Parallel Processing (Computers); Parallel Programming; Computer Techniques*

**20010119237** Army Research Lab., Human Research and Engineering Directorate, Aberdeen Proving Ground, MD USA

**An Application of Statistics to Algorithm Development in Image Analysis** ***Final Report***

Bodt, Barry; David, Philip; Hillis, David; Aug. 2001; 25p; In English

Report No.(s): AD-A395055; ARL-TR-2333; No Copyright; Avail: CASI; A03, Hardcopy; A01, Microfiche

We gathered and processed infrared (IR) images taken by a quantum well infrared photodetector (QWIP) camera to support the development of an algorithm for airborne target detection. This report addresses the statistical aspects of this effort. Digitized images consisted of background clutter alone and background clutter with a small aircraft target. We used a template-matching technique to detect the small aircraft amidst the background clutter. We propose a reasonable statistic for use in our algorithm. Our primary focus is to describe the experimental design and analysis used in determining parameter settings for the detection algorithm and to report those results.

DTIC

*Algorithms; Photometers; Quantum Wells; Image Analysis; Statistical Analysis*

**20010119529** Sandia National Labs., Albuquerque, NM USA

**Validation Methodology in Computational Fluid Dynamics**

Oberkampf, W. L.; Trucano, T. G.; Jul. 14, 2000; 37p; In English

Report No.(s): DE2000-760805; SAND2000-1656C; No Copyright; Avail: Department of Energy Information Bridge

Verification and validation are the primary means to assess accuracy and reliability in computational simulations. This paper presents an extensive review of the literature in computational validation and develops a number of extensions to existing ideas. We discuss the early work in validation by the operations research, statistics, and CFD communities. The emphasis in our review is to bring together the diverse contributors to validation methodology and procedures.

NTIS

*Computational Fluid Dynamics; Reliability; Accuracy; Computerized Simulation*

**20010119613** Air Command and Staff Coll., Maxwell AFB, AL USA

**The Software Maintenance Spectrum: Using More than Just New Toys**

Sward, Ricky E.; Apr. 2000; 43p; In English

Report No.(s): AD-A394972; AU/ACSC/173/2000-04; No Copyright; Avail: CASI; A03, Hardcopy; A01, Microfiche

As the Air Force enters the 21st century, the software that runs our information systems continues to age and become harder to maintain. Organizations that maintain this legacy software are faced with the challenge of rising software maintenance costs. This paper presents a spectrum of software maintenance options that can be used to reduce the cost of maintenance. The software understanding and programmer unfamiliarity factors from the COCOMO II model are compared to graphically show the effect good software understandability can have on the cost of maintenance. The structure, application clarity, and self-descriptiveness of a software module affect its understandability. The cost of software maintenance is quantified by combining factors from the COCOMO II model and the Software Reengineering Assessment Handbook reengineering decision model that affect understandability. A spectrum of software maintenance options include status quo, redocument, reverse engineer, translate source code, restructure within a paradigm, restructure into a new paradigm, and new acquisition is presented. The benefits of each option are presented in terms of their effect on understandability. Organizations faced with rising maintenance costs should consider the full spectrum of software maintenance options before choosing to replace a software module through new acquisition. by using automated tools, some of the reengineering options present a cost-effective way to reduce the cost of software maintenance. DTIC

*Maintenance; Software Engineering; Information Systems; Cost Reduction*

**20010119931** Carnegie-Mellon Univ., Software Engineering Inst., Pittsburgh, PA USA

**Developing a Product Line Acquisition Strategy for a DoD Organization: A case Study**

Bergey, John K.; Goethert, Wolfhart B.; Apr. 2001; 39p; In English

Contract(s)/Grant(s): F19628-00-C-0003

Report No.(s): AD-A395202; CMU/SEI-2001-TN-021; No Copyright; Avail: CASI; A03, Hardcopy; A01, Microfiche

Industrial experience clearly demonstrates that a product line approach for software-intensive systems can save money and result in faster time to field higher quality systems. Many within the DoD recognize the benefits of product lines, but also recognize that there are significant challenges to adopting such an approach. One of several challenges that confront a DoD organization is developing and implementing a suitable acquisition strategy. to be effective, the DoD organization must balance its product line aspirations against the ability of potential contractors (having varying levels of product line experience and ”hands-on” knowledge of related legacy systems) to meet its needs. It also must balance them against the requirements of DoD policy and regulatory documents that govern the entire acquisition process. Several key questions are: ”What does developing an acquisition strategy involve?” and ”How does a DoD organization develop an effective strategy for acquiring a software product line?” This case study focuses on a recent effort that shows how one DoD organization answered these questions. This technical note describes the approach a DoD organization used to develop alternative acquisition strategies and analyzes the pros and cons of each. It summarizes the acquisition context. It also presents a number of alternative product line acquisition strategies, a method for comparing the merits of each approach, and some risk reduction measures. Although this case study purposely disguises the actual organization and product line, it reflects the considerations involved in developing a software product line acquisition strategy. DTIC

*Government Procurement; Defense Program*

**20010119932** Carnegie-Mellon Univ., Software Engineering Inst., Pittsburgh, PA USA

**Options Analysis for Reengineering (OAR): A Method for Mining Legacy Assets**

Bergey, John; O’Brien, Liam; Smith, Dennis; Jun. 2001; 35p; In English

Contract(s)/Grant(s): F19628-00-C-0003

Report No.(s): AD-A395201; CMU/SEI-2001-TN-013; No Copyright; Avail: CASI; A03, Hardcopy; A01, Microfiche

Options Analysis for Reengineering (OAR) is a systematic, architecture-centric, decision making method for mining existing components for a product line or new software architecture. OAR’s five activities identify potential components, estimate the mining cost, and evaluate the effort required to reuse legacy components. OAR reveals implicit stakeholder assumptions, constraints, and other major drivers that affect component mining, thereby giving managers insight into this complex task. DTIC

*Software Engineering; Systems Engineering*

**20010119933** Carnegie-Mellon Univ., Software Engineering Inst., Pittsburgh, PA USA

**Using Quality Attribute Workshops to Evaluate Architectural Design Approaches in a Major System Acquisition: A Case Study** ***Final Report***

Bergey, John; Barbacci, Mario; Wood, William; Jul. 2000; 35p; In English

Contract(s)/Grant(s): F19628-00-C-0003

Report No.(s): AD-A395200; CMU/SEI-2000-TN-010; No Copyright; Avail: CASI; A03, Hardcopy; A01, Microfiche

To a large extent, a system's software architecture determines the quality attributes of both the software and the entire system. It is also one of the earliest artifacts available for evaluation. For a Department of Defense (DoD) or government acquisition organization, the ability to evaluate software architectures early in the acquisition cycle can positively affect the delivered system. to assist a government organization in evaluating architectures, a series of Quality Attribute Workshops (QAWs) were planned and an initial set conducted as part of a competitive acquisition of a complex, integrated command and control system. The QAW is a "lightweight" (i.e., non-intrusive) version of the Architecture Tradeoff Analysis Method(SM) (ATAM(SM)) developed by the Software Engineering Institute (SEI). The QAWs provided the acquiring government agency with a means to evaluate each contractor's software architectural approach and determine whether it satisfied the system's quality attribute requirements (e.g., performance, interoperability, security). Since the acquisition is ongoing, follow-on workshops are currently being scheduled to evaluate the architectural designs as they evolve. This technical note provides an overview of the QAW process and the results of the first set of workshops, including the perceived benefits of the workshops to both the acquirer and the contractors. It also discusses future opportunities for applying a full-scale architecture evaluation (e.g., an ATAM evaluation) in early stages of system acquisition, and identifies the benefits that could be obtained.

DTIC

*Command and Control; Complex Systems; Defense Program*

**20010119934** Carnegie-Mellon Univ., Software Engineering Inst., Pittsburgh, PA USA

**Beyond the Black Box: A Case Study in C to Java Conversion and Product Extensibility**

Huy, Pisey; Lewis, Grace A.; Liu, Ming-hsun; Aug. 2001; 51p; In English

Contract(s)/Grant(s): F19628-00-C-0003

Report No.(s): AD-A395199; CMU/SEI-2001-TN-017; No Copyright; Avail: CASI; A04, Hardcopy; A01, Microfiche

This case study describes the experience of converting and enhancing NDBS 1.0 (Netscape Database Keystore), a programmatic library to extract private keys and digital certificates from a Netscape database written in C and Java. The result of this work is NDBS 2.0, a 100% Java version of NDBS 1.0 designed to support other keystores easily. NDBS 2.0 also includes write and delete capabilities, features that were not present in NDBS 1.0. The case study describes the experience of the conversion and development process, difficulties, and lessons learned.

DTIC

*Data Bases; Computer Programming; Information Retrieval*

**20010119935** Carnegie-Mellon Univ., Software Engineering Inst., Pittsburgh, PA USA

**Architecture Reconstruction Guidelines**

Kazman, Rick; O'Brien, Liam; Verhoef, Chris; Aug. 2001; 41p; In English

Contract(s)/Grant(s): F19628-00-C-0003

Report No.(s): AD-A395198; CMU/SEI-2001-TR-026; ESC-TR-2001-026; No Copyright; Avail: CASI; A03, Hardcopy; A01, Microfiche

Architecture reconstruction is the process where the "as-built" architecture of an implemented system is obtained from the existing legacy system. This is done through a detailed analysis of the system using tool support. The tools extract information about the system and aid in building and aggregating successive levels of abstraction. If the reconstruction is successful, the end result is an architectural representation of the system that aids in reasoning about the system. In some cases, it may not be possible to generate a useful representation due to the system. Architecture reconstruction generates an architectural representation that can be used in several ways. One of the main uses is for documenting the existing architecture. If no documentation exists or it is out of date, the recovered architectural representation can be used as a basis for redocumenting the architecture. The recovered "as-built" architecture of the system can be used to check conformance against an "as-designed" architecture. The architectural representation can also be used as a starting point for reengineering the system to a new desired architecture. Finally, the representation can be used to help identify components for reuse, or to help establish a software product line. In this report, we describe the process of architecture reconstruction using the Dali architecture reconstruction workbench. We outline guidelines

for reconstructing the architectural representations of existing systems. The process that is undertaken to reconstruct an architecture can be supported by other tools and in fact can be done manually.
DTIC
*Architecture (Computers); Systems Analysis*

**20010120021** Argonne National Lab., IL USA
**Collaborative virtual reality environments for computational science and design**
Papka, M. E.; Feb. 17, 1998; 14p; In English
Report No.(s): DE2001-10657; ANL/MCS-P707-0298; No Copyright; Avail: Department of Energy Information Bridge

The authors are developing a networked, multi-user, virtual-reality-based collaborative environment coupled to one or more petaFLOPs computers, enabling the interactive simulation of 10(sup 9) atom systems. The purpose of this work is to explore the requirements for this coupling. Through the design, development, and testing of such systems, they hope to gain knowledge that allows computational scientists to discover and analyze their results more quickly and in a more intuitive manner.
NTIS
*Computer Systems Simulation; Virtual Reality; Systems Engineering; Computer Networks*

**20010120044** Research Inst. for Advanced Computer Science, Automated Software Engineering Group, Moffett Field, CA USA
**Circular Coinduction**
Rosu, Grigore, Research Inst. for Advanced Computer Science, USA; Goguen, Joseph, California Univ., San Diego, USA; [2001]; 16p; In English; No Copyright; Avail: CASI; A03, Hardcopy; A01, Microfiche

Circular coinduction is a technique for behavioral reasoning that extends cobasis coinduction to specifications with circularities. Because behavioral satisfaction is not recursively enumerable, no algorithm can work for every behavioral statement. However. algorithms using circular coinduction can prove every practical behavioral result that we know. This paper proves the correctness of circular coinduction and some consequences.
Author
*Algorithms; Programming Languages; Computer Techniques*

**20010120055** Computer Sciences Corp., Moffett Field, CA USA
**A Portable Debugger for Parallel and Distributed Programs**
Cheng, Doreen Y., Computer Sciences Corp., USA; Hood, Robert, Computer Sciences Corp., USA; [1994]; 1p; In English; Supercomputing 1994, 14-18 Nov. 1994, Washington, DC, USA
Contract(s)/Grant(s): NAS2-12961; RTOP 536-01-11; No Copyright; Avail: Issuing Activity; Abstract Only

In this paper, we describe the design and implementation of a portable debugger for parallel and distributed programs. The design incorporates a client-server model in order to isolate non-portable debugger code from the user interface. The precise definition of a protocol for client-server interaction permits a high degree of portability of the client user interface. Replication of server components permits the implementation of a debugger for distributed computations. Portability across message passing implementations is achieved with a protocol that dictates the interaction between a message passing library and the debugger. This permits the same debugger to be used both on PVM and MTI programs. The process abstractions used for debugging message-passing programs can be easily adapted to debug HPF programs at the source level. This allows the debugger to present information hidden in tool-generated code in a meaningful manner.
Author
*Program Verification (Computers); Parallel Processing (Computers); Distributed Processing*

**20010120056** Computer Sciences Corp., Moffett Field, CA USA
**Programming Tools: Status, Evaluation, and Comparison**
Cheng, Doreen Y., Computer Sciences Corp., USA; [1994]; 1p; In English; Supercomputing 1994, 14-18 Nov. 1994, Washington, DC, HI, USA, USA
Contract(s)/Grant(s): NAS2-12961; RTOP 536-01-11; No Copyright; Avail: Issuing Activity; Abstract Only

In this tutorial I will first describe the characteristics of scientific applications and their developers, and describe the computing environment in a typical high-performance computing center. I will define the user requirements for tools that support application portability and present the difficulties to satisfy them. These form the basis of the evaluation and comparison of the tools. I will then describe the tools available in the market and the tools available in the public domain. Specifically, I will describe the tools for converting sequential programs, tools for developing portable new programs, tools for debugging and performance tuning, tools for partitioning and mapping, and tools for managing network of resources. I will introduce the main goals and

approaches of the tools, and show main features of a few tools in each category. Meanwhile, I will compare tool USAbility for real-world application development and compare their different technological approaches. Finally, I will indicate the future directions of the tools in each category.
Author
*Supercomputers; Computer Programming; Software Development Tools*

**20010120082** Sandia National Labs., Albuquerque, NM USA
**Investigation of Two-Dimensional CAD Generated Models with Body Decoupled Cartesian Grids for DSMC**
Otahal, T. J.; Gallis, M. A.; Bartel, T. J.; Jun. 27, 2000; 11p; In English
Report No.(s): DE2000-760790; SAND2000-1562C; No Copyright; Avail: Department of Energy Information Bridge

This paper presents an investigation of a technique for using two-dimensional bodies composed of simple polygons with a body decoupled uniform Cartesian grid in the Direct Simulation Monte Carlo method (DSMC). The method employs an automated grid pre-processing scheme beginning form a CAD geometry definition file, and is based on polygon triangulation using a trapezoid algorithm. A particle-body intersection time comparison is presented between the Icarus DSMC code using a body-fitted structured grid and using a structured body-decoupled Cartesian grid with both linear and logarithmic search techniques. A comparison of neutral flow over a cylinder is presented using the structured body fitted grid and the Cartesian body de-coupled grid.
NTIS
*Computerized Simulation; Monte Carlo Method; Two Dimensional Models; Computer Aided Design*

**20010120127** University of West Florida, Pensacola, FL USA
**Dynamic Analysis of Test and Evaluation Software** ***Final Report, Dec. 1998-Jul. 2001***
Wilde, Norman; Aug. 13, 2001; 69p; In English
Contract(s)/Grant(s): F49620-99-1-0057; Proj-2304
Report No.(s): AD-A394982; AFRL-SR-BL-TR-01-0463; No Copyright; Avail: CASI; A04, Hardcopy; A01, Microfiche

Large legacy software systems are extremely difficult to keep up to date because they are so difficult to understand. Software Reconnaissance is a technique to aid in the understanding of such software by locating where each user 'feature' is implemented. This project explored the application of Software Reconnaissance to the legacy FORTRAN 77 code that forms a large part of the Air Force Test and Evaluation software inventory. Two software tools, a FORTRAN 77 instrumentor and the TraceGraph visualization tool, were developed and are now publicly available on the internet. A case study was performed showing how the Reconnaissance could be used to aid in understanding and maintaining the CONVERT3 program which is typical of legacy FORTRAN code. A systematic methodology for reengineering such code into object-oriented C++ was then developed. The methodology prepares a domain class model and elaborates it by assigning features of the old program to the new object classes. Test cases are used both for Software Reconnaissance feature location and to validate the correctness of the new C++ version. A case study was performed showing how the methodology could be applied to CONVERT3, and providing several insights into this kind of reengineering task.
DTIC
*Computer Programs; Dynamic Characteristics; Applications Programs (Computers); Evaluation; Performance Tests*

**20010120131** Carnegie-Mellon Univ., Software Engineering Inst., Pittsburgh, PA USA
**Quality Attribute Workshops**
Barbacci, Mario R.; Ellison, Robert; Stafford, Judith A.; Weinstock, Charles B.; Wood, William G.; May 2001; 33p; In English
Contract(s)/Grant(s): F19628-00-C-0003
Report No.(s): AD-A395197; CMU/SEI-2001-TR-010; ESC-TR-2001-010; No Copyright; Avail: CASI; A03, Hardcopy; A01, Microfiche

Quality attribute workshops (QAW) provide a method for evaluating the architecture of a software-intensive system during the acquisition phase of major programs. The architecture is evaluated against a number of critical quality attributes, such as availability, performance, security, interoperability, and modifiability. The evaluation is based on test cases that capture questions and concerns elicited from various stakeholders associated with the system. The process of eliciting questions allows stakeholders to communicate directly, thereby exposing assumptions that may not have surfaced during requirements capture. Our experience to date includes twelve quality attribute workshops that were held with three different U.S. Government acquisition programs.

In this report, we provide a rationale for developing the process and describe it in detail. We follow this with a list of lessons learned and discuss how these lessons have helped us evolve the process to its current state.
DTIC
*Quality Control; Architecture (Computers)*

**20010120136** Air Command and Staff Coll., Maxwell AFB, AL USA
**The Military Decision-Making Process: A Software Tutorial**
Akins, Elton; Dodge, Hank; Duffy, Colleen; Gollsneider, Brian; Imlay, James; Apr. 1999; 25p; In English
Report No.(s): AD-A395175; AU/ACSC/002/1999-04; No Copyright; Avail: CASI; A03, Hardcopy; A01, Microfiche

This HTML-based tutorial provides a comprehensive and in-depth program of instruction on key Army concepts for the student. It may be used and easily understood by both the novice and the experienced, singly or in-groups. It is designed to operate over a number of popular browsers, with a final goal of running in a stand-alone configuration from a CD-ROM. It also hosts online features, such as hot links to informational web sites, if Internet connectivity is available. The software architecture allows easy modification of current scenarios and introduction of additional scenarios without major code rewriting. This course of instruction was produced over two generations of Air Command and Staff College student officers, with its target audience of both Army and other services' officers. A major emphasis of this project was to add a second scenario to the previous product. Its focus on a multi-MTW (Major Theater War) has direct applicability to the AWC/ACSC wargame, Tandem Challenge. The lesson hosts four main areas: Military Decision-Making Process; Exercises; Reference; and Help. This tutorial draws its references from the most current editions of Field Manual 100-5 Operations (June 1993), and Field Manual 101-5 Staff Organization and Operations (May 1997). This tutorial has been organized in a user-friendly manner to promote learning. A document outlining the software architecture and programming code is provided for future maintenance activities. The universality of this tutorial is assured, as all information herein is of a non-classified origin and approved for public distribution.
DTIC
*Decision Making; Document Markup Languages; Computer Programs; Education*

**20010120138** Carnegie-Mellon Univ., Software Engineering Inst., Pittsburgh, PA USA
**SEI Workshop on Software Architecture Representation, 16-17 January 2001** ***Final Report***
Bachmann, Felix; Clements, Paul; Garlan, David; Ivers, James; Little, Reed; May 2001; 64p; In English
Contract(s)/Grant(s): F19628-00-C-0003
Report No.(s): AD-A395172; CMU/SEI-2001-SR-010; No Copyright; Avail: CASI; A04, Hardcopy; A01, Microfiche

To further its work in architecture related ideas, the SEI held its first Architecture Representation Workshop, January 16-17, 2001. Five leading software architects and practitioners were invited to discuss aspects of architecture representation with senior members of the SEI technical staff. The workshop articulated best practices, identified gaps in the available technology, and set the direction for future efforts.
DTIC
*Software Engineering; Architecture (Computers); Computer Systems Programs*

**20010120139** Carnegie-Mellon Univ., Software Engineering Inst., Pittsburgh, PA USA
**Architecture Reconstruction to Support a Product Line Effort: Case Study** ***Final Report***
O'Brien, Liam; Jul. 2001; 27p; In English
Contract(s)/Grant(s): F19628-OO-C-0003
Report No.(s): AD-A395167; CMU/SEI-2001-TN-015; No Copyright; Avail: CASI; A03, Hardcopy; A01, Microfiche

Recently, technical staff members of the SEI performed architecture reconstructions on three small automotive motor systems. One system has an interface to an external bus within the automobile (the Controller Area Network CAN bus). The other systems do not have this interface. This technical note describes the architecture reconstruction process that was followed. It provides an overview of the Dali workbench used to support this process, presents the various activities in each phase of the process, and outlines the results that were produced.
DTIC
*Automobiles; Architecture (Computers); Products; Controllers*

**20010120140** Carnegie-Mellon Univ., Software Engineering Inst., Pittsburgh, PA USA
**Case Study: Building and Communicating a Business Case for a DoD Product Line** ***Final Report***
Cohen, Sholom; Apr. 2001; 31p; In English
Contract(s)/Grant(s): F19628-00-C-0003
Report No.(s): AD-A395155; CMU/SEI-2001-TN-020; No Copyright; Avail: CASI; A03, Hardcopy; A01, Microfiche

This case study describes a US Department of Defense (DoD) weapon system development effort and compares the current way of developing software systems to the product line approach. The report describes a product line business case acquisition context, alternative development paths, and a comparison of their merits. While the report ”sanitizes” the actual organization and product line, it typifies the process of building a product line business case.
DTIC
*Defense Program; Software Engineering; Commerce; Weapon Systems*

**20010120156** Computer Sciences Corp., Moffett Field, CA USA
**Portability Support for High Performance Computing**
Cheng, Doreen Y., Computer Sciences Corp., USA; [1994]; 1p; In English; Supercomputing 1994, 14-18 Nov. 1994, Washington, DC, USA
Contract(s)/Grant(s): NAS2-12961; RTOP 536-01-11; No Copyright; Avail: Issuing Activity; Abstract Only

While a large number of tools have been developed to support application portability, high performance application developers often prefer to use vendor-provided, non-portable programming interfaces. This phenomena indicates the mismatch between user priorities and tool capabilities. This paper summarizes the results of a user survey and a developer survey. The user survey has revealed the user priorities and resulted in three criteria for evaluating tool support for portability. The developer survey has resulted in the evaluation of portability support and indicated the possibilities and difficulties of improvements.
Author
*Parallel Processing (Computers); Protocol (Computers); Supercomputers; Applications Programs (Computers)*

**20010120261** Oak Ridge Y-12 Plant, TN USA
**Application of High Performance Computing for Automotive Design and Manufacturing**
Zacharia, T.; Apr. 01, 1999; 6p; In English
Report No.(s): DE2001-10665; Y/AMT-623; No Copyright; Avail: Department of Energy Information Bridge

This project developed new computer simulation tools which can be used in DOE internal combustion engine and weapons simulation programs currently being developed. Entirely new massively parallel computer modeling codes for chemically reactive and incompressible fluid mechanics with interactive physics sub-models were developed. Chemically reactive and aerodynamic flows are central parts in many DOE systems. Advanced computer modeling codes with new chemistry and physics capabilities can be used on massively parallel computers to handle more complex problems associated with chemically reactive propulsion systems, energy efficiency, enhanced performance and durability, multi-fuel capability and reduced pollutant emissions. The work for this project is also relevant to the design, development and application of advanced user-friendly computer codes for new high-performance computing platforms for manufacturing and which will also impact and interact with the U.S.’s advanced communications program. Finite element method (FEM) formulations were developed that are directly USAble in simulating rapid deformation resulting from collision, impact, projectiles, etc. This simulation capability is applicable to both DOE (e.g., surety and penetration) and DoD (e.g., armor) applications. The models of plate and shell composite structures were developed for simulation of glass continuous strand mat and braided composite in thermoset polymer matrix. The developed numerical tools based upon the fundamental mechanisms responsible for damage evolution in continuous-fiber organic-matrix composites. This class of materials is especially relevant because of their high strength to mass ratio, anisotropic behavior, and general application in most transportation and weapon delivery systems. The high-performance computational tools developed are generally applicable to a broad spectrum of materials with similar fiber structures.
NTIS
*Automobiles; Computerized Simulation; Manufacturing; Internal Combustion Engines; Applications Programs (Computers)*

**20010120466** NASA Ames Research Center, Moffett Field, CA USA
**Numerical Simulations of Self-Focused Pulses Using the Nonlinear Maxwell Equations**
Goorjian, Peter M., NASA Ames Research Center, USA; Silberberg, Yaron, Bellcore, USA; [1994]; 1p; In English; Nonlinear Optics: Materials, Fundamentals, and Applications, 24-29 Jul. 1994, Waikaloa, HI, USA; Sponsored by Institute of Electrical and Electronics Engineers, USA
Contract(s)/Grant(s): RTOP 505-59-53; No Copyright; Avail: Issuing Activity; Abstract Only

This paper will present results in computational nonlinear optics. An algorithm will be described that solves the full vector nonlinear Maxwell's equations exactly without the approximations that are currently made. Present methods solve a reduced scalar wave equation, namely the nonlinear Schrodinger equation, and neglect the optical carrier. Also, results will be shown of calculations of 2-D electromagnetic nonlinear waves computed by directly integrating in time the nonlinear vector Maxwell's equations. The results will include simulations of 'light bullet' like pulses. Here diffraction and dispersion will be counteracted by nonlinear effects. The time integration efficiently implements linear and nonlinear convolutions for the electric polarization, and can take into account such quantum effects as Kerr and Raman interactions. The present approach is robust and should permit modeling 2-D and 3-D optical soliton propagation, scattering, and switching directly from the full-vector Maxwell's equations. Abstract of a proposed paper for presentation at the meeting NONLINEAR OPTICS: Materials, Fundamentals, and Applications, Hyatt Regency Waikaloa, Waikaloa, Hawaii, July 24-29, 1994, Cosponsored by IEEE/Lasers and Electro-Optics Society and Optical Society of America

Author

*Diffraction; Electro-Optics; Nonlinear Optics; Optical Properties; Physical Optics; Wave Equations*

**20010120786** Computer Sciences Corp., Moffett Field, CA USA

**Virtual Environments in Scientific Visualization**

Bryson, Steve, Computer Sciences Corp., USA; [1994]; 1p; In English; ICAT 1992, Jul. 1992, Tokyo, Winchester, Japan, UK, Singapore

Contract(s)/Grant(s): RTOP 536-01-11; No Copyright; Avail: Issuing Activity; Abstract Only

Virtual environment technology is a new way of approaching the interface between computers and humans. Emphasizing display and user control that conforms to the user's natural ways of perceiving and thinking about space, virtual environment technologies enhance the ability to perceive and interact with computer generated graphic information. This enhancement potentially has a major effect on the field of scientific visualization. Current examples of this technology include the Virtual Windtunnel being developed at NASA Ames Research Center. Other major institutions such as the National Center for Supercomputing Applications and SRI International are also exploring this technology. This talk will be describe several implementations of virtual environments for use in scientific visualization. Examples include the visualization of unsteady fluid flows (the virtual windtunnel), the visualization of geodesics in curved spacetime, surface manipulation, and examples developed at various laboratories.

Author

*Scientific Visualization; Graphs (Charts); Human-Computer Interface; Computer Aided Design*

**20010120843** Carnegie-Mellon Univ., Software Engineering Inst., Pittsburgh, PA USA

**The Team Software ProcessSM (TSPSM): An Overview and Preliminary Results of Using Disciplined Practices *Final Report***

McAndrews, Donald R.; Nov. 2000; 53p; In English

Contract(s)/Grant(s): F19628-00-C-0003

Report No.(s): AD-A395283; CMU/SEI-2000-TN-015; ESC*-TR-2000-015; No Copyright; Avail: CASI; A04, Hardcopy; A01, Microfiche

The Software Engineering Institute has developed the Team Software Process(SM) (TSP(SM)) to help engineering teams more effectively build software-intensive products. The TSP addresses many of the current problems of building software-intensive products and shows teams and managers explicitly how to address these problems. This report describes the TSP technology as an implementation strategy for teams that are attempting to apply disciplined software process methods. It provides some of the background and rationale for the TSP approach, as well as an overview of the technology. Then, the report presents initial results of the use of the TSP technology in four different organizational settings. In each of these organizations, the data show that defect densities found in system-level test activities and the actual duration of these system-level tests were reduced significantly with the use of the TSP. In addition, the accuracy of software estimates improved, and the variation in estimation accuracy was significantly reduced. Based on the analysis of these results, some assertions are made to help organizations set goals for improvement.

DTIC

*Software Engineering; Computer Programs; Procedures*

**20010120844** Carnegie-Mellon Univ., Software Engineering Inst., Pittsburgh, PA USA

**Volume 1: Market Assessment of Component-Based Software Engineering *Final Report***

Bass, Len; Buhman, Charles; Comella-Dorda, Santiago; Long, Fred; Robert, John; May 2000; 43p; In English

Contract(s)/Grant(s): F19628-00-C-0003
Report No.(s): AD-A395250; CMU/SEI-2001-TN-007; No Copyright; Avail: CASI; A03, Hardcopy; A01, Microfiche

To assess the market for component-based software engineering, the Software Engineering Institute (SEI) studied industry trends in the use of software components. The study, conducted from September 1999 to February 2000, examined software components from both technical and business perspectives. The results of this study are summarized in the following technical notes and reports: Volume I: Market Assessment of Component-Based Software Engineering Volume II: Technical Concepts of Component-Based Software Engineering Volume III: SEI Role in Component-Based Software Engineering This technical note, Volume I, examines software component technology from a business perspective. It synthesizes the views of economists, industry analysts, information technology (IT) managers, and engineers. It presents evidence that software component technology is indeed being adopted by commercial industry. It also explains what lies behind the adoption of software component technology, and what industry expects from software component technology.

DTIC

*Software Engineering; Computer Programming*

**20010120847** Georgia Univ., Athens, GA USA

**Remote Distributed Simulation Kits for Team Decision Making** ***Final Report, 1 Feb. 1998 - 30 Nov. 2000***

Mahan, Robert P.; Jul. 13, 2001; 56p; In English
Contract(s)/Grant(s): F49620-98-1-0200; AF Proj. 2313
Report No.(s): AD-A395170; AFRL-SR-BL-TR-01-0510; No Copyright; Avail: CASI; A04, Hardcopy; A01, Microfiche

The first of its kind prototype Internet-based distributed team simulation software offering full portability and based exclusively on the Java programming language has been completed. SynTEAM (Synthetic Team Evaluation and Modeling), an inexpensive research/training simulator, will allow commanders to remotely configure scenario 'kits' from a library of kit exercises in an effort to study a variety of team-based command and control decision behaviors. While the current simulator is programmed as an AWACS weapon director's platform, it has been designed to provide rapid prototyping for other military applications. The simulator development program includes: audio/video streaming, intelligent agent applications, graphical measures of quantitative information, and telephony and other messaging vehicles to keep commanders abreast of real-time and off-line scenario events. We are currently developing extensions to the SynTEAM Internet Simulator for the 'SynTEAM Federated Internet 2 Architecture Project (SFIA)'. The goal of SFIA development will be creating network technology that will make it possible to: (1) unite AFOSR simulation programs by creating a common set of protocol standards and tools that will allow integration of multiple simulators in support of Joint Battle space training directives, and (2) configure these standards to be directly compatible with the broad-band connectivity provided by ATM Internet 2 technology.

DTIC

*Decision Making; Training Devices; Command and Control; Computerized Simulation*

**20010121509** Sandia National Labs., Albuquerque, NM USA

**Parallel Prediction-Augmented Classical Least Squares/Partial Least Squares Hybrid Algorithm: CPLS 1.0 Code**

Drewien, C. A.; Jun. 01, 2000; 42p; In English
Report No.(s): DE2000-759455; SAND2000-1529; No Copyright; Avail: Department of Energy Information Bridge, Microfiche

A parallel code or CPLS 1.0, based upon the recently invented prediction-augmented Classical Least Squares/Partial Least Squares (PA-CLS/PLS) hybrid algorithm, was developed in order to perform quantitative analyses of spectral data. A parallel routine was desired for fast calculation of full calibration models, cross-validation verification, and true prediction results from large data collections, which are expected to result from two-dimensional infrared (IR) imaging spectroscopy. This report contains a summary of the parallel PA-CLS/PLS hybrid algorithm, the mathematical formulation, and software libraries used in the implementation of the parallel algorithm. An explanation of how to use the three routines in the CPLS 1.0 code - full calibration, cross-validation, and true prediction - is provided along with variable definitions, input file requirements, and output file data formats. In order to demonstrate parallel speed-up, the added advantage of multiple processors, and communication versus computation times, timing results for each of the three routines are reported for a representative (but small) sample set.

NTIS

*Algorithms; Least Squares Method; Quantitative Analysis; Mathematical Models; Parallel Processing (Computers)*

**20010121511** Sandia National Labs., Albuquerque, NM USA

**System Analysis Tool**

Campbell, P. L.; Espinoza, J.; Jun. 01, 2000; 18p; In English
Report No.(s): DE2000-759453; SAND2000-1465; No Copyright; Avail: Department of Energy Information Bridge, Microfiche

In this paper we describe a tool for analyzing systems. The analysis is based on program slicing. It answers the following question for the software: if the value of a particular variable changes, what other variable values also change, and what is the path in between. program slicing was developed based on intra-procedure control and data flow. It has been expanded commercially to inter-procedure flow. However, we extend slicing to collections of programs and non-program entities, which we term multi-domain systems. The value of our tool is that an analyst can model the entirety of a system, not just the software, and we believe that this makes for a significant increase in power. We are building a prototype system.
NTIS
*Systems Analysis; Artificial Intelligence; Software Engineering*

**20010121538** Computer Sciences Corp., USA
**Parallel Sparse Cholesky Factorization with Spectral Nested Dissection Ordering, Chapter 1**
Pothen, Alex, Old Dominion Univ., USA; Rothberg, Edward, INTEL Corp., USA; Simon, Horst, Computer Sciences Corp., USA; Wang, Lie, Pennsylvania State Univ., USA; [1994]; 1p; In English; 5th SIAM Conference on Applied Linear Algebra, 15-18 Jun. 1994, Snowbird, UT, USA; Sponsored by Society for Industrial and Applied Mathematics, USA
Contract(s)/Grant(s): NAS2-12961; DE-FG02-91ER-25095; NSERC-OGP-0008111; NSF CCR-90-24954; RTOP 536-01-11; No Copyright; Avail: Issuing Activity; Abstract Only

We show that the use of a new ordering computed from the spectral nested dissection (SND) algorithm leads to efficient parallel sparse Cholesky factorization on an Intel Paragon multiprocessor.
Author
*Multiprocessing (Computers); Massively Parallel Processors; Cholesky Factorization*

**20010121545** North Carolina State Univ., Dept. of Electrical and Computer Engineering, Raleigh, NC USA
**Floating-Point Modules Targeted for Use with RC Compilation Tools**
Sahin, Ibrahin, North Carolina State Univ., USA; Gloster, Clay S., Howard Univ., USA; [2000]; 6p; In English; Sponsored by Association for Computing Machinery, USA; Diskette: 1 3.5-inch DSHD diskette
Contract(s)/Grant(s): NAG5-7942
Report No.(s): ACM-1-58113-000-0; NONP-NASA-DK-2001164501; ISBN 1-58113-000-0; Copyright; Avail: Issuing Activity

Reconfigurable Computing (RC) has emerged as a viable computing solution for computationally intensive applications. Several applications have been mapped to RC system and in most cases, they provided the smallest published execution time. Although RC systems offer significant performance advantages over general-purpose processors, they require more application development time than general-purpose processors. This increased development time of RC systems provides the motivation to develop an optimized module library with an assembly language instruction format interface for use with future RC system that will reduce development time significantly. In this paper, we present area/performance metrics for several different types of floating point (FP) modules that can be utilized to develop complex FP applications. These modules are highly pipelined and optimized for both speed and area. Using these modules, and example application, FP matrix multiplication, is also presented. Our results and experiences show, that with these modules, 8-10X speedup over general-purpose processors can be achieved.
Author
*Floating Point Arithmetic; Reconfigurable Hardware; Assembly Language; Computer Programs*

**20010121548** Computer Sciences Corp., Moffett Field, CA USA
**High Performance Programming Using Explicit Shared Memory Model on the Cray T3D**
Saini, Subhash, Computer Sciences Corp., USA; Simon, Horst D., Computer Sciences Corp., USA; [1994]; 1p; In English; Supercomputing 1994, Nov. 1994, Washington, DC, USA
Contract(s)/Grant(s): RTOP 536-01-11
Report No.(s): RNR-94-012; No Copyright; Avail: Issuing Activity; Abstract Only

The Cray T3D is the first-phase system in Cray Research Inc.'s (CRI) three-phase massively parallel processing program. In this report we describe the architecture of the T3D, as well as the CRAFT (Cray Research Adaptive FORTRAN) programming model, and contrast it with PVM, which is also supported on the T3D We present some performance data based on the NAS Parallel Benchmarks to illustrate both architectural and software features of the T3D.
Author
*Computer Programming; Massively Parallel Processors*

**20010121559** NASA Ames Research Center, Moffett Field, CA USA

**Cpt 2.0: A 2-D Fluid Visualization Program for Unsteady Data**

Levit, Creon, NASA Ames Research Center, USA; Shermer, Russ, Naval Surface Weapons Center, USA; Krystynak, John, NASA Ames Research Center, USA; [1994]; 1p; In English

Contract(s)/Grant(s): RTOP 536-01-11; No Copyright; Avail: Issuing Activity; Abstract Only

Cpt is an interactive two dimensional fluid visualization program for unsteady data sets. Cpt is capable of showing the velocity and scalar fields, calculating streaml@nes and contours, advecting particles, bubblers and more. The user interface is simple point and click and most of its operations are deducible from a few minutes of experimentation.

Author

*Two Dimensional Flow; Velocity Distribution; Computer Programs; Flow Visualization*

**20010122269** NASA Ames Research Center, Moffett Field, CA USA

**The Visibility of DCT Quantization Noise: Spatial Frequency Summation**

Peterson, H. A., International Business Machines Corp., USA; Ahumada, A. J., Jr., NASA Ames Research Center, USA; Watson, A. B., NASA Ames Research Center, USA; [1994]; 1p; In English; Society for Information Display (SID '94} Symposium, 12-17 Jun. 1994, San Jose, CA, USA

Contract(s)/Grant(s): RTOP 199-06-31; RTOP 505-64-53; No Copyright; Avail: Issuing Activity; Abstract Only

Computational models of the ability to detect image compression artifacts facilitate the optimization of compression parameters, such as the JPEG quantization matrix. For simplicity, some models assume that the visibility of artifacts containing different spatial frequency components is determined by the most visible component, that is, no summation over components. Using the type of noise generated by quantization in the Discrete Cosine Transform (DCT) domain, we find a degree of summation between that of probability summation and contrast energy summation.

Author

*Discrete Cosine Transform; Noise Measurement*

**20010122387** Carnegie-Mellon Univ., Software Engineering Inst., Pittsburgh, PA USA

**DoD Software Migration Planning** ***Final Report***

Bergey, John; O'Brien, Liam; Smith, Dennis; Aug. 2001; 23p; In English

Contract(s)/Grant(s): F19628-00-C-0003

Report No.(s): AD-A395251; CMU/SEI-2001-TN-012; No Copyright; Avail: CASI; A03, Hardcopy; A01, Microfiche

The DoD often faces the challenge of migrating from legacy systems to new target systems. Such migration efforts represent a complex engineering problem. These efforts call for a migration plan to supplement the development plan. The migration plan addresses issues associated with phasing out legacy systems and moving to the new system. These issues include user interface compatibility, database compatibility, transition support, system interface compatibility, and training. by producing and implementing a migration plan, a development organization can help a user community make the transition in an orderly fashion. This note describes migration planning, identifies influencing factors, outlines a set of migration planning activities, and offers a set of guidelines for the migration planning process.

DTIC

*Defense Program; Software Engineering; Computer Programs*

**20010122390** Army Construction Engineering Research Lab., Champaign, IL USA

**Design Review and Checking System (DrChecks)** ***Final Report***

East, E. W.; Kirby, Jeffrey G.; Kelly, Jana; Sep. 2001; 114p; In English

Contract(s)/Grant(s): MIPR-WX3JR902219476

Report No.(s): AD-A395194; ERDC/CERL-SR-01-20; No Copyright; Avail: CASI; A06, Hardcopy; A02, Microfiche

Design Review and Checking System (DrChecks), developed by the Engineer Research and Development Center's Construction Engineering Research Laboratory (CERL), is Government-Off-the-Shelf software that supports the capture and use of organizational experience in the context of the design review process. DrChecks and its companion, Corporate Lessons Learned (CLL), are being used to turn personal experience, lessons learned, success stories, and good work practices identified by experienced staff members into corporate knowledge that can be shared throughout the organization.

DTIC

*Computer Programs; Software Engineering; Systems Engineering; Design Analysis*

**20010122395** Army Engineer Research and Development Center, Information Technology Lab., Vicksburg, MS USA
**Development of Geodetic Conversion Routines** ***Final Report***
Danuskhkodi, Vaiyapuri, Army Engineer Research and Development Center, USA; September 2001; 29p; In English
Report No.(s): AD-A394986; ERDC/ITL-TR-01-5; No Copyright; Avail: CASI; A03, Hardcopy; A01, Microfiche

The Geodetic Conversion Routines Report is the final report of the Center Project 01.008. The report facilitates data conversion between various horizontal and vertical datums in the USA. It provides examples to invoke the Dynamic Link Library and use conversion functions in various programming languages, such as Visual Basic, C, and C++.
DTIC
*Data Processing; Programming Languages; Data Conversion Routines; Geodesy*

**20010122396** CFD Research Corp., Huntsville, AL USA
**Generation of Reduced Parametric Models of Microdevices from High Fidelity Tools for System Level Composite Computer-Aided Design (CAD)** ***Final Report, Aug. 1997 - Aug. 2000***
Turowski, Marek; Pzekwas, Andrzej; Chen, Zhijan; Tan, Zhiqiang; Yu, Enchao; July 2001; 170p; In English; Original contains color images
Contract(s)/Grant(s): F30602-97-2-0332
Report No.(s): AD-A394960; AFRL-IF-RS-TR-2001-141; No Copyright; Avail: CASI; A08, Hardcopy; A02, Microfiche

Microelectromechanical Systems (MEMS), also Known as microsystems, consist of interconnected arrays of mechanical, electrostatic, thermal, structural, optical, fluidic, magnetic, and electronic components. Individual components can be simulated using multi-dimensional high fidelity computational tools based on first principles and Partial Differential Equations. For system level design, where large numbers of devices are interconnected, use of detailed 3-D models of each component is unrealistic. A more practical approach is to develop simplified but accurate sub models. A software system for the automated generation of reduced or compact models of microdevices from high fidelity 3-D simulations was developed, demonstrated, and validated. During this effort: fluidic, electromechanical, and thermal phenomena were examined; new concepts for reduced models were pursued; the burden of generating 3-D models from Electronic Design Automation (EDA) layouts and process data was eased; and procedures to exploit interface and import/export CAD/EDA standards were defined. Results of this effort were incorporated into CFD Research Corporation's commercial Computer-Aided Design (CAD) tool suite along with Carnegie Mellon University's NODAS system-level CAD tool. The results of this effort have been applied to a variety of real problems of interest to both the defense industry and commercial Market.
DTIC
*Computer Aided Design; Finite Element Method; Partial Differential Equations; Microelectromechanical Systems; Computational Fluid Dynamics*

**20010122646** Sandia National Labs., Albuquerque, NM USA
**SIENA Customer Problem Statement and Requirements**
Sauer, L.; Clay, R.; Adams, C.; Walther, H.; Allan, B.; Aug. 01, 2000; 33p; In English
Report No.(s): DE2000-763045; SAND2000-8255; No Copyright; Avail: Department of Energy Information Bridge, Microfiche

This document describes the problem domain and functional requirements of the SIENA framework. The software requirements and system architecture of SIENA are specified in separate documents (called SIENA Software Requirement Specification and SIENA Software Architecture, respectively). While currently this version of the document describes the problems and captures the requirements within the Analysis domain (concentrating on finite element models), it is our intention to subsequently expand this document to describe problems and capture requirements from the Design and Manufacturing domains. In addition, SIENA is designed to be extendible to support and integrate elements from the other domains.
NTIS
*Architecture (Computers); Functional Design Specifications; Computer Programs*

**20010122651** Sandia National Labs., Albuquerque, NM USA
**Taming the Viper: Software Upgrade for VFAUser and Viper**
Dorin, R. T.; Moser, J. C.; Aug. 08, 2000; 10p; In English
Report No.(s): DE2000-761857; SAND2000-2021C; No Copyright; Avail: Department of Energy Information Bridge, Microfiche

This report describes the procedure and properties of the software upgrade for the Vibration Performance Recorder. The upgrade will check the 20 memory cards for proper read/write operation. The upgrade was successfully installed and uploaded into the Viper and the field laptop. The memory checking routine must run overnight to complete the test, although the laptop need

only be connected to the Viper unit until the downloading routine is finished. The routine has limited ability to recognize incomplete or corrupt header and footer files. The routine requires 400 Megabytes of free hard disk space. There is one minor technical flaw detailed in the conclusion.
NTIS
*Computer Programs; Vibration; Recording Instruments*

**20010122925** Computer Sciences Corp., Moffett Field, CA USA
**Multi-dimensional Color Mapping: Display of Vector Field Data Using Color Spaces**
Uselton, Samuel P., Computer Sciences Corp., USA; [1994]; 1p; In English; SIGGRAPH '94 Technical Sketches Program, 29-30 Jul. 1994, Orlando, FL, USA
Contract(s)/Grant(s): RTOP 536-01-11; No Copyright; Avail: Issuing Activity; Abstract Only

User controlled mapping of vector fields to color spaces permits expressive and effective visualization of data that is otherwise difficult to display and analyze.
Author
*Mapping; Color; Vector Spaces*

**20010123095** Brookhaven National Lab., Upton, NY USA
**Simlink: a software substrate for physical simulations**
Brown,; Chiueh,; Sep. 11, 2000; 7p; In English
Report No.(s): DE2000-767189; BNL-67459; No Copyright; Avail: Department of Energy Information Bridge

The simlink server is an HTTP (hypertext transfer protocol)/1.1 server which doesn't serve html (hypertext markup language) documents, but instead, serves the output of a physical simulator. A host system user defines what simulator will be run by the server through a short simple configuration file, which can be specified at invocation time. Since the server uses http protocol it is capable of sending data out to http clients. A library is provided with the distribution which allows new clients to be constructed using the simlink API (applications programming interface). This paper will describe the system and its design and demonstrate how it is used with BNL's Collider Accelerator online modeling environment.
NTIS
*Computer Programs; Particle Accelerators; Protocol (Computers)*

**20010123542** Argonne National Lab., IL USA
**Evaluation of Smalltalk, C++, and ADA95 for use in a major DoD application**
Hummel, J. R.; May 05, 1998; 8p; In English
Report No.(s): DE2001-10637; ANL/DIS/CP-95613; No Copyright; Avail: Department of Energy Information Bridge, Microfiche

The choice of a programming language can have a significant impact on the development of effective software. Numerous programming languages are available in the computer science community and supporters of specific languages often defend their choices with a religious zeal. Argonne National Laboratory (ANL) was recently tasked to assist in the selection of a programming language and development environment for a major DoD software development effort. Three candidate programming languages were identified by the sponsor for evaluation: Smalltalk, C++, and Ada95. (At the time the evaluation was performed, Java was regarded as being too immature.) Smalltalk is a pure object-oriented language that was originally developed by Xerox. C++ originated at AT and T and is not a pure object-oriented language. Ada95 is an object-oriented version of Ada, a language that was developed to support the defense community. The purpose of this paper is to describe the process that was used to evaluate the three languages and to describe the results of the evaluation.
NTIS
*Programming Languages; C++ (Programming Language); Object-Oriented Programming*

**20010123729** Lawrence Livermore National Lab., Livermore, CA USA
**Overture: Object-oriented tools for overset grid applications**
Brown, D. L.; Henshaw, W. D.; Quinlan, D. J.; Apr. 28, 1999; 14p; In English
Report No.(s): DE2001-11309; UCRL-JC-134018; No Copyright; Avail: Department of Energy Information Bridge

The Overture framework is an object-oriented environment for solving partial differential equations in two and three space dimensions. It is a collection of C++ libraries that enables the use of finite difference and finite volume methods at a level that hides the details of the associated data structures. Overture can be used to solve problems in complicated, moving geometries using

the method of overlapping grids. It has support for grid generation, difference operators, boundary conditions, data-base access and graphics. Short sample code segments are presented to show the power of this approach.
NTIS
*Object-Oriented Programming; Partial Differential Equations; Data Bases*

**20010124102** Computer Sciences Corp., Moffett Field, CA USA
**Scientific Computing Paradigm**
VanZandt, John, Computer Sciences Corp., USA; January 1994; 9p; In English
Contract(s)/Grant(s): RTOP 536-01-50
Report No.(s): RND-94-002; No Copyright; Avail: CASI; A02, Hardcopy; A01, Microfiche

The USAge model of supercomputers for scientific applications, such as computational fluid dynamics (CFD), has changed over the years. Scientific visualization has moved scientists away from looking at numbers to looking at three-dimensional images, which capture the meaning of the data. This change has impacted the system models for computing. This report details the model which is used by scientists at NASA's research centers.
Author
*Computational Fluid Dynamics; Scientific Visualization; Supercomputers*

**20010124980** California Univ., Lawrence Berkeley Lab., Berkeley, CA USA
**High-speed Wide Area, Data Intensive Computing: A Ten Year Retrospective**
Johnston, W. E.; May 01, 1998; 12p; In English
Report No.(s): DE2000-765126; LBNL-41862; No Copyright; Avail: Department of Energy Information Bridge

Modern scientific computing involves organizing, moving, visualizing, and analyzing massive amounts of data from around the world, as well as employing large-scale computation. The distributed systems that solve large-scale problems will always involve aggregating and scheduling many resources. Data must be located and staged, cache and network capacity must be available at the same time as computing capacity, etc. Every aspect of such a system is dynamic: locating and scheduling resources, adapting running application systems to availability and congestion in the middleware and infrastructure, responding to human interaction, etc. The technologies, the middleware services, and the architectures that are used to build useful high-speed, wide area distributed systems, constitute the field of data intensive computing. This paper explores some of the history and future directions of that field.
NTIS
*Computer Networks; Data Transfer (Computers); Data Transmission*

**20010124982** RECOM Technologies, Inc., Moffett Field, CA USA
**Mobile Computing for Aerospace Applications**
Alena, Richard, RECOM Technologies, Inc., USA; [1994]; 1p; In English; AIAA Aerospace 10th Conference, 28-30 Mar. 1995, San Antonio, TX, USA; Sponsored by American Inst. of Aeronautics and Astronautics, USA
Contract(s)/Grant(s): RTOP 241-02-00; No Copyright; Avail: Issuing Activity; Abstract Only

The use of commercial computer technology in specific aerospace mission applications can reduce the cost and project cycle time required for the development of special-purpose computer systems. Additionally, the pace of technological innovation in the commercial market has made new computer capabilities available for demonstrations and flight tests. Three areas of research and development being explored by the Portable Computer Technology Project at NASA Ames Research Center are the application of commercial client/server network computing solutions to crew support and payload operations, the analysis of requirements for portable computing devices, and testing of wireless data communication links as extensions to the wired network. This paper will present computer architectural solutions to portable workstation design including the use of standard interfaces, advanced flat-panel displays and network configurations incorporating both wired and wireless transmission media. It will describe the design tradeoffs used in selecting high-performance processors and memories, interfaces for communication and peripheral control, and high resolution displays. The packaging issues for safe and reliable operation aboard spacecraft and aircraft are presented. The current status of wireless data links for portable computers is discussed from a system design perspective. An end-to-end data flow model for payload science operations from the experiment flight rack to the principal investigator is analyzed using capabilities provided by the new generation of computer products. A future flight experiment on-board the Russian MIR space station will be described in detail including system configuration and function, the characteristics of the spacecraft operating environment, the flight qualification measures needed for safety review, and the specifications of the computing devices to be used in the experiment. The software architecture chosen shall be presented. An analysis of the performance characteristics of wireless

data links in the spacecraft environment will be discussed. Network performance and operation will be modeled and preliminary test results presented. A crew support application will be demonstrated in conjunction with the network metrics experiment.
Author
*Aerospace Engineering; Numerical Analysis; Systems Engineering; Computer Techniques; Wireless Communication*

**20010125149** MCAT Inst., Moffett Field, CA USA
**Recent Developments in Grid Generation and Force Integration Technology for Overset Grids**
Chan, William M., MCAT Inst., USA; [1994]; 1p; In English; 2nd Overset Composite Grid and Solution Technology Symposium, 25-28 Oct. 1994, Fort Walton Beach, FL, USA
Contract(s)/Grant(s): RTOP 505-59-00; No Copyright; Avail: Issuing Activity; Abstract Only

Recent developments in algorithms and software tools for generating overset grids for complex configurations are described. These include the overset surface grid generation code SURGRD and version 2.0 of the hyperbolic volume grid generation code HYPGEN. The SURGRD code is in beta test mode where the new features include the capability to march over a collection of panel networks, a variety of ways to control the side boundaries and the marching step sizes and distance, a more robust projection scheme and an interpolation option. New features in version 2.0 of HYPGEN include a wider range of boundary condition types. The code also allows the user to specify different marching step sizes and distance for each point on the surface grid. A scheme that takes into account of the overlapped zones on the body surface for the purpose of forces and moments computation is also briefly described, The process involves the following two software modules: MIXSUR - a composite grid generation module to produce a collection of quadrilaterals and triangles on which pressure and viscous stresses are to be integrated, and OVERINT - a forces and moments integration module.
Author
*Algorithms; Grid Generation (Mathematics); Applications Programs (Computers); Systems Integration*

**20010125166** California Univ., Lawrence Berkeley Lab., Berkeley, CA USA
**Comparison of Three Programming Models for Adaptive Applications on the Origin2000**
Shan, H.; Singh, J. P.; Oliker, L.; Biswas, R.; Jun. 28, 2000; 20p; In English; Super Computing 2000, 4-10 Nov. 2000, Dallas, TX, USA
Report No.(s): DE2000-767610; LBNL-46242-REV; No Copyright; Avail: Department of Energy Information Bridge, Microfiche

Adaptive applications have computational workloads and communication patterns which change unpredictably at runtime, requiring dynamic load balancing to achieve scalable performance on parallel machines. Efficient parallel implementations of such adaptive applications is therefore a challenging task. In this paper, we compare the performance of and the programming effort required for two major classes of adaptive applications under three leading parallel programming models on an SGI Origin2000 system, a machine which supports all three models efficiently. Results indicate that the three models deliver comparable performance; however, the implementations differ significantly beyond merely using explicit messages versus implicit loads/stores even though the basic parallel algorithms are similar. Compared with the message-passing (using MPI) and SHMEM programming models, the cache-coherent shared address space (CC-SAS) model provides substantial ease of programming at both the conceptual and program orchestration levels, often accompanied by performance gains. However, CC-SAS currently has portability limitations and may suffer from poor spatial locality of physically distributed shared data on large numbers of processors.
NTIS
*Dynamic Loads; Computer Programs; Parallel Programming*

**20010125454** Lawrence Livermore National Lab., Livermore, CA USA
**Sizing oracle applications projects: a technical perspective**
Rivenes, A.; Feb. 01, 1999; 17p; In English
Report No.(s): DE2001-8321; UCRL-JC-133071; No Copyright; Avail: Department of Energy Information Bridge, Microfiche

This paper will review the issues involved in sizing an Oracle Applications project. The topics include initial machine sizing, the different environments required, refresh procedures, and final system sizing. Installation and patching requirements will be addressed along with a methodology for handling long term capacity planning.
NTIS
*Computers; Computer Programs; Data Base Management Systems*

**20010125461** Sandia National Labs., Albuquerque, NM USA

**ISIS++ Reference Guide (Iterative Scalable Implicit Solver in C++) Version 1.1**

Williams, A. B.; Allan, B. A.; Mish, K. D.; Clay, R. L.; Apr. 01, 1999; 67p; In English

Report No.(s): DE2001-8238; SAND99-8231; No Copyright; Avail: Department of Energy Information Bridge, Microfiche

ISIS++ (Iterative Scalable Implicit Solver in C++) Version 1.1 is a portable, object-oriented framework for solving sparse linear systems of equations. It includes a collection of Krylov solution methods and preconditioners, as well as both uni-processor (serial) and multi-processor (scalable) matrix and vector classes. Though it was developed to solve systems of equations originating from large-scale, 3-D (three dimensional), finite element analyses, it has application in many other fields. This document supersedes the ISIS++ V1.0 Reference Guide, defines the V1.1 interface specification, and includes the necessary instructions for building and running ISIS++ V1.1 on UNIX platforms. The interface is presented in annotated header format, along with background on design and implementation considerations. A finite difference modeling example problem is included to demonstrate the overall setup and use.

NTIS

*Linear Systems; Computer Programs; Iterative Solution; User Manuals (Computer Programs); Interfaces*

**20010125462** Sandia National Labs., Albuquerque, NM USA

**Annotated Reference Guide to the Finite-Element Interface Specification Version 1.0**

Williams, A. B.; Otero, I. J.; Mish, K. D.; Tayor, L. M.; Clay, R. L.; Apr. 01, 1999; 71p; In English

Report No.(s): DE2001-8236; SAND99-8229; No Copyright; Avail: Department of Energy Information Bridge, Microfiche

The Finite-Element Interface (FEI) specification provides a layered abstraction that permits finite-element analysis codes to utilize various linear-algebra solution packages with minimal concern for the internal details of the solver modules. Alternatively, this interface can be viewed as a way for solver developers to provide solution services to finite-element clients without having to embed finite-element abstractions within their solver libraries. The purpose of this document is to provide some level of documentation between the bare interface specification itself, which consists only of C/C++ header files, and the full documentation suite that supports the interface definition by providing considerable detail as to its design and implementation. This document primarily provides the 'how' of calling the interface member functions, so that programmers can readily learn how to utilize the interface implementation without having to consider all the details contained in the interface's definition, design, and motivation. The interface specification is presented three times in this document, each time with an increasing level of detail. The first presentation provides a general overview of the calling sequence, in order to acquaint the programmer with a basic introduction to how the interface is used to 'train' the underlying solver software on the particular finite-element problem that is to be solved. The second pass through the interface definition provides considerable detail on each method, including specific considerations as to the structure of the underlying data, and an exposition of potential pitfalls that may occur as a byproduct of either the finite-element modeling process, or of the use of the associated interface implementation. Finally, a third description of the interface is given implicitly via the discussion of sample problems that provide concrete examples of the use of the finite-element interface.

NTIS

*Finite Element Method; Interfaces; Software Engineering; Computerized Simulation*

**20010125513** Sandia National Labs., Albuquerque, NM USA

**Accurate Time-Linked Data Acquisition System Field Deployment and Operational Experience**

Berg, D. E.; Zayas, J. R.; Nov. 15, 2000; 11p; In English

Report No.(s): DE2001-767882; SAND2000-2855C; No Copyright; Avail: Department of Energy Information Bridge, Microfiche

The Accurate Time-Linked Data Acquisition System (ATLAS) became fully operational on the Long-Term Inflow and Structural Test (LIST) turbine at Bushland, Texas in May of 2000. In the LIST configuration, one data acquisition unit is mounted on the rotor and two additional acquisition units are mounted near the base of the turbine. All communication between the rotor unit and the ground is via telemetry. Data acquisition on all three units is synchronized (within +/- 1 microsecond) by slaving the units to universal time with the Sandia-developed Programmable Accurate Time Synchronization Module. A total of 74 channels of instrumentation is monitored by the three acquisition units. Data acquisition occurs at a 30 Hz rate for a continuous data throughput of over 35,000 bits per second, resulting in over 2 GB of ASCII data per day. Implementation of the system is discussed and operational experience is reviewed.

NTIS

*Data Acquisition; Deployment*

**20010125517** Tech-X Corp., Boulder, CO USA
**Final Report: Java Clients for Analyses and Design of Accelerator and Other Systems, September 3, 1997-March 17, 1998**
Shasharina, S.; Sep. 29, 1998; 7p; In English
Report No.(s): DE2001-765180; No Copyright; Avail: Department of Energy Information Bridge

Completed the development of a basic client that can edit input data in a hierarchy form. The hierarchial form of the data is specified by a simple resource file that defines the container element by the line.

NTIS
*Accelerators; Java (Programming Language); Design Analysis*

**20010125610** NASA Ames Research Center, Moffett Field, CA USA
**Analysis and Optimization of Parallel Software Pipeline Performance**
VanderWijngaart, Rob F., MCAT Inst., USA; Sarukkai, Sekhar R., RECOM Technologies, Inc., USA; Mehra, Pankaj N., RECOM Technologies, Inc., USA; [1994]; 1p; In English
Contract(s)/Grant(s): RTOP 509-10-00; No Copyright; Avail: Issuing Activity; Abstract Only

Pipelining is a common strategy for extracting parallelism from a collection of independent computational tasks, each of which is spread among a number of processors and has an implied data dependence. When implemented on MIMD parallel computers with finite process interrupt times, pipeline algorithms suffer from slowdown--in addition to the expected pipeline fill time--due to a wave-like propagation of delays. This phenomenon, which has been observed experimentally using the performance monitoring system AIMS, is investigated analytically, and an optimal correction is derived to eliminate the wave. Efficiency increase through the correction is verified experimentally.

Author
*Pipelining (Computers); Parallel Programming; Optimization*

## 62
## COMPUTER SYSTEMS

*Includes computer networks and distributed processing systems. For information systems see 82 Documentation and Information Science. For computer systems applied to specific applications, see the associated category.*

**20010117732** NASA Ames Research Center, Moffett Field, CA USA
**Performance and the NAS Parallel Benchmarks**
Bailey, David H., NASA Ames Research Center, USA; [1994]; 1p; In English; Supercomputing 1994 Conference, 14-18 Nov. 1994, Washington, DC, USA
Contract(s)/Grant(s): RTOP 536-01-11; No Copyright; Avail: Issuing Activity; Abstract Only

This talk will describe the NAS (National Aerospace Standards) Parallel Benchmarks, which are now widely cited in the high performance computing field as a measure of sustained performance on realistic scientific applications. The latest performance results will be included. It will be shown that significant progress has been made by several systems during the past year or so, with sustained performance on a par with the best conventional systems, and with performance per dollar significantly exceeding the conventional systems. This talk will also describe many of the pitfalls of performance reporting, and will give advice on how to avoid such pitfalls. The overall state of the field of high performance computing will also be discussed.

Author
*Data Processing; Computers; Aerospace Systems*

**20010117866** Computer Sciences Corp., Moffett Field, CA USA
**Six Years of Parallel Computing at NAS (1987 - 1993): What Have we Learned?**
Simon, Horst D., Computer Sciences Corp., USA; Apr. 04, 1994; 1p; In English; Cray Research/CUG Board of Directors, 10-13 Apr. 1994, USA; Sponsored by Cray Research
Contract(s)/Grant(s): RTOP 536-01-11; No Copyright; Avail: Issuing Activity; Abstract Only

In the fall of 1987 the age of parallelism at NAS began with the installation of a 32K processor CM-2 from Thinking Machines. In 1987 this was described as an ”experiment” in parallel processing. In the six years since, NAS acquired a series of parallel machines, and conducted an active research and development effort focused on the use of highly parallel machines for applications in the computational aerosciences. In this time period parallel processing for scientific applications evolved from a fringe research topic into the one of main activities at NAS. In this presentation I will review the history of parallel computing at NAS in the context of the major progress, which has been made in the field in general. I will attempt to summarize the lessons we have learned

so far, and the contributions NAS has made to the state of the art. Based on these insights I will comment on the current state of parallel computing (including the HPCC effort) and try to predict some trends for the next six years.
Author
*Parallel Processing (Computers); Aerospace Sciences; Computer Networks; Supercomputers*

**20010118355** RECOM Technologies, Inc., Moffett Field, CA USA
**Methodologies and Tools for Tuning Parallel Programs: Facts and Fantasies**
Yan, Jerry C., RECOM Technologies, Inc., USA; [1994]; 1p; In English; SuperComputing 1994, 14-18 Nov. 1994, Washington, DC, USA
Contract(s)/Grant(s): RTOP 509-10-31; No Copyright; Avail: Issuing Activity; Abstract Only

The need for computing power has forced a migration from serial computation on a single processor to parallel processing on multiprocessors. However, without effective means to monitor (and analyze) program execution, tuning the performance of parallel programs becomes exponentially difficult as program complexity and machine size increase. The recent introduction of performance tuning tools from various supercomputer vendors (Intel's ParAide, TMC's PRISM, CRI's Apprentice, and Convex's CXtrace) seems to indicate the maturity of performance tool technologies and vendors'/customers' recognition of their importance. However, a few important questions remain: What kind of performance bottlenecks can these tools detect (or correct)? How time consuming is the performance tuning process? What are some important technical issues that remain to be tackled in this area? This workshop reviews the fundamental concepts involved in analyzing and improving the performance of parallel and heterogeneous message-passing programs. Several alternative strategies will be contrasted, and for each we will describe how currently available tuning tools (e.g. AIMS, ParAide, PRISM, Apprentice, CXtrace, ATExpert, Pablo, IPS-2) can be used to facilitate the process. We will characterize the effectiveness of the tools and methodologies based on actual user experiences at NASA Ames Research Center. Finally, we will discuss their limitations and outline recent approaches taken by vendors and the research community to address them.
Author
*Parallel Processing (Computers); Multiprocessing (Computers); Supercomputers; Computation*

**20010119583** California Univ., Radiation Lab., Livermore, CA USA
**Accessing the CIAC Computer Security Archive CIAC-2301 R.1**
Jan. 1995; 40p; In English; Prepared in cooperation with Booz Allen and Hamilton, McLean, VA
Report No.(s): AD-A394337; UCRL-MA-119769; No Copyright; Avail: CASI; A03, Hardcopy; A01, Microfiche

CIAC maintains an archive of Computer security information for the DOE community. You can obtain documents and software in this archive through several access severs. This guide describes how to connect to these systems and obtain files from them.
DTIC
*Computer Information Security; Computers*

**20010122223** Computer Sciences Corp., Moffett Field, CA USA
**Evaluation Metrics for the Paragon XP/S-15**
Traversat, Bernard, NASA Ames Research Center, USA; McNab, David, Computer Sciences Corp., USA; Nitzberg, Bill, Computer Sciences Corp., USA; Fineberg, Sam, Computer Sciences Corp., USA; December 1993; 19p; In English
Contract(s)/Grant(s): NAS2-12961; RTOP 536-01-50
Report No.(s): RND-93-017; No Copyright; Avail: CASI; A03, Hardcopy; A01, Microfiche

On February 17th 1993, the Numerical Aerodynamic Simulation (NAS) facility located at the NASA Ames Research Center installed a 224 node Intel Paragon XP/S-15 system. After its installation, the Paragon was found to be in a very immature state and was unable to support a NAS users' workload, composed of a wide range of development and production activities. As a first step towards addressing this problem, we implemented a set of metrics to objectively monitor the system as operating system and hardware upgrades were installed. The metrics were designed to measure four aspects of the system that we consider essential to support our workload: availability, utilization, functionality, and performance. This report presents the metrics collected from February 1993 to August 1993. Since its installation, the Paragon availability has improved from a low of 15% uptime to a high of 80%, while its utilization has remained low. Functionality and performance have improved from merely running one of the NAS Parallel Benchmarks to running all of them faster (between 1 and 2 times) than on the iPSC/860. In spite of the progress accomplished, fundamental limitations of the Paragon operating system are restricting the Paragon from supporting the NAS workload. The maximum operating system message passing (NORMA IPC) bandwidth was measured at 11 Mbytes/s, well below the peak hardware bandwidth (175 Mbytes/s), limiting overall virtual memory and UNIX services (i.e. Disk and HiPPI I/O)

performance. The high NX application message passing latency (184 microns), three times than on the iPSC/860, was found to significantly degrade performance of applications relying on small message sizes. The amount of memory available for an application was found to be approximately 10 Mbytes per node, indicating that the OS is taking more space than anticipated (6 Mbytes per node).
Author
*Evaluation; Computerized Simulation; Research Facilities; Virtual Memory Systems; Installing; Computational Fluid Dynamics*

**20010122279** Odyssey Research Associates, Inc., Ithaca, NY USA
**Extensible Requirements Management Architecture** ***Final Report, Mar. 2000-Mar. 2001***
Rosenthal, David, Odyssey Research Associates, Inc., USA; June 2001; 64p; In English
Contract(s)/Grant(s): F30602-00-C-0066; DARPA ORDER-J779; Proj-IAST
Report No.(s): AD-A394992; AFRL-IF-RS-TR-2001-129; No Copyright; Avail: CASI; A04, Hardcopy; A01, Microfiche

The goal of this effort is to facilitate the appropriate control of security configuration parameters based on goals and available systems after a cyber attack. This report addresses a method to aid in the reconfiguration of systems after a cyber attack. Most current research on requirements focuses on how to satisfy requirements under some small set of circumstances- possibly an expected situation and/or a safe fallback position. When some systems and components have been disabled by enemy attacks, it may not be possible to meet some predetermined set of system security requirements. In this case, the cyber commander needs automated assistance in choosing an alternative that represents the best compromise between the 'required' and the achievable. to do this, we have to relate system between the 'required' and the achievable. to do this, we have to relate system requirements to configurable parameter settings and describe precisely how the satisfaction of low-level requirements affects the satisfaction of requirements at the system level. This will help present decision-makers with a picture of what configurations are possible and what trade-offs they involve. This work is a first step towards systematizing this process.
DTIC
*Configuration Management; Disabilities; Images; Security*

**20010122707** Louisville Univ., Computer Vision and Image Processing Lab., KY USA
**Integration of Multiple Cues for Robust 3D Object Description: A Computational and Psychophysical Study with Applications** ***Final Report, 14 Nov. 1997 - 14 Feb. 2001***
Farag, Aly A.; Feb. 2001; 47p; In English
Contract(s)/Grant(s): N00014-97-1-1076; Proj. 01PR02894-00
Report No.(s): AD-A395273; No Copyright; Avail: CASI; A03, Hardcopy; A01, Microfiche

The project involves a comprehensive study of object description using multi-sensors. The study examines two basic scenarios for surface reconstruction. The first scenario provides a 2D - to - 3D mapping from images to surfaces and will include stereo, focus, zoom, vergence, shape from shading, and shape from texture. The second scenario uses active range finders to provide direct depth information about the object, i.e., provides a 3D - to - 3D mapping. The research focuses on the representation and fusion of information form differing image sources and the use of machine learning techniques to perform the fusion. Psychophysical studies conducted include investigating the applicability of the recently introduced" quasi 2D coding hypothesis for 3D surface representation" in machine vision; and the behavioral evaluation of human performance with 3D fused imagery. The investigations of 3D surface reconstruction in human, computer and robot vision have an important applications in military, manufacturing and medical areas. As described in technical report this research has been conducted in the Computer Vision and Image Processing Laboratory (CVIP Lab) at the University of Louisville. The "vision environment" created in the CVIP Lab enabled integration of multiple cues to sense, explore and reconstruct the environment layout. As a result, an active vision system called the CardEye was created.
DTIC
*Computer Vision; Information Systems; Human Performance*

**20010122799** California Univ., Lawrence Berkeley Lab., Berkeley, CA USA
**Intergroup protocols: Scalable group communication for the internet**
Berket, K.; Nov. 01, 2000; 114p; In English
Report No.(s): DE2001-775165; LBNL-47152; No Copyright; Avail: Department of Energy Information Bridge

Reliable group ordered delivery of multicast messages in a distributed system is a useful service that simplifies the programming of distributed applications. Such a service helps to maintain the consistency of replicated information and to coordinate the activities of the various processes. With the increasing popularity of the Internet, there is an increasing interest in scaling the protocols that provide this service to the environment of the Internet. The InterGroup protocol suite, described in this

dissertation, provides such a service, and is intended for the environment of the Internet with scalability to large numbers of nodes and high latency links. The InterGroup protocols approach the scalability problem from various directions. They redefine the meaning of group membership, allow voluntary membership changes, add a receiver-oriented selection of delivery guarantees that permits heterogeneity of the receiver set, and provide a scalable reliability service. The InterGroup system comprises several components, executing at various sites within the system. Each component provides part of the services necessary to implement a group communication system for the wide-area. The components can be categorized as: (1) control hierarchy, (2) reliable multicast, (3) message distribution and delivery, and (4) process group membership. We have implemented a prototype of the InterGroup protocols in Java, and have tested the system performance in both local-area and wide-area networks.
NTIS
*Internets; Protocol (Computers); Architecture (Computers); Data Transmission*

**20010122913** Department of Energy, National Petroleum Technology Office, Tulsa, OK USA
**Develop Data Management System for Assistance in Conducting Areas of Review in Kansas**
Korphage, M. L.; Oct. 30, 2000; 13p; In English
Report No.(s): DE2000-766120; DOE/MT/95002-7; No Copyright; Avail: Department of Energy Information Bridge, Microfiche

Continued debugging and program enhancements were made to the project. The finished product is a functional, 32-bit version of RBDMS, accessed via a Microsoft Access 97 user interface, with ODBC connectivity to a Microsoft SQL Server 6.5 database engine. The system utilized the client/server model which is implemented on a Microsoft Windows NT Server 4.0 network operating system, with clients utilizing Windows 95 desktops. Connection of the remote site (the KCC District Offices) to the RBDMS data set in Wichita via the Wide Area Network (WAN) was realized during the First Quarter of 1998.
NTIS
*Data Management; Management Systems; Program Verification (Computers); Data Bases; Computer Programs*

**20010124886** Lunar and Planetary Inst., Houston, TX USA
**The Geological History of Mercury**
Spudis, Paul D., Lunar and Planetary Inst., USA; Mercury: Space Environment, and Surface and Interior; 2001, pp. 100-101; In English; See also 20010124826; No Copyright; Abstract Only; Available from CASI only as part of the entire parent document

The Mariner 10 mission in 1974 mapped about half the surface of Mercury. On the basis of these data, we have a first-order understanding of the geology and history of the planet. Mercury's surface shows intercrater plains, basins, smooth plains, craters, and tectonic features. Additional information is contained in the original extended abstract.
Author
*Geology; Mercury (Planet); Mercury Surface; Planetary Evolution*

**20010125091** Sandia National Labs., Albuquerque, NM USA
**Security Services Discovery by ATM Endsystems**
Sholander, P.; Tarman, T.; Jul. 15, 1999; 7p; In English
Report No.(s): DE2001-9013; SAND99-1795C; No Copyright; Avail: Department of Energy Information Bridge, Microfiche

This contribution proposes strawman techniques for Security Service Discovery by ATM endsystems in ATM networks. Candidate techniques include ILMI extensions, ANS extensions and new ATM anycast addresses. Another option is a new protocol based on an IETF service discovery protocol, such as Service Location Protocol (SLP). Finally, this contribution provides strawman requirements for Security-Based Routing in ATM networks.
NTIS
*Computer Networks; Protocol (Computers); Security; Asynchronous Transfer Mode*

## 63
## CYBERNETICS, ARTIFICIAL INTELLIGENCE AND ROBOTICS

*Includes feedback and control theory, information theory, machine learning, and expert systems. For related information see also 54 Man/System Technology and Life Support.*

**20010117645** NASA Goddard Space Flight Center, Greenbelt, MD USA
**Control of Flexible Systems in the Presence of Failures**
Magahami, Peiman G., NASA Goddard Space Flight Center, USA; Cox, David E., NASA Langley Research Center, USA; [2001]; 7p; In English; AIAA Conference, 6-9 Aut. 2001, USA; Sponsored by American Inst. of Aeronautics and Astronautics, USA

Report No.(s): AIAA Paper 01-4096; Copyright Waived; Avail: CASI; A02, Hardcopy; A01, Microfiche

Control of flexible systems under degradation or failure of sensors/actuators is considered. A Linear Matrix Inequality framework is used to synthesize H(sub infinity)-based controllers, which provide good disturbance rejection while capable of tolerating real parameter uncertainties in the system model, as well as potential degradation or failure of the control system hardware. In this approach, a one-at-a-time failure scenario is considered, wherein no more than one sensor or actuator is allowed to fail at any given time. A numerical example involving control synthesis for a two-dimensional flexible system is presented to demonstrate the feasibility of the proposed approach.

Author

*Actuators; Controllers; Degradation; Failure Analysis; Flexible Bodies*

**20010118901** Brookhaven National Lab., Upton, NY USA

**Effects of parametric variations on seismic analysis methods for non-classically damped coupled systems**

Xu,; Degrassi,; Apr. 02, 2000; 10p; In English

Report No.(s): DE2000-755032; BNL-NUREG-67224; No Copyright; Avail: Department of Energy Information Bridge

A comprehensive benchmark program was developed by Brookhaven National Laboratory (BNL) to perform an evaluation of state-of-the-art methods and computer programs for performing seismic analyses of coupled systems with non-classical damping. The program, which was sponsored by the US Nuclear Regulatory Commission (NRC), was designed to address various aspects of application and limitations of these state-of-the-art analysis methods to typical coupled nuclear power plant (NPP) structures with non-classical damping, and was carried out through analyses of a set of representative benchmark problems. One objective was to examine the applicability of various analysis methods to problems with different dynamic characteristics unique to coupled systems. The examination was performed using parametric variations for three simple benchmark models. This paper presents the comparisons and evaluation of the program participants' results to the BNL exact solutions for the applicable ranges of modeling dynamic characteristic parameters.

NTIS

*Nuclear Power Plants; Earthquake Damage; Seismic Energy*

**20010119229** Booz-Allen and Hamilton, Inc., McLean, VA USA

**Elliptic Curve Cryptography on Smart Cards Without Coprocessors**

Woodbury, Adam D.; Bailey, Daniel V.; Paar, Christof; Sep. 20, 2000; 21p; In English

Report No.(s): AD-A395092; No Copyright; Avail: CASI; A03, Hardcopy; A01, Microfiche

This contribution describes how an elliptic curve cryptosystem can be implemented on very low cost microprocessors with reasonable performance. We focus in this paper on the Intel 8051 family of microcontrollers popular in smart cards and other cost-sensitive devices. The implementation is based on the use of the finite field GF((28)).

DTIC

*Cryptography; Microprocessors; Computer Programming*

**20010119241** North Carolina Agricultural and Technical State Univ., Dept. of Mechanical Engineering, Greensboro, NC USA

**Experimental Intelligent Structures** ***Final Report, 1 Apr. 2000-31 Mar. 2001***

Schulz, Mark J.; Sunderesan, Mannur J.; Ghoshal, Anindya; Jul. 2001; 14p; In English

Contract(s)/Grant(s): F49620-00-1-0232; Proj-3484

Report No.(s): AD-A395047; AFRL-SR-BL-TR-01-0469; No Copyright; Avail: CASI; A03, Hardcopy; A01, Microfiche

This instrumentation grant requested equipment to establish an Intelligent Structures Laboratory for the R&D of cybernetic or artificially intelligent structures. The equipment requested included a mechanical testing machine, signal processing instrumentation, piezoceramic materials, software for a laser vibrometer, oscilloscopes, and other instrumentation. Experimentation was performed using some of the equipment purchased in this grant. Salary support for the research was from other research grants. The equipment purchased will be the basis for long-term experimental research in the area of intelligent structures. The equipment and instrumentation requested was ordered and received and all is operating except for the mechanical testing machine which is being installed. Analytical studies and simulations of intelligent structures and no-load testing of an artificial neural system are being performed and some interesting results from these activities are highlighted in this report. The next step in the work is to test an artificial neural system under loading using the mechanical testing system. The intelligent structure to be tested is a composite component with the neural system attached. The structure will be tested under realistic load conditions to verify that the neural system can detect initiating damage in the panel. Further studies will be to develop the algorithms and the sensor system architecture needed to provide strain and acoustic emission information that can be used to

optimize the performance while minimizing the fatigue of the structure. Development of a self-regulating or intelligent structure that can sense and optimize its performance while minimizing fatigue damage is the goal of this research.
DTIC
*Smart Structures; Cybernetics; Mechanical Properties; Composite Materials*

**20010120085** Sandia National Labs., Albuquerque, NM USA
**Minimalist Approach to Design of Walking Robots**
Moses, M. S.; Jun. 13, 2000; 11p; In English
Report No.(s): DE2000-760782; SAND2000-1498C; No Copyright; Avail: Department of Energy Information Bridge
A minimalist approach to the design of walking robots is presented, in which emphasis is placed on the simplification of control, the use of mechanics to solve problems, and the use of biologically inspired designs. Control is realized by artificial neurons, arranged to mimic neural control circuits found in animals. An artificial neuron consists of an RC circuit and an inverting Schmidt trigger. Pulses will travel along loops or chains of neurons. Actuators can be driven in a coordinated manner by the amplified outputs of neurons. The pattern of motion a given network creates in a set of actuators can be modified by changing the number and duration of pulses, and by changing the topology of a network. A simple network controlling properly designed mechanics can result in a robot capable of a wide range of motions, including stepping and various gaits. A nervous network can independently control a walking robot, and it can be interfaced to other devices. A network is described that is interfaced to a microprocessor and controls a physical robot.
NTIS
*Robots; Walking; Robot Control; Simplification*

**20010120472** Robotic Systems Technology, Westminster, MD USA
**Demo III Operational Concept**
May 29, 2001; 22p; In English; 2001 Vehicle Technologies Symposium: Intelligent Systems for the Objective, 29-31 May 2001, USA
Report No.(s): AD-A394561; No Copyright; Avail: CASI; A03, Hardcopy; A01, Microfiche
The viewgraphs for the Demo III Operational Concept is presented.
DTIC
*Software Engineering; Combat; Military Vehicles*

**20010120473** Army Tank-Automotive Research and Development Command, Warren, MI USA
**Crew Integration and Automation Testbed and Robotic Follower Programs**
Brendle, Bruce, Army Tank-Automotive Research and Development Command, USA; May 30, 2001; 12p; In English; 2001 Vehicle Technologies Symposium: Intelligent Systems for the Objective Force, 29-31 May 2001, USA; Original contains color images
Report No.(s): AD-A394575; No Copyright; Avail: CASI; A03, Hardcopy; A01, Microfiche
The viewgraphs for the crew integration and automation testbed and robotic follower programs are presented.
DTIC
*Robotics; Crews; Man Machine Systems*

**20010120474** Army Tank-Automotive Research and Development Command, Warren, MI USA
**Vetronics Overview**
Adams, Curt, Army Tank-Automotive Research and Development Command, USA; May 30, 2001; 9p; In English; 2001 Vehicle Technologies Symposium: Intelligent Systems for the Objective Force, 29-31 Nay 2001, USA; Original contains color images
Report No.(s): AD-A394576; No Copyright; Avail: CASI; A02, Hardcopy; A01, Microfiche
The viewgraphs for the Vetronics Overview briefing are presented.
DTIC
*Robotics; Artificial Intelligence; Man Machine Systems*

**20010120475** Public Univ. of Navarre, Dept. de Automatica y Computacion, Pamplona, Spain
**5th International Symposium on Quantitative Feedback Theory and Robust Frequency Domain Methods**
January 2001; 319p; In English, 24-24 Aug. 2001, Pamplona, Spain
Contract(s)/Grant(s): F61775-01-WF049
Report No.(s): AD-A394625; EOARD-CSP-01-5049; No Copyright; Avail: CASI; A14, Hardcopy; A03, Microfiche

The Final Proceedings for International Symposium on Quantitative Feedback Theory and Robust Frequency Domain Methods, 23 August 2001 - 24 August 2001. This is an interdisciplinary conference. Topics include: (1) Quantitative Feedback Theory, (2) Robust Control, (3) Frequency-based Methods; (4) Robust Stability and Performance, (5) Uncertain Dynamic Systems, (6) Identification for Robust Control, (7) Fault Detection in Uncertain Systems, and (8) Applications.
DTIC
*Control Theory; Feedback Control; Fault Detection*

**20010120483** California Univ., San Diego, La Jolla, CA USA
**Quantum and Classical Cryptography for Security and Privacy of Photonic Networks** ***Final Report, 1 Jun. 1997 - 31 May 2001***
Fainman, Y.; Jan. 2001; 18p; In English
Contract(s)/Grant(s): F49620-97-1-0389
Report No.(s): AD-A395011; AFRL-SR-BL-TR-01-0484; No Copyright; Avail: CASI; A01, Microfiche; A03, Hardcopy
We have developed rigorous definitions and mathematical formalism for information leakage through possible eavesdropping on the quantum channel. We have investigated classical cryptograph using nonlinear optical processor based on three-wave and four-wave mixing in nonlinear crystals. The processors operate with femtosecond response time and unlike commonly used autocorrelators, allows time-to-space conversion of both amplitude and phase information carried by ultrashort pulses. Pulse position modulation is combined with CDMA techniques to allow enhanced privacy optical networking with ultrahigh bandwidth utilization.
DTIC
*Cryptography; Quantum Electronics; Quantum Cryptography; Pulse Position Modulation*

**20010120834** Carnegie-Mellon Univ., Dept. of Computer Science, Pittsburgh, PA USA
**Basic Research in Computer Science: Image Understanding** ***Final Report, Dec. 1993-Jan. 2000***
Kanade, Takeo; Shafer, Steven; Ikeuchi, Katsushi; Oct. 01, 2001; 15p; In English
Contract(s)/Grant(s): DAAH04-94-G-0006
Report No.(s): AD-A395319; ARO-32567.38-CI; No Copyright; Avail: CASI; A03, Hardcopy; A01, Microfiche
The CMU Image Understanding program performed basic research and technology development toward robust, flexible, and precise vision systems to impact a wide variety of military and civilian applications. The accomplished results include: hypergeometric filter-based image matching; multi-body factorization for structure from motion; a trainable face detection system; 3D surface representation from multiple range images; learning of an object appearance model: recognition of 3D objects in range images by the Spin Image method; eigen window method for SAR image recognition; and shape matching technique and its medical application.
DTIC
*Computer Vision; Pattern Recognition; Image Analysis; Machine Learning*

**20010121968** Argonne National Lab., IL USA
**Models of Reality: The Unconscious Tattletale**
Brown-VanHoozer, S. A.; VanHoozer, W. R.; Aug. 29, 2000; 10p; In English
Report No.(s): DE2000-761249; ANL/ED/CP-101897; No Copyright; Avail: Department of Energy Information Bridge
Humans are constantly subjected to enormous amounts of information greatly exceeding our conscious ability to sense fully experiences vis-a-vis reality. As a consequence, we assimilate this vast array of information at the unconscious level so it can later be considered useful during the process of identifying belief systems and behaviors for learning, decision-making, memory, language, and knowledge. These assimilations are ordered using internal strategies that can be externally observed as analog feedback behavior(s) from an individual's unconscious. These can then be concisely expressed in models for application regarding effective choices in decision-making and learning strategies, memory access, and the actualization of other understandings and applied as knowledge. How we can learn from the unconscious is the focus of this paper.
NTIS
*Assimilation; Decision Making; Learning*

**20010123545** Argonne National Lab., IL USA
**Simulation of dynamic processes with adaptive neural networks**
Tzanos, C. P.; Feb. 03, 1998; 8p; In English
Report No.(s): DE2001-10633; ANL/RE/CP-95587; No Copyright; Avail: Department of Energy Information Bridge, Microfiche

Many industrial processes are highly non-linear and complex. Their simulation with first-principle or conventional input-output correlation models is not satisfactory, either because the process physics is not well understood, or it is so complex that direct simulation is either not adequately accurate, or it requires excessive computation time, especially for on-line applications. Artificial intelligence techniques (neural networks, expert systems, fuzzy logic) or their combination with simple process-physics models can be effectively used for the simulation of such processes. Feedforward (static) neural networks (FNNs) can be used effectively to model steady-state processes. They have also been used to model dynamic (time-varying) processes by adding to the network input layer input nodes that represent values of input variables at previous time steps. The number of previous time steps is problem dependent and, in general, can be determined after extensive testing. This work demonstrates that for dynamic processes that do not vary fast with respect to the retraining time of the neural network, an adaptive feedforward neural network can be an effective simulator that is free of the complexities introduced by the use of input values at previous time steps. NTIS

*Simulation; Neural Nets; Feedforward Control; Fuzzy Systems; Dynamic Characteristics*

**20010125089** Sandia National Labs., Albuquerque, NM USA

**Mobile Surveillance and Monitoring Robots**

Kimberly, H. R.; Shipers, L. R.; Jul. 14, 1999; 11p; In English

Report No.(s): DE2001-9012; SAND99-1788C; No Copyright; Avail: Department of Energy Information Bridge, Microfiche

Long-term nuclear material storage will require in-vault data verification, sensor testing, error and alarm response, inventory, and maintenance operations. System concept development efforts for a comprehensive nuclear material management system have identified the use of a small flexible mobile automation platform to perform these surveillance and maintenance operations. In order to have near-term wide-range application in the Complex, a mobile surveillance system must be small, flexible, and adaptable enough to allow retrofit into existing special nuclear material facilities. The objective of the Mobile Surveillance and Monitoring Robot project is to satisfy these needs by development of a human scale mobile robot to monitor the state of health, physical security and safety of items in storage and process; recognize and respond to alarms, threats, and off-normal operating conditions; and perform material handling and maintenance operations. The system will integrate a tool kit of onboard sensors and monitors, maintenance equipment and capability, and SNL developed non-lethal threat response technology with the intelligence to identify threats and develop and implement first response strategies for abnormal signals and alarm conditions. System versatility will be enhanced by incorporating a robot arm, vision and force sensing, robust obstacle avoidance, and appropriate monitoring and sensing equipment. NTIS

*Monitors; Robots; Surveillance; Automatic Control*

## 64
## NUMERICAL ANALYSIS

*Includes iteration, differential and difference equations, and numerical approximation.*

**20010119227** NASA Ames Research Center, Moffett Field, CA USA

**Analytical Methods to Evaluate Failure Potential During High-Risk Component Development**

Tumer, Irem Y., NASA Ames Research Center, USA; Stone, Robert B., Missouri Univ., USA; 2001; 11p; In English; DETC'01: 2001 ASME Design Engineering Technical Conferences, 9-12 Sep. 2001, Pittsburgh, PA, USA; Sponsored by American Society of Mechanical Engineers, USA; Copyright; Avail: Issuing Activity

Communicating failure mode information during design and manufacturing is a crucial task for failure prevention. Most processes use Failure Modes and Effects types of analyses, as well as prior knowledge and experience, to determine the potential modes of failures a product might encounter during its lifetime. When new products are being considered and designed, this knowledge and information is expanded upon to help designers extrapolate based on the similarity with existing products. This paper makes use of similarities that exist between different failure modes based on the functionality of each component/product. In this light, a function-failure method is developed to help the design of new products with solutions for functions that eliminate or reduce the potential of a failure mode. The method is applied to rotating machinery components and is proposed as a means to account for helicopter failure modes, addressing stringent safety and performance requirements for NASA applications. Author

*Numerical Analysis; Component Reliability; Failure Modes; Prevention*

**20010119586** Air Force Office of Scientific Research, Bolling AFB, Washington, DC USA

**Numerical Analysis of a Singular Integral Equation Arising from Electromagnetic Interior Scattering** ***Final Report, Jan. 1998-Oct. 2000***

Samn, Sherwood; Jun. 15, 2001; 26p; In English

Contract(s)/Grant(s): Proj-2304

Report No.(s): AD-A394884; AFRL-HE-BR-TR-2001-0138; No Copyright; Avail: CASI; A03, Hardcopy; A01, Microfiche

Solving interior scattering problems of electromagnetic waves in biological media using a volume integral equation approach gives rise naturally to an integral equation with unbounded coefficients and with strongly singular kernel. The numerical solution of an analogous 1-D integral equation of the second kind is studied and a convergence proof for the numerical solution is given. DTIC

*Numerical Analysis; Electromagnetic Scattering; Singular Integral Equations*

**20010120102** Aerospace Corp., Lab. Operations, El Segundo, CA USA

**Unitary Integration with Operator Splitting for Weakly Dissipative Systems**

Shadwick, B. A.; Buell, W. F.; Jun. 20, 2001; 20p; In English

Contract(s)/Grant(s): F04701-00-C-0009; Proj-TR-2001(8555)-1

Report No.(s): AD-A395111; SMC-TR-01-17; No Copyright; Avail: CASI; A03, Hardcopy; A01, Microfiche

Unitary integration is a numerical method that preserves the structure of the quantum Liouville equation by evolving the density via unitary transformations. Unitary integrators preserve the kinematic invariants C(sub j) = trp(sup j), j = 1,..., n to all orders in the time step. Here we extend unitary integration to weakly dissipative systems. We apply the technique of operator splitting, using a unitary integrator for the Hamiltonian evolution and a conventional integrator for the dissipative piece. In this way, we guarantee that all dissipation and decoherence (variation of the C(sub j)) is due to the new non-Hamiltonian terms and not to any numerical artifacts. We illustrate the method with examples. DTIC

*Dissipation; Systems Integration; Numerical Analysis; Integrators; Quantum Theory*

**20010120111** Naval Undersea Warfare Center, Newport, RI USA

**User Manual for the Generic Directivity Index (GenDI) Program (Version 1.0. 5)**

Hull, Andrew J.; Aug. 03, 2001; 45p; In English

Report No.(s): AD-A395054; NUWC-NPT-TD-11301; No Copyright; Avail: CASI; A03, Hardcopy; A01, Microfiche

This document is the user manual for the Generic Directivity Index (GenDI) Program. Designed to calculate the directivity index of 10 predefined geometry shapes for linear, planar, and volumetric arrays, the program is also able to read a user-prescribed sensor geometry file for irregularly shaped or weighted arrays. Included in the manual are a description of the basic theory behind GenDI, the program commands and flowcharts, and validation procedures. DTIC

*Directivity; User Manuals (Computer Programs); Linear Arrays*

**20010120149** Stanford Univ., Dept. of Mathematics, Stanford, CA USA

**Signals, Waves and Transport** ***Final Report, 1 Feb. 1998-31 Jan. 2001***

Papanicolaou, George C.; Jan. 2001; 3p; In English

Contract(s)/Grant(s): F49620-98-1-0211

Report No.(s): AD-A395137; AFRL-SR-BL-TR-01-0525; No Copyright; Avail: CASI; A01, Hardcopy; A01, Microfiche

We carry out theoretical and numerical studies of resolution limits for imaging and beam-forming (time reversal) with an active array when the ambient medium is noisy. We analyze in detail some new problems that emerge in the asymptotics of stochastic differential equations, which play an essential role in the formulation of imaging methods. We also analyze the phenomenon of super-resolution in time reversal, where the random medium improves the resolution beyond the diffraction limit, and contrast this with image degradation. Applications range from foliage and ground penetrating radar to secure wireless communications in noisy environments. DTIC

*Differential Equations; Stochastic Processes; Wireless Communication; Numerical Analysis; Asymptotic Methods*

**20010120476** Vassilios Theofilis, Gottingen, Germany

**On Steady Laminar Basic Flows and Their Global Eigenmodes: An Elliptic Cone in Compressible Flow** ***Final Report***

Theofilis, Vassilios, Vassilios Theofilis, Germany; Oct. 31, 2000; 95p; In English; Original contains color images

Contract(s)/Grant(s): F61775-99-W-E049

Report No.(s): AD-A394719; EOARD-SPC 99-4049; No Copyright; Avail: CASI; A05, Hardcopy; A01, Microfiche

The present report is the first step towards global linear instability analysis of three-dimensional flowfields over elliptic cones at hypersonic speeds. The report discusses basic flows which form the variable coefficients of the partial differential equation eigenvalue problem at a small representative class of the parameter values at which the analyses will ultimately be performed. The report illustrates characteristic compressible flowfields recovered at constant Reynolds number and increasing angle of attack and Mach number, keeping for the most part of this work the same resolution of three-dimensional space. The contract tasking states: The contractor will perform a three-dimensional inviscid analysis of the nonparallel steady compressible basic flow over an elliptic cone. A Compressible direct numerical simulation (DNS) code will be developed. The work will show a comparison between the basic flow results obtained with experimental and independently obtained results. The deliverables are the steady-state flow results and the code used to obtain them.

DTIC

*Laminar Flow; Compressible Flow; Flow Distribution*

**20010122219** California Univ., Lawrence Berkeley Lab., Berkeley, CA USA

**Effect of stoichiometry on vortex flame interactions**

Bell, J. B.; Brown, N. J.; Day, M. S.; Frenklach, M.; Grcar, J. F.; Dec. 01, 1999; 14p; In English

Report No.(s): DE2000-764363; LBNL-44730; No Copyright; Avail: Department of Energy Information Bridge, Microfiche

The interaction of a vortex pair with a premixed flame serves as an important prototype for premixed turbulent combustion. In this study, the authors investigate the interaction of a counter-rotating vortex pair with an initially flat premixed methane flame. The authors focus on characterizing the mechanical nature of the flame-vortex interaction and on the features of the interaction strongly affected by fuel equivalence ratio. The authors compare computational solutions obtained using a time-dependent, two-dimensional adaptive low Mach number combustion algorithm that incorporates GRI-Mech 1.2 for the chemistry, thermodynamics and transport of the chemical species. The authors find that the circulation around the vortex scours gas from the preheat zone in front of the flame, making the interaction extremely sensitive to equivalence ratio. For nearly stoichiometric cases, the peak mole fraction of CH across the flame is relatively insensitive to the vortex whereas for richer flames they observe a substantial and rapid decline in the peak CH mole fraction, commencing early in the flame-vortex interaction. The peak concentration of HCO is found to correlate, in both space and time, with the peak heat release across a broad range of equivalence ratios. The model also predicts a measurable increase in C2H2 as a result of interaction with the vortex, and a marked increase in the low temperature chemistry activity.

NTIS

*Combustion; Reaction Kinetics; Vortices; Premixed Flames*

**20010124071** NASA Goddard Space Flight Center, Greenbelt, MD USA

**Comparison of Implicit Collocation Methods for the Heat Equation**

Kouatchou, Jules, NASA Goddard Space Flight Center, USA; Jezequel, Fabienne, Paris VI Univ., France; [2001]; 12p; In English

Contract(s)/Grant(s): NAS5-3508; No Copyright; Avail: CASI; A03, Hardcopy; A01, Microfiche

We combine a high-order compact finite difference scheme to approximate spatial derivatives arid collocation techniques for the time component to numerically solve the two dimensional heat equation. We use two approaches to implement the collocation methods. The first one is based on an explicit computation of the coefficients of polynomials and the second one relies on differential quadrature. We compare them by studying their merits and analyzing their numerical performance. All our computations, based on parallel algorithms, are carried out on the CRAY SV1.

Author

*Finite Difference Theory; Difference Equations; Iterative Solution; Collocation*

## 65
## STATISTICS AND PROBABILITY

*Includes data sampling and smoothing; Monte Carlo method; time series and analysis; and stochastic processes.*

**20010119925** Army Materiel Systems Analysis Activity, Aberdeen Proving Ground, MD USA
**Mathematica Templates for Sequential Reliability/Maintainability Test Design and Analysis**
Cushing, Michael; Jun. 2001; 232p; In English; Original contains color images
Report No.(s): AD-A395237; TR-687; No Copyright; Avail: CASI; A11, Hardcopy; A03, Microfiche

This report documents the recent design and/or analysis of sequential reliability test plans for three systems. Also included in this report is a new, simulation-based method for designing a hypergeometric test plan for acceptance of maintenance troubleshooting procedures based on sequential sampling. The design and analysis of sequential test plans is computationally challenging thus implementation in software is essential. For this reason, each chapter and appendix of this report was written in Mathematica, a leading commercial mathematics software. The test designs and analyses contained within this report constitute a basic set of templates for sequential test planning in the future.
DTIC
*Design Analysis; Reliability Analysis; Sequential Analysis*

**20010120487** Naval Postgraduate School, Monterey, CA USA
**Stochastic Models for Promoting and Testing System Reliability Evolution**
Gaver, Donald P.; Jacobs, Patricia A.; Seglie, Ernest A.; Sep. 2001; 17p; In English
Contract(s)/Grant(s): MIPR-DVAM10001
Report No.(s): AD-A395058; NPS-OR-01-011; No Copyright; Avail: CASI; A03, Hardcopy; A01, Microfiche

Many systems and systems-of-systems function in sequential-stage fashion, and are constantly on when operative, but are failure-susceptible. Communication systems, power generation and transmission, and vehicular transportation systems tend to fall into this category. We propose a reliability growth model for such systems that is based on design defect removal under a Test-Fix-Test (TFT) protocol: a system is assembled and put under test, for example for a fixed mission time, or multiple thereof. If the system fails during the test time its failure source in some stage is diagnosed, the stage is re-designed, and the new prototype system reassembled (system design is 'fixed') and the system is re-tested. The test (TFT) process is repeated until a pre-determined test period elapses with no failures. This is analogous to the run-test criteria analyzed for one-shot devices 1. In this model we also allow for occasional defective re-design: response to a test failure can actually (and realistically) increase the number of failure-generating design defects. Our model allows quick numerical assessment of TFT operating characteristics, given defining parameter values. It thus provides a planning tool for test designers.
DTIC
*Reliability Analysis; Stochastic Processes; Telecommunication; Systems Engineering*

**20010122938** NASA Ames Research Center, Moffett Field, CA USA
**AutoClass: A Bayesian Approach to Classification**
Stutz, John, NASA Ames Research Center, USA; Cheeseman, Peter, Research Inst. for Advanced Computer Science, USA; Hanson, Robin, RECOM Technologies, Inc., USA; Taylor, Will, RECOM Technologies, Inc., USA; [1994]; 1p; In English; Fourteenth International MaxEnt Workshop (MaxEnt-94), 1-5 Aug. 1994, Cambridge, UK
Contract(s)/Grant(s): RTOP 233-01-02; No Copyright; Avail: Issuing Activity; Abstract Only

We describe a Bayesian approach to the untutored discovery of classes in a set of cases, sometimes called finite mixture separation or clustering. The main difference between clustering and our approach is that we search for the "best" set of class descriptions rather than grouping the cases themselves. We describe our classes in terms of a probability distribution or density function, and the locally maximal posterior probability valued function parameters. We rate our classifications with an approximate joint probability of the data and functional form, marginalizing over the parameters. Approximation is necessitated by the computational complexity of the joint probability. Thus, we marginalize w.r.t. local maxima in the parameter space. We discuss the rationale behind our approach to classification. We give the mathematical development for the basic mixture model and describe the approximations needed for computational tractability. We instantiate the basic model with the discrete Dirichlet distribution and multivariant Gaussian density likelihoods. Then we show some results for both constructed and actual data.
Author
*Classifications; Bayes Theorem; Probability Distribution Functions*

**20010123920** Los Alamos National Lab., NM USA

**Application of Fuzzy Set Theory for Exposure Control in Beryllium Part Manufacturing**

Parkinson, W. J.; Abeln, S. P.; Jan. 01, 2000; 25p; In English

Report No.(s): DE2001-763326; LA-UR-00-326; No Copyright; Avail: Department of Energy Information Bridge

We have applied fuzzy set theory to some exposure control problems encountered in the machining and the manufacturing of beryllium parts. A portion of that work is presented in this paper. The major driving force for using fuzzy techniques in this case rather than classical statistical process control is that beryllium exposure is very task dependent and our manufacturing plant is quite atypical. We believe that standard statistical techniques will produce too many false alarms. The beryllium plant produces parts on a daily basis, but every day is different. Some days many parts are produced and some days only a few. Some times the parts are large and sometimes the parts are small. Some machining cuts are rough and some are fine. These factors and others make it hard to define a typical day. The problem of concern, for this study, is the worker beryllium exposure. Even though the plant is new and very modern and the exposure levels are expected to be well below the required levels, the Department of Energy has demanded that the levels for this plant be well below required levels. The control charts used to monitor this process are expected to answer two questions: 1. Is the process out of Control. Do we need to instigate special controls such as requiring workers to use respirators. 2. Are new, previously untested, controls making a difference. The standard Shewhart type control charts, based on consistent plant operating conditions do not adequately answer this question. The approach described here is based upon a fuzzy modification to the Shewhart X Bar-R chart. This approach is expected to yield better results than work based upon the classical probabilistic control chart.

NTIS

*Fuzzy Sets; Air Pollution; Statistical Analysis; Beryllium*

**20010125236** Oak Ridge National Lab., TN USA

**Robust Detection of Dynamical Change in Scalp EEG**

Gailey, P. C.; Hively, L. M.; Protopopescu, V. A.; Jun. 28, 1999; 6p; In English

Report No.(s): DE2001-11469; ORNL/CP-103699; No Copyright; Avail: Department of Energy Information Bridge

We present a robust, model-independent technique for measuring changes in the dynamics underlying nonlinear time-serial data. We define indicators of dynamical change by comparing distribution functions on the attractor via L(sub 1)-distance and X(sup 2) statistics. We apply the measures to scalp EEG data with the objective of capturing the transition between non-seizure and epileptic brain activity in a timely, accurate, and non-invasive manner. We find a clear superiority of the new metrics in comparison to traditional nonlinear measures as discriminators of dynamical change.

NTIS

*Electroencephalography; Seizures; Distribution Functions*

**20010125460** Sandia National Labs., Albuquerque, NM USA

**Can Data Recognize Its Parent Distribution**

Marshall, A. W.; Meza, J. C.; Olkin, I.; May 01, 1999; 64p; In English

Report No.(s): DE2001-8244; SAND99-8241; No Copyright; Avail: Department of Energy Information Bridge, Microfiche

This study is concerned with model selection of lifetime and survival distributions arising in engineering reliability or in the medical sciences. We compare various distributions, including the gamma, Weibull and lognormal, with a new distribution called geometric extreme exponential. Except for the lognormal distribution, the other three distributions all have the exponential distribution as special cases. A Monte Carlo simulation was performed to determine sample sizes for which survival distributions can distinguish data generated by their own families. Two methods for decision are by maximum likelihood and by Kolmogorov distance. Neither method is uniformly best. The probability of correct selection with more than one alternative shows some surprising results when the choices are close to the exponential distribution.

NTIS

*Mortality; Service Life; Mathematical Models; Statistical Distributions; Probability Density Functions*

**20010125496** Sandia National Labs., Albuquerque, NM USA

**Data Torturing and the Misuse of Statistical Tools**

Abate, M. L.; Aug. 16, 1999; 13p; In English

Report No.(s): DE2001-10185; SAND99-2178C; No Copyright; Avail: Department of Energy Information Bridge

Statistical concepts, methods, and tools are often used in the implementation of statistical thinking. Unfortunately, statistical tools are all too often misused by not applying them in the context of statistical thinking that focuses on processes, variation, and data. The consequences of this misuse may be data torturing or going beyond reasonable interpretation of the facts due to a

misunderstanding of the processes creating the data or the misinterpretation of variability in the data. In the hope of averting future misuse and data torturing, examples are provided where the application of common statistical tools, in the absence of statistical thinking, provides deceptive results by not adequately representing the underlying process and variability. For each of the examples, a discussion is provided on how applying the concepts of statistical thinking may have prevented the data torturing. The lessons learned from these examples will provide an increased awareness of the potential for many statistical methods to mislead and a better understanding of how statistical thinking broadens and increases the effectiveness of statistical tools.
NTIS
*Statistical Analysis; Variability; Procedures*

## 67
## THEORETICAL MATHEMATICS

*Includes algebra, functional analysis, geometry, topology set theory, group theory and and number theory.*

**20010119610** Pittsburgh Univ., Pittsburgh, PA USA
**Upper and Lower Bounds for the Eigenvalues of Vibrating Beams with Linearly Varying Axial Load**
Laird, William M.; Fauconneau, Guy; Nov. 1966; 77p; In English
Contract(s)/Grant(s): NSG-634
Report No.(s): AD-A394967; NASA-CR-653; No Copyright; Avail: CASI; A05, Hardcopy; A01, Microfiche

Previous investigations have demonstrated the importance of the effect of linearly varying axial or in-plane loading on the vibration characteristics of beams and flat plates. It has already been established that the problem reduces to solving for the eigenvalues of a fourth order, variable coefficient differential equation that can not be solved in closed form. Beginning with a variational representation of the eigenvalue problem, methods are discussed by which both upper and lower bounds for the eigenvalues may be formed, The true eigenvalues may thus be estimated as being bracketed by the upper and lower bounds which are shown to approach each other. The bounds for the eigenvalues may also be estimated by an averaging procedure which may or may not compare favorably with the true values depending on the values of the loading parameters. Finally, numerical values for upper bounds, lower bounds, and average lumped end-load eigenvalues are computed on an IBM 7090 Computer.
DTIC
*Eigenvalues; Vibration; Beams (Supports); Loads (Forces); Flat Plates*

**20010122273** NASA Ames Research Center, Moffett Field, CA USA
**Electron Correlation in 4-Component Relativistic Calculations**
Visscher, Luuk, NASA Ames Research Center, USA; [1994]; 1p; In English; Relativistic Pseudopotentials, 7-9 May 1994, Toulouse, France; Sponsored by European Science Foundation, Unknown
Contract(s)/Grant(s): RTOP 232-01-04; No Copyright; Avail: Issuing Activity; Abstract Only

The full 4-component Dirac-Coulomb equation can nowadays be used in molecular calculations, The first step in solving this relativistic many-electron equation usually consists of solving the closed or open-shell Diarc-Fock equations. Like in non-relativistic calculations the outcome does not account for the effects of electron correlation. This can in principle be remedied by developing relativistic variants of electron correlation methods like Configuration Interaction or Coupled Cluster. In this talk the differences and similarities of such relativistic approaches as compared to non-relativistic methods will be reviewed. Results of Configuration Interaction calculations on the PtH molecule and on the MeF(sub 6, sup 2-) (Me= Co, Rh, Ir) complexes will be presented to give an impression of the kind of results that currently can be obtained.
Author
*Dirac Equation; Correlation; Computation; Electron Scattering*

## 70
## PHYSICS (GENERAL)

*Includes general research topics related to mechanics, kinetics, magnetism, and electrodynamics. For specific areas of physics see categories 71 through 77. For related instrumentation see 35 Instrumentation and Photography; for geophysics, astrophysics or solar physics see 46 Geophysics, 90 Astrophysics, or 92 Solar Physics.*

**20010117649** Los Alamos National Lab., NM USA
**Optical Signatures from Magnetic 2-D Electron Gases in High Magnetic Fields to 60 Tesla**
Crooker, S. A.; Kikkawa, J. M.; Awschalom, D. D.; Smorchikova, I. P.; Samarth, N.; Nov. 08, 1998; 18p; In English
Report No.(s): DE2000-760140; LA-UR-98-4115; No Copyright; Avail: Department of Energy Information Bridge

We present experiments in the 60 Tesla Long-Pulse magnet at the Los Alamos National High Magnetic Field Lab (NHMFL) focusing on the high-field, low temperature photoluminescence (PL) from modulation-doped ZnSe/Zn(Cd,Mn)Se single quantum wells. High-speed charge-coupled array detectors and the long (2 second) duration of the magnet pulse permit continuous acquisition of optical spectra throughout a single magnet shot. High-field PL studies of the magnetic 2D electron gases at temperatures down to 350 mK reveal clear intensity oscillations corresponding to integer quantum Hall filling factors, from which we determine the density of the electron gas.
NTIS
*Continuous Spectra; Doped Crystals; Electron Gas; Photoluminescence; Quantum Wells*

**20010117655** Los Alamos National Lab., NM USA
**2 Hz, 30 T Split Pulse Water Cooled Magnet for Neutron Scattering Experiments (Materials Characterization and Design Options)**
Eyssa, Y. M.; Walsh, R. P.; Miller, J. R.; Miller, G. E.; Pernambuco-Wise, P.; Aug. 26, 1997; 55p; In English
Report No.(s): DE2000-760057; LA-SUB-00-47; No Copyright; Avail: Department of Energy Information Bridge

The Manuel Lujan Jr. Neutron Scattering Center at LANL has a need of an engineering design study for a split-pair, pulse magnet that would provide a 30 T field in a 30 mm bore, 10 mm split gap, 3 ms pulse width at a repetition rate of 2 Hz. The use of such magnet would enable the use of neutron diffraction in determining the arrangements (magnetic structures) of magnetic moments in solids, the spatial extent of the magnetic electrons around their parent ions, and the full moment-density distribution function in real space. This report covers a study for a conceptual design and material characterization for a fatigue life up to 107 cycles of charge and discharge.
NTIS
*Distribution Functions; Magnetic Field Configurations; Moment Distribution; Neutron Diffraction; Neutron Scattering*

**20010117656** Sandia National Labs., Albuquerque, NM USA
**Magnetic Anticrossing of 1D Subbands in Coupled Ballistic Double Quantum Wires: SIMD'99 Proceedings**
Blount, M. A.; Moon, J. S.; Simmons, J. A.; Lyo, S. K.; Wendt, J. R.; Jul. 13, 2000; 8p; In English
Report No.(s): DE2000-760048; SAND99-2769C; No Copyright; Avail: Department of Energy Information Bridge

We study the low-temperature in-plane magnetoconductance of vertically coupled double quantum wires. Using a novel flip-chip technique, the wires are defined by two pairs of mutually aligned split gates on opposite sides of a 1 micron thick AlGaAs/GaAs double quantum well heterostructure. We observe quantized conductance steps due to each quantum well and demonstrate independent control of each 1D wire. A broad dip in the magnetoconductance at -6 T is observed when a magnetic field is applied perpendicular to both the current and growth directions. This conductance dip is observed only when 1D subbands are populated in both the top and bottom constrictions. This data is consistent with a counting model whereby the number of subbands crossing the Fermi level changes with field due to the formation of an anticrossing in each pair of 1D subbands.
NTIS
*Quantum Wells; Quantum Wires; Magnetic Properties*

**20010117852** Los Alamos National Lab., NM USA
**PHERMEX, REX, and Thomson-Generated XUV Calculations**
Hughes, T. P.; Clark, R. M.; Carlson, R. L.; Moir, D. C.; May 01, 1993; 48p; In English
Report No.(s): DE2000-760073; LA-SUB-00-52; No Copyright; Avail: Department of Energy Information Bridge

We report on calculations carried out during 1990 in support of on-going and planned beam experiments at M-4. A higher-current injector for PHERMEX is under consideration and we have modeled a REX-like diode geometry which can deliver 1-1.5 kA. A three-coil focusing configuration has been designed to maintain low beam emittance in the diode region. We show

that the existing two transport magnets are marginally capable of transporting a 1 kA beam to the a-cavity. This work is described. We look at the possibility of accelerating a 4 kA, 4 MV beam, which could be provided by the REX machine, through the PHERMEX a cavity. Simulation results indicate that this is feasible. Because of the high cost and limited pulse length of a REX injector, however, a 1-1.5 kA upgrade is a more attractive option at this time. Computations in support of ongoing REX experiments are described. We have modeled the generation of transverse beam oscillations through the excitation of an electromagnetic dipole mode in the diode cavity. Results show that oscillating magnetic fields on the order of 1-2 gauss are sufficient to cause the oscillation amplitudes observed. A simulation was carried to look at the effect of placing iron rings inside the windings of the REX anode magnet. We conclude that this causes no significant degradation of beam emittance. We have also looked at the focusing produced when the REX beam is injected into a laser-ionized plasma channel. This is a possible alternative to a magnetic lens to obtain a small spot-size. Finally, we give results of preliminary calculations of extreme ultraviolet and X-ray photon production through laser backscattering off a relativistic electron beam. There are plans to carry out such an experiment on REX in the near future.
NTIS
*Cavities; Electron Beams; Magnetic Fields*

**20010118271** California Univ., Lawrence Berkeley Lab., Berkeley, CA USA
**Attenuation and fluctuations of elastic waves due to random scattering from inclusions**
Korneev, V.; Johnson, L. R.; May 01, 1999; 46p
Report No.(s): DE2000-760320; LBNL-43341; No Copyright; Avail: Department of Energy Information Bridge, Microfiche

Exact solutions for elastic compressional and shear waves scattered from a homogeneous sphere are used to obtain formulas for velocity and attenuation of plane waves propagating through a layer of randomly distributed inclusions. Analytical expressions are obtained for the mean transmitted wave and fluctuations in its amplitude and phase over the complete range of frequencies. The size and contrast of the inclusions are arbitrary, but interactions between scatterers are not considered and the concentration of scatterers is assumed to be small. The results are compared with effective media expressions for velocities in the low frequency limit. The analytical solutions are also compared with numerical simulations and it is demonstrated that they satisfactorily explain the effects of scattering on both the mean and variance of the phase and the mean and variance of the attenuation for all frequencies. The need for spatial averaging of observational data and methods of interpreting such averaged data in terms of the material properties of the scattering medium are discussed.
NTIS
*Wave Attenuation; Variations; Elastic Waves; Elastic Scattering*

**20010118516** Brookhaven National Lab., Upton, NY USA
**Magnetic Excitations and Double Gap in the S = 1/2 Linear Chain Quantum Antiferromagnet BaCu2Si2O7**
Raymond,; Zheludev,; Masuda,; Kakurai,; Ressouche,; Mar. 16, 2000; 2p; In English
Report No.(s): DE2000-759036; BNL-67296; No Copyright; Avail: Department of Energy Information Bridge

The magnetic excitation spectrum of the ideal S=1/2 1-dimensional quantum antiferromagnet (AF), contains no single-mode contributions, and, in fact, can be described as a 2-particle continuum of spinons. Chain-MF theory predicts that a weakly coupled chains system becomes ordered at low temperatures. In the ordered state a sharp magnon excitation is present. The continuum persists, but is separated from the magnon branch by an appreciable energy gap. On the other hand, if weakly coupled chains are described through the 1/S expansion of the conventional Holstein-Primakov spin wave theory, one finds a longitudinal 2-magnon continuum and a transverse 3-magnon continuum that start immediately above the spin wave energy.
NTIS
*Magnetic Properties; Antiferromagnetism; Excitation*

**20010119203** Oak Ridge National Lab., TN USA
**Enhanced Luminescence in Epitaxial Oxide Thin-Film Phosphors**
Lee, Y. E.; Norton, D. P.; Budai, J. D.; Park, C.; Kim, M.; Nov. 08, 1999; 15p; In English
Report No.(s): DE2000-751501; ORNL/CP-105278; No Copyright; Avail: Department of Energy Information Bridge, Microfiche

Undoped and Mn-doped ZnGa(sub 2)O(sub 4) thin-film phosphors were grown using pulsed laser ablation on (100) MgO single crystal and glass substrates. X-ray results showed the films on (100) MgO are well aligned both out-of plane and in-plane. Epitaxial films show superior photoluminescent intensity as compared to randomly oriented polycrystalline films, indicating that

intragranular crystallinity strongly influences luminescent properties. Li-doped ZnGa(sub 2)O(sub 4) exhibited significantly enhanced photoluminescence intensity.
NTIS
*Phosphors; Photoluminescence; Additives; Thin Films; Epitaxy; Doped Crystals*

**20010119209** Brookhaven National Lab., Upton, NY USA
**Centrality and E(sub T) Fluctuations from P+Be to Au+Au at AGS Energies**
Tannenbaum, M. J.; Aug. 09, 1999; 9p; In English
Report No.(s): DE2000-751160; BNL-67066; No Copyright; Avail: Department of Energy Information Bridge

Measurements by the E802 Collaboration of the A-dependence and pseudorapidity interval (delta-n) dependence of mid-rapidity E(sub T) distributions in a half-azimuth electromagnetic calorimeter are presented. The shapes of E(sub T) distributions are observed to vary systematically with the size of the delta-n interval, like multiplicity. by plotting the E(sub T) distributions for a given delta-n interval scaled by the measured (E(sub T)(delta-n))(sub p+Au) on the same interval for p+Au collisions, the distributions become nearly universal in the physically meaningful units of 'number of average p+Au collisions', effectively Wounded Projectile Nucleons. This shows that the centrality characterization remains valid even in relatively small mid-rapidity pseudo-rapidity intervals.
NTIS
*Collisions; Beryllium*

**20010119213** Brookhaven National Lab., Upton, NY USA
**Flux Mapping and Magnetic Behavior of Grain Boundaries in Nd-Fe-B Magnets**
Volkov, V. V.; Nov. 29, 1999; 6p; In English
Report No.(s): DE2000-751121; BNL-66920; No Copyright; Avail: Department of Energy Information Bridge

Advanced Fresnel- and Foucault-Lorentz microscopy were applied to analyze magnetic behavior of the grain boundaries in Nd-Fe-B hard magnets. In-situ transmission electron microscopic magnetizing experiments combined with these imaging methods revealed the process of magnetization reversal in polycrystalline sintered and die-upset Nd-Fe-B under various magnetic fields. Fine details of magnetic flux distribution, derived from the magnetic interferograms created by phase-coherent Foucault imaging, provide a quantitative description of the local variation of magnetic flux. Our study suggests that the grain boundaries play an important multi-functional role in the reversal of magnetization, by acting as pinning centers of domain walls, centers of nucleation of reversal domains, and sinks or sources for migrating magnetostatic charges and/or dipoles. They also ensure a smooth transient for irreversible remagnetization in polycrystalline samples.
NTIS
*Flux Density; Grain Boundaries; Imaging Techniques; Magnetic Flux; Magnetization; Magnets*

**20010119419** Argonne National Lab., IL USA
**Note on RHIC Polarimetry**
Spinka, H.; Nov. 12, 1999; 18p; In English
Report No.(s): DE2000-750790; ANL-HEP-TR-99-113; No Copyright; Avail: Department of Energy Information Bridge

For physics measurements with polarized colliding beams, beam polarizations and relative luminosities must both be determined. Predictions for spin observables of many interesting physics processes at RHIC are quite small in magnitude. This requires high statistics measurements of relative luminosities and careful control of systematic errors. Discussions about the polarized beams at RHIC often presume that the polarization and intensity of each bunch within a will be known quite well from measurements by the RHIC polarimeters. The purpose of this note is to give a description of the knowledge that can actually be obtained from these polarimeters.
NTIS
*Luminosity; Polarimetry; Particle Beams*

**20010119420** Brookhaven National Lab., Upton, NY USA
**Conceptual Design of a Magnet System to Generate 20 T in a 0.15 m Diameter Bore, Employing an Inductor Precooled by Liquid Nitrogen**
Weggel, R. J.; Sep. 26, 1999; 5p; In English
Report No.(s): DE2000-750783; BNL-67007; No Copyright; Avail: Department of Energy Information Bridge

The research program for an eventual neutrino factory or muon collider needs a magnet of approximately 0.15 m diameter bore to generate approximately 20 T over a length of approximately 0.3 m. Downstream for approximately 3 m the field should

fall gradually to approximately 1.25 T, while the bore increases four-fold inversely as the square root of the field. A conventional magnet would require approximately 40 MW; a superconducting or hybrid magnet might cost tens of millions of dollars. An economically feasible system employs a pulse magnet precoded by liquid nitrogen, with two sets of coils energized sequentially. NTIS

*Cavities; Muons; Neutrinos; Superconducting Magnets*

**20010119427** Brookhaven National Lab., Upton, NY USA

**AGS Experiment 945a Radiation Damage in Metals at Liquid Helium Temperature by GeV Protons**

Greene, G. A.; Aug. 01, 1999; 130p; In English

Report No.(s): DE2000-750770; BNL-66931; No Copyright; Avail: Department of Energy Information Bridge

The purpose of this experiment was to provide data for the validation and improvement of models used in computer codes which are being used to predict radiation-induced damage in target and blanket materials of APT and similar technologies when the materials are irradiated with GeV-range protons. The experiment was performed at the BNL AGS at liquid helium temperatures, employing a commercially-available flow cryostat for the mounting of the samples. The shaft of the cryostat is mounted on a 2.75-inch conflat flange around which the vacuum chamber was constructed. The target chamber of the vacuum vessel was a six-inch diameter six-way cross. Two flanges on this cross were for the 0.010-inch beam windows; a third flange was for the cryostat mount; a fourth flange was for the vacuum valve and turbo-roughing pump assembly; a fifth flange was for the vacuum gauge assembly, and the sixth flange was for the electrical feed through for the instrumentation wires to the data-acquisition system. Target samples were prepared from copper and tungsten wire and mounted to the cryostat tip. Each sample consisted of 0.002-inch diameter wire, wrapped around U-shaped posts, and anchored to OFHC copper bases. The U-shaped posts were made of anodized aluminum threaded rods which insulated the wires electrically while providing good thermal contact to the base. The radiation damage was determined indirectly by measuring changes in the resistivities of the samples using the four-wire current reversal technique. The temperature of the target assembly was monitored during the experiments by a Cernox(tm) model CX-1070-AA-4L resistor attached to the copper base. The data-acquisition instrumentation used to measure the resistance changes of the sample wires was also used to measure the resistance of the Cernox resistor as well. A series of experiments were performed with both 1.94-GeV and 1.10-GeV protons with the sample wires at 4.7 K to freeze the radiation-induced defects into the samples in order to measure the defect-induced changes in electrical resistivity. NTIS

*Cryostats; Flanges; Radiation Damage; Wire*

**20010119566** Fermi National Accelerator Lab., Batavia, IL USA

**Effects of inflow on NuMI groundwater concentrations**

Cossairt, J. D.; Sep. 08, 1999; 11p; In English

Report No.(s): DE2001-10502; FERMILAB-TM-2092; No Copyright; Avail: Department of Energy Information Bridge, Microfiche

Recent discussions of the NuMI groundwater problem have been concerned with the effect of inflow of water into the tunnel on the overall groundwater concentration. The purpose of this note is to document calculations of these effects using simple mathematical models. These results can, then, be compared with the results obtained using more elaborate methods such as computer modeling techniques. At Fermilab, a concentration model has been developed to address groundwater activation concerns. While this model has evolved to some degree over time, the main features have remained stable. NTIS

*Radiation Detectors; Ground Water*

**20010119983** Argonne National Lab., IL USA

**Complex magnetic behavior and the role of dynamic structural fluctuations in La(1.2)SR(1.8)Mn2O7 crystals**

Sharma, R. P.; Jan. 12, 1998; 19p; In English

Report No.(s): DE2001-10557; ANL/MSD/CP-95294; No Copyright; Avail: Department of Energy Information Bridge

The layered perovskite double sheet La(sub 1.2)SR(sub 1.8)Mn(sub 2)O(sub 7) crystals have shown an unusual magnetic behavior. They are found to be fully ferromagnetic below 120 K, with a small ferromagnetic component ((le) 0.3% by volume) persisting above 120 K and extending up to 320 K along with a paramagnetic phase and becoming fully paramagnetic above 320 K. A large magnetoresistance is seen around 120 K. Ion channeling investigations in these crystals show clearly a change of 1.5 picometers in the atomic displacement from 70 to 150 K, which is twice that expected due to the change in the thermal vibrational amplitude and the lattice parameters a and c, observed by neutron diffraction. This provides a clear indication of dynamic distortion occurring around the ferromagnetic transition. Even in the wide temperature region between 120 to 320 K, anomalous

displacement of ions can be seen, correlating well with the features observed in magnetization measurements. These displacements are again larger than those due to thermal motion, thereby supporting the idea of dynamic fluctuations in the Jahn-Teller distorted MnO(sub 6) octahedra playing an important role at the magnetic phase transitions in this material. There is a large magneto-crystalline anisotropy with the hard axis along the c-direction. The material seems to be an inhomogeneous magnetic system with the presence of small regions of highly correlated spins parallel to the ab plane and appears to be in a state of two dimensional magnetic order in the region 120 to 320 K.
NTIS
*Manganese Oxides; Neutron Diffraction; Ferromagnetism; Crystals*

**20010120000** Sandia National Labs., Albuquerque, NM USA
**Z-Pinch Generated X-Rays in Static-Wall Hohlraum Geometry Demonstrate Potential for Indirect-Drive ICF Studies**
Sandord, T. W. L.; Olson, R. E.; Chandler, G. A.; Hebron, D. E.; Mock, R. C.; Aug. 25, 1999; 17p; In English
Report No.(s): DE2001-10341; SAND99-0662C; No Copyright; Avail: Department of Energy Information Bridge, Microfiche

Hohlraums of full ignition scale (6-mm diameter by 7-mm length) have been heated by x-rays from a z-pinch target on Z to a variety of temperatures and pulse shapes which can be used to simulate the early phases of the National Ignition Facility (NIF) temperature drive. The pulse shape is varied by changing the on-axis target of the z pinch in a static-wall-hohlraum geometry. A 2-(micro)m-thick walled Cu cylindrical target of 8-mm diameter filled with 10 mg/cm(sup 3) CH, for example, produces foot-pulse conditions of (minus)85 eV for a duration of (approximately) 10 ns, while a solid cylindrical target of 5-mm diameter and 14-mg/cm(sup 3) CH generates first-step-pulse conditions of (approximately) 122 eV for a duration of a few ns. Alternatively, reducing the hohlraum size (to 4-mm diameter by 4-mm length) with the latter target has increased the peak temperature to (approximately) 150 eV, which is characteristic of a second-step-pulse temperature. In general, the temperature T of these x-ray driven hohlraums is in agreement with the Planckian relation (T-(P/A)(sup 1/4)). P is the measured x-ray input power and A is the surface area of the hohlraum. Fully-integrated 2-D radiation-hydrodynamic simulations of the z pinch and subsequent hohlraum heating show plasma densities within the useful volume of the hohlraums to be on the order of air or less.
NTIS
*Cylindrical Bodies; Ignition Temperature; Zeta Pinch*

**20010120028** Argonne National Lab., IL USA
**Stratified Source-Sampling Techniques for Monte Carlo Eigenvalue Analysis**
Mohamed, A.; Jul. 10, 1998; 11p; In English
Report No.(s): DE2001-10648; ANL/RA/CP-95657; No Copyright; Avail: Department of Energy Information Bridge

In 1995, at a conference on criticality safety, a special session was devoted to the Monte Carlo 'Eigenvalue of the World' problem. Argonne presented a paper, at that session, in which the anomalies originally observed in that problem were reproduced in a much simplified model-problem configuration, and removed by a version of stratified source-sampling. In this paper, stratified source-sampling techniques are generalized and applied to three different Eigenvalue of the World configurations which take into account real-world statistical noise sources not included in the model problem, but which differ in the amount of neutronic coupling among the constituents of each configuration. It is concluded that, in Monte Carlo eigenvalue analysis of loosely-coupled arrays, the use of stratified source-sampling reduces the probability of encountering an anomalous result over that if conventional source-sampling methods are used. However, this gain in reliability is substantially less than that observed in the model-problem results.
NTIS
*Eigenvalues; Monte Carlo Method; Sampling*

**20010120048** Brookhaven National Lab., Upton, NY USA
**Crystalline beams**
Ruggiero, A. G.; Nov. 09, 1999; 24p; In English
Report No.(s): DE2000-752964; BNL-66946; No Copyright; Avail: Department of Energy Information Bridge

Crystalline Beams are an ordered state of an ensemble of ions circulating in a Storage Ring with very small velocity fluctuations. They can be obtained from ordinary warm ion beams with the application of intense cooling techniques, namely electron and/or laser cooling. A phase transition occurs when sufficiently small velocity spreads are reached, freezing the particle-to-particle spacing in strings, zig-zags, and helices. The properties and feasibility of Crystalline Beams depend on the choice of the lattice of the Storage Ring. There are three issues closely related to the design of the Storage Ring, namely: the determination of Equilibrium Configurations, Confinement Conditions, and Stability Conditions. of particular concern is the effect of the trajectory curvature and of the beam momentum spread. They both set the requirements on the amount of momentum

cooling, on the focussing, and on the distribution of bending in the lattice of the Storage Ring. The practical demonstration of Crystalline Beams may create the basis for an advanced technology of particle accelerators. The limitations due to Coulomb intra-beam scattering and space-charge forces would be finally be brought under control, so that ordered beams of ions can be achieved for a variety of new applications.
NTIS
*Crystallinity; Ion Beams; Particle Accelerators; Momentum*

**20010120052** Brookhaven National Lab., Upton, NY USA
**Symposium on QCD physics at Riken BNL Research Center**
Yazaki, K.; Nov. 23, 1999; 183p; In English; QCD physics, 23 Sep. 1999, Matsue, Japan
Report No.(s): DE2000-752959; BNL-52578; No Copyright; Avail: Department of Energy Information Bridge
The symposium, 'QCD Physics at RIKEN-BNL Research Center' was held at Shimane University, Matsue, Japan, on September 23, 1999, both as a topical symposium of the biannual meeting of the Physical Society of Japan and a RIKEN-BNL Research Center (RBRC) workshop.
NTIS
*Conferences; Quantum Chromodynamics; Quantum Mechanics*

**20010120076** Argonne National Lab., IL USA
**Review of the recent applications of the stochastic variational method**
Varga, K.; Aug. 11, 2000; 11p; In English
Report No.(s): DE2000-761264; ANL/PHY/CP-102560; No Copyright; Avail: Department of Energy Information Bridge
The recent applications of the stochastic variational method is reported. Besides the review of the earlier calculations for atomic, nuclear and subnuclear systems, recent developments on quantum dots, quantum wells and on atoms in strong magnetic field is presented.
NTIS
*Stochastic Processes; Quantum Theory; Calculus of Variations*

**20010120116** Army Research Lab., Human Research and Engineering Directorate, Aberdeen Proving Ground, MD USA
**A Study of the Phase-Lock Phenomenon for a Circular Slingatron**
Cooper, Gene R.; Tidman, Derek A.; Sep. 2001; 26p; In English; Original contains color images; Prepared in collaboration with ALCorp., McLean, VA
Contract(s)/Grant(s): Proj-1L162618AH80
Report No.(s): AD-A395010; ARL-TR-2566; No Copyright; Avail: CASI; A03, Hardcopy; A01, Microfiche
The phase-lock phenomenon of a mass sled sliding along in a circular slingatron is studied both numerically and analytically. Parameters that describe a slingatron, in which the phase angle of the swing arms increases quadratically in time, are found to be simply related to the sled's speed during phase lock. The time required for phase lock to occur is related to a simple exponential function of the gyration speed and the coefficient of friction between the sled and track. Accurate time histories describing the motion of the accelerating sled are expressed in terms of confluent hypergeometric functions 1F1. These results are then used to obtain physical insight into why the phase-lock phenomenon takes place and to describe the important role that friction plays by damping the oscillatory motion of the sled.
DTIC
*Friction; Sliding; Sleds; Coefficient of Friction*

**20010120845** Space and Naval Warfare Systems Center, San Diego, CA USA
**Best Windband Impedance Matching Bounds for Lossless 2-Ports**
Allen, J. C.; Schwartz, D. F.; Sep. 2001; 71p; In English
Report No.(s): AD-A395248; TR-1859; No Copyright; Avail: CASI; A04, Hardcopy; A01, Microfiche
The selection of a lossless 2-port to maximize the wideband power transfer from a generator to a load is a ubiquitous problem in electrical engineering. The mathematical problem is to maximize the wideband transducer power gain over a class of lossless 2-ports. As a numerical optimization problem, wideband impedance matching is difficult because the wideband transducer power gain is a nonlinear, nondifferentiable badly scaled multivariable function. Therefore, any information on the global solution is valuable to the engineer for assessing the quality of suboptimal solutions computed by numerical optimizers. In his classic 1950 paper, Fano determined a theoretical upper bound on the transducer power gain 16. Specifically, the transducer power gain of any lossless 2-port cannot exceed Fano's bound. Development of Fano's approach continued through the 1960s, However, computing

these bounds required solving a highly nonlinear system of multivariate inequalities amenable only for simple cases. In the early 1970s, Helton made the amazing connection between operator theory and electrical engineering. Powerful Hardy space techniques were coupled to the electrical engineer's Smith chart computations. In this framework, Nehari's Theorem gave an upper bound on the transducer power gain computable as an (easy) eigenvalue problem. This report shows that continuity conditions make this Nehari bound tight.
DTIC
*Impedance Matching; Electric Generators; Power Gain; Transducers*

**20010121958** California Univ., Lawrence Berkeley Lab., Berkeley, CA USA
**Submicron X-ray diffraction**
MacDowell, A.; Celestre, R.; Tamura, N.; Spolenak, R.; Valek, B.; Aug. 17, 2000; 21p; In English
Report No.(s): DE2000-764370; LBNL-45241; No Copyright; Avail: Department of Energy Information Bridge, Microfiche

At the Advanced Light Source in Berkeley the authors have instrumented a beam line that is devoted exclusively to x-ray micro diffraction problems. By micro diffraction they mean those classes of problems in Physics and Materials Science that require x-ray beam sizes in the sub-micron range. The instrument is for instance, capable of probing a sub-micron size volume inside micron sized aluminum metal grains buried under a silicon dioxide insulating layer. The resulting Laue pattern is collected on a large area CCD detector and automatically indexed to yield the grain orientation and deviatoric (distortional) strain tensor of this sub-micron volume. A four-crystal monochromator is then inserted into the beam, which allows monochromatic light to illuminate the same part of the sample. Measurement of diffracted photon energy allows for the determination of d spacings. The combination of white and monochromatic beam measurements allow for the determination of the total strain/stress tensor (6 components) inside each sub-micron sized illuminated volume of the sample.
NTIS
*Light Sources; Beams (Radiation); X Ray Diffraction*

**20010121961** California Univ., Lawrence Berkeley Lab., Berkeley, CA USA
**First synchrotron infrared beamlines at the Advanced Light Source: Spectromicroscopy and fast timing**
Martin, M. C.; McKinney, W. R.; Sep. 01, 1999; 10p; In English
Report No.(s): DE2000-764347; LBNL-44208; No Copyright; Avail: Department of Energy Information Bridge, Microfiche

Two recently commissioned infrared beamlines on the 1.4 bending magnet port at the Advanced Light Source, LBNL, are described. Using a synchrotron as an IR source provides three primary advantages: increased brightness, very fast light pulses, and enhanced far-IR flux. The considerable brightness advantage manifests itself most beneficially when performing spectroscopy on a microscopic length scale. Beamline (BL) 1.4.3 is a dedicated FTIR spectromicroscopy beamline, where a diffraction-limited spot size using the synchrotron source is utilized. BL 1.4.2 consists of a vacuum FTIR bench with a wide spectral range and step-scan capability. This BL makes use of the pulsed nature of the synchrotron light as well as the far-IR flux. Fast timing is demonstrated by observing the pulses from the electron bunch storage pattern at the ALS. Results from several experiments from both IR beamlines will be presented as an overview of the IR research currently being done at the ALS.
NTIS
*Light Sources; Infrared Radiation; Beams (Radiation)*

**20010121977** Sandia National Labs., Albuquerque, NM USA
**Design and Optimization of a Complete Stokes Polarimeter for the MWIR**
Dereniak, E. L.; Sabatke, D. S.; Locke, A. M.; Descour, M. R.; Sweatt, W. C.; Aug. 11, 2000; 8p; In English
Report No.(s): DE2000-761867; SAND2000-2042C; No Copyright; Avail: Department of Energy Information Bridge, Microfiche

A figure of merit for optimization of a complete Stokes polarimeter based on its measurement matrix is described from the standpoint of singular value decomposition and analysis of variance. It is applied to optimize a system featuring a rotatable retarder and fixed polarizer, and to study the effects of non-ideal retarder properties. A retardance of 132 degrees (approximately three-eighths wave) and retarder orientation angles of +/- 51.7 degrees and +/- 15.1 degrees are favorable when four measurements are used. An achromatic, form-birefringent retarder for the 3-5 micron spectral region has been fabricated and characterized. The effects of non-idealities in the form-birefringent retarder are moderate, and performance superior to that of a quarter-wave plate is expected.
NTIS
*Polarimeters; Design Optimization; Retarders (Devices)*

**20010122260** Argonne National Lab., IL USA

**Operation of the APS RD Gun**

Lewellen, J. W.; Sep. 11, 1998; 5p; In English

Report No.(s): DE2001-10801; ANL/ASD/CP-96444; No Copyright; Avail: Department of Energy Information Bridge, Microfiche

The Advanced Photon Source (APS) has a thermionic-cathode radio frequency (rf) gun system capable of providing beams to the APS linac. The gun system consists of a 1.6-cell thermionic-cathode rf gun, a fast kicker for beam current control, and an alpha magnet for bunch compression and injection into the APS linac line. This system is intended for use both as an injector for positron creation, and as a first beam source for the Low-Energy Undulator Test Line (LEUTL) project. The first measured performance characteristics of the gun are presented.

NTIS

*Radio Frequencies; Thermionic Cathodes; Electron Guns*

**20010122382** Argonne National Lab., IL USA

**New diffractometer for high energy synchrotron radiation at the elliptical multipole wiggler at the APS**

Ruett, U.; Aug. 06, 1998; 14p; In English

Report No.(s): DE2001-10703; ANL/MSD/CP-95961; No Copyright; Avail: Department of Energy Information Bridge, Microfiche

The use of high energy synchrotrons radiation (above 80 keV) for diffraction experiments offers many advantages resulting from the high penetration depth of the high energy photons and the small Bragg angles. The main features are: the possibility for the study of large sample crystals in transmission geometry, simple sample environments, high instrumental resolution in reciprocal space, the ability to utilize high momentum transfers and small correction factors for scattered intensities. The experiments performed at this kind of diffractometer are mainly flux experiments, in which the only requirement is a relatively small angular divergence for the incident beam in the scattering plane. The new triple crystal diffractometer introduced here will be installed at the elliptical multipole wiggler beamline at the Advanced Photon Source (APS), Because of the high critical energy of this device, 32 keV, the wiggler will produce high intensities at very high photon energies. to collect up to 1 mrad of the horizontal divergence of the beam, a bent annealed silicon monochromator will scatter and focus in the horizontal scattering plane. The diffractometer will be operated in the vertical scattering plane taking advantage of the small vertical beam divergence.

NTIS

*Diffractometers; Synchrotron Radiation; Aerospace Environments*

**20010122383** Fermi National Accelerator Lab., Batavia, IL USA

**Lattice determinations of the strange quark mass**

Ryan, S.; Aug. 25, 1999; 9p; In English

Report No.(s): DE2001-10343; FERMILAB-CONF-99/222-T; No Copyright; Avail: Department of Energy Information Bridge, Microfiche

The importance of the strange quark mass, as a fundamental parameter of the Standard Model (SM) and as an input to many interesting quantities, has been highlighted in many reviews, eg in Ref (1). A first principles calculation of m(sub s) is possible in lattice QCD but to date there has been a rather large spread in values from lattice calculations. This review aims to clarify the situation by explaining the particular systematic errors and their effects and illustrating the emerging consensus. In addition, a discussion of the strange quark mass is timely given the recent results from KTeV (2) and NA48 (3) for (epsilon)(prime)/(epsilon) which firmly establish direct CP-violation in the SM and when combined with previous measurements give a world average (epsilon)(prime)/(epsilon) (21:2 (+/-) 2:8) x 10(exp -4). This is in stark disagreement with the theoretical predictions which favor a low (epsilon)(prime)/(epsilon) (4). Although in principle (epsilon)(prime)/(epsilon) does not depend directly on m(sub s) in practice it has been an input in current phenomenological analyses. In this talk I will focus on some recent and careful lattice determinations of m(sub s), illustrating the reasons for the large spread in earlier results.

NTIS

*Quantum Chromodynamics; Quarks; Phenomenology*

**20010122394** BAE Systems, Nashua, NH USA

**Correlated Hopping Enhanced Spread Spectrum (CHESS) Study** ***Final Report, Jun. 2000-Feb. 2001***

Mills, Diane, BAE Systems, USA; August 2001; 54p; In English

Contract(s)/Grant(s): F30602-00-C-0157; DARPA ORDER-K037; Proj-CHES

Report No.(s): AD-A394991; AFRL-IF-RS-TR-2001-159; No Copyright; Avail: CASI; A04, Hardcopy; A01, Microfiche

This report describes a study to identify and quantify the advantages of Correlated Hopping Enhanced Spread Spectrum (CHESS) and enhanced-CHESS in the presence of Additive White Gaussian Noise and fading channels. Performance is compared to Direct Sequence Spread Spectrum and fixed frequency hopped methods.
DTIC
*Radio Equipment; Spread Spectrum Transmission; Frequencies*

**20010122642** Sandia National Labs., Albuquerque, NM USA
**Surface Morphology and Dynamics: Using Ab-Initio Total Energies to Make the Most of STM Data**
Feibelman,; Sep. 21, 2000; 14p; In English
Report No.(s): DE2000-763138; SAND2000-2321C; No Copyright; Avail: Department of Energy Information Bridge, Microfiche

Scanning Tunneling Microscopy (STM) has revolutionized surface science by providing atomic-resolution images of a broad range of surfaces, Still, STM data is often as challenging to interpret as any from the host of techniques used to understand surface structure and dynamics. I offer examples here that reveal the power of modem first-principles total-energy calculations to help derive maximum value from STM observations of surface morphology and its time-evolution, whether in the form of reliable, quantitative surface energetic information or a plausible mechanistic scenario.
NTIS
*Morphology; Scanning Tunneling Microscopy; Topology*

**20010122790** Arizona Univ., Dept. of Physics, Tucson, AZ USA
**Final Technical Report May 1, 1986-January 31, 1995 (Research in Theoretical High Energy Physics at University of Arizona)**
Jan. 31, 1995; 405p; In English
Report No.(s): DE2001-761217; DOE/ER/40213-12; No Copyright; Avail: Department of Energy Information Bridge

This document summarizes progress made on this project during the third year (February 1, 1994--January 31, 1995) of the current three-year grant period and outlines proposed renewal period activities of the theoretical high energy physics group at the University of Arizona.
NTIS
*Theoretical Physics; Universities; Arizona*

**20010122793** Los Alamos National Lab., NM USA
**Latest Results from the LSND Experiment**
Tayloe, R.; Feb. 14, 1999; 12p; In English
Report No.(s): DE2001-761202; LA-UR-99-2289; No Copyright; Avail: Department of Energy Information Bridge

The LSND experiment at Los Alamos has searched for anti-(nu)(sub (mu)) (r-arrow) anti-(nu)(sub e) oscillations using anti-(nu)(sub (mu)) from (mu)(sup +) decay at rest and (nu)(sub (mu)) (r-arrow) (nu)(sub e) oscillations using (nu)(sub (mu)) from (pi)(sup +) decay in flight. An excess of events attributable to neutrino oscillations has been observed in both of these channels in data collected in 1993-1995. A recent preliminary analysis of the decay at rest anti-(nu)(sub (mu)) (r-arrow) anti-(nu)(sub e) data collected in 1996-1998 with a different (nu) source configuration is consistent with the earlier data. The BooNE experiment that is planned to run at FNAL will further test these results.
NTIS
*Neutrinos; Oscillations; Detectors; Reaction Kinetics*

**20010122795** Los Alamos National Lab., NM USA
**Hyperon Particle Physics at the Joint Project**
Mischke, R. E.; Mar. 17, 1999; 16p; In English
Report No.(s): DE2001-761187; LA-UR-99-2267; No Copyright; Avail: Department of Energy Information Bridge

This paper presents a summary of information available on hyperon decays and some of the relevant physics issues for these decays.
NTIS
*Hyperons; Particle Decay; Field Theory (Physics)*

**20010122801** California Univ., Lawrence Berkeley Lab., Berkeley, CA USA

**Exploring the microscopic origin of exchange bias with photo-electron emission microscopy (PEEM)**

Scholl, A.; Nolting, F.; Stohr, J.; Regan, T.; Luning, J.; Jan. 22, 2001; 11p; In English

Report No.(s): DE2001-775145; LBNL-46504; No Copyright; Avail: Department of Energy Information Bridge

It is well known that magnetic exchange coupling across the ferromagnet--antiferromagnet interface results in a unidirectional magnetic anisotropy of the ferromagnetic layer, called exchange bias. Despite large experimental and theoretical efforts, the origin of exchange bias is still controversial, mainly because detection of the interfacial magnetic structure is difficult. We have applied photoelectron emission microscopy (PEEM) on several ferromagnet - antiferromagnet thin-film structures and microscopically imaged the ferromagnetic and the antiferromagnetic structure with high spatial resolution. Taking advantage of the surface sensitivity and elemental specificity of PEEM, the magnetic configuration and critical properties such as the Neel temperature were determined on LaFeO(sub 3) and NiO thin films and single crystals. On samples coated with a ferromagnetic layer, we microscopically observe exchange coupling across the interface, causing a clear correspondence of the domain structures in the adjacent ferromagnet and antiferromagnet. Field dependent measurements reveal a strong uniaxial anisotropy in individual ferromagnetic domains. A local exchange bias was observed even in not explicitly field-annealed samples, caused by interfacial uncompensated magnetic spins. These experiments provide highly desired information on the relative orientation of electron spins at the interface between ferromagnets and antiferromagnets.

NTIS

*Antiferromagnetism; Ferromagnetic Materials; Microscopy; Photoelectrons; Electron Emission*

**20010122828** Fermi National Accelerator Lab., Batavia, IL USA

**What, Why, and Who, is ICFA**

Rubinstein, R.; Oct. 24, 2000; 7p; In English

Report No.(s): DE2000-765653; FERMILAB-TM-2130; No Copyright; Avail: Department of Energy Information Bridge, Microfiche

ICFA (International Committee for Future Accelerators) plays an important role as a forum for discussions transcending national or regional boundaries on the future of high-energy accelerators and their associated particle physics, detectors and technology. It is probably true that, to paraphrase an old expression, if ICFA didn't exist, something very similar would have to be invented. As appeared to be true in the 1970s, projects in our field are becoming so large and costly that no single country or group of countries can carry them out alone; more and more international discussion and cooperation is needed. This will be especially relevant if the next major accelerator is a linear e + e - collider in the hundreds of GeV energy range.

NTIS

*Particle Accelerators; Theoretical Physics; Nuclear Research*

**20010122829** Fermi National Accelerator Lab., Batavia, IL USA

**Recent results from SELEX**

Russ, J. S.; Oct. 24, 2000; 3p; In English

Report No.(s): DE2000-765651; FERMILAB-CONF-00/252-E; No Copyright; Avail: Department of Energy Information Bridge, Microfiche

Charm physics explores QCD (quantum chromodynamics) phenomenology in both perturbative and nonperturbative regimes. Charm lifetime measurements test models based on 1/Mq QCD expansions and evaluate corrections from non-spectator W-annihilation and Pauli interference to perturbative QCD matrix elements. Production studies test leading order (LO) and next to leading order (NLO) perturbative QCD.

NTIS

*Quantum Chromodynamics; Charm (Particle Physics); Perturbation Theory*

**20010122830** Fermi National Accelerator Lab., Batavia, IL USA

**Top physics from Run 1 and Run 2 prospects at CDF**

Blusk, S. R.; Oct. 24, 2000; 3p; In English

Report No.(s): DE2000-765648; FERMILAB-CONF-00/241-E; No Copyright; Avail: Department of Energy Information Bridge, Microfiche

We present a summary of top quark physics results from Run 1. In addition to the precursory measurements of the top quark mass and cross section, we have performed a number of other analyses which test the consistency of the data sample with the standard model (SM). Deviations from SM expectations could provide hints for new physics. We show that the data are consistent with the SM. While the Run 1 data are statistically limited, we have shown that the systematic uncertainties are under control and

thus have layed the groundwork for higher precision tests of the SM in Run 2. This report describes the Run 1 top quark analyses and expectations and prospects for top quark measurements in Run 2.
NTIS
*Particle Collisions; Theoretical Physics; Research Facilities*

**20010122832** California Univ., Lawrence Berkeley Lab., Berkeley, CA USA
**RTA betatron-node experiment: Limiting cumulative BBU growth in a linear periodic system**
Lidia, S. M.; Houck, T. L.; Westenskow, G.; Aug. 01, 2000; 3p; In English
Report No.(s): DE2000-765497; LBNL-46703; No Copyright; Avail: Department of Energy Information Bridge, Microfiche

The successful operation of a Two-Beam accelerator based on extended relativistic klystrons hinges upon decreasing the cumulative dipole BBU (beam break up) growth from an exponential to a more manageable linear growth rate. The authors describe the theoretical scheme to achieve this, and a new experiment to test this concept. The experiment utilizes a 1-MeV, 600-Amp, 200-ns electron beam and a short beamline of periodically-spaced RF (radio frequency) dipole-mode pillbox cavities and solenoid magnets for transport. Descriptions of the beamline are presented, followed by theoretical studies of the beam transport and dipole-mode growth.
NTIS
*Klystrons; Electron Beams; Electric Dipoles*

**20010122876** Argonne National Lab., IL USA
**Symmetry breaking at magnetic surfaces and interfaces**
Qiu, Z. Q.; Nov. 20, 1998; 32p; In English
Report No.(s): DE2001-11055; ANL/MSD/CP-97486; No Copyright; Avail: Department of Energy Information Bridge, Microfiche

Examples represented of how symmetry breaking enters into consideration of the physical properties of magnetic surfaces and ultrathin films. The role of magnetic anisotropy is discussed to understand: (i) the existence of two-dimensional (2D) magnetic long-ranged order at finite temperature, (ii) magnetization scaling behavior at the Curie transition, (iii) the 2D spin reorientation transition, and (iv) step-induced magnetic behavior. Experimental examples cited include ultrathin magnetic Fe and Co overlayer and wedge structures grown onto single crystal substrates that are either flat or curved to produce vicinal surfaces with a continuous gradient in the step density. Also included is an example of an atomically flat manganite intergrowth that appears as a stacking fault in a bulk single crystal of a naturally layered structure.
NTIS
*Broken Symmetry; Single Crystals; Magnetization*

**20010122894** Argonne National Lab., IL USA
**Deep x-ray lithography fabrication of mm Wave cavities at the Advanced Photon Source**
Song, J. J.; Sep. 11, 1998; 5p; In English
Report No.(s): DE2001-10960; ANL/ASD/CP-97263; No Copyright; Avail: Department of Energy Information Bridge, Microfiche

Millimeter-wave (mmWave) accelerating cavity structures have been manufactured using the deep x-ray lithography (DXRL) technique. These cavity structures have potential applications as parts of linear accelerators, microwave undulatory, and mm-wave amplifiers. The microfabrication process includes manufacturing of precision x-ray masks, exposure of positive resist by x-rays through the mask, resist development, and electroforming of the final microstructure. Prototypes of a 32-cell, 108-GHz constant-impedance cavity and a 66-cell, 94-GHz constant-gradient cavity were fabricated at APS. Using an HP8510C 26-GHz vector network analyzer, rf measurements are being prepared with a frequency up- and down-converter before and after a test cavity structure. Preliminary design parameters for a 91-GHz multi-module klystron along with an overview of the DXRL technology are also discussed.
NTIS
*Cavity Resonators; Manufacturing; Lithography; Microstructure*

**20010122905** Fermi National Accelerator Lab., Batavia, IL USA
**Double Diffraction Dissociation in pbar-p Collisions at the Fermilab Tevatron**
Convery, M. E.; Nov. 01, 2000; 3p; In English
Report No.(s): DE2000-766387; FERMILAB-CONF-00/283-E; No Copyright; Avail: Department of Energy Information Bridge, Microfiche

We present results from a study of double diffraction dissociation in pp collisions at the Fermilab Tevatron performed by the CDF Collaboration. The production cross section for events with a central pseudorapidity gap (overlapping n=o) of width (carot)n greater than 3 is found to be 4.57 +0.02(stat)+99(syst) mb (5.45+0.02(stat)+1.10(syst) mb)at 3=630 (1800) GeV. Our results are compared with previous measurements and with predictions based on Regge theory and factorization.
NTIS
*Diffraction; Dissociation; Particle Collisions*

**20010122907** Fermi National Accelerator Lab., Batavia, IL USA
**Soft and Hard Interactions in p(bar p) Collisions at (radical)s = 1800 and 630 GeV**
Rimondi, F.; Oct. 31, 2000; 8p; In English
Report No.(s): DE2000-766205; FERMILAB-CONF-00/259-E; No Copyright; Avail: Department of Energy Information Bridge, Microfiche

Proton-antiproton events collected with the CDF minimum-bias trigger at (radical)(s) = 1800 and 630 GeV are studied splitting the full event sample in a soft subsample of events with no energy clusters above 1.1 GeV and in the subsample of the remaining events. Detailed and precise analyses of the multiplicity and transverse momentum distributions as well as of the correlation of the average pt and of its dispersion with the multiplicity are performed for the two samples. Comparisons of the results and of their dependence from the center of mass energy show clear differences in their behaviors. The results support important and unexpected scaling properties of the soft sample.
NTIS
*Collisions; Transverse Momentum; Proton Beams*

**20010122908** Fermi National Accelerator Lab., Batavia, IL USA
**Measurement of d(sigma)/dy for High Mass Drell-Yan e+ e- Pairs at CDF**
Bodek, A.; Oct. 31, 2000; 3p; In English
Report No.(s): DE2000-766203; FERMILAB-CONF-00/249-E; No Copyright; Avail: Department of Energy Information Bridge, Microfiche

Most measurements at high energy proton-antiproton colliders are performed in the central rapidity production region, yis less than 1. A model dependent extrapolation for y>1 is needed to extract the total cross section for hard processes such as top quark production or W and Z boson production. This extrapolation is made using Monte Carlo programs (e.g., PYTHIA), which incorporate quantum chromodynamics (QCD) calculations in leading order (LO) or next to leading order (NLO). A previous measurement of the rapidity distribution, d(sigma)/dy, for dimuon pairs in the Z-boson mass region was limited to yis less than 1. In this communication, we present the first measurement of d(sigma)/dy for e+e- pairs in the z-boson mass and high mass region over nearly the entire kinematic region of rapidity. At the Tevatron pp collider, the kinematic limit at the Z-boson mass is y = 3.0, while we measure y up to 2.8. The d(sigma)/dy distributions are compared to the predictions of QCD in LO and NLO. The measurement is also relevant for precision W boson mass measurements at hadron colliders, where W's reconstructed using ev and pv pairs from the Drell-Yan process.
NTIS
*Bosons; Proton-Antiproton Interactions; Quantum Chromodynamics*

**20010122909** Fermi National Accelerator Lab., Batavia, IL USA
**E781 Hyperon Beam and Targeting System**
Lach, J. T.; Oct. 31, 2000; 6p; In English
Report No.(s): DE2000-766200; FERMILAB-TM-2129; No Copyright; Avail: Department of Energy Information Bridge, Microfiche

The E781 beamline included a set of dipole magnets that directed the 800 GeV/c proton beam from the Tevatron onto a target just inside the aperture of the Hyperon magnet.
NTIS
*Hyperons; Magnets; Proton Beams*

**20010122912** Fermi National Accelerator Lab., Batavia, IL USA
**Estimates of Dispersive Effects in a Bent NLC Main Linac**
Syphershers, M.; Michelotti, L.; Oct. 31, 2000; 3p; In English
Report No.(s): DE2000-766190; FERMILAB-CONF-00/199; No Copyright; Avail: Department of Energy Information Bridge, Microfiche

An alternative being considered for the Next Linear Collider (NLC) is not to tunnel in a straight line but to bend the Main Linac into an arc so as to follow a gravitational equipotential. The authors begin here an examination of the effects that this would have on vertical dispersion, with its attendant consequences on synchrotron radiation and emittance growth by looking at two scenarios: a gentle continuous bending of the beam to follow an equipotential surface, and an introduction of sharp bends at a few sites in the linac so as to reduce the maximum sagitta produced.
NTIS
*Bending; Equipotentials; Linear Accelerators*

**20010122914** Thomas Jefferson National Accelerator Facility, Newport News, VA USA
**Measurements of the Deuteron Elastic Structure Function A(Q(sup 2)) at the Jefferson Laboratory**
Chudakov, E. A.; Sep. 01, 1998; 3p; In English
Report No.(s): DE2000-765741; JLAB-PHY-98-07; DOE/ER/40150-1756; No Copyright; Avail: Department of Energy Information Bridge, Microfiche

The deuteron elastic structure function A(Q(sup 2)) has been extracted in a range of 0.7 (le) Q(sup 2) (le) 6.0 (GeV/c)(sup 2) from measurements of elastic electron-deuteron cross section.
NTIS
*Particle Accelerators; Deuterons*

**20010122941** Brookhaven National Lab., Upton, NY USA
**RIKEN BNL Research Center Workshop on OSCAR II: Predictions for RHIC, Volume 22.**
Pang, Y.; Gyulassy, M.; Jun. 06, 2000; 259p; In English
Report No.(s): DE2000-767145; BNL-52591; KB0201; No Copyright; Avail: Department of Energy Information Bridge

The sessions discuss the need for and implementation of open standards for codes and routines for application to Relativistic Heavy Ion Collider (RHIC) physics. A critical review of the physics assumptions and algorithmic implementations of several of the OSCAR event generators are covered. The working groups members workshop objectives are to refine and extend the observables predicted for RHIC at QM99 and tests the hydrodynamic concepts and numerical simulations. The OSCAR needs of the RHIC experimental community is also discussed. The recent developments in parton (pre-hadronization) transport simulations that solve specific non-linear ultrarelativistic transport equations, speculative aspects of transport models, and the challenging aspects of AA dynamics are covered.
NTIS
*Partons; Computerized Simulation; Standardization*

**20010122943** Thomas Jefferson National Accelerator Facility, Newport News, VA USA
**Interactions, Currents and the Structure of Few-Nucleon Systems**
Schiavilla, R.; Oct. 01, 2000; 10p; In English
Report No.(s): DE2000-765543; JLAB-THY-00-32; DOE/ER/40150-1753,NUCL-TH/0010; No Copyright; Avail: Department of Energy Information Bridge, Microfiche

The current understanding of the structure of nuclei with up to A=8, including energy spectra, electromagnetic form factors, and weak transitions, is reviewed within the context of a realistic approach to nuclear dynamics based on two- and three-nucleon interactions and associated electro-weak currents. Low-energy radiative and weak capture reactions of astrophysical relevance involving these light systems are also discussed.
NTIS
*Nucleon-Nucleon Interactions; Nuclear Physics; Electron Capture*

**20010122945** Fermi National Accelerator Lab., Batavia, IL USA
**Jet Production at D-Zero**
Varelas, N.; Oct. 17, 2000; 3p; In English
Report No.(s): DE2000-765283; FERMILAB-CONF-00/237-E; No Copyright; Avail: Department of Energy Information Bridge, Microfiche

The authors report on a new measurement of the rapidity dependence of the inclusive jet production cross section in p(bar p) collisions at (radical)s = 1:8 TeV using 92 pb(sup (minus)1) of data collected by the DO detector at the Tevatron collider. The differential cross sections, d(sup 2)(sigma)/dE(sub T)d(eta) are presented as a function of jet transverse energy (E(sub T)) in five pseudorapidity ((eta)) intervals, up to (vert bar)(eta)(vert bar) = 3, significantly extending previous measurements beyond (vert bar)(eta)(vert bar) = 0.7. They also present recent results on the ratio of central ((vert bar)(eta)(vert bar) 0.5) inclusive cross

sections from two center-of-mass energies, 0.63 TeV and 1.8 TeV, as a function of jet x(sub T). Experimental results are compared to next-to-leading order QCD predictions.
NTIS
*Proton-Antiproton Interactions; Collisions*

**20010123030** Fermi National Accelerator Lab., Batavia, IL USA
**Design and construction of the CDF central outer tracker**
Burkett, K.; Nov. 14, 2000; 3p; In English
Report No.(s): DE2000-767237; FERMILAB-CONF-00/128-E; No Copyright; Avail: Department of Energy Information Bridge
A new tracking chamber, the Central Outer Tracker (COT), has been built as part of the upgrade of the CDF (Collider Detector Facility) detector at the Fermilab Tevatron. The COT is a cylindrical open-cell drift chamber, segmented into 96 layers. High voltage and readout electronics are mounted on the chamber endplates, providing timing and charge deposition information. The COT is designed to operate in the high luminosity environment of the upgraded Tevatron. With the addition of the Main Injector and the Recycler Ring, the Tevatron will be capable of providing luminosity as high as 2 X 10 (sup 32) cm(sup -2) s(sup -1) at a bunch spacing of 132 ns. We discuss the design of the detector, as well as the assembly. Construction of the COT was completed in Spring 2000, and the first data will be taken during a commissioning run in late Summer 2000.
NTIS
*Research Facilities; Particle Accelerators; Detection; Tracking (Position)*

**20010123032** Brookhaven National Lab., Upton, NY USA
**Rare kaon decays**
Littenberg,; Mar. 11, 2000; 11p; In English
Report No.(s): DE2000-767192; BNL-67772; No Copyright; Avail: Department of Energy Information Bridge
The current status of the study of rare kaon decays is reviewed. Future prospects are discussed.
NTIS
*Kaons; Particle Decay*

**20010123033** Brookhaven National Lab., Upton, NY USA
**Multiparticle simulation of adiabatic excitation of longitudinal parametric resonances**
Brown,; Bai,; Fischer,; Roser,; Sep. 11, 2000; 9p; In English
Report No.(s): DE2000-767190; BNL-67485; No Copyright; Avail: Department of Energy Information Bridge
In order to further understand phenomena observed during studies of adiabatic excitation of longitudinal bunch shape oscillations, we have developed a simple simulation using a one-turn map. In this report we will present the physical foundations for the simulation and the methods used in the simulator. We will present simulations using parameters of actual experiments, along with the corresponding experimental results.
NTIS
*Adiabatic Conditions; Excitation; Simulation*

**20010123034** Brookhaven National Lab., Upton, NY USA
**Heating of nuclear matter and multifragmentation: antiprotons vs. pions**
Beaulieu,; Lefort,; Gushue,; Remsberg,; Jan. 09, 1999; 14p; In English
Report No.(s): DE2000-767186; BNL-67736; No Copyright; Avail: Department of Energy Information Bridge
The 'quest' for the liquid gas phase transition in nuclear matter using heavy ion collisions at intermediate energies has been punctuated by heated debates in recent years, ranging from the very small cross section for fusion of the two partners to the dominance of dynamical effects over thermal equilibrium.
NTIS
*Antiprotons; Pions; Nucleons; Particle Collisions; Heavy Ions*

**20010123035** Brookhaven National Lab., Upton, NY USA
**Further studies on the prospects for many-tev muon colliders**
King,; Sep. 20, 2000; 4p; In English
Report No.(s): DE2000-767182; BNL-67742; No Copyright; Avail: Department of Energy Information Bridge
New self-consistent parameter sets are presented and discussed for muon collider rings at center-of-mass energies of 10, 30 and 100 TeV. All three parameter sets attain luminosities of L = 3 x 10(sup 35) cm(sup -2) .s(sup -l). The parameter sets benefit

from new insights gained at the HEMC (High Energy Muon Collider) '99 workshop that considered the feasibility of many-TeV muon colliders.
NTIS
*Muons; Storage Rings (Particle Accelerators)*

**20010123037** Brookhaven National Lab., Upton, NY USA
**Muscat: The muon scattering experiment**
Attwood,; Bell,; McMahon,; Wilson,; Fernow,; Sep. 20, 2000; 10p; In English
Report No.(s): DE2000-767180; BNL-67710; No Copyright; Avail: Department of Energy Information Bridge
The MUSCAT (mesoscale chemistry-transport model) experiment has been created to measure the one dimensional (1-D) scattering distribution of muons in the momentum range 100-180 Me V/c from a number of elements of low atomic number. These measurements will be used to test various multiple scattering theories employed in ionization cooling studies and elsewhere.
NTIS
*Muons; Scattering*

**20010123038** Brookhaven National Lab., Upton, NY USA
**Polarization effects in the front end of the neutrino factory**
Fernow,; Gallardo,; Fukui,; Sep. 20, 2000; 9p; In English
Report No.(s): DE2000-767179; BNL-67711; No Copyright; Avail: Department of Energy Information Bridge
We summarize the methods used for simulation of polarization effects in the front end of a possible neutrino factory. We first discuss the helicity of muons in the pion decay process. We find that, neglecting acceptance considerations, the average helicity asymptotically approaches a magnitude of 0.185 at large pion momenta. Next we describe the methods used for tracking the spin through the complicated electromagnetic field configurations in the front end of the neutrino factory, including rf (radio frequency) phase rotation and ionization cooling channels. Various depolarizing effects in matter are then considered, including multiple Coulomb scattering and elastic scattering from atomic electrons. Finally, we include all these effects in a simulation of a 480 m long, double phase rotation front end scenario.
NTIS
*Muons; Neutrinos; Polarization (Spin Alignment)*

**20010123039** Brookhaven National Lab., Upton, NY USA
**Riken bnl research center workshops on predictions and uncertainties for rhic spin physics and event generator for rhic spin physics iii - towards precision spin physics at rhic - march 6-31, 2000**
Qiu,; Saito,; Schafer,; Vogelsang,; Mar. 31, 2000; 235p; In English
Report No.(s): DE2000-767174; BNL-52596; No Copyright; Avail: Department of Energy Information Bridge
This volume archives the presentations made at the joint RIKEN BNL (Brookwood National Laboratory) Research Center workshops on 'Predictions and Uncertainties for RHIC Spin Physics' and 'Event Generator for RHIC Spin Physics III - towards precision spin physics at RHIC', held in March 2000 at BNL. The RHIC (Relativistic Heavy Ion Collider) spin physics program will start in early 2001. RHIC-Spin will be the first polarized-proton collider and will thus represent a new and unique laboratory for studying the spin structure of the proton. There are important further applications of RHIC-Spin, among them the search for physics beyond the Standard Model. The RHIC spin program will mark a completely new era of spin physics and hadron physics because of its high energy, high luminosity, and high polarization, and because of the versatility of the machine.
NTIS
*Theoretical Physics; Particle Spin; Heavy Ions; Ionic Collisions*

**20010123040** Brookhaven National Lab., Upton, NY USA
**X-ray Resonant Scattering Studies of Charge and Orbital Ordering in Pr(sub 1-x)Ca(sub x)MnO(sub 3)**
Zimmermann,; Nelson,; Hill,; Gibbs,; Blume,; Aug. 14, 2000; 17p; In English
Report No.(s): DE2000-767169; BNL-67705; No Copyright; Avail: Department of Energy Information Bridge
We present the results of x-ray scattering studies of the charge and orbital ordering in the manganite series Pr(sub 1(minus)z), Ca(sub x), MnO(sub 3) with x = 0.25, 0.4 and 0.5. The polarization and azimuthal dependence of the charge and orbital ordering in these compounds is characterized both in the resonant and nonresonant limits, and compared with the predictions of current theories. The results are qualitatively consistent with both cluster and LDA+U calculations of the electronic structure.
NTIS
*Magnetic Materials; Scattering; Manganese Compounds*

**20010123045** Brookhaven National Lab., Upton, NY USA

**AGS Proposal 923: Search for T Violating Muon Polarization in Kappa(+) Yields mu(+)pi(0)nu mu Decay**

Diwan, M. V.; Frank, J.; Gordeev, A.; Kettell, S.; Leipuner, L.; Sep. 30, 1996; 87p; In English

Report No.(s): DE2000-767153; BNL-67611; KA0401; No Copyright; Avail: Department of Energy Information Bridge

We propose a new search for the time reversal violating polarization of the muon normal to the decay plane of the decay. The value of such a polarization in the Standard Model is zero. However, it is now accepted that the baryon asymmetry of the universe requires a source of CP (charge conjugate and parity transformation) violation stronger than that embodied in the quark mixing matrix. Models of non-standard CP violation that produce the baryon asymmetry could also produce effects observable in the transverse polarization. Moreover, because of the very high sensitivity of the experiment the possibility of discovering unexpected new physics should not be underestimated.

NTIS

*Muons; Particle Decay; Nuclear Physics*

**20010123048** Brookhaven National Lab., Upton, NY USA

**Rare Kaon Decay Experiments**

Kettell, S.; May 12, 2000; 7p; In English

Report No.(s): DE2000-767148; BNL-67589; KA0401; No Copyright; Avail: Department of Energy Information Bridge

The current status of rare kaon decay experiments is reviewed. A large number of new results are available from several very sensitive experiments at Brookhaven National Laboratory, Fermi National Acceleration Laboratory, and CEBN. New limits in the search for Lepton Flavor Violation are discussed, as are new measurements of the Cabibbo-Kobayashi-Maskawa matrix.

NTIS

*Kaons; Decay*

**20010123049** Brookhaven National Lab., Upton, NY USA

**Developments in Rare Kaon Decay Physics**

Barker, A. R.; Kettell, S. H.; Dec. 01, 2000; 47p; In English

Report No.(s): DE2000-767147; BNL-67590; KA0401; No Copyright; Avail: Department of Energy Information Bridge

We review the current status of the field of rare Kahn decays. The study of rare kaon decays has played a key role in the development of the standard model, and the field continues to have significant impact. The two areas of greatest import are the search for physics beyond the standard model and the determination of fundamental standard-model parameters. Due to the exquisite sensitivity of rare kaon decay experiments, searches for new physics can probe very high mass scales. Studies of the K + xvrii modes in particular, where the first event has recently been seen, will permit tests of the standard-model picture of quark mixing and CP violation.

NTIS

*Kaons; Models; Quarks*

**20010123050** Brookhaven National Lab., Upton, NY USA

**ERHIC Workshop (2nd) Workshop Proceedings. Held at Yale University on June 21, 2000**

Venugopalan, A.; Apr. 04, 2000; 423p; In English

Report No.(s): DE2000-767146; BNL-52592; KB03; No Copyright; Avail: Department of Energy Information Bridge

This Workshop on eRHIC (Relativistic Heavy Ion Collider) at Yale is the second one on the topic of studying electron-nucleon and electron-nucleus collisions at Brookhaven National Laboratory (BNL) using the RHIC rings and an additional electron ring to be built in the RHIC tunnel. This facility is designated eRHK. The first workshop was held at BNL on December 3-4, 1999 and focused primarily on the physics motivations for electron-ion(e-A) scattering at eRHIC. The present workshop at Yale deals with e-A physics as well as polarized e-p physics. In addition, the accelerator design options for the electron ring in the RHIC tunnel were discussed in some detail. The conceptual design for a e-p/A collider detector for eRHIC were considered for the first time. It is expected that in the next few months, through formal and informal meetings of those who attended this workshop, a more detailed physics program possible at RHIC will be developed. A third workshop will take place at BNL from June 26 to July 14.

NTIS

*Conferences; Design Analysis; Electron Scattering*

**20010123053** Brookhaven National Lab., Upton, NY USA

**Beam Profile Measurements on RHIC**

Connolly, R.; Michnoff, R.; Moore, T.; Shea, T.; Tepikian, S.; Jun. 02, 2000; 6p; In English

Report No.(s): DE2000-767141; BNL-67475; KC0204019; No Copyright; Avail: Department of Energy Information Bridge

The Relativistic Heavy Ion Collider (RHIC) at Brookhaven National Lab was commissioned during the summer of 1999. Transverse beam profiles on RHIC are measured with ionization profile monitors (IPMs). An IPM measures beam profiles by collecting the electrons liberated by residual gas ionization by the beam. The detector is placed in the gap of a dipole magnet to force the electrons to travel in straight lines from the beamline center to the collector. One IPM was tested and it measured the profiles of a single gold bunch containing 108 ions on consecutive turns. We show an example of one of these profiles giving transverse emittance. Also several profiles are combined into a mountain-range plot which shows betatron oscillations at injection.

NTIS

*Monitors; Particle Beams; Dynamic Characteristics*

**20010123054** Brookhaven National Lab., Upton, NY USA

**SNS Project-Wide Beam Current Monitors**

Kesselman, M.; Witkover, R.; Doolittle, L.; Power, J.; May 03, 2000; 8p; In English

Report No.(s): DE2000-767140; BNL-67457; No Copyright; Avail: Department of Energy Information Bridge

A consortium of national laboratories are constructing the Spallation Neutron Source (SNS) to be installed at Oak Ridge National Laboratory. There are signal similarities that exist in the beam diagnostic instrumentation that could permit common designs. This paper will focus on the beam current monitoring requirements, and the methods beam current in various locations throughout the SNS facility.

NTIS

*Beam Currents; Neutron Sources; Spallation; Fabrication*

**20010123055** Brookhaven National Lab., Upton, NY USA

**Intra-Undulator Measurements at VISA FEL**

Murokh, A.; Frigola, P.; Johnson, E.; Wang, X. J.; Yakimenko, V.; Aug. 13, 2000; 4p; In English

Report No.(s): DE2000-767128; BNL-67738; KA0403000; No Copyright; Avail: Department of Energy Information Bridge

We describe a diagnostics system developed, to measure exponential gain properties and the electron beam dynamics inside the strong focusing 4-m long undulator for the VISA (Visible to Infrared SASE (self-amplification of spontaneous emission) Amplifier) free-electron laser (FEL). The technical challenges included working inside the small undulator gap, optimizing the electron beam diagnostics in the high background environment of the spontaneous undulator radiation, multiplexing and transporting the photon beam. Initial results are discussed.

NTIS

*Diagnosis; Free Electron Lasers; Infrared Lasers*

**20010123057** Brookhaven National Lab., Upton, NY USA

**Photo-Electron Beam Longitudinal Phase Space Tomography Studies at the ATF**

Kashiwagi, S.; Washio, M.; Wang, X. J.; Ben-Zvi, I.; Malone, R.; Aug. 20, 2000; 5p; In English

Report No.(s): DE2000-767126; BNL-67740; KA0403000; No Copyright; Avail: Department of Energy Information Bridge

The longitudinal phase space distribution of electron beam plays critical role in ultrashort electron bunch production, coherent radiation, free electron laser (FEL), and many other applications. Photocathode radio frequency (RF) gun is capable of not only controlling the transverse emittance of electron beam, but also longitudinal emittance. The longitudinal phase space distribution of photoelectron beam was investigated at the Brookhaven Accelerating Test Facility (BNL-ATF) using tomography technique. The longitudinal phase space distribution is reconstructed by measuring the energy spectrums of the beam for different RF phase. We will first briefly describe the principle of tomography technique and the ATF experiment set-up. The longitudinal emittance as function of RF gun phase was measured first time. The longitudinal emittance growth caused by the space charge effect was observed.

NTIS

*Electron Beams; Emittance; Photocathodes; Spatial Distribution*

**20010123097** Brookhaven National Lab., Upton, NY USA
**Measurement of Beta(Kappa(+) Yields pi(+)nu nu(bar))**
Kettell,; May 22, 2000; 6p; In English
Report No.(s): DE2000-767157; BNL-67630; No Copyright; Avail: Department of Energy Information Bridge

The experimental measurement of K(+) that yields pi(+) nu-nu(bar) is reviewed. New results from experiment E787 at Brookhaven National Laboratory are presented: with data from 1995-97 the branching ratio has been measured to be B(K(+) that yields pi(+) nu-nu(bar) = (1.5(sub -1.2)(sup +3.4)) x 10(exp -10). The future prospects for additional data in this mode are examined.
NTIS
*Nuclear Physics; Branching (Physics)*

**20010123135** Brookhaven National Lab., Upton, NY USA
**High-Resolution Beam Profile Monitor R and D at the BNL ATF**
Wang, X. J.; Ben-Zvi, I.; Malone, R.; Yakimenko, V.; Jun. 26, 2000; 5p; In English
Report No.(s): DE2000-767103; BNL-67636; KA0403000; No Copyright; Avail: Department of Energy Information Bridge

Beam profile monitor (BPM) is widely used at the Brookhaven accelerator test facility (ATF) for machine operation and beam studies. BPM is also critical for many ATF experiments, such as laser acceleration and single pass FEL (free electron laser) experiments where both laser and electron beams profiles and positions measurements are required. We will first describe at ATF video and BPM system, the performance of the BPM is presented. The two-lens telescope optics was adopted for the most ATF BPM optics, the experimental data for variable resolution BPM is presented from laser acceleration experiment Stella. We will also present two special BPM, one is the BPM and Faraday combination for photocathode RF (radio frequency) gun injection system, and other is dual arm OTR (Optical Transition Radiation) BPM.
NTIS
*Monitors; Free Electron Lasers; Laser Beams*

**20010123139** Brookhaven National Lab., Upton, NY USA
**SNS project-wide beam current monitors**
Kesselman, M.; Witkover, R.; Doolittle, L.; Power, J.; May 03, 2000; 8p; In English
Report No.(s): DE2000-767083; BNL-67457; No Copyright; Avail: Department of Energy Information Bridge

A consortium of national laboratories is constructing the Spallation Neutron Source (SNS) to be installed at Oak Ridge National Laboratory. There are signal similarities that exist in the beam diagnostic instrumentation that could permit common designs. This paper will focus on the beam current monitoring requirements, and the methods under consideration to measure beam current in various locations throughout the SNS facility.
NTIS
*Beam Currents; Spallation*

**20010123140** Los Alamos National Lab., NM USA
**Chain-Length Distribution in Subcritical Systems**
Nolen, S. D.; Jun. 01, 2000; 128p; In English
Report No.(s): DE2000-766762; LA-13721-T; No Copyright; Avail: Department of Energy Information Bridge

The individual fission chains that appear in any neutron multiplying system provide a means, via neutron noise analysis, to unlock a wealth of information regarding the nature of the system. This work begins by determining the probability density distributions for fission chain lengths in zero-dimensional systems over a range of prompt neutron multiplication constant (K) values. This section is followed by showing how the integral representation of the chain-length distribution can be used to obtain an estimate of the system's subcritical prompt multiplication (MP). The lifetime of the chains is then used to provide a basis for determining whether a neutron noise analysis will be successful in assessing the neutron multiplication constant, k, of the system in the presence of a strong intrinsic source. A Monte Carlo transport code, MC++, is used to model the evolution of the individual fission chains and to determine how they are influenced by spatial effects. The dissertation concludes by demonstrating how experimental validation of certain global system parameters by neutron noise analysis may be precluded in situations in which the system K is relatively low and in which realistic detector efficiencies are simulated.
NTIS
*Chains; Density Distribution; Fission; Neutrons*

**20010123142** Princeton Univ., Plasma Physics Lab., NJ USA

**Numerical Study of Global Stability of Oblate Field-Reversed Configurations**

Belova, E. V.; Jardin, S. C.; Ji, H.; Yamada, M.; Kulsrud, R.; Oct. 27, 2000; 31p; In English

Report No.(s): DE2000-766640; PPPL-3500; No Copyright; Avail: Department of Energy Information Bridge

Global stability of the oblate (small elongation) Field-Reversed Configuration (FRC) has been investigated numerically using both three-dimensional magnetohydrodynamic (MHD) and hybrid (fluid electrons and kinetic ions) simulations. For every non-zero value of the toroidal mode number n, there are three MHD modes that must be stabilized. For n = 1, these are the interchange, the tilt and the radial shift; while for n*1 these are the interchange and two co-interchange modes with different polarization. It is shown that the n = 1 tilt mode becomes an external mode and it can be effectively stabilized by close-fitting conducting shells, even in the small Larmor radii (MHD) regime. The tilt mode stability improves with increasing oblateness, however at sufficiently small elongations the radial shift mode becomes more unstable than the tilt mode. The interchange mode stability is strongly profile dependent, and all n*1 interchange modes can be stabilized for a class of pressure profile with separatrix beta larger than 0.035. Our results show that all three n = 1 modes can be stabilized in the MHD regime, but the stabilization of the co-interchange modes still remains an open question.

NTIS

*Attitude (Inclination); Magnetic Field Configurations; Magnetohydrodynamics; Stability*

**20010123143** Princeton Univ., Plasma Physics Lab., NJ USA

**Experimental Study of Ion Heating and Acceleration During Magnetic Reconnection**

Hsu, S. C.; Carter, T. A.; Fiksel, G.; Ji, H.; Kulsrud, R. M.; Oct. 24, 2000; 48p; In English

Report No.(s): DE2000-766638; PPPL-3499; No Copyright; Avail: Department of Energy Information Bridge

Ion heating and acceleration has been studied in the well-characterized reconnection layer of the Magnetic Reconnection Experiment. Ion temperature in the layer rises substantially during null-helicity reconnection in which reconnecting field lines are anti-parallel. The plasma out flow is sub-Alfvonic due to a downstream back pressure. An ion energy balance calculation based on the data and including classical viscous heating indicates that the ions are heated largely due to non-classical mechanisms. The Ti rise is much smaller during co-helicity reconnection in which field lines reconnect obliquely. This is consistent with a slower reconnection rate and a smaller resistivity enhancement over the Spitzer value. These observations indicate strongly that non-classical dissipation mechanisms can play an important role both in heating the ions and in facilitating the reconnection process.

NTIS

*Energy Budgets; Heating; Magnetic Field Reconnection*

**20010123217** Fermi National Accelerator Lab., Batavia, IL USA

**B and D mesons in lattice QCD**

Kronfeld, A. S.; Oct. 17, 2000; 7p; In English

Report No.(s): DE2000-765299; FERMILAB-CONF-00/256-T; No Copyright; Avail: Department of Energy Information Bridge, Microfiche

Computational and theoretical developments in lattice QCD calculations of B and D mesons are surveyed. Several topical examples are given: new ideas for calculating the HQET parameters (bar (Lambda)) and (lambda)(sub 1); form factors needed to determine (vert bar)V(sub cb)(vert bar) and (vert bar)V(sub ub)(vert bar); bag parameters for the mass differences of the B mesons; and decay constants. Prospects for removing the quenched approximation are discussed.

NTIS

*Mesons; Quantum Chromodynamics*

**20010123218** Fermi National Accelerator Lab., Batavia, IL USA

**Random walk through models of nonlinear clustering**

Sheth, R. K.; Oct. 17, 2000; 12p; In English; Sponsored in party by the US DOE Energy Information Administration

Report No.(s): DE2000-765285; FERMILAB-CONF-00/253-A; No Copyright; Avail: Department of Energy Information Bridge, Microfiche

The authors present a few simple models of the mass function of collapsed objects. The emphasis is on apparently unrelated models which end up giving the same answer for the number density and merger histories of virialized clumps. They also comment briefly on models of the spatial distribution of the clumps, and how they can be used to model the spatial distribution of the mass.

NTIS

*Mathematical Models; Mass Distribution; Spatial Distribution; Nonlinearity*

**20010123225** Los Alamos National Lab., NM USA
**Microcanonical Ensembles and Molecular Dynamics**
Baker, G.; Johnson, J.; Feb. 01, 2000; 8p; In English
Report No.(s): DE2000-763358; LA-UR-00-812; No Copyright; Avail: Department of Energy Information Bridge
We show that the O(Nsup -1) finite-size correction derived by Ray and Zhang can be arrived at in an alternate and simpler way. An application to the hard-sphere system inspires a quasi-ergodic hypothesis linking the molecular dynamics averages to those of the appropriate microcanonical ensemble.
NTIS
*Molecular Dynamics; Ergodic Process*

**20010123228** Los Alamos National Lab., NM USA
**Globally Optimized Fourier Finite-Difference Migration Method**
Fehler, M.; Huang, L.; Jan. 01, 2000; 5p; In English
Report No.(s): DE2000-763348; LA-UR-00-786; No Copyright; Avail: Department of Energy Information Bridge
To image complex structures with strong lateral velocity variations and steep dips, we use a rational approximation of the square-root operator in the one-way wave equation to develop a globally optimized Fourier finite-difference method. The two coefficients in the rational approximation are obtained by an optimization scheme that maximizes the maximum dip angle of the Fourier finite-difference method for a given model. Our optimized method uses the same coefficients throughout a model in contrast to Ristow-Ruhl's locally optimized Fourier finite difference scheme which uses coefficients varying with lateral velocity contrast. The table of coefficients could be huge for a highly accurate optimized scheme. The computational cost of our optimized method is the same as other Fourier finite difference methods. Our optimized method is accurate for dips with angles of approximately 15 degrees larger than that of Ristow-Ruhl's unoptimized Fourier finite-difference method, while Ristow-Ruhl's optimized scheme can handle approximately 16 degrees larger dip angles than their unoptimized scheme.
NTIS
*Coefficients; Finite Difference Theory; Migration; Fourier Analysis*

**20010123229** Sandia National Labs., Albuquerque, NM USA
**New Linear Inductive Voltage Adder Driver for the Saturn Accelerator**
Mazarakis,; Spielman,; Struve,; Long,; Sep. 25, 2000; 5p; In English
Report No.(s): DE2000-763347; SAND2000-2343C; No Copyright; Avail: Department of Energy Information Bridge
Saturn is a dual-purpose accelerator. It can be operated as a large-area flash x-ray source for simulation testing or as a Z-pinch driver especially for K-line x-ray production. In the first mode, the accelerator is fitted with three concentric-ring 2-MV electron diodes, while in the Z-pinch mode the current of all the modules is combined via a post-hole convolute arrangement and driven through a cylindrical array of very fine wires. We present here a point design for a new Saturn class driver based on a number of linear inductive voltage adders connected in parallel. A technology recently implemented at the Institute of High Current Electronics in Tomsk (Russia) is being utilized.
NTIS
*X Ray Sources; Zeta Pinch; Linear Accelerators*

**20010123251** Department of Energy, Oak Ridge, TN USA
**Nuclear Studies with Intermediate Energy Probes. Final Report**
Norum, B. E.; Aug. 23, 2000; 21p; In English
Report No.(s): DE2001-762258; No Copyright; Avail: Department of Energy Information Bridge
Outlines research in intermediate energy nuclear physics.
NTIS
*Nuclear Physics; Energy Technology; Probes*

**20010123254** Texas Univ., Austin, TX USA
**Studies in Medium Energy Physics. Final technical report**
Hoffmann, G. W.; Ray, R. L.; McDonough, J.; Betts, W.; Chen, X.; Sep. 01, 1994; 167p; In English
Report No.(s): DE2001-761656; DE/ER/40444-6; No Copyright; Avail: Department of Energy Information Bridge
This document constitutes the (1991 - 1994) technical Progress Report for the ongoing medium/high energy nuclear physics research program supported by the U.S. Department of Energy. The experiments discussed were/are conducted at the Los Alamos National Laboratorys (LANL) Clinton P. Anderson Meson Physics Facility (LAMPF) and the Alternating Gradient Synchrotrons

(AGS) facility of the Brookhaven National Laboratory (BNL). Considerable design, fabrication, setup, testing, and support work was/is done at The University of Texas at Austin as part of the research program. The overall motivation for the work done over the past three years was driven by four main objectives: (1) provide proton-nucleon and proton-nucleus scattering data which serve to facilitate the study of effective two-body interactions, test (and possibly determine) nuclear structure, and help study reaction mechanisms and dynamics; (2) provide unique, first-of-a-kind exploratory proton-nucleus scattering data in the hope that such data will lead to discovery of new phenomena and new physics; (3) perform precision tests of fundamental interactions, such as rare decay searches, whose observation would imply new physics; and, (4) begin work associated with the Solenoidal Tracker at RHIC (STAR) project at the Relativistic Heavy-Ion Collider (RHIC) and phase in major work associated with relativistic heavy ion physics.
NTIS
*Energy Technology; High Energy Interactions; Reaction Kinetics; Synchrotrons; Nuclear Physics*

**20010123256** Los Alamos National Lab., NM USA
**Pi(sup+) Decay of Light Hypernuclei**
Gibson, B. F.; Feb. 19, 1999; 13p; In English
Report No.(s): DE2001-761231; LA-UR-99-2294; No Copyright; Avail: Department of Energy Information Bridge

The observed (pi)(sup +) emission from the weak decay of the (sup 4)(sub (Lambda))He hypernucleus has been an intriguing puzzle for more than 30 years, because the Lambda decays in free space only by emission of a (pi)(sup (minus)) or a (pi)(sup 0). We re-examine this puzzling weak decay with our focus upon a decay mechanism involving the (Sigma)(sup +)N (r-arrow) (pi)(sup +)nN decay of a virtual (Sigma)(sup +), stemming from (Lambda)N to (Sigma)N conversion (mixing) within the hypernucleus. We emphasize the observed energy distribution of the observed (pi)(sup +)s compared to that of (pi)(sup -)s in standard mesonic decay as well as the isotropic angular distribution of the (pi) (sup +)s. Competing suggestions to explain the positive pion weak decay have been offered. A possible search for (pi)(sup +) decay from the other (Lambda) hypernuclei is explored as means to test our hypothesis.
NTIS
*Hypernuclei; Particle Decay; Electron Energy; Theoretical Physics*

**20010123260** Brookhaven National Lab., Upton, NY USA
**Development of a Novel Superconducting RF Photocathode Electron Gun**
Cole, M.; Bluem, H.; Rathke, J.; Schultheiss, J.; Ben-Zvi, I.; Aug. 21, 2000; 4p; In English
Report No.(s): DE2000-767294; BNL-67644; No Copyright; Avail: Department of Energy Information Bridge

Over the past year Advanced Energy Systems Inc, and Brookhaven National Laboratory have undertaken a program to develop a Superconducting Photocathode Electron Gun utilizing a unique cathode concept. The cathode concept is much simpler than many other approaches and should avoid many complications which might otherwise be encountered. This cathode concept does not utilize an insert of any kind and is fully integrated with the Nb cavity. The results of experiments which demonstrate the feasibility of the cathode concept will be presented. We will review the important gun design parameters, discuss how they play against each other, and present results of an optimization of the design. Anticipated beam output parameters will be given, based on the optimized design and experimental results. Finally we will review our plans to continue the development program. This program will include the design and fabrication of the cavity and associated cryostat at Advanced Energy Systems Inc, integration of the entire system, and testing of the full system at BNL.
NTIS
*Electron Guns; Photocathodes; Superconductivity; Design Analysis; Design Optimization*

**20010123262** Brookhaven National Lab., Upton, NY USA
**Future Kaon Programs at BNL, FNAL**
Kettell, S. H.; May 22, 2000; 6p; In English
Report No.(s): DE2000-767292; BNL-67629; No Copyright; Avail: Department of Energy Information Bridge

Future kaon decay programs at BNL (Brookhaven National Laboratory) and FNAL (Fermi National Accelerator Laboratory) are discussed. The primary focus of these programs is the measurement of the golden modes, K: -+ n(sup 1)v and K+ -/+ m+VD . The observation of K+ -+ T+VD by E787 at BNL is the first step in a series of measurements which will completely determine the unitarity triangle within the kaon system. The next step after E787 in the measurement of B(K+ + n+vfi) will be the E949 experiment at BNL that is currently under construction. This experiment, building on the experience of E787 and making use of the intense AGS (Alternating Gradient Synchrotron) proton beam, is scheduled to run in FY01L03 and to observe 0(10) SM (standard model) events with a small and well-understood background. The proposed CKM (Cabibbo-Kobayashi-Maskawa)

experiment at JNAL (Jefferson National Accelerator Laboratory) would take the next step, using a decay-in-flight technique and a 22 GeV/c RF (radio frequency)-separated kaon beam from the Main Injector, to observe 0(100) SM events.
NTIS
*Kaons; Nuclear Physics; Synchrotrons*

**20010123263** Fermi National Accelerator Lab., Batavia, IL USA
**Physics potential and status of D-Zero upgrade at Fermilab**
Yu, J.; Nov. 14, 2000; 3p; In English
Report No.(s): DE2000-767254; FERMILAB-CONF-00/275-E; No Copyright; Avail: Department of Energy Information Bridge

The D experiment is one of the two collider experiments at Fermilab. The D detector is a multi-purpose detector and took its data during Fermilab TeVatron collider run in 1992-1996. Both the D detector and the Tevatron accelerator at Fermilab are currently undergoing significant upgrade to extend the reach to new physics and to further probe Standard Model. In this paper, physics potential of the upgraded D detector and the upgrade status are discussed.
NTIS
*Particle Accelerators; Theoretical Physics*

**20010123427** Virginia Polytechnic Inst. and State Univ., Blacksburg, VA USA
**Partial-wave Analyses of Scattering Reactions below 3 GeV, May 31, 1997-May 31, 1999. Final Technical Report**
Arndt, R. A.; Workman, R. L.; Jun. 26, 2000; 7p; In English
Report No.(s): DE2001-763229; No Copyright; Avail: Department of Energy Information Bridge

Over the period that the Department of Energy has funded the Partial Wave Analysis effort at VPI&SU, it has grown from an analysis of elastic NN scattering, below 500 Me'V, to include 10 separate reactions which are summarized below. The group has maintained a repository for scattering data from these important reactions as well as a primary source for partial-wave solutions, including those of 'competitors' around the world. Perhaps the most important contribution of the VPI effort has been the development of interactive (Scattering Analysis Interactive Dialin) programs that make accessible both the data bases and the solutions to the Nuclear Physics community.
NTIS
*Nuclear Physics; Wave Scattering; Data Processing*

**20010123432** Los Alamos National Lab., NM USA
**Accelerator Production of Tritium - Design Execution Plan**
Gattoni, W. C.; Sep. 01, 1998; 162p; In English
Report No.(s): DE2001-763185; LA-UR-98-4612; APT-PPO-0005-REV-1; No Copyright; Avail: Department of Energy Information Bridge, Microfiche

The APT Project, sponsored by DOE's (Department of Energy) Defense Programs (DO EIDP60) provides an accelerator-based system to produce tritium for the nation's stockpile of nuclear weapons. The mission of the APT program is to produce tritium by means of a fully integrated accelerator plant. The process is based on proven accelerator, target blanket, tritium extraction, and balance of plant technologies. The APT plant is being designed to produce 3 kilograms (nominal) per year of tritium. The Plant will be built at the Savannah River Site (SRS) and will be fully operational no later than the end of FY (fiscal year) 2007. The APT facility is designed for a minimum lifetime of 40 years.
NTIS
*Tritium; Design Analysis; Production Engineering; Linear Accelerators; Systems Engineering*

**20010123433** Los Alamos National Lab., NM USA
**Accelerator Production of Tritium - Project Execution Plan**
Fultonberg, D. N.; Jul. 01, 1997; 56p; In English
Report No.(s): DE2001-763184; LA-UR-98-4610; APT-PDO-001; No Copyright; Avail: Department of Energy Information Bridge, Microfiche

Tritium is an essential ingredient in US nuclear weapons. Because tritium has a radioactive half-life of 12.3 years, it must be replenished periodically for weapons to operate as designed. Tritium does not occur in useful quantities in nature and must be produced in specialized facilities that use nuclear reactions to transform another element into tritium. The US has been without such a facility since 1988, but has been able to maintain the tritium stockpile using tritium recovered from dismantled weapons. This approach cannot be sustained indefinitely. Presidential direction requires an Accelerator Production of Tritium (APT) System to come on line by fiscal year FY2007 to maintain the nations nuclear deterrent, if APT is chosen for construction by the

Department of Energy (DOE). Until recently, the only practical approach to producing the required amount of tritium has been use of a nuclear reactor, with nuclear fission generating the neutrons that drive tritium-producing reactions. Accelerator technology offers an alternative to nuclear reactors for this mission. Energetic protons from a linear accelerator strike a tungsten and lead target producing neutrons in quantities comparable to those in reactors. This approach to neutron production avoids the use of fissile materials (uranium or plutonium), which in turn simplifies design and licensing and offers numerous safety and environmental advantages.
NTIS
*Linear Accelerators; Nuclear Reactors; Tritium; Particle Collisions*

**20010123434** Los Alamos National Lab., NM USA
**Accelerator Production of Tritium Software Management Plan**
Olsen, B.; Jun. 01, 1998; 29p; In English
Report No.(s): DE2001-763183; LA-UR-98-4611; APT-PPO-0013-REV-0; No Copyright; Avail: Department of Energy Information Bridge, Microfiche
This Software Management Plan documents the process used to manage computer software-related activities pertaining to the Accelerator Production of Tritium (APT) design. These activities include development, acquisition, leasing, modification, configuration management, and controlled use of Engineering & Scientific software and Real Time software on the APT project. The management of software by the APT design and development team members and others, including suppliers, performing tasks during the preliminary and final design, construction, startup and testing of the APT plant shall be compatible with the approach developed in this Plan.
NTIS
*Management Planning; Particle Accelerators; Tritium; Software Engineering*

**20010123441** Virginia Polytechnic Inst. and State Univ., Blacksburg, VA USA
**Physics of low-lying hadrons in quark model and effective hadronic approaches** ***Final Report, 1 Sep. 1996 - 31 Mar. 2000***
Mizutani, T.; Jun. 19, 2000; 7p; In English
Report No.(s): DE2001-761066; DOE/ER/40994-3; No Copyright; Avail: Department of Energy Information Bridge, Microfiche
There were basically three theoretical projects supported by this grant: (1) Use of confined quark models to study low energy hadronic processes; (2) Production of strangeness by Electromagnetic Probes; and (3) Diffractive dissociative production of vector mesons by virtual photons on nucleons. Each of them is summarized in the paper.
NTIS
*Quark Models; Strangeness; Particle Production*

**20010123450** Los Alamos National Lab., NM USA
**Four Pulse Drive System for the Beam Induction Cells for DARHT Axis 2**
Downing, J.; Carlson, R.; Melton, J.; Fockler, J.; Jun. 28, 1999; 9p; In English
Report No.(s): DE2001-761019; LA-UR-99-3383; No Copyright; Avail: Department of Energy Information Bridge, Microfiche
The proposed drive system allows for the generation of up to four (4) high-quality radiographic pulses along one line-of-sight, having arbitrary pulse spacing (approx.500 ns), using demonstrated technologies. This concept uses a four-pulse drive system to drive both a 16-MeV ensemble of 250-kV, 4-kA induction cells and a four-pulse, 4-MeV injector. The key to this approach lies in the method used to combine four pulses from different generators in a manner that does not compromise the voltage flatness requirement of +/- 1%. The induction cells use core material for only a single pulse. A simple reverse bias circuit is used to reset the cores between pulses, and the insulator has been redesigned to withstand the reverse reset voltage. This approach can be installed in stages so that the facility can be used for dual axis radiography while implementing the multi-pulsing capability. A dual double-pulse format has been identified which provides a sequence of two pulses along one line-of-sight within a 2-(micro)sec window. The 2-(micro)sec windows can be separated by arbitrary time intervals of 2- to 10-(micro)sec.
NTIS
*Beams (Radiation); Pulsed Radiation*

**20010123625** Fermi National Accelerator Lab., Batavia, IL USA
**Energy Distribution in a Relativistic DC Electron Beam**
Nagaitsev, S.; Alexey, A. S.; Nov. 15, 2000; 9p; In English
Report No.(s): DE2000-767336; FERMILAB-TM-2133; No Copyright; Avail: Department of Energy Information Bridge, Microfiche

Electron cooling of the 8.9 GeV/c antiprotons in the Recycler ring requires a high-quality dc electron beam with the current of several hundred mA and the kinetic energy of 4.3 MeV. The only technically feasible way to attain such high electron currents is through beam recirculation (charge recovery). The primary current path is from the cathode at high voltage terminal to ground where the electron beam interacts with the antiproton beam and cooling takes place, then to the collector located in the terminal, and finally through the collector power supply back to the cathode. The energy distribution function of the electron beam after the deceleration determines the required collector energy acceptance. Multiple and single intra-beam scattering as well as the dissipation of density micro-fluctuations during the beam transport are studied as factors forming a core and tails of the electron energy distribution. For parameters of the Fermilab electron cooling project 1, the single intra-beam scattering (Touschek effect) is found to be of the most importance.
NTIS
*Accumulators; Distribution Functions; Electron Energy; Relativistic Electron Beams*

**20010123630** Princeton Univ., Plasma Physics Lab., NJ USA
**National Spherical Torus Experiment (NSTX) Engineering Overview and Research Results, *1999 - 2000***
Neumeyer, C.; Oct. 06, 2000; 7p; In English
Report No.(s): DE2000-765036; PPPL-3491; No Copyright; Avail: Department of Energy Information Bridge
The National Spherical Torus Experiment (NSTX) is a new US facility for the study of plasma confinement, heating, and current drive in a low aspect ratio, spherical torus (ST) configuration. The ST configuration is an alternate magnetic confinement concept which is characterized by high beta (ratio plasma pressure to magnetic field pressure) and low toroidal field compared to conventional tokamaks, and could provide a pathway to the realization of a practical fusion power source. NSTX achieved first plasma in February 1999, and since that time has completed and commissioned all components and systems within the machine proper. Routine operation with inductively driven plasma current less than or equal to 1 MA and flat top less than or equal to 0.3 seconds has been established, and the ohmic characterization phase of the research program is underway. Radio Frequency (RF) and Neutral Beam Injection (NBI) systems have been installed and are presently being commissioned. This paper describes the NSTX mission, gives an overview of the engineering design, and summarizes the research results obtained thus far.
NTIS
*Tokamak Devices; Toroidal Plasmas; Design Analysis; Plasma Control*

**20010123631** Fermi National Accelerator Lab., Batavia, IL USA
**Last Meson**
Devlin, T.; Oct. 10, 2000; 9p; In English
Report No.(s): DE2000-765032; FERMILAB-CONF-00/232-E; No Copyright; Avail: Department of Energy Information Bridge
The authors describe the observation of the B(sub c) meson through its semileptonic decays, B(sub c) (r arrow) J/(psi)(ell)(nu), and the measurements of the B(sub c) mass, lifetime and production rate in the CDF detector at Fermilab. They also present estimates for B(sub c) production and decay into other final states in the forthcoming run of the upgraded CDF and Tevatron.
NTIS
*Mesons; Particle Decay*

**20010123632** Fermi National Accelerator Lab., Batavia, IL USA
**Color Transparency and Pion Valence Quark Distributions from Di-Jet Events in Fermilab E791**
Appel, J. A.; Oct. 10, 2000; 3p; In English
Report No.(s): DE2000-765030; FERMILAB-CONF-00/226-E; No Copyright; Avail: Department of Energy Information Bridge
Diffractive, exclusive di-jet events produced by 500 GeV/c (pi-) scattered off nuclei were used to measure their A-dependence, and to make the first direct measurement of the valence-quark momentum distribution in pions. Data on the latter are compared to two limiting predictions for the pion light-cone wave-function. The results show that the asymptotic wave-function of perturbative quantum chromodynamics describes the data well for Q(sup 2) of 10 GeV(sup 2) and above. The measured A-dependence is consistent with observation of point-like configurations in the pion and color-transparency calculations.
NTIS
*Pions; Quarks; Valence; Quantum Chromodynamics*

**20010123639** Fermi National Accelerator Lab., Batavia, IL USA

**Search for rare and forbidden charm meson decays at Fermilab E791**

Summers, D. J.; Sep. 29, 2000; 7p; In English

Report No.(s): DE2000-764140; FERMILAB-CONF-00/223-E; No Copyright; Avail: Department of Energy Information Bridge

The authors report the results of a blind search for flavor-changing neutral current, lepton-flavor violating, and lepton-number violating decays of D(sup +), D(sub s)(sup +), and D(sup 0) mesons (and their antiparticles) into modes containing muons and electrons. Using data from Fermilab charm hadroproduction experiment E791, they examine the (pi)(ell)(ell) and K(ell)(ell) decay modes of D(sup +) and D(sub s)(sup +) and the (ell)(sup +)(ell)(sup (minus)) decay modes of D(sup 0). No evidence for any of these decays is found. Therefore, they present branching-fraction upper limits at 90% confidence level for the 24 decay modes examined. Eight of these modes have no previously reported limits, and fourteen are reported with significant improvements over previously published results.

NTIS

*Leptons; Mesons; Charm (Particle Physics); Particle Decay*

**20010123902** Prairie View Agricultural and Mechanical Coll., TX USA

**Final Report on Heavy Quark Studies by the Prairie View High Energy Physics Group and Research in Theoretical High Energy Physics to Department of Energy for Prairie View A and M University High Energy Physics**

Judd, D. J.; Wagoner, D. E.; Wu, D. D.; Dec. 15, 1996; 19p; In English

Report No.(s): DE2001-764182; DOE/ER/40728-1-VOL-1; No Copyright; Avail: Department of Energy Information Bridge

The High Energy Physics (HEP) group at Prairie View has been involved with experiment E771 at Fermilab since its inception. Prior to the run, group members did a number of Monte Carlo studies of the E771 triggers, designed and programmed a large part of the E771 data acquisition system, and acquired and installed the Fastbus readout system for the PWC Central Chambers. During the run, our major responsibility was the smooth operation of the data acquisition system. Since the run ended, we have been involved in the offline data analysis of the dimuon trigger data. We also wrote a section of Proposal P867 at Fermilab, a continuation of the E771 study of B mesons. Our part of the proposal was a redesign of the data acquisition system to improve its efficiency in dealing with the high multiplicity events typical of E771. Our work on P867 was discontinued when the Program Advisory Committee at Fermilab recommended against the proposal, and our work on E771 is now winding down.

NTIS

*Data Acquisition; Energy Technology; High Energy Interactions*

**20010123903** Houston Univ., TX USA

**Development of Singularities in Riemann Invariants**

Keyfitz, B. L.; May 22, 1992; 14p; In English

Report No.(s): DE2001-764165; UH/MD-129; DOE/ER/25102-1-VOL-1B; No Copyright; Avail: Department of Energy Information Bridge

Shocks form in a finite time in systems of quasilinear hyperbolic equations in one space variable which are genuinely nonlinear. The authors write down a simple geometric construction for systems of two equations, and use it to obtain a priori estimates for the growth of the derivatives. They also find realistic bounds on the maximum and minimum time of existence of smooth solutions for large amplitude waves in a model system of an unusual type.

NTIS

*Hyperbolic Differential Equations; Singularity (Mathematics); Riemann Manifold*

**20010123904** Maryland Univ., Inst. for Plasma Research, College Park, MD USA

**Proposal for the Development of Techniques for the Implementation of Control to Experimental Chaotic Systems: Final Technical Report**

Grebogi, C.; Feb. 29, 2000; 12p; In English

Report No.(s): DE2001-764163; DOE/ER/25166-F; No Copyright; Avail: Department of Energy Information Bridge

This is the final report on a research project that explored: (1) controlling complex dynamical systems; (2) using controlled chaotic signals for communication; (3) methods of controlling chaos via targeting; (4) deterministic modeling; (5) miscellaneous work on the interface between chaotic and stable periodic behavior as system parameters vary, bifurcations of non-smooth systems that describe impact oscillators; and (6) phenomena that occur in quasiperiodically forced systems, and the fractal and topological properties of chaotic inveriant sets, in particular those arising in fluid flow.

NTIS

*Complex Systems; Oscillators; Mathematical Models; Fractals*

**20010123913** Los Alamos National Lab., NM USA

**Envelope Oscillations and Halo Formation in Bunched Beams: A Perturbational Approach**

Allen, C. K.; Feb. 01, 2000; 23p; In English

Report No.(s): DE2001-763362; LA-UR-00-885; No Copyright; Avail: Department of Energy Information Bridge

We examine in detail the first-order vibration modes of a bunched beam then apply the results to the analysis of halo formation using the particle-core model. The three-dimensional envelope equations are derived from first principle in order to avoid some discrepancies currently found in the literature. From the full envelope equations, we employ perturbation analysis to compute analytic expressions for the natural oscillation frequencies and corresponding oscillation modes of a beam bunch. Moreover, the mode excitations due to a periodic accelerator structure can be estimated. We then use the results of the envelope analysis as a starting point in the study of halo formation in bunched beams. An overview of the current nonlinear analysis using the particle-core model is presented. The collected results of this study are to be published at a later time.

NTIS

*Electron Beams; Bunching; Vibration Mode; Oscillations; Halos*

**20010123929** Fermi National Accelerator Lab., Batavia, IL USA

**Emittance Measurements at the A0 Photo-Injector**

Carneiro, J. P.; Oct. 10, 2000; 3p; In English

Report No.(s): DE2000-765037; FERMILAB-CONF-00/233-E; No Copyright; Avail: Department of Energy Information Bridge

The A0 photo-injector produces electron bunches of 1-14 nC charge with an energy of 18 MeV. Detailed measurements and optimization of emittance have been carried out for a number of gun and laser operating conditions, beam line optics conditions, and at a number of beam line locations. Results are compared with the predictions of simulations using HOMDYN.

NTIS

*Electron Bunching; Emittance; Electron Beams*

**20010124090** Oak Ridge National Lab., TN USA

**Support Facility for a Graphite Target Neutrino Factory**

Spampinato, P. T.; Chesser, J. B.; Gabriel, T. A.; Gallmeier, F. X.; Haines, J. R.; Aug. 01, 2000; 48p; In English

Report No.(s): DE2001-769367; ORNL/TM-2000/153; No Copyright; Avail: Department of Energy Information Bridge

The Target Support Facility for a Neutrino Producing Research Facility extends from the pretarget, primary beam focusing region to the end of the decay channel. Technical components include the target, beam absorber, and solenoid magnetic-field focusing system. While the ultimate goal is to target about 4 MW of proton beam in the target area, smaller values and different target materials (e.g., low Z) are considered to facilitate the first step. As detailed in this report, a carbon target was chosen with an incident primary beam power of 1.5 MW, The target is embedded in a high-field solenoid magnet of 20 T, followed by a transition section channel, where the field tapers down to 1.25 T. An iterative design process has been carried out which optimizes Monte Carlo code flux projections with realistic magnetic-field parameters. The severe radiation environment and component shielding requirements strongly influence design choices. The overall system design includes the capture and decay channel solenoids, the design parameters of which were provided by the National High Magnetic Field Laboratory. This design balances resistive and superconducting magnet contributions. Facility requirements, including shielding, remote handling, radioactive water system, etc. are based on the final design goal of 4 MW. The extent of the Target Support Facility and radiation-handling equipment includes the 50 m decay channel, where remote-handling operations are also required.

NTIS

*Neutrinos; Systems Engineering; Nuclear Research and Test Reactors; Equipment Specifications*

**20010124108** NASA Ames Research Center, Moffett Field, CA USA

**Time-to-Passage Judgments under Violations of Various Constancy Assumptions**

Kaiser, Mary K., NASA Ames Research Center, USA; Hecht, Heiko, NASA Ames Research Center, USA; [1994]; 1p; In English; Psychonomic Society, Inc. 35th Annual Meeting, 11-13 Nov. 1994, Saint Louis, MO, USA; Sponsored by Psychonomic Society, Inc., USA

Contract(s)/Grant(s): RTOP 538-04-11; No Copyright; Avail: Issuing Activity; Abstract Only

Time-to-passage (TTP) derivations typically assume constant translational velocities and consistent object orientation. In our first study, we examined the impact of acceleration, and observer roll and heading (relative to track vector) on TTP judgments.

Judgments reflected an insensitivity to acceleration; roll did not affect performance, but the decoupling of observer heading and track vector did. Our second study examined the effect of multi-axis target rotation on TTP and time-to-contact judgments. Author

*Judgments; Variability; Time Measurement; Parameter Identification*

**20010125005** Sandia National Labs., Albuquerque, NM USA

**Investigation of the Effects of Waterline Switch Capacitance on the Electrical Prepulse of the Z-Accelerator**

Shoup, R. W.; Spielman, R. B.; Struve, K. W.; Stygar, W. A.; Aug. 02, 1999; 6p; In English

Report No.(s): DE2001-9681; SAND99-1986C; No Copyright; Avail: Department of Energy Information Bridge, Microfiche

The Z-accelerator at the Sandia National Laboratories (SNL) was modified in 1996 to deliver a 20 MA pulse to a z-pinch load in 100 ns. The pulsed-power driver is a 36-module waterline accelerator. Each waterline contains four self-break switches as part of the pulse-forming section. A study was conducted to investigate the effects of increasing the capacitance of the waterline switches on the shape of the electrical prepulse at the load. Past studies have shown that increasing the prepulse at the z-pinch load increases the x-ray output power. In this study, one set of switches with its surrounding waterline hardware was modeled in 3-D and capacitance calculated using the electrostatic code, COULOME. The capacitance values were used in a SCREAMER model of the Z-accelerator. SCREAMER an SNL developed, lumped-element circuit code was used to calculate the time-dependent current waveforms delivered to the z-pinch load. The design was changed and a new capacitance matrix and output waveforms were calculated. This paper presents the results of the COULOMB 3-D modeling, and the SCREAMER circuit-model analyses. NTIS

*Capacitance Switches; Three Dimensional Models; Zeta Pinch; Electrostatics; Electric Networks; Accelerators*

**20010125032** California Univ., Lawrence Berkeley Lab., Berkeley, CA USA

**Baryon Stopping and Charged Particle Production from Lead-Lead Collisions at 158 GeV per Nucleon**

Toy, M. Y.; Jul. 01, 1999; 97p; In English

Report No.(s): DE2000-767742; LBNL-45935; No Copyright; Avail: Department of Energy Information Bridge, Microfiche

Net proton (proton minus antiproton) and negative charge hadron spectra (h-) from central Pb+Pb collisions at 158 GeV per nucleon at the CERN Super Proton Synchrotron were measured and compared to spectra from central collisions of the lighter S+S system. Net baryon distributions were derived from those of net protons and net lambdas. Stopping, or rapidity shift with respect to the beam, of net protons and net baryons increase with system size. The mean transverse momentum (PT); of net protons also increase with system size. The h- rapidity density scales with the number of participant nucleons for nuclear collisions, where their (PT); is independent of system size. The (PT); dependence upon particle mass and system size is consistent with larger transverse flow velocity at midrapidity for central collisions of Pb+Pb compared to that of S+S. NTIS

*Baryons; Collisions; Particle Mass; Particle Production; Transverse Momentum*

**20010125068** Fermi National Accelerator Lab., Batavia, IL USA

**CDF Silicon Vertex Tracker**

Cerri, A.; Oct. 10, 2000; 7p; In English

Report No.(s): DE2000-765040; FERMILAB-CONF-00/238-E; No Copyright; Avail: Department of Energy Information Bridge

Real time pattern recognition is becoming a key issue in many position sensitive detector applications. The CDF collaboration is building SVT: a specialized electronic device designed to perform real time track reconstruction using the silicon vertex detector (SVX II). This will strongly improve the CDF capability of triggering on events containing b quarks, usually characterized by the presence of a secondary vertex. SVT is designed to reconstruct in real time charged particles trajectories using data coming from the Silicon Vertex detector and the Central Outer Tracker drift chamber. The SVT architecture and algorithm have been specially tuned to minimize processing time without degrading parameter resolution. NTIS

*Charged Particles; Pattern Recognition; Quarks; Real Time Operation*

**20010125110** Helsinki Univ. of Technology, Electromagnetics Lab., Espoo, Finland

**Wave Equation and Solution in Time Varying and Frequency Dependent Medium: Plane Case**

Sengoer, T.; December 2000; 36p; In English; Prepared in cooperation with Yildiz Technical University, Istanbul, Turkey, Dept. of Electronics and Communications Engineering

Report No.(s): PB2001-107372; Copyright; Avail: National Technical Information Service (NTIS), Microfiche

This report covers different aspects of frequency dependent and time varying materials in electromagnetic wave theory applications. The purpose is to introduce a method, which is suitable to use in different applications of the wave phenomena in dispersive and time varying media. The perspective of the report includes convenient transforms for waves in dispersive materials and covers most types of environments. Planar waves in time the frequency dependent media are considered in this report. Modified separation method is given. The solution is obtained for non-gradient medium.
NTIS
*Plane Waves; Wave Equations; Transformations (Mathematics)*

**20010125142** NASA Ames Research Center, Moffett Field, CA USA
**The Bond Dissociation Energies of 1-Butene**
Bauschlicher, Charles W., Jr., NASA Ames Research Center, USA; [1994]; 1p; In English
Contract(s)/Grant(s): RTOP 232-01-04; No Copyright; Avail: Issuing Activity; Abstract Only
The bond dissociation energies of 1-butene and several calibration systems are computed using the G2(MP2) approach. The agreement between the calibration systems and experiment is very good. The computed values for 1-butene are compared with calibration systems and the agreement between the computed results for 1-butene and the ”rule of thumb” values from the smaller systems is remarkably good.
Author
*Butenes; Dissociation; Binding Energy*

**20010125169** California Univ., Lawrence Berkeley Lab., Berkeley, CA USA
**Stopping: From Peripheral to Central Nuclear Collisions at the SPS**
Cooper, G. E.; Jul. 15, 1999; 4p; In English; 14th; Fourteenth International Conference on Ultra-Relativistic Nucleus-Nucleus Collisions, 5-10 May, 1999, Turin, Italy
Report No.(s): DE2000-767531; LBNL-43836; No Copyright; Avail: Department of Energy Information Bridge, Microfiche
In the early phase of a nuclear collision, participating nucleons convert a large fraction of their kinetic energy into other degrees of freedom. How this occurs sets the baryon density created in the collision and determines the energy available for particle production and expansion. At the CERN SPS, baryon stopping in collisions using light nuclear projectiles (NA35) and in central Pb+Pb collisions (NA49) were studied previously. The results presented here extend these studies over nearly the full range of nuclear system size.
NTIS
*Kinetic Energy; Nucleons; Stopping; Particle Collisions*

**20010125170** California Univ., Lawrence Berkeley Lab., Berkeley, CA USA
**Baryon Stopping and Hadronic Spectra in Pb-Pb Collisions at 158 GeV/Nucleon**
Cooper, G. E.; Apr. 12, 2000; 130p; In English
Report No.(s): DE2000-765129; LBNL-45467; No Copyright; Avail: Department of Energy Information Bridge
Baryon stopping and particle production in Pb+Pb collisions at 158 GeV/nucleon are studied as a function of the collision centrality using new proton, antiproton, charged kaon and charged pion production data measured with the NA49 experiment at the CERN Super Proton Synchrotron (SPS). Stopping, which is measured by the shift in rapidity of net protons or baryons from the initial beam rapidity, increases in more central collisions. This is expected from a geometrical picture of the collisions. The stopping data are quantitatively compared to models incorporating various mechanisms for stopping. In general, microscopic transport calculations which incorporate current theoretical models of baryon stopping or use phenomenological extrapolations from simpler systems overestimate the dependence of stopping on centrality. Approximately, the yield of produced pions scales with the number of nucleons participating in the collision. A small increase in yield beyond this scaling, accompanied by a small suppression in the yield of the fastest pions, reflects the variation in stopping with centrality. Consistent with the observations from central collisions of light and heavy nuclei at the SPS, the transverse momentum distributions of all particles are observed to become harder with increasing centrality. This effect is most pronounced for the heaviest particles. This hardening is discussed in terms of multiple scattering of the incident nucleons of one colliding nucleus as they traverse the other nucleus and in terms of rescattering within the system of produced particles.
NTIS
*Baryons; Nucleons; Particle Production; Particle Collisions*

**20010125177** National Renewable Energy Lab., Golden, CO USA
**Comprehensive Research on Stability of Amorphous Silicon and Alloy Materials and Devices**
Dalal, V. K.; Han, K.; Maxson, T.; Girvan, R.; Kaushal, S.; Sep. 29, 2000; 61p; In English
Report No.(s): DE2000-765093; NREL/SR-520-28989; No Copyright; Avail: Department of Energy Information Bridge

In this report, the authors describe the work done to improve the material and device properties of a-Si:H and a-(Si,Ge):H alloys prepared using electron cyclotron resonance (ECR) plasma deposition and to understand the growth chemistry. Major results were obtained in the following areas: (1) Influence of plasma chemistry on properties and stability of a-Si:H single-junction solar cells; (2) Fabrication of good-quality tandem-junction cells. The authors made tandem-junction a-Si/a-Si cells with excellent voltages and fill factors using the H-ECR process; (3) Growth of high-quality a-(Si,Ge):H films using the ECR deposition process; (4) Fabrication of single-junction devices in a-(Si,Ge):H for diagnosing the material; and (5) Graded-gap cells in a-(Si,Ge):H. Good devices were produced using a graded-gap I-layer. In summary, the most important finding from this research has been that plasma chemistry plays a very important role in determining the properties of the materials, particularly the properties of the a-(Si,Ge):H alloy system. Even in a-Si:H, plasma chemistry plays a role in determining stability. This result suggests that by deliberately changing the chemistry of deposition, one may be able to further improve the a-(Si,Ge):H materials system and make its properties comparable to the properties of a-Si:H. The ECR reactor has proved to be a very useful chemical tool, with excellent control over growth chemistry.

NTIS
*Electron Cyclotron Resonance; Amorphous Silicon; Silicon Alloys*

**20010125230** Fermi National Accelerator Lab., Batavia, IL USA
**B Physics at CDF**
Paus, C.; Oct. 10, 2000; 3p; In English
Report No.(s): DE2000-765042; FERMILAB-CONF-00/235-E; No Copyright; Avail: Department of Energy Information Bridge

From 1992 to 1995 the CDF experiment has taken 110 pb(sup -1) of p(anti p) collisions at a center-of-mass energy of 1.8 TeV. These data gave rise to a variety of important B physics measurements. Most importantly B mass, lifetime and mixing measurements, the observation of the last missing meson, the B(sub c), and a measurement of the CP violation parameter sin(2(beta)). The highlights of those results are described and a perspective for the upcoming Run 2 period is given.

NTIS
*Collisions; Mesons; Proton-Antiproton Interactions; Atomic Physics*

**20010125231** Fermi National Accelerator Lab., Batavia, IL USA
**Dark Matter Distribution in the Universe and Ultra-High Energy Cosmic Rays**
Blasi, P.; Oct. 10, 2000; 15p; In English
Report No.(s): DE2000-765041; FERMILAB-CONF-00/247-A; No Copyright; Avail: Department of Energy Information Bridge

Two of the greatest mysteries of modern physics are the origin of the dark matter in the universe and the nature of the highest energy particles in the cosmic ray spectrum. The authors discuss here possible direct and indirect connections between these two problems, with particular attention to two cases: in the first they study the local clustering of possible sources of ultra-high energy cosmic rays (UHECRs) driven by the local dark matter overdensity. In the second case they study the possibility that UHECRs are directly generated by the decay of weakly unstable super heavy dark matter.

NTIS
*Cosmic Rays; Dark Matter; Energy Spectra*

**20010125232** Fermi National Accelerator Lab., Batavia, IL USA
**Supersymmetry Searches at the Tevatron**
LeCompte, T. J.; Oct. 10, 2000; 4p; In English
Report No.(s): DE2000-765039; FERMILAB-CONF-00/236-E; No Copyright; Avail: Department of Energy Information Bridge

The CDF and D0 experiments have each collected over 110 pb(sup -1) of proton-antiproton collision data with (radical)s = 1,800 GeV during the period 1992-1995. Limits on the production of supersymmetric particles are presented here.

NTIS
*Particle Collisions; Proton-Antiproton Interactions; Supersymmetry*

**20010125233** Fermi National Accelerator Lab., Batavia, IL USA
**Charm and Beauty Production and Polarization at CDF**
Papadimitriou, V.; Oct. 10, 2000; 13p; In English

Report No.(s): DE2000-765038; FERMILAB-CONF-00/234-E; No Copyright; Avail: Department of Energy Information Bridge

In this paper the authors present results on Charm and Beauty production as well as on production and polarization of Quarkonia at (radical)s = 1.8 TeV. These results were obtained from data taken with the CDF detector at Fermilab. They cover recently completed analyses of the 1992-96 collider run.

NTIS

*Charm (Particle Physics); Particle Production*

**20010125401** Argonne National Lab., IL USA

**Toward a fourth-generation x-ray source**

Monction, D. E.; May 19, 1999; 6p; In English

Report No.(s): DE2001-11809; ANL/OTD-APS/CP-99036; No Copyright; Avail: Department of Energy Information Bridge

The field of synchrotron radiation research has grown rapidly over the last 25 years due to both the push of the accelerator and magnet technology that produces the x-ray beams and the pull of the extraordinary scientific research that is possible with them. Three successive generations of synchrotrons radiation facilities have resulted in beam brilliances 11 to 12 orders of magnitude greater than the standard laboratory x-ray tube. However, greater advances can be easily imagined given the fact that x-ray beams from present-day facilities do not exhibit the coherence or time structure so familiar with the optical laser. Theoretical work over the last ten years or so has pointed to the possibility of generating hard x-ray beams with laser-like characteristics. The concept is based on self-amplified spontaneous emission (SASE) in free-electron lasers. A major facility of this type based upon a superconducting linac could produce a cost-effective facility that spans wave-lengths from the ultraviolet to the hard x-ray regime, simultaneously servicing large numbers experimenters from a wide range of disciplines. As with each past generation of synchrotrons facilities, immense new scientific opportunities would result from fourth-generation sources.

NTIS

*X Ray Sources; Synchrotron Radiation*

**20010125427** Argonne National Lab., IL USA

**Deformations and stress in PMMA during hard x-ray exposure for deep lithography**

Moldovan, N.; Aug. 17, 1999; 11p; In English

Report No.(s): DE2001-11742; ANL/XFD/CP-98715; No Copyright; Avail: Department of Energy Information Bridge, Microfiche

The availability of high-energy, high-flux, collimated synchrotrons radiation has extended the application of deep X-ray lithography (DXRL) to thickness values of the PMMA (polymethyl methacrylate) resist of several millimeters. Some of the most severe limitations come from plastic deformation, stress, and cracks induced in PMMA during exposure and development. We have observed and characterized these phenomena quantitatively. Profilometry measurements revealed that the PMMA is subjected either to local shrinkage or to expansion, while compression and expansion evolve over time. Due to material loss and crosslinking, the material undergoes a shrinkage, while the radiation-induced decomposition generates gases expanding the polymer matrix. The overall dynamics of the material microrelief and stress during and after the exposure depend on the balance between compaction and outgassing. These depend in turn on the exposure conditions (spectrum; dose, dose rate, seaming, temperature), post-exposure storage conditions, PMMA material properties and thickness, and also on the size and geometry of the exposed patterns.

NTIS

*Plastic Deformation; Polymethyl Methacrylate; Synchrotron Radiation; Lithography*

**20010125444** Lawrence Livermore National Lab., Livermore, CA USA

**Work-Op IV summary: lessons from iron opacities**

Davidson, S. J.; Iglesias, C. A.; Minguez, E.; Serduke, F. J. D.; Apr. 16, 1999; 21p; In English

Report No.(s): DE2001-8392; UCRL-JC-133915; DP0101017; No Copyright; Avail: Department of Energy Information Bridge, Microfiche

The fourth international LTE (Local Thermodynamic Equilibrium) opacity workshop and code comparison study, WorkOp-IV, was held in Madrid in 1997. Results of this workshop are summarized with a focus on iron opacities. In particular, the astrophysically important photon absorption region between 50 and 80 eV is emphasized for a sequence of iron plasmas at densities and temperatures that produce nearly the same average ionization stage (Z* (approximately) 8.6). Experimental data that addressed this spectral region is also reviewed.

NTIS

*Iron; Opacity; Local Thermodynamic Equilibrium*

**20010125491** Argonne National Lab., IL USA

**Thermodynamics of lattice QCD with 2 quark flavours: Chiral symmetry and topology**

Lagae, J. F.; Jun. 09, 1998; 14p; In English

Report No.(s): DE2001-10846; ANL-HEP-CP-98-49; No Copyright; Avail: Department of Energy Information Bridge

We have studied the restoration of chiral symmetry in lattice QCD (quantum chromodynamics) at the finite temperature transition from hadronic matter to a quark-gluon plasma. by measuring the screening masses of flavor singlet and non-singlet meson excitations, we have seen evidence that, although flavor chiral symmetry is restored at this transition, flavor singlet (U(1)) axial symmetry is not. We conclude that this indicates that instantons continue to play an important role in the quark-gluon plasma phase.

NTIS

*Chirality; Quantum Chromodynamics; Thermodynamics; Flavor (Particle Physics)*

**20010125493** Argonne National Lab., IL USA

**QCD bound states and their response to extremes of temperature and density**

Maris, P.; Jun. 09, 1998; 22p; In English

Report No.(s): DE2001-10844; ANL/PHY/CP-96653; No Copyright; Avail: Department of Energy Information Bridge

We describe the application of Dyson-Schwinger equations to the calculation of hadron observable. The studies at zero temperature (T) and quark chemical potential ((mu)) provide a springboard for the extension to finite-(T, (mu)). Our exemplars highlight that much of hadronic physics can be understood as simply a manifestation of the nonperturbative, momentum-dependent dressing of the elementary Schwinger functions in QCD (quantum chromodynamics).

NTIS

*Hadrons; Quantum Chromodynamics*

**20010125502** Princeton Univ., Plasma Physics Lab., NJ USA

**Energetic Ion Loss Diagnostic for the Wendelstein 7-AS Stellarator**

Darrow, D. S.; Werner, A.; Weller, A.; Dec. 07, 2000; 35p; In English

Report No.(s): DE2001-769181; PPPL-3525; No Copyright; Avail: Department of Energy Information Bridge, Microfiche

A diagnostic to measure the loss of energetic ions from the Wendelstein 7-AS (W7-AS) stellarator has been built. It is capable of measuring losses of both neutral beam ions and energetic ions arising from ion cyclotron resonant heating. The probe can measure losses of both clockwise and counterclockwise-going energetic ions simultaneously, and accepts a wide range of pitch angles in both directions. Initial measurements by the diagnostic are reported.

NTIS

*Ion Beams; Neutral Beams; Stellarators; Cyclotrons*

**20010125504** Thomas Jefferson National Accelerator Facility, Newport News, VA USA

**Diagnostics for the CEBAF FEL Injector**

Kehne, D.; Engwall, D.; Jordan, K.; Benson, S.; Bohn, C.; Dec. 01, 1995; 10p; In English

Report No.(s): DE2001-769173; JLAB-ACT-96-07; DOE/ER/40150-1781; No Copyright; Avail: Department of Energy Information Bridge, Microfiche

A test stand for the 10 MeV, 5 mA average current injector for the Continuous Electron Beam Accelerator Facility (CEBAF) free-electron laser (FEL) is currently under construction. The injector tests will progress through two phases. The first phase will be devoted to characterizing the gun transverse and longitudinal emittance performance as a function of bunch charge, beam size, and energy. The goal of the second phase is to achieve the nominal requirements of the 10 MeV injector, including bunch length, emittance, charge per bunch, and energy stability. This paper summarizes the diagnostics planned to be used in these experiments.

NTIS

*Electron Beams; Free Electron Lasers; Injectors; Linear Accelerators*

**20010125505** Thomas Jefferson National Accelerator Facility, Newport News, VA USA

**Measuring and Controlling Energy Spread in CEBAF**

Krafft, G.; Denard, J. C.; Dickson, R.; Kazimi, R.; Lebedev, V.; Aug. 01, 2000; 5p; In English

Report No.(s): DE2001-769168; JLAB-ACC-00-13; JLAB-ACP-00-05,PSYSICS/0009087; No Copyright; Avail: Department of Energy Information Bridge, Microfiche

As compared to the electron storage rings, one advantage of recirculating linacs is that the beam properties at a target are no longer dominated by the equilibrium between quantum radiative diffusion and radiation damping because new beam is continually

injected into the accelerator. This allows the energy spread from a Continuous Electron Beam Accelerator Facility (CEBAF)-type machine to be relatively small; the measured energy spread from CEBAF at 4 GeV is less than 100 parts per million accumulated over times of order several days. In this paper, the various subsystems contributing to the energy spread of a CEBAF-type accelerators are reviewed, as well as the machine diagnostics and controls that are used in CEBAF to ensure that a small energy spread is provided during routine running. Examples of relevant developments are: (1) stable short bunches emerging from the injector; (2) precision timing and phasing of the linacs with respect to the centroid of the beam bunches on all passes; (3) implementing 2 kHz sampling rate feedback systems for final energy stabilization; and (4) continuous beam energy spread monitoring with optical transition radiation devices. We present measurement results showing that small energy spreads are achieved over extended periods.
NTIS
*Linear Accelerators; Electron Beams; Energy Distribution*

**20010125506** Thomas Jefferson National Accelerator Facility, Newport News, VA USA
**Superconducting Linac for the SNS**
Stovall, J.; Nath, S.; Billen, J.; Young, L.; Lynch, M.; Aug. 01, 2000; 3p; In English
Report No.(s): DE2001-769166; JLAB-ACC-00-11; DOE/ER/40150-1776; No Copyright; Avail: Department of Energy Information Bridge, Microfiche

The Spallation Neutron Source (SNS) linac is comprised of both normal and superconducting radio frequency (SRF) accelerating structures. The SRF linac is accelerates the beam from 186 to 1250 MeV through 117 elliptical, multi-cell niobium cavities. This paper describes the SRF linac architecture, physics design considerations, cavity commissioning, and the expected beam dynamics performance.
NTIS
*Linear Accelerators; Neutron Sources; Dynamic Characteristics*

**20010125507** Fermi National Accelerator Lab., Batavia, IL USA
**Radioactivation of Coolant in the E-823 D-Zero Silicon Tracker**
Freeman, W. S.; Dec. 12, 2000; 6p; In English
Report No.(s): DE2001-769162; FERMILAB-TM-2135; No Copyright; Avail: Department of Energy Information Bridge, Microfiche

The DO Silicon Microstrip Tracker (SMT) for E-823 surrounds the beam pipe at the interaction region of the DO straight section. The central part of the detector consists of six barrel/disk modules with an additional three 'F-disks' on each end. There also are two additional, larger disks outside each end of the central detector, called the 'H disks'. Each barrel contains four concentric layers of silicon ladders at radial distances ranging from 2.7 to 9.4 cm from the beam centerline, while the associated F-disks (H-disks) are constructed of wedge-shaped silicon pieces and span the range from 2.6 to 10.5 cm (9.5 to 26 cm).
NTIS
*Coolants; Silicon*

**20010125508** Fermi National Accelerator Lab., Batavia, IL USA
**Time of Flight Detector at CDF**
Grozis, C.; Kephart, R.; Stanek, R.; Dec. 12, 2000; 4p; In English
Report No.(s): DE2001-769161; FERMILAB-CONF-00/326-E; No Copyright; Avail: Department of Energy Information Bridge, Microfiche

A Time-of-Flight detector (TOD) has been incorporated into the CDF-II experiment in order to provide charged kaon identification to improve neutral B meson flavor determination. with an expected time-of-flight resolution of 100 ps, the system will be able to provide two standard deviation separations between K(+/-) and Pi(+/-) for momenta p less than 1.6 GeV/c, complementing the specific ionization energy loss dE/dx measured with the new drift chamber.
NTIS
*Energy Dissipation; Kaons; Mesons*

**20010125509** Argonne National Lab., IL USA
**Report of the Tevatron Higgs Working Group**
Carena, M.; Conway, J. S.; Haber, H. E.; Hobbs, J. D.; Harris, B. W.; Nov. 14, 2000; 187p; In English
Report No.(s): DE2001-768619; ANL-HEP-CP-00-118; No Copyright; Avail: Department of Energy Information Bridge, Microfiche

Despite the success of the Standard Model (SM), which provides a superb description of a wide range of experimental particle physics data, the dynamics responsible for electroweak symmetry breaking is still unknown. Its elucidation remains one of the primary goals of future high energy physics experimentation. Present day global fits to precision electroweak data based on the Standard Model favor the existence of a weakly-interacting scalar Higgs boson, which is a remnant of elementary scalar dynamics that drives electroweak symmetry breaking. The only known viable theoretical framework incorporating light elementary scalar fields employs low-energy supersymmetry, where the scale of supersymmetry breaking is (Omicron) (1 TeV). The Higgs sector of the Minimal Supersymmetric extension of the Standard Model (MSSM) is of particular interest because it predicts the existence of a light CP-even neutral Higgs boson with a mass below about 130 GeV. Moreover, over a significant portion of the MSSM parameter space, the properties of this scalar are indistinguishable from those of the SM Higgs boson.
NTIS
*Broken Symmetry; Electroweak Interactions (Field Theory); Supersymmetry; Higgs Bosons*

**20010125516** YY Labs, Inc., Freemont, CA USA
**Final Report: A Multi-Channel Recirculating Loop Signal Regenerator for High Frequency Single-Shot Bench Length Measurement, August 13, 1998-March 17, 1999**
Yin, Y.; Jun. 15, 1999; 17p; In English
Report No.(s): DE2001-765220; No Copyright; Avail: Department of Energy Information Bridge
The project is to design and bench test a multi-channel single shot transient electrical or optical pulses or pulse trains. A special gating function has been used to select a specific pulse for detail measurement. A study has been done to learn the dynamic physics in the recirculative loop. The proposed technique has been able to let signal circulate more than 1000 turns in the recirculative loop.
NTIS
*Dimensional Measurement; Electromagnetic Pulses; High Frequencies; Regenerators; Multichannel Communication*

**20010125533** Ames Lab., IA USA
**Characterization of the Dilute Ising Antiferromagnet**
Wiener, T.; Sep. 12, 2000; 132p; In English
Report No.(s): DE2001-764680; IS-T 1910; No Copyright; Avail: Department of Energy Information Bridge
A spin glass is a magnetic ground state in which ferromagnetic and antiferromagnetic exchange interactions compete, thereby creating frustration and a multidegenerate state with no long range order. An Ising system is a system where the spins are constrained to lie parallel or antiparallel to a primary axis. There has been much theoretical interest in the past ten years in the effects of applying a magnetic field transverse to the primary axis in an Ising spin glass at low temperatures and thus study phase transitions at the T=0 limit. The focus of this study is to search for and characterize a new Ising spin glass system. This is accomplished by site diluting yttrium for terbium in the crystalline material TbNi(sub 2)Ge(sub 2). The first part of this work gives a brief overview of the physics of rare earth magnetism and an overview of experimental characteristics of spin glasses. This is followed by the methodology used to manufacture the large single crystals used in this study, as well as the measurement techniques used. Next, a summary of the results of magnetic measurements on across the dilution series from pure terbium to pure yttrium is presented. This is followed by detailed measurements on particular dilutions which demonstrate spin glass behavior. Pure TbNi(sub 2)Ge(sub 2) is an Ising antiferromagnet with a several distinct metamagnetic states below 17 K. As the terbium is alloyed with yttrium, these magnetic states are weakened in a consistent manner, as is seen in measurements of the transition temperatures and analysis of Curie-Weiss behavior at high temperature. At low concentrations of terbium, below 35%, long range order is no longer present and a spin-glass-like state emerges. This state is studied through various measurements, dc and ac susceptibility, resistivity, and specific heat. This magnetic behavior was then compared to that of other well characterized spin glasses. It is concluded that there is a region of concentration s for which a spin glass state is formed with the best spin glasses existing between the concentration of 25% and 30%.
NTIS
*Antiferromagnetism; Crystallinity; Ising Model; Spin Glass; Rare Earth Elements; Dilution*

**20010125563** Argonne National Lab., IL USA
**Photon Structure and the Production of Jets, Hadrons, and Prompt Photons**
Klasen, M.; Jul. 22, 1999; 14p; In English
Report No.(s): DE2001-11906; ANL-HEP-CP-99-73; No Copyright; Avail: Department of Energy Information Bridge, Microfiche

We give a pedagogical introduction to hard photoproduction processes at HERA, including the production of jets, hadrons, and prompt photons. Recent theoretical developments in the three areas are reviewed. In summary, hard photoproduction processes can provide very useful information on the hadronic structure of the photon, in particular on the gluon density, which is complimentary to the information coming from deep inelastic photon-photon scattering at electron-positron colliders. Among the different hadronic final states, jets are most easily accessible experimentally and phenomenologically. On the other hand, inclusive hadron production offers the possibility to test the universality of hadron fragmentation functions and measure the photon structure down to very low values of p(sub T) and x(sub gamma). Prompt photon production suffers from a reduced cross section and limited data, but allows for the additional testing of photon fragmentation functions.
NTIS
*Gluons; Hadrons; Photons; Photoproduction*

**20010125577** Argonne National Lab., IL USA
**Production of (phi) meson in Au+Au collisions at 11.7 A GeV/c**
Back, B. B.; Betts, R. R.; Chang, J.; Chang, W. C.; Chi, C. Y.; Jun. 29, 1999; 8p; In English
Report No.(s): DE2001-11870; ANL/PHY/CP-99369; No Copyright; Avail: Department of Energy Information Bridge, Microfiche

First Measurement of (phi) meson production in Au+Au collisions has been conducted by E917 at BNL-AGS via selecting events with identified K(sup +)K(sup (minus)) pairs. Preliminary results on the invariant mass spectra of K(sup +)K(sup (minus)) pairs and the m(sub T) spectra are presented. Also, the inverse slope T, dN/dy, the ratio of (phi)/K(sup (minus)), ratio of (phi)/K(sup +)K(sup (minus)) and their centrality dependences are extracted in a rapidity range of y = 0.9-1.4. Indications on the possible mechanisms of (phi) production are discussed.
NTIS
*Gold; Mesons; Pair Production; Atomic Collisions*

**20010125578** Argonne National Lab., IL USA
**Atmospheric neutrinos in Soudan 2**
Goodman, M. C.; Jun. 22, 1999; 6p; In English
Report No.(s): DE2001-11869; ANL-HEP-CP-99-63; No Copyright; Avail: Department of Energy Information Bridge, Microfiche

The value and zenith angle dependence of the atmospheric neutrino flavor ratio is interpreted as evidence for neutrino oscillations. The latest values from the Soudan 2 detector are presented. From 4.2 kt-years fiducial exposure, Soudan 2 measures R = 0.66 (+-) 0.11(stat) + 0.05--0.06(syst). Using a subset of the data with the best angular resolution, they plot the L/E distribution and use this to find the allowed region in oscillation parameter space. Their fit suggests that delta m-squared is greater than 10(sup (minus)3) eV(sup 2) at 90% CL.
NTIS
*Neutrinos; Oscillations; Zenith; Flavor (Particle Physics)*

**20010125580** Argonne National Lab., IL USA
**Measurement of the light quark flavor asymmetry in the nucleon sea**
Awes, T. C.; Beddo, M. E.; Brown, C. N.; Bush, J. D.; Geesaman, D. F.; Jun. 25, 1999; 14p; In English
Report No.(s): DE2001-11867; ANL/PHY/CP-99361; No Copyright; Avail: Department of Energy Information Bridge, Microfiche

Fermilab experiment E866 has performed a precision measurement of the ratio of Drell-Yan yields from 800 GeV/c protons incident on deuterium and hydrogen targets. The measurement is used to determine the ratio of down antiquarks((bar d)) to up antiquarks((bar u)) in the proton over a broad range in the fraction of the proton momentum carried by the antiquark, 0.02 greater than x greater than 0.345. For x greater than 0.15, the data is in reasonable agreement with pre-existing parton distributions while for x less than 0.20 the data is much closer to unity than these parton functions had indicated. The light quark asymmetry provides valuable information on the relative role perturbative and non-perturbative mechanisms play in generating the nucleon sea. A proposal to extend the Drell-Yan measurement to higher values of x using 120 GeV protons from the Fermilab main injector will be discussed.
NTIS
*Asymmetry; Nucleons; Quarks; Flavor (Particle Physics)*

**20010125581** Argonne National Lab., IL USA

**Dependence of HBT source parameters on beam energy and reaction plane at AGS**

Back, B. B.; Betts, R. R.; Chang, J.; Chang, W. C.; Chi, C. Y.; Jun. 29, 1999; 8p; In English

Report No.(s): DE2001-11866; ANL/PHY/CP-99360; No Copyright; Avail: Department of Energy Information Bridge, Microfiche

Two-particle correlations between pions in Au+Au collisions have been measured at beam kinetic energies of 6, 8, and 10.6 GeV/u at the Alternating Gradient Synchrotron (AGS) over a wide range of rapidities using a magnetic spectrometer. The data have been analyzed in the Hanbury-Brown and Twiss (HBT) framework to extract source parameters as functions of the reaction plane as well as beam energy.

NTIS

*Ionic Collisions; Synchrotrons; Beams (Radiation); Gold; Metal Ions*

**20010125583** Argonne National Lab., IL USA

**Searching for R-parity violation at run-II of the tevatron**

Allanach, B.; Banerjee, S.; Berger, E. L.; Chertok, M.; Diaz, M. A.; Jun. 22, 1999; 41p; In English

Report No.(s): DE2001-11862; ANL-HEP-CP-99-74; No Copyright; Avail: Department of Energy Information Bridge, Microfiche

The authors present an outlook for possible discovery of supersymmetry with broken R-parity at Run II of the Tevatron. They first present a review of the literature and an update of the experimental bounds. In turn they then discuss the following processes: (1) resonant slepton production followed by R(sub P) decay, (a) via LQD(sup c) and (b) via LLE(sup c); (2) how to distinguish resonant slepton production from Z(prime) or W(prime) production; (3) resonant slepton production followed by the decay to neutralino LSP, which decays via LQD(sup c); (4) resonant stop production followed by the decay to a chargino, which cascades to the neutralino LSP; (5) gluino pair production followed by the cascade decay to charm squarks which decay directly via L(sub 1)Q(sub 2)D(sub 1)(sup c); (6) squark pair production followed by the cascade decay to the neutralino LSP which decays via L(sub 1)Q(sub 2)D(sub 1)(sup c); (7) MSSM pair production followed by the cascade decay to the LSP which decays (a) via LLE(sup c), (b) via LQD(sup c), and (c) via U(sup c)D(sup c)D(sup c), respectively; and (8) top quark and top squark decays in spontaneous R(sub P).

NTIS

*Particle Accelerators; Supersymmetry; Elementary Particles; Quarks; Fermions*

**20010125584** Argonne National Lab., IL USA

**Reproducible measurements of MPI performance characteristics**

Gropp, W.; Lusk, E.; Jun. 25, 1999; 10p; In English

Report No.(s): DE2001-11859; ANL/MCS/CP-99345; No Copyright; Avail: Department of Energy Information Bridge, Microfiche

In this paper, we describe the difficulties inherent in making accurate, reproducible measurements of message-passing performance. We describe some of the mistakes often made in attempting such measurements and the consequences of such mistakes. We describe mpptest, a suite of performance measurement programs developed at Argonne National Laboratory, that attempts to avoid such mistakes and obtain reproducible measures of MPI performance that can be useful to both MPI implementers and MPI application writers. We include a number of illustrative examples of its use.

NTIS

*Data Transmission; Applications Programs (Computers); Message Processing; Performance Tests*

**20010125624** Thomas Jefferson National Accelerator Facility, Newport News, VA USA

**Specifying HOM-Power Extraction in a High Average Current Short Bunch Length SRF Environment**

Merminga, L.; Krafft, G.; Leemann, C.; Sundelin, R.; Bisognano, B.; Aug. 01, 2000; 3p; In English

Report No.(s): DE2001-769186; JLAB-ACP-00-04; DOE/ER/40150-1786; JLAB-ACC-00-10; No Copyright; Avail: Department of Energy Information Bridge, Microfiche

High average current, short bunch length beams in superconducting cavities can excite significant amounts of higher-order mode (HOM) power. The fraction that is dissipated in the cavity walls is of primary relevance as it can potentially limit the peak and average current due to the finite cryogenic capacity. A model has been developed which estimates the amount of power dissipated on the walls based on the dependence of the cavity's quality factor Q on frequency, due to Bardeen-Cooper-Schrieffer (BCS) losses, and an analytic expression for the cavity impedance in the high frequency limit. Specifications for the HOM power

extraction efficiency are derived so that the cryogenic load due to the HOM excitation is of similar magnitude as the load due to the accelerating fields.
NTIS
*Cavities; Extraction; Superconductivity*

## 71
## ACOUSTICS

*Includes sound generation, transmission, and attenuation. For noise pollution see 45 Environment Pollution. For aircraft noise see also 02 Aerodynamics and 07 Aircraft Propulsion Propulsion and Power.*

**20010117660** Sandia National Labs., Albuquerque, NM USA
**Radiation of Elastic Waves from Point Sources in a Uniform Wholespace**
Adridge, D. F.; Jul. 01, 2000; 73p; In English
Report No.(s): DE2000-759486; SAND2000-1767; No Copyright; Avail: Department of Energy Information Bridge

The elastic waves radiated from a point source in a homogeneous and isotropic wholespace have been described, with varying degrees of completeness and generality, by numerous investigators. However, it is difficult (if not impossible) to locate a comprehensive mathematical treatment of the subject that could form the basis of a reasonably general synthetic seismogram algorithm. In the present study, the equations characterizing the elastic wavefields produced by a variety of different point sources are assembled in a tiled mathematical notation. Derivations of the formulae are not provided. All possible point force sources (represented by an orientation vector) and point moment sources (represented by an orientation tensor) are included. Arbitrary source activation waveforms are allowed. The radiated elastic waves are expressed in terms of the particle velocity and particle rotation vectors, and the acoustic pressure. Mathematical formulae describing these wavefield quantities contain all near-field, intermediate-field, and far-field terms. In the limiting case of vanishing shear wave speed, the expressions are applicable to an ideal fluid (i.e., acoustic) medium.
NTIS
*Elastic Waves; Wave Propagation; Elastic Scattering*

**20010119231** National Center for Physical Acoustics, University, MS USA
**NCPA Enhancement for Physical Acoustics** ***Final Report, 15 Sep. 1998-14 Sep 1999***
Bass, Henry E.; Oct. 09, 2001; 3p; In English
Contract(s)/Grant(s): N00014-98-1-0880
Report No.(s): AD-A395088; No Copyright; Avail: CASI; A01, Hardcopy; A01, Microfiche

The overall objective of this grant is to enhance and maintain a strong physical acoustics research program at the National Center for Physical Acoustics that will improve our ability to recruit first-rate scientists and students and carry out effective, ONR-supported research. Specific objectives of this grant are to support research and recruitment by enhancing the infrastructure in physical acoustics through (a) graduate fellowship support, (b) modernization of scientific presentation capabilities, and (c) publishing a monograph series on the elastic properties of materials.
DTIC
*Acoustics; Augmentation; Research Management; Physical Properties*

**20010119238** State Univ. of New York, Marine Sciences Research Center, Stony Brook, NY USA
**High Resolution Bathymetry and Backscatter of a High-Frequency Test Area** ***Final Report, 15 May 1999-31 Dec. 2000***
Flood, Roger D.; Feb. 10, 2001; 7p; In English
Contract(s)/Grant(s): N00014-98-1-0867
Report No.(s): AD-A395053; No Copyright; Avail: CASI; A02, Hardcopy; A01, Microfiche

High-resolution multibeam bathymetry was collected in the SAX99 study area (18 m deep, offshore western Florida) prior to instrument deployment to ensure that moorings were located within a uniform region. The multibeam data defined a region of similar bottom type on a ridge between two muddy depressions, and the moorings were deployed on the ridge. Analysis of backscatter patterns from the 300 kHz EM3000 multibeam echosounder show that backscatter at 15 to 30 degrees from vertical on the ridge is higher on east-west tracks than on north-south tracks. This is due to the presence of east-west trending wave-generated ripples with amplitudes of about 15 cm and wavelengths of about 75 cm on the ridge, with backscatter being

higher when the sound beams are perpendicular to the ripples. The backscatter patterns on multi beam records may thus be used for determining the presence and orientation of small-scale topographic relief.
DTIC
*Backscattering; Bathymeters; High Resolution; Topography; High Frequencies*

**20010119431** Oak Ridge National Lab., TN USA
**Approximate Identification of Boundary Properties in a Wave Equation by Optimal Control Techniques**
Lenhart, S.; Protopopescu, V.; Yong, J.; Jun. 07, 1999; 13p; In English
Report No.(s): DE2000-15060; ORNL/CP-105497; No Copyright; Avail: Department of Energy Information Bridge, Microfiche
We apply optimal control techniques to find approximate solutions to an inverse problem for the acoustic wave equation. The inverse problem is to determine the shape and reflection coefficient of a part of the boundary from partial measurements of the acoustic signal. The sought functions are treated as controls and the goal is to drive the model solution close to the experimental data by adjusting these functions.
NTIS
*Approximation; Boundary Conditions; Optimal Control; Wave Equations*

**20010119436** Oak Ridge National Lab., TN USA
**Static and Transient Cavitation Threshold Measurements for Mercury**
Moraga, F.; Taleyarkhan, R. P.; Nov. 14, 1999; 7p; In English
Report No.(s): DE2000-15055; ORNL/CP-105500; No Copyright; Avail: Department of Energy Information Bridge, Microfiche
Transient and static cavitation thresholds for mercury as a function of the cover gas (helium or air) and pressure are reported. Both static and transient cavitation onset pressure thresholds increase linearly with cover gas pressure. Additionally, the cavitation thresholds as a function of dissolved gases were also measured and are reported.
NTIS
*Cavitation Flow; Gas Pressure; Transient Pressures; Mercury (Metal)*

**20010119561** Atomic Energy Commission, Idaho Operations Office, Idaho Falls, ID USA
**Dynamic Holographic Lock-In Imaging of Ultrasonic Waves**
Telschow, K. L.; Datta, S. K.; Deason, V. A.; May 01, 1999; 9p; In English
Report No.(s): DE2001-10487; INEEL/CON-99-00472; No Copyright; Avail: Department of Energy Information Bridge, Microfiche
A laser imaging approach is presented that utilizes the adaptive property of photorefractive materials to produce a real-time measurement of ultrasonic traveling wave surface displacement and phase in all planar directions simultaneously without scanning. The imaging method performs optical lock-in operation. A single antisymmetric Lamb wave mode image produces direct quantitative determination of the phase velocity in all planar directions showing plate stiffness anisotropy. Excellent agreement was obtained with modeling calculations of the phase velocity in all planar directions for an anisotropic sheet material. The approach functions with diffusely scattering surfaces, subnanometer motions and at frequencies from Hz to GHz.
NTIS
*Anisotropy; Lasers; Ultrasonic Radiation; Holography*

**20010120109** General Accounting Office, Washington, DC USA
**AVIATION AND THE ENVIRONMENT: Transition to Quieter Aircraft Occurred as Planned, but Concerns About Noise Persist**
Sep. 2001; 48p; In English
Report No.(s): AD-A395076; GAO-01-1053; No Copyright; Avail: CASI; A03, Hardcopy; A01, Microfiche
Aircraft noise is a major concern in communities around airports despite considerable reductions in such noise and a corresponding decrease in the population exposed to it. Moreover, concern about noise remains a constraint on efforts to expand airport capacity to meet the growing demand for air travel. The Congress has authorized the Federal Aviation Administration (FAA) to regulate aircraft noise. The Airport Noise and Capacity Act (ANCA) of 1990 established December 31, 1999, as the deadline for airlines to phase out the use of existing jet aircraft weighing more than 75,000 pounds that had not been modified to comply with current aircraft noise standards, called Stage 3. 1 Until ANCA's passage, only newly designed or newly manufactured aircraft were required to comply with the Stage 3 aircraft noise standards. Recently, the USA participated with other countries in the International Civil Aviation Organization (ICAO) to develop a more stringent aircraft noise standard for subsonic

jets and large propeller-driven aircraft. On June 27, 2001, the ICAO Council approved the adoption of a new noise certification standard called Chapter 4.
DTIC
*Aircraft Noise; Airports; Civil Aviation; Commercial Aircraft*

**20010122265** Lawrence Livermore National Lab., Livermore, CA USA
**Classification of Heart Valve Sounds from Experiments in an Anechoic Water Tank**
Axelrod, M. C.; Clark, G. A.; Scott, D.; Jun. 01, 1999; 46p; In English
Report No.(s): DE2001-10789; UCRL-ID-134634; AC1005000; No Copyright; Avail: Department of Energy Information Bridge, Microfiche

In vivo studies in both sheep and humans were plagued by a number of problems including movement artifacts, biological noise, low signal-to-noise ratio (SNR), chest-wall reverberation, and limited bandwidth recordings. To overcome these problems it was decided to record heart valve sounds under controlled conditions deep in an anechoic water tank, free from reverberation noise. The main goal of this experiment was to obtain measurements of 'pure' heart valve sounds free of the scattering effects of the body. Experiments were conducted at the Transdec facility in San Diego. We used a high quality hydrophone together with a wide-band data acquisition system. We recorded sounds from 100 repetitions of the opening-closing cycles on each of 50 different heart valves, including 21 SLS valves and 29 intact valves. The power spectrum of the opening and closing phases of each cycle were calculated and outlier spectra removed as described by Candy. In this report, we discuss the results of our classification of the heart valve sound measurements. The goal of this classification task was to apply the fundamental classification algorithms developed for the clinical data in 1994 and 1996 to the measurements from the anechoic water tank. From the beginning of this project, LLNL's responsibility has been to process and classify the heart valve sounds. For this experiment, however, we processed both the opening sounds and closing sounds for comparison purposes. The results of this experiment show that the classifier did not perform well because of low signal-to-noise ratio and excessive variability in signal power from beat-to-beat for a given valve.
NTIS
*Acoustic Measurement; Acoustic Properties; Classifications; Heart Valves*

**20010122266** Lawrence Livermore National Lab., Livermore, CA USA
**Classification of Heart Valve Sounds from Experiments in an Anechoic Water Tank**
Axelrod, M. C.; Clark, G. A.; Scott, D.; Jun. 01, 1999; 51p; In English
Report No.(s): DE2001-10788; UCRL-ID-134634-REV-1; AC1005000; No Copyright; Avail: Department of Energy Information Bridge, Microfiche

In vivo studies in both sheep and humans were plagued by a number of problems including movement artifacts, biological noise, low signal-to-noise ratio (SNR), chest-wall reverberation, and limited bandwidth recording. To overcome these problems it was decided to record heart valve sounds under controlled conditions deep in an anechoic water tank, free from reverberation noise, including surface reflections. Experiments were conducted in a deep water tank at the Transdec facility in San Diego, which satisfies these requirements. The Transdec measurements are free of reverberations, but not totally free of acoustic and electrical noise. We used a high quality hydrophone together with a wide-band data acquisition system. We recorded sounds from 100 repetitions of the opening-closing cycles on each of 50 different heart valves, including 21 SLS valves and 29 intact valves. The power spectrum of the opening and closing phases of each cycle were calculated and outlier spectra removed as described by Candy. In this report, we discuss the results of our classification of the heart valve sound measurements. The goal of this classification task was to apply the fundamental classification algorithms developed for the clinical data in 1994 and 1996 to the measurements from the anechoic water tank. From the beginning of this project, LLNL's responsibility has been to process and classify the heart valve opening sounds. For this experiment, however, we processed both the opening sounds and closing sounds for comparison purposes. The results of this experiment show that the classifier did not perform well. We believe this is because of low signal-to-noise ratio and excessive variability in signal power from beat-to-beat for a given valve.
NTIS
*Acoustic Properties; Classifications; Heart Valves; Acoustic Measurement*

**20010122711** Massachusetts Inst. of Tech., Dept. of Electrical Engineering and Computer Science, Cambridge, MA USA
**Acoustic Characterization of a Stationary Field Synchronous Motor**
Woodward, E. C., Jr.; Aug. 2001; 59p; In English
Report No.(s): AD-A395279; No Copyright; Avail: CASI; A04, Hardcopy; A01, Microfiche

The stationary field synchronous motor (SFSM) has been described and analyzed previously. This machine usually consists of a stationary, direct current field winding and a rotating, alternating current armature winding. The field winding is superconducting. This topology presents certain advantages and disadvantages. One of the greatest theoretical advantages is reduced acoustic emission. The precise nature of such reductions has not been considered in previous work. We investigate the gross acoustic signature of a notional stationary field synchronous motor utilized as a marine propulsion motor in a naval combatant using the following methodology: (1) model the forces (harmonic by harmonic) of electromagnetic origin using solutions of the two dimensional Laplace Equation arising from the scalar potential of a magnetic field, (2) Develop a force spectrum based upon this modeling, (3) Develop appropriate acoustic transfer functions describing the acoustic propagation of the machine components, equipment mounting structures, and other pertinent items in the machine-to-sea sound conduction path, (4) Apply the force spectrum to the acoustic transfer function(s), and (5) obtain a meaningful far-field acoustic signature due to the SFSM.
DTIC
*Armatures; Acoustic Emission; Marine Propulsion*

**20010124128** NASA Goddard Space Flight Center, Greenbelt, MD USA
**Orbital Noise in the Earth System and Climate Fluctuations**
Liu, Han-Shou, NASA Goddard Space Flight Center, USA; [2001]; 4p; In English; 16th International Conference on Noise in Physical Systems and 1/f Fluctuations, Unknown; No Copyright; Avail: CASI; A01, Hardcopy; A01, Microfiche

Frequency noise in the variations of the Earth's obliquity (tilt) can modulate the insolation signal for climate change. Including this frequency noise effect on the incoming solar radiation, we have applied an energy balance climate model to calculate the climate fluctuations for the past one million years. Model simulation results are in good agreement with the geologically observed paleoclimate data. We conclude that orbital noise in the Earth system may be the major cause of the climate fluctuation cycles.
Author
*Climate Change; Climate Models; Simulation; Solar Radiation; Electromagnetic Noise*

**20010125027** National Defence Research Establishment, Div. of Systems and Underwater Technology, Stockholm, Sweden
**Analysis of Active Sonar Data using the ARTES Ray-Trace Model. Methodology Report**
Ivansson, S.; Karasalo, I.; December 2000; 30p; In English
Report No.(s): PB2001-107295; FOA-R-00-01753-409-SE; No Copyright; Avail: CASI; A01, Microfiche; A03, Hardcopy

Data from an active sonar array collected at a sea trial in shallow water are compared with theoretical predictions by the ARTES (Acoustic Ray Tracing Target Echo Strength) model. The data originate from three sources, a Baretta sphere towed across the line of sight of the sonar, and two noise sources at fixed bearings. A Baretta sphere target option for ARTES is developed, based on the theoretic target strength of a fluid-filled steel shell, and used for the data analysis. The dominating features of the data are found to agree satisfactorily well, to within a few dB, with the model predictions for all pings.
NTIS
*Sonar; Targets; Mathematical Models; Predictions*

**20010125137** NASA Ames Research Center, Moffett Field, CA USA
**Microphone Corrections for Accurate In-Flow Acoustic Measurements at High Frequency**
Allen, Christopher S., Sterling Federal Systems, Inc., USA; Vandra, Kartik, Sterling Federal Systems, Inc., USA; Soderman, Paul T., NASA Ames Research Center, USA; [1994]; 3p; In English; 1995 AIAA Aeroacoustics Conference, 12-15 Jun. 1995, Munich, Germany; Sponsored by American Inst. of Aeronautics and Astronautics, USA
Contract(s)/Grant(s): RTOP 505-59-52; No Copyright; Avail: Issuing Activity; Abstract Only

Acoustic analysis of aircraft components through small-scale experiments in wind tunnels requires in-flow acoustic measurements at high frequencies. This high frequency information is shifted to lower frequencies during the geometric scaling process. As a result, models of scale one tenth and smaller require frequency information of up to at least 100 kHz to resolve the midpoint of the full-scale equivalent audible range. Farfield acoustic measurements of frequencies higher than 100 kHz are prohibitively difficult to make due to the physical limitations of atmospheric propagation over large distances and the delicacy of the required instruments. Even measurements up to 100 kHz require special corrections and calibration procedures to maintain sufficient accuracy. In-flow microphone measurements at high frequencies require additional consideration due to the presence of the aerodynamic microphone forebody which protects the microphone diaphragm from flow impingement. The screen located at the forebody surface attenuates the high frequency acoustic waves and must be accounted for. The purpose of this paper is to present procedures for calibrating and correcting high frequency acoustic measurements to retain high accuracy. Specifically, this

paper gives calibration procedures and examples of typical data for calibrating or correcting for five physical effects. These effects include the frequency response of the entire acoustic data acquisition system, intrusion of the microphone into the acoustic field, forebody screen attenuation, directionality of microphone forebody response and atmospheric absorption.
Author
*Acoustic Measurement; High Frequencies; Microphones; Data Acquisition*

**20010125443** Lawrence Livermore National Lab., Livermore, CA USA
**Temporal imaging system demonstrates 103x magnification**
Bennett, C. V.; Kolner, B. H.; Nov. 11, 1998; 9p; In English
Report No.(s): DE2001-8403; UCRL-JC-132413; No Copyright; Avail: Department of Energy Information Bridge, Microfiche
A temporal imaging system obtaining 103x magnification and 300 fs resolution was demonstrated. This system consists of dispersive delay lines and a time lens produced by sum-frequency generation with a chirped pump.
NTIS
*Imaging Techniques; Images; Optical Equipment*

**20010125445** Lawrence Livermore National Lab., Livermore, CA USA
**Elastic constants of B-HMX and tantalum, equations of state of supercritical fluids and fluid mixtures and thermal transport determinations**
Zaug, J. M.; Aug. 21, 1998; 12p; In English
Report No.(s): DE2001-8390; UCRL-JC-131658; No Copyright; Avail: Department of Energy Information Bridge, Microfiche
Ultrasonic sound speed measurements via Impulsive Stimulated Light Scattering (ISLS) were made in single crystals of b-HMX and tantalum over an extended range of temperatures. Elastic constants are consequently determined for b-HMX. Sound speeds are calculated for tantalum, from known elastic constants, and compare favorably with the results presented here. ISLS time-domain fits of tantalum records allowed for thermal diffusion determinations and, correspondingly, thermal conductivity. Measurements of the speed of sound and of the thermal diffusivities of fluid oxygen up to pressures of 13 GPa and at several temperatures are presented. Between 0.1 and 13 GPa the fluid's density increases by a factor of three. Thermal diffusivities rise slowly over this range, and are substantially smaller than those previously measured for the solid b-phase. Additional sound speed measurements were made along the 250 C isotherm in a 1:1 molar ratio mixture of liquid oxygen and nitrogen. These experiments demonstrate the versatility and potential application of a new laboratory within the U.S. DOD (Department of Defense) and DOE (Department of Energy) complex.
NTIS
*Equations of State; Tantalum; Thermal Conductivity; HMX; Elastic Properties; Supercritical Fluids; Ultrasonic Tests*

## 72
## ATOMIC AND MOLECULAR PHYSICS

*Includes atomic and molecular structure, electron properties, and atomic and molecular spectra. For elementary particle physics see 73 Nuclear Physics.*

**20010117636** Brookhaven National Lab., Upton, NY USA
**Yields of Ions and Excited States in Nonpolar Liquids Exposed to X-Rays of 1 to 30 keV Energy**
Holroyd,; Aug. 18, 1999; 8p; In English
Report No.(s): DE2000-759006; BNL-66640; No Copyright; Avail: Department of Energy Information Bridge, Microfiche
When x-rays from a synchrotron source are absorbed in a liquid, the x-ray energy (E(sub x)) is converted by the photoelectric effect into the kinetic energy of the electrons released. For hydrocarbons, absorption by the K-electrons of carbon dominates. Thus the energy of the photoelectron (E(sub pe)) is E(sub x)-E(sub b), where E(sub b) is the K-shell binding energy of carbon. Additional electrons with energy equal to E(sub b) is released in the Auger process that fills the hole in the K-shell. These energetic electrons will produce many ionizations, excitations and products. The consequences of the high density of ionizations and excitations along the track of the photoelectron and special effects near the K-edge are examined here.
NTIS
*Electrons; Excitation; Hydrocarbons; Ions; Photoelectrons*

**20010117733** NASA Ames Research Center, Moffett Field, CA USA

**Cr2 Revisited**

Bauschlicher, Charles W., Jr., NASA Ames Research Center, USA; Partridge, Harry, NASA Ames Research Center, USA; [1994]; 1p; In English

Contract(s)/Grant(s): RTOP 232-01-04; No Copyright; Avail: Issuing Activity; Abstract Only

Abstract Cr2 is studied at the coupled cluster singles and doubles level of theory, including a perturbational estimate of the connected triples [CCSD(T)]. Both spin restricted, RCCSD(T), and spin unrestricted, UCCSD(T), approaches are used. The UCCSD(T) bond length is much longer than the experimental value, while the RCCSD(T) bond length is shorter. This difference is due to the inability of the spin restricted Hartree-Fock reference to describe the antiferromagnetic coupling at larger r values. In contrast with the results obtained using density functional theory in conjunction with older functionals, the results obtained with recently developed functionals are in agreement with the UCCSD(T) results.

Author

*Computational Chemistry; Chromium; Functionals*

**20010118919** Brookhaven National Lab., Upton, NY USA

**Superconducting dipole magnets for the lhc insertion regions**

Willen,; Anerella,; Cozzolino,; Ganetis,; Ghosh,; Jun. 26, 2000; 3p; In English

Report No.(s): DE2000-760993; BNL-67549; No Copyright; Avail: Department of Energy Information Bridge

Dipole bending magnets are required to change the horizontal separation of the two beams in the LHC (Large hadron colliders). In Intersection Regions (IR) 1, 2, 5, and 8, the beams are brought into collision for the experiments located there. In IR4, the separation of the beams is increased to accommodate the machine's particle acceleration hardware. As part of the US contribution to the LHC Project, BNL (Brookhaven National Laboratory) is building the required superconducting magnets. Designs have been developed featuring a single aperture cold mass in a single cryostat, two single aperture cold masses in a single cryostat, and a dual aperture cold mass in a single cryostat. All configurations feature the 80 mm diameter, 10 m long superconducting coil design used in the main bending magnets of the Relativistic Heavy Ion Collider recently completed at Brookhaven. The magnets for the LHC, to be built at Brookhaven, are described and results from the program to build two dual aperture prototypes are presented.

NTIS

*Superconducting Magnets; Beam Interactions; Particle Collisions; Magnetic Dipoles*

**20010119923** Purdue Univ., Dept. of Earth and Atmospheric Sciences, West Lafayette, IN USA

**Exploring Physics beyond the Standard Model: Astrophysical Motivations and Accelerator Applications**

Javorsek, Daniel, II; Sep. 06, 2001; 412p; In English

Report No.(s): AD-A395241; CI01-215; No Copyright; Avail: CASI; A18, Hardcopy; A04, Microfiche

We report the motivation and results of a search for beryllium, Be, with electrons which violate the Pauli exclusion principle. We then present the run by run results of completed search for the Pauli-forbidden 1s(sup 4) state of Be, denoted by Be'. In contrast to most experiments of this type we have obtained unique samples with higher probability of Be' retention. We set limits on the abundance of Be' in metallic Be, Be ore, natural gas, and air with abundances around 10(exp -11). Our results improve on those obtained in a previous search for Be' by a factor of approximately 300.

DTIC

*Quantum Theory; Beryllium; Fermions; Elementary Particles; Pauli Exclusion Principle*

**20010120006** Sandia National Labs., Albuquerque, NM USA

**Diffusion-Time-Resolved Ion-Beam-Induced Charge Collection from Stripe-Like Test Junctions Induced by Heavy-Ion Microbeams**

Guo,; Bouanani,; Renfrow,; Nigam,; Walsh,; Sep. 18, 2000; 19p; In English

Report No.(s): DE2000-763111; SAND2000-2291C; No Copyright; Avail: Department of Energy Information Bridge, Microfiche

To design more radiation-tolerant Integrated Circuits (ICS), it is necessary to design and test accurate models of ionizing radiation induced charge collection dynamics with microcircuits. A new technique, Diffusion Time Resolved Ion Beam Induced Charge Collection (DTNBICC), is used to measure the average arrival time of the diffused charge, which can be related to the first moment (or the average time) of the arrival carrier density at the junction. Specially designed stripe-like test junctions are experimentally studied using a 12 MeV carbon microbeam with a spot size of about 0.1 micrometer. The relative arrival time of ion-generated charge and the collected charge are measured using a multiple parameter data acquisition system. A 2-D device

simulation code, MEDIC1, is used to calculate the charge collection dynamics on the stripe-like test junctions. The simulations compare very well with experimental microbeam measurements. The results show the importance of the diffused charge collection by junctions, which is especially significant for Single Event Upsets (SEUS) and Multiple Event Upset (MEUS) in digital devices. The charge sharing results also indicate that stripe-like junctions may be used as position sensitive detectors with a resolution of about 0.1 micrometer.
NTIS
*Integrated Circuits; Ionizing Radiation; Ion Beams*

**20010120029** Argonne National Lab., IL USA
**Exclusive Studies of the GDR in Excited Nuclei**
Nanal, V.; Sep. 07, 1998; 6p; In English
Report No.(s): DE2001-10647; ANL/PHY/CP-95650; No Copyright; Avail: Department of Energy Information Bridge
The GDR in Er-164 at 62 MeV excitation energy has been studied in coincidence with the evaporation residues, selected using the Argonne fragment mass analyzer (FMA). The Er-164* has a prolate shape with deformation statistical model fit to the data indicate that similar to the ground state.
NTIS
*Erbium Isotopes; Residues; Mathematical Models*

**20010122304** Brookhaven National Lab., Upton, NY USA
**Intensity Dependent Effects in RHIC**
Wei,; Sep. 02, 1999; 16p; In English
Report No.(s): DE2000-761068; BNL-66781; No Copyright; Avail: Department of Energy Information Bridge
The Relativistic Heavy Ion Collider (RHIC) is currently under commissioning after a seven-year construction cycle. Unlike conventional hadron colliders, this machine accelerates, stores, and collides heavy ion beams of various combinations of species. The dominant intensity dependent effects are intra-beam scattering at both injection and storage, and complications caused by crossing transition at a slow ramp rate. In this paper, the authors present theoretical formalisms that have been used for the study, and discuss mechanisms, impacts, and compensation methods including beam cooling and transition jump schemes. Effects of space charge, beam-beam, and ring impedances are also summarized.
NTIS
*Ion Beams; Beam Injection; Cooling*

**20010123726** Lawrence Livermore National Lab., Livermore, CA USA
**Direct observation of resonance effects in laser cluster interactions**
Zweiback, J.; Jun. 01, 1999; 164p; In English
Report No.(s): DE2001-11313; UCRL-LR-134008; DP0214000; No Copyright; Avail: Department of Energy Information Bridge
Time resolved dynamics of high intensity laser interactions with atomic clusters have been studied with both theoretical analysis and experiment. A short-pulse Ti:sapphire laser system, which could produce 50 mJ of energy in a 50 fs pulse, was built to perform these experiments. The laser used a novel single grating stretcher and was pumped, in part, by a custom Nd:YLF laser system, including 19 mm Nd:YLF amplifiers. It was found that there is an optimal pulse width to maximize absorption for a given cluster size. This optimal pulse width ranged from 400 fs for 85 A radius xenon clusters to 1.2 ps for 205 (angstrom) radius xenon clusters. Using a pump-probe configuration, the absorption of the probe radiation was observed to reach a maximum for a particular time delay between pump and probe, dependent on the cluster size. The delay for peak absorption was 800, 1400, and 2100 fs for 85 (angstrom), 130 (angstrom), and 170 (angstrom) radius xenon clusters respectively. Model calculations suggest that these effects are due to resonant heating of the spherical plasma in agreement with the hydrodynamic interpretation of cluster interactions. While this simple hydrodynamic code produces reasonable agreement with data, it does not include bulk plasma or non-linear propagation effects and is limited to the regime where resonant behavior dominates. We also measured the scattered laser light from the laser-cluster interaction. Similar to the absorption measurements, there is an optimal pulse width which maximizes the scattered signal. This pulse width is larger than the optimal pulse width for absorption. This disagrees with model calculations which show both pulse widths being similar. Further experiments measuring the scattered light in a pump-probe configuration should help to resolve this disagreement.
NTIS
*Atomic Clusters; High Power Lasers; Electromagnetic Interactions; Pulsed Lasers*

**20010123736** Argonne National Lab., IL USA
**Coulomb excitation of a (78)Rb radioactive beam**
Schwartz, J.; Nov. 18, 1998; 6p; In English
Report No.(s): DE2001-11111; ANL/PHY/CP-97688; No Copyright; Avail: Department of Energy Information Bridge, Microfiche

In order to test the feasibility of Coulomb excitation of radioactive projectiles with low beam energies and intensities, they have produced a secondary radioactive beam of (sup 78)Rb and Coulomb re-excited it. The beam was produced in the fusion evaporation reaction (sup 24)Mg((sup 58)Ni,3pn)(sup 78)Rb at a beam energy of 260 MeV, using the Argonne National Laboratory ATLAS accelerator. The residues of interest were separated from other reaction products and non-interacting beam using the Fragment Mass Analyzer (FMA). The beam leaving the FMA was (sup 78)Kr and (sup 78)Rb(sup gs,m1,m2), which was refocused onto a (sup 58)Ni secondary target. They have extracted a spectrum of (gamma)-rays associated with re-excitation of A = 78 isobars. The re-excitation of stable (sup 78)Kr was observed, which serves as a reference. Gamma-rays associated with excitation of (sup 78)Rb(sup gs,m1,m2) were also seen. The measured yields indicate that all the (sup 78)Rb states are highly deformed.
NTIS
*Excitation; Radioactivity; Deformation*

**20010123741** Argonne National Lab., IL USA
**Lifetime measurements and dipole transition rates for superdeformed states in (sup 190)Hg**
Amro, H.; Mar. 24, 1999; 7p; In English
Report No.(s): DE2001-11090; ANL/PHY/CP-97616; No Copyright; Avail: Department of Energy Information Bridge, Microfiche

The Doppler-shift attenuation method was used to measure life-times of superdeformed (SD) states for both the yrast and the first excited superdeformed band of (sup 190)Hg. Intrinsic quadruple moments Q(sub 0) were extracted. For the first time, the dipole transition rates have been extracted for the inter-band transitions which connect the excited SD band to the yrast states in the second minimum. The results support the interpretation of the excited SD band as a rotational band built on an octupole vibration.
NTIS
*Nuclei (Nuclear Physics); Doppler Effect*

**20010124096** Argonne National Lab., IL USA
**PNC in hydrogen. different prospects using helium-like ions**
Dunford, R. W.; Sep. 25, 1998; 11p; In English
Report No.(s): DE2001-10980; ANL/PHY/CP-97343; No Copyright; Avail: Department of Energy Information Bridge, Microfiche

The motivation for parity experiments in simple atomic systems is that the atomic physics is known precisely so they directly test the weak interactions. We review the status of the parity experiments that have been done in atomic hydrogen and suggest some possibilities for experiments in helium like ions.
NTIS
*Atomic Physics; Weak Energy Interactions*

**20010125143** NASA Ames Research Center, Moffett Field, CA USA
**Large Atomic Natural Orbital Basis Sets for the First Transition Row Atoms**
Bauschlicher, Charles W., Jr., NASA Ames Research Center, USA; [1994]; 1p; In English
Contract(s)/Grant(s): RTOP 232-01-04; No Copyright; Avail: Issuing Activity; Abstract Only

Large atomic natural orbital (ANO) basis sets are tabulated for the Sc to Cu. The primitive sets are taken from the large sets optimized by Partridge, namely (21s 13p 8d) for Sc and Ti and (20s 12p 9d) for V to Cu. These primitive sets are supplemented with three p, one d, six f, and four g functions. The ANO sets are derived from configuration interaction density matrices constructed as the average of the lowest states derived from the 3d(sup n)4s(sup 2) and 3d(sup n+1)4s(sup 1) occupations. For Ni, the 1S(3d(sup 10)) state is included in the averaging. The choice of basis sets for molecular calculations is discussed.
Author
*Electron Orbitals; Electronic Structure; Configuration Interaction*

**20010125159** Argonne National Lab., IL USA

**Heating Au-197 nuclei with 8 GeV antiproton and pi- beams**

Back, B.; Beaulieu, L.; Breuer, H.; Gushue, S.; Hsi, W. C.; May 03, 1999; 14p; In English

Report No.(s): DE2001-11782; ANL/PHY/CP-98922; No Copyright; Avail: Department of Energy Information Bridge

This contribution stresses results recently obtained from experiment E900 performed at the Brookhaven AGS accelerator with 8 GeV/c antiproton and negative pion beams using the Indiana Silicon Sphere detector array. An investigation of the reaction mechanism is presented, along with source characteristics deduced from a two-component fit to the spectra. An enhancement of deposition energy with the antiproton beam with respect to the pion beam is observed. The results are qualitatively consistent with predictions of an intranuclear cascade code.

NTIS

*Antiprotons; Pion Beams; Gold Isotopes*

**20010125160** Argonne National Lab., IL USA

**Isolating the thermal degree of freedom in nuclear multifragmentation**

Back, B.; Beaulieu, L.; Breuer, H.; Gushue, S.; Hsi, W. C.; May 03, 1999; 14p; In English

Report No.(s): DE2001-11779; ANL/PHY/CP-98913; No Copyright; Avail: Department of Energy Information Bridge

Multifragmentation studies induced by GeV light-ion beams permit investigation of the influence of intrinsic thermal properties of hot nuclear matter, with minimal interference from the compression/decompression cycle and rotational instabilities. We summarize recent results obtained with He-3, proton and pion beams up to 15 GeV/c and present the initial results from a recent experiment with 8 GeV/c antiproton and pion beams. The results are compared with INC simulations coupled to EES and SMM models and the caloric curve for the He-3 data will also be discussed.

NTIS

*Fragmentation; Degrees of Freedom; Thermodynamic Properties*

**20010125391** NASA Ames Research Center, Moffett Field, CA USA

**The Molecular Structure of cis-FONO**

Lee, Timothy J., NASA Ames Research Center, USA; Dateo, Christopher E., Thermoscience Inst., USA; Rice, Julia E., International Business Machines Corp., USA; [1994]; 1p; In English

Contract(s)/Grant(s): RTOP 537-02-20; No Copyright; Avail: Issuing Activity; Abstract Only

The molecular structure of cis-FONO has been determined with the CCSD(T) correlation method using an spdf quality basis set. In agreement with previous coupled-cluster calculations but in disagreement with density functional theory, cis-FONO is found to exhibit normal bond distances. The quadratic and cubic force fields of cis-FONO have also been determined in order to evaluate the effect of vibrational averaging on the molecular geometry. Vibrational averaging is found to increase bond distances, as expected, but it does not affect the qualitative nature of the bonding. The CCSD(T)/spdf harmonic frequencies of cis-FONO support our previous assertion that a band observed at 1200 /cm is a combination band (upsilon(sub 3) + upsilon(sub 4)), and not a fundamental.

Author

*Molecular Structure; Field Theory (Physics)*

**20010125574** Argonne National Lab., IL USA

**Design and Performance of the ASAXS Instrument at the Advanced Photon Source**

Seifert, S.; Thiyagarajan, P.; Tiede, D. M.; Winans, R. E.; Jul. 06, 1999; 13p

Report No.(s): DE2001-11888; ANL/IPNS/CP-99465; No Copyright; Avail: Department of Energy Information Bridge, Microfiche

The small-angle X-ray scattering (SAXS) instrument on the high brilliance undulator beam line (ID-12, BESSRC-CAT) at APS has been designed to produce high-resolution scattering patterns in the millisecond time domain. This instrument is equipped with a 20 cm x 20 cm position sensitive gas detector and a 15 cm x 15 cm high-resolution position sensitive CCD mosaic detector. A photodiode detector mounted on a 3 mm diameter beam stop permits quick alignment of the instrument as well as precise measurement of the transmitted beam intensity. The ease of changing the sample to detector distance and tuning of x-ray energy enables easy access to different Q ranges. With this instrument we routinely measure data in a Q range of 0.001 to 1/angstrom. The exposure time with the CCD detector varies from 0.1 sec to 10 sec depending on the scattering cross-section of the samples. Techniques to interface ancillary equipment for time-resolved studies and software for faster online analysis of the data have also

been developed. We have obtained excellent data on the unfolding of proteins in the millisecond time domain, ASAXS of metallic alloys by using this instrument.
NTIS
*Photons; X Ray Scattering*

**20010125576** Argonne National Lab., IL USA
**Antibaryon Production in AU+AU Collisions at the AGS**
Back, B. B.; Betts, R. R.; Chang, J.; Chang, W. C.; Chi, C. Y.; Jul. 02, 1999; 7p; In English
Report No.(s): DE2001-11886; ANL/PHY/CP-99439; No Copyright; Avail: Department of Energy Information Bridge, Microfiche

Experiment E917 at the Brookhaven Alternating Gradient Synchrotron (AGS) has made a measurement of near-mid-rapidity antibaryon production in both the antiproton and antilambda channel. Results on dN/dy and inverse slope parameters are shown. A preliminary measurement of the ratio (bar Lambda)/(bar p) is also presented.
NTIS
*Antiprotons; Collisions; Particle Production*

## 73
## NUCLEAR PHYSICS

*Includes nuclear particles; and reactor theory. For space radiation see 93 Space Radiation. For atomic and molecular physics see 72 Atomic and Molecular Physics. For elementary particle physics see 77 Physics of Elementary Particles and Fields. For nuclear astrophysics see 90 Astrophysics.*

**20010118260** Oak Ridge National Lab., TN USA
**Review of ENDF/B-VI Fission-Product Cross Sections (Evaluated Nuclear Data File)**
Wright, R. Q.; MacFarlane, R. E.; Apr. 01, 2000; 52p; In English
Report No.(s): DE2000-760512; ORNL/TM-13723; No Copyright; Avail: Department of Energy Information Bridge, Microfiche

In response to concerns raised in the Defense Nuclear Facilities Safety Board (DNFSB) Recommendation 93-2, the US Department of Energy (DOE) developed a comprehensive program to help assure that the DOE maintain and enhance its capability to predict the criticality of systems throughout the complex. Tasks developed to implement the response to DNFSB recommendation 93-2 included Critical Experiments, Criticality Benchmarks, Training, Analytical Methods, and Nuclear Data. The Nuclear Data Task consists of a program of differential measurements at the Oak Ridge Electron Linear Accelerator (ORELA), precise fitting of the differential data with the generalized least-squares fitting code SAMMY to represent the data with resonance parameters using the Reich-Moore formalism along with covariance (uncertainty) information, and the development of complete evaluations for selected nuclides for inclusion in the Evaluated Nuclear Data File (ENDFB).
NTIS
*Critical Experiments; Nuclear Research; Safety Management*

**20010118514** Brookhaven National Lab., Upton, NY USA
**Chiral symmetries in nuclear physics**
Zschiesche,; Papazoglou,; Schramm,; Beckmann,; Schaffner-Bielich,; Jun. 12, 2000; 20p; In English
Report No.(s): DE2000-759044; BNL-67510; No Copyright; Avail: Department of Energy Information Bridge

The theoretical concepts of a chirally symmetric meson field theory are reviewed and an overview of the most relevant applications in nuclear physics is given. This includes a unified description of the vacuum properties of hadrons, finite nuclei and hot, dense and strange nuclear matter in an extended chiral SU(3)(sub L)/SU(3)(sub R) (sigma)-(omega) model.
NTIS
*Enantiomers; Hadrons; Mesons; Nuclear Physics*

**20010118519** Brookhaven National Lab., Upton, NY USA
**Questions of the nuclear level density and the E1 photon strength functions**
Mughabghab,; Dunford,; Nov. 15, 1999; 20p; In English
Report No.(s): DE2000-759026; BNL-NCS-66978; No Copyright; Avail: Department of Energy Information Bridge

New results were derived from average level spacings of neutron resonances for the spin dispersion parameter of the nuclear level density, which demonstrated the influence of shell effects, as well as the interplay of nucleon pairing correlations for nuclei

in the mass range from (sup 29)Si to (sup 241)Pu. The volume and surface components of the nuclear level density parameter, as well as the shell-damping factor, were determined as, a(sub v) = 0.076 +/- 0.009 MeV(sup (minus)1) , a(sub s) = 0.180 +/- 0.047 MeV(sup (minus)1), and y(sub 0) = 0.047 +/- 0.04 MeV, respectively. The effective nucleon mass at the Fermi surface is derived as m*/m = 1.09 +/- 0.13. New evidence is presented for a dipole-quadrupole interaction term in the primary E1 transitions of average resonance capture data. This evidence is obtained by testing a proposed generalized Landau Fermi liquid model for spherical and deformed nuclei, which includes the effect of the dipole-quadrupole interaction. The Landau-Migdal interaction constant and the effective nucleon mass, are determined as F(sub 0)(prime) = 1.49 +/- 0.08, and m*/m= 1.04 +/- 0.07, respectively.
NTIS
*Nuclear Capture; Nuclear Deformation; Nuclear Transformations; Photons*

**20010118539** Brookhaven National Lab., Upton, NY USA
**P-Shell (Lambda) Hypernuclei and the (Lambda)N Effective Interaction**
Millener,; Dec. 02, 2000; 14p; In English
Report No.(s): DE2000-757142; BNL-67385; No Copyright; Avail: Department of Energy Information Bridge, Microfiche

Empirical data on the spectra of light hypernuclei, especially the data from recent (gamma)-ray experiments, is used to constrain the parameters which govern the P(sub N)s(sub (Lambda)) and p(sub N)p(sub (Lambda))j two-body matrix elements that enter into shell-model calculations.
NTIS
*Hypernuclei; Matrix Methods; Two Body Problem*

**20010118911** Sandia National Labs., Albuquerque, NM USA
**M and S for Life Cycle Management at Sandia National Laboratories: From Engineering Simulations to Enterprise Modeling**
Chavez, P. F.; Nielan, P. E.; Skocypec, R. D.; Yarrington, P.; Jul. 12, 2000; 8p; In English
Report No.(s): DE2000-760799; SAND2000-1623C; No Copyright; Avail: Department of Energy Information Bridge

Sandia National Laboratories has responsibility for designing all non-nuclear components for the U.S. nuclear weapons program, as well as performing a wide variety of energy research and development projects. More generically, Sandia works on assignments that broadly respond to military and economic national security threats. In conjunction with this work, Sandia encourages and seeks partnerships with appropriate U.S. industry and U.S. government groups to collaborate on emerging technologies that support our mission. The breadth and depth of Sandia's scientific endeavors span every discipline required to fulfill our national defense mission and have consistently contributed to the U.S.'s technological and economic well being. This broad focus has led to revolutionary advances in multiple science and technology areas including for example, advanced manufacturing, materials and processes, modeling and simulation, computational and information sciences, nanotechnology, electronics, pulsed power, and engineering sciences.
NTIS
*Research and Development; Defense Program; Government/Industry Relations; Nuclear Weapons*

**20010119212** Brookhaven National Lab., Upton, NY USA
**Reflections on the Two-State Electron Transfer Model**
Brunschwig, B. S.; Jan. 12, 2000; 40p; In English
Report No.(s): DE2000-751122; BNL-67079; No Copyright; Avail: Department of Energy Information Bridge

There is general agreement that the two most important factors determining electron transfer rates in solution are the degree of electronic interaction between the donor and acceptor sites, and the changes in the nuclear configurations of the donor, acceptor, and surrounding medium that occur upon the gain or loss of an electron L1-51. The electronic interaction of the sites will be very weak, and the electron transfer slow, when the sites are far apart or their interaction is symmetry or spin forbidden. Since electron motion is much faster than nuclear motion, energy conservation requires that, prior to the actual electron transfer, the nuclear configurations of the reactants and the surrounding medium adjust from their equilibrium values to a configuration (generally) intermediate between that of the reactants and products. In the case of electron transfer between two metal complexes in a polar solvent, the nuclear configuration changes involve adjustments in the metal-ligand and intraligand bond lengths and angles, and changes in the orientations of the surrounding solvent molecules. In common with ordinary chemical reactions, an electron transfer reaction can then be described in terms of the motion of the system on an energy surface from the reactant equilibrium

configuration (initial state) to the product equilibrium configuration (final state) via the activated complex (transition state) configuration.
NTIS
*Electron Transfer; Solvents; Mathematical Models*

**20010119217** Brookhaven National Lab., Upton, NY USA
**Two Dimensional Studies of Dynamics of Electron Clouds in Silicon Drift Detectors**
Bellwied, R.; Nov. 08, 1998; 6p; In English
Report No.(s): DE2000-751108; BNL-66889; No Copyright; Avail: Department of Energy Information Bridge
The dynamics of electrons generated in silicon drift detectors is studied using an infrared LED. Electrons were generated at different drift distances. In this way the evolution of the cloud in anode and drift directions as a function of drift time was measured. For the anode direction the method of cumulative functions was used to extract the electron cloud profiles. The cloud width was obtained also from measurements of the charge collected on a single anode as a function of the coordinate of the light spot. We present the first report of the experimental measurements of the cloud width in drift direction extracted from signal waveforms. The evolution of the electron cloud width with drift time is compared with theoretical calculations. Theoretical expectations agree with our experimental results.
NTIS
*Anodes; Electron Clouds; Time Dependence*

**20010119218** Brookhaven National Lab., Upton, NY USA
**Fast Loss Electron Proton Instability**
Blaskiewicz, M.; Jun. 28, 1999; 10p; In English
Report No.(s): DE2000-751105; BNL-66810; No Copyright; Avail: Department of Energy Information Bridge
The fast loss electron proton instability is described. It is shown that electron multi-pactoring is required for fast beam loss.
NTIS
*Losses; Protons; Stability*

**20010119402** Brookhaven National Lab., Upton, NY USA
**Measurement and basic physics committee of the US Cross-Section Evaluation Working Group** ***Annual Report, 1997***
Smith,; McLane,; Oct. 20, 1998; 42p; In English
Report No.(s): DE2000-760972; No Copyright; Avail: Department of Energy Information Bridge
The Cross-Section Evaluation Working Group (CSEWG) is a long-standing committee charged with responsibility for organizing and overseeing the US cross-section evaluation effort. Its main product is the official US evaluated nuclear data file, ENDF. The current version of this file is Version VI. All evaluations included in ENDF, as well as periodic modifications and updates to the file, are reviewed and approved by CSEWG and issued by the US Nuclear Data Center, Brookhaven National Laboratory. CSEWG is comprised of volunteers from the US nuclear data community who possess expertise in evaluation methodologies and who collectively have been responsible for producing most of the evaluations included in ENDF. In 1992 CSEWG added the Measurements Committee to its list of standing committees and subcommittees. This action was based on a recognition of the importance of experimental data in the evaluation process as well as the realization that measurement activities in the US were declining at an alarming rate and needed considerable encouragement to avoid the loss of this resource. The mission of the Committee is to maintain contact with experimentalists in the US and to encourage them to contribute to the national nuclear data effort. Improved communication and the facilitation of collaborative activities are among the tools employed in achieving this objective. In 1994 the Committee was given an additional mission, namely, to serve as an interface between the applied interests represented in CSEWG and the basic nuclear science community. Accordingly, its name was changed to the Measurement and Basic Physics Committee. The present annual report is the third such document issued by the Committee. It contains voluntary contributions from several laboratories in the US. Their contributions were submitted to the Chairman for compilation and editing.
NTIS
*Nuclear Research; Neutron Cross Sections; Data Management*

**20010119416** Brookhaven National Lab., Upton, NY USA
**RHIC Beam Abort Kicker System**
Hahn, H.; Mar. 29, 1999; 2p; In English
Report No.(s): DE2000-751102; BNL-66411; No Copyright; Avail: Department of Energy Information Bridge

The energy stored in the RHIC beam is about 200 KJ per ring at design energy and intensity. to prevent quenching of the superconducting magnets or material damage, the beam will be safety disposed of by an internal beam abort system, which includes the kicker magnets, the pulsed power supplies, and the dump absorber. Disposal of heavy ions, such as gold, imposes design constraints more severe than those for proton beams of equal intensity. In order to minimize the thermal shock in the carbon-fiber dump block, the bunches must be laterally dispersed.
NTIS
*Proton Beams; Superconducting Magnets*

**20010119424** Brookhaven National Lab., Upton, NY USA
**Production of Double-A Hypernuclei: BNL-AGS E906**
Fukuda, T.; Feb. 19, 1999; 8p; In English
Report No.(s): DE2000-750778; BNL-66991; No Copyright; Avail: Department of Energy Information Bridge
We have carried out an experiment at BNL-AGS (E906) to search for double-A hypernuclei by observing sequential pionic decays. We will describe the principle of the experiment and report the present status.
NTIS
*Hypernuclei; Pions*

**20010119558** Atomic Energy Commission, Idaho Operations Office, Idaho Falls, ID USA
**Model for Molten Fuel-Coolant Interaction during Melt Slumping in a Nuclear Reactor**
Siefken, L. J.; Sohal, M. S.; Oct. 01, 1999; 31p; In English
Report No.(s): DE2001-10480; INEEL/CON-99-00151; No Copyright; Avail: Department of Energy Information Bridge, Microfiche
This paper describes a simple fuel melt slumping model to replace the current parametric model in SCDAP/RELAP5. Specifically, a fuel-coolant interaction (FCI) model is developed to analyze the slumping molten fuel, molten fuel breakup, heat transfer to coolant, relocation of the molten droplets, size of the partially solidified particles that settle to the bottom of the lower plenum, and melt-plenum interaction, if any. Considering our objectives, the molten fuel jet breakup model, and fuel droplets Lagrangian model as included in a code TEXAS-V with Eulerian thermal hydraulics for water and steam from SCDAP/RELAP5 were used. The model was assessed with experimental data from MAGICO-2000 tests performed at University of California at Santa Barbara, and FARO Test L-08 performed at Joint Research Center, Ispra, Italy. The comparison was found satisfactory.
NTIS
*Fuels; Coolants; Slumping*

**20010119571** Argonne National Lab., IL USA
**Evaluation of reactor kinetic parameters without the need for perturbation codes**
Bretscher, M. M.; Jan. 14, 1998; 15p; In English
Report No.(s): DE2001-10571; ANL/TD/CP-95381; No Copyright; Avail: Department of Energy Information Bridge, Microfiche
The analysis of research reactor transients depends on the effective delayed neutron fraction (k(sub eff)), its family-dependent components ((beta)(sub eff,i)), the prompt neutron lifetime (l(sub p)), and the decay constants ((lambda)(sub i)) for each delayed neutron family. Beginning with ENDF (Evaluated Nuclear Data File)/B-V data, methods are presented for accurately calculating these kinetic parameters within the framework of diffusion theory but without the need for a perturbation code. For heavy water systems these methods can be extended to include the delayed photoneutron component of (beta)(sub eff). However, a separate calculation is needed to estimate the fractional loss of fission product gamma rays, energetic enough to dissociate the deuteron, from leakage, energy degradation and absorption in fuel and structural materials. These methods are illustrated for a light-water Oak Ridge Research Reactor (ORR) LEU (low-enriched uranium) core and for a heavy-water Georgia Tech Research Reactor (GTRR) HEU (high-enriched uranium) core where calculated and measured values of the prompt neutron decay constant ((beta)(sub eff)/l(sub p)) are compared.
NTIS
*Nuclear Reactors; Nuclear Reactions; Reaction Kinetics; Perturbation; Parameterization*

**20010119994** Oak Ridge National Lab., TN USA
**Neutron Capture and Neutron Total Cross Sections Measurements for (27)Al at the Oak Ridge Electron Linear Accelerator**
Guber, K. H.; Harvey, J. A.; Hill, N. W.; Koehler, P. E.; Leal, L. C.; Aug. 30, 1999; 3p; In English
Report No.(s): DE2001-10536; ORNL/CP-104444; No Copyright; Avail: Department of Energy Information Bridge

We have used the Oak Ridge Electron Linear Accelerator (ORELA) to measure neutron total and capture cross sections of (sup 27)Al in the energy range from 100 eV to (approximately)400 keV. We report the resonance parameters as well as the Maxwellian average capture cross sections.
NTIS
*Electron Beams; Neutrons; Capture Effect*

**20010120022** Argonne National Lab., IL USA
**Nuclear data evaluation for explosive hydrogen burning on A = 30-50 nuclei**
Smith, D. L.; Feb. 17, 1998; 12p; In English
Report No.(s): DE2001-10656; ANL/TD/CP-95683; No Copyright; Avail: Department of Energy Information Bridge

A research program to develop a reaction-rate (RR) data base for stellar explosive hydrogen burning via (p,(gamma)) and (p,(alpha)) reactions involving stable-isotope target elements in the mass range A = 30-50 (phosphorus to titanium) is described. This project includes: (1) a survey of the literature; (2) preparation of written summaries for pertinent contributions; (3) compilation of alpha-numeric information into computer-platform-independent data files; (4) tabulation of reaction resonance parameters (and uncertainties); (5) determination of resonance RRs (and uncertainties) for Maxwellian-distributed reactant energies corresponding to temperatures in the range T(sub 9)=0.01-10 GK (1 GK=10(sup 9) degrees Kelvin); (6) fitting of these calculated RRs with an empirical formula, thereby converting the basic data into a form that is convenient for astrophysical network calculations; (7) examination of deviations between fitted curves and these RRs in the context of the uncertainties. The results of this work are made available to the nuclear astrophysics community through formal laboratory reports and computer files which are distributed to data centers. The procedures used in this work are discussed and some representative examples of products from the activity are given.
NTIS
*Hydrogen; Nuclear Astrophysics; Isotopes; Combustion; Reaction Kinetics*

**20010120046** Brookhaven National Lab., Upton, NY USA
**E949: An Experiment to Measure the Branching Ratio B Kappa(+) yields pi(+)nu nu(-) at Brookhaven National Laboratory**
Kettell, A.; Oct. 08, 1998; 38p; In English
Report No.(s): DE2000-752966; BNL-67247; No Copyright; Avail: Department of Energy Information Bridge

A new, more precise measurement of the Kappa(sup +) yields Pi(sup +)Nu Nu(bar) branching ratio is proposed. Improvements to the E787 apparatus and modifications to the Alternating Gradient Synchrotrons (AGS) operating mode will be made to reach a sensitivity of (8-15)x10(sup -12), an order of magnitude below the Standard Model (SM) prediction of approximately 1x10(sup -10). This will result in a determination of (V(sub td)) to better than 30 percent. Experiment E787 presented evidence for this decay based on the observation of a clean event from data collected in the 1995 run of the AGS.
NTIS
*Nuclear Physics; Standard Model (Particle Physics); Branching (Physics); Synchrotron Radiation*

**20010120091** Argonne National Lab., IL USA
**Nuclear data requirements for fission reactor neutronics calculations**
Finck, P.; Jun. 29, 1998; 11p; In English
Report No.(s): DE2001-10620; ANL/RA/CP-95531; No Copyright; Avail: Department of Energy Information Bridge, Microfiche

The paper discusses current European nuclear data measurement and evaluation requirements for fission reactor technology applications and problems involved in meeting the requirements. Reference is made to the NEA High Priority Nuclear Data Request List and to the production of the new JEFF-3 library of evaluated nuclear data. There are requirements for both differential (or basic) nuclear data measurements and for different types of integral measurement critical facility measurements and isotopic sample irradiation measurements. Cross-section adjustment procedures are being used to take into account the simpler types of integral measurement, and to define accuracy needs for evaluated nuclear data.
NTIS
*Nuclear Fission; Data Acquisition*

**20010120092** Argonne National Lab., IL USA

**Recent developments pertinent to processing of ENDF/B-6 type resonance cross section data**

Hwang, R. N.; Jul. 07, 1998; 13p; In English

Report No.(s): DE2001-10618; ANL/RA/CP-95513; No Copyright; Avail: Department of Energy Information Bridge, Microfiche

In view of our increasing dependence on computations rather than construction and operation of more costly experimental facilities, the rigor and accuracy achievable by calculational methods certainly deserve more attention. This is particularly so for the Monte Carlo methods which are generally regarded as the ultimate computational standard for the entire nuclear community around the globe. One obvious question that one may raise is whether the numerical algorithms deployed to process cross sections accurately reflect the rigor of the state-of-the-art nuclear data. The case in point is particularly essential in the resolved and the unresolved resonance regions, which constitute the most demanding task in all processing codes for reactor applications. For the resolved energy region, the point-wise cross sections are highly fluctuating functions of energy and temperature. In light of the availability of a large body of resonance data spanning over the much expanded energy ranges for most of major nuclides, critical examinations and improvement where appropriate, of the existing methods are apparently in order. For the unresolved energy region, improvement of traditional methods based on statistical approaches for treating the self-shielding effects is also desirable. From the perspective of the Monte Carlo approach, an alternative means for generating the probability tables without the inevitable difficulties associated with statistical uncertainties and/or those with concerns of uniqueness is needed. The accuracy considerations provide the motivation for the recent efforts at ANL to upgrade the existing VIMB processing code developed in early 70's in order to deal processing codes with these issues. Various tasks of upgrading are still at various stages of development. The purpose of this paper is to present an up-to-date account of the work in progress.

NTIS

*Resonance; Monte Carlo Method*

**20010120529** Los Alamos National Lab., NM USA

**Analytical Benchmark Test Set for Criticality Code Verification**

Sood, A.; Parsons, D. K.; Forster, R. A.; Jul. 01, 1999; 57p; In English

Report No.(s): DE2001-10601; LA-13511; No Copyright; Avail: Department of Energy Information Bridge, Microfiche

A number of published numerical solutions to analytic eigenvalue (k(sub eff)) and eigenfunction equations are summarized for the purpose of creating a criticality verification benchmark test set. The 75-problem test set allows the user to verify the correctness of a criticality code for infinite medium and simple geometries in one- and two-energy groups, one- and two-media, and both isotropic and anisotropic neutron scattering. The problem specifications will produce both k(sub eff) = 1 and the quoted k(sub (infinity)) to at least five decimal places. Additional uses of the test set for code verification are also discussed. A list of 45 references and an appendix with k(sub (infinity)) derivations is also included.

NTIS

*Program Verification (Computers); Numerical Analysis; Computer Program Integrity; Proving*

**20010120532** Argonne National Lab., IL USA

**Janus reactor d and d project**

Fellhauer, C. R.; Feb. 16, 1998; 17p; In English

Report No.(s): DE2001-10611; ANL/TD/CP-94774; No Copyright; Avail: Department of Energy Information Bridge, Microfiche

Argonne National Laboratory (ANL-E) has recently completed the decontamination and decommissioning (D and D) of the JANUS Reactor Facility located in Building 202. The 200 KW reactor operated from August 1963 to March 1992. The facility was used to study the effects of both high and low doses of fission neutrons in animals. There were two exposure rooms on opposite sides of the reactor and the reactor was therefore named after the two-faced Roman god. The High Dose Room was capable of specimen exposure at a dose rate of 3,600 rads per hour. During calendar year 1996 a detailed characterization of the facility was performed by ANL-E Health Physics personnel. ANL-E Analytical Services performed the required sample analysis. An Auditable Safety Analysis and an Environmental Assessment were completed. D and D plans, procedures and procurement documents were prepared and approved. A D and D subcontractor was selected and a firm, fixed price contract awarded for the field work and final survey effort. The D and D subcontractor was mobilized to ANL-E in January 1997. Electrical isolation of all reactor equipment and control panels was accomplished and the equipment removed. A total of 207,230 pounds (94,082 Kg) of lead shielding was removed, surveyed and sampled, and free-released for recycle. All primary and secondary piping was removed, size reduced and packaged for disposal or recycled as appropriate. The reactor vessel was removed, size reduced and packaged as radioactive waste in April. The activated graphite block reflector was removed next, followed by the bioshield concrete and steel. All of this material was packaged as low level waste. Total low level radioactive waste generation was 4002.1

cubic feet (113.3 cubic meters). Mixed waste generation was 538 cubic feet (15.2 cubic meters). The Final Release Survey was completed in September. The project field work was completed in 38 weeks without any lost-time accidents, personnel contaminations or unplanned exposures. The project was managed by the ANL-E Technology Development Division's D and D Program personnel. Total cost of the project was $2,095,000.00. Total project exposure was 0.482 person rem (4.82 mSv). Detailed information on D and D methods and lessons learned are presented.
NTIS
*Janus Reactor; Radioactive Wastes; Waste Disposal; Decommissioning; Decontamination*

**20010120792** Argonne National Lab., IL USA
**Imprinted spiral structures as neutron polarizers**
Lohstroh, W.; Oct. 07, 1998; 11p; In English
Report No.(s): DE2001-10825; ANL/MSD/CP-96572; No Copyright; Avail: Department of Energy Information Bridge

Neutron diffraction from magnetic spiral structures is governed by strong selection rules for the polarization of the outgoing beam. When the sample is entirely of one chirality--for instance a right handed spiral--the neutrons diffracted by some Bragg reflections are fully polarized. While the scattering theory has been formulated long ago, attempts to controllably modify the population of left handed and right handed spiral domains in natural magnetic structures (which for instance occur in some rare earth metals) have been largely unsuccessful. In contrast, we have been able to imprint helical magnetic structures in La/Fe multilayers (each layer approximately 30 (angstrom) thick) simply by rotating the growing sample in a weak external field (30e). A first estimate is given of the efficiency of these multilayers as polarizers of neutron beams.
NTIS
*Chirality; Neutron Beams; Neutron Diffraction; Polarizers; Rare Earth Elements*

**20010121522** Oak Ridge National Lab., TN USA
**P threads Versus MPI Parallel Performance of Angular-Domain Decomposed S**
Azmy, Y. Y.; Barnett, D. A.; May 07, 2000; 10p; In English
Report No.(s): DE2000-754815; ORNL/P00-106228; No Copyright; Avail: Department of Energy Information Bridge

Two programming models for parallelizing the Angular Domain Decomposition (ADD) of the discrete ordinates (S(sub n)) approximation of the neutron transport equation are examined. These are the shared memory model based on the POSIX threads (Pthreads) standard, and the message passing model based on the Message Passing Interface (MPI) standard. These standard libraries are available on most multiprocessor platforms thus making the resulting parallel codes widely portable. The question is: on a fixed platform, and for a particular code solving a given test problem, which of the two programming models delivers better parallel performance. Such comparison is possible on Symmetric Multi-Processors (SMP) architectures in which several CPUs physically share a common memory, and in addition are capable of emulating message passing functionality. Implementation of the two-dimensional,(S(sub n)), Arbitrarily High Order Transport (AHOT) code for solving neutron transport problems using these two parallelization models is described. Measured parallel performance of each model on the COMPAQ AlphaServer 8400 and the SGI Origin 2000 platforms is described, and comparison of the observed speedup for the two programming models is reported. For the case presented in this paper it appears that the MPI implementation scales better than the Pthreads implementation on both platforms.
NTIS
*Neutrons; Transport Properties; Parallel Processing (Computers)*

**20010121525** Brookhaven National Lab., Upton, NY USA
**Scattering of real photons and the structure of baryons**
Hoblit, S.; Sep. 17, 1999; 11p; In English
Report No.(s): DE2000-752151; BNL-67031; No Copyright; Avail: Department of Energy Information Bridge

The transient dipole moments of the proton, induced by the electric and magnetic fields of a photon during Compton scattering, are described by six polarizability parameters that are sensitive to the protons internal structure. We review here the extraction of a particular linear combination of these spin polarizabilities that characterizes backward Comptom scattering.
NTIS
*Photons; Electron Scattering; Compton Effect*

**20010121553** Sandia Corp., Albuquerque, NM USA

**Rover/Nerva Destruct System Test Results, Aberdeen Proving Ground-3, 3** ***Final Report***

Berry, R. E.; Martin, J. P.; Dec. 1965; 227p; In English

Report No.(s): AD-A395169; SC-RR-65-620; No Copyright; Avail: CASI; A11, Hardcopy; A03, Microfiche

The ROVER/NERVA Nuclear Propulsion Engine destruct test was performed to determine the distribution, particle size and mass, and particle velocity of the debris. These debris data are the input data for a computer analysis of the safety aspects of using the NERVA reactor for space flight. Reported in this document are the debris distribution, size, mass, and velocity measured during the destruct test. These data are presented as tables and as graphs.

DTIC

*Destructive Tests; Particle Size Distribution; Nuclear Engine For Rocket Vehicles; Engine Tests; Nuclear Propulsion*

**20010122358** Argonne National Lab., IL USA

**Thermal hydraulic calculations to support increase in operating power in McClellen Nuclear Radiation Center(MNRC) TRIGA reactor**

Jensen, R. T.; May 05, 1998; 11p; In English

Report No.(s): DE2001-10763; ANL/ED/CP-96366; No Copyright; Avail: Department of Energy Information Bridge, Microfiche

The RELAP5/Mod3.1 computer program has been used to successfully perform thermal-hydraulic analyses to support the Safety Analysis for increasing the MNRC (McClellen Nuclear Radiation Center) reactor from 1.0 MW to 2.0 MW. The calculation results show the reactor to have operating margin for both the fuel temperature and critical heat flux limits. The calculated maximum fuel temperature of 705 C is well below the 750 C operating limit. The critical heat flux ratio was calculated to be 2.51.

NTIS

*Thermal Analysis; Nuclear Reactor Control; Nuclear Reactors; Reactor Safety; Hydraulic Control*

**20010122375** Argonne National Lab., IL USA

**Thermal hydraulic calculations in the SAS-DIF3DK coupled reactor physics and thermal hydraulics code**

Dunn, F. E., Argonne National Lab., USA; Jul. 22, 1998; 9p; In English

Report No.(s): DE2001-10736; ANL/RA/CP-96117; No Copyright; Avail: Department of Energy Information Bridge, Microfiche

The SAS-DIF3DK code couples a detailed 3-D neutron kinetics treatment with a detailed thermal hydraulics treatment. One goal of the work on SAS-DIF3DK is to produce a detailed code that will run a wide range of transients in real time. Achieving this goal will require efficient numerical methods and efficient coding, and it will probably require the use of multiple processors for larger problems. It has previously been reported that the thermal hydraulics treatment in the code achieves the required speed for typical PWR and BWR cases. This paper presents results from thermal hydraulic analysis of severe LOCA cases in a Soviet design RBMK reactor, and shows that the computing speed goals are also met in these cases.

NTIS

*Thermal Analysis; Reactor Physics; Computerized Simulation; Applications Programs (Computers); Thermohydraulics*

**20010122877** Argonne National Lab., IL USA

**Quantum Monte Carlo calculations for light nuclei**

Wiringa, R. B.; Oct. 23, 1998; 19p; In English

Report No.(s): DE2001-11054; ANL/PHY/CP-97477; No Copyright; Avail: Department of Energy Information Bridge, Microfiche

Quantum Monte Carlo calculations of ground and low-lying excited states for nuclei with A (le) 8 are made using a realistic Hamiltonian that fits NN scattering data. Results for more than 40 different (J(pi), T) states, plus isobaric analogs, are obtained and the known excitation spectra are reproduced reasonably well. Various density and momentum distributions and electromagnetic form factors and moments have also been computed. These are the first microscopic calculations that directly produce nuclear shell structure from realistic NN interactions.

NTIS

*Density Distribution; Hamiltonian Functions; Monte Carlo Method*

**20010122881** Argonne National Lab., IL USA

**Neutronics feasibility study for the LEU conversion of Poland's Maria research reactor**

Bretscher, M. M.; Oct. 14, 1998; 12p; In English

Report No.(s): DE2001-11047; ANL/TD/CP-97463; No Copyright; Avail: Department of Energy Information Bridge, Microfiche

The MARIA reactor is a high-flux multipurpose research reactor which is water-cooled and moderated with both beryllium and water. Standard HEU (80% (sup 235)U)fuel assemblies consist of six concentric fuel tubes of a U-Al alloy clad in aluminum. Although the inventory of HEU (80%) fuel is nearly exhausted, a supply of highly-loaded 36%-enriched fuel assemblies is available at the reactor site. Neutronic equilibrium studies have been made to determine the relative performance of fuels with enrichments of 80%, 36% and 19.7%. These studies indicate that LEU (19.7%) densities of about 2.5 gU/cm(sup 3) and 3.8 gU/cm(sup 3) are required to match the performance of the MARIA reactor with 80%-enriched and with 36%-enriched fuels, respectively.

NTIS

*Nuclear Reactors; Liquid Cooling; Fuels*

**20010122882** Argonne National Lab., IL USA

**Upgrades to the WIMS-ANL code**

Woodruff, W. L.; Oct. 14, 1998; 11p; In English

Report No.(s): DE2001-11045; ANL/TD/CP-97461; No Copyright; Avail: Department of Energy Information Bridge, Microfiche

The dusty old source code in WIMS-D4M has been completely rewritten to conform more closely with current FORTRAN coding practices. The revised code contains many improvements in appearance, error checking and in control of the output. The output is now tabulated to fit the typical 80 column window or terminal screen. The Segev method for resonance integral interpolation is now an option. Most of the dimension limitations have been removed and replaced with variable dimensions within a compile-time fixed container. The library is no longer restricted to the 69 energy group structure, and two new libraries have been generated for use with the code. The new libraries are both based on ENDF/B-VI data with one having the original 69 energy group structure and the second with a 172 group structure. The common source code can be used with PCs using both Windows 95 and NT, with a Linux based operating system and with UNIX based workstations. Comparisons of this version of the code to earlier evaluations with ENDF/B-V are provided, as well as, comparisons with the new libraries.

NTIS

*Coding; FORTRAN; Interpolation*

**20010122883** Argonne National Lab., IL USA

**Use of WIMS-ANL lumped fission product cross sections for burned core analysis with the MCNP Monte Carlo code**

Hanan, N. A.; Oct. 14, 1998; 9p; In English

Report No.(s): DE2001-11044; ANL/TD/CP-97460; No Copyright; Avail: Department of Energy Information Bridge, Microfiche

Most Monte Carlo neutronics analyses are performed for fresh cores. To model snapshots of the cores at different stages during burnup using MCNP, a method is presented that uses lumped fission product (LFP) cross sections generated by the WIMS-ANL code and processed for use in MCNP. Results of analyses for four very different reactor cores using MTR-type and Russian-designed fuel assemblies, with LEU and HEU fuels, are provided to demonstrate the use of this method.

NTIS

*Reactor Cores; Fuels*

**20010122885** Argonne National Lab., IL USA

**In-beam (gamma)-ray spectroscopy in the vicinity of (100)Sn**

Seweryniak, D.; Sep. 29, 1998; 9p; In English

Report No.(s): DE2001-10974; ANL/PHY/CP-97335; No Copyright; Avail: Department of Energy Information Bridge, Microfiche

In recent years, in-beam x-ray experiments supplied a vast amount of data on high-spin states in nuclei in the vicinity of (sup 100)Sn. The present contribution reviews spectroscopic information obtained recently for N (ge) 50 nuclei around (sup 100)Sn, with emphasis on isomer studies, and discusses selected results in the frame of the shell model.

NTIS

*Isomers; Spectroscopy; Gamma Ray Spectrometers; Nuclear Spin; Nuclear Models; Tin Isotopes*

**20010123214** Argonne National Lab., IL USA

**Study of the high-j states in (sup 249)Cm**

Ahmad, I.; Jul. 16, 1998; 6p; In English

Report No.(s): DE2001-10889; ANL/PHY/CP-96827; No Copyright; Avail: Department of Energy Information Bridge, Microfiche

The authors have performed the reaction (sup 248)Cm((sup 4)He, (sup 3)He) using 98.5-MeV alpha particles from the IUCF (Indiana University Cyclotron Facility) cyclotron to populate high-j states in (sup 249)Cm. A tentative assignment of the K(sub 17/2) component of the 1/2(sup +)(880) Nilsson state has been made.

NTIS

*Curium; Alpha Particles; Helium Isotopes*

**20010123457** Oak Ridge National Lab., TN USA

**Irradiation, Annealing, and Reirradiation Effects on American and Russian Reactor Pressure Vessel Steels**

Chernobaeva, A. A.; Korolev, Y. N.; Nanstad, R. K.; Nikolaev, Y. A.; Sokolov, M. A.; Jun. 16, 1998; 21p; In English

Report No.(s): DE2001-11010; ORNL/CP-104207; No Copyright; Avail: Department of Energy Information Bridge

One of the options to mitigate the effects of irradiation on reactor pressure vessels (RPVs) is to thermally anneal them to restore the toughness properties that have been degraded by neutron irradiation. Even though a postirradiation anneal may be deemed successful, a critical aspect of continued RPV operation is the rate of embrittlement upon reirradiation. There are insufficient data available to allow for verification of available models of reirradiation embrittlement or for the development of a reliable predictive methodology. This is especially true in the case of fracture toughness data. Under the U.S.-Russia Joint Coordinating Committee for Civilian Nuclear Reactor Safety (JCCCNRS), Working Group 3 on Radiation Embrittlement, Structural Integrity, and Life Extension of Reactor Vessels and Supports agreed to conduct a comparative study of annealing and reirradiation effects on RPV steels. The Working Group agreed that each side would irradiate, anneal, reirradiate (if feasible ), and test two materials of the other. Charpy V-notch (CVN) and tensile specimens were included. Oak Ridge National Laboratory (ORNL) conducted such a program (irradiation and annealing, including static fracture toughness) with two weld metals representative of VVER-440 and VVER-1000 RPVs, while the Russian Research Center-Kurchatov Institute (RRC-KI) conducted a program (irradiation, annealing, reirradiation, and reannealing) with Heavy-Section Steel Technology (HSST) Program Plate 02 and Heavy-Section Steel Irradiation (HSSI) Program Weld 73W. The results for each material from each laboratory are compared with those from the other laboratory. The ORNL experiments with the VVER welds included irradiation to about 1 x 10(exp 19) n/square cm (>1 MeV), while the RRC-KI experiments with the U.S. materials included irradiations from about 2 to 18 x 10(exp 19) n/square cm (>l MeV). In both cases, irradiations were conducted at (approximately)290 C and annealing treatments were conducted at (approximately)454 C. The ORNL and RRC-RI experiments have shown generally good agreement for both the Russian and U.S. steels. While recoveries of the Charpy 41-J transition temperatures were substantial in all cases, significantly less recovery of the lateral expansion and shear fracture in some cases (no recovery in one case) deserves further attention. The RRC-KI results for the U.S. steels showed reirradiation embrittlement rates which are conservative relative to the lateral shift prediction based on Charpy impact energy.

NTIS

*Hardness Tests; Pressure Vessels; Steels; Charpy Impact Test*

**20010123548** Argonne National Lab., IL USA

**Analysis of ANS LWR physics benchmark problems**

Taiwo, T. A.; Jul. 29, 1998; 10p; In English

Report No.(s): DE2001-10629; ANL/RA/CP-95551; No Copyright; Avail: Department of Energy Information Bridge, Microfiche

Various Monte Carlo and deterministic solutions to the three PWR Lattice Benchmark Problems recently defined by the ANS Ad Hoc Committee on Reactor Physics Benchmarks are presented. These solutions were obtained using the VIM continuous-energy Monte Carlo code and the DIF3D/WIMS-D4M code package implemented at the Argonne National Laboratory. The code results for the K(sub eff) and relative pin power distribution are compared to measured values. Additionally, code results for the three benchmark-prescribed infinite lattice configurations are also intercompared. The results demonstrate that the codes produce very good estimates of both the K(sub eff) and power distribution for the critical core and the lattice parameters of the infinite lattice configuration.

NTIS

*Lattice Parameters; Monte Carlo Method; Pins; Reactor Physics*

**20010123738** Argonne National Lab., IL USA

**Determining Pu-239 content by resonance transmission analysis using a filtered reactor beam**

Klann, R. T.; Nov. 25, 1998; 23p; In English

Report No.(s): DE2001-11109; ANL/TD/CP-97678; No Copyright; Avail: Department of Energy Information Bridge, Microfiche

A novel technique has been developed at Argonne National Laboratory to determine the (sup 239)Pu content in EBR-II blanket elements using resonance transmission analysis (RTA) with a filtered reactor beam. The technique uses cadmium and gadolinium filters along with a (sup 239)Pu fission chamber to isolate the 0.3 eV resonance in (sup 239)Pu. In the energy range from 0.1 to 0.5 eV, the total microscopic cross-section of (sup 239)Pu is significantly larger than the cross-sections of (sup 238)U and (sup 235)U. This large difference in cross-section allows small amounts of (sup 239)Pu to be detected in uranium samples. Tests using a direct beam from a 250 kW TRIGA reactor have been performed with stacks of depleted uranium and (sup 239)Pu foils. Preliminary measurement results are in good agreement with the predicted results up to about two weight percent of (sup 239)Pu in the sample. In addition, measured (sup 239)Pu masses were in agreement with actual sample masses with uncertainties less than 3.8 percent.

NTIS

*Reactors; Spent Fuels; Cadmium; Fission*

**20010123742** Argonne National Lab., IL USA

**Study of thermal stratification in the cold legs during the subcooled blowdown phase of a loss of coolant accident in the OSU APEX thermal hydraulic testing facility**

Wachs, D. M.; Nov. 04, 1998; 37p; In English

Report No.(s): DE2001-11088; ANL/ED/CP-97607; No Copyright; Avail: Department of Energy Information Bridge, Microfiche

Thermal stratification, which has been linked to the occurrence of pressurized thermal shock (PTS), is observed to occur during the early stages of simulated loss of coolant accidents (LOCAS) in the Oregon State University Advanced Plant Experiment (OSU APEX) Thermal Hydraulic Test Facility. The OSU APEX Test Facility is a scaled model of the Westinghouse AP600 nuclear power plant. Analysis of the OSU APEX facility data has allowed the determination of an onset criteria for thermal stratification and has provided support for the postulated mechanisms leading to thermal stratification. CFX 4.1, a computational fluid dynamics code, was used to generate a model of the cold legs and the downcomer that described the phenomena occurring within them. Some mixing phenomena were predicted that lead to non-uniformity between the two cold legs attached to the steam generator on the side of the facility containing the Passive Residual Heat Removal (PRHR) injection system. The stratification was found to be two phase and unlikely to be a factor in PTS.

NTIS

*Loss of Coolant; Nuclear Power Plants; Stratification; Thermal Shock; Computational Fluid Dynamics*

**20010123965** Argonne National Lab., IL USA

**Incident spectrum determination for time-of-flight neutron powder diffraction data analysis**

Hodges, J. P.; Aug. 27, 1998; 13p; In English

Report No.(s): DE2001-10921; ANL/MSD/CP-97036; No Copyright; Avail: Department of Energy Information Bridge, Microfiche

Accurate characterization of the incident neutron spectrum is an important requirement for precise Rietveld analysis of time-of-flight powder neutron diffraction data. Without an accurate incident spectrum the calculated model for the measured relative intensities of individual Bragg reflections will possess systematic errors. We describe a method for obtaining an accurate numerical incident spectrum using data from a transmitted beam monitor.

NTIS

*Beams (Radiation); Incident Radiation; Neutron Spectra*

**20010124089** Oak Ridge National Lab., TN USA

**SCALE-4 Analysis of LaSalle Unit 1 BWR Commercial Reactor Critical Configurations**

Gauld, I. C.; Mar. 01, 2000; 98p; In English

Report No.(s): DE2001-769368; ORNL/TM-1999/247; No Copyright; Avail: Department of Energy Information Bridge

Five commercial reactor criticals (CRCs) for the LaSalle Unit 1 boiling-water reactor have been analyzed using KENO V.a, the Monte Carlo criticality code of the SCALE 4 code system. The irradiated fuel assembly isotopics for the criticality analyses were provided by the Waste Package Design team at the Yucca Mountain Project in the US, who performed the depletion calculations using the SAS2H sequence of SCALE 4. The reactor critical measurements involved two beginning-of-cycle and three middle-of-cycle configurations. The CRCs involved relatively low-cycle burnups, and therefore contained a relatively high

gadolinium poison content in the reactor assemblies. This report summarizes the data and methods used in analyzing the critical configurations and assesses the sensitivity of the results to some of the modeling approximations used to represent the gadolinium poison distribution within the assemblies. The KENO V.a calculations, performed using the SCALE 44GROUPNDF5 ENDF/B-V cross-section library, yield predicted k(sub eff) values within about 1% (Delta)k/k relative to reactor measurements for the five CRCs using general 8-pin and 9-pin heterogeneous gadolinium poison pin assembly models.
NTIS
*Reactor Safety; Gadolinium; Boiling Water Reactors; Numerical Analysis*

**20010125235** Oak Ridge National Lab., TN USA
**Posteriori Error Estimation for a Nodal Method in Neutron Transport Calculations**
Azmy, Y. Y.; Buscaglia, G. C.; Zamonsky, O. M.; Nov. 03, 1999; 8p; In English
Report No.(s): DE2001-11468; ORNL/CP-104570; No Copyright; Avail: Department of Energy Information Bridge
An a posteriori error analysis of the spatial approximation is developed for the one-dimensional Arbitrarily High Order Transport-Nodal method. The error estimator preserves the order of convergence of the method when the mesh size tends to zero with respect to the L(sup 2) norm. It is based on the difference between two discrete solutions that are available from the analysis. The proposed estimator is decomposed into error indicators to allow the quantification of local errors. Some test problems with isotropic scattering are solved to compare the behavior of the true error to that of the estimated error.
NTIS
*Error Analysis; Neutrons*

**20010125400** Argonne National Lab., IL USA
**Benchmarking D and D procurement best practices at four commercial nuclear power plants**
Arflin, J.; Baker, G.; Bidwell, B.; Bugielski, D.; Cavanagh, J.; May 11, 1999; 35p; In English
Report No.(s): DE2001-11810; ANL/OCF/CP-99038; No Copyright; Avail: Department of Energy Information Bridge
The Department of Energy (DOE) has as two of its strategic objectives to safely accomplish the world's largest environmental clean-up of contaminated sites and the adoption of the best management practices of the private sector to achieve business-like results efficiently and effectively. An integral part of the strategic response to the challenges facing the Department has been the use of benchmarking and best practice management to facilitate identifying and implementing leading-edge thinking, practices, approaches, and solutions.
NTIS
*Contamination; Nuclear Power Plants; Project Management*

**20010125632** Argonne National Lab., IL USA
**Computer simulation of FCC riser reactors**
Chang, S. L.; Golchert, B.; Lottes, S. A.; Petrick, M.; Zhou, C. Q.; Apr. 20, 1999; 12p; In English
Report No.(s): DE2001-11756; ANL/ES/CP-98784; No Copyright; Avail: Department of Energy Information Bridge, Microfiche
A three-dimensional computational fluid dynamics (CFD) code, ICRKFLO, was developed to simulate the multiphase reacting flow system in a fluid catalytic cracking (FCC) riser reactor. The code solves flow properties based on fundamental conservation laws of mass, momentum, and energy for gas, liquid, and solid phases. Useful phenomenological models were developed to represent the controlling FCC processes, including droplet dispersion and evaporation, particle-solid interactions, and interfacial heat transfer between gas, droplets, and particles. Techniques were also developed to facilitate numerical calculations. These techniques include a hybrid flow-kinetic treatment to include detailed kinetic calculations, a time-integral approach to overcome numerical stiffness problems of chemical reactions, and a sectional coupling and blocked-cell technique for handling complex geometry. The copyrighted ICRKFLO software has been validated with experimental data from pilot- and commercial-scale FCC units. The code can be used to evaluate the impacts of design and operating conditions on the production of gasoline and other oil products.
NTIS
*Computational Fluid Dynamics; Computerized Simulation; Multiphase Flow; Cracking (Chemical Engineering)*

## 74
## OPTICS

*Includes light phenomena and the theory of optical devices. For lasers see 36 Lasers and Masers.*

**20010118511** NASA Ames Research Center, Moffett Field, CA USA
**Color Breakup In Sequentially-Scanned LC Displays**
Arend, L., David Sarnoff Research Center, USA; Lubin, J., David Sarnoff Research Center, USA; Gille, J., Western Aerospace Labs., Inc., USA; Larimer, J., NASA Ames Research Center, USA; [1994]; 1p; In English
Contract(s)/Grant(s): RTOP 506-59-00; No Copyright; Avail: Issuing Activity; Abstract Only

In sequentially-scanned liquid-crystal displays the chromatic components of color pixels are distributed in time. For such displays eye, head, display, and image-object movements can cause the individual color elements to be visible. We analyze conditions (scan designs, types of eye movement) likely to produce color breakup.
Author
*Liquid Crystals; Display Devices; Pixels; Color*

**20010118923** Brookhaven National Lab., Upton, NY USA
**Precise angle monitor based on the concept of pencil-beam interferometry**
Qian,; Takacs,; Jul. 30, 2000; 11p; In English
Report No.(s): DE2000-760999; BNL-67423; No Copyright; Avail: Department of Energy Information Bridge

The precise angle monitoring is a very important metrology task for research, development and industrial applications. Autocollimator is one of the most powerful and widely applied instruments for small angle monitoring, which is based on the principle of geometric optics. In this paper the authors introduce a new precise angle monitoring system, Pencil-beam Angle Monitor (PAM), based on pencil beam interferometry. Its principle of operation is a combination of physical and geometrical optics. The angle calculation method is similar to the autocollimator. However, the autocollimator creates a cross image but the precise pencil-beam angle monitoring system produces an interference fringe on the focal plane. The advantages of the PAM are: high angular sensitivity, long-term stability character making angle monitoring over long time periods possible, high measurement accuracy in the order of sub-microradian, simultaneous measurement ability in two perpendicular directions or on two different objects, dynamic measurement possibility, insensitive to the vibration and air turbulence, automatic display, storage and analysis by use of the computer, small beam diameter making the alignment extremely easy and longer test distance. Some test examples are presented.
NTIS
*Pencil Beams; Interferometry*

**20010118931** Sandia National Labs., Albuquerque, NM USA
**Student Internship Program Report**
Cassidy, T. A.; Aug. 04, 2000; 6p; In English
Report No.(s): DE2000-761848; SAND2000-1963C; No Copyright; Avail: Department of Energy Information Bridge

This is the author's third summer working at Sandia National Laboratories in organization 5712. He is a physics major at Reed College in Portland, Oregon. His work at Sandia began during his senior year at Eldorado High School, when he worked part time and received school credit for participating in the internship program. During that time and two ensuing summers he worked on a variety of projects. These experiences included testing a number of optical-electronic systems, performing such tasks as determining the spectral responsivity of photodiodes and placing optical/electronic systems in front of a variety of light-sources in order to generate calibration curves. He also contributed to the computer generation of data to model a hypothetical satellite-mounted detection system using SSGM (Synthetic Scene Generation Model) and the Khoros visual programming software Cantata on a UNIX operating system. Other experiences included pre-flight satellite testing, and work in the field deploying a suite of sensors and data collection equipment in Nevada. This summer he is involved in image analysis using the software development tools of the Khoros programming environment. He is working on a project whose goal is to identify superimposed spectra obtained from remote-sensing equipment. The spectra to be identified are those of chemical warfare agents and precursor chemicals from the industrial processes used to manufacture them. Identifying these spectra is a challenge when they are mixed with each other and with incident light from the ground and atmosphere--photons that are both reflected from the sun and emitted as blackbody radiation. In order to model this process, he is working on a Khoros program that will add noise to laboratory-obtained spectra from a variety of chemicals. This altered data will mimic what a remote sensing device is likely

to record in the field. Given this example of likely field results, developing an ideal sensor and a method to identify spectra from such data will continue for a number of years.
NTIS
*Computer Techniques; Programming Environments; Remote Sensing; Education*

**20010119052** Moscow State Univ., Russia
**ICONO 2001 - International Conference on Coherent and Nonlinear Optics (XVII): Technical Digest (Part 2) Held in Belarus Cultural Center, Minsk, Belarus on June 26-July 1, 2001; Technical Exhibit, June 28-30, 2001**
Jan. 2001; 363p; In English
Contract(s)/Grant(s): F61775-01-W-F015
Report No.(s): AD-A394912; EOARD-CSP 01-5015; No Copyright; Avail: CASI; A16, Hardcopy; A03, Microfiche

The Final Proceedings for XVII International Conference on Coherent and Nonlinear Optics (ICONO 2001), 28 June - 1 July 2001. This is a multi-disciplinary conference. Topics of discussion include fundamental aspects of laser-matter interaction, ultrafast phenomena, quantum and atomic optics, nonlinear optical phenomena, novel trends in nonlinear laser spectroscopy and optical diagnostics, physics of nanostructures, high-precision measurements in optics, laser in chemistry, biophysics and biomedicine, optical information processing and storage, strong laser fields and high field physics, nonlinear dynamics of optical physics.
DTIC
*Coherence; Nonlinear Optics; Electromagnetic Interactions; Nanostructures (Devices)*

**20010119192** Oak Ridge National Lab., TN USA
**Dynamic Pressure of Liquid Mercury Target During 800-MeV Proton Thermal Shock Tests**
Allison, S. W.; Andriulli, J. B.; Cates, M. R.; Earl, D. D.; Haines, J. R.; Feb. 01, 2000; 11p; In English
Report No.(s): DE2000-754360; ORNL/TM-2000/46; No Copyright; Avail: Department of Energy Information Bridge

Described here are efforts to diagnose transient pressures generated by a short-pulse (about 0.5 microseconds) high intensity proton ((approximately) 2 * 10 14 per pulse) beam. Proton energy is 800-MeV. The tests were performed at the Los Alamos Neutron Science Center - Weapons Neutron Research (LANSCE-WNR). Such capability is required for understanding target interaction for the Spallation Neutron Source project as described previously at this conference. The main approach to effect the pressure measurements utilized the deflection of a diaphragm in intimate contact with the mercury. There are a wide variety of diaphragm-deflection methods used in scientific and industrial applications. Many deflection-sensing approaches are typically used, including, for instance, capacitive and optical fiber techniques. It was found, however, that conventional pressure measurement using commercial pressure gages with electrical leads was not possible due to the intense nuclear radiation environment. Earlier work with a fiber optic strain gauge demonstrated the viability of using fiber optics for this environment.
NTIS
*Mercury (Metal); Thermal Shock; Protons; Dynamic Pressure; Nuclear Radiation*

**20010119426** Brookhaven National Lab., Upton, NY USA
**FEL Development at the Advanced Photon Source**
Milton, S. V.; Jan. 26, 1999; 14p; In English
Report No.(s): DE2000-750771; BNL-66945; No Copyright; Avail: Department of Energy Information Bridge

Construction of a single-pass He-electron laser (FEL) based on the self-amplified spontaneous emission (SASE) mode of operation is nearing completion at the Advanced Photon Source (APS) with initial experiments imminent. The APS SASE FEL is a proof-of-principle fourth-generation light source. As of January 1999 the undulator hall, end-station building, necessary transfer lines, electron and optical diagnostics, injectors, and initial undulatory have been constructed and, with the exception of the undulators, installed. All preliminary code development and simulations have also been completed. The undulator hall is now ready to accept tirst beam for characterization of the output radiation. It is the project goal to push towards full FEL saturation, initially in the visible, but ultimately to ultraviolet and VUV wavelengths.
NTIS
*Free Electron Lasers; Spontaneous Emission*

**20010119428** Brookhaven National Lab., Upton, NY USA
**Proceedings of the Workshop on Siberian Snakes and Spin Rotators (3rd).**
Luccio, A.; Roser, T.; Sep. 12, 1994; 242p; In English
Report No.(s): DE2000-750767; BNL-52453; No Copyright; Avail: Department of Energy Information Bridge

The aim of the workshop was to provide a forum to discuss new developments in the area of Siberian snakes and spin rotators, also in preparation for the SPIN 94 Conference. In the workshop we had presentations followed by in-depth discussions in working groups: (1) Snake/Spin Rotator Design: Physics and Engineering Aspects; (2) Spin Dynamics: Tracking of Polarized Beams, Resonances, Stability; and (3) Accelerator Optics: Effects of Insertion of Snakes/Rotators in the Lattice. The following proceedings contain the contributions to the workshop. They are copies of the transparencies that were presented and discussed.
NTIS
*Conferences; Stability; Spin Dynamics*

**20010119531** Sandia National Labs., Albuquerque, NM USA
**High-Power Single Mode Operation of Hybrid Ion-Implanted/Selectively-Oxidized VCSELs**
Hadley, G. R.; Choquette, K. D.; Fischer, A. J.; Geib, K. M.; Allerman, A. A.; Aug. 01, 2000; 5p; In English
Report No.(s): DE2000-761854; SAND2000-2006C; No Copyright; Avail: Department of Energy Information Bridge

We report the design and testing of a novel 850nrn hybrid vertical cavity laser employing ion implantation and selective oxidation to independently define the gain region and mode size for optimal high-power single-mode operation.
NTIS
*Ion Implantation; Laser Cavities; Oxidation; Amplification*

**20010119543** Lawrence Livermore National Lab., Livermore, CA USA
**High-Accuracy Calibration of an Adaptive Optics System Using a Phase Shifting Diffraction Interferometer**
Bauman, B. J.; Campbell, E. W.; Olivier, S. S.; Sweider, D. R.; Jun. 23, 1999; 10p; In English
Report No.(s): DE2001-10421; UCRL-JC-134805; Rept-97-ERD-037; No Copyright; Avail: Department of Energy Information Bridge

A phase-shifting diffraction interferometer (PSDI) has been integrated into an adaptive optics (AO) system developed by LLNL for use on the three meter Shane telescope at Lick Observatory. The interferometer is an all fiber optic design, which is extremely compact. It is useful for calibrating the control sensors, measuring the aberrations of the entire AO optical train, and measuring the influence functions of the individual actuators on the deformable mirror. The PSDI is particularly well suited for this application because it measures converging, quasi-spherical wavefronts, such as are produced by an AO imaging system. Thus, a PSDI can be used to measure the aberrations of the entire AO system, in-situ and without errors introduced by auxiliary optics. This provides an extremely accurate measurement (approximately 5 nm RMS) of the optical properties of the AO system.
NTIS
*Adaptive Optics; Fiber Optics; Interferometers*

**20010119576** Argonne National Lab., IL USA
**Novel laser doppler linear encoder using multiple-reflection optical design for high-resolution linear actuator**
Shu, D.; Jul. 16, 1998; 10p; In English
Report No.(s): DE2001-10577; ANL/XFD/CP-95415; No Copyright; Avail: Department of Energy Information Bridge, Microfiche

A novel laser Doppler linear encoder system (LDLE) has been developed at the Advanced Photon Source, Argonne National Laboratory. A self-aligning 3-D multiple-reflection optical design was used for the laser Doppler displacement meter (LDDM) to extend the encoder system resolution. The encoder is compact (about 70 mm(H) x 100 mm(W) x 250 mm(L)) and it has sub-Angstrom resolution, 100 mm/sec measuring speed, and 300 mm measuring range. Because the new device affords higher resolution, as compared with commercial laser interferometer systems, and yet costs less, it will have good potential for use in scientific and industrial applications.
NTIS
*Lasers; Doppler Effect; Optical Equipment; High Resolution*

**20010119594** Moscow State Univ., Russia
**ICONO 2001 - International Conference on Coherent and Nonlinear Optics (XVII): Advance Program (Part 1) Held in Belarus Cultural Center, Minsk, Belarus on June 26-July 1, 2001; Technical Exhibit, June 28-30, 2001**
Jan. 2001; 111p; In English
Contract(s)/Grant(s): F61775-01-W-F015
Report No.(s): AD-A394913; EOARD-CSP 01-5015; No Copyright; Avail: CASI; A06, Hardcopy; A02, Microfiche

The Final Proceedings for XVII International Conference on Coherent and Nonlinear Optics (ICONO 2001), 28 June - 1 July 2001. This is a multi-disciplinary conference. Topics of discussion include fundamental aspects of laser-matter interaction,

ultrafast phenomena, quantum and atomic optics, nonlinear optical phenomena, novel trends in nonlinear laser spectroscopy and optical diagnostics, physics of nanostructures, high-precision measurements in optics, laser in chemistry, biophysics and biomedicine, optical information processing and storage, strong laser fields and high field physics, nonlinear dynamics of optical physics.
DTIC
*Coherence; Nonlinear Optics; Nanostructures (Devices); Medical Science; Electromagnetic Interactions; Biophysics*

**20010119956** NASA Stennis Space Center, Bay Saint Louis, MS USA
**Determining CDOM Absorption Spectra in Diverse Aquatic Environments Using a Multiple Pathlength, Liquid Core Waveguide System**
Miller, Richard L., NASA Stennis Space Center, USA; Belz, Mathias, World Precision Instruments, Inc., USA; DelCastillo, Carlos, NASA Stennis Space Center, USA; Trzaska, Rick, GB Technology, Inc., USA; Aug. 06, 2001; 27p; In English
Report No.(s): SE-2001-08-00044; No Copyright; Avail: CASI; A03, Hardcopy; A01, Microfiche

We evaluated the accuracy, sensitivity and precision of a multiple pathlength, liquid core waveguide (MPLCW) system for measuring colored dissolved organic matter (CDOM) absorption in the UV-visible spectral range (370-700 nm). The MPLCW has four optical paths (2.0, 9.8, 49.3, and 204 cm) coupled to a single Teflon AF sample cell. Water samples were obtained from inland, coastal and ocean waters ranging in salinity from 0 to 36 PSU. Reference solutions for the MPLCW were made having a refractive index of the sample. CDOM absorption coefficients, aCDOM, and the slope of the log-linearized absorption spectra, S, were compared with values obtained using a dual-beam spectrophotometer. Absorption of phenol red secondary standards measured by the MPLCW at 558 nm were highly correlated with spectrophotometer values and showed a linear response across all four pathlengths. Values of aCDOM measured using the MPLCW were virtually identical to spectrophotometer values over a wide range of concentrations. The dynamic range of aCDOM for MPLCW measurements was 0.002 - 231.5 m-1. At low CDOM concentrations spectrophotometric aCDOM were slightly greater than MPLCW values and showed larger fluctuations at longer wavelengths due to limitations in instrument precision. In contrast, MPLCW spectra followed an exponential to 600 nm for all samples.
Author
*Evaluation; Accuracy; Sensitivity Analysis; Liquid Flow; Color; Dissolved Organic Matter; Measure and Integration*

**20010120049** Brookhaven National Lab., Upton, NY USA
**Can free electron lasers answer critical questions in ultraviolet photobiology**
Sutherland, J. C.; Jan. 20, 2000; 9p; In English
Report No.(s): DE2000-752963; BNL-67205; No Copyright; Avail: Department of Energy Information Bridge

DNA and other biological macromolecules are sensitive to damage by ultraviolet light with wavelengths less than about 320 nm. Fortunately, such wavelengths are efficiently absorbed by ozone in the stratosphere. DNA can also be damaged by longer wavelength ultraviolet and (perhaps) visible light, albeit with far lower efficiencies. Indeed, the cross section for damage induction in DNA by longer wavelengths is so low that it has been difficult to measure easily in controlled experiments using monochromatic laboratory sources. However, the flux of solar photons reaching the biosphere is far higher than at the shorter wavelengths. Thus the damage induced by wavelengths greater than 320 nm may constitute a significant fraction of the total UV burden in a particular organism or ecosystem. Understanding the nature and extent of this long wavelength induced damage is crucial in several important societal problems including: (1) Evaluating the biological impact of depletion of stratospheric ozone; (2) Determining if sunscreen preparations offer the same protection against long term effects such as cutaneous malignant melanoma as they do against prompt effects such as erythema (sunburn); and (3) Determining the safest spectrum for use in indoor tanning. The light sources required for such studies must provide high intensities of nearly monochromatic light that can be tuned to any wavelength in the required spectral range. This paper will evaluate the potential of ultraviolet free electron lasers, and particularly the soon to be available UV-FEL at the Thomas Jefferson National Accelerator Facility for such experiments.
NTIS
*Free Electron Lasers; Ultraviolet Lasers; Molecular Biology; Photolysis; Ecosystems*

**20010120075** Argonne National Lab., IL USA
**Photorefractivity in ferroelectric liquid crystals**
Wiederrecht, G. P.; Wasielewski, M. R.; Fuller, M.; Aug. 15, 2000; 9p; In English
Report No.(s): DE2000-761265; ANL/CHM/CP-102579; No Copyright; Avail: Department of Energy Information Bridge

The first observation of photorefractivity in ferroelectric liquid crystals (FLC) is reported. The FLCs are doped with the easily oxidized chromophore perylene, which also functions as the sensitizer. The electron acceptor di-butyl-pyromellitirnide is added

to induce photoconductivity through an efficient intermolecular electron transfer reaction to produce mobile ions. A strong dependence on the orientation of the wavevector of the optical interference pattern and polarization of the writing beams relative to the orientation of the FLC molecules is observed. The results are interpreted as an orientational photorefractive effect in which the net polarization of the FLC couples linearly to the space-charge field as opposed to nematic liquid crystals in which the dielectric anisotropy couples to the square of the space charge field.
NTIS
*Ferroelectric Materials; Liquid Crystals; Photorefractivity*

**20010120079** Argonne National Lab., IL USA
**Nonlinear harmonics in the high-gain harmonic generation (HGHG) experiment**
Biedron, S. G.; Freund, H. P.; Wang, X.; Yu, L. H.; Aug. 22, 2000; 20p; In English
Report No.(s): DE2000-761254; ANL/AOD/CP-102079; No Copyright; Avail: Department of Energy Information Bridge
A single-pass, high-gain free-electron laser (FEL) experiment based on the high-gain harmonic generation (HGHG) theory is underway at the Accelerator Test Facility (ATF) at Brookhaven National Laboratory (BNL) in collaboration with the Advanced Photon Source (APS) at Argonne National Laboratory (ANL). This project achieved first lasing in August 1999, when gain of 107 above spontaneous was measured. It has been shown through both the 1D and 3D analytical models and in 3D simulations that the higher nonlinear harmonics are expected to grow at rates that scale in inverse proportion to the harmonic number in all single-pass, high-gain FELs. Also, the powers in these harmonics are expected to be substantial. An HGHG FEL configuration already implements frequency up-conversion (as explained briefly in the next section), and, in such a system, these higher nonlinear harmonics are unusually interesting, as even shorter wavelengths can be exploited simultaneously. The specific case of the simulated higher nonlinear harmonic output for the BNL/APS HGHG experiment will be examined here.
NTIS
*Free Electron Lasers; Harmonic Generations; High Gain; Nonlinearity*

**20010120080** Argonne National Lab., IL USA
**Solution to the initial value problem for a high-gain FEL via Van Kampen's method**
Huang, Z.; Kim, K. J.; Aug. 22, 2000; 16p; In English
Report No.(s): DE2000-761253; ANL/ASD/CP-101972; No Copyright; Avail: Department of Energy Information Bridge
Using Van Kampen's normal mode expansion, we solve the initial value problem for a high-gain free-electron laser (FEL) described by the three-dimensional Maxwell-Klimontovich equations. An expression of the radiation spectrum is given for the process of coherent amplification and self-amplified spontaneous emission. It is noted that the input coupling coefficient for either process increases with the initial beam energy spread. The effective start-up noise is identified as the coherent fraction of the spontaneous undulator radiation in one field gain length, and is larger with increasing energy spread and emittance mainly because of the increase in gain length.
NTIS
*Free Electron Lasers; Boundary Value Problems; High Gain*

**20010120089** Sandia National Labs., Albuquerque, NM USA
**Feasibility of Fundamental-Mode Operation in Unstable-Resonator InGaN Lasers**
Chow, W. W.; Amano, H.; Akasaki, I.; Aug. 01, 2000; 7p; In English
Report No.(s): DE2000-760772; SAND2000-1245C; No Copyright; Avail: Department of Energy Information Bridge
A wave-optical model that is coupled to a microscopic gain theory is used to explore solutions to the filamentation problem in group-III nitride quantum well lasers. A negative-branch unstable resonator is found to mitigate filament effects, enabling high-power fundamental-mode operation in broad-area lasers.
NTIS
*Nitrides; Quantum Well Lasers*

**20010120098** NASA Ames Research Center, Moffett Field, CA USA
**FPA Needs for NASA Missions**
McCreight, Craig R., NASA Ames Research Center, USA; Krabach, Timothy N., Jet Propulsion Lab., California Inst. of Tech., USA; [1994]; 1p; In English; Infrared Information Symposium Detector Specialty Group Meeting, 17-18 Aug. 1994, Boulder, CO, USA
Contract(s)/Grant(s): RTOP 233-02-05-01; No Copyright; Avail: Issuing Activity; Abstract Only

NASA has identified needs for a broad range of specialized, optimized infrared detectors and IR detector arrays to meet its future mission requirements. Space infrared missions will be conducted in a number of discipline areas, including astrophysics, earth and atmospheric science, planetary systems, and space physics. to allow investigators to meet scientific goals, specific technical requirements for infrared detectors have been developed. These challenging and often unique requirements include, for example, achieving background-limited performance in a cryogenic space telescope; developing long-wave IR arrays which achieve near background-limited performance at elevated (approximately 60 kelvin) operating temperatures; achieving IR arrays with large two-dimensional formats, excellent uniformity and linearity, and low power dissipation; demonstrating an imaging array technology for very long-wavelength (less than 100 microns) IR sensing, and IR devices with extremely low dark current levels; and demonstrating stable, low-noise, low-dissipation readouts. These requirements can in some cases be met by adaptation or extension of technologies originally developed by DoD. In other cases, the novel spectral range or other characteristics require unique solutions. Examples are given of recent scientific results which have been made possible with IR arrays. These serve as a preview of the kinds of science return which can be enabled by advanced IR focal plane technology from space platforms.
Author
*Arrays; Atmospheric Physics; Imaging Techniques; Infrared Detectors; Infrared Radiation*

**20010120262** Argonne National Lab., IL USA
**Optimization of the design for the LCLS undulator line**
Gluskin, E.; Vinokurov, N. A.; Dejus, R. J.; Emma, P.; Moog, E. R.; Aug. 25, 2000; 13p; In English
Report No.(s): DE2000-761255; ANL/XFD/CP-102080; No Copyright; Avail: Department of Energy Information Bridge

The Linac Coherent Light Source (LCLS) undulator line will consist of undulator segments separated by breaks of various lengths. Focusing quadrupoles, in a FODO lattice, and electron beam diagnostics will be located in the breaks, and every third break will be longer to also accommodate photon diagnostics. The electron beam beta function and the undulator period were selected to minimize the saturation length. The FEL (free electron laser) simulation code RON has been used to optimize parameters such as the length of the undulatory and the break lengths between undulatory. Different break lengths after the first three undulatory have been found to help reduce the overall undulator line saturation length. Tolerances for individual undulatory have also been determined.
NTIS
*Design Optimization; Free Electron Lasers; Linear Accelerators; Coherent Light; Light Sources*

**20010121497** Sandia National Labs., Albuquerque, NM USA
**Pivoting Micromirror Designs for Large Orientation Angles**
Garcia, E. J.; Jul. 18, 2000; 13p; In English
Report No.(s): DE2000-760770; SAND2000-0865C; No Copyright; Avail: Department of Energy Information Bridge, Microfiche

This paper describes mechanical design concepts for a class of pivoting micromirrors that permit relatively large angles of orientation to be obtained when configured in large arrays. Micromirror arrays can be utilized in a variety of applications ranging from optical switching to beam-front correction in a variety of technologies. This particular work is concerned with silicon surface micromachining (SMM). The multi-layer polysilicon surface micromachining process developed at Sandia National Laboratories is used to fabricate micromirror arrays that consist of capacitive electrode pairs which are used to electrostatically actuate mirrors to their desired positions and suitable elastic suspensions which support the 2 micron thick mirror structures. The designs described have been fabricated and successfully operated.
NTIS
*Micromachining; Mirrors; Mechanical Engineering; Equipment Specifications; Silicon Polymers*

**20010122278** Argonne National Lab., IL USA
**First Measurements of Subpicosecond Electron Beam Structure by Autocorrelation of Coherent Diffraction Radiation**
Lumpkin, A. H.; Sereno, N. S.; Rule, D. W.; Aug. 22, 2000; 19p; In English
Report No.(s): DE2000-761251; ANL/AOD/CP-101967; No Copyright; Avail: Department of Energy Information Bridge

We report the initial measurements of subpicosecond electron beam structure using a nonintercepting technique based on the autocorrelation of coherent diffraction radiation (CDR). A far infrared (FIR) Michelson interferometer with a Golay detector was used to obtain the autocorrelation. The radiation was generated by a thermionic rf gun beam at 40 MeV as it passed through a 5-mm-tall slit/aperture in a metal screen whose surface was at 45 deg to the beam direction. For the observed bunch lengths of about 450 fs (FWHM) with a shorter time spike on the leading edge, peak currents of about 100 A are indicated. Also a model was developed and used to calculate the CDR from the back of two metal strips separated by a 5-mm vertical gap. The

demonstrated nonintercepting aspect of this method could allow on-line bunch length characterizations to be done during free-electron laser experiments.
NTIS
*Coherent Radiation; Electron Beams; Atomic Structure*

**20010122384** University of Central Florida, School of Optics, Orlando, FL USA
**Equipment for Research on True Three Dimensional Displays** ***Final Report, 1 May 2000 - 30 Apr. 2001***
Bass, Michael; Apr. 2001; 7p; In English
Contract(s)/Grant(s): DAAD19-00-1-0132
Report No.(s): AD-A395261; ARO-40734.1-EL-RIP; No Copyright; Avail: CASI; A02, Hardcopy; A01, Microfiche

Equipment is described that was purchased for the study of nonlinear absorption in dyes for use in true, three dimensional displays. A pair of optical parametric oscillators pumped by the same frequency tripled, Q-switched Nd:YAG laser was purchased from Spectra Physics Inc. and installed with appropriate beam control optics. LabView drivers for the laser and the OPOs were written and combined in a master driver controlling the diagnostic equipment and, thus, the data acquisition. This system was tested out and will be used in the study of dye doped media for true three-dimensional displays.
DTIC
*Optical Equipment; Nonlinear Systems; Optical Pumping; Neodymium Lasers; Doped Crystals; Display Devices*

**20010122831** California Univ., Lawrence Berkeley Lab., Berkeley, CA USA
**Analysis of longitudinal bunching in an FEL driven two-beam accelerator**
Lidia, S.; Gardelle, J.; Lefevre, T.; Donohue, J. T.; Gouard, P.; Aug. 01, 2000; 3p; In English
Report No.(s): DE2000-765498; LBNL-46704; No Copyright; Avail: Department of Energy Information Bridge, Microfiche

Recent experiments have explored the use of a free-electron laser (FEL) as a buncher for a microwave two-beam accelerator, and the subsequent driving of a standing-wave rf (radio frequency) output cavity. Here the authors present a deeper analysis of the longitudinal dynamics of the electron bunches as they are transported from the end of the FEL and through the output cavity. In particular, the authors examine the effect of the transport region and cavity aperture to filter the bunched portion of the beam.
NTIS
*Free Electron Lasers; Linear Accelerators; Electron Bunching*

**20010122890** Argonne National Lab., IL USA
**Development of a 3D FEL code for the simulation of a high-gain harmonic generation experiment**
Biedron, S. G.; Feb. 26, 1999; 16p; In English
Report No.(s): DE2001-10967; ANL/ASD/CP-97292; No Copyright; Avail: Department of Energy Information Bridge, Microfiche

Over the last few years, there has been a growing interest in self-amplified spontaneous emission (SASE) free-electron lasers (FELs) as a means for achieving a fourth-generation light source. In order to correctly and easily simulate the many configurations that have been suggested, such as multi-segmented wigglers and the method of high-gain harmonic generation, we have developed a robust three-dimensional code. The specifics of the code, the comparison to the linear theory as well as future plans will be presented.
NTIS
*Free Electron Lasers; Harmonic Generations; Light Sources; Computerized Simulation*

**20010122942** Brookhaven National Lab., Upton, NY USA
**Single-pass high-gain free electron laser electron beam diagnostics**
Wang, X. J.; May 08, 2000; 20p; In English
Report No.(s): DE2000-767102; BNL-67638; KA0403000; No Copyright; Avail: Department of Energy Information Bridge

Consensus reached in the last few years that fourth generation light source will most likely be an X ray or a UV coherent source based on single pass high gain free electron laser (FEL), such as Self Amplified Spontaneous Emission (SASE), or seeded high gain harmonic generation (HGHG) free electron lasers. High gain (greater than 10 7) required for single pass FEL puts great constraint on the quality of electron beam, and demands detailed distribution information of electron beam in six-dimension. The typical accelerator system for single pass FEL consists of a photocathode RF (radio frequency) gun injection system, a linac and magnetic bunch compressors, and a long undulator. The major challenges in beam diagnostics for single pass FEL are to characterize the picoseconds high brightness electron beam in six dimension produced by photocathode RF gun injector, and improve the stability and reliability of the photocathode RF gun injection system. Characterization of short electron bunch (100

fs) produced by the compressors, and co-align the electron beam with FEL radiation inside long undulator are also critical for FEL performance. We will discuss many diagnostic techniques developed at the Brookhaven Accelerator Test Facility (ATF) for the photocathode RF gun injection system, present several techniques for femtoseconds bunch length measurement, especially RF kicker cavity. Tomography technique for both transverse and longitudinal phase space measurements is discussed. Concept of multiple alignment laser stations is present for beam alignment in the long undulator.
NTIS
*Electron Beams; Free Electron Lasers*

**20010123041** Brookhaven National Lab., Upton, NY USA
**Deep Ultra-Violet Free Electron Laser (DUV-FEL) at Brookhaven National Laboratory**
Johnson,; Ben-Zvi,; Diamauro,; Graves,; Heese,; Feb. 15, 2000; 3p; In English
Report No.(s): DE2000-767166; BNL-67669; No Copyright; Avail: Department of Energy Information Bridge
Brookhaven National Laboratory has established an initiative in free-electron laser (FEL) science and technology development which includes the Deep Ultra-Violet Free Electron Laser (DUV-FEL) experiment. It is configured as a sub-harmonically seeded High Gain Harmonic Generator (HGHG) to improve coherence and pulse control as contrasted with other schemes that start up from noise. In its initial configuration the DUV-FEL will allow operation at wavelengths down to 200 nm at pulse lengths below a picosecond. The DUV-FEL will be used as a test-bed for experiments to utilize the ultraviolet radiation it produces, and serve as model for extending its principles to much shorter wavelengths (x-rays).
NTIS
*Free Electron Lasers; Ultraviolet Radiation*

**20010123042** Brookhaven National Lab., Upton, NY USA
**Applications of the Jefferson Lab Free Electron Laser for Photobiology**
Dylla,; Benson,; Neil,; Shinn,; Austin,; Feb. 15, 2000; 10p; In English
Report No.(s): DE2000-767165; BNL-67683; No Copyright; Avail: Department of Energy Information Bridge
A versatile free electron laser (FEL) user facility has recently come on line at the Thomas Jefferson National Accelerator Facility (Jefferson Lab) providing high average (kilowatt-level) power laser light in the infrared (IR). A planned upgrade of the FEL in this facility will extend the wavelength range through the visible to the deep ultraviolet (UV) and provide the photobiology community with a unique light source for a variety of studies. Planned and potential applications of this FEL include: IR studies of energy flow in biomolecules, IR and visible imaging of biomedical systems, IR and visible studies of photodynamic effects and UV and near visible studies of DNA photodamage.
NTIS
*Free Electron Lasers; Imaging Techniques; Infrared Radiation*

**20010123056** Brookhaven National Lab., Upton, NY USA
**Initial Gain Measurements of a 800 nm SASE FEL, VISA**
Frigola, P.; Murokh, A.; Musumeci, P.; Babzien, M.; Ben-Zvi, I.; Aug. 13, 2000; 9p; In English
Report No.(s): DE2000-767127; BNL-67739; KA0403000; No Copyright; Avail: Department of Energy Information Bridge
The VISA (Visible to Infrared SASE Amplifier) free-electron laser (FEL) is designed to obtain high gain at a radiation wavelength of 800 nm. The FEL uses the high brightness electron beam of the Accelerator Test Facility (ATF), with energy of 72MeV. VISA uses a novel, 4 m long, strong focusing undulator with a gap of 6 mm and a period of 1.8 cm. to obtain large gain the beam and undulator axis have to be aligned to better than 50 micrometers. Results from initial measurements on the alignment, gain, and spectrum will be presented and compared to theoretical calculations and simulations.
NTIS
*Free Electron Lasers; Infrared Lasers; Spectra*

**20010123058** Chitose Inst. of Science and Technology, Chitose, Japan
**2nd Chitose International Forum on Photonic Science and Technology (CIF'2). International Forum on Nanotechnology: Toward the Organic Photonics**
September 2001; 113p; In English; 2nd Chitose International Forum on Photonic Science and Technology (CIF'2). International Forum on Nanotechnology: Toward the Organic Photonics, 6-8 Sep. 2001, Hokkaido, Japan
Contract(s)/Grant(s): F62562-01-M-9086
Report No.(s): AD-A395309; No Copyright; Avail: CASI; A06, Hardcopy; A02, Microfiche

This report presents the proceedings of the International Forum on Nanotechnology: Toward the Organic Photonics, held 6-8 September 2001 at Chitose, Hokkaido, Japan. This is an interdisciplinary conference. Its aim is to achieve international cooperation among researchers and to stimulate the field of nonlinear polymers as photonic materials and devices.
DTIC
*Photonics; Nanotechnology*

**20010123134** Brookhaven National Lab., Upton, NY USA
**FEL Technologies R and D and SASE Gain Enhancement Observation at the BNL ATF**
Wang, X. J.; Babzien, M.; Ben-Zvi, I.; Malone, R.; Yakimenko, V.; Jun. 26, 2000; 5p; In English
Report No.(s): DE2000-767104; BNL-67635; KA0403000; No Copyright; Avail: Department of Energy Information Bridge

The research at the Brookhaven Accelerator Test Facility (ATF) covers all major aspects of the future light source (LS) technologies, from high-brightness electron beam source, beam diagnostics to FEL (free electron laser) experiments. The ATF itself is the testing ground for photocathode RF (radio frequency) gun technologies; it is the only multi-user facility based on the photocathode RF gun injection system. Using vacuum based laser-cleaning technique, 0.5% quantum efficiency (QE) was measured for an Mg cathode. The best emittance (normalized rms) for a 0.5nC charge with peak current 110 A is measured to be 1.5 mm-mrad. The ATF is the only facility where both laser seeded (HGHG) and SASE (self-amplified spontaneous emission) FEL experiments are performed. SASE was observed at the ATF from 5.3 microns to visible. A record of seven orders of magnitude gain was observed at the ATF high-gain harmonic-generation (HGHG) experiment. An order of magnitude SASE gain enhancement by optical klystron was observed at the ATF.
NTIS
*Free Electron Lasers; High Gain*

**20010123641** Lawrence Livermore National Lab., Livermore, CA USA
**Ion-optics calculations of the LLNL AMS system for biochemical 14C measurements**
Ognibene, T. J.; Brown, T. A.; Knezovich, J. P.; Roberts, M. L.; Southon, J. R.; Oct. 27, 1999; 13p; In English
Report No.(s): DE2000-757340; UCRL-JC-134095; No Copyright; Avail: Department of Energy Information Bridge, Microfiche

A dedicated AMS (Accelerator Mass Spectrometry) system for biochemical (sup 14)C measurements is being built at the Center for Accelerator Mass Spectrometry. The system is centered around a National Electrostatics Corporation Model 3SDH-1 1-MV Pelletron accelerator and is designed to accept two ion sources. The LLNL (Lawrence Livermore National Laboratory) 64-sample Cs-sputter ion source with its zoom lens beam line is attached to one port of the electrostatic switching element. to ensure efficient coupling of the source to the acceptance of the accelerator, ion-optics calculations of the low-energy injection beam line have been conducted; the results of which were used to determine the layout of the ion optical components of the beam line. Beam tests of the low-energy injection line show that beam behavior was accurately predicted by the calculations.
NTIS
*Ion Optics; Mass Spectroscopy; Ion Sources; Carbon 14*

**20010123659** Texas Univ., Houston, TX USA
**Diagnostic and Therapeutic Applications of Diode Lasers and Solids State Lasers in Medicine. Final Report, 1994**
Sep. 17, 1999; 29p; In English
Report No.(s): DE2001-764420; DOE/ER/61226-1-VOL-1; No Copyright; Avail: Department of Energy Information Bridge

The research has focused on five projects: (1) Spectroscopy; (2) Imaging; (3) PhotoDynamic Therapy; (4) Controlled Photocoagulation; and (5) Laser Surgery. A major goal is to bring specific projects to the clinic during the proposed funding period. Therefore, the projects me specifically tied to several examples of clinical translation.
NTIS
*Imaging Techniques; Laser Applications; Spectroscopy; Therapy*

**20010124087** California Univ., Lawrence Berkeley Lab., Berkeley, CA USA
**Ultrahigh resolution multicolor colocalization of single fluorescent nanocrystals**
Michalet, X.; Lacoste, T. D.; Pinaud, F.; Chemla, D. S.; Alivisatos, A. P.; Dec. 20, 2000; 8p; In English
Report No.(s): DE2001-775176; LBNL-47233; No Copyright; Avail: Department of Energy Information Bridge

A new method for in vitro and possibly in vivo ultrahigh-resolution colocalization and distance measurement between biomolecules is described, based on semiconductor nanocrystal probes. This ruler bridges the gap between FRET and far-field (or near-field scanning optical microscope) imaging and has a dynamic range from few nanometers to tens of micrometers. The ruler is based on a stage-scanning confocal microscope that allows the simultaneous excitation and localization of the excitation

point-spread-function (PSF) of various colors nanocrystals while maintaining perfect registry between the channels. Fit of the observed diffraction and photophysics-limited images of the PSFs with a two-dimensional Gaussian allows one to determine their position with nanometer accuracy. This new high-resolution tool opens new windows in various molecular, cell biology and biotechnology applications.
NTIS
*Biotechnology; Fluorescence; High Resolution; Nanocrystals; Molecular Biology; Semiconductors (Materials)*

**20010124094** Argonne National Lab., IL USA
**Design for a high resolution very-low-Q time-of flight diffractometer**
Hjelm, R. P.; Sep. 29, 1998; 17p; In English
Report No.(s): DE2001-10982; ANL/IPNS/CP-97349; No Copyright; Avail: Department of Energy Information Bridge, Microfiche

The design of a high resolution view low-Q time of flight diffractometer was motivated by the anticipated need to perform small-angle neutron scattering measurements at far lower momentum transfer and higher precision than currently available at either pulsed or steady state sources. In addition, it was recognized that flexibility in the configuration of the instrument and ease in which data is acquired are important. The design offers two configurations, a high intensity/very low Q geometry employing a focusing mirror and a medium to high Q-precision/low Q configuration using standard pinhole collimation geometry. The quality of the mirror optics is very important to the performance of the high intensity/very low Q configuration. We believe that the necessary technology exists to fabricate the high quality mirror optics required for the instrument.
NTIS
*Diffractometers; Neutron Scattering; Q Factors*

**20010124142** Argonne National Lab., IL USA
**Fourth Generation Light Source Instrumentation Discussion Group Number 6**
Lumpkin, A.; Sep. 24, 1998; 4p; In English
Report No.(s): DE2001-10984; ANL/ASD/CP-97354; No Copyright; Avail: Department of Energy Information Bridge, Microfiche

This working group on 4th Generation Light Source (4GLS) Instrumentation was a follow-up to the opening-discussion on Challenges in Beam Profiling. It was in parallel with the Feedback Systems session. We filled the SSRL Conference Room with about 25 participants. The session opened with an introduction by Lumpkin. The target beam parameter values for a few-angstrom, self-amplified spontaneous emissions (SASE) experiment and for a diffraction-limited soft x-ray storage ring source were addressed. Instrument resolution would of course need to be 2-3 times better than the value measured, if possible. The nominal targeted performance parameters are emittance (1-2(pi) mm mrad), bunch length (100 fs), peak-current (l-5 kA), beam size (10 (micro)m), beam divergence (1 (micro)rad), energy spread (2 x 10(exp -4)), and beam energy (10 of GeV). These are mostly the SASE values, and the possible parameters for a diffraction-limited soft x-ray source would be relaxed somewhat. Beam stability and alignment specifications in the sub-micron domain for either device are anticipated.
NTIS
*Light Sources; X Ray Sources; Storage Rings (Particle Accelerators)*

**20010124837** Osservatorio Astronomico, Padova, Italy
**A Wide Angle Camera for Bepi Colombo**
Cremonese, G., Osservatorio Astronomico, Italy; Achilli, V., Osservatorio Astronomico, Italy; Barbieri, C., Osservatorio Astronomico, Italy; Caporali, A., Osservatorio Astronomico, Italy; Capria, M. T., Osservatorio Astronomico, Italy; Colangeli, L., Osservatorio Astronomico, Italy; Forlani, G., Osservatorio Astronomico, Italy; Fornasier, S., Osservatorio Astronomico, Italy; Lazzarin, M., Osservatorio Astronomico, Italy; Marzari, F., Osservatorio Astronomico, Italy; Mercury: Space Environment, and Surface and Interior; 2001, pp. 18; In English; See also 20010124826; No Copyright; Abstract Only; Available from CASI only as part of the entire parent document

In the frame of the ESA (European Space Agency) Cornerstone Mission BepiColombo to planet Mercury, we are working on the concept for a Wide Angle Camera (WAC) aiming to fulfill the main scientific goals set forth in the ESA document (ESA-SCI[2000]1) about surface morphology, mineralogy and exosphere. A primary requirement is the complete coverage of the surface with a resolution of about 50 m in all three coordinates. Relying on previous experience in advanced imaging systems,

both in our Institutes and in consulting industries, novel technological solutions are investigated for optics, detectors and data acquisition and analysis. A conceptual design of the WAC will be presented.
Author
*Cameras; European Space Agency; Mercury (Planet); Space Missions; Mercury Surface*

**20010124838** Rutherford Appleton Lab., Space Science and Technology Dept., Chilton, UK
**X-Ray Science on ESA's BepiColombo Mission to Mercury**
Dunkin, S. K., Rutherford Appleton Lab., UK; Grande, M., Rutherford Appleton Lab., UK; Kellett, B. J., Rutherford Appleton Lab., UK; Mercury: Space Environment, and Surface and Interior; 2001, pp. 19-20; In English; See also 20010124826; No Copyright; Abstract Only; Available from CASI only as part of the entire parent document

Mercury has been visited only once by a spacecraft, with Mariner 10 completing three flybys in 1974/5. Its closeness to the Sun makes ground based observations very difficult, and hence our knowledge of Mercury is extremely limited. This paper outlines the science drivers of an X-ray instrument (i.e. CIXS) to fly on a spacecraft such as ESA's (European Space Agency) BepiColombo mission. Additional information is contained in the original extended abstract.
Author
*Mercury (Planet); Space Missions; Spacecraft Equipment; X Ray Spectrometers*

**20010125016** Lawrence Livermore National Lab., Livermore, CA USA
**Developing solid state experiments on the Nova laser**
Chandler, E. A.; Colvin, J. D.; Failor, B. H.; Gold, D. M.; Hauer, A.; Aug. 06, 1999; 25p; In English
Report No.(s): DE2001-11330; UCRL-JC-131851; No Copyright; Avail: Department of Energy Information Bridge

An x-ray drive has been developed to shock compress metal foils in the solid state using an internally shielded hohlraum with a high contrast shaped pulse from the Nova laser. The drive has been characterized and hydrodynamics experiments designed to study growth of the Rayleigh-Taylor (RT) instability in Cu foils at 3 Mbar peak pressures in the plastic flow regime have been started. Pre-imposed modulations with an initial wavelength of 20-50 micrometers, and amplitudes of 1.0-2.5 micrometers show growth consistent with simulations. In the Nova experiments, the fluid and solid states are expected to behave similarly for Cu. An analytic stability analysis is used to motivate an experimental design with an Al foil where the effects of material strength on the RT growth are significantly enhanced. The conditions reached in the metal foils at peak compression are similar to those predicted at the core of the earth.
NTIS
*Metal Foils; Solid State; Hohlraums; Pulsed Lasers*

**20010125018** Oak Ridge National Lab., TN USA
**Hyperthermal Pulsed-Laser Ablation Beams for Film Deposition and Surface Microstructural Engineering**
Lowndes, D. H.; Nov. 08, 1999; 6p; In English
Report No.(s): DE2001-11465; ORNL/CP-104571; No Copyright; Avail: Department of Energy Information Bridge

This paper presents an overview of pulsed-laser ablation for film deposition and surface microstructure formation. by changing the ambient gas pressure from high vacuum to several Torr (several hundred Pa) and by selecting the pulsed-laser wavelength, the kinetic energy of ablated atoms/ions can be varied from several hundred eV down to (approximately)0.1 eV and films ranging from superhard to nanocrystalline may be deposited. Furthermore, cumulative (multi-pulse) irradiation of a semiconductor surface (e.g. silicon) in an oxidizing gas (O2, SF6) et atmospheric pressure can produce dense, self-organized arrays of high-aspect-ratio microcolumns or microcones. Thus, a wide range of materials synthesis and processing opportunities result from the hyperthermal flux and reactive growth conditions provided by pulsed-laser ablation.
NTIS
*Deposition; Pulsed Lasers; Laser Ablation; Microstructure*

**20010125165** California Univ., Lawrence Berkeley Lab., Berkeley, CA USA
**Variable Included Angle Plane Grating Monochromator on an Undulator for Spectroscopy and Microscopy at the Advanced Light Source**
Warwick, T.; Cambie, D.; Padmore, H.; Howells, M.; Aug. 01, 2000; 5p; In English; 7th; 7th International Conference on Synchrotron Radiation Instrumentation, 21-25 Aug. 2000, Berlin, Germany, USA
Report No.(s): DE2000-767635; LBNL-46881; No Copyright; Avail: Department of Energy Information Bridge, Microfiche

A new beam line (beam line 11.0) at the Advanced Light Source has been designed to employ a Variable-Included-Angle Plane-Grating-Monochromator. The extended range available from a specific grating is exploited to cover energies from the

carbon 1s absorption edge to the oxygen 1s absorption edge with two different gratings (150 l/mm and 1200 l/mm) with dispersion different by a factor of three. The phase space of a zone plate microscope can then be efficiently filled either at low or high resolution (R = 2500 and R = 7500). At the same time the monochromator is designed to cover the energy range from 75 eV to 1500 eV using the same two gratings at high resolution for spectroscopy. A deformable mirror pair will re-focus to a monochromatic spot, matched into the acceptance of a fluorescence spectrometer. The monochromator will operate in vertically collimated light and the free choice of focussing parameter provides a guarantee of high resolution even when the power loading is high. However, we will provide a thermally engineered pre-mirror so that the high resolution requirement at low photon energy can be met without loss of efficiency.
NTIS
*High Resolution; Light Sources; Monochromators*

**20010125234** Idaho National Engineering and Environmental Lab., Idaho Falls, ID USA
**Remote Laser Diffraction PSD Analyzer**
Batcheller, T. A.; Huestis, G. M.; Bolton, S. M.; Jun. 01, 2000; 12p; In English
Report No.(s): DE2000-764162; INEEL/EXT-2000-00479; No Copyright; Avail: Department of Energy Information Bridge
Particle size distribution (PSD) analysis of radioactive slurry samples were obtained using a modified off-the-shelf classical laser light scattering particle size analyzer. A Horiba Instruments Inc. Model La-300 PSD analyzer, which has a 0.1 to 600 micron measurement range, was modified for remote application in a hot cell (gamma radiation) environment. The general details of the modifications to this analyzer are presented in this paper. This technology provides rapid and simple PSD analysis, especially down in the fine and microscopic particle size regime. Particle size analysis of these radioactive slurries down in this smaller range was not achievable - making this technology far superior than the traditional methods used previously. Remote deployment and utilization of this technology is in an exploratory stage. The risk of malfunction in this radiation environment is countered by gaining of this tremendously useful fundamental engineering data. Successful acquisition of this data, in conjunction with other characterization analyses, provides important information that can be used in the myriad of potential radioactive waste management alternatives.
NTIS
*Light Scattering; Particle Size Distribution; Radioactivity; Laser Beams; Measuring Instruments*

**20010125406** Argonne National Lab., IL USA
**Nonlinear harmonic generation and proposed experimental verification in SASE FELs**
Biedron, S. G.; Freund, H. P.; Milton, S. V.; Aug. 24, 1999; 20p; In English
Report No.(s): DE2001-11802; ANL/ASD/CP-98998; No Copyright; Avail: Department of Energy Information Bridge
Recently, a 3D, polychromatic, nonlinear simulation code was developed to study the growth of nonlinear harmonics in self-amplified spontaneous emission (SASE) free-electron lasers (FELs). The simulation was applied to the parameters for each stage of the Advanced Photon Source (APS) SASE FEL, intended for operation in the visible, UV, and short UV wavelength regimes, respectively, to study the presence of nonlinear harmonic generation. Significant nonlinear harmonic growth is seen. Here, a discussion of the code development, the APS SASE FEL, the simulations and results, and, finally, the proposed experimental procedure for verification of such nonlinear harmonic generation at the APS SASE FEL will be given.
NTIS
*Harmonic Generations; Computerized Simulation; Spontaneous Emission; Free Electron Lasers*

**20010125407** Argonne National Lab., IL USA
**Parameter analysis for a high-gain harmonic generation FEL using a recently developed 3D polychromatic code**
Biedron, S. G.; Freund, H. P.; Yu, L. H.; Sep. 10, 1999; 21p; In English
Report No.(s): DE2001-11800; ANL/ASD/CP-98996; No Copyright; Avail: Department of Energy Information Bridge
One possible design for a fourth-generation light source is the high-gain harmonic generation (HGHG) free-electron laser (FEL). Here, a coherent seed with a wavelength at a subharmonic of the desired output radiation interacts with the electron beam in an energy-modulating section. This energy modulation is then converted into spatial bunching while traversing a dispersive section (a three-dipole chicane). The final step is passage through a radiative section, an undulator tuned to the desired higher harmonic output wavelength. The coherent seed serves to remove noise and can be at a much lower subharmonic of the output radiation, thus eliminating the concerns found in self-amplified spontaneous emission (SASE) and seeded FELs, respectively. Recently, a 3D code that includes multiple frequencies, multiple undulatory (both in quantity and/or type), quadruple magnets, and dipole magnets was developed to easily simulate HGHG. Here, a brief review of the HGHG theory, the code development,

the Accelerator Test Facility's (ATF) HGHG FEL experimental parameters, and the parameter analysis from simulations of this specific experiment will be discussed.
NTIS
*Free Electron Lasers; High Gain; Harmonic Generations; Light Sources*

**20010125417** Argonne National Lab., IL USA
**Vacuum chambers for the VUV SASE FEL at the TESLA test facility (TFF FEL) at DESY**
Den Hartog, P. K.; Erdmann, M.; Hahn, U.; Pfluger, J.; Ruter, M.; Apr. 20, 1999; 6p; In English
Report No.(s): DE2001-11760; ANL/XFD/CP-98792; No Copyright; Avail: Department of Energy Information Bridge, Microfiche

A vacuum chamber for the VUV (Vacuum ultraviolet) SASE (self-amplified spontaneous emission) FEL (free-electron laser) undulatory at the TESLA Test Facility (TTF) was designed, a prototype was built and tested, and seven complete chambers were manufactured. The chambers use the aluminum extrusion technology developed for the insertion device vacuum chambers of the Advanced Photon Source. Each chamber is 4.5 m long with a beam aperture of 9.5 mm and an external thickness of 11.5 mm. Three of the chambers include ports for integral beam position monitors (10 horizontal and vertical pairs) inserted into the chambers, and all of the chambers include grooves for mounting correction coils. Bimetallic flanges (stainless steel to aluminum) are welded to the ends of the chamber for connection to the beamline. Special processing was performed to meet the stringent vacuum and particle-free requirements of the TTF.
NTIS
*Vacuum Systems; Free Electron Lasers*

**20010125428** Brookhaven National Lab., Upton, NY USA
**Developments in synchrotron x-ray computed microtomography at the national synchrotron light source**
Dowd,; Jul. 23, 1999; 15p; In English
Report No.(s): DE2001-11723; BNL-66660; No Copyright; Avail: Department of Energy Information Bridge, Microfiche

Last year, the X27A beamline at the National Synchrotron Light Source (NSLS) became dedicated solely to X-Ray Computed Microtomography (XCMT). This is a third-generation instrument capable of producing tomographic volumes of 1-2 micron resolution over a 2-3mm field of view. Recent enhancements will be discussed. These have focused on two issues: the desire for real-time data acquisition and processing and the need for highly monochromatic beam (.1 % energy bandpass). The latter will permit k-edge subtraction studies and will provide improved image contrast from below the Cr (6 keV) up to the Cs (36 keV) k-edge. A range of applications that benefit from these improvements will be discussed as well. These two goals are somewhat counterproductive, however; higher monochromaticity yields a lower flux forcing longer data acquisition times. to balance the two, a more efficient scintillator for X-ray conversion is being developed. Some testing of a prototype scintillator has been performed; preliminary results will be presented here. In the meantime, data reconstruction times have been reduced, and the entire tomographic acquisition, reconstruction and volume rendering process streamlined to make efficient use of synchrotron beam time. A Fast Filtered Back Transform (FFBT) reconstruction program recently developed helped to reduce the time to reconstruct a volume of 150 x 150 x 250 pixels(sup 3) (over 5 million voxels) from the raw camera data to 1.5 minutes on a dual R10,000 CPU. With these improvements, one can now obtain a 'quick look' of a small tomographic volume ((approximately)10(sup 6)voxels) in just over 15 minutes from the start of data acquisition.
NTIS
*Computer Aided Tomography; Synchrotrons; X Ray Analysis; Light Sources; Monochromators*

**20010125447** Lawrence Livermore National Lab., Livermore, CA USA
**Automated damage test facilities for materials development and production optic quality assurance at Lawrence Livermore National Laboratory**
Battersby, C.; Dickson, R.; Jennings, R.; Kimmons, J.; Kozlowski, M. R.; Dec. 22, 1998; 14p; In English
Report No.(s): DE2001-8360; UCRL-JC-131230; DP0212000; No Copyright; Avail: Department of Energy Information Bridge, Microfiche

The Laser Program at LLNL (Lawrence Livermore National Laboratory) has developed automated facilities for damage testing optics up to 1 meter in diameter. The systems were developed to characterize the statistical distribution of localized damage performance across large-aperture National Ignition Facility optics. Full aperture testing is a key component of the quality assurance program for several of the optical components. The primary damage testing methods used are R:1 mapping and raster

scanning. Automation of these test methods was required to meet the optics manufacturing schedule. The automated activities include control and diagnosis of the damage-test laser beam as well as detection and characterization of damage events.
NTIS
*Optical Equipment; Laser Damage; Automatic Test Equipment; Test Facilities*

**20010125448** Lawrence Livermore National Lab., Livermore, CA USA
**Effects of wet etch processing on laser-induced damage of fused silica surfaces**
Battersby, C. L.; Kozlowski, M. R.; Sheehan, L. M.; Dec. 22, 1998; 12p; In English
Report No.(s): DE2001-8359; UCRL-JC-131224; DP0212000; No Copyright; Avail: Department of Energy Information Bridge, Microfiche

Laser-induced damage of transparent fused silica optical components by 355 nm illumination occurs primarily at surface defects produced during the grinding and polishing processes. These defects can either be surface defects or sub-surface damage. Wet etch processing in a buffered hydrogen fluoride (HF) solution has been examined as a tool for characterizing such defects. A study was conducted to understand the effects of etch depth on the damage threshold of fused silica substrates. The study used a 355 nm, 7.5 ns, 10 Hz Nd:YAG laser to damage test fused silica optics through various wet etch processing steps. Inspection of the surface quality was performed with Nomarski microscopy and Total Internal Reflection Microscopy. The damage test data and inspection results were correlated with polishing process specifics. The results show that a wet etch exposes subsurface damage while maintaining or improving the laser damage performance. The benefits of a wet etch must be evaluated for each polishing process.
NTIS
*Laser Damage; Silicon Dioxide; Etching; Optical Equipment; Destructive Tests*

**20010125449** Lawrence Livermore National Lab., Livermore, CA USA
**Extrapolation of damage test data to predict performance of large-area NIF optics at 355 nm**
Schwartz, S.; Feit, M. D.; Genin, F. Y.; Kozlowski, M. R.; Rubenchik, A. M.; Dec. 22, 1998; 10p; In English
Report No.(s): DE2001-8358; UCRL-JC-131222; DP0212000; No Copyright; Avail: Department of Energy Information Bridge, Microfiche

For the aggressive fluence requirements of the NIF (National Ignition Facility) laser, some level of laser-induced damage to the large (40 x 40 cm) 351 nm final optics is inevitable. Planning and utilization of NIF therefore requires reliable prediction of the functional degradation of the final optics. Laser damage tests are typically carried out with Gaussian beams on relatively small test areas. The tests yield a damage probability vs. energy fluence relation. These damage probabilities are shown to depend on both the beam fluence distribution and the size of area tested. Thus, some analysis is necessary in order to use these test results to determine expected damage levels for large aperture optics. The authors present a statistical approach which interprets the damage probability in terms of an underlying intrinsic surface density of damaging defects. This allows extrapolation of test results to different sized areas and different beam shapes (NIF has a flattop beam). The defect density is found to vary as a power of the fluence (Weibull distribution).
NTIS
*Lasers; Optical Equipment; Laser Damage; Probability Theory; Statistical Analysis*

**20010125450** Lawrence Livermore National Lab., Livermore, CA USA
**Single-beam photothermal microscopy: a new diagnostic tool for optical materials**
Feit, M. D.; Kozlowski, M.; Natoli, J. Y.; Rubenchik, A. M.; Sheehan, L.; Dec. 22, 1998; 12p; In English
Report No.(s): DE2001-8354; UCRL-JC-131212; DP0212000; No Copyright; Avail: Department of Energy Information Bridge, Microfiche

A novel photothermal microscopy (PTM) is developed which uses only one laser beam, working as both the pump and the probe. The principle of this single-beam PTM is based on the detection of the second harmonic component of the laser modulated scattering (LMS) signal. This component has a linear dependence on the optical absorptance of the tested area and a quadratic dependence on the pump laser power. Using a pump laser at the wavelengths of 514.5 and 532 nm, high-resolution photothermal scans are performed for polished fused silica surfaces and HfO(sub 2)/SiO(sub 2) multilayer coatings. The results are compared with those from traditional two-beam PTM mapping. It is demonstrated that the single-beam PTM is more user-friendly (i.e. no alignment is needed) than conventional two-beam PTM, and offers a higher spatial resolution for defect detection.
NTIS
*Laser Beams; Microscopy; Laser Pumping*

**20010125452** Lawrence Livermore National Lab., Livermore, CA USA

**Interaction of plasmas with intense lasers**

Kruer, W.; Apr. 30, 1999; 35p; In English

Report No.(s): DE2001-8350; UCRL-JC-132222; DP0210000; No Copyright; Avail: Department of Energy Information Bridge, Microfiche

The interaction of plasmas with intense lasers is an excellent example of how different fields of physics are inter-connected. Invention of the laser and its ongoing development has allowed the creation and study of high temperature, dense matter in the laboratory. The results both advance the underlying plasma science and are relevant to many fields ranging from astrophysics to fusion and nonlinear physics. A brief overview of the interaction physics is given. Selected topics are discussed to illustrate the exciting progress in experimental, theoretical and computational investigations with focused laser intensities up to 10(sup 21) W/cm(sup 2).

NTIS

*Lasers; Plasmas (Physics); Laser Plasma Interactions*

**20010125459** Kansas City Plant, Kansas City, MO USA

**Flyer Velocity Characteristics of the Laser-Driven Miniflyer System**

Gehr, R. J.; Harper, R. W.; Robbins, D. L.; Rupp, T. D.; Sheffield, S. A.; Jul. 01, 1999; 7p; In English

Report No.(s): DE2001-8283; KCP-613-6209; No Copyright; Avail: Department of Energy Information Bridge, Microfiche

The laser-driven MiniFlyer system is used to launch a small, thin flyer plate for impact on a target. Consequently, it is an indirect drive technique that de-couples the shock from the laser beam profile. The flyer velocity can be controlled by adjustment of the laser energy. The upper limits on the flyer velocity involve the ability of the substrate window to transmit the laser light without absorbing, reflecting, etc.; i.e., a maximum amount of laser energy is directly converted into kinetic energy of the flyer plate. We have investigated the use of sapphire, quartz, and BK-7 glass as substrate windows. In the past, a particular type of sapphire has been used for nearly all MiniFlyer experiments. Results of this study in terms of the performance of these window materials, based on flyer velocity, are discussed.

NTIS

*Lasers; Laser Applications; Launchers; Laser Propulsion; Velocity; Thin Plates; Materials Selection*

**20010125503** Thomas Jefferson National Accelerator Facility, Newport News, VA USA

**Diagnostics for Ultrashort Bunches**

Krafft, G. A.; Dec. 01, 1997; 5p; In English

Report No.(s): DE2001-769179; JLAB-ACP-97-11; DOE/ER/40150-1785; No Copyright; Avail: Department of Energy Information Bridge, Microfiche

Recently, producing and maintaining short bunches in accelerators has become a forefront issue. Examples of accelerators that require short bunches are high quality nuclear physics accelerators, free electron laser driver accelerators, next generation linear colliders, and linac-based fourth generation light sources. Large bodies of work have accumulated at various sites on producing, measuring, and maintaining ultrashort bunches. In this paper such work is reviewed, with particular emphasis placed on diagnostic techniques that may be applied in the subpicosecond rms bunch duration domain. Instrumentation based on both time domain and frequency domain methods are discussed: in the frequency domain and coherent radiation detection techniques in the far infrared receive special emphasis. In addition to the usual problem of measuring the bunch longitudinal distribution function, it is also important to have efficient ways to control the bunch length in short bunch machines. Solving this problem involves instruments with somewhat different properties than the standard ones. Consequently, some space is devoted to several devices, both in use and proposed, that are useful in the problem of controlling ultrashort bunches.

NTIS

*Electron Accelerators; Free Electron Lasers; Frequency Domain Analysis*

**20010125598** Argonne National Lab., IL USA

**First lasing of a high-gain harmonic generation free-electron laser experiment**

Babzien, M.; Ben-Zvi, I.; Biedron, S. G.; DiMauro, L. F.; Douryan, A.; Sep. 11, 1999; 25p; In English

Report No.(s): DE2001-11801; ANL/ASD/CP-98997; No Copyright; Avail: Department of Energy Information Bridge

We report on the first lasing of a high-gain harmonic generation (HGHG) free-electron laser (FEL). The experiment was conducted at the Accelerator Test Facility (ATF) at Brookhaven National Laboratory (BNL). This is a BNL experiment in collaboration with the Advanced Photon Source (APS) at Argonne National Laboratory. A preliminary measurement gives a high-gain harmonic generation (HGHG) pulse energy that is 2 x 10(exp 7) times larger than the spontaneous radiation, In a purely

self-amplified spontaneous emission (SASE) mode of operation, the signal was measured as 10 times larger than the spontaneous radiation in the same distance (approximately 2 m) through the same wiggler. This means the HGHG signal is 2 x 10(exp 6) times larger than the SASE signal. To obtain the same saturated output power by the SASE process, the radiator would have to be 3 times longer (6 m).
NTIS
*Lasing; Free Electron Lasers; Harmonic Generations*

**20010125603** Bechtel Nevada Corp., Las Vegas, NV USA
**Photonic Power Delivery Through Optical Fiber Using Very High Power Laser Diode Arrays**
Heino, M.; Jun. 01, 1999; 6p; In English
Report No.(s): DE2001-8270; DOE/NV/11718-281; No Copyright; Avail: Department of Energy Information Bridge, Microfiche

Described is a system that will provide isolated electric power for a circuit that drives the core reset of a pulsed power modulator. This can be accomplished by coupling light from a number of diode laser bars to bundles of 200 (micro)m multimode optical fibers. This is then coupled to photo-voltaic power converters that will deliver 16V 29mA of electricity from 1 watt of optical power. Spot size at the bundle face is a Gaussian ellipse with a major axis of 0.9 mm radius and a minor axis of 0.118mm with a maximum full angle divergence of 16 X 2.4 degrees. Data is presented from four 20W laser bars coupled to four bundles of 12 fibers generating a total of 24W of electric power. Various schemes are used to maximize coupling into the optical fiber while limiting the number of optical components, and comparing components such as fresnel and aspheric lenses and lens ducts for effectiveness and cost. This will provide a completely isolated low power source for high voltage, high current environments where traditional isolation techniques yield inadequate isolation or prove too cumbersome.
NTIS
*Laser Beams; Laser Power Beaming; Systems Engineering*

## 75
## PLASMA PHYSICS

*Includes magnetohydrodynamics and plasma fusion. For ionospheric plasmas see 46 Geophysics. For space plasmas see 90 Astrophysics.*

**20010117863** Eloret Corp., Palo Alto, CA USA
**Collisional-Radiative Nonequilibrium and Precursor Effects in a Nitrogen Shock Wave**
Cambier, Jean-Luc, Eloret Corp., USA; [1994]; 1p; In English; 26th AIAA Plasmadynamics and Lasers Conference, 19-22 Jun. 1995, San Diego, CA, USA; Sponsored by American Inst. of Aeronautics and Astronautics, USA
Contract(s)/Grant(s): RTOP 232-01-04; No Copyright; Avail: Issuing Activity; Abstract Only

Improvements to a plasma code with a Collisional-Radiative (CR) non-equilibrium model are made, allowing for a more accurate description of the physical processes. The code allows for non-Boltzmann distributions of the electronic excited states by convecting separately each excited state, as a pseudo-specie. Each molecular state has also its own vibrational temperature, while a global rotational temperature is assumed. The free electron temperature is different from those of the excited states, and the electron heat conduction is also included. The CR model also uses a unique coupling between chemistry and vibrational energy (C-V coupling), which is fully coherent, and has the property of establishing thermal equilibrium as well as chemical equilibrium, on its own. We have also included a coupling between electronic excitations and vibrational energy (X-V coupling), which can have a strong influence on the vibrational temperature of some states. The recent improvements include the multi- temperature dependence of the chemical rates for associative ionization, as well as the estimation of the internal energies transferred during this process. Additionally, the distribution of energy into different translational modes (electron and heavy particles) is now correctly modeled. This provides a very rapid heating mechanism for the free electrons, since it is found that the electrons are generated with an average thermal energy of the same order as the heavy particle translational energy. This effect was observed by Gorelov et al in a recent paper, and lead to pronounced peaks in electron temperature immediately behind the shock. We will attempt ro reproduce this phenomenon. The last modification concerns the inclusion of the radiative terms into the calculations, thus enabling us to observe the effect of radiative losses and radiation transport. Preliminary tests have shown that the radiative losses are not negligible, i.e. the shock velocity drops when the radiative emission is included. In addition, we have observed some precursor excitation and ionization phenomena. These may be important at high shock velocities, and this will be investigated

in detail. Precursor phenomena were also observed (in air) by Gorelov et al, and our results (for pure nitrogen) will be qualitatively compared with theirs.
Author
*Nitrogen; Shock Waves; Electron States; Electron Energy; Excitation; Plasmas (Physics)*

**20010118930** Sandia National Labs., Albuquerque, NM USA
**Design of the PST: A Diagnostic for 1-D Imaging of Fast Z-Pinch Power Emissions**
Rochau, G. A.; Derzon, M. S.; Chandler, G. A.; Lazier, S. E.; Aug. 03, 2000; 11p; In English
Report No.(s): DE2000-761847; SAND2000-1960C; No Copyright; Avail: Department of Energy Information Bridge

Fast Z-pinch technology developed on the Z machine at Sandia National Laboratories can produce up to 230 TW of thermal x-ray power for applications in inertial confinement fusion (ICF) and weapons physics experiments. During implosion, these Z-pinches develop Rayleigh-Taylor (R-T) instabilities which are very difficult to diagnose and which functionally diminish the overall pinch quality. The Power-Space-Time (PST) instrument is a newly configured diagnostic for measuring the pinch power as a function of both space and time in a Z-pinch. Placing the diagnostic at 90 degrees from the Z-pinch axis, the PST provides a new capability in collecting experimental data on R-T characteristics for making meaningful comparisons to magneto-hydrodynamic computer models. This paper is a summary of the PST diagnostic design. by slit-imaging the Z-pinch x-ray emissions onto a linear scintillator/fiber-optic array coupled to a streak camera system, the PST can achieve (approximately)100 (micro)m spatial resolution and (approximately)1.3 ns time resolution. Calculations indicate that a 20 (micro)m thick scintillating detection element filtered by 1,000 (angstrom) of Al is theoretically linear in response to Plankian x-ray distributions corresponding to plasma temperatures from 40 eV to 150 eV, by calibrating this detection element to x-ray energies up to 5,000 eV, the PST can provide pinch power as a function of height and time in a Z-pinch for temperatures ranging from (approximately)40 eV to (approximately)400 eV. With these system pm-meters, the PST can provide data for an experimental determination of the R-T mode number, amplitude, and growth rate during the late-time pinch implosion.
NTIS
*Imaging Techniques; Zeta Pinch; Computerized Simulation; X Ray Imagery*

**20010119194** Princeton Univ., Plasma Physics Lab., NJ USA
**Princeton Plasma Physics Laboratory Annual Site Environmental Report for Calendar Year 1998**
Finley, V.; Mar. 06, 2000; 100p; In English
Report No.(s): DE2000-753854; PPPL-3440; No Copyright; Avail: Department of Energy Information Bridge

The results of the 1998 environmental surveillance and monitoring program for the Princeton Plasma Physics Laboratory (PPPL) are presented and discussed. The purpose of this report is to provide the US Department of Energy and the public with information on the level of radioactive and non-radioactive pollutants, if any, that are added to the environment as a result of PPPL's operations. The report also summarizes environmental initiatives, assessments, and programs that were undertaken in 1998. One significant initiative is the Integrated Safety Management (ISM) program that embraces environment, safety, and health principles as one.
NTIS
*Plasma Physics; Environmental Monitoring; Health Physics; Contaminants*

**20010119421** Brookhaven National Lab., Upton, NY USA
**Possible Striking Signals for a Quark-Gluon Plasma at RHIC**
Lindenbaum, S. J.; Dec. 01, 1999; 31p; In English
Report No.(s): DE2000-750782; BNL-52580; No Copyright; Avail: Department of Energy Information Bridge

We believe that one can have serious reservations as to whether heavy ion collisions can lead to thermal and chemical equilibrium over large regions (particularly if it is assumed this happens whenever quark-gluon plasma (QGP) is produced at RHIC, that is, if it is produced). It is at present not clear that the collision dynamics and times available will lead to this. An alternate scenario proposed by Van Hove where localized in rapidity bubbles of plasma may well be more probable, and may well occur at least some of the time, and some of the time mainly survive to the final state. If this occurs we have developed a series of reasonable event generators to extend and describe these phenomena. They predict (with reasonable assumption) Striking Signals which may allow strong evidence for a QGP which cannot be explained by alternative conventional physical arguments, and thus may be crucial elements in establishing a QGP. We are also applying these techniques to investigating Kharzeev and Pisarski bubbles of metastable vacua with odd CP.
NTIS
*Gluons; Ionic Collisions; Quarks; Particle Interactions*

**20010119435** Oak Ridge National Lab., TN USA

**Production and Innovative Applications of Cryogenic Solid Pellets**

Baylor, L. R.; Combs, S. K.; Fisher, P. W.; Foster, C. A.; Foust, C. R.; Jul. 12, 1999; 10p; In English

Report No.(s): DE2000-15056; ORNL/CP-105101; No Copyright; Avail: Department of Energy Information Bridge, Microfiche

For over two decades Oak Ridge National Laboratory has been developing cryogenic pellet injectors for fueling hot, magnetic fusion plasmas. Cryogenic solid pellets of all three hydrogen isotopes have been produced in a size range of 1 to 10 mm diameter and accelerated to speeds from 100 to approximately 3000 m/s. The pellets have been formed discretely by cryocondensation in gun barrels and also by extrusion of cryogenic solids at mass flow rates up to approximately 0.26 g/s and production rates up to ten pellets per second. The pellets traverse the hot plasma in a fraction of a millisecond and continuously ablate, providing fresh hydrogenic fuel to the interior of the plasma. From this initial application, uses of this technology have expanded to include: (1) cryogenic xenon drops or solids for use as a debris-less target in a laser plasma source of x-rays for advanced lithography systems; (2) solid argon and carbon dioxide pellets for surface cleaning or decontamination; and (3) methane pellets in a liquid hydrogen bath for use as an innovative moderator of cold neutrons. Methods of production and acceleration transport of these cryogenic solids will be described, and examples will be given of their use in prototype systems.

NTIS

*Cryogenics; Pellets; High Temperature Plasmas*

**20010120018** Princeton Univ., Plasma Physics Lab., NJ USA

**In-situ Tritium Measurements of the Tokamak Fusion Test Reactor Bumper Limiter Tiles Post D-T Operations**

Gentile, C. A.; Skinner, C. H.; Young, K. M.; Nishi, M.; Langish, S.; Sep. 01, 1999; 6p; In English

Report No.(s): DE2001-10662; PPPL-3355; No Copyright; Avail: Department of Energy Information Bridge

The Princeton Plasma Physics Laboratory (PPPL) Engineering and Research Staff in collaboration with members of the Japan Atomic Energy Research Institute (JAERI), Tritium Engineering Laboratory have commenced in-situ tritium measurements of the TFTR bumper limiter. The Tokamak Fusion Test Reactor (TFTR) operated with tritium from 1993 to 1997. During this time (approximately) 53,000 Ci of tritium was injected into the TFTR vacuum vessel. After the cessation of TFTR plasma operations in April 1997 an aggressive tritium cleanup campaign lasting (approximately) 3 months was initiated. The TFTR vacuum vessel was subjected to a regimen of glow discharge cleaning (GDC) and dry nitrogen and 'moist air' purges. Currently (approximately) 7,500 Ci of tritium remains in the vacuum vessel largely contained in the limiter tiles. The TFTR limiter is composed of 1,920 carbon tiles with an average weight of (approximately) 600 grams each. The location and distribution of tritium on the TFTR carbon tiles are of considerable interest. Future magnetically confined fusion devices employing carbon as a limiter material may be considerably constrained due to potentially large tritium inventories being tenaciously held on the surface of the tiles. In-situ tritium measurements were conducted in TFTR bay L during August and November 1998. During the bay L measurement campaign open wall ion chambers and ultra thin thermoluminescent dosimeters (TLD) affixed to a boom and end effector were deployed into the vacuum vessel. The detectors were designed to make contact with the surface of the bumper limiter tile and to provide either real time (ion chamber) or passive (TLD) indication of the surface tritium concentration. The open wall ion chambers were positioned onto the surface of the tile in a manner which employed the surface of the tile as one of the walls of the chamber. The ion chambers, which are (electrically) gamma insensitive, were landed at four positions per tile. The geometry for landing the TLD's provided measurement at 24 positions per tile. The instrumentation was positioned on the tiles (96 tiles in each bay) by technicians who manipulated the boom and end effector from outside the vacuum vessel port. In addition to obtaining bay L tile measurements, 3 bumper limiter tiles were collected from the vacuum vessel for further analysis. During the bay L measurement campaign it was observed that several of the tiles in the lower third of the bumper limiter exhibited considerable surface flaking.

NTIS

*Energy Technology; In Situ Measurement; Thermoluminescence; Tokamak Devices; Tritium; Cushions*

**20010120063** Sandia National Labs., Albuquerque, NM USA

**Techniques for Equation-of-State Measurements on a Three-Stage Light-Gas Gun**

Reinhart,; Chhabildas,; Thornhill,; Sep. 14, 2000; 14p; In English

Report No.(s): DE2000-763102; SAND2000-2269C; No Copyright; Avail: Department of Energy Information Bridge, Microfiche

Understanding high pressure behavior materials is necessary in order to address the physical processes associated with hypervelocity impact events related to space science applications including orbital debris impact and impact lethality. Until recently the highest-pressure states in materials have been achieved from impact loading techniques from two-stage light gas guns with velocity limitations of approximately 81 cm/s. In this paper, techniques that are being developed and implemented to obtain

the needed shock loading parameters (Hugoniot states) for material characterization studies, namely shock velocity and particle velocity, will be described at impact velocities up to 11 kds. The determination of equation-of-state (EOS) and thermodynamic states of materials in the regimes of extreme high pressures is now attainable utilizing the three-stage launcher. What is new in this report is that these techniques are being implemented for use at engagement velocities never before attained utilizing two-stage light-gas gun technology. The design and test methodologies used to determine Hugoniot states are described in this paper.
NTIS
*Light Gas Guns; Hypervelocity Impact*

**20010120542** Argonne National Lab., IL USA
**Performance and lifetime assessment of reactor wall and nearby components during plasma instabilities**
Hassanein, A.; Mar. 10, 1998; 29p; In English
Report No.(s): DE2001-10680; ANL/TD/CP-95857; No Copyright; Avail: Department of Energy Information Bridge

Surface and structural damage to plasma-facing components due to the frequent loss of plasma confinement is a serious problem for the tokamak reactor concept. The plasma energy deposited on these components during loss of confinement causes significant surface erosion, possible structural failure, and frequent plasma contamination. Surface damage consists of vaporization, spallation, and liquid splatter of metallic materials. Comprehensive multidimensional models that include thermodynamics and thermal hydraulics of plasma-facing materials, eroded-debris/vapor atomic physics and magnetohydrodynamics, resulting photon radiation and photon transport, as well as liquid splashing and brittle destruction of materials, are used self-consistently to evaluate and assess our current understanding of the lifetime of plasma-facing materials and the various forms of damage they experience. Models are developed to study the stability of the vapor shielding layer, erosion of the melt-layer, brittle destruction/explosive erosion, and the issues involved therein.
NTIS
*Plasmas (Physics); Magnetohydrodynamic Stability; Tokamak Devices; Service Life; Reactor Materials*

**20010121500** Sandia National Labs., Albuquerque, NM USA
**NIF Total Neutron Yield Diagnostic**
Cooper, G. W.; Ruiz, C. L.; Jun. 15, 2000; 12p; In English
Report No.(s): DE2000-760767; SAND2000-0723C; No Copyright; Avail: Department of Energy Information Bridge, Microfiche

We have designed a total neutron yield diagnostic for NIF (National Ignition Facility) which is based on the activation of In and Cu samples. The particular approach that we have chosen to use is the calibration factor method in which we calibrate the entire counting system. In this method, In and/or Cu samples are exposed to known sources of DD and DT neutrons. The activated samples are then counted with the appropriate system, an HPGe detector for In and a NaI coincidence system for Cu. We can then calculate a calibration factor, which relates measured activity to total neutron yield. The advantage of this approach is that specific knowledge of such factors as cross sections and detector efficiencies are not needed. The disadvantage is that it may be difficult to mock-up in a calibration experiment the actual scattering environment of NIF. As a result, the experimentally obtained calibration factor may have to be modified using the results of a numerical simulation of the scattering environment. In this paper, the calibration factor methodology will be discussed and experimental results for the calibration factors will be presented.
NTIS
*Neutrons; Scattering; Calibrating*

**20010121502** Sandia National Labs., Albuquerque, NM USA
**X-Ray Imaging Techniques on Z using the Z-Beamlet Laser Backlighter System**
Bennett, G. R.; Porter, J. L.; Ruggles, L. E.; Simpson, W. W.; Wakefield, C.; Jul. 20, 2000; 21p; In English
Report No.(s): DE2000-760765; SAND2000-0621C; No Copyright; Avail: Department of Energy Information Bridge, Microfiche

The Z-Beamlet Laser Backlighter System at Sandia National Laboratories, which will be operational in 2001, will create a point- or area-source of high (or moderate) energy x-rays behind a Z-accelerator. This high-energy source, as either a single point or four separate spots, will be used directly for four-frame point projection x-ray imaging, and will attain spatial resolutions and signal-to-noise levels significantly better than presently possible on Z using existing methods, In combination with a - 1 cm field-of-view, the technique will be well suited to the large, relatively opaque objects characteristic of Z experiments. This addition is anticipated to have a major impact upon the basic physics of z-pinch implosions, and therefore possibly the ultimate x-ray powers and hohlraum (vacuum or dynamic) radiation temperatures that may be attainable. Furthermore, in combination with a

slightly defocused point source and a medium energy grazing incidence microscope, Z-Beamlet may allow various inertial confinement fusion and high energy density physics experiments to be studied at even higher spatial resolution and signal-to-noise levels.
NTIS
*Lasers; Plasma Diagnostics; Point Sources; X Rays*

**20010121957** Princeton Univ., Plasma Physics Lab., NJ USA
**Cosmic Ray Pitch Angle Scattering Through 90(degree)**
Kulsrud, R. M.; Felice, G. M.; Sep. 19, 2000; 48p; In English
Report No.(s): DE2000-764465; PPPL-3488; No Copyright; Avail: Department of Energy Information Bridge, Microfiche

The authors study the problem of cosmic ray diffusion in the galactic disk with particular attention to the problem of particle scattering through the (theta) = cos(sup (minus)1))((nu)(sub (parallel))/(nu) = 90(degree) pitch angle in momentum space by wave-particle mirror interaction here (nu)(sub (parallel)) is the cosmic ray velocity parallel to the average galactic magnetic field). They consider the case in which cosmic rays are the only source of magnetic turbulence, which originates as the relativistic particles try to stream through the interstellar plasma faster than the local Alfven speed. The wave growth rate is proportional to the cosmic ray anisotropy and the amplitude of hydro-magnetic waves generated by this streaming instability is limited by the presence of various damping mechanisms. They study the propagation of cosmic rays in the different phases of the I.S.M., in particular the coronal regions (where the main form of wave dissipation is non-linear Landau damping) and the warm regions (where charge exchange between the ions and the neutral atoms gives rise to the dominant form of wave dissipation). They also account for ion-cyclotron damping of small wavelength waves. The effect of a spectrum of waves is to limit the anisotropy of the cosmic ray distribution function, and hence to limit their drift velocity. They show that quasi-linear resonant scattering cannot account for particle diffusion everywhere in momentum space, and that particles with (theta) (approximately) 90 degrees must change their pitch angle by mirror interaction with long wavelength waves generated by the (theta) (approximately) 0 particles. The authors match the quasi-linear scattering with the adiabatic mirroring in a small boundary layer in momentum space close to the (theta) (approximately) 90 degree point and then they calculate the diffusion coefficient together with the cosmic ray drift velocity. They show that scattering through the 90 degree point is very efficient and they calculate the correction to the particle diffusion coefficient due to the presence of mirroring.
NTIS
*Cosmic Rays; Scattering; Wave-Particle Interactions; Angular Distribution*

**20010122253** Argonne National Lab., IL USA
**Erosion/redeposition analysis: status of modeling and code validation for semi-detached tokamak edge plasmas**
Brooks, J. N.; Jan. 19, 1999; 27p; In English
Report No.(s): DE2001-10811; ANL/TD/CP-96490; No Copyright; Avail: Department of Energy Information Bridge, Microfiche

We are analyzing erosion and tritium codeposition for ITER, DIII-D, and other devices with a focus on carbon divertor and metallic wall sputtering, for detached and semi-detached edge plasmas. Carbon chemical-sputtering hydrocarbon-transport is computed in detail using upgraded models for sputtering yields, species, and atomic and molecular processes. For the DIII-D analysis this includes proton impact and dissociative recombination for the full methane and higher hydrocarbon chains. Several mixed material (Si-C doping and Be/C) effects on erosion are examined. A semi-detached reactor plasma regime yields peak net wall erosion rates of (approximately)1.0 (Be), (approximately)0.3 (Fe), and (approximately)0.01 (W) cm/burn-yr, and (approximately)50 cm/burn-yr for a carbon divertor. Net carbon erosion is dominated by chemical sputtering in the (approximately)1-3 eV detached plasma zone. Tritium codeposition in divertor-sputtered redeposited carbon is high ((approximately)10-20 g-T/1000 s ). Silicon and beryllium mixing tends to reduce carbon erosion. Initial hydrocarbon transport calculations for the DIII-D DiMES-73 detached plasma experiment show a broad spectrum of redeposited molecules with (approximately)90% redeposition fraction.
NTIS
*Plasmas (Physics); Tokamak Devices; Sputtering; Diverters; Deposition; Erosion*

**20010122267** Lawrence Livermore National Lab., Livermore, CA USA
**Laser Glass: A Key Material in the Search for Fusion Energy**
Campbell, J. H.; Jun. 02, 1999; 20p; In English
Report No.(s): DE2001-10784; UCRL-JC-134385; No Copyright; Avail: Department of Energy Information Bridge, Microfiche

Nuclear fusion is the energy source that powers the sun. For more than four decades man has sought to develop this essentially inexhaustible, clean power source for use on Earth. Unfortunately the conditions needed to initiate fusion are daunting; the nuclear

fuel, consisting of isotopes of hydrogen, must be heated to temperatures in excess of 100,000,000 C and maintained at that temperature long enough for the nuclear fuel to ignite and burn. Lasers are being used as one of the tools to achieve these conditions. The best lasers for this work are those that derive their energy from a unique set of optical glasses called laser glasses. The work to develop, manufacture, and test these glasses has involved a partnership between university and industry that has spanned more than 25 years. During this time lasers used in fusion development have grown from small systems that could fit on the top of a table to systems currently under construction that are approximately the size of a municipal sports stadium. A brief historical and anecdotal account of the development of laser glasses for fusion energy research applications is the subject of the presentation.
NTIS
*Glass; Nuclear Fusion; Laser Materials*

**20010122650** Sandia National Labs., Albuquerque, NM USA
**DD Neutron Yield Measurements on Z Using Lead Probes**
Gerken, E. S.; Aug. 09, 2000; 11p; In English
Report No.(s): DE2000-761862; SAND2000-2030C; No Copyright; Avail: Department of Energy Information Bridge, Microfiche

A series of inertial confinement fusion (ICF) capsule experiments were run on the Z machine at Sandia's Pulsed Power directorate. These experiments were designed specifically to implode a 2 mm diameter hollow plastic capsule filled with deuterium gas. The implosion of the capsule should raise the temperature (kinetic energy) of the deuterium gas ions, which will interact with each other and produce 2.45 MeV fusion neutrons. The author is reporting on one diagnostic technique used to measure the yield of these fusion neutrons. The technique chosen to measure the DD neutron yield is the use of lead (Pb) probe detectors. The assignment was to calibrate two detectors for the 2.50-MeV neutrons produced by the deuterium-deuterium fusion reactions on Z. The author introduces ICF, and then describes the theory, the design, and the calibration of the lead probe. Finally, she presents the results of the ICF experiments and explains the difficulties inherent in analyzing the data.
NTIS
*Zeta Pinch; Inertial Confinement Fusion; Plasma Diagnostics; Implosions*

**20010122833** Princeton Univ., Plasma Physics Lab., NJ USA
**Shear-Alfven Waves in Gyrokinetic Plasmas**
Lee, W. W.; Lewandowski, J. L. V.; Hahm, T. S.; Lin, Z.; Oct. 18, 2000; 14p; In English
Report No.(s): DE2000-765443; PPPL-3495; No Copyright; Avail: Department of Energy Information Bridge, Microfiche

It is found that the thermal fluctuation level of the shear-Alfven waves in a gyrokinetic plasma decreases with plasma b(* cs2/uA2), where cs is the ion acoustic speed and uA is the Alfven velocity. This unique thermodynamic property based on the fluctuation-dissipation theorem is verified in this paper using a new gyrokinetic particle simulation scheme, which splits the particle distribution function into the equilibrium part as well as the adiabatic and nonadiabatic parts.
NTIS
*Plasmas (Physics); Magnetohydrodynamic Waves; S Waves*

**20010122834** Princeton Univ., Plasma Physics Lab., NJ USA
**Acceleration and Compression of Charged Particle Bunches Using Counter-Propagating Laser Beams**
Shvets, G.; Fisch, N. J.; Pukhov, A.; Oct. 17, 2000; 11p; In English
Report No.(s): DE2000-765442; PPPL-3496; No Copyright; Avail: Department of Energy Information Bridge, Microfiche

The nonlinear interaction between counter-propagating laser beams in a plasma results in the generation of large (enhanced) plasma wakes. The two beams need to be slightly detuned in frequency, and one of them has to be ultra-short (shorter than a plasma period). Thus produced wakes have a phase velocity close to the speed of light and can be used for acceleration and compression of charged bunches. The physical mechanism responsible for the enhanced wake generation is qualitatively described and compared with the conventional laser wakefield mechanism. The authors also demonstrate that, depending on the sign of the frequency difference between the lasers, the enhanced wake can be used as a 'snow-plow'; to accelerate and compress either positively or negatively charged bunches. This ability can be utilized in an electron-positron injector.
NTIS
*Particle Beams; Charged Particles*

**20010122875** Argonne National Lab., IL USA

**Monte Carlo burnup code linking MCNP and REBUS**

Hanan, N. A.; Oct. 19, 1998; 10p; In English

Report No.(s): DE2001-11059; ANL/TD/CP-97492; No Copyright; Avail: Department of Energy Information Bridge, Microfiche

The REBUS-3 burnup code, used in the ANL RERTR Program, is a very general code that uses diffusion theory (DIF3D) to obtain the fluxes required for reactor burnup analyses. Diffusion theory works well for most reactors. However, to include the effects of exact geometry and strong absorbers that are difficult to model using diffusion theory, a Monte Carlo method is required. MCNP, a general-purpose, generalized-geometry, time-dependent, Monte Carlo transport code, is the most widely used Monte Carlo code. This paper presents a linking of the MCNP code and the REBUS burnup code to perform these difficult burnup analyses. The linked code will permit the use of the full capabilities of REBUS which include non-equilibrium and equilibrium burnup analyses. Results of burnup analyses using this new linked code are also presented.

NTIS

*Diffusion Theory; Time Dependence*

**20010122899** Argonne National Lab., IL USA

**Integrated models for plasma/material interaction during loss of plasma confinement**

Hassanein, A.; Jul. 29, 1998; 7p; In English

Report No.(s): DE2001-10900; ANL/TD/CP-96900; No Copyright; Avail: Department of Energy Information Bridge, Microfiche

A comprehensive computer package, High Energy Interaction with General Heterogeneous Target Systems (HEIGHTS), has been developed to evaluate the damage incurred on plasma-facing materials during loss of plasma confinement. The HEIGHTS package consists of several integrated computer models that follow the start of a plasma disruption at the scrape-off layer (SOL) through the transport of the eroded debris and splashed target materials to nearby locations as a result of the energy deposited. The package includes new models to study turbulent plasma behavior in the SOL and predicts the plasma parameters and conditions at the divertor plate. Full two-dimensional comprehensive radiation magnetohydrodynamic models are coupled with target thermodynamics and liquid hydrodynamics to evaluate the integrated response of plasma-facing materials. A brief description of the HEIGHTS package and its capabilities are given in this work with emphasis on turbulent plasma behavior in the SOL during disruptions.

NTIS

*Computer Programs; Plasma Control; Magnetohydrodynamics; Divertors (Fusion Reactors)*

**20010123144** Princeton Univ., Plasma Physics Lab., NJ USA

**Engineering Status of the Fusion Ignition Research Experiment (FIRE)**

Heitzenroeder, P. J.; Meade, D.; Thome, R. J.; Oct. 24, 2000; 7p; In English

Report No.(s): DE2000-766637; PPPL-3498; No Copyright; Avail: Department of Energy Information Bridge

Fusion Ignition Research Experiment (FIRE) is a compact, high field tokamak being studied as an option for the next step in the US magnetic fusion energy program. FIRE's programmatic mission is to attain, explore, understand, and optimize alpha-dominated plasmas to provide the knowledge necessary for the design of attractive magnetic fusion energy systems. This study began in 1999 with broad participation of the US fusion community, including several industrial participants. The design under development has a major radius of 2 m, a minor radius of 0.525 m, a field on axis of 10 T and capability to operate at 12 T with upgrades to power supplies. Toroidal and poloidal field magnets are inertially cooled with liquid nitrogen. An important goal for FIRE is a total project cost in the $1 billion range. This paper presents an overview of the engineering details which were developed during the FIRE preconceptual design study in FY99 and 00.

NTIS

*Ignition; Tokamak Devices; Nuclear Fusion*

**20010123253** Los Alamos National Lab., NM USA

**Tritium Production from Palladium Alloys**

Claytor, T. N.; Schwab, M. J.; Thoma, D. J.; Teter, D. F.; Tuggle, D. G.; Apr. 19, 1998; 9p; In English

Report No.(s): DE2001-761707; LA-UR-98-2697; No Copyright; Avail: Department of Energy Information Bridge

A number of palladium alloys have been loaded with deuterium or hydrogen under low energy bombardment in a system that allows the continuous measurement of tritium. Long run times (up to 200 h) result in an integration of the tritium and this, coupled with the high intrinsic sensitivity of the system ((approx.) 0.1 nCi/l), enables the significance of the tritium measurement to be many sigma (10). We will show the difference in tritium generation rates between batches of palladium alloys (Rh, Co, Cu, Cr,

Ni, Be, B, Li, Hf, Hg and Fe) of various concentrations to illustrate that tritium generation rate is dependent on alloy type as well as within a specific alloy, dependent on concentration.
NTIS
*Palladium Alloys; Tritium; Deuterium; Intermetallics*

**20010123410** Florida Univ., Gainesville, FL USA
**Final Technical Report for the Period October 1, 1996-September 30, 1998**
Hooper, C. F.; May 28, 1999; 40p; In English
Report No.(s): DE2001-765111; No Copyright; Avail: Department of Energy Information Bridge

The body of this report is contained in two appendices that deal with time-resolved spectroscopic analysis of microballoon implosions. The first paper introduces the experimental observation of plasma-induced line shifts in recent implosion experiments together with our theoretical analysis. These observations provide a new parameter with which to diagnose very dense laser-produced plasmas. It also indicates that at even higher densities shift-effects can be expected to be more prominent. The second paper represents an application of our analytical tools to the analysis of mix experiments. Interesting results are discussed.
NTIS
*Plasmas (Physics); Microballoons; Implosions*

**20010123546** Argonne National Lab., IL USA
**U.S. Assessment of advanced limiter-divertor plasma-facing systems (ALPS) design, analysis, and R and D needs**
Mattas, R. F.; Jun. 17, 1998; 8p; In English
Report No.(s): DE2001-10631; ANL/TD/CP-95569; No Copyright; Avail: Department of Energy Information Bridge, Microfiche

The purpose of the ALPS program is to identify and evaluate advanced limiter/diverter systems that will enhance the attractiveness of fusion power. The highest priority goals at present are achieving high power density, up to 50 MW/m(sup 2), and showing compatibility of plasma-facing surfaces with plasma operation. Personnel representing a wide range of disciplines from a number of institutions are engaged in the program, where an evaluation phase of the program is planned for three years. Successful identification of promising concepts in the evaluation phase should lead to an R and D phase that includes proof-of-principle experiments.
NTIS
*Plasma Control; Proving; Diverters*

**20010123633** Princeton Univ., Plasma Physics Lab., NJ USA
**Ohmic Flux Consumption During Initial Operation of the NSTX Spherical Torus**
Menard, J.; LeBlanc, B.; Sabbagh, S. A.; Bell, M.; Bell, R.; Oct. 05, 2000; 13p; In English
Report No.(s): DE2000-764943; PPPL-3490; No Copyright; Avail: Department of Energy Information Bridge

The spherical tokamak (ST), because of its slender central column, has very limited volt-second capability relative to a standard aspect ratio tokamak of similar plasma cross-section. Recent experiments on the National Spherical Torus Experiment (NSTX) have begun to quantify and optimize the ohmic current drive efficiency in a MA-class ST device. Sustainable ramp-rates in excess of 5 MA/sec during the current rise phase have been achieved on NSTX, while faster ramps generate significant magnetohydrodynamic activity. Discharges with Ip exceeding 1 MA have been achieved in NSTX with nominal parameters: aspect ratio A = 1.3-1.4, elongation k = 2-2.2, triangularity d = 0.4, internal inductance li = 0.6, and Ejima coefficient CE = 0.35. Flux consumption efficiency results, performance improvements associated with first boronization, and comparisons to neoclassical resistivity are described.
NTIS
*Aspect Ratio; Tokamak Devices; Electrical Resistivity*

**20010123957** Argonne National Lab., IL USA
**Comprehensive Physical Models and Simulation Package for Plasma/Material Interactions During Plasma Instabilities**
Hassanein, A.; Aug. 26, 1998; 21p; In English
Report No.(s): DE2001-10935; ANL/TD/CP-97103; No Copyright; Avail: Department of Energy Information Bridge

Damage to plasma-facing components (PFCS) from plasma instabilities remains a major obstacle to a successful tokamak concept. The extent of the damage depends on the detailed physics of the disrupting plasma, as well as on the physics of plasma-material interactions. A comprehensive computer package called High Energy Interaction with General Heterogeneous Target Systems (HEIGHTS) has been developed and consists of several integrated computer models that follow the beginning

of a plasma disruption at the scrape-off layer (SOL) through the transport of the eroded debris and splashed target materials to nearby locations as a result of the deposited energy. The package can study, for the first time, plasma-turbulent behavior in the SOL and predict the plasma parameters and conditions at the divertor plate. Full two-dimensional (2-D) comprehensive radiation magnetohydrodynamic (MHD) models are coupled with target thermodynamics and liquid hydrodynamics to evaluate the integrated response of plasma-facing materials. Factors that influence the lifetime of plasma-facing and nearby components, such as loss of vapor-cloud confinement and vapor removal due to MHD effects, damage to nearby components due to intense vapor radiation, melt splashing, and brittle destruction of target materials, are also modeled and discussed.
NTIS
*Computerized Simulation; Magnetohydrodynamic Stability; Magnetohydrodynamics; Plasmas (Physics); Tokamak Devices; Plasma Interactions*

**20010124081** Sandia National Labs., Albuquerque, NM USA
**2-D Self-Consistent DSMC Model for Chemically Reacting Low Pressure Plasma Reactors**
Bartel, T. J.; Economou, D.; Johannes, J. E.; Jun. 17, 1999; 10p; In English
Report No.(s): DE2001-7900; SAND99-1532C; No Copyright; Avail: Department of Energy Information Bridge

This paper will focus on the methodology of using a 2D plasma Direct Simulation Monte Carlo technique to simulate the species transport in an inductively coupled, low pressure, chemically reacting plasma system. The pressure in these systems is typically less than 20 mtorr with plasma densities of approximately 10(sup 17) (number-sign)/m(sup 3) and an ionization level of only 0.1%. This low ionization level tightly couples the neutral, ion, and electron chemistries and interactions in a system where the flow is subsonic. We present our strategy and compare simulation results to experimental data for Cl(sub 2) in a Gaseous Electronics Conference (GEC) reference cell modified with an inductive coil.
NTIS
*Computerized Simulation; Low Pressure; Monte Carlo Method; Plasmas (Physics); Two Dimensional Models; Chemical Reactions*

**20010124083** Sandia National Labs., Albuquerque, NM USA
**Large Distributed Data Acquisition System at the Z Facility**
Mills, J. A.; Potter, J. E.; Jun. 15, 1999; 6p; In English
Report No.(s): DE2001-7896; SAND99-1504C; No Copyright; Avail: Department of Energy Information Bridge

Experiments at the Z machine generate over four hundred channels of waveform data on each accelerator shot. Most experiments require timing accuracy to better than one nanosecond between multiple distributed recording locations throughout the facility. Experimental diagnostics and high speed data recording equipment are typically located within a few meters of the 200 to 300 terawatt X-ray source produced during Z-pinch experiments. This paper will discuss techniques used to resolve the timing of the several hundred data channels acquired on each shot event and system features which allow viewing of waveforms within a few minutes after a shot. Methods for acquiring high bandwidth signals in a severe noise environment will also be discussed.
NTIS
*Zeta Pinch; Channels (Data Transmission); Data Acquisition; Linear Systems*

**20010124097** Argonne National Lab., IL USA
**Resonant excitation of plasma wakefields using multiple electron bunches**
Conde, M. E.; Sep. 25, 1998; 5p; In English
Report No.(s): DE2001-10979; ANL-HEP-CP-98-99; No Copyright; Avail: Department of Energy Information Bridge, Microfiche

We plan to resonantly excite plasma wakefields using a train of electron bunches separated by an-integer number of plasma wavelengths. The multiple electron bunches are generated by a photocathode based RF gun by splitting the laser beam into temporally separated pulses. The amplitude of the wakefields generated by the sequence of bunches is expected to be higher than that generated if all charge had been in only one bunch, because this single bunch would be considerably longer than the individual sub-bunches due to space charge effects in our gun.
NTIS
*Linear Accelerators; Excitation; Plasmas (Physics)*

**20010125004** Sandia National Labs., Albuquerque, NM USA

**ZX Pulsed-Power Design**

Corley, J. P.; Johnson, D. L.; McDaniel, D. H.; Spielman, R. B.; Struve, K. W.; Aug. 02, 1999; 6p; In English

Report No.(s): DE2001-9680; SAND99-1985C; No Copyright; Avail: Department of Energy Information Bridge, Microfiche

ZX is a new z-pinch accelerator planned as the next generation z-pinch driver at SNL, and as an intermediate step towards X-1. It is planned to drive either a single 50 MA z-pinch load, or two 25 to 30 MA z pinches. Three designs for the ZX accelerator are presented. All require 7 to 8 MV at the insulator stack to drive the z-pinch load to implosion in 100 to 120 ns. Two of the designs are based on the Z accelerator, and use water-line technology; a transit-time-isolated water adder, and a water transformer. The third design uses inductive-voltage adders in water. They also describe a low-inductance insulator stack design that helps minimize voltage requirements. This design is evaluated for water and vacuum break-down using JCM, THM, and magnetic-flashover-inhibition criteria.

NTIS

*Zeta Pinch; Electric Potential; Systems Engineering; Plasma Accelerators*

**20010125418** Argonne National Lab., IL USA

**Dyson-Schwinger equations and the quark-gluon plasma**

Roberts, C. D.; Schmidt, S.; Apr. 20, 1999; 15p; In English

Report No.(s): DE2001-11757; ANL/PHY/CP-98787; No Copyright; Avail: Department of Energy Information Bridge, Microfiche

The authors review applications of Dyson-Schwinger equations at nonzero temperature, T, and chemical potential, (mu), touching topics such as: deconfinement and chiral symmetry restoration; the behavior of bulk thermodynamic quantities; the (T,(mu))-dependence of hadron properties; and the possibility of diquark condensation.

NTIS

*Plasmas (Physics); Particle Interactions; Gluons; Quarks*

**20010125488** Sandia National Labs., Albuquerque, NM USA

**Proceedings of US/Japan Workshop (97FT5-06) on High Heat Flux Components and Plasma Surface Interactions for Next Fusion Devices**

Kureczko, D.; Nygren, R.; Nov. 01, 1998; 867p; In English; US/Japan Workshop (97FT5-06) on High Heat Flux Components and Plasma Surface Interactions for Next Fusion Devices

Contract(s)/Grant(s): AC04-94AL85000

Report No.(s): DE2001-1117; SAND98-2252; No Copyright; Avail: Department of Energy Information Bridge, Microfiche

The 1997 US-Japan Workshop on High Heat Flux Components and Plasma Surface Interactions for Next Step Fusion Devices was held at the Warwick Regis Hotel in San Francisco, California, on December 8-11, 1997. There were 53 presentations as well as discussions on technical issues and on planning for future collaborations, and 35 researchers from Japan and the US participated in the workshop. Over the last few years, with the strong emphasis in the US on technology for ITER, there has been less work done in the US fusion program on basic plasma-materials interactions and this change in emphasis workshops. The program this year emphasized activities that were not carried out under the ITER program and a new element this year in the US program was planning and some analysis on liquid surface concepts for advanced plasma facing components.

NTIS

*Conferences; Fusion Reactors; Plasma Interactions; Plasmas (Physics)*

**20010125521** California Univ., Irvine, CA USA

**Final Report: Controlled Thermonuclear Fusion in a Staged Z-Pinch, August 1, 1993-December 31, 1998**

Wessel, F. J.; Rostoker, N.; Mar. 30, 2000; 69p; In English

Report No.(s): DE2001-765161; No Copyright; Avail: Department of Energy Information Bridge

In a 'Staged Z-Pinch' electric energy is converted to kinetic energy of a plasma liner and then efficiently transferred to a coaxial-target plasma. Magnetic fields interior to the plasma liner stabilize the implosion and provide a means to amplify current in the target while heating it to ICF conditions. Thermonuclear break-even is predicted in a compact-laboratory device.

NTIS

*Kinetic Energy; Plasmas (Physics); Zeta Pinch; Thermonuclear Reactions*

**20010125522** Nevada Univ., Reno, NV USA
**Final Report: Atomic Resonances in Plasmas, September 24, 1993-November 30, 1998**
Winkler, P.; Nov. 30, 1998; 8p; In English
Report No.(s): DE2001-765156; No Copyright; Avail: Department of Energy Information Bridge

The long-term goal of the project has been the extension of the theory of at omit processes in plasmas with emphasis on various resonance phenomena. This encompasses the inclusion of stochastic plasma fluctuations into atomic structure calculations as well as the extension of standard electron propagator techniques to multichannel propagator methods for resonant and direct scattering calculations. Conventional atomic structure programs require substantial modifications if they are to be linked with high temperature and/or high density plasma research. The development and testing of these modifications has been an important part of the research project which also has provided new insights into the theory of atomic processes in plasmas to be discussed.
NTIS
*Atomic Physics; Plasmas (Physics); Stochastic Processes; Propagation; Resonance Scattering*

**20010125531** Ames Lab., IA USA
**Development and Evaluation of an Externally Air-Cooled Low-Flow torch and the Attenuation of Space Charge and Matrix Effects in Inductively Coupled Plasma Mass Spectrometry**
Praphairaksit, N.; Sep. 12, 2000; 112p; In English
Report No.(s): DE2001-764685; IS-T 1893; No Copyright; Avail: Department of Energy Information Bridge

An externally air-cooled low-flow torch has been constructed and successfully demonstrated for applications in inductively coupled plasma mass spectrometry (ICP-MS). The torch is cooled by pressurized air flowing at (approximately)70 L/min through a quartz air jacket onto the exterior of the outer tube. The outer gas flow rate and operating RF forward power are reduced considerably. Although plasmas can be sustained at the operating power as low as 400 W with a 2 L/min of outer gas flow, somewhat higher power and outer gas flows are advisable. A stable and analytical useful plasma can be obtained at 850 W with an outer gas flow rate of (approximately)4 L/min. Under these conditions, the air-cooled plasma produces comparable sensitivities, doubly charged ion ratios, matrix effects and other analytical merits as those produced by a conventional torch while using significantly less argon and power requirements. Metal oxide ion ratios are slightly higher with the air-cooled plasma but can be mitigated by reducing the aerosol gas flow rate slightly with only minor sacrifice in analyte sensitivity. A methodology to alleviate the space charge and matrix effects in ICP-MS has been developed. A supplemental electron source adapted from a conventional electron impact ionizer is added to the base of the skimmer. Electrons supplied from this source downstream of the skimmer with suitable amount and energy can neutralize the positive ions in the beam extracted from the plasma and diminish the space charge repulsion between them. As a result, the overall ion transmission efficiency and consequent analyte ion sensitivities are significantly improved while other important analytical aspects, such as metal oxide ion ratio, doubly charged ion ratio and background ions remain relatively unchanged with the operation of this electron source. This technique not only improves the ion transmission efficiency but also minimizes the matrix effects drastically. The matrix-induced suppression of signal for even the most troublesome combination of light analyte and heavy matrix elements can be attenuated from 90-99% to only 2-10% for 2 mM matrix solutions with an ultrasonic nebulizer. The supplemental electron current can be adjusted to titrate; out the matrix effects as desired.
NTIS
*Air Cooling; Gas Flow; Inductively Coupled Plasma Mass Spectrometry; Metal Oxides; Space Charge; Attenuation; Heavy Elements*

**20010125537** Auburn Univ., AL USA
**Experimental Studies of Radio Frequency Wave and Confinement in the Auburn Torsatron** ***Final Report***
Gandy, R.; Jul. 03, 2000; 11p; In English
Report No.(s): DE2001-763951; No Copyright; Avail: Department of Energy Information Bridge, Microfiche

The report explains work done by Auburn University research personnel in the area of fluctuation physics with application to magnetic fusion research.
NTIS
*Nuclear Fusion; Stellarators*

**20010125649** Texas Univ., Inst. for Fusion Studies, Austin, TX USA
**Final Report: Establishment of an Institute for Fusion Studies, June 1, 1980-March 1, 1998**
Hazeltine, R. D.; Dec. 03, 1999; 25p; In English
Report No.(s): DE2001-765162; No Copyright; Avail: Department of Energy Information Bridge

The mission of the Institute for Fusion Studies has been to serve as a national center for theoretical fusion and plasma physics research. As an independent scientific group of critical size, its objectives were to conduct research on fundamental phenomena important to fusion; to serve as a center for fusion theory exchange activities with other countries; to exchange scientific developments with other academic disciplines; and to train students and postdoctoral fellows in fusion and plasma physics research.
NTIS
*Plasma Physics; Nuclear Fusion; Education*

## 76
## SOLID-STATE PHYSICS

*Includes condensed matter physics, crystallography, and superconductivity. For related information see also 33 Electronics and Electrical Engineering and 36 Lasers and Masers.*

**20010117653** Los Alamos National Lab., NM USA
**Pressure Effects on Magneto-Optical Properties in Cadmium Telluride/(Cadmium, Manganese) Telluride Single Quantum Well with High Manganese Concentration**
Yokoi, H.; Tozer, S.; Kim, Y.; Rickel, D.; Kakudate, Y.; Nov. 09, 1998; 17p; In English
Report No.(s): DE2000-760126; LA-UR-98-4157; No Copyright; Avail: Department of Energy Information Bridge
Photoluminescence (PL) measurements under hydrostatic pressures up to 1.07 GPa and long pulsed magnetic fields up to 60 T with a pulse duration of 2 seconds are reported. The pressures were generated in a plastic diamond anvil cell (DAC). A bend toward lower energies (additional red shift) is observed above 28.5 T in magnetic field dependence of the exciton energy for a 13 Aring thick quantum well. We attribute this red shift to a phenomenon preceding the type 1-type 2 transition after a comparison with a simple quantum mechanical calculation. The onset field of the additional red shift increases by 3.4 T by applying a pressure of 1.07 GPa. Spin-spin coupling between the exciton and the Mn ion in the interface region is also investigated and found to be enhanced by pressure.
NTIS
*Cadmium Tellurides; Magnetic Effects; Magneto-Optics; Photoluminescence; Pressure Effects; Quantum Wells*

**20010118265** California Univ., Lawrence Berkeley Lab., Berkeley, CA USA
**Ga Self-Diffusion in Isotopically Enriched GaAs Heterostructures Doped with Si and Zn**
Norseng, M. S.; Dec. 16, 1999; 95p; In English
Report No.(s): DE2000-760338; LBNL-45257; No Copyright; Avail: Department of Energy Information Bridge, Microfiche
The tremendous advances in semiconductor process and device technology over the last few decades have been much chronicled, and such reviews usually focus on the commercial success of silicon based solid state integrated circuits. While it is undisputed that Si is commercially the most utilized semiconductor, GaAs and related compound semiconductors have been the standard materials for optoelectronic devices such as light emitting diodes and lasers, high electron mobility transistors promise of allowing integrated circuits which operate using (HEMT's) and hold the photons in addition to electrons and holes. Among the advantages of GaAs based materials for such advanced devices is a direct band gap allowing single event emission and absorption of photons, the possibility to create layered structures with varying band gaps and alloy composition, and band gap energies covering the full spectrum of visible light.
NTIS
*Doped Crystals; Gallium Arsenides; Semiconductors (Materials)*

**20010118267** California Univ., Lawrence Berkeley Lab., Berkeley, CA USA
**DC SQUID Spectrometers for Nuclear Quadrupole and Low-Field Nuclear Magnetic Resonance Spectroscopy**
TonThat, D. M.; Apr. 01, 1998; 124p; In English
Report No.(s): DE2000-760336; LBNL-44249; No Copyright; Avail: Department of Energy Information Bridge, Microfiche
The dc Superconducting Quantum Interference Device (SQUID) is a very sensitive detector of magnetic flux. This inherent flux sensitivity of the SQUID is used in a spectrometer for the detection of nuclear magnetic resonance (NMR)and nuclear quadruple resonance (NQR). The processing magnetic field from the nuclear spins is coupled to the SQUID by mean of a flux

transformer. An NMR probe configuration consists of a static field coil, an audio frequency (af) pulsing coil, and a pickup coil coupled to the SQUID.
NTIS
*Nuclear Magnetic Resonance; Quadrupoles; Squid (Detectors); Magnetic Flux*

**20010118510** NASA Ames Research Center, Moffett Field, CA USA
**Laboratory Investigation of the Growth and Crystal Structure of Nitric Acid Hydrates by Transmission Electron Microscopy (TEM)**
Blake, David F., NASA Ames Research Center, USA; [1994]; 1p; In English; Atmospheric Effects of Aviation Project, 24 Jun. - 1 Jul. 1994, Virginia Beach, VA, USA
Contract(s)/Grant(s): RTOP 152-13-60; No Copyright; Avail: Issuing Activity; Abstract Only

A great deal of recent laboratory work has focussed on the characterization of the nitric acid hydrates, thought to be present in type I Polar Stratospheric Clouds (PSCs). Phase relationships and vapor pressure measurements (1-3) and infrared characterizations (4-5) have been made. However, the observed properties of crystalline solids (composition, melting point, vapor pressure, surface reactivity, thermodynamic stability, extent of solid solution with other components, etc.) are controlled by their crystal structure. The only means of unequivocal structural identification for crystalline solids is diffraction (using electrons, X-rays, neutrons, etc.). Other observed properties of crystalline solids, such as their infrared spectra, their vapor pressure as a function of temperature, etc. yield only indirect information about what phases are present, their relative proportions, or whether they are crystalline or amorphous.
Derived from text
*Nitric Acid; Hydrates; Crystal Structure; Vapor Pressure; Transmission Electron Microscopy; Melting Points; Infrared Radiation*

**20010118903** Brookhaven National Lab., Upton, NY USA
**Resonant and non-resonant inelastic x-ray scattering in CuGeO3**
Zimmermann,; Hill,; Kao,; Gog,; Venkataraman,; Dec. 31, 1999; 4p; In English
Report No.(s): DE2000-755035; BNL-67265; No Copyright; Avail: Department of Energy Information Bridge

Transition metal oxides are presently the focus of much attention in condensed matter physics because of the diverse phenomena exhibited by these materials. Examples include antiferromagnetism, superconductivity and colossal magnetoresistance. The origin of these phenomena lies in the strong electron correlations present in these materials which place them between the well understood limits of band insulators and simple metals. The presence of these correlations makes these materials hard to handle theoretically, and there is a need for more detailed experimental work, in particular in regard to the electronic structure and excitations.
NTIS
*X Ray Scattering; Metal Oxides; Transition Metals; Electronic Structure; Excitation*

**20010118917** Brookhaven National Lab., Upton, NY USA
**Magnetic exchange-coupling in CoPt/Co bilayer thin films**
Kim,; Barmak,; Lewis,; Crew,; Welch,; Apr. 05, 1999; 6p; In English
Report No.(s): DE2000-760983; BNL-66024; No Copyright; Avail: Department of Energy Information Bridge

Thin film CoPt/Co bilayers have been prepared as a model system to investigate the relationship between microstructure and exchange coupling in two-phase hard/soft composite magnets. CoPt films, with a thickness of 25 nm, were sputter-deposited from a nearly equiatomic alloy target onto oxidized Si wafers. The films were subsequently annealed at 700 C and fully transformed from the FCC (face centered cubic) phase to the magnetically hard, ordered L1(sub 0) phase. The coercivity of the films increased rapidly with annealing time until it reached a plateau at approximately 9.5 kOe. Fully-ordered CoPt films were then used as substrates for deposition of Co layers, with thicknesses in the range of 2.8-225 nm, in order to produce the hard/soft composite bilayers. As predicted by theory, the magnetic coherency between the soft Co phase and the hard, ordered CoPt phase decreased as the thickness of the soft phase increased. This decrease in coupling was clearly seen in the magnetic hysteresis loops of the bilayers. At small thicknesses of Co (a few nanometers), the shape of the loop was one of a uniform material showing no indication of the presence of two phases with extremely different coercivities. At larger Co thicknesses, constricted loops, i.e., ones showing the presence of a mixture of two ferromagnetic phases of different hardnesses, were obtained. The magnetic exchange present in the bilayer samples was qualitatively analyzed using magnetic recoil curves and the dependence of exchange coupling on the soft phase dimension in the bilayer hard/soft composite magnet films is discussed.
NTIS
*Magnetic Properties; Thin Films; Microstructure; Electromagnetic Coupling; Hardness*

**20010118926** Sandia National Labs., Albuquerque, NM USA
**Surfactant Templated Mesoporous Hybrid Thin Films**
Fan, H.; Lu, Y.; Assink, R. A.; Lopez, G.; Brinker, C. J.; Jul. 14, 2000; 8p; In English
Report No.(s): DE2000-761832; SAND2000-1884C; No Copyright; Avail: Department of Energy Information Bridge

Organic/inorganic hybrid films exhibiting ordered mesophases were prepared by a simple dip-coating procedure. Beginning with a homogeneous solution of tetraethyl orthosilicate, organoalkoxysilane ((R Si(OR)3), R is a non-hydrolyzable functional ligand) surfactant, we relied on solvent evaporation to induce micellization and continuous self-assembly into hybrid silica-surfactant thin film mesophases. Surface acoustic wave (SAW)-based nitrogen sorption measurements indicate that the films have high surface areas and unimodal pore diameters after removal of surfactants.
NTIS
*Surfactants; Thin Films; Porous Materials; Silicon Dioxide; Solid State Physics*

**20010119059** Brookhaven National Lab., Upton, NY USA
**Monopoles and dyons in the pure Einstein Yang Mills Theory**
Hosotani,; Bjoraker,; Aug. 16, 1999; 9p; In English
Report No.(s): DE2000-755034; BNL-67267; No Copyright; Avail: Department of Energy Information Bridge

In the pure Einstein-Yang-Mills theory in four dimensions there exist monopole and dyon solutions. The spectrum of the solutions is discrete in asymptotically flat or de Sitter space, whereas it is continuous in asymptotically anti-de Sitter space. The solutions are regular everywhere and specified with their mass, and non-Abelian electric and magnetic charges. In asymptotically anti-de Sitter space a class of monopole solutions have no node in non-Abelian magnetic fields, and are stable against spherically symmetric perturbations.
NTIS
*Monopoles; Elementary Particles*

**20010119061** Oak Ridge National Lab., TN USA
**Alternative Gate Dielectrics on Semiconductors for MOSFET Device Applications**
Norton, D. P.; Budai, J. D.; Chisholm, M. F.; Pennycook, S. J.; McKee, R.; Dec. 06, 1999; 9p; In English
Report No.(s): DE2000-751435; ORNL/CP-105771; No Copyright; Avail: Department of Energy Information Bridge, Microfiche

We have investigated the synthesis and properties of deposited oxides on Si and Ge for use as alternative gate dielectrics in MOSFET (metal oxide semiconductors field effect transistors) applications. The capacitance and leakage current behavior of polycrystalline Y(sub 2)O(sub 3) films synthesized by pulsed-laser deposition is reported. In addition, we also discuss the growth of epitaxial oxide structures. In particular, we have investigated the use of silicide termination for oxide growth on (001) Si using laser-molecular beam epitaxy. In addition, we discuss a novel approach involving the use of hydrogen to eliminate native oxide during initial dielectric oxide nucleation on (001) Ge.
NTIS
*Dielectrics; Field Effect Transistors; Metal Oxide Semiconductors; Molecular Beam Epitaxy; Pulsed Laser Deposition; Silicon; Germanium*

**20010119190** Oak Ridge National Lab., TN USA
**Recent Studies of Proton Drip-Line Nuclei Using the Berkeley Gas-Filled Separator**
Rowe, M. W.; Batchelder, J. C.; Ninov, V.; Gregorich, K. E.; Toth, K. S.; Oct. 07, 1999; 10p; In English
Report No.(s): DE2000-754814; ORNL/P00-106090; No Copyright; Avail: Department of Energy Information Bridge

The Berkeley Gas-filled Separator provides new research opportunities at Lawrence Berkeley National Laboratory's X-Inch Cyclotron. The use of this apparatus for the study of proton drip-line nuclides is discussed. Preliminary results of (sup 78)Kr bombardments of (sup 102)Pd targets at mid-target energies of 360, 375 and 385 MeV are presented. Improvements planned partially as a result of this measurement are also discussed.
NTIS
*Cyclotrons; Nuclides; Protons; Transition Metals; Rare Gases*

**20010119198** Brookhaven National Lab., Upton, NY USA
**Properties of silicon on defect layer material**
Li, H.; Nov. 27, 1996; 4p; In English
Report No.(s): DE2000-752969; BNL-61310-00/02-REV; BNL-C-92-02O; No Copyright; Avail: Department of Energy Information Bridge

A new silicon material, silicon-on-defect-layer (SODL), has been measured by secondary ion mass spectrometry (SIMS) and spreading resistivity (SR) measurements. SIMS data show that the buried defect-layer in SODL consists of silicon oxide due to the gettering of intrinsic oxygen by proton-implanted damage. Furthermore, SODL procedure makes a silicon wafer contain much fewer oxygen in surface-layer on the defect-layer, resulting in a purified surface-layer. Measurements of SR indicate that the surface-layer of n-type silicon wafer was converted to p-type silicon after SODL procedure. A metal oxide semiconductor (MOS) device with a value of the electron mobility in the inversion mode of 714 cm(squared)/(V.s) was fabricated on SODL material. Like isolation function of a well in a complementary MOS (CMOS) device, the p-n junction in SODL material could play a role of isolation between the surface-layer and bulk. In addition, by reducing the implantation energy, SODL technology for making p-n junction, in which built-in field separates light-generated electrons and holes, is a candidate to make cheap solar cells by using low-quality low-cost silicon.
NTIS
*Defects; Energy Technology; Secondary Ion Mass Spectrometry; Silicon; Metal Oxide Semiconductors*

**20010119202** Oak Ridge National Lab., TN USA
**Surface Intensive Materials Processing for Multi-Functional Purposes**
Ila, D.; Williams, E. K.; Muntele, C. I.; George, M. A.; Poker, D. B.; Mar. 06, 2000; 10p; In English
Report No.(s): DE2000-751502; ORNL/CP-105988; No Copyright; Avail: Department of Energy Information Bridge, Microfiche

We have chosen silicon carbide (SiC) as a multi-functional material to demonstrate the application of surface intensive processing for device fabrication. We will highlight two devices which are produced in house at the Center for Irradiation of materials of Alabama A and M University: (A) High temperature electronic gas sensor, (B) High temperature optical properties/sensor.
NTIS
*Silicon Carbides; Semiconductor Devices*

**20010119204** Oak Ridge National Lab., TN USA
**3-D Measurement of Deformation Microstructure of Al(0.2%)Mg Using Submicron Resolution White X-Ray Microbeams**
Larson, B. C.; Tamura, N.; Chung, J. S.; Ice, G. E.; Budai, J. D.; Nov. 29, 1999; 7p; In English
Report No.(s): DE2000-751483; ORNL/CP-105769; No Copyright; Avail: Department of Energy Information Bridge, Microfiche

We have used submicron-resolution white x-ray microbeams on the MHATT (University of Michigan, Howard University, AT&T)-CAT (Collaborative Access Team) beamline 7-ID at the Advanced Photon Source to develop techniques for three-dimensional investigation of the deformation microstructure in a 20% plane strain compressed Al(0.2%)Mg tri-crystal. Kirkpatrick-Baez mirrors were used to focus white radiation from an undulator to a 0.7 x 0.7 (micro)m(sup 2) beam that was scanned over bi- and tri-crystal regions near the triple-junction of the tri-crystal. Depth resolution along the x-ray microbeam of less than 5 microns was achieved by triangulation to the diffraction source point using images taken at a series of CCD (charge coupled device) distances from the microbeam. Computer indexing of the deformation cell structure in the bi-crystal region provided orientations of individual subgrains to (approximately) 0.01 degrees, making possible detailed measurements of the rotation axes between individual cells.
NTIS
*Deformation; Microstructure; Photons; Crystals; Microbeams*

**20010119205** Oak Ridge National Lab., TN USA
**Study of Chromium-Doped Diamond-Like Carbon by Z-Contrast Imaging and Electron Energy Loss Spectroscopy**
Fax, X.; Dickey, E. C.; Pennycook, S. J.; Nov. 29, 1999; 7p; In English
Report No.(s): DE2000-751482; ORNL/CP-105679; No Copyright; Avail: Department of Energy Information Bridge, Microfiche

Metal-doped diamond-like carbon films were produced for the purpose of an electrochemical nano-electrode. In this study we use Z-contrast scanning transmission electron microscopy to directly observe metal cluster formation and distributions within the chromium-doped carbon films. At low doping ((approximately) 6 at % Cr), Cr is uniformly distributed; at high doping ((approximately) 12 at % Cr), Cr-rich clusters are formed. Using electron energy loss spectroscopy, we find that the Cr clusters tend to be metallic-like at low doping levels and carbide-like at high doping levels according to the Cr L, white line ratios. The

carbon is more diamond-like at low doping and more graphite/carbide like at high doping according to the sp1/sp3 electron percentage measurements.
NTIS
*Diamonds; Chromium; Transmission Electron Microscopy; Doped Crystals; Diamond Films*

**20010119206** Oak Ridge National Lab., TN USA
**Z-Contrast STEM Imaging and Ab-Initio Calculations of Grain Boundaries in SRTiO**
Kim, M.; Browning, N. D.; Pennyscook, S. J.; Sohlberg, K.; Pantelides, S. T.; Nov. 29, 1999; 7p; In English
Report No.(s): DE2000-751481; ORNL/CP-105693; No Copyright; Avail: Department of Energy Information Bridge, Microfiche

The understanding of electrical properties of grain boundaries in perovskites is essential for their application to capacitors, varistors and positive-temperature coefficient resistors. The origin of the electrical activity is generally attributed to the existence of charged defects in grain boundaries, usually assumed to be impurities, which set up a double Schottky barrier as they are screened by dopants in the adjacent bulk crystal. Microscopic understanding of the origin of the grain boundary charge, however, has not been achieved. It is not known yet if the charged grain boundary states are an intrinsic property of a stoichiometric grain boundary, arise from nonstoichiometry, or are caused by impurities. Here, the relation between atomic structure and electronic properties is studied by combining experiment with ab-initio calculations. The starting structures for theoretical calculations were obtained from Z-contrast images combined with electron energy loss spectroscopy to resolve the dislocation core structures comprising the boundary. Dislocation core reconstructions are typical of all grain boundaries so far observed in this material. They avoid like-ion repulsion, and provide alternative sites for cation occupation in the grain boundaries. Optimized atomic positions are found by total energy calculations. Calculated differences in vacancy formation energies between the grain boundaries and the bulk suggest that vacancy segregation can account for the postulated grain boundary charge.
NTIS
*Electrical Properties; Grain Boundaries; Titanium Oxides; Strontium Oxides; Perovskites*

**20010119207** Oak Ridge National Lab., TN USA
**Epitaxial Electronic Oxides on Semiconductors Using Pulsed-Laser Deposition**
Norton, D. P.; Budai, J. D.; Chisholm, M. F.; Dec. 01, 1999; 6p; In English
Report No.(s): DE2000-751431; ORNL/CP-105770; No Copyright; Avail: Department of Energy Information Bridge, Microfiche

We describe the growth and properties of epitaxial (001) CeO (sub 2) on a (001) Ge surface using a hydrogen-assisted pulsed-laser deposition method. Hydrogen gas is introduced during film growth to eliminate the presence of the GeOs from the semiconductor surface during the initial nucleation of the metal oxide film. The hydrogen partial pressure and substrate temperature are selected to be sufficiently high such that the germanium native oxides are thermodynamically unstable. The Gibbs free energy of CeO(sub 2) is larger in magnitude than that of the Ge native oxides, making it more favorable for the metal oxide to reside at the interface in comparison to the native Ge oxides. By satisfying these criteria. the metal oxide/semiconductor interface is shown to be atomically abrupt with no native oxide present. Preliminary structural and electrical properties are reported.
NTIS
*Germanium Oxides; Metal Oxide Semiconductors; Thin Films; Oxide Films; Pulsed Laser Deposition; Cerium Oxides*

**20010119208** Oak Ridge National Lab., TN USA
**Pulsed-Laser Deposition of Electronic Oxides: Superconductor and Semiconductor Applications**
Norton, D. P.; Park, C.; Lee, Y. E.; Budai, J. D.; Chisholm, M. F.; Jan. 24, 2000; 8p; In English
Report No.(s): DE2000-751428; ORNL/CP-105775; No Copyright; Avail: Department of Energy Information Bridge

Over the past decade, pulsed-laser deposition (PLD) has proven to be one of the most versatile and effective methods for obtaining high-quality electronic oxide thin-film materials. Much of this success can be attributed to its initial use in depositing high temperature superconducting materials. However, pulsed-laser deposition is now a leading research tool in the development of various electronic oxide thin-film technologies. In this paper, recent progress in the deposition of oxide materials on dissimilar materials for both superconductor and semiconductor applications is discussed. Recent developments in the synthesis of superconducting wires via epitaxial growth of superconducting oxides on biaxially textured metal tapes is described. In addition, efforts to integrate high-k dielectric oxides on semiconductor surfaces using pulsed-laser deposition are highlighted.
NTIS
*Oxides; Pulsed Laser Deposition; Thin Films; Vapor Deposition*

**20010119210** Brookhaven National Lab., Upton, NY USA

**Towards a Damage Mechanics of High-T(c) Superconductors**

Welch, D. O.; Dec. 01, 1999; 11p; In English

Report No.(s): DE2000-751158; BNL-66981; No Copyright; Avail: Department of Energy Information Bridge

Stresses in superconductors arise in various ways, ranging from the stresses on a macroscopic scale which arise from Lorentz forces in the operation of high field superconducting magnets to the stresses on a microscopic scale which arise from defects such as dislocations in the microstructure of superconductors. Stresses arise during various steps in the manufacture of composite superconductors, such as the essential processes of rolling and pressing that occur during the fabrication of silver-sheathed bismuth cuprate superconducting tapes by the so-called powder-in-tube process, and significant levels of stress can arise from differential thermal contraction between the elements of a composite superconductor such as the normally-conducting metallic matrix and the embedded superconducting filaments during the process of cooling from the high temperatures employed in fabrication to the cryogenic temperatures of operation of the superconductor.

NTIS

*High Field Magnets; High Temperature Superconductors; Damage Assessment*

**20010119544** Lawrence Livermore National Lab., Livermore, CA USA

**Growth Phenomena in the Surface Layer and Step Generation from the Edges of Faceted Crystals**

Carman, L.; Smolsky, I.; Zaitseva, N. P.; Jul. 29, 1999; 34p; In English

Report No.(s): DE2001-10423; UCRL-JC-133048; No Copyright; Avail: Department of Energy Information Bridge

The mechanism of growth step generation from the edges of faceted crystals obtained from experimental results with KDP crystals is described. It shows that growth from the crystal edges is initiated by the deviation of the edges from their crystallographic orientation and formation of incomplete shapes of singular facets. The conditions for formation of the incomplete faceted shapes during dislocation growth are considered. It is shown that the process of step generation from the edges is determined by the mutual positions of the vicinal slopes on the adjacent faces.

NTIS

*Crystals; Edges; Surface Layers; Crystal Growth; Flat Surfaces*

**20010119569** Argonne National Lab., IL USA

**Recent advances in fabrication of high-Tc superconductors for electric power applications**

Balachandran, U.; Mar. 25, 1998; 20p; In English

Report No.(s): DE2001-10562; ANL/ET/CP-95330; No Copyright; Avail: Department of Energy Information Bridge, Microfiche

The U.S. Department of Energy (DOE) supports an applied superconductivity program entitled 'Superconductivity Program for Electric Power Systems.' Activities within this program contribute to development of the high-temperature superconductor (HTS) technology needed for industry to proceed with the commercial development of electric power applications such as motors, generators, transformers, transmission cables, and current limiters. Research is conducted in three categories: wire development, systems technology development, and Superconductivity Partnership Initiative (SPI). Wire development activities are devoted to improving the critical current density (J(sub c)) of short-length HTS wires, whereas systems technology development focuses on fabrication of long-length wires, coils, and on magnets. The SPI activities are aimed at development of prototype products. Significant progress has been made in the development of HTSs for various applications: some applications have already made significant strides in the marketplace, while others are still in the developmental stages. For successful electric power applications, it is very important that the HTS be fabricated into long-length conductors that exhibit desired superconducting and mechanical properties. Several parameters of the PIT (powder in tube) technique must be carefully controlled to obtain the desired properties. Long lengths of Bi-2223 tapes with respectable superconducting properties have been fabricated by a carefully designed thermomechanical treatment process. A 1-MVA capacity fault current limiter, a 286-hp motor, and 630-kVA transformers, and a 50-m-long conductor, all using HTSs, have already been demonstrated. While the use of HTS devices in the electric utility area has clear advantages, impediments to successful commercialization remain. Issues such as AC losses, conductor cost, and reliable superconducting joints must be addressed. The cost of HTS conductors are still quite high, and significant research and development efforts must be focused on this issue. The general acceptance of HTS power equipment will ultimately be based on system performance, reliability and maintenance, efficiency, and installed cost relative to those of conventional technologies.

NTIS

*Critical Current; High Temperature Superconductors; Product Development; Superconductivity; Electronic Equipment*

**20010119570** Argonne National Lab., IL USA

**Evolution of magnetic and superconducting fluctuations with doping of high-Tc superconductors: an electronic Raman scattering study**

Blumberg, G.; Jan. 14, 1998; 8p; In English

Report No.(s): DE2001-10570; ANL/MSD/CP-95380; No Copyright; Avail: Department of Energy Information Bridge, Microfiche

For YBa(sub 2)Cu(sub 3)O(sub 6+(delta)) and Bi(sub 2)SR(sub 2)CaCu(sub 2)O(sub 3(+/-)(delta)) superconductors, electronic Raman scattering from high- and low-energy excitations has been studied in relation to the hole doping level, temperature, and energy of the incident photons. For underdoped superconductors, it is concluded that short range antiferromagnetic (AF) correlations persist with hole doping and doped single holes are incoherent in the AF environment. Above the superconducting (SC) transition temperature T(sub c) the system exhibits a sharp Raman resonance of B(sub 1g) symmetry and about 75 meV energy and a pseudogap for electron-hole excitations below 75 meV, a manifestation of a partially coherent state forming from doped incoherent quasi-particles. The occupancy of the coherent state increases with cooling until phase ordering at T(sub c) produces a global SC state.

NTIS

*High Temperature Superconductors; Raman Spectroscopy; Doped Crystals; Barium Oxides; Copper Oxides; Bismuth Oxides; Strontium Oxides; Calcium Oxides; Yttrium Oxides*

**20010119575** Argonne National Lab., IL USA

**Nucleation of nanocrystalline diamond by fragmentation of fullerene precursors**

Gruen, D. M.; May 04, 1998; 13p; In English

Report No.(s): DE2001-10576; ANL/CHM/CP-95414; No Copyright; Avail: Department of Energy Information Bridge, Microfiche

Growth of diamond films from C(sub 60)/Ar microwave discharges results in a nanocrystalline microstructure with crystallite sizes in the range 3-10 nm. Heterogeneous nucleation rates of 10(sup 10) cm(sup (minus)2) sec are required to account for the results. The nucleation mechanism presented here fulfills this requirement and is based on the insertion of carbon dimer, C(sub 2), molecules, produced by fragmentation of C(sub 60), into the n-bonded dimer rows of the reconstructed (100) surface of diamond. Density functional theory is used to calculate the energetic of C(sub 2) insertion into carbon clusters that model the (100) surface. The reaction of singlet C(sub 2) with the double bond of the C(sub 9)H(sub 12) cluster leads to either carbene structures or a cyclobutynelike structure. At the HF/6-31G* level, the carbene product has a C(sub 2v) structure, while at the B3LYP/6-31G* levels of theory, it has a C(sub s) structure with the inserted C(sub 2) tilted. No barrier for insertion into the C=C double bond of the C(sub 9)H(sub 12) cluster was found at the HF/6-31G* and B3LYP/6-31G* levels of theory. Thus, calculations including correlation energy and geometry optimization indicate that insertion of C(sub 2) into a C=C double bond leads to a large energy lowering, (approximately) 120 kcal/mol for a C(sub 9)H(sub 12) cluster, and there is no barrier for insertion.

NTIS

*Diamonds; Nucleation; Nanostructure (Characteristics); Crystal Growth*

**20010119953** Sandia National Labs., Albuquerque, NM USA

**Collective Collision Operator for DSMC**

Gallis, M. A.; Torczynski, J. R.; Jun. 21, 2000; 7p; In English

Report No.(s): DE2000-760784; SAND2000-1538C; No Copyright; Avail: Department of Energy Information Bridge

A new scheme to simulate elastic collisions in particle simulation codes is presented. The new scheme aims at simulating the collisions in the highly collisional regime, in which particle simulation techniques typically become computationally expensive.The new scheme is based on the concept of a grid-based collision field. According to this scheme, the particles perform a single collision with the background grid during a time step. The properties of the background field are calculated from the moments of the distribution function accumulated on the grid. The collision operator is based on the Langevin equation. Based on comparisons with other methods, it is found that the Langevin method overestimates the collision frequency for dilute gases.

NTIS

*Particle Interactions; Particle Collisions; Computerized Simulation; Elastic Scattering*

**20010119954** Argonne National Lab., IL USA

**Unconventional cyclotron resonance in the organic superconductor (beta)-(ET)(sub 2)SF(sub 5)CH(sub 2)CF(sub 2)SO(sub 3)**

Edwards, R. S.; Symington, J. A.; Rzepniewski, E.; Ardavan, A.; Singleton, J.; Aug. 22, 2000; 4p; In English

Report No.(s): DE2000-761270; ANL/CHM/CP-102620; No Copyright; Avail: Department of Energy Information Bridge

No abstract prepared.

NTIS

*Cyclotron Resonance; Organic Superconductors*

**20010120065** Los Alamos National Lab., NM USA

**Investigation of the Initial Stages of Processing Bi-2223 Multifilamentary Tapes by Analytical Electron Microscopy**

Holesinger, T. G.; Ayala, A.; Sep. 19, 2000; 7p; In English

Report No.(s): DE2000-762843; LA-UR-00-4424; No Copyright; Avail: Department of Energy Information Bridge, Microfiche

Analytical transmission electron microscopy (TEM) was used to probe the formation of liquid phases in multifilamentary Bi-2223 tapes. Silver was found to nucleate small amounts of lead-rich liquid phase formation in these tapes. The compositions of the lead-rich liquid phases were measured quantitatively. The data presented is consistent with a mechanism whereby Bi-2223 can precipitate from a liquid phase.

NTIS

*Precipitates; Silver; Transmission Electron Microscopy*

**20010120066** Los Alamos National Lab., NM USA

**Non-Destructive Evaluation with a Linear Array of 11 HTS SQUIDs**

Espy, M. A.; Matlachov, A. N.; Kraus, R. H.; Sep. 15, 2000; 7p; In English

Report No.(s): DE2000-762304; LA-UR-00-4323; No Copyright; Avail: Department of Energy Information Bridge, Microfiche

The linear array of 11 HTS SQUIDs discussed in this paper has been developed into a non-destructive evaluation (NDE) tool we refer to as the SQUID array microscope (SAMi). The SAMi is a second-generation device, developed after we built and successfully deployed a single-SQUID NDE instrument. Both the SAMi and its single SQUID predecessor were designed for stockpile stewardship applications at Los Alamos National Laboratory. The stockpile stewardship application is well suited to SQUID NDE techniques. The features of interest are in conductive material, typically small in spatial extent, generally deeply buried (>1 cm), and the cost of destructively evaluating a sample is sufficiently high to render the overhead of a SQUID system negligible.

NTIS

*Linear Arrays; Nondestructive Tests; Squid (Detectors)*

**20010120073** Argonne National Lab., IL USA

**High-resolution atomic distribution functions of disordered materials by high-energy x-ray diffraction**

Petkov, V.; Billinge, S. J. L.; Shastri, S. D.; Himmel, B.; Aug. 15, 2000; 14p; In English

Report No.(s): DE2000-761267; ANL/UPD/CP-102591; No Copyright; Avail: Department of Energy Information Bridge

Knowledge of the atomic-scale structure is a prerequisite to understanding the physical properties and technological characteristics of materials. Also, many technologically important materials contain significant disorder on an atomic scale. Often this disorder has a direct effect on the properties which make the material technologically and/or scientifically important. It is clearly advantageous to characterize the structure of disordered materials with high resolution. A fruitful experimental approach is the combination of the high-energy x-ray diffraction and the atomic Pair Distribution Function (PDF) technique.

NTIS

*X Ray Diffraction; Atomic Structure; Distribution Functions*

**20010120078** Argonne National Lab., IL USA

**Measurement and minimization of wing tilt in laterally overgrown GaN on a SiO(sub 2) mask**

Fini, P.; Zhao, L.; Speck, J. S.; DenBaars, S. P.; Munkholm, A.; Aug. 04, 2000; 7p; In English

Report No.(s): DE2000-761259; ANL/MSD/CP-102479; No Copyright; Avail: Department of Energy Information Bridge

The utility of x-ray diffraction measurements in characterizing the tilt that occurs during lateral growth of GaN on a stripe-patterned SiO mask is demonstrated. These measurements, in conjunction with additional structural characterization, have led to the minimization of 'wing' tilt via careful control of stripe cross-section. In addition, in situ grazing-incidence x-ray

diffraction studies have revealed that 'wing' tilt evolves early during lateral growth, thus demonstrating the importance of initial growth conditions in determining tilt magnitude.
NTIS
*X Ray Diffraction; Crystal Growth; Silicon Oxides; Gallium Nitrides; Characterization; Thin Films*

**20010120094** Argonne National Lab., IL USA
**Oxidation dynamics of nanophase aluminum clusters: a molecular dynamics study**
Ogata, S.; Jan. 27, 1998; 8p; In English
Report No.(s): DE2001-10615; ANL/IPNS/CP-95508; No Copyright; Avail: Department of Energy Information Bridge, Microfiche

Oxidation of an aluminum nanocluster (252,158 atoms) of radius 100(angstrom) placed in gaseous oxygen (530,727 atoms) is investigated by performing molecular-dynamics simulations on parallel computers. The simulation takes into account the effect of charge transfer between Al and O based on the electronegativity equalization principles. We find that the oxidation starts at the surface of the cluster and the oxide layer grows to a thickness of (approximately)28(angstrom). Evolutions of local temperature and densities of Al and O are investigated. The surface oxide melts because of the high temperature resulting from the release of energy associated with Al-O bondings. Amorphous surface-oxides are obtained by quenching the cluster. Vibrational density-of-states for the surface oxide is analyzed through comparisons with those for crystalline Al, Al nanocluster, and (alpha)-Al2O3.
NTIS
*Aluminum; Oxidation; Molecular Dynamics*

**20010120118** California Univ., Dept. of Materials, Santa Barbara, CA USA
**Periodic Lattices of Interacting Self-Assembled Quantum Dots** ***Final Report, 15 Mar. 1998 - 14 Nov. 2000***
Speck, James S.; Petroff, Pierre M.; Beltz, Glenn E.; Sep. 2001; 25p; In English
Contract(s)/Grant(s): F49620-98-1-0367; Proj-2305
Report No.(s): AD-A395008; AFRL-SR-BL-TR-01-0494; No Copyright; Avail: CASI; A01, Microfiche; A03, Hardcopy

Overall, in this program, we developed high quality 2D and 3D periodic quantum dot lattices that show strong photoluminescence. In the initial stages of the program, we worked on QD growth on a periodic stressor lattice formed by ordered subsurface dislocations. The dislocation grid was formed by twist bonding.
DTIC
*Quantum Dots; Photoluminescence; Lattice Vibrations*

**20010120132** Iowa Univ., Dept. of Physics and Astronomy, Iowa City, IA USA
**Nanoscale Coherence Near Defects: Superconductivity, Spin Ordering, and Their Coexistence** ***Annual Report, 1 Jul. 2000-30 Jun. 2001***
Flatte, Michael E.; Oct. 08, 2001; 18p; In English
Contract(s)/Grant(s): N00014-99-1-0313
Report No.(s): AD-A395196; No Copyright; Avail: CASI; A03, Hardcopy; A01, Microfiche

This is a report of progress in theoretical calculations of the influence of impurities on tunneling spectroscopy in high-temperature superconductors. The calculations have been improved by the addition of energy-dependent linewidths and bilayer splitting. Notable results include the use of Ni as a local probe for superconductivity, the lack of splitting from the bilayer of the quasiparticle resonances, and the independence of low-energy quasiparticles from bilayer splitting. Preliminary theoretical views of noise in tunnel junctions have been presented as well.
DTIC
*Superconductivity; High Temperature Superconductors; Scanning Tunneling Microscopy*

**20010120259** Argonne National Lab., IL USA
**Structure and property relationship in the mixed-conducting SR-Fe-Co-O system**
Ma, B.; May 18, 1998; 15p; In English
Report No.(s): DE2001-10561; ANL/ET/CP-95329; No Copyright; Avail: Department of Energy Information Bridge

Mixed-conducting ceramic oxides have potential uses in high-temperature electrochemical applications such as solid oxide fuel cells, advanced batteries, sensors, and oxygen-permeable membranes. The SR-Fe-Co-O system combines high electronic/ionic conductivity with appreciable oxygen permeability at elevated temperatures. Dense ceramic membranes made of this material can be used to separate high-purity oxygen from air without the need for external electrical circuitry, or to partially

oxidize methane to produce syngas. Samples of SR(sub 2)Fe(sub 3(minus)x)Co(sub x)O(sub y) (with x = 0, 0.6, 1.0, and 1.4) were prepared by solid-state reaction in atmospheres with various oxygen partial pressures (pO(sub 2)) and were characterized by X-ray diffraction, scanning electron microscopy, and electrical conductivity measurements. Phase components of the samples are dependent on cobalt concentration and synthesis pO(sub 2). Total conductivity increases with increasing temperature and cobalt content in the material. Higher ionic transference numbers have been observed in samples with lower cobalt contents. Current-voltage characteristics determined in a gas-tight cell indicate that a bulk effect, rather than a surface exchange effect, is the main limiting factor for oxygen permeation through membranes made of SR(sub 2)Fe(sub 2)CoO(sub y). Oxygen permeability measurements at various temperatures showed that oxygen permeability increases with increasing temperature, as expected. At 900 C, an oxygen permeation flux of 2.5 scc(center-dot)cm(sup (minus)2)(center-dot)min(sup (minus)1) was obtained for a SR(sub 2)Fe(sub 2)CoO(sub y) disk of 2.9 mm thickness.
NTIS
*Cobalt Oxides; Ceramics; Solid Oxide Fuel Cells*

**20010120260** Argonne National Lab., IL USA
**Cryocooler applications for high-temperature superconductor magnetic bearings**
Niemann, R. C.; May 22, 1998; 23p; In English
Report No.(s): DE2001-10552; ANL/ET/CP-95266; No Copyright; Avail: Department of Energy Information Bridge
The efficiency and stability of rotational magnetic suspension systems are enhanced by the use of high-temperature superconductor (HTS) magnetic bearings. Fundamental aspects of the HTS magnetic bearings and rotational magnetic suspension are presented. HTS cooling can be by liquid cryogen bath immersion or by direct conduction, and thus there are various applications and integration issues for cryocoolers. Among the numerous cryocooler aspects to be considered are installation; operating temperature; losses; and vacuum pumping.
NTIS
*Magnetic Bearings; Cryogenic Cooling; High Temperature Superconductors; Magnetic Suspension*

**20010120269** Sandia National Labs., Albuquerque, NM USA
**Particle Transport in Parallel-Plate Reactors**
Rader, D. J.; Geller, A. S.; Aug. 01, 1999; 100p; In English
Report No.(s): DE2001-10355; SAND99-1539; No Copyright; Avail: Department of Energy Information Bridge, Microfiche
A major cause of semiconductor yield degradation is contaminant particles that deposit on wafers while they reside in processing tools during integrated circuit manufacturing. This report presents numerical models for assessing particle transport and deposition in a parallel-plate geometry characteristic of a wide range of single-wafer processing tools: uniform downward flow exiting a perforated-plate showerhead separated by a gap from a circular wafer resting on a parallel susceptor. Particles are assumed to originate either upstream of the showerhead or from a specified position between the plates. The physical mechanisms controlling particle deposition and transport (inertia, diffusion, fluid drag, and external forces) are reviewed, with an emphasis on conditions encountered in semiconductor process tools (i.e., sub-atmospheric pressures and submicron particles). Isothermal flow is assumed, although small temperature differences are allowed to drive particle thermophoresis. Numerical solutions of the flow field are presented which agree with an analytic, creeping-flow expression for Re less than 4. Deposition is quantified by use of a particle collection efficiency, which is defined as the fraction of particles in the reactor that deposit on the wafer. Analytic expressions for collection efficiency are presented for the limiting case where external forces control deposition (i.e., neglecting particle diffusion and inertia). Deposition from simultaneous particle diffusion and external forces is analyzed by an Eulerian formulation; for creeping flow and particles released from a planar trap, the analysis yields an analytic, integral expression for particle deposition based on process and particle properties. Deposition from simultaneous particle inertia and external forces is analyzed by a Lagrangian formulation, which can describe inertia-enhanced deposition resulting from particle acceleration in the showerhead. An approximate analytic expression is derived for particle velocity at the showerhead exit as a function of showerhead geometry, flow rate, and gas and particle properties. The particle showerhead-exit velocity is next used as an initial condition for particle transport between the plates to determine whether the particle deposits on the wafer, as a function of shower-head-exit particle velocity, the plate separation, flow rate, and gas and particle properties. Based on the numerical analysis, recommendations of best practices are presented that should help tool operators and designers reduce particle deposition in real tools. These guidelines are not intended to replace detailed calculations, but to provide the user with a general feel for inherently-clean practices.
NTIS
*Particles; Deposition; Integrated Circuits; Numerical Analysis; Semiconductors (Materials)*

**20010120540** Argonne National Lab., IL USA

**Stresses in thermally grown alumina scales near edges and corners**

Grimsditch, M.; Jun. 03, 1998; 12p; In English

Report No.(s): DE2001-10677; ANL/MSD/CP-95844; No Copyright; Avail: Department of Energy Information Bridge

We have investigated the residual stress near edges and corners of thermally grown alumina scales. Micro-fluorescence measurements, performed on alloys with composition Fe-5Cr-28Al (at.%, bal. Fe) oxidized at 900 C, showed a large (>50%) reduction in hydrostatic stress in the vicinity of edges and corners. Surprisingly, stress relaxation persists out to distances ten times the scale thickness from the edge. Finite element analysis calculations confirm the experimental results and provide a considerably more detailed picture of the stress distribution and its components.

NTIS

*Aluminum Alloys; Stress Distribution; Aluminum Oxides; Edges; Corners*

**20010120544** Argonne National Lab., IL USA

**Growth of Alumina Scale on Fe-Cr-Al: A Multiprobe Study**

Veal, B. W.; Jun. 03, 1998; 14p; In English

Report No.(s): DE2001-10684; ANL/MSD/CP-95864; No Copyright; Avail: Department of Energy Information Bridge, Microfiche

The use of local probes at specific spatial locations provides a clear picture of the scale growth. The thermal evolution of the oxide scale on Fe(72)-Cr(18)-Al(10)-Hf(0.15) (at.%) has been investigated using a number of spectroscopic techniques. Well defined regions (approximately 70 mm in diameter) were probed by a battery of techniques as a function of oxidation at different temperatures (between 800-1100 C). This study provides information about the dependence of scale evolution on fluctuations in the local composition and/or grain structure of the starting material. Results suggest that properties of the starting material, which were not investigated in this study, strongly influence the scale evolution, even to the stage of mature scales.

NTIS

*Oxidation; Spectroscopy; Probes*

**20010120548** Argonne National Lab., IL USA

**Two-Dimensional Ferromagnetic Correlations Above Tc in the Naturally Layered CMR Manganite (La(2-2x)SR(1+2x))Mn2O7 (x = 0.3-0.4)**

Argyriou, D. N.; Mar. 23, 1998; 22p; In English

Report No.(s): DE2001-10689; ANL/MSD/CP-95904; No Copyright; Avail: Department of Energy Information Bridge, Microfiche

Neutron diffuse scattering in the form of rod-like features are observed in single crystals of the layered CMR material (La(2-2x)SR(1+2x)Mn2O7 (x=0.4,0.36), consistent with the presence of two dimensional ferromagnetic spin correlations. These diffuse features are observed over a wide temperature region, however, their coherence length does not appear to diverge at T(sub c), although there is evidence of the development of three-dimensional correlations around ferromagnetic reflections of the 3D-ordered magnetic structure close to T(sub c). Quasi-elastic neutron scattering on a ceramic sample of x = 0.3 shows that the lifetime of these ferromagnetic correlations increases at T going to T(sub c). They exhibit a spin-diffusion constant above T(sub c) of approximately 5 meV square angstroms, much lower than that reported for La(2/3)Ca(1/3)MnO3. We discuss the relationship of these magnetic correlations to models of the ferromagnetic transition in CMR compounds.

NTIS

*Correlation; Diffusion; Ferromagnetic Materials; Manganese Compounds; Neutron Scattering*

**20010120549** Argonne National Lab., IL USA

**Gravimeter Using High-Temperature Superconductor Bearing**

Hull, J. R.; Sep. 11, 1998; 16p; In English

Report No.(s): DE2001-10690; ANL/ET/CP-95921; No Copyright; Avail: Department of Energy Information Bridge, Microfiche

We have developed a sensitive gravimeter concept that uses an extremely low-friction bearing based on a permanent magnet (PM) levitated over a high-temperature superconductor (HTS). A mass is attached to the PM by means of a cantilevered beam, and the combination of PM and HTS forms a bearing platform that has low resistance to rotational motion but high resistance to horizontal, vertical, or tilting motion. The combination acts as a low-loss torsional pendulum that can be operated in any orientation. Gravity acts on the cantilevered beam and attached mass, accelerating them. Variations in gravity can be detected by time-of-flight acceleration, or by a control coil or electrode that would keep the mass stationary. Calculations suggest that the HTS

gravimeter would be as sensitive as present-day superconducting gravimeters that need cooling to liquid helium temperatures, but the HTS gravimeter needs cooling only to liquid nitrogen temperatures.
NTIS
*Gravimeters; High Temperature Superconductors; Superconducting Devices*

**20010120550** Argonne National Lab., IL USA
**Trapped-Flux Internal-Dipole Superconducting Motor/Generator**
Hull, J. R.; Sep. 03, 1998; 17p; In English
Report No.(s): DE2001-10691; ANL/ET/CP-95922; No Copyright; Avail: Department of Energy Information Bridge, Microfiche
A new class of motor/generator (M/G) utilizes the magnetic flux trapping capability of high-temperature superconductors (HTSs). The rotor consists of a cylindrical shell composed of HTS segments. These segments act as trapped-field magnets, magnetized in such a way that a dipole magnetic field is produced in the interior of the shell. A stator coil assembly is placed in the interior of the shell and current passing through the conductors of the coil produce a rotational torque, either as a hysteresis motor or as a synchronous motor. The coil may be either conventional, with copper wires and an iron core, or composed of superconductors and can be used to establish the trapped fields in the HTSs.
NTIS
*High Temperature Superconductors; Magnetic Flux; Superconductors (Materials); Superconducting Magnets*

**20010120789** Argonne National Lab., IL USA
**Oscillation period of the interlayer coupling in epitaxial Fe/1-xVx(100) and (211) superlattices**
You, C. Y.; Sep. 22, 1998; 14p; In English
Report No.(s): DE2001-10829; ANL/MSD/CP-96580; No Copyright; Avail: Department of Energy Information Bridge
The microscopic origin of the 18-(angstrom) period in the oscillatory interlayer exchange coupling of Fe/Cr( 100) and (211) superlattices is investigated by alloying the Cr spacer with V to alter its Fermi surface. The addition of V increases or decreases in size the various Fermi surface calipers that are candidates for governing the oscillation period, such as those that span the ellipse, lens, octahedron, and nested sheets. Epitaxial sputtered superlattices of (100) and (211) orientation were grown and characterized via magnetoresistance measurements as a function of spacer layer thickness for different V-doping levels. A small decrease of the oscillation period is found experimentally which strongly implicates the N-centered ellipse as the origin of the 18-(angstrom) period in Fe/Cr superlattices.
NTIS
*Epitaxy; Interlayers; Oscillations; Superlattices; Magnetoresistivity; Iron Alloys*

**20010120791** Argonne National Lab., IL USA
**Magnetic profile in Nb/Si superconducting multilayers**
Yusuf, S. M.; Feb. 04, 1999; 26p; In English
Report No.(s): DE2001-10826; ANL/MSD/CP-96574; No Copyright; Avail: Department of Energy Information Bridge
Polarized neutron reflectivity measurements were conducted on (Nb(100(angstrom)) /Si(15(angstrom)))xN superconducting multilayers with a T(sub c) (approximately) 7.5 K. Scope of the experiment was to verify the existence of arrays of vortices parallel to the surface above the critical field H(sub cl) = 400 Oe when a magnetic field was applied parallel to the film plane. Measurements at 1.6 K and 700 Oe in the zero-field-cooled condition, and at 30 Oe after field cooling, indicated that reflectivity close to the first Bragg reflection of the multilayer was significantly dependent on the neutron spin. This effect was interpreted as due to Josephson type vortices at and around the silicon layers.
NTIS
*Bragg Angle; Magnetic Fields; Silicon; Superconductivity*

**20010120793** Argonne National Lab., IL USA
**Novel structural phenomena at the maximum Tc in 123 and HgBa2CuO4 + Delta superconductors: Evidence for a structural response that competes with superconductivity**
Jorgensen, J. D.; Jun. 03, 1998; 12p; In English
Report No.(s): DE2001-10824; ANL/MSD/CP-96567; No Copyright; Avail: Department of Energy Information Bridge
Structural distortions that compete with superconductivity have been investigated in two systems where oxygen content can be used to vary the doping continuously from the under doped state, through the maximum T(sub c) into the over doped state. In the 123 system, (La(sub 1(minus)x)Ca(sub x))(Ba(sub 1.75(minus)x)La(sub 0.25+x))Cu(sub 3)O(sub 7+(delta)), the buckling of the CuO(sub 2) planes goes through a maximum at the maximum T(sub c). In HgBa(sub 2)CuO(sub 4+(delta)), where buckling

of the CuO(sub 2) planes is not available as a structural degree of freedom, there is a plateau at the maximum T(sub c) where the unit cell volume expands as oxygen is added while the charge transfer and T(sub c) remain constant. These unusual structural phenomena upon crossing through the maximum T(sub c) are hypothesized to be a response of the crystal structure to the electronic structure, with the structural distortions competing with superconductivity, or lowering the T(sub c) from what it would otherwise be.
NTIS
*Crystal Structure; Superconductors (Materials); Copper; Mercury (Metal); Barium; Chemical Reactions*

**20010120794** Argonne National Lab., IL USA
**Magnetic spiral structures in La/Fe multilayers**
Lohstroh, W.; Sep. 25, 1998; 12p; In English
Report No.(s): DE2001-10823; ANL/MSD/CP-96563; No Copyright; Avail: Department of Energy Information Bridge
The magnetic properties of La/Fe multilayers were tested by magneto-optical Kerr effect and polarized neutron reflectometry. The experiments indicated that above a layer thickness t(sub la) = 25(angstrom) the magnetic state of the virgin sample is represented by a spiral-like arrangement of magnetizations of subsequent Fe layers, whereas each Fe layer itself is ferromagnetic. Polarized neutron reflectometry shows that the helix has predominantly one chirality over the entire surface area of several cm(sup 2). Tine magnetic spiral structure is imprinted during the growth process by rotating the sample in a small residual magnetic field. External magnetic field of 90 Oe are sufficient to erase the magnetic structure irreversibly.
NTIS
*Ferromagnetic Materials; Iron; Lanthanum; Kerr Magnetooptical Effect; Chirality*

**20010121877** Argonne National Lab., IL USA
**Short Range Spin Correlations in the CMR Material La(1.4)SR(1.6)Mn2O7**
Kelley, T. M.; Mar. 23, 1998; 9p; In English
Report No.(s): DE2001-10687; ANL/MSD/CP-95884; No Copyright; Avail: Department of Energy Information Bridge, Microfiche
The La(sub 1-x)SR(sub x)3Mn2O7 compounds are layered materials that exhibit higher magneto-resistance than the corresponding three dimensional manganite perovskites. Quasi-elastic neutron scattering on a polycrystalline sample of La(sub 1.4)SR(sub 1.6)Mn2O7 shows that the spin fluctuation spectrum of the these layered CMR materials is qualitatively similar to those found in the perovskite manganites (La,Ca)MnO3; their concentration, lifetime, and coherence length increase as T decreases to T(sub c). Unlike the perovskites we find a lower spin-diffusion constant above T(sub c) of approximately 5 meV square angstroms.
NTIS
*Correlation; Elastic Scattering; Manganese Compounds; Perovskites; Spin*

**20010121882** Argonne National Lab., IL USA
**Measurement of the critical current and transient characteristics of a high-temperature superconductor tube using a pulsed current supply**
Cha, Y. S.; Aug. 27, 1998; 22p; In English
Report No.(s): DE2001-10671; ANL/ET/CP-95791; No Copyright; Avail: Department of Energy Information Bridge
The transient response of a melt-cast-processed BSCCO-2212 superconductor tube is investigated by using a pulsed current source. It was found that (1) the maximum induced current and the excitation current at field penetration increase with the maximum excitation current, and (2) there is a time delay between peak excitation current and peak magnetic field inside the superconductor. These observations can be explained by the concept of magnetic diffusion. The ac (alternating current) steady-state critical current of the superconductor was found to depend on the magnitude of the current increment. The critical current determined by using the pulsed current system agrees fairly well with the ac steady-state critical current determined by using relatively large current increment.
NTIS
*Critical Current; BSCCO Superconductors; Transient Response*

**20010121946** Los Alamos National Lab., NM USA
**Development of Meter-Long YBCO Coated Conductors Produced by Ion Beam Assisted Deposition and Pulsed Laser Deposition**
Foltyn, S. R.; Arendt, P. N.; Jan. 01, 2000; 7p; In English
Report No.(s): DE2000-763334; LA-UR-00-646; No Copyright; Avail: Department of Energy Information Bridge, Microfiche

A 'second-generation' of high T(sub c) conductors, consisting of YBCO coatings on flexible metal substrates, has recently reached a milestone with meter-long tapes capable of carrying over 100 A in a 1 cm width at liquid nitrogen temperature. Having reached this level of performance, however, we have encountered difficulties in the self-field characterization of such high current material. In particular, measurement of critical current uniformity along the tape length has in some cases resulted in damage to weaker tape segments during measurement of higher-current ones. to address this problem we have developed a novel measurement technique that uses permanent magnets to locally suppress the critical current of the tape section being measured to a level that is safe for the rest of the tape.
NTIS
*YBCO Superconductors; Critical Current*

**20010121964** Sandia National Labs., Albuquerque, NM USA
**GaN High Power Devices**
Pearton, S. J.; Ren, F.; Zhang, A. P.; Dang, G.; Cao, X. A.; Jul. 17, 2000; 17p; In English
Report No.(s): DE2000-761448; SAND2000-1869C; No Copyright; Avail: Department of Energy Information Bridge
A brief review is given of recent progress in fabrication of high voltage GaN and AlGaN rectifiers, GaN/AlGaN heterojunction bipolar transistors, GaN heterostructure and metal-oxide semiconductor field effect transistors. Improvements in epitaxial layer quality and in fabrication techniques have led to significant advances in device performance.
NTIS
*Gallium Nitrides; Metal Oxide Semiconductors; Fabrication; Heterojunctions; Aluminum Nitrides*

**20010121965** Argonne National Lab., IL USA
**Importance of Interlayer Effects for Tc in kappa-(ET)2 X Superconductors**
Muller, J.; Lang, M.; Schlueter, J. A.; Geiser, U.; Schweitzer, D.; Aug. 22, 2000; 4p; In English
Report No.(s): DE2000-761392; ANL/CHM/CP-102623; No Copyright; Avail: Department of Energy Information Bridge
We report high-resolution measurements of the linear thermal-expansion coefficient perpendicular to the conducting planes, (alpha)(perpendicular)(T), on single crystals of the superconductors (kappa)-(ET)(sub 2)X with X=I(sub 3), CU(NCS)(sub 2) and Cu(N(CN)(sub 2))Br. For all three compounds we find pronounced negative phase-transition anomalies at (Tc). Using the Ehrenfest relation, the uniaxial-pressure coefficients of (Tc) can be determined. We find that interlayer effects are of crucial importance for (Tc) in this class of materials. Regarding also interlayer effects we compare our results with recent theories addressing the p-T phase diagram.
NTIS
*Interlayers; Superconductors (Materials); Thermal Expansion; Anomalies; Phase Transformations*

**20010121967** Argonne National Lab., IL USA
**Interplane transport effects in layered organic conductors**
Symington, J. A.; Singleton, J.; Harrison, N.; Clayton, N.; Schlueter, J. A.; Aug. 22, 2000; 4p; In English
Report No.(s): DE2000-761272; ANL/CHM/CP-102622; No Copyright; Avail: Department of Energy Information Bridge
Detailed studies of the magnetic field orientation on magnetic quantum oscillations in two charge transfer salts of the molecule ET have been carried out. After all conventional mechanisms affecting quantum oscillations have been accounted for, we find that the amplitude of the oscillations has an underlying dependence exp((minus)(alpha) tan 0), where (theta) is the angle between the normal to the highly-conducting layers and the magnetic field, and a is a constant.
NTIS
*Magnetic Fields; Quantum Mechanics; Superconductors (Materials); Oscillations*

**20010121972** Los Alamos National Lab., NM USA
**Comparison of Buffer Layer Architectures on Continuously Processed YBCO Coated Conductors Based on the IBAD YSZ Process**
Holesinger, T. G.; Foltyn, S. R.; Sep. 19, 2000; 9p; In English
Report No.(s): DE2000-762850; LA-UR-00-4395; No Copyright; Avail: Department of Energy Information Bridge, Microfiche
The microstructures of continuously processed Yba2Cu3Oy (YBCO) coated conductors processed with three different architectures are presented. YBCO films were deposited directly on ion-beam-assisted deposition (IBAD) yttria-stabilized zirconia (YSZ) or on intervening layers of Y2O3 or CeO2. Different interfacial reactions were observed in each case. The volume changes that occur with the interfacial reactions were calculated based on the identified reaction products. The calculated volume

changes correlate with the in determining an optimal buffer layer system. The interfacial reactions do not preclude the attainment of high I(c) and J(c) values in these coated conductors.
NTIS
*Coatings; Conductors; Microstructure; Superconducting Films; YBCO Superconductors*

**20010121974** Los Alamos National Lab., NM USA
**Competing Quantum Orderings in Cuprate Superconductors: A Minimal Model**
Martin, I.; Ortiz, G.; Sep. 19, 2000; 8p; In English
Report No.(s): DE2000-762846; LA-UR-00-4406; No Copyright; Avail: Department of Energy Information Bridge, Microfiche
We present a minimal model for cuprate superconductors. At the unrestricted mean-field level, the model produces homogeneous superconductivity at large doping, striped superconductivity in the underdoped regime and various antiferromagnetic phases at low doping and for high temperatures. On the underdoped side, the superconductor is intrinsically inhomogeneous and global phase coherence is achieved through Josephson-like coupling of the superconducting stripes. The model is applied to calculate experimentally measurable ARPES spectra.
NTIS
*Cuprates; Superconductors (Materials); Mathematical Models; Superconductivity*

**20010122226** Argonne National Lab., IL USA
**Deposition of biaxially textured yttria-stabilized zirconia by ion-beam-assisted deposition**
Chudzik, M. P.; Sep. 17, 1998; 7p; In English
Report No.(s): DE2001-10705; ANL/ET/CP-95981; No Copyright; Avail: Department of Energy Information Bridge, Microfiche
Biaxially textured yttria (8 mol %)-stabilized zirconia (YSZ) thin films were deposited on randomly oriented Hastelloy C and Stainless Steel 304 at room temperature as a buffer layer for subsequent deposition of oriented YBa(sub 2)Cu(sub 3)O(sub x) films. The 0.16-1.3 (micro)m thick YSZ films were deposited by e-beam evaporation at rates of 1.2-3.2 (angstrom)/sec. Biaxially textured films were produced with an Ar/O(sub 2) ion beam directed at the substrate during film growth. X-ray diffraction was used to study in-plane and out-of-plane orientation as a function of ion-bombardment angle, film thickness, ion-to-atom flux ratio, and substrate material. In-plane and out-of-plane average-misorientation angles on these YSZ films that were deposited by ion-beam-assisted deposition were as low as 17 and 5.4(degree), respectively, on as-received substrates.
NTIS
*Deposition; Ion Beams; Thin Films; Steels; Electron Beams*

**20010122231** Argonne National Lab., IL USA
**Optical Properties of beta(sup 1) - (ET)2SF5CH2CF2SO3: A novel superconductor with large discrete counterions**
Dong, J.; Aug. 06, 1998; 4p; In English
Report No.(s): DE2001-10753; ANL/CHM/CP-96217; No Copyright; Avail: Department of Energy Information Bridge, Microfiche
The optical spectra of the organic superconductor (beta)(double prime)-(ET)(sub 2)SF(sub 5)CH(sub 2)CF(sub 2)SO(sub 3) are measured over a wide spectral range (30-35000 cm(sup (minus)1)) as a function of temperature and polarization. The optical anisotropy is quite large compared with other ET-based organic superconductors, and the spectra are far from Drude-like over the full temperature range. A broad electronic band centered near 1000 cm(sup (minus)1) is observed at low temperature along the a axis, prior to the superconducting transition. The changes of vibrational features near 120 K are attributed to a weak reorientation of the counterion, which may affect hydrogen bonding in the material.
NTIS
*Anisotropy; Optical Properties; Organic Superconductors*

**20010122242** Argonne National Lab., IL USA
**Layered manganites: Magnetic Structure at Extreme Doping Levels**
Mitchell, J. F.; Sep. 11, 1998; 17p; In English
Report No.(s): DE2001-10953; ANL/MSD/CP-97235; No Copyright; Avail: Department of Energy Information Bridge, Microfiche
We report powder neutron diffraction results on the crystal and magnetic structures of the bilayer Ruddlesden-Popper phase SR(sub 3)Mn(sub 2)O(sub 7(minus)(delta)) ((delta) = 0.0, 0.45) and correlate these structures with their magnetic and transport properties. The (delta) = 0.45 compound contains a large number of oxygen vacancies that are disordered in the MnO(sub 2) planes. As a result of this disordered vacancy structure, SR(sub 3)Mn(sub 2)O(sub 6.55) is a nonmagnetic insulator. SR(sub

3)Mn(sub 2)O(sub 7.0) ((delta) = 0) is an antiferromagnetic insulator whose magnetic structure is related to that of the SRMnO(sub 3) perovskite. Comparison of this end-member compound to its doped congeners in the La(sub 2(minus)2x)SR(sub 1+2x)Mn(sub 2)O(sub 7) series highlights the extreme sensitivity of magnetic structure to dopant concentration in these layered materials.
NTIS
*Manganese Compounds; Neutron Diffraction; Doped Crystals; Magnetic Properties*

**20010122264** Lawrence Livermore National Lab., Livermore, CA USA
**Surface Dynamics During Environmental Degradation of Crystal Surfaces**
De Yoreo, J.; Smolsky, I.; Apr. 03, 1999; 29p; In English
Report No.(s): DE2001-10791; UCRL-CR-134532; DP0202000; No Copyright; Avail: Department of Energy Information Bridge, Microfiche

The Final Report describes results of further investigation of nature of vicinal sectorality in potassium dihydrogen phosphate (KDP) crystals. Part 1 contains data of quantitative estimation of distinctions between the lattice parameters in the neighbor growth sectors and vicinal sectors of some rapidly grown KDP and deuterated KDP crystals. It demonstrates opportunities of the plane wave X-ray topography for quantitative characterization of crystals grown in known conditions. Part 2 gives description of some mechanisms of striations formation in which the vicinal sectorality takes an important part.
NTIS
*Crystal Surfaces; Crystals; Degradation; Surface Properties*

**20010122354** Oak Ridge National Lab., TN USA
**Fuzzy Logic Connectivity in Semiconductor Defect Clustering**
Gleason, S. S.; Kamowski, T. P.; Tobin, K. W.; Jan. 24, 1999; 9p; In English
Report No.(s): DE2001-10780; No Copyright; Avail: Department of Energy Information Bridge, Microfiche

In joining defects on semiconductor wafer maps into clusters, it is common for defects caused by different sources to overlap. Simple morphological image processing tends to either join too many unrelated defects together or not enough together. Expert semiconductor fabrication engineers have demonstrated that they can easily group clusters of defects from a common manufacturing problem source into a single signature. Capturing this thought process is ideally suited for fuzzy logic. A system of rules was developed to join disconnected clusters based on properties such as elongation, orientation, and distance. The clusters are evaluated on a pair-wise basis using the fuzzy rules and are joined or not joined based on a defuzzification and threshold. The system continuously re-evaluates the clusters under consideration as their fuzzy memberships change with each joining action. The fuzzy membership functions for each pair-wise feature, the techniques used to measure the features, and methods for improving the speed of the system are all developed. Examples of the process are shown using real-world semiconductor wafer maps obtained from chip manufacturers. The algorithm is utilized in the Spatial Signature Analyzer (SSA) software, a joint development project between Oak Ridge National Lab (ORNL) and SEMATECH.
NTIS
*Defects; Fuzzy Systems; Semiconductors (Materials); Wafers*

**20010122362** Argonne National Lab., IL USA
**Fermiology of the organic superconductor beta(sup 1) -(ET)2SF5CH2CF2SO3**
Wosnitza, J.; Jul. 29, 1998; 4p; In English
Report No.(s): DE2001-10757; ANL/CHM/CP-96266; No Copyright; Avail: Department of Energy Information Bridge, Microfiche

We present a detailed Fermi-surface (FS) investigation of the quasi two-dimensional (2D) organic superconductor (T(sub c) (approx) 4.5 K) (beta)(double prime)(ET)(sub 2)SF(sub 5)CH(sub 2)CF(sub 2)SO(sub 3). In line with previous investigations, de Haas-van Alphen measurements in pulsed fields up to 60 T show a single oscillation frequency, F(sub 0) = 200 T, which corresponds to a FS size of about 5% of the first Brillouin zone. Angular dependent magnetoresistance oscillations (AMROs) are utilized for the exact determination of the in-plane FS, which is found to be a strongly elongated ellipsoid with an axes ratio of about 1:9. Transport measurements in static fields up to 33 T show an unusual temperature dependence of the Shubnikov-de Haas (SdH) signal, i.e., a decrease of the SdH amplitude with decreasing temperature.
NTIS
*Organic Superconductors; Oscillations; Fermi Surfaces*

**20010122363** Argonne National Lab., IL USA

**Modeling coherent cherenkov radio emissions from high energy electromagnetic showers**

Schoessow, P.; Apr. 24, 1998; 15p; In English

Report No.(s): DE2001-10756; ANL-HEP-CP-98-35; No Copyright; Avail: Department of Energy Information Bridge, Microfiche

A technique currently under study for the detection of ultrahigh energy cosmic ray neutrinos involves the measurement of radio emissions from the electromagnetic shower generated by the neutrino in a large volume of naturally occurring dielectric such as the Antarctic ice cap or salt domes. The formation of an electron excess in the shower leads to the emission of coherent Cherenkov radiation, an effect similar to the generation of wakefields in dielectric loaded structures. We have used the finite difference time domain (FDTD) wakefield code ARRAKIS to model coherent Cherenkov radiation fields from high energy showers; we present as an example calculations of expected signals in a proof of principle experiment proposed for the Fermilab Main Injector.

NTIS

*Neutrinos; Cerenkov Radiation; Cosmic Ray Showers; Finite Difference Time Domain Method*

**20010122370** Argonne National Lab., IL USA

**Crystal phases, microstructure and surface chemistry of industry-relevant nanostructured metal oxides**

Loong, C. K., Argonne National Lab., USA; Apr. 17, 1998; 10p; In English

Report No.(s): DE2001-10744; ANL/IPNS/CP-96196; No Copyright; Avail: Department of Energy Information Bridge, Microfiche

Industries response keenly to two factors: the costs of materials and processing, and regulatory forces imposed by governments. The method of neutron scattering maybe applied to address these concerns. Slow (cold to epithermal) neutrons probe the organization and dynamic response of atomic nuclei and electrons in a substance thereby providing valuable knowledge toward the development of cost-effective means for materials preparation and possessing. Neutron facilities for basic research are funded by governments, thus these organizations are obliged to provide technical support to industries for the fulfillment of governmental policies. I hope to argue, based on these premises, the mutual beneficialness of a close collaboration between the industrial-research and neutron-scattering communities. In order to limit the scope of discussion, I shall illustrate the potential applications of neutron scattering for industrial problems by some recent studies of nanostructured metal-oxide catalysts.

NTIS

*Crystal Structure; Surface Properties; Microstructure; Neutron Scattering; Nanostructure (Characteristics); Metal Oxides*

**20010122380** Argonne National Lab., IL USA

**Advances in fabrication of Ag-clad Bi-2223 superconductors**

Balachandran, U.; Sep. 04, 1998; 8p; In English

Report No.(s): DE2001-10712; ANL/ET/CP-96010; No Copyright; Avail: Department of Energy Information Bridge, Microfiche

Powder-in-tube (PIT) processing was used to fabricate multifilamentary Ag-clad Bi(sub 2)SR(sub 2)Ca(sub 2)Cu(sub 3)O(sub y) (Bi-2223) superconductors for various electric power applications. Enhancements in the transport current properties of long lengths of multifilament tapes were achieved by increasing the packing density of the precursor powder, improving the mechanical deformation, and adjusting the cooling rate. The dependence of the critical current density on magnetic field and temperature for the optimally processed tapes was measured. J(sub c) was greater than 10(sup 4) (A/cm(sup 2)) at 20 K for magnetic field up to 3 T and parallel to the c-axis which is of interest for use in refrigerator coded magnets. An attempt was made to combine the good alignment of Bi-2223 grains in Ag-sheathed superconducting tapes to obtain high J(sub c) values at high temperature and low field, and good intrinsic pinning of YBa(sub 2)Cu(sub 3)O(sub 7(minus)d) (Y-123) thin film to maintain high J(sub c) values in high fields. A new composite multifilament tape was fabricated such that the central part contained Bi-2223 filaments, with the primary function of conducting the transport current. The central Bi-2223 filaments were surrounded by Y-123 thin film to shield the applied magnetic field and protect the Bi-2223 filaments. The J(sub c) values of the composite tape were better than those of an uncoated tape. In the case of 77 K applications, an I(sub c) of about 60 A was obtained in a 150 m long tape and zero applied magnetic field. In-situ strain characteristics of the mono- and multifilament tapes were conducted.

NTIS

*Fabrication; Critical Current; High Temperature; Superconductors (Materials); Superconductivity*

**20010122385** New Mexico Univ., Center for High Technology Materials, Albuquerque, NM USA

**Advanced RHEED Instrumentation for the Analysis of the Initial Stages of MBE Quantum Dot Growth for Semiconductor Lasers** ***Final Report, 17 Aor 2000-16 Apr. 2001***

Lester, Luke F.; Aug. 10, 2001; 4p; In English

Contract(s)/Grant(s): DAAD19-00-1-0139

Report No.(s): AD-A395259; 3-16651-FT; ARO-40879.1-EL-RIP; No Copyright; Avail: CASI; A01, Hardcopy; A01, Microfiche

The Staib Instruments EK-15-R RHEED System purchased on this DURIP grant has been mounted in the University of New Mexico's (UNM) Vacuum Generators VH80 MBE system and used extensively for RHEED studies during the growth of antimony-bearing semiconductors. The beam rocking feature in this unit has been critical in establishing the exact angle of incidence needed for clear observation of reconstruction patterns during the growth of bulk and digital alloy materials, and for the observation of RHEED oscillations to determine the precise growth rate. Observation of RHEED reconstruction patterns is particularly crucial in the growth of Digital Alloy (DA) materials. Arsenic-free GaInSb quantum well lasers for 2-5 nanometer applications were fabricated by growing a graded digital alloy AlInSb metamorphic buffer layer on GaSb to tailor the lattice constant The relaxation of the AlInSb DA buffer layer generates dislocations that are turned along the slip plane at strained heterojunctions. By increasing the number of heterojunctions, filtering of dislocations is possible. Below 200K the laser threshold was virtually constant, and a characteristic temperature T0 of 107K was found above 200K. This is the highest reported T0 for a semiconductor laser at this wavelength.

DTIC

*Semiconductor Lasers; Indium Antimonides; Molecular Beam Epitaxy*

**20010122660** National Academy of Sciences - National Research Council, Washington, DC USA

**Final progress report for the period 4/1/92 through 3/31/95 to the Department of Energy on the Solid State Sciences Committee (National Academy of Sciences - National Research Council)** ***Final Report, 1 Apr. 1992 - 31 Mar. 1995***

Sep. 30, 1995; 10p; In English

Report No.(s): DE2000-764577; No Copyright; Avail: Department of Energy Information Bridge, Microfiche

The Solid State Sciences Committee is a standing committee under the auspices of the Board on Physics and Astronomy, Commission on Physical Sciences, Mathematics, and Applications of the National Academy of Sciences-National Research Council. The SSSC is a multidisciplinary committee with membership drawn from universities, industry, government, and national laboratories. Its members' areas of expertise include condensed matter physics, solid state chemistry, and materials research aspects of ceramics, electronic materials, metallurgy, and polymers. The Committee is broadly representative of the community, providing perspective on issues that affect the progress and vitality of the materials sciences. A special effort has been made to ensure that the committee takes into account the roles in the field of both the science and engineering communities. The SSSC identifies and makes recommendations on issues of concern to the materials research, development, and applications community, particularly in connection with research opportunities, and provides guidance to federal agencies regarding their materials sciences research programs. Since its organization in 1971, the Committee's operating guidelines have included the following objectives: (1) to respond to requests for technical advice and assistance from federal agencies; (2) to initiate and oversee the conduct and publication of studies in the solid state sciences and its strong multidisciplinary connections to other fields of science and technology; (3) to act as an educational resource for the community of solid state scientists and materials scientists in the USA by identifying critical scientific issues and opportunities; and (4) to provide a forum for discussion among solid state and materials scientists and Washington policy makers. Several mechanisms are used to achieve these objectives. The Committee organizes and conducts special technical studies, surveys, workshops, and other meetings. It also functions as an oversight committee for ad hoc panels charged with the task of preparing reports on specific issues or topics. Symposia held at the National Academy of Sciences or at research centers have been used to focus attention on particular issues connected with facilities, programs, or other matters of concern to the community.

NTIS

*Semiconductors (Materials); Solid State; Research and Development*

**20010122672** Sandia National Labs., Albuquerque, NM USA

**Thick Sol-Gel Derived YBa2Cu3O7-x Films**

Dawley,; Clem,; Siegal,; Overmyer,; Rodriguez,; Sep. 21, 2000; 6p; In English

Report No.(s): DE2000-763141; SAND2000-2324C; No Copyright; Avail: Department of Energy Information Bridge, Microfiche

Sol-gel deposition of YBa2Cu3O7-8 (YBCO) holds great potential as a fast and efficient method of producing large-scale, biaxially-textured superconducting films at a lower cost than physical and chemical vapor deposition techniques. However, one difficulty in applying traditional sol-gel processing schemes, such as metal-organics (alkoxides, acetates, etc.) dissolved in alcohols, organic acids, and ethers, is the need for an organic pyrolysis step prior to YBCO crystallization to remove the bound carbonaceous species.
NTIS
*YBCO Superconductors; Sol-Gel Processes; Superconducting Films*

**20010122821** Los Alamos National Lab., NM USA
**Non-Magnetic Substrates for Low Cost YBCO Coated Conductors**
Thieme, C. L.; Annavarapu, S.; Sep. 01, 2000; 8p; In English
Report No.(s): DE2000-763930; LA-UR-00-4520; No Copyright; Avail: Department of Energy Information Bridge

CuNiAl and NiCr alloys were made and processed to non-magnetic bi-axially textured substrates. Epitaxial YSZ (Yttria-Stabilized Zirconia) and YBCO were deposited by pulsed laser deposition on the CuNiAl. Samples were cross sectioned and investigated with TEM (tunneling electron microscopy). It appears that Al forms a thin oxide layer at the CuNA surface that acts as a template for the subsequent YSZ layer. The 1.2 micrometer YBCO layer had a current density of 0.16MA/ at 75K and self field. On the NiCr substrates an Y(sub 2)O(sub 3) seed layer was deposited with E-beam evaporation, followed by RF (radio frequency) sputter deposition of YSZ and a CeO(sub 2) cap layer. These substrates were coated with a 0.4 YBCO layer using a trifluoroacetate process, a very cost effective metal-organic solution process. These samples carried critical currents exceeding 0.7MA/cm(sup 2) at 77K self field.
NTIS
*Substrates; Superconducting Devices; Pulsed Laser Deposition; YBCO Superconductors; Yttria-Stabilized Zirconia*

**20010122879** Argonne National Lab., IL USA
**Recent applications of the stochastic variational method**
Varga, K.; Oct. 20, 1998; 12p; In English
Report No.(s): DE2001-11051; ANL/PHY/CP-97470; No Copyright; Avail: Department of Energy Information Bridge, Microfiche

The stochastic variational method has proved to be useful in various fields of physics, including atomic, molecular, solid state, nuclear and subnuclear physics. This paper only reviewed a small part of the applications. Other contributions to this volume will show its usefulness in studies related to the structure of the baryons. Its main application is in nuclear physics, which has not been covered here but the interested reader can find examples in the references. We would like to extend its applicability to larger systems and for more complicated interactions. Such developments are under way. This paper overviews the most recent developments and applications of the stochastic variational method for different physical systems.
NTIS
*Stochastic Processes; Solid State; Nuclear Physics*

**20010122884** Argonne National Lab., IL USA
**Thermodynamic and nonstoichiometric behavior of promising Hi-Tc cuprate systems via EMF measurements: A short review**
Tetenbaum, M.; Feb. 24, 1999; 21p; In English
Report No.(s): DE2001-10975; ANL/CMT/CP-97336; No Copyright; Avail: Department of Energy Information Bridge, Microfiche

Electromotive force (EMF) measurements of oxygen fugacities as a function of stoichiometry have been made on the YBa(sub 2)Cu(sub 3)O(sub x), GdBa(sub 2)Cu(sub 3)O(sub x), NdBa(sub 2)Cu(sub 3)O(sub x) and bismuth cuprate systems in the temperature range (approximately)400-750 C by means of an oxygen titration technique with an yttria-stabilized zirconia electrolyte. The shapes of the 400 C isotherms as a function of oxygen stoichiometry for the Gd and Nd cuprate systems suggest the presence of miscibility gaps at values of x that are higher than those in the YBa(sub 2)Cu(sub 3)O(sub x) system. For a given oxygen stoichiometry, oxygen partial pressures above GdBa(sub 2)Cu(sub 3)O(sub x) and NdBa(sub 2)Cu(sub 3)O(sub x) are higher (above x=6.5) than that for the promising YBa(sub 2)Cu(sub 3)O(sub x) system. A thermodynamic assessment and intercomparison of our partial pressure measurements with the results of related measurements will be presented.
NTIS
*High Temperature Superconductors; Cuprates; Electromotive Forces; Stoichiometry; Yttria-Stabilized Zirconia; Copper Oxides; Thermodynamic Properties*

**20010122896** Argonne National Lab., IL USA

**Crystal field in the heavy fermion compound CeAl3**

Goremychkin, E. A.; Sep. 11, 1998; 17p; In English

Report No.(s): DE2001-10958; ANL/MSD/CP-97254; No Copyright; Avail: Department of Energy Information Bridge, Microfiche

Although the crystal field has a strong influence on the heavy fermion properties of CeAl(sub 3), the parameters of the crystal field Hamiltonian have not been established. We present the results of an analysis of inelastic neutron scattering data on CeAl(sub 3) to resolve this issue. by combining the neutron scattering results with measurements of the single crystal magnetic susceptibility, we have obtained an unambiguous set of crystal field parameters in CeAl(sub 3): B(sub 2)(sup 0) = (5.8 (+/-) 0.2) x 10(sup (minus)2) meV and B(sub 4)(sup 0) = (2.3 (+/-) 0.1) x 10(sup (minus)2) meV. The corresponding level scheme of the ground multiplet of the Ce(sup 3+) ion is characterized by a (Lambda)(sub 9) (vert-bar) (+/-) 3/2amp gt; ground state doublet and two close-lying excited doublets (Lambda)(sub 8) (vert-bar) (+/-) 5/2amp gt; and (Lambda)(sub 7) (vert-bar) (+/-) 1/2; at an energy of (approximately) 6.4 meV at 20 K. A comparison of the crystal field parameters along the RAl(sub 3) (R = Ce, Pr and Nd) series of isostructural compounds shows that in CeAl(sub 3), A(sub 2)(sup 0) r(sup 2); is an order of magnitude larger, and A(sub 4)(sup 0) R(sup 4); is three times larger, than in PrAl(sub 3) and NdAl(sub 3). These increases cannot be explained by changes in lattice parameters but are more likely to result from the enhancement of the hybridization of the cerium 4f electrons with the conduction electrons in CeAl(sub 3). This conclusion is in an agreement with the results of our study of the RCu(sub 2)Si(sub 2) series.

NTIS

*Crystal Field Theory; Heavy Fermion Systems; Inelastic Scattering; Magnetic Permeability; Neutron Scattering; Cerium Compounds*

**20010122897** Argonne National Lab., IL USA

**Inelastic neutron scattering study of the spin dynamics of Yb1-xLuxAl3**

Osborn, R.; Sep. 11, 1998; 17p; In English

Report No.(s): DE2001-10957; ANL/MSD/CP-97253; No Copyright; Avail: Department of Energy Information Bridge, Microfiche

We present the results of a systematic inelastic neutron scattering study of the spin dynamics of the mixed valent compound YbAl(sub 3) doped with nonmagnetic lutetium. The aim of the investigation is to clarify the origin of the unusual gap-like magnetic response observed in YbAl(sub 3), which can be modeled by two inelastic peaks: a narrow peak at 34 meV with HWHM, r = 6.4 (+/-) 0.8 meV and a broad peak at 44 meV with (Lambda) = 30 (+/-) 1 meV. Lutetium substitution leads to a substantial increase in the linewidth ((Lambda) = 9 (+/-) 1 meV at x = 0.1) and a decrease in the intensity (down by 60% at x = 0.1) of the narrow component, with a negligible effect on the broad inelastic peak. This trend is confirmed with higher doping resulting in the complete suppression of the narrow peak at x (ge) 0.35. The results indicate that the narrow component arises from coherent excitation processes within the hybridized 4f-band, which are destroyed by disorder, while the broad component is not so sensitive to the loss of coherence.

NTIS

*Doped Crystals; Inelastic Scattering; Spin Dynamics; Neutron Scattering; Superconductors (Materials)*

**20010122901** Princeton Univ., Plasma Physics Lab., NJ USA

**Performance Enhancement of Negative Ion Sources for the JT-60U Tokamak**

Oct. 27, 2000; 4p; In English

Report No.(s): DE2000-766456; CFPAPER-4267; No Copyright; Avail: Department of Energy Information Bridge

The negative ion based neutral beam system now operating for plasma heating and current drive on the large JT-60U tokamak marked the first application of negative ion source technology to the production of high current, high voltage beams for conversion to neutral atomic beams. This pioneering system has demonstrated the technical feasibility of negative ion based neutral beams for future fusion devices. Because this was a very large advance in the state of the art with respect to all system parameters, the principal physical processes governing the performance of the ion source and accelerator were somewhat different than had been the case with earlier much smaller negative ion sources. We have explored the physical mechanisms limiting the power and pulse length capability of these large sources, and have implemented ameliorating changes to reduce power loading on the accelerator grids and increase the transmitted power fraction.

NTIS

*Atomic Beams; Ion Beams; Ion Sources; Negative Ions*

**20010123046** Brookhaven National Lab., Upton, NY USA

**232U Content of Sapphire Material**

Kane, W. R.; Lemley, J. R.; Vanier, P. E.; Forman, L.; Jul. 18, 2000; 4p; In English

Report No.(s): DE2000-767151; BNL-67157; GJ1200; No Copyright; Avail: Department of Energy Information Bridge

Under Project Sapphire the governments of the USA and Kazahkstan arranged for the removal of high-enriched uranium (HEU) material from Kazahkstan to the USA as a nonproliferation measure. Brookhaven National Laboratory measured high-resolution gamma ray spectra (HRGS) of some of the Sapphire material in the same sealed containers in which it was transported from Kazahkstan. These measurements were made at BWX Technologies (Lynchburg, VA) shortly before the material was processed there for recovery of HEU. As a result of feeding reprocessed uranium to gaseous diffusion plants, U-232 may become preferentially concentrated in HEU. The very penetrating 2614-keV gamma ray associated with radioactive decay of a U-232 daughter can provide a signature of HEU that may be useful, for U-232 concentration relative to total uranium example, in arms control applications. The average for 20 samples of Sapphire material was 396 +/- 140 (one standard deviation) parts per trillion (10(exp 12)).

NTIS

*Gamma Ray Spectra; Sapphire; Concentration (Composition)*

**20010123066** Argonne National Lab., IL USA

**Simultaneous quasiparticle and Josephson tunneling in BSCCO-2212 break junctions**

Ozyuzer, L.; Oct. 27, 1998; 7p

Report No.(s): DE2001-11069; ANL/MSD/CP-97514; No Copyright; Avail: Department of Energy Information Bridge, Microfiche

Tunneling measurements are reported for superconductor- insulator-superconductor (SIS) break junctions on underdoped, optimally-doped, and overdoped single crystals of Bi2SR2CaCu2O(sub 8+(delta)) (Bi-2212). The junction I-V characteristics exhibit well-defined quasiparticle current jumps at eV =2A as well as hysteretic Josephson currents. The quasiparticle branch has been analyzed in the framework of d(sub x(sup 2)-y(sup 2)) (d-wave) superconductivity and indicates that there is preferential tunneling along the lobe directions of the d-wave gap. For overdoped Bi-2212 with T(sub c) = 62 K, the Josephson current is measured as a function of junction resistance, R(sub n), which varied by two orders of magnitude (1 k(Omega) to 100 k(Omega)). I(sub c)R(sub n) product is proportional to the 0.47 power of I(sub c) and displays a maximum of 7.0 mV. When thehole doping is decreased from overdoped (T(sub c) = 62 K) to the underdoped regime (T(sub c) = 70 K), the average I(sub c)R(sub n) product increases as does the quasiparticle gap. The maximum I(sub c)R(sub n) is (approximately) 40% of the (Delta)/e at each doping level,with a value as high as 25 mV in underdoped Bi-2212.

NTIS

*Superconductivity; Josephson Junctions; SIS (Superconductors); BSCCO Superconductors; Doped Crystals*

**20010123068** Argonne National Lab., IL USA

**Pinning effect on critical dynamics in Tl2Ba2CaCu2O8 films before and after introducing columnar defects**

Kim, J. T.; Oct. 27, 1998; 7p; In English

Report No.(s): DE2001-11066; ANL/MSD/CP-97511; No Copyright; Avail: Department of Energy Information Bridge, Microfiche

The effect of columnar defects on the critical dynamics of superconducting Tl2Ba2CaCa2O8 (Tl-2212) film has been investigated. The Tl-2212 film was irradiated at 0 C by 1.3 GeV U-ions along the normal of the film surface. The dose of 6.0 x 10(exp 10) ions/square cm of the U-ion irradiation corresponds to a matching field of 1.2 T. The in-plane longitudinal resistivity of the irradiated Tl-2212 has been measured as a function of magnetic field H and temperature T. The extracted fluctuation part of the conductivity (sigma)(sub xx)(T, H) of the unirradiated sample exhibits 3D-XY scaling behavior that reveals dynamic critical exponent z = 1.8 (+/-) 0.1 and static critical exponent v (approx) 1.338. The results indicate that the weak interlayer coupling along the c-axis of Tl-2212 significantly influences static critical exponent v and does not change dynamical critical exponent. After the irradiation, the fluctuation conductivities are enhanced by the strong pinnings and do not exhibit the same 3D-XY scaling behavior as for the unirradiated Tl-2212. Particularly at the low magnetic field values near the matching field of 1.2 T, the fluctuation conductivities show a clear deviation from the critical dynamics, suggesting that the pinning effect on the critical dynamics is significant.

NTIS

*Superconductivity; Superconducting Films; Crystal Defects*

**20010123070** Argonne National Lab., IL USA

**In situ spectroscopic ellipsometry as a surface sensitive tool to probe thin film growth**

Liu, C.; Feb. 19, 1999; 28p; In English

Report No.(s): DE2001-11063; ANL/XFD/CP-97499; No Copyright; Avail: Department of Energy Information Bridge, Microfiche

Sputtered thin film and multilayer x-ray mirrors are made routinely at the Advanced Photon Source (APS) for the APS users. Precise film growth control and characterization are very critical in fabricating high-quality x-ray mirrors. Film thickness calibrations are carried out using in situ and ex situ spectroscopic ellipsometry, interferometry, and x-ray scattering. to better understand the growth and optical properties of different thin film systems, we have carried out a systematic study of sputtered thin films of Au, Rh, Pg Pd, Cu, and Cr, using in situ ellipsometry. Multiple data sets were obtained in situ for each film material with incremental thicknesses and were analyzed with their correlation in mind. We found that in situ spectroscopic ellipsometry as a surface-sensitive tool can also be used to probe the growth and morphology of the thin film system. This application of in situ spectroscopic ellipsometry for metal thin film systems will be discussed.

NTIS

*Photons; Thin Films; X Rays; Mirrors; Ellipsometry*

**20010123092** Argonne National Lab., IL USA

**Influence of vortex pinning and grain boundary structure on critical currents across grain boundaries in YBa2Cu3Ox**

Miller, D. J.; Oct. 27, 1998; 7p; In English

Report No.(s): DE2001-11067; ANL/MSD/CP-97512; No Copyright; Avail: Department of Energy Information Bridge, Microfiche

We have used studies of single grain boundaries in YBCO thin films and bulk bicrystals to study the influence of vortex pinning along a grain boundary on dissipation. The critical current density for transport across grain boundaries in thin films is typically more than an order of magnitude larger than that measured for transport across grain boundaries in bulk samples. For low disorientation angles, the difference in critical current density within the grains that form the boundary can contribute to the substantial differences in current density measured across the boundary. However, substantial differences exist in the critical current density across boundaries in thin film compared to bulk bicrystals even in the higher angle regime in which grain boundary dissipation dominates. The differences in critical current density in this regime can be understood on the basis of vortex pinning along the boundary.

NTIS

*Critical Current; Grain Boundaries; Thin Films; Yttrium Oxides; Barium Oxides; Copper Oxides*

**20010123133** Brookhaven National Lab., Upton, NY USA

**Variable momentum compaction lattice studies**

Kramer, S.; Murphy, J. B.; Mar. 29, 1999; 5p; In English

Report No.(s): DE2000-767106; BNL-67691; KC0204011; No Copyright; Avail: Department of Energy Information Bridge

The VUV (Vacuum Ultraviolet) storage ring at the National Synchrotron Light Source was used to study the impact of changes in the momentum compaction factors over a large range from positive to negative values. Changes in bunch length and synchrotron tune were measured versus current and RF (radio frequency) parameters for these different lattices. by controlling both the first and second-order momentum compaction factors, a lattice was developed in which a pair of alpha buckets was created within the energy aperture of the vacuum chamber and beam was stored simultaneously in both buckets.

NTIS

*Compacting; Storage Rings (Particle Accelerators); Far Ultraviolet Radiation*

**20010123249** Old Dominion Univ., Norfolk, VA USA

**Dynamics of surface melting. Final report for period 1 September, 1993-30 April, 1996**

Elsayed-Ali, H. E.; Apr. 01, 1996; 230p; In English

Report No.(s): DE2001-762939; DOE/ER/45505-3; DOE/OR/45505-FIN; No Copyright; Avail: Department of Energy Information Bridge

The research supported by this DOE grant deals with the study of the dynamics of surface melting. Both conventional surface probes and picosecond time-resolved surface electron diffraction are used in our studies. The goal is to develop a better understanding of the nature of the order-disorder phase transformation that the top few atomic layers undergo with the increase

in temperature. We have studied the temperature induced disorder of the surface of single-crystals of metals and epitaxially grown metal thin films. In the following we summarize work performed on this grant.
NTIS
*Epitaxy; Melting; Electron Diffraction; Metal Films; Single Crystals*

**20010123255** Los Alamos National Lab., NM USA
**US DOE Grand Challenge in Computational Accelerator Physics**
Ryne, R.; Habib, S.; Qiang, J.; Ko, K.; Li, Z.; Mar. 01, 1998; 8p; In English
Report No.(s): DE2001-761619; LA-UR-98-4743; No Copyright; Avail: Department of Energy Information Bridge

Particle accelerators are playing an increasingly important role in basic and applied science, and are enabling new accelerator-driven technologies. But the design of next-generation accelerators, such as linear colliders and high intensity linacs, will require a major advance in numerical modeling capability due to extremely stringent beam control and beam loss requirements, and the presence of highly complex three-dimensional accelerator components. to address this situation, the U.S. Department of Energy has approved a 'Grand Challenge' in Computational Accelerator Physics, whose primary goal is to develop a parallel modeling capability that will enable high performance, large scale simulations for the design, optimization, and numerical validation of next-generation accelerators. In this paper we report on the status of the Grand Challenge.
NTIS
*Mathematical Models; Particle Accelerators; Computerized Simulation; Field Theory (Physics)*

**20010123428** Los Alamos National Lab., NM USA
**Development of a Fundamental Understanding of Chemical Bonding and Electronic Structure in Spinel Compounds**
Sickafus, K. E.; Wills, J. M.; Chen, S. P.; Terry, J. H.; Hartmann, T.; May 14, 1999; 61p; In English
Report No.(s): DE2001-763216; LA-UR-99-2227; No Copyright; Avail: Department of Energy Information Bridge

This is the final report of a three-year, Laboratory-Directed Research and Development (LDRD) project at the Los Alamos national Laboratory (LANL). Hundreds of ceramic compounds possess the spinel crystal structure and exhibit a remarkable variety of properties, ranging from compounds that are electrical insulators to compounds that are superconducting, or from compounds with ferri- and antiferromagnetic behavior to materials with colossal magnetoresistive characteristics. The unique crystal structure of spinel compounds is in many ways responsible for the widely varying physical properties of spinels. The objective of this project is to investigate the nature of chemical bonding, point defects, and electronic structure in compounds with the spinel crystal structure. Our goal is to understand and predict the stability of the spinel structure as a function of chemical composition, stoichiometry, and cation disorder. The consequences of cation disorder in spinel materials can be profound. The ferromagnetic characteristics of magnesioferrite, for instance, are entirely attributable to disorder on the cation sublattices. Our studies provide insight into the mechanisms of point defect formation and cation disorder and their effects on the electronic band structure and crystal structure of spinel-structure materials. our ultimate objective is to develop a more substantive knowledge of the spinel crystal structure and to promote new and novel uses for spinel compounds. The technical approach to achieve our goals is to combine first-principles calculations with experimental measurements. The structural and electronic properties of spinel samples were experimentally determined primarily with X-ray and neutron scattering, optical and X-ray absorption, and electron energy-loss spectroscopy. Total energy electronic structure calculations were performed to determine structural stability, band structure, density of states, and electron distribution. We also used shell-model total-energy calculations to assess point-defect formation and migration energies in magnesio-aluminate spinel.
NTIS
*Antiferromagnetism; Chemical Bonds; Crystal Structure; Electronic Structure; Spinel; Superconductivity; Cations*

**20010123453** Argonne National Lab., IL USA
**Measurement of oxygen disorder and nano-twin microstructure associated with columnar defects in YBCO**
Yan, Y.; Dec. 18, 1998; 9p; In English
Report No.(s): DE2001-11026; ANL/MSD/CP-96876; No Copyright; Avail: Department of Energy Information Bridge, Microfiche

Studies of defects generated by high energy (GeV) heavy ion irradiation in high-Tc superconductors have been performed by transmission electron microscopy (TEM). Our study shows that high dose irradiation leads to the formation of nano-twins, by which the columnar defects are connected. An analysis of the local Fourier components of the image intensity in (001) lattice images indicates that these new twin boundaries are much more diffuse than pre-existing twin boundaries in YBCO. The

mechanism of the formation of nano-twin boundaries on (l-brace)110(r-brace) planes and their possible relation to superconducting properties are discussed.
NTIS
*YBCO Superconductors; Ion Irradiation; Microstructure; Crystal Defects*

**20010123460** Lawrence Livermore National Lab., Livermore, CA USA
**Electronic sputtering of solids by slow, highly charged ions: fundamentals and applications**
Banks, J. C.; Barnes, A. V.; Doyle, B. L.; Hamza, A. V.; Machioane, G. A.; Jul. 20, 1999; 26p; In English
Report No.(s): DE2001-10998; UCRL-JC-133729; No Copyright; Avail: Department of Energy Information Bridge, Microfiche

Electronic sputtering in the interaction of slow (v<v(sub Bohr)), highly charged ions (SHCI) with solid surfaces have been subject of controversial discussions for almost 20 years. We review results from recent studies of total sputtering yields and discuss distinct microscopic mechanisms (such as defect mediated desorption, Coulomb explosions and effects of intense electronic excitation) in the response of insulators and semiconductors to the impact of SHCI. We then describe an application of ions like Xe(sup 44+) and Au(sup 69+) as projectiles in time-of-flight secondary ion mass spectrometry for surface characterization of semiconductors.
NTIS
*Sputtering; Ions; Solid Surfaces*

**20010123466** Argonne National Lab., IL USA
**Anisotropy of the sublattice magnetization and magnetoresistance in Co/Re superlattices on Al2O(1120)**
Charloton, T.; Sep. 29, 1998; 13p; In English
Report No.(s): DE2001-10985; ANL/MSD/CP-97361; No Copyright; Avail: Department of Energy Information Bridge, Microfiche

Co(20 (angstrom))/Re(6(angstrom))(sub 20) superlattices were grown on a (11(bar 2)0) surface of a Al2O3 single crystal, with the (0001) direction of their hcp structure in the plane of the film. The Co layers were found to be antiferromagnetically coupled (AF), with a saturating field of 6 kOe. Polarized neutron reflectivity was used to determine the direction of the sublattice magnetization. In zero applied field, the AF moments are aligned along the Co(0001) axis. In a magnetic field H perpendicular to the Co(0001) axis, the sublattices moments evolve to a canted arrangement, with the AF component always perpendicular to the field. With H along the Co(0001) axis, the AF moments flop in a direction perpendicular to Co(0001) axis. The spin flop transition is not abrupt, but can be described as a gradual rotation that is completed at 2 kOe. The anisotropy of the sublattice magnetization is related to the anisotropy of the magnetoresistance. This has the conventional dumbbell behavior with the field applied perpendicular to the Co(0001) axis, but exhibits an extended plateau near H = 0, and a slight increase up to H (approximately) 2 kOe, when H is parallel to Co(0001) axis.
NTIS
*Aluminum Oxides; Magnetization; Superlattices; Magnetoresistivity*

**20010123510** National Renewable Energy Lab., Golden, CO USA
**Studies of Band Structure and Free Carrier Scattering in Transparent Conducting Oxides Based on Combined Measurements of Electron Transport Phenomena**
Kaydanov, V. I.; Coutts, T. J.; Young, D. L.; Oct. 31, 2000; 23p; In English
Report No.(s): DE2000-767313; NREL/CP-520-29064; No Copyright; Avail: Department of Energy Information Bridge, Microfiche

Experimental methods are discussed for studying band structure, effective mass, and other electronic properties relevant to mobility, including scattering mechanisms, relaxation time, and the influence of grain boundaries (GBs) in polycrystalline transparent conducting oxide (TCO) films. Impedance spectroscopy permits evaluation of the GB potential barrier height and density-of-states. These studies enable an estimate of the limiting mobility achievable for practical transparent conducting oxides to be made. The equipment for measurement of the four transport coefficients is discussed, and examples of its application to films of ZnO, SnO2, and Cd2SnO4 are given.
NTIS
*Electrical Properties; Electron Transfer; Grain Boundaries; Scattering; Transparence; Transport Properties*

**20010123533** Argonne National Lab., IL USA

**Magnetic imaging of interlayer Josephson vortices**

Kirtley, J. A.; Jan. 15, 1999; 8p; In English

Report No.(s): DE2001-10913; ANL/CHM/CP-96989; No Copyright; Avail: Department of Energy Information Bridge, Microfiche

The authors have magnetically imaged interlayer Josephson vortices emerging parallel to the planes of single crystals of the organic superconductor (kappa)-(BEDT-TTF)(sub 2) Cu(NCS)(sub 2), and the single layer cuprate high-T(sub c) superconductors Tl(sub 2)Ba(sub 2)CuO(sub 6+(delta)) (Tl-2201) and (Hg,Cu)Ba(sub 2)CuO(sub 6+(delta)) (Hg-1201), using a scanning Superconducting Quantum Interference Device (SQUID) microscope. These images provide a direct measurement of the interlayer penetration depth, which is approximately 63 (micro)m for (kappa)-(BEDT-TTF)(sub 2) Cu(NCS)(sub 2), 18 (micro)m for Tl-2201 and 8 (micro)m for Hg-1201. The lengths for the cuprates are about a factor of 10 larger than originally predicted by the interlayer tunneling model for the mechanism of superconductivity in layered compounds, indicating that this mechanism alone cannot account for the high critical temperatures in these materials.

NTIS

*Cuprates; Organic Superconductors; Single Crystals; Josephson Effect; Imaging Techniques; Critical Temperature*

**20010123535** Argonne National Lab., IL USA

**Electron-phonon coupling in (kappa)-(BEDT-TTF)(sub 2)Cu(NCS)(sub 2) organic superconductor studied by Raman scattering spectroscopy**

Pedron, D.; Jul. 31, 1998; 6p; In English

Report No.(s): DE2001-10909; ANL/CHM/CP-96970; No Copyright; Avail: Department of Energy Information Bridge, Microfiche

Low frequency Raman data for (kappa)-(ET)(sub 2)Cu(NCS)(sub 2)(T(sub c) = 10.4 K) are reported. Measurements have been performed in a wide range of temperatures (1.5-100 K) and frequency hardening related to the superconducting transition has been observed for all the low-lying coupled phonons. The measured relative frequency shifts are lower than those previously reported for (kappa)-(ET)(sub 2)Cu(N(CN)(sub 2))Br (T(sub c) = 11.67 K), but the behavior of the two systems is similar and indicates a significant strength of the intermolecular electron-phonon coupling. The effects of isotopic substitutions ((sup 13)C(sub 4) (sup 34)S(sub 8) and (sup 2)H(sub 8)) in ET molecules on the low frequency Raman active phonons of (kappa)-(ET(sub 2)Cu(NCS)(sub 2)) are also reported. They give the first direct experimental confirmation to the suggested lattice softening induced by deuteration.

NTIS

*Thermodynamic Coupling; Electron Phonon Interactions; Organic Superconductors*

**20010123536** Argonne National Lab., IL USA

**Techniques for inelastic x-ray scattering with (mu)eV resolution**

Rohlsberger, R.; Oct. 23, 1998; 6p; In English

Report No.(s): DE2001-10907; ANL/XFD/CP-96959; No Copyright; Avail: Department of Energy Information Bridge, Microfiche

We introduce a novel type of spectrometer that provides a (micro)eV bandpass together with a tunability over a few meV. The technique relies on nuclear resonant scattering (Moessbauer effect) of synchrotrons radiation at the 14.4-keV resonance of (sup 57)Fe. Energy tuning is achieved by the Doppler effect in high speed rotary motion. The resonantly scattered monochromatic radiation is extracted by a polarization filtering technique or by spatial separation due to the nuclear lighthouse effect.

NTIS

*Monochromatic Radiation; X Ray Spectrometers; Inelastic Scattering; X Ray Spectroscopy; Resonance Scattering; Equipment Specifications*

**20010123537** Argonne National Lab., IL USA

**Vibrational density of states of thin films measured by inelastic scattering of synchrotron radiation**

Rohlsberger, R.; Sep. 18, 1998; 6p; In English

Report No.(s): DE2001-10906; ANL/XFD/CP-96955; No Copyright; Avail: Department of Energy Information Bridge, Microfiche

Vibrational spectra of thin films were measured by inelastic nuclear resonant scattering of synchrotrons radiation in grazing incidence geometry. A strong enhancement of the inelastic signal was obtained by designing the layer system as x-ray waveguide

and coupling the incident beam into a guided mode. This effect opens the possibility to study vibrational excitations in thin films that were so far impossible to obtain due to flux limitations.
NTIS
*Thin Films; Vibrational States*

**20010123628** National Renewable Energy Lab., Golden, CO USA
**Nanostructure of a-Si:H and Related Alloys by Small-Angle Scattering of Neutrons and X-Rays** ***Progress Report, May 22, 1999 - Aug. 21, 2000***
Williamson, D.; Oct. 30, 2000; 48p; In English
Report No.(s): DE2000-767314; NREL/SR-520-29121; No Copyright; Avail: Department of Energy Information Bridge, Microfiche

This report describes work being performed to provide details of the microstructure in high-quality hydrogenated amorphous and microcrystalline silicon and related alloys on the nanometer size scale. The materials under study are being prepared by current state-of-the-art deposition methods, as well as by new and emerging deposition techniques. The purpose is to establish the role of nanostructural features in controlling the opto-electronic and photovoltaic properties. The approach centers around the use of the uncommon technique of small-angle scattering of both X-rays (SAXS) and neutrons (SANS). SAXS has already been established as highly sensitive to microvoids and columnar-like microstructure. A major goal of this research is to establish how sensitive SANS is to the hydrogen nanostructure. Conventional X-ray diffraction techniques are being used to examine medium-range order and microcrystallinity, particularly near the boundary between amorphous and microcrystalline material.
NTIS
*Amorphous Silicon; Crystallinity; Microcrystals; Nanostructure (Characteristics); Scattering*

**20010123732** Argonne National Lab., IL USA
**Large NMR signals and polarization asymmetries**
Penttila, S. I.; Nov. 25, 1998; 11p; In English
Report No.(s): DE2001-11122; ANL-HEP-CP-98-135; No Copyright; Avail: Department of Energy Information Bridge, Microfiche

A large modulation in the series Q-meter can lead to nonlinear NMR signals and asymmetric polarization values. With a careful circuit analysis the nonlinearity can be estimated and corrections to polarization can be determined as a function of the strength of the modulation. We describe the recent LAMPF polarized proton target experiment, its NMR measurement and corrections to the measured polarizations.
NTIS
*Nuclear Magnetic Resonance; Polarization Modulation; Electric Networks; Network Analysis*

**20010123737** Argonne National Lab., IL USA
**Vortex melting and the liquid state in YBa2Cu3Ox**
Crabtree, G. W.; Nov. 18, 1998; 32p; In English
Report No.(s): DE2001-11110; ANL/MSD/CP-97683; No Copyright; Avail: Department of Energy Information Bridge, Microfiche

The experimental vortex phase diagram of YBa(sub 2)Cu(sub 3)O(sub x) is reviewed, with emphasis on first order vortex melting, the upper and lower critical points on the melting line, and the effect of disorder arising from twin boundary and point defect pinning.
NTIS
*Critical Point; Melting; Boundaries*

**20010123744** Argonne National Lab., IL USA
**Local topological and chiral properties of QCD**
de Forcrand, P.; Oct. 30, 1998; 5p; In English
Report No.(s): DE2001-11085; ANL-HEP-CP-98-65; No Copyright; Avail: Department of Energy Information Bridge, Microfiche

To elucidate the role played by instantons in chiral symmetry breaking, the authors explore their properties, in full QCD, around the critical temperature. They study in particular, spatial correlations between low-lying Dirac eigenmodes and instantons. Their measurements are compared with the predictions of instanton-based models.
NTIS
*Chirality; Quantum Chromodynamics; Broken Symmetry*

**20010123746** Argonne National Lab., IL USA
**Xe precipitates at grain boundaries in Al under 1 MeV electron irradiation**
Allen, C. W.; Oct. 23, 1998; 19p; edm226776; In English
Report No.(s): DE2001-11082; ANL/MSD/CP-97585; No Copyright; Avail: Department of Energy Information Bridge, Microfiche

Crystalline nanoprecipitates of Xe have been produced by ion implantation into mazed bicrystalline Al at 300 K, in which the matrix grain boundaries are mainly 90 deg tilt boundaries. Within Al grains, Xe nanocrystals are fee, isotactic with the Al and cuboctohedral in shape with (l brace)111(r brace) and (l brace)100(r brace) facets. With an off-axial imaging technique, the nanocrystals were structure imaged against a relatively featureless matrix background. In contrast to metal precipitates in Al, such as Pb, Xe precipitates straddling a matrix grain boundary are bicrystals as small as approximately 2 nm in diameter. Larger Xe precipitates tend to avoid boundaries which are inclined away from asymmetrical orientation and which thus have a significant twist component. Under the 1 MeV electron irradiation employed for HREM observation, small Xe nanocrystals near a grain boundary may migrate to the boundary and coalesce with other Xe precipitates. The structural observations are rationalized on a simple geometrical interpretation.
NTIS
*Grain Boundaries; Ion Implantation; Nanocrystals; Xenon*

**20010123747** Argonne National Lab., IL USA
**Influence of strain on the dielectric behavior of Ba, SR Ti1+xO3 thin films grown by LS-MOCVD on Pt/SiO2/Si**
Streiffer, S. K.; Oct. 14, 1998; 7p; In English
Report No.(s): DE2001-11043; ANL/MSD/CP-97459; No Copyright; Avail: Department of Energy Information Bridge

The strain state and its coupling to dielectric behavior have been investigated for (100) BST thin films deposited on Pt/SiO2/Si at 640 C. It is estimated from x-ray diffraction that the in-plane biaxial strain is approximately 0.7%. We postulate that this is of sufficient magnitude to confine any spontaneous polarization to the plane of the film. The thickness-corrected dielectric behavior perpendicular to the substrate for these samples shows evidence of coupling to such an in-plane phase transition at approximately 390K, as manifested by deviation from Curie-Weiss-like behavior at this temperature.
NTIS
*Metalorganic Chemical Vapor Deposition; Dielectric Properties; Thin Films*

**20010123762** Lawrence Livermore National Lab., Livermore, CA USA
**Electron field emission from undoped and doped DLC films**
Chakhovskoi, A. G.; EvtukhmAAKlyui, N. I.; Felter, T. E.; Kudzinocaky, S. Y.; Litovchenko, V. G.; Apr. 01, 1999; 8p; In English
Report No.(s): DE2001-11327; UCRL-JC-134060; No Copyright; Avail: Department of Energy Information Bridge

In this presentation the electron field emission and electrical conductivity of undoped and nitrogen doped DLC films have been investigated. Undoped and nitrogen doped DLC films were grown by PE CVD from CH4:H2 and CH4:H2:N2 gas mixtures, correspondingly. During nitrogen doped DLC film deposition, the nitrogen content in the gas mixture was varied within the range 0 to 45%. In-situ gas-phase doping allowed them to deposit DLC films with different content nitrogen. DLC films were deposited under three different levels of gas pressure in the chamber: 0.2, 0.6 and 0.8 Torr. The measurements of emission current from samples were performed in the vacuum system which could be pumped to a stable pressure of 10(sup (minus)6) Torr. The emission current was measured in the diode structure. The emitter-anode spacing L was constant and equal to 20 (micro)m. The current-voltage characteristics of the Si field electron emission arrays covered with undoped and nitrogen doped DLC films show that at the beginning the threshold voltage (V(sub th)) increases remarkably with nitrogen content, then V(sub th) is observed to decrease and finally V(sub th) increases. Corresponding Fowler-Nordheim (F-N) plots follow F-N tunneling over a wide range. The F-N plots were used for determination of the work functions, threshold voltage, field enhancement factors, and effective emission areas. For the qualitative explanation of experimental results, they treat the DLC film as a diamond-like (sp(sup 3)-bonds) matrix with graphite-like inclusions in it.
NTIS
*Electrical Resistivity; Electron Emission; Gas Pressure*

**20010123928** Argonne National Lab., IL USA

**Angular dependence of the Josephson critical current across c-axis twist junctions of layered superconductors**

Klemm, R. A.; Jul. 31, 1998; 14p; In English

Report No.(s): DE2001-10908; ANL/MSD/CP-96961; No Copyright; Avail: Department of Energy Information Bridge, Microfiche

The authors studied theoretically the c-axis Josephson critical current for bicrystals of high temperature superconductors twisted an angle (phi)(sub 0) about the c-axis with respect to each other. They used the effective Lawrence-Doniach models appropriate for the cases of pure s-wave or d(sub x(sup 2)-y(sup 2))-wave order parameters, and of a dominant d(sub x(sup 2)-y(sup 2))-wave order parameter combined with a subdominant one of either s-wave or d(sub xy)-wave form, as a function of the temperature and (phi)(sub 0). The results demonstrate that this new phase-sensitive experiment can serve as a very useful test of order parameter symmetry. In particular, the recent zero-field experiments in the vicinity of T(sub c) by Li et al. on c-axis twist junctions of Bi(sub 2)SR(sub 2)CaCu(sub 2)O(sub 8+(delta)) are very difficult to explain with a dominant d(sub x(sup 2)-y(sup 2))-wave order parameter.

NTIS

*Josephson Junctions; Bicrystals; Critical Current; High Temperature Superconductors; Proximity Effect (Electricity)*

**20010123930** Argonne National Lab., IL USA

**Thermodynamics of lattice QCD with massless quarks and chiral 4-fermion interactions**

Kogut, J. B.; Oct. 30, 1998; 5p; In English

Report No.(s): DE2001-11087; ANL-HEP-CP-98-101; No Copyright; Avail: Department of Energy Information Bridge, Microfiche

N(sub f) = 2 lattice QCD with massless quarks and a weak 4-fermion interaction appears to have the expected second order transition, at least for N(sub t) (ge) 6. More work is needed to clarify the N(sub t) = 4 case. With more statistics the N(sub t) = 6 simulations should produce an accurate determination of the critical exponent (beta)(sub m). Moving to finite mass at (beta) = (beta)(sub c) should allow an accurate determination of (sigma). Hadronic screening masses need further analysis. Other order parameters remain to be analyzed. Unfortunately, there is no obvious way to include 4-fermion interactions with full SU(2) x SU(2) chiral flavor symmetry.

NTIS

*Quantum Chromodynamics; Thermodynamics; Quarks*

**20010123961** Argonne National Lab., IL USA

**High-Spin States in As-71, Se-72, and Br-72**

Fotiades, N.; Aug. 25, 1998; 6p; In English

Report No.(s): DE2001-10929; ANL/PHY/CP-97066; No Copyright; Avail: Department of Energy Information Bridge

The O-16 + Ni-58 reaction was used to study yrast and non-yrast excitations in As-71, Se-72, and Br-72. High-spin yrast and negative-parity non-yrast bands were observed in Se-72. The F(sub 7/2) proton extruder orbital was identified in As-71. The odd-even staggering in the (pi)g(sub 9/2)(nu)g(sub 9/2) decoupled band in Br-72 is compared with similar structures in heavier Br isotopes.

NTIS

*Arsenic Isotopes; Bromine Isotopes; Particle Spin; Radioactive Isotopes*

**20010123963** Argonne National Lab., IL USA

**Enhancement of Critical Currents in (Bi,Pb)2SR2Ca2Cu3O(y) (Bi-2223) Superconducting Tapes**

Balachandran, U.; Nov. 11, 1998; 7p; In English

Report No.(s): DE2001-10926; ANL/ET/CP-97046; No Copyright; Avail: Department of Energy Information Bridge

The performance of (Bi,Pb)2SR2Ca2Cu3O(y) (Bi-2223) superconducting tapes in magnetic fields at 77 K is critical for winding this material into high-field magnets. We have recently enhanced the transport current (I(sub c)) of multifilament Ag-clad Bi-2223 tapes in a self-field at 77 K by increasing the packing density of the precursor powder improving the mechanical deformation, optimizing the conductor design, and adjusting the cooling rate. I(sub c) values of 40 A were obtained repeatedly. However, a transport current of 42 A in a self-field declined to 4 A in a 0.2 T magnetic field applied parallel to the c-axis at 77 K. A new composite tape was then fabricated in which a YBa2Cu3O(7-delta) (Y-123) film was deposited on the top of the Ag-sheathed Bi-2223 tape to shield the applied magnetic field and protect the central Bi-2223 filaments. Magnetization measurements showed that the critical current densities of the Y-123-coated, Ag-sheathed Bi-2223 tapes were higher than those

of an uncoated tape. These preliminary results may provide the basis for further improving the processing of long-length Bi-2223 tapes for high-field applications.
NTIS
*Critical Current; Current Density; Magnetic Fields; Superconductivity; YBCO Superconductors*

**20010124065** Meyer Tool and Mfg. Co., Inc., Oak Lawn, IL USA
**Cost Reduction for Production of Superconducting Niobium Cavities** ***Final Report***
Meyer, F. J.; Apr. 23, 1998; 11p; In English
Report No.(s): DE2001-761126; DOE/ER82431; No Copyright; Avail: Department of Energy Information Bridge, Microfiche

Nine-cell superconducting niobium radio-frequency cavities are used in Linear Colliders. The current manufacturing processes for fabrication of nine-cell niobium cavities requires the deep drawing of eighteen half cells and nineteen electron beam welds. The manufacturing operations required to prepare the half cells for electron beam welding are labor intensive and expensive. Cost reductions in cavity fabrication would provide substantial savings and increase the economic viability of numerous Scientific Research Projects. This project investigated the feasibility of substantially reducing fabrication costs through the use of a spinning manufacturing process that would ultimately result in the fabrication of three-cell cavities. Fabrication of three-cell cavities would substantially reduce cost by reducing the number of electron beam welds and associated machining weld preparations from nineteen to four. The major goal of this investigation was to demonstrate that multi-cell cavities could be produced by spinning. Important spinning process parameters were developed. One and two cell cavities were successfully spun. Problems with the developing process were identified and solutions requiring further investigation were developed. Requirements for continuation of efforts to develop a spinning process to consistently achieve uniform thickness in the niobium material and a smooth surface finish without inclusions or tears were determined.
NTIS
*Superconductivity; Niobium; Cavities*

**20010124141** Argonne National Lab., IL USA
**Role of selected f ions in the suppression of high-Tc superconductivity**
Soderholm, L.; Sep. 25, 1998; 41p; In English
Report No.(s): DE2001-10976; ANL/CHM/CP-97337; No Copyright; Avail: Department of Energy Information Bridge, Microfiche

The initial observations of superconductivity at temperatures above 77 K in copper-oxide based materials was surprising from a variety of different perspectives. Among the unexpected findings were reports of superconductivity for the series RBa2Cu3O7 where R is a rare earth (Y, Nd-Tm), which may carry a large, local magnetic moment. Superconductivity was subsequently demonstrated for all 4f analogs in this series except Ce, Pr, and Tb. In addition to the RBa2Cu3O7 series, there are several other CuO based series of superconductors that are formed by substituting R ions. The most studied of these are listed in a table, together with the f ions that form isostructural compounds and their superconducting critical temperatures (T(sub c)). The presence of an R ion with a large magnetic moment does not significantly influence the superconductivity. In contrast, even the presence of small concentrations of magnetic impurity ions in a conventional superconductor inhibits superconductivity by interfering with the formation of Cooper pairs. Most R ions substitute into an isostructural series with no observable effect on the superconducting properties of the material. As can be seen from the presented table, there are notable exceptions to this observation. In particular, the rare-earth ions Ce, Pr, and Tb, together with the 5f-actinide ions Am and Cm, sometimes behave anomalously. These ions either do not form an isostructural phase, or if the phase forms it may not be superconducting. The fact that an f-ion can suppress superconductivity is clearly demonstrated in the isostructural series Y(sub 1(minus)x)Pr(sub x)Ba2Cu3O7 (0 < x < 1)(sup 3), in which the critical temperature decreases with increasing x, such that for concentrations of Pr greater than x (approx) 0.5, the samples no longer superconduct.
NTIS
*High Temperature Superconductors; Superconductivity; Copper Oxides; Rare Earth Elements*

**20010125002** Sandia National Labs., Albuquerque, NM USA
**Distributed Sensing and Shape Control of Piezoelectric Bimorph Mirrors**
Redmond, J. M.; Barney, P. S.; Henson, T. D.; Jul. 28, 1999; 10p; In English
Report No.(s): DE2001-9676; SAND99-1974C; No Copyright; Avail: Department of Energy Information Bridge, Microfiche

As part of a collaborative effort between Sandia National Laboratories and the University of Kentucky to develop a deployable mirror for remote sensing applications, research in shape sensing and control algorithms that leverage the distributed nature of electron gun excitation for piezoelectric bimorph mirrors is summarized. A coarse shape sensing technique is developed

that uses reflected light rays from the sample surface to provide discrete slope measurements. Estimates of surface profiles are obtained with a cubic spline curve fitting algorithm. Experiments on a PZT bimorph illustrate appropriate deformation trends as a function of excitation voltage. A parallel effort to effect desired shape changes through electron gun excitation is also summarized. A one dimensional model-based algorithm is developed to correct profile errors in bimorph beams. A more useful two dimensional algorithm is also developed that relies on measured voltage-curvature sensitivities to provide corrective excitation profiles for the top and bottom surfaces of bimorph plates. The two algorithms are illustrated using finite element models of PZT bimorph structures subjected to arbitrary disturbances. Corrective excitation profiles that yield desired parabolic forms are computed, and are shown to provide the necessary corrective action.
NTIS
*Algorithms; Mirrors; Piezoelectricity; Remote Sensing; Shape Control; Spline Functions*

**20010125021** Argonne National Lab., IL USA
**Simple method for simulation of coherent synchrotron radiation in a tracking code**
Borland, M.; Aug. 15, 2000; 5p; In English
Report No.(s): DE2000-764211; LS-286; No Copyright; Avail: Department of Energy Information Bridge
Coherent synchrotron radiation (CSR) is of great interest to those designing accelerators as drivers for free-electron lasers (FELs). Although experimental evidence is incomplete, CSR is predicted to have potentially severe effects on the emittance of high-brightness electron beams. The performance of an FEL depends critically on the emittance, current, and energy spread of the beam. Attempts to increase the current through magnetic bunch compression can lead to increased emittance and energy spread due to CSR in the dipoles of such a compressor. The code elegant was used for design and simulation of the bunch compressor for the Low-Energy Undulator Test Line (LEUTL) FEL at the Advanced Photon Source (APS). In order to facilitate this design, a fast algorithm was developed based on the 1-D formalism of Saldin and coworkers. In addition, a plausible method of including CSR effects in drift spaces following the chicane magnets was developed and implemented. The algorithm is fast enough to permit running hundreds of tolerance simulations including CSR for 50 thoUSAnd particles. This article describes the details of the implementation and shows results for the APS bunch compressor.
NTIS
*Coherent Radiation; Computerized Simulation; Algorithms; Synchrotron Radiation; Photons*

**20010125063** Argonne National Lab., IL USA
**Measurement and calculation of PZT thin film longitudinal piezoelectric coefficients**
Christman, J. A.; Kim, S. H.; Kingon, A. I.; Maiwa, H.; Maria, J. P.; Apr. 26, 1999; 10p; In English
Report No.(s): DE2001-11777; ANL/MSD/CP-98896; No Copyright; Avail: Department of Energy Information Bridge
The ferroelectric and piezoelectric properties of 2000 (angstrom) thick chemical solution deposited Pb(Zr(sub x)Ti(sub 1 - x))O3 (PZT) thin films were investigated. Several Zr/Ti ratios were studied: 30/70, 50/50 and 65/35, which correspond to tetragonal, near-morphotropic, and rhombohedral symmetries. In all samples, a (l-brace)111(r-brace)-texture is predominant. Longitudinal piezoelectric coefficients and their dc field dependence were measured using the contact AFM method. The expected trend of a maximum piezoelectric coefficient at or near to the MPB was not observed. The composition dependence was small, with the maximum d(sub 33) occurring in the tetragonal material. to explain the results, crystallographic texture and film thickness effects are suggested. Using a modified phenomenological approach, derived electrostrictive coefficients, and experimental data, d(sub 33) values were calculated. Qualitative agreement was observed between the measured and calculated coefficients. Justifications of modifications to the calculations are discussed.
NTIS
*Thin Films; Ferroelectricity; Piezoelectricity*

**20010125088** Sandia National Labs., Albuquerque, NM USA
**Experiment-Based Computational Investigation of Thermomechanical Stresses in Flip Chip BGA Using the ATC4.2 Test Vehicle**
Burchett, S. N.; Nguyen, L.; Peterson, D. W.; Sweet, J. N.; Aug. 02, 1999; 11p; In English
Report No.(s): DE2001-9685; SAND99-1999C; No Copyright; Avail: Department of Energy Information Bridge, Microfiche
Stress measurement test chips were flip chip assembled to organic BGA substrates containing micro-vias and epoxy build-up interconnect layers. Mechanical degradation observed during temperature cycling was correlated to a damage theory developed based on 3D finite element method analysis. Degradation included die cracking, edge delamination and radial fillet cracking.
NTIS
*Chips; Finite Element Method; Stress Measurement; Test Vehicles; Degradation; Thermodynamics*

**20010125095** Sandia National Labs., Albuquerque, NM USA

**Optically-Activated GaAs Switches for Ground Penetrating Radar and Firing Set Applications**

Aurand, J.; Brown, D. J.; Carin, L.; Denison, G. J.; Helgeson, W. D.; Jul. 14, 1999; 6p; In English

Report No.(s): DE2001-8995; SAND99-0116C; No Copyright; Avail: Department of Energy Information Bridge, Microfiche

Optically activated, high gain GaAs switches are being tested for many different applications. TWO such applications are ground penetrating radar (GPR) and firing set switches. The ability of high gain GaAs Photoconductive Semiconductor Switches (PCSs) to deliver fast risetime pulses makes them suitable for their use in radars that rely on fast impulses. This type of direct time domain radar is uniquely suited for the detection of buried items because it can operate at low frequency, high average power, and close to the ground, greatly increasing power on target. We have demonstrated that a PCSs based system can be used to produce a bipolar waveform with a total duration of about 6 ns and with minimal ringing. Such a pulse is radiated and returns from a 55 gallon drum will be presented. For firing sets, the switch requirements include small size, high current, dc charging, radiation hardness and modest longevity. We have switched 1 kA at 1 kV and 2.8 kA at 3 kV dc charge.

NTIS

*Gallium Arsenides; Ground Penetrating Radar; Photoconductivity; Switches; Semiconductors (Materials)*

**20010125112** Helsinki Univ. of Technology, Electromagnetics Lab., Espoo, Finland

**Analytical Classification of the Time and Frequency Dependence Basics in Dielectric Materials**

Sengoer, T.; November 2000; 28p; In English; Prepared in cooperation with Yildiz Technical University, Istanbul, Turkey, Dept. of Electronics and Communications Engineering

Report No.(s): PB2001-107370; Copyright; Avail: National Technical Information Service (NTIS)

This paper contributes new perspectives including convenient transformations for waves in dispersive materials and covers most types of structures. Some conditions related with the constitutive parameters put some limits on calculations. Formalisms in literature use some extra extensions to overcome the analytical difficulties related with the application of Fourier transform. All of known extensions accept certain discontinuities postulated in time domain. Although, frequency domain characteristic has pole singularities at certain frequencies such a sharp discontinuity may not be acceptable in discussions related with physical point of view. For example, if we want to explain the discontinuity of time domain susceptibility for Debye materials then we have to discuss the generation of the material in atomic level since the susceptibility is not an effect of external sources. We consider solving such inconveniences by giving the constitutive relations of a time varying and dispersive medium by convenient transformations. We give the exact definitions of medial parameters by these transformations.

NTIS

*Dielectrics; Time Dependence; Frequency Distribution; Fourier Transformation; Discontinuity*

**20010125243** Argonne National Lab., IL USA

**Toward crystal design in organic conductors and superconductors**

Geiser, U.; Apr. 23, 1999; 18p; In English

Report No.(s): DE2001-11769; ANL/CHM/CP-98831; No Copyright; Avail: Department of Energy Information Bridge

We have seen that many different types of intermolecular interactions in organic conducting cation radical salts. Hydrogen bonding between the donor molecules and the anions is weak but not negligible. The ionic Madelung energy is insufficient to completely intersperse anions and cations, thus the layers favored by the van der Waals interactions remain intact. The search for new conducting and superconducting salts has been mainly by trial-and-error methods, even though simple substitutions have been employed in order to obtain isostructural analogs of successful (e.g., superconducting) salts. However, even seemingly minor substitutions sometimes destroy the packing type, and different crystal structures result. Simulations with the aim at predicting crystal structures have not succeeded, mainly because the different interaction types are of comparable energy, and the delocalized and partial charges render the calculations of the ionic terms extremely unreliable. Clearly, the development of suitable crystal modeling techniques with predictive capabilities is one of the great needs of the field.

NTIS

*Crystal Structure; Molecular Interactions; Organic Superconductors; Superconductors (Materials)*

**20010125395** Argonne National Lab., IL USA

**Advances in processing of Ag-sheathed (Bi,Pb)(sub 2)SR2Ca2Cu3O(sub x) superconductors**

Balachandran, U.; Eror, N. G.; Haldar, P.; Lelovic, M.; Mar. 05, 1998; 9p; In English

Report No.(s): DE2001-8124; ANL/ET/CP-94379; No Copyright; Avail: Department of Energy Information Bridge, Microfiche

Advances in the processing and fabrication of Ag-sheathed (Bi,Pb)(sub 2)SR2Ca2)Cu3O(sub x) (Bi-2223) high-T(sub c) superconductors by the powder-in-tube technique continue to bring this material closer to commercial applications. Enhancement

of the transport critical current density (J(sub c)) of Ag-sheathed Bi-2223 tapes was achieved by increasing the packing density of the precursor powder, improving mechanical deformation, and adjusting the cooling rate. Long lengths (greater than 150 m) of multifilamentary Bi-2223 tapes have been fabricated and carry critical currents (I(sub c)) of greater than 50 A (J(sub c) (approx) 25 kA/square cm) at 77 K in self-field. A 1260-m-long tape carried an I(sub c) of 18 A (J(sub c) (approx) 12 kA/square cm) from end-to-end. Several prototype coils have been assembled from these long-length tapes. Recent progress in the fabrication of Bi-2223 tapes is presented in this paper.
NTIS
*High Temperature Superconductors; Silver*

**20010125405** Argonne National Lab., IL USA
**Magnetic properties of Dy in Pb2SR2DyCu3O8**
Movshovich, R.; Skanthakumar, S.; Soderholm, L.; Jul. 02, 1999; 18p; In English
Report No.(s): DE2001-11803; ANL/CHM/CP-99005; No Copyright; Avail: Department of Energy Information Bridge

Superconductivity can be induced at high temperatures in Pb2SR2RCu3O8 (R - rare earth) by partially doping Ca(sup 2+) for R(sup 3+). In order to understand the interplay between magnetism and superconductivity, the magnetic properties of the parent compounds, Pb2SR2RCu3O8, have been studied. The work presented here includes magnetic susceptibility and specific heat measurements on R = Dy and extends our previous studies on R = Ce, Pr, Tb, Ho and Er. Specific heat experiments suggest that the Dy ions order antiferromagnetically with an ordering temperature of 1.3K. The magnetic susceptibility data are in good agreement with the susceptibility calculated using crystal field parameters that are extrapolated from previous modeling of the R = Er and Ho analogs of this series.
NTIS
*Magnetic Properties; Superconductivity; Dysprosium*

**20010125416** Argonne National Lab., IL USA
**Phase-space quantization of field theory**
Curtright, T.; Zachos, C.; Apr. 20, 1999; 16p; In English
Report No.(s): DE2001-11761; ANL-HEP-CP-99-06; No Copyright; Avail: Department of Energy Information Bridge, Microfiche

In this lecture, a limited introduction of gauge invariance in phase-space is provided, predicated on canonical transformations in quantum phase-space. Exact characteristic trajectories are also specified for the time-propagating Wigner phase-space distribution function: they are especially simple, indeed, classical, for the quantized simple harmonic oscillator. This serves as the underpinning of the field theoretic Wigner functional formulation introduced. Scalar field theory is thus reformulated in terms of distributions in field phase-space. This is a pedagogical selection from work published and reported at the Yukawa Institute Workshop 'Gauge Theory and Integrable Models', 26-29 January, 1999.
NTIS
*Canonical Forms; Gauge Theory; Field Theory (Physics); Distribution (Property); Quantum Theory*

**20010125425** Argonne National Lab., IL USA
**Construction and testing of an 11.4 GHz dielectric structure based travelling wave accelerator**
Gai, W.; Konecny, R.; Wong, T.; Zou, P.; Mar. 26, 1999; 5p; In English
Report No.(s): DE2001-11746; ANL-HEP-CP-99-31; No Copyright; Avail: Department of Energy Information Bridge, Microfiche

One major challenge in constructing a dielectric loaded traveling wave accelerator powered by an external rf (radio frequency) power source is the difficulty in achieving efficient coupling. In this paper, we report that we have achieved high efficiency broadband coupling by using a combination of a tapered dielectric section and a carefully adjusted coupling slot. We are currently constructing an 11.4 GHz accelerator structure loaded with a permitivity=20 dielectric. Bench testing has demonstrated a coupling efficiency in excess of 95% with bandwidth of 600 MHz. The final setup will be tested at high power at SLAC (Stanford Linear Accelerator Center) using an X-band klystron rf source.
NTIS
*Dielectrics; Linear Accelerators; Traveling Waves*

**20010125446** Sandia National Labs., Albuquerque, NM USA

**Wafer Fusion for Integration of Semiconductor Materials and Devices**

Choquette, K. D.; Geib, K. M.; Hou, H. Q.; Allerman, A. A.; Kravitz, S.; May 01, 1999; 36p; In English

Report No.(s): DE2001-8371; SAND99-0923; No Copyright; Avail: Department of Energy Information Bridge, Microfiche

We have developed a wafer fusion technology to achieve integration of semiconductor materials and heterostructures with widely disparate lattice parameters, electronic properties, and/or optical properties for novel devices not now possible on any one substrate. Using our simple fusion process which uses low temperature (400-600 C) anneals in inert N(sub 2) gas, we have extended the scope of this technology to examine hybrid integration of dissimilar device technologies. As a specific example, we demonstrate wafer bonding vertical cavity surface emitting lasers (VCSELs) to transparent AlGaAs and GaP substrates to fabricate bottom-emitting short wavelength VCSELs. As a baseline fabrication technology applicable to many semiconductor systems, wafer fusion will revolutionize the way we think about possible semiconductor devices, and enable novel device configurations not possible by epitaxial growth.

NTIS

*Electrical Properties; Lattice Parameters; Optical Properties; Semiconductors (Materials); Bonding; Wafers*

**20010125465** Argonne National Lab., IL USA

**Mn K-edge X-ray absorption spectroscopy (XAS) studies of La(sub 1-x)SR(sub x)MnO(sub 3)**

Mini, S. M.; Mitchell, J.; Hinks, D. G.; Alatas, A.; Rosenmann, D.; Mar. 06, 1998; 9p; In English

Report No.(s): DE2001-8109; ANL/MSD/CP-93881; No Copyright; Avail: Department of Energy Information Bridge, Microfiche

Systematic Mn K-edge x-ray absorption spectroscopy (XAS) measurements on samples of La(sub 1 - x)SR(sub x)MnO3, which are precursors to colossal magnetoresistive (CMR) materials, are reported. Detailed results on the edge or chemical shift as a function of SR concentration (hole doping) and sample preparation (air vs oxygen annealed), are discussed. For comparison, a systematic XANES study of the Mn K-edge energy shift, denoting valence change in Mn, has been made in standard manganese oxide systems. Contrary to expectations, the variation in near-edge energies for Mn in La(sub 0.725)SR(sub 0.275)MnO3 were small when compared to the difference between that for manganese oxide standards of nominal valence of +3 and +4 (Mn2O3 and MnO2).

NTIS

*X Ray Absorption; Absorption Spectroscopy; Magnetoresistivity; Chemical Equilibrium*

**20010125466** Argonne National Lab., IL USA

**Spectroscopic determination of C2 in Ar/H2/CH4 and Ar/H2/C60 microwave plasmas for nanocrystalline diamond synthesis**

Goyette, A. N.; Lawler, J. E.; Anderson, L. W.; Gruen, D. M.; McCauley, T. G.; Feb. 05, 1998; 9p; In English

Report No.(s): DE2001-8108; ANL/CHM/CP-93845; No Copyright; Avail: Department of Energy Information Bridge, Microfiche

We have measured the steady state concentration of gas phase C2 in Ar/H2/CH4 and Ar/H2/C60 microwave plasmas used for the deposition of nanocrystalline diamond films. High sensitivity white light absorption spectroscopy is used to monitor the C2 density using the d(sup 3)II (l arrow) A(sup 3)II (0,0) vibrational band of C2 as chamber pressure, microwave power, substrate temperature and feed gas mixtures are varied in both chemistries. Understanding how these parameters influence the C2 density in the plasma volume provides insight into discharge mechanisms relevant to the deposition of nanocrystalline diamond.

NTIS

*Carbon; Plasmas (Physics); Diamonds; Concentration (Composition)*

**20010125467** Argonne National Lab., IL USA

**Redox behavior below 1000K of Pt-impregnated CeO2-ZrO2 solid solutions: an in-situ neutron diffraction study**

Loong, C. K.; Short, S. M.; Ozawa, M.; Suzuki, S.; Jan. 12, 1998; 9p; In English

Report No.(s): DE2001-8107; ANL/IPNS/CP-93843; No Copyright; Avail: Department of Energy Information Bridge, Microfiche

The Ce(sup 3+) yields Ce(sup 4+) redox process in automotive three-way catalysts such as Ce-ZrO(sub 2)/Pt provides an essential mechanism to oxygen storage/release under dynamic air-to-fuel ratio cycling. Such a function requires a metal-support interaction which is not completely understood. We have carried out an in-situ neutron powder diffraction study to monitor the crystal structures (a mixture of a major tetragonal and a minor monoclinic phase) of 10mol% Ce-doped ZrO2 with and without Pt (1wt%) impregnation under oxidizing and reducing conditions over the temperature range of 25 - 7000 C. The samples were

heated first in flowing 2%O(sub 2)/Ar from room temperature to 400 C and then in 1%CO/Ar to about 700 C. A discontinued increase of the tetragonal unit-cell volume, a decrease of tetragonality (c/a), and a change of color from light yellow to gray when changing from oxidizing to reducing atmosphere were observed only in the sample containing Pt. This result supports the model which assumes the formation of oxygen vacancies initially near the Pt atoms. As more Ce ions are reduced from 4+ to 3+ oxidation states at high temperatures, oxygen vacancies migrate to the bulk of the oxide particles.
NTIS
*Oxidation-Reduction Reactions; Cerium Oxides; Zirconium Oxides; Neutron Diffraction; Crystal Structure*

**20010125468** Argonne National Lab., IL USA
**Crystal structures of mixed-conducting oxides present in the SR-Fe-Co-O system**
Hodges, J. P.; Jorgensen, J. D.; Miler, D. J.; Ma, B.; Balachandran, U.; Jan. 14, 1998; 9p; In English
Report No.(s): DE2001-8106; ANL/MSD/CP-93842; No Copyright; Avail: Department of Energy Information Bridge, Microfiche

The potential applications of mixed-conducting ceramic oxides include solid-oxide fuel cells, rechargeable batteries, gas sensors and oxygen-permeable membranes. Several perovskite-derived mixed SR-Fe-Co oxides show not only high electrical-conductivity but also appreciable oxygen-permeability at elevated temperatures. For example, dense ceramic membranes of SRFeCo(sub 0.5)O(sub 3 - delta) can be used to separate oxygen from air without the need for external electrical circuitry. The separated oxygen can be directly used for the partial oxidation of methane to produce syngas. Quantitative phase analysis of the SRFeCo(sub 0.5)O(sub 3 - delta) material has revealed that it is predominantly composed of two SR-Fe-Co-O systems, SR4Fe(sub 6 - x)Co(sub x)O13 and SRFe(sub 1 - x)Co(sub x)O(sub 3 - delta). Here we report preliminary structural findings on the SRFe(sub 1 - x)Co(sub x)O(sub 3 - delta) (0 (le) x (le) 0.3) system.
NTIS
*Ceramics; Perovskites; Crystal Structure; Mixed Oxides*

**20010125476** Argonne National Lab., IL USA
**Growth and Characterization of Epitaxial fcc Fe Wedges on Diamond (100)**
Bader, S. D.; Keavneu, D. J.; Keune, W.; Li, D.; Pearson, J.; Dec. 05, 1997; 17p; In English
Report No.(s): DE2001-8093; ANL/MSD/CP-93481; No Copyright; Avail: Department of Energy Information Bridge, Microfiche

Epitaxial Fe wedges with a thickness gradation from 0-20 angstroms were grown on diamond(100) at room temperature, subsequently annealed, and investigated with reflection high-energy electron diffraction and the surface magneto-optical Kerr effect. The results indicate that for less than monolayer thicknesses the Fe grows on C(100) as smooth, epitaxial fcc films, which are not ferromagnetic, but that thicker films undergo a transition to become rough and the ordinary bcc ferromagnetic phase.
NTIS
*Diamonds; Epitaxy; Wedges; Iron; Face Centered Cubic Lattices; Thin Films*

**20010125564** Argonne National Lab., IL USA
**Synchrotron X-Ray Reflectivity Study of Oxidation/Passivation of Copper and Silicon**
Chu, Y.; Nagy, Z.; Parkhutik, V.; You, H.; Jul. 21, 1999; 9p; In English
Report No.(s): DE2001-11901; ANL/MSD/CP-99610; No Copyright; Avail: Department of Energy Information Bridge, Microfiche

Synchrotron x-ray-scattering technique studies of copper and silicon electrochemical interfaces are reported. These two examples illustrate the application of synchrotron x-ray techniques for oxidation, passivation, and dissolution of metals and semiconductors.
NTIS
*Copper; Oxidation; Passivity; Reflectance; Silicon; X Ray Scattering*

**20010125587** Argonne National Lab., IL USA
**Fermi surfaces, Fermi patches, and Fermi arcs in high T(c) superconductors**
Norman, M. R.; May 19, 1999; 8p; In English
Report No.(s): DE2001-11811; ANL/MSD/CP-99040; No Copyright; Avail: Department of Energy Information Bridge

A defining property of metals is the existence of a Fermi surface: for two dimensions, a continuous contour in momentum space which separates occupied from unoccupied states. In this paper, I discuss angle resolved photoemission data on the cuprate superconductor BSCCO and argue that it is not best thought of in this conventional picture. Rather, the data are consistent with

patches of finite area connected by more conventional arcs. Novel physics is associated with the patches, in that the states contained in a patch are dispersionless and thus interaction dominated. In the pseudogap phase, the patches are gapped out, leaving the Fermi arcs disconnected. This unusual situation may be the key to understanding the microscopic physics of the high temperature superconductors, in that the pairing correlations are strongest in the patches, yet the superfluid density lives only on the arcs.
NTIS
*Fermi Surfaces; BSCCO Superconductors; Photoelectric Emission*

**20010125631** Argonne National Lab., IL USA
**Morphology and electron emission properties of nanocrystalline CVD diamond thin films**
Krauss, A. R.; Gruen, D. M.; Zhou, D.; McCauley, T. G.; Qin, L. C.; Jan. 30, 1998; 15p; In English
Report No.(s): DE2001-8120; ANL/CHM/CP-94250; No Copyright; Avail: Department of Energy Information Bridge, Microfiche

Nanocrystalline diamond thin films have been produced by microwave plasma-enhanced chemical vapor deposition (MPECVD) using C60/Ar/H) or CH4/Ar/H2 plasmas. Films grown with H2 concentration (le) 20% are nanocrystalline, with atomically abrupt grain boundaries and without observable graphitic or amorphous carbon phases. The growth and morphology of these films are controlled via a high nucleation rate resulting from low hydrogen concentration in the plasma. Initial growth is in the form of diamond, which is the thermodynamic equilibrium phase for grains (le)5 nm in diameter. Once formed, the diamond phase persists for grains up to at least 15-20 nm in diameter. The renucleation rate in the near-absence of atomic hydrogen is very high (approximately 10(exp 10) square cm/sec), limiting the average grain size to a nearly constant value as the film thickness increases, although the average grain size increases as hydrogen is added to the plasma. For hydrogen concentrations less than approximately 20%, the growth species is believed to be the carbon dimer, C2, rather than the CH3 growth species associated with diamond film growth at higher hydrogen concentrations. For very thin films grown from the C60 precursor, the threshold field (2 to approximately 60 volts/micron) for cold cathode electron emission depends on the electrical conductivity and on the surface topography, which in turn depends on the hydrogen concentration in the plasma. A model of electron emission, based on quantum well effects at the grain boundaries is presented. This model predicts promotion of the electrons at the grain boundary to the conduction band of diamond for a grain boundary width (approximately) 3-4 angstroms, a value within the range observed by TEM.
NTIS
*Morphology; Electron Emission; Diamond Films; Vapor Deposition*

**20010125648** Argonne National Lab., IL USA
**Prototype 350 MHz niobium spoke-loaded cavities**
Delayen, J. R.; Kedzie, M.; Mammosser, J.; Piller, C.; Shepard, K. W.; May 10, 1999; 4p; In English
Report No.(s): DE2001-11798; ANL/PHY/CP-98993; No Copyright; Avail: Department of Energy Information Bridge

This paper reports the development of 350 MHz superconducting cavities of a spoke-loaded geometry, intended for the velocity range 0.2 to 0.6 v/c. Two prototype single-cell cavities have been designed, one optimized for velocity v/c = 0.4, and the other for v/c = 0.29. Construction of the prototype niobium cavities is nearly complete. Details of the design and construction are discussed, along with the results of cold tests.
NTIS
*Niobium; Cavities; Superconducting Devices*

## 77
## PHYSICS OF ELEMENTARY PARTICLES AND FIELDS

*Includes quantum mechanics; theoretical physics; and statistical mechanics. For related information see also 72 Atomic and Molecular Physics, 73 Nuclear Physics, and 25 Inorganic, Organic and Physical Chemistry.*

**20010117634** Brookhaven National Lab., Upton, NY USA
**Superconducting solenoids for the muon collider**
Green,; Eyssa,; Kenny,; Miller,; Prestemon,; Jun. 12, 2000; 8p; In English
Report No.(s): DE2000-759051; BNL-67540; No Copyright; Avail: Department of Energy Information Bridge

The muon collider is a new idea for lepton colliders. The ultimate energy of an electron ring is limited by synchrotron radiation. Muons, which have a rest mass that is 200 times that of an electron can be stored at much higher energies before

synchrotron radiation limits ring performance. The problem with muons is their short life time (2.1 (micro)s at rest). In order to operate a muon storage ring large numbers of muon must be collected, cooled and accelerated before they decay to an electron and two neutrinos. As the authors see it now, high field superconducting solenoids are an integral part of a muon collider muon production and cooling systems. This report describes the design parameters for superconducting and hybrid solenoids that are used for pion production and collection, RF phase rotations of the pions as they decay into muons and the muon cooling (reduction of the muon emittance) before acceleration.
NTIS
*Muons; Solenoids; Superconductivity; Storage Rings (Particle Accelerators)*

**20010117635** Brookhaven National Lab., Upton, NY USA
**QCD at high parton density**
Kovchegov,; Apr. 25, 2000; 4p; In English
Report No.(s): DE2000-759048; BNL-67525; No Copyright; Avail: Department of Energy Information Bridge
The authors derive an equation determining the small-x evolution of the F(sub 2) structure function of a large nucleus which resumes a cascade of gluons in the leading logarithmic approximation using Mueller's color dipole model. In the traditional language it corresponds to resummation of the pomeron fan diagrams, originally conjectured in the GLR equation. The authors show that the solution of the equation describes the physics of structure functions at high partonic densities, thus allowing them to gain some understanding of the most interesting and challenging phenomena in small-x physics--saturation.
NTIS
*Quantum Chromodynamics; Field Theory (Physics); Logarithms; Quark Parton Model*

**20010117639** Brookhaven National Lab., Upton, NY USA
**BNL Activities in Advanced Neutron Source Development: Past and Present**
Hastings,; Ludewig,; Montanez,; Todosow,; Smith,; Jun. 14, 1998; 8p; In English
Report No.(s): DE2000-758988; BNL-66295; No Copyright; Avail: Department of Energy Information Bridge, Microfiche
Brookhaven National Laboratory (BNL) has been involved in advanced neutron sources almost from its inception in 1947. These efforts have mainly focused on steady state reactors beginning with the construction of the first research reactor for neutron beams, the Brookhaven Graphite Research Reactor. This was followed by the High Flux Beam Reactor that has served as the design standard for all the subsequent high flux reactors constructed worldwide. In parallel with the reactor developments BNL has focused on the construction and use of high energy proton accelerators. The first machine to operate over 1 GeV in the world was the Cosmotron. The machine that followed this, the AGS, is still operating and is the highest intensity proton machine in the world and has nucleated an international collaboration investigating liquid metal targets for next generation pulsed spallation sources. Early work using the Cosmotron focused on spallation product studies for both light and heavy elements into the several GeV proton energy region. These original studies are still important today. The authors discuss the facilities and activities at BNL focused on advanced neutron sources. BNL is involved in the proton source for the Spallation Neutron source, spectrometer development at LANSCE, target studies using the AGS, and state-of-the-art neutron detector development.
NTIS
*Neutron Sources; Spallation; Particle Accelerators*

**20010117640** Brookhaven National Lab., Upton, NY USA
**Circular RFQ Storage Ring**
Ruggiero,; Oct. 20, 1998; 14p; In English
Report No.(s): DE2000-758975; BNL-65920; No Copyright; Avail: Department of Energy Information Bridge, Microfiche
This paper presents a novel idea of storage ring for the accumulation of intense beams of light and heavy ions at low energy. The new concept is a natural development of the combined features used in a conventional storage ring and an ion trap, and is basically a linear RFQ bend on itself. In summary, the advantages are smaller beam dimensions, higher beam intensity, and a more compact storage device.
NTIS
*Light Beams; Storage Rings (Particle Accelerators); Ion Beams*

**20010117642** Brookhaven National Lab., Upton, NY USA
**Power Spectrum Calculation for the Cornell Wiggler: A SASE Experiment at BNL**
Yu,; Aug. 16, 1998; 16p; In English
Report No.(s): DE2000-758973; BNL-65854; No Copyright; Avail: Department of Energy Information Bridge, Microfiche

Recently the authors showed that the widely used simulation code TDA3D, even though a single frequency code, can be used to determine the power spectrum in the self-amplification of spontaneous emission (SASE) process with excellent approximation in the exponential growth regime. In this paper, they apply this method to the BNL Cornell Wiggler A SASE experiment as an example. When the gain is not very high, there are many modes in the radiation, which seems to make the analytical calculation very difficult. However, they show that the increment of the radiation due to SASE over the spontaneous radiation can be expanded in terms of guided modes with rapid convergence. Thus when the spontaneous radiation is subtracted from the SASE power during the calculation, there is a good agreement between the analytical theory and the numerical simulation.
NTIS
*Spontaneous Emission; Free Electron Lasers; Power Spectra*

**20010117643** Brookhaven National Lab., Upton, NY USA
**VISA FEL Undulator**
Carr,; Cornacchia,; Emma,; Nuhn,; Fuland,; Aug. 16, 1998; 10p; In English
Report No.(s): DE2000-758972; BNL-65842; No Copyright; Avail: Department of Energy Information Bridge, Microfiche
The Visible-Infrared SASE Amplifier (VISA) FEL is an experimental device designed to show Self Amplified Spontaneous Emission (SASE) to saturation in the visible light energy range. It will generate a resonant wavelength output from 800-600 nm, so that silicon detectors may be used to characterize the optical properties of the FEL radiation. VISA is the first SASE FEL designed to reach saturation, and its diagnostics will provide important checks of theory. This paper includes a description of the VISA undulator, the magnet measuring and shimming system, and the alignment strategy. VISA will have a 4 m pure permanent magnet undulator comprising four 99 cm segments, each with 55 periods of 18 mm length. The undulator has distributed focusing built into it, to reduce the average beta function of the 70-85 MeV electron beam to about 30 cm. There are four FODO cells per segment. The permanent magnet focusing lattice consists of blocks mounted on either side of the electron beam, in the undulator gap. The most important undulator error parameter for a free electron laser is the trajectory walkoff or lack of overlap of the photon and electron beams. Using pulsed wire magnet measurements and magnet shimming, the authors expect to be able to control trajectory walkoff to less than +/- 50 pm per field gain length.
NTIS
*Free Electron Lasers; Optical Properties; Design Analysis*

**20010117707** Brookhaven National Lab., Upton, NY USA
**Simulation Study of Three-Dimensional Laser Cooling Schemes for Fast Stored Beams**
Kihara,; Okamoto,; Iwashita,; Oide,; Lamanna,; Jun. 22, 1998; 3p; In English
Report No.(s): DE2000-758969; BNL-65652; No Copyright; Avail: Department of Energy Information Bridge, Microfiche
Molecular dynamics (MD) approach is employed to study laser cooling of fast circulating beams in a storage ring. The authors compare several three-dimensional cooling methods, examining achievable minimum beam temperature. In particular, the stress is put upon the three coupling schemes, i.e., the dispersion-coupling scheme, the coupling-cavity scheme, and the tapered cooling scheme. The authors show that beam temperatures much lower than the currently achievable level could be reached with these schemes.
NTIS
*Laser Cooling; Molecular Dynamics; Computerized Simulation; Three Dimensional Models; Particle Beams*

**20010117708** Brookhaven National Lab., Upton, NY USA
**Stability Measurements on Cored Cables in Normal and Superfluid Helium**
Ghosh,; Sampson,; Kim,; Leroy,; Oberli,; May 10, 1998; 6p; In English
Report No.(s): DE2000-758968; BNL-65650; No Copyright; Avail: Department of Energy Information Bridge, Microfiche
The relative stability of LHC type cables has been measured by the direct heating of one of the individual strands with a short duration current pulse. The minimum energy required to initiate a quench has been determined for a number of cables which have a central core to increase the effective inter-strand cross-over resistance. Experiments were performed in both normal helium at 4.4 K and superfluid at 1.9 K. Conductors in general are less stable at the lower temperature when measured at the same fraction of critical current. Results show that the cored-cables, even when partially filled with solder or with a porous-metal filler exhibit a relatively low stability at currents close to the critical current. It is speculated that the high inter-strand electrical and thermal resistance inherent in these cables may effect the stability at high currents.
NTIS
*Fillers; Stability; Strands; Cores; Power Lines*

**20010118273** California Univ., Lawrence Berkeley Lab., Berkeley, CA USA

**Magnetic Performance of the Advanced Light Source EPU5.0 Elliptically Polarizing Undulator**

Marks, S.; DeVries, J.; Hoyer, E.; Kincaid, B. M.; Plate, D.; Mar. 26, 1999; 6p; In English

Report No.(s): DE2000-760302; LBNL-43049; No Copyright; Avail: Department of Energy Information Bridge, Microfiche

An elliptically polarizing undulator (EPU) has been assembled, tested, and installed in the Advanced Light Source (ALS) storage ring. It is a 2 m long pure permanent magnet device with a 5.0 cm period capable of providing polarized radiation of any ellipticity. This paper reports on the program of magnetic measurements and field tuning, and final magnetic and chive system performance. A summary of measurement results, calculated radiation spectral performance, and a description of the magnetic shimming procedure used for field tuning are included.

NTIS

*Storage Rings (Particle Accelerators); Light Sources; Ellipticity; Polarized Radiation*

**20010118275** California Univ., Lawrence Berkeley Lab., Berkeley, CA USA

**Identification of hadronic tau decays in ATLAS**

Coadou, Y.; Hinchliffe, I.; LozanoBahilo, J.; Loveridge, L. C.; Shapiro, M. D.; Sep. 01, 1998; 25p; In English

Report No.(s): DE2000-760283; LBNL-41757; ATL-PHYS-98-126; No Copyright; Avail: Department of Energy Information Bridge, Microfiche

Taus can be an important signature for Supersymmetry at the LHC. They can be produced copiously in the decays of supersymmetric particles. Measurement of their momentum and of the tau-tau invariant mass distribution, would provide detailed information regarding the masses of supersymmetric particles. It is demonstrated using full simulation that it will be possible for ATLAS to make a cut on the reconstructed tau invariant mass using information from the tracking and the electromagnetic calorimeter. The measured energy and momentum of tau's that pass this selection can then be used to infer information about the tau-tau invariant mass.

NTIS

*Leptons; Supersymmetry; Simulation*

**20010118505** Brookhaven National Lab., Upton, NY USA

**LHC interaction region quadrupole error impact studies**

Fischer,; Ptitsin,; Wei,; Sep. 07, 1999; 4p; In English

Report No.(s): DE2000-759018; BNL-66793; No Copyright; Avail: Department of Energy Information Bridge

The performance of the Large Hadron Collider (LHC) at collision energy is limited by the field quality of the interaction region (IR) quadrupoles and dipoles. In this paper the authors study the impact of the expected field errors of these magnets on the dynamic aperture. The authors investigate different magnet arrangements and error strength. Based on the results they propose and evaluate a corrector layout to meet the required dynamic aperture performance in a companion paper.

NTIS

*Apertures; Correction; Beams (Radiation); Errors*

**20010118515** Brookhaven National Lab., Upton, NY USA

**Muon polarization effects in the front end of the neutrino factory**

Fernow,; Gallardo,; Fukui,; Jun. 12, 2000; 18p; In English

Report No.(s): DE2000-759043; BNL-67511; No Copyright; Avail: Department of Energy Information Bridge

The authors summarize the methods used for simulation of polarization effects in the front end of a possible neutrino factory. They first discuss the helicity of muons in the pion decay process. They find that, neglecting acceptance considerations, the average helicity asymptotically approaches a magnitude of 0.185 at large pion momenta. Next they describe the methods used for tracking the spin through the complicated electromagnetic field configurations in the front end of the neutrino factory, including rf phase rotation and ionization cooling channels. Various depolarizing effects in matter are then considered, including multiple Coulomb scattering and elastic scattering from atomic electrons. Finally, they include all these effects in a simulation of a 480 m long, double phase rotation front end scenario.

NTIS

*Coulomb Collisions; Particle Decay; Elastic Scattering; Electromagnetic Fields*

**20010118517** Brookhaven National Lab., Upton, NY USA
**Time-Resolved Infrared Spectroscopy in the U121R Beamline at the NSLS**
Carr,; Laveigne,; Lobo,; Reitze,; Tanner,; Jul. 19, 1999; 12p; In English
Report No.(s): DE2000-759028; BNL-66995; No Copyright; Avail: Department of Energy Information Bridge
A facility for performing time-resolved infrared spectroscopy has been developed at the NSLS, primarily at beamline U12IR. The pulsed IR light from the synchrotron is used to perform pump-probe spectroscopy. The authors present here a description of the facility and results for the relaxation of photoexcitations in both a semiconductor and superconductor.
NTIS
*Infrared Spectroscopy; Photoexcitation; Semiconductors (Materials); Superconductors (Materials)*

**20010118524** Brookhaven National Lab., Upton, NY USA
**LHC interaction region correction scheme studies**
Fischer,; Ptitsin,; Wei,; Sep. 07, 1999; 4p; In English
Report No.(s): DE2000-759017; BNL-66794; No Copyright; Avail: Department of Energy Information Bridge
In a companion paper the authors showed that the performance of the Large Hadron Collider (LHC) at collision energy is limited by the field quality of the interaction region quadrupoles and dipoles. In this situation, the dynamic aperture can be increased through local multipole correctors. Since the betatron phase advance is well defined for magnets that are located in regions of large beta functions, local corrections can be very effective and robust. They compare possible compensation schemes and propose a corrector layout to meet the required dynamic aperture performance.
NTIS
*Apertures; Betatrons; Correction; Magnetic Dipoles*

**20010118525** Brookhaven National Lab., Upton, NY USA
**Principle of interaction region local correction**
Wei,; Sep. 07, 1999; 6p; In English
Report No.(s): DE2000-759016; BNL-66795; No Copyright; Avail: Department of Energy Information Bridge
For hadron storage rings like the Relativistic Heavy Ion Collider (RHIC) and the Large Hadron Collider (LHC), the machine performance at collision is usually limited by the field quality of the interaction region (IR) magnets. A robust local correction for the IR region is valuable in improving the dynamic aperture with practically achievable magnet field quality. The authors present in this paper the action-angle kick minimization principle on which the local IR correction for both RHIC and the LHC are based.
NTIS
*Apertures; Optical Correction Procedure; Beams (Radiation); Hadrons*

**20010118526** Brookhaven National Lab., Upton, NY USA
**LHC interaction region correction in heavy ion operation**
Ptitsin,; Fischer,; Wei,; Sep. 07, 1999; 4p; In English
Report No.(s): DE2000-759015; BNL-66796; No Copyright; Avail: Department of Energy Information Bridge
In heavy ion operation the LHC interaction region at IP2 will have a low-(beta) optics for collisions. The dynamic aperture is therefore sensitive to magnetic field errors in the interaction region quadrupoles and dipoles. The authors investigate the effect of the magnetic field errors on the dynamic aperture and evaluate the effectiveness of local interaction region correctors. The dynamic aperture and the tune space are computed for different crossing angles.
NTIS
*Heavy Ions; Apertures; Magnetic Fields; Errors*

**20010118527** Brookhaven National Lab., Upton, NY USA
**Local decoupling in the LHC interaction regions**
Pilat,; Sep. 07, 1999; 4p; In English
Report No.(s): DE2000-759014; BNL-66797; No Copyright; Avail: Department of Energy Information Bridge
Local decoupling is a technique to correct coupling locally and operationally, that is, without a prior knowledge of the underlying skew quadrupole errors. The method is explained and applied to the correction of coupling in the interaction regions of the LHC at collision.
NTIS
*Decoupling; Errors; Beam Interactions*

**20010118530** Brookhaven National Lab., Upton, NY USA
**PHENIX experiment**
Read,; Jan. 09, 1999; 8p; In English
Report No.(s): DE2000-759009; BNL-66670; No Copyright; Avail: Department of Energy Information Bridge
The PHENIX experiment at RHIC is currently under construction with data collection planned to start in 1999. The heavy ion and spin physics goals of PHENIX are described. The authors discuss the experiment's capabilities to address these physics goals. Highlights of the present status of construction and installation are presented.
NTIS
*Heavy Ions; Spin*

**20010118531** Brookhaven National Lab., Upton, NY USA
**Structure of p-shell hypernuclei**
Millener,; Feb. 19, 1999; 10p; In English
Report No.(s): DE2000-759007; BNL-66639; No Copyright; Avail: Department of Energy Information Bridge
New (gamma)-ray data for (sub (Lambda))Li-7 from KEK E419 and new ((pi)(sup +), K(sup +)) data on C-12, C-13, and O-16 targets from KEK E336 and E369 is used to update Millener, Gal, Dover and Dalitz's 1985 analysis of the spin dependence of the effective AN interaction.
NTIS
*Hypernuclei; Targets; Electronic Structure*

**20010118534** Brookhaven National Lab., Upton, NY USA
**Prospects for colliders and collider physics to the 1 pev energy scale**
King,; May 05, 2000; 37p; In English
Report No.(s): DE2000-757147; BNL-67410; No Copyright; Avail: Department of Energy Information Bridge, Microfiche
A review is given of the prospects for future colliders and collider physics at the energy frontier. A proof-of-plausibility scenario is presented for maximizing the authors progress in elementary particle physics by extending the energy reach of hadron and lepton colliders as quickly and economically as might be technically and financially feasible. The scenario comprises 5 colliders beyond the LHC--one each of e(sup +)e(sup (minus)) and hadron colliders and three (mu)(sup +)(mu)(sup (minus)) colliders--and is able to hold to the historical rate of progress in the log-energy reach of hadron and lepton colliders, reaching the 1 PeV constituent mass scale by the early 2040's. The technical and fiscal requirements for the feasibility of the scenario are assessed and relevant long-term R and D projects are identified. Considerations of both cost and logistics seem to strongly favor housing most or all of the colliders in the scenario in a new world high energy physics laboratory.
NTIS
*High Energy Interactions; Particle Accelerators; Linear Energy Transfer (LET)*

**20010118535** Brookhaven National Lab., Upton, NY USA
**Parameter sets for 10 tev and 100 tev muon colliders, and their study at the hemc 99 workshop**
King,; May 05, 2000; 21p; In English
Report No.(s): DE2000-757146; BNL-67409; No Copyright; Avail: Department of Energy Information Bridge, Microfiche
A focal point for the HEMC'99 workshop was the evaluation of straw-man parameter sets for the acceleration and collider rings of muon colliders at center of mass energies of 10 TeV and 100 TeV. These self-consistent parameter sets are presented and discussed. The methods and assumptions used in their generation are described and motivations are given for the specific choices of parameter values. The assessment of the parameter sets during the workshop is then reviewed and the implications for the feasibility of many-TeV muon colliders are evaluated. Finally, a preview is given of plans for iterating on the parameter sets and, more generally, for future feasibility studies on many-TeV muon colliders.
NTIS
*Muons; Feasibility; Particle Accelerators*

**20010118536** Brookhaven National Lab., Upton, NY USA
**Neutrino radiation challenges and proposed solutions for many-tev muon colliders**
King,; May 05, 2000; 17p; In English
Report No.(s): DE2000-757145; BNL-67408; No Copyright; Avail: Department of Energy Information Bridge, Microfiche
Neutrino radiation is expected to impose major design and siting constraints on many-TeV muon colliders. Previous predictions for radiation doses at TeV energy scales are briefly reviewed and then modified for extension to the many-TeV energy

regime. The energy-cubed dependence of lower energy colliders is found to soften to an increase of slightly less than quadratic when averaged over the plane of the collider ring and slightly less than linear for the radiation hot spots downstream from straight sections in the collider ring. Despite this, the numerical values are judged to be sufficiently high that any many-TeV muon colliders will likely be constructed on large isolated sites specifically chosen to minimize or eliminate human exposure to the neutrino radiation. It is pointed out that such sites would be of an appropriate size scale to also house future proton-proton and electron-positron colliders at the high energy frontier, which naturally leads to conjecture on the possibilities for a new world laboratory for high energy physics. Radiation dose predictions are also presented for the speculative possibility of linear muon colliders. These have greatly reduced radiation constraints relative to circular muon colliders because radiation is only emitted in two pencil beams directed along the axes of the opposing linacs.
NTIS
*Neutrino Beams; Linear Accelerators; Radiation Dosage*

**20010118537** Brookhaven National Lab., Upton, NY USA
**Potential for neutrino physics at muon colliders and dedicated high current muon storage rings**
Bigi,; Bolton,; Formaggio,; Harris,; Morfin,; May 11, 2000; 152p; In English
Report No.(s): DE2000-757144; BNL-67404; No Copyright; Avail: Department of Energy Information Bridge, Microfiche

Conceptual design studies are underway for both muon colliders and high-current non-colliding muon storage rings that have the potential to become the first true neutrino factories. Muon decays in long straight sections of the storage rings would produce uniquely intense and precisely characterized two-component neutrino beams--muon neutrinos plus electron antineutrinos from negative muon decays and electron neutrinos plus muon antineutrinos from positive muons. This article presents a long-term overview of the prospects for these facilities to greatly extend the capabilities for accelerator-based neutrino physics studies for both high rate and long baseline neutrino experiments. As the first major physics topic, recent experimental results involving neutrino oscillations have motivated a vigorous design effort towards dedicated neutrino factories that would store muon beams of energies 50 GeV or below. These facilities hold the promise of neutrino oscillation experiments with baselines up to intercontinental distances and utilizing well understood beams that contain, for the first time, a substantial component of multi-GeV electron-flavored neutrinos. In deference to the active and fast-moving nature of neutrino oscillation studies, the discussion of long baseline physics at neutrino factories has been limited to a concise general overview of the relevant theory, detector technologies, beam properties, experimental goals and potential physics capabilities. The remainder of the article is devoted to the complementary high rate neutrino experiments that would study neutrino-nucleon and neutrino-electron scattering and would be performed at high performance detectors placed as close as is practical to the neutrino production straight section of muon storage rings in order to exploit beams with transverse dimensions as small as a few tens of centimeters.
NTIS
*Neutrino Beams; Design Analysis; Storage Rings (Particle Accelerators)*

**20010118538** Brookhaven National Lab., Upton, NY USA
**BNL accelerator-based radiobiology facilities**
Lowenstein,; May 28, 2000; 9p; In English
Report No.(s): DE2000-757143; BNL-67119; No Copyright; Avail: Department of Energy Information Bridge, Microfiche

For the past several years, the Alternating Gradient Synchrotron (AGS) at Brookhaven National Laboratory (USA) has provided ions of iron, silicon and gold, at energies from 600 MeV/nucleon to 10 GeV/nucleon, for the US National Aeronautics and Space Administration (NASA) radiobiology research program. NASA has recently funded the construction of a new dedicated ion facility, the Booster Applications Facility (BAF). The Booster synchrotron will supply ion beams ranging from protons to gold, in an energy range from 40--3,000 MeV/nucleon with maximum beam intensities of 10(exp 10) to 10(exp 11) ions per pulse. The BAF Project is described and the future AGS and BAF operation plans are presented.
NTIS
*Ion Beams; Radiobiology; Research Projects*

**20010118542** Brookhaven National Lab., Upton, NY USA
**Focusing and acceleration of bunched beams**
Parsa,; Zadorozhny,; Apr. 07, 2000; 12p; In English
Report No.(s): DE2000-757134; BNL-67348; No Copyright; Avail: Department of Energy Information Bridge, Microfiche

A new approach to solving the kinetic equation for the beam distribution function, (very useful from the practical point of view), is discussed, in which the authors also obtain a complement to the Skrinsky's condition for the self-focused bunched beam. This problem belongs to the theory of nonlinear systems in which both regular and chaotic motion is possible. The kinetic

approach, based on Vlasov-Poisson equations, are used to investigate the focusing and acceleration of bunched beam. Special attention is given to the studies of stability in a bunched beam by means of the two norm, which may be used to describe the motion of high-energy particles.
NTIS
*Particle Beams; Focusing; Acceleration (Physics); Kinetic Equations*

**20010118700** Brookhaven National Lab., Upton, NY USA
**Rare kaon decays**
Kettell,; Dec. 07, 1999; 8p; In English
Report No.(s): DE2000-759034; BNL-67141; No Copyright; Avail: Department of Energy Information Bridge
The current status of rare kaon decay experiments is reviewed. New limits in the search for Lipton Flavor Violation are discussed, as are new measurements of the CKM matrix.
NTIS
*Kaons; Decay*

**20010118900** Brookhaven National Lab., Upton, NY USA
**Interactions of heavy quarkonium: Some recent results**
Kharzeev,; Jan. 17, 2000; 8p; In English
Report No.(s): DE2000-755031; BNL-67222; No Copyright; Avail: Department of Energy Information Bridge
Some recent developments in the theory of heavy quarkonium interactions are presented. First, the authors consider quarkonium-quarkonium scattering at very low energies--an analog of the Van der Waals interaction. These long-range forces have very surprising properties in QCD (quantum chromodynamics); in particular, as a consequence of scale anomaly, the strength of the interaction at large distances appears independent of the coupling constant and is entirely determined by the non-perturbative vacuum energy density. Second, they argue that the scale anomaly can play a dominant role also in high-energy scattering, and discuss the possible origin of the soft Pomeron.
NTIS
*Quantum Chromodynamics; Quarks*

**20010118904** Brookhaven National Lab., Upton, NY USA
**Ultra-Relativistic Nuclei: A New Frontier**
McLerran,; Oct. 29, 1999; 10p; In English
Report No.(s): DE2000-755036; BNL-67252; No Copyright; Avail: Department of Energy Information Bridge
The collisions of ultra-relativistic nuclei provide a window on the behavior of strong interactions at asymptotically high energies. They also will allow the authors to study the bulk properties of hadronic matter at very high densities.
NTIS
*Collisions; Hadrons; Nuclei (Nuclear Physics)*

**20010118905** Brookhaven National Lab., Upton, NY USA
**Pion production models and neutrino factories**
Collot,; Kirk,; Mokhov,; Feb. 11, 2000; 8p; In English
Report No.(s): DE2000-755037; BNL-67251; No Copyright; Avail: Department of Energy Information Bridge
Scenarios for the building of muon colliders or storage rings suitable for the generation of robust neutrino beams call for the generation of a prodigious quantity of pions. These pions are then conducted into a decay channel where the resulting muon decay products can be collected for cooling and subsequent acceleration. Central to this concept is the design and construction of a target which will be highly efficient in producing pions of both signs while mitigating the absorption of these pions before they decay. This design effort is being facilitated by using two computer codes FLUKA and MARS. The authors present comparisons of the two computer codes and also present a comparison of these codes with available data.
NTIS
*Neutrino Beams; Particle Production*

**20010118915** Brookhaven National Lab., Upton, NY USA

**Quarkonium Production in Relativistic Nuclear Collisions: Proceedings of Riken BNL Research Center Workshop, Volume 12**

Kharzeev,; Apr. 20, 1999; 252p; In English; Quarkonium Production in Relativistic Nuclear Collisions, 28 Sep. - 2 Oct. 1998, Upton, NY, USA

Report No.(s): DE2000-760969; BNL-52559-Vol-12; No Copyright; Avail: Department of Energy Information Bridge

The RIKEN-BNL Workshop on Quarkonium Production in Relativistic Nuclear Collisions was held September 28 - October 2, 1998, at Brookhaven National Laboratory. The Workshop brought together about 50 invited participants from around the world and a number of Brookhaven physicists from both particle and nuclear physics communities.

NTIS

*Nuclear Physics; Conferences*

**20010118918** Brookhaven National Lab., Upton, NY USA

**Case for a 500 Gev e+e-linear collider**

Bagger,; Baltay,; Marciano,; Paige,; Turcot,; Jun. 30, 2000; 64p; In English

Report No.(s): DE2000-760991; BNL-67545; No Copyright; Avail: Department of Energy Information Bridge

There are now several proposals that have been put forward from around the world for an e(sup +)e(sup (minus)) linear collider with an initial center of mass energy of 500 GeV. In this paper, the authors discuss why a project of this type deserves priority as the next, major initiative in high energy physics.

NTIS

*High Energy Interactions; Particle Collisions; Electron Beams; Positrons*

**20010118920** Brookhaven National Lab., Upton, NY USA

**Parity partner of the nucleon in quenched QCD with domain wall fermions**

Sasaki,; Jul. 12, 2000; 3p; In English

Report No.(s): DE2000-760994; BNL-67560; No Copyright; Avail: Department of Energy Information Bridge

The authors present preliminary results for the mass spectrum of the nucleon and its low-lying excited states from quenched lattice QCD (quantum chromodynamics) using the domain wall fermion method which preserves the chiral symmetry at finite lattice cutoff. Definite mass splitting is observed between the nucleon and its parity partner. This splitting grows with decreasing valence quark mass. They also present preliminary data regarding the first positive-parity excited state.

NTIS

*Fermions; Quantum Chromodynamics; Parity; Nucleons; Domain Wall*

**20010118921** Brookhaven National Lab., Upton, NY USA

**Riken BNL Research Center Workshop on Gauge-Invariant Variables in Gauge Theories, Volume 20**

VanBaal,; Orland,; Pisarski,; Jun. 01, 2000; 159p; In English; Riken BNL Research Center Workshop on Gauge-Invariant Variables in Gauge Theories, Upton, NY, USA

Report No.(s): DE2000-760995; BNL-52590-Vol-20; No Copyright; Avail: Department of Energy Information Bridge

This four-day workshop focused on the wide variety of approaches to the non-perturbative physics of QCD (quantum chromodynamics). The main topic was the formulation of non-Abelian gauge theory in orbit space, but some other ideas were discussed, in particular the possible extension of the Maldacena conjecture to nonsupersymmetric gauge theories. The idea was to involve most of the participants in general discussions on the problem. Panel discussions were organized to further encourage debate and understanding. Most of the talks roughly fell into three categories: (1) Variational methods in field theory; (2) Anti-de Sitter space ideas; (3) The fundamental domain, gauge fixing, Gribov copies and topological objects (both in the continuum and on a lattice). In particular some remarkable progress in three-dimensional gauge theories was presented, from the analytic side by V.P. Nair and mostly from the numerical side by O. Philipsen. This work may ultimately have important implications for RHIC (Relativistic Heavy Ion Collider) experiments on the high-temperature quark-gluon plasma.

NTIS

*Gauge Invariance; Gauge Theory; Quantum Chromodynamics*

**20010118922** Brookhaven National Lab., Upton, NY USA

**Proceedings of Riken BNL Research Center Workshop Circum-Pan-Pacific Riken Symposium on High Energy Spin Physics, Volume 25**

Kumano,; Shibata,; Yazaki,; Jun. 28, 2000; 235p; In English; Riken BNL Research Center Workshop Circum-Pan-Pacific Riken Symposium on High Energy Spin Physics, 3-6 Nov. 1999, Riken, Japan

Report No.(s): DE2000-760997; BNL-52588-Vol-25; No Copyright; Avail: Department of Energy Information Bridge

The Circum-Pan-Pacific Riken Symposium on High Energy Spin Physics was held at Oukouchi Memorial Hall in Riken from November 3 through 6, 1999. It was held as a joint meeting of the 2nd Circum-Pan-Pacific Symposium on High Energy Spin Physics and the 3rd of the series of Riken Symposia related to the RHIC (Relativistic Heavy Ion Collider)-SPIN. The 1st Circum-Pan-Pacific Symposium on High Energy Spin Physics was held at Kobe in 1996 and the RHIC-SPIN Riken Symposia had been held every two years since 1995. As Prof. Ozaki mentioned in his talk at the beginning of this meeting, the RHIC was ready for the first beam, physics experiments scheduled in 2000, and the RHIC-SPIN would start in 2001. It was therefore considered to be very timely for the researchers in the field of high energy spin physics to get together, clarifying the present status of the field and discussing interesting and important topics as well as experimental subjects to be pursued. It is especially important for the success of the RHIC-SPIN project that the researchers in the neighboring countries surrounding the Pacific are actively involved in it. This is why the above two series were joined in this symposium. The subjects discussed in the symposium include: Hard processes probing spin-structure functions, polarization mechanisms in high energy reactions, lattice studies of polarized structure functions, theoretical models for the nucleon and its spin structure, RHIC and RHIC-SPIN projects, results and future projects of existing experimental facilities. Totally 73 scientists participated in the symposium, 27 from abroad and 46 from Japan. It consisted of 13 main sessions, with 33 invited and contributed talks, and four discussion sessions covering recent experimental and theoretical developments and important topics in high energy spin physics and closely related fields.

NTIS

*Particle Spin; High Energy Interactions; Theoretical Physics; Conferences*

**20010119051** Fermi National Accelerator Lab., Batavia, IL USA

**CDF B Spectroscopy Results: B(asterik)(asterik) and B(+/c)**

Bauer, G.; Sep. 08, 1999; 5p; In English

Report No.(s): DE2001-10500; FERMILAB-CONF-99/227-E; No Copyright; Avail: Department of Energy Information Bridge, Microfiche

The authors report on two spectroscopy results from CDF. First, they observe the orbitally excited B(star)(star) mesons in B (r-arrow) (ell)D(star) X events. They find 28 (+-) 6 (+-) 3% of light B mesons produced are B** states. A collective mass fit results in a B(sub 1) mass of 5.71 (+-) 0.02 GeV/c(sup 2). Secondly, they observe 20.4(sub (minus)5.5)(sup +0.18) (+-) 0.03 ps lifetime. The production rate is in reasonable accordance with expectations.

NTIS

*Mesons; Particle Production*

**20010119056** Brookhaven National Lab., Upton, NY USA

**Convergence of Basis Expansions**

Blaskiewicz, M.; Jun. 28, 1999; 10p; In English

Report No.(s): DE2000-751106; BNL-66809; No Copyright; Avail: Department of Energy Information Bridge

An exactly solvable model of longitudinal bunched beam stability is used to test the convergence of the basis expansion formalism. It is found that basis expansions can predict instability for equations that have no unstable solutions.

NTIS

*Convergence; Longitudinal Stability; Beams (Radiation)*

**20010119057** Brookhaven National Lab., Upton, NY USA

**High Rate Physics at Neutrino Factories**

King, B. J.; Jun. 10, 1999; 20p; In English

Report No.(s): DE2000-750775; BNL-66976; No Copyright; Avail: Department of Energy Information Bridge

Both muon colliders and non-colliding muon storage rings using muon collider technology have the potential to become the first true 'neutrino factories', with uniquely intense and precisely characterized neutrino beams that could usher in a new era of high rate and long baseline neutrino physics studies at accelerators. This paper gives an overview of the predicted capabilities of

neutrino factories for high rate neutrino physics analyses that will use huge event samples collected with novel, high performance neutrino detectors.
NTIS
*Muons; Neutrinos; Neutrino Beams*

**20010119058** Brookhaven National Lab., Upton, NY USA
**Possible synchrotron light beam profile monitor in RHIC**
Trbojevic, D.; Jun. 26, 1998; 5p; In English
Report No.(s): DE2001-10380; BNL-65134; KB0202000; No Copyright; Avail: Department of Energy Information Bridge, Microfiche

This report examines the possibility of observing transverse beam profiles by using synchrotron light emission from the 100 GeV/nucleon heavy-ion gold beam in the Relativistic Heavy Ion Collider (RHIC). Synchrotron radiation experiences a shift towards higher photon energy when the magnetic field at the end of a dipole varies rapidly over a short distance. Synchrotron light signals from high energy (larger than 400 GeV) proton beams have already been routinely used to observe the transverse beam profiles at the SPS (Super Proton Synchrotron) in CERN (European Center for Nuclear Research) and at the TEVATRON at Fermilab. Because of the modest relativistic factor of the fully stripped stored gold ions in RHIC this 'push' towards higher critical energy is not large enough to place the synchrotron light within the visible region of the spectrum. The critical wavelength remains within the infrared region. A 77K cooled infrared array detector with 160 elements, made of PbSe (Lead salt) could be used for beam profile detection. It would cover the wavelength range between 1 and 6 microns, with maximum sensitivity at a wavelength of 4.5 microns.
NTIS
*Ion Beams; Synchrotron Radiation; Ionic Collisions; Synchrotrons*

**20010119196** Brookhaven National Lab., Upton, NY USA
**Proton boron colliding beams for nuclear fusion**
Ruggiero, A. G.; Apr. 02, 2000; 14p; In English
Report No.(s): DE2000-752976; BNL-67212; No Copyright; Avail: Department of Energy Information Bridge

This paper describes a method of extracting energy from the fusion events occurring during collision of a beam of protons with a beam of ions of (sup 11)B. The two beams circulate in separated and intersecting storage rings of the same geometry and size where they collide head-on in a common long straight-section. Requirements of the beam parameters and of the collider are presented and discussed for a total production of 10 kW of power. to allow small beam dimension and higher intensity, the storage ring itself is a novel concept based on a linear Radio-Frequency Quadrupole bent on itself and closed mechanically: the Circular RFQ. Stringent engineering limitations are encountered. Moreover, the collider performance is disrupted by Space-Charge forces, Intra-Beam and Beam-Beam Scattering. to alleviate and counter-come these limitations, the use of colliding Crystalline Beams is proposed. This has the benefit to enhance the Luminosity of the collision by several orders of magnitude. But it also requires fast and effective Laser and/or Electron Cooling. Sympathetic cooling of ions, as that demonstrated in ion traps, can also be used to avoid partially-stripped boron ions and negative-hydrogen ions.
NTIS
*Boron; Nuclear Fusion; Proton Beams; Ion Beams*

**20010119197** Brookhaven National Lab., Upton, NY USA
**Detector challenges for mu+mu- colliders in the 10-100 tev range**
Rehak, P.; Sep. 27, 1999; 30p; In English
Report No.(s): DE2000-752975; BNL-67213; No Copyright; Avail: Department of Energy Information Bridge

The challenges to design, construct, and operate a detector system in an interaction region at a high energy u+u=collider are briefly summarized. A new solution, based on an extensive use of liquefied rare gases, is proposed for the vertex detector and for the inner tracker. The proposed solution takes a full advantage of the small size of the collision region. The region has radial dimensions below the um range, while its extent in the beam direction is of the order of 1mm depending on the energy of the machine and on the details of the design. In the energy range considered in this workshop, the momenta of charged particles are high enough to be bent only slightly in the solenoidal magnetic field. The tracks are basically straight lines emerging from a known common point. The proposed solution is based on a projective geometry matched to the desired tracks. The aim of the design is to achieve a background blind radiation hard detector.
NTIS
*Muons; Radiation Detectors; Solenoids; Atomic Collisions; Energy Technology*

**20010119215** Brookhaven National Lab., Upton, NY USA

**Acceleration Stages for a Muon Collider**

Berg, J. S.; Mar. 29, 1999; 6p; In English

Report No.(s): DE2000-751112; BNL-66929; No Copyright; Avail: Department of Energy Information Bridge

Using muons in high energy colliders has an advantage in that the muons emit negligible synchrotrons radiation, but has the disadvantage that the lifetime of the muons is very short. The latter requires that the muons be accelerated as rapidly as possible to prevent particle loss. The former allows one to use something other than a single long, straight linac to achieve that acceleration, and thereby achieve potentially significant cost advantages. Some of the acceleration systems will use recirculating linacs to achieve the reuse of the accelerating structures. However, the large longitudinal beam emittances make it difficult to simultaneously achieve large gradients by using high frequency RF and design an arc with a sufficient energy acceptance. The current state of the design for the acceleration stages for a muon collider will be presented, with emphasis on systems accelerating to 70 GeV per beam. Known difficulties will be described as will their possible solutions. In particular, the use of an FFAG-like lattice for the arcs of a recirculating linac will be described which accepts a beam with a very large energy spread over a wide range of energies, allowing a single arc to be used instead of multiple arcs.

NTIS

*Linear Accelerators; Muons; Beams (Radiation)*

**20010119219** Brookhaven National Lab., Upton, NY USA

**Impedance Group Summary**

Blaskiewicz, M.; Jun. 28, 1999; 6p; In English

Report No.(s): DE2000-751104; BNL-66811; No Copyright; Avail: Department of Energy Information Bridge

The impedance working group was charged to reply to the eight questions relevant to the design of high-intensity proton machines such as the SNS or the FNAL driver. These questions were first discussed one by one in the whole group, then each one of them assigned to one member to summarize. On the last morning these contributions were publicly read, re-discussed, and re-written where required - hence they are not the opinion of a particular person, but rather the averaged opinion of all members of the working group.

NTIS

*Impedance; Proton Beams; Particle Beams*

**20010119417** Brookhaven National Lab., Upton, NY USA

**Polarization and Luminosity Requirements for the First Muon Collider**

Parsa, Z.; Jul. 05, 1998; 11p; In English

Report No.(s): DE2000-751101; BNL-66097; No Copyright; Avail: Department of Energy Information Bridge

The muon polarization and luminosity requirement for physics studies at a muon collider are discussed. An overview of a muon collider concepts and design parameters for 0.1, 0.5, and 4 TeV muon colliders are also presented.

NTIS

*Luminosity; Muons*

**20010119423** Brookhaven National Lab., Upton, NY USA

**K Yields pp and e/e using Domain Wall Fermions**

Blum, T.; Jun. 29, 1999; 6p; In English

Report No.(s): DE2000-750779; BNL-66985; No Copyright; Avail: Department of Energy Information Bridge

Due to the good chiral properties of domain wall fermions we attempt to calculate K going to 2(pi) decay amplitudes and Re(e'/e), on the lattice, in the quenched approximation, and using lowest order chiral perturbation theory. Since the first results for Re(e'/e) have been reported recently, we include them here although they were not presented at the time of LATTICE '99. Improvements now underway are briefly described.

NTIS

*Domain Wall; Fermions; Particle Production; Kaons*

**20010119425** Brookhaven National Lab., Upton, NY USA

**Acceleration and Storage of Polarized Proton Beam at RHIC**

Roser, T.; Sep. 12, 1999; 11p; In English

Report No.(s): DE2000-750774; BNL-66969; No Copyright; Avail: Department of Energy Information Bridge

High energy polarized beam collisions will open up the unique physics opportunities of studying spin effects in hard processes. However, the acceleration of polarized beams in circular accelerators is complicated by the numerous depolarizing spin resonances. Using a partial Siberian Snake and a rf dipole that ensure stable adiabatic spin motion during acceleration has made it possible to accelerate polarized protons to 25 GeV at the Brookhaven AGS. Full Siberian Snakes and polarimeters are being developed for RHIC to make the acceleration of polarized protons to 250 GeV possible. Spin rotators around two RHIC interaction regions will allow for the collision of longitudinally polarized protons at the STAR and PHENIX detectors.
NTIS
*Collisions; Polarimeters; Proton Beams*

**20010119429** Brookhaven National Lab., Upton, NY USA
**Quantum Fields In and Out of Equilibrium. Volume 14**
Boyanovsky, B.; Oct. 26, 1998; 101p; In English
Report No.(s): DE2000-750763; BNL-52560; KB0201; No Copyright; Avail: Department of Energy Information Bridge
This is the proceedings of 'Quantum Fields In and Out of Equilibrium', a workshop held October 26-30, 1998.
NTIS
*Conferences; Quantum Mechanics; Equilibrium*

**20010119533** Brookhaven National Lab., Upton, NY USA
**Rhic longitudinal parameter revision**
Wei, J.; Jun. 26, 1998; 5p; In English
Report No.(s): DE2001-10376; BNL-65139; KB0202000; No Copyright; Avail: Department of Energy Information Bridge, Microfiche
Recent experience showed that bunch rotations are needed in the AGS (Alternating Gradient Synchrotron) for gold as well as proton operations before the beams are injected into RHIC (Relativistic Heavy Ion Collider). The longitudinal bunch area is increased for gold operation from 0.3 up to 0.5 eV (center-dot)s/u at design intensity. This paper reviews the revised longitudinal parameters in RHIC during injection, acceleration, transition crossing, rebucketing, and storage for gold and proton beams, accommodating for the change in injection conditions at the AGS.
NTIS
*Beam Injection; Synchrotrons; Heavy Ions; Ionic Collisions*

**20010119534** Brookhaven National Lab., Upton, NY USA
**US-LHC IR Magnet Error Analysis and Compensation**
Wei, J.; Jun. 26, 1998; 5p; In English
Report No.(s): DE2001-10377; BNL-65138; KA0204000; No Copyright; Avail: Department of Energy Information Bridge, Microfiche
This paper studies the impact of the insertion-region (IR) magnet field errors on LHC (Large Hadron Collider) collision performance. Compensation schemes including magnet orientation optimization, body-end compensation, tuning shims, and local nonlinear correction are shown to be highly effective.
NTIS
*Magnets; Linear Accelerators; Particle Collisions; Hadrons*

**20010119535** Brookhaven National Lab., Upton, NY USA
**Colliding crystalline beams**
Wei, J.; Jun. 26, 1998; 5p; In English
Report No.(s): DE2001-10378; BNL-65137; KB0202000; No Copyright; Avail: Department of Energy Information Bridge, Microfiche
The understanding of crystalline beams has advanced to the point where one can now, with reasonable confidence, undertake an analysis of the luminosity of colliding crystalline beams. Such a study is reported here. It is necessary to observe the criteria, previously stated, for the creation and stability of crystalline beams. This requires, firstly, the proper design of a lattice. Secondly, a crystal must be formed, and this can usually be done at various densities. Thirdly, the crystals in a colliding-beam machine are brought into collision. We study all of these processes using the molecular dynamics (MD) method. The work parallels what was done previously, but the new part is to study the crystal-crystal interaction in collision. We initially study the zero-temperature situation. If the beam-beam force (or equivalent tune shift) is too large then overlapping crystals can not be created (rather two spatially separated crystals are formed). However, if the beam-beam force is less than but comparable to that of the space-charge

forces between the particles, we find that overlapping crystals can be formed and the beam-beam tune shift can be of the order of unity. Operating at low but non-zero temperature can increase the luminosity by several orders of magnitude over that of a usual collider. The construction of an appropriate lattice, and the development of adequately strong cooling, although theoretically achievable, is a challenge in practice.
NTIS
*Linear Accelerators; Molecular Dynamics; Beam Interactions; Particle Collisions; Crystallinity*

**20010119536** Brookhaven National Lab., Upton, NY USA
**Bunched beam echos in the AGS**
Kewisch, J.; Jun. 26, 1998; 5p; In English
Report No.(s): DE2001-10379; BNL-65136; KB0202000; No Copyright; Avail: Department of Energy Information Bridge, Microfiche

Beam echos have been measured at FNAL (Fermi National Accelerator Laboratory) and CERN (European Center for Nuclear Research) in coasting beams. A coherent oscillation introduced by a short RF (radio frequency) burst decoheres quickly, but a coherent echo of this oscillation can be observed if the decohered oscillation is 'bounced off' a second RF burst. In this report we describe first longitudinal echo measurements of bunched beam in the AGS (Alternating Gradient Synchrotron) accelerator. We applied a method proposed by Stupakov for transverse beam echos, where the initial oscillation is produced by a dipole kick and is bounced off a quadrupole kick. In the longitudinal case the dipole and quadrupole kicks are produced by a cavities operating at a 90(degree) and 0(degree) phase shift, respectively.
NTIS
*Oscillations; Particle Beams*

**20010119537** Brookhaven National Lab., Upton, NY USA
**Lattice for the 50 gev muon collider ring**
Trbojevic,; Jun. 28, 1998; 5p; In English
Report No.(s): DE2001-10384; BNL-65130; KB0202000; No Copyright; Avail: Department of Energy Information Bridge, Microfiche

A recent progress report on the lattice design of the 50-50 GeV muon collider is presented. The ring circumference needs to be as small as possible due to the short lifetime of the 50 GeV muons. The background at the detector is affected by the continuous decay of muons into electrons which requires a dipole between the high focusing quadrupoles and the detector. to obtain a luminosity on the order of 1 x 10(sup 33) cm(sup -2) S(sup -1) it is required to have beam intensities on the order of 1 x 10(sup 12) particles per bunch. The rms (root mean square) momentum spread of the beam is equal to 0.12% and the beta functions at the interaction point are equal to 4 cm. The maxima of the betatron functions at these quadrupoles are 1300 m, resulting in large chromaticities which must be corrected by local chromatic correction. Pairs of horizontal and vertical chromatic sextupoles are located at locations where the corresponding betatron functions are 100 m and the values of the horizontal dispersion functions are 3 and 2 m, respectively. They are carefully placed so that most of their nonlinear effects are canceled. The dynamic aperture is larger than 7 times the mean size of the beam for the momentum offsets larger than -6 and +10 sigmas.
NTIS
*Linear Accelerators; Particle Collisions; Particle Beams; Muons*

**20010119539** Brookhaven National Lab., Upton, NY USA
**Emittance control of a beam by shaping the transverse charge distribution, using a tomography diagnostic**
Yakimenko,; Jun. 26, 1998; 5p; In English
Report No.(s): DE2001-10387; BNL-65675; No Copyright; Avail: Department of Energy Information Bridge, Microfiche

A high-brightness beam is very important for many applications. A diagnostic that measures the multi-dimensional phase-space density-distribution of the electron bunch is a must for obtaining such beams. Measurement of a slice emittance has been achieved. Tomographic reconstruction of phase space was suggested and implemented using a single quadrupole scan. In the present work we give special attention to the accuracy of the phase space reconstruction and present an analysis using a transport line with nine focusing magnets and techniques to control the optical functions and phases. This diagnostic, coupled with control of the radial charge distribution presents an opportunity to improve the beam brightness. Combining the slice emittance and tomography diagnostics lead to an unprecedented visualization of phase space distributions in five dimensional phase-space and an opportunity to perform high-order emittance corrections.
NTIS
*Particle Beams; Luminosity; Tomography; Beamforming; Charge Distribution*

**20010119547** Lawrence Livermore National Lab., Livermore, CA USA

**Simulation of Ceramic Windows for the APT/LEDA CCDTL**

Daily, L. D.; Mar. 01, 1999; 15p; In English

Report No.(s): DE2001-10439; UCRL-ID-134051; DP0404012; No Copyright; Avail: Department of Energy Information Bridge

Development of a robust, high-average-power (up to 1 MW, CW) microwave transmission line system for the Accelerator Production of Tritium (APT) linac (linear accelerator) facility is a stringent engineering and operational requirement. One key component in this RF (radio frequency) transmission system is the vacuum barrier window. The requirement of high-power handling capability coupled to the desirability of low probability of failure over lengthy time scales can be treated substantially with a set of microwave, thermomechanical, and Weibull analysis codes. This paper examines engineering models of ceramic windows for the Coupled-Cavity Drift-Tube Linac (CCDTL) segment of the APT Normal Conducting (NC) linac. The detailed cooling circuit is modeled and accurate heat deposition models for the RF are implemented. This simulation is then used to analyze the thermomechanically induced stresses on the CCDTL window configuration. A Weibull-distribution failure prediction code is used to integrate experimentally obtained ceramic material failure data and structural analysis calculations to infer reliability of the structure.

NTIS

*Ceramics; Transmission Lines; Computerized Simulation; Cooling Systems*

**20010119549** Lawrence Livermore National Lab., Livermore, CA USA

**Spherical Harmonic Results for the 3D Kobayashi Benchmark Suite**

Brown, P. N.; Chang, B.; Hanebutte, U. R.; Mar. 02, 1999; 6p; In English

Report No.(s): DE2001-10442; UCRL-JC-133372; REPT-98-ERD-022; No Copyright; Avail: Department of Energy Information Bridge

Spherical harmonic solutions are presented for the Kobayashi benchmark suite. The results were obtained with Ardra, a scalable, parallel neutron transport code developed at Lawrence Livermore National Laboratory (LLNL). The calculations were performed on the IBM ASCI Blue-Pacific computer at LLNL.

NTIS

*Computer Programs; Spherical Harmonics*

**20010119552** Fermi National Accelerator Lab., Batavia, IL USA

**Progress in leptonic and semileptonic decays in lattice QCD**

Ryan, S. M.; Sep. 02, 1999; 9p; In English

Report No.(s): DE2001-10461; FERMILAB-CONF-99/054-T; No Copyright; Avail: Department of Energy Information Bridge, Microfiche

The status of lattice calculations of heavy quark phenomenology is reviewed. Particular emphasis is placed on the understanding and control of the calculational uncertainties. The ensuring implications for constraining the CKM matrix elements are discussed.

NTIS

*Quantum Chromodynamics; Quarks*

**20010119553** Fermi National Accelerator Lab., Batavia, IL USA

**Design and test of a beam transformer as a chopper**

Mori, Y.; Muto, M.; Shirakabe, Y.; Takagi, A.; Sep. 02, 1999; 5p; In English

Report No.(s): DE2001-10463; FERMILAB-CONF-99/102; No Copyright; Avail: Department of Energy Information Bridge, Microfiche

This paper introduces a new type of chopper, which is similar to a beam transformer first discussed by R. Wideroe. It is based on the fact that the RFQ has a rather small energy window. A pulsed beam transformer that provides 10% energy modulation to the beam in front of an RFQ can effectively chop the beam. It has fast rise- and fall-time and a short physical length. A prototype, which consists of a cavity and a high voltage pulsed power supply, has been constructed and tested. Two types of magnetic materials were tried for making the core of the cavity--the Finemet and the ferrite Philips 4M2. While the former gave good performance, the latter failed the test. Results from the bench measurements and a plan for beam tests are briefly described.

NTIS

*Beams (Radiation); Magnetic Materials; Transformers*

**20010119554** Fermi National Accelerator Lab., Batavia, IL USA
**Electroweak results from hadron colliders**
Demarteau, M.; Sep. 02, 1999; 7p; In English
Report No.(s): DE2001-10464; FERMILAB-CONF-99/126-E; No Copyright; Avail: Department of Energy Information Bridge, Microfiche

A very brief summary of recent electroweak results from hadron colliders is given. The emphasis is placed on inclusive W(sup (+-)) and Z(sup 0) production, the measurement of the mass of the W boson and the measurement of trilinear gauge boson couplings.
NTIS
*Hadrons; Electroweak Interactions (Field Theory); Bosons*

**20010119556** Fermi National Accelerator Lab., Batavia, IL USA
**Intensity Dependent Instability Issues for Electron Rings**
Ng, K. Y.; Sep. 02, 1999; 42p; In English
Report No.(s): DE2001-10468; FERMILAB-TM-2090; No Copyright; Avail: Department of Energy Information Bridge, Microfiche

A bunch of electrons has a spread of energy because of many reasons, for example, random quantum excitation which changes the energy of the particles randomly, intrabeam scattering which is just Coulomb scattering among the particles, and Touschek scattering which is large-angle Coulomb scattering which converts the transverse momentum of a particle into longitudinal.
NTIS
*Electron Bunching; Storage Rings (Particle Accelerators)*

**20010119565** Fermi National Accelerator Lab., Batavia, IL USA
**Online monitoring in the upcoming Fermilab Tevatron Run II**
Canal, P.; Sep. 08, 1999; 6p; In English
Report No.(s): DE2001-10501; FERMILAB-CONF-99/235-E; No Copyright; Avail: Department of Energy Information Bridge, Microfiche

We describe the online event monitoring systems using ROOT (1) for the CDF and D0 collaborations in the upcoming Fermilab Tevatron runII. The CDF and D0 experiments consist of many detector subsystems and will run in a high rate large bandwidth data transfer environment. In the experiments, it is crucial to monitor the performance of each subsystem and the integrity of the data, in real time with minimal interruption. ROOT is used as the main analysis tool for the monitoring systems and its GUI is used to browse the results via socket, allowing multiple GUI client connections.
NTIS
*On-Line Systems; Particle Accelerators; Data Acquisition*

**20010119573** Argonne National Lab., IL USA
**B physics at CDF**
Wicklund, A. B.; Jan. 20, 1998; 20p; In English
Report No.(s): DE2001-10574; ANL-HEP-CP-98-01; No Copyright; Avail: Department of Energy Information Bridge, Microfiche

The CDF (Collider Detector Facility) experiment at the Fermilab Tevatron has proven to be well suited for precision studies of b physics. Thanks to the excellent performance of the Tevatron Collider and the detector, CDF has accumulated very large data samples and roughly a decade of experience with b physics in p(bar p) collisions. With the much higher luminosities expected for the Main Injector era, the next decade promises to be an even more fruitful period for CDF. Here we offer a brief overview of issues in hadron-collider b physics and a summary of CDF's accomplishments and future plans.
NTIS
*Particle Collisions; Particle Accelerators; Research Facilities; Particle Theory*

**20010119574** Argonne National Lab., IL USA
**Multi-neutron transfer reactions at sub-barrier energies**
Rehm, K. E.; Jan. 20, 1998; 12p; In English
Report No.(s): DE2001-10575; ANL/PHY/CP-95412; No Copyright; Avail: Department of Energy Information Bridge, Microfiche

The optimum conditions for multi-neutron transfer have been studied in the system (sup 58)Ni + (sup 124)Sn at bombarding energies at and below the Coulomb barrier. The experiments were performed in inverse kinematics with a (sup 124)Sn beam bombarding a (sup 58)Ni target. The particles were identified with respect to mass and Z in the split-pole spectrograph with a hybrid focal plane detector with mass and Z-resolutions of A/(Delta)A = 150 and Z/(Delta)Z = 70. At all energies the transfer of up to six neutrons was observed. The yields for these transfer reactions are found to decrease by about a factor of four for each transferred neutron.
NTIS
*Neutron Physics; Nuclear Reactions; Inverse Kinematics; Neutrons*

**20010119982** Argonne National Lab., IL USA
**Kaon electroproduction on deuterium**
Reinhold, J.; Jan. 12, 1998; 10p; In English
Report No.(s): DE2001-10558; ANL/PHY/CP-95316; No Copyright; Avail: Department of Energy Information Bridge
Kaon electroproduction on deuterium and hydrogen targets has been measured at beam energies of 3.245 and 2.445 GeV and momentum transfer Q(sup 2)=0.38 and 0.5 GeV(sup 2). Associated (Lambda) production off a proton in the deuteron exhibits a quasifree production mechanism. The production of (Sigma)(sup (minus)) off the neutron could be extracted for the first time with reasonable errors.
NTIS
*Deuterium; Deuterons; Kaons; Hydrogen*

**20010119985** Argonne National Lab., IL USA
**Tunneling from super- to normal-deformed minima in nuclei**
Khoo, T. L.; Jan. 08, 1998; 48p; In English
Report No.(s): DE2001-10550; ANL/PHY/CP-95250; No Copyright; Avail: Department of Energy Information Bridge
An excited minimum, or false vacuum, gives rise to a highly elongated superdeformed (SD) nucleus. A brief review of superdeformation is given, with emphasis on the tunneling from the false to the true vacuum, which occurs in the feeding and decay of SD bands. During the feeding process the tunneling is between hot states, while in the decay it is from a cold to a hot state. The (gamma) spectra connecting SD and normal-deformed (ND) states provide information on several physics issues: the decay mechanism; the spin/parity quantum numbers, energies and microscopic structures of SD bands; the origin of identical SD bands; the quenching of pairing with excitation energy; and the chaoticity of excited ND states at 2.5-5 MeV. Other examples of tunneling in nuclei, which are briefly described, include the possible role of tunneling in (Delta)I = 4 bifurcation in SD bands, sub-barrier fusion and proton emitters.
NTIS
*Nuclei (Nuclear Physics); Nuclear Deformation*

**20010119989** Argonne National Lab., IL USA
**Accelerator development for a radioactive beam facility based on ATLAS**
Shepard, K. W.; Jan. 08, 1998; 7p; In English
Report No.(s): DE2001-10544; ANL/PHY/CP-95196; No Copyright; Avail: Department of Energy Information Bridge
The existing superconducting linac ATLAS is in many respects an ideal secondary beam accelerator for an ISOL (Isotope separator on-line) type radioactive beam facility. Such a facility would require the addition of two major accelerator elements: a low charge state injector for the existing heavy ion linac, and a primary beam accelerator providing 220 MV of acceleration for protons and light ions. Development work for both of these elements, including the option of superconducting cavities for the primary beam accelerator is discussed.
NTIS
*Heavy Ions; Light Ions; Linear Accelerators; Fabrication; Ion Beams*

**20010119993** Argonne National Lab., IL USA
**Photon scattering in muon collisions**
Klasen, M.; Dec. 18, 1997; 12p; In English
Report No.(s): DE2001-10540; ANL-HEP-CP-97-96; No Copyright; Avail: Department of Energy Information Bridge
The authors estimate the benefit of muon colliders for photon physics. They calculate the rate at which photons are emitted from muon beams in different production mechanisms. Bremsstrahlung is reduced, breamsstrahlung disappears, and laser backscattering suffers from a bad conversion of the incoming to the outgoing photon beam in addition to requiring very short

wavelengths. As a consequence, the cross sections for jet photoproduction in (mu)p and (mu)(sup +) (mu)(sup (minus)) collisions are reduced by factors of 2.2 and 5 compared to ep and e(sup +) e(sup (minus)) machines. However, the cross sections remain sizable and measurable giving access to the photon and proton parton densities down to x values of 10(sup (minus)3) to 10(sup (minus)4).
NTIS
*Photons; Muons; Collisions; Scattering*

**20010120007** Argonne National Lab., IL USA
**Linac-beam characterizations at 600 MeV using optical transition radiation diagnostics**
Lumpkin, A. H.; May 27, 1998; 10p; In English
Report No.(s): DE2001-10700; ANL/ASD/CP-95937; No Copyright; Avail: Department of Energy Information Bridge, Microfiche

Selected optical diagnostics stations were upgraded in anticipation of low-emittance, bright electron beams from a thermionic rf gun or a photoelectric rf gun on the Advanced Photon Source (APS) injector linac. These upgrades include installation of optical transition radiation (OTR) screens, transport lines, and cameras for use in transverse beam size measurements and longitudinal profile measurements. Using beam from the standard thermionic gun, tests were done at 50 MeV and 400 to 650 MeV. Data were obtained on the limiting spatial ((sigma) (approximately) 200 (micro)m) and temporal resolution (300 ms) of the Chromox (Al2O3 : Cr) screen (250-(micro)n thick) in comparison to the OTR screens. Both charge-coupled device (CCD) and charge-injection device (CID) video cameras were used as well as the Hamamatsu C5680 synchroscan streak camera operating at a vertical deflection rate of 119.0 MHz (the 24th subharmonic of the S-band 2856-MHz frequency). Beam transverse sizes as small as (sigma)(sub x) = 60 (micro)m for a 600-MeV beam and micropulse bunch lengths of (sigma)(sub (tau)) less than ps have been recorded for macropulse-averaged behavior with charges of about 2 to 3 nC per macropulse. These techniques are applicable to linac-driven, fourth-generation light source R and D experiments including the APS's SASE FEL experiment.
NTIS
*Photons; Optical Transition; Diagnosis; Electron Beams; Linear Accelerators*

**20010120008** Argonne National Lab., IL USA
**Optimization of four-button BPM configuration for small-gap beam chambers**
Kim, S. H.; May 27, 1998; 10p; In English
Report No.(s): DE2001-10699; ANL/ASD/CP-95936; No Copyright; Avail: Department of Energy Information Bridge, Microfiche

Configuration of four-button beam position monitors (BPMs) employed in small-gap beam chambers is optimized from 2-D electrostatic calculation of induced charges on the button electrodes. The calculation shows that for a narrow chamber of width/height (2w/2h) much greater than 1, over 90% of the induced charges are distributed within a distance of 2h from the charged beam position in the direction of the chamber width. The most efficient configuration for a four-button BPM is to have a button diameter of (2-2.5) h with no button offset from the beam. The button sensitivities in this case are maximized and have good linearity with respect to the beam positions in the horizontal and vertical directions. The button sensitivities and beam coefficients are also calculated for the 8-mm and 5-mm chambers used in the insertion device straight sections of the 7-GeV Advanced Photon Source.
NTIS
*Optimization; Beams (Radiation); Monitors*

**20010120009** Argonne National Lab., IL USA
**Fundamental limits on beam stability at the Advanced Photon Source**
Decker, G. A.; Jun. 18, 1998; 11p; In English
Report No.(s): DE2001-10698; ANL/ASD/CP-95935; No Copyright; Avail: Department of Energy Information Bridge, Microfiche

Orbit correction is now routinely performed at the few-micron level in the Advanced Photon Source (APS) storage ring. Three diagnostics are presently in use to measure and control both AC and DC orbit motions: broad-band turn-by-turn rf beam position monitors (BPMs), narrow-band switched heterodyne receivers, and photoemission-style x-ray beam position monitors. Each type of diagnostic has its own set of systematic error effects that place limits on the ultimate pointing stability of x-ray beams supplied to users at the APS. Limiting sources of beam motion at present are magnet power supply noise, girder vibration, and thermal

timescale vacuum chamber and girder motion. This paper will investigate the present limitations on orbit correction, and will delve into the upgrades necessary to achieve true sub-micron beam stability.
NTIS
*Photons; Beams (Radiation); Stability; Storage Rings (Particle Accelerators)*

**20010120010** Argonne National Lab., IL USA
**Design of the digitizing beam position limit detector**
Merl, R.; May 27, 1998; 11p; In English
Report No.(s): DE2001-10696; ANL/ASD/CP-95933; No Copyright; Avail: Department of Energy Information Bridge, Microfiche

The Digitizing Beam Position Limit Detector (DBPLD) is designed to identify and react to beam missteering conditions in the Advanced Photon Source (APS) storage ring. The high power of the insertion devices requires these missteering conditions to result in a beam abort in less than 2 milliseconds. Commercially available beam position monitors provide a voltage proportional to beam position immediately upstream and downstream of insertion devices. The DBPLD is a custom VME board that digitizes these voltages and interrupts the heartbeat of the APS machine protection system when the beam position exceeds its trip limits.
NTIS
*Beams (Radiation); Storage Rings (Particle Accelerators); Photons*

**20010120011** Argonne National Lab., IL USA
**Calibration of an Advanced Photon Source linac beam position monitor used for positron position measurement of a beam containing both positrons and electrons**
Sereno, N. S.; May 19, 1998; 9p; In English
Report No.(s): DE2001-10695; ANL/ASD/CP-95931; No Copyright; Avail: Department of Energy Information Bridge, Microfiche

The Advanced Photon Source (APS) linac beam position monitors can be used to monitor the position of a positron beam also containing electrons. To accomplish this task, both the signal at the bunching frequency of 2856 MHz and the signal at 2 x 2856 MHz are acquired and processed for each stripline. The positron beam position is obtained by forming a linear combination of both 2856- and 5712-MHz signals for each stripline and then performing the standard difference over sum computation. The required linear combination of the 2856- and 5712-MHz signals depends on the electrical calibration of each stripline/cable combination. In this paper, the calibration constants for both 2856-MHz and 5712-MHz signals for each stripline are determined using a pure beam of electrons. The calibration constants are obtained by measuring the 2856- and 5712-MHz stripline signals at various electron beam currents and positions. Finally, the calibration constants measured using electrons are used to determine positron beam position for the mixed beam case.
NTIS
*Photon Beams; Electron Beams; Positrons*

**20010120012** Argonne National Lab., IL USA
**Characterizing transverse beam dynamics at the APS storage ring using a dual-sweep streak camera**
Yang, B.; May 27, 1998; 11p; In English
Report No.(s): DE2001-10694; ANL/ASD/CP-95930; No Copyright; Avail: Department of Energy Information Bridge, Microfiche

We present a novel technique for characterizing transverse beam dynamics using a dual-sweep streak camera. The camera is used to record the front view of successive beam bunches and/or successive turns of the bunches. This extension of the dual-sweep technique makes it possible to display non-repeatable beam transverse motion in two fast and slow time scales of choice, and in a single shot. We present a study of a transverse multi-bunch instability in the APS storage ring. The positions, sizes, and shapes of 20 bunches (2.84 ns apart) in the train, in 3 to 14 successive turns (3.68 (micro)s apart) are recorded in a single image, providing rich information about the unstable beam. These include the amplitude of the oscillation ((approximately)0.0 at the head of the train and (approximately)2 mm towards the end of the train), the bunch-to-bunch phase difference, and the significant transverse size growth within the train. In the second example, the technique is used to characterize the injection-kicker induced beam motion, in support of the planned storage ring top-up operation. By adjusting the time scale of the dual sweep, it clearly shows the amplitude ((+-)1.8mm) and direction of the kick, and the subsequent decoherence ((approximately) 500 turns) and damping ((approximately) 20 ms) of the stored beam. Since the storage ring has an insertion device chamber with full vertical aperture of 5 mm, it is of special interest to track the vertical motion of the beam. An intensified gated camera was used for this

purpose. The turn-by-turn x-y motion of a single-bunch beam was recorded and used as a diagnostic for coupling correction. Images taken with uncorrected coupling will be presented.
NTIS
*Photons; Beams (Radiation); Storage Rings (Particle Accelerators); Streak Cameras*

**20010120013** Argonne National Lab., IL USA
**First multi-GeV particle-beam measurements using a synchroscan and dual-sweep x-ray streak camera**
Lumpkin, A. H.; May 27, 1998; 10p; In English
Report No.(s): DE2001-10693; ANL/ASD/CP-95929; No Copyright; Avail: Department of Energy Information Bridge, Microfiche

Particle-beam characterizations of a multi (7)-GeV storage ring beam have been done for the first time using a synchroscan and dual-sweep x-ray streak camera at the Advanced Photon Source (APS). The hard x-rays (2-20 keV) from a bending magnet source were imaged using an adjustable pinhole aperture, and both the horizontal size, (sigma)(sub x) (approximately) 190 (micro)m, and bunch length, (sigma)(sub t) (approximately) 28 ps, were measured simultaneously. The Au photocathode provides sensitivity from 10 eV to 10 keV covering the three orders of magnitude in wavelength from the UV to hard x-rays.
NTIS
*Photons; Sensitivity; Storage Rings (Particle Accelerators); Streak Cameras; Streak Photography; Particle Beams*

**20010120014** Argonne National Lab., IL USA
**Real-time orbit feedback at the APS**
Carwardine, J.; Jun. 18, 1998; 22p; In English
Report No.(s): DE2001-10692; ANL/ASD/CP-95927; No Copyright; Avail: Department of Energy Information Bridge, Microfiche

A real-time orbit feedback system has been implemented at the Advanced Photon Source in order to meet the stringent orbit stability requirements. The system reduces global orbit motion below 30Hz by a factor of four to below 5(micro)m rms horizontally and 2(micro)m rms vertically. This paper focuses on dynamic orbit stability and describes the all-digital orbit feedback system that has been implemented at the APS. Implementation of the global orbit feedback system is described and its latest performance is presented. Ultimately, the system will provide local feedback at each x-ray source point using installed photon BPMs to measure x-ray beam position and angle directly. Technical challenges associated with local feedback and with dynamics of the associated corrector magnets are described. The unique diagnostic capabilities provided by the APS system are discussed with reference to their use in identifying sources of the underlying orbit motion.
NTIS
*Photons; Real Time Operation; Feedback; Dynamic Stability; Digital Systems*

**20010120031** Argonne National Lab., IL USA
**Threshold Resummation of Soft Gluons in Hadronic Reactions: An Introduction**
Berger, E. L.; Feb. 17, 1998; 18p; In English
Report No.(s): DE2001-10645; ANL-HEP-CP-98-03; No Copyright; Avail: Department of Energy Information Bridge

The authors discuss the motivation for resummation of the effects of initial-state soft gluon radiation, to all orders in the strong coupling strength, for processes in which the near-threshold region in the partonic subenergy is important. The author summarizes the method of perturbative resummation and its application to the calculation of the total cross section for top quark production at hadron colliders. Comments are included on the differences between the treatment of subleading logarithmic terms in this method and in other approaches.
NTIS
*Gluons; Hadrons; Perturbation*

**20010120045** Brookhaven National Lab., Upton, NY USA
**Classical methods in DIS and nuclear scattering at small x**
Venugopalan, R.; May 29, 1999; 40p; In English
Report No.(s): DE2000-752967; BNL-67244; No Copyright; Avail: Department of Energy Information Bridge

In hadrons and nuclei at very small x, parton distributions saturate at a scale Q(sub s)(x). Since the occupation number is large, and Q(sub s)(x) much greater than Lambda(sub QCD), classical weak coupling methods may be used to study this novel regime

of nonlinear classical fields in QCD. In these lectures, we apply these methods to compute structure functions in deeply inelastic scattering (DIS) and the energy densitiy of gluons produced in high energy nuclear collisions.
NTIS
*Quantum Chromodynamics; Partons; High Energy Electrons; Inelastic Scattering*

**20010120047** Brookhaven National Lab., Upton, NY USA
**Detector backgrounds for a high energy muon collider**
Benary, O.; Sep. 27, 1999; 13p; In English
Report No.(s): DE2000-752965; BNL-67248; No Copyright; Avail: Department of Energy Information Bridge
The potentially large background produced from the decay products of muons could affect the quality of the physics in a high energy muon collider. This paper examines the kinds of background present and their expected rate. The results are based on a simulation of muon colliders with center of mass energies of 100 GeV, 500 GeV and 4 TeV.
NTIS
*Muons; Computerized Simulation; Detectors; High Energy Electrons*

**20010120070** Los Alamos National Lab., NM USA
**Computation of Charged-Particle Transfer Maps for General Fields and Geometries Using Electromagnetic Boundary-Value Data**
Stasevich, T. J.; Bodoh-Creed, A.; Walstrom, P.; Roberts, P.; Dragt, A. J.; Sep. 07, 2000; 15p; In English
Report No.(s): DE2000-762078; LA-UR-00-4248; No Copyright; Avail: Department of Energy Information Bridge, Microfiche
The passage of a charged particle through a region of nonvanishing electromagnetic fields (e.g., a bending magnet, multipole magnet, spectrometer, electrostatic lens, electromagnetic velocity separator, etc. ) can be described by a transfer map. In general, the map is a six-vector-valued function that relates the final six phase-space coordinates of a beam particle to its initial six phase-space coordinates. The map can be represented in either Taylor- or Lie-series form. The series-expansion variables for the map are deviations from a nominal or reference trajectory, which in general is curved and must be found by numerical integration of the equations of motion of a reference particle. The reference particle is represented by a particular point in the initial phase space and a corresponding point in the final phase space. Calculation of aberration terms (terms beyond lowest order) in the series form of the map requires knowledge of multiple derivatives of the electromagnetic fields along the reference trajectory.
NTIS
*Charged Particles; Electromagnetic Fields; Taylor Series*

**20010120077** Argonne National Lab., IL USA
**Progress in the linear beam dynamics study of ionization cooling channel**
Kim, K. J.; Wang, C. X.; Aug. 04, 2000; 33p; In English
Report No.(s): DE2000-761262; ANL/ASD/CP-102519; No Copyright; Avail: Department of Energy Information Bridge
We review recent progresses in the study of linear beam dynamics of the ionization cooling in solenoidal focusing channels. The topics included are: understanding of the solenoidal focusing in the rotating frame; beam parameterization in terms of the envelope functions, emittance, and angular momentum; the coupled equation for emittance and angular momentum in periodic focusing channels; general solution and comparison with simulation; analytic approach for calculating the stability criteria and envelope function in periodic focusing channels.
NTIS
*Ionization; Beams (Radiation); Cooling Systems*

**20010120090** Brookhaven National Lab., Upton, NY USA
**First Fermi in a high energy nuclear collision**
Krasnitz, A.; Aug. 09, 1999; 6p; In English
Report No.(s): DE2000-752968; BNL-67240; No Copyright; Avail: Department of Energy Information Bridge
At very high energies, weak coupling, non-perturbative methods can be used to study classical gluon production in nuclear collisions. One observes in numerical simulations that after an initial formation time, the produced partons are on shell, and their subsequent evolution can be studied using transport theory. At the initial formation time, a simple non-perturbative relation exists between the energy and number densities of the produced partons, and a scale determined by the saturated parton density in the nucleus.
NTIS
*Collisions; Transport Theory; Partons; Fermions; Standard Model (Particle Physics)*

**20010120100** Argonne National Lab., IL USA

**Second crystal cooling on cryogenically cooled undulator and wiggler double crystal monochromators**

Knapp, G. S.; Aug. 03, 1998; 11p; In English

Report No.(s): DE2001-10702; ANL/MSD/CP-95959; No Copyright; Avail: Department of Energy Information Bridge, Microfiche

Simple methods for the cooling of the second crystals of cryogenically cooled undulator and wiggler double crystal monochromators are described. Copper braids between the first and second crystals are used to cool the second crystals of the double crystal monochromators. The method has proved successful for an undulator monochromator and we describe a design for a wiggler monochromator.

NTIS

*Crystals; Monochromators; Cooling*

**20010120264** Argonne National Lab., IL USA

**Recent observations on the APS storage ring using synchrotron radiation monitors**

Borland, M.; Jul. 30, 1998; 5p; In English

Report No.(s): DE2001-10625; ANL/ASD/CP-95539; No Copyright; Avail: Department of Energy Information Bridge, Microfiche

The Advanced Photon Source (APS) 7-GeV storage ring and the synchrotron radiation diagnostics have matured noticeable in the past year. The monitors now include information from two separate bending-magnet sources (one at a dispersive point in the lattice) as well as a 198-period diagnostic undulator. Data logging via EPICS of the observed transverse beam size is coupled with the measured lattice parameters to calculate emittance on-line as well. Information on the beam emittance (7 (+/-) 1 nm rad) in both the standard lattice and a low (beta)(sub y) lattice, the vertical coupling (1 to 4%), and beam position and jitter are logged. In addition, measurements of divergence, (3 to 7 (micro)rad), beam bunch length (approximately 35 ps), and even effects of the moon's gravity on the source point image position have been performed.

NTIS

*Beams (Radiation); Monitors; Storage Rings (Particle Accelerators); Synchrotron Radiation*

**20010120267** Argonne National Lab., IL USA

**Advanced Photon Source monopulse RF beam position monitor front-end upgrade**

Lill, R. M.; May 27, 1998; 10p; In English

Report No.(s): DE2001-10697; ANL/ASD/CP-95934; No Copyright; Avail: Department of Energy Information Bridge, Microfiche

This paper will describe and analyze the rf beam position monitor (RFBPM) front-end upgrade for the Advanced Photon Source (APS) storage ring. This system is based on amplitude-to-phase (AM/PM) conversion monopulse receivers. The design and performance of the existing BPM front-end will be considered as the baseline design for the continuous effort to improve and upgrade the APS beam diagnostics. The upgrade involves redesigning the in-tunnel filter comparator units to improve insertion loss, return loss, and bandpass filter matching that presently limit the different fill patterns used at APS.

NTIS

*Photons; Beams (Radiation); Monitors; Storage Rings (Particle Accelerators)*

**20010120533** Argonne National Lab., IL USA

**Study of hyperon-nucleon interactions with d(e,e(sup 1)K) reactions**

Lee, T. S. H.; Jan. 29, 1998; 6p; In English

Report No.(s): DE2001-10612; ANL/PHY/CP-95494; No Copyright; Avail: Department of Energy Information Bridge, Microfiche

The dependence of the d(e,e(prime)K(sup +)) reaction cross sections on the hyperon-nucleon interactions is investigated. It is shown that the data obtained with Longitudinal-Transverse separation or polarized photons can distinguish a class of Nijmegen models of hyperon-nucleon interactions which are (chi)(sup 2)-equivalent in fitting the existing 35 data points of hyperon-nucleon reactions.

NTIS

*Nucleons; Particle Interactions; Hyperons*

**20010120547** Argonne National Lab., IL USA
**Physics Results from Polarized DIS**
Ramsey, G. P.; Mar. 23, 1998; 6p; In English
Report No.(s): DE2001-10688; ANL-HEP-CP-98-19; No Copyright; Avail: Department of Energy Information Bridge, Microfiche

We have extracted polarized nucleon distributions from recent data at CERN, SLAC and DESY. The flavor-dependent valence and sea quark spin distributions are determined for each experiment. We take into account possible differences in the up and down sea distributions, and assume that the strange sea contribution is suppressed by mass effects. Physics results determined from different experiments are compared, including higher order corrections.
NTIS
*Nucleons; Quarks; Valence; Inelastic Scattering*

**20010120554** Argonne National Lab., IL USA
**Rotating crystal cube as a variable shutter for use with synchrotron radiation**
McPherson, A., Argonne National Lab., USA; Jul. 08, 1998; 9p; In English
Report No.(s): DE2001-10730; ANL/XFD/CP-96074; No Copyright; Avail: Department of Energy Information Bridge, Microfiche

A beam chopper together with the temporal structure of x-rays emitted by a synchrotrons storage ring can be utilized to generate x-ray bursts of variable length and time separation. A Si cube, cut for diffraction from the (220) planes, was mounted to a low-speed motor to produce a beam chopper based upon the Darwin width of the crystal. An x-ray pulse, consisting of an envelope of individual pulses characterizing the loading pattern of the storage ring, was transmitted. The width of the transmitted pulse and the time between pulses was varied by varying the rotation frequency of the Si cube. Pulses as short as (approx) 75 ps or as long as (approx) 4 (micro)s were transmitted with pulse separation spanning from 4 ms to 167 ms.
NTIS
*Crystals; Synchrotron Radiation; X Rays; Beam Splitters; Pulsed Radiation*

**20010120557** Argonne National Lab., IL USA
**Low-(beta) SC Linacs: Past, Present, and Future**
Bollinger, L. M., Argonne National Lab., USA; Nov. 18, 1998; 7p; In English
Report No.(s): DE2001-10733; ANL/PHY/CP-96083; No Copyright; Avail: Department of Energy Information Bridge, Microfiche

This paper is a general review of superconducting low-(beta) technology and applications from its beginning in 1969 into the near-term future. The emphasis is on studies of accelerating resonators and on SC linacs that boost the energy of heavy-ion beams from tandem electrostatic accelerators used for nuclear-physics research. Other topics are positive-ion SC injectors to replace tandems and the need for accelerating structures with (beta) outside of the present proven range, 0.008 less than (beta) less than 0.2.
NTIS
*Superconductivity; Technology Utilization; Linear Accelerators; Superconducting Cavity Resonators*

**20010120560** Argonne National Lab., IL USA
**Improved Temperature Regulation of APS Linac RF Components**
Dortwegt, R.; Sep. 21, 1998; 5p; In English
Report No.(s): DE2001-10765; ANL/ASD/CP-96378; No Copyright; Avail: Department of Energy Information Bridge, Microfiche

The temperature of the APS S-Band linac's high-power radio frequency (rf) components is regulated by water from individual closed-loop deionized (DI) water systems. The rf components are all made of oxygen-free high-conductivity copper and respond quickly to temperature changes. The SLED cavities are especially temperature-sensitive and cause beam energy instabilities when the temperature is not well regulated. Temperature regulation better than +/- 0.1 F is required to achieve good energy stability. Improvements in the closed-loop water systems have enabled them to achieve a regulation of +/- 0.05 F over long periods. Regulation philosophy and equipment are discussed and numerical results are presented.
NTIS
*Feedback Control; Linear Accelerators; Radio Equipment; Cooling Systems; Temperature Control*

**20010120790** Argonne National Lab., IL USA

**Effect of small radiation divergence on measurements of the source size**

Ilinski, P.; Oct. 01, 1998; 6p; In English

Report No.(s): DE2001-10827; ANL/XFD/CP-96577; No Copyright; Avail: Department of Energy Information Bridge

Third-generation storage rings have small particle beam emittances. The size of the particle beam can be determined from the measured image size of the focused radiation source. Undulators are preferred as radiation sources at third-generation storage rings, the radiation emitted by an undulator has both small size and divergence. The effect of the small beam divergence on determination of the source size is discussed here. The analysis is performed in an approximation of a Gaussian distribution of the radiation intensity. The partial approximation and matrix methods were also used for this derivation. It was found that the effect of the small beam divergence depends on the ratio of the angular acceptance of the source to the divergence of the emitted radiation. NTIS

*Radiation Sources; Storage Rings (Particle Accelerators); Particle Beams; Divergence; Approximation*

**20010120798** Argonne National Lab., IL USA

**Electron Beam Charge State Amplifier (EBQA): A Conceptual Evaluation**

Dooling, J. C.; Oct. 12, 1998; 5p; In English

Report No.(s): DE2001-10773; ANL/IPNS/CP-96397; No Copyright; Avail: Department of Energy Information Bridge, Microfiche

A concept is presented for stripping low-energy, radioactive ions from 1+ to higher charge states. Referred to as an Electron Beam Charge State Amplifier (EBQA), this device accepts a continuous beam of singly-charged, radioactive ions and passes them through a high-density electron beam confined by a solenoidal magnetic field. Singly-charged ions may be extracted from standard Isotope-Separator-Online (ISOL) sources. An EBQA is potentially useful for increasing the charge state of ions prior to injection into post-acceleration stages at ISOL radioactive beam facilities. The stripping efficiency from q=1+ to 2+ ((eta)(sub 12)) is evaluated as a function of electron beam radius at constant current with solenoid field, injected ion energy, and ion beam emittance used as parameters. Assuming a 5 keV, 1 A electron beam, (eta)(sub 12) = 0.38 for 0.1 keV, Xe132 ions passing through an 8 Tesla solenoid, 1 m in length. Multi-pass configurations to achieve 3+ or 4+ charge states are also conceivable. The calculated efficiencies depend inversely on the initial ion beam emittances. The use of a helium-buffer-gas, ion-guide stage to improve the brightness of the 1+ beams may enhance the performance of an EBQA. NTIS

*Charged Particles; Electron Beams; Emittance; Ion Beams*

**20010120799** Argonne National Lab., IL USA

**Time-Resolved Imaging for the APS Linac Beams**

Lumpkin, A. H.; Sep. 29, 1998; 5p

Report No.(s): DE2001-10769; ANL/ASD/CP-96385; No Copyright; Avail: Department of Energy Information Bridge, Microfiche

The particle-beam imaging diagnostics for the Advanced Photon Source (APS) injector time have been enhanced by the installation of optical transition radiation (OTR) screens and the use of Ce-doped YAG crystals as beam profile monitors. Both converters have improved spatial resolution and time responses compared to the standard Chromox (Al2O3:Cr) screens used elsewhere in the linac. These enhancements allow us to address the smaller beam sizes (less than 100 micrometers) and the critical micropulse bunch length of higher brightness gun sources. For the Linac macropulse of 30-ns duration composed of 86 micropulses at S-band frequency intervals, only the OTR mechanism is prompt enough to separate individual micropulses and to allow streak camera measurements of the micropulse averaged bunch length. Tests have been performed at 400 to 625 MeV using the gated DC thermionic gun source. Beam sizes less than sigma(sub x) = 30 micrometers have been observed with a micropulse bunch length of sigma = 2-3 ps using OTR. First results on the lower-emittance rf thermionic gun are briefly discussed. NTIS

*Imaging Techniques; Injectors; Linear Accelerators; Micropulsations*

**20010120800** Argonne National Lab., IL USA

**Implementation of Improved Interactive Image Analysis at the Advanced Photon Source (APC) Linac**

Arnold, N.; Sep. 11, 1998; 5p; In English

Report No.(s): DE2001-10768; ANL/ASD/CP-96383; No Copyright; Avail: Department of Energy Information Bridge, Microfiche

An image-analysis system, based on commercially available data visualization software (IDL), allows convenient interaction with image data while still providing calculated beam parameters at a rate of up to 2 Hz. Image data are transferred from the IOC to the workstation via EPICS channel access. A custom EPICS record was created in order to overcome the channel access limit of 16 kilobytes per array. The user can conveniently calibrate optical transition radiation (OTR) and fluorescent screens, capture background images, acquire and average a series of images, and specify several other filtering and viewing options. The images can be saved in either IDL format or APS-standard format (SDDS), allowing for rapid postprocessing of image data by numerous other software tools.
NTIS
*Image Analysis; Linear Accelerators; Computer Programs*

**20010120801** Argonne National Lab., IL USA
**High Peak Power S-Band Switching System for the Advanced Photon Source (APS) Linear Accelerator (Linac)**
Grelick, A. E.; Sep. 11, 1998; 5p; In English
Report No.(s): DE2001-10767; ANL/ASD/CP-96380; No Copyright; Avail: Department of Energy Information Bridge, Microfiche

An S-band linear accelerator is the source of particles and front end of the Advanced Photon Source injector. Additionally, it will be used to support a low-energy undulator test line (LEUTL) and to drive a free-electron laser (FEL). To provide maximum linac availability for all uses, an additional modulator-klystron subsystem has been built, and a waveguide-switching and distribution subsystem is now under construction. The combined subsystems provide a hot spare for any of the five S-band transmitters that power the linac and have been given the additional function of powering a radio frequency gun test stand whenever they are not otherwise needed. Design considerations for the waveguide-switching subsystem, topology selection, timing, control, and system protection provisions are described.
NTIS
*Linear Accelerators; Photons; Switching; Waveguides*

**20010121501** Sandia National Labs., Albuquerque, NM USA
**Measurement of the Efficiency of Gold Transmission Gratings in the 100 to 5000 eV Photon Energy Range**
Ruggles, L. E.; Cuneo, M. E.; Porter, J. L.; Wenger, D. F.; Simpson, W. W.; Jul. 20, 2000; 20p; In English
Report No.(s): DE2000-760766; SAND2000-0635C; No Copyright; Avail: Department of Energy Information Bridge, Microfiche

Three x-ray spectrometers, each with a transmission grating dispersion element, are routinely used at the Z soft x-ray facility to measure the spectrum and temporal history of the absolute soft x-ray power emitted from z-pinch and hohlraum radiation sources. Our goal is to make these measurements within an accuracy of +/- 10%. We periodically characterize the efficiency of the gratings used in the spectrometers by using an electron-impact soft x-ray source, a monochromator, grazing-incidence mirrors, thin filters, and an x-ray CCD (charge coupled device) detector. We measure the transmission efficiency of the gratings at many photon energies for several grating orders. For each grating, we calculate efficiency as a function of photon energy using published optical constants of gold and multiple-slit Fraunhofer diffraction theory and fit the calculation to the measurements using the physical parameters of the grating as variables. This article describes the measurement apparatus and calibration techniques, discusses the grating efficiency calculation and fitting procedure, and presents recent results.
NTIS
*Gratings (Spectra); Photons; Transmission Efficiency; X Ray Spectrometers; Calibrating*

**20010121517** Brookhaven National Lab., Upton, NY USA
**Parton saturation, production, and equilibration in high energy nuclear collisions**
Venugopalan,; Mar. 20, 1999; 6p; In English
Report No.(s): DE2000-755028; BNL-67239; No Copyright; Avail: Department of Energy Information Bridge

Deeply inelastic scattering of electrons off nuclei can determine whether parton distributions saturate at HERA energies. If so, this phenomenon will also tell us a great deal about how particles are produced, and whether they equilibrate, in high energy nuclear collisions.
NTIS
*Partons; Collisions; Nuclear Scattering; Concentration (Composition); Stability*

**20010121518** Brookhaven National Lab., Upton, NY USA
**Making glue in high energy nuclear collisions**
Krasnitz,; Venugopalan,; Nov. 20, 1998; 9p; In English
Report No.(s): DE2000-755027; BNL-67242; No Copyright; Avail: Department of Energy Information Bridge
The authors discuss a real time, non-perturbative computation of the transverse dynamics of gluon fields at central rapidities in very high energy nuclear collisions.
NTIS
*Gluons; Real Time Operation; Nuclear Physics; Collisions*

**20010121520** Brookhaven National Lab., Upton, NY USA
**Event generator for RHIC spin physics**
Saito,; Schaefer,; Mar. 15, 1999; 88p; In English
Report No.(s): DE2000-754977; BNL-52571; No Copyright; Avail: Department of Energy Information Bridge
This volume archives the reports from the RIKEN BNL Research Center workshop on Event Generator for RHIC Spin Physics II; held during the week March 15, 1999 at Brookhaven National Laboratory. It was the second meeting on the subject following a first one in last September. This workshop has been initiated to establish a firm collaboration between theorists and experimentalists involved in RHIC spin physics with the aim of developing a reliable, high-precision event generator for RHIC spin physics. Needless to say, adequate event generators are indispensable tools for high energy physics programs in general, especially in the process of: planning the experimental programs; developing algorithms to extract the physics signals of interest; estimating the background in the extracted results, and connecting the final particle kinematics to the fundamental i.e. partonic level processes. Since RHIC is the first polarized collider, dedicated efforts are required to obtain a full-fledged event generator which describes spin dependent reactions in great detail.
NTIS
*Kinematics; High Energy Interactions; Spin Dynamics*

**20010121523** Brookhaven National Lab., Upton, NY USA
**Rotating band pion production targets for muon colliders and neutrino factories**
King, B. J.; Jan. 24, 2000; 15p; In English
Report No.(s): DE2000-752154; BNL-67162; No Copyright; Avail: Department of Energy Information Bridge
Conceptual design studies for muon colliders that have taken place since the mid-1990's have motivated the design of pion production targets that can operate and survive with metawatt-scale pulsed proton beams. Over the past few months, the design timescale and potential learning curve for such targets has effectively been abbreviated by the expanded interest in neutrino factories-muon storage rings dedicated to producing neutrino beams that will require similarly large muon currents to muon colliders and that have prospects for being built on a shorter timescale-perhaps to be ready within the next decade. We present an update on a previous report describing a conceptual design for a cupronickel rotating band pion production target for muon colliders that was proposed as a relatively conservative extrapolation from existing targets. A more detailed write-up on this target is in progress.
NTIS
*Muons; Neutrinos; Storage Rings (Particle Accelerators)*

**20010121526** Brookhaven National Lab., Upton, NY USA
**Acceleration for a high energy muon collider**
Berg, J. S.; Jan. 05, 2000; 11p; In English
Report No.(s): DE2000-752150; BNL-67115; No Copyright; Avail: Department of Energy Information Bridge
We describe a method for designing the acceleration systems for a muon collider, with particular application and examples for a high energy muon collider. This paper will primarily concentrate on design considerations coming from longitudinal motion, but some transverse issues will be briefly discussed.
NTIS
*Muons; Particle Acceleration*

**20010121529** Brookhaven National Lab., Upton, NY USA
**Higgs and heavy quarks diffractive production**
Levin, E.; Nov. 03, 1999; 4p; In English
Report No.(s): DE2000-752147; BNL-67022; No Copyright; Avail: Department of Energy Information Bridge

In this report we give the highest of reasonable estimates for the value of cross section of the double Pomeron Higgs meson production and suggest a new mechanism for heavy quark diffractive production which will dominate at the Tevatron energies.
NTIS
*Quantum Chromodynamics; Quarks*

**20010121530** Brookhaven National Lab., Upton, NY USA
**Cost of survival for large rapidity gaps**
Levin, E.; Nov. 03, 1999; 4p; In English
Report No.(s): DE2000-752146; BNL-67023; No Copyright; Avail: Department of Energy Information Bridge
In this document we report on calculations of the survival probability of the large rapidity gap (LRG) processes and its energy behaviour.
NTIS
*Quantum Chromodynamics; Bosons*

**20010121883** Argonne National Lab., IL USA
**Bremsstrahlung Pair-Production of Positrons with Low Neutron Background**
Lessner, E.; Sep. 16, 1998; 5p; In English
Report No.(s): DE2001-10766; ANL/ASD/CP-96379; No Copyright; Avail: Department of Energy Information Bridge, Microfiche
Minimization of component activation is highly desirable at accelerator-based positron sources. Electrons in the 8- to 14-MeV energy range impinging on a target produce photons energetic enough to create electron-positron pairs; however, few of the photons are energetic enough to produce photoneutrons. Slow positron production by low-energy electrons impinging on a multilayer tungsten target with and without electromagnetic extraction between the layers was studied by simulation. The neutron background from 14-MeV electrons is expected to be significantly lower than that encountered with higher-energy electron beams. Numerical results are presented and some ideas for a low-activation slow-positron source are discussed.
NTIS
*Bremsstrahlung; Electrons; Pair Production; Positrons*

**20010121963** Maryland Univ., College Park, MD USA
**Advanced methods for the computation of particle beam transport and the computation of electromagnetic fields and beam-cavity interactions. Progress report, September 1997 - January 1999, and final report, September 1995 - January 1999**
Dragt, A. J.; Gluckstern, R. L.; Apr. 01, 1999; 41p; In English
Report No.(s): DE2000-761566; DOE/ER/40949-3; No Copyright; Avail: Department of Energy Information Bridge
No abstract prepared.
NTIS
*Electromagnetic Fields; Particle Beams; Field Theory (Physics); Cavity Resonators*

**20010121969** Argonne National Lab., IL USA
**Heavy-Ion Beam Acceleration of Two-Charge States from an ECR Ion Source**
Ostroumov, P. N.; Shepard, K. W.; Aseev, V. N.; Kolomiets, A. A.; Aug. 15, 2000; 6p; In English
Report No.(s): DE2000-761246; ANL/PHY/CP-101747; No Copyright; Avail: Department of Energy Information Bridge
No abstract prepared.
NTIS
*Ion Beams; Ion Sources; Electron Density (Concentration)*

**20010121970** Los Alamos National Lab., NM USA
**Spectroscopy 'Windows' of Quark-Antiquark Mesons and Glueballs with Effective Regge Trajectories**
Goldman, J. T.; Brisudova, M.; Burakovsky, L.; Sep. 20, 2000; 6p; In English
Report No.(s): DE2000-762928; LA-UR-00-4404; No Copyright; Avail: Department of Energy Information Bridge, Microfiche
Regge trajectories of quark-antiquark mesons can be well approximated for phenomenology purposes by a specific nonlinear form, reflecting that the flux tubes cannot be arbitrarily large, but breaks due to the effect of pair-production. If confirmed, this

would imply that there is only a finite number of bound states on each trajectory, and consequently, an existence of 'spectroscopy windows' for each flavor. Here we present our results for these windows.
NTIS
*Gluons; Mesons; Quarks; Spectroscopy*

**20010122240** Argonne National Lab., IL USA
**Design of an accelerator for advanced pulse radiolysis experiments**
Jonah, C. D.; Sep. 11, 1998; 7p; In English
Report No.(s): DE2001-10956; ANL/CHM/CP-97252; No Copyright; Avail: Department of Energy Information Bridge, Microfiche

New accelerator techniques have made it possible to make shorter and shorter electron pulses. If appropriate detection techniques are available, these pulses make it possible to measure many important sub-picosecond chemical processes. We are proposing an accelerator system that can be used to measure important sub-picosecond chemical processes, such as solvation, vibrational relaxation, excited state relaxations and molecular fragmentation.
NTIS
*Radiolysis; Linear Accelerators; Electron Beams; Pulsed Radiation; Picosecond Pulses*

**20010122241** Argonne National Lab., IL USA
**High power test results of the first SRRC/ANL high current L-band RF gun**
Ho, C. H.; Sep. 11, 1998; 5p; In English
Report No.(s): DE2001-10954; ANL-HEP-CP-98-94; No Copyright; Avail: Department of Energy Information Bridge, Microfiche

A joint program is underway between the SRRC (Synchrotrons Radiation Research Center, Taiwan) and ANL (Argonne National Laboratory, USA) for developing a high current L-band photocathode rf guns. We have constructed an L-Band (1.3 Ghz), single cell rf photocathode gun and conducted low power tests at SRRC. High power rf conditioning of the cavity has been completed at ANL. In this paper we report on the construction and high power test results. So far we have been able to achieve > 120 MV/m axial electric field with minimal dark current. This gun will be used to replace the AWA (Argonne Wakefield Accelerator)(l) high current gun.
NTIS
*Electron Guns; Linear Accelerators; Photocathodes; Performance Tests*

**20010122244** Argonne National Lab., IL USA
**Detector limitations, STAR**
Underwood, D. G.; Jul. 13, 1998; 24p; In English
Report No.(s): DE2001-10879; ANL-HEP-CP-98-52; No Copyright; Avail: Department of Energy Information Bridge

Every detector has limitations in terms of solid angle, particular technologies chosen, cracks due to mechanical structure, etc. If all of the presently planned parts of STAR (Solenoidal Tracker At RHIC) were in place, these factors would not seriously limit our ability to exploit the spin physics possible in RHIC. What is of greater concern at the moment is the construction schedule for components such as the Electromagnetic Calorimeters, and the limited funding for various levels of triggers.
NTIS
*Construction; Mechanical Properties; Detection*

**20010122248** Argonne National Lab., IL USA
**Quantum fluctuations in beam dynamics**
Kim, K. J.; Jun. 04, 1998; 17p; In English
Report No.(s): DE2001-10832; ANL/APS-LS-271; No Copyright; Avail: Department of Energy Information Bridge

Quantum effects could become important for particle and photon beams used in high-luminosity and high brightness applications in the current and next generation accelerators and radiation sources. This paper is a review of some of these effects.
NTIS
*Particle Beams; Photon Beams; Quantum Mechanics*

**20010122255** Argonne National Lab., IL USA

**Production of negative hydrogen and deuterium ions in microwave-driven ion sources**

Spence, D.; Sep. 11, 1998; 5p; In English

Report No.(s): DE2001-10809; ANL/TD/CP-96484; No Copyright; Avail: Department of Energy Information Bridge, Microfiche

The authors report progress they have made in the production of negative hydrogen and deuterium atomic ions in magnetically-confined microwave-driven (2.45 GHz) ion sources. The influence of source surface material, microwave power, source gas pressure and magnetic field configuration on the resulting ion current is discussed. Results strongly suggest that, at least in the source, vibrationally excited molecular hydrogen, the precursor to atomic negative ion production, is produced via a surface mechanism suggested by Hall et al. rather than via a gas phase reaction as is generally believed to be the case in most ion sources.

NTIS

*Deuterium; Ions; Hydrogen Ions; Ion Sources*

**20010122261** Argonne National Lab., IL USA

**Magnetic and Diagnostic Systems for the Advanced Photon Source Self-Amplified Spontaneously Emitting FEL**

Gluskin, E.; Dec. 23, 1998; 24p; In English

Report No.(s): DE2001-10799; ANL/XFD/CP-96425; No Copyright; Avail: Department of Energy Information Bridge, Microfiche

A self-amplified spontaneously emitting (SASE) free-electron laser (FEL) for the visible-to-ultraviolet spectral range is under construction at the Advanced Photon Source at Argonne National Laboratory. The amplifier part of the FEL consists of twelve identical 2.7-meter-long sections. Each section includes a 2.4-meter-long, 33-mm-period hybrid undulator, a quadruple lens, and a set of electron beam and radiation diagnostics equipment. The undulatory will operate at a fixed magnetic gap (approximately 9.3 mm) with K = 3.1. The electron beam position will be monitored using capacitive beam position monitors, YAG scintillators with imaging optics, and secondary emission detectors. The spatial distribution of the photon beam will be monitored by position sensitive detectors equipped with narrow-band filters. A high-resolution spectrograph will be used to observe the spectral distribution of the FEL radiation.

NTIS

*Free Electron Lasers; Design Analysis*

**20010122284** Argonne National Lab., IL USA

**Status of RNB facilities in North America**

Nolen, J.; Sep. 16, 1998; 10p; In English

Report No.(s): DE2001-10819; ANL/PHY/CP-96536; No Copyright; Avail: Department of Energy Information Bridge, Microfiche

This paper presents the status of accelerator facilities in North America that are involved in research using radioactive nuclear beams (RNB), including existing and operating facilities, ones currently under construction or undergoing major upgrades, and ones being planned or proposed for the future. Existing RNB facilities are located at TRIUMF (TISOL) in Vancouver, B.C., the Holifield Radioactive Ion Beam Facility (HRIBF) at Oak Ridge National Laboratory, the Argonne Tandem Linear Accelerator System (ATLAS) at Argonne National Laboratory, the National Superconducting Cyclotron Laboratory (NSCL) at Michigan State University, the Nuclear Structure Laboratory at The University of Notre Dame, the 88 Cyclotron at Lawrence Berkeley National Laboratory, and the Cyclotron Institute at Texas A and M University. Currently, there are two major RNB facility upgrades in progress in North America, one at TRIUMF, the ISAC project, and one at NSCL the Intensity Upgrade project. For the future the U. S. Nuclear Science Advisory Committee has given high priority for an advanced RNB facility of the ISOL type. Concepts for such a facility, currently being developed at Argonne National Laboratory and Oak Ridge National Laboratory, are presented. Plans are also being developed in Canada at TRIUMF for a major upgrade of the ISAC facility.

NTIS

*Particle Accelerators; North America; Technology Assessment*

**20010122298** Argonne National Lab., IL USA

**Design and Performance Simulations of the Bunch Compressor for the APS LEUTL FEL**

Borland, M.; Aug. 03, 2000; 5p; In English

Report No.(s): DE2000-761244; ANL/AOD/CP-101631; No Copyright; Avail: Department of Energy Information Bridge

A magnetic bunch compressor was designed and is being commissioned to provide higher peak current for the Advanced Photon Source's (APS) Low-Energy Undulator Test Line (LEUTL) free-electron laser (FEL). of great concern is limiting emittance growth due to coherent synchrotron radiation (CSR). Tolerances must also be carefully evaluated to find stable operating conditions and ensure that the system can meet operational goals. Automated matching and tolerance simulations allowed consideration of numerous configurations, pinpointing those with reduced error sensitivity. Simulations indicate tolerable emittance growth up to 600 A peak current, for which the normalized emittance will increase from 5 to about 6.8 micrometers. The simulations also provide predictions of emittance variation with chicane parameters which we hope to verify experimentally.
NTIS
*Coherent Radiation; Emittance; Magnetic Compression; Tolerances (Mechanics)*

**20010122299** Argonne National Lab., IL USA
**Highly Flexible Bunch Compressor for the APS LEUTL FEL**
Borland, M.; Lewellen, J.; Milton, S.; Aug. 03, 2000; 5p; In English
Report No.(s): DE2000-761243; ANL/AOD/CP-101630; No Copyright; Avail: Department of Energy Information Bridge
The Low-Energy Undulator Test Line (LEUTL) free-electron laser (FEL) at the Advanced Photon Source (APS) has achieved gain at 530 nm with an electron beam current of about 100 A. In order to push to 120 nm and beyond, we have designed and are commissioning a bunch compressor using a four-dipole chicane at 100-210 MeV to increase the current to 600 A or more. to provide options for control of emittance growth due to coherent synchrotron radiation (CSR), the chicane is also variable via longitudinal motion of the final dipole, which is predicted to have an effect on emittance growth. Following the chicane, a three-screen emittance measurement system should permit resolution of he difference in emittance growth between various chicane configurations. A vertical bending magnet analysis line will permit imaging of correlations between transverse and energy coordinates. A comparison paper discusses the physics design in detail.
NTIS
*Compressors; Free Electron Lasers; Beam Currents*

**20010122300** Argonne National Lab., IL USA
**Automated Operation of the APS Linear Using the Procedure Execution Manager**
Soliday, R.; Pasky, S.; Borland, M.; Aug. 22, 2000; 5p; In English
Report No.(s): DE2000-761242; ANL/AOD/CP-101629; No Copyright; Avail: Department of Energy Information Bridge
The Advanced Photon Source (APS) linear accelerator has two thermionic cathode rf guns and one photocathode rf gun. The thermionic cathode rf guns are used primarily for APS operations while the photocathode gun is used as a free-electron laser (FEL) driver. With each gun requiring different lattice and timing configuration, the need to change quickly between guns puts great demands on the accelerator operators. Using the Procedure Execution Manager (PEM), a software environment for managing automated procedures, we have made start-up and switchover of the linac systems both easier and more reliable. The PEM is a graphical user interface written in Tcl/Tk that permits the user to invoke 'machine procedures' and control their execution. It allows construction of procedures in a hierarchical, parallel fashion, which makes for efficient execution and development. In this paper, we discuss the features and advantages of the PEM environment as well as the specifics of our procedures for the APS linac.
NTIS
*Photocathodes; Thermionic Cathodes; Linear Accelerators; Procedures*

**20010122301** Argonne National Lab., IL USA
**Recent Developments in Measurement and Tracking of the APS Storage Ring Beam Emittance**
Yang, B.; Lumpkin, A. H.; Emery, L.; Borland, M.; Jul. 31, 2000; 10p; In English
Report No.(s): DE2000-761240; ANL/AOD/CP-101382; No Copyright; Avail: Department of Energy Information Bridge
The x-ray pinhole camera is used at the MS storage ring to measure the beam emittance. The measured data are archived during user operation. At 1-Hz bandwidth, we have achieved better than l-pm stability in the measured horizontal beam size, typically of 143 m, corresponding to 48 nm rad. During user runs, beam size variations up to 2.5 micrometers were observed (corresponding to emittance variations of 0.4 nm rad), which were strongly correlated and attributed to the variation of electron energy loss in the insertion devices. In other words, the user-initiated insertion device gap changes are the major factor in observed beam emittance variations during user runs.
NTIS
*Emittance; Photon Beams*

**20010122302** Argonne National Lab., IL USA
**High Accuracy Momentum Compaction Measurement for the APS Storage Ring with Undulator Radiation**
Yang, B.; Borland, M.; Emery, L.; Jul. 31, 2000; 10p; In English
Report No.(s): DE2000-761239; ANL/AOD/CP-101381; No Copyright; Avail: Department of Energy Information Bridge

We developed a new technique to measure the electron beam energy centroid and spread. It takes advantage of a sharp feature in the Advanced Photon Source (APS) diagnostic: undulator spectrum, the drop-off in the angle-integrated flux near its fundamental photon energy. The measurement technique has a high resolution and is nearly independent of the storage ring lattice functions. In this work, we present the results of electron beam energy measurements as a function of rf frequency and obtain the momentum compaction factor of the AI% storage ring. We will also discuss methods to further reduce experimental errors, making the technique potentially the most accurate one for measuring momentum compaction factors of a storage ring.
NTIS
*Centroids; Electron Beams; Momentum; Spreading*

**20010122357** Argonne National Lab., IL USA
**First tests of a traveling-wave chopper for the ATLAS positive ion linac**
Pardo, R. C.; Nov. 18, 1998; 5p; In English
Report No.(s): DE2001-10764; ANL/PHY/CP-96373; No Copyright; Avail: Department of Energy Information Bridge, Microfiche

A ten segment traveling-wave chopper has been constructed and successfully tested at 5% of the design 12 MHz repetition rate. The chopper must remove unbunched tails from a partially bunched heavy-ion beam in order to avoid undue emittance growth in the linac and the production of undesirable satellite beam bunches. When poorly bunched beams traverse the traditional sine-wave chopper, it produces unacceptable transverse emittance growth and unnecessary beam loss. These effects are expected to be much reduced in the traveling wave chopper. First tests have confirmed the validity of these claims, clearly showing much reduced transverse emittance growth as compared to the original sine wave chopper and excellent selectivity for the desired beam. Details of these tests will be presented and compared to calculations. Operation of the new chopper at the full 12 MHz rate is the next goal. Development of a driver power supply capable of full CW (continuous wave) operation will also be described.
NTIS
*Linear Accelerators; Ion Beams; Emittance; Superconductivity*

**20010122364** Argonne National Lab., IL USA
**AGS experiment to test bunching for the proton driver of the muon collider**
Norem, J.; Apr. 27, 1998; 8p; In English
Report No.(s): DE2001-10750; ANL-HEP-CP-98-32; No Copyright; Avail: Department of Energy Information Bridge, Microfiche

The proton driver for the muon collider must produce short pulses of protons in order to facilitate muon cooling and operation with polarized beams. In order to test methods of producing these bunches they have operated the AGS (Alternating Gradient Synchrotron) near transition and studied procedures which involved moving the transition energy (gamma) to the beam energy. They were able to produce stable bunches with RMS (root mean square) widths of (sigma) = 2.2 - 2.7 ns for longitudinal bunch areas of (minus)1.5 V-s, in addition to making measurements of the lowest two orders of the momentum compaction factor.
NTIS
*Muons; Protons; Bunching*

**20010122365** Argonne National Lab., IL USA
**e(+)e(-) and ep options for the very large hadron collider**
Norem, J.; Apr. 27, 1998; 5p; In English
Report No.(s): DE2001-10749; ANL-HEP-CP-98-33; No Copyright; Avail: Department of Energy Information Bridge, Microfiche

Although the linear collider is ultimately capable of higher energies, a circular e(sup +)e(sup (minus)) collider installed in the large tunnels of a Very Large Hadron Collider (VLHC) has attractive features, including very light magnet system and unchallenging vacuum requirements. An ep collider, built either in the 3 TeV booster or the large tunnel, could extend the HERA (Hadron-Elektron-Ring-Analage) program beyond (radical)s (approximately) 1 TeV. Both machines could perhaps use the same rf (radio frequency) system, first in the booster tunnel and then as part of the large collider.
NTIS
*Hadrons; Linear Accelerators; Particle Collisions*

**20010122378** Argonne National Lab., IL USA

**Measurements of the Argonne Wakefield Accelerator's low charge, 4 MeV RF photocathode witness beam**

Power, J.; Apr. 01, 1998; 11p; In English

Report No.(s): DE2001-10715; ANL-HEP-CP-98-26; No Copyright; Avail: Department of Energy Information Bridge, Microfiche

The Argonne Wakefield Accelerator's (AWA) witness RF photocathode gun produced its first electron beam in April of 1996. We have characterized the charge, energy, emittance and bunch length of the witness beam over the last several months. The emittance was measured by both a quad scan that fitted for space charge using an in house developed Mathematica routine and a pepper pot technique. The bunch length was measured by imaging Cherenkov light from a quartz plate to a Hamamatsu streak camera with 2 psec resolution. A beam energy of 3.9 Mev was measured with a 6 inch round pole spectrometer while a beam charge was measured with both an ICT and a Faraday Cup. Although the gun will normally be run at 100 pC it has produced charges from 10 pC to 4 nc. All results of the measurements to date are presented here.

NTIS

*Microstructure; Electron Beams; Imaging Techniques; Quartz*

**20010122480** Los Alamos National Lab., NM USA

**Update on the Commissioning of the Low-Energy Demonstration Accelerator (LEDA) Radio-Frequency Quadrupole (RFQ)**

Smith, H. V.; Gilpatrick, J. D.; Jan. 01, 2000; 17p; In English

Report No.(s): DE2000-763328; LA-UR-00-413; No Copyright; Avail: Department of Energy Information Bridge, Microfiche

The Low-Energy Demonstration Accelerator (LEDA) Radio-Frequency Quadrupole (RFQ) is a 100% duty factor (cw) linac capable of delivering greater than 100-mA of H(+) beam at 6.7-MeV. The 8-m-long, 350-MHz RFQ structure is designed to accelerate the dc 75-keV, 110-mA H 9(+) beam from the LEDA injector with greater than 90% transmission. The primary objective of LEDA is to verify the design codes, gain fabrication knowledge, understand beam operation, and improve prediction of costs and operational availability for the full 1000- to 1700-MeV APT accelerator. Even though the output energy is low (6.7 MeV), the average beam power (670 kW) of LEDA ranks it with the LANSCE accelerator as the two highest power proton linacs in the world. Clearly, radiation shielding and power handling are important design issues. Preliminary RFQ commissioning results for pulsed beams with low rep-rate and short pulse lengths are given.

NTIS

*Computer Programs; Linear Accelerators; Quadrupoles*

**20010122656** Argonne National Lab., IL USA

**Use of Coherent Transition Radiation to Set Up the APS RF Thermionic Gun to Produce High-Brightness Beams for SASE FEL Experiments**

Sereno, N. S.; Borland, M.; Lumpkin, A. H.; Aug. 03, 2000; 5p; In English

Report No.(s): DE2000-761245; ANL/AOD/CP-101672; No Copyright; Avail: Department of Energy Information Bridge

We describe use of the Advanced Photon Source (APS) rf thermionic gun Alpha-magnet beamline, and linac to produce a stable high-brightness beam in excess of 100 amperes peak current with normalized emittance of 10 pi mm-mrad. To obtain peak currents greater than 100 amperes, the rf gun system must be tuned to produce a FWHM bunch length on the order of 350 fs. Bunch lengths this short are produce when the rf gun beam, accelerated to 40 MeV, strikes a metal foil. The CTR is detected using a Golay detector attached to one arm of a Michelson interferometer. The alpha-magnet current and gun rf phase are adjusted so as to maximize the CTR signal at the Golay detector, which corresponds to the minimum bunch length. This interferometer is used to measure the autocorrelation of the CTR. The minimum Phase approximation is used to derive the bunch profile from the autocorrelation. The high-brightness beam is accelerated to 217 meV and used to produce self-amplified spontaneous emission (SASE) in five APS undulators installed in the Low-Energy Undulator Test Line (LEUTL) experiment hall. Initial optical measurements showed a gain length of 1.3 m at 530 nm.

NTIS

*Coherent Radiation; Electron Beams; Thermionic Emission*

**20010122796** Argonne National Lab., IL USA

**Luminosity monitor**

Underwood, D. G.; Jul. 16, 1998; 7p; In English

Report No.(s): DE2001-10883; ANL-HEP-CP-98-53; No Copyright; Avail: Department of Energy Information Bridge

Luminosity monitors are needed in each experiment doing spin physics at RHIC. They concentrate on the luminosity aspects here because, for example, with a 10(sup (minus)3) raw asymmetry in an experiment, an error of 10(sup (minus)4) in the luminosity is as significant as a 10% polarization error. Because luminosity is a property of how two beams overlap, the luminosity at an interaction region must be measured at that interaction region in order to be relevant to the experiment at that interaction region. The authors will have to do the physics and the luminosity measurements by using labels on the event sums according to the polarization labels on the colliding bunches. Most likely they will not have independent polarization measurement on each bunch, but only on all the filled bunches in a ring, or perhaps all the bunches that are actually used in an experiment. Most analyses can then be handled by using the nine combinations gotten from three kinds of bunches in each ring, +, (minus) and empty bunches. The empty bunches are needed to measure beam-gas background, (and some, like six in a row, are needed for the beam abort). Much of the difficulty comes from the fact that they must use a physics process to represent the luminosity. This process must have kinematic and geometric cuts both to reduce systematics such as beam-gas backgrounds, and to make it representative of the part of the interaction diamond from which the physics events come.
NTIS
*Asymmetry; Diamonds; Luminosity*

**20010122878** Argonne National Lab., IL USA
**Heavy meson observables and Dyson Schwinger equations**
Ivanov, M. A.; Oct. 20, 1998; 13p; In English
Report No.(s): DE2001-11052; ANL/PHY/CP-97471; No Copyright; Avail: Department of Energy Information Bridge, Microfiche

Dyson-Schwinger equation (DSE) studies show that the b-quark mass-function is approximately constant, and that this is true to a lesser extent for the c-quark. This observation provides the basis for a study of the leptonic and semileptonic decays of heavy pseudoscalar mesons using a heavy-quark; limit of the DSES, which, when exact, reduces the number of independent form factors. Semileptonic decays with light mesons in the final state are also accessible because the DSES provide a description of light-quark propagation characteristics and light-meson structure. A description of B-meson decays is straightforward, however, the study of decays involving the D-meson indicates that c-quark mass-corrections are quantitatively important.
NTIS
*Decay; Particle Decay; Quarks; Mesons*

**20010122887** Argonne National Lab., IL USA
**New hydrostatic leveling system developed for the Advanced Photon Source**
Kivioja, L. A.; Sep. 18, 1998; 8p; In English
Report No.(s): DE2001-10971; ANL/ASD/CP-97314; No Copyright; Avail: Department of Energy Information Bridge, Microfiche

As a result of the calibration tests performed with the first prototype units using the new measurement principle, we believe that the described leveling method is stable and accurate to the micron level with a sufficiently large range for the expected elevation changes of the support girders used in the Advanced Photon Source (APS) storage ring. Although long-term studies with this system have not been conducted, we believe that after installation this system requires little or no servicing for long periods of time. The methods described in this paper cover only the elevation changes of individual vessels. However, changes in the tilt of a girder must also be known. Therefore, a combination of tiltmeters in conjunction with this hydrostatic level system (HLS) would be most suitable for measuring the tilt and elevation changes of the APS girders.
NTIS
*Hydrostatics; Leveling; Storage Rings (Particle Accelerators); Tiltmeters; Instrument Compensation; Calibrating*

**20010122888** Argonne National Lab., IL USA
**Poisson alignment reference system implementation at the Advanced Photon Source**
Feier, I.; Sep. 21, 1998; 11p; In English
Report No.(s): DE2001-10970; ANL/ASD/CP-97313; No Copyright; Avail: Department of Energy Information Bridge, Microfiche

The Poisson spot was established using a collimated laser beam from a 3-mW diode laser. It was monitored on a quadrant detector and found to be very sensitive to vibration and air disturbances. Therefore, for future work we strongly recommend a sealed vacuum tube in which the Poisson line may be propagated. A digital single-axis feedback system was employed to generate an straight line reference (SLR) on the X axis. Pointing accuracy was better than 8 (+/-) 2 microns at a distance of 5 m. The digital system was found to be quite slow with a maximum bandwidth of 47 (+/-) 9 Hz. Slow drifts were easily corrected but any vibration

over 5 Hz was not. We recommend an analog proportional-integral-derivative (PID) controller for high bandwidth and smooth operation of the kinematic mirror. Although the Poisson alignment system (PAS) at the Advanced Photon Source is still in its infancy, it already shows great promise as a possible alignment system for the low-energy undulator test line (LEUTL). Since components such as wigglers and quadruples will initially be aligned with respect to each other using conventional means and mounted on some kind of rigid rail, the goal would be to align six to ten such rails over a distance of about 30 m. The PAS could be used to align these rails by mounting a sphere at the joint between two rails. These spheres would need to be in a vacuum pipe to eliminate the refractive effects of air. Each sphere would not be attached to either rail but instead to a flange connecting the vacuum pipes of each rail. Thus the whole line would be made up of straight, rigid segments that could be aligned by moving the joints. Each sphere would have its own detector, allowing the operators to actively monitor the position of each joint and therefore the overall alignment of the system.
NTIS
*Alignment; Research Facilities; Particle Accelerators; Vacuum Tubes*

**20010122889** Argonne National Lab., IL USA
**Status report on the long-term stability of the Advanced Photon Source**
Friedsam, H.; Sep. 21, 1998; 10p; In English
Report No.(s): DE2001-10969; ANL/ASD/CP-97312; No Copyright; Avail: Department of Energy Information Bridge, Microfiche

A table summarizes the average elevation changes and standard deviations as well as the points with the largest changes for each year. On average, hardly any settlements can be detected; however, local changes of +2.90 mm to -2.31 mm have been measured. Looking at the low and high points, the settlement process is slowing down over time. Overall, the settlements observed match the expectations for this type of construction. to date no major realignment of the Advanced Photon Source (APS) storage ring has been necessary. The particle beam tracks with the settlements of the floor as long as these changes occur in a smooth fashion and not as sudden discontinuities. It is also apparent that settlements affect larger areas in the storage ring and experiment hall that impact the location of the source point as well as the location of the beamline user equipment. The limiting apertures of the insertion device chambers will make realignment of the APS storage ring a necessity at some point in the future. Currently simulations and machine studies we underway to provide an estimate of tolerable settlement limits before a realignment of certain sections of the storage ring would be required. In conclusion, the APS has been constructed on solid ground with an excellent foundation. Only small settlement changes are being observed; so far they are not impacting the operation of the accelerator. We are continuing to monitor deformations of the APS floor in anticipation of a future realignment of the accelerator components.
NTIS
*Research Facilities; Particle Accelerators; Foundations; Geotechnical Engineering; Settling*

**20010122891** Argonne National Lab., IL USA
**Theories of electromagnetic productions of pions**
Lee, T. S. H.; Sep. 11, 1998; 10p; In English
Report No.(s): DE2001-10964; ANL/PHY/CP-97274; No Copyright; Avail: Department of Energy Information Bridge, Microfiche

The current theoretical approaches for investigating the (gamma)N (r-arrow) (pi)N and N(e,e(prime)(pi)) reactions are reviewed. It is shown that the dynamical approach can be used to test the predictions from hadron structure calculations. Some N* form factors calculated from using various chiral constituent quark models are presented.
NTIS
*Chirality; Pions; Quark Models; Dynamical Systems*

**20010122892** Argonne National Lab., IL USA
**Study of the Delta structure and N Delta interactions with N(e,e'pi) and d(e,e'pi) reactions**
Lee, T. S. H.; Sep. 11, 1998; 17p; In English
Report No.(s): DE2001-10963; ANL/PHY/CP-97268; No Copyright; Avail: Department of Energy Information Bridge, Microfiche

A dynamical approach for using the (gamma)N (r-arrow) (pi)N and N(e,e(prime)(pi)) reactions to test the chiral constituent quark model is reviewed. Recent results for the (Delta) excitations and predictions for future experiments are presented. It is shown that the polarization observables of d(e,e(prime)(pi)) reactions are useful for investigating the N(Delta) interactions which are

crucial in exploring the (Delta) components in nuclei and the properties of (Delta)-rich systems created in relativistic heavy-ion collisions.
NTIS
*Chirality; Ionic Collisions; Quark Models*

**20010122947** Argonne National Lab., IL USA
**RF power generation and coupling measurements for the dielectric wakefield step-up transformer**
Conde, M. E.; Jun. 16, 1998; 7p; In English
Report No.(s): DE2001-10881; ANL-HEP-CP-98-86; No Copyright; Avail: Department of Energy Information Bridge

The dielectric wakefield transformer (DWT) is one route to practical high energy wakefield-based accelerators. Progress has been made in a number of areas relevant to the demonstration of this device. In this article we describe recent bench measurements and beam experiments using 7.8 and 15.6 GHz structures and discuss some remaining technical challenges in the development of the DWT.
NTIS
*Dielectrics; Transformers*

**20010123067** Argonne National Lab., IL USA
**Reliability and availability of high power proton accelerators**
Cho, Y.; Oct. 27, 1998; 12p; In English
Report No.(s): DE2001-11068; ANL/APS/CP-97513; No Copyright; Avail: Department of Energy Information Bridge, Microfiche

It has become increasingly important to address the issues of operational reliability and availability of an accelerator complex early in its design and construction phases. In this context, reliability addresses the mean time between failures and the failure rate, and availability takes into account the failure rate as well as the length of time required to repair the failure. Methods to reduce failure rates include reduction of the number of components and over-design of certain key components. Reduction of the on-line repair time can be achieved by judiciously designed hardware, quick-service spare systems, and redundancy. In addition, provisions for easy inspection and maintainability are important for both reduction of the failure rate as well as reduction of the time to repair. The radiation safety exposure principle of ALARA (As Low As Reasonably Achievable) is easier to comply with when easy inspection capability and easy maintainability are incorporated into the design. Discussions of past experience in improving accelerator availability, some recent developments, and potential R and D items are presented.
NTIS
*Particle Accelerators; Design Analysis; Reliability*

**20010123069** Argonne National Lab., IL USA
**Waveguide harmonic damper for klystron amplifier**
Kang, Y.; Oct. 27, 1998; 5p; In English
Report No.(s): DE2001-11064; ANL/ASD/CP-97509; No Copyright; Avail: Department of Energy Information Bridge, Microfiche

A waveguide harmonic damper was designed for removing the harmonic frequency power from the klystron amplifiers of the APS linac. Straight coaxial probe antennas are used in a rectangular waveguide to form a damper. A linear array of the probe antennas is used on a narrow wall of the rectangular waveguide for damping klystron harmonics while decoupling the fundamental frequency in dominent TE(sub 01) mode. The klystron harmonics can exist in the waveguide as waveguide higher-order modes above cutoff. Computer simulations are made to investigate the waveguide harmonic damping characteristics of the damper.
NTIS
*Waveguides; Harmonics; Damping; Klystrons*

**20010123089** Argonne National Lab., IL USA
**Coherent multimoded dielectric wakefield accelerators**
Power, J.; Jul. 16, 1998; 6p; In English
Report No.(s): DE2001-10892; ANL-HEP-CP-98-87; No Copyright; Avail: Department of Energy Information Bridge, Microfiche

There has recently been a study of the potential uses of multimode dielectric structures for wakefield acceleration. This technique is based on adjusting the wakefield modes of the structure to constructively interfere at certain delays with respect to

the drive bunch, thus providing an accelerating gradient enhancement over single mode devices. In this report we examine and attempt to clarify the issues raised by this work in the light of the present state of the art in wakefield acceleration.
NTIS
*Particle Acceleration; Dielectrics; Particle Accelerators*

**20010123212** Argonne National Lab., IL USA
**Design of a high charge (10 - 100 nC) and short pulse (2 - 5 ps) rf photocathode gun for wakefield acceleration**
Gai, W.; Jul. 16, 1998; 9p; In English
Report No.(s): DE2001-10891; ANL-HEP-CP-98-85; No Copyright; Avail: Department of Energy Information Bridge, Microfiche

In this paper we present a design report on a 1-1/2 cell, L Band RF (radio frequency) photocathode gun that is capable of generating and accelerating electron beams with peak currents 10 kA. We have performed simulation for bunch intensities in the range of 10-100 nC with peak axial electrical field at the photocathode of 30-100 MV/m. Unlike conventional short electron pulse generation, this design does not require magnetic pulse compression. Based on numerical simulations using SUPERFISH and PARMELA, this design will produce 20-100 nC beam at 18 MeV with rms (root mean square) bunch length 0.6-1.25 mm and normalized transverse emittance 30-108 mm mrad. Applications of this beam for wakefield acceleration is also discussed.
NTIS
*Particle Acceleration; Particle Accelerators; Electron Beams; Photocathodes*

**20010123213** Argonne National Lab., IL USA
**Solving QCD using multi-regge theory**
White, A. R.; Jul. 13, 1998; 14p; In English
Report No.(s): DE2001-10890; ANL-HEP-CP-98-67; No Copyright; Avail: Department of Energy Information Bridge, Microfiche

This talk outlines the derivation of a high-energy, transverse momentum cut-off, solution of QCD (quantum chromodynamics) in which the Regge pole and 'single gluon' properties of the pomeron are directly related to the confinement and chiral symmetry breaking properties of the hadron spectrum. In first approximation, the pomeron is a single reggeized gluon plus a 'wee parton' component that compensates for the color and particle properties of the gluon. This solution corresponds to a supercritical phase of Reggeon Field Theory.
NTIS
*Gluons; Hadrons; Quantum Chromodynamics; Regge Poles; Chirality*

**20010123230** Los Alamos National Lab., NM USA
**Particle-Core Model for Transverse Dynamics of Beam Halo in Periodic-Focusing Channels**
Wang, T. F.; Jan. 01, 2000; 16p; In English
Report No.(s): DE2000-763346; LA-UR-00-779; No Copyright; Avail: Department of Energy Information Bridge

This work is a numerical study of the particle dynamics in the halo region of mismatched charged-particle beams propagating through periodic-focusing channels using a recently developed technique based on the particle core model. Numerical examples and preliminary results of finding the boundaries of the resonant region in the phase space where particles can be driven into the beam halo will be presented.
NTIS
*Charged Particles; Halos; Particle Beams*

**20010123248** Argonne National Lab., IL USA
**SRRC/ANL high current l-band single cell photocathode RF gun**
Ho, C. H.; Jul. 16, 1998; 5p; In English
Report No.(s): DE2001-10884; ANL-HEP-CP-98-60; No Copyright; Avail: Department of Energy Information Bridge

A high current L-band photocathode rf gun is under development at SRRC (Synchrotron Radiation Research Center, Taiwan) in collaboration with ANL (Argonne National Laboratory, USA). The goal is to produce up to 100 nC charge with the surface field gradient of over 90 MV/m at the center of the photocathode. In this report, they present the detailed design and initial test results. If successful, this gun will be used as the future AWA (Argonne Wakefield Accelerator)(1) high current gun.
NTIS
*Particle Accelerators; Photocathodes*

**20010123398** Argonne National Lab., IL USA
**Equation of Motion of an Electron**
Kim, K. J.; Sep. 02, 1998; 18p; In English
Report No.(s): DE2001-10944; ANL/APS/LS-270; No Copyright; Avail: Department of Energy Information Bridge

We review the current status of understanding of the equation of motion of an electron. Classically, a consistent linearized theory exists for an electron of finite extent, as long as the size of the electron is larger than the classical electron radius. Nonrelativistic quantum mechanics seems to offer a fine theory even in the point particle limit. Although there is as yet no convincing calculation, it is probable that a quantum electrodynamical result will be at least as well-behaved as is the nonrelativistic quantum mechanical results.

NTIS
*Equations of Motion; Nonrelativistic Mechanics; Electrons; Quantum Electrodynamics*

**20010123461** Argonne National Lab., IL USA
**Low-neutron background slow-positron source**
White, M. M.; Oct. 09, 1998; 6p; In English
Report No.(s): DE2001-10993; ANL/ASD/CP-97408; No Copyright; Avail: Department of Energy Information Bridge, Microfiche

The addition of a thermionic rf gun and a photocathode rf gun will allow the Advanced Photon Source (APS) linear accelerator (linac) to become a free-electron laser (FEL) driver. As the FEL project progresses, the existing high-charge DC thermionic gun will no longer be critical to APS operation and could be used to generate high-energy or low-energy electrons to drive a slow-positron source. We investigated possibilities to create a useful low-energy source that could operate semi-independently and would have a low neutron background.

NTIS
*Photons; Photocathodes; Linear Accelerators; Free Electron Lasers*

**20010123532** Argonne National Lab., IL USA
**Measurements with radioactive beams at ATLAS**
Rehm, K. E.; Aug. 06, 1998; 9p; In English
Report No.(s): DE2001-10916; ANL/PHY/CP-97005; No Copyright; Avail: Department of Energy Information Bridge, Microfiche

Reactions of interest to nuclear astrophysics have been studied with radioactive beams at the ATLAS (Argonne Tandem Linac Accelerator System) accelerator. Using a modified ISOL (isotope separation on-line) technique, beams of (sup 18)F (T(sub 1/2) = 110 min) and (sup 56)Ni (T(sub 1/2) = 6.1d) were produced and the reactions (sup 18)F(p,(alpha))(sup 15)O, (sup 18)F(p,(gamma))(sup 19)Ne, and (sup 56)Ni(d,p)(sup 57)Ni have been investigated. The results indicate that the (sup 18)F(p,(gamma)) route is a small contributor to the breakout from the hot CNO cycle into the rp process, while the (sup 56)Ni(p,(gamma))(sup 57)Cu rate is about ten times larger than previously assumed.

NTIS
*Linear Accelerators; Ion Beams; Nuclear Astrophysics*

**20010123544** Argonne National Lab., IL USA
**Microscopic calculations of (lambda) single-particle energies**
Usmani, Q. N.; Feb. 12, 1998; 12p; In English
Report No.(s): DE2001-10634; ANL/PHY/CP-95594; No Copyright; Avail: Department of Energy Information Bridge

(Lambda) binding energy data for total baryon number A (le) 208 and for (Lambda) angular momenta (ell)(sub (Lambda)) (le) 3 are analyzed in terms of phenomenological (but generally consistent with meson-exchange) (Lambda)N and (Lambda)NN potentials. The Fermi-Hypernetted-Chain technique is used to calculate the expectation values for the (Lambda) binding to nuclear matter. Accurate effective (Lambda)N and (Lambda)NN potentials are obtained which are folded with the core nucleus nucleon densities to calculate the (Lambda) single particle potential U(sub (Lambda))(r). We use a dispersive (Lambda)NN potential but also include an explicit (rho) dependence to allow for reduced repulsion in the surface, and the best fits have a large (rho) dependence giving consistency with the variational Monte Carlo calculations for (sub (Lambda))(sup 5)He. The exchange fraction of the (Lambda)N space-exchange potential is found to be 0.2-0.3 corresponding to m(sub (Lambda))* (approx equal)

(0.74-0.82)m(sub (Lambda)). Charge symmetry breaking is found to be significant for heavy hypernuclei with a large neutron excess, with a strength consistent with that obtained from the A = 4 hypernuclei.
NTIS
*Binding Energy; Computation; Microscopy; Particle Energy; Baryons*

**20010123643** Brookhaven National Lab., Upton, NY USA
**Why color-flavor locking is just like chiral symmetry breaking**
Pisarski,; Rischke,; May 10, 2000; 9p; In English
Report No.(s): DE2000-757157; BNL-67421; No Copyright; Avail: Department of Energy Information Bridge, Microfiche
The authors review how a classification into representations of color and flavor can be used to understand the possible patterns of symmetry breaking for color superconductivity in dense quark matter. In particular, the authors show how for three flavors, color-flavor locking is precisely analogous to the usual pattern of chiral symmetry breaking in the QCD (quantum chromodynamics) vacuum.
NTIS
*Quarks; Superconductivity*

**20010123644** Brookhaven National Lab., Upton, NY USA
**Characterization of the coherent noise, electromagnetic compatibility and electromagnetic interference of the atlas EM calorimeter front end board**
Chase,; Citterio,; Lanni,; Makowiecki,; Radeka,; Sep. 20, 2000; 6p; In English
Report No.(s): DE2000-757155; BNL-67429; No Copyright; Avail: Department of Energy Information Bridge, Microfiche
The ATLAS (Argonne Tandem Linac Accelerator System) Electromagnetic (EM) calorimeter (EMCAL) Front End Board (FEB) will be located in custom-designed enclosures solidly connected to the feedtroughs. It is a complex mixed signal board which includes the preamplifier, shaper, switched capacitor array analog memory unit (SCA), analog to digital conversion, serialization of the data and related control logic. It will be described in detail elsewhere in these proceedings. The electromagnetic interference (either pick-up from the on board digital activity, from power supply ripple or from external sources) which affects coherently large groups of channels (coherent noise) is of particular concern in calorimetry and it has been studied in detail.
NTIS
*Calorimeters; Linear Accelerators; Control Systems Design*

**20010123645** Brookhaven National Lab., Upton, NY USA
**Muon storage rings: neutrino factories**
Parsa,; May 30, 2000; 17p; In English
Report No.(s): DE2000-757154; BNL-67466; No Copyright; Avail: Department of Energy Information Bridge, Microfiche
The concept of a muon storage ring-based Neutrino Source (Neutrino Factory) has sparked considerable interest in the High Energy Physics community. Besides providing a first phase of a muon collider facility, it would generate more intense and well collimated neutrino beams than currently available. The BNL (Brookhaven National Laboratory)-AGS (Alternating Gradient Synchrotron) or some other proton driver would provide an intense proton beam that hits a target, produces pions that decay into muons. The muons must be cooled, accelerated and injected into a storage ring with a long straight section where they decay. The decays occurring in the straight sections of the ring would generate neutrino beams that could be directed to detectors located thoUSAnds of kilometers away, allowing studies of neutrino oscillations with precisions not currently accessible. For example, with the neutrino source at BNL, detectors at Soudan, Minnesota (1,715 km), and Gran SASso, Italy (6,527 km) become very interesting possibilities. The feasibility of constructing and operating such a muon-storage-ring based Neutrino-Factory, including geotechnical questions related to building non-planar storage rings (e.g. at 8 (degree) angle for BNL-Soudan, and 3 (degree) angle for BNL-Gran SASso) along with the design of the muon capture, cooling, acceleration, and storage ring for such a facility is being explored by the growing Neutrino Factory and Muon Collider Collaboration (NFMCC). The authors present overview of Neutrino Factory concept based on a muon storage ring, its components, physics opportunities, possible upgrade to a full muon collider, latest simulations of front-end, and a new bowtie-muon storage ring design.
NTIS
*Muons; Storage Rings (Particle Accelerators); Particle Acceleration; Particle Production; High Energy Interactions*

**20010123646** Brookhaven National Lab., Upton, NY USA
**Future lepton colliders and laser acceleration**
Parsa,; May 30, 2000; 13p; In English
Report No.(s): DE2000-757153; BNL-67467; No Copyright; Avail: Department of Energy Information Bridge, Microfiche

Future high energy colliders along with their physics potential, and relationship to new laser technology are discussed. Experimental approaches and requirements for New Physics exploration are also described.

NTIS
*Particle Acceleration; Lasers; Electron Scattering*

**20010123647** Brookhaven National Lab., Upton, NY USA
**What is new at small x**
Venugopalan,; Jan. 03, 2000; 12p; In English
Report No.(s): DE2000-757149; BNL-67413; No Copyright; Avail: Department of Energy Information Bridge, Microfiche

The authors discuss some recent developments in small x physics. Current understanding of small x physics is that pQCD (quantum chromodynamics) works at HERA (Hadron-Elektron-Ring-Analage) and the Tevatron, but perhaps even better than expected. There is much flexibility in parton distributions to hide interesting new effects. Indeed, there are strong hints from HERA that one is on the threshold of a new regime of truly high parton densities, where one may expect qualitative changes in the behavior of distributions.

NTIS
*Elementary Particles; Quantum Chromodynamics; Theoretical Physics*

**20010123648** Brookhaven National Lab., Upton, NY USA
**Mighty murines: neutrino physics at very high energy muon colliders**
King,; May 05, 2000; 24p; In English
Report No.(s): DE2000-757148; BNL-67411; No Copyright; Avail: Department of Energy Information Bridge, Microfiche

An overview is given of the potential for neutrino physics studies through parasitic use of the intense high energy neutrino beams that would be produced at future many-TeV muon colliders. Neutrino experiments clearly cannot compete with the collider physics. Except at the very highest energy muon colliders, the main thrust of the neutrino physics program would be to improve on the measurements from preceding neutrino experiments at lower energy muon colliders, particularly in the fields of B physics, quark mixing and CP (Charge conjugation and Parity transfer) violation. Muon colliders at the 10 TeV energy scale might already produce of order 10(sup 8) B hadrons per year in a favorable and unique enough experimental environment to have some analytical capabilities beyond any of the currently operating or proposed B factories. The most important of the quark mixing measurements at these energies might well be the improved measurements of the important CKM (Cabibbo-Kobayashi-Maskawa) matrix elements (vert bar)V(vert bar) and (vert bar)V(sub cb)(vert bar) and, possibly, the first measurements of (vert bar)V(sub td)(vert bar) in the process of flavor changing neutral current interactions involving a top quark loop. Muon colliders at the highest center-of-mass energies that have been conjectured, 100-1,000 TeV, would produce neutrino beams for neutrino-nucleon interaction experiments with maximum center-of-mass energies from 300-1,000 GeV. Such energies are close to, or beyond, the discovery reach of all colliders before the turn-on of the LHC (large hadron collider). In particular, they are comparable to the 314 GeV center-of-mass energy for electron-proton scattering at the currently operating HERA (Hadron-Elektron-Ring-Analage) collider and so HERA provides a convenient benchmark for the physics potential. It is shown that these ultimate terrestrial neutrino experiments, should they eventually come to pass, would have several orders of magnitude more luminosity than HERA. This would potentially open up the possibility for high statistics studies of any exotic particles, such as leptoquarks, that might have been previously discovered at these energy scales.

NTIS
*Muons; Neutron Physics; Neutrino Beams; High Energy Interactions; Particle Collisions*

**20010123731** Argonne National Lab., IL USA
**Hot-spare injector for the APS linac**
Lewellen, J. W.; Apr. 13, 1999; 5p; In English
Report No.(s): DE2001-11123; ANL/ASD/CP-97717; No Copyright; Avail: Department of Energy Information Bridge, Microfiche

Last year a second-generation SSRL-type thermionic cathode rf gun was installed in the Advanced Photon Source (APS) linac. This gun (referred to as 'gun') has been successfully commissioned and now serves as the main injector for the APS linac, essentially replacing the Koontz-type DC gun. to help ensure injector availability, particularly with the advent of top-up mode

operation at the APS, a second thermionic-cathode rf gun will be installed in the APS linac to act as a hot-spare beam source. The hot-spare installation includes several unique design features, including a deep-orbit Panofsky-style alpha magnet. Details of the hot-spare beamline design and projected performance are presented, along with some plans for future performance upgrades.
NTIS
*Guns; Thermionic Cathodes; Radio Frequencies; Photons*

**20010123733** Argonne National Lab., IL USA
**Measurement of sextupole orbit offsets in the APS storage ring**
Borland, M.; Apr. 16, 1999; 5p; In English
Report No.(s): DE2001-11118; ANL/ASD/CP-97708; No Copyright; Avail: Department of Energy Information Bridge, Microfiche

Horizontal orbit errors at the sextuples in the Advanced Photon Source (APS) storage ring can cause changes in tune and modulation of the beta functions around the ring. to determine the significance of these effects requires knowing the orbit relative to the magnetic center of the sextuples. The method considered here to determine the horizontal beam position in a given sextupole is to measure the tune shift caused by a change in the sextupole strength. The tune shift and a beta function for the same plane uniquely determine the horizontal beam position in the sextupole. The beta function at the sextupole was determined by propagating the beta functions measured at nearby quadrupoles to the sextupole location. This method was used to measure the sextupole magnetic center offset relative to an adjacent beam position monitor (BPM) at a number of sextupole locations. We report on the successes and problems of the method as well as an improved method.
NTIS
*Beams (Radiation); Modulation*

**20010123734** Argonne National Lab., IL USA
**Bunch cleaning strategies and experiments at the Advanced Photon Source**
Sereno, N. S.; Apr. 15, 1999; 5p; In English
Report No.(s): DE2001-11117; ANL/ASD/CP-97707; No Copyright; Avail: Department of Energy Information Bridge, Microfiche

The Advanced Photon Source (APS) design incorporated a positron accumulator ring (PAR) as part of the injector chain. In order to increase reliability and accommodate other uses of the injector, APS will run with electrons, eliminating the need for the PAR, provided another method of eliminating rf bucket pollution in the APS is found. Satellite bunches captured from an up to 30-ns-long beam from the linac need to be removed in the injector synchrotron and storage ring. The bunch cleaning method considered here relies on driving a stripline kicker with an amplitude modulated (AM) carrier signal where the carrier is at a revolution harmonic sideband corresponding to the vertical tune. The envelope waveform is phased so that all bunches except a single target bunch (eventually to be injected into the storage ring) are resonated vertically into a scraper. The kicker is designed with a large enough shunt impedance to remove satellite bunches from the injection energy of 0.4 GeV up to 1 GeV. Satellite bunch removal in the storage ring relies on the single bunch current tune shift resulting from the machine impedance. Small bunches remaining after initial preparation in the synchrotron may be removed by driving the beam vertically into a scraper using a stripline kicker operating at a sideband corresponding to the vertical tune for small current bunches. In this paper both design specifications and bunch purity measurements are reported for both the injector synchrotron and storage ring.
NTIS
*Linear Accelerators; Storage Rings (Particle Accelerators); Photons; Positrons; Amplitude Modulation*

**20010123740** Argonne National Lab., IL USA
**Solving QCD via multi-Regge theory**
White, A. R.; Nov. 04, 1998; 17p; In English
Report No.(s): DE2001-11092; ANL-HEP-CP-98-121; No Copyright; Avail: Department of Energy Information Bridge, Microfiche

To solve QCD at high-energy the authors must simultaneously find the hadronic states and the exchanged pomeron (IP) giving UNITARY scattering amplitudes. Experimentally, the IP (approximately) a Regge pole at small Q(sup 2) and a single gluon at larger Q(sup 2). (F(sub 2)(sup D)-H1, dijets-ZEUS). In the solution which the author describes, these non-perturbative properties of the IP are directly related to the non-perturbative confinement and chiral symmetry breaking properties of hadrons.
NTIS
*Quantum Chromodynamics; Regge Poles; Pomerons*

**20010123743** Argonne National Lab., IL USA
**Domain wall fermions at finite temperature**
Lagae, J. F.; Oct. 30, 1998; 5p; In English
Report No.(s): DE2001-11086; ANL-HEP-CP-98-66; No Copyright; Avail: Department of Energy Information Bridge, Microfiche

We investigate the properties of domain wall fermions on a set of quenched configurations at non-zero temperature. In particular, we compute the low lying eigenvalues of the DWF operator and study their relation with topology, level crossings and chiral symmetry breaking. We also measure the screening correlators and discuss the dependence on the extent of the extra dimension and the quark mass.
NTIS
*Eigenvalues; Domain Wall; Fermions*

**20010123748** Argonne National Lab., IL USA
**Metrology of a mirror at the Advanced Photon Source: Comparison between optical and x-ray measurements**
Assoufid, L.; Oct. 14, 1998; 14p; In English
Report No.(s): DE2001-11040; ANL/XFD/CP-97435; No Copyright; Avail: Department of Energy Information Bridge

This paper describes methology of a vertically focusing mirror on the bending magnet beamline in sector-1 of the Advanced Photon Source, Argonne National Laboratory. The mirror was evaluated using measurements from both an optical long trace profiler and x-rays. Slope error profiles obtained with the two methods were compared and were found to be in a good agreement. Further comparisons were made between x-ray measurements and results from the SHADOW ray-tracing code.
NTIS
*Photons; Magnetic Mirrors*

**20010123749** Argonne National Lab., IL USA
**Measurement of the CP asymmetry parameter sin2 beta at CDF**
LeCompte, T. J.; Oct. 14, 1998; 11p; In English
Report No.(s): DE2001-11039; ANL-HEP-CP-98-102; No Copyright; Avail: Department of Energy Information Bridge

We present a measurement of the time-dependent asymmetry in the rate for (bar B)(sub d)(sup 0) versus B(sub d)(sup 0) decays to J/(psi)K(sub S)(sup 0). In the context of the Standard Model this is interpreted as a measurement of the CP-violation parameter sin(2(beta)). A total of 198 +/- 17 B(sub d)(sup 0)/(bar B)(sub d)(sup 0) decays were observed in p(bar p) collisions at (radical)s = 1.8 TeV by the CDF detector at the Fermilab Tevatron. The initial b-flavor is determined by a same side flavor tagging technique. Our analysis results in sin(2(beta)) = 1.8 +/- 1.1(stat) +/- 0.3(syst).
NTIS
*Asymmetry; Time Dependence; Mesons; Particle Decay*

**20010123752** Argonne National Lab., IL USA
**Quantum Monte Carlo calculations of light nuclei**
Pieper, S. C.; Aug. 25, 1998; 10p; In English
Report No.(s): DE2001-11035; ANL/PHY/CP-97110; No Copyright; Avail: Department of Energy Information Bridge

Quantum Monte Carlo calculations using realistic two- and three-nucleon interactions are presented for nuclei with up to eight nucleons. We have computed the ground and a few excited states of all such nuclei with Greens function Monte Carlo (GFMC) and all of the experimentally known excited states using variational Monte Carlo (VMC). The GFMC calculations show that for a given Hamiltonian, the VMC calculations of excitation spectra are reliable, but the VMC ground-state energies are significantly above the exact values. We find that the Hamiltonian we are using (which was developed based on H-3, He-4, and nuclear matter calculations) underpredicts the binding energy of p-shell nuclei. However our results for excitation spectra are very good and one can see both shell-model and collective spectra resulting from fundamental many-nucleon calculations. Possible improvements in the three-nucleon potential are also be discussed.
NTIS
*Nucleons; Elementary Particle Interactions; Monte Carlo Method; Nucleon Potential*

**20010123753** Argonne National Lab., IL USA
**Rotating target wheel system for gammasphere**
Greene, J. P.; Jan. 04, 1999; 5p; In English
Report No.(s): DE2001-11034; ANL/PHY/CP-96977; No Copyright; Avail: Department of Energy Information Bridge

A description is given for a low-mass, rotating target wheel to be used within the Gammasphere target chamber. This system was developed for experiments employing high beam currents in order to extend lifetimes of targets using low-melting point target material. The design is based on a previously successful implementation of rotating target wheels for the Argonne Positron Experiment (APEX) as well as the Fragment Mass Analyser (FMA) at ATLAS (Argonne Tandem Linac Accelerator System). A brief history of these rotating target wheel systems is given as well as a discussion on target preparation and performance.
NTIS
*Linear Accelerators; Targets*

**20010123956** Argonne National Lab., IL USA
**Preparation of a 1 mg/cm(sup 2) C-13 Target**
Greene, J. P.; Nov. 18, 1998; 10p; In English
Report No.(s): DE2001-10937; ANL/PHY/CP-97115; No Copyright; Avail: Department of Energy Information Bridge

We give a description for the production of C-13 foils and the preparation of an approximately 1 mg/sq cm thick target. A recent experiment to measure the mass of Ca-36 via the Ca-40(He-4,He-8)Ca-36 reaction at the S800 magnetic spectrometer at MSU, needed a precise determination of the beam energy and calibration of the focal plane of the magnetic spectrometer in order to achieve the most accurate value for the Ca-36 mass. The 1 mg/sq cm C-13 target was essential for these purposes. Target performance along with some preliminary results will also be discussed.
NTIS
*Carbon 13; Magnetic Spectroscopy; Targets; Foils (Materials)*

**20010123962** Argonne National Lab., IL USA
**Measurement of the Mass of the W Boson from the Tevatron**
Thurman-Keup, R.; Aug. 25, 1998; 14p; In English
Report No.(s): DE2001-10928; ANL-HEP-CP-98-89; No Copyright; Avail: Department of Energy Information Bridge

This paper presents measurements of the mass of the W vector boson from the CDF and D0 experiments using data collected at (radical)s = 1.8 TeV during the 1994-1995 data taking run. CDF finds a preliminary mass of M(sub W) = 80.43 +/- 0.16 GeV and D0 measures a mass of M(sub W) = 80.44 +/- 0.12 GeV.
NTIS
*Bosons; Mass*

**20010124082** Sandia National Labs., Albuquerque, NM USA
**Effect of Near-Interface Network Strain on the Mobility of Protons in SiO2**
Fleetwood, D. M.; Karna, S. P.; Korambath, P. P.; Kurtz, H. A.; Pugh, R. D.; Jun. 17, 1999; 7p; In English
Report No.(s): DE2001-7899; SAND99-1531C; No Copyright; Avail: Department of Energy Information Bridge

Our data suggest a correlation between near-interface strain in SiO(sub 2) and the ratio of fixed vs. mobile positive charge generated at the interface during forming gas annealing. A model based on first-principles quantum mechanical calculations supports this correlation.
NTIS
*Protons; Quantum Mechanics; Silicon Dioxide; Mathematical Models; Mobility*

**20010124098** Argonne National Lab., IL USA
**High charge short electron bunches for wakefield accelerator structures development**
Conde, M. E.; Sep. 25, 1998; 5p; In English
Report No.(s): DE2001-10978; ANL-HEP-CP-98-100; No Copyright; Avail: Department of Energy Information Bridge, Microfiche

The Argonne Wakefield Accelerator group develops accelerating structures based on dielectric loaded waveguides. We use high charge short electron bunches to excite wakefields in dielectric loaded structures, and a second (low charge) beam to probe the wakefields left behind by the drive beam. We report measurements of beam parameters and also initial results of the dielectric loaded accelerating structures. We have studied acceleration of the probe beam in these structures and we have also made measurements on the RF pulses that are generated by the drive beam. Single drive bunches, as well as multiple bunches separated by an integer number of RF periods have been used to generate the accelerating wakefields.
NTIS
*Linear Accelerators; Dielectrics; Waveguides*

**20010124099** Argonne National Lab., IL USA
**Laser system for a subpicosecond electron linac**
Crowell, R. A.; Sep. 25, 1998; 6p; In English
Report No.(s): DE2001-10977; ANL/CHM/CP-97338; No Copyright; Avail: Department of Energy Information Bridge, Microfiche

At the Argonne Chemistry Division efforts are underway to develop a sub-picosecond electron beam pulse radiolysis facility for chemical studies. The target output of the accelerator is to generate electron pulses that can be adjusted from 3nC in 0.6ps to 100nC in 45ps. In conjunction with development of the accelerator a state-of-the-art ultrafast laser system is under construction that will drive the linacs photocathode and provide probe pulses that are tunable from the UV to IR spectral regions.
NTIS
*Picosecond Pulses; Electron Beams; Radiolysis; Linear Accelerators*

**20010124136** Argonne National Lab., IL USA
**Development of niobium spoke cavities for a superconducting light-ion Linac**
Shepard, K. W.; Nov. 18, 1998; 5p; In English
Report No.(s): DE2001-11112; ANL/PHY/CP-97690; No Copyright; Avail: Department of Energy Information Bridge, Microfiche

This paper reports the development of 350 MHz niobium superconducting cavities for the velocity range 0.2< v/c less than 0.6. Such cavities could be used to form a linac of exceptional flexibility, capable of efficiently accelerating beams of either protons, deuterons, or any of a wide range of light ions, at intensities sufficient for a production beam for a radioactive beam facility. Results of numerical modeling for several resonator geometries are presented. The design and construction status of prototype niobium cavities is discussed.
NTIS
*Niobium; Superconducting Magnets; Light Ions; Linear Accelerators*

**20010124138** Argonne National Lab., IL USA
**Dispersion and betatron function correction in the Advanced Photon Source storage ring using singular value decomposition**
Emery, L.; Apr. 13, 1999; 5p; In English
Report No.(s): DE2001-11119; ANL/ASD/CP-97709; No Copyright; Avail: Department of Energy Information Bridge, Microfiche

Magnet errors and off-center orbits through sextuples perturb the dispersion and beta functions in a storage ring (SR), which affects machine performance. In a large ring such as the Advanced Photon Source (APS), the magnet errors are difficult to determine with beam-based methods. Also the non-zero orbit through sextuples result from user requests for steering at light source points. For expediency, a singular value decomposition (SVD) matrix method analogous to orbit correction was adopted to make global corrections to these functions using strengths of several quadrupoles as correcting elements. The direct response matrix is calculated from the model of the perfect lattice. The inverse is calculated by SVD with a selected number of singular vectors. Resulting improvement in the lattice functions and machine performance will be presented.
NTIS
*Storage Rings (Particle Accelerators); Matrix Methods; Photons; Matrices (Mathematics)*

**20010124139** Brookhaven National Lab., Upton, NY USA
**ARTUS: The Tune Measurement System at RHIC**
Drees,; Brennan,; Connolly,; Michnoff,; DeLong,; May 08, 2000; 8p; In English
Report No.(s): DE2000-757156; BNL-67428; No Copyright; Avail: Department of Energy Information Bridge, Microfiche

The super-conducting Relativistic Heavy Ion Collider (RHIC) with two separate rings and six combined interaction regions will provide collisions between equal and unequal heavy ion species up to Au ions in typically 60 bunches. The betatron tunes of the two beams are among the most important parameters to be measured. The tunes have to be acquired at any moment during accelerator operation and in particular during the acceleration process. At RHIC the tune measurement device (ARTUS) consists of a fast horizontal and vertical kicker magnet and a dedicated beam position monitor in each ring. The system layout is described and first experiences from operation is reported.
NTIS
*Heavy Ions; Particle Accelerators; Ionic Collisions*

**20010125014** Argonne National Lab., IL USA

**Solving QCD via multi-Regge theory**

White, A. R.; Nov. 04, 1998; 13p; In English; 4th; 4th Workshop on Quantum Chromodynamics, 1-6 Jun. 1998, Paris, France

Report No.(s): DE2001-11094; ANL-HEP-CP-98-130; No Copyright; Avail: Department of Energy Information Bridge, Microfiche

A high-energy, transverse momentum cut-off, solution of QCD is outlined. Regge pole and single gluon properties of the pomeron are directly related to the confinement and chiral symmetry breaking properties of the hadron spectrum. This solution, which corresponds to a supercritical phase of Reggeon Field Theory, may only be applicable to QCD with a very special quark content.

NTIS

*Quantum Chromodynamics; Quarks; Regge Poles*

**20010125156** Argonne National Lab., IL USA

**Summary of experimental electroweak physics**

Nodulman, L.; May 03, 1999; 9p; In English

Report No.(s): DE2001-11788; ANL-HEP-CP-99-33; No Copyright; Avail: Department of Energy Information Bridge

Progress continues on many fronts of experimental testing of electroweak symmetry breaking. Updates were presented on LEP, SLC, Brookhaven g-2 ring, Tevatron Collider, HERA, CESR and Tevatron neutrino experiments. Perhaps most exciting is the Higgs search at LEP2, complementing the indirect constraints. However, the standard model with one Higgs doublet remains viable.

NTIS

*Electroweak Interactions (Field Theory); Higgs Bosons*

**20010125157** Argonne National Lab., IL USA

**Status of the new muon g - 2 experiment**

Carey, R. M.; Earle, W.; Efstathiadis, E.; Hare, M. F.; Nodulman, L.; May 03, 1999; 7p; In English

Report No.(s): DE2001-11787; ANL-HEP-CP-99-41; No Copyright; Avail: Department of Energy Information Bridge

The new muon (g - 2) experiment is now fully operational The goal of the experiment is to obtain a relative error on (g - 2) of +/- 0.35 ppm to measure the electroweak contribution for the first time, and to observe, or place stringent limits on physics beyond the standard model which can contribute to (g - 2). A brief status report is presented.

NTIS

*Muons; Neutrinos*

**20010125158** Argonne National Lab., IL USA

**Single-top-squark production via baryon-number-violating couplings at the Fermilab Tevatron Collider**

Berger, E. L.; Harris, B. W.; Sullivan, Z.; Apr. 29, 1999; 12p; In English

Report No.(s): DE2001-11786; ANL-HEP-CP-99-40; No Copyright; Avail: Department of Energy Information Bridge

We consider the s-channel R-parity-violating production of a single light top squark (tilde t)(sub 1) and its subsequent R-parity-conserving decay. For masses in the range 180-325 GeV, and R-parity-violating couplings (lambda)(sub 3ij)(double-prime) > 0.02-0.05, we show that discovery of the top squark is possible with 2 fb(sup (minus)1) of integrated luminosity at run II. If no evidence for the top squark is found, the bound on (lambda)(sub 3ij)(double-prime) can be reduced by up to an order of magnitude with existing data from run I, and by two orders of magnitude at run II.

NTIS

*Particle Accelerators; Quarks*

**20010125163** Argonne National Lab., IL USA

**Toward a fourth-generation light source**

Moncton, D. E.; May 03, 1999; 10p; In English

Report No.(s): DE2001-11775; ANL/OTD-APS/CP-98889; No Copyright; Avail: Department of Energy Information Bridge

Historically, x-ray research has been propelled by the existence of urgent and compelling scientific questions and the push of powerful and exquisite source technology. These two factors have gone hand in hand since Rontgen discovered x-rays. Here we review the progress being made with existing third-generation synchrotron-radiation light sources and the prospects for a fourth-generation light source with dramatically improved laser-like beam characteristics. The central technology for high-brilliance x-ray beams is the x-ray undulator, a series of alternating-pole magnets situated above and below the particle beam.

When the particle beam is oscillated by the alternating magnetic fields, a set of. interacting and interfering wave fronts is produced, which leads to an x-ray beam with extraordinary properties. Third-generation sources of light in the hard x-ray range have been constructed at three principal facilities: the European Synchrotrons Radiation Facility (ESRF) in France; the Super Photon Ring 8-GeV (or Spring-8) in Japan; and the Advanced Photon Source (APS) in the US. Undulator technology is also used on a number of low-energy machines for radiation in the ultraviolet and soft x-ray regimes. At the APS, these devices exceed all of our original expectations for beam brilliance, tunability, spectral range, and operational flexibility. Shown in Fig. 1 are the tuning curves of the first few harmonics, showing x-ray production from a few kV to better than 40 keV. High-brilliance radiation extends to over 100 keV.
NTIS
*Light Sources; Synchrotron Radiation; X Rays*

**20010125238** Oak Ridge National Lab., TN USA
**Computational Benchmark Calculations Relevant to the Neutronic Design of the Spallation Neutron Source (SNS)**
Gallmeier, F. X.; Glasgow, D. C.; Jerde, E. A.; Johnson, J. O.; Yugo, J. J.; Nov. 14, 1999; 8p; In English
Report No.(s): DE2001-11471; ORNL/CP-104532; No Copyright; Avail: Department of Energy Information Bridge

The Spallation Neutron Source (SNS) will provide an intense source of low-energy neutrons for experimental use. The low-energy neutrons are produced by the interaction of a high-energy (1.0 GeV) proton beam on a mercury (Hg) target and slowed down in liquid hydrogen or light water moderators. Computer codes and computational techniques are being benchmarked against relevant experimental data to validate and verify the tools being used to predict the performance of the SNS. The LAHET Code System (LCS), which includes LAHET, HTAPE ad HMCNP (a modified version of MCNP version 3b), have been applied to the analysis of experiments that were conducted in the Alternating Gradient Synchrotron (AGS) facility at Brookhaven National Laboratory (BNL). In the AGS experiments, foils of various materials were placed around a mercury-filled stainless steel cylinder, which was bombarded with protons at 1.6 GeV. Neutrons created in the mercury target, activated the foils. Activities of the relevant isotopes were accurately measured and compared with calculated predictions. Measurements at BNL were provided in part by collaborating scientists from JAERI as part of the AGS Spallation Target Experiment (ASTE) collaboration. to date, calculations have shown good agreement with measurements.
NTIS
*Spallation; Neutron Sources; Computer Programs*

**20010125239** Brookhaven National Lab., Upton, NY USA
**Requirements and guidelines for NSLS experimental beam line vacuum systems**
Foerster,; May 01, 1999; 102p; In English
Report No.(s): DE2001-11472; BNL-28073-99/05-Rev; No Copyright; Avail: Department of Energy Information Bridge

Typical beam lines are comprised of an assembly of vacuum valves and shutters referred to as a front end, optical elements to monochromatize, focus and split the photon beam, and an experimental area where a target sample is placed into the photon beam and data from the interaction is detected and recorded. Windows are used to separate sections of beam lines that are not compatible with storage ring ultra high vacuum. Some experimental beam lines share a common vacuum with storage rings. Sections of beam lines are only allowed to vent up to atmospheric pressure using pure nitrogen gas after a vacuum barrier is established to protect ring vacuum. The front end may only be bled up when there is no current in the machine. This is especially true on the VUV storage ring where for most experiments, windows are not used. For the shorter wavelength, more energetic photons of the x-ray ring, beryllium windows are used at various beam line locations so that the monochromator, mirror box or sample chamber may be used in a helium atmosphere or rough vacuum. The window separates ring vacuum from the environment of the downstream beam line components. The stored beam lifetime in the storage rings and the maintenance of desirable reflection properties of optical surfaces depend upon hydrocarbon-free, ultra-high vacuum systems. Storage ring vacuum systems will operate at pressures of (approximately) 1 x 10(exp -10) Torr without beam and (approximately) 1 x 10(exp -9) Torr with beam. Systems are free of hydrocarbons in the sense that no pumps, valves, etc. containing organics are used. Components are all-metal, chemically cleaned and bakeable. to the extent that beam lines share a common vacuum with the storage ring, the same criteria will hold for beam line components. The design philosophy for NSLS beam lines is to use all-metal, hydrocarbon-free front end components and recommend that experimenters use this approach for common vacuum hardware downstream of front ends. O-ring-sealed valves, if used, are not permitted upstream of the monochromator exit aperture. It will be the responsibility of users to demonstrate that their experiment will not degrade the pressure or quality of the storage ring vacuum. As a matter of operating

policy, all beam lines will be monitored for prescribed pressure and the contribution of high mass gases to this pressure each time a beam line has been opened to ring vacuum.
NTIS
*Photon Beams; Vacuum Systems*

**20010125245** Argonne National Lab., IL USA
**Nuclear Excitation by Electronic Transition (NEET)**
Ahmad, I.; Dunford, R. W.; Esbensen, H.; Gemmell, D. S.; Kanter, E. P.; Apr. 28, 1999; 13p; In English
Report No.(s): DE2001-11772; ANL/PHY/CP-98882; No Copyright; Avail: Department of Energy Information Bridge
We present a report on recent measurements using the Advanced Photon Source at Argonne National Laboratory to explore the phenomenon of Nuclear Excitation by Electronic Transition (NEET) in the (sup 189)Os atomic/nuclear system.
NTIS
*Photons; Excitation; Electron Transitions*

**20010125246** Argonne National Lab., IL USA
**Updated calculations of the reach of Fermilab Tevatron upgrades for Higgs Bosons in the MSSM, mSUGRA, and mGMSB models**
Baer, H.; Harris, B. W.; Tata, X.; Apr. 23, 1999; 16p; In English
Report No.(s): DE2001-11773; ANL-HEP-CP-99-34; No Copyright; Avail: Department of Energy Information Bridge
One of the crucial predictions of supersymmetric models that reduce to the Minimal Supersymmetric Standard Model (MSSM) at the weak scale is that the lightest Higgs scalar should have mass m(sub h) (approx-lt) 125-130 GeV(1). Recent results on the reach of Fermilab Tevatron upgrades for Standard Model (SM) Higgs bosons show that masses of order 120-180 GeV may be probed (2, 3, 4, 5), depending on integrated luminosity, detector performance and signal and background modeling. Thus, the discovery of a Higgs boson (or a new limit of around 120-130 GeV on its mass) will severely constrain supersymmetric models as well. In this report, we update previous calculations made by our group pertaining to the reach of Fermilab Tevatron upgrades for Higgs bosons in supersymmetric models. We present reach results for SUSY Higgs bosons within the MSSM, the minimal Supergravity model (mSUGRA) and in the minimal Gauge Mediated SUSY Breaking model (mGMSB). In this update, 95% CL exclusion contours and 5(sigma) discovery contours are presented for integrated luminosity values of 2, 5 and 20 fb(sup -1).
NTIS
*Particle Accelerators; Supersymmetry; Higgs Bosons*

**20010125387** Argonne National Lab., IL USA
**R-parity-violating production of single top squarks with R-parity-conserving decays**
Berger, E. L.; Harris, B. W.; Sullivan, Z.; Apr. 30, 1999; 8p; In English
Report No.(s): DE2001-11795; ANL-HEP-CP-99-42; No Copyright; Avail: Department of Energy Information Bridge
Single-top-squark production probes R-parity-violating extensions of the minimal supersymmetric standard model though the (lambda)(sub 3ij)(double-prime) coupling. For top-squark masses in the range 180-325 GeV, and (lambda)(sub 3ij)(double-prime) greater than 0.02-0.06, we show that discovery of the top squark is possible with 2 fb(sup -1) of integrated luminosity at run II of the Fermilab Tevatron. The bound on (lambda)(sub 3ij)(double-prime) can be reduced by up to an order of magnitude with existing data from run I, and by two orders of magnitude at run II if the top squark is not found.
NTIS
*Particle Production; Supersymmetry; Parity*

**20010125399** Brookhaven National Lab., Upton, NY USA
**Experience with polarized proton acceleration at cosy (julich)**
Lehrach,; May 20, 1999; 7p; In English
Report No.(s): DE2001-11476; BNL-66702; No Copyright; Avail: Department of Energy Information Bridge, Microfiche
The Cooler Synchrotrons and storage ring COSY at the Forschungszentrum Juelich accelerates protons to momenta between 600 MeV/c and 3300 MeV/c. At present the beam is used at four internal and three external target places. In addition, a polarized beam can be produced and accelerated at COSY. A colliding beams source, developed by a collaboration of the universities of Bonn, Erlangen, and Cologne is in operation. The polarized H(sup (minus)) beam delivered by this source is pre-accelerated in a cyclotron to 295 MeV/c and injected via stripping injection into the COSY ring. The polarization of the circulating proton beam

in COSY is measured continuously during acceleration with the internal EDDA detector. In this paper the methods to overcome depolarizing resonances in COSY are discussed and the progress to preserve polarization during acceleration is presented.
NTIS
*Synchrotron Radiation; Beam Interactions; Storage Rings (Particle Accelerators); Proton Beams*

**20010125408** Argonne National Lab., IL USA
**Quasi-realtime x-ray microtomography system at the Advanced Photon Source**
DeCarlo, F.; Foster, I.; Insley, J.; Kesselman, C.; Lane, P.; Jul. 16, 1999; 12p; In English
Report No.(s): DE2001-11799; ANL/XFD/CP-98995; No Copyright; Avail: Department of Energy Information Bridge

The combination of high-brilliance x-ray sources, fast detector systems, wide-bandwidth networks, and parallel computers can substantially reduce the time required to acquire, reconstruct, and visualize high-resolution three-dimensional tomographic datasets. A quasi-realtime computed x-ray microtomography system has been implemented at the 2-BM beamline at the Advanced Photon Source at Argonne National Laboratory. With this system, a complete tomographic data set can be collected in about 15 minutes. Immediately after each projection is obtained, it is rapidly transferred to the Mathematics and Computing Sciences Division where preprocessing and reconstruction calculations are performed concurrently with the data acquisition by a SGI parallel computer. The reconstruction results, once completed, are transferred to a visualization computer that performs the volume rendering calculations. Rendered images of the reconstructed data are available for viewing back at the beamline experiment station minutes after the data acquisition was complete. The fully pipelined data acquisition and reconstruction system also gives us the option to acquire the tomographic data set in several cycles, initially with coarse then with fine angular steps. At present the projections are acquired with a straight-ray projection imaging scheme using 5-20 keV hard x rays in either phase or amplitude contrast mode at a 1-10 pm resolution. In the future, we expect to increase the resolution of the projections to below 100 nm by using a focused x-ray beam at the 2-ID-B beamline and to reduce the combined acquisition and computation time to the 1 min scale with improvements in the detectors, network links, software pipeline, and computation algorithms.
NTIS
*Tomography; Photons; X Ray Sources; Parallel Computers*

**20010125413** Argonne National Lab., IL USA
**Beam tests of the 12 MHz RFQ RIB injector for ATLAS**
Clifft, B. E.; Kaye, R. A.; Kedzie, M.; Shepard, K. W.; May 06, 1999; 5p; In English
Report No.(s): DE2001-11792; ANL/PHY/CP-98959; No Copyright; Avail: Department of Energy Information Bridge

Beam tests of the ANL 12 MHz Radio-Frequency Quadruple (RFQ), designed for use as the initial element of an injector system for radioactive beams into the existing ATLAS accelerators, are in progress. Recent high-voltage tests of the RFQ without beam achieved the design intervane voltage of 100 kV CW, enabling beam tests with A/q as large as 132 using beams from the ANL Physics Division 4 MV Dynamitron accelerator facility. Although the RFQ was designed for bunched beams, initial tests have been performed with unbunched beams. Experiments with stable, unbunched beams of singly-charged Xe-132 and Kr-84 measured the output beam energy distribution as a function of the RFQ operating voltage. The observed energies are in excellent agreement with numerical beam simulations.
NTIS
*Ion Beams; Injectors; Particle Accelerators*

**20010125420** Argonne National Lab., IL USA
**Wakefield excitation in multimode structures by a train of electron bunches**
Conde, M. E.; Gai, W.; Konecny, R.; Power, J. G.; Schoessow, P.; Mar. 26, 1999; 5p; In English
Report No.(s): DE2001-11751; ANL-HEP-CP-99-27; No Copyright; Avail: Department of Energy Information Bridge, Microfiche

We discuss wakefield excitation and propagation in dielectric structures, particularly concentrating on the case of multiple drive beam excitation in multimode structures. We emphasize calculations of the energy loss of the drive bunch train, the amplitude of the wakefield, and the relation between power flow and stored energy in the dielectric wakefield device. We show that for a collinear multimode structure the amplitude of the wakefield generated by a bunch train is less than or equal to the wakefield generated by a single bunch of the same total charge. Furthermore, the transformer ratio, R, is shown to be always less than 2, even in the multiple drive beam case. Plans for an experiment to measure wakes in a multimode structure at AWA (Argonne Wakefield Accelerator) are presented.
NTIS
*Electron Bunching; Excitation; Field Theory (Physics); Wave Excitation*

**20010125421** Argonne National Lab., IL USA

**Ep collider with E(sub cm) = 1 TeV in a VLHC booster tunnel**

Barber, D. P.; Chojnacki, E.; Derrick, M.; Friedsam, H.; Gorski, A.; Mar. 26, 1999; 5p; In English

Report No.(s): DE2001-11750; ANL-HEP-CP-99-28; No Copyright; Avail: Department of Energy Information Bridge, Microfiche

The low field option for the VLHC (Very Large Hadron Collider) includes a 3 TeV proton booster with a circumference of 34 km. The authors are studying the option of an electron ring to fit in this tunnel which can produce ep collisions with a luminosity of 1 fb(sup (minus)1)/yr with a center of mass energy of 1 TeV. The machine would utilize superconducting rf (radio frequency) and small low field magnets for the (approximately) 80 GeV electron beam. They describe the vacuum chamber/magnet system, rf power supply requirements, vacuum chamber cooling, interaction regions and installation of the facility in the tunnel, as well as provide preliminary estimates of beam stability and lifetimes.

NTIS

*Hadrons; Protons; Particle Accelerators; Particle Collisions*

**20010125422** Argonne National Lab., IL USA

**Design and construction of a high charge and high current 1-1/2 cell L-Band RF photocathode gun**

Conde, M. E.; Gai, W.; Konecny, R.; Power, J. G.; Schoessow, P.; Mar. 26, 1999; 5p; In English

Report No.(s): DE2001-11749; ANL-HEP-CP-99-26; No Copyright; Avail: Department of Energy Information Bridge, Microfiche

The Argonne Wakefield Accelerator has been successfully commissioned and used for conducting wakefield experiments in dielectric loaded structures and plasmas. Although the initial wakefield experiments were successful, higher drive beam quality would substantially improve the wakefield accelerating gradients. In this paper we present a new 1-1/2 cell L-band photocathode RF (radio frequency) gun design. This gun will produce 10-100 nC beam with 2-5 ps rms (root mean square) pulse length and normalized emittance less than 100 mm mrad. The final gun design and numerical simulations of the beam dynamics are presented.

NTIS

*Photocathodes; Plasma Guns; Radio Frequency Discharge*

**20010125423** Argonne National Lab., IL USA

**Design of a liquid lithium lens for a muon collider**

Balbekov, V.; Geer, S.; Hassanein, A.; Holtkamp, N.; Lebrun, P.; Mar. 26, 1999; 5p; In English

Report No.(s): DE2001-11748; ANL-HEP-CP-99-29; No Copyright; Avail: Department of Energy Information Bridge, Microfiche

The last stage of ionization cooling for the muon collider requires a multistage liquid lithium lens. This system uses a large ((approximately)0.5 MA) pulsed current through liquid lithium to focus the beam while energy loss in the lithium removes momentum which is replaced by linacs. The beam optics are designed to maximize the 6 dimensional transmission from one lens to the next while minimizing emittance growth. The mechanical design of the lithium vessel is constrained by a pressure pulse due to the sudden ohmic heating, and the stress on the Be window. The authors describe beam optics, the liquid lithium pressure vessel, pumping, power supplies, as well as the overall optimization of the system.

NTIS

*Linear Accelerators; Muons; Particle Collisions; Liquid Lithium; Lenses*

**20010125424** Argonne National Lab., IL USA

**Bent solenoids for spectrometers and emittance exchange sections**

Norem, J.; Mar. 26, 1999; 5p; In English

Report No.(s): DE2001-11747; ANL-HEP-CP-99-30; No Copyright; Avail: Department of Energy Information Bridge, Microfiche

Bent solenoids can be used to transport low energy beams as they provide both confinement and dispersion of particle orbits. Solenoids are being considered both as emittance exchange sections and spectrometers in the muon cooling system as part of the study of the muon collider. They present the results of a study of bent solenoids which considers the design of coupling sections between bent solenoids to straight solenoids, drift compensation fields, aberrations, and factors relating to the construction, such as field ripple, stored energy, coil forces and field errors.

NTIS

*Solenoids; Spectrometers*

**20010125429** Brookhaven National Lab., Upton, NY USA
**Polarized protons tracking in the ags and rhic**
Luccio,; May 20, 1999; 7p; In English
Report No.(s): DE2001-11477; BNL-66689; No Copyright; Avail: Department of Energy Information Bridge, Microfiche

A code, SPINK, to track polarized particles in a circular accelerator, in particular RHIC (Relativistic Heavy Ion Collider), has been used to: find conditions for safely crossing depolarizing resonances, using Siberian Snakes; find the best conditions to match the spin of the injected beam to the ring lattice; study the operation of Spin Rotators and study the beam-beam effects in a polarized proton collider.

NTIS
*Proton Beams; Polarized Radiation; Particle Accelerators; Computer Programs*

**20010125430** Brookhaven National Lab., Upton, NY USA
**Rhic spin program: machine aspects and recent progress**
Roser,; Jul. 20, 1999; 10p; In English
Report No.(s): DE2001-11475; BNL-66668; No Copyright; Avail: Department of Energy Information Bridge, Microfiche

High energy polarized beam collisions will open up the unique physics opportunities of studying spin effects in hard processes. However, the acceleration of polarized beams in circular accelerators is complicated by the numerous depolarizing spin resonances. Using a partial Siberian Snake and a rf (radio frequency) dipole that ensure stable adiabatic spin motion during acceleration has made it possible to accelerate polarized protons to 25 GeV at the Brookhaven AGS (Alternating Gradient Synchrotron). Full Siberian Snakes and polarimeters are being developed for RHIC (Relativistic Heavy Ion Collider) to make the acceleration of polarized protons to 250 GeV possible.

NTIS
*Beam Interactions; Particle Collisions; Charged Particles; Heavy Ions; Ionic Collisions; Research Facilities*

**20010125431** Brookhaven National Lab., Upton, NY USA
**Metrological challenges of synchrotron radiation optics**
Sostero,; May 25, 1999; 8p; In English
Report No.(s): DE2001-11474; BNL-66662; No Copyright; Avail: Department of Energy Information Bridge, Microfiche

Modern third generation storage rings, require state-of-the-art grazing incidence x-ray optics, in order to monochromate the Synchrotrons Radiation (SR) source photons, and focus them into the experimental stations. Slope error tolerances in the order of 0.5 (micro)Rad RMS (root mean square), and surface roughness well below 5 (angstrom) RMS, are frequently specified for mirrors and gratings exceeding 300 mm in length. Non-contact scanning instruments were developed, in order to characterize SR optical surfaces, of spherical and aspherical shape. Among these, the Long Trace Profiler (LTP), a double pencil slope measuring interferometer, has proved to be particularly reliable, and was adopted by several SR optics metrology laboratories. The ELETTRA soft x-rays and optics metrology laboratory, has operated an LTP since 1992. We review the basic operating principles of this instrument, and some major instrumental and environmental improvements, that were developed in order to detect slope errors lower than 1 (micro)Rad RMS on optical surfaces up to one meter in length. A comparison among measurements made on the same reference flat, by different interferometers (most of them were LTPs) can give some helpful indications in order to optimize the quality of measurement.

NTIS
*Interferometers; Mirrors; Synchrotron Radiation; Optical Equipment*

**20010125432** Argonne National Lab., IL USA
**State-of-the-Art Developments in Accelerator Controls at the APS**
Lenkszus, F.; Apr. 13, 1999; 7p; In English; 1999 Particle Accelerator Conference, 3 Mar. - 2 Apr. 1999, New York, NY, USA
Contract(s)/Grant(s): W-31109-ENG-38
Report No.(s): DE2001-11108; ANL/ASD/CP-97677; No Copyright; Avail: Department of Energy Information Bridge, Microfiche

The performance requirements of the Advanced Photon Source (APS) challenge the control system in a number of areas. This paper will review a few applications of advanced technology in the control and monitoring of the APS. The application of digital signal processors (DSPs) and techniques will be discussed, both from the perspective of a large distributed multiprocessor system and from that of embedded systems. In particular, two embedded applications will be highlighted, a beam position monitor processor and a DSP-based power supply controller. Fast data distribution is often a requirement. The application of a high-speed network based on reflective memory will also be discussed in the context of the APS global orbit feedback system. Timing systems

provide opportunities to apply technologies such as high-speed logic and fiber optics. Examples of the use of these technologies will also be included. Finally, every modern accelerator control system of any size requires networking. Features of the APS accelerator controls network will be discussed.
NTIS
*Linear Accelerators; Control Equipment; Data Processing; Signal Processing*

**20010125433** Argonne National Lab., IL USA
**PHOBOS Experiment at RHIC: Physics and Capabilities**
Back, B. B.; Nov. 17, 1998; 12p; In English; Workshop on Particle Distributions in Hadronic and Nuclear Collisions, 11-13 Jun. 1998, Chicago, IL, USA
Report No.(s): DE2001-11107; ANL/PHY/CP-97675; No Copyright; Avail: Department of Energy Information Bridge, Microfiche

The PHOBOS experiment at RHIC is designed to study multiplicity distributions and fluctuations over all of 4(pi), as well as particle spectra and correlations at mid rapidity, with a particular emphasis on physics at low p(sub T). The experiment is relatively small and relies almost entirely on silicon pad detector technology. The flexibility of the design, the conservative nature of the technologies used, and the ability to take data at high rates place the experiment in a good position to search for exotic physics from heavy-ion collisions at the early stages of RHIC operations.
NTIS
*Ionic Collisions; Relativistic Particles; Research Facilities*

**20010125435** Argonne National Lab., IL USA
**High-brightness electron beams for production of high intensity, coherent radiation for scientific and industrial applications**
Kim, K. J.; Jan. 15, 1999; 12p; In English; ECOMAP-98, 24-27 Nov. 1998, Heiankaikan, Japan
Report No.(s): DE2001-11100; ANL/ASD/CP-97648; No Copyright; Avail: Department of Energy Information Bridge, Microfiche

Relativistic electron beams with high six-dimensional phase space densities, i.e., high-brightness beams, are the basis for efficient generation of intense and coherent radiation beams for advanced scientific and industrial applications. The remarkable progress in synchrotrons radiation facilities from the first generation to the current, third-generation capability illustrates this point. With the recent development of the high-brightness electron gun based on laser-driven rf photocathodes, linacs have become another important option for high-brightness electron beams. With linacs of about 100 MeV, megawatt-class infrared free-electron lasers can be designed for industrial applications such as power beaming. With linacs of about 10 GeV, 1-(angstrom) x-ray beams with brightness and time resolution exceeding by several orders of magnitude the current synchrotrons radiation sources can be generated based on self-amplified spontaneous emission. Scattering of a high-brightness electron beam by high power laser beams is emerging as a compact method of generating short-pulse, bright x-rays. In the high-energy frontier, photons of TeV quantum energy could be generated by scattering laser beams with TeV electron beams in future linear colliders.
NTIS
*Coherent Radiation; Electron Beams; Electron Guns*

**20010125436** Argonne National Lab., IL USA
**Experimental Tests of the Standard Model**
Nodulman, L.; Nov. 11, 1998; 48p; In English; 1998 Advanced Study Institute on Techniques and Concepts of High Energy Physics, I, 18-29 Jun. 1998, St. Croix, VI, USA
Contract(s)/Grant(s): W-31109-ENG-38
Report No.(s): DE2001-11099; ANL-HEP-CP-98-129; No Copyright; Avail: Department of Energy Information Bridge, Microfiche

The title implies an impossibly broad field, as the Standard Model includes the fermion matter states, as well as the forces and fields of SU(3) x SU(2) x U(1). For practical purposes, I will confine myself to electroweak unification, as discussed in the lectures of M. Herrero. Quarks and mixing were discussed in the lectures of R. Aleksan, and leptons and mixing were discussed in the lectures of K. Nakamura. I will essentially assume universality, that is flavor independence, rather than discussing tests of it. I will not pursue tests of QED beyond noting the consistency and precision of measurements of (alpha)(sub EM) in various processes including the Lamb shift, the anomalous magnetic moment (g-2) of the electron, and the quantum Hall effect. The fantastic precision and agreement of these predictions and measurements is something that convinces people that there may be something to this science enterprise. Also impressive is the success of the 'Universal Fermi Interaction' description of beta decay

processes, or in more modern parlance, weak charged current interactions. With one coupling constant G(sub F), most precisely determined in muon decay, a huge number of nuclear instabilities are described. The slightly slow rate for neutron beta decay was one of the initial pieces of evidence for Cabbibo mixing, now generalized so that all charged current decays of any flavor are covered.
NTIS
*Electroweak Interactions (Field Theory); Standard Model (Particle Physics)*

**20010125437** Argonne National Lab., IL USA
**Quarkonium at STAR**
LeCompte, T. J.; Nov. 11, 1998; 12p; In English; Workshop on Quarkonium Production in Relativistic Nuclear Collisions, 11-15 May 1998, Seattle, WA, USA
Contract(s)/Grant(s): W-31109-ENG-38
Report No.(s): DE2001-11098; ANL-HEP-CP-98-131; No Copyright; Avail: Department of Energy Information Bridge, Microfiche

The STAR detector is capable of reconstruction the J/(psi) meson in its dielectron decay channel, along with continuum dielectrons from heavy quark decay. The limitation is not instrumental--the ability of the STAR detector to identify electrons--rather, the primary limitation is yield. We expect to reconstruct of order 10,000 events per year in the bin of highest centrality, with perhaps ten times that many integrated over all bins of centrality. This is enough for a rather detailed study of J/(psi) production. The yields for (psi)(prime) and the high p(sub T) (chi) mesons which are in a low enough background region of phase space to permit reconstruction are too small for precision measurements. The only parent of the J/(psi) with a large enough yield for clear observation is the b quark. Even limited to just the J/(psi), there is a rich physics program available to STAR: the yield provides information on the gluon flux as well as color screening, especially when compared to the open charm and b (r arrow) J/(psi)X yields. The p(sub T) distribution measures energy loss in a nuclear medium, either by comparison with pp data or across different bins in centrality. The STAR quarkonium program should provide several unique windows into the physics of heavy ion collisions at RHIC.
NTIS
*Radiation Counters; Particle Decay*

**20010125438** Argonne National Lab., IL USA
**CVD-diamond-based position sensitive photoconductive detector for high-flux x-rays and gamma rays**
Shu, D.; Apr. 19, 1999; 5p; 1999 Particle Accelerator Conference, 29 Mar. - 2 Apr. 1999, New York, NY, USA
Contract(s)/Grant(s): W-31109-ENG-38
Report No.(s): DE2001-11097; ANL/XFD/CP-97643; No Copyright; Avail: Department of Energy Information Bridge, Microfiche

A position-sensitive photoconductive detector (PSPCD) using insulating-type CVD diamond as its substrate material has been developed at the Advanced Photon Source (APS). Several different configurations, including a quadrant pattern for a x-ray-transmitting beam position monitor (TBPM) and 1-D and 2-D arrays for PSPCD beam profilers, have been developed. Tests on different PSPCD devices with high-heat-flux undulator white x-ray beam, as well as with gamma-ray beams from (sup 60)Co sources have been done at the APS and National Institute of Standards and Technology (NIST). It was proven that the insulating-type CVD diamond can be used to make a hard x-ray and gamma-ray position-sensitive detector that acts as a solid-state ion chamber. These detectors are based on the photoconductivity principle. A total of eleven of these TBPMs have been installed on the APS front ends for commissioning use. The linear array PSPCD beam profiler has been routinely used for direct measurements of the undulator white beam profile. More tests with hard x-rays and gamma rays are planned for the CVD-diamond 2-D imaging PSPCD. Potential applications include a high-dose-rate beam profiler for fourth-generation synchrotrons radiation facilities, such as free-electron lasers.
NTIS
*Vapor Deposition; Diamonds; Detectors; Beams (Radiation)*

**20010125439** Argonne National Lab., IL USA
**Search for new physics in D(+-) --> K(sub s)X(+-) and D(+-) --> K(sub s)K(sub s)K(+-)**
Lipkin, H. J.; Nov. 09, 1998; 11p; Workshop on Heavy Quarks at Fixed Target (HQ'98), 10-12 Oct. 1998, Batavia, IL, USA
Contract(s)/Grant(s): W-31109-ENG-38
Report No.(s): DE2001-11096; ANL-HEP-CP-98-122; No Copyright; Avail: Department of Energy Information Bridge, Microfiche

Direct CP violation beyond the standard model can be produced in charged D decays to final states with a K(sub S) by small new physics contributions to the transitions D(sup +) (r-arrow) K(sup 0)X(sup +), where X(sup +) denotes any positively charged hadronic state or transitions D(sup +) (r-arrow) K(sup 0)(bar K)(sup 0)K(sup (*)+), denotes any positive strange state. These transitions are doubly-Cabibbo suppressed and color suppressed in the standard model and branching ratios are experimentally observed to be suppressed by two orders of magnitude relative to the allowed D(sup +) (r-arrow) (bar K)(sup 0)X(sup +) or D(sup +) (r arrow) (bar K)(sup 0)(bar K)(sup 0)K(sup (star)+), branching ratio. An even smaller new physics contribution might produce an observable CP asymmetry in D(sup (+-)) (r arrow) K(sub S)X(sup (+-)) or D(sup (+-)) (r-arrow) K(sub S)K(sub S)K(sup (star)(+-)) decays. Since such asymmetries are easily checked in the early stages of any charm production experiment, it seems worth while to check them before the opportunity is lost in later stages of the analysis, even if no theoretical model predicts such an asymmetry.
NTIS
*Standard Model (Particle Physics); Quarks; Branching (Physics); Asymmetry*

**20010125474** Argonne National Lab., IL USA
**Accelerator Controls Network Designed for Reliability and Flexibility**
McDowell, W. P.; Sidorowicz, K. V.; Dec. 02, 1997; 5p; In English
Report No.(s): DE2001-8095; ANL/ASD/CP-93577; No Copyright; Avail: Department of Energy Information Bridge, Microfiche

The APS accelerator control system is a typical modern system based on the standard control system model, which consists of operator interfaces to a network and computer-controlled interfaces to hardware. The network provides a generalized communication path between the host computers, operator workstations, input/output crates, and other hardware that comprise the control system. The network is an integral part of all modern control systems and network performance will determine many characteristics of a control system. This paper describes the methods used to provide redundancy for various network system components as well as methods used to provide comprehensive monitoring of this network. The effect of archiving tens of thoUSAnds of data points on a regular basis and the effect on the controls network will be discussed. Metrics are provided on the performance of the system under various conditions.
NTIS
*Versatility; Reliability; Workstations; Control Systems Design*

**20010125586** Argonne National Lab., IL USA
**Effects of bunch density gradient in high-gain free-electron lasers**
Huang, Z.; Kim, K. J.; Sep. 01, 1999; 12p; In English
Report No.(s): DE2001-11812; ANL/ASD/CP-99048; No Copyright; Avail: Department of Energy Information Bridge

The authors investigate effects of the bunch density gradient in self-amplified spontaneous emission (SASE), including the role of coherent spontaneous emission (CSE) in the evolution of the free-electron laser (FEL) process. In the exponential gain regime, the authors solve the coupled Maxwell-Vlasov equations and extend the linear theory to a bunched beam with energy spread. A time-dependent, nonlinear simulation algorithm is used to study the CSE effect and the nonlinear evolution of the radiation pulse.
NTIS
*Electron Bunching; Free Electron Lasers; Electron Beams*

**20010125650** Brookhaven National Lab., Upton, NY USA
**AGS Experiments in Nuclear/QCD Physics at Medium Energies 1988-2000**
Lo Presti, P.; Jul. 01, 1999; 90p; In English
Contract(s)/Grant(s): AC02-98CH10886
Report No.(s): DE2001-11437; BNL-65732; KA0202; No Copyright; Avail: Department of Energy Information Bridge, Microfiche

The report contains experiments performed at the Brookhaven AGS facility on nuclear physics and quantum chromodynamics physics.
NTIS
*Nuclear Physics; Quantum Chromodynamics; Research Facilities*

## 80
## SOCIAL AND INFORMATION SCIENCES (GENERAL)

*Includes general research topics related to sociology; educational programs and curricula.*

**20010120407** Arizona State Univ., East Mesa, AZ USA
**University Aviation Education: An Integrated Model**
Karp, Merrill R., Arizona State Univ., USA; Collegiate Aviation Review; October 2000; Volume 18, No. 1, pp. 1-10; In English; See also 20010120406; Copyright; Avail: Issuing Activity

As indicated at the Regional Air Transport Training Convention and Tradeshow (RATS 2000) at Daytona Beach, FL, on February 8-9, 2000, the United States regional airlines fully recognize that the frequently-discussed shortage of regional airline pilots is now a fact rather than a forecast. The regional airline conference attendees also felt that potential pilot shortages in the major airlines are probably not far behind. Over the past few decades, the airline industry has relied upon the military for its primary source of experienced pilots. However, with increased commercial airline expansion, coupled with the Vietnam era trained pilots approaching retirement age and the recent low military pilot training production, the USA now faces a shortage of highly experienced pilots in both the military and the commercial airline industry. While flight programs have been developed to meet these shortfalls with increased training, consideration should also be given to improving the aviation education process itself, which is the foundation of flight training. University aviation training programs, because of their comprehensive academic environments, offer excellent opportunities to develop and deliver state-of-the-art aviation curricula and become the new primary resource for commercial airline pilots. A key question to help resolve the impact of the commercial pilot shortage should be: Can an enhanced aviation academic education and flight training program help accelerate university-trained pilots into airline cockpits. This paper draws upon research conducted in the Aeronautical Management Technology Department at Arizona State University and addresses potential educational enhancements through the implementation of an integrated aviation teaming model, the Aviation Education Reinforcement Option (AERO). The AERO model is a teaming strategy that incorporates elements of the adult education paradigm, teaming style theory, cooperative and collaborative teaming techniques, and personal computer-based aviation training devices (PCATDs), to span the long-term retention and application gap that can occur between the classroom and the flight line. This paper suggests that the AERO model, when combined with flight training that emphasizes airline procedures from the very beginning, has the potential to reduce the pilot training time required between the universities' academic classrooms and flight training environments, and the commercial airline cockpit.
Author
*Education; Airline Operations; Aircraft Pilots; University Program; Universities; Learning*

**20010120409** Bowling Green State Univ., OH USA
**The Relationship of Document and Quantitative Literacy with Learning Styles and Selected Personal Variables for Aviation University Students**
Martin, Royce Ann, Bowling Green State Univ., USA; Collegiate Aviation Review; October 2000; Volume 18, No. 1, pp. 26-40; In English; See also 20010120406; Copyright; Avail: Issuing Activity

The purpose of this study was to determine the extent to which university student scores on a researcher-constructed quantitative and document literacy test were associated with learning style, program of study, cumulative grade point average, and year in school. Instruments used for the study were the 35 question Aviation Documents Delineator (ADD) and the Learning Type Measure (LTM). Data collected were analyzed using a step-wise multiple regression analysis technique. The ADD was designed to identify a student's ability and preference for interpreting and using graphic or tabular data. Study results reveal that year in school and GPA were significant predictors of literacy scores on the ADD while learning style and the student's program of study were not.
Author
*Universities; Reading; Education*

**20010120418** Auburn Univ., AL USA
**The Impact of Ground Schools in a Collegiate Aviation Program on FAA Written Exam Scores**
Flouris, Triant G., Auburn Univ., USA; Collegiate Aviation Review; October 2001; Volume 19, No. 1, pp. 49-61; In English; See also 20010120414; Copyright; Avail: Issuing Activity

This is a longitudinal study, tracing student FAA written exam test scores in a collegiate environment. The exams surveyed were administered in the War Eagle CATS testing center located at Auburn University from January 1, 1999 to December 31, 2000. The purpose of the study was to test the significance of ground schools offered at Auburn University on FAA written exam test scores. In addition, it examined the difference on test scores of Auburn students versus non-Auburn University students. The

independent variable was set as the group corresponding to each FAA test ground school. The dependent variable was student performance based on each corresponding FAA written exam score. Statistical analysis revealed that there is no significance on the impact of the independent to the dependent variable, or the impact of ground schools on FAA written test performance is not significant.
Author
*Civil Aviation; Education; Statistical Analysis*

**20010120425** Nebraska Univ., Omaha, NE USA
**Evaluation and Action: Sustaining Excellence in Collegiate Aviation Distance Education**
Scarpellini, Nanette M., Nebraska Univ., USA; Bowen, Brent D., Nebraska Univ., USA; Collegiate Aviation Review; October 2001; Volume 19, No. 1, pp. 140-167; In English; See also 20010120414; Copyright; Avail: Issuing Activity

This study assesses the role of the evaluation process in sustaining and developing quality distance education programs in collegiate aviation. Distance education encompasses distance learning and distributive learning as well as e-learning and multiple method crossover delivery that includes some form of electronic delivery. The research explores the sanctioned position of evaluation procedures and their practical application in the outcomes assessment process within collegiate aviation distance education programs as compared to traditional delivery methods. Additionally, the study investigates the criteria for determining outcomes assessment based on establishing methods for interpolating contact hours, applied testing, and gauging learning. The methodological approach includes a literature review and a survey instrument implemented by semi-structured phone interviews. The gathered data are based on a review of accredited graduate and undergraduate collegiate aviation distance programs. The findings demonstrate that evaluation is an underutilized method for sustaining and ensuring a high-level academic product is delivered via distance education. The lack of consistent terminology for classifying and measuring distance education, and more specifically, the meaning of quality, further complicate this. Further research is recommended in order to reach a consensus on defining vocabulary of distance education elements and the role and application of evaluation. Additionally, the recommendations provide guidance in modifying the curriculum for achieving consistent results commensurate with accreditation standards.
Author
*Civil Aviation; Education; Distance*

**20010123759** Nebraska Univ., Aviation Inst., Omaha, NE USA
**The Aeronautics Education, Research, and Industry Alliance (AERIAL): A Proposal to NASA EPSCoR 2000**
Bowen, Brent D., Nebraska Univ., USA; Alexander, Dennis R., Nebraska Univ., USA; Bartle, John R., Nebraska Univ., USA; Carstenson, Larry, Nebraska Univ., USA; Deichert, Jerome A., Nebraska Univ., USA; Gogos, George, Nebraska Univ., USA; Larson, Michael K., Nebraska Univ., USA; Narayanan, Ram M., Nebraska Univ., USA; Palmer, Robert D., Nebraska Univ., USA; Reed, B. J., Nebraska Univ., USA; 2000; 110p; In English
Report No.(s): UNOAI-2000-5; Copyright; Avail: Issuing Activity

The State of Nebraska proposes the Aeronautics Education, Research, and Industry Alliance (AERIAL): a comprehensive, multi-faceted NASA EPSCoR 2000 initiative that will contribute substantially to the strategic research and technology priorities of NASA while also intensifying the state's rapidly growing aeronautics research and development endeavors. AERIAL will enable Nebraska researchers to: (1) continue strengthening their collaborative relationships with NASA Field Centers, Codes, and Enterprises; (2) increase the capacity of higher education throughout Nebraska to invigorate and expand aeronautics research; and (3) expedite the development of aeronautics-related research infrastructure and industry in the state. This multi-institutional alliance will both form the foundation of a new statewide center for aeronautics research and elevate the state's activities in this regard to national prominence and impact. In the past ten years, Nebraska has initiated a series of specific strategies and initiatives-notably the Nebraska Space Grant Consortium, the Nebraska Initiative for Aerospace Research and Industrial Development (NIARID), and the NASA Nebraska EPSCoR Preparation Grant - designed to foster and sustain productive collaborations with NASA personnel. These efforts have resulted in a proliferation of research activity that continues to benefit NASA's Strategic Enterprises and Centers as well as the state of Nebraska. Specifically, these initiatives have directly or indirectly resulted in 42 new or expanded collaborations with NASA; $3,315,000 in non-NASA research funding; and approximately 86 undergraduate, graduate, and doctoral assistantships. They have also contributed to the development of several new industrial efforts in Nebraska, including collaboration with the J.A. Woollam company, manufacturer of ellipsometers.
Author
*Aeronautics; Education; Research and Development; Industries*

## 81
## ADMINISTRATION AND MANAGEMENT

*Includes management planning and research.*

**20010118261** Oak Ridge National Lab., TN USA
**Survey of LTR Program Industry Partner Satisfaction at Oak Ridge National Lab**
Payne, T. L.; Kniel, C.; Feb. 01, 2000; 7p; In English
Report No.(s): DE2000-760509; ORNL/TM-2000/62; No Copyright; Avail: Department of Energy Information Bridge, Microfiche

As a US Department of Energy (DOE) Office of Science (SC) National Laboratory, the Oak Ridge National Lab (ORNL) participates in the Laboratory Technology Research (LTR) Program. The mission of the LTR Program is to advance science and technology, in support of DOE missions, toward innovative applications through cost-shared partnerships with the private sector. The benefits to industry participants include gaining access to world-class researchers and facilities, while the benefits to the ORNL researchers includes leveraging the declining government-provided funds. Thus, the importance placed upon industry partner satisfaction is large, especially if the LTR Program is to be sustained during episodes of government budget constraints. Realizing the critical nature of partner satisfaction, in 1998 the DOE-SC National Laboratories surveyed industrial partners to assess their satisfaction with the cooperative research projects in which they were involved. This paper will describe the survey methodology including development of the questionnaire and a summary of the responses (particularly those which are germane to the ORNL.) The results of the survey will be categorized as follows: (1) Desire to partner again with ORNL; (2) Benefits obtained by the company from the partnership; and (3) LTR Program ratings assigned in 11 key areas (i.e.,quality of work, expertise, protection of intellectual property, value, facilities, understanding company needs, reliability of funding, schedule responsiveness, project management, contract negotiation, and contract administration.) More information about the LTR Program can be found at http://www.er.doe.gov/production/octr/aentr/aeptrnr.html.
NTIS
*Industries; Agreements; Research and Development; Energy Technology*

**20010118906** Brookhaven National Lab., Upton, NY USA
**Surveys of organizational culture and safety culture in nuclear power**
Brown,; Jul. 30, 2000; 5p; In English
Report No.(s): DE2000-755040; BNL-67231; No Copyright; Avail: Department of Energy Information Bridge

The results of a survey of organizational culture at a nuclear power plant are summarized and compared with those of a similar survey which has been described in the literature on high-reliability organizations. A general-purpose cultural inventory showed a profile of organizational style similar to that reported in the literature; the factor structure for the styles was also similar to that of the plant previously described. A specialized scale designed to measure safety culture did not distinguish among groups within the organization that would be expected to differ.
NTIS
*Nuclear Power Plants; Operations Research; Organizations; Personnel; Management*

**20010119054** Norwegian Defence Research Establishment, Kjeller, Norway
**Communicating Reform Processes in the Creation of the Australian Defence Materiel Organization**
Warberg, Erik Normann, Norwegian Defence Research Establishment, Norway; Aug. 27, 2001; 48p; In English; Original contains color illustrations
Contract(s)/Grant(s): FFIN Proj. 782/732
Report No.(s): FFI/RAPPORT-2001/04415; ISBN 82-464-0543-8; No Copyright; Avail: CASI; A03, Hardcopy; A01, Microfiche

This report is based on the report ”The creation of the Australian Defence Materiel Organization - The Communication Strategy” for the Masters program; ”Strategic reforms in the public sector” at the Norwegian school of Management made by Erik Normann Warberg, Norwegian Defence Research Establishment (FFI). The report looks into how reform processes are communicated to employees within Australian Defence Materiel Organization (DMO). The starting point for the report is the Communication Strategy developed by the DMO. A survey was conducted to verify the effect of this Strategy. The results show the importance of giving enough information as early as possible and also involve employees in the reform processes. It also gives a clear indication that the DMO did not perform particular well in the early stages when creating the DMO.
Author
*Communicating; Strategy; Management*

**20010119947** NASA Ames Research Center, Moffett Field, CA USA

**Decision Making in Action: Applying Research to Practice**

Orasanu, Judith, NASA Ames Research Center, USA; [1994]; 1p; In English; ICAO Seventh Regional Flight and Human Factors Seminar, 18-21 Oct. 1994, Addis Ababa, Ethiopia; Sponsored by International Civil Aviation Organization, Unknown

Contract(s)/Grant(s): RTOP 199-06-12-04; No Copyright; Avail: Issuing Activity; Abstract Only

The importance of decision-making to safety in complex, dynamic environments like mission control centers, aviation, and offshore installations has been well established. NASA-ARC has a program of research dedicated to fostering safe and effective decision-making in the manned spaceflight environment: Because access to spaceflight is limited, environments with similar characteristics, including aviation and nuclear power plants, serve as analogs from which space-relevant data can be gathered and theories developed. Analyses of aviation accidents cite crew judgement and decision making as causes or contributing factors in over half of all accidents. Yet laboratory research on decision making has not proven especially helpful in improving the quality of decisions in these kinds of environments. One reason is that the traditional, analytic decision models are inappropriate to multi-dimensional, high-risk environments, and do not accurately describe what expert human decision makers do when they make decisions that have consequences. A new model of dynamic, naturalistic decision making is offered that may prove useful for improving decision making in complex, isolated, confined and high-risk environments. Based on analyses of crew performance in full-mission simulators and accident reports, features that define effective decision strategies in abnormal or emergency situations have been identified. These include accurate situation assessment (including time and risk assessment), appreciation of the complexity of the problem, sensitivity to constraints on the decision, timeliness of the response, and use of adequate information. More effective crews also manage their workload to provide themselves with time and resources to make good good decisions are appropriate to the demands of the situation. Effective crew decision making and overall performance are mediated by crew communication. Communication contributes to performance because it assures that all crew members have essential information, but it also regulates and coordinates crew actions and is the medium of collective thinking in response to a problem. This presentation will examine the relations between leadership, communication, decision making and overall crew performance. Implications of these findings for training will be discussed.

Author

*Abnormalities; Aircraft Accidents; Decision Making; Dynamic Control; Environmental Control; Human Performance; Mathematical Models; Safety*

**20010120411** University of Southern Illinois, Carbondale, IL USA

**A Follow-up Survey of 1985-1996 Graduates of the Aviation Management Program Bachelor of Science Degree at Southern Illinois University Carbondale**

Ruiz, Jose R., University of Southern Illinois, USA; Worrells, D. Scott, University of Southern Illinois, USA; Kaps, Robert W., University of Southern Illinois, USA; NewMyer, David A., University of Southern Illinois, USA; Liberto, Joe, University of Southern Illinois, USA; Bowman, Terry S., University of Southern Illinois, USA; Collegiate Aviation Review; October 2000; Volume 18, No. 1, pp. 49-69; In English; See also 20010120406; Copyright; Avail: Issuing Activity

During 1997 and 1998, researchers conducted a follow-up study of graduates earning a Bachelor of Science Degree in Aviation Management (AVM) from the College of Applied Sciences and Arts (ASA) at Southern Illinois University Carbondale (SIUC). The purpose of the study was twofold: (1) to determine a demographic, educational, and occupational profile of the graduates and (2) to obtain an evaluation of the program in terms of the degree to which it helped graduates achieve their occupational and/or life goals. The follow-up study population was composed of students who graduated from the aviation management degree program between 1985 and 1996. A population of 2,663 graduates was identified. A mail-in survey instrument was used to gather data for the follow-up study. Three mailings were conducted, resulting in 806 USAble returns and a 31 % response rate. Key findings of the study were: (1) eighty-six percent indicated that the degree was an asset that assisted them in achieving their occupational and/or life goals, (2) ninety percent indicated that they would recommend the program to others, (3) fifty-nine percent reported that they are employed within the aviation industry, (4) sixty-eight percent reported earning annual salaries in excess of $35,000.00, and (5) sixty-three percent indicated that they were satisfied with their current levels of employment.

Author

*Universities; Illinois; Students; Aircraft Industry; Surveys*

**20010120424** University of Southern Illinois, Carbondale, IL USA

**Risk Analysis, Pilot Motivation, and Decision-Making: Application of the PAVE Personal Minimums Checklist to Pilot Decision-Making in Three General Aviation Accidents**

Ruiz, Lorelei E., University of Southern Illinois, USA; Collegiate Aviation Review; October 2001; Volume 19, No. 1, pp. 121-139; In English; See also 20010120414; Copyright; Avail: Issuing Activity

This paper addresses the relative effects of risk and pilot motivation on decisions made by three general aviation pilots. Using the PAVE (Pilot, Aircraft, environment, External pressures) personal minimums checklist, various risk elements related to the flights and information available to the pilots prior to/during flight are considered. The motivation behind each pilot's decision to go ahead with the flight in spite of adverse conditions is also discussed. Use of the checklist as an in-flight decision-making tool, as well as go/no-go decision-making are considered, and suggestions for further research are offered.

Author

*Aircraft Accidents; Decision Making; General Aviation Aircraft; Risk; Aircraft Pilots*

**20010120835** Carnegie-Mellon Univ., Software Engineering Inst., Pittsburgh, PA USA

**People Capability Maturity Model (P-CMM) Version 2.0**

Curtis, Bill; Hefley, William E.; Miller, Sally A.; Jul. 2001; 730p; In English

Contract(s)/Grant(s): F19628-00-C-0003

Report No.(s): AD-A395316; CMU/SEI-2001-MM-01; No Copyright; Avail: CASI; A99, Hardcopy; A06, Microfiche

This document describes the People CMM, the key practices that constitute each of its maturity levels, and information on how to apply it in guiding organizational improvements. It describes an organization's capability for developing its workforce at each maturity level. It describes how the People CMM can be applied as a standard for assessing workforce practices and as a guide in planning and implementing improvement activities. This document provides guidance on how to interpret its practices. It also presents case studies of organizations that have used the People CMM.

DTIC

*Organizations; Procedures; Personnel Management; Software Development Tools*

**20010121489** NASA Ames Research Center, Moffett Field, CA USA

**Decision Making in Action: Applying Research to Practice**

Orasanu, Judith, NASA Ames Research Center, USA; [1994]; 1p; In English; International Civil Aviation Organization Flight Safety and Human Factors Seminar, 17-19 May 1994, Amsterdam, Netherlands; Sponsored by International Civil Aviation Organization, Unknown

Contract(s)/Grant(s): RTOP 199-06-12-04; No Copyright; Avail: Issuing Activity; Abstract Only

The importance of decision-making to safety in complex, dynamic environments like mission control centers and offshore installations has been well established. NASA-ARC has a program of research dedicated to fostering safe and effective decision-making in the manned spaceflight environment. Because access to spaceflight is limited, environments with similar characteristics, including aviation and nuclear power plants, serve as analogs from which space-relevant data can be gathered and theories developed. Analyses of aviation accidents cite crew judgement and decision making as causes or contributing factors in over half of all accidents. A similar observation has been made in nuclear power plants. Yet laboratory research on decision making has not proven especially helpful in improving the quality of decisions in these kinds of environments. One reason is that the traditional, analytic decision models are inappropriate to multidimensional, high-risk environments, and do not accurately describe what expert human decision makers do when they make decisions that have consequences. A new model of dynamic, naturalistic decision making is offered that may prove useful for improving decision making in complex, isolated, confined and high-risk environments. Based on analyses of crew performance in full-mission simulators and accident reports, features that define effective decision strategies in abnormal or emergency situations have been identified. These include accurate situation assessment (including time and risk assessment), appreciation of the complexity of the problem, sensitivity to constraints on the decision, timeliness of the response, and use of adequate information. More effective crews also manage their workload to provide themselves with time and resources to make good decisions. In brief, good decisions are appropriate to the demands of the situation. Effective crew decision making and overall performance are mediated by crew communication. Communication contributes to performance because it assures that all crew members have essential information, but it also regulates and coordinates crew actions and is the medium of collective thinking in response to a problem. This presentation will examine the relations between leadership, communication, decision making and overall crew performance. Implications of these findings for spaceflight and training for offshore installations will be discussed.

Author

*Decision Making; Safety; Assessments; Space Flight*

**20010121490** NASA Ames Research Center, Moffett Field, CA USA

**Decision Making in Action**

Orasanu, Judith, NASA Ames Research Center, USA; [1994]; 1p; In English; Third Offshore Installation Management Conference, 28-29 Apr. 1994, Aberdeen, UK; Sponsored by Robert Gordon Univ., UK

Contract(s)/Grant(s): RTOP 199-06-12-04; No Copyright; Avail: Issuing Activity; Abstract Only

The importance of decision-making to safety in complex, dynamic environments like mission control centers and offshore installations has been well established. NASA-ARC has a program of research dedicated to fostering safe and effective decision-making in the manned spaceflight environment. Because access to spaceflight is limited, environments with similar characteristics, including aviation and nuclear power plants, serve as analogs from which space-relevant data can be gathered and theories developed. Analyses of aviation accidents cite crew judgement and decision making as causes or contributing factors in over half of all accidents. A similar observation has been made in nuclear power plants. Yet laboratory research on decision making has not proven especially helpful in improving the quality of decisions in these kinds of environments. One reason is that the traditional, analytic decision models are inappropriate to multidimensional, high-risk environments, and do not accurately describe what expert human decision makers do when they make decisions that have consequences. A new model of dynamic, naturalistic decision making is offered that may prove useful for improving decision making in complex, isolated, confined and high-risk environments. Based on analyses of crew performance in full-mission simulators and accident reports, features that define effective decision strategies in abnormal or emergency situations have been identified. These include accurate situation assessment (including time and risk assessment), appreciation of the complexity of the problem, sensitivity to constraints on the decision, timeliness of the response, and use of adequate information. More effective crews also manage their workload to provide themselves with time and resources to make good decisions. In brief, good decisions are appropriate to the demands of the situation. Effective crew decision making and overall performance are mediated by crew communication. Communication contributes to performance because it assures that all crew members have essential information, but it also regulates and coordinates crew actions and is the medium of collective thinking in response to a problem. This presentation will examine the relations between leadership, communication, decision making and overall crew performance. Implications of these findings for spaceflight and training for offshore installations will be discussed.

Author

*Decision Making; Safety; Assessments; Space Flight*

**20010121516** Brookhaven National Lab., Upton, NY USA

**Organizational culture, safety culture, and safety performance at research facilities**

Brown,; Jul. 30, 2000; 6p; In English

Report No.(s): DE2000-755029; BNL-67230; No Copyright; Avail: Department of Energy Information Bridge

Organizational culture surveys of research facilities conducted several years ago and archival occupational injury reports were used to determine whether differences in safety performance are related to general organizational factors or to safety culture as reflected in specific safety-related dimensions. From among the organizations surveyed, a pair of facilities was chosen that were similar in size and scientific mission while differing on indices of work-related injuries. There were reliable differences in organizational style between the facilities, especially among workers in environment, safety, and health functions; differences between the facilities (and among job categories) on the safety scale were more modest and less regular.

NTIS

*Research Facilities; Organizations; Safety; Human Performance*

**20010122668** Los Alamos National Lab., NM USA

**Is There Room for Durable Analog Information Storage in a Digital World**

Stutz, R. A.; Hereth, L. G.; Jan. 01, 2000; 19p; In English

Report No.(s): DE2000-763339; LA-UR-00-750; No Copyright; Avail: Department of Energy Information Bridge, Microfiche

Information technology has completely changed our concept of record keeping - the advent of digital records was a momentous discovery, as significant as the invention of the printing press. Digital records allowed huge amounts of information to be stored in a very small space and to be examined quickly. However, digital documents are much more vulnerable to the passage of time than printed documents, because the media on which they are stored are easily affected by physical phenomena, such as magnetic fields, oxidation, material decay, and by various environmental factors that may erase the information. Even more important, digital information becomes obsolete, because even if future generations maybe able to read it, they may not necessarily be able to interpret it. Over the centuries analog documents have been written on solid materials such as stone, clay, and metal plates using tools to inscribe the characters. These archival methods have preserved records for centuries, and even millennia, but suffer from low information density. Modern methods facilitate writing pages on smooth material surfaces at high information

densities. This writing can generate from about 25 to 100,000 times the area information density of microfilm and work with either analog or digital storage methods. Information of all types is becoming more dependent on digital records. These records are often created and stored on computer systems by scanning in documents or creating them directly on the system. Often analog information (human viewable information) is forced into binary form (ones and zeros). The necessity for the accurate and accessible storage of these documents is increasing for a number of reasons, including legal and environment issues. This paper will discuss information storage life, methods of information storage, media life considerations, and life cycle costs associated with several methods of storage.
NTIS
*Analog Data; Data Storage; Digital Data; Information Systems; Physical Factors; Storage Stability*

**20010123226** Los Alamos National Lab., NM USA
**Virtual Environments as Constraints on Decision Making in Agent Models of Human Organizations**
Joslyn, C.; Feb. 01, 2000; 9p; In English
Report No.(s): DE2000-763357; LA-UR-00-811; No Copyright; Avail: Department of Energy Information Bridge
We consider agent-based modeling from a semiotics perspective, with application to the simulation of Socio-Technical Organizations. After outlining our semiotic approach, we consider the role of constraints present in the virtual environment, including the virtual physics, common communication structures, and shared knowledge, for constraining the decision-making capabilities of the constituent agents.
NTIS
*Decision Making; Models*

**20010123924** Oak Ridge National Lab., TN USA
**U.S. Atomic Energy Commission's Environmental Research Programs Established in the 1950s**
Reichle, D. E.; Sep. 22, 1999; 18p; In English
Report No.(s): DE2001-11007; ORNL/CP-104816; No Copyright; Avail: Department of Energy Information Bridge, Microfiche
In 1946 the USA (U.S.) Congress passed the Atomic Energy Act and with it created the Atomic Energy Commission. For the ensuing half-century the AEC and its successors have pursued biological and environmental research with an unwavering mandate to exploit the use of fissionable and radioactive material for medical purposes and, at the same time, to ensure the health of its workers, the public, and the environment during energy technology development and use. The following pages are testimony to the success of this undeviating vision. From the early days of the AEC, cooperation has also linked researchers from the national laboratories, the academic community, and the private sector. The AEC-sponsored research both at national laboratories and universities, and also supported graduate students to develop a cadre of health physicists, radiation biologists, and nuclear engineers. Coordinating these diverse performers has been crucial to the unique teaming that has made many of the successes possible. The success of the biological and environmental research program has often been shared with other federal agencies. The future will demand even stronger and more substantive intraagency, interagency, and international collaborations.
NTIS
*Medical Science; Technology Utilization; Nuclear Electric Power Generation*

## 82
## DOCUMENTATION AND INFORMATION SCIENCE

*Includes information management; information storage and retrieval technology; technical writing; graphic arts; and micrography. For computer documentation see 61 Computer Programming and Software.*

**20010118272** California Univ., Lawrence Berkeley Lab., Berkeley, CA USA
**Building life-cycle information system for tracking building performance metrics**
Hitchcock, R. J.; Piette, M. A.; Selkowitz, S. E.; Apr. 01, 1999; 10p; In English
Report No.(s): DE2000-760308; LBNL-43136; No Copyright; Avail: Department of Energy Information Bridge, Microfiche
Buildings often do not perform as well in practice as expected during pre-design planning, nor as intended at the design stage. While this statement is generally considered to be true, it is difficult to quantify the impacts and long-term economic implications of a building in which performance does not meet expectations. This leads to a building process that is devoid of quantitative feedback that could be used to detect and correct problems both in an individual building and in the building process itself. One key element in this situation is the lack of a standardized method for documenting and communicating information about the intended performance of a building. This paper describes the Building Life-cycle Information System (BLISS); designed to

manage a wide range of building related information across the life cycle of a building project. BLISS is based on the Industry Foundation Classes (IFC) developed by the International Alliance for Interoperability. A BLISS extension to th e IFC that adds classes for building performance metrics is described. Metracker, a prototype tool for tracking performance metrics across the building life cycle, is presented.
NTIS
*Buildings; Structural Design; Architecture; Economics; Feedback*

**20010118276** Oak Ridge National Lab., TN USA
**Database Development of Land Use Characteristics Along Major U.S. Highways**
Xiong, D.; Jun. 01, 2000; 53p; In English
Report No.(s): DE2000-760255; ORNL/TM-2000/160; No Copyright; Avail: Department of Energy Information Bridge, Microfiche

Information about land use by and adjacent to transportation systems is essential to understanding the environmental impacts of transportation systems. Nevertheless, such data are presently sparse and incomplete, especially at the national scale. to address the need for land use data, the Bureau of Transportation Statistics (BTS) and Oak Ridge National Laboratory (ORNL) undertook the development of land use data for major U.S. highways. This report describes data sources, methodology and preliminary results of this research.
NTIS
*Transportation Networks; Land Use; Information Systems*

**20010118929** Sandia National Labs., Albuquerque, NM USA
**Reducing Information Overload in Large Seismic Data Sets**
Hampton, J. W.; Young, C. J.; Merchant, J.; Carr, D. B.; Aguilar-Chang, J.; Aug. 02, 2000; 12p; In English
Report No.(s): DE2000-761844; SAND2000-1952C; No Copyright; Avail: Department of Energy Information Bridge

Event catalogs for seismic data can become very large. Furthermore, as researchers collect multiple catalogs and reconcile them into a single catalog that is stored in a relational database, the reconciled set becomes even larger. The sheer number of these events makes searching for relevant events to compare with events of interest problematic. Information overload in this form can lead to the data sets being under-utilized and/or used incorrectly or inconsistently. Thus, efforts have been initiated to research techniques and strategies for helping researchers to make better use of large data sets. In this paper, the authors present their efforts to do so in two ways: (1) the Event Search Engine, which is a waveform correlation tool and (2) some content analysis tools, which area combination of custom-built and commercial off-the-shelf tools for accessing, managing, and querying seismic data stored in a relational database.
NTIS
*Seismology; Algorithms; Relational Data Bases; Information Retrieval*

**20010119559** Atomic Energy Commission, Idaho Operations Office, Idaho Falls, ID USA
**Database for Reviewing and Selecting Radioactive Waste Treatment Technologies and Vendors**
Marushia, P. C.; Schwinkendorf, W. E.; Jul. 01, 1999; 12p; In English
Report No.(s): DE2001-10484; INEEL/CON-99-00450; No Copyright; Avail: Department of Energy Information Bridge, Microfiche

Several attempts have been made in past years to collate and present waste management technologies and solutions to waste generators. These efforts have been manifested as reports, buyers' guides, and databases. While this information is helpful at the time it is assembled, the principal weakness is maintaining the timeliness and accuracy of the information over time. In many cases, updates have to be published or developed as soon as the product is disseminated. The recently developed National Low-Level Waste Management Program's Technologies Database is a vendor-updated Internet based database designed to overcome this problem. The National Low-Level Waste Management Program's Technologies Database contains information about waste types, treatment technologies, and vendor information. Information is presented about waste types, typical treatments, and the vendors who provide those treatment methods. The vendors who provide services update their own contact information, their treatment processes, and the types of wastes for which their treatment process is applicable. This information is queriable by a generator of low-level or mixed low-level radioactive waste who is seeking information on waste treatment methods and the vendors who provide them. Timeliness of the information in the database is assured using time clocks and automated messaging to remind featured vendors to keep their information current. Failure to keep the entries current results in a vendor being warned and then

ultimately dropped from the database. This assures that the user is dealing with the most current information available and the vendors who are active in reaching and serving their market.
NTIS
*Information Systems; Radioactive Wastes; Waste Management; Waste Treatment*

**20010119564** Pacific Northwest National Lab., Richland, WA USA
**PNNL information technology benchmarking**
Hostetler, D. D.; Sep. 08, 1999; 11p; In English
Report No.(s): DE2001-10498; PNNL-13008; No Copyright; Avail: Department of Energy Information Bridge, Microfiche

Benchmarking is a methodology for searching out industry best practices that lead to superior performance. It is exchanging information, not just with any organization, but with organizations known to be the best within PNNL, in industry, or in dissimilar industries with equivalent functions. It is used as a continuous improvement tool for business and technical processes, products, and services. Information technology--comprising all computer and electronic communication products and services--underpins the development and/or delivery of many PNNL products and services. This document describes the Pacific Northwest National Laboratory's (PNNL's) approach to information technology (IT) benchmarking. The purpose is to engage other organizations in the collaborative process of benchmarking in order to improve the value of IT services provided to customers. TM document's intended audience consists of other US Department of Energy (DOE) national laboratories and their IT staff. Although the individual participants must define the scope of collaborative benchmarking, an outline of IT service areas for possible benchmarking is described.
NTIS
*Information Dissemination; Information Systems; Procedures*

**20010119578** Defense Technical Information Center, Fort Belvoir, VA USA
**The DTIC Review. Volume 5, Number 4. Homeland Defense** ***Final Report***
Jul. 2001; 279p; In English
Report No.(s): AD-A389848; DTIC-BR-TR--2001/03; No Copyright; Avail: CASI; A13, Hardcopy; A03, Microfiche

Homeland defense is a vital aspect of our national security strategy. In recent years, threats against the homeland have become the greatest danger to national security. The documents included within this edition of The DTIC Review seek to provide some clarity regarding current homeland security policies, doctrine for carrying these policies out, and potential improvements to the current homeland defense strategy.
DTIC
*Civil Defense; Bibliographies; Hazards*

**20010119587** Analytic Sciences Corp., Fairborn, OH USA
**Feasibility of Direct Conversion of Page-Based Information** ***Final Report, Jul. 1997-Mar. 1998***
McClellan, Sherrise L.; Stute, Nicholas J.; Woolley, Colleen; Azar, Maurice C.; Mar. 1998; 86p; In English; Prepared in cooperation with TAMSCO, Fairborn, OH
Contract(s)/Grant(s): F41624-97-D-5002; Proj-2950
Report No.(s): AD-A394890; AFRL-HE-WP-TR-2001-0064; No Copyright; Avail: CASI; A05, Hardcopy; A01, Microfiche

Feasibility of Direct Conversion of Page-Based Information is a study to determine the feasibility of using low cost Commercial Off-the-Shelf (COTS) software packages to convert paper based technical information to HyperText Markup Language (HTML) and viewed via low cost web browsers. As well as determining feasibility, the project evaluated multiple methods of conversion with alternate electronic file formats (i.e., Standard Generalized Markup Language (SGML) and Portable Document Format (PDF). Each method was investigated and a recommended process to convert paper technical manuals to HTML using specific COTS software packages is presented. Costs to convert the paper to HTML using this process were quantified and compared to costs for electronic formats (Interactive Electronic Technical Manuals (IETMs)). A demonstration of the resulting HTML files was conducted and is described in this final report.
DTIC
*Information Management; Applications Programs (Computers); Commercial Off-The-Shelf Products*

**20010119588** Army Research Lab., Human Research and Engineering Directorate, Aberdeen Proving Ground, MD USA
**Human Factors Military Lexicon: Auditory Displays** ***Final Report***
Letowski, Tomasz; Karsh, Robert; Vause, Nancy; Shilling, Russell D.; Ballas, James; Sep. 2001; 49p; In English
Report No.(s): AD-A394902; ARL-TR-2526; No Copyright; Avail: CASI; A03, Hardcopy; A01, Microfiche

This report is a lexicon of terms developed by the Department of Defense Spatial Audio Display Working Group in an attempt to standardize terminology used by human factors researchers working in the area of auditory displays and human-machine communication. The lexicon has been primarily developed for the U. S. armed forces research groups, but it is hoped that it will be also useful for other Government, academic, and industrial organizations. In addition to definitions specific to auditory displays, speech communication, and audio technology, the lexicon includes several terms unique to military operational environments and human factors engineering applications. Furthermore, human factors researchers appear to be increasingly interested in conducting integrated studies of auditory and visual perception in order to answer broad questions related to human situational awareness and performance. Therefore, the lexicon also includes some definitions related to visual perception, particularly in the areas of visual displays, virtual reality, and communication symbology.
DTIC
*Display Devices; Human Factors Engineering; Terminology*

**20010119601** Syracuse Univ., NY USA
**Twin Evils: Government Copyright and Copyright-like Controls Over Government Information**
Gellman, Robert M.; Jan. 1995; 66p; In English
Report No.(s): AD-A394923; No Copyright; Avail: CASI; A04, Hardcopy; A01, Microfiche

The policy of the USA against government copyright is clearly stated in the Copyright Act of 1976. Other statutes, most notably the Freedom of Information Act, support public access to government information and should limit the ability of federal agencies to restrict or regulate public use of agency data. Regulatory policies, such as OMB Circular A-130, also direct agencies to share information resources with the public. Nevertheless, several factors work together to allow agencies to deny public access to or effective use of uncopyrighted government information, restrict use of that information, or charge royalties. The result can be the effective imposition of copyright-like controls that restrict government information despite the Copyright Act's prohibition against government copyright and the FOIA's support for public availability of government information. This article has attempted to show that the exercise of control by government over public information generated or compiled by government can have political, economic, and bureaucratic effects that are inconsistent with existing statutory policies supporting openness in government.
DTIC
*Law (Jurisprudence); Copyrights*

**20010119615** National Inst. of Standards and Technology, Gaithersburg, MD USA
**US Government Traffic-Filter Firewall Protection Profile for Low-Risk Environments *Final Report***
Jansen, Wayne; Walsh, Jack; Dolan, Kathy V.; Wright, Patricia A.; Apr. 1999; 61p; In English
Report No.(s): AD-A395023; No Copyright; Avail: CASI; A04, Hardcopy; A01, Microfiche

This traffic-filter firewall Protection Profile defines the minimum security requirements for firewalls used by U.S Government organizations handling unclassified information in a low-risk environment. Firewalls may consist of one or more devices that act as part of an organization s overall security defense by isolating an organization s internal network from the Internet or other external networks. Firewalls pass and block information flows based on a set of screening rules defined by an authorized administrator. This Protection Profile applies to firewalls that are capable of screening network traffic at the network and transport protocol levels, authenticating the authorized administrator for actions at the firewall, and auditing security-relevant events that occur. For clarification of terms, see terminology section.
DTIC
*Governments; Traffic; Computer Networks; Computer Information Security*

**20010119621** Booz-Allen and Hamilton, Inc., McLean, VA USA
**U.S. Department of Defense Application-Level Firewall Protection Profile for Medium Robustness Environments *Final Report***
Dolan, Kathy V.; Wright, Patricia A.; Montequin, Rita R.; Jun. 28, 2000; 65p; In English
Report No.(s): AD-A395046; No Copyright; Avail: CASI; A04, Hardcopy; A01, Microfiche

This Application Level Firewall Protection Profile defines the minimum security requirements for firewalls used by U. S. Government organizations, specifically the Department of Defense, handling unclassified or sensitive but unclassified information for Mission-Critical Categories in a moderate-risk environment. Firewalls may consist of one or more devices that act as part of an organization s overall security defense by isolating an organization s internal network from the Internet or other external networks. The Protection Profile defines the assumptions about the security aspects of the environment in which the firewall will be used, defines the threats that are to be addressed by the firewall, defines implementation-independent security

objectives of the firewall and its environment, defines the functional and assurance requirements to meet those objectives, and provides a rationale demonstrating how the requirements meet the security objectives.
DTIC
*Defense Program; Robustness (Mathematics); Applications Programs (Computers); Computer Program Integrity*

**20010120106** Booz-Allen and Hamilton, Inc., McLean, VA USA
**U.S. Department of Defense Application-Level Firewall Protection Profile for Basic Robustness Environments** ***Final Report***
Jansen, Wayne; Walsh, Jack; Dolan, Kathy V.; Wright, Patricia A.; Montequin, Rita R.; Jun. 22, 2000; 54p; In English
Report No.(s): AD-A395104; No Copyright; Avail: CASI; A04, Hardcopy; A01, Microfiche

This Application Level Firewall Protection Profile defines the minimum security requirements for firewalls used by U. S. Government organizations handling unclassified information in a low-risk environment. Firewalls may consist of one or more devices that act as part of an organization s overall security defense by isolating an organization's internal network from the Internet or other external networks. The Protection Profile defines the assumptions about the security aspects of the environment in which the firewall will be used, defines the threats security objectives of the firewall and its environment, defines the functional and assurance requirements to meet those objectives, and provides a rationale demonstrating how the requirements meet the security objectives.
DTIC
*Defense Program; Computer Information Security; Computer Networks; Internets*

**20010120110** General Accounting Office, Washington, DC USA
**USER FEES: DOD Fees for Providing Information Not Current and Consistent**
Oct. 2001; 20p; In English
Report No.(s): AD-A395071; GAO-02-34; No Copyright; Avail: CASI; A03, Hardcopy; A01, Microfiche

Section 1085 of the National Defense Authorization Act for Fiscal Year 2001 authorized the military department secretaries to (1) charge fees to persons requesting information from the primary military archives and (2) retain collected fees to help defray costs associated with providing the information. The military archives also have authority under the User Charge Statute (31 U.S. C. 9701) and the Freedom of Information Act(FOIA) (5 U.S.C. 552) to charge for general information provided to the public. A major distinction, however, is that the fees collected under these two provisions are to be deposited with the Department of the Treasury.
DTIC
*Defense Program; Congressional Reports; Financial Management*

**20010121540** RECOM Technologies, Inc., Moffett Field, CA USA
**A Semantic Theory of Abstractions: A Preliminary Report**
Nayak, P. Pandurang, RECOM Technologies, Inc., USA; Levy, Alon Y., Bell Telephone Labs., Inc., USA; [1994]; 1p; In English; Workshop on Theory Reformulation and Abstraction, 22-24 May 1994, Jackson Hole, WY, USA
Contract(s)/Grant(s): RTOP 232-01-03; No Copyright; Avail: Issuing Activity; Abstract Only

In this paper we present a semantic theory of abstractions based on viewing abstractions as interpretations between theories. This theory captures important aspects of abstractions not captured in the theory of abstractions presented by Giunchiglia and Walsh. Instead of viewing abstractions as syntactic mappings, we view abstractions as a two step process: the intended domain model is first abstracted and then a set of (abstract) formulas is constructed to capture the abstracted domain model. Viewing and justifying abstractions as model level transformations is both natural and insightful. We provide a precise characterization of the abstract theory that exactly implements the intended abstraction, and show that this theory, while being axiomatizable, is not always finitely axiomatizable. A simple corollary of the latter result disproves a conjecture made by Tenenberg that if a theory is finitely axiomatizable, then predicate abstraction of that theory leads to a finitely axiomatizable theory.
Author
*Abstracts; Theories*

**20010121573** Brookhaven National Lab., Upton, NY USA
**Quality Control and Checking of Electronically Submitted Papers to Accelerator Conferences**
MacKay, W. W.; Jan. 13, 2000; 4p; In English; Workshop on Electronic Publication of Proceedings of Particle Accelerator Conferences, 1-4 Dec. 1999, Upton, NY, USA
Report No.(s): DE2000-752153; BNL-67130; No Copyright; Avail: Department of Energy Information Bridge

Recent conferences and workshops have been producing proceedings in paper and electronic forms in both CD-ROM and Web formats. In order to have a readable paper with some uniformity in a given publication, certain rules must be followed by authors to ensure a USAble final product. This paper discusses the quality control process.
NTIS
*Accelerators; Quality Control; Documents*

**20010121976** Sandia National Labs., Albuquerque, NM USA
**Survivability via Control Objectives**
Campbell, P. L.; Aug. 11, 2000; 6p; In English
Report No.(s): DE2000-761868; SAND2000-2047C; No Copyright; Avail: Department of Energy Information Bridge, Microfiche

Control objectives open an additional front in the survivability battle. A given set of control objectives is valuable if it represents good practices, it is complete (it covers all the necessary areas), and it is auditable. CobiT and BS 7799 are two examples of control objective sets.
NTIS
*Information Systems; Control Theory; Survival*

**20010122274** Army Research Inst. Field Unit, Fort Hood, TX USA
**ARI Working Papers. Fort Hood Field Unit 1987-1990**
Jul. 2001; 4p; In English
Report No.(s): AD-A395258; No Copyright; Avail: CASI; A01, Hardcopy; A01, Microfiche

ARI working papers were originally unofficial documents intended for limited distribution to obtain comments. These working papers are being archived in order to preserve material that was not included in other ARI publications. The material contained herein may not meet ARI's usual scientific or professional standards for publication. Twenty-two working papers dealing with air defense, MANPRINT, SINCGARS, mobile subscriber equipment, HMMWV-HV, and remotely piloted vehicles.
DTIC
*Bibliographies; Air Defense*

**20010122294** Defence Science and Technology Organisation, Information Technology Div., Salisbury, Australia
**Information Visualisation Using Composable Layouts and Visual Sets**
Pattison, Tim, Defence Science and Technology Organisation, Australia; Vernik, Rudi, Defence Science and Technology Organisation, Australia; Phillips, Matthew, Defence Science and Technology Organisation, Australia; August 2001; 40p; In English; Original contains color illustrations
Report No.(s): DSTO-RR-0216; DODA-AR-011-960; Copyright; Avail: Issuing Activity

A modern military enterprise is characterized not only by its people, physical infrastructure and geography, but also by its business processes, knowledge management practices and fluid organizational structures. Management, coordination, planning and development of the enterprise all require awareness of its current state. to aid these functions, the DSTO task JNT 00/130 entitled "Assembly and Deployment of Defence Visualisation Solutions" (ADDVIS) proposes the use of information visualisation techniques to produce integrated enterprise situation awareness pictures tailored to meet the requirements of ADF functions such as capability development, system management and self-synchronisation. To this end, Information Technology Division (ITD) is performing research and development (R&D) into the next generation of information visualisation systems which will enable the rapid assembly and deployment of Defence visualisation solutions. InVision is a component-based software architecture for the rapid prototyping of information visualisation solutions. Its evolutionary implementation has given rise to an experimental component infrastructure with the aid of which the assumptions and goals of the ADDVIS task are being tested. This report describes the CLOVIS class of views, along with the associated supporting InVision infrastructure. The versatility and generality of the CLOVIS class of views described in this report makes it ideal for rapid prototyping of information visualizations. Its subsumption of a number of existing information layouts constitutes significant progress towards one of the key goals of InVision: the integration of various visual representations, with each chosen on the basis of its particular suitability to the task at hand.
Author
*Information Systems; Visual Control; Management Planning; Management Methods*

**20010122713** Alaska Univ., Office of Arctic Programs, Fairbanks, AK USA
**Planning for Alaska DEPSCoR** ***Final Report, 10 May 2000 - 9 Aug. 2001***
Happ, George; Jan. 2000; 15p; In English
Contract(s)/Grant(s): DAAD19-00-1-0354
Report No.(s): AD-A395282; ARO-41422.1-RT-DP; No Copyright; Avail: CASI; A03, Hardcopy; A01, Microfiche

In its planning phase, Alaska EPSCoR aims to develop a statewide, integrated EPSCoR program to build research in science and technology for Alaska and to serve national needs in scientific research, education, and technology transfer. Our process includes careful consideration of the research strengths on the university campuses, the growth potential of various sectors of the state's economy, the needs of the people of Alaska for more education in science and engineering, and the integration of university research priorities. The specific aims of the DEPSCoR planning effort are: I. to hold workshops on DEPSCoR opportunities for Alaskan scientists and engineers. 2. to fund travel for Alaska scientists and engineers to visit DOD program officers. 3. to fund travel for Alaska scientists and engineers to develop collaborations in DOD priority areas for research. In the project period, Alaska EPSCoR has accomplished the following: 1. Provided administrative planning and leadership to support faculty, in the development and submission of DOD research proposals. 2. Provided coordination and logistical support for three workshops related to EPSCoR Research Focus Areas and DOD funding priorities. 3. Provided travel support to seven scientists to attend workshops, develop collaborative proposals, or meet with program officers. 4. Supported faculty in the submission of four FY 2001 DEPSCoR proposals, three of which were funded in February 2001. 5. Provided DEPSCoR website publicity for FY 2001 and FY 2002 solicitations, including guidance on proposal development and submission.

DTIC
*Research and Development; Project Management; Engineers; Coordination; Education*

**20010122798** California Univ., Lawrence Berkeley Lab., Berkeley, CA USA
**Use of the singular value decomposition for text retrieval**
Husbands, P.; Simon, H. D.; Ding, C.; Dec. 04, 2000; 12p; In English
Report No.(s): DE2001-775166; LBNL-47170; No Copyright; Avail: Department of Energy Information Bridge

The use of the Singular Value Decomposition (SVD) has been proposed for text retrieval in several recent works. This technique uses the SVD to project very high dimensional document and query vectors into a low dimensional space. In this new space it is hoped that the underlying structure of the collection is revealed thus enhancing retrieval performance. Theoretical results have provided some evidence for this claim and to some extent experiments have confirmed this. However, these studies have mostly used small test collections and simplified document models. In this work we investigate the use of the SVD on large document collections. We show that, if interpreted as a mechanism for representing the terms of the collection, this technique alone is insufficient for dealing with the variability in term occurrence. Section 2 introduces the text retrieval concepts necessary for our work. A short description of our experimental architecture is presented in Section 3. Section 4 describes how term occurrence variability affects the SVD and then shows how the decomposition influences retrieval performance. A possible way of improving SVD-based techniques is presented in Section 5 and concluded in Section 6.

NTIS
*Information Retrieval; Architecture (Computers); Applications Programs (Computers)*

**20010123051** Brookhaven National Lab., Upton, NY USA
**EXFOR Systems Manual Nuclear Reaction Data Exchange Format**
McLane, V.; May 19, 2000; 122p; In English
Report No.(s): DE2000-767144; BNL-NCS-63330-00/04-REV; KB0401040; No Copyright; Avail: Department of Energy Information Bridge

EXFOR is an exchange format designed to allow transmission of nuclear reaction data between the members of the Nuclear Data Centers Network. This document has been written for use by the members of the Network and includes matters of procedure and protocol, as well as detailed rules for the compilation of data. Users may prefer to consult EXFOR Basics for a brief description of the format.

NTIS
*Information Systems; Protocol (Computers); Computer Programs; Data Flow Analysis*

**20010123059** Environmental Protection Agency, Washington, DC USA

**Uniform Federal Policy for Implementing Environmental Quality Systems. Evaluating, Assessing, and Documenting Environmental Data Collection/Use and Technology Programs** ***Final Report***

November 2000; 110p; In English; Original contains color images

Report No.(s): AD-A395303; No Copyright; Avail: CASI; A06, Hardcopy; A02, Microfiche

The Uniform Federal Policy for Implementing Environmental Quality Systems (UFP) outlines essential elements of a Quality System for management of environmental data collection and use and environmental technology programs. The UFP will serve as a high-level policy for documenting and implementing acceptable Quality Systems for Federal agencies. The UFP provided a framework to ensure that essential elements are addressed. The UFP must be used to develop a new Quality System or to evaluate the adequacy of an existing Quality System. The results of that evaluation must then be used to develop plans for correcting identified deficiencies.

DTIC

*Data Acquisition; Environmental Quality*

**20010123137** Brookhaven National Lab., Upton, NY USA

**EXFOR Systems Manual Nuclear Reaction Data Exchange Format**

McLane, V.; May 19, 2000; 122p; In English

Report No.(s): DE2000-767087; BNL-NCS-63330-00/04-REV; KB0401040; No Copyright; Avail: Department of Energy Information Bridge

EXFOR (exchange format) is an exchange format designed to allow transmission of nuclear reaction data between the members of the Nuclear Data Centers Network. This document has been written for use by the members of the Network and includes matters of procedure and protocol, as well as detailed rules for the compilation of data. Users may prefer to consult EXFOR Basics for a brief description of the format.

NTIS

*Nuclear Reactions; Data Transmission; Format; Nuclear Research*

**20010123418** Ames Lab., IA USA

**Generalized Portable SHMEM Library for High Performance Computing**

Parzyszek, K.; Nieplocha, J.; Kendall, R. A.; Sep. 15, 2000; 12p; In English

Report No.(s): DE2001-764612; IS-M 893; No Copyright; Avail: Department of Energy Information Bridge

This paper describes a portable one-sided communication library GPSHMEM that follows the interfaces of the successful SHMEM library introduced by Cray Research Inc. for their distributed memory systems: the Cray T3D and T3E. The portability is achieved by relying on ARMCI, a low-level communication library developed to support one-sided communication in distributed array libraries and compiler run-time systems, and the MPI message passing interface. The paper discusses implementation, requirements, and initial experience with GPSHMEM.

NTIS

*Distributed Memory; Libraries*

**20010125011** Sandia National Labs., Albuquerque, NM USA

**Knowledge Base Interface for Parametric Grid Information**

Hipp, J. R.; Simons, R. W.; Young, C. J.; Aug. 03, 1999; 11p; In English

Report No.(s): DE2001-9689; SAND99-2008C; No Copyright; Avail: Department of Energy Information Bridge, Microfiche

The parametric grid capability of the Knowledge Base (KBase) provides an efficient robust way to store and access interpolatable information that is needed to monitor the Comprehensive Nuclear Test Ban Treaty. to meet both the accuracy and performance requirements of operational monitoring systems, we use an approach which combines the error estimation of kriging with the speed and robustness of Natural Neighbor Interpolation. The method involves three basic steps: data preparation, data storage, and data access. In past presentations we have discussed in detail the first step. In this paper we focus on the latter two, describing in detail the type of information which must be stored and the interface used to retrieve parametric grid data from the Knowledge Base. Once data have been properly prepared, the information (tessellation and associated value surfaces) needed to support the interface functionality, can be entered into the KBase. The primary types of parametric grid data that must be stored include (1) generic header information; (2) base model, station, and phase names and associated ID's used to construct surface identifiers; (3) surface accounting information; (4) tessellation accounting information; (5) mesh data for each tessellation; (6) correction data defined for each surface at each node of the surfaces owning tessellation (7) mesh refinement calculation set-up and flag information; and (8) kriging calculation set-up and flag information. The eight data components not only represent the

results of the data preparation process but also include all required input information for several population tools that would enable the complete regeneration of the data results if that should be necessary.
NTIS
*Grid Generation (Mathematics); Robustness (Mathematics); Parameterization; Information Retrieval*

**20010125518** Scientific Digital Visions, Inc., San Jose, CA USA
**Final Report: Advanced Methods for Accessing and Disseminating Nuclear Data, August 13, 1996-March 15, 1999**
Stone, C. A.; Mar. 15, 1999; 30p; In English
Report No.(s): DE2001-765179; No Copyright; Avail: Department of Energy Information Bridge

Scientific Digital Visions, Inc. developed methods of accessing and dissemination nuclear data contained within the databases of the National Data Center (NNDC) at the Brookhaven National Laboratory supporting a long standing and important DOE Program to provide scientists access to NNDC Databases. The NNDC participated as a partner in this effort.
NTIS
*Data Bases; Information Dissemination; Nuclear Research*

## 83
## ECONOMICS AND COST ANALYSIS

*Includes cost effectiveness studies.*

**20010120410** Saint Louis Univ., Parks Coll. of Engineering and Aviation, Cahokia, IL USA
**Memory Strategies for the Pilot**
Northam, Gary J., Saint Louis Univ., USA; Collegiate Aviation Review; October 2000; Volume 18, No. 1, pp. 41-48; In English; See also 20010120406; Copyright; Avail: Issuing Activity

Theorists have studied the problem of forgetting for a number of years; however, very little application has been made to the general aviation pilot. This paper considers some concepts for understanding the processes involved when important tasks are forgotten and/or certain ”actionsnot-as-planned” are executed. While there are numerous ways suggested by memory specialists, a few may be particularly applicable to flight. Forgetting can be explained as an activation issue as defined in the concepts of action theory. A structural model of three stages is used to explain some psychological processes of the memory system. Finally, some suggestions for the practical enhancements of memory are offered along with recommendations for further memory research.
Author
*Aircraft Pilots; General Aviation Aircraft; Retention (Psychology); Memory*

## 84
## LAW, POLITICAL SCIENCE AND SPACE POLICY

*Includes: aviation law; space law and policy; international law; international cooperation; and patent policy*

**20010117641** Brookhaven National Lab., Upton, NY USA
**US DOE Laboratory Views on U.S.-Russian Partnership for Nuclear Security**
Kempf,; Jul. 26, 1998; 10p; In English
Report No.(s): DE2000-758974; BNL-65764-98/10-REV; No Copyright; Avail: Department of Energy Information Bridge, Microfiche

This paper summarizes an analysis of the US-Russian Nuclear Material Protection, Control and Accounting (MPC and A) Program, developed on the basis of extensive discussions with US laboratory participants as well as personal experience. Results of the discussions have been organized into three main areas: (1) Technical/MPC and A Progress; (2) Programmatic and Administrative Issues; and (3) Professional Aspects, Implications for MPC and A effectiveness, for MPC and A sustainability, and for future relations and collaboration are derived. Suggested next steps are given.
NTIS
*Protection; Security; International Cooperation; Nuclear Devices; Management Systems*

**20010118520** Brookhaven National Lab., Upton, NY USA

**Recruitment of US Citizens for Vacancies in IAEA Safeguards**

Pepper,; DeCaro,; Williams,; Carelli,; Assur,; Jul. 25, 1999; 6p; In English

Report No.(s): DE2000-759024; BNL-66944; No Copyright; Avail: Department of Energy Information Bridge

The International Atomic Energy Agency (IAEA) relies on its member states to assist with recruiting qualified individuals for positions within the IAEA's secretariat. It is important that persons within and outside the US nuclear and safeguards industries become aware of career opportunities available at the IAEA, and informed about important vacancies. The IAEA has established an impressive web page to advertise opportunities for employment. However, additional effort is necessary to ensure that there is sufficient awareness in the US of these opportunities, and assistance for persons interested in taking positions at the IAEA. In 1998, the Subgroup on Safeguards Technical Support (SSTS) approved a special task under the US Support Program to IAEA Safeguards (USSP) for improving US efforts to identify qualified candidates for vacancies in IAEA's Department of Safeguards. The International Safeguards Project Office (ISPO) developed a plan that includes increased advertising, development of a web page to support US recruitment efforts, feedback from the US Mission in Vienna, and interaction with other recruitment services provided by US professional organizations. The main purpose of this effort is to educate US citizens about opportunities at the IAEA so that qualified candidates can be identified for the IAEA's consideration.

NTIS

*Occupation; Personnel; Nuclear Electric Power Generation; Industries; Marketing*

**20010119930** Army Command and General Staff Coll., Fort Leavenworth, KS USA

**By Deploying Weapons in Space, Is the USA Opening a Theater of Engagement That Could Disadvantage the USA in the Long Term?**

Baldauff, Regis J.; Jun. 2001; 114p; In English

Report No.(s): AD-A395205; No Copyright; Avail: CASI; A06, Hardcopy; A02, Microfiche

Since man's initial contact with space in 1957, the U.S. and Russia have flirted with putting weapons in space. Today, two camps exist in the space weapons debate: sanctuary and weaponization. The sanctuary camp argues that space should remain free of weapons because it is in the best interest of the USA. The weaponization camp feels the U.S. dependence on space is too great to leave assets there unprotected. Weaponization is especially important because of the large dependence of the U.S. military on space for force enhancement purposes. This thesis examines some of the major arguments by evaluating them against the U.S. instruments of national power: diplomatic, information, military, and economic. According to this thesis' research, deploying weapons in space would disadvantage the USA in the long term. The evaluation of the options presented in chapter 3 led to the choice of continuing research and development with a limiting treaty (Option 3A) as the highest scoring option.

DTIC

*International Relations; Space Weapons*

**20010120153** Army Command and General Staff Coll., School of Advanced Military Studies, Fort Leavenworth, KS USA

**Arming the Skies: The Right Time Has Not Arrived**

Taylor, Kirk D.; Dec. 15, 2000; 51p; In English

Report No.(s): AD-A395132; No Copyright; Avail: CASI; A04, Hardcopy; A01, Microfiche

The crux of the debate as to whether the USA (US) should immediately field space weapons is not whether another nation will eventually field like weapons of its own. Rather, the primary issue is whether an immediate space weaponization program best serves national security interests. The economic significance of the civilian space sector further complicates the issue. In the year 2000, economic activity in space is anticipated to exceed $150 billion. The majority of the profits that will accrue from space activities will benefit the US. Additionally, the implications of weaponizing space far exceed immediate space control issues. The United Nations and both the Russian and Chinese governments have tried to link existing space law to proposed space weapon capabilities not inclusive in any treaty to which the US is a signatory. The anti-satellite weapons inherent in the proposed Nation Missile Defense program pose a threat to missile launch early warning assets and subsequently to nuclear deterrence. An adequate evaluation of the utility of fielding space weapons must take into consideration several factors beyond technological feasibility and military applications. This monograph examines the benefits and drawbacks of an aggressive US space weaponization program. The US possesses a lead in space capabilities that places it in a position to field space weapons first and guarantee the security of national space assets for the foreseeable future. Additionally, the dependence of US military forces on space enablers poses a vulnerability that an adversary will likely attempt to exploit in any future conflict. Advocates of weaponizing space view the failure to weaponize space first would represent an abdication of responsibility by US government officials. The risks

associated with weaponizing space include the possibility of an increase in nuclear tensions and a diminishment of US national power in terms of diplomatic, information and economic influence.
DTIC
*Defense Program; Early Warning Systems; Military Technology; Economics*

**20010121955** National Renewable Energy Lab., Golden, CO USA
**Technology Cooperation Agreement Pilot Project (TCAPP)**
Keegan, P.; Benioff, R.; Oct. 20, 1999; 54p; In English
Report No.(s): DE2000-764484; NREL/BK-710-26841; No Copyright; Avail: Department of Energy Information Bridge, Microfiche

The Technology Cooperation Agreement Pilot Project (TCAPP) is helping developing countries design and implement actions to attract investment in clean energy technologies that will meet their economic development goals, while mitigating greenhouse gas emissions. TCAPP was launched by three US government agencies -- the US Agency for International Development (USAID), the US Environmental Protection Agency (USEPA), and the US Department of Energy (USDOE) -- in August 1997 to establish a model for climate change technology cooperation with developing and transition countries. This report describes the TCAPP approach and the significant progress made by the participating countries.
NTIS
*International Cooperation; Pollution Control; Climate Change; Energy Technology*

**20010124088** Sandia National Labs., Albuquerque, NM USA
**Scientific Meetings Database: A New Tool for CTBT-Related International Cooperation**
Knapik, J. F.; Girven, M. L.; Aug. 20, 1999; 18p; In English
Report No.(s): DE2001-10181; SAND99-2149C; No Copyright; Avail: Department of Energy Information Bridge

The mission of international cooperation is defined in the Comprehensive Nuclear-Test-Ban Treaty (CTBT). Ways and means of implementation were the subject of discussion during the International Cooperation Workshop held in Vienna in November 1998, and during the Regional Workshop for CTBTO International Cooperation held in Cairo, Egypt in June 1999. In particular, a database of 'Scientific and Technical Meetings Directly or Indirectly Related to CTBT Verification-Related Technologies' was developed by the CTBTO PrepCom/PTS/International Cooperation section and integrated into the organization's various web sites in cooperation with the U.S. Department of Energy CTBT Research and Development Program. This database, the structure and use of which is described in this paper/presentation is meant to assist the CTBT-related scientific community in identifying worldwide expertise in the CTBT verification-related technologies and should help experts, particularly those of less technologically advanced States Signatories, to strengthen contacts and to pursue international cooperation under the Treaty regime. Specific opportunities for international cooperation, in particular those provided by active participation in the use and further development of this database, are presented in this paper and/or presentation.
NTIS
*International Cooperation; Nuclear Weapons*

## 88
## SPACE SCIENCES (GENERAL)

*Includes general research topics related to the natural space sciences. For specific topics in Space Sciences see categories 89 through 93.*

**20010120495** Colorado Univ., Dept. of Aerospace Engineering Sciences, Boulder, CO USA
**Data Assimilation for Thermospheric Density Forecasting with Application to Satellite Ephemeris Prediction** ***Final Report, 1 Sep. 1997 - 31 Aug. 2001***
Forbes, Jeffrey M.; Sep. 01, 2001; 4p; In English
Contract(s)/Grant(s): F49620-97-1-0047
Report No.(s): AD-A395134; AFRL-SR-BL-TR-01-0524; No Copyright; Avail: CASI; A01, Hardcopy; A01, Microfiche

Climatological density patterns derived from low-orbit accelerometer data are shown to be consistent with meridional advection of disturbances originating at high latitudes. Long-term (11-year) and short-term (daily and 27-day) variations in thermospheric density are deliberated in terms of the MG II solar index.
DTIC
*Drag; Thermosphere; Climatology; Ephemerides*

## 89
## ASTRONOMY

*Includes observations of celestial bodies, astronomical instruments and techniques; radio, gamma-ray, x-ray, ultraviolet, and infrared astronomy; and astrometry.*

**20010118356** NASA Goddard Space Flight Center, Greenbelt, MD USA
**Galactic Noise and Passive Microwave Remote Sensing from Space at L-Band**
LeVine, D. M., NASA Goddard Space Flight Center, USA; Abraham, S., NASA Goddard Space Flight Center, USA; [2001]; 1p; In English; International Geoscience for Remote Sensing Symposium, 9-13 Jul. 2001, Sydney, Australia; No Copyright; Avail: Issuing Activity; Abstract Only

The spectral window at L-band (1.4 GHz) is important for passive remote sensing of parameters such as soil moisture and ocean salinity best measured at long wavelengths. At L-band, radiation from extraterrestrial (galactic) sources is strong enough to warrant inclusion in calibration and retrieval algorithms and unlike the constant cosmic background is spatially variable. Previous estimates of the magnitude and distribution of this background radiation have been rather coarse, However, recent surveys of the radio sky at 1.4 GHz have made it possible to produce maps with sufficient spatial and radiometric accuracy to be relevant to remote sensing applications. This is of particular concern for remote sensing of sea surface salinity because the surface (water) is a good reflector and the salinity signal is relatively small. This paper presents a modem map of the radiometric sky at L-band and a solution to the problem of determining the portion of the sky seen by a radiometer in orbit. The data is derived from recent radio astronomy surveys and is presented as equivalent brightness temperature suitable for remote sensing applications. Examples using orbits and antennas representative of those contemplated for remote sensing of soil moisture and sea surface salinity from space are presented to illustrate the signal levels to be expected. Radiation near the galactic plane can exceed several kelvin.
Author
*Remote Sensing; Microwave Imagery; Ultrahigh Frequencies; Radio Astronomy; Soil Moisture; Salinity*

**20010118509** NASA Ames Research Center, Moffett Field, CA USA
**Types of Information Expected from a Photometric Search for Extra-Solar Planets**
Borucki, William, NASA Ames Research Center, USA; Koch, David, NASA Ames Research Center, USA; Bell, James, III, Washington Univ., USA; [1994]; 1p; In English; ASP Meeting, 28-30 Jun. 1994, Flagstaff, AZ, USA
Contract(s)/Grant(s): RTOP 186-06-01-04; No Copyright; Avail: Issuing Activity; Abstract Only

The current theory postulates that planets are a consequence of the formation of stars from viscous accretion disks. Condensation from the hotter, inner portion of the accretion disk favors the formation of small rocky planets in the inner portion and the formation of gas giants in the cuter, cooler part. Consequently, terrestrial-type planets in inner orbits must be commonplace (Wetheril 1991). From the geometry of the situation (Borucki and Summers 1984), it can be shown that 1% of those planetary systems that resemble our solar system should show transits for Earth-sized (or larger) planets. Thus a photometric satellite that uses a wide field of view telescope and a large CCD array to simultaneously monitor 5000 target stars should detect 50 planetary systems. to verify that regularly recurring transits are occurring rather than statistical fluctuations of the stellar flux, demands observations that extend over several orbital periods so that the constancy of the orbital period, signal amplitude, and duration can be measured. Therefore, to examine the region from Mercury's orbit to that of the Earth requires a duration of three years whereas a search out to the orbit of mars requires about six years. The results of the observations should provide estimates of the distributions of planetary size and orbital radius, and the frequency of planetary systems that have Earth-sized planets in inner orbits. Because approximately one half of the star systems observed will be binary systems, the frequency of planetary systems orbit ' ing either one or both of the stars can also be determined. Furthermore, the complexity of the photometric signature of a planet transiting a pair of stars provides enough information to estimate the eccentricities of the planetary orbits. In summary, the statistical evidence from a photometric search of solar-like stars should be able to either confirm or deny the applicability of the current theory of planet formation and provide new information about the stability of planetary orbits in binary star systems.
Author
*Extrasolar Planets; Planetary Evolution; Planetary Systems; Charge Coupled Devices; Terrestrial Planets; Photometry*

**20010119917** NASA Ames Research Center, Moffett Field, CA USA
**Physical State of Ices in the Outer Solar System**
Roush, Ted L., NASA Ames Research Center, USA; [2001]; 1p; In English
Contract(s)/Grant(s): RTOP 344-30-30-01; Copyright; Avail: Issuing Activity; Abstract Only

Comparison of the identity and abundances of ices observed around protostars and those associated with comets clearly suggests that comets preserve the heritage of the interstellar materials that aggregated to form them. However, the ability to identify these same species on icy satellites in the outer solar system is a complex function of the composition of the original ices, their subsequent thermal histories, and their exposure to various radiation environments. Our ability to identify the ices currently present on objects in the outer solar system relies upon observational and laboratory, and theoretical efforts. to date there is ample observational evidence for crystalline water ice throughout the outer solar system. In addition, there is growing evidence that amorphous ice may be present on some bodies. More volatile ices, e.g. N2, CH4. CO, and other species, e.g. ammonia hydrate, are identified on objects lying at and beyond Uranus. Both photolysis and radiolysis play important roles in altering the original surfaces due to chemical reactions and erosion of the surface. Ultraviolet photolysis appears to dominate alteration of the upper few hundred Angstroms, although sputtering the surface can sometimes be a significantly competitative process; dominating on icy surfaces embedded in a strong planetary magnetospheric field. There is growing observational evidence that the by-products of photolysis and radiolysis, suggested on a theoretical basis, are present on icy surfaces.
Author
*Crystallinity; Gas Giant Planets; Icy Satellites; Photolysis; Planetary Surfaces*

**20010120465** NASA Ames Research Center, Moffett Field, CA USA
**Imaging of the PAH Emission Bands in the Orion Bar**
Bregman, Jesse, NASA Ames Research Center, USA; Harker, David, Lick Observatory, USA; Rank, David, Lick Observatory, USA; Temi, Pasqiale, Lick Observatory, USA; [1994]; 1p; In English; Airborne Astronomy Symposium, 5-8 Jul. 1994, Moffett Field, CA, USA
Contract(s)/Grant(s): RTOP 352-02-03; No Copyright; Avail: Issuing Activity; Abstract Only

The infrared spectrum of many planetary nebulae, HII regions, galactic nuclei, reflection nebulae, and WC stars are dominated by a set of narrow and broad features which for many years were called the ”unidentified infrared bands”. These bands have been attributed to several carbon-rich molecular species which all contain only carbon and hydrogen atoms, and fall into the class of PAH molecules or are conglomerates of PAH skeletons. If these bands are from PAHs, then PAHs contain 1-10% of the interstellar carbon, making them the most abundant molecular species in the interstellar medium after CO. From ground based telescopes, we have studied the emission bands assigned to C-H bond vibrations in PAHs (3.3, 11.3 microns) in the Orion Bar region, and showed that their distribution and intensities are consistent with a quantitative PAH model. We have recently obtained spectral images of the Orion Bar from the KAO at 6.2 and 7.7 microns using a 128 x 128 Si:Ga array camera in order to study the C-C modes of the PAH molecules. We will show these new data along with our existing C-H mode data set, and make a quantitative comparison of the data with the existing PAH model.
Author
*Infrared Spectra; Planetary Nebulae; Molecular Gases; Interstellar Matter; H II Regions*

**20010121535** NASA Ames Research Center, Moffett Field, CA USA
**The Next Generation Airborne Observatory: SOFIA**
Erickson, E. F., NASA Ames Research Center, USA; [1994]; 1p; In English; International Workshop on IR/Submillimeter Space Astronomy for the Coming Decade, 25-27 Apr. 1994, Saclay, France; No Copyright; Avail: Issuing Activity; Abstract Only

NASA, DARA, and the astronomical community have planned SOFIA (Stratospheric Observatory for Infrared Astronomy) to extend and expand the capabilities of airborne astronomy. Just as the Kuiper Airborne Observatory telescope has three times the aperture of its Learjet predecessor, SOFIA’s aperture (2.5 m) will be three times that of the KAO. Thus SOFIA will surpass the angular resolution of the KAO by a factor of three and its per-pixel sensitivity by a factor approximately 10 at wavelengths beyond 10 micrometers. Following the tradition of the KAO and Learjet programs, the user community will provide most of the SOFIA focal plane instruments. Scientists will fly their new instruments as soon as they become operational, assuring immediate application of state-of-the-art technology throughout the anticipated 20 year observatory lifetime. Annual peer review of submitted proposals guarantees a vigorous observing program. Armed by 15-20 different instrument teams, reinforced by an additional approximately 50 guest investigator groups, and flying 160 8-hour sorties per year, SOFIA will be used to attack a very broad range of astronomical problems. to name just a few, observations made from SOFIA will: greatly extend our understanding of the star-formation process, including collapse, accretion, and outflow phenomena; penetrate the obscuring dust of the Milky way to reveal gas motions, the luminosity distribution, and possibly the powerful excitation mechanism at the center of our Galaxy; and probe km-scale structure of planetary atmospheres and ring systems. The Astronomy and Astrophysics Survey (Bahcall) committee ranked SOFIA as the highest priority moderate cost new mission for NASA in the 1990s. SOFIA has been thoroughly

studied and is ready to start development. If funding is available in 1996 as currently planned by NASA and DARA Astrophysics Offices, SOFIA could be flying by the end of the decade.
Author
*Sofia (Airborne Observatory); Spaceborne Astronomy; Focal Plane Devices*

**20010122296** NASA Ames Research Center, Moffett Field, CA USA
**FRESIP: A Discovery Mission Concept to Find Earth-Sized Planets Around Solar Like Stars**
Borucki, William, NASA Ames Research Center, USA; Koch, D., NASA Ames Research Center, USA; Dunham, E., NASA Ames Research Center, USA; Cullers, D., NASA Ames Research Center, USA; Webster, L., NASA Ames Research Center, USA; Granados, A., Search for Extraterrestrial Intelligence Inst., USA; Ford, C., Search for Extraterrestrial Intelligence Inst., USA; Reitsema, H., Ball Aerospace Systems Div., USA; Cochran, W., Texas Univ., USA; Bell, J., Washington Univ., USA; [1994]; 1p; In English; Division for Planetary Sciences Meeting, 30 Oct. - 4 Nov. 1994, Washington, DC, USA; Sponsored by Lunar and Planetary Inst., USA; No Copyright; Avail: Issuing Activity; Abstract Only

The current nebular theory postulates that planets are. a consequence of the formation of stars from viscous accretion disks. Condensation from the accretion disk favors the formation of small rocky planets in the hot inner region, and the formation of gas giants in the cool outer region. Consequently, terrestrial-type planet in inner orbits should be commonplace. From geometrical considerations , Borucki and Summers have shown that 1% of planetary systems resembling our solar system should show transits for Earth-sized (or larger) planets. Thus a photometric satellite that uses a wide field of view telescope and a large detector array to simultaneously monitor 5000 target stars should detect 50 planetary systems. to differentiate regularly recurring transits from statistical fluctuations of the stellar flux, one must observe over several orbital periods so that the false positive rate can be reduced to one event or less. A one-meter aperture telescope placed in a halo orbit about either the L1 or L2 Lagrange points and viewing perpendicular to both the orbital and ecliptic planes can view continuously for the required period because neither the Sun, Earth, or Moon would enter the field of view. Model calculations show that the observations should provide statistically significant estimates of the distributions of planetary size, orbital radius, coplanarity, and the frequency of planetary systems that have Earth-sized planets in inner orbits. Because approximately one half of the star systems observed will be binary systems, the frequency of planetary systems orbiting either one or both of the stars can also be determined.
Author
*Coplanarity; Ecliptic; Mission Planning; Planetary Evolution; Planetary Systems; Solar System; Terrestrial Planets*

**20010122924** NASA Ames Research Center, Moffett Field, CA USA
**Explosion Calculations of SN1087**
Wooden, Diane H., NASA Ames Research Center, USA; [1994]; 1p; In English; Airborne Astronomy Symposium, 5-8 Jul. 1994, Moffett Field, CA, USA
Contract(s)/Grant(s): RTOP 352-02-03; No Copyright; Avail: Issuing Activity; Abstract Only

Explosion calculations of SNT1987A generate pictures of Rayleigh-Taylor fingers of radioactive Ni-56 which are boosted to velocities of several thoUSAnd km/s. From the KAO observations of the mid-IR iron lines, a picture of the iron in the ejecta emerges which is consistent with the ”frothy iron fingers” having expanded to fill about 50% of the metal-rich volume of the ejecta. The ratio of the nickel line intensities yields a high ionization fraction of greater than or equal to 0.9 in the volume associated with the iron-group elements at day 415, before dust condenses in the ejecta. From the KAO observations of the dust’s thermal emission, it is deduced that when the grains condense their infrared radiation is trapped, their apparent opacity is gray, and they have a surface area filling factor of about 50%. The dust emission from SN1987A is featureless: no 9.7 micrometer silicate feature, nor PAH features, nor dust emission features of any kind are seen at any time. The total dust opacity increases with time even though the surface area filling factor and the dust/gas ratio remain constant. This suggests that the dust forms along coherent structures which can maintain their radial line-of-sight opacities, i.e., along fat fingers. The coincidence of the filling factor of the dust and the filling factor of the iron strongly suggests that the dust condenses within the iron, and therefore the dust is iron-rich. It only takes approximately 4 x 10(exp -4) solar mass of dust for the ejecta to be optically thick out to approximately 100 micrometers; a lower limit of 4 x 10(exp -4) solar mass of condensed grains exists in the metal-rich volume, but much more dust could be present. The episode of dust formation started at about 530 days and proceeded rapidly, so that by 600 days 45% of the bolometric luminosity was being emitted in the IR; by 775 days, 86% of the bolometric luminosity was being reradiated by the dust. Measurements of the bolometric luminosity of SN1987A from 1000 - 1800 days are based on 10 micrometers and 20 micrometers photometry and rely on the suppositions that the IR emission is a greybody (proven to be true by the KAO observations at 615 and 775 days) and

that the dust temperature drops to and remains at 150 K. The late time bolometric luminosity is stronger than that expected from the radioactive decay of Co-56, Co-57, Ti-44, and Na-22 and the possibility of an embedded compact object will be discussed. Author

*Stellar Activity; Stellar Mass Ejection; Supernova 1987A; Ejecta; Thermal Emission; Opacity; Dust; Luminosity*

**20010124104** Smithsonian Astrophysical Observatory, Cambridge, MA USA

**Temperature Maps of Clusters of Galaxies** ***Annual Report, 1 Jan. - 31 Dec. 2001***

Forman, William R., Smithsonian Astrophysical Observatory, USA; October 2001; 3p; In English

Contract(s)/Grant(s): NAG5-6749; No Copyright; Avail: CASI; A01, Hardcopy; A01, Microfiche

We have progressed on our analysis of the temperature structure of clusters of galaxies. This report addresses the following areas: (1) merging clusters; (2) mass distributions; (3) temperature structures of clusters.

Derived from text

*Galactic Clusters; Thermal Mapping*

**20010125135** NASA Ames Research Center, Moffett Field, CA USA

**Search Space Characterization for a Telescope Scheduling Application**

Bresina, John, RECOM Technologies, Inc., USA; Drummond, Mark, RECOM Technologies, Inc., USA; Swanson, Keith, NASA Ames Research Center, USA; [1994]; 1p; In English; Sponsored by American Inst. of Aeronautics and Astronautics, USA

Contract(s)/Grant(s): RTOP 233-02-07; No Copyright; Avail: Issuing Activity; Abstract Only

This paper presents a technique for statistically characterizing a search space and demonstrates the use of this technique within a practical telescope scheduling application. The characterization provides the following: (i) an estimate of the search space size, (ii) a scaling technique for multi-attribute objective functions and search heuristics, (iii) a ”quality density function” for schedules in a search space, (iv) a measure of a scheduler’s performance, and (v) support for constructing and tuning search heuristics. This paper describes the random sampling algorithm used to construct this characterization and explains how it can be used to produce this information. As an example, we include a comparative analysis of an heuristic dispatch scheduler and a look-ahead scheduler that performs greedy search.

Author

*Algorithms; Heuristic Methods; Telescopes; Artificial Intelligence*

## 90
## ASTROPHYSICS

*Includes cosmology; celestial mechanics; space plasmas; and interstellar and interplanetary gases and dust.*

**20010117717** Brookhaven National Lab., Upton, NY USA

**High rate neutrino detectors for neutrino factories**

King, B. J.; Jan. 24, 2000; 13p; In English

Report No.(s): DE2000-752155; BNL-67161; No Copyright; Avail: Department of Energy Information Bridge

Muon colliders and other proposed high-current muon storage rings can be collectively referred to as neutrino factories. As well as the long baseline neutrino oscillation studies that are currently garnering much of the attention, neutrino factories also have considerable potential for wide-ranging studies involving the physics of neutrino interactions. Exciting and unique high rate (HR) neutrino physics could be performed using detectors placed as close as is practical to the storage ring in order to maximize the event rate and to subtend the neutrino beam with the narrowest possible target. Rather than studying the properties of the neutrinos themselves, such experiments would instead investigate their interactions with the quarks inside nucleons and with electrons. HR detectors needed for these studies form the topic of this paper.

NTIS

*Neutron Counters; Muons; Neutrinos; Storage Rings (Particle Accelerators)*

**20010117731** NASA Ames Research Center, Moffett Field, CA USA

**More Consequences of the Collision of a Comet and Jupiter**

Zahnle, Kevin, NASA Ames Research Center, USA; MacLow, M.-M., Chicago Univ., USA; [1994]; 1p; In English; Division for Planetary Sciences Meeting, 30 Oct. - 4 Nov. 1994, Washington, DC, USA; Sponsored by Lunar and Planetary Inst., USA; No Copyright; Avail: Issuing Activity; Abstract Only

The impending collision of P/Shoemaker-Levy 9 with Jupiter has excited a wide spectrum of large amplitude predictions. Although the prediction waves themselves have been easily detected propagating through diverse media here on Earth, their future manifestation at Jupiter may prove mostly undetectable. In this talk we may or may not attempt to explain what may or may not have been observed. We will doubtless emphasize our most successful predictions, if any.
Author
*Collisions; Comets; Jupiter (Planet)*

**20010117735** NASA Ames Research Center, Moffett Field, CA USA
**Excitation of the E2 and W1 "Arched" Filaments Near the Galactic Center as Deduced from Far-Infrared Spectroscopy**
Colgan, Sean W.J., NASA Ames Research Center, USA; Erickson, Edwin F., NASA Ames Research Center, USA; Simpson, Janet P., NASA Ames Research Center, USA; Haas, Michael R., NASA Ames Research Center, USA; Morris, Mark, California Univ., USA; Jun. 14, 1994; 1p; In English; Airborne Astronomy, 5-8 Jul. 1994, Moffett Field, CA, USA
Contract(s)/Grant(s): RTOP 352-02-03; No Copyright; Avail: Issuing Activity; Abstract Only

We present measurements of the far-infrared (FIR) fine structure lines [S III] (33 microns), [Si II] (35 microns), [O III] (51, 88 microns), [O I] (63 microns) and [C II] (158 microns) and the adjacent continua along a scan crossing the E2 and W1 thermal radio filaments in the Galactic center 'Arc'. The deduced electron density and excitation vary along the scan by less than factors of two and three, respectively. The properties of the two filaments are similar: the line and continuum fluxes peak at the radio ridge, and the ridge/off-ridge contrast is greatest for the FIR continuum and ionized lines, lower for the single dish radio measurements (Sofue et al. 1986), and smallest for the low excitation lines. The spatial coincidence of the FIR and radio peaks demonstrates that any excitation mechanism for the radio continuum filaments must also account for the FIR line and continuum emission. The FIR luminosity of approx. 3 x 10(exp 5) Solar Luminosity per beam, and the association of [O III] emission with the filaments poses difficulties for shock and MHD models. Photoionization of molecular cloud edges by a random distribution of stars is the most likely excitation mechanism among those proposed. The continuum and the low excitation line fluxes are consistent with an origin in photodissociated molecular material adjacent to the photoionized gas.
Author
*Fine Structure; Infrared Spectroscopy; Filaments; Excitation; Continuums; A Stars*

**20010117738** NASA Ames Research Center, Moffett Field, CA USA
**Multiple Core Galaxies**
Miller, R.H., NASA Ames Research Center, USA; Apr. 04, 1994; 1p; In English; Dynamical Astronomy/DDA Committee, 27-29 Mar. 1994, Kingsville, TX, USA; Sponsored by Texas A&M Univ., USA
Contract(s)/Grant(s): RTOP 188-44-53-02; No Copyright; Avail: Issuing Activity; Abstract Only

Nuclei of galaxies often show complicated density structures and perplexing kinematic signatures. In the past we have reported numerical experiments indicating a natural tendency for galaxies to show nuclei offset with respect to nearby isophotes and for the nucleus to have a radial velocity different from the galaxy's systemic velocity. Other experiments show normal mode oscillations in galaxies with large amplitudes. These oscillations do not damp appreciably over a Hubble time. The common thread running through all these is that galaxies often show evidence of ringing, bouncing, or sloshing around in unexpected ways, even though they have not been disturbed by any external event. Recent observational evidence shows yet another phenomenon indicating the dynamical complexity of central regions of galaxies: multiple cores (M31, Markarian 315 and 463 for example). These systems can hardly be static. We noted long-lived multiple core systems in galaxies in numerical experiments some years ago, and we have more recently followed up with a series of experiments on multiple core galaxies, starting with two cores. The relevant parameters are the energy in the orbiting clumps, their relative.masses, the (local) strength of the potential well representing the parent galaxy, and the number of cores. We have studied the dependence of the merger rates and the nature of the final merger product on these parameters. Individual cores survive much longer in stronger background potentials. Cores can survive for a substantial fraction of a Hubble time if they travel on reasonable orbits.
Author
*Galactic Nuclei; Markarian Galaxies; Andromeda Galaxy*

**20010118353** NASA Ames Research Center, Moffett Field, CA USA
**The Disruption and Demise of Periodic Comet Shoemaker-Levy 9**
Asphaug, Erik, NASA Ames Research Center, USA; Benz, Willy, Arizona Univ., USA; [1994]; 1p; In English; Small Bodies in the Solar System and Their Interactions with the Planets, 8-12 Aug. 1994, Marienhamn, Finland
Contract(s)/Grant(s): RTOP 151-01-60-07; No Copyright; Avail: Issuing Activity; Abstract Only

The impact of the fragmented comet Shoemaker-Levy 9 (SL9) into Jupiter this July promises to change our understanding of the outer solar system. More than twenty mountain-sized conglomerates of ice and rock will hit the atmosphere at approx. 50 km/s over the course of a week beginning July 16, releasing approx. 10(exp 4) to 10(exp8) megatons of energy per burst, and providing unique and perhaps pivotal clues to the properties of comets and the physics of massive atmospheres. Because the fragments will strike the far side of Jupiter, data acquisition, analysis and interpretation will be quite sensitive to the actual size and energy of the fragments. We therefore examine an event which took place two summers ago, unnoticed and unobserved: the disruption of SL9 into a ”string of pearls’ as it passed within the Roche limit at perijove. We first demonstrate, on the basis of timescales of tidal interaction, that the comet could not have broken into 20+ fragments through a hierarchy of brittle fracture events. Next, noting that the tidal stress was too weak to have even fragmented an uncompressed mass of freshly fallen snow, we run models for a strengthless comet held together only by self-gravity. We explore the initial size, density, and rotation. We conclude that a 4 km diameter comet (smaller if a prograde rotator) of density approx. 0.5 g/cu cm disrupts and disperses into a chain of fragments similar to Shoemaker-Levy 9, whether we begin with 21, 85, 169, 700 or 2000 sub-grains. Gravitational reaccumulation is evidently the answer, and there is no need to invoke the presence of 21 ”cometesimals” as the subscale of the comet. to explain how a comet can be weaker than uncompacted snow, we show that the ring-plane crossing prior to perijove could have caused total damage. Finally, we compute the tidal stress on impactors as they approach Jupiter this July. Objects of various density are moderately distorted but not disrupted by the time they strike the planet.
Author
*Shoemaker-Levy 9 Comet; Cometary Collisions; Impact; Fracturing*

**20010119563** Oak Ridge National Lab., TN USA
**Recent Nuclear Astrophysics Data Activities in the US**
Bardayan, D. W.; Blackmon, J. C.; Browne, E.; Firestone, R. B.; Hale, G. M.; Aug. 30, 1999; 9p; In English
Report No.(s): DE2001-10491; ORNL/CP-104603; KB-04-01-02-1; No Copyright; Avail: Department of Energy Information Bridge, Microfiche

Measurements in nuclear physics laboratories form the empirical foundation for new, realistic, sophisticated theoretical models of a wide variety of astrophysical systems. The predictive power of these models has, in many instances, a strong dependence on the input nuclear data, and more extensive and accurate nuclear data is required for these models than ever before. Progress in astrophysics can be aided by providing scientists with more USAble, accurate, and significant amounts of nuclear data in a timely fashion in formats that can be easily incorporated into their models. A number of recent data compilations, evaluations, calculations, and disseminations that address nuclear astrophysics data needs will be described.
NTIS
*Data Management; Nuclear Astrophysics*

**20010119946** NASA Ames Research Center, Moffett Field, CA USA
**Laboratory Comparisons of Organic Materials to Those Observed in the Interstellar Medium**
Pendleton, Yvonne J., NASA Ames Research Center, USA; [1994]; 1p; In English; International Conference on Dust, Molecules and Backgrounds: From Laboratory to Space, 12-15 Sep. 1994, Capri, Catania, Italy, Italy
Contract(s)/Grant(s): RTOP 188-44-21-04; No Copyright; Avail: Issuing Activity; Abstract Only

Spectra of objects which lie along several lines of sight through the diffuse interstellar medium (ISM) all contain an absorption feature near 3.4 Pm which has been attributed to saturated aliphatic hydrocarbons on interstellar grains. The similarity of the absorption bands near 3.4 microns (2950 /cm) along different lines of sight reveal that the carrier of this band lies in the diffuse dust. Several materials have been proposed as ”fits” to the 3.4 microns feature over the years. A comparison of these identifications is presented. A remarkable similarity between the spectrum of the diffuse dust and an organic extract from the Murchison meteorite suggests that some of the interstellar organic material may be preserved in primitive solar system bodies. Recent detections of the hydrocarbon absorption feature in external galaxies are presented. These results indicate the widespread availability of the organic material for incorporation into planetary systems. Recent detections of the X-CN absorption feature in dense molecular clouds are also presented. The preliminary results suggest that the X-CN band is only observed toward embedded sources and is not distributed throughout the molecular cloud. If so, this has profound effects on the production mechanism of this component of the organic material in space.
Author
*Absorption Spectra; Cosmic Dust; Hydrocarbons; Interstellar Matter; Molecular Clouds; Organic Materials*

**20010120054** NASA Ames Research Center, Moffett Field, CA USA

**The Infrared Spectrum of Matrix-Isolated Hexamethylenetetramine in Argon at 12 K**

Bernstein, Max P., NASA Ames Research Center, USA; Sandford, Scott A., NASA Ames Research Center, USA; Allamandola, Louis J., NASA Ames Research Center, USA; Chang, Sherwood, NASA Ames Research Center, USA; [1994]; 1p; In English

Contract(s)/Grant(s): RTOP 452-33-93-03; No Copyright; Avail: Issuing Activity; Abstract Only

It is commonly accepted that constant exposure of comets and ice grains to ultraviolet (UV) radiation causes an organic crust to form on their surface, but the exact molecules that comprise the crust remains a mystery. Based on our lab simulations of interstellar and cometary ices (a paper to be submitted this spring) we believe that Hexamethylenetetramine (HMT) may be a major component of the organic crust on the surface of comets and ice grains. The enclosed paper presents the laboratory infrared spectra and UV photochemistry of HMT under conditions akin to that of the interstellar medium.

Author

*Argon; Hexamethylenetetramine; Infrared Spectra; Photochemical Reactions; Interstellar Matter*

**20010120057** NASA Ames Research Center, Moffett Field, CA USA

**Solid and Gas-Phase Spectroscopy of Cosmic Carbon Analogs: Results and Perspectives**

Salama, Farid, NASA Ames Research Center, USA; [2001]; 1p; In English; International Space Science Institute Workshop on Laboratory Astrophysics, 7-11 May 2001, Bern, Switzerland; Sponsored by International Space Science Inst., Unknown

Contract(s)/Grant(s): RTOP 344-01-57-41; No Copyright; Avail: Issuing Activity; Abstract Only

The laboratory studies of interstellar carbon materials analogs (PAHs, Fullerenes, chains) will be discussed with their advantages and limitations from the point of view of the application to astrophysical processes. The discussion will focus on the newest generation of laboratory experiments that has been developed in order to provide a closer simulation of space environments and a better support to space missions. The astrophysical implications and future perspectives will be stressed.

Author

*Astrophysics; Carbon; Interstellar Matter; Solid Phases; Gas Spectroscopy*

**20010120134** NASA Ames Research Center, Ames Research Center, Moffett Field, CA USA

**Theory of Tumbling Bodies Entering Planetary Atmospheres with Application to Probe Vehicles and the Australian Tektites**

Tobak, Murray; Peterson, Victor L.; Jul. 1964; 44p; In English

Report No.(s): AD-A395187; NASA-TR-R-203; No Copyright; Avail: CASI; A03, Hardcopy; A01, Microfiche

The tumbling motion of aerodynamically stable bodies entering planetary atmospheres is analyzed considering that the tumbling, its arrest, and the subsequent oscillatory motion are governed by the equation for the fifth Painleve' transcendent. Results based on the asymptotic behavior of the transcendent are applied to study (1) the oscillatory behavior of planetary probe vehicles in relation to aerodynamic heating and loads and (2) the dynamic behavior of the Australian tektites on entering the Earth's atmosphere, under the hypothesis that their origin was the Moon.

DTIC

*Australia; Planetary Atmospheres; Tektites; Tumbling Motion; Asymptotic Properties; Space Probes*

**20010120158** NASA Ames Research Center, Moffett Field, CA USA

**Progress in the Laboratory Study of Interstellar Analogs**

Salama, Farid, NASA Ames Research Center, USA; [2001]; 1p; In English, 18-28 Jun. 2001, Jena, Germany

Contract(s)/Grant(s): RTOP 344-01-57-41; No Copyright; Avail: Issuing Activity; Abstract Only

Recent progress in the laboratory study of cosmic carbon analogs will be discussed. After a brief review of the history of laboratory studies of interstellar carbon molecules and ions, new gas-phase results will be discussed and contrasted to previous studies that used the techniques of matrix isolation spectroscopy. Finally, the impact of these new laboratory studies on the field of astrophysics will be discussed.

Author

*Astrophysics; Interstellar Matter; Carbon; Spectroscopy*

**20010121547** NASA Ames Research Center, Moffett Field, CA USA

**Encounter with Asteroids Gaspra and Ida: Imaging Results**

Morrison, David, NASA Ames Research Center, USA; [1994]; 1p; In English; IAU 22nd General Assembly, 13-27 Aug. 1994, The Hague, Netherlands; Sponsored by International Astronomical Union, Unknown

Contract(s)/Grant(s): RTOP 196-41-67-06; No Copyright; Avail: Issuing Activity; Abstract Only

A progress report is given on imaging science results from the Galileo spacecraft flybys of the S-type main-belt asteroids Gaspra and Ida. Images were obtained in six colors of both asteroids, a few at resolutions better than 100 m. The overall sizes, shapes, and spin vectors of both objects are defined, and more detailed geological studies are possible for approximately half the surface of each (the hemisphere facing the spacecraft at closest approach). Each is elongated and highly irregular in profile, with heavily cratered surfaces. A number of grooves, other linear features, and surface blocks may also be associated with a recent history of impacts. Modest variations in surface albedo and color are probably due to differences in regolith development rather than compositional differences across the surfaces of each. Both the density and the size distributions of craters differ from Gaspra to Ida, in spite of its younger anticipated dynamical age, Ida is more density cratered. Ida also has a small satellite in a roughly 100-km orbit, allowing the possibility of determining the density of Ida with sufficient precision to constrain alternative models of its bulk composition.
Author
*Asteroids; Density Distribution; Geology; Imaging Techniques*

**20010121552** NASA Ames Research Center, Moffett Field, CA USA
**Observations of High Rotational Excitation of CO Lines in AGB and Post-AGB Stars**
Justtanont, K., NASA Ames Research Center, USA; Tielens, A. G. G. M., NASA Ames Research Center, USA; Skinner, C. J., Lawrence Livermore National Lab., USA; [1994]; 1p; In English; Circumstellar Matter Conference, 28 Aug. - 2 Sep. 1994, Edinburgh, Scotland, UK
Contract(s)/Grant(s): RTOP 399-20-10-27; No Copyright; Avail: Issuing Activity; Abstract Only

We present ground based observations of AGB stars for CO J=6-5; 4-3; 3-2; 2-1 and 1-0 lines. Radiative transfer modelling of these lines suggests that the stars do not lose mass continuously, but undergo discrete bursts of significant mass loss. Ratio of brightness of different fines show a wide range of behaviours in different stars, with higher transition lines probing deeper into the circumstellar envelope. We also obtained higher CO rotational transitions for post-AGB stars at J=22-21; 17-16 and 13-12. These lines can be used as probes for the warm medium at the inner part of the envelope. From these results, we can trace the history of mass loss in these stars.
Author
*Asymptotic Giant Branch Stars; Brightness; Excitation; Observation*

**20010122401** NASA Ames Research Center, Moffett Field, CA USA
**Organic Material in the ISM**
Pendleton, Yvonne, NASA Ames Research Center, USA; [1994]; 1p; In English, 6-17 Jun. 1994, Erice, Sicily, Italy
Contract(s)/Grant(s): RTOP 188-44-21-04; No Copyright; Avail: Issuing Activity; Abstract Only

Spectra of objects which lie along several lines of sight through the diffuse interstellar medium (ISM) all contain an absorption feature near 3.4 micrometers which has been attributed to saturated aliphatic hydrocarbons on interstellar grains. The similarity of the absorption bands near 3.4 micrometers along different lines of sight reveal that the carrier of this band lies in the diffuse dust. Several materials have been proposed as ”fits” to the 3.4 micrometers feature over the years. A comparison of these identifications is presented. A remarkable similarity between the spectrum of the diffuse dust and an organic extract from the Murchison meteorite suggests that some of the interstellar organic material may be preserved in primitive solar system bodies. The optical depth/extinction tau /A(sub v) ratio for the 3.4 micrometers band is higher toward the Galactic center than toward sources which sample the interstellar medium in the local neighborhood. A similar trend has been observed previously for silicates, indicating that the two materials may be simultaneously enhanced in the Galactic center.
Author
*Organic Materials; Interstellar Matter; Absorption Spectra*

**20010123541** Argonne National Lab., IL USA
**Zr and Mo isotopes in single presolar graphite grains: a record of stellar nucleosynthesis**
Nicolussi, G. K.; Feb. 10, 1998; 15p; In English
Report No.(s): DE2001-10639; ANL/CHM/CP-95617; No Copyright; Avail: Department of Energy Information Bridge, Microfiche

Thirty-two individual graphite grains from the Murchison meteorite were analyzed for their Mo and/or Zr isotopic compositions by laser ablation resonant ionization mass spectrometry. (sup 96)Zr/(sup 94)Zr ratios range from 0.074 times to 10 times the solar value. Five grains have depletions in (sup 96)Zr, suggestive of the s-process, and two grains have extraordinary

enrichments in (sup 96)Zr, suggestive of the r-process. Most graphite grains have close-to-terrestrial Mo isotopic imposition, but five have s-process Mo nucleosynthesis signatures.
NTIS
*Graphite; Meteorites; Zirconium Isotopes; Molybdenum Isotopes*

**20010124105** NASA Ames Research Center, Moffett Field, CA USA
**Evidence for Gravity as a Cue for Absolute Size and Distance**
Hecht, Heiko, NASA Ames Research Center, USA; Kaiser, Mary K., NASA Ames Research Center, USA; Banks, Martin S., California Univ., USA; [1994]; 1p; In English; Psychonomic Society, Inc. 35th Annual Meeting, 11-13 Nov. 1994, Saint Louis, MO, USA; Sponsored by Psychonomic Society, Inc., USA
Contract(s)/Grant(s): RTOP 538-04-11; No Copyright; Avail: Issuing Activity; Abstract Only

The constant force of gravity constrains the motion of objects in natural environments. In principle, gravity could provide valuable scaling information about size and distance of unfamiliar objects. We supply empirical evidence that observers use some of the information provided by gravity to scale objects. However, scaling judgments based on retinal size and event duration alone are nearly as accurate as those made with gravitational acceleration information.
Author
*Cues; Gravitation; Judgments; Dimensional Analysis; Space Perception*

**20010124892** Uppsala Univ., Inst. fuer Astronomi och Rymfysik, Uppsala, Sweden
**A Study of Mercury-Like Orbits**
Warell, J., Uppsala Univ., Sweden; Karlsson, O., Uppsala Univ., Sweden; Skogloev, E., Uppsala Univ., Sweden; Mercury: Space Environment, and Surface and Interior; 2001, pp. 109-110; In English; See also 20010124826; No Copyright; Abstract Only; Available from CASI only as part of the entire parent document

We have performed a series of n-body numerical integrations of particles in heliocentric orbits which are closely similar to that of Mercury (in a, e and i). The calculations have been performed with the 15th order integrator RADAU with a variable step size, including the perturbations of the eight major planets. The purpose of the study was to determine the dynamics of objects near Mercury's heliocentric distance, the possibility of temporary captures by Mercury, routes of transfer of Near Earth Objects (NEOs) within the inner solar system, and the effect of resonances in this region. After an initial integration to determine what types of orbital elements are susceptible to close encounters with Mercury, a total of 10,000 objects were integrated for 15,000 years. From this sample, 675 objects were selected which spent a minimum of 10 days within the Hill radius of Mercury (at a Hermeocentric radius of about 200,500 km) during at least one approach, and an integration of 100,000 years was performed. A subset of 17 objects whose approaches were extraordinarily long or numerous was then selected and integrated for 1,200 years, to study the dynamics of the encounters in detail. Two follow-up integrations lasting 10(exp 8) years were finally made to study objects whose secular evolution in a and e caused longterm excursions from the Mercury zone, and those objects whose orbits were found to be Hermeocentric for extended periods of time. We find that (1) there exists retrograde Hermeocentric orbits which are stable for at least 100,000 years (Hermeocentric elements around a(sub H) = 111,000 km, e(sub H) = 0.38 with anomalistic periods P(sub H) = 16 days), thus numerically verifying the analytical work of Rawal; (2) objects originally in closely Hermean heliocentric orbits may secularly increase the semi-major axis due to numerous encounters with Mercury, followed by passages through the secular v(sub 2) resonances with Venus which increase the eccentricity to attain Venus crossing orbits; this evolution forms a possible way of producing NEOs from orbits inferior to Earth's; (3) objects may be repeatedly intermittently locked in the 1:1 mean motion resonance with Mercury and follow Trojan-like horse-shoe orbits for up to at least 23,000 years with periods of around 80 years in the Hermeocentric frame of motion; (4) objects may be subject to temporary satellite captures by Mercury with orbits within the Hill sphere for durations of at least 90 days. Based on the estimated number of kilometer size Amor asteroids, as well as on Weidenschilling's model of the solar nebula and the retainment of objects larger than 10 km within Mercury's perihelion distance, we also estimate that the number of objects in Mercury-like orbits existing today is less than 10(exp -3).
Author
*Celestial Bodies; Many Body Problem; Mercury (Planet); Solar Orbits; Natural Satellites; Numerical Integration; Planetary Orbits; Orbital Mechanics*

**20010125148** NASA Ames Research Center, Moffett Field, CA USA
**Meteoritic Constraints on Models of the Solar Nebula: The Abundances of Moderately Volatile Elements**
Cassen, Patrick, NASA Ames Research Center, USA; [1994]; 1p; In English; Division for Planetary Sciences Meeting, 30 Oct. - 4 Nov. 1994, Washington, DC, USA; Sponsored by Lunar and Planetary Inst., USA; No Copyright; Avail: Issuing Activity; Abstract Only

The ”moderately volatile” elements are those which condense (or evaporate) in the temperature range 650 - 1350 K, as a mix of material with solar abundances is cooled (or heated) tinder equilibrium conditions. Their relative abundances in chondritic meteorites are solar (or ”cosmic”, as defined by the composition of Cl meteorites) to within a factor of several, but vary within that range in a way that correlates remarkably well with condensation temperature, independent of chemical affinity. It has been argued that this correlation reflects a systematically selective process which favored the accretion of refractory material over volatile material from a cooling nebula. Wasson and Chou (Meteoritics 9, 69-94, 1974, and Wasson and co-authors in subsequent papers) suggested that condensation and settling of solids contemporaneously with the cooling and removal of nebular gas could produce the observed abundance patterns, but a quantitative model has been lacking. We show that the abundance patterns of the moderately volatile elements in chondritic meteorites can be produced, in some degree of quantitative detail, by models of the solar nebula that are designed to conform to observations of T Tauri stars and the global conservation laws. For example, even if the local surface density of the nebula is not decreasing, condensation and accretion of solids from radially inflowing gas in a cooling nebula can result in depletions of volatiles, relative to refractories, like those observed, The details of the calculated abundance patterns depend on (but are not especially sensitive to) model parameters, and can exhibit the variations that distinguish the meteorite classes. Thus it appears that nebula characteristics such as cooling rates, radial flow velocities, and particle accumulation rates can be quantitatively constrained by demanding that they conform to meteoritic data; and the models, in turn, can produce testable hypotheses regarding the time and location of the formation of the chondrite parent bodies and the planets. Author

*Chondrites; Solar Nebula; Meteoritic Composition; Mathematical Models; Abundance*

**20010125162** Argonne National Lab., IL USA

**Measurement of the Ti-44 half-life and its significance for supernova**

Ahmad, I.; Greene, J. P.; Kutschera, W.; Paul, M.; Aug. 28, 1999; 10p; In English

Report No.(s): DE2001-11776; ANL/PHY/CP-98892; No Copyright; Avail: Department of Energy Information Bridge

In 1998, we reported the three-laboratory measurement of the Ti-44 half-life which was determined relative to the well known value (5.2714 +/- 0.0005 yr) of the Co-60 half-life. We have continued the measurement at Argonne and JerUSAlem and inclusion of data points for additional two years does not change our published value of 59.0 +/- 0.6 yr.

NTIS

*Supernovae; Titanium Isotopes; Radioactive Isotopes*

**20010125579** Argonne National Lab., IL USA

**Search for neutrinos from active galactic nuclei in Soudan 2**

DeMuth, D. M.; Jun. 22, 1999; 6p; In English

Report No.(s): DE2001-11868; ANL-HEP-CP-99-55; No Copyright; Avail: Department of Energy Information Bridge, Microfiche

Models for AGN neutrino production suggest a measurable muon flux in underground detectors. In this paper, we comment on neutrino point sources and discuss our methods for determining an upper limit on the intensity of horizontal, neutrino induced muons with energy above 1 TeV at the Soudan 2 detector. We set a limit of 1.8 x 10(sup (minus)13) (cm(sup 2) sr s)(sup (minus)) for detecting 5 TeV (nu)-induced muons from AGN.

NTIS

*Active Galactic Nuclei; Neutrinos; Point Sources; Particle Production*

**20010125582** Argonne National Lab., IL USA

**Observation of the moon shadow in deep underground muon flux**

Allison, W. W. M.; Alner, G. J.; Ayres, D. S.; Cobb, J. H.; Fields, T. H.; Jun. 22, 1999; 6p; In English

Report No.(s): DE2001-11864; ANL-HEP-CP-99-58; No Copyright; Avail: Department of Energy Information Bridge, Microfiche

A shadow of the moon, with a statistical significance of 5(sigma), has been observed in the underground muon flux at a depth of 2090 mwe using the Soudan 2 detector. The angular resolution of the detector is well described by a Gaussian with (sigma) (le)0.3(degree). The position of the shadow confirms the alignment of the detector to better than 0.15(degree). This alignment has remained stable during 10 years of data taking from 1989 through 1998.

NTIS

*Moon; Muons; Cosmic Rays; Shadows; Astrophysics*

**20010125612** NASA Ames Research Center, Moffett Field, CA USA

**Organic Signature of Dust from the Interstellar Medium (ISM)**

Freund, Friedemann, NASA Ames Research Center, USA; Freund, Minoru, NASA Goddard Space Flight Center, USA; Staple, Aaron, Stanford Univ., USA; Scoville, John, Kentucky Univ., USA; [2001]; 1p; In English; 197th Meeting of the American Astronomical Society, 7-11 Jan. 2001, San Diego, CA, USA; Sponsored by American Astronomical Society, USA; No Copyright; Avail: Issuing Activity; Abstract Only

Dust in the ISM carries an ”organic” signature in form of a distinct group of C-H stretching bands, both in emission and absorption, around 3.4 micrometers. These bands agree with the symmetrical and asymmetrical C-H stretching vibrations of aliphatic -CH2- entities and are thought to be associated with organic molecules on the surface of dust grains. We show that this interpretation is inconsistent with laboratory experiments. Synthetic MgO and natural olivine single crystals, grown from a CO/CO2/H2O-saturated melt, exhibit the same C-H stretching bands but those bands are clearly associated with C-H entities inside the dense mineral matrix. The multitude of C-H stretching bands suggests that the C-H bonds arise from polyatomic C(sub n) entities. We heated the MgO and olivine crystals to temperatures between 550-1000 K to pyrolyze the C-H bonds and to cause the C-H stretching bands to disappear. Upon annealing at moderate temperatures between 300-390 K the C-H stretching bands reappear within a few days to weeks. The C-H stretching band intensity increases linearly with the square root of time. Thus, while the pyrolysis broke the C-H bonds and caused the H to disperse in the mineral matrix, the H atoms (or H2 molecules) are sufficiently mobile to return during annealing and reestablish the C-H bonds. Dust grains that condense in a gas-laden environment (outflow of late-stage stars or in dense molecular clouds) probably incorporate the same type of Cn-H entities. Imbedded in and in part bonded to the surrounding mineral matrix, the Cn-H entities display C-H stretching bands in the 3.4 micrometer region, but their lower frequency librational modes are so strongly coupled to the lattice modes that they broaden excessively and thus become unobservable.

Author

*Spectral Signatures; Organic Materials; Interstellar Matter; Hydrocarbons; Bonding*

## 91
## LUNAR AND PLANETARY SCIENCE AND EXPLORATION

*Includes planetology; selenology; meteorites; comets; and manned and unmanned planetary and lunar flights. For spacecraft design or space stations see 18 Spacecraft Design, Testing and Performance.*

**20010121542** NASA Ames Research Center, Moffett Field, CA USA

**Measurement Capabilities of Single-Pulse Planar Doppler Velocimetry**

McKenzie, Robert L., NASA Ames Research Center, USA; [1994]; 2p; In English; 33rd AIAA Aerospace Sciences Meeting, 9-12 Jan. 1995, Reno, NV, USA; Sponsored by American Inst. of Aeronautics and Astronautics, USA

Contract(s)/Grant(s): RTOP 505-59-53; No Copyright; Avail: Issuing Activity; Abstract Only

Preliminary investigations are described of a method that is capable of measuring instantaneous, 3-D, velocity vectors everywhere in a light sheet generated by a pulsed laser. The technique, here called Planar Doppler Velocimetry (PDV), is a variation of a new concept for velocity measurements that was called Doppler Global Velocimetry (DGV) in its original disclosure. The concept relies on the use of a narrowband laser and measurements of the Doppler shift of scattered light from particles moving with a flow. The Doppler shift is recorded as a variation in transmission through a sharp-edged spectral filter provided by iodine vapor in a cell. Entire fields of velocity can be determined by using a solid-state camera to record the intensity variations throughout the field of view. However, the implementation of DGV has been centered principally on the use of high power, continuous-wave, ion lasers and measurement times that are determined by the 30-ms framing times of standard video cameras. Hence, they provide velocity fields that are averaged in time at least over that period. On the other hand, the PDV concept described in this presentation incorporates a high energy, repetitively pulsed, Nd-YAG laser that is injection-seeded to make it narrowband and then frequency-doubled to provide light at frequencies absorbed by the iodine vapor. The duration of each pulse is less than 10 nanoseconds. When used in combination with nonstandard, scientific quality, solid state cameras, a sequence of images can be obtained that provides instantaneous velocity vectors everywhere in the field of view. The investigations described in this paper include an accurate characterization of the iodine cell spectral behavior and its influence on the PDV measurements, a derivation of the PDV signal analysis requirements, and the unique aspects of the pulsed laser behavior related to this application. In addition, PDV measurements are to be demonstrated using data from a rotating wheel target and from the flow of a subsonic jet. Initially, single optical fiber light collection and photomultiplier detectors will be substituted for solid state cameras. Those results will allow the determination of the fundamental limitations of the PDV technique without the complications of image acquisition and processing. They will then be used to provide an analysis of the measurement capabilities of PDV both in small aerodynamic

research wind tunnels and in large wind tunnels designed for production airframe and propulsion testing. Future plans include the implementation of solid state cameras and the development of the required image acquisition and processing software. Eventually, the PDV technique will be applied to an aerodynamic research program related to transonic wing flutter.
Author
*Velocity Measurement; Pulsed Lasers; Doppler Effect; Narrowband*

**20010121971** Los Alamos National Lab., NM USA
**3rd Dimension of Planetary Exploration: Deep Subsurface Sampling**
Blacic, J. D.; Dreesen, D. S.; Mockler, T. T.; Sep. 20, 2000; 15p; In English
Report No.(s): DE2000-762915; LA-UR-00-4392; No Copyright; Avail: Department of Energy Information Bridge, Microfiche

Strategic planning for the exploration of the Martian subsurface to search for evidence of life, sources of water, and to determine the geologic makeup and history of the planet has begun. A mission to explore and sample the Martian subsurface hydrosphere, which may be 4-km deep will be more complex than any mission accomplished to date. In order to reduce risk, a phased approach is being planned with shallow and intermediate depth precursor mission. We researchers at Los Alamos National Laboratory are conducting a conceptual system study of a 200-m, intermediate-depth penetration and sampling mission on Mars. We constrained the study with a reasonable set of surface and subsurface environmental conditions and science requirements. Mission requirements include a 200-day duration, a soft lander which will fit within a Delta III payload fairing, a 250-kg drilling system mass limit, and a maximum available energy for drilling technologies are compared, and the down-selection process results in mechanical drilling/sampling subsystems that can be mixed to produce a number of specific systems that can be studied in more detail. Promising technology areas that need further investigation are identified.
NTIS
*Drilling; Mission Planning; Sampling; Mars Missions*

**20010122728** Lunar and Planetary Inst., Houston, TX USA
**Field Trip and Workshop on the Martian Highlands and Mojave Desert Analogs**
2001; 66p; In English; Martian Highlands and Mojave Desert Analogs, 20-27 Oct. 2001, Las Vegas, NV and Barstow, CA, USA; Sponsored by Lunar and Planetary Inst., USA; See also 20010122729 through 20010122753
Contract(s)/Grant(s): NASW-4574
Report No.(s): LPI-Contrib-1101; No Copyright; Avail: CASI; A04, Hardcopy; A01, Microfiche

This volume contains the program and abstracts that have been accepted for presentation at the Field Trip and Workshop on the Martian Highlands and Mojave Desert Analogs, October 20-27, 2001.
Derived from text
*Mars (Planet); Highlands; Mojave Desert (CA)*

**20010122729** Massachusetts Inst. of Tech., Dept. of Earth, Atmospheric and Planetary Science, Cambridge, MA USA
**Topography of Drainage Basins and Channels: Mars and Terrestrial Analogs**
Aharonson, O., Massachusetts Inst. of Tech., USA; Zuber, M. T., Massachusetts Inst. of Tech., USA; Rothman, D. H., Massachusetts Inst. of Tech., USA; Whipple, K. X., Massachusetts Inst. of Tech., USA; Schorghofer, N., Massachusetts Inst. of Tech., USA; Field Trip and Workshop on the Martian Highlands and Mojave Desert Analogs; 2001, pp. 7-8; In English; See also 20010122728; No Copyright; Avail: CASI; A01, Hardcopy; A01, Microfiche

Valley networks and channels on Mars were discovered during the Mariner 9 mission. Alternatives for their origin have been suggested, but the most widely accepted formation hypotheses is by erosion, and the most likely erosive agent is water. Morphometric criteria have been developed to detect incision by groundwater sapping and surface runoff. A distinction can be made by the change of valley widths, which increases downstream for runoff features but remains essentially constant for sapping features; by the shape of valley heads, which are tapered in rivers but theater-formed for sapping features; and by dendritic networks that are indicative of surface runoff. Such criteria require only planimetric images. Knowledge of the topography permits extension of such analyses using additional quantitative criteria. Longitudinal stream profiles, locations of channels relative to surface topography, and transverse cross-sections of valleys may now be used to constrain the genesis and evolution of Martian valleys. The analysis here proceeds by watershed computation of the of drainage systems, has been developed and tested extensively in terrestrial landscapes, and is also applied on Mars.
Author
*Topography; Structural Basins; Mars Surface; Erosion; Ground Water*

**20010122730** Jet Propulsion Lab., California Inst. of Tech., Pasadena, CA USA

**Noachian Faulting: What Do Faults Tell Us About the Tectonic History of Tharsis?**

Anderson, R. C., Jet Propulsion Lab., California Inst. of Tech., USA; Dohm, J. M., Arizona Univ., USA; Field Trip and Workshop on the Martian Highlands and Mojave Desert Analogs; 2001, pp. 9-10; In English; See also 20010122728; No Copyright; Avail: CASI; A01, Hardcopy; A01, Microfiche

The western hemisphere of Mars is dominated by the formation of Tharsis, which is an enormous high-standing region (roughly 25% of the surface area of the planet) capped by volcanics, including the solar system's largest shield volcanoes. Tharsis is surrounded by an enormous radiating system of grabens and a circumferential system of wrinkle ridges that extends over the entire western hemisphere of Mars. This region is perhaps the largest and most long lived tectonic and volcanic province of any of the terrestrial planets with a well-preserved history of magmatic-driven activity that began in the Noachian and has lasted throughout Martian geologic time. Tharsis and the surrounding regions comprise numerous components, including volcanic constructs of varying sizes and extensive lava flow fields, large igneous plateaus, fault and ridge systems of varying extent and relative age of formation, gigantic outflow channel systems, vast system of canyons, and local and regional centers of tectonic activity. Many of these centers are interpreted to be the result of magmatic-related activity, including uplift, faulting, dike emplacement, volcanism, and local hydrothermal activity. Below we present a summary of our work for Tharsis focusing primarily on the earliest stage of development, the Noachian period. Here we hone in on the early centers and how they relate to the early development of the Tharsis Magmatic Complex (TMC).

Author

*Mars Surface; Geological Faults; Volcanoes; Volcanology; Tectonics*

**20010122731** University of Central Florida, Dept. of Physics, Orlando, FL USA

**Impact Cratering on Mars During the Noachian Period**

Barlow, N. G., University of Central Florida, USA; Field Trip and Workshop on the Martian Highlands and Mojave Desert Analogs; 2001, pp. 11-12; In English; See also 20010122728; No Copyright; Avail: CASI; A01, Hardcopy; A01, Microfiche

The Martian highlands have been affected by numerous geologic processes, many of localized extent, but impact cratering was of major importance throughout the entire highlands. The Noachian-aged highlands materials formed during the period of late heavy bombardment when impact crater rates were substantially higher than during recent times. The craters in the highlands extend over a wider range of crater diameters than is seen for craters on post heavy bombardment aged terrains. In addition craters in the highlands display a wider range of degradation, suggesting that erosional and depositional processes were heightened during this time. Impact craters in the Martian highlands thus allow us to study (1) the population of impacting objects dominating at Mars during this early time, and (2) the degradational environment affecting the planet throughout its history.

Author

*Mars Craters; Mars Surface; Highlands; Degradation; Impact Damage*

**20010122732** Jet Propulsion Lab., California Inst. of Tech., Pasadena, CA USA

**Rock Abrasion and Ventifact Formation on Mars from Field Analog, Theoretical, and Experimental Studies**

Bridges, N. T., Jet Propulsion Lab., California Inst. of Tech., USA; Laity, J. E., California State Univ., USA; Field Trip and Workshop on the Martian Highlands and Mojave Desert Analogs; 2001, pp. 13; In English; See also 20010122728; No Copyright; Abstract Only; Available from CASI only as part of the entire parent document

Rocks observed by the Viking Landers and Pathfinder Lander/Sojourner rover exhibit a suite of perplexing rock textures. Among these are pits, spongy textures, penetrative flutes, lineaments, crusts, and knobs Fluvial, impact, chemical alteration, and aeolian mechanisms have been proposed for many of these. In an effort to better understand the origin and characteristics of Martian rock textures, abraded rocks in the Mojave Desert and other regions have been studied. We find that most Martian rock textures, as opposed to just a few, bear close resemblance to terrestrial aeolian textures and can most easily be explained by wind, not other, processes. Flutes, grooves, and some pits on Mars are consistent with abrasion by saltating particles, as described previously. However, many other rock textures probably also have an aeolian origin. Sills at the base of rocks that generally lie at high elevations, such as Half Dome, are consistent with such features on Earth that are related to moats or soil ramps that shield the basal part of the rock from erosion. Crusts consisting of fluted fabrics, such as those on Stimpy and Chimp, are similar to fluted crusts on Earth that spall off over time. Knobby and lineated rocks are similar to terrestrial examples of heterogeneous rocks that differentially erode. The location of specific rock textures on Mars also gives insight into their origin. Many of the most diagnostic ventifacts found at the Pathfinder site are located on rocks that lie near the crests or the upper slopes of ridges. On Earth, the most active ventifact formation occurs on sloped or elevated topography, where windflow is accelerated and particle kinetic energy and flux are increased. Integrated 0 together, these observations point to significant aeolian 0 modification of rocks on Mars and cast doubt on whether many primary textures resulting from other processes are preserved. Experimental simulations of abrasion in

the presence of abundant sand indicate that rocks on Mars should erode at a rate of 7.7 to 210 micrometers/yr. These rates cannot have operated over the entire history of the Pathfinder site or elsewhere on Mars, because craters, knobs, and other obstacles would be quickly worn away. More likely, rock abrasion occurs over short time periods when sand supplies are sufficient and saltation friction speeds are frequently reached. Depletion or exhaustion of sand and a decline in wind fluxes at speeds greater than that of saltation friction will then act to reduce the rate of further abrasion. We are currently engaged in a new set of wind tunnel experiments coupled with theoretical models and field studies that address rock abrasion and ventifact formation on Mars and Earth. These studies have implications for the Noachian, when sand supplies were probably more plentiful and the threshold friction speed was possibly lower because of a more dense atmosphere. Under these conditions, erosion rates from the wind could have been much greater than to day, contributing, along with probable fluvial erosion, to the Noachian landscape that is in limited preservation today.
Author
*Mars Surface; Rocks; Textures; Mojave Desert (CA); Abrasion; Planetary Geology; Sands*

**20010122734** National Air and Space Museum, Center for Earth and Planetary Studies, Washington, DC USA
**Martian Drainage Densities: Analyses from MOLA Digital Elevation Models**
Craddock, Robert A., National Air and Space Museum, USA; Irwin, Rossman P., National Air and Space Museum, USA; Howard, Alan D., Virginia Univ., USA; Field Trip and Workshop on the Martian Highlands and Mojave Desert Analogs; 2001, pp. 17-18; In English; See also 20010122728; No Copyright; Avail: CASI; A01, Hardcopy; A01, Microfiche

Martian valley networks indicate that at least geologic conditions were different in the past, if not the climate. It is commonly believed that valley networks must be the result of groundwater sapping because their apparent drainage densities are lower than terrestrial runoff channels. It has also been suggested that valley networks are not uniformly distributed on topography, which would also argue in favor of groundwater sapping. When coupled to the belief that early Mars was cold and dry such observations have led many investigators to suggest that valley networks were fed by geothermal heating of ground ice. This interpretation has become so entrenched in the planetary community that geothermal heating has essentially become a panacea. Valley networks are no longer seen as some of the best evidence for past surface water. Rather, they are automatically equated to a cold, dry climate. Unfortunately, however, plotting the densities of valley networks from imagery data is easily influenced by observational bias and image interpretation. Using topographic data from Mars Global Surveyor, we are in the process of making a more impartial analysis of valley network drainage densities and morphometric characteristics.
Author
*Mars Surface; Valleys; Topography*

**20010122736** North Carolina Univ., Dept. of Geography and Earth Sciences, Charlotte, NC USA
**Evolving Perspectives on the Geologic Evolution of Early Martian Crater Basins**
Forsythe, R. D., North Carolina Univ., USA; Blackwelder, C. R., North Carolina Univ., USA; Field Trip and Workshop on the Martian Highlands and Mojave Desert Analogs; 2001, pp. 21-22; In English; See also 20010122728; No Copyright; Avail: CASI; A01, Hardcopy; A01, Microfiche

This contribution continues to explore a model first proposed by Forsythe and Zimbleman, 1995 and expanded upon in the work of Forsythe and Blackwelder, 1998. The model views the ancient southern highlands of Mars as having formed under a climatic and hydrologic regime akin to semi-arid and and lands on Earth. Within this regime a groundwater table existed within the upper regolith, sufficiently shallow to be easily intercepted by impact basins a few kilometers in diameter. These depressions, when isolated from regional surface drainage networks, represent closed-drainage watersheds. Where positioned along outflow systems, the crater basins formed lakes, within which fluvial and lacustrine evidence exists for baselevel-controlled hydrology/geomorphology (e.g. terraces). The case for closed drainage crater basins is essentially a case for evaporite basins, and was further explored in detail in Forsythe and Blackwelder, 1998, wherein approximately 140 evaporite basins were identified by locating craters with inflow, but no surface water outflow, channels. Baselevel indicators, stream channel hydraulics, and nominal assumptions regarding hydrogeologic properties for Martian regolith were used in this study to constrain a MODFLOW simulation of a generic Martian Noachian evaporite basin. This simulation yielded evaporation rates of approximately 10-20 cm/yr and precipitation rates of 10-20 mm/yr. Here we explore the geologic implications of the early work and attempt to build a more evolutionary scheme for crater basin evolution.
Author
*Mars Craters; Mathematical Models; Mars Surface; Simulation; Planetary Geology*

**20010122737** Smithsonian Institution, Center for Earth and Planetary Studies, Washington, DC USA

**Exploring the Martian Highlands using a Rover-Deployed Ground Penetrating Radar**

Grant, J. A., Smithsonian Institution, USA; Schutz, A. E., Geophysical Survey Systems, Inc., USA; Campbell, B. A., Smithsonian Institution, USA; Field Trip and Workshop on the Martian Highlands and Mojave Desert Analogs; 2001, pp. 23-24; In English; See also 20010122728

Contract(s)/Grant(s): NAG5-9658; No Copyright; Avail: CASI; A01, Hardcopy; A01, Microfiche

The Martian highlands record a long and often complex history of geologic activity that has shaped the planet over time. Results of geologic mapping and new data from the Mars Global Surveyor spacecraft reveal layered surfaces created by multiple processes that are often mantled by eolian deposits. Knowledge of the near-surface stratigraphy as it relates to evolution of surface morphology will provide critical context for interpreting rover/lander remote sensing data and for defining the geologic setting of a highland lander. Rover-deployed ground penetrating radar (GPR) can directly measure the range and character of in situ radar properties, thereby helping to constrain near-surface geology and structure. As is the case for most remote sensing instruments, a GPR may not detect water unambiguously on Mars. Nevertheless, any local, near-surface occurrence of liquid water will lead to large, easily detected dielectric contrasts. Moreover, definition of stratigraphy and setting will help in evaluating the history of aqueous activity and where any water might occur and be accessible. GPR data can also be used to infer the degree of any post-depositional pedogenic alteration or weathering, thereby enabling assessment of pristine versus secondary morphology. Most importantly perhaps, GPR can provide critical context for other rover and orbital instruments/data sets. Hence, rover-deployment of a GPR deployment should enable 3-D mapping of local stratigraphy and could guide subsurface sampling. Author

*Mars Surface; Highlands; Ground Penetrating Radar; Remote Sensing; Weathering*

**20010122739** Washington Univ., Dept. of Earth and Planetary Sciences, Saint Louis, MO USA

**The Enigmatic Arabia Terra, Mars**

Hynek, B. M., Washington Univ., USA; Phillips, R. J., Washington Univ., USA; Field Trip and Workshop on the Martian Highlands and Mojave Desert Analogs; 2001, pp. 27-28; In English; See also 20010122728; No Copyright; Avail: CASI; A01, Hardcopy; A01, Microfiche

High-resolution altimetry and gravity data from Mars Global Surveyor (MGS) shed new light on the already perplexing province of Arabia Terra (0 deg - 45 deg N, -25 deg E eastward across the prime meridian to 40 deg E). Traditionally, this region has been considered a part of the ancient highlands that cover the southern part of Mars that are thought to represent the final stages of heavy bombardment, over 3.7 G.A. However, recent results from MGS reveal that Arabia Terra has several unique properties, indicating that it may have a history considerably different than the rest of the uplands.
Author

*Mars Surface; Planetary Geology*

**20010122740** Virginia Univ., Dept. of Environmental Sciences, Charlottesville, VA USA

**Drainage Basin Integration in the Martian Highlands**

Irwin, R. P., III, Virginia Univ., USA; Craddock, R. A., National Air and Space Museum, USA; Field Trip and Workshop on the Martian Highlands and Mojave Desert Analogs; 2001, pp. 29-30; In English; See also 20010122728; No Copyright; Avail: CASI; A01, Hardcopy; A01, Microfiche

Martian ancient valley networks commonly have short valley lengths compared to their terrestrial counterparts, which suggests that the martian landscape has poorly integrated drainage or that the valley networks are poorly developed within their catchments. Superposition relationships and crater counts hold that valley network development occurred contemporaneously with highland crater degradation. MOLA topographic data and stereo photography have been used to delimit drainage basins on the quadrangle and larger map scales. Here we discuss the effect of cratering on valley network development and the response of the networks to disruption by impacts.
Author

*Structural Basins; Mars Surface; Highlands; Valleys; Cratering; Impact Damage*

**20010122742** Lunar and Planetary Inst., Houston, TX USA

**Detecting Minerals on Mars using TES, THEMIS, and Mini-TES**

Kirkland, L. E., Lunar and Planetary Inst., USA; Herr, K. C., Aerospace Corp., USA; Salisbury, J. W., Johns Hopkins Univ., USA; Keim, E. R., Aerospace Corp., USA; Adams, P. M., Aerospace Corp., USA; Hackwell, J. A., Aerospace Corp., USA; Field Trip and Workshop on the Martian Highlands and Mojave Desert Analogs; 2001, pp. 33-34; In English; See also 20010122728; No Copyright; Avail: CASI; A01, Hardcopy; A01, Microfiche

There has been no definitive infrared spectral evidence for carbonates on Mars, and this result affects early Mars ”dry” vs. ”wet” hypotheses. The near-term search for minerals is being conducted by the 1996 Thermal Emission Spectrometer (TES), the 2001 9-band radiometer THEMIS, and the 2003 lander Mini-TES. Christensen et al. conclude that TES has recorded the signature of surface silicates and hematite. However, TES has not detected definitive signatures of minerals such as carbonates and sulfates, although they are predicted to be present, and TES was expected to be able to detect them. Current explanations for the puzzling lack of carbonate detections include that they were never there; are buried; altered by UV radiation; occur exclusively in small deposits (exposed over less than one-tenth of the TES -3 km x 5 km field of view); or are rough and weathered, and so exhibit low spectral contrast. If Mars had a denser atmosphere in its past and liquid water on its surface, then large deposits of carbonates likely formed. Thus the lack of carbonate detections affects interpretations of Mars' geologic and climatic history, even though its cause is poorly understood. It may also affect landing site selections. Interpretations of TES spectra typically use laboratory spectra of smooth, fresh mineral surfaces. However, spectra of fresh mineral surfaces are frequently a poor match to spectra measured of rough and weathered surfaces. For TES, THEMIS, and Mini-TES to attain their predicted mineral detection limits, minerals must be present under specific conditions: well-crystalline, uncoated, smooth-surfaced at several scales, and low atmospheric downwelling radiance contribution. These issues raise the question of whether non-silicate minerals are rare on Mars, or whether smooth, uncoated deposits of well-crystalline minerals are rare. These caveats should be considered when using a lack of mineral detections to interpret the geologic and climatic history of Mars.
Author
*Minerals; Mars Surface; Thermal Emission; Spectrometers; Radiometers; Remote Sensing*

**20010122743** Academy of Sciences (USSR), IGEM, Moscow, USSR
**The Composition of the Martian Highlands as a Factor of Their Effective Uplifting, Destruction and Production of Voluminous Debris**
Kochemasov, G. G., Academy of Sciences (USSR), USSR; Field Trip and Workshop on the Martian Highlands and Mojave Desert Analogs; 2001, pp. 35-36; In English; See also 20010122728; No Copyright; Avail: CASI; A01, Hardcopy; A01, Microfiche

As was predicted before ”Pathfinder” launch the composition of the martian highlands is principally different from that of the martian lowlands (earlier the majority of scientists believed that both crusts are basaltic: altered and fresh). The wave planetology precludes similar compositions (similar densities) for uplifted and subsided blocks of a rotating celestial body. The higher global relief range, the higher density range of mean lithologies of raised and fallen planetary blocks. At Venus it is the range between magnesium and alkali basalts, at Earth between tholeiltes and andesites (the mean composition of continents), at Mars between Fe-basalts and rocks of granitic, syenitic, albititic affinities. The new discoveries at Mars support this natural requirement. Fractionated Si, Al, K-rich rocks occur in the contact between lowlands and highlands (something similar to the intermediate andesites between basaltic oceans and light -not dense continents at Earth). The MGS gravity data indicate that the thick highland crust is much less dense than the thin lowland crust. The high chlorine content in the martian rocks and soils (0.3-0.6 weight %) is a geochemical indicator of acid and more probably alkaline igneous compositions of highlands. In terrestrial rocks such Cl contents as 0.2-2.5 % can be found in nepheline and sodalite syenites of Lovozero massif (Kola peninsula), in sodalite-bearing lavas in Latium (Italy), in France, at Mount Suswe (Kenya) [6]. Chlorine contents in intermediate and basic terrestrial rocks are much lower (0.005-0.01 weight %). The martian cratered highlands, composed of ”not dense” relative to basalts igneous material, due to tendency of uplifting and hence intensive destruction produce huge amounts of detrital material obliterating small craters, smoothing crater rims, giving landslides and lobes, dry (and wet?) debris flows and layered deposits.
Author
*Mars Surface; Highlands; Debris; Crusts; Planetary Geology*

**20010122744** Jet Propulsion Lab., California Inst. of Tech., Pasadena, CA USA
**SNOOPY: Student Nanoexperiments for Outreach and Observational Planetary Inquiry**
Kuhlma, K. R., Jet Propulsion Lab., California Inst. of Tech., USA; Hecht, M. H., Jet Propulsion Lab., California Inst. of Tech., USA; Brinza, D. E., Jet Propulsion Lab., California Inst. of Tech., USA; Feldman, J. E., Jet Propulsion Lab., California Inst. of Tech., USA; Fuerstenau, S. D., Jet Propulsion Lab., California Inst. of Tech., USA; Friedman, L., Planetary Society, USA; Kelly, L., Planetary Society, USA; Oslick, J., Planetary Society, USA; Polk, K., Planetary Society, USA; Moeller, L. E., Planetary Society, USA; Field Trip and Workshop on the Martian Highlands and Mojave Desert Analogs; 2001, pp. 37-38; In English; See also 20010122728; No Copyright; Avail: CASI; A01, Hardcopy; A01, Microfiche

As scientists and engineers primarily employed by the public, we have a responsibility to ”communicate the results of our research so that the average American could understand that NASA is an investment in our future...”. Not only are we employed by the public, but they are also the source of future generations of scientists and engineers. Teachers typically don't have the time or expertise to research recent advances in space science and reduce them to a form that students can absorb. Teachers are also

often intimidated by both the subject and the researchers themselves. Therefore, the burden falls on us - the space scientists and engineers of the world - to communicate our findings in ways both teachers and students can understand. Student Nanoexperiments for Outreach and Observational Planetary InquirY (SNOOPY) provides just such an opportunity to directly involve our customers in planetary science missions.
Author
*Education; Space Missions; Students; Spaceborne Experiments*

**20010122747** Pittsburgh Univ., Dept. of Geology and Planetary Science, Pittsburgh, PA USA
**Fluvial Degradation of the Circum-Hellas Highlands of Mars**
Mest, S. C., Pittsburgh Univ., USA; Crown, D. A., Pittsburgh Univ., USA; Field Trip and Workshop on the Martian Highlands and Mojave Desert Analogs; 2001, pp. 43-44; In English; See also 20010122728; No Copyright; Avail: CASI; A01, Hardcopy; A01, Microfiche

Geologic mapping and geomorphic analyses of Noachian-to Amazonian-aged terrains in the highlands east and north of Hellas basin have revealed the effects of volcanic, fluvial, aeolian, and mass wasting processes. Mars Global Surveyor (MGS) and Viking Orbiter data sets are currently being used to qualitatively and quantitatively analyze highland evolution, particularly degradation resulting from fluvial processes. Fluvial features include small highland gullies, well-integrated valley networks, and extensive outflow channels systems. These features represent different types of fluvial activity, and their presence in units of different ages indicates fluvial activity spans a large portion of the region's history. It is necessary to characterize the features and units in which they occur in order to fully understand the nature of Martian fluvial activity and ultimately the history of Mars' climate. The results of these studies support the Goal of NASA's Mars Exploration program by determining: (1) locations for future landing sites; (2) areas in which water may be present in the subsurface; and (3) areas where life may have developed and its fossilized remnants may have been preserved.
Author
*Degradation; Highlands; Mars Surface; Planetary Geology; Geomorphology*

**20010122749** California Univ., Space Sciences Lab., Berkeley, CA USA
**Surficial Studies of Mars Using Cosmogenic Nuclides**
Nishiizumi, K., California Univ., USA; Field Trip and Workshop on the Martian Highlands and Mojave Desert Analogs; 2001, pp. 47-48; In English; See also 20010122728; No Copyright; Avail: CASI; A01, Hardcopy; A01, Microfiche

Cosmogenic nuclides (CNs) are produced by cosmic-ray nuclear interactions with target nuclei in rocks, soils, ice, and the atmosphere. Cosmogenic nuclides have been widely used for investigation of solar system matter for several decades. Stable nuclides, such as He-3, Ne-21, and Ar-38, are built up over time as the surface is exposed to cosmic rays. The concentrations of cosmogenic radionuclides, such as Be-10, Al-26, and C-14 also build up with exposure time but reach saturation values after several half-lives. Especially since the development of accelerator mass spectrometry (AMS), CNs in terrestrial samples have been routinely used for geomorphic studies such as glaciation, surface erosion, and tectonics, and studies of atmospheric and ocean circulation. Cosmogenic nuclides on Mars will be able to answer questions of exposure ages, erosion rates, tectonic events, and deposition rates of sediments and/or volatiles. The concentrations of cosmogenic stable nuclides give the integrated exposure time of the rock/mineral, and the activities of radionuclides give recent records for times back as long as a few half-lives.
Author
*Cosmic Rays; Nuclear Interactions; Nuclides; Mars (Planet); Mars Atmosphere; Mars Surface*

**20010122750** Geological Survey, Flagstaff, AZ USA
**Possible Formation Processes for Martian Crystalline Hematite**
Noreen, Eric D., Geological Survey, USA; Chapman, M. G., Geological Survey, USA; Tanaka, K. L., Geological Survey, USA; Field Trip and Workshop on the Martian Highlands and Mojave Desert Analogs; 2001, pp. 49-50; In English; See also 20010122728; No Copyright; Avail: CASI; A01, Hardcopy; A01, Microfiche

The Thermal Emission Spectrometer (TES) on the Mars Global Surveyor (MGS) has detected large concentrations of bulk crystalline hematite within the western equatorial region of Mars. The hematite represents a unique and enigmatic spectral signature of surface rock distinct from basalt or basaltic andesite. Analysis of the spectral data also suggests that the hematite grains are axis-oriented. This discovery of large concentrations of hematite is interesting because on Earth, production of iron oxides at this scale would require large quantities of liquid water, a known requirement for life. While no one hypothesis as to how the hematite formed has been excluded at this time, examination of the morphology of the deposits may favor a hydrothermal origin.
Author
*Crystallinity; Hematite; Mars Surface; Morphology; Mineral Deposits*

**20010122751** Jet Propulsion Lab., California Inst. of Tech., Pasadena, CA USA

**Accessing Martian Fluvial and Lacustrine Sediments by Landing in Holden Crater, Margaritifer Sinus**

Parker, T. J., Jet Propulsion Lab., California Inst. of Tech., USA; Grant, J. A., National Air and Space Museum, USA; Field Trip and Workshop on the Martian Highlands and Mojave Desert Analogs; 2001, pp. 51-52; In English; See also 20010122728; No Copyright; Avail: CASI; A01, Hardcopy; A01, Microfiche

Rover missions to the surface of Mars after MER 2003, are likely to be centered around focused geologic field mapping. One objective with high priority in selecting landing sites for these missions will be to characterize the nature, spatial distribution, internal structure, composition, and depositional history of exposed sedimentary layered deposits by visiting a number of distributed outcrops identified previously (and with a high degree of certainty) from orbit. These deposits may contain prebiotic material, even fossil organisms, but their primary value will be to enable an assessment of the planet's climate at the time they were emplaced. High resolution imaging from a mobile rover will enable the detailed study of these deposits over a wide area, their internal structure and mineralogy at distributed localities, and could resolve biologically-derived structures (such as stromatolite-like textures) if they are present. With the addition of a spectrometer, it should be possible to ascertain the presence of carbonates, sulfates, organics, water (liquid, frost, and bound water), as well as a variety of silicate minerals in the context of the collected imagery. Such a mission approach is directly relevant to future exploration of Mars, because it provides the geologic context comparable to what a field geologist visiting a site for the first time would acquire. Rover missions after MER will likely have much better targeting and hazard avoidance landing systems, enabling access to planimetrically-challenged sites of high scientific interest. These vehicles will also likely have greater mobility than MER, capable of driving greater distances in a shorter amount of time. Many scientists and mission planners have realized the need to design a rover whose mobility can be comparable to the dimensions of its 3-sigma landing error ellipse.

Author

*Mars (Planet); Mars Surface; Sediments; Mars Craters; Geological Surveys*

**20010122752** Arizona State Univ., Dept. of Geological Sciences, Tempe, AZ USA

**High Latitude Terrestrial Lacustrine and Fluvial Field Analogs for the Martian Highlands**

Rice, J. W., Jr., Arizona State Univ., USA; Field Trip and Workshop on the Martian Highlands and Mojave Desert Analogs; 2001, pp. 53-54; In English; See also 20010122728; No Copyright; Avail: CASI; A01, Hardcopy; A01, Microfiche

"Study nature not books" was the overriding philosophy of Louis Agassiz, the first geologist to formulate and advance the theory of Ice Ages. His work was primarily based on his field observations. J. Harlan Bretz also followed this philosophy in determining that catastrophic floods formed the Channeled Scabland in Washington state. It is with this philosophy in mind that Mars analog field investigations are being conducted in regions on earth that approximate Martian climatic, geologic, and geomorphic conditions. High latitude field investigations conducted in Iceland, the ice-free regions of Antarctica and the High Arctic are a very useful aid and tool to understanding certain Martian geological processes and landforms. These regions will also be used one day to train astronauts in preparation for manned missions to Mars within the next 15-20 years. Analog field studies do have limitations after all they are conducted on earth. However, a catastrophic flood, for example on either Mars or earth (Iceland), will leave behind similar landforms and deposits. The value of conducting field investigations in terrestrial geologic studies is obvious and unquestioned despite advancements in remote sensing capabilities. Planetary geologic studies are conducted in a 'reverse format' compared to terrestrial geologic studies. These differences can be summarized by the following: terrestrial geologic studies go from local to global explanations and planetary geologic studies go from global to local explanations. Therefore, in order to understand Mars we should first attempt to understand our own terrestrial backyard. This is not as easy as it appears take the Channeled Scabland; although everyone now agrees that catastrophic floods formed this landscape, there is no agreement on the quantity and magnitude of these floods. This landscape was formed only about 13,000 years ago and is easily accessible for field studies. It is interesting to conjecture that some processes and landforms on Mars may be distinctly and uniquely Martian. Nevertheless, the value of fieldwork in deciphering Martian geologic processes will be crucial to the planning and operations of any future surface missions to Mars.

Author

*Mars Surface; Highlands; Geological Surveys; Iceland; Mars (Planet); Polar Regions*

**20010123757** Mercury Seven Foundation, Titusville, FL USA

**Moon Shot: The Inside Story of America's Race to the Moon**

Shepard, Alan, Mercury Seven Foundation, USA; Slayton, Donald, Slayton (Donald), USA; Barbree, Jay, Consultant, USA; Benedict, Howard, Mercury Seven Foundation, USA; [1994]; 383p; In English

Report No.(s): LC-94-3027; ISBN 1-878685-54-6; Copyright; Avail: Issuing Activity

July 20, 1969. Eight short years after President John F. Kennedy promised America that the newly formed NASA would land a man on the moon, the crew of Apollo 11 touched down on the Sea of Tranquility in triumph. Three months on the New York Times bestseller list, "Moon Shot" is the never-before-told story of the courage, dedication, and teamwork that made that journey to the moon possible. Astronauts Alan Shepard and Deke Slayton, members of the original Mercury Seven team, were part of America's pioneering space program from the beginning and were perfectly placed to tell this inside story. An intense human drama of the sacrifices and risks asked of a small but remarkable group of astronauts, "Moon Shot" takes us back to the days of discovery and achievement, revealing the men behind the heroes, and the successes, bitter disappointments, and even tragedy that shaped the world of those who risked everything to tackle the unknown.
Derived from text
*Astronauts; Apollo 11 Flight; Lunar Landing*

**20010124826** Lunar and Planetary Inst., Houston, TX USA
**Workshop on Mercury: Space Environment, Surface, and Interior**
Mercury: Space Environment, and Surface and Interior; 2001; 130p; In English, 4-5 Oct. 2001, Chicago, IL, USA; Sponsored by Lunar and Planetary Inst., USA; See also 20010124827 through 20010124898
Contract(s)/Grant(s): NASW-4574
Report No.(s): LPI-Contrib-1097; No Copyright; Avail: CASI; A07, Hardcopy; A02, Microfiche

This volume contains abstracts that have been accepted for presentation at the Workshop on Mercury: Space Environment, Surface, and Interior, October 4-5, 2001. The Scientific Organizing Committee consisted of Mark Robinson (Northwestern University), Marty Slade (Jet Propulsion Laboratory), Jim Slavin (NASA Goddard Space Flight Center), Sean Solomon (Carnegie Institution), Ann Sprague (University of Arizona), Paul Spudis (Lunar and Planetary Institute), G. Jeffrey Taylor (University of Hawai'i), Faith Vilas (NASA Johnson Space Center), Meenakshi Wadhwa (The Field Museum), and Thomas Watters (National Air and Space Museum). Logistics, administrative, and publications support were provided by the Publications and Program Services Departments of the Lunar and Planetary Institute.
Author
*Abstracts; Conferences; Mercury (Planet)*

**20010124827** Jet Propulsion Lab., California Inst. of Tech., Pasadena, CA USA
**Mercury's Global Topography from Radar Ranging Data**
Anderson, J. D., Jet Propulsion Lab., California Inst. of Tech., USA; Schubert, G., California Univ., USA; Asmar, S. W., Jet Propulsion Lab., California Inst. of Tech., USA; Jurgens, R. F., Jet Propulsion Lab., California Inst. of Tech., USA; Lau, E. L., Jet Propulsion Lab., California Inst. of Tech., USA; Moore, W. B., California Univ., USA; Slade, M. A., III, Jet Propulsion Lab., California Inst. of Tech., USA; Standish, E. M., Jr., Jet Propulsion Lab., California Inst. of Tech., USA; Mercury: Space Environment, and Surface and Interior; 2001, pp. 1; In English; See also 20010124826; No Copyright; Abstract Only; Available from CASI only as part of the entire parent document

When Mercury's radius is expanded in Legendre functions to the second degree and order, the systematic error in radar ranging data is reduced substantially. Previously, data spanning an observing interval from 1966 to 1990 were used to infer an equatorial ellipticity (a - b)/a = (540 +/- 54) X 10(exp -6) and a center-of-figure minus center-of-mass offset of (640 +/- 78) m. The magnitude of this equatorial center of figure offset implies an excess crustal thickness of 12 km or less, comparable to the Moon's excess. by comparing the equatorial ellipticity with the Mariner 10 gravity field, and assuming Airy isostatic compensation, bounds on crustal thickness can be derived. Mercury's crustal thickness is in the range from 100 to 300 km. The Mercury radar ranging observing interval has been extended from 1966 to the present. In addition, improvements in data reduction techniques have resulted in a set of Mercury ranging data less affected by systematic error, in particular the biases introduced by local topographic variations. We use this new set of reduced ranging data to improve Mercury's global topography and center-of-figure minus center-of-mass offset. New results on crustal thickness are derived, and prospects for further improvement with Mercury Orbiter data are discussed.
Author
*Mercury (Planet); Radar Data; Data Reduction; Mercury Surface; Radar Range*

**20010124828** Carnegie Institution of Washington, Dept. of Terrestrial Magnetism, Washington, DC USA
**Applying Numerical Dynamo Models to Mercury**
Aurnou, J. M., Carnegie Institution of Washington, USA; Al-Shamali, F. M., Alberta Univ., Canada; Mercury: Space Environment, and Surface and Interior; 2001, pp. 2-3; In English; See also 20010124826; No Copyright; Abstract Only; Available from CASI only as part of the entire parent document

Measurements made during the Mariner 10 fly-bys detected that Mercury has an intrinsic magnetic field. It was inferred that the field is dominantly dipolar with an average equatorial field intensity of 0.003 gauss. This corresponds to a dipole moment or 5 x 10(exp 12) T cu m, roughly 0.07% that of the Earth. In dynamo theory, the magnetic field intensity is often non-dimensionalized by the Elsasser number, Lambda = sigma Beta(exp 2)/2rho Omega, where sigma is the electrical conductivity, Beta is the magnetic induction, rho is the density and Omega is the angular velocity of planetary rotation. The Elsasser number represents the ratio of the Lorentz forces produced by the magnetic field and the Coriolis forces due to planetary rotation. Estimates of Lambda for most of the known planetary dynamos in our solar system are of order unity. For Mercury, we estimate that Lambda is approximately 5 x 10(exp -4) using core parameter values of sigma is approximately 10(exp 6) rho m(exp -1), Beta is approximately 0.03 gauss, rho is approximately 7 x 10(exp 3) kg/cu m, and Omega = 2pi/58.6 days. Clearly, this Lambda estimate is far less than unity. This indicates that the Hermean field is weak, not only in absolute magnitude, but also dynamically, in that the Lorentz forces are far smaller than the Coriolis forces generated by planetary rotation. Two main explanations have been put forward to explain the weak magnetic field of Mercury. The first argues that the magnetic field measured by Mariner 10 is produced by global-scale remanent magnetization of Mercury's crust. In this theory, the presently observed field has been frozen into magnetic minerals contained in the crust. The remanent magnetization was acquired when the crust cooled in the presence of an early dynamo field. This scenario is similar to those proposed to explain the strong magnetic anomalies detected in the southern hemisphere of Mars. If this theory is correct, then Mercury's magnetic field should remain fixed in time, with no detectable secular variation occurring over any timescale of measurement. In addition, strong short-wavelength crustal signals may also be detected, similar to the magnetic anomalies on Mars. The second possibility is that Mercury's magnetic field is internally-generated by an active fluid dynamo within the planet's huge, iron-rich core. The necessary (but not sufficient) conditions for the possible existence of a planetary dynamo require 1) a sufficiently large region of electrically conducting fluid present within the planet, 2) an energy source to drive motions of the conducting fluid and 3) a planetary rotation rate that is strong enough to appropriately organize the net fluid motions. Thermal evolution models of Mercury show that the core can remain partially liquid depending on the amount of sulfur present. For non-zero values of the core sulfur content, the melting point of the core material will be strongly depressed such that a spherical shell of liquid core material may exist. Assuming that such a liquid layer exists, and is not exceedingly thin, thermochemical convection is likely to occur. Experiments in liquid metals show that for even very weakly supercritical thermal convection, the fluid motions tend to be turbulent. Thus, if there is sufficient energy such that convective motions exist in the core fluid layer, then those motions may be able to sustain dynamo action. In addition, the rotation rate of Mercury is sufficiently rapid to organize the turbulent flow in all but the thinnest fluid layers. This claim is based on the findings of the present generation of geodynamo simulations which are all run at numerical rotation rates far slower than that of Mercury. In these simulations, the flow field remains strongly controlled by rotation even for Lambda approximately equals 10. Additional information is contained in the original extended abstract.

Author

*Dynamo Theory; Mathematical Models; Mercury (Planet); Planetary Magnetic Fields; Planetary Rotation; Planetary Cores*

**20010124829** Innovative Technical Solutions, Honolulu, HI USA

**Reflectance Spectra of Lunar Pure Anorthosites and of Mercury**

Blewett, D. T., Innovative Technical Solutions, USA; Hawke, B. R., Hawaii Univ., USA; Lucey, P. G., Hawaii Univ., USA; Mercury: Space Environment, and Surface and Interior; 2001, pp. 4-5; In English; See also 20010124826; No Copyright; Abstract Only; Available from CASI only as part of the entire parent document

Remote sensing measurements at a variety of wavelengths indicate that the surface of Mercury must be low in iron and titanium, with FeO + TiO2 approximately less than 6 wt.%. Earth-based reflectance spectrometry has discovered portions of the lunar surface that are extremely low in FeO, less than 2-3 wt.%, and are believed to be composed of pure anorthosite (greater than 90% plagioclase). Global imaging from the Clementine mission, along with a method for the determination of FeO abundance from multispectral measurements has led to the identification of large regions of the lunar farside that are low in FeO content. The present work extends a previous study comparing spectra of Mercury to those of lunar anorthosites. The newly identified mature areas of very low iron content on the Moon may be analogs for much of Mercury. Additional information is contained in the original extended abstract.

Author

*Anorthosite; Lunar Surface; Mercury Surface; Reflectance; Spectrometers*

**20010124830** Johns Hopkins Univ., Applied Physics Lab., Laurel, MD USA

**ENA Imaging at Mercury? Lessons from IMAGE/HENA**

Brandt, P. C., Johns Hopkins Univ., USA; Mitchell, D. G., Johns Hopkins Univ., USA; Barabash, S., Swedish Inst. of Space Physics, Sweden; Mercury: Space Environment, and Surface and Interior; 2001, pp. 6; In English; See also 20010124826; No Copyright; Abstract Only; Available from CASI only as part of the entire parent document

Due to the extremely dynamic nature of the Hermean magnetosphere there is a demand for global imaging techniques in a future mission to Mercury. Energetic neutral atom (ENA) imaging is a new technique that allows space plasma to be imaged. A few mission has utilized this technique at Earth and it has proven to be a powerful tool for space plasma diagnostics. There are plans to apply ENA imaging to investigate the Hermean magnetosphere. Questions have been raised what ENA imaging really can measure at Mercury and simulations have been trying to partly answer those questions. In this presentation we will present ENA images from the Terrestrial magnetosphere and explore what lessons can be given when applied to the Hermean magnetosphere.

Author

*Imaging Techniques; Mercury (Planet); Plasma Diagnostics; Earth Magnetosphere; Planetary Magnetospheres*

**20010124831** National Museum of Natural History, Dept. of Mineral Sciences, Washington, DC USA

**Reflectance Spectra of Aubrites, Sulfides, and E Asteroids: Possible Implications for Mercury**

Burbine, T. H., National Museum of Natural History, USA; McCoy, T. J., National Museum of Natural History, USA; Cloutis, E. A., Winnipeg Univ., Canada; Mercury: Space Environment, and Surface and Interior; 2001, pp. 7-8; In English; See also 20010124826; No Copyright; Abstract Only; Available from CASI only as part of the entire parent document

One of the science objectives of the proposed missions to Mercury is to determine its surface composition. Telescopic observations of Mercury from Earth are extremely difficult due to Mercury's proximity to the Sun. Previous spectral measurements show a weak feature centered at approximately 0.9 microns; however, it is not entirely certain if this feature is due to Fe(2+) in the silicates or due to the incomplete removal of an atmospheric water feature in the spectra. Many researchers have noted the spectral similarity in shape and slope of Mercury to the lunar highlands. Analyses of the 'best' telescopic spectra have led to estimates of FeO contents of Mercury's surface to be between 3-6 wt.%, assuming Mercury has a surface composition similar to lunar anorthosites. However, it has also been postulated that Mercury's crust contains lower amounts of FeO. One possibility is that it has a surface composed predominately of enstatite (a Mg-rich pyroxene). Enstatite found in meteorites has a featureless spectrum due to the almost complete absence of iron in the silicates. Mercury's location at 0.4 AU may be consistent with its formation out of highly reduced material, possibly similar to the enstatite chondrites, which then experienced significant degrees of melting. These meteorites contain minerals (primarily enstatite) that condense out of the solar nebula at relatively high temperatures. Sulfur, volatilized from sulfides in Mercury's crust, has been proposed as a possible alternative to water ice as the cause of Mercury's bright radar spots at its poles. Our closest analog to Mercury's composition could be the differentiated enstatite-rich meteorites called the aubrites and their proposed asteroidal parent bodies, the E asteroids. Aubrites are composed of essentially iron-free enstatite plus minor accessory phases such as metallic iron and sulfides. Sulfides found in aubrites include troilite (FeS), oldhamite (CaS), ferromagnesian alabandite ((Mn,Fe)S), and daubreelite (FeCr2S4). These questions on Mercury's surface compositions should be answered by the MESSENGER and Bepi-Colombo missions. Both spacecrafts will obtain visible and near-infrared reflectance spectra and elemental ratios from X-ray and gamma-ray measurements of Mercury. Elemental ratios such as Al/Si, Ca/Si, Fe/Si, and Mg/Si can easily distinguish between a surface composition similar to the lunar highlands and one similar to the aubrites. If Mercury has an enstatite-rich surface, what would be its spectral properties? to investigate the spectral properties of an enstatite-rich surface, we have done a spectral survey of aubrites and their constituent minerals. We will focus on sulfur and sulfides, which have distinctive spectral characteristics. Additional information is contained in the original extended abstract.

Author

*Mercury (Planet); Mercury Surface; Spectral Reflectance; Planetary Composition*

**20010124832** California Inst. of Tech., Pasadena, CA USA

**The Nature of the Mercury Polar Radar Features**

Muhleman, D. O., California Inst. of Tech., USA; Mercury: Space Environment, and Surface and Interior; 2001, pp. 9-10; In English; See also 20010124826; No Copyright; Abstract Only; Available from CASI only as part of the entire parent document

In 1991, two new radar techniques were used for the first time to probe the surface of Mercury, by two different groups. The results were quite unexpected, and puzzling. In both experiments, the regions of the surface which had the highest radar albedo (were the best radar reflectors) were very near the north and south poles. These polar features also had the very unusual characteristic that more signal was received in the same circular polarization sense as had been transmitted, rather than the opposite

sense. This is an unexpected occurrence (radar astronomers call it a 'polarization inversion'), since single reflections of the radar will result in a polarization reversal, and so more signal is generally received in the opposite sense than that transmitted. This peculiar radar signature is generally only observed in regions on solar system bodies which are known to have some kind of ice present, like the large moons of Jupiter, the polar caps of Mars, and portions of glaciers and ice and snow fields in Greenland and the Himalayas and Andes on Earth. From the initial Arecibo observations, it was clear that the feature near the south pole was related to the large (150 km diameter) crater Chao Meng-Fu. The feature near the north pole seemed to be composed of several smaller features, and was somewhat more confusing and harder to interpret with the initial data. Further experiments from Arecibo (after the power upgrade) produced extremely good, high resolution (1.5-3 km) images of the north polar region. Unfortunately, the south polar region has not been accessible to Arecibo since the upgrade, and so the images of that region are not quite so good (resolution only about 15 km), but are still quite spectacular. Where these radar images could be compared to the photographs from Mariner 10, it was immediately apparent (even from the lower resolution images) that the high albedo, polarization inversion regions were all located within the boundaries of craters. Additional information is contained in the original extended abstract.
Author
*Mercury (Planet); Mercury Surface; Radar Imagery; Radar Echoes; Polar Regions*

**20010124834** Osservatorio Astronomico, Capodimonte, Naples, Italy
**A Multi-Colour Imaging System for the Bepi Colombo Mercury Lander**
Colangeli, L., Osservatorio Astronomico, Capodimonte, Italy; Palumbo, P., Naples Univ., Italy; Barbieri, C., Osservatorio Astronomico, Italy; Bellucci, G., Consiglio Nazionale delle Ricerche, Italy; Bini, A., Alenia Difesa, Italy; Blanco, A., Lecce Univ., Italy; Cremonese, G., Osservatorio Astronomico, Italy; DellaCorte, V., Osservatorio Astronomico, Capodimonte, Italy; Fonti, S., Lecce Univ., Italy; Epifani, E. Mazzotta, Osservatorio Astronomico, Capodimonte, Italy; Mercury: Space Environment, and Surface and Interior; 2001, pp. 13; In English; See also 20010124826; No Copyright; Abstract Only; Available from CASI only as part of the entire parent document

The ESA (European Space Agency) 'Bepi Colombo' space mission to Mercury includes a lander system for the study of planet surface characteristics. Surface-based geology and mineralogy measurements are needed to expand and complement remote sensing observations. In the complement of the lander payload, cameras are required to provide (multicolor) images of the landing site during and after descent. The study of Mercury surface morphology and composition is particularly relevant in the context of the Solar System exploration due to the heavy evolution/processing of this planet. However, available information is rather poor and in situ multi-spectral imaging investigation of the local environment will provide essential clues to the understanding of Mercury present state and past evolution. In this work we present a preliminary study of a multi-spectral imaging system, potentially candidate for the lander camera. Technical details must be defined considering the stringent requirements imposed by the mission profile, harsh environment and foreseen limited resources. Therefore, selected technologies are aimed at a miniaturized system.
Author
*Cameras; Mercury (Planet); Mercury Surface; Space Missions; Surface Properties; Color Photography*

**20010124835** National Air and Space Museum, Center for Earth and Planetary Studies, Washington, DC USA
**Digital Elevation Model Mosaic of Mercury**
Cook, A. C., National Air and Space Museum, USA; Watters, T. R., National Air and Space Museum, USA; Robinson, M. S., Northwestern Univ., USA; Mercury: Space Environment, and Surface and Interior; 2001, pp. 14-15; In English; See also 20010124826
Contract(s)/Grant(s): NAG5-9076; NAG5-1029; No Copyright; Abstract Only; Available from CASI only as part of the entire parent document

At CEPS (Center for Earth and Planetary Studies) work has been underway since 2000 to semi-automatically stereo match all Mariner 10 stereo pairs. The resulting matched image coordinates are converted into longitude, latitude, and height points and then combined to form a map projected Digital Elevation Model (DEM) mosaic of the planet's surface. Stereo images from Mariner 10 cover one quarter of the planet's surface, mostly in the southern hemisphere. Additional information is contained in the original extended abstract.
Author
*Coordinates; Mariner 10 Space Probe; Mercury (Planet); Stereophotography; Mercury Surface*

**20010124836** NASA, Washington, DC USA

**Mid-Infrared Spectra of Mercury**

Cooper, B., Oceaneering Space Systems, USA; Potter, A. E., National Solar Observatory, USA; Killen, R. M., Southwest Research Inst., USA; Morgan, T. H., NASA, USA; Mercury: Space Environment, and Surface and Interior; 2001, pp. 16-17; In English; See also 20010124826; No Copyright; Abstract Only; Available from CASI only as part of the entire parent document

Mid-infrared (8-13 microns) spectra of radiation emitted from the surface of solar system objects can be interpreted in terms of surface composition. However, the spectral features are weak, and require exceptionally high signal-to-noise ratio spectra to detect them. Ground-based observations of spectra in this region are plagued by strong atmospheric absorptions from water and ozone. High-altitude balloon measurements that avoid atmospheric absorptions can be affected by contamination of the optics by dust. We have developed a technique to obtain mid-infrared spectra of Mercury that minimizes these problems. The resulting spectra show evidence of transparency features that can be used to qualitatively characterize the surface composition. Additional information is contained in the original extended abstract.

Author

*Spectral Emission; Mercury (Planet); Infrared Radiation; Mercury Surface*

**20010124839** Centre d'Etude Spatiale des Rayonnements, Toulouse, France

**Measuring the Chemical Composition of the Surface of Mercury Using Orbital Gamma-Ray and Neutron Spectroscopy**

dUston, C., Centre d'Etude Spatiale des Rayonnements, France; Brueckner, J., Max-Planck-Inst. fuer Chemie, Germany; Feldman, W. C., Los Alamos National Lab., USA; Gasnault, O., Los Alamos National Lab., USA; Hasebe, N., Waseda Univ., Japan; Lawrence, D. J., Los Alamos National Lab., USA; Maurice, S., Observatoire de Midi-Pyrenees, France; Mercury: Space Environment, and Surface and Interior; 2001, pp. 21-22; In English; See also 20010124826; No Copyright; Abstract Only; Available from CASI only as part of the entire parent document

Many of the fundamental questions regarding the formation and evolution of Mercury can be addressed by measuring the global chemical composition of its surface. For example, the FeO composition of the Mercury surface can reveal information about the condensation temperature of Mercury during its accretion along with information about its volcanic history after formation. Knowledge of the iron abundance will in turn enable discrimination between different models that explain the formation and evolution of Mercury. Abundance measurements of refractory elements such as Ca, Mg, Al, Ti and radioactive elements such as K, Th, and U can also help to discriminate between various models of formation and enable us to better understand the environment in which Mercury formed. In addition to measuring the global abundance of these elements, it is also important to derive abundance maps to be able to characterize the degree of composition inhomogeneity that exists on the surface of Mercury. Abundance measurements of volatile elements, such as hydrogen, are important to understand the origin and nature of the radar-bright spots located in the permanently shaded regions of the north and south poles. In particular, hydrogen abundance measurements may help to determine if these regions are populated by large amounts of water ice. One of the best ways to carry out all these measurement objectives is to use orbital gamma-ray and neutron spectroscopy to make measurements of absolute elemental abundances on the surface of Mercury. Additional information is contained in the original extended abstract.

Author

*Chemical Composition; Mercury (Planet); Mercury Surface; Planetary Evolution*

**20010124841** Southwest Research Inst., San Antonio, TX USA

**The Electron Environment at Mercury**

Frahm, R. A., Southwest Research Inst., USA; Link, R., Southwest Research Inst., USA; Winningham, J. D., Southwest Research Inst., USA; Coates, A. J., Mullard Space Science Lab., UK; Norberg, O., Esrange, Sweden; Mercury: Space Environment, and Surface and Interior; 2001, pp. 25; In English; See also 20010124826; No Copyright; Abstract Only; Available from CASI only as part of the entire parent document

The Electron environment at Mercury is unique. The planet has a magnetic field, which is similar to that of Earth, but Mercury's magnetic field is significantly smaller than that of Earth, so the planetary body dominates a larger area of Mercury's field compared to the Earth system. The solar wind interacts with the magnetic field of Mercury and an Earth-like plasma interaction with the solar wind is expected to occur. However, Mercury has no substantial ionosphere, so that the mechanism by which the magnetospheric currents are closed remains a matter of debate. Additional information is contained in the original extended abstract.

Author

*Mercury (Planet); Planetary Magnetic Fields; Planetary Environments*

**20010124842** Washington Univ., Dept. of Earth and Planetary Sciences, Saint Louis, MO USA

**Using Remotely Sensed Observations of Ancient Mare Deposits on the Moon as Possible Analogs to the Intercrater Plains on Mercury**

Gillis, J. J., Washington Univ., USA; Robinson, M. S., Northwestern Univ., USA; Mercury: Space Environment, and Surface and Interior; 2001, pp. 26-27; In English; See also 20010124826

Contract(s)/Grant(s): NAG5-8905; No Copyright; Abstract Only; Available from CASI only as part of the entire parent document

Two commonly held models for the formation of the mercurian intercrater plains are: a global volcanic resurfacing event or basin-ejecta material. Although Mariner 10 images have provided morphologic and limited compositional information of the intercrater plains, the origin of these materials remains ambiguous. We examine whether Mariner 10 image at 355 (UV (ultraviolet)) and 575 nm (orange) can be used to distinguish between these models. Here we use Clementine image data (415 and 750 nm) for ancient lunar mare deposits to evaluate this suggestion. The inventorying of 'hidden' volcanic deposits is important to mercurian studies because they provide evidence of ancient volcanism, which yields clues to the thermal evolution of the planet. The greater abundance of intercrater plains on Mercury, relative to the intercrater plains observed within the lunar highlands, suggests that the resurfacing was comparably more intense. Mercury may represent an intermediate member of planet resurfacing; with the extremes being the Moon (approximately 17% resurfacing) and Venus (global resurfacing). Additional information is contained in the original extended abstract.
Author

*Mercury (Planet); Plains; Planetary Craters; Planetary Surfaces; Remote Sensing; Mercury Surface; Planetary Evolution; Maria*

**20010124846** European Space Agency. European Space Research and Technology Center, ESTEC, Space Science Dept., Noordwijk, Netherlands

**The Charged Particle Environment of Mercury and Related Electric Phenomena**

Grard, R., European Space Agency. European Space Research and Technology Center, ESTEC, Netherlands; Laakso, H., European Space Agency. European Space Research and Technology Center, ESTEC, Netherlands; Mercury: Space Environment, and Surface and Interior; 2001, pp. 33; In English; See also 20010124826; No Copyright; Abstract Only; Available from CASI only as part of the entire parent document

Like the Moon, Mercury has a vestigial atmosphere and no ionosphere, but it possesses a small intrinsic magnetic field. Due to the weakness of this field, of the order of few 100 nT at the equator, and the relatively high solar wind pressure which prevails at the orbit of Mercury, the size of the magnetospheric cavity is much smaller that that of the Earth. The solar wind may even reach the surface of Mercury when its pressure is sufficiently large. The formation of radiation belts is probably impeded for lack of a sufficiently strong magnetic confinement. The environment is permeated by a current system which is basically unknown and the plasma is extremely rarefied, like in the lobes of the Earth magnetosphere. The absence of an atmosphere permits the circulation of electric currents directly between the solid planet and its space environment. Due to the proximity of the Sun, the emission rate of photoelectrons is up to 10 times larger than at the Earth orbit and leads to unique electrostatic phenomena on orbiting spacecraft and at the planetary surface.
Author

*Charged Particles; Electrostatics; Magnetic Fields; Mercury (Planet); Solar Wind; Mercury Atmosphere*

**20010124848** Pittsburgh Univ., Dept. of Geology and Planetary Science, Pittsburgh, PA USA

**Space Weathering and the Composition of the Crust of Mercury**

Hapke, B., Pittsburgh Univ., USA; Mercury: Space Environment, and Surface and Interior; 2001, pp. 35; In English; See also 20010124826; No Copyright; Abstract Only; Available from CASI only as part of the entire parent document

The vapor deposition model of space weathering is now widely accepted. The changes in the optical properties of pulverized crustal material of a planet, including spectral darkening, reddening and obscuration of absorption bands, are caused by vapor deposits containing submicroscopic metallic iron (SMFe) particles; the vapor is generated by both solar wind sputtering and micrometeorite vaporization. Mercury's magnetic field stands off the solar wind most of the time. However, Cintala estimates that micrometeorite vapor generation is 20 times greater on Mercury than on the moon, which implies that vapor deposits probably make up more than half of the Mercurian regolith. This paper discusses the implications of these deposits on the interpretation of observations that bear on the composition of the regolith. Additional information is contained in the original extended abstract.
Author

*Mercury (Planet); Space Weathering; Mercury Surface; Planetary Crusts; Planetary Composition*

**20010124849** Jet Propulsion Lab., California Inst. of Tech., Pasadena, CA USA

**Radar Imaging of Mercury's North and South Poles at 3.5 cm Wavelength**

Harcke, L. J., Stanford Univ., USA; Zebker, H. A., Stanford Univ., USA; Jurgens, R. F., Jet Propulsion Lab., California Inst. of Tech., USA; Mercury: Space Environment, and Surface and Interior; 2001, pp. 36-37; In English; See also 20010124826; No Copyright; Abstract Only; Available from CASI only as part of the entire parent document

The Goldstone Solar System Radar has been used to image the north and south poles of Mercury during the inferior conjunctions of February 2001 and June 2001. The sub-Earth latitude was -10.7 degrees in February during observations of the southern hemisphere, and +8.4 degrees in June during observations of the northern hemisphere. These excellent viewing angles provided an opportunity to resolve the radar bright material in polar craters at 6 km range resolution. Fine-scale (1.5 km) resolution images of the northern craters have previously been obtained at 13 cm wavelengths during the July 1999 inferior conjunction. However, due to geometric constraints, the Arecibo radar cannot observe the southern polar region of Mercury until 2004. Our new Goldstone 6 km data are a factor of two higher resolution than Arecibo data collected in March 1992 at 15 km range resolution, and will remain the most highly resolved images of the south polar region for the next few years. Additional information is contained in the original extended abstract.

Author

*Mercury (Planet); Polar Regions; Radar Imagery*

**20010124850** Arecibo Ionospheric Observatory, Arecibo, Puerto Rico

**Mercury Radar Imaging at Arecibo**

Harmon, J. K., Arecibo Ionospheric Observatory, Puerto Rico; Mercury: Space Environment, and Surface and Interior; 2001, pp. 38-39; In English; See also 20010124826; No Copyright; Abstract Only; Available from CASI only as part of the entire parent document

Until 10 years ago, Mercury radar studies consisted primarily of CW (Continuous Wave) and delay-Doppler observations of the polarized echo for altimetry, scattering analysis, and imaging of the equatorial region near the subradar track. The last decade has seen a shift in emphasis to full-disk imaging of both the polarized and depolarized echoes. Several advances have made this more practicable. One of these was the advent of bistatic radar synthesis imaging with Goldstone/VLA (Very Large Array), which circumvented the north-south ambiguity and overspread aliasing problems inherent in delay-Doppler radar. Another advance was the development of the long-code method, which mitigates echo overspreading in delay-Doppler. Both of these methods were developed for observing Mars, but were immediately adaptable to Mercury. Finally, there has been the recent upgrading of the Arecibo telescope. This upgrade has given a more than five-fold improvement in the sensitivity of the Arecibo S-band radar, enabling delay-Doppler imaging with better quality and resolution. In this talk I review recent Arecibo delay-Doppler radar imaging results for Mercury, concentrating mainly on data obtained with the newly upgraded system. I will begin with a discussion of the putative 'ice' features that have been seen at the poles, and then go on to a discussion of the major nonpolar radar features seen in the Mariner-unimaged hemisphere. Some of the results discussed in this abstract are based on preliminary analysis of new data. The final images resulting from more complete analysis will be presented at the meeting. Additional information is contained in the original extended abstract.

Author

*Imaging Techniques; Mercury (Planet); Radar Imagery; Polar Regions; Mercury Surface*

**20010124851** Washington Univ., McDonnell Center for the Space Sciences, Saint Louis, MO USA

**Mercury's Thermal, Tectonic, and Magmatic Evolution**

Hauck, Steven A., II, Washington Univ., USA; Dombard, Andrew J., Carnegie Institution of Washington, USA; Phillips, Roger J., Washington Univ., USA; Solomon, Sean C., Carnegie Institution of Washington, USA; Mercury: Space Environment, and Surface and Interior; 2001, pp. 40-41; In English; See also 20010124826; No Copyright; Abstract Only; Available from CASI only as part of the entire parent document

An important problem in the understanding of Mercury's history is the reconciliation of thermal evolution models with interpretations of its surface geology. This is true on two specific fronts regarding: (1) the surface contractional history (especially as recorded in lobate scarps such as Discovery Rupes), and (2) the origin and significance of plains materials. Estimates of contractional strain recorded in the lobate scarps range between approximately 0.04 and 0.10%, the most recent analysis favoring values near the lower end of this range. Such strain suggests approximately 1-2 km of planetary radial contraction, yet thermal models predict at least 2-6 times as much contraction. The origin of widespread intercrater plains and younger smooth plains and the nature of volcanism on Mercury are points of some debate. On the basis of surface reflectance at visible, infrared and microwave wavelengths, Mercury's surface is inferred to be generally low in Fe(2+). Some workers have interpreted this result to mean that high-albedo regions (at visible wavelengths) have a surface composition that is devoid of basaltic material. If this

inference were true, despite the presence of Fe-poor lavas (e.g., some komatiites) on Earth, it would have profound consequences for the thermal evolution of Mercury. However, re-analysis of Mariner 10 color images illustrates that some plains units are spectrally distinguishable on the basis of their opaque mineral content and that these units are stratigraphically and morphologically consistent with volcanic emplacement. This result is contrary to some thermal models that suggest that volcanism is not an important part of Mercury's energy budget. Additional information is contained in the original extended abstract.
Author
*Mercury (Planet); Mercury Surface; Planetary Evolution; Tectonics; Volcanoes; Planetary Composition; Planetary Geology; Planetary Temperature; Remote Sensing*

**20010124853** Brown Univ., Dept. of Geological Sciences, Providence, RI USA
**Theoretical Aspects of Magma Generation, Ascent and Eruption on Mercury and Comparison with Composition and Morphology of Surface Features**
Head, James W., Brown Univ., USA; Wilson, Lionel, Lancaster Univ., UK; Mercury: Space Environment, and Surface and Interior; 2001, pp. 44-45; In English; See also 20010124826; No Copyright; Abstract Only; Available from CASI only as part of the entire parent document

Despite exploration of Mercury by Mariner 10, some fundamental questions remain about the basic surface processes on the planet. Did Mercury, like the Moon, experience crustal intrusion and surface extrusion, resulting in the formation of volcanic deposits and landforms during its early thermal evolution? Did secondary crustal formation occupy a significant part of the resurfacing history of Mercury as it did for the Moon? How did the environmental parameters associated with Mercury modify and change the geologic record and eruptions styles there, relative to the Moon? and how can the better-known lunar record be used to address these issues? Fundamental questions remain as to whether there are any unambiguous signs of volcanism visible on Mercury's surface. This debate stems from the initial analyses of Mariner 10 monochrome images (approximately 1 km / pixel over about half the planet). Workers identified the existence of widespread plains deposits, occurring as relatively smooth surfaces between craters and as apparently ponded material, somewhat analogous to lunar mare units. It was proposed that at least some of these units were volcanic in origin. Others argued that the plains deposits must be considered to be basin ejecta, similar to those found at the lunar Apollo 16 landing site, raising the possibility that there are no identifiable volcanic units on Mercury. Recalibrated Mariner 10 mosaics made by combining images taken through various filters and having significantly increased signal-to-noise ratio have been interpreted to indicate that indeed color units correspond to mapped plains units on Mercury, and further that some color units are the result of compositional heterogeneities in the mercurian crust. From these new data, color units can be identified that correspond with previously mapped smooth plains deposits. The dark blue material associated with the crater Homer exhibits diffuse boundaries consistent with fragmental material emplaced ballistically, and a pyroclastic origin is favored. A similar deposit is seen northwest of the crater Lermontov; examination of the iron-maturity parameter and opaque index images reveal that the darkest and bluest material in this deposit is not associated with an ejecta pattern. The relatively blue color, high opaque index, and low albedo of these materials (for both areas) is consistent with a more mafic material, possibly analogous to a basaltic or gabbroic composition. A tentative identification of basalt-like material in this hemisphere was made with Earth-based thermal IR (infrared) measurements, whereas later microwave measurements were interpreted to indicate a total lack of areally significant basaltic materials on Mercury. From the data currently available it is not possible to make an unambiguous identification of basaltic material or indeed of any rock type; however the spectral parameters, stratigraphic relations and morphology of various units are consistent with volcanically emplaced materials. Regardless of the mode of emplacement, the presence of the materials found around the craters Homer and Lermontov, and of the plains units identified above, argues that significantly different compositional units occur within the mercurian crust and that at least some of them were emplaced during volcanic eruptions. Additional information is contained in the original extended abstract.
Author
*Craters; Crusts; Ejecta; Mercury (Planet); Mercury Surface; Planetary Evolution; Planetary Crusts; Planetary Composition; Volcanic Eruptions; Planetary Structure; Planetary Geology*

**20010124854** Academy of Sciences (USSR), Inst. of Radioengineering, Moscow, USSR
**Estimation of Mercury's Obliquity and Physical Librations by Earth-Based Radar Speckle Displacement Interferometry**
Holin, I. V., Academy of Sciences (USSR), USSR; Mercury: Space Environment, and Surface and Interior; 2001, pp. 46; In English; See also 20010124826; No Copyright; Abstract Only; Available from CASI only as part of the entire parent document

In accordance with 'A Procedure for Determining the Nature of Mercury's Core,' four parameters should be known to find out internal constitution of Mercury including the size and state of its core. Two of them, the obliquity and the amplitude of physical librations, are not known even roughly. MESSENGER mission includes solving this problem. In addition we consider an approach based on the radar speckle displacement effect. If we illuminate Mercury by a monochromatic radio wave then due to its

rotational-progressive motion the spatial distribution (speckle pattern) of a reflected radar field will run in a 'freezed' state on the surface of Earth at a velocity of 200...300 km/s. From measuring this speckle velocity vector it is possible to calculate tangential (with respect to the line of sight) components of the instantaneous spin-vector of Mercury's mantle. A variety of Earth-based communication and radio facilities are suitable for this goal. For example, near the May 2002 inferior conjunction of Mercury NRAO (National Radio Astronomy Observatory) VLBA (Very Long Baseline Array) antennae at Pie Town and Hancock as the receiving interferometer under Goldstone 3.5 cm illumination may give one-look relative accuracy for the instantaneous tangential spin vector near to one...three parts in 100,000 while for the spin-radar Goldstone/Mauna Kea - Hancock it is by nearly another two times higher. This is well enough for obliquity. to measure librations one should repeat the experiment for 10...15 days (a few minutes a day for each baseline) near the same inferior conjunction. Further improvements in accuracy are obtainable through using several inferior conjunctions and additional VLBA and large antennae at Arecibo, Green Bank, Madrid.
Author
*Librational Motion; Mercury (Planet); Speckle Interferometry; Solar Orbits; Planetary Rotation; Space Observations (From Earth)*

**20010124855** Swedish Inst. of Space Physics, Kiruna, Sweden
**Neutral Atom Imaging Near Mercury**
Holmstroem, M., Swedish Inst. of Space Physics, Sweden; Barabash, S., Swedish Inst. of Space Physics, Sweden; Lukyanov, A., Coventry Univ., UK; Mercury: Space Environment, and Surface and Interior; 2001, pp. 47; In English; See also 20010124826; No Copyright; Abstract Only; Available from CASI only as part of the entire parent document

The interaction between energetic ions and a planetary atmosphere produces energetic neutral atoms (ENA) when an ion charge-exchange with a neutral atom, e.g., H(+) + O yields H + O(+). Since momentum is conserved the neutral will have the same velocity as the ion. A property of ENAs is that they, in the absence of gravity, travel in straight lines since they, as neutrals, are unaffected by magnetic and electric fields. Thus, using an ENA imager it is possible to extract global information about the plasma and neutral populations that generated the ENAs. ENA imaging has successfully been applied for Earth's magnetosphere, the most recent example being NASA's IMAGE (Imager for Magnetopause-to-Aurora Global Exploration) mission. The next planet to be imaged in ENAs will be Mars. There are two ENA imagers, as parts of the ASPERA (Analyzer of Space Plasma and Energetic Atoms)-3 instrument, onboard ESA's Mars Express mission (launch 2003). Due to its global nature, ENA imaging is an attractive method of exploring the largely unknown Hermean exospheric and magnetospheric environment on future Mercury missions. Given the phase space distribution of ions and neutrals, and the charge-exchange cross sections, one can compute ENA images. One purpose of such simulated images is to predict typical fluxes that can be expected, and thereby provide design constraints for instruments. Simulated images can also help in interpreting large scale features in observed images. For a more detailed, quantitative analysis of observed images one can use inversion techniques to extract parameters from a mathematical model. For Mercury, this is a challenging problem for future research. Additional information is contained in the original extended abstract.
Author
*Imaging Techniques; Neutral Atoms; Space Plasmas; Mercury (Planet); Planetary Magnetospheres; Mercury Atmosphere*

**20010124856** Arizona Univ., Lunar and Planetary Lab., Tucson, AZ USA
**Diurnal Variation of Na and K at Mercury**
Hunten, D. M., Arizona Univ., USA; Sprague, A. L., Arizona Univ., USA; Mercury: Space Environment, and Surface and Interior; 2001, pp. 48-49; In English; See also 20010124826; No Copyright; Abstract Only; Available from CASI only as part of the entire parent document

We have published data showing a strong morning enhancement in the abundances of both Na and K. Sprague has proposed an explanation, that these elements accumulate on the cold, dark night side and are released in the morning as the surface warms up. Killen and Morgan, however, present a derivation, showing that such a mechanism cannot produce any enhancement greater than a factor of three. We show that their derivation contains a subtle error; when this error is corrected, no such limit exists. Their data do not show an obvious morning enhancement. The disagreement in the data is harder to understand; we suggest some possible explanations but do not come to any definite conclusion.
Author
*Diurnal Variations; Sodium; Potassium; Mercury (Planet); Mercury Surface; Temperature Effects*

**20010124857** Finnish Meteorological Inst., Geophysical Research, Helsinki, Finland
**On the Modeling of the Mercury-Solar Wind Interaction by a Quasineutral Hybrid Model**
Kallio, Esa, Finnish Meteorological Inst., Finland; Janhunen, Pekka, Finnish Meteorological Inst., Finland; Mercury: Space Environment, and Surface and Interior; 2001, pp. 50; In English; See also 20010124826; No Copyright; Abstract Only; Available from CASI only as part of the entire parent document

The Hermean magnetosphere is anticipated to have certain unique features compared with other planetary magnetospheres. The planet's intrinsic magnetic field is strong enough to form a magnetosphere around the planet. However, it is not clear how the processes in the Hermean magnetosphere resemble the processes that take place in the other magnetospheres. Especially the questions: How effectively the magnetosphere can shield the planet against the solar wind particles, how effectively the magnetosphere can store energy in the magnetotail, and how the interaction between the magnetosphere and the planet's surface, which can take place because of the very tenuous atmosphere, are unknown. Modeling of the solar wind-Mercury interaction is therefore a challenging problem because a physically realistic model should include processes between three highly different components: the solar wind, the magnetosphere,and the planetary surface. We have developed a 3-D (three-dimensional) quasi-neutral hybrid model to study the Hermean magnetosphere. The recently developed self-consistent hybrid model, which has been used earlier to study the Mars-solar wind interaction, includes ions which are moved by the Lorentz force, while electrons are a massless charge neutralizing fluid. The model includes solar wind protons and planetary ions, say, Na(+), or K(+) ions. Planetary ions are produce from two sources, by photoionization from a neutral corona, and by ion sputtering from the surface. A fully 3-D neutral corona density model, and fully 2-D (two-dimensional) (latitude and longitude dependence on the surface) ion emission model from the surface can be used. The hybrid simulation approach makes it possible to study several plasma physical processes in the vicinity of the planet that are difficult or impossible to model by other self consistent approaches, such as effects associated with ion finite gyroradius, the velocity difference between different ion species, the large loss cone, or the non-maxwellian velocity distribution function. Especially, the model can be used to study magnetosphere-planetary surface interaction because ions can precipitate to the surface. Our work has two primary goals. First, the global hybrid model will be used to study basic global plasma physical processes in the vicinity of Mercury. Second, it will provide a tool that will be used to optimize of the performance of an ENA (energetic neutral atom) instrument planned for BepiColombo mission, and in the future for interpreting the measurements. ENA instrument will measure Energetic Neutral Atoms, ENAs. In the presentation we will show some preliminary results of our hybrid model runs.

Author

*Three Dimensional Models; Mercury Surface; Mercury (Planet); Solar Wind; Astronomical Models*

**20010124858** Eoetvoes LORANd Univ., Dept. of Physical Geography, Budapest, Hungary

**In Search of Lunar Like Rilles on Mercury**

Kereszturi, A., Eoetvoes LORANd Univ., Hungary; Mercury: Space Environment, and Surface and Interior; 2001, pp. 51-52; In English; See also 20010124826; No Copyright; Abstract Only; Available from CASI only as part of the entire parent document

Lunar rilles or rimae can be divided into two classes: 1. near straight tectonic structures and 2. sinuous lunar rilles which are traces of ancient lava flows on the Moon's surface. They were carved by thermal erosion of lava flows and/or subsequent collapse of lava tubes on the mare basalt terrains of the Moon. Because of the several connection between the surface and planetary evolution of the Moon and Mercury there is reason that on Mercury we can find rilles too. However only some rill like structures are published in the scientific literature. It is interesting to search of rilles on Mercury because if we find some, comparing them with the Moon's we can estimate some characteristics of the lava flows. Additional information is contained in the original extended abstract.

Author

*Mercury (Planet); Planetary Evolution; Terrain; Valleys; Mercury Surface; Planetary Geology; Lava; Fissures (Geology)*

**20010124859** NASA, Washington, DC USA

**Ar Atmosphere: Implications for Structure and Composition of Mercury's Crust**

Killen, R. M., Southwest Research Inst., USA; Morgan, T. H., NASA, USA; Mercury: Space Environment, and Surface and Interior; 2001, pp. 53; In English; See also 20010124826; No Copyright; Abstract Only; Available from CASI only as part of the entire parent document

We examine the possibilities of sustaining an argon atmosphere by diffusion from the upper 10 km of crust, and alternatively by effusion from a molten or previously molten area at great depth . Ar-40 in the atmospheres of the planets is a measure of potassium abundance in the interiors since Ar-40 is a product of radiogenic decay of K-40 by electron capture with the subsequent emission of a 1.46 eV gamma-ray. Although the Ar-40 in the earth's atmosphere is expected to have accumulated since the late bombardment, Ar-40 in surface-bounded exospheres is eroded quickly by photoionization and electron impact ionization. Thus, the argon content in the exospheres of the Moon, Mercury and probably Europa is representative of current effusion rather than accumulation over the lifetime of the body. Argon content will be a function of K content, temperature, grain size distribution, connected pore volume and possible seismic activity. Although Mercury and the Moon differ in many details, we can train the solutions to diffusion equations to predict the average lunar atmosphere. Then these parameters can be varied for Hermean conditions. Assuming a lunar crustal potassium abundance of 300 ppm, the observed argon atmosphere requires equilibrium

between the argon production in the upper 9 Km of the moon (1.135 x 10(exp -3) cm(exp -3) s(exp -1)) and its loss. Hodges et al. conclude that this loss rate and the observed time variability requires argon release through seismic activity, tapping a deep argon source. An important observation is that the extreme surface of the Moon is enhanced in argon rather than depleted, as one would expect from outgassing of radiogenic argon. Manka and Michel concluded that ion implantation explains the surface enhancement of Ar-40. About half of the argon ions produced in the lunar atmosphere would return to the surface, where they would become embedded in the rocks. Similarly, at Mercury we expect the surface rocks to be enhanced in Ar-40 wherever the magnetosphere has been open over time. Thus the measurement of surface composition will reveal the long-term effects of solar wind-magnetosphere interaction. Additional information is contained in the original extended abstract.
Author
*Argon Isotopes; Mercury Surface; Planetary Atmospheres; Potassium 40; Radiogenic Materials; Atmospheric Composition; Planetary Crusts; Earth Atmosphere*

**20010124860** Michigan Univ., Atmospheric, Oceanic and Space Sciences Dept., Ann Arbor, MI USA
**Measuring the Plasma Environment at Mercury: The Fast Imaging Plasma Spectrometer**
Koehn, P. L., Michigan Univ., USA; Zurbuchen, T. H., Michigan Univ., USA; Fisk, L. A., Michigan Univ., USA; Gloeckler, G., Maryland Univ., USA; Mercury: Space Environment, and Surface and Interior; 2001, pp. 54; In English; See also 20010124826; No Copyright; Abstract Only; Available from CASI only as part of the entire parent document

The plasma environment at Mercury is a rich laboratory for studying the interaction of the solar wind with a planetary magnetosphere. Three primary populations of ions exist at Mercury: solar wind, magnetospheric and pickup ions. An instrument to measure the composition of these ion populations and their three dimensional velocity distribution functions must be lightweight, fast, and have a very large field of view. Composition instruments, however, are traditionally bulky and massive. This provides an opportunity for miniaturization to reduce costs in both mass and power. The Fast Imaging Plasma Spectrometer (FIPS) is an imaging mass spectrometer proposed for, accepted by, and expected to be launched aboard NASA's MESSENGER (Mercury Surface, Space, Environment, Geochemistry, and Ranging) spacecraft, a Mercury orbiter. This versatile instrument has a very small footprint, requires 2W of power, and has a mass a full order of magnitude less than current, similarly performing systems. It maintains a nearly full-hemisphere field of view, equally suitable for either spinning or three-axis-stabilized platforms. Its unique cylindrical mirror entrance system and position-sensing time-of-flight telescope allows the rapid imaging of phase-space and identification of particle species. For magnetospheric and planetary missions, where events happen on timescales of minutes or even seconds, this is especially valuable. This instrument has been extensively simulated with the ray-tracing software package SimIon. A prototype of the entrance system has been constructed at the University of Michigan's Space Physics Research Laboratory, and fully tested at the Goddard Space Flight Center (GSFC) Beam Facility. We will present and compare the results of simulation and testing of the FIPS prototype. It will show that the FIPS instrument is an ideal solution for measuring the plasma environment at Mercury.
Author
*Imaging Spectrometers; Planetary Magnetospheres; Plasmas (Physics); Prototypes; Solar Wind; Space Missions; Spacecraft Instruments; Mercury (Planet); Mass Spectroscopy*

**20010124861** Academy of Sciences (USSR), Space Research Inst., Moscow, USSR
**Resolved Ground Based Observation of Mercury**
Ksanfomality, L. V., Academy of Sciences (USSR), USSR; Mercury: Space Environment, and Surface and Interior; 2001, pp. 55; In English; See also 20010124826; No Copyright; Abstract Only; Available from CASI only as part of the entire parent document

The results of investigations of astronomical climate in several observatories have shown that the amplitudes of scintillation (flicker) decrease for stars with higher frequency spectra. This means that a short exposure may substantially improve the image resolution of planetary astronomical objects. The use of a high sensitivity CCD (charge coupled device) detector permits the exposure to be radically diminished. This improves the sharpness of the image, however it does not improve picture distortion. Nevertheless it is possible to find a low distortion picture amid many obtained in observations. 15 short exposure (10 ms) images of the planet Mercury were obtained in December 1999, with a zenith angle of 83-78 degrees, at the Abastumany astrophysical observatory (Republic of Georgia), placed at an altitude 1700 m a.s.l.. Only one image (wavelength 533 nm, Delta lambda = 24 nm) is of low distortion. The telescope was an AZT-11 (D = 1.25 m, F = 16 m). Mercury was at a geocentric distance of 1.007 a.u., a heliocentric distance of 0.39 a.u. and had a phase of 76 degrees. The coordinates of the subterrestrial point at 03:30 UT, 3.12.1999 were 108 degrees W, 2 degrees 26 minutes S. The CCD pixel size was 12 by 14 mcm. The photometric readings were about 1000 counts per pixel. All images are additionally distorted by refraction in their eastern parts. Despite the fact that the observations were made far from the zenith, about 80 degrees, photometrical sections along the subterrestrial meridian show some details seen in the curve. The suggestion was made that the details seen in the image reveal large blocks of Hermean surface,

normally not seen in ground based images of Mercury. Occasionally the phase of the planet and the subterrestrial point position were almost the same as when MARINER 10 encountered Mercury in 1974. This coincidence permits a comparison of the images obtained with the MARINER 10 data, proving the reality of the details. The large dark area 1 was identified with crater Beethoven (20 degrees S, 124 degrees W, center). The three dark spots 2 in the disk center and 120-140 degrees W are also seen in section (b), as is spot 3. Spot 4 was tentatively identified with the Caloris Planitia (30 degrees S, 177 degrees W, center) partly seen in section (b). Using very short exposures for Mercury ground based observations allows resolved images of the planet to be obtained that are not available using any other ground based techniques. The image resolution is up to 0.4 arc sec instead of 1 to 1.5 arc sec for a moderate sized telescope. The method has much in common with speckle interferometry.
Author
*Charge Coupled Devices; Exposure; Image Resolution; Mercury (Planet); Imaging Techniques; Space Observations (From Earth); Astronomical Photometry*

**20010124862** Academy of Sciences (USSR), Space Research Inst., Moscow, USSR
**Properties of the Hermean Surface**
Ksanfomality, L., Academy of Sciences (USSR), USSR; Sprague, A., Arizona State Univ., USA; Cremonese, C., Osservatorio Astronomico, Italy; Jorda, L., Max-Planck-Inst. fuer Aeronomie, Germany; Thomas, N., Max-Planck-Inst. fuer Aeronomie, Germany; Warell, J., Astronomical Observatory, Sweden; Mercury: Space Environment, and Surface and Interior; 2001, pp. 56; In English; See also 20010124826; No Copyright; Abstract Only; Available from CASI only as part of the entire parent document

There are two Mercury missions projects intended for nearest years, NASA's 'Messenger' (2004) and ESA's (European Space Agency) 'BepiColombo' (2009). The Mercury Orbiter is the European Space Agency cornerstone. There are many aspects of Mercury which require further study such as the origin and composition of the regolith, processes of surface cratering, the origin of the planet, its internal structure, its magnetosphere, its very rarefied atmosphere (exosphere), its orbital and rotational dynamics, and its thermal history. Despite the signs found for presence of rock-types that widely distributed on the Moon (feldspathoids, anorthosites), the huge differences in the mean density and crust/mantle thickness of the two bodies point to peculiarities of Mercury's surface. There is a good evidence of past volcanic flows. The mid-infrared spectroscopy found indications of heterogeneous crustal composition that is FeO-poor - less than 3% and possibly feldspar-rich, with the possibility of low iron pyroxenes and alkali basalts. The only spectral near-infrared feature indicated at some longitudes is a possible pyroxene absorption feature at 0.95 microns, which may be used to investigate the abundance distribution of FeO in the regolith. Mercury reveals as a geologically interesting planet. It has abundant Na and K in a thin atmosphere which appears to have Mercury's surface materials as its source. The physical properties of a regolith, its structure, grain sizes, refraction coefficient and even sizes of boulders may been estimated by methods of spectrozonal photometry and polarimetry. It is possible that there are deposits of buried water ice and/or elemental sulfur. The results of the study of the structure, physical properties and composition of Mercury's regolith, may be used to detect principal features on the origin of Mercury. Thermal infrared spectra have features, too, indicating the possible presence of feldspars, pyroxenes and igneous nepheline-bearing alkali syenite. The wavelength of the thermal emissivity maxima indicate intermediate or slightly mafic rock types as well as considerable heterogeneity in composition. The Fe absorption is used as a proxy for FeO, the abundance of which in the Hermean crust and mantle can be used to infer whether or not the planet accreted material from just a narrow feeding zone near its current heliocentric distance. To a lesser extent, the physical properties of crustal layers may be associated with the strange magnetic field of the planet. The existence of Mercury's dipole magnetic field may be the greatest challenge for the basic principles of the theory. There is the hypothesis on Mercury's magnetic field appearing in light of the Mars remnant fields that have been found by MGS (Mars Global Surveyor). The hypothesis states that the same data on the Hermean resulting magnetic field may be produced, at least partly, by separate magnetized blocks of crust with a random orientation of the field.
Author
*Mercury (Planet); Mercury Surface; Space Missions; Planetary Geology; Infrared Spectroscopy; Planetary Crusts; Planetary Composition; Chemical Composition*

**20010124865** Academy of Sciences (Russia), Inst. of Experimental Mineralogy, Chernogolovka, Russia
**Specific Character of the Formation of Mercury as the Densest Planet**
Marakushev, A. A., Academy of Sciences (Russia), Russia; Chaplygin, O. V., Academy of Sciences (Russia), Russia; Bobrov, A. V., Academy of Sciences (Russia), Russia; Mercury: Space Environment, and Surface and Interior; 2001, pp. 59; In English; See also 20010124826; No Copyright; Abstract Only; Available from CASI only as part of the entire parent document

Earth-type planets were initially formed as giant planets, similarly to the planets of the group of Jupiter and simultaneously with the solar mass by the accumulation of aqueous-hydrogen planetesimals, which were similar by physical state to Pluto, Charon, and comets. Gravitational compression was accompanied by melting of the planets whose size increases with the

approach to the Sun, with which they are also similar in composition. Development of hydrogen-water-silicate liquid immiscibility in planets was accompanied by their layering to heavy cores and gigantic fluid envelopes. The impulses of high-spin motion of these envelopes resulted in separation of satellites under the action of centrifugal forces. Satellite density varies widely, growing with the approach to dense iron-silicate cores of their parental giant planets. The maximum density of satellites of the peripheral, remote from the Sun planets (Neptune, Uranus, Saturn) does not exceed 1.9 g/cc, but for near-solar giant planets it reaches 3.5 g/cc (Io, the satellite of Jupiter) and 3.3 g/cc (Moon, the satellite of proto-Earth). In contrast to peripheral near-solar giant planets underwent surface degassing under the action of solar wind. Jupiter in this case lost the part of hydrogen of its fluid envelope, which can be judged from its anomalously high density (1.3 g/cc), almost two times higher than that of Saturn (0.7 g/cc). The giant planets located nearer to the Sun, completely lost fluid envelopes being transformed into terrestrial planets. They lost satellite systems because of decrease of gravity. Only relics of their satellites (Moon, Phobos and Deimos) remained. Several dozens of analogs of near-solar giant planets (figure) was revealed in the last years (1995-2001) in the surroundings of the stars, similar to the Sun. The degree of surface degassing of these planets is traced by the effect of the decrease of their massiveness with the approach to the stars. Terrestrial planets initially were formed as iron-silicate cores of parental giant protoplanets simultaneously with the separation of lighter silicate material into their satellite systems. Cores were formed in the protoplanets in the sequence of the development of chondrite systems, starting with the iron meteorites (I) of the corresponding genetic groups: I (type Netschaevo) - HH - H - L - LL. This development was determined by the increase of H2O/H2 ratio in the fluid envelopes of the protoplanets, which were undergoing degassing under the action of the solar wind. The development ceased at the different stages upon the complete degassing of planets in the sequence of moving away from the Sun. Proto-Mercury was the first giant planet, which lost its fluid envelope. Therefore Mercury has the most primitive composition, extremely rich in iron (I-HH). Furthermore the content in earth-type planets of nickel-iron phase is found in dependence on the degree of the development of their satellite systems. It increases with the approach to the Sun in the row: Neptune - Uranus - Saturn - Jupiter. The propagation of this regularity to the giant protoplanets of terrestrial group explains well the unique nature of Mercury, whose silicate phase to a considerable extent went away into the satellite system of its parental protoplanet, which the latter then lost. Additional information is contained in the original extended abstract.
Author
*Protoplanets; Planetary Evolution; Planetary Structure; Planetary Composition; Density (Mass/Volume); Mercury (Planet); Planets; Solar System Evolution*

**20010124866** Jet Propulsion Lab., California Inst. of Tech., Pasadena, CA USA
**Radar Techniques for the Measurement of Mercury's Obliquity and Librations**
Margot, J. L., California Inst. of Tech., USA; Peale, S. J., California Univ., USA; Slade, M. A., Jet Propulsion Lab., California Inst. of Tech., USA; Mercury: Space Environment, and Surface and Interior; 2001, pp. 60-61; In English; See also 20010124826; No Copyright; Abstract Only; Available from CASI only as part of the entire parent document

Evidence for a global magnetic field at Mercury has raised perplexing questions regarding the existence and nature of the planet's core. The problems related to Mercury's core are of great interest because of their implications on how planets evolve thermally and on how they generate magnetic fields. Peale showed that the measurement of four quantities could place constraints on the size and state of Mercury's core. The required parameters in Peale's experiment are the C(sub 20) and C(sub 22) coefficients in the spherical harmonic expansion of the gravity field, the planet's obliquity theta, and the amplitude phi of the forced libration in longitude. While the gravitational harmonics are best determined from an orbiting spacecraft, Earth-based radar observations may provide refined estimates of the obliquity and amplitude of the libration. We describe several techniques and attempt to quantify their potential for the proposed measurements. Additional information is contained in the original extended abstract.
Author
*Librational Motion; Mercury (Planet); Radar Measurement; Planetary Rotation; Axes of Rotation; Speckle Interferometry*

**20010124868** Brown Univ., Dept. of Geological Sciences, Providence, RI USA
**Identification of Mercurian Volcanism: Resolution Effects and Implications for MESSENGER**
Milkovich, S. M., Brown Univ., USA; Head, J. W., Brown Univ., USA; Mercury: Space Environment, and Surface and Interior; 2001, pp. 63-64; In English; See also 20010124826; No Copyright; Abstract Only; Available from CASI only as part of the entire parent document

Ever since the arrival of Mariner 10 at Mercury in 1974-5 there has been debate over the existence of volcanic features on the surface of the planet. Mercury has two types of plains, smooth and intercrater. Through comparisons with lunar mare, many researchers have concluded that these plains were formed through volcanic processes. Others consider that they are closer to some of the lunar light plains formed by crater ejecta. The identification of landforms typical of extrusive volcanism (e. g. domes, shields, sinuous rilles, calderas, flow fronts) is key to resolving this debate. Work by Malin indicates that the viewing geometry

of Mariner 10 may have been insufficient for the identification of such volcanic features. He addressed this issue by analyzing lunar images under Mariner 10 resolutions (approximately 1-2 km) and various lighting conditions (0-30 degrees) for volcanic features. Since the mercurian images are at about the same resolution as pre-1964 Earth-based telescopic images of the Moon, Malin used such images from the Consolidated Lunar Atlas with approximately the same viewing conditions as the Mariner 10 data. Malin was only able to identify lunar volcanic domes and flow fronts under these conditions, and found that volcanic features cannot be identified in images with sun elevation angles above 25 degrees. Due to the limited coverage of mercurian plains at low sun angles (only 15% of the surface was imaged with sun elevation angles greater than 20 degrees while smooth plains were identified in 40% of the images, or 18% of the surface), Malin was not surprised that volcanic landforms have not been identified on Mercury. He concludes that the only way to identify volcanic landforms in the Mariner 10 data is to look near the terminator. In such images he identifies two possible volcanic domes on Mercury; these are positive topographic features which are reminiscent of lunar domes but are near scarps and other structural features. Recent recalibration of Mariner 10 color data has allowed identification of several features spectrally similar to volcanic flows and pyroclastic fissure eruptions. The question of the mode of formation of the mercurian plains remains unanswered. The upcoming MESSENGER mission to Mercury will address this question. The MESSENGER mission will meet the resolution and lighting geometry conditions necessary for identification of any lunar-like volcanic features on Mercury. Additional information is contained in the original extended abstract.
Author

*Landforms; Mercury (Planet); Planetary Craters; Planetary Surfaces; Volcanic Eruptions; Topography*

**20010124869** Deutsche Forschungsanstalt fuer Luft- und Raumfahrt, Inst. of Space Sensor Technology and Planetary Exploration, Berlin, Germany

**Crater Production Function and Cratering Chronology for Mercury**

Neukum, G., Deutsche Forschungsanstalt fuer Luft- und Raumfahrt, Germany; Ivanov, B. A., Academy of Sciences (USSR), USSR; Wagner, R., Deutsche Forschungsanstalt fuer Luft- und Raumfahrt, Germany; Mercury: Space Environment, and Surface and Interior; 2001, pp. 65-66; In English; See also 20010124826; No Copyright; Abstract Only; Available from CASI only as part of the entire parent document

The well investigated size-frequency distributions (SFD) for lunar craters may be used to estimate the SFD for projectiles which formed craters on terrestrial planets and on asteroids. The result shows the relative stability of these distributions during the past 4 Gyr. The derived projectile size-frequency distribution is found to be very close to the size-frequency distribution of Main-Belt asteroids as compared with the recent Spacewatch asteroid data and astronomical observations as well as data from close-up imagery by space missions. It means that asteroids (or, more generally, collisionally evolved bodies) are the main component of the impactor family. A cratering chronology model is established which can be used as a safe basis for modeling the impact chronology of other terrestrial planets, especially Mercury. Additional information is contained in the original extended abstract.
Author

*Projectile Cratering; Size Distribution; Frequency Distribution; Mercury (Planet); Mercury Surface; Planetary Surfaces; Craters*

**20010124870** NASA Ames Research Center, Moffett Field, CA USA

**Constraining the Mean Crustal Thickness on Mercury**

Nimmo, F., NASA Ames Research Center, USA; Mercury: Space Environment, and Surface and Interior; 2001, pp. 67; In English; See also 20010124826; No Copyright; Abstract Only; Available from CASI only as part of the entire parent document

The topography of Mercury is poorly known, with only limited radar and stereo coverage available. However, radar profiles reveal topographic contrasts of several kilometers over wavelengths of approximately 1000 km. The bulk of Mercury's geologic activity took place within the first 1 Ga of the planet's history), and it is therefore likely that these topographic features derive from this period. On Earth, long wavelength topographic features are supported either convectively, or through some combination of isostasy and flexure. Photographic images show no evidence for plume-like features, nor for plate tectonics; I therefore assume that neither convective support nor Pratt isostasy are operating. The composition and structure of the crust of Mercury are almost unknown. The reflectance spectrum of the surface of Mercury is similar to that of the lunar highlands, which are predominantly plagioclase. Anderson et al. used the observed center-of-mass center-of-figure offset together with an assumption of Airy isostasy to infer a crustal thickness of 100-300 km. Based on tidal despinning arguments, the early elastic thickness (T(sub e)) of the (unfractured) lithosphere was approximately equal to or less than 100 km. Thrust faults with lengths of up to 500 km and ages of about 4 Ga B.P. are known to exist on Mercury. Assuming a semicircular slip distribution and a typical thrust fault angle of 10 degrees, the likely vertical depth to the base of these faults is about 45 km. More sophisticated modelling gives similar or slightly smaller answers. The depth to the base of faulting and the elastic layer are usually similar on Earth, and both are thought to be

thermally controlled. Assuming that the characteristic temperature is about 750 K, the observed fault depth implies that the heat flux at 4 Ga B.P. is unlikely to be less than 20 mW m(exp -2) for a linear temperature gradient. For an elastic thickness of 45 km, topography at 1000 km wavelength is likely to be about 60% compensated. There are thus likely to be considerable lateral variations in crustal thickness. Additional information is contained in the original extended abstract.
Author
*Mercury (Planet); Mercury Surface; Thickness; Topography; Planetary Crusts*

**20010124871** Brown Univ., Dept. of Geological Sciences, Providence, RI USA
**Space Weathering in the Mercurian Environment**
Noble, S. K., Brown Univ., USA; Pieters, C. M., Brown Univ., USA; Mercury: Space Environment, and Surface and Interior; 2001, pp. 68-69; In English; See also 20010124826
Contract(s)/Grant(s): NAG5-4303; No Copyright; Abstract Only; Available from CASI only as part of the entire parent document

Space weathering processes are known to be important on the Moon. These processes both create the lunar regolith and alter its optical properties. Like the Moon, Mercury has no atmosphere to protect it from the harsh space environment and therefore it is expected that it will also incur the effects of space weathering. However, there are many important differences between the environments of Mercury and the Moon. These environmental differences will almost certainly affect the weathering processes and the products of those processes. It should be possible to observe the effects of these differences in Vis (visible)/NIR (near infrared) spectra of the type expected to be returned by MESSENGER. More importantly, understanding these weathering processes and their consequences is essential for evaluating the spectral data returned from MESSENGER and other missions in order to determine the mineralogy and the Fe content of the Mercurian surface. Additional information is contained in the original extended abstract.
Author
*Aerospace Environments; Regolith; Space Weathering; Mercury (Planet); Mercury Surface; Mercury Atmosphere*

**20010124874** NASA, Washington, DC USA
**Ratio of Sodium to Potassium in the Mercurian Exosphere**
Potter, A. E., National Solar Observatory, USA; Anderson, C. M., New Mexico State Univ., USA; Killen, R. M., Southwest Research Inst., USA; Morgan, T. H., NASA, USA; Mercury: Space Environment, and Surface and Interior; 2001, pp. 75-76; In English; See also 20010124826; No Copyright; Abstract Only; Available from CASI only as part of the entire parent document

Sodium (Na) and Potassium (K) atoms can be seen in the exosphere of Mercury and the Moon because they are extremely efficient at scattering sunlight. These species must be derived from surface materials, so that we might expect the ratio of sodium to potassium to reflect the ratio of these elements in the surface crust. This expectation is approximately born out for the Moon, where the ratio of sodium to potassium in the lunar exosphere averages to be about 6, not too far from the ratio in lunar rocks of 2 to 7. However, the ratio in the Mercury exosphere was found to be in the range 80 to 190, and at least once, as high as 400. The sodium and potassium atoms seen in the Mercury exosphere represent a balance between production from the surface and loss to space. Only if the production efficiencies and loss rates for Na and K were equal, would the ratio of Na to K in the exosphere reflect the ratio in the surface rocks. Since a value of 100 or more for the ratio of sodium to potassium in the surface rocks seems very unlikely, the high values of the observed ratios suggests that either production efficiencies or loss processes for the two elements are not equivalent. It does not seem likely that source processes should be different on the Moon and Mercury by an order of magnitude. This suggests that loss processes rather than source processes are the cause of the difference between the two. The major loss processes for sodium and potassium on Mercury are radiation pressure and trapping of photoions by the solar wind. Radiation pressure can reach 50-70% of surface gravity, and can sweep sodium and potassium atoms off the planet, provided they are sufficiently hot. Photoionization followed by trapping of the ions in the solar wind is the other major loss process. Photoions are accelerated to keV energies in the magnetosphere, and may either intercept the magnetopause, and be lost from the planet, or impact the planetary surface. Ions that impact the surface are neutralized, and are then available for resupply to the exosphere. The loss efficiency depends on characteristics of the magnetosphere that determine the fraction of the ions that are recycled by neutralization on the surface. Over the preceding decade, we have collected sodium and potassium data for Mercury at irregular intervals. We analyzed these data to extract values for the Na/K ratio at a variety of conditions on Mercury. Additional information is contained in the original extended abstract.
Author
*Mercury (Planet); Mercury Atmosphere; Mercury Surface; Atmospheric Composition; Potassium; Sodium; Chemical Composition; Ratios*

**20010124875** NASA, Washington, DC USA

**The Distant Sodium Tail of Mercury**

Potter, A. E., National Solar Observatory, USA; Killen, R. M., Southwest Research Inst., USA; Morgan, T. H., NASA, USA; Mercury: Space Environment, and Surface and Interior; 2001, pp. 77-78; In English; See also 20010124826; No Copyright; Abstract Only; Available from CASI only as part of the entire parent document

Models of the sodium atmosphere of Mercury predict the possible existence of a cornet-like sodium tail. Detection and mapping of the predicted sodium tail would provide quantitative data on the energy of the process that produces sodium atoms from the planetary surface. Previous efforts to detect the sodium tail by means of observations done during daylight hours have been only partially successful because scattered sunlight obscured the weak sodium emissions in the tail. However, at greatest eastern elongation around the March equinox in the northern hemisphere, Mercury can be seen as an evening star in astronomical twilight. At this time, the intensity of scattered sunlight is low enough that sodium emissions as low as 500 Rayleighs can be detected. Additional information is contained in the original extended abstract.

Author

*Mercury Atmosphere; Planetary Surfaces; Sodium; Mercury (Planet); Planetary Structure*

**20010124876** Ohio State Univ., Lab. for Space Geodesy and Remote Sensing Research, Columbus, OH USA

**Rheological Inferences on the Mercurian Crust from Crater Morphometric Analyses of the Moon, Mars, and Mercury**

Potts, L. V., Ohio State Univ., USA; vonFrese, R. R., Ohio State Univ., USA; Shum, C. K., Ohio State Univ., USA; Mercury: Space Environment, and Surface and Interior; 2001, pp. 79-80; In English; See also 20010124826; No Copyright; Abstract Only; Available from CASI only as part of the entire parent document

Analysis of lunar free-air and terrain gravity correlations reveals distinct trends in transient cavity diameter estimates for the multi-ring basins. These trends clearly differentiate the farside crust as having been significantly more rigid than the nearside crust during bombardment time. The lunar crustal dichotomy is also reflected in local estimates of surface roughness developed from the root-mean-squared topography over 64 degrees x 64 degrees patches centered on the basins. For Mercury where gravity observations are lacking, this approach may be useful for developing insight on the rheological properties of the crust. As a test, the roughness values for multi-ring basins on Mercury and the highlands of Mars were evaluated. The trend for Mars is comparable to the trend noted for the less rigid lunar nearside crust. This result is also supported by the analysis of gravity data from the Mars Global Surveyor that suggests superisostatic mantle plugs may underlie the highland basins much like they appear to underlie the prominent basins of the lunar nearside. For Mercury the roughness trend is more comparable to the trend for the more rigid lunar farside crust. While the crust for Mercury was probably much hotter than the lunar crust during bombardment time, its dryness may have promoted strong rigidity. Additional information is contained in the original extended abstract.

Author

*Mercury (Planet); Planetary Surfaces; Rheology; Planetary Crusts; Planetary Craters*

**20010124877** Monash Univ., Dept. of Mathematics and Statistics, Australia

**Gas Ring Condensation Model for the Origin and Bulk Chemical Composition of Mercury**

Prentice, Andrew J. R., Monash Univ., Australia; Mercury: Space Environment, and Surface and Interior; 2001, pp. 81-82; In English; See also 20010124826; No Copyright; Abstract Only; Available from CASI only as part of the entire parent document

Mercury's mean uncompressed density approximately 5.3 g/cc greatly exceeds that of its neighbor Venus, viz. approximately 3.9 g/cc, suggesting bulk metal to rock mass fractions of 0.67:0.33 instead of 0.33:0.67. The latter values coincide with the ones expected on the basis of solar elemental abundances. Lewis discovered that a natural explanation for Mercury's high metal content existed within his equilibrium chemical condensation model applied to the solar nebula. Reconstruction of the mid-plane temperature T and pressure p(sub neb) spatial distributions from all of the planetary density data, including the observation of water ice at Jupiter's orbit, suggested that T and p (sub neb) vary with heliocentric distance R (in AU) according as T(R) = 550 R(exp -1.1 +/- 0.2) K and p(sub neb)(R) = 10(exp -4) R(exp -3.85) bar. At the orbit of Mercury (R = R(sub n), n = 1), p(sub neb) = 0.004 bar and the condensation temperatures of the dominant metal (Fe-Ni) and rock (MgSiO3) species are T(sub 1,1) = 1,520 K and T(sub 1,2) = 1490 K, respectively. Hence if T(R(sub 1)) lies just below T(sub 1,2) only a small quantity of MgSiO3 can condense and so a relative enrichment of metals occurs. Unfortunately, numerical studies of planetary accretion in a condensate disc show that Mercury drew its mass from a wide range of orbital radii. Any initial chemical inhomogeneity at Mercury's distance would soon be blended out. Also, we need T(sub 1,1) - T(sub 1,2) is greater than 60 K if the density enhancement is to be noticeable, even in the absence of radial mixing. Additional information is contained in the original extended abstract.

Author

*Mercury (Planet); Planetary Composition; Density (Mass/Volume); Chemical Composition; Condensates*

**20010124878** Northwestern Univ., Evanston, IL USA

**Low Albedo, Blue, and Opaque Rich Spectral Anomalies in the Mercurian Crust**

Robinson, M. S., Northwestern Univ., USA; Hawke, B. R., Hawaii Univ., USA; Mercury: Space Environment, and Surface and Interior; 2001, pp. 83-84; In English; See also 20010124826; No Copyright; Abstract Only; Available from CASI only as part of the entire parent document

Newly calibrated UV (ultraviolet) (375 nm) and orange (575 nm) Mariner 10 mosaics were interpreted to indicate compositional heterogeneities in the mercurian crust. These studies interpreted the calibrated color data according to the view that ferrous iron lowers the albedo and reddens (relative decrease in the UV/visible ratio) a lunar or mercurian soil. Soil maturation has a similar effect with increasing maturity: darkening and reddening a soil with addition of submicroscopic iron metal. In contrast, addition of spectrally neutral opaque minerals (i.e. ilmenite) results in a nearly perpendicular trend to that of iron and maturity: opaque minerals lower the albedo and increase the UV/visible ratio. by transforming the Mariner 10 color data (UV and orange mosaics) and thus separating these color trends into two separate parameter images sensitive to relative abundances of opaque minerals and combined maturity-and-iron spectral anomalies on the surface can be mapped. Utilizing these parameter maps and the color mosaics, we extend the previous work by identifying occurrences of a relatively low albedo, blue, and opaque rich material (LBO). In addition to the distinct spectral properties of the LBOs we find that this unit typically exhibits diffuse and patchy boundaries. The four best exposures are found stratigraphically below the Rudaki (4 degrees S, 52 degrees W) and Tolstoj (15 degrees S, 165 degrees) plains, and in the areas of Lermomtov crater (16 degrees N, 49 degrees W) and Homer basin (1 degree S, 37 degrees W). With the limited spectral and spatial resolution of the Mariner 10 dataset we cannot uniquely determine the origin of these deposits. However, our observations are most consistent with two theories. 1) The LBOs are a volumetrically significant rock type that composes portions of the crust though compositionally distinct from the average crust or 2) they are relatively thin blankets of pyroclastic material. In the rest of this paper we will briefly describe the four best occurrences and discuss the merits of the two possible origins and their significance. Additional information is contained in the original extended abstract.

Author

*Mercury (Planet); Planetary Crusts; Planetary Composition; Image Analysis; Ultraviolet Astronomy; Soils; Mercury Surface*

**20010124879** Northwestern Univ., Evanston, IL USA

**Complexity of the Mercurian Crust**

Robinson, M. S., Northwestern Univ., USA; Taylor, G. J., Hawaii Univ., USA; Lucey, P. G., Northwestern Univ., USA; Hawke, B. R., Hawaii Univ., USA; Mercury: Space Environment, and Surface and Interior; 2001, pp. 85-86; In English; See also 20010124826; No Copyright; Abstract Only; Available from CASI only as part of the entire parent document

Mercury has been visited by only one reconnaissance spacecraft, Mariner 10, over 25 years ago. This mission executed three flybys, but only imaged one hemisphere of the planet and carried no instruments capable of making direct compositional measurements of Mercury. Thus, our current state of knowledge concerning Mercury is in many ways similar to what we knew about the Earth's moon at the dawn of the space age. From the Mariner 10 dataset it is known that Mercury underwent a complex and rich geologic history. The planet is heavily cratered, tectonically deformed, volcanically resurfaced, and has an anomalously high bulk density, suggesting an iron rich core that occupies a greater percent of its volume than that of the other terrestrial planets. One of the outstanding problems remaining from the Mariner 10 mission is a first order cataloging of the compositional diversity of the mercurian crust. Additional information is contained in the original extended abstract.

Author

*Mercury (Planet); Planetary Crusts; Planetary Composition; Mercury Surface; Chemical Composition; Ultraviolet Astronomy*

**20010124880** California Univ., Inst. of Geophysics and Planetary Physics, Los Angeles, CA USA

**The Magnetic Field and Magnetosphere of Mercury**

Russell, C. T., California Univ., USA; Mercury: Space Environment, and Surface and Interior; 2001, pp. 87; In English; See also 20010124826; No Copyright; Abstract Only; Available from CASI only as part of the entire parent document

The most naive picture of planetary magnetism is that a planet is hottest at initial accretion, the iron sinks to the center, if there is sufficient energy a magnetic field is generated, and when the planet cools the dynamo stops. In this picture, the large rocky planets, such as the Earth, should have active dynamos and the small rocky planets such as Mercury should not. In fact Mercury does appear to have an active dynamo while larger bodies such as Mars and Venus do not. The dynamos in the cores of these two planets either ceased or in the case of Venus perhaps never began. Thus the story of the generation of a planetary magnetic field is more complicated than the naive picture and includes the effect of the crust and mantle in allowing the core to cool so that a solid inner core can condense and provide the energy for the dynamo. We can learn about the interior of Mercury from its gravitational and magnetic fields but from the Mariner 10 flybys these have been but poorly constrained. In the case of the magnetic field the solution for the quadrupole moment is almost totally unconstrained. Orbiter measurements such as planned on

the Messenger and Bepi Columbo missions are essential to determine the high order magnetic field. The solar wind plasma confines Mercury's magnetic field to a teardrop-shaped region with a long tail in the antisolar direction. The solar wind is so strong at Mercury's orbit and the planetary magnetic moment so weak that the standoff distance of the solar wind flow at the subsolar point is very close to the planet's surface. Thus relative to the size of Mercury, already the smallest of the terrestrial planets, its magnetosphere is small. There is not much room for a radiation belt as we have on Earth. Nevertheless, the magnetosphere of Mercury is of great interest to magnetospheric physicists because of something else Mercury lacks, a significant atmosphere. In the terrestrial magnetosphere the magnetic field is rooted in a highly electrically conducting ionosphere caused by the ionization of the Earth's ionosphere. This ionosphere enables the coupling of the solar wind momentum with the atmosphere through the generation of current systems that close in the ionosphere. Since this coupling is not expected at Mercury, the nature of the solar wind magnetosphere interaction might be quite different at Mercury than at Earth. These differences in turn can provide insights into how the various magnetospheric processes work. Thus, one of the overall objectives of the Messenger and Bepi Columbo missions is to examine these magnetospheric processes. The sparse data obtained from the Mariner 10 missions in 1974 and 1975 indicates that analogs of terrestrial processes do occur at Mercury but that there are important differences in the ways in which these processes work.

Author

*Gravitational Fields; Mercury (Planet); Terrestrial Planets; Planetary Structure; Space Missions; Planetary Magnetospheres; Planetary Magnetic Fields*

**20010124881** Jet Propulsion Lab., California Inst. of Tech., Pasadena, CA USA

**Repeat-Orbit Interferometric Precision Measurement of Mercury Obliquity**

Slade, M. A., Jet Propulsion Lab., California Inst. of Tech., USA; Jurgens, R. F., Jet Propulsion Lab., California Inst. of Tech., USA; Margot, J.-L., California Inst. of Tech., USA; Standish, E. M., Jet Propulsion Lab., California Inst. of Tech., USA; Mercury: Space Environment, and Surface and Interior; 2001, pp. 88-89; In English; See also 20010124826; No Copyright; Abstract Only; Available from CASI only as part of the entire parent document

Repeat-orbit or time-delayed interferometry has been widely used for SAR (Synthetic Aperture Radar)-based observations of such terrestrial phenomena as flow of glaciers and post-seismic displacements from radar on Earth-orbiting satellites and spacecraft. Repeat-orbit interferometry has also obtained fringes while investigating the measurement of topography of the Moon from Arecibo radar observations. Because of the unique spin-orbit resonance of Mercury, the locus of the sub-radar point on Mercury crosses over itself many times per year. Moreover, the locus of the sub-radar track repeats these crossings from year to year over many years. Given the proper geometry, these subradar point crossings offer the opportunity for interplanetary repeat-orbit interferometry via Earth-based radar observations. The ephemerides of Mercury and Earth, and the orientation of the Earth, are all known to sufficiently high-precision with respect to 'inertial space' to enable this kind of interferometry. This capability would merely be a curiosity, since Earth-based radar lacks the signal-to-noise to measure planetary-scale topography, except that the technique can be used to measure Mercury's obliquity (and possibly the forced libration in longitude). Combining very accurate measurements of the obliquity and the forced libration in longitude with Mercury-orbiter-based measurements of the low-order and degree Mercury gravity field can place constraints on the size and state of Mercury's fluid core. Additional information is contained in the original extended abstract.

Author

*Mercury (Planet); Synthetic Aperture Radar; Astronomical Interferometry; Radar Astronomy; Planetary Rotation; Axes of Rotation; Attitude (Inclination)*

**20010124882** NASA Goddard Space Flight Center, Greenbelt, MD USA

**Estimating the Libration of Mercury by Remote Sensing of Gravity and Altimetry**

Smith, D. E., NASA Goddard Space Flight Center, USA; Zuber, M. T., Massachusetts Inst. of Tech., USA; Peale, S. J., California Univ., USA; Phillips, R. J., Washington Univ., USA; Solomon, S. C., Carnegie Institution of Washington, USA; Mercury: Space Environment, and Surface and Interior; 2001, pp. 90-91; In English; See also 20010124826; No Copyright; Abstract Only; Available from CASI only as part of the entire parent document

One of the most intriguing scientific questions about Mercury is whether the planet possesses a liquid core. One way that this can be ascertained is through the measurement of the longitudinal libration of Mercury about its rotation axis. The MESSENGER (Mercury Surface, Space, Environment, Geochemistry, and Ranging) mission to Mercury will attempt this measurement by deriving the rotation of the planet from remotely sensed observations of the Mercury gravity field and the planet's shape. For a fully fluid core the libration is expected to be an approximately 350-m-amplitude oscillation (at the equator) about the mean rotation of the planet. Thus, the shape of the planet undergoes a librational oscillation in the same way that features on the surface participate in the motion. In this sense altimetric topography can be considered analogous to imaging, with the important exception

that for altimetry, the long wavelengths corresponding to low degrees and orders in a spherical harmonic expansion, can be precisely determined from orbital measurements. The rotation of the planet thus introduces a time dependence of the topographic image in an inertial (i.e. fixed) reference frame and the libration is a variation in the planetary rotation rate, manifest as an oscillation of the topographic image. Similarly, gravity measures the distribution of mass within a planet and as such can be viewed as providing a vertically integrated 'image' of the internal density structure. For a librating planet the gravitational field will also reveal a variation in the rotation rate, manifest as an oscillation of the field with respect to an inertial reference frame. While the long-wavelength gravity field contains contributions from the radial distribution of mass with depth, the long wavelength terms are most sensitive to the mass distribution of the deep interior. Thus, both the topography and the gravity independently can be used to determine the (irregular) rotation of a planet, although the topographical method measures the rotation of the crust while the gravity measures the rotation of the distributed mass, and these are not necessarily identical. For example, for a planet that contains a fluid outer core that is effectively decoupled from the mantle the gravity field will not librate in the manner of a solid body. The libration obtained from the variable rotation of the gravity field will represent a combination of contributions due to a librating mantle and a differentially rotating fluid core. Differential rotation of the Earth's inner core had been theoretically predicted from three dimensional geodynamical models and subsequently reported from seismic observations. A difference between the libration of the lithosphere as determined from altimetry and the deep interior as determined from gravity, if it could be detected, might provide further insight into the nature of core-mantle coupling. Additional information is contained in the original extended abstract.
Author
*Altimetry; Libration; Mercury (Planet); Planetary Cores; Space Missions; Remote Sensing*

**20010124883** New Mexico State Univ., Dept. of Physics, Las Cruces, NM USA
**Mantle Convection and Thermal Evolution of Mercury Revisited**
Solomatov, V. S., New Mexico State Univ., USA; Reese, C. C., New Mexico State Univ., USA; Mercury: Space Environment, and Surface and Interior; 2001, pp. 92-93; In English; See also 20010124826; No Copyright; Abstract Only; Available from CASI only as part of the entire parent document

The question of whether mantle heat transport in Mercury occurs by conduction or convection was eventually settled in favor of convection. Indeed, quantitative estimates of convective instability and convective heat transport showed that convection must occur although not as vigorously as on Earth. Some observational support for convection was argued to be the presence of a magnetic field on Mercury which is easier to explain with mantle convection than without it. Rapid solidification of the iron core predicted by convective models and the cessation of generation of the magnetic field can be avoided if a sufficiently large amount of antifreeze is present (it can be anything, but sulfur is the most likely candidate). Although convection seems to be a reasonable theory, results based mainly on studies of constant viscosity convection can substantially overestimate the vigor of convection. Since previous models predicted a marginally unstable mantle with weak convection one might wonder if convection occurs at all for realistic rheologies. The goal of this study is to investigate models of mantle convection and thermal evolution of Mercury, which take into account realistic temperature- and pressure-dependent viscosity, partial melting and differentiation. Additional information is contained in the original extended abstract.
Author
*Antifreezes; Planetary Mantles; Mercury (Planet); Convection; Heat Transmission*

**20010124884** Carnegie Institution of Washington, Dept. of Terrestrial Magnetism, Washington, DC USA
**The MESSENGER Mission to Mercury**
Solomon, Sean C., Carnegie Institution of Washington, USA; McNutt, Ralph L., Jr., Johns Hopkins Univ., USA; Gold, Robert E., Johns Hopkins Univ., USA; Santo, Andrew G., Johns Hopkins Univ., USA; Mercury: Space Environment, and Surface and Interior; 2001, pp. 94-95; In English; See also 20010124826; No Copyright; Abstract Only; Available from CASI only as part of the entire parent document

Mercury is an extraordinary planet. The closest planet to the Sun, Mercury has the largest diurnal range in surface temperature yet has polar deposits that may consist of water ice. Mercury is the only planet locked in a spin-orbit resonance, an important though poorly understood constraint on dynamical and internal evolution. It has the largest uncompressed density and, by inference, the greatest mass fraction of iron-nickel of any planet or satellite, a compositional anomaly that is a critical clue, not yet deciphered, to the processes by which the inner planets formed. Mercury has a strong internal magnetic field and presumably a hydromagnetic dynamo in a fluid outer core, yet the known portion of the surface has a density of impact craters indicating that geological activity largely ceased early in planetary history. Mercury's magnetic field gives rise to a small magnetosphere with many similarities to that of the Earth, yet the presence of only a tenuous atmosphere and ionosphere and the greater proximity to the Sun affect the nature of solar wind interaction with the planet in ways still poorly discerned. Mercury is also the least

explored planet save Pluto. Most of what is known comes from the three flybys of Mercury by Mariner 10 in 1974 and 1975. With the recognition that gravity-assisted trajectories, using available launch and propulsion systems, now permit the insertion of a spacecraft into Mercury orbit, the need for the intensive exploration of the innermost planet has recently been recognized by both NASA and the European Space Agency. MESSENGER, a Mercury Surface, Space Environment, Geochemistry, and Ranging mission to orbit Mercury for one Earth year after completing two flybys of that planet and two flybys of Venus, was selected for flight under NASA's Discovery Program in July 1999. The lead institutions for MESSENGER are the Carnegie Institution of Washington and the Applied Physics Laboratory of The Johns Hopkins University. Additional members of the MESSENGER consortium include Composite Optics, Inc., a leader in lightweight spacecraft structures, GenCorp Aerojet, a leader in spacecraft propulsion systems, Goddard Space Flight Center, the University of Colorado, and the University of Michigan. Co-engineered with planetary scientists from twelve institutions, MESSENGER has been designed to accommodate the severe near-Sun thermal environment and supply the required large spacecraft velocity change while enabling all scientific observations. Additional information is contained in the original extended abstract.
Author
*Mercury (Planet); Space Missions; Space Exploration; Spacecraft Design; Planetary Evolution; Planetary Structure*

**20010124885** Arizona Univ., Lunar and Planetary Lab., Tucson, AZ USA
**Mercury's Atmospheric Species**
Sprague, A. L., Arizona Univ., USA; Mercury: Space Environment, and Surface and Interior; 2001, pp. 96-97; In English; See also 20010124826; No Copyright; Abstract Only; Available from CASI only as part of the entire parent document

Several attempts with ground-based spectrographs were made to find CO2 in Mercury's atmosphere during the 1960s and 1970s. But no atmosphere was discovered until Mariner 10 identified H, He, and possibly O with the Broadfoot et al. airglow polychromater, and made several upper limit measurements with the solar occultation instrument. In these experiments, limited wavelength bands were pre-determined based upon optical requirements and expectations of what might exist in an entirely unknown atmosphere. In 1985, Potter and Morgan were studying a phenomenon called the Ring effect observed as infilling of Fraunhofer lines in the reflected continuum from the lunar surface. For comparison, they shifted their view to Mercury and beheld significant emission lines, high above the continuum at 5890 and 5896 A, the wavelengths of the Na resonance lines. This discovery renewed groundbased spectroscopic search efforts that have resulted in discoveries of K and Ca and set an upper limit on Li. The pressure of the known atmosphere is approximately 10(exp -12) b. Mercury's atmospheric atoms do not collide appreciably with one another, only with the surface. For this reason it is called a surface-bounded-atmosphere. If the atmosphere were homogeneously distributed and its atoms assumed a Maxwellian speed distribution it would be called a surface-bounded-exosphere. But Mercury's atmosphere has multiple speed distributions with some and perhaps all species having multiple speed components that result from differing source, release, and recycling mechanisms. All of the known species were discovered by measuring emission of some, but not all, strong resonance lines in the ultraviolet and visible wavelengths. It is likely that MESSENGER will make new discoveries with its atmospheric and surface composition spectrograph (MASCS) because it covers the region from 1150 to 6000 A with no breaks and a resolving power sufficient to observe very faint resonant emissions above Mercury's limb. Additional information is contained in the original extended abstract.
Author
*Atmospheric Composition; Mercury (Planet); Mercury Atmosphere; Spectroscopy; Ultraviolet Astronomy; Chemical Composition*

**20010124887** Arizona Univ., Lunar and Planetary Lab., Tucson, AZ USA
**Mid-Infrared Spectroscopy of Mercury's Surface with BASS**
Sprague, A. L., Arizona Univ., USA; Russell, R. W., Aerospace Corp., USA; Lynch, D. K., Aerospace Corp., USA; Mazuk, A. L., Aerospace Corp., USA; Donaldson, K. L., Arizona Univ., USA; Mercury: Space Environment, and Surface and Interior; 2001, pp. 98-99; In English; See also 20010124826; No Copyright; Abstract Only; Available from CASI only as part of the entire parent document

Measurements of Mercury's thermal emission spectrum were made at the 3 m NASA Infrared Telescope Facility (IRTF) in Mauna Kea, Hawaii on March 21 and 22, 1998, and on May 11 and 12, 1998. The major purpose of the observations was to obtain information regarding the physical and chemical properties of Mercury's surface materials. In theory telescopic mid-infrared observations of planetary surfaces should yield spectral features that can be assigned to know Reststrahlen and other mineralogically caused features. When taken as a whole, however, differences between the 14 published spectra obtained with different instruments exhibit differences which cannot be explained easily by differences in the chemical make up of Mercury's soils, rocks and minerals observed. Thus, another purpose of these observations was to compare thermal emission spectra from the BroadBand Array Spectrograph (BASS) on the IRTF to those obtained by four other telescope, circular variable filter (CVF),

and spectrograph configurations: 1) the AT1 CVF on the IRTF; 2) the High Resolution Grating Spectrometer (HIFOGS) from the IRTF that exhibited spectral features resembling silicate Reststrahlen bands, transparency features, and from the 1m, Kuiper Airborne Observatory (KAO), in one case from 5 - 7 microns, a significantly high emission feature. The BASS spectra are also compared to those obtained with the McMath Pierce 1.5 m Solar Telescope on Kitt Peak with the Fourier transform spectrometer (FTS), and to a spectral composite from mid-infrared (8 - 13 microns) images obtained with the Mid-Infrared Array Camera (MIRAC) and the Steward Observatory 2.4 m telescope on Kitt Peak. All comparisons are inexact because of different viewing geometry on Mercury (sub-solar longitude and sub-Earth longitude), spectrograph aperture size (which can either isolate a portion of the illuminated surface or include the entire Earth-facing disk of Mercury), diffraction limit of the telescope used which is a function of telescope mirror diameter (limits the spatial resolution on the surface), and spectrograph resolving power (lambda/Delta lambda). Additional information is contained in the original extended abstract.
Author
*Infrared Astronomy; Mercury (Planet); Mercury Surface*

**20010124889** Hawaii Univ., Hawaii Inst. of Geophysics and Planetology, Honolulu, HI USA
**Mercury: An End-Member Planet or a Cosmic Accident?**
Taylor, G. J., Hawaii Univ., USA; Scott, E. R. D., Hawaii Univ., USA; Mercury: Space Environment, and Surface and Interior; 2001, pp. 104-105; In English; See also 20010124826; No Copyright; Abstract Only; Available from CASI only as part of the entire parent document

Mercury is unique. It is the densest planet, undoubtedly because it has a large metallic core. Spectral observations indicate that its surface is low in FeO (the best guess is around 3 wt%, but it might have none). Unambiguous lava plains have low FeO, indicating that their source regions in the mercurian mantle also contain little FeO, 2-3 wt%; we infer that the entire mercurian mantle is low in FeO. In contrast, the bulk silicate Earth and Venus contain more FeO (about 8 wt%), and Mars contains about 18 wt%. Do these compositional features of Mercury reflect its location near the Sun? Lewis suggested that temperature gradients in the solar nebula led to variations in chemical composition of the planets. The FeO variation from Mercury to Earth and Venus to Mars is consistent with this idea. Alternatively, could Mercury simply be the product of stochastic events? In this view, the terrestrial planets accreted from material from the whole inner solar system, and Mercury's high density is due to a large impact that removed much of its original mantle or other processes that fractionated metal from silicate. So, is Mercury an end-member planet that contains a record of its formation near the Sun? Or is it an accident of accretion and giant impacts? Additional information is contained in the original extended abstract.
Author
*Chemical Composition; Mercury (Planet); Position (Location); Solar System; Sun; Terrestrial Planets; Planetology; Planetary Evolution; Planetary Composition*

**20010124890** Deutsche Forschungsanstalt fuer Luft- und Raumfahrt, Inst. of Space Sensor Technology and Planetology Exploration, Berlin, Germany
**Application of an Updated Impact Cratering Chronology Model to Mercury's Time-Stratigraphic System**
Wagner, R. J., Deutsche Forschungsanstalt fuer Luft- und Raumfahrt, Germany; Wolf, U., Deutsche Forschungsanstalt fuer Luft- und Raumfahrt, Germany; Ivanov, B. A., Academy of Sciences (USSR), USSR; Neukum, G., Deutsche Forschungsanstalt fuer Luft- und Raumfahrt, Germany; Mercury: Space Environment, and Surface and Interior; 2001, pp. 106-107; In English; See also 20010124826; No Copyright; Abstract Only; Available from CASI only as part of the entire parent document

During three close encounters with Mercury in 1974-1975, the camera onboard the Mariner 10 spacecraft acquired images of 40-45 % of the total surface at spatial resolutions between 1 and 4 km/pxl, with highest resolutions obtained in selected areas down to about 100 m/pxl. In this work we present results from crater size-frequency measurements carried out on various geologic units, using a recently updated crater production function polynomial and impact cratering chronology model derived for Mercury in order to reassess the time-stratigraphic system established for Mercury. These investigations are prerequisite for further studies during two upcoming orbiting missions to Mercury, ESA's (European Space Agency) Bepi-Colombo and NASA's Messenger. Additional information is contained in the original extended abstract.
Author
*Cratering; Craters; Mercury (Planet); Space Missions; Stratigraphy; Chronology; Planetary Evolution; Geographic Distribution*

**20010124891** Uppsala Univ., Inst. fuer Astronomi och Rymdfysik, Uppsala, Sweden

**Disk-Resolved Multicolor Photometry and Spectroscopy of Mercury**

Warell, J., Uppsala Univ., Sweden; Mercury: Space Environment, and Surface and Interior; 2001, pp. 106; In English; See also 20010124826; No Copyright; Abstract Only; Available from CASI only as part of the entire parent document

Multicolor photometric observations of the poorly known (in terms of Mariner 10 coverage) hemisphere of Mercury have been performed with the Swedish Vacuum Solar Telescope (SVST) on La Palma at maximal elongations from the Sun in 1997 and 1998. The photometry was obtained in twilight and calibrated with standard star observations made shortly following the Mercury observations. The work is based on a subset, in the longitude range 160-310 degrees, of high resolution CCD (charge coupled device) image data covering the global surface of Mercury obtained by Warell and Limaye. The disk-integrated spectrum of Mercury displays a linear slope from 650 to 940 nm with the same reddening (approximately 17% / 1000 A) as the CCD spectrum by Vilas. The slopes of these two spectra are larger than previously published spectrophotometry, and indicate that the average Hermean regolith is considerably more mature than lunar anorthosite regions. The spectrophotometry presented here provides negative evidence for the presence of the putative absorption feature at 930 nm. due to presence of Fe(2+) in pyroxenes, though a band depth of 4% is possible within the photometric error budget. No effect of phase reddening is observed between phase angles of 63 degrees and 84 degrees. Multicolor photometry of resolved bright and dark albedo features on the Hermean disk shows a variation in spectral slopes for these features which is smaller than that from laboratory bidirectional reflectance spectra of lunar maria and highland soils for the same geometries. This indicates that the scattering properties are more homogeneous for Mercury and that there is no clear relation between reflectivity and chemical properties at spatial scales of approximately 300 km on the poorly known hemisphere. There is an inverse relation of spectral slope with emission angle for Hermean albedo features; i.e. the spectral slope increases as the terminator is approached. The relation is the same for the brightest and darkest features. This property of the Hermean regolith is most similar to that of Apollo 14 mature highland bulk surface soil. The inclination of the spectral slope-emission angle relation is larger for Mercury than for the Moon, indicating that the average Hermean regolith is more back-scattering and that this effect increases for longer wavelengths. Filter ratio images of the Hermean disk show that color variations are less than 2% with respect to the surroundings at a spatial scale of approximately 300 km. All slight color variations visible in the data are attributable to seeing effects and the spatial location of sampling CCD pixels with respect to the regolith albedo pattern. Low resolution spectroscopic observations in the 5,000-11,000 A range were carried out with the 2.6-m Nordic Optical Telescope (NOT) in June 1999. The seeing ranged from 0.8 to 1.3 arcseconds, allowing spectra from rather well-defined surface regions in the longitude range 200-300 degrees to be obtained. Very good correction for telluric absorptions has been possible thanks to extensive calibration observations. The increase in spectral slope with emission angle found by the disk-resolved spectrophotometry with the SVST is verified with the NOT spectroscopy. The spectra are practically featureless and no obvious absorption bands are visible; there are however possible very broad and shallow absorption features shortward of 6000 A and longward of 8500 A. The disk integrated spectral slope is somewhat smaller than that determined from the SVST spectrophotometry. Further results of the current analysis of the NOT spectra will be presented.

Author

*Spectrophotometry; Mercury Surface; Mercury (Planet); Charge Coupled Devices; Space Observations (From Earth); Regolith*

**20010124893** National Air and Space Museum, Center for Earth and Planetary Studies, Washington, DC USA

**Mechanical Modeling of the Discovery Rupes Thrust Fault: Implications for the Thickness of the Elastic Lithosphere of Mercury**

Watters, T. R., National Air and Space Museum, USA; Schultz, R. A., Nevada Univ., USA; Robinson, M. S., Northwestern Univ., USA; Cook, A. C., National Air and Space Museum, USA; Mercury: Space Environment, and Surface and Interior; 2001, pp. 111-112; In English; See also 20010124826; No Copyright; Abstract Only; Available from CASI only as part of the entire parent document

One of the most remarkable discoveries of the Mariner 10 mission to Mercury was the existence of hundreds of landforms described as lobate scarps. Based on morphology and offsets in crater wall and floor materials, lobate scarps are interpreted to be the surface expression of thrust faulting. The largest lobate scarp on the hemisphere imaged by Mariner 10 is Discovery Rupes. Located in the southern hemisphere, Discovery Rupes is over 500 km in length. New topographic data for Mercury, derived from digital stereoanalysis, using updated Mariner 10 camera orientations indicates that Discovery Rupes is up to approximately 1.5 km. high. These data are also providing the first quantitative measurements about the morphometry of Discovery Rupes. Using the new topographic data, it is possible to test the validity of kinematic models proposed for lobate scarps by mechanically modeling the long and short wavelength topography across Discovery Rupes. Additional information is contained in the original extended abstract.

Author

*Escarpments; Mercury (Planet); Mercury Surface; Geological Faults; Kinematics; Lithosphere*

**20010124895** Boston Univ., Boston, MA USA

**High Definition Imaging of Mercury's Surface and Atmosphere**

Wilson, J. K., Boston Univ., USA; Mendillo, M., Boston Univ., USA; Baumgardner, J., Boston Univ., USA; Mercury: Space Environment, and Surface and Interior; 2001, pp. 115; In English; See also 20010124826; No Copyright; Abstract Only; Available from CASI only as part of the entire parent document

High Definition Imaging (HDI) is a means of obtaining nearly diffraction-limited images of telescopic targets through a turbulent atmosphere without adaptive optics. The method involves taking thoUSAnds of high-speed (1/60th second) video images of an object, and then selecting the small fraction of those images which occurred during instances of 'perfect seeing' to construct a final, high-resolution image. In 1998 we obtained nearly diffraction-limited images of Mercury's surface using a digital imaging video system on the Mt. Wilson 1.5m telescope. These images reveal dark 'mare-like' areas punctuated by brighter spots. In November of 2000 we tested our complete HDI system on Mercury, including an image slicer/spectrograph, using the 2.1m telescope at McDonald Observatory. Our ultimate goal is to obtain high-resolution, monochromatic images of Mercury's sodium atmosphere to better understand the surface distribution and variability of the atmospheric source mechanisms.

Author

*Imaging Techniques; Mercury Atmosphere; Mercury Surface; High Speed Photography; Digital Cameras; Space Observations (From Earth)*

**20010124896** Rutgers - The State Univ., Dept. of Physics and Astronomy, NJ USA

**Photon- and Electron-Stimulated Desorption of Alkalis from Model Mineral Surfaces: Relation to Planetary Atmospheres**

Yakshinskiy, B. V., Rutgers - The State Univ., USA; Madey, T. E., Rutgers - The State Univ., USA; Mercury: Space Environment, and Surface and Interior; 2001, pp. 116; In English; See also 20010124826; No Copyright; Abstract Only; Available from CASI only as part of the entire parent document

To investigate source mechanisms for the origin of Na and K in the tenuous atmospheres of the planet Mercury and the Moon, we are studying the photon- and electron-stimulated desorption (PSD and ESD) of alkali atoms from amorphous silicon dioxide films grown on a metal substrate. The ultrahigh vacuum measurement scheme for ESD and PSD of alkalis includes an efficient pulsed low energy electron source, as well as mechanically chopped UV (ultraviolet) light from a mercury arc source, a highly sensitive detector based on surface ionization, and the use of a time-of-flight technique. We find that bombardment of Na (K) covered silica surface by ultraviolet photons or by low energy electrons (E is greater than 4 eV) causes desorption of supra-thermal Na and K atoms with velocity distribution peaks at 1000 m/s and 650 m/s, respectively. These values are consistent with the 'hot' components of the lunar and Mercurian atmospheres. The ESD yield demonstrates a resonance-like feature at approximately 11 eV and a shoulder at 25 eV excitation energy (O2s excitation). The mechanism of desorption is identified as an electronically excited charge-transfer from the silica substrate to neutralize the surface alkali ion, followed by desorption of the alkali atom [1]. These data strongly suggest that PSD by UV solar photons (E is greater than 4 eV) is a dominant source process for Na and K in the tenuous lunar atmosphere. Although there are insufficient electrons in the solar wind to produce the observed lunar sodium atmosphere, there appear to be sufficient UV solar photons to maintain the atmosphere by desorbing Na from the surface. In the case of Mercury, where long-wavelength solar photons cause significant heating of the surface (approximately 700 K) at the sub solar point, thermal desorption of Na and K is believed to contribute to the tenuous atmosphere, but PSD is likely to play a major role in that case also.

Author

*Alkalies; Lunar Atmosphere; Sodium; Potassium; Mercury Atmosphere; Desorption*

**20010124897** Michigan Univ., Atmospheric, Oceanic and Space Sciences Dept., Ann Arbor, MI USA

**The Mercury Plasma Environment: MHD Predictions and Mercury Pickup Ions**

Zurbuchen, T. H., Michigan Univ., USA; Koehn, P. L., Michigan Univ., USA; Fisk, L. A., Michigan Univ., USA; Gloeckler, G., Maryland Univ., USA; Kabin, K., Alberta Univ., Canada; Mercury: Space Environment, and Surface and Interior; 2001, pp. 117; In English; See also 20010124826; No Copyright; Abstract Only; Available from CASI only as part of the entire parent document

The Mercury environment is dominated by two particle populations: the solar wind and ions originating from Mercury. The absence of any significant ionosphere and atmosphere creates a magnetosphere that differs from the Earth's and may affect the transfer of energy from the solar wind to magnetospheric plasma. We use three-dimensional MHD (magnetohydrodynamics) simulations from Kabin et al. to model fundamental magnetospheric processes in the planet's vicinity. Due to its close vicinity to the Sun, the solar wind momentum flux is approximately 10 times larger than the momentum flux at Earth. At the same time, Mercury's intrinsic magnetic field is relatively weak. Under normal solar wind conditions, this magnetic field is able to hold off the solar wind, preventing it from striking the planet's surface. This is not always the case, however. For example, during fast coronal mass ejections the solar wind ram pressure can be sufficient to compress the magnetopause to the surface. This direct

interaction gives rise to sputtered particles that provide a direct probe of the surface composition. Most of these particles are released in a neutral state and are eventually ionized. The resulting pickup ions move through Mercury's magnetosphere. We apply the results of recently modeled three-dimensional MHD interactions of the solar wind and Mercury's magnetosphere to predict the plasma and composition measurements on MESSENGER, a Mercury orbiter scheduled for launch in 2004. We then use this simulated MHD structure of the magnetosphere to record the trajectories of newly created magnetospheric and near-surface pickup ions. During certain parts of the MESSENGER orbit, these ions are observed during their first gyration. The observed particles therefore provide a good measure for the neutral particle environment near Mercury. During other, more distant parts of the MESSENGER orbit, the spatial distribution of particles depends on the large-scale structure of the Mercury magnetosphere. Detailed pickup ion measurements, therefore provide direct information about the Mercury surface composition, and the structure of the Mercury magnetosphere. We will present the simulated trajectories and spatial distributions of these pickup ions, as well as predictions of particle fluxes measured by the Fast Imaging Plasma Spectrometer (FIPS), one of the mass spectrometers on board the MESSENGER spacecraft.
Author
*Magnetohydrodynamics; Mercury (Planet); Mercury Surface; Plasmas (Physics); Three Dimensional Models; Plasma Interactions; Planetary Magnetospheres*

**20010124898** NASA Goddard Space Flight Center, Greenbelt, MD USA
**A Procedure for Determining the Nature of Mercury's Core**
Peale, S. J., California Univ., USA; Phillips, R. J., Washington Univ., USA; Solomon, S. C., Carnegie Institution of Washington, USA; Smith, D. E., NASA Goddard Space Flight Center, USA; Zuber, M. T., Massachusetts Inst. of Tech., USA; Mercury: Space Environment, and Surface and Interior; 2001, pp. 73-74; In English; See also 20010124826; No Copyright; Abstract Only; Available from CASI only as part of the entire parent document

We review past assertions that the determinations of the four parameters, C(20), C(22), theta, phi, are sufficient to determine the size and state of Mercury's core. C(20) and C(22) are gravitational harmonics, theta is Mercury's obliquity and phi is the amplitude of the forced, 88 day period libration in longitude. The upcoming MESSENGER orbiter mission to Mercury with onboard instrumentation capable of measuring these four parameters, and the possibility of precision measurements of Mercury's spin geometry with radar interferometry techniques make a reexamination of this proposal particularly relevant. The two necessary conditions on the core-mantle interaction for the experiment to work are: 1. The core must not follow the 88 day physical librations of the mantle. 2. The core must follow the mantle on the time scale of the 250,000 year precession of the spin in Cassini state 1. We shall assume these two conditions are satisfied to develop the method and later establish the constraints on the core viscosity for which they are satisfied. Proposed mechanisms of core mantle coupling other than a viscous coupling do not frustrate the first condition. The physical libration of the mantle about the mean resonant angular velocity arises from the periodically reversing torque on the permanent deformation as Mercury rotates relative to the Sun. Additional information is contained in the original extended abstract.
Author
*Mercury (Planet); Planetary Cores; Planetary Rotation; Gravitation; Axes of Rotation; Libration*

**20010125026** Museum of Arts and Sciences, Macon, CA USA
**Hands On Universe: Astronomy project for museums. Final report**
Nov. 30, 1993; 9p; In English
Report No.(s): DE2000-764176; DOE/ER/75843-1-VOL-1; No Copyright; Avail: Department of Energy Information Bridge

The goal of the Hands On Universe project is to bring a sense of wonder about the Universe to children and adults in light-polluted and technology-deprived, culturally under-served environments. The beauty and magnificence of the heavens have been a source of wonder to humans from the earliest times. This appeal remains today, but for many people it is never realized. As humans have moved indoors and into urban areas, they have become less and less aware of the heavens. This program was designed introduce teachers, students, and the general community, to image processing and automated astronomy. There were two levels to the program at the Macon Museum of Arts and Sciences: a teacher enhancement /teacher training program and a program for school children which would also serve the general public.
NTIS
*Museums; Universe; Astronomy; Image Processing; Autonomy*

**20010125134** Jet Propulsion Lab., California Inst. of Tech., Pasadena, CA USA

**Energetic Ion and Electron Irradiation of the Icy Galilean Satellites**

Cooper, John F., Raytheon Information Technology and Scientific Services, USA; Johnson, Robert E., Virginia Univ., USA; Mauk, Barry H., Johns Hopkins Univ., USA; Garrett, Henry B., Jet Propulsion Lab., California Inst. of Tech., USA; Gehrels, Neil, NASA Goddard Space Flight Center, USA; Icarus; 2001; ISSN 0019-1035; Volume 149, pp. 133-159; In English
Contract(s)/Grant(s): NASW-99029; NAS5-97059; NAS5-98156; Copyright; Avail: Issuing Activity

Galileo Orbiter measurements of energetic ions (20 keV to 100 MeV) and electrons (20-700 keV) in Jupiter's magnetosphere are used, in conjunction with the JPL electron model (less than 40 MeV), to compute irradiation effects in the surface layers of Europa, Ganymede, and Callisto. Significant elemental modifications are produced on unshielded surfaces to approximately centimeter depths in times of less than or equal to 10(exp 6) years, whereas micrometer depths on Europa are fully processed in approximately 10 years. Most observations of surface composition are limited to optical depths of approximately 1 mm, which are indirect contact with the space environment. Incident flux modeling includes Stormer deflection by the Ganymede dipole magnetic field, likely variable over that satellite's irradiation history. Delivered energy flux of approximately 8 x 10(exp 10) keV/square cm-s at Europa is comparable to total internal heat flux in the same units from tidal and radiogenic sources, while exceeding that for solar UV energies (greater than 6 eV) relevant to ice chemistry. Particle energy fluxes to Ganymede's equator and Callisto are similar at approximately 2-3 x 10(exp 8) keV/square cm-s with 5 x 10(exp 9) at Ganymede's polar cap, the latter being comparable to radiogenic energy input. Rates of change in optical reflectance and molecular composition on Europa, and on Ganymede's polar cap, are strongly driven by energy from irradiation, even in relatively young regions. Irradiation of nonice materials can produce SO2 and CO2, detected on Callisto and Europa, and simple to complex hydrocarbons. Iogenic neutral atoms and meteoroids deliver negligible energy approximately 10(exp 4-5) keV/square cm-s but impacts of the latter are important for burial or removal of irradiation products. Downward transport of radiation produced oxidants and hydrocarbons could deliver significant chemical energy into the satellite interiors for astrobiological evolution in putative sub-surface oceans.
Author

*Radiation Chemistry; Europa; Ganymede; Callisto; Ion Irradiation; Electron Irradiation; Surface Layers*

## 92
## SOLAR PHYSICS

*Includes solar activity, solar flares, solar radiation and sunspots. For related information see 93 Space Radiation.*

**20010119228** Virginia Polytechnic Inst. and State Univ., Dept. of Mechanical Engineering, Blacksburg, VA USA

**Determination of the Thermal Offset of the Eppley Precision Spectral Pyranometer**

Haeffelin, Martial, Virginia Polytechnic Inst. and State Univ., USA; Kato, Seiji, Hampton Univ., USA; Smith, Amie M., Virginia Polytechnic Inst. and State Univ., USA; Rutledge, C. Ken, Analytical Sciences Corp., USA; Charlock, Thomas P., NASA Langley Research Center, USA; Mahan, J. Robert, Virginia Polytechnic Inst. and State Univ., USA; Applied Optics; Feb. 01, 2001; ISSN 0003-6935; Volume 40, No. 4, pp. 472-484; In English
Contract(s)/Grant(s): NAG1-2106; Copyright; Avail: Issuing Activity

Eppley's precision spectral pyranometer (PSP) is used in networks around the world to measure downwelling diffuse and global solar irradiance at the surface of the Earth. In recent years several studies have shown significant discrepancy between irradiances measured by pyranometers and those computed by atmospheric radiative transfer models. Pyranometer measurements have been questioned because observed diffuse irradiances sometimes are below theoretical minimum values for a pure molecular atmosphere, and at night the instruments often produce nonzero signals ranging between + 5 and - 10 W/sq m. We install thermistor sondes in the body of a PSP as well as on its inner dome to monitor the temperature gradients within the instrument, and we operate a pyrgeometer (PIR) instrument side by side with the PSP. We derive a relationship between the PSP output and thermal radiative exchange by the dome and the detector and a relationship between the PSP output and the PIR thermopile output (net-IR). We determine the true PSP offset by quickly capping the instrument at set time intervals. For a ventilated and shaded PSP, the thermal offset can reach - 15 W/sq m under clear skies, whereas it remains close to zero for low overcast clouds. We estimate the PSP thermal offset by two methods: (1) using the PSP temperatures and (2) using the PIR net-IR signal. The offset computed from the PSP temperatures yields a reliable estimate of the true offset (+/- 1 W/sq m). The offset computed from net-IR is consistent with the true offset at night and under overcast skies but predicts only part of the true range under clear skies.
Author

*Solar Radiation; Radiation Measuring Instruments; Terrestrial Radiation; Temperature Gradients; Radiative Transfer; Pyranometers*

## 93
## SPACE RADIATION

*Includes cosmic radiation; and inner and outer Earth radiation belts. For biological effects of radiation on plants and animals see 52 Aerospace Medicine. For theory see 73 Nuclear Physics.*

**20010122281** NASA Ames Research Center, Moffett Field, CA USA
**The FU Orionis Outburst as a Thermal Disk Accretion Event: Detailed Calculations and Comparison to Observations**
Bell, K. R., NASA Ames Research Center, USA; [1994]; 1p; In English; Disks and Outflows Around Young Stars Meeting, 6-9 Sep. 1994, Heidelberg, Germany
Contract(s)/Grant(s): RTOP 399-20-10-12; No Copyright; Avail: Issuing Activity; Abstract Only

FU Orionis outbursts are temporary large increases in luminosity: x (40 - 250) thought to occur repeatedly in all low mass young stellar systems. We discuss detailed calculations of viscous accretion disks suggesting that FU Ori events signify the existence of a protostellar disk transporting mass at a rate of (1 - 10) x 10(exp 6) solar mass / yr, in agreement with theoretical and observational estimates of molecular cloud core collapse rates. Accretion through the inner edge of disks subject to outburst is self-regulated through the thermal ionization instability such that long periods (approx. 1000 yrs) of low mass flux: (1 - 10) x 10(exp -5) solar mass / yr, are punctuated by short periods (approx. 100 yrs) of high mass flux: (1-10) x 10(exp -5) solar mass / yr. The unstable region of the disk extends radially only to a distance of approx. = 1/4 AU. Beyond this region matter is transported stably at the infall rate. In systems for which M(sum *) = 1 solar mass with an inner disk edge of 3 solar radius, the critical rate for outbursts is 5 x 10(exp -7) solar mass / yr independent of the magnitude of the viscous ce parameter consistent with estimates of boundary layer mass flux in T Tauri stars. We use timescales of observed outbursts to constrain the magnitude of the alpha parameter to be 10(exp -4) where hydrogen is neutral and 10(exp -3) where ionized. Light curves of V1515 Cyg, FU Ori, and V1057 Cya are reproduced; the latter two require application of a small perturbation in surface density to produce observed rapid rise times. Detailed reply is made to objections to the accretion disk model for outbursts. Comparison to observations are made of time dependent spectral energy distributions, colors, and line-width velocity evolution.
Author
*Accretion Disks; Cygnus Constellation; Estimates; Stellar Systems; Stellar Mass; Thermal Instability; Computation*

**20010125164** California Univ., Lawrence Berkeley Lab., Berkeley, CA USA
**Guide to Using the Berkeley Lab Cosmic Ray Detector**
Twitty, C.; Matis, H.; Jun. 30, 2000; 15p; In English
Report No.(s): DE2000-767637; LBNL-46909; No Copyright; Avail: Department of Energy Information Bridge, Microfiche

Cosmic rays are particles that strike the Earth at high speeds, and consequently high energies, from sources within our galaxy and beyond. To measure primary cosmic rays (these particles that come directly from sources in outer space) you would need to travel very high into the Earth's atmosphere. These primary cosmic rays collide with particles in our atmosphere and produce particles called secondary cosmic rays - many of which are muons or electrons. The Berkeley Lab detector measures secondary cosmic rays, which can be found at, and even below, the surface of the earth.
NTIS
*Earth Atmosphere; Primary Cosmic Rays; Secondary Cosmic Rays*

## 99
## GENERAL

*Includes aeronautical, astronautical, and space science related histories, biographies, and pertinent reports too broad for categorization; histories or broad overviews of NASA programs such as Apollo, Gemini, and Mercury spacecraft, Earth Resources Technology Satellite (ERTS), and Skylab; NASA appropriations hearings.*

**20010123756** Chaikin (Andrew), Arlington, MA USA
**A Man on the Moon: The Voyages of the Apollo Astronauts**
[1998]; In English
Report No.(s): LC-93-48680; ISBN 0-670-81446-6; Copyright; Avail: Issuing Activity

This full-length book chronicles NASA's Apollo space program. Based on interviews with astronauts and others involved in the program, each mission is carefully described. In Apollo 8, astronauts orbited the Moon for the first time. In Apollo 11, human

beings first walked on the lunar surface. Behind the scenes details from these and other Apollo missions are laid bare in this highly readable and comprehensive account, upon which a popular television miniseries was based.
CASI
*NASA Space Programs; Apollo Project; Apollo Flights*

**20010123760** Slayton (Donald K.), League City, TX USA
**Deke! US Manned Space: From Mercury to the Shuttle**
Slayton, Donald K., Slayton (Donald K.), USA; Cassutt, Michael; [1994]; 353p; In English
Report No.(s): LC-94-2463; ISBN 0-312-85918-X; Copyright; Avail: Issuing Activity

Deke Slayton was one of the first seven Mercury astronauts, and he might have been the first American in space. Instead, he became the first chief of America's Astronaut Corps. It was Deke Slayton who selected the crews who flew the Gemini, Apollo, and Skylab missions. It was Deke Slayton who made Neil Armstrong the first man on the moon. "Deke!" is Deke Slayton's story, told in his own words and in the voices of the men and women who worked with him and knew him best. Deke Slayton's knowledge of how the U.S. manned space program worked is the missing piece of every space buff's puzzle. Now, after decades of silence, he tells his priceless stories of those years when America was engaged in the greatest voyage of exploration in human history.
Derived from text
*Astronauts; Space Programs*

**20010123761** Kranz (Eugene F.), Houston, TX USA
**Failure Is Not an Option: Mission Control from Mercury to Apollo 13 and Beyond**
Krantz, Eugene F., Kranz (Eugene F.), USA; May 2001; 415p; In English; ISBN 0-425-17987-7; Copyright; Avail: Issuing Activity

This novel recounts the stories of the astronauts aboard space missions, specifically Apollo 11 and Apollo 13. The electrical fire that killed three Apollo astronauts is described, as well as what went wrong and how ground control fixed it. The stories are told from the point of view of mission control.
CASI
*Astronauts; Apollo 11 Flight; Apollo 13 Flight; Ground Based Control*

# Subject Term Index


## A

A STARS, 561
ABNORMALITIES, 543
ABRASION, 291, 570
ABSORPTION COOLING, 161
ABSORPTION SPECTRA, 204, 562, 564
ABSORPTION SPECTROSCOPY, 34, 60, 80, 130, 486
ABSORPTIVITY, 71
ABSTRACTS, 312, 550, 575
ABUNDANCE, 566
ACCELERATION (PHYSICS), 29, 495
ACCELERATORS, 359, 398, 551
ACCELEROMETERS, 202, 221, 223, 230
ACCESS CONTROL, 170
ACCRETION DISKS, 600
ACCUMULATORS, 255, 395
ACCURACY, 214, 343, 431
ACETALS, 90
ACETYL COMPOUNDS, 317
ACETYLENE, 56
ACID RAIN, 281
ACIDITY, 36, 41
ACOUSTIC EMISSION, 123, 410
ACOUSTIC MEASUREMENT, 230, 409, 411
ACOUSTIC PROPERTIES, 409
ACOUSTICS, 19, 407
ACTINIDE SERIES, 40, 64
ACTIVATION ENERGY, 118
ACTIVE GALACTIC NUCLEI, 566
ACTUATORS, 118, 363
ADAPTATION, 318, 319
ADAPTIVE FILTERS, 156
ADAPTIVE OPTICS, 430
ADDITIVES, 374
ADHESION, 177
ADHESIVE BONDING, 117
ADHESIVES, 42, 115, 117
ADIABATIC CONDITIONS, 385
ADMIXTURES, 237
ADRENOCORTICOTROPIN (ACTH), 325
ADSORBENTS, 333
ADSORPTION, 65, 82, 333
AERODYNAMIC COEFFICIENTS, 6, 190
AERODYNAMIC CONFIGURATIONS, 19, 199
AERODYNAMIC DRAG, 3, 6
AERODYNAMIC HEATING, 87, 190
AERODYNAMIC LOADS, 190
AERODYNAMIC STABILITY, 3
AERODYNAMICS, 3, 4, 6, 190
AEROELASTICITY, 17
AEROGELS, 41
AERONAUTICAL ENGINEERING, 5, 15
AERONAUTICS, 1, 2, 541
AEROSOLS, 240, 274, 275, 277, 281, 283, 287, 299
AEROSPACE ENGINEERING, 108, 156, 357
AEROSPACE ENVIRONMENTS, 24, 379, 589
AEROSPACE INDUSTRY, 24
AEROSPACE MEDICINE, 317, 321, 325, 326, 328
AEROSPACE SCIENCES, 360
AEROSPACE SYSTEMS, 5, 24, 25, 342, 359
AEROTHERMODYNAMICS, 4, 190, 193
AFTERBODIES, 188
AGING (MATERIALS), 172
AGREEMENTS, 148, 542
AGRICULTURE, 77, 133, 138, 233, 300, 301
AIR BREATHING ENGINES, 4
AIR CONDITIONING, 159
AIR CONDITIONING EQUIPMENT, 159
AIR COOLING, 453
AIR DEFENSE, 551
AIR FILTERS, 277
AIR FLOW, 68, 87, 191, 265, 272
AIR INTAKES, 68
AIR LAND INTERACTIONS, 293
AIR MASSES, 271
AIR POLLUTION, 154, 272, 273, 276, 278, 279, 280, 281, 283, 284, 286, 370
AIR QUALITY, 245, 279, 281
AIR SAMPLING, 244, 275, 282
AIR TO AIR REFUELING, 7
AIR TRAFFIC, 14
AIR TRANSPORTATION, 11, 12, 13, 14
AIR WATER INTERACTIONS, 62, 299
AIRBORNE EQUIPMENT, 20
AIRCRAFT, 5
AIRCRAFT ACCIDENT INVESTIGATION, 8
AIRCRAFT ACCIDENTS, 8, 543, 544
AIRCRAFT CONTROL, 20
AIRCRAFT FUEL SYSTEMS, 18
AIRCRAFT INDUSTRY, 2, 10, 23, 328, 329, 543
AIRCRAFT LANDING, 18
AIRCRAFT MAINTENANCE, 20
AIRCRAFT NOISE, 409
AIRCRAFT PILOTS, 328, 540, 544, 554
AIRCRAFT SAFETY, 7
AIRCRAFT STRUCTURES, 20
AIRFOILS, 3
AIRLINE OPERATIONS, 7, 8, 9, 16, 328, 540
AIRPORT SECURITY, 10
AIRPORTS, 10, 11, 12, 13, 14, 23, 31, 409
ALABAMA, 236
ALANINE, 318
ALCOHOLS, 146
ALFALFA, 138
ALGEBRA, 340
ALGORITHMS, 162, 167, 186, 195, 200, 207, 214, 220, 226, 234, 331, 335, 336, 337, 338, 339, 340, 343, 346, 351, 357, 483, 547, 560
ALIGNMENT, 203, 212, 521
ALKALIES, 276, 597
ALKALINE EARTH METALS, 68
ALKENES, 37
ALKYL COMPOUNDS, 68
ALLOYING, 94, 99
ALLOYS, 47, 63, 75, 97, 100, 104, 106, 108, 109, 110, 224
ALPHA PARTICLES, 46, 425
ALTERNATING CURRENT, 167, 208
ALTERNATIVES, 139, 255
ALTIMETRY, 593
ALTITUDE SICKNESS, 313
ALUMINUM, 54, 89, 93, 104, 106, 462
ALUMINUM ALLOYS, 15, 99, 102, 464
ALUMINUM ISOTOPES, 65
ALUMINUM NITRIDES, 175, 467
ALUMINUM OXIDES, 41, 85, 89, 95, 96, 112, 464, 477
AMAZON REGION (SOUTH AMERICA), 239
AMINO RADICAL, 323
AMMONIA, 72, 276, 278, 286
AMORPHOUS MATERIALS, 41, 45, 113, 119, 182, 229
AMORPHOUS SILICON, 400, 479

AMPHIBIOUS VEHICLES, 289
AMPLIFICATION, 430
AMPLIFIERS, 183
AMPLITUDE MODULATION, 527
ANAEROBES, 153
ANALOG DATA, 546
ANALOGIES, 199
ANALYSIS OF VARIANCE, 315
ANALYTICAL CHEMISTRY, 36, 41, 76, 263
ANCHORS (FASTENERS), 258
ANDROMEDA GALAXY, 561
ANGLE OF ATTACK, 3, 18, 192
ANGULAR DISTRIBUTION, 447
ANGULAR MOMENTUM, 28
ANIMALS, 312
ANIONS, 38
ANISOTROPY, 68, 97, 408, 468
ANNEALING, 110, 117
ANNUAL VARIATIONS, 282, 295, 305
ANNULI, 32
ANODES, 106, 113, 245, 248, 257, 269, 418
ANOMALIES, 185, 467
ANORTHOSITE, 576
ANTARCTIC REGIONS, 290
ANTENNA ARRAYS, 167
ANTIFERROMAGNETISM, 373, 381, 404, 476
ANTIFREEZES, 593
ANTIGRAVITY, 319
ANTIOXIDANTS, 309
ANTIPROTONS, 385, 415, 416
APERTURES, 491, 492
APOLLO 11 FLIGHT, 575, 601
APOLLO 13 FLIGHT, 25, 601
APOLLO FLIGHTS, 601
APOLLO PROJECT, 601
APPLICATIONS PROGRAMS (COMPUTERS), 17, 138, 155, 226, 339, 342, 347, 349, 357, 406, 423, 548, 550, 552
APPROXIMATION, 6, 408, 511
AQUEOUS SOLUTIONS, 45
AQUIFERS, 231
ARC LAMPS, 172
ARCHAEBACTERIA, 291
ARCHITECTURE, 547
ARCHITECTURE (COMPUTERS), 166, 168, 341, 346, 348, 354, 362, 552
ARCTIC REGIONS, 275
ARGON, 563
ARGON ISOTOPES, 585
ARID LANDS, 294
ARIZONA, 251, 281, 380
ARMATURES, 410
ARMED FORCES (UNITED STATES), 24, 162, 313
ARRAYS, 433
ARSENIC ISOTOPES, 481
ARTERIES, 325
ARTIFICIAL INTELLIGENCE, 52, 274, 352, 364, 560
ARTIFICIAL SATELLITES, 28
ASHES, 150
ASPECT RATIO, 450
ASSAYING, 309
ASSEMBLY LANGUAGE, 352
ASSESSMENTS, 544, 545
ASSIMILATION, 286, 365
ASTEROIDS, 564
ASTRONAUTS, 25, 318, 325, 575, 601
ASTRONOMICAL INTERFEROMETRY, 592
ASTRONOMICAL MODELS, 584
ASTRONOMICAL PHOTOMETRY, 586
ASTRONOMY, 598
ASTROPHYSICS, 563, 566
ASYMMETRY, 218, 331, 405, 520, 528, 539
ASYMPTOTIC GIANT BRANCH STARS, 564
ASYMPTOTIC METHODS, 367
ASYMPTOTIC PROPERTIES, 563
ASYNCHRONOUS TRANSFER MODE, 362
ATMOSPHERIC BOUNDARY LAYER, 187, 298
ATMOSPHERIC CHEMISTRY, 235, 275, 279, 280, 281, 284, 287, 294
ATMOSPHERIC CIRCULATION, 282, 298, 301
ATMOSPHERIC COMPOSITION, 4, 141, 205, 206, 306, 585, 589, 594
ATMOSPHERIC CORRECTION, 234
ATMOSPHERIC MODELS, 234, 235, 286, 288
ATMOSPHERIC MOISTURE, 296
ATMOSPHERIC PHYSICS, 293, 433
ATMOSPHERIC RADIATION, 235, 239, 242, 295, 297, 299, 301
ATMOSPHERIC TEMPERATURE, 297
ATOMIC BEAMS, 473
ATOMIC CLUSTERS, 413
ATOMIC COLLISIONS, 405, 498
ATOMIC ENERGY LEVELS, 98
ATOMIC EXCITATIONS, 126
ATOMIC FORCE MICROSCOPY, 81
ATOMIC PHYSICS, 88, 400, 414, 453
ATOMIC STRUCTURE, 263, 434, 461
ATOMIZING, 21, 40
ATROPHY, 327
ATTENUATION, 453
ATTITUDE (INCLINATION), 4, 390, 592
ATTITUDE CONTROL, 20
AUDITORY PERCEPTION, 332
AUDITORY SIGNALS, 17
AUGMENTATION, 146, 228, 407
AUSTENITIC STAINLESS STEELS, 48, 95, 110
AUSTRALIA, 290, 563
AUTOMATA THEORY, 198
AUTOMATIC CONTROL, 16, 17, 23, 76, 156, 326, 366
AUTOMATIC TEST EQUIPMENT, 441
AUTOMATIC WEATHER STATIONS, 163
AUTOMOBILE FUELS, 148, 152
AUTOMOBILES, 53, 141, 144, 149, 150, 269, 348, 349
AUTONOMIC NERVOUS SYSTEM, 328
AUTONOMY, 154, 207, 306, 329, 598
AUTOROTATION, 4
AXES OF ROTATION, 587, 592, 598
AXIAL FLOW, 191

## B

BACKSCATTERING, 176, 408
BACTERIA, 274, 308
BALLAST (MASS), 258
BARIUM, 466
BARIUM OXIDES, 460, 475
BARRIER LAYERS, 33, 177
BARS, 113
BARYONS, 398, 399, 525
BASALT, 119
BATHYMETERS, 306, 408
BATTERY CHARGERS, 251, 260
BAYES THEOREM, 221, 369
BEACHES, 289
BEAM CURRENTS, 388, 389, 517
BEAM INJECTION, 413, 500
BEAM INTERACTIONS, 412, 492, 501, 534, 536
BEAM SPLITTERS, 510
BEAMFORMING, 501
BEAMS (RADIATION), 210, 211, 215, 225, 378, 394, 406, 426, 491, 492, 497, 499, 502, 505, 506, 507, 508, 509, 527, 538
BEAMS (SUPPORTS), 223, 371
BED REST, 325
BEDS (GEOLOGY), 289
BENDING, 22, 384
BENDING MOMENTS, 22
BENZENE, 79
BERYLLIUM, 93, 112, 370, 374, 412

BETATRONS, 492
BIBLIOGRAPHIES, 548, 551
BICRYSTALS, 481
BIMETALS, 78
BINARY ALLOYS, 269
BINARY MIXTURES, 43, 189
BINARY SYSTEMS (MATERIALS), 47
BINAURAL HEARING, 163
BINDING ENERGY, 399, 525
BIOASTRONAUTICS, 318, 325
BIOFILMS, 308, 314, 315
BIOGEOCHEMISTRY, 239, 285, 291, 306, 308
BIOINSTRUMENTATION, 312
BIOLOGICAL EVOLUTION, 291
BIOLOGY, 41, 312, 319
BIOMASS, 77, 83, 133, 134, 135, 142, 145, 149, 153, 233, 255, 261, 268, 308
BIOMASS BURNING, 271, 284, 285
BIOMASS ENERGY PRODUCTION, 149
BIOMEDICAL DATA, 317
BIOPHYSICS, 431
BIOPROCESSING, 140
BIOTECHNOLOGY, 149, 437
BIPOLAR TRANSISTORS, 175, 178, 180
BISMUTH COMPOUNDS, 102
BISMUTH OXIDES, 113, 460
BLANKETS (FUSION REACTORS), 120
BLINDNESS, 324
BLOOD CIRCULATION, 319
BLOOD PRESSURE, 325
BLOWOUTS, 160
BODIES OF REVOLUTION, 192
BODY CENTERED CUBIC LATTICES, 98, 106
BODY FLUIDS, 320
BODY TEMPERATURE, 334
BODY WEIGHT, 327
BOEING 747 AIRCRAFT, 2
BOILERS, 75, 139, 142, 286
BOILING WATER REACTORS, 427
BONDING, 220, 486, 567
BONE MINERAL CONTENT, 323
BONES, 316, 322
BOREHOLES, 245
BORIC ACIDS, 121
BORON, 207, 498
BORON COMPOUNDS, 93
BORON NITRIDES, 127, 222
BORON-EPOXY COMPOSITES, 19, 20
BOSONS, 383, 503, 514, 529
BOUNDARIES, 192, 340, 479
BOUNDARY CONDITIONS, 157, 189, 408
BOUNDARY ELEMENT METHOD, 91
BOUNDARY LAYERS, 4, 285, 286, 299
BOUNDARY VALUE PROBLEMS, 432
BRAGG ANGLE, 465
BRAIN, 317
BRANCHING (PHYSICS), 389, 420, 539
BRAZIL, 239, 271, 284
BRAZING, 158
BREAKDOWN, 119
BREMSSTRAHLUNG, 514
BRIGHTNESS, 564
BRIGHTNESS TEMPERATURE, 293
BRINES, 188
BROADBAND, 171
BROKEN SYMMETRY, 382, 404, 480
BROMINE ISOTOPES, 481
BRONZES, 263
BSCCO SUPERCONDUCTORS, 466, 474, 488
BUBBLES, 151, 304
BUFFETING, 18, 22, 194
BUILDINGS, 156, 246, 272, 283, 547
BUNCHING, 397, 518
BUOYANCY, 187
BURNERS, 21
BUTENES, 399

## C

C++ (PROGRAMMING LANGUAGE), 355
CADMIUM, 426
CADMIUM SULFIDES, 266
CADMIUM TELLURIDES, 256, 266, 454
CALCIUM, 316, 322, 324
CALCIUM CARBONATES, 62
CALCIUM OXIDES, 460
CALCULUS OF VARIATIONS, 377
CALIBRATING, 19, 180, 207, 234, 253, 268, 446, 512, 520
CALIFORNIA, 148, 161, 270, 283, 284
CALLISTO, 599
CALORIMETERS, 155, 221, 525
CAMERAS, 205, 438, 578
CAMS, 336
CANCER, 309, 310
CANONICAL FORMS, 485
CANOPIES (VEGETATION), 320
CAPACITANCE SWITCHES, 398
CAPACITORS, 129, 177
CAPILLARY WAVES, 304
CAPTURE EFFECT, 420
CARBIDES, 127
CARBON, 52, 82, 91, 113, 121, 256, 267, 275, 306, 486, 563
CARBON 13, 529
CARBON 14, 436
CARBON CYCLE, 306, 316
CARBON DIOXIDE, 44, 47, 57, 90, 131, 136, 141, 211, 262, 273, 276, 286, 318, 333
CARBON DIOXIDE CONCENTRATION, 141
CARBON DIOXIDE LASERS, 72, 100
CARBON FIBERS, 53, 116
CARBON ISOTOPES, 314
CARBON MONOXIDE, 37, 250, 253
CARBON STEELS, 47
CARBON-CARBON COMPOSITES, 54
CARBONACEOUS MATERIALS, 267
CARBONATES, 232, 270
CARCINOGENS, 34
CARDIOVASCULAR SYSTEM, 319, 326, 327
CARRIER FREQUENCIES, 170, 183
CASTING, 94, 102, 109
CATALYSIS, 47, 79, 80, 132
CATALYSTS, 37, 78, 90, 151, 269, 282, 287
CATALYTIC ACTIVITY, 60, 90
CATHODES, 91, 245, 250, 265
CATHODIC COATINGS, 259
CATHODOLUMINESCENCE, 61
CATIONS, 68, 84, 476
CAVES, 35, 136, 228
CAVITATION CORROSION, 47
CAVITATION FLOW, 408
CAVITIES, 47, 105, 211, 373, 375, 407, 482, 488
CAVITY RESONATORS, 67, 382, 514
CELESTIAL BODIES, 565
CELESTIAL REFERENCE SYSTEMS, 292
CELL MEMBRANES (BIOLOGY), 317
CELLS (BIOLOGY), 321
CELLULOSE, 77
CEMENTS, 123
CENTRAL NERVOUS SYSTEM, 312
CENTRIFUGES, 235
CENTRIFUGING, 320
CENTROIDS, 518
CERAMIC FIBERS, 51, 123
CERAMIC MATRIX COMPOSITES, 16, 21, 51, 111, 114, 122
CERAMICS, 46, 52, 54, 74, 85, 86, 114, 115, 118, 119, 120, 121, 122, 123, 124, 125, 126, 127, 129, 214, 463, 487, 502
CERENKOV RADIATION, 470
CERIUM COMPOUNDS, 473

CERIUM OXIDES, 118, 458, 487
CERMETS, 123, 130, 245
CERTIFICATION, 28
CESIUM, 55
CESIUM 137, 47
CESSNA 172 AIRCRAFT, 20
CHAIN REACTIONS (CHEMISTRY), 68
CHAINS, 389
CHALCOGENIDES, 116, 121
CHANNELS (DATA TRANSMISSION), 451
CHARACTERIZATION, 45, 53, 180, 230, 237, 462
CHARGE CARRIERS, 67
CHARGE COUPLED DEVICES, 173, 557, 586, 596
CHARGE DISTRIBUTION, 501
CHARGED PARTICLES, 398, 448, 508, 511, 523, 536, 580
CHARM (PARTICLE PHYSICS), 381, 396, 401
CHARPY IMPACT TEST, 425
CHARTS, 191
CHECKOUT, 185
CHEMICAL ANALYSIS, 39, 41, 43, 45, 49, 274, 275
CHEMICAL BONDS, 476
CHEMICAL COMPOSITION, 33, 38, 82, 87, 142, 287, 579, 586, 589, 590, 591, 594, 595
CHEMICAL EQUILIBRIUM, 486
CHEMICAL EXPLOSIONS, 71
CHEMICAL PROPERTIES, 34, 49
CHEMICAL REACTIONS, 43, 68, 78, 121, 150, 189, 451, 466
CHEMICALS, 75
CHEMISORPTION, 66
CHINA, 279, 297
CHINESE SPACE PROGRAM, 24
CHIPS, 483
CHIPS (ELECTRONICS), 181
CHIRALITY, 402, 422, 466, 480, 521, 522, 523
CHLORINE, 109
CHOLESKY FACTORIZATION, 352
CHOLESTEROL, 315
CHOLINESTERASE, 317
CHONDRITES, 566
CHROMATOGRAPHY, 77
CHROMIUM, 15, 63, 412, 458
CHROMIUM ALLOYS, 101, 110
CHRONOLOGY, 595
CIRCADIAN RHYTHMS, 330
CIRCUITS, 174
CIRRUS CLOUDS, 288
CIVIL AVIATION, 2, 9, 10, 12, 328, 329, 333, 409, 541
CIVIL DEFENSE, 548
CLASSIFICATIONS, 167, 369, 409
CLATHRATES, 132
CLAYS, 226, 267
CLEAN ENERGY, 148, 284
CLEAN FUELS, 148, 152, 284
CLIFFS, 290
CLIMATE CHANGE, 135, 283, 296, 300, 303, 410, 556
CLIMATE MODELS, 282, 303, 410
CLIMATOLOGY, 278, 283, 294, 297, 300, 301, 305, 556
CLINICAL MEDICINE, 311, 327
CLOSED ECOLOGICAL SYSTEMS, 315, 333
CLOSING, 132, 141
CLOUD COVER, 302
CLOUD-TO-GROUND DISCHARGES, 300
CLOUDS (METEOROLOGY), 202, 296, 297, 299, 302, 306
CLUTCHES, 218
COAL, 141, 142, 143, 145, 151, 268, 276, 279
COAL DERIVED GASES, 145
COAL GASIFICATION, 145, 249
COAL LIQUEFACTION, 43
COASTAL WATER, 187
COASTS, 260
COATINGS, 323, 468
COBALT 60, 207
COBALT ALLOYS, 97
COBALT OXIDES, 463
COCKPITS, 17
CODING, 424
COEFFICIENT OF FRICTION, 377
COEFFICIENTS, 391
COGNITION, 334
COHERENCE, 429, 431
COHERENT LIGHT, 213, 433
COHERENT RADIATION, 316, 434, 483, 517, 519, 537
COKE, 144, 151, 221
COLD NEUTRONS, 212
COLD ROLLING, 113
COLLAPSE, 112
COLLIMATORS, 212
COLLISION AVOIDANCE, 8
COLLISIONS, 374, 383, 385, 398, 400, 416, 495, 500, 505, 508, 512, 513, 561
COLLOCATION, 368
COLOR, 67, 355, 428, 431
COLOR PHOTOGRAPHY, 578
COLORADO, 265, 297
COLUMBIA RIVER BASIN (ID-OR-WA), 227
COMBAT, 17, 364
COMBUSTION, 71, 73, 77, 141, 144, 368, 420
COMBUSTION CHAMBERS, 21, 154, 195, 279
COMBUSTION PHYSICS, 67, 71
COMBUSTION PRODUCTS, 131, 143
COMBUSTION SYNTHESIS, 120
COMETARY COLLISIONS, 562
COMETS, 561
COMMAND AND CONTROL, 162, 334, 345, 351
COMMERCE, 70, 160, 349
COMMERCIAL AIRCRAFT, 16, 20, 409
COMMERCIAL ENERGY, 246
COMMERCIAL OFF-THE-SHELF PRODUCTS, 24, 548
COMMERCIALIZATION, 140
COMMUNICATING, 542
COMMUNICATION, 169
COMMUNICATION NETWORKS, 168, 169, 289
COMMUNICATION SATELLITES, 170
COMPACTING, 475
COMPARISON, 239
COMPLEX COMPOUNDS, 42
COMPLEX SYSTEMS, 71, 335, 337, 338, 345, 396
COMPONENT RELIABILITY, 109, 366
COMPOSITE MATERIALS, 21, 51, 52, 54, 55, 64, 96, 120, 217, 364
COMPOSITION (PROPERTY), 255, 259, 314
COMPRESSED GAS, 132
COMPRESSIBILITY, 192
COMPRESSIBLE FLOW, 188, 198, 368
COMPRESSION LOADS, 224
COMPRESSION RATIO, 180
COMPRESSION TESTS, 104
COMPRESSORS, 166, 517
COMPTON EFFECT, 422
COMPUTATION, 101, 342, 360, 371, 525, 600
COMPUTATIONAL CHEMISTRY, 412
COMPUTATIONAL FLUID DYNAMICS, 6, 38, 66, 144, 146, 147, 151, 186, 187, 189, 190, 193, 195, 196, 197, 198, 199, 343, 354, 356, 361, 426, 427
COMPUTATIONAL GRIDS, 2, 192, 335, 338, 342
COMPUTER AIDED DESIGN, 16, 178, 347, 350, 354
COMPUTER AIDED TOMOGRAPHY, 440

COMPUTER INFORMATION SECURITY, 343, 360, 549, 550
COMPUTER NETWORKS, 342, 346, 356, 360, 362, 549, 550
COMPUTER PROGRAM INTEGRITY, 421, 550
COMPUTER PROGRAMMING, 155, 190, 336, 345, 347, 351, 352, 363
COMPUTER PROGRAMS, 6, 24, 48, 66, 340, 342, 347, 348, 350, 352, 353, 354, 355, 357, 358, 362, 449, 502, 512, 519, 532, 536, 552
COMPUTER STORAGE DEVICES, 177
COMPUTER SYSTEMS DESIGN, 17
COMPUTER SYSTEMS PERFORMANCE, 165
COMPUTER SYSTEMS PROGRAMS, 348
COMPUTER SYSTEMS SIMULATION, 346
COMPUTER TECHNIQUES, 343, 346, 357, 429
COMPUTER VISION, 339, 361, 365
COMPUTERIZED SIMULATION, 38, 44, 63, 87, 94, 146, 147, 150, 164, 169, 186, 192, 207, 215, 217, 235, 265, 269, 285, 298, 339, 343, 347, 349, 351, 358, 361, 384, 423, 427, 434, 439, 444, 451, 460, 476, 483, 490, 502, 508
COMPUTERS, 196, 357, 359, 360
CONCENTRATION (COMPOSITION), 474, 486, 512
CONCENTRATORS, 39, 44, 247
CONCRETES, 34, 49, 212
CONDENSATES, 124, 590
CONDENSED MATTER PHYSICS, 69
CONDUCTIVE HEAT TRANSFER, 40, 193
CONDUCTORS, 162, 468
CONFERENCES, 1, 34, 69, 139, 188, 253, 280, 301, 309, 312, 377, 387, 430, 452, 496, 497, 500, 575
CONFIDENCE, 221
CONFIGURATION INTERACTION, 58, 414
CONFIGURATION MANAGEMENT, 361
CONFINEMENT, 84
CONGRESSIONAL REPORTS, 550
CONIFERS, 233
CONJUGATION, 48
CONNECTION MACHINE, 197
CONSERVATION EQUATIONS, 189
CONSERVATION LAWS, 72, 339
CONSTRUCTION, 43, 515
CONTAINMENT, 84, 125
CONTAMINANTS, 34, 131, 232, 233, 271, 272, 315, 444
CONTAMINATION, 232, 305, 427
CONTINENTAL SHELVES, 306
CONTINUOUS RADIATION, 210
CONTINUOUS SPECTRA, 372
CONTINUUM MODELING, 60, 238
CONTINUUMS, 561
CONTOURS, 84
CONTRACTORS, 148
CONTROL BOARDS, 260
CONTROL EQUIPMENT, 537
CONTROL SYSTEMS DESIGN, 145, 315, 331, 525, 539
CONTROL THEORY, 365, 551
CONTROLLED ATMOSPHERES, 320
CONTROLLERS, 348, 363
CONVECTION, 295, 593
CONVECTIVE HEAT TRANSFER, 190, 288
CONVERGENCE, 497
COOLANTS, 95, 180, 403, 419
COOLING, 109, 161, 413, 509
COOLING SYSTEMS, 34, 215, 502, 508, 510
COORDINATES, 578
COORDINATION, 169, 552
COPLANARITY, 559
COPOLYMERIZATION, 37
COPPER, 58, 66, 96, 104, 106, 112, 257, 466, 487
COPPER INDIUM SELENIDES, 257
COPPER OXIDES, 96, 460, 472, 475, 482
COPPER SELENIDES, 260
COPYRIGHTS, 549
CORES, 490
CORN, 142
CORNEA, 323
CORNERS, 464
CORRECTION, 162, 210, 234, 491, 492
CORRELATION, 199, 371, 464, 466
CORRELATION COEFFICIENTS, 307
CORROSION, 65, 87, 104, 119, 188
CORROSION PREVENTION, 15, 75, 161
CORROSION RESISTANCE, 46, 47, 74, 75
CORROSION TESTS, 73, 75, 109, 150
CORRUGATED PLATES, 188
CORTICOSTEROIDS, 325
COSMIC DUST, 562
COSMIC RAY SHOWERS, 470
COSMIC RAYS, 400, 447, 566, 573
COST EFFECTIVENESS, 88
COST ESTIMATES, 264
COST REDUCTION, 266, 344
COSTA RICA, 283
COSTS, 142, 153, 311
COULOMB COLLISIONS, 491
COULOMB POTENTIAL, 63
COUNTERFLOW, 188
COUNTERMEASURES, 315
COUNTERS, 221
CRACK INITIATION, 101
CRACK PROPAGATION, 19, 100, 101, 110, 114, 130
CRACK TIPS, 111
CRACKING (CHEMICAL ENGINEERING), 38, 66, 146, 147, 427
CRANES, 156
CRASHWORTHINESS, 18
CRATERING, 571, 595
CRATERS, 582, 588, 595
CREEP PROPERTIES, 54, 95, 96, 110
CREEP STRENGTH, 95
CREW PROCEDURES (INFLIGHT), 29
CREW PROCEDURES (PREFLIGHT), 29
CREWS, 364
CRITICAL CURRENT, 113, 459, 466, 467, 470, 475, 481, 482
CRITICAL EXPERIMENTS, 416
CRITICAL POINT, 479
CRITICAL TEMPERATURE, 478
CROP GROWTH, 315
CRUDE OIL, 32, 87, 136, 138, 148, 151
CRUSHING, 116
CRUSTS, 572, 582
CRYOGENIC COOLING, 156, 463
CRYOGENIC EQUIPMENT, 243
CRYOGENIC TEMPERATURE, 208
CRYOGENICS, 40, 163, 445
CRYOSTATS, 375
CRYPTOGRAPHY, 363, 365
CRYSTAL DEFECTS, 83, 112, 474, 477
CRYSTAL FIELD THEORY, 473
CRYSTAL GROWTH, 459, 460, 462
CRYSTAL STRUCTURE, 49, 91, 265, 266, 455, 466, 470, 476, 484, 487
CRYSTAL SURFACES, 78, 469
CRYSTALLINITY, 120, 184, 229, 266, 377, 404, 479, 501, 558, 573
CRYSTALLIZATION, 44, 63
CRYSTALLOGRAPHY, 81, 176, 266
CRYSTALS, 62, 376, 457, 459, 469, 509, 510
CUES, 565
CULTURE TECHNIQUES, 323
CUPRATES, 468, 472, 478
CURIUM, 425
CURRENT DENSITY, 113, 482
CUSHIONS, 445
CYANIDES, 318

CYBERNETICS, 364
CYCLIC LOADS, 100, 123, 323
CYCLOGENESIS, 297
CYCLONES, 297, 298, 306
CYCLOTRON RESONANCE, 461
CYCLOTRONS, 402, 456
CYGNUS CONSTELLATION, 600
CYLINDRICAL BODIES, 157, 218, 376
CYLINDRICAL CHAMBERS, 159
CYTOLOGY, 317

## D

DAMAGE, 18, 44, 111, 222
DAMAGE ASSESSMENT, 53, 459
DAMPING, 522
DARK MATTER, 400
DATA ACQUISITION, 154, 202, 219, 234, 235, 260, 358, 396, 411, 420, 451, 503, 553
DATA BASE MANAGEMENT SYSTEMS, 166, 357
DATA BASES, 25, 342, 345, 356, 362, 554
DATA CONVERSION ROUTINES, 354
DATA FLOW ANALYSIS, 552
DATA LINKS, 9
DATA MANAGEMENT, 41, 295, 362, 418, 562
DATA PROCESSING, 93, 220, 354, 359, 393, 537
DATA PROCESSING EQUIPMENT, 251
DATA REDUCTION, 575
DATA RETRIEVAL, 296
DATA STORAGE, 546
DATA SYSTEMS, 9
DATA TRANSFER (COMPUTERS), 356
DATA TRANSMISSION, 165, 166, 169, 179, 343, 356, 362, 406, 553
DEATH VALLEY (CA), 240, 241
DEBRIS, 25, 572
DECAY, 387, 495, 520
DECISION MAKING, 7, 170, 342, 348, 351, 365, 543, 544, 545, 546
DECOMMISSIONING, 135, 422
DECOMPOSITION, 64, 113, 154, 282
DECONTAMINATION, 59, 82, 212, 422
DECOUPLING, 492
DEFECTS, 38, 86, 93, 130, 174, 185, 457, 469
DEFENSE PROGRAM, 159, 209, 248, 249, 344, 345, 349, 353, 417, 550, 556
DEFORMATION, 49, 54, 96, 104, 116, 127, 224, 293, 414, 457
DEGRADATION, 127, 363, 469, 483, 569, 573
DEGREES OF FREEDOM, 415
DELTA LAUNCH VEHICLE, 25
DEMOGRAPHY, 12
DENSITY (MASS/VOLUME), 41, 187, 587, 590
DENSITY DISTRIBUTION, 389, 423, 564
DENSITY MEASUREMENT, 40
DEPLOYMENT, 7, 8, 163, 313, 358
DEPOSITION, 89, 235, 257, 290, 438, 447, 463, 468
DEPOSITS, 94
DEPTH MEASUREMENT, 208
DERMATOLOGY, 311
DESERTS, 280
DESIGN, 156
DESIGN ANALYSIS, 158, 165, 175, 181, 183, 202, 252, 278, 353, 359, 369, 387, 392, 393, 395, 490, 494, 516, 522
DESIGN OPTIMIZATION, 378, 392, 433
DESORPTION, 333, 597
DESTRUCTION, 59, 224
DESTRUCTIVE TESTS, 423, 441
DETECTION, 28, 37, 43, 80, 147, 148, 181, 200, 208, 288, 385, 515
DETECTORS, 202, 380, 508, 538
DETONATION, 72, 147
DEUTERIUM, 450, 504, 516
DEUTERIUM COMPOUNDS, 316
DEUTERONS, 86, 384, 504
DIAGNOSIS, 166, 191, 388, 505
DIAMOND FILMS, 182, 458, 488
DIAMONDS, 83, 458, 460, 486, 487, 520, 538
DIATOMIC MOLECULES, 76
DIELECTRIC PROPERTIES, 129, 480
DIELECTRICS, 60, 119, 456, 484, 485, 522, 523, 529
DIESEL ENGINES, 60, 137, 145, 214, 217, 272
DIESEL FUELS, 135, 145, 154, 261, 269
DIETS, 315, 324
DIFFERENCE EQUATIONS, 368
DIFFERENTIAL EQUATIONS, 367
DIFFRACTION, 186, 350, 383
DIFFRACTOMETERS, 212, 379, 437
DIFFUSION, 3, 69, 464
DIFFUSION FLAMES, 56, 57, 58, 59, 62
DIFFUSION THEORY, 449
DIFFUSION WELDING, 220
DIFFUSIVITY, 110
DIGITAL CAMERAS, 597
DIGITAL DATA, 546
DIGITAL SYSTEMS, 219, 507
DIGITAL TECHNIQUES, 162
DILUTION, 404
DIMENSIONAL ANALYSIS, 565
DIMENSIONAL MEASUREMENT, 404
DIPOLES, 71
DIRAC EQUATION, 371
DIRECT NUMERICAL SIMULATION, 198
DIRECTIVITY, 367
DISABILITIES, 361
DISCONTINUITY, 484
DISCRETE COSINE TRANSFORM, 353
DISPLACEMENT, 330
DISPLAY DEVICES, 31, 170, 330, 428, 434, 549
DISSIPATION, 367
DISSOCIATION, 58, 60, 383, 399
DISSOLVED GASES, 110
DISSOLVED ORGANIC MATTER, 306, 431
DISTANCE, 541
DISTORTION, 109, 198
DISTRIBUTED MEMORY, 553
DISTRIBUTED PROCESSING, 168, 341, 346
DISTRIBUTION (PROPERTY), 485
DISTRIBUTION FUNCTIONS, 370, 372, 395, 461
DIURNAL VARIATIONS, 297, 583
DIVERGENCE, 511
DIVERTERS, 447, 450
DIVERTORS (FUSION REACTORS), 449
DIVIDERS, 186
DOCUMENT MARKUP LANGUAGES, 348
DOCUMENTS, 551
DOMAIN WALL, 496, 499, 528
DOMES (GEOLOGY), 138
DOMINANCE, 239
DOPED CRYSTALS, 41, 42, 48, 287, 372, 374, 434, 454, 458, 460, 469, 473, 474
DOPPLER EFFECT, 414, 430, 568
DOPPLER RADAR, 207
DOSAGE, 272
DRAG, 556
DRILLING, 209, 231, 267, 568
DROPS (LIQUIDS), 66, 67
DRUGS, 311
DRYING, 264
DUCTILE-BRITTLE TRANSITION, 100
DUCTS, 214
DURABILITY, 119
DUST, 283, 560
DYADICS, 171

DYNAMIC CHARACTERISTICS, 30, 150, 236, 347, 366, 388, 403
DYNAMIC CONTROL, 543
DYNAMIC LOADS, 357
DYNAMIC MODELS, 174
DYNAMIC MODULUS OF ELASTICITY, 225
DYNAMIC PRESSURE, 429
DYNAMIC RESPONSE, 223
DYNAMIC STABILITY, 507
DYNAMIC STRUCTURAL ANALYSIS, 28, 54, 224
DYNAMICAL SYSTEMS, 198, 521
DYNAMO THEORY, 576
DYSPROSIUM, 485

## E

E GLASS, 25
EARLY WARNING SYSTEMS, 556
EARTH (PLANET), 30
EARTH ATMOSPHERE, 278, 585, 600
EARTH CRUST, 293
EARTH MAGNETOSPHERE, 577
EARTH ORIENTATION, 292
EARTH RADIATION BUDGET, 240, 288
EARTH RADIATION BUDGET EXPERIMENT, 240
EARTH SCIENCES, 303
EARTH SURFACE, 292
EARTHQUAKE DAMAGE, 363
EARTHQUAKES, 158, 225, 230, 293
ECLIPTIC, 559
ECOLOGY, 153
ECONOMIC ANALYSIS, 217
ECONOMIC IMPACT, 250
ECONOMICS, 11, 13, 24, 84, 300, 547, 556
ECONOMY, 14
ECOSYSTEMS, 239, 285, 301, 308, 316, 334, 431
EDDY VISCOSITY, 272
EDGE DETECTION, 339
EDGE DISLOCATIONS, 104
EDGES, 459, 464
EDUCATION, 1, 2, 169, 316, 328, 329, 348, 429, 454, 540, 541, 552, 573
EFFICIENCY, 16, 172, 260
EFFLUENTS, 229
EIGENVALUES, 371, 376, 528
EJECTA, 560, 582
ELASTIC PROPERTIES, 106, 214, 411
ELASTIC SCATTERING, 86, 373, 407, 460, 466, 491
ELASTIC WAVES, 373, 407
ELASTOHYDRODYNAMICS, 217
ELASTOMERS, 158, 225
ELECTRIC ARCS, 172
ELECTRIC BATTERIES, 80, 248, 254, 256, 258, 269
ELECTRIC CURRENT, 174
ELECTRIC DIPOLES, 382
ELECTRIC ENERGY STORAGE, 250
ELECTRIC FIELDS, 181, 183
ELECTRIC GENERATORS, 272, 378
ELECTRIC MOTOR VEHICLES, 159, 256, 264, 270
ELECTRIC MOTORS, 173, 178, 216
ELECTRIC NETWORKS, 398, 479
ELECTRIC POTENTIAL, 70, 452
ELECTRIC POWER PLANTS, 149, 266, 284
ELECTRIC POWER TRANSMISSION, 137
ELECTRICAL ENGINEERING, 160
ELECTRICAL MEASUREMENT, 93
ELECTRICAL PROPERTIES, 117, 120, 126, 167, 458, 477, 486
ELECTRICAL RESISTIVITY, 93, 100, 105, 237, 450, 480
ELECTRICITY, 250, 276
ELECTRIFICATION, 300
ELECTRO-OPTICS, 120, 179, 350
ELECTROCARDIOGRAPHY, 321
ELECTROCATALYSTS, 80
ELECTROCHEMICAL CELLS, 67, 116, 245
ELECTROCHEMICAL SYNTHESIS, 117
ELECTROCHEMISTRY, 70, 91, 113, 263, 267
ELECTROCHROMISM, 73, 117
ELECTRODES, 80, 89, 181, 252, 256, 262, 263, 264, 269, 312
ELECTROENCEPHALOGRAPHY, 370
ELECTROFORMING, 177
ELECTROLYTES, 44, 116, 250
ELECTROLYTIC CELLS, 138, 245, 249, 250
ELECTROMAGNETIC COUPLING, 455
ELECTROMAGNETIC FIELDS, 171, 491, 508, 514
ELECTROMAGNETIC INTERACTIONS, 30, 413, 429, 431
ELECTROMAGNETIC NOISE, 410
ELECTROMAGNETIC PULSES, 404
ELECTROMAGNETIC RADIATION, 164, 171, 241, 293, 304
ELECTROMAGNETIC SCATTERING, 367
ELECTROMAGNETISM, 105
ELECTROMETERS, 118
ELECTROMOTIVE FORCES, 126, 472
ELECTRON ACCELERATION, 183
ELECTRON ACCELERATORS, 442
ELECTRON BEAM WELDING, 160
ELECTRON BEAMS, 203, 213, 373, 382, 388, 397, 402, 403, 420, 434, 435, 468, 496, 505, 506, 511, 515, 518, 519, 523, 530, 537, 539
ELECTRON BUNCHING, 203, 397, 434, 503, 534, 539
ELECTRON CAPTURE, 384
ELECTRON CLOUDS, 418
ELECTRON CYCLOTRON RESONANCE, 400
ELECTRON DENSITY (CONCENTRATION), 514
ELECTRON DIFFRACTION, 176, 229, 476
ELECTRON EMISSION, 381, 480, 488
ELECTRON ENERGY, 61, 98, 392, 395, 444
ELECTRON GAS, 372
ELECTRON GUNS, 182, 379, 392, 515, 537
ELECTRON IRRADIATION, 47, 185, 599
ELECTRON MICROSCOPES, 157
ELECTRON ORBITALS, 414
ELECTRON PHONON INTERACTIONS, 478
ELECTRON SCATTERING, 371, 387, 422, 526
ELECTRON SPECTROSCOPY, 76
ELECTRON STATES, 58, 444
ELECTRON TRANSFER, 60, 77, 173, 418, 477
ELECTRON TRANSITIONS, 533
ELECTRON TUNNELING, 175
ELECTRONIC EQUIPMENT, 175, 181, 459
ELECTRONIC STRUCTURE, 54, 66, 83, 98, 105, 414, 455, 476, 493
ELECTRONS, 161, 181, 201, 411, 514, 524
ELECTROSTATIC CHARGE, 118
ELECTROSTATIC PRECIPITATORS, 151
ELECTROSTATICS, 398, 580
ELECTROWEAK INTERACTIONS (FIELD THEORY), 404, 503, 531, 538
ELECTROWINNING, 106
ELEMENTARY PARTICLE INTERACTIONS, 528
ELEMENTARY PARTICLES, 406, 412, 456, 526
ELEVATION, 243
ELEVONS, 17
ELLIPSOMETRY, 475

ELLIPTICITY, 491
ELONGATION, 319
EMISSION, 246, 284
EMISSIVITY, 63, 94
EMITTANCE, 203, 242, 388, 397, 511, 517, 518
EMITTERS, 211
ENANTIOMERS, 416
ENCAPSULATING, 115, 119, 125, 172
END-TO-END DATA SYSTEMS, 166
ENDEAVOUR (ORBITER), 29
ENDOCRINE SYSTEMS, 327
ENERGETIC PARTICLES, 35, 63, 72, 206
ENERGY BUDGETS, 134, 390
ENERGY CONSERVATION, 135, 137, 148, 159, 161, 244, 265, 296
ENERGY CONSUMPTION, 72, 270, 281
ENERGY CONVERSION, 152
ENERGY CONVERSION EFFICIENCY, 145, 253, 284
ENERGY DISSIPATION, 98, 187, 403
ENERGY DISTRIBUTION, 403
ENERGY POLICY, 135, 244, 246, 283
ENERGY SPECTRA, 400
ENERGY STORAGE, 144
ENERGY TECHNOLOGY, 133, 135, 152, 156, 195, 248, 249, 251, 391, 392, 396, 445, 457, 498, 542, 556
ENGINE TESTS, 423
ENGINEERS, 552
ENHANCED VISION, 333
ENTHALPY, 84, 157
ENVIRONMENT EFFECTS, 95, 114, 141, 283
ENVIRONMENT MODELS, 274
ENVIRONMENT POLLUTION, 284
ENVIRONMENT PROTECTION, 123, 146, 153, 231, 232, 296
ENVIRONMENTAL CHEMISTRY, 80
ENVIRONMENTAL CLEANUP, 256
ENVIRONMENTAL CONTROL, 256, 543
ENVIRONMENTAL MONITORING, 244, 245, 275, 343, 444
ENVIRONMENTAL QUALITY, 343, 553
ENZYMES, 77, 309, 311
EPHEMERIDES, 556
EPIDEMIOLOGY, 228
EPITAXY, 182, 374, 465, 476, 487
EPOXY RESINS, 34
EQUATIONS OF MOTION, 28, 524
EQUATIONS OF STATE, 103, 187, 224, 411
EQUILIBRIUM, 500
EQUIPMENT SPECIFICATIONS, 172, 185, 397, 433, 478
EQUIPOTENTIALS, 384
ERBIUM ISOTOPES, 413
ERGODIC PROCESS, 391
EROSION, 289, 290, 447, 568
ERROR ANALYSIS, 139, 296, 427
ERRORS, 307, 491, 492
ESCARPMENTS, 596
ESTIMATES, 337, 600
ESTIMATING, 271, 283
ETCHING, 441
ETHANE, 82
ETHERS, 68
ETHYL ALCOHOL, 133, 140, 142, 143, 145, 149
ETHYLENE, 57, 58, 62, 70
EUROPA, 599
EUROPEAN SPACE AGENCY, 26, 204, 438
EVALUATION, 262, 347, 361, 431
EVAPORATIVE COOLING, 334
EVAPOTRANSPIRATION, 242
EXCITATION, 40, 61, 77, 79, 373, 385, 411, 414, 444, 451, 455, 533, 534, 561, 564
EXHAUST EMISSION, 131, 145, 253, 271, 280, 282, 284, 287
EXHAUST GASES, 131, 145, 215, 253, 284, 285
EXOBIOLOGY, 322, 323
EXOSPHERE, 292
EXPERIMENTATION, 164
EXPERT SYSTEMS, 154
EXPLOSIVES, 59, 71, 136, 147, 148, 150, 152
EXPOSURE, 586
EXTRACTION, 32, 77, 407
EXTRASOLAR PLANETS, 557
EXTRUDING, 53

## F

F-18 AIRCRAFT, 18, 22
FABRICATION, 39, 45, 61, 108, 115, 123, 155, 156, 181, 184, 388, 467, 470, 504
FABRICS, 38
FACE CENTERED CUBIC LATTICES, 106, 112, 487
FAILURE, 28, 130
FAILURE ANALYSIS, 50, 174, 221, 363
FAILURE MODES, 366
FAR INFRARED RADIATION, 87
FAR ULTRAVIOLET RADIATION, 475
FASTENERS, 113
FATIGUE (BIOLOGY), 330
FATIGUE (MATERIALS), 51, 93, 101
FATIGUE LIFE, 94, 110, 114
FAULT DETECTION, 365
FEASIBILITY, 304, 493
FEASIBILITY ANALYSIS, 101
FEEDBACK, 17, 507, 547
FEEDBACK CONTROL, 145, 261, 365, 510
FEEDFORWARD CONTROL, 366
FEMALES, 328, 329
FERMENTATION, 77, 133
FERMI SURFACES, 469, 488
FERMIONS, 406, 412, 496, 499, 508, 528
FERROELECTRIC MATERIALS, 70, 432
FERROELECTRICITY, 62, 70, 177, 483
FERROMAGNETIC MATERIALS, 381, 464, 466
FERROMAGNETISM, 175, 376
FERROUS METALS, 95
FIBER COMPOSITES, 54
FIBER OPTICS, 430
FIBERS, 53, 222
FIBROBLASTS, 323
FIELD EFFECT TRANSISTORS, 175, 179, 456
FIELD EMISSION, 182
FIELD TESTS, 90
FIELD THEORY (PHYSICS), 380, 415, 476, 485, 489, 514, 534
FIELD-PROGRAMMABLE GATE ARRAYS, 340
FIGHTER AIRCRAFT, 17
FILAMENTS, 53, 561
FILLERS, 490
FILM THICKNESS, 199, 217
FINANCIAL MANAGEMENT, 12, 23, 311, 550
FINE STRUCTURE, 73, 561
FINITE DIFFERENCE THEORY, 197, 368, 391
FINITE DIFFERENCE TIME DOMAIN METHOD, 222, 470
FINITE ELEMENT METHOD, 52, 54, 112, 113, 139, 217, 226, 288, 336, 354, 358, 483
FINITE VOLUME METHOD, 193
FIRES, 231, 255
FISHES, 227, 228
FISSION, 389, 426
FISSURES (GEOLOGY), 584
FLAMMABLE GASES, 75
FLANGES, 375
FLASH LAMPS, 81
FLAT PANEL DISPLAYS, 182
FLAT PLATES, 371

FLAT SURFACES, 459
FLAVOR (PARTICLE PHYSICS), 402, 405
FLEXIBILITY, 258
FLEXIBLE BODIES, 363
FLIGHT CREWS, 169, 323
FLIGHT SIMULATORS, 328
FLIGHT TESTS, 18, 28
FLIGHT TRAINING, 323, 328, 329
FLOATING POINT ARITHMETIC, 352
FLOW, 68
FLOW CHARACTERISTICS, 66, 68, 191, 197
FLOW DISTRIBUTION, 5, 31, 151, 272, 368
FLOW MEASUREMENT, 188, 193
FLOW VELOCITY, 87, 188
FLOW VISUALIZATION, 18, 191, 198, 353
FLOWMETERS, 232
FLUE GASES, 279, 280, 282
FLUID FILMS, 199
FLUID FLOW, 232, 238
FLUID MECHANICS, 188, 190, 193
FLUORESCENCE, 437
FLUORIDES, 135
FLUX (RATE), 31
FLUX DENSITY, 247, 374
FLYWHEELS, 217
FOAMS, 340
FOCAL PLANE DEVICES, 200, 559
FOCUSING, 495
FOG, 202
FOILS (MATERIALS), 529
FOREST MANAGEMENT, 283
FORESTS, 231, 233, 303
FORMALDEHYDE, 318
FORMAT, 553
FORTRAN, 342, 424
FOSSIL FUELS, 29, 57, 148, 276
FOULING, 44, 48, 259
FOUNDATIONS, 521
FOURIER ANALYSIS, 391
FOURIER TRANSFORMATION, 484
FRACTALS, 396
FRACTIONATION, 130
FRACTOGRAPHY, 48
FRACTURE MECHANICS, 111, 123, 130
FRACTURE STRENGTH, 96, 109, 111
FRACTURES (MATERIALS), 226, 238
FRACTURING, 225, 562
FRAGMENTATION, 415
FREE ELECTRON LASERS, 213, 388, 389, 402, 429, 431, 432, 433, 434, 435, 436, 439, 440, 442, 443, 490, 516, 517, 524, 539
FREE ENERGY, 187
FREE FALL, 4
FREE FLOW, 3, 186, 189
FREE VIBRATION, 225
FREQUENCIES, 380
FREQUENCY DISTRIBUTION, 484, 588
FREQUENCY DOMAIN ANALYSIS, 442
FREQUENCY RANGES, 225
FRESH WATER, 229, 316
FRICTION, 218, 377
FRICTION FACTOR, 118, 199
FRICTION WELDING, 218
FUEL CELL POWER PLANTS, 248
FUEL CELLS, 130, 133, 138, 150, 248, 249, 250
FUEL COMBUSTION, 281
FUEL CONSUMPTION, 86, 137
FUEL CORROSION, 66
FUEL INJECTION, 60
FUEL PRODUCTION, 142, 145, 273
FUEL SYSTEMS, 144
FUEL TESTS, 21, 261
FUELS, 72, 83, 102, 135, 139, 146, 149, 244, 419, 424
FULL SCALE TESTS, 18, 21
FUNCTIONAL ANALYSIS, 48
FUNCTIONAL DESIGN SPECIFICATIONS, 354
FUNCTIONALS, 94, 412
FURNACES, 21, 73, 144, 158, 159, 199, 221
FUSION REACTORS, 65, 167, 452
FUZZY SETS, 370
FUZZY SYSTEMS, 366, 469

## G

GADOLINIUM, 126, 427
GALACTIC CLUSTERS, 560
GALACTIC NUCLEI, 561
GALLIUM, 41
GALLIUM ARSENIDES, 247, 454, 484
GALLIUM COMPOUNDS, 180
GALLIUM NITRIDES, 175, 462, 467
GAMMA RAY SPECTRA, 48, 474
GAMMA RAY SPECTROMETERS, 424
GAMMA RAYS, 33
GANYMEDE, 599
GAS ANALYSIS, 37
GAS CHROMATOGRAPHY, 45
GAS COMPOSITION, 58, 62
GAS DETECTORS, 33, 37, 43
GAS DYNAMICS, 189
GAS EXCHANGE, 333
GAS FLOW, 197, 453
GAS GENERATORS, 32
GAS GIANT PLANETS, 558
GAS LASERS, 210
GAS PRESSURE, 408, 480
GAS RECOVERY, 141
GAS SPECTROSCOPY, 563
GAS TEMPERATURE, 58, 62
GAS TRANSPORT, 132
GAS TURBINE ENGINES, 21, 22
GAS TURBINES, 21, 249
GASES, 68
GASIFICATION, 134, 141, 258
GASOLINE, 269
GAUGE INVARIANCE, 496
GAUGE THEORY, 485, 496
GENE EXPRESSION, 310
GENERAL AVIATION AIRCRAFT, 8, 10, 11, 12, 13, 14, 544, 554
GENES, 310
GENESIS MISSION, 255
GENETIC ENGINEERING, 310
GENETICS, 90, 311
GEOCHEMISTRY, 142, 237
GEODESY, 292, 354
GEOGRAPHIC DISTRIBUTION, 595
GEOLOGICAL FAULTS, 229, 569, 596
GEOLOGICAL SURVEYS, 227, 231, 235, 312, 574
GEOLOGY, 228, 362, 564
GEOMETRIC RECTIFICATION (IMAGERY), 20
GEOMORPHOLOGY, 573
GEOPHYSICS, 237, 238
GEOTECHNICAL ENGINEERING, 236, 521
GEOTHERMAL RESOURCES, 245
GEOTHERMAL TECHNOLOGY, 217
GERMANIUM, 456
GERMANIUM OXIDES, 458
GLASS, 74, 116, 119, 124, 125, 128, 448
GLASS FIBERS, 160
GLASS TRANSITION TEMPERATURE, 113
GLOBAL POSITIONING SYSTEM, 15, 29, 243, 293
GLOBAL WARMING, 57, 283, 300
GLUONS, 405, 444, 452, 507, 513, 515, 523
GOGGLES, 18
GOLD, 38, 58, 234, 405, 406
GOLD ALLOYS, 98
GOLD COATINGS, 73
GOLD ISOTOPES, 415

GOVERNMENT PROCUREMENT, 344
GOVERNMENT/INDUSTRY RELATIONS, 417
GOVERNMENTS, 549
GRAIN BOUNDARIES, 95, 374, 458, 475, 477, 480
GRAPHITE, 258, 565
GRAPHITE-EPOXY COMPOSITES, 50
GRAPHS (CHARTS), 350
GRASSES, 133, 153
GRASSLANDS, 228
GRATINGS (SPECTRA), 122, 512
GRAVIMETERS, 465
GRAVITATION, 293, 565, 598
GRAVITATIONAL EFFECTS, 318, 320
GRAVITATIONAL FIELDS, 592
GRAVITATIONAL WAVES, 304
GRAVITY WAVES, 288
GREENHOUSE EFFECT, 283
GRID GENERATION (MATHEMATICS), 294, 338, 357, 554
GROUND BASED CONTROL, 601
GROUND PENETRATING RADAR, 186, 484, 571
GROUND TESTS, 315
GROUND TRUTH, 260
GROUND WATER, 226, 227, 232, 235, 236, 237, 245, 274, 275, 375, 568
GROUP DYNAMICS, 9, 342
GUNS, 139, 527

## H

H II REGIONS, 558
HABITATS, 228, 315
HADRONS, 402, 405, 416, 492, 495, 500, 503, 507, 518, 523, 535
HALL THRUSTERS, 181
HALOGENS, 81
HALOS, 397, 523
HAMILTONIAN FUNCTIONS, 423
HARDNESS, 455
HARDNESS TESTS, 425
HARMONIC GENERATIONS, 81, 432, 434, 439, 440, 443
HARMONICS, 522
HARTREE APPROXIMATION, 58, 105
HAZARDOUS MATERIALS, 36
HAZARDOUS WASTES, 232, 255, 277
HAZARDS, 34, 548
HEAD DOWN TILT, 325
HEALTH PHYSICS, 444
HEART, 325, 337
HEART FUNCTION, 319
HEART RATE, 320, 321
HEART VALVES, 409
HEAT AFFECTED ZONE, 108
HEAT EXCHANGERS, 48, 193
HEAT FLUX, 31, 52, 219
HEAT MEASUREMENT, 162
HEAT PIPES, 216
HEAT PUMPS, 217
HEAT RESISTANT ALLOYS, 152
HEAT SHIELDING, 31, 199
HEAT STORAGE, 267
HEAT TRANSFER, 147, 180, 189, 226
HEAT TRANSFER COEFFICIENTS, 190
HEAT TRANSMISSION, 593
HEAT TREATMENT, 102, 108
HEATING, 390
HEATING EQUIPMENT, 144
HEAVY ELEMENTS, 453
HEAVY FERMION SYSTEMS, 473
HEAVY IONS, 324, 385, 386, 492, 493, 500, 504, 530, 536
HEAVY METALS, 73
HELICOPTERS, 18
HELIUM, 156
HELIUM ISOTOPES, 83, 425
HELMET MOUNTED DISPLAYS, 332
HELMETS, 332
HEMATITE, 573
HETEROGENEITY, 78, 245
HETEROJUNCTION DEVICES, 178, 180
HETEROJUNCTIONS, 467
HEURISTIC METHODS, 560
HEXAMETHYLENETETRAMINE, 563
HIGGS BOSONS, 404, 531, 533
HIGH ENERGY ELECTRONS, 508
HIGH ENERGY FUELS, 136
HIGH ENERGY INTERACTIONS, 392, 396, 493, 496, 497, 513, 525, 526
HIGH FIELD MAGNETS, 459
HIGH FREQUENCIES, 221, 289, 404, 408, 411
HIGH GAIN, 432, 436, 440
HIGH POLYMERS, 117
HIGH POWER LASERS, 209, 210, 413
HIGH PRESSURE, 208
HIGH RESOLUTION, 408, 430, 437, 439
HIGH SPEED PHOTOGRAPHY, 597
HIGH TEMPERATURE, 96, 126, 470
HIGH TEMPERATURE ENVIRONMENTS, 251
HIGH TEMPERATURE GASES, 85, 129
HIGH TEMPERATURE PLASMAS, 445
HIGH TEMPERATURE SUPERCONDUCTORS, 134, 163, 175, 459, 460, 462, 463, 465, 472, 481, 482, 485
HIGH TEMPERATURE TESTS, 159
HIGHLANDS, 568, 569, 571, 572, 573, 574
HINDLIMB SUSPENSION, 318
HISTORIES, 74
HMX, 411
HOHLRAUMS, 438
HOLOCENE EPOCH, 294
HOLOGRAPHY, 408
HOMOGENEOUS TURBULENCE, 198
HONEYCOMB STRUCTURES, 223
HOT WORKING, 107
HUMAN BEHAVIOR, 7, 9
HUMAN BEINGS, 323, 326
HUMAN BODY, 325, 332
HUMAN FACTORS ENGINEERING, 18, 329, 331, 332, 334, 549
HUMAN PERFORMANCE, 330, 333, 335, 361, 543, 545
HUMAN TOLERANCES, 326, 328
HUMAN-COMPUTER INTERFACE, 341, 350
HUMIDITY, 136
HUNGARY, 161
HYBRID CIRCUITS, 43
HYDRATES, 132, 455
HYDRAULIC CONTROL, 218, 423
HYDRAULICS, 237
HYDRIDES, 58
HYDROCARBON COMBUSTION, 79
HYDROCARBON FUELS, 67, 250, 269
HYDROCARBONS, 32, 56, 59, 78, 81, 82, 149, 250, 275, 411, 562, 567
HYDROCHLORIC ACID, 276
HYDRODYNAMICS, 151, 188
HYDROFLUORIC ACID, 73
HYDROGEN, 33, 41, 43, 46, 61, 65, 117, 119, 144, 145, 150, 420, 504
HYDROGEN ATOMS, 57
HYDROGEN FUELS, 141, 269
HYDROGEN IONS, 516
HYDROGEN PEROXIDE, 90
HYDROGEN PRODUCTION, 85, 139, 141
HYDROGEN SULFIDE, 121
HYDROLOGY, 227, 228, 236
HYDROLOGY MODELS, 237
HYDROLYSIS, 127, 146
HYDROMETALLURGY, 135
HYDROPONICS, 320
HYDROSTATIC PRESSURE, 325
HYDROSTATICS, 520
HYDROTHERMAL SYSTEMS, 270
HYDROXIDES, 262
HYPERBOLIC DIFFERENTIAL EQUATIONS, 396
HYPERCAPNIA, 318

HYPERNUCLEI, 392, 417, 419, 493
HYPERONS, 380, 383, 509
HYPERSONIC FLIGHT, 195
HYPERSONIC SPEED, 21
HYPERSONIC WIND TUNNELS, 265
HYPERVELOCITY IMPACT, 103, 446
HYPOKINESIA, 325
HYPOTENSION, 325
HYPOTHESES, 324
HYPOXIA, 177
HYSTERESIS, 83

## I

ICE, 41, 208, 229
ICELAND, 574
ICY SATELLITES, 558
IGNEOUS ROCKS, 230
IGNITION, 32, 72, 73, 154, 183, 449
IGNITION SYSTEMS, 60
IGNITION TEMPERATURE, 376
ILLINOIS, 543
ILLUMINATING, 161
ILLUMINATORS, 210
IMAGE ANALYSIS, 343, 365, 512, 591
IMAGE CORRELATORS, 204
IMAGE PROCESSING, 173, 204, 339, 598
IMAGE RESOLUTION, 243, 586
IMAGERY, 204, 243
IMAGES, 361, 411
IMAGING RADAR, 240
IMAGING SPECTROMETERS, 63, 204, 293, 585
IMAGING TECHNIQUES, 38, 69, 119, 122, 157, 175, 181, 186, 202, 205, 240, 374, 411, 433, 435, 436, 444, 478, 511, 519, 564, 577, 581, 583, 586, 597
IMPACT, 562
IMPACT ACCELERATION, 223
IMPACT DAMAGE, 569, 571
IMPACT LOADS, 78, 118
IMPACT TESTS, 27, 103
IMPEDANCE, 165, 499
IMPEDANCE MATCHING, 378
IMPLANTATION, 89
IMPLOSIONS, 40, 227, 448, 450
IMPURITIES, 255
IN SITU MEASUREMENT, 106, 243, 445
IN SITU RESOURCE UTILIZATION, 27
IN VITRO METHODS AND TESTS, 319
INCIDENT RADIATION, 426
INCOMPRESSIBLE FLOW, 192
INCONEL (TRADEMARK), 94
INDICATING INSTRUMENTS, 148
INDIUM ANTIMONIDES, 471
INDIUM COMPOUNDS, 180
INDUCTIVELY COUPLED PLASMA MASS SPECTROMETRY, 453
INDUSTRIAL AREAS, 258
INDUSTRIAL PLANTS, 138
INDUSTRIES, 245, 541, 542, 555
INELASTIC SCATTERING, 65, 473, 478, 508, 510
INERTIAL CONFINEMENT FUSION, 448
INFECTIOUS DISEASES, 311
INFILTRATION, 114
INFORMATION DISSEMINATION, 548, 554
INFORMATION MANAGEMENT, 548
INFORMATION RESOURCES MANAGEMENT, 262
INFORMATION RETRIEVAL, 345, 547, 552, 554
INFORMATION SYSTEMS, 162, 344, 361, 546, 547, 548, 551, 552
INFRARED ASTRONOMY, 205, 595
INFRARED DETECTORS, 37, 433
INFRARED IMAGERY, 122, 202, 292
INFRARED INSPECTION, 54
INFRARED LASERS, 211, 388, 435
INFRARED RADIATION, 19, 282, 292, 378, 433, 435, 455, 579
INFRARED SIGNATURES, 19
INFRARED SPECTRA, 43, 558, 563
INFRARED SPECTROMETERS, 204
INFRARED SPECTROSCOPY, 87, 211, 492, 561, 586
INJECTORS, 402, 511, 534
INKS, 257
INLET FLOW, 195
INSPECTION, 38
INSTALLING, 260, 361
INSTRUMENT COMPENSATION, 520
INSTRUMENTS, 176
INTEGRATED CIRCUITS, 185, 413, 463
INTEGRATORS, 367
INTELLIGIBILITY, 163
INTERCALATION, 258
INTERFACES, 358
INTERFEROMETERS, 28, 430, 536
INTERFEROMETRY, 290, 428
INTERFERON, 312
INTERGRANULAR CORROSION, 48
INTERLAYERS, 465, 467
INTERMETALLICS, 50, 75, 111, 200, 252, 257, 269, 450
INTERMOLECULAR FORCES, 78
INTERNAL COMBUSTION ENGINES, 86, 138, 144, 215, 349
INTERNAL WAVES, 196
INTERNATIONAL COOPERATION, 554, 556
INTERNATIONAL RELATIONS, 555
INTERNATIONAL SPACE STATION, 315
INTERNETS, 171, 362, 550
INTERPOLATION, 424
INTERPROCESSOR COMMUNICATION, 168
INTERSTELLAR MATTER, 558, 562, 563, 564, 567
INTERSTITIALS, 316
INTESTINES, 324
INVERSE KINEMATICS, 504
INVERTERS, 244
INVISCID FLOW, 196
ION BEAMS, 33, 38, 86, 184, 324, 377, 402, 413, 468, 473, 489, 494, 498, 504, 511, 514, 518, 524, 534
ION EMISSION, 201
ION EXCHANGE MEMBRANE ELECTROLYTES, 130
ION EXCHANGE RESINS, 55, 77
ION EXCHANGING, 130
ION EXTRACTION, 68
ION IMPACT, 38
ION IMPLANTATION, 33, 96, 430, 480
ION IRRADIATION, 52, 86, 98, 185, 477, 599
ION MICROSCOPES, 201
ION MOBILITY SPECTROSCOPY, 33
ION OPTICS, 436
ION SOURCES, 436, 473, 514, 516
ION TRAPS (INSTRUMENTATION), 76, 275
IONIC COLLISIONS, 386, 406, 444, 498, 500, 522, 530, 536, 537
IONIZATION, 40, 508
IONIZING RADIATION, 88, 340, 413
IONS, 33, 411, 477, 516
IRON, 63, 89, 207, 221, 401, 466, 487
IRON ALLOYS, 110, 465
IRON ALUMINIDES, 75
IRON COMPOUNDS, 93
IRRADIANCE, 308
IRRADIATION, 38, 40, 48, 90, 100, 101, 102, 105, 110, 174, 179, 207
ISING MODEL, 404
ISOLATION, 64, 158
ISOLATORS, 221
ISOMERS, 424
ISOTOPE EFFECT, 79, 92
ISOTOPE RATIOS, 48, 237
ISOTOPES, 79, 420

ISOTOPIC LABELING, 79
ITERATIVE SOLUTION, 358, 368

## J

JANUS REACTOR, 422
JAVA (PROGRAMMING LANGUAGE), 359
JET AIRCRAFT, 7
JET ENGINE FUELS, 136
JET FLOW, 56, 57, 58, 59, 62, 87
JOINTS (JUNCTIONS), 152
JOSEPHSON EFFECT, 478
JOSEPHSON JUNCTIONS, 175, 474, 481
JUDGMENTS, 398, 565
JUPITER (PLANET), 561

## K

KANSAS, 242
KAONS, 385, 387, 393, 403, 495, 499, 504
KERR MAGNETOOPTICAL EFFECT, 186, 466
KETENES, 90
KINEMATICS, 513, 596
KINETIC ENERGY, 63, 190, 399, 452
KINETIC EQUATIONS, 495
KINETICS, 106, 146, 147, 258
KLYSTRONS, 382, 522
KNOWLEDGE BASED SYSTEMS, 274
KNOWLEDGE BASES (ARTIFICIAL INTELLIGENCE), 334

## L

LABORATORIES, 76, 157
LABORATORY EQUIPMENT, 155
LAMINAR BOUNDARY LAYER, 5, 186
LAMINAR FLOW, 5, 56, 58, 59, 62, 368
LAMINATES, 127, 266
LAND SURFACE TEMPERATURE, 293
LAND USE, 239, 547
LANDFILLS, 241
LANDFORMS, 588
LANDSAT 7, 242
LANGMUIR-BLODGETT FILMS, 81
LANTHANUM, 89, 466
LARGE EDDY SIMULATION, 286
LASER ABLATION, 40, 212, 438
LASER ALTIMETERS, 206
LASER APPLICATIONS, 436, 442
LASER BEAMS, 94, 165, 209, 211, 389, 439, 441, 443
LASER CAVITIES, 430
LASER COOLING, 490
LASER DAMAGE, 441
LASER INDUCED FLUORESCENCE, 40, 313
LASER MATERIALS, 213, 448
LASER OUTPUTS, 209, 210
LASER PLASMA INTERACTIONS, 442
LASER POWER BEAMING, 443
LASER PROPULSION, 442
LASER PUMPING, 441
LASER SPECTROSCOPY, 211
LASER WEAPONS, 209
LASER WELDING, 212
LASER-INDUCED BREAKDOWN SPECTROSCOPY, 41
LASERS, 165, 203, 211, 313, 408, 430, 441, 442, 447, 526
LASING, 213, 443
LATENT HEAT, 320
LATTICE PARAMETERS, 425, 486
LATTICE VIBRATIONS, 462
LAUNCHERS, 442
LAVA, 584
LAW (JURISPRUDENCE), 549
LEACHING, 104
LEAD ALLOYS, 93, 94
LEAD SELENIDES, 237
LEAD SULFIDES, 237
LEAKAGE, 85, 135, 155, 214
LEARNING, 365, 540
LEAST SQUARES METHOD, 351
LENSES, 535
LEPTONS, 396, 491
LEVELING, 520
LIBRARIES, 553
LIBRATION, 593, 598
LIBRATIONAL MOTION, 206, 583, 587
LICENSING, 160
LIFE (DURABILITY), 134
LIFE CYCLE COSTS, 137
LIFE SCIENCES, 316, 322
LIFT, 6
LIGHT BEAMS, 489
LIGHT EMISSION, 67
LIGHT GAS GUNS, 103, 446
LIGHT IONS, 504, 530
LIGHT SCATTERING, 37, 176, 275, 439
LIGHT SOURCES, 180, 378, 433, 434, 437, 439, 440, 491, 532
LIGHT WATER REACTORS, 101
LIGHTNING, 293
LINE OF SIGHT, 202
LINEAR ACCELERATORS, 203, 384, 391, 393, 394, 402, 403, 433, 434, 451, 485, 494, 499, 500, 501, 504, 505, 510, 511, 512, 515, 517, 518, 519, 524, 525, 527, 529, 530, 535, 537
LINEAR ARRAYS, 367, 461
LINEAR ENERGY TRANSFER (LET), 493
LINEAR POLARIZATION, 330
LINEAR SYSTEMS, 195, 197, 358, 451
LIPIDS, 309, 312, 314
LIQUEFIED NATURAL GAS, 131, 132, 152
LIQUID ALLOYS, 98, 113
LIQUID CHROMATOGRAPHY, 64
LIQUID COOLING, 424
LIQUID CRYSTALS, 48, 120, 122, 428, 432
LIQUID FLOW, 431
LIQUID LITHIUM, 535
LIQUID METAL COOLED REACTORS, 88
LIQUID METALS, 215, 216
LIQUID OXYGEN, 55
LIQUID PHASES, 71
LIQUID SURFACES, 83
LIQUIDS, 79, 84
LITHIUM, 42, 57, 91, 105, 248, 254, 256, 264, 265
LITHIUM BATTERIES, 113, 251, 252, 256, 257, 262, 265, 267, 269
LITHIUM COMPOUNDS, 82, 102
LITHIUM NIOBATES, 62
LITHIUM OXIDES, 91, 113
LITHOGRAPHY, 177, 382, 401
LITHOLOGY, 229, 290
LITHOSPHERE, 596
LOADS (FORCES), 20, 156, 271, 327, 371
LOCAL THERMODYNAMIC EQUILIBRIUM, 401
LOGARITHMS, 489
LONG DURATION SPACE FLIGHT, 27, 333
LONGITUDINAL STABILITY, 223, 497
LOSS OF COOLANT, 426
LOSSES, 162, 209, 418
LOSSY MEDIA, 171
LOW COST, 182
LOW EARTH ORBITS, 29
LOW PRESSURE, 238, 451
LOW TEMPERATURE, 177
LOWER BODY NEGATIVE PRESSURE, 320, 325, 326
LUBRICANTS, 214
LUBRICATION, 217
LUMINAIRES, 183
LUMINESCENCE, 136
LUMINOSITY, 374, 499, 501, 520, 560

LUNAR ATMOSPHERE, 597
LUNAR LANDING, 575
LUNAR SURFACE, 576

## M

MACH NUMBER, 3
MACHINE LEARNING, 365
MADDEN-JULIAN OSCILLATION, 294
MAGNESIUM, 54, 58, 102
MAGNESIUM ALLOYS, 100
MAGNETIC BEARINGS, 463
MAGNETIC COMPRESSION, 517
MAGNETIC DIPOLES, 412, 492
MAGNETIC DISKS, 45
MAGNETIC EFFECTS, 454
MAGNETIC FIELD CONFIGURATIONS, 89, 113, 167, 372, 390
MAGNETIC FIELD RECONNECTION, 390
MAGNETIC FIELDS, 69, 159, 373, 465, 467, 482, 492, 580
MAGNETIC FLUX, 166, 374, 455, 465
MAGNETIC INDUCTION, 105
MAGNETIC MATERIALS, 99, 173, 386, 502
MAGNETIC MIRRORS, 528
MAGNETIC PERMEABILITY, 473
MAGNETIC PROPERTIES, 90, 93, 97, 372, 373, 455, 469, 485
MAGNETIC RESONANCE, 230
MAGNETIC SPECTROSCOPY, 529
MAGNETIC SUSPENSION, 463
MAGNETIZATION, 89, 374, 382, 477
MAGNETO-OPTICS, 186, 454
MAGNETOHYDRODYNAMIC STABILITY, 446, 451
MAGNETOHYDRODYNAMIC WAVES, 448
MAGNETOHYDRODYNAMICS, 263, 390, 449, 451, 598
MAGNETORESISTIVITY, 465, 477, 486
MAGNETOSTATIC FIELDS, 62
MAGNETS, 374, 383, 500
MAGNITUDE, 209
MAINTENANCE, 154, 217, 344
MAMMALS, 321
MAMMARY GLANDS, 309, 310
MAN MACHINE SYSTEMS, 331, 364
MANAGEMENT, 542
MANAGEMENT METHODS, 14, 551
MANAGEMENT PLANNING, 8, 9, 394, 551
MANAGEMENT SYSTEMS, 246, 362, 554
MANGANESE COMPOUNDS, 386, 464, 466, 469
MANGANESE OXIDES, 264, 376
MANIPULATORS, 158
MANUFACTURING, 20, 84, 138, 220, 250, 252, 264, 266, 349, 382
MANY BODY PROBLEM, 565
MAPPING, 243, 355
MAPS, 227
MARIA, 580
MARINE BIOLOGY, 273
MARINE PROPULSION, 410
MARINER 10 SPACE PROBE, 243, 292, 578
MARKARIAN GALAXIES, 561
MARKET RESEARCH, 178, 265
MARKETING, 555
MARKING, 80, 227, 228
MARKOV CHAINS, 276
MARKOV PROCESSES, 338
MARS (PLANET), 568, 573, 574
MARS ATMOSPHERE, 573
MARS CRATERS, 290, 569, 570, 574
MARS MISSIONS, 568
MARS PHOTOGRAPHS, 291
MARS SURFACE, 290, 291, 568, 569, 570, 571, 572, 573, 574
MARSHLANDS, 300
MARTENSITE, 108
MARTENSITIC TRANSFORMATION, 103
MASKS, 115, 334
MASS, 529
MASS DISTRIBUTION, 390
MASS SPECTROMETERS, 80, 275
MASS SPECTROSCOPY, 64, 76, 436, 585
MASS TRANSFER, 155
MASSIVELY PARALLEL PROCESSORS, 195, 352
MATERIALS HANDLING, 84, 131
MATERIALS RECOVERY, 27
MATERIALS SCIENCE, 41
MATERIALS SELECTION, 255, 442
MATHEMATICAL MODELS, 28, 39, 44, 53, 78, 83, 84, 85, 93, 94, 112, 116, 158, 168, 190, 192, 193, 194, 196, 198, 216, 219, 224, 232, 247, 271, 288, 289, 294, 300, 301, 323, 338, 351, 370, 390, 396, 410, 413, 418, 468, 476, 529, 543, 566, 570, 576
MATRICES (MATHEMATICS), 195, 223, 530
MATRIX METHODS, 417, 530
MEASURE AND INTEGRATION, 431
MEASUREMENT, 19, 22
MEASURING INSTRUMENTS, 183, 200, 213, 219, 222, 306, 439
MECHANICAL DEVICES, 221
MECHANICAL DRIVES, 216
MECHANICAL ENGINEERING, 160, 161, 433
MECHANICAL PROPERTIES, 54, 78, 93, 101, 102, 103, 104, 107, 118, 122, 126, 136, 214, 222, 224, 237, 340, 364, 515
MEDICAL SCIENCE, 317, 431, 546
MEDICAL SERVICES, 309
MELTING, 242, 476, 479
MELTING POINTS, 455
MEMBRANES, 46, 61, 90, 119, 323
MEMORY, 554
MENTAL PERFORMANCE, 332
MERCURY (METAL), 108, 280, 408, 429, 466
MERCURY (PLANET), 26, 27, 30, 183, 204, 205, 206, 292, 362, 438, 565, 575, 576, 577, 578, 579, 580, 581, 582, 583, 584, 585, 586, 587, 588, 589, 590, 591, 592, 593, 594, 595, 596, 598
MERCURY ALLOYS, 98
MERCURY ATMOSPHERE, 205, 206, 580, 583, 589, 590, 594, 597
MERCURY SURFACE, 205, 206, 362, 438, 575, 576, 577, 578, 579, 580, 581, 582, 583, 584, 585, 586, 588, 589, 591, 595, 596, 597, 598
MESONS, 390, 395, 396, 400, 403, 405, 416, 497, 515, 520, 528
MESOSCALE PHENOMENA, 288, 297
MESSAGE PROCESSING, 406
MESSAGES, 171
METABOLISM, 318
METAL CLUSTERS, 105
METAL FATIGUE, 114
METAL FILMS, 35, 476
METAL FOILS, 93, 96, 438
METAL FUELS, 40
METAL HYDRIDES, 83
METAL IONS, 73, 74, 91, 98, 184, 256, 264, 265, 406
METAL MATRIX COMPOSITES, 49, 51, 54
METAL OXIDE SEMICONDUCTORS, 175, 184, 456, 457, 458, 467
METAL OXIDES, 453, 455, 470
METAL STRIPS, 108
METAL SURFACES, 87, 312
METAL WORKING, 107, 113
METALLIC GLASSES, 25, 39, 94, 116
METALLOGRAPHY, 155
METALLOIDS, 39
METALORGANIC CHEMICAL VAPOR DEPOSITION, 119, 480
METALS, 53, 98, 108, 212, 222

METEORITES, 565
METEORITIC COMPOSITION, 566
METEOROLOGICAL INSTRUMENTS, 235, 303
METEOROLOGICAL PARAMETERS, 235, 297, 298
METEOROLOGICAL RADAR, 301, 302
METEOROLOGICAL SATELLITES, 294
METEOROLOGY, 295, 297, 301, 303
METHANE, 57, 82, 131, 153, 291
METHYL ALCOHOL, 133
METHYL POLYSILOXANES, 340
MICROANALYSIS, 290
MICROBALLOONS, 450
MICROBEAMS, 457
MICROBIOLOGY, 153
MICROCHANNELS, 180
MICROCLIMATOLOGY, 297
MICROCRYSTALS, 479
MICROELECTROMECHANICAL SYSTEMS, 174, 178, 181, 214, 216, 354
MICROELECTRONICS, 178
MICROGRAVITY, 56, 57, 318, 320, 321, 325, 326, 327
MICROINSTRUMENTATION, 118, 178
MICROMACHINING, 174, 433
MICROMECHANICS, 116, 178
MICROORGANISMS, 308, 314, 315, 316
MICROPHONES, 411
MICROPROCESSORS, 363
MICROPULSATIONS, 511
MICROSCOPY, 201, 381, 441, 525
MICROSEISMS, 226
MICROSTRUCTURE, 54, 86, 97, 99, 101, 102, 106, 108, 112, 114, 126, 127, 216, 238, 382, 438, 455, 457, 468, 470, 477, 519
MICROWAVE EQUIPMENT, 166
MICROWAVE FREQUENCIES, 164
MICROWAVE IMAGERY, 307, 557
MICROWAVES, 157
MIDAIR COLLISIONS, 8
MIGRATION, 391
MILITARY HELICOPTERS, 332
MILITARY OPERATIONS, 7, 8, 16, 17, 24, 164, 170, 313
MILITARY TECHNOLOGY, 24, 169, 175, 556
MILITARY VEHICLES, 364
MILLIMETER WAVES, 299
MINERAL DEPOSITS, 228, 241, 573
MINERAL EXPLORATION, 204
MINERALS, 67, 572
MINIATURIZATION, 30, 45, 147
MINING, 104, 234
MIRRORS, 215, 433, 475, 483, 536
MISSILE CONFIGURATIONS, 3
MISSILES, 3
MISSION PLANNING, 30, 559, 568
MIXED OXIDES, 34, 130, 487
MIXING HEIGHT, 298
MIXING LAYERS (FLUIDS), 189, 298
MIXING RATIOS, 298
MIXTURES, 151
MOBILE COMMUNICATION SYSTEMS, 169
MOBILITY, 529
MODELS, 111, 194, 233, 264, 311, 387, 546
MODULATION, 527
MODULATORS, 179
MODULES, 202
MOISTURE CONTENT, 136
MOJAVE DESERT (CA), 240, 289, 291, 568, 570
MOLECULAR BEAM EPITAXY, 99, 176, 456, 471
MOLECULAR BEAMS, 77
MOLECULAR BIOLOGY, 431, 437
MOLECULAR CLOUDS, 562
MOLECULAR DYNAMICS, 54, 69, 72, 121, 127, 391, 462, 490, 501
MOLECULAR GASES, 558
MOLECULAR INTERACTIONS, 484
MOLECULAR ORBITALS, 82, 248
MOLECULAR STRUCTURE, 84, 87, 415
MOLECULES, 49, 77, 312
MOLTEN CARBONATE FUEL CELLS, 250, 252, 254
MOLYBDENUM, 107
MOLYBDENUM ALLOYS, 105
MOLYBDENUM ISOTOPES, 46, 565
MOMENT DISTRIBUTION, 372
MOMENTUM, 79, 377, 518
MOMENTUM TRANSFER, 109
MONITORS, 31, 221, 282, 296, 366, 388, 389, 505, 509
MONOCHROMATIC RADIATION, 478
MONOCHROMATORS, 215, 439, 440, 509
MONOPOLES, 456
MONSOONS, 297
MONTE CARLO METHOD, 105, 121, 276, 347, 376, 421, 423, 425, 451, 528
MOON, 566
MORPHOLOGY, 319, 380, 488, 573
MORTALITY, 370
MOTION, 4
MOTION SICKNESS, 321, 323, 326
MOUNTAINS, 313
MULTICHANNEL COMMUNICATION, 404
MULTIGRID METHODS, 338
MULTIPATH TRANSMISSION, 289
MULTIPHASE FLOW, 194, 226, 228, 238, 427
MULTIPROCESSING (COMPUTERS), 352, 360
MULTISPECTRAL BAND SCANNERS, 20
MULTIVARIATE STATISTICAL ANALYSIS, 201
MUONS, 375, 386, 387, 489, 493, 498, 499, 501, 505, 508, 513, 518, 525, 526, 531, 535, 560, 566
MURCHISON METEORITE, 92
MUSCULOSKELETAL SYSTEM, 323, 327
MUSEUMS, 598

## N

NANOCOMPOSITES, 126
NANOCRYSTALS, 112, 185, 437, 480
NANOSTRUCTURE (CHARACTERISTICS), 80, 460, 470, 479
NANOSTRUCTURES (DEVICES), 178, 429, 431
NANOTECHNOLOGY, 68, 93, 436
NARCOTICS, 16
NARROWBAND, 568
NASA PROGRAMS, 10, 11, 12, 13, 14
NASA SPACE PROGRAMS, 601
NATURAL GAS, 132, 144, 146, 248
NATURAL GAS EXPLORATION, 267
NATURAL SATELLITES, 565
NAVIER-STOKES EQUATION, 2, 3, 4, 197, 294
NAVIGATION SATELLITES, 29
NEAR FIELDS, 164
NEBRASKA, 10, 11, 12, 13, 14
NEGATIVE IONS, 473
NEODYMIUM, 207
NEODYMIUM COMPOUNDS, 93
NEODYMIUM LASERS, 33, 100, 434
NETHERLANDS, 135
NETWORK ANALYSIS, 479
NEURAL NETS, 366
NEUROLOGY, 312
NEURONS, 331
NEUTRAL ATOMS, 206, 583
NEUTRAL BEAMS, 402
NEUTRAL PARTICLES, 206
NEUTRINO BEAMS, 272, 494, 495, 498, 526
NEUTRINOS, 375, 380, 386, 397, 405, 470, 498, 513, 531, 560, 566

NEUTRON BEAMS, 422
NEUTRON COUNTERS, 560
NEUTRON CROSS SECTIONS, 65, 418
NEUTRON DIFFRACTION, 90, 122, 372, 376, 422, 469, 487
NEUTRON PHYSICS, 504, 526
NEUTRON SCATTERING, 113, 122, 127, 267, 372, 437, 464, 470, 473
NEUTRON SOURCES, 388, 403, 489, 532
NEUTRON SPECTRA, 426
NEUTRONS, 41, 83, 200, 272, 389, 420, 422, 427, 446, 504
NEVADA, 132, 141, 227, 229, 231, 259
NEW YORK, 236
NICKEL, 265
NICKEL ALLOYS, 22, 92, 110
NIGHT VISION, 18, 173
NIOBIUM, 482, 488, 530
NITRATION, 36
NITRIC ACID, 455
NITRIC OXIDE, 64
NITRIDES, 127, 432
NITROGEN, 65, 315, 444
NITROGEN OXIDES, 286
NITROGENATION, 286
NITROUS OXIDES, 282
NOISE (SOUND), 163
NOISE MEASUREMENT, 272, 353
NOISE REDUCTION, 272
NONDESTRUCTIVE TESTS, 51, 54, 55, 111, 122, 129, 222, 461
NONLINEAR OPTICS, 350, 429, 431
NONLINEAR SYSTEMS, 196, 434
NONLINEARITY, 224, 336, 390, 432
NONRELATIVISTIC MECHANICS, 524
NORMALIZED DIFFERENCE VEGETATION INDEX, 242
NORMALIZING (STATISTICS), 194
NORTH AMERICA, 293, 516
NUCLEAR ASTROPHYSICS, 420, 524, 562
NUCLEAR CAPTURE, 417
NUCLEAR DEFORMATION, 417, 504
NUCLEAR DEVICES, 554
NUCLEAR ELECTRIC POWER GENERATION, 546, 555
NUCLEAR ENGINE FOR ROCKET VEHICLES, 423
NUCLEAR EXPLOSIONS, 227
NUCLEAR FISSION, 420
NUCLEAR FUSION, 448, 449, 453, 454, 498
NUCLEAR INTERACTIONS, 573
NUCLEAR MAGNETIC RESONANCE, 71, 142, 455, 479
NUCLEAR MEDICINE, 324
NUCLEAR MODELS, 424
NUCLEAR PHYSICS, 324, 384, 387, 389, 391, 392, 393, 416, 420, 472, 496, 513, 539
NUCLEAR POWER PLANTS, 331, 363, 426, 427, 542
NUCLEAR PROPULSION, 423
NUCLEAR RADIATION, 429
NUCLEAR REACTIONS, 316, 419, 504, 553
NUCLEAR REACTOR CONTROL, 423
NUCLEAR REACTORS, 102, 394, 419, 423, 424
NUCLEAR RESEARCH, 381, 416, 418, 553, 554
NUCLEAR RESEARCH AND TEST REACTORS, 46, 397
NUCLEAR SCATTERING, 512
NUCLEAR SPIN, 424
NUCLEAR STRUCTURE, 158
NUCLEAR TRANSFORMATIONS, 417
NUCLEAR WEAPONS, 88, 417, 556
NUCLEATION, 78, 105, 460
NUCLEI (NUCLEAR PHYSICS), 414, 495, 504
NUCLEIC ACIDS, 90
NUCLEON POTENTIAL, 528
NUCLEON-NUCLEON INTERACTIONS, 384
NUCLEONS, 385, 399, 405, 496, 509, 510, 528
NUCLIDES, 456, 573
NUMERICAL ANALYSIS, 19, 40, 68, 73, 76, 101, 118, 190, 209, 357, 366, 367, 421, 427, 463
NUMERICAL INTEGRATION, 565
NUMERICAL WEATHER FORECASTING, 296

## O

OBJECT-ORIENTED PROGRAMMING, 168, 355, 356
OBSERVATION, 564
OCCUPATION, 328, 555
OCEAN BOTTOM, 192, 304
OCEAN CURRENTS, 303
OCEAN DYNAMICS, 196, 303
OCEAN MODELS, 303
OCEAN SURFACE, 15, 285
OCEANOGRAPHY, 196, 284, 306
OCEANS, 306
OIL FIELDS, 34, 35, 254, 277
OILS, 21
ON-LINE SYSTEMS, 166, 503
OPACITY, 401, 560
OPEN CIRCUIT VOLTAGE, 246
OPERATING COSTS, 264
OPERATIONS RESEARCH, 542
OPTICAL COMMUNICATION, 211
OPTICAL CORRECTION PROCEDURE, 492
OPTICAL EQUIPMENT, 178, 202, 411, 430, 434, 441, 536
OPTICAL INTERCONNECTS, 211
OPTICAL MEASUREMENT, 136
OPTICAL PROPERTIES, 266, 350, 468, 486, 490
OPTICAL PUMPING, 434
OPTICAL RADAR, 163, 165, 170, 213
OPTICAL THICKNESS, 240
OPTICAL TRANSITION, 505
OPTICS, 210, 211
OPTIMAL CONTROL, 408
OPTIMIZATION, 55, 104, 122, 137, 144, 199, 338, 359, 505
ORBITAL MECHANICS, 565
ORDER-DISORDER TRANSFORMATIONS, 91
ORDNANCE, 51
ORGANIC COMPOUNDS, 33, 80, 248
ORGANIC MATERIALS, 61, 306, 307, 562, 564, 567
ORGANIC SUPERCONDUCTORS, 461, 468, 469, 478, 484
ORGANIZATIONS, 542, 544, 545
ORGANOMETALLIC COMPOUNDS, 37, 38, 78
ORTHOSTATIC TOLERANCE, 327
OSCILLATIONS, 380, 397, 405, 465, 467, 469, 501
OSCILLATORS, 210, 396
OXIDATION, 75, 92, 94, 96, 112, 149, 150, 291, 430, 462, 464, 487
OXIDATION RESISTANCE, 75, 94, 252
OXIDATION-REDUCTION REACTIONS, 57, 117, 251, 487
OXIDE DISPERSION STRENGTHENING, 106
OXIDE FILMS, 458
OXIDES, 37, 97, 127, 129, 458
OXYGEN, 57, 65, 109, 287, 291
OZONE, 68, 285
OZONE DEPLETION, 278

## P

PACIFIC OCEAN, 285
PACKAGING, 123, 124, 174
PAIR PRODUCTION, 405, 514
PALEOBIOLOGY, 291
PALEONTOLOGY, 291
PALLADIUM, 33, 85

PALLADIUM ALLOYS, 450
PAPER (MATERIAL), 42
PARABOLIC REFLECTORS, 265, 267
PARALLEL COMPUTERS, 199, 534
PARALLEL PLATES, 188
PARALLEL PROCESSING (COMPUTERS), 168, 194, 195, 338, 339, 340, 343, 346, 349, 351, 360, 422
PARALLEL PROGRAMMING, 343, 357, 359
PARAMETER IDENTIFICATION, 97, 398
PARAMETERIZATION, 419, 554
PARAMETRIC AMPLIFIERS, 62
PARITY, 496, 533
PARKS, 273
PARTIAL DIFFERENTIAL EQUATIONS, 337, 338, 354, 356
PARTICLE ACCELERATION, 335, 513, 523, 525, 526
PARTICLE ACCELERATORS, 355, 377, 381, 384, 385, 393, 394, 406, 476, 489, 493, 503, 516, 521, 522, 523, 530, 531, 533, 534, 535, 536
PARTICLE BEAMS, 203, 374, 388, 448, 490, 495, 499, 501, 507, 511, 514, 515, 523
PARTICLE COLLISIONS, 382, 383, 385, 394, 399, 400, 412, 460, 496, 500, 501, 503, 518, 526, 535, 536
PARTICLE DECAY, 380, 385, 387, 392, 395, 396, 491, 520, 528, 538
PARTICLE DIFFUSION, 276
PARTICLE ENERGY, 525
PARTICLE IMAGE VELOCIMETRY, 3, 191
PARTICLE INTERACTIONS, 79, 198, 444, 452, 460, 509
PARTICLE MASS, 398
PARTICLE PRODUCTION, 394, 398, 399, 401, 416, 495, 497, 499, 525, 533, 566
PARTICLE SIZE DISTRIBUTION, 423, 439
PARTICLE SPIN, 386, 481, 497
PARTICLE THEORY, 503
PARTICLES, 274, 463
PARTICULATES, 196, 277, 307
PARTONS, 384, 508, 512
PASSENGER AIRCRAFT, 9
PASSIVITY, 9, 92, 487
PATTERN RECOGNITION, 198, 204, 337, 365, 398
PAULI EXCLUSION PRINCIPLE, 412
PAYLOAD CONTROL, 156
PAYLOADS, 30
PELLETS, 445
PENCIL BEAMS, 428
PENETRATION, 190
PENETROMETERS, 43
PERFLUORO COMPOUNDS, 80
PERFORMANCE, 259
PERFORMANCE PREDICTION, 183, 214, 263, 335
PERFORMANCE TESTS, 46, 119, 155, 165, 203, 221, 244, 250, 252, 254, 262, 282, 347, 406, 515
PERMANENT MAGNETS, 207
PERMEABILITY, 245
PEROVSKITES, 86, 177, 458, 466, 487
PERSONNEL, 542, 555
PERSONNEL MANAGEMENT, 544
PERTURBATION, 419, 507
PERTURBATION THEORY, 58, 381
PETROLOGY, 230
PH, 63
PHARMACOLOGY, 323
PHASE DIAGRAMS, 121
PHASE MATCHING, 179
PHASE TRANSFORMATIONS, 47, 68, 467
PHENOMENOLOGY, 175, 379
PHONONS, 103, 126
PHOSPHORS, 374
PHOSPHORUS, 39
PHOTOCATHODES, 388, 392, 515, 517, 523, 524, 535
PHOTOCHEMICAL REACTIONS, 59, 74, 78, 285, 301, 563
PHOTOCONDUCTIVITY, 175, 484
PHOTODIODES, 180
PHOTOELECTRIC EFFECT, 174
PHOTOELECTRIC EMISSION, 488
PHOTOELECTRONS, 381, 411
PHOTOEXCITATION, 492
PHOTOLITHOGRAPHY, 201
PHOTOLUMINESCENCE, 372, 374, 454, 462
PHOTOLYSIS, 81, 278, 431, 558
PHOTOMETERS, 200, 240, 343
PHOTOMETRY, 557
PHOTOMICROGRAPHY, 85
PHOTON BEAMS, 506, 515, 517, 533
PHOTONICS, 436
PHOTONS, 148, 201, 207, 405, 416, 417, 422, 457, 475, 483, 505, 506, 507, 509, 512, 524, 527, 528, 530, 533, 534
PHOTOPRODUCTION, 405
PHOTOREFRACTIVITY, 48, 122, 432
PHOTOSYNTHESIS, 291, 306, 308
PHOTOVOLTAIC CELLS, 184, 202, 246, 252, 258, 264, 266
PHOTOVOLTAIC CONVERSION, 245, 246, 251, 253, 254, 260, 265
PHYSICAL CHEMISTRY, 135
PHYSICAL EXERCISE, 334
PHYSICAL FACTORS, 67, 546
PHYSICAL OPTICS, 350
PHYSICAL PROPERTIES, 407
PHYSIOLOGICAL EFFECTS, 325
PHYSIOLOGICAL RESPONSES, 313, 319, 322, 327, 328
PHYTOTRONS, 315
PICOSECOND PULSES, 515, 530
PIEZOELECTRICITY, 221, 483
PILOT PLANTS, 145, 259, 279
PILOTLESS AIRCRAFT, 16, 25, 242
PINS, 425
PION BEAMS, 415
PIONS, 385, 395, 419, 521
PIPELINES, 95, 197, 198
PIPELINING (COMPUTERS), 359
PIPES (TUBES), 139
PITCH (INCLINATION), 6
PITTING, 47, 89, 93
PIXELS, 428
PLAINS, 580
PLANE WAVES, 399
PLANETARY ATMOSPHERES, 563, 585
PLANETARY BOUNDARY LAYER, 298
PLANETARY COMPOSITION, 4, 205, 577, 580, 582, 586, 587, 590, 591, 595
PLANETARY CORES, 576, 593, 598
PLANETARY CRATERS, 580, 588, 590
PLANETARY CRUSTS, 27, 580, 582, 585, 586, 589, 590, 591
PLANETARY ENVIRONMENTS, 579
PLANETARY EVOLUTION, 291, 362, 557, 559, 579, 580, 582, 584, 587, 594, 595
PLANETARY GEOLOGY, 570, 571, 572, 573, 582, 584, 586
PLANETARY MAGNETIC FIELDS, 576, 579, 592
PLANETARY MAGNETOSPHERES, 292, 577, 583, 585, 592, 598
PLANETARY MANTLES, 27, 593
PLANETARY MAPPING, 243
PLANETARY NEBULAE, 558
PLANETARY ORBITS, 565
PLANETARY ROTATION, 576, 583, 587, 592, 598
PLANETARY STRUCTURE, 582, 587, 590, 592, 594
PLANETARY SURFACES, 558, 580, 588, 590
PLANETARY SYSTEMS, 557, 559
PLANETARY TEMPERATURE, 582

PLANETOLOGY, 595
PLANETS, 587
PLANFORMS, 17
PLANT DISEASES, 315
PLANT STRESS, 313
PLANTS (BOTANY), 286, 333
PLASMA ACCELERATORS, 452
PLASMA CONTROL, 167, 395, 449, 450
PLASMA DIAGNOSTICS, 447, 448, 577
PLASMA GUNS, 535
PLASMA INTERACTIONS, 451, 452, 598
PLASMA PHYSICS, 444, 454
PLASMAS (PHYSICS), 52, 77, 264, 442, 444, 446, 447, 448, 450, 451, 452, 453, 486, 585, 598
PLASTIC DEFORMATION, 107, 401
PLASTIC FLOW, 38
PLASTICS, 128
PLATES (TECTONICS), 292
PLUTONIUM, 80, 121, 130
PLUTONIUM 238, 42
PLUTONIUM OXIDES, 41, 84
PNEUMATICS, 21
POINT DEFECTS, 50, 112
POINT SOURCES, 447, 566
POINT TO POINT COMMUNICATION, 171
POLAR REGIONS, 574, 578, 581
POLARIMETERS, 378, 500
POLARIMETRY, 374
POLARIZATION (SPIN ALIGNMENT), 386
POLARIZATION MODULATION, 479
POLARIZED RADIATION, 491, 536
POLARIZERS, 83, 422
POLICIES, 8, 9, 11, 149
POLLUTION CONTROL, 253, 271, 280, 305, 556
POLLUTION TRANSPORT, 272, 281
POLYATOMIC MOLECULES, 37
POLYCARBONATES, 115
POLYCHLORINATED BIPHENYLS, 73
POLYCRYSTALS, 112, 119, 121, 261
POLYETHYLENES, 125
POLYIMIDES, 50
POLYMER MATRIX COMPOSITES, 49, 53, 116
POLYMERIZATION, 61
POLYMERS, 43, 120, 138
POLYMETHYL METHACRYLATE, 177, 401
POLYPEPTIDES, 309
POLYSTYRENE, 53
POLYURETHANE FOAM, 130
POMERONS, 527
PONDS, 242
POPULATIONS, 308
POROSITY, 39, 94, 196, 225
POROUS MATERIALS, 196, 238, 456
POSITION (LOCATION), 595
POSITIONING, 157, 215
POSITRONS, 496, 506, 514, 527
POSTURE, 318, 325
POTASSIUM, 583, 589, 597
POTASSIUM 40, 585
POWDER (PARTICLES), 94, 126
POWER EFFICIENCY, 270
POWER GAIN, 378
POWER LINES, 490
POWER PLANTS, 280
POWER SPECTRA, 22, 490
PREAMPLIFIERS, 184
PRECAMBRIAN PERIOD, 291
PRECIPITATES, 461
PRECIPITATION (METEOROLOGY), 302
PREDICTION ANALYSIS TECHNIQUES, 247, 339
PREDICTIONS, 303, 410
PREGNANCY, 313
PREMIXED FLAMES, 57, 368
PRESSURE DISTRIBUTION, 3
PRESSURE EFFECTS, 454
PRESSURE GRADIENTS, 199, 325
PRESSURE MEASUREMENT, 4, 70
PRESSURE OSCILLATIONS, 295
PRESSURE REGULATORS, 315
PRESSURE SENSORS, 208
PRESSURE VESSELS, 95, 425
PRESSURIZED WATER REACTORS, 107
PRETREATMENT, 45
PREVENTION, 366
PRIMARY COSMIC RAYS, 600
PROBABILITY DENSITY FUNCTIONS, 370
PROBABILITY DISTRIBUTION FUNCTIONS, 369
PROBABILITY THEORY, 335, 441
PROBES, 391, 464
PROBLEM SOLVING, 189
PROCEDURES, 146, 350, 371, 517, 544, 548
PRODUCT DEVELOPMENT, 142, 315, 459
PRODUCTION COSTS, 142
PRODUCTION ENGINEERING, 104, 144, 160, 393
PRODUCTS, 348
PROGRAM VERIFICATION (COMPUTERS), 339, 346, 362, 421
PROGRAMMING ENVIRONMENTS, 429
PROGRAMMING LANGUAGES, 346, 354, 355
PROGRESS, 74
PROJECT MANAGEMENT, 148, 427, 552
PROJECTILE CRATERING, 588
PROJECTILES, 139
PROPAGATION, 453
PROPELLANT COMBUSTION, 77, 154
PROPELLANT CONSUMPTION, 154
PROPELLANTS, 64, 77
PROPELLER BLADES, 6
PROPULSION, 4, 28, 32, 134
PROPULSION SYSTEM CONFIGURATIONS, 192, 217
PROPULSION SYSTEM PERFORMANCE, 21, 249
PROPULSIVE EFFICIENCY, 249
PROTECTION, 554
PROTECTIVE CLOTHING, 115, 334
PROTECTIVE COATINGS, 15, 34, 39, 45, 90
PROTEINS, 310
PROTOBIOLOGY, 311
PROTOCOL (COMPUTERS), 168, 171, 349, 355, 362, 552
PROTON BEAMS, 383, 419, 498, 499, 500, 534, 536
PROTON-ANTIPROTON INTERACTIONS, 383, 385, 400
PROTONS, 88, 116, 418, 429, 456, 518, 529, 535
PROTOPLANETS, 587
PROTOTYPES, 16, 38, 43, 134, 144, 153, 163, 585
PROVING, 5, 19, 41, 421, 450
PROXIMITY EFFECT (ELECTRICITY), 481
PSYCHOPHYSIOLOGY, 328
PUBLIC HEALTH, 154, 278, 311
PULSE DETONATION ENGINES, 32
PULSE GENERATORS, 183, 263
PULSE POSITION MODULATION, 365
PULSED LASER DEPOSITION, 456, 458, 472
PULSED LASERS, 61, 316, 413, 438, 568
PULSED RADIATION, 394, 510, 515
PULSEJET ENGINES, 21
PUMPING, 75
PUMPS, 153
PYRANOMETERS, 599
PYRITES, 143

PYROHELIOMETERS, 253

## Q

Q FACTORS, 437
QUADRATIC PROGRAMMING, 336
QUADRUPOLES, 455, 519
QUALITY CONTROL, 148, 235, 348, 551
QUANTITATIVE ANALYSIS, 41, 96, 155, 351
QUANTUM CHEMISTRY, 69, 90
QUANTUM CHROMODYNAMICS, 377, 379, 381, 383, 390, 395, 402, 480, 481, 489, 495, 496, 502, 508, 514, 523, 526, 527, 531, 539
QUANTUM CRYPTOGRAPHY, 365
QUANTUM DOTS, 462
QUANTUM EFFICIENCY, 182
QUANTUM ELECTRODYNAMICS, 524
QUANTUM ELECTRONICS, 365
QUANTUM MECHANICS, 335, 377, 467, 500, 515, 529
QUANTUM THEORY, 367, 377, 412, 485
QUANTUM WELL LASERS, 432
QUANTUM WELLS, 200, 343, 372, 454
QUANTUM WIRES, 372
QUARK MODELS, 394, 521, 522
QUARK PARTON MODEL, 489
QUARKS, 379, 387, 395, 398, 405, 406, 444, 452, 481, 495, 502, 510, 514, 515, 520, 525, 531, 539
QUARTZ, 519
QUENCHING (COOLING), 91, 93, 108
QUINOXALINES, 36

## R

RADAR, 299
RADAR ASTRONOMY, 592
RADAR CROSS SECTIONS, 164
RADAR DATA, 162, 164, 575
RADAR DETECTION, 169, 302
RADAR ECHOES, 578
RADAR IMAGERY, 169, 578, 581
RADAR MEASUREMENT, 222, 587
RADAR RANGE, 575
RADAR SCATTERING, 164
RADIANCE, 239
RADIATION CHEMISTRY, 599
RADIATION COUNTERS, 299, 538
RADIATION DAMAGE, 52, 53, 375
RADIATION DETECTORS, 184, 185, 274, 288, 375, 498
RADIATION DOSAGE, 99, 494
RADIATION EFFECTS, 47, 99, 110, 124, 174, 340
RADIATION MEASUREMENT, 235, 239, 242, 295, 296, 297, 301, 302
RADIATION MEASURING INSTRUMENTS, 599
RADIATION PROTECTION, 158
RADIATION SOURCES, 511
RADIATIVE TRANSFER, 599
RADICALS, 71
RADIO ASTRONOMY, 557
RADIO EQUIPMENT, 380, 510
RADIO FREQUENCIES, 170, 173, 180, 183, 186, 379, 527
RADIO FREQUENCY DISCHARGE, 535
RADIO PROBING, 222
RADIO TELEMETRY, 230
RADIOACTIVE CONTAMINANTS, 212, 277
RADIOACTIVE ISOTOPES, 45, 64, 225, 324, 481, 566
RADIOACTIVE MATERIALS, 95, 277
RADIOACTIVE WASTES, 33, 45, 46, 47, 55, 75, 82, 84, 95, 115, 119, 121, 123, 124, 125, 128, 130, 198, 234, 236, 254, 277, 304, 422, 548
RADIOACTIVITY, 414, 439
RADIOBIOLOGY, 494
RADIOCHEMICAL SEPARATION, 46
RADIOGENIC MATERIALS, 585
RADIOGRAPHY, 88, 219
RADIOLYSIS, 90, 515, 530
RADIOMETERS, 572
RADIOSONDES, 296
RAIN, 282, 297
RAIN GAGES, 302
RAMAN SPECTRA, 37
RAMAN SPECTROSCOPY, 87, 460
RAPID PROTOTYPING, 178
RARE EARTH COMPOUNDS, 42
RARE EARTH ELEMENTS, 135, 287, 404, 422, 482
RARE GASES, 456
RATIOS, 589
RATS, 318, 321
RDX, 147
REACTION KINETICS, 59, 66, 71, 78, 79, 96, 147, 154, 368, 380, 392, 419, 420
REACTION PRODUCTS, 36
REACTIVITY, 65, 78, 97, 176
REACTOR CORES, 424
REACTOR DESIGN, 65, 88
REACTOR MATERIALS, 446
REACTOR PHYSICS, 423, 425
REACTOR SAFETY, 423, 427
REACTORS, 426
READING, 540
REAL TIME OPERATION, 154, 398, 507, 513
RECEIVERS, 171
RECIPROCITY THEOREM, 165
RECONFIGURABLE HARDWARE, 352
RECONNAISSANCE, 24
RECORDERS, 20
RECORDING INSTRUMENTS, 355
RECTANGULAR PLATES, 4
RECYCLING, 42, 279, 280
REFINING, 146
REFLECTANCE, 35, 487, 576
REFRIGERANTS, 155, 217
REFRIGERATORS, 157, 161
REFUELING, 7
REGENERATION (ENGINEERING), 279
REGENERATORS, 404
REGGE POLES, 523, 527, 531
REGIONS, 91
REGOLITH, 290, 292, 589, 596
REGULATIONS, 170, 284, 306
RELATIONAL DATA BASES, 547
RELATIVISTIC EFFECTS, 58
RELATIVISTIC ELECTRON BEAMS, 395
RELATIVISTIC PARTICLES, 537
RELIABILITY, 221, 343, 522, 539
RELIABILITY ANALYSIS, 166, 214, 335, 369
REMOTE CONTROL, 158
REMOTE SENSING, 15, 20, 204, 207, 240, 241, 242, 243, 278, 284, 285, 296, 299, 302, 306, 307, 312, 429, 483, 557, 571, 572, 580, 582, 593
REMOVAL, 214, 280
RENEWABLE ENERGY, 144, 149, 156, 247, 251, 257, 261, 284
RENORMALIZATION GROUP METHODS, 124
REPLACING, 23
REPORTS, 251
RESEARCH AIRCRAFT, 298
RESEARCH AND DEVELOPMENT, 11, 24, 51, 76, 135, 157, 417, 471, 541, 542, 552
RESEARCH FACILITIES, 88, 157, 277, 361, 382, 385, 503, 521, 536, 537, 539, 545
RESEARCH MANAGEMENT, 76, 407
RESEARCH PROJECTS, 4, 494
RESERVES, 140
RESERVOIRS, 44, 232, 245, 256, 267
RESIDENTIAL ENERGY, 159
RESIDUAL STRESS, 35, 44, 109, 113

RESIDUES, 413
RESIN TRANSFER MOLDING, 51
RESINS, 115
RESONANCE, 421
RESONANCE SCATTERING, 453, 478
RESONANT FREQUENCIES, 332
RESPIRATORS, 334
RESTORATION, 231
RESUSCITATION, 309
RETARDERS (DEVICES), 378
RETENTION (PSYCHOLOGY), 324, 554
REUSABLE LAUNCH VEHICLES, 28
REVENUE, 23
REVISIONS, 340
REYNOLDS STRESS, 151
RHENIUM, 107
RHENIUM COMPOUNDS, 182
RHEOLOGY, 198, 590
RIEMANN MANIFOLD, 396
RISERS, 66, 146
RISK, 273, 544
RIVERS, 77, 228, 229
ROBOT CONTROL, 364
ROBOTICS, 364
ROBOTS, 161, 364, 366
ROBUSTNESS (MATHEMATICS), 550, 554
ROCKET PROPELLANTS, 29
ROCKS, 229, 230, 232, 238, 570
RODENTS, 309
ROLLERS, 218
ROOFS, 4, 258
ROTARY WING AIRCRAFT, 17, 18
ROTATING DISKS, 54
ROTATING FLUIDS, 294
ROTOR BLADES (TURBOMACHINERY), 3, 6, 17
ROTORS, 247
RUBBER, 128
RUPTURING, 92
RURAL AREAS, 12, 13

## S

S WAVES, 448
SAFETY, 23, 85, 543, 544, 545
SAFETY FACTORS, 141
SAFETY MANAGEMENT, 416
SALINITY, 557
SALT BEDS, 34, 138
SAMARIUM COMPOUNDS, 97
SAMPLING, 49, 376, 568
SANDS, 290, 291, 570
SANDWICH STRUCTURES, 82
SAPPHIRE, 474
SATELLITE ANTENNAS, 183, 247
SATELLITE COMMUNICATION, 164
SATELLITE CONSTELLATIONS, 247
SATELLITE IMAGERY, 242, 243, 294, 296
SATELLITE INSTRUMENTS, 278, 307
SATELLITE OBSERVATION, 296
SATELLITE TRACKING, 29
SCALE (CORROSION), 112
SCALING LAWS, 194
SCANNERS, 203, 206
SCANNING ELECTRON MICROSCOPY, 157, 290
SCANNING TUNNELING MICROSCOPY, 380, 462
SCATTERING, 37, 87, 164, 386, 446, 447, 477, 479, 505
SCHEDULING, 154, 168
SCHOOLS, 217
SCIENTIFIC VISUALIZATION, 198, 341, 350, 356
SCINTILLATION, 77
SCRAP, 95
SEA FLOOR SPREADING, 304
SEA ICE, 242, 243, 307
SEA SURFACE TEMPERATURE, 282, 305
SEA WATER, 306
SEAS, 297, 304
SEATS, 332
SECONDARY COSMIC RAYS, 600
SECONDARY ION MASS SPECTROMETRY, 457
SECURITY, 361, 362, 554
SEDIMENTARY ROCKS, 241, 294
SEDIMENTS, 229, 230, 233, 236, 304, 305, 574
SEGMENTS, 223
SEISMIC ENERGY, 363
SEISMIC WAVES, 27
SEISMOGRAPHS, 27
SEISMOLOGY, 230, 547
SEIZURES, 370
SELF ASSEMBLY, 216
SEMICONDUCTING FILMS, 182
SEMICONDUCTOR DEVICES, 126, 457
SEMICONDUCTOR LASERS, 211, 471
SEMICONDUCTORS (MATERIALS), 175, 176, 178, 180, 184, 185, 437, 454, 463, 469, 471, 484, 486, 492
SENSITIVITY, 507
SENSITIVITY ANALYSIS, 130, 431
SENSORIMOTOR PERFORMANCE, 318
SENSORS, 43
SEQUENTIAL ANALYSIS, 369
SERPENTINE, 270
SERVICE LIFE, 370, 446
SERVOMECHANISMS, 173
SETTLING, 521
SHADOWS, 566
SHAFTS (MACHINE ELEMENTS), 22, 208
SHAPE CONTROL, 483
SHAPE MEMORY ALLOYS, 103
SHAPE OPTIMIZATION, 336
SHAPES, 56, 114
SHEAR FLOW, 187
SHEAR STRESS, 222
SHOCK LAYERS, 4
SHOCK LOADS, 224
SHOCK TUBES, 81
SHOCK TUNNELS, 195
SHOCK WAVES, 444
SHOEMAKER-LEVY 9 COMET, 562
SHOWERS, 221
SIGNAL PROCESSING, 162, 169, 201, 338, 537
SIGNAL REFLECTION, 15
SIGNATURES, 337
SILANES, 117
SILICON, 99, 184, 215, 403, 456, 457, 465, 487
SILICON ALLOYS, 400
SILICON CARBIDES, 33, 65, 96, 117, 152, 457
SILICON DIOXIDE, 270, 441, 456, 529
SILICON NITRIDES, 123, 126, 127, 156, 222
SILICON OXIDES, 53, 261, 462
SILICON POLYMERS, 177, 216, 433
SILVER, 58, 461, 485
SIMPLIFICATION, 364
SIMULATION, 15, 31, 44, 118, 194, 195, 196, 201, 257, 366, 385, 410, 491, 570
SIMULATORS, 168
SINE WAVES, 331
SINGLE CRYSTALS, 382, 476, 478
SINGLE EVENT UPSETS, 340
SINGLE STAGE TO ORBIT VEHICLES, 31
SINGULAR INTEGRAL EQUATIONS, 367
SINGULARITY (MATHEMATICS), 396
SINTERING, 113, 114
SIS (SUPERCONDUCTORS), 474
SITES, 229
SITUATIONAL AWARENESS, 330
SIZE DISTRIBUTION, 274, 287, 299, 588
SKIN (ANATOMY), 323

SKIN TEMPERATURE (BIOLOGY), 322
SLABS, 6
SLEDS, 377
SLEEP, 330
SLENDER BODIES, 192
SLIDING, 377
SLUDGE, 83
SLUMPING, 419
SLURRIES, 151, 156, 198
SMART MATERIALS, 217
SMART STRUCTURES, 364
SNAKES, 319
SODALITE, 127
SODAR, 299, 301
SODIUM, 286, 324, 583, 589, 590, 597
SODIUM VAPOR, 172
SOFIA (AIRBORNE OBSERVATORY), 559
SOFTWARE DEVELOPMENT TOOLS, 198, 341, 347, 544
SOFTWARE ENGINEERING, 24, 76, 199, 226, 246, 344, 348, 349, 350, 351, 352, 353, 358, 364, 394
SOI (SEMICONDUCTORS), 179, 251
SOIL MOISTURE, 557
SOIL SAMPLING, 36
SOIL SCIENCE, 289
SOILS, 233, 236, 237, 238, 591
SOL-GEL PROCESSES, 472
SOLAR CELLS, 247, 250, 253, 256, 257, 260, 261, 262
SOLAR COLLECTORS, 265
SOLAR ENERGY, 247, 257
SOLAR ENERGY CONVERSION, 266
SOLAR FLUX, 4
SOLAR HEATING, 265
SOLAR NEBULA, 566
SOLAR ORBITS, 565, 583
SOLAR POWER SATELLITES, 247
SOLAR RADIATION, 282, 296, 410, 599
SOLAR SYSTEM, 559, 595
SOLAR SYSTEM EVOLUTION, 587
SOLAR THERMAL ELECTRIC POWER PLANTS, 265, 266
SOLAR WIND, 255, 580, 584, 585
SOLDERS, 96, 216
SOLENOIDS, 203, 489, 498, 535
SOLID ELECTROLYTES, 267
SOLID OXIDE FUEL CELLS, 249, 254, 260, 463
SOLID PHASES, 563
SOLID SOLUTIONS, 90
SOLID STATE, 96, 161, 176, 209, 438, 471, 472
SOLID STATE LASERS, 210, 211
SOLID STATE PHYSICS, 456
SOLID SURFACES, 477
SOLIDS FLOW, 197
SOLUTES, 155
SOLVENT EXTRACTION, 45, 47, 64, 82, 135
SOLVENTS, 36, 44, 47, 80, 418
SONAR, 410
SOOT, 56, 57, 79
SORPTION, 70, 280
SOUTHERN OSCILLATION, 294, 295
SPACE CHARGE, 48, 453
SPACE ENVIRONMENT SIMULATION, 324
SPACE EXPLORATION, 594
SPACE FLIGHT, 316, 318, 544, 545
SPACE HEATING (BUILDINGS), 156, 217, 246
SPACE MISSIONS, 26, 27, 30, 204, 205, 206, 207, 438, 573, 578, 585, 586, 592, 593, 594, 595
SPACE OBSERVATIONS (FROM EARTH), 583, 586, 596, 597
SPACE PERCEPTION, 565
SPACE PLASMAS, 583
SPACE PROBES, 183, 563
SPACE PROGRAMS, 601
SPACE TRANSPORTATION SYSTEM, 322
SPACE WEAPONS, 555
SPACE WEATHERING, 580, 589
SPACEBORNE ASTRONOMY, 559
SPACEBORNE EXPERIMENTS, 321, 573
SPACECRAFT DESIGN, 594
SPACECRAFT EQUIPMENT, 26, 30, 154, 204, 205, 438
SPACECRAFT INSTRUMENTS, 205, 206, 585
SPACECRAFT LAUNCHING, 29
SPACECREWS, 25, 29, 327
SPACELAB, 322, 326
SPALLATION, 388, 389, 489, 532
SPATIAL DISTRIBUTION, 91, 192, 226, 298, 388, 390
SPATIAL RESOLUTION, 241, 243
SPECIFIC IMPULSE, 32
SPECKLE INTERFEROMETRY, 583, 587
SPECTRA, 288, 435
SPECTRAL BANDS, 241
SPECTRAL EMISSION, 579
SPECTRAL REFLECTANCE, 240, 577
SPECTRAL RESOLUTION, 242
SPECTRAL SIGNATURES, 567
SPECTROMETERS, 33, 77, 205, 535, 572, 576
SPECTROPHOTOMETRY, 596
SPECTRORADIOMETERS, 240
SPECTROSCOPY, 41, 49, 313, 424, 436, 464, 515, 563, 594
SPECTRUM ANALYSIS, 225
SPEECH, 338
SPEECH RECOGNITION, 338
SPEED CONTROL, 216
SPEED INDICATORS, 208
SPENT FUELS, 86, 128, 226, 426
SPHERICAL HARMONICS, 165, 502
SPIN, 466, 493
SPIN DYNAMICS, 74, 430, 473, 513
SPIN GLASS, 404
SPINAL CORD, 312, 317
SPINEL, 124, 125, 259, 476
SPLINE FUNCTIONS, 483
SPONTANEOUS EMISSION, 213, 429, 439, 490
SPORES, 274
SPREAD SPECTRUM TRANSMISSION, 380
SPREADING, 518
SPRITES (ATMOSPHERIC PHYSICS), 301
SPUTTERING, 447, 477
SQUID (DETECTORS), 455, 461
STABILITY, 21, 72, 129, 305, 390, 418, 430, 490, 506, 512
STABILIZATION, 95, 252
STACKS, 282
STAINLESS STEELS, 36, 63, 94, 97, 99, 103, 104, 107, 108, 114
STANDARD MODEL (PARTICLE PHYSICS), 420, 508, 538, 539
STANDARDIZATION, 267, 384
STANDARDS, 280
STATIC THRUST, 6
STATISTICAL ANALYSIS, 72, 202, 268, 292, 315, 329, 343, 370, 371, 441, 541
STATISTICAL DISTRIBUTIONS, 370
STEADY STATE, 219
STEELS, 95, 101, 107, 139, 161, 220, 425, 468
STELLAR ACTIVITY, 560
STELLAR MASS, 600
STELLAR MASS EJECTION, 560
STELLAR SYSTEMS, 600
STELLARATORS, 402, 453
STEREOCHEMISTRY, 68
STEREOPHOTOGRAPHY, 206, 243, 578
STEREOSCOPIC VISION, 202
STIRLING ENGINES, 216
STOCHASTIC PROCESSES, 194, 367, 369, 377, 453, 472

STOICHIOMETRY, 472
STOPPING, 399
STORAGE, 132
STORAGE BATTERIES, 248
STORAGE RINGS (PARTICLE ACCELERATORS), 386, 437, 475, 489, 491, 494, 503, 506, 507, 509, 511, 513, 520, 525, 527, 530, 534, 560
STORAGE STABILITY, 248, 546
STORAGE TANKS, 85, 135, 241, 261
STRAIN RATE, 54, 59, 111, 112
STRANDS, 490
STRANGENESS, 394
STRATEGY, 542
STRATIFICATION, 426
STRATIFIED FLOW, 294
STRATIGRAPHY, 227, 229, 595
STREAK CAMERAS, 507
STREAK PHOTOGRAPHY, 507
STREAMS, 229, 289
STRESS CONCENTRATION, 44
STRESS CORROSION CRACKING, 48, 92
STRESS DISTRIBUTION, 235, 245, 464
STRESS INTENSITY FACTORS, 19
STRESS MEASUREMENT, 483
STRESS-STRAIN RELATIONSHIPS, 222, 223
STRESSES, 106
STRONTIUM 90, 47
STRONTIUM ISOTOPES, 237
STRONTIUM OXIDES, 458, 460
STRUCTURAL ANALYSIS, 217, 225
STRUCTURAL BASINS, 232, 241, 568, 571
STRUCTURAL DESIGN, 547
STRUCTURAL STABILITY, 287
STRUCTURED GRIDS (MATHEMATICS), 2
STUDENTS, 543, 573
SUBSTITUTES, 135
SUBSTRATES, 89, 99, 177, 472
SUBSTRUCTURES, 104
SUGARS, 78
SULFIDATION, 96
SULFONATES, 70
SULFUR, 109
SULFUR COMPOUNDS, 125
SULFUR DIOXIDES, 60
SULFUR HEXAFLUORIDE, 37
SUN, 30, 595
SUNLIGHT, 282
SUPERCOMPUTERS, 342, 347, 349, 356, 360
SUPERCONDUCTING CAVITY RESONATORS, 510
SUPERCONDUCTING DEVICES, 465, 472, 488
SUPERCONDUCTING FILMS, 468, 472, 474
SUPERCONDUCTING MAGNETS, 375, 412, 419, 465, 530
SUPERCONDUCTING POWER TRANSMISSION, 163
SUPERCONDUCTIVITY, 392, 407, 459, 462, 465, 468, 470, 474, 476, 482, 485, 489, 510, 518, 525
SUPERCONDUCTORS (MATERIALS), 465, 466, 467, 468, 470, 473, 484, 492
SUPERCRITICAL FLUIDS, 32, 47, 411
SUPERCRITICAL PRESSURES, 67
SUPERLATTICES, 465, 477
SUPERNOVA 1987A, 560
SUPERNOVAE, 566
SUPERSONIC COMBUSTION RAMJET ENGINES, 21
SUPERSONIC FLOW, 3, 188
SUPERSONIC JET FLOW, 77
SUPERSONIC SPEED, 5
SUPERSONIC TRANSPORTS, 5
SUPERSONIC WIND TUNNELS, 5
SUPERSYMMETRY, 400, 404, 406, 491, 533
SURFACE LAYERS, 81, 459, 599
SURFACE PROPERTIES, 70, 80, 90, 128, 469, 470, 578
SURFACE REACTIONS, 66
SURFACE ROUGHNESS, 213
SURFACE TEMPERATURE, 242
SURFACE TREATMENT, 33, 80, 99, 104, 117, 261
SURFACE VEHICLES, 29
SURFACE WATER, 232, 236, 304
SURFACE WAVES, 298, 306
SURFACTANTS, 456
SURVEILLANCE, 244, 366
SURVEYS, 140, 237, 267, 272, 543
SURVIVAL, 227, 228, 551
SWELLING, 107
SWEPT WINGS, 5
SWITCHES, 173, 175, 484
SWITCHING, 512
SYNCHROTRON RADIATION, 46, 207, 379, 401, 420, 483, 498, 509, 510, 532, 534, 536
SYNCHROTRONS, 43, 87, 88, 212, 392, 393, 406, 440, 498, 500
SYNTHESIS (CHEMISTRY), 68, 120
SYNTHETIC APERTURE RADAR, 164, 592
SYSTEM EFFECTIVENESS, 138
SYSTEMS ANALYSIS, 346, 352
SYSTEMS ENGINEERING, 13, 16, 18, 25, 88, 144, 145, 180, 202, 234, 250, 260, 332, 344, 346, 353, 357, 369, 393, 397, 443, 452
SYSTEMS INTEGRATION, 357, 367
SYSTEMS SIMULATION, 249

## T

TALKING, 163
TANKER AIRCRAFT, 7
TANKS (CONTAINERS), 55
TANTALUM, 111, 411
TARGET ACQUISITION, 202
TARGET RECOGNITION, 164, 169, 170
TARGETS, 330, 410, 493, 529
TATB, 81
TAYLOR SERIES, 508
TECHNETIUM, 55
TECHNETIUM ISOTOPES, 77
TECHNOLOGIES, 24, 76
TECHNOLOGY ASSESSMENT, 2, 86, 253, 283, 516
TECHNOLOGY TRANSFER, 28, 256
TECHNOLOGY UTILIZATION, 107, 156, 245, 510, 546
TECTONICS, 569, 582
TEKTITES, 563
TELECOMMUNICATION, 9, 24, 164, 369
TELESCOPES, 560
TEMPERATURE CONTROL, 149, 220, 247, 510
TEMPERATURE DEPENDENCE, 37
TEMPERATURE DISTRIBUTION, 6, 202
TEMPERATURE EFFECTS, 193, 209, 334, 583
TEMPERATURE GRADIENTS, 246, 599
TEMPERATURE INVERSIONS, 296, 298
TEMPERATURE MEASUREMENT, 63, 220, 246
TEMPERATURE PROFILES, 162
TEMPLATES, 336
TEMPORAL DISTRIBUTION, 203, 226
TENSILE CREEP, 95
TENSILE PROPERTIES, 72, 100
TENSORS, 86
TERMINOLOGY, 549
TERRAIN, 313, 584
TERRESTRIAL PLANETS, 557, 559, 592, 595
TERRESTRIAL RADIATION, 599
TEST CHAMBERS, 193
TEST FACILITIES, 441
TEST RANGES, 132, 141

TEST STANDS, 72
TEST VEHICLES, 483
TETHERLINES, 28
TEXTURES, 570
THEMATIC MAPPERS (LANDSAT), 243
THEORETICAL PHYSICS, 380, 381, 382, 386, 392, 393, 497, 526
THEORIES, 550
THERAPY, 436
THERMAL ANALYSIS, 70, 91, 116, 139, 158, 288, 423
THERMAL COMFORT, 322
THERMAL CONDUCTIVITY, 97, 103, 411
THERMAL CONTROL COATINGS, 34, 39, 44
THERMAL CYCLING TESTS, 39
THERMAL DECOMPOSITION, 53, 130
THERMAL EMISSION, 560, 572
THERMAL ENERGY, 215
THERMAL ENVIRONMENTS, 159
THERMAL EXPANSION, 139, 467
THERMAL FATIGUE, 96
THERMAL INSTABILITY, 600
THERMAL MAPPING, 114, 560
THERMAL PROTECTION, 189, 251
THERMAL RADIATION, 288
THERMAL SHOCK, 426, 429
THERMAL SIMULATION, 108, 150
THERMAL STRESSES, 39, 112
THERMIONIC CATHODES, 379, 517, 527
THERMIONIC EMISSION, 161, 519
THERMOACOUSTIC EFFECTS, 193
THERMOCHEMISTRY, 70
THERMODYNAMIC COUPLING, 478
THERMODYNAMIC CYCLES, 293
THERMODYNAMIC EFFICIENCY, 149, 215
THERMODYNAMIC EQUILIBRIUM, 138
THERMODYNAMIC PROPERTIES, 50, 105, 116, 126, 263, 415, 472
THERMODYNAMICS, 83, 88, 135, 402, 481, 483
THERMOGRAPHY, 222
THERMOGRAVIMETRY, 64
THERMOHYDRAULICS, 88, 423
THERMOLUMINESCENCE, 445
THERMONUCLEAR REACTIONS, 452
THERMOPHILES, 153, 314
THERMOPHYSICAL PROPERTIES, 212
THERMOPILES, 288
THERMOSPHERE, 556
THICKNESS, 39, 208, 222, 589
THIN FILMS, 45, 47, 73, 78, 85, 111, 117, 119, 129, 176, 177, 182, 186, 257, 260, 266, 374, 455, 456, 458, 462, 468, 475, 479, 480, 483, 487
THIN PLATES, 442
THREADS, 113
THREE DIMENSIONAL MODELS, 337, 338, 398, 490, 584, 598
THRUST, 218
THUNDERSTORMS, 300
THYRATRONS, 180
THYRISTORS, 173
TILTMETERS, 520
TIME DEPENDENCE, 71, 339, 418, 449, 484, 528
TIME MEASUREMENT, 398
TIN, 257
TIN ALLOYS, 93, 94
TIN ISOTOPES, 424
TITANATES, 121
TITANIUM ALLOYS, 100, 101
TITANIUM ISOTOPES, 566
TITANIUM OXIDES, 264, 458
TOKAMAK DEVICES, 52, 167, 395, 445, 446, 447, 449, 450, 451
TOLERANCES (MECHANICS), 18, 517
TOMOGRAPHY, 186, 233, 340, 501, 534
TOPOGRAPHY, 182, 229, 291, 294, 408, 568, 570, 588, 589
TOPOLOGY, 380
TOROIDAL PLASMAS, 395
TOROIDS, 67
TORSION, 223
TORSIONAL VIBRATION, 223
TOWERS, 34
TOXICITY, 36, 154
TOXICOLOGY, 273
TRACE ELEMENTS, 39, 40, 92, 275, 306
TRACKING (POSITION), 385
TRAFFIC, 549
TRAINING DEVICES, 351
TRAJECTORY ANALYSIS, 25
TRANSDUCERS, 378
TRANSFORMATIONS (MATHEMATICS), 399
TRANSFORMERS, 172, 502, 522
TRANSIENT PRESSURES, 408
TRANSIENT RESPONSE, 217, 466
TRANSISTORS, 173, 174, 177, 181, 183, 184
TRANSITION METALS, 37, 61, 98, 455, 456
TRANSMISSION, 171
TRANSMISSION EFFICIENCY, 512
TRANSMISSION ELECTRON MICROSCOPY, 70, 106, 171, 455, 458, 461
TRANSMISSION LINES, 167, 502
TRANSPARENCE, 477
TRANSPORT PROPERTIES, 422, 477
TRANSPORT THEORY, 508
TRANSPORTATION, 135, 143, 146, 148, 268
TRANSPORTATION ENERGY, 268
TRANSPORTATION NETWORKS, 547
TRANSVERSE MOMENTUM, 383, 398
TRANSVERSE WAVES, 78
TRAVELING WAVES, 485
TREES (PLANTS), 233
TRIBOLOGY, 214
TRIBUTARIES, 229
TRINITROTOLUENE, 147, 152
TRITIUM, 120, 393, 394, 445, 450
TROPICAL STORMS, 298, 299, 306
TRUCKS, 86, 137, 149, 152
TUBE HEAT EXCHANGERS, 157
TUBES, 186
TUMBLING MOTION, 563
TUMORS, 309
TURBINE BLADES, 51, 193
TURBINE ENGINES, 195
TURBINE PUMPS, 32
TURBOMACHINERY, 191
TURBULENCE, 187, 189, 190, 192, 193, 271
TURBULENCE MODELS, 6, 187, 191
TURBULENT FLOW, 3, 188
TWO BODY PROBLEM, 417
TWO DIMENSIONAL FLOW, 353
TWO DIMENSIONAL MODELS, 347, 451
TWO PHASE FLOW, 71, 195, 196, 197

## U

UGANDA, 300
ULTRAHIGH FREQUENCIES, 557
ULTRASONIC RADIATION, 408
ULTRASONIC SCANNERS, 222
ULTRASONIC TESTS, 237, 411
ULTRASONICS, 114, 220
ULTRAVIOLET ASTRONOMY, 205, 591, 594
ULTRAVIOLET LASERS, 431
ULTRAVIOLET RADIATION, 301, 435
UNDERGROUND EXPLOSIONS, 227
UNDERGROUND STORAGE, 35, 44, 136, 140, 234, 241
UNDERGROUND STRUCTURES, 140, 235
UNITED STATES, 8, 209

UNIVERSE, 598
UNIVERSITIES, 2, 329, 380, 540, 543
UNIVERSITY PROGRAM, 540
UNSTEADY AERODYNAMICS, 21
UNSTEADY FLOW, 192
URANIUM, 65, 66, 73
URANIUM 233, 85
URANIUM ALLOYS, 40, 105
URANIUM COMPOUNDS, 78
URANIUM ISOTOPES, 48, 200
URBAN PLANNING, 278
UREAS, 90, 315
URINE, 324
USER MANUALS (COMPUTER PROGRAMS), 358, 367
UTILITIES, 250, 255

## V

VACCINES, 311
VACUUM CHAMBERS, 159
VACUUM SYSTEMS, 159, 440, 533
VACUUM TUBES, 521
VALENCE, 395, 510
VALLEYS, 227, 570, 571, 584
VALVES, 214
VANADIUM ALLOYS, 100, 101, 102, 110
VANES, 193
VAPOR DEPOSITION, 35, 229, 458, 488, 538
VAPOR PHASES, 45, 68, 72, 200, 280
VAPOR PRESSURE, 455
VARIABILITY, 192, 298, 371, 398
VARIATIONAL PRINCIPLES, 181
VARIATIONS, 373
VECTOR SPACES, 355
VEGETATION, 239, 297
VEINS, 325
VELOCITY, 139, 442
VELOCITY DISTRIBUTION, 4, 191, 353
VELOCITY MEASUREMENT, 62, 68, 568
VENUS (PLANET), 4
VERSATILITY, 539
VERTEBRATES, 319
VERTICAL TAKEOFF AIRCRAFT, 17
VESTIBULAR TESTS, 321
VIBRATION, 54, 332, 355, 371
VIBRATION EFFECTS, 215
VIBRATION MODE, 397
VIBRATIONAL STATES, 479
VIRIAL COEFFICIENTS, 187
VIRTUAL MEMORY SYSTEMS, 361
VIRTUAL REALITY, 341, 346
VIRUSES, 312
VISCOMETERS, 84, 198
VISCOUS FLOW, 3, 116
VISIBILITY, 273
VISION, 332
VISUAL CONTROL, 551
VISUAL PERCEPTION, 202
VOIDS, 111
VOLATILE ORGANIC COMPOUNDS, 255
VOLCANIC ERUPTIONS, 582, 588
VOLCANOES, 569, 582
VOLCANOLOGY, 569
VOLTAGE REGULATORS, 174
VOLUME, 136
VORTEX BREAKDOWN, 194
VORTICES, 3, 368
VULNERABILITY, 164

## W

WAFERS, 469, 486
WALKING, 325, 364
WALLS, 222
WARFARE, 313
WARNING SYSTEMS, 10
WASTE DISPOSAL, 34, 35, 43, 49, 95, 123, 124, 127, 128, 254, 277, 304, 422
WASTE MANAGEMENT, 33, 35, 59, 73, 74, 124, 130, 259, 277, 548
WASTE TREATMENT, 86, 115, 236, 548
WASTE UTILIZATION, 144
WASTE WATER, 132, 268
WASTES, 86
WATER, 66, 70, 83, 188, 305, 333
WATER POLLUTION, 229, 233, 273
WATER QUALITY, 72, 232, 236
WATER RECLAMATION, 72
WATER RESOURCES, 236
WATER SAMPLING, 244, 274, 275
WATER TREATMENT, 268
WATER VAPOR, 235, 296
WATER WAVES, 304, 306
WATERSHEDS, 231
WAVE ATTENUATION, 373
WAVE EQUATIONS, 350, 399, 408
WAVE EXCITATION, 534
WAVE FRONTS, 211, 339
WAVE PROPAGATION, 407
WAVE SCATTERING, 393
WAVE-PARTICLE INTERACTIONS, 447
WAVEFORMS, 293
WAVEGUIDES, 157, 171, 512, 522, 529
WAVELENGTH DIVISION MULTIPLEXING, 173, 183
WAVELENGTHS, 213
WAVELET ANALYSIS, 204, 243, 337
WAXES, 33
WEAK ENERGY INTERACTIONS, 414
WEAPON SYSTEMS, 349
WEATHER, 202
WEATHER FORECASTING, 297, 301
WEATHERING, 290, 571
WEDGES, 330, 487
WEIGHTLESSNESS, 325
WEIGHTLESSNESS SIMULATION, 325
WELDABILITY, 22
WELDING, 100, 108
WELDING MACHINES, 218
WELLS, 227, 231
WICKS, 216
WIND (METEOROLOGY), 187, 262, 291, 298
WIND DIRECTION, 31
WIND EFFECTS, 289, 291
WIND PRESSURE, 298
WIND PROFILES, 15, 288, 301
WIND TUNNEL NOZZLES, 5
WIND TUNNEL TESTS, 18, 22
WIND TUNNELS, 23
WIND TURBINES, 51, 247, 259, 260, 268, 271
WIND VELOCITY, 31, 213, 291
WINDPOWER UTILIZATION, 251, 260, 261, 262
WING TIP VORTICES, 4
WIRE, 375
WIRELESS COMMUNICATION, 170, 357, 367
WOOD, 83
WORK HARDENING, 100
WORKING FLUIDS, 263
WORKLOADS (PSYCHOPHYSIOLOGY), 329, 334
WORKSTATIONS, 539

## X

X RAY ABSORPTION, 73, 80, 486
X RAY ANALYSIS, 440
X RAY ASTRONOMY, 206
X RAY DIFFRACTION, 35, 81, 98, 265, 290, 378, 461, 462
X RAY FLUORESCENCE, 40, 97
X RAY IMAGERY, 444
X RAY SCATTERING, 35, 109, 148, 416, 455, 487
X RAY SOURCES, 391, 401, 437, 534

X RAY SPECTROMETERS, 204, 438, 478, 512
X RAY SPECTROSCOPY, 60, 206, 478
X RAYS, 177, 447, 475, 510, 532
XENON, 47, 112, 185, 274, 480

## Y

YAG LASERS, 33, 100, 210, 211
YBCO SUPERCONDUCTORS, 467, 468, 472, 477, 482
YTTRIA-STABILIZED ZIRCONIA, 126, 472
YTTRIUM OXIDES, 460, 475

## Z

ZENITH, 405
ZEOLITES, 70, 82, 127
ZERO POWER REACTORS, 65
ZETA PINCH, 376, 391, 398, 444, 448, 451, 452
ZINC OXIDES, 126
ZIRCONIUM, 42, 71
ZIRCONIUM ALLOYS, 98, 113
ZIRCONIUM ISOTOPES, 565
ZIRCONIUM OXIDES, 53, 287, 487

# Personal Author Index


## A

Aase, S. B., 130
Abate, M. L., 370
Abboud, R. G., 54
Abeln, S. P., 370
Abraham, S., 557
Abramo, M. T., 184
Abrefah, J., 52
Abshire, James B., 163
Aceves, A., 195
Aceves, S. M., 91, 215
Acheson, Densel K., 2
Achilli, V., 437
Adamowicz, L., 89
Adams, C., 354
Adams, Curt, 364
Adams, F., 233
Adams, J., 124, 125
Adams, J. W., 124, 125
Adams, P. M., 25, 571
Adams, R. J., 24
Adelman, H. G., 31
Adridge, D. F., 407
Adzic, R., 80
Agarwal, D. A., 171
Ager, J. W., 44, 182
Aguilar-Chang, J., 547
Aharonson, O., 568
Ahmad, I., 425, 533, 566
Ahmed, S., 149, 268
Ahumada, A. J., Jr., 353
Aidala, K., 173, 182
Aires, Claudia Boian, 271
Akasaki, I., 432
Akermark, H., 169
Akins, Elton, 348
Al-Shamali, F. M., 575
Alatas, A., 486
Alber, M., 195
Alderman, J., 207
Aldridge, D. F., 226
Aleksandrov, A. V., 152
Alena, Richard, 356
Alexander, Aaron, 193
Alexander, Dennis R., 541
Alexey, A. S., 394
Alford, O. J., 88
Alivisatos, A. P., 436
Allamandola, Louis J., 563
Allan, B., 354
Allan, B. A., 358
Allan, M. L., 34
Allanach, B., 406
Allen, B. M., 229
Allen, C. K., 397
Allen, C. W., 46, 70, 107, 112, 480
Allen, Christopher S., 410
Allen, D. A., 299
Allen, J. C., 377
Allen, J. S., 195
Allen, T., 110
Allen, T. R., 107, 109
Allerman, A. A., 430, 486
Allgood, G. O., 220
Allison, S. W., 219, 429
Allison, W. W. M., 566
Ally, M. R., 85
Almusaiteer, K., 282
Alner, G. J., 566
Alonso, J. R., 324
Altamimi, Zuheir, 292
Alvarado, J. S., 73
Amano, H., 432
Amine, K., 262
Amro, H., 414
An, F., 270
Anderson, C. M., 589
Anderson, J. D., 575
Anderson, L. W., 486
Anderson, R. C., 569
Anderson, S. E., 196
Andesrson, B., 285
Andreassen, Oyvind, 4
Andreev, A. V., 90
Andreev, Alexander A., 210
Andrews, J. W., 214
Andrews, W. H., 219
Andriulli, J. B., 429
Anerella,, 412
Angel, E., 339
Angermann, Detlef, 292
Anitescu, M., 336
Annavarapu, S., 472
Anovitz, L. M., 187
Antelo, Maria A., 34
Antoniou, N., 184
Appel, J. A., 203, 395
Apseloff, G., 315
Aratow, Michael, 325
Ardavan, A., 461
Arduini, R., 296
Arend, L., 428
Arendt, P. N., 466
Arflin, J., 427
Argus, Don, 292
Argyriou, D. N., 464
Arisholm, Gunnar, 208
Armstrong,, 342
Arnaud, S. B., 324
Arndt, R. A., 393
Arnold, B. W., 225
Arnold, James O., 20
Arnold, N., 511
Arnott, P., 299
Aro, C., 150
Arris, H. W., 172
Arturo, G., 283
Asay, J. R., 224
Aseev, V. N., 514
Asmar, S. W., 575
Asphaug, Erik, 561
Asrat, 152
Assink, R. A., 456
Assoufid, L., 528
Assur,, 555
Atchison, W. L., 263
Attanasio, S. A., 91
Attwood,, 386
Atwater, H. A., 184
Auciello, O. H., 129
Auflick, J. L., 334
Aurand, J., 484
Aurnou, J. M., 575
Austin,, 435
Awes, T. C., 405
Awschalom, D. D., 372
Axelrad, P., 243
Axelrod, M. C., 409
Ayala, A., 461
Ayres, D. S., 566
Azar, Maurice C., 548
Azmy, Y. Y., 422, 427
Azofeifa, S., 283

## B

Babzien, M., 435, 436, 442
Baca, A. G., 178, 179
Bachmann, Felix, 348
Back, B., 415
Back, B. B., 405, 406, 416, 537

Bader, S. D., 487
Baer, H., 533
Baer, L., 318
Baer, Tomas, 72
Bagger,, 496
Baginski, Thomas A., 176
Bai,, 385
Bailey, Daniel V., 363
Bailey, David H., 341, 342, 359
Bailey, R., 233
Baird, R. Scott, 27
Baker, G., 391, 427
Balachandran, U., 46, 113, 129, 459, 470, 481, 484, 487
Balasubramanian, M., 72
Balbekov, V., 535
Baldauff, Regis J., 555
Baldo, P., 129
Baldridge, A., 240
Ballard, R. E., 319, 320, 326
Ballard, S., 138
Ballas, James, 548
Baltay,, 496
Bamford, Douglas J., 86
Banerjee, S., 406
Banks, J. C., 477
Banks, Martin S., 565
Barabash, S., 206, 577, 583
Barbacci, Mario, 345
Barbacci, Mario R., 347
Barber, D. P., 535
Barber, N. L., 235
Barbieri, C., 437, 578
Barbour,, 93, 95
Barbour, J. C., 89
Barbree, Jay, 574
Bardayan, D. W., 562
Barker, A. R., 387
Barker, Ballard M., 1
Barlow, N. G., 569
Barmak,, 455
Barnes, A. V., 477
Barnes, Norman P., 213
Barnes, P. D., 88
Barnett, D. A., 422
Barney, P. S., 482
Barr-Kumarakulasinghe,, 304
Barr-Kumarakulasinghe, S. A., 294, 295
Barraza, J., 215
Barrett, J., 308
Bartel, T. J., 347, 451
Bartle, John, 10
Bartle, John R., 10, 11, 12, 541
Barton, C. A., 245
Basilevsky,, 60
Basol, B., 257
Bass, Henry E., 407
Bass, Len, 350
Bass, Michael, 434
Bassani, J. L., 104
Bassett, Bob, 15
Batchelder, J. C., 456
Batcheller, T. A., 439
Bateman, B. I., 222
Bateman, K. J., 127
Bateman, V. I., 220
Battaile,, 213
Battersby, C., 440
Battersby, C. L., 441
Bauer, G., 497
Bauer, R. C., 199
Bauman, B. J., 430
Baumann, P., 129
Baumgardner, J., 597
Bauschlicher, Charles W., Jr., 58, 76, 98, 399, 412, 414
Bautista, Abigail B., 330
Baylor, L. R., 445
Beale, B., 114
Beasley, C. E., 198
Beasley, M. R., 175
Beatty, John H., 51
Beauchamp, E. K., 130
Beaudoin, A. J., 107
Beaulieu,, 385
Beaulieu, L., 415
Bechtold, M., 316
Beck, D. L., 294
Becker, Andrew, 21
Beckmann,, 416
Beddo, M. E., 405
Belak, J., 111
Bell,, 386
Bell, J., 559
Bell, J. B., 368
Bell, James, III, 557
Bell, K. R., 600
Bell, M., 450
Bell, R., 450
Bell, Thomas L., 292
Bellamy, Al, 9
Bellucci, G., 578
Bellwied, R., 418
Belova, E. V., 390
Beltz, Glenn E., 462
Belz, Mathias, 431
Ben-Zvi,, 435
Ben-Zvi, I., 388, 389, 392, 435, 436, 442
Benaissa, M., 97
Benary, O., 508
Benavides,, 213
Benavides, G. L., 174
Bender,, 79
Bender, James M., 51
Benedek, R., 90, 262
Benedict, Howard, 574
Benedikt, B., 50
Benioff, R., 556
Bennett, C. V., 411
Bennett, G. R., 446
Benoit, R., 245
Benson,, 435
Benson, S., 402
Benton, Bernard J., 316
Bentz, J. H., 159
Benz, Willy, 561
Berg, D. E., 358
Berg, J. S., 499, 513
Berge, P., 236
Berge, P. A., 238
Berger, E. L., 406, 507, 531, 533
Bergey, John, 344, 345, 353
Bergey, John K., 344
Bergstrom, R., 287
Berket, K., 361
Bernstein, Max P., 563
Berry, R. E., 423
Berryman, K. G., 238
Beshears, D. L., 219
Betts, R. R., 405, 406, 416
Betts, W., 391
Beus, S. G., 199
Beutter, B. R., 331
Bhattacharya, Pallab, 210
Bidwell, B., 427
Biedron, S. G., 213, 432, 434, 439, 442
Bierwagen, Gordon P., 15
Bigi,, 494
Billen, J., 403
Billinge, S. J. L., 461
Billone, M. C., 110
Binder, Michael J., 248, 249
Bini, A., 578
Birtcher, R. C., 38, 46, 112
Bishop, J. K., 306
Bishop, James, 329
Bisognano, B., 406
Biswas, R., 357
Bjerke, Todd W., 190
Bjoraker,, 456
Blacic, J. D., 568
Black, P. G., 305
Blackmon, J. C., 562
Blackwelder, C. R., 570
Blackwell, B. F., 96, 103

Blackwell, C., 315
Blaisdell, G. A., 198
Blake, D. R., 285
Blake, David F., 229, 455
Blanchat,, 219
Blanchat, T. K., 235
Blanco, A., 578
Blasi, P., 400
Blaskiewicz, M., 418, 497, 499
Bleck, R., 303
Blencoe, J. G., 187
Blewett, D. T., 576
Blewitt, Geoff, 292
Blok, K., 134
Bloom, A., 286
Bloom, I., 249
Blotter, J., 188
Blount, M. A., 372
Bluem, H., 392
Bluem, H. P., 181
Blum, T., 499
Blumberg, G., 460
Blume,, 386
Blusk, S. R., 381
Boatner, L. A., 85
Bobrov, A. V., 586
Bodek, A., 383
Boden, T. A., 262
Bodoh-Creed, A., 508
Bodt, Barry, 343
Boehnlein, D. J., 272
Bogetti, Travis A., 51
Bohle, David S., 63
Bohler, Jeffrey A., 175
Bohn, C., 402
Boice, M., 260, 261
Boldt, J. D., 204
Bollig, Aliccia B., 310
Bollinger, L. M., 510
Bolton,, 494
Bolton, S. M., 439
Bond, A. H., 74
Bonn, R. H., 244, 252
Bonner, B. P., 236, 238
Bonner, R., 318
Bordallo, H. N., 90
Borden, Brett, 164
Borders, B., 233
Borland, M., 483, 509, 516, 517, 518, 519, 527
Boro, C., 236
Borucki, W. J., 301
Borucki, William, 557, 559
Borup, R. L., 139
Bouanani,, 412
Boucher, Claude, 292
Boudreaux, J. F., 282
Bourke, M., 112
Bousnani,, 201
Bowen, Brent, 10
Bowen, Brent D., 1, 2, 8, 10, 11, 541
Bower,, 252
Bower, W. I., 252
Bowman, Terry S., 543
Boyanovsky, B., 500
Boyle, T. K., 290
Boynton, W. V., 206
Boyse, R., 41
Boyson, W. E., 253
Bradshaw, J. D., 285
Braithwaite,, 95
Branagan,, 92
Brandt, P. C., 577
Branning, J. M., 340
Branum, Lonnie, 6
Brass, James A., 284, 285
Braun, Barry, 312
Braun, James E., 193
Bregman, Jesse, 558
Breit, G. A., 320, 323, 326
Brelsford, D. L., 145
Brendle, Bruce, 364
Brennan,, 530
Brentnall, W. D., 21
Bresina, John, 560
Bretscher, M. M., 419, 424
Breuer, H., 415
Brewster, L. Tom, 328
Brewster, S. B., 20
Bridges, N. T., 290, 569
Brieger, E. F., 226
Brinker, C. J., 178, 456
Brinza, D. E., 572
Brisudova, M., 514
Broadbelt, L. J., 42
Brock,, 164
Brookhart, M., 37
Brooks, C., 166
Brooks, Ian M., 187
Brooks, J. A., 94
Brooks, J. N., 447
Browell, E., 285
Brown,, 131, 331, 355, 385, 542, 545
Brown, C. N., 405
Brown, D. J., 484
Brown, D. L., 355
Brown, F. A., 220, 222
Brown, Gerald E., 30
Brown, H., 140, 255
Brown, M. J., 278
Brown, N. J., 368
Brown, P. N., 502
Brown, Scott M., 71
Brown, T. A., 436
Brown-VanHoozer, S. A., 331, 365
Browne, E., 562
Browning, N. D., 458
Browning, R. Y., 136
Brueckner, J., 579
Bruesselbach, Hans, 209
Brunett, B. A., 185
Brunett, J. O., 235
Brunett, S., 341
Brunschwig, B. S., 417
Bryson, Steve, 341, 350
Buchele, S. F., 339
Bucher, Merideth A., 313
Buchheit,, 213
Buckley, T. M., 326
Budai, J. D., 373, 456, 457, 458
Buell, W. F., 367
Bugbee, Bruce, 319
Bugielski, D., 427
Buhler, C. R., 118
Buhman, Charles, 350
Bullock,, 79
Bunker, B. C., 89
Burakovsky, L., 514
Burbine, T. H., 577
Burchett,, 96
Burchett, S. N., 483
Burke, J. D., 289
Burke, S. K., 100
Burkett, K., 385
Burns, A. W., 235
Busby, J. T., 109, 110
Buscaglia, G. C., 427
Busch, C., 283
Bush, J. D., 405
Buss, R. J., 264
Bustamante, A. C., 4
Butcher,, 21
Byren, Robert W., 209
Byrnes, M. E., 49

## C

Cabibil, H., 49
Cabosky, Steven R., 299
Cadwallader, L. C., 141
Cady, Sherry, 314
Caffrey, M., 340
Cairns,, 51
Calaway, W. F., 254
Calderone, J. J., 235

Cale, M. C., 133
Calle, Carlos I., 118
Callinan, R. J., 18
Camassa, R., 195
Cambie, D., 438
Cambier, Jean-Luc, 31, 443
Campbell, A. N., 184
Campbell, B. A., 571
Campbell, E. W., 430
Campbell, J. A., 32
Campbell, J. H., 447
Campbell, James, 163
Campbell, Jonathan W., 218
Campbell, P. L., 351, 551
Canal, P., 503
Cao, H., 125
Cao, X. A., 175, 467
Cap,, 28
Capelle, G., 313
Caporali, A., 437
Capria, M. T., 437
Carelli,, 555
Carena, M., 403
Carey, R. M., 531
Carin, L., 484
Carlson, R., 394
Carlson, R. L., 372
Carman, L., 459
Carneiro, J. P., 397
Carney, Thomas Q., 1
Carpenter, P. J., 237
Carr,, 490, 492
Carr, B. J., 237
Carr, D. B., 547
Carrado, K., 267
Carrado, K. A., 91
Carroll, Carol W., 23
Carroll, D. E., 103
Carstenson, Larry, 541
Carstenson, Larry G., 1
Carte, M. D., 134
Carter, D. H., 49
Carter, Grace M., 310
Carter, J. D., 149
Carter, Robert W., 218
Carter, T. A., 390
Carwardine, J., 507
Casalnuovo, S. A., 45
Case, Jeff, 342
Cassen, Patrick, 565
Cassidy, T. A., 428
Cassutt, Michael, 601
Castaneda, J. N., 78
Catalano, George D., 188
Cates, M. R., 219, 429
Cavalieri, Donald J., 242, 307
Cavanagh, J., 427
Cederwall, R. T., 286
Celebi,, 21
Celestre, R., 378
Cereda, E., 162
Cerri, A., 398
Cesarano, J., 156
Cha, Y. S., 466
Chaiko, D. J., 45
Chakhovskoi, A. G., 480
Chalk, S., 149
Chan, Helen M., 95
Chan, S. T., 272
Chan, William M., 357
Chandler, E. A., 438
Chandler, G. A., 376, 444
Chandler, T., 161
Chang, B., 502
Chang, J., 405, 406, 416
Chang, P. C., 178, 179
Chang, S., 90
Chang, S. G., 276
Chang, S. L., 38, 66, 146, 147, 427
Chang, Sherwood, 563
Chang, W. C., 405, 406, 416
Chang-Diaz, J. P., 134
Chao, Ben, 292
Chaplygin, O. V., 586
Chapman, John J., 208
Chapman, M. G., 573
Chargin, A. K., 88
Charlock, Thomas P., 296, 599
Charloton, T., 477
Charron, Tammy M., 312
Chase,, 525
Chatfield, Robert B., 284, 285
Chaturvedi,, 60
Chavez, P. F., 417
Cheeseman, Peter, 369
Chemla, D. S., 436
Chen, C. H., 112
Chen, F., 43, 259
Chen, Mingwei, 97
Chen, N., 118
Chen, R. F., 307
Chen, Ray T., 179
Chen, S. P., 476
Chen, X., 391
Chen, Zhijan, 354
Cheng, Doreen Y., 346, 349
Chernobaeva, A. A., 425
Chertok, M., 406
Chesser, J. B., 397
Cheung, Bob, 322
Cheung, Samson H., 199
Chhabildas,, 139, 445
Chhabildas, L. C., 78, 103
Chi, C. Y., 405, 406, 416
Chiarizia, R., 68
Chien, H. T., 37
Chinn, D., 220
Chiodini, G., 203
Chisholm, M. F., 456, 458
Chitwood, L. D., 107
Chiueh,, 355
Cho, D. H., 71
Cho, Y., 522
Choi, S. U. S., 180
Chojnacki, E., 535
Choo, Teck H., 26
Chopra, O. K., 95, 101, 110
Choquette, K. D., 430, 486
Chou, Ming-Dah, 292
Chow, C. L., 93
Chow, W. W., 432
Christini, R. A., 244
Christman, J. A., 483
Chu, D. A., 239
Chu, S., 306
Chu, Y., 487
Chuang, S. S. C., 282
Chubb, Gerald P., 1
Chudakov, E. A., 384
Chudzik, M. P., 468
Chung, H. M., 47, 100, 102, 110
Chung, J. S., 457
Cialella, A. T., 297
Ciborowski, Steven, 115
Ciszek, T., 184
Citterio,, 525
Clark, B. F., 36
Clark, G. A., 409
Clark, Joseph F., III, 328
Clark, R. M., 372
Clarksean, R., 73
Clauss, S. A., 32
Clauss, T. W., 32
Clay, R., 354
Clay, R. L., 358
Clayton, N., 467
Claytor, T. N., 449
Clem,, 471
Clements, J. W., 185
Clements, Paul, 348
Clifft, B. E., 534
Cloer,, 7
Cloutis, E. A., 577
Clucas, Jean, 197
Co, Elizabeth L., 330

Coadou, Y., 491
Coates, A. J., 579
Cobb, J. H., 566
Coburn, T., 264
Cochran, W., 559
Cohen, R. H., 196
Cohen, Sholom, 349
Colangeli, L., 437, 578
Cole,, 174
Cole, E. I., 185
Cole, J. I., 99
Cole, M., 392
Cole, Paul, 15
Cole-Rhodes, Arlene, 203
Colella, P., 337, 339
Coleman, G. N., 198
Coletta, C., 162
Colgan, Sean W.J., 561
Collier, H. A., 230
Collins, Charlene L., 58
Collins, M., 40
Collins, Paul, 15
Collot,, 495
Colvin, J. D., 438
Combs, S. K., 445
Comella-Dorda, Santiago, 350
Comerford, N. B., 233
Conde, M. E., 451, 522, 529, 534, 535
Conner, C., 46
Connolly,, 530
Connolly, R., 388
Convery, M. E., 382
Conway, B., 115
Conway, J. S., 403
Cook,, 131
Cook, A. C., 243, 578, 596
Cook, B. K., 194
Cooper, B., 579
Cooper, D. M., 341
Cooper, G. E., 399
Cooper, G. W., 446
Cooper, Gene R., 377
Cooper, John F., 599
Corcoran, M., 317
Corley, J. P., 452
Cornacchia,, 490
Cossairt, J. D., 272, 375
Coulter, R. L., 298, 299, 300
Coutts, T. J., 247, 477
Covington, M. Alan, 20
Cowgill,, 200
Cowgill, M., 124, 125
Cowings, P. S., 321, 326
Cowings, P.S., 327
Cox, Charles, 303
Cox, David E., 362
Cozzolino,, 412
Crabtree, G. W., 479
Craddock, R. A., 571
Craddock, Robert A., 570
Craig, K., 142, 255
Craighead, Harold G., 312
Crawford, D., 266
Crawford, J., 285
Cremonese, C., 586
Cremonese, G., 437, 578
Crew,, 455
Crisalle, O. D., 84
Crooker, S. A., 372
Cross, Charles, 5
Crossno, P., 339
Croweley, Barbara K., 188
Crowell, R. A., 530
Crowley, B., 166
Crown, D. A., 573
Cuenca, R. M., 264
Cugini, A. V., 46
Cullan, Tracey M., 10
Cullers, D., 559
Cumbest, R. J., 228
Cummings, P. T., 44
Cuneo, M. E., 512
Cunningham, D. W., 266
Cunningham, G. S., 337
Curtis, B. C., 196
Curtis, Bill, 544
Curtiss, L. A., 66, 82
Curto, Paul A., 30
Curtright, T., 485
Cushing, Michael, 369
Cushman, R. M., 262

## D

D, 312
DaCosta, Stacey, 309
Daglis, I. A., 206
Dai, Z., 57
Daily, L. D., 502
Dalal, V. K., 400
Dallman, M. F., 325
Dalton, B., 308
Dang, G., 175, 467
Daniel, R. B., 234
Daniels, E. J., 53
Danilov, Oleg B., 210
Dannevik, W. P., 196
Danuskhkodi, Vaiyapuri, 354
Darlington, E. H., 204
Darrow, D. S., 402
Das, R., 198
Dateo, Christopher E., 415
Datta, S. K., 408
Dattoli, G., 213
Daulton, T. L., 106, 111
Daum,, 245
Daunton, N. G., 317
David, Philip, 343
David-Bajar, Kathleen, 311
Davidson, John R., 6
Davidson, S. J., 401
Davie, N. T., 235
Davis, D. A., 260
Davis, D. D., 285
Davis, R. E., 306
Davis, S. C., 268
Dawley,, 471
Day, M. S., 368
Daymond, M., 112
de Almeida, V. F., 187
de Forcrand, P., 479
De Geronimo, G., 181
De Witt, M. J., 42
De Yoreo, J., 469
Dean,, 7
DeAngelis, E., 206
DeArellano-Lopez, A. R., 96
Deason, V. A., 408
Debarber, Peter A., 67
DeCarlo, F., 176, 534
DeCaro,, 555
Decker, G. A., 505
Deemer, C., 53, 111, 114, 128
Deemer, C. M., 222
Dees, D. W., 267
Deffeyes, Joan E., 15
Degrassi,, 363
Deichert, Jerome, 10
Deichert, Jerome A., 11, 541
Deiwert, G. S., 194
Deiwert, George S., 20
Dejus, R. J., 433
Dekin, W. D., 88
Del Cul, G. D., 73
DeLay, Thomas K., 54
Delayen, J. R., 488
DelCastillo, Carlos, 431
Delcourt, D., 206
DellaCorte, V., 578
DeLong,, 530
Demarteau, M., 503
Deming, R., 185
Demko, J. A., 163
DeMuth, D. M., 566

Den Hartog, P. K., 440
Denard, J. C., 402
DenBaars, S. P., 461
Dendy, J. E., 338
Deng,, 174
Denham, M. E., 228
Denison, G. J., 484
Dennis, Henry J., Jr., 32
Dereniak, E. L., 378
Derniak, Eustace L., 63
Derrick, M., 535
Derzon, M. S., 444
Descour, M. R., 378
DesMarais, David J., 308, 314
Despe, O., 173
Deutsch, P. W., 66
Devaney, A. J., 185
Devlin, T., 395
DeVries, J., 491
Diamauro,, 435
Diaz, M. A., 406
Dibble, R., 215
Dickey, E. C., 457
Dickey, F. M., 177
Dickson, R., 402, 440
Dietz, M. L., 64
DiLellis, A. M., 206
Dimasi, E., 98
DiMauro, L. F., 442
Dimits, A. M., 196
Ding, C., 552
Ding, C. H. Q., 226
Ding, R. Jeffrey, 218
Dingfelder, M., 83
Dinus, R. J., 233
DiSanto, T., 127
DiStefano, J. R., 103, 107
Diwan, M. V., 387
Dlott, Dana D., 69
Doctor, R. D., 141, 145
Dodd,, 179
Dodge, Hank, 348
Doebling, S. W., 224
Dohm, J. M., 569
Dolan, Kathy V., 549, 550
Dolin, R. M., 221
Doll, W. E., 237
Dombard, Andrew J., 581
Donaldson, K. L., 594
Donato,, 305
Dong, J., 468
Donnelly, S. E., 46
Donohue, J. T., 434
Dooley, J. J., 134
Dooling, J. C., 511
Doolittle, L., 388, 389
Dorin, R. T., 354
Dorman, Clive E., 187
Dorris, S. E., 46
Dorsch,, 245
Dorsett, Helen E., 36
Dortwegt, R., 510
Dosluoglu, Taner, 172
Doss, E. D., 137
Doty, K. J., 295
Doty, L., 23
Dougherty, Lamar F., 29
Doughty, D. H., 265
Douryan, A., 442
Dowd,, 440
Dowding, K. J., 96, 103
Downing, J., 394
Doyle,, 201
Doyle, B. L., 477
Dragoi, D., 50
Dragt, A. J., 508, 514
Drees,, 530
Dreesen, D. S., 568
Drellack, S. L., 229
Dress, W. B., 335
Drewes, Hermann, 292
Drewien, C. A., 351
Drummond, Mark, 560
Dua, S. K., 282
Dubinovsky, Michael, 179
Duda, A., 247
Duffy, Colleen, 348
Duncan, Michael A., 211
Dunford,, 416
Dunford, R. W., 414, 533
Dungan, Jennifer L., 273
Dunham, E., 559
Dunkin, S. K., 204, 438
Dunn, F. E., 423
Dunn, W., 23
Durfee, D. J., 217
dUston, C., 579
Duvel, Jean Philippe, 239
Dyall, Kenneth G., 58
Dylla,, 435

## E

Eamus, Derek, 274
Eanes, Richards, 292
Earl, D. D., 429
Earle, W., 531
Easler, T. E., 114
East, E. W., 353
Easterling, R. G., 103
Eastman, J. A., 263
Eastman, Roger, 203
Eatough, C. N., 144
Ebadian, M. A., 198, 282
Eberhardt, J. J., 154
Ebert, W. L., 45, 128
Eckert, J., 64, 65
Economou, D., 451
Edger, Wolfgang, 313
Edmonds, R., 229
Edwards, J. G., 278
Edwards, R. S., 461
Efstathiadis, E., 531
Eglinton, T. I., 307
Ehgartner,, 228
Ehgartner, B. L., 138
Eiffert, P., 245
Ein-Eli, Y., 258
Eisgruber, I., 260
Ekblad, U., 170
Elcock, D., 34, 35
Eller, P., 84
Elling, J., 146
Ellingson, W. A., 51, 111, 122, 128, 222, 339
Elliott, S., 306
Ellison, Robert, 347
Elmroth, E., 226
Elsayed-Ali, H. E., 475
Emert, ScottE., 201
Emery, K., 246
Emery, L., 517, 518, 530
Emma,, 490
Emma, P., 433
Emory, S., 37
Engelhardt, G. R., 47
Engwall, D., 402
Ensz,, 213
Epifani, E. Mazzotta, 578
Erard, S., 204
Erck, R. A., 129
Erdmann, M., 440
Erickson, E. F., 558
Erickson, Edwin F., 561
Ericson, Mark A., 163
Eriksson, J., 221
Eror, N. G., 484
Ertl, A. C., 324
Esbensen, H., 533
Esh, D. W., 86, 127
Eslinger, S., 24
Espinoza, J., 351
Espy, M. A., 461
Estill, J., 62
Evans, J., 324, 325

Evans, N. D., 290
Evans, R. P., 188
Eveleigh, D. E., 77
EvtukhmAAKlyui, N. I., 480
Eyssa,, 488
Eyssa, Y. M., 372

## F

Fabris, G., 195
Faeth, G. M., 55, 56, 57, 58, 61
Failor, B. H., 438
Fainman, Y., 365
Falco, Charles M., 176
Fan, F., 178
Fan, H., 456
Fang,, 213
Fang, H. E., 93
Fanjoy, Richard O., 328
Farag, Aly A., 361
Farhar, B., 264
Farmer, J., 62, 240
Farmer, M. T., 87
Farr, Tom G., 240
Farrington, R., 159
Fauconneau, Guy, 371
Fawley, W. M., 213
Fax, X., 457
Fehler, M., 391
Feibelman,, 380
Feier, I., 520
Feissel, Martine, 292
Feit, M. D., 441
Feldman, J. E., 572
Feldman, L. C., 184
Feldman, W. C., 579
Felice, G. M., 447
Felix,, 173
Fellhauer, C. R., 421
Felter, T. E., 480
Feltes, Carolyn, 310
Feng, W., 167
Ferber, M. K., 21
Ferland, Remi, 292
Fernow,, 386, 491
Feron, Eric, 14
Ferris, David L., 25
Ferry, G. V., 299
Ficker, C., 139
Fields, T. H., 566
Fiksel, G., 390
Finch, J. L., 222
Finck, P., 420
Fineberg, Sam, 360
Fini, P., 461
Fink, Mary M., 2
Finkelman, R. B., 143
Finley,, 230
Finley, V., 444
Finn, Cory K., 332
Finn, John E., 333
Firestone, R. B., 562
Fisch, N. J., 180, 181, 448
Fischer,, 385, 491, 492
Fischer, A. J., 430
Fischer, J. E., 258
Fischer, T., 200
Fish, J. S., 91
Fisher, B. L., 113
Fisher, E. P., 46
Fisher, L. M., 166
Fisher, P. W., 445
Fisk, L. A., 585, 597
Fitzgerald, M., 276
Fjeldly,, 174
Flach, G. P., 231
Flatte, Michael E., 462
Fleetwood,, 173
Fleetwood, D. M., 184, 529
Fleming, S. W., 155
Flemming, J. H., 39
Flood, Roger D., 407
Flouris, Triant G., 329, 540
Flowers, D., 215
Flynn, Mark E., 332
Flynn, Michael T., 71
Fockler, J., 394
Foerster,, 532
Fogelman, R. P., 235
Fogelson, A., 337
Foltyn, S. R., 466, 467
Fonti, S., 578
Forbes, Jeffrey M., 556
Ford, C., 559
Fore, L. B., 199
Forlani, G., 437
Formaggio,, 494
Forman, L., 474
Forman, William R., 560
Fornasier, S., 437
Forster, R. A., 421
Forsyth, T., 259
Forsythe, R. D., 570
Fortner, J. A., 42
Fossum,, 96
Foster, C. A., 445
Foster, I., 534
Foster, T. C., 299
Fotiades, N., 481
Foust, C. R., 445
Fox, R. A., 317
Frahm, R. A., 579
Frainier, Richard J., 154
Frank, J., 387
Frank, M. V., 23
Frank, S. M., 86
Fraser, J. A., 80
Frederick, W. J., 43, 259
Freeman, J., 180
Freeman, W. S., 403
Frehlich, Rod G., 207
Freitag,, 60
Frenklach, M., 368
Freund, Friedemann, 293, 567
Freund, H. P., 213, 432, 439
Freund, Minoru, 567
Fricke, A. K., 84
Fridrich, C. J., 227
Fried, L. E., 147
Friedman, L., 572
Friedsam, H., 521, 535
Friessnegg, T., 177
Frigo, A. A., 199
Frigola, P., 388, 435
Fruchtman, A., 180, 181
Fry,, 245
Frye-Mason, G. C., 39, 45
Fthenakis,, 245
Fuerstenau, S. D., 572
Fujita, A., 273
Fujita, E., 56, 135
Fukuda, T., 419
Fukui,, 386, 491
Fuland,, 490
Fulco, Charles S., 312
Fulkerson, E. S., 183
Fuller, E., 340
Fuller, M., 431
Fultonberg, D. N., 393
Fung, Bing M., 120
Fung, P., 318, 324
Furuya, K., 46, 112, 184

## G

Gabriel, T. A., 397
Gaffney, J. S., 281
Gai, W., 485, 523, 534, 535
Gailey, P. C., 370
Gaines, L., 86, 137
Gaines, L. L., 264
Galambos, P. C., 174
Galbreath, C. J., 256

Galea, S. C., 18, 100
Gallardo,, 386, 491
Gallis, M. A., 347, 460
Gallmeier, F. X., 397, 532
Galloway, B. J., 1
Gander, Philippa H., 330
Gandy, R., 453
Ganetis,, 412
Ganter,, 7
Garcia, A. W., 305
Garcia, E. J., 433
Garcia, John P., 63
Gardelle, J., 434
Garlan, David, 348
Garrett, Henry B., 599
Garrison, James L., 14
Gasnault, O., 579
Gates, Stephen S., 27
Gatski, T. B., 187
Gattoni, W. C., 393
Gauglitz, P. A., 75
Gauld, I. C., 426
Gaver, Donald P., 369
Gazda, J., 101
Gee, J., 184
Geenen, Robert, 22
Geer, S., 535
Geesaman, D. F., 405
Gehr, R. J., 442
Gehrels, Neil, 599
Geib, K. M., 430, 486
Geiser, U., 467, 484
Geller, A. S., 463
Gelles, D. S., 101
Gellman, Robert M., 549
Gemmell, D. S., 533
Genin, F. Y., 441
Gentile, C. A., 445
George,, 230
George, M. A., 457
Gerald, R., 91
Gerald, R. E., 67
Gerken, E. S., 448
Gherardi, L., 162
Ghosh,, 412, 490
Ghoshal, Anindya, 363
Gianoulakis, S. E., 158
Giardini, D., 26
Gibbs,, 386
Gibson, B. F., 392
Gidaspow, D., 151
Gierman, S. M., 203
Gill,, 219
Gill, W., 96, 103
Gille, J., 428
Gillies, D. C., 235
Gillis, J. J., 580
Gilpatrick, J. D., 519
Ginn, J. W., 244
Ginsberg, I. W., 336
Girten, B., 308, 315
Girvan, R., 400
Girven, M. L., 556
Giumarra, J., 129
Giver, Lorraine J., 316
Gjerleov, J. W., 291
Glasgow, D. C., 532
Glass, R. S., 259
Gleason, S. S., 469
Glissmeyer, J. A., 282
Gloeckler, G., 585, 597
Glosi, J. N., 121
Gloster, Clay S., 352
Gluckstern, R. L., 514
Gluskin, E., 433, 516
Goethert, Wolfhart B., 344
Goff, F., 270
Goff, K. M., 86, 127
Goforth, J. H., 263
Gog,, 455
Gogos, George, 10, 541
Goguen, Joseph, 346
Golchert, B., 427
Golchert, B. M., 196
Gold, D. M., 438
Gold, R. E., 206
Gold, Robert E., 30, 593
Goldberg, A., 200
Goldberg, Allan, 248
Goldman, J. T., 514
Goldsmith, S. Y., 168
Goldsten, J. O., 206
Gollsneider, Brian, 348
Gomes, I. C., 65
Gomez, L. S., 304
Gomory, F., 162
Gonzales, A. A., 314
Gonzalez, S., 244
Goodman, Allen D., 330
Goodman, M. C., 405
Goodwin, Warren E., 19
Goorjian, Peter M., 349
Gordeev, A., 387
Gordon, S., 62
Goremychkin, E. A., 473
Goretta, K. C., 113, 123
Gorski, A., 535
Gosselink, Kristin L., 327
Gouard, P., 434
Gouge, M. J., 163
Goyette, A. N., 486
Graham, R. L., 231
Graham, W. J., 46
Grams, G. W., 302
Granados, A., 559
Grande, M., 204, 438
Grandhi, Ramana V., 190
Grann, E. B., 219
Grant, J. A., 571, 574
Grard, R., 26, 183, 580
Graves,, 435
Gray, P. C., 36
Grcar, J. F., 368
Grebogi, C., 396
Green,, 245, 488
Green, Mavis F., 1, 329
Green, Michael J., 4
Greene, G. A., 94, 375
Greene, J. P., 528, 529, 566
Gregorich, K. E., 456
Gregory, G. L., 285
Gregory, Kevin B., 330
Gregory, R. B., 116
Grelick, A. E., 512
Grey, M. P., 204
Griffin, T. P., 76
Grimes, R., 84
Grimsditch, M., 464
Grindeland, Richard E., 327
Groleau, Nicolas, 154
Groom, K. N., 156
Groop, E. E., 118
Gropp, W., 406
Gross, Steven, 115
Grossman, R. F., 280
Grozis, C., 403
Grubisic, V., 294
Gruen, D. M., 460, 486, 488
Grymes, Rosalind A., 323
Guan, J., 119
Guber, K. H., 419
Guerin, M. R., 80
Guild, Liane, 285
Guild, Liane S., 284
Gunsel, S., 217
Guo,, 412
Gupta, A., 54, 224
Gurevich,, 132
Gurevich, Serguei A., 211
Gushue,, 385
Gushue, S., 415
Gustafsson, K. K., 86
Guthrie, G., 270
Gyulassy, M., 384

## H


Haas, Michael R., 561
Haber, H. E., 403
Habib, S., 476
Hablanian, David A., 7
Hackert, C. L., 230
Hackwell, J. A., 571
Hadley, G. R., 430
Haeffelin, Martial, 239, 599
Haeffelin, Martial P. A., 240
Hafez, Ismail, 312
Haggerty, R., 155
Hahm, T. S., 448
Hahn, H., 418
Hahn, H. T., 52
Hahn, U., 440
Haines, J. R., 397, 429
Haining, J., 126
Halani, A., 257
Haldar, P., 484
Hale, G. M., 562
Hall, C. A., 224
Hallett, J., 299
Hamill, P., 287
Hammond, J., 183
Hampton, J. W., 547
Hamza, A. V., 477
Han, K., 400
Hanamean, James R., Jr., 297
Hanan, N. A., 424, 449
Hanbey, Glenn T., 24
Handley, Lawrence R., 312
Hanebutte, U. R., 502
Hannum, D. W., 147
Hanrahan, R. J., 78
Hansen, A. C., 260
Hansen, Frederick, 11
Hanson, A., 60
Hanson, Robin, 369
Hapke, B., 580
Happ, George, 552
Harbell, John, 319
Harben, P. E., 105
Harcke, L. J., 581
Hardy, E., 236
Hare, M. F., 531
Hargens, A. R., 319, 320, 326
Hargens, Alan R., 325
Harjes, H. C., 183
Harker, David, 558
Harmer, Martin P., 95
Harmon, J. K., 581
Haroldsen, David J., 3
Harper, J. S., 324
Harper, R. W., 442
Harris,, 494
Harris, B. W., 403, 531, 533
Harris, C. L., 219
Harris, N. C., 113
Harris, Robert S., Jr., 6
Harrison, N., 467
Harrison, W. B., 232
Hart,, 33
Hartman, J. H., 294
Hartmann, T., 476
Hartouni, E. P., 88
Hartshorn, D. C., 229
Harvey, J. A., 419
Harvey, R. P., 289
Hasebe, N., 579
Hassanein, A., 52, 446, 449, 450, 535
Hastings,, 489
Hatalis, Miliadis K., 177
Hatton, T. A., 45
Hauck, Steven A., II, 581
Hauer, A., 438
Hawke, B. R., 576, 591
Hawkins, S. E., III, 204
Haworth, Loran, 17
Hawthorne, S. B., 32
Hayahsi,, 79
Hayashi, Y., 125
Hayes, John M., 313
Hayter, S. J., 155
Hazeltine, R. D., 453
He, G. P., 156
Head, J. W., 587
Head, James W., 582
Head, Larry, 21
Headrick, R. L., 109
Heavey, Karen R., 189
Hebner, G. A., 264
Hebron, D. E., 376
Hecht, Heiko, 397, 565
Hecht, M. H., 572
Heese,, 435
Hefley, William E., 544
Heineck, James T., 3
Heino, M., 443
Heiser,, 33
Heitzenroeder, P. J., 449
Helgeland, Anders, 4
Helgeson, W. D., 484
Helgeson, W. E., 175
Heller, E. J., 45
Hembree, C. E., 184
Hemez, F. M., 224
Hemker, Kevin J., 97
Hendrick, R., 233
Hendron, B., 159
Henfling,, 250
Henley, R. J., 43
Henline, Bill, 189
Henline, William D., 3
Henriksen, G. L., 256, 267
Henshaw, W. D., 355
Hensley, D. K., 33
Henson, T. D., 482
Hereth, L. G., 545
Herndon, Marcia, 15
Herr, K. C., 571
Herring, J. S., 141
Herzog, J. P., 28
Heuer, J., 111
Hickman, S. H., 245
Hietala, V. M., 45
Higgins,, 331
Higuera, F., 189
Hilbrandt, N., 96
Hill,, 386, 455
Hill, D. J., 87
Hill, N. W., 419
Hillis, David, 343
Himmel, B., 461
Hinchliffe, I., 491
Hinks, D. G., 486
Hinrichs, Kai-Uwe, 313
Hinton, David W., 10, 11
Hipp, J. R., 553
Hirschfeld, D. A., 156
Hiskey, M. A., 81
Hissam, D. Andy, 32
Hitchcock, R. J., 546
Hively, L. M., 370
Hjalmarson,, 174
Hjelm, R. P., 437
Hlava, P. F., 66
Hlavka, Christine, 285
Hlavka, Christine A., 284
Ho, C. H., 515, 523
Ho, G. C., 206
Ho, Jim, 274
Hobbs, J. D., 403
Hobbs, J. L., 191
Hobbs, M. L., 130
Hoblit, S., 422
Hochhaus, Larry, 323
Hodges, J. P., 129, 426, 487
Hoffmann, G. W., 391
Hoffmann, H., 205
Hogan, S. J., 266
Hogden, J. E., 338
Hogue, M. D., 118
Hoisie, A., 338

Holben, B. N., 239
Holcomb, Franklin H., 248, 249
Holding, M., 166
Holdridge, D. J., 235
Holesinger, T. G., 461, 467
Holin, I. V., 582
Holland, O. W., 116
Holm, D. D., 195
Holmes, Bruce J., 10, 11, 13, 14
Holmstroem, M., 583
Holroyd,, 411
Holsclaw, Gregory M., 205
Holswade, S. C., 177
Holtkamp, N., 535
Hoo, G., 166
Hood, Robert, 346
Hook, Jack A., Jr., 164
Hook, L. A., 262
Hooper, C. F., 450
Hope, Janet M., 314
Hopkins, Mark F., 63
Hoppel, Christopher, 51
Horsley, C. J., 325
Horwitz, E. P., 47
Hosking, F. M., 158, 262
Hosotani,, 456
Hostetler, D. D., 548
Hou, Arthur Y., 292
Hou, H. Q., 486
Houck, T. L., 382
Houston, S. H., 305
Hovland, P., 343
Howard, Alan D., 570
Howard, David E., 207
Howard, S. D., 299
Howard, W. M., 147
Howells, M., 438
Hoyer, E., 491
Hrbek,, 60
Hryn, J. N., 106
Hsi, W. C., 415
Hsieh, B. J., 216
Hsieh, G., 43, 259
Hsu, S. C., 390
Huang, H. P., 276
Huang, L., 391
Huang, Z., 213, 432, 539
Huber, Robert, 313
Huckaby, J. L., 75
Hudson, J., 299
Hudson, Thomas H., 19
Huestis, G. M., 439
Huff, D. D., 231
Hughes, P. J., 217
Hughes, T. P., 372
Hughey, R. L., 163
Hulbert, Greg, 342
Hulet, M., 23
Hull, Andrew J., 367
Hull, J. R., 54, 464, 465
Hummel, J. R., 355
Humphries,, 219
Hund,, 253
Hunt, J. E., 87
Hunten, D. M., 583
Husbands, P., 552
Hutcheson, Ralph L., 213
Huy, Pisey, 345
Hwang, R. N., 421
Hynek, B. M., 571

## I

Iannucci, J., 250
Ibsen, K., 142
Ice, G. E., 457
Icenhour, A. S., 73
Icenhower, J. P., 120
Ichoku, C., 239
Iglesias, C. A., 401
Ikeuchi, Katsushi, 365
Ila, D., 33, 457
Ilias, S., 84
Ilinski, P., 511
Ilton, E. S., 237
Imlay, James, 348
Inbody, M. A., 139
Ingersoll, D., 265
Inokuti, M., 88
Insley, J., 534
Intrator, T., 167
Irwin, R. P., III, 571
Irwin, Rossman P., 570
Ivanoff, Alvaro, 242, 307
Ivanov, B. A., 588, 595
Ivanov, M. A., 520
Ivansson, S., 410
Ivers, James, 348
Iwashita,, 490

## J

Jacobs, Patricia A., 369
Jacobson, Kathy, 15
Jahnke, Linda L., 291, 313
Jakeway, L., 145, 260, 268
James, Kevin, 22
James, Richard, 118
Janesick, James R., 172
Janhunen, Pekka, 583
Janney, M. A., 172
Jansen, A. N., 112, 256
Jansen, Wayne, 549, 550
Jardin, S. C., 390
Jaumann, R., 205
Javorsek, Daniel, II, 412
Jean-Prost, F., 104
Jen, E., 198
Jen, Julia S., 26
Jendrowski, P., 301
Jendrzejczyk, J. A., 215
Jenior, M. M., 155
Jenkins, James, 333
Jennings, R., 440
Jenniskens, Peter, 229
Jensen, M. P., 64
Jensen, R. T., 423
Jerde, E. A., 532
Jespersen, Dennis C., 197
Jezequel, Fabienne, 368
Ji, H., 390
Jiang, W., 85
Jin, O., 39
Jirsak,, 60
Job, P. K., 207
Jodalen, Vivianne, 289
Jody, B. J., 53, 276
Joensson, C., 169
Johannes, J. E., 451
Johlander, B., 183
Johnson,, 435
Johnson, C. E., 119
Johnson, C. R., 337
Johnson, C. S., 263, 269
Johnson, D. L., 452
Johnson, D. R., 217
Johnson, E., 388
Johnson, J., 391
Johnson, J. O., 532
Johnson, Julie M., 330
Johnson, Kisha, 203
Johnson, L. R., 373
Johnson, R., 114
Johnson, R. W., 262
Johnson, Robert E., 599
Johnson, S., 161
Johnson, S. G., 86, 119, 127
Johnson, T. M., 237
Johnson, W. C., 106
Johnson, W. L., 113
Johnsrud, Steiner, 162
Johnston, James C., 323
Johnston, W., 166
Johnston, W. E., 166, 356

Jonah, C. D., 515
Jones,, 305
Jones, J. L., 216
Jones, S., 313
Jones, S. B., 262
Jorda, L., 586
Jordan, K., 402
Jorgensen, J. D., 129, 465, 487
Joslyn, C., 546
Judd, D. J., 396
Judkoff, R., 155
Jurgens, R. F., 575, 581, 592
Justtanont, K., 564

## K

Kabin, K., 597
Kad, B. K., 105
Kahaian, A. J., 269
Kailath, Thomas, 200
Kaiser, D. P., 262
Kaiser, Mary K., 333, 397, 565
Kakudate, Y., 454
Kakurai,, 373
Kalb,, 115
Kalb, P. D., 124, 125
Kalia, Rajiv K., 54
Kallio, E., 206
Kallio, Esa, 583
Kamath,, 21
Kamowski, T. P., 469
Kanade, Takeo, 365
Kandasamy,, 184
Kandra, J. T., 114
Kane, W. R., 474
Kang, M., 52
Kang, Y., 522
Kanki, Barbara G., 168
Kanske, Craig A., 328
Kanter, E. P., 533
Kao,, 79, 455
Kao, W. H., 25
Kapat, J. S., 193
Kaps, Robert W., 23, 543
Karasalo, I., 410
Kardian, C. J., Jr., 204
Karlsen, T. M., 47
Karlsson, C., 213
Karlsson, O., 565
Karna, S. P., 529
Karp, Merrill R., 1, 329, 540
Karsh, Robert, 548
Karthikeyan, Annamalai, 116, 121
Kasha, M., 49
Kashiwagi, S., 388
Kassab, A. J., 193
Kassner, T. F., 110
Kato, Seiji, 599
Katz, Joseph, 190
Katzberg, S. J., 243
Kaufman, Y. J., 239
Kaufmann, M. R., 231
Kaufmann, R. D., 237
Kaun, T. D., 252
Kaushal, S., 400
Kavicky, J. A., 137
Kawai, Yasuaki, 325
Kawamoto, K., 296
Kaydanov, V. I., 477
Kaye, R. A., 534
Kazimi, R., 402
Kazman, Rick, 345
Keating, Christine D., 68
Keavneu, D. J., 487
Keavney, David J., 176
Kedzie, M., 488, 534
Keefe, Tony, 311
Keegan, P., 556
Keelen, L., 251
Kehne, D., 402
Keil, L., 324
Keil, L. C., 325
Keim, E. R., 571
Keiser, J. R., 21
Keller, J. G., 188
Keller, Richard M., 273
Kellett, B. J., 204, 438
Kelley, N. D., 247
Kelley, T. M., 466
Kelly, D. S., 301
Kelly, Jana, 353
Kelly, L., 572
Kempf,, 554
Kendall, R. A., 553
Kenik, E. A., 109, 110
Kennerly, S., 200
Kenny,, 488
Kephart, R., 403
Kepler, K. D., 257, 269
Kereszturi, A., 290, 584
Kern, E. C., 257
Kern, G., 244
Kesick, Christina M., 322
Kesier, J., 138
Kesselman, C., 534
Kesselman, M., 388, 389
Ketcham, M. S., 155
Kettell,, 389, 495
Kettell, A., 420
Kettell, S., 387
Kettell, S. H., 387, 392
Keune, W., 487
Kewisch, J., 501
Keyfitz, B. L., 396
Khachaturyan, A. G., 83
Kharzeev,, 495, 496
Khoo, T. L., 504
Kihara,, 490
Kikkawa, J. M., 372
Killen, R., 206
Killen, R. M., 579, 584, 589, 590
Kim,, 455, 490
Kim, J. T., 474
Kim, K. J., 432, 508, 515, 524, 537, 539
Kim, M., 373, 458
Kim, S. H., 483, 505
Kim, Y., 454
Kimberly, H. R., 366
Kimmons, J., 440
Kincaid, B. M., 491
King,, 202, 385, 493, 526
King, B. J., 497, 513, 560
King, D. L., 253, 262
King, F. G., 84
King, K., 62
King, Lyndell S., 4
King, R. P., 142
King, W. D., 55
Kingon, A. I., 483
Kinne, S. A., 275
Kirby, Jeffrey G., 353
Kiris, Cetin, 192
Kirk,, 495
Kirk, M. A., 111
Kirkendall, B. A., 105
Kirkland, L. E., 571
Kirtley, J. A., 478
Kiss, G., 245
Kittel, P., 157
Kivioja, L. A., 520
Kladitis, Paul E., 215
Klann, R. T., 426
Klasen, M., 404, 504
Klazura, G. E., 301
Klemm, R. A., 481
Klibanov, Michael V., 167
Klinge, D., 183
Klinger, G. S., 32, 52
Kluger, Jeffrey, 25
Kmeoka, Jun, 312
Knapik, J. F., 556
Knapp, G. S., 509
Knezovich, J. P., 436
Kniel, C., 542

Knorovsky, G. A., 209
Knudson, M. D., 78, 224
Knupp,, 335
Ko, K., 476
Kober, E. M., 126
Koch, D., 559
Koch, David, 557
Kochemasov, G. G., 572
Koehl, E. R., 128
Koehler, P. E., 419
Koehn, P. L., 585, 597
Kogut, J. B., 481
Kolachina, S., 185
Kolesnikov, A. I., 41
Kolka, Margaret A., 322
Kolker, A., 143
Kolner, B. H., 411
Kolomiets, A. A., 514
Komjathy, A., 243
Komjathy, Attila, 14
Konecny, R., 485, 534, 535
Konrad,, 139
Kopasz, J. P., 149
Korambath, P. P., 529
Korneev, V., 373
Korolev, Y. N., 425
Korphage, M. L., 362
Korzekwa, D. A., 104
Koshelev, I., 97
Kottenstette, R. J., 39, 45
Kouatchou, Jules, 368
Kovchegov,, 489
Koviak, Thomas A., 316
Kozlowski, M., 441
Kozlowski, M. R., 440, 441
Krabach, Timothy N., 432
Krabill, W. B., 305
Krafft, G., 402, 406
Krafft, G. A., 442
Krajewski, R. F., 246
Kramer,, 92
Kramer, S., 475
Krane, Dale, 10
Krantz, Eugene F., 601
Krasnitz,, 513
Krasnitz, A., 508
Kratochvil,, 202
Kratochvil, J. A., 262
Kraus, R. H., 461
Krauss, A. R., 488
Kravitz, S., 486
Kremenetsky, Mark D., 195
Krishna, C. R., 272
Krishnamurthy, R., 282
Kristl, Joseph A., 19
Kronfeld, A. S., 390
Kropf, A. J., 80, 130
Kroposki,, 252
Kroposki, B., 252
Krueger, S. K., 302
Kruer, W., 442
Krumpelt, M., 149, 254, 268
Krystynak, John, 353
Ksanfomality, L., 586
Ksanfomality, L. V., 585
Kudzinocaky, S. Y., 480
Kuehn, D. D., 294
Kuhlma, K. R., 572
Kuhlman, K. R., 290
Kulak, R. F., 158
Kulsrud, R., 390
Kulsrud, R. M., 390, 447
Kumano,, 497
Kumar, R., 149, 249
Kumosa, L., 50
Kumosa, Maciej S., 50
Kureczko, D., 452
Kurtz, H. A., 529
Kurtz, S. R., 247
Kutschera, W., 566
Kwak, Dochan, 192

## L

Laakso, H., 183, 580
Lach, J. T., 383
Lackner,, 141
Lacoste, T. D., 436
Lagae, J. F., 402, 528
Lageraaen, P. R., 124
Lagerraaen,, 115
Lagoudas, Dimitris C., 5, 155
Laguna, G. R., 185
Laird, C., 104
Laird, William M., 371
Laity, J. E., 290, 569
Lam, N. Q., 111
Lamanna,, 490
Lambrakos, S. G., 163
Lane, P., 534
Lang, C., 318
Lang, M., 467
Langevin, Y., 26
Langhoff, Stephen R., 76, 98
Langish, S., 445
Lanman, Richard T., 23
Lanni,, 525
Lanyi, Janos K., 311
Lapides, M. E., 191
Laporte, Nadine, 243
Larimer, J., 428
Laroche, J. R., 178, 179
Larson, B. C., 457
Larson, Kristine M., 292
Larson, Michael K., 2, 541
Larson, William E., 27
Latham, Donald C., 209
Lau, Angela, 315
Lau, E. L., 575
Lau, William K. M., 281
Lauf, R. J., 114
Laveigne,, 492
Law, D., 44
Lawler, J. E., 486
Lawrence, D. J., 579
Lazier, S. E., 444
Lazrov, R. D., 196
Lazzarin, M., 437
Leal, L. C., 419
Leax, T. R., 114
Lebacqz, J. Victor, 330
Leban, F., 156
Lebedev, V., 402
Lebien,, 165
LeBlanc, B., 450
Lebreton, J.-P., 183
Lebrun, P., 535
LeCocq, C. M., 203
LeCompte, T. J., 400, 528, 538
Lee,, 132, 245
Lee, H., 128
Lee, H. C., 260, 261
Lee, H. K., 115
Lee, J. M., 157
Lee, J. R., 166
Lee, R. L., 272
Lee, S. H. D., 250
Lee, T. H., 259
Lee, T. S. H., 509, 521
Lee, Timothy J., 415
Lee, W. W., 448
Lee, Y. E., 373, 458
Lee, Y. Y., 146
Leemann, C., 406
Lees, A. J., 78
Lefevre, T., 434
Lefort,, 385
Lehman, S. K., 222
Lehovich, A., 337
Lehrach,, 533
Lehrer, Hank, 12
Lehrer, Henry, 10
Lehrer, Henry R., 2, 10
Leidholm, C., 257

Leipuner, L., 387
Lelovic, M., 484
LeMay, J. D., 126
Lemley, J. R., 474
LeMoigne, Jacqueline, 203, 243
Lenhart, S., 408
Lenkszus, F., 536
Leong, K. H., 99, 211
Lerner, Narcinda R., 318
Leroy,, 490
Lesoinne,, 336
Lessner, E., 514
Lester, Luke F., 471
Letalick, D., 213
Letowski, Tomasz, 548
Levin, E., 513, 514
LeVine, D. M., 293, 557
Levine, Leslie, 322
Levinski, Oleg, 194
Levit, Creon, 197, 353
Levy, Alon Y., 550
Lewandowski, J. L. V., 448
Lewellen, J., 517
Lewellen, J. W., 379, 526
Lewis,, 92, 455
Lewis, E. R., 266
Lewis, Grace A., 345
Lewis, J. P., 105
Lewis, M. A., 45, 130
Lewis, N. S., 200
Li, D., 99, 487
Li, H., 456
Li, N. Y., 178, 179
Li, W., 276
Li, Z., 476
Liberatore, M. W., 46
Liberto, Joe, 543
Lichtner, P. C., 238
Lidia, S., 434
Lidia, S. M., 382
Lien, S., 43, 259
Lill, R. M., 509
Lillywhite, H. B., 319
Lillywhite, Harvey B., 319
Lin, K.-C., 55, 57, 58, 61
Lin, M., 52
Lin, Z., 448
Lindau, Manfred, 312
Lindell, I. V., 170
Lindemuth, I. R., 263
Lindenbaum, S. J., 444
Linderman, Jon K., 327
Lindseth, Paul D., 1
Lindzen, Richard S., 292
Link, R., 579
Linker, K. L., 147
Linteris, G. T., 57
Lipkin, H. J., 538
Lippert, Espen, 208
Liscum-Powell, J., 335
Litovchenko, V. G., 480
Littenberg,, 385
Little, Reed, 348
Litzinger, Thomas A., 77
Liu, C., 475
Liu, C. L., 109
Liu, C. T., 94, 116
Liu, H., 49
Liu, Han-Shou, 410
Liu, Ming-hsun, 345
Liu, P. K. T., 90
Livi, S., 206
Livingston, J. M., 287, 299
Lloyd, Steven A., 278
Lo Presti, P., 539
Lobo,, 492
Lochert, Ian J., 36
Locke, A. M., 378
Loffler, J. F., 113
Lognonne, P., 26
Logotetta, L., 62
Lohstroh, W., 89, 422, 466
Long,, 391
Long, Fred, 350
Long, M., 214
Loong, C. K., 122, 126, 127, 287, 470, 486
Lopez, G., 456
Lopez, G. P., 178
Lorence, L. J., 335
Los, S., 180
Lottes, S. A., 427
Loubriel, G. M., 175
Lovell, Jim, 25
Loveridge, L. C., 491
Lowe, L. L., 340
Lowenstein,, 494
Lowndes, D. H., 438
Lowther, A. B., 227
Loy, D. A., 61
Lozano, J., 49
LozanoBahilo, J., 491
Lu, Xuejun, 179
Lu, Y., 178, 456
Lubeck, O., 338
Lubin, J., 428
Lucas, Thomas R., 167
Luccio,, 536
Luccio, A., 429
Lucey, P. G., 576, 591
Ludewig,, 489
Ludwig, D. A., 324
Lue, J. W., 163
Lueck, Dale E., 27
Luedtke, Jacqueline R., 1
Luiten, E. E. M., 134
Lukyanov, A., 583
Lumpkin, A., 437
Lumpkin, A. H., 433, 505, 507, 511, 517, 519
Lund, J. C., 185
Luning, J., 381
Luo, J. S., 119
Lusk, E., 406
Luskin, Mitchell, 118
Lutte, Rebecca K., 2, 8
Luttge, A., 290
Lyman, J., 84
Lynch, D. K., 288, 594
Lynch, M., 403
Lyo, S. K., 372
Lyon, L. A., 68

## M

Ma, B., 129, 462, 487
MacCallum, D. O., 209
MacCarley, C. A., 144
Macdonald, D. D., 47
MacDonald, R. G., 71
MacDowell, A., 378
MacFarlane, R. E., 416
Machioane, G. A., 477
MacKay, W. W., 550
MacLow, M.-M., 560
Macmillan, J. D., 77
Macrander, A., 35
Macrander, A. T., 109
Madaras, Eric, 55
Madey, T. E., 78, 597
Magahami, Peiman G., 362
Mahajan,, 132, 133
Mahan, G. D., 161
Mahan, J. E., 182
Mahan, J. Robert, 599
Mahan, Robert P., 351
Mahood, R. O., 94, 95
Mahrt, Larry, 298
Mailunas, Raymond, 15
Mainieri, R., 181
Maiwa, H., 483
Makowiecki,, 525
Malone, R., 388, 389, 436
Mammosser, J., 488

Manges, W. W., 220
Manginell, R. P., 39
Mankinen, E. A., 227
Mann, M. K., 133
Manneschmidt, E. T., 103
Mansour, N. N., 198
Mantovani, J. G., 118
Manuel, L., 270
Mao, F., 198
Mar, A., 175
Marakushev, A. A., 586
Marchukov, V. A., 152
Marciano,, 496
Margolin, L. G., 294
Margot, J. L., 587
Margot, J.-L., 592
Maria, J. P., 483
Mariani, Ugo, 18
Maris, P., 402
Markes, B. M., 244
Marks, F. D., 305
Marks, S., 491
Markus, Thorsten, 242, 307
Marshall, A. W., 370
Marshall, J., 290
Martin, C. R., 80
Martin, I., 468
Martin, J. A., 113
Martin, J. P., 423
Martin, M. A., 217
Martin, M. C., 378
Martin, P. F., 120
Martin, R., 163
Martin, Royce Ann, 540
Martin, Steve W., 116, 121
Martindale, Chad A., 116, 121
Martinez,, 93
Martinez, M. A., 41, 89
Martinez-Frias, J. M., 215
Marushia, P. C., 547
Marzari, F., 437
Maslanik, J. A., 243
Masuda,, 373
Matis, H., 600
Matlachov, A. N., 461
Matsui, H., 110
Matsukawa, Y., 111
Mattas, R. F., 450
Maughan, A. D., 282
Mauk, Barry H., 599
Maurice, S., 579
Maxson, T., 400
May, David, 115
Mays, J., 126
Mazarakis,, 391
Mazuk, A. L., 594
Mazuk, S., 288
McAlister, Kenneth W., 3
McAloon, A., 142
McAndrews, Donald R., 350
McBride, Sharon A., 322
McCaffery, Michael R., 162
McCallen, R. C., 150
McCallum,, 92
McCarthy, John F., 273
McCarty, John L., 223
McCauley, T. G., 486, 488
McClellan, Sherrise L., 548
McClintock, William E., 205
McCoig, T. M., 80
McCormack, Ann, 319
McCoy, T. J., 577
McCreight, Craig R., 432
McDaniel, D. H., 452
McDeavitt, S. M., 102
McDonald, D., 143
McDonough, J., 391
McDonough, John H., 316
McDowell, W. P., 539
McGowan, V. R., 228
McGrail, B. P., 120
McHood, M., 236
McIntosh, R. E., 299
McKee, R., 456
McKenna, S. A., 155
McKenzie, Robert L., 567
McKinley, Richard L., 163
McKinney, S. D., 244
McKinney, W. R., 378
McLane,, 418
McLane, V., 552, 553
McLeod, Raymond S., 297
McLerran,, 124, 495
McMahon,, 202, 386
McMillan, A. D., 114
McNab, David, 360
McNeely, Michael T., 23
McNutt, Ralph L., Jr., 593
McNutt, Ralph, L., Jr., 30
McPherson, A., 510
Meade, D., 449
Medgyesi-Mitschang, L. N., 163
Mehra, Pankaj N., 359
Mehta, V. M., 281
Meier, Gerd E., 188, 190, 193
Meldrum, A., 85
Melendres, C. A., 87
Melloch, Michael R., 156
Melson, E., 315
Melton, J., 394
Menard, J., 450
Mendillo, M., 597
Menees, G. P., 31
Meneveau, Charles, 190
Menter, F. R., 5
Merchant, J., 547
Merl, R., 506
Merminga, L., 406
Messing, Gary L., 176
Mest, S. C., 573
Meyer, F. J., 482
Meyer, M. K., 40
Meyer, Mark, 6
Meyer, T., 136
Meyers, S., 271
Meyn, Larry, 22
Meza, J. C., 370
Michael, J. V., 81
Michalet, X., 436
Michelotti, L., 383
Michnoff,, 530
Michnoff, R., 388
Miksicek, Richard J., 310
Miler, D. J., 487
Milian, L. W., 124
Milillo, A., 206
Milkovich, S. M., 587
Millener,, 417, 493
Miller,, 488
Miller, D. J., 129, 475
Miller, Donna L., 330
Miller, G. E., 372
Miller, J. D., 81
Miller, J. R., 372
Miller, N. E., 326
Miller, R.H., 561
Miller, Richard L., 431
Miller, Roger E., 72
Miller, Sally A., 544
Miller, T. A., 276
Milliken, J., 149
Mills, Diane, 379
Mills, J. A., 451
Milton, S., 517
Milton, S. V., 429, 439
Minervini, L., 84
Minguez, E., 401
Mini, S. M., 486
Minnis, P., 296
Minnis, Patrick, 296
Minor, S. A., 227
Mintsev, V., 165, 166
Miriyala, N., 21
Mischke, R. E., 380
Mish, K. D., 358

Misra, A., 35, 182
Missert,, 93
Missert, N. A., 89
Mitchell,, 335
Mitchell, D. G., 577
Mitchell, J., 486
Mitchell, J. F., 468
Mitchell, R., 314
Mitchell, R. M., 244
Mitchell, T. E., 182
Mitsuishi, K., 112
Mizutani, H., 26
Mizutani, T., 394
Mock, R. C., 376
Mockler, T. T., 568
Modiano, D., 339
Moelhman, M., 133
Moeller, L. E., 572
Moersch, J. E., 240
Mohamed, A., 376
Moir, D. C., 372
Mokhov,, 495
Moldovan, N., 401
Monction, D. E., 401
Moncton, D. E., 531
Mongeau, Luc, 193
Monier, C., 178
Monje, O. A., 319
Montaner, E. P., 52
Montanez,, 489
Montequin, Rita R., 549, 550
Montgomery, Jonathan S., 51
Moog, E. R., 433
Moon, J. S., 372
Moore, P. G., 163
Moore, T., 388
Moore, W. B., 575
Moore, W. B. S., 183
Moraga, F., 408
More, K. L., 21
Morel, J. E., 335
Morey-Holton, E., 317, 321
Morfin,, 494
Morgan, T. H., 579, 584, 589, 590
Mori, Y., 502
Moriarty, T., 246
Morisette, Jeffrey, 203
Morokuma, Keiji, 68
Morris, Mark, 561
Morris, William R., 24
Morrison, David, 563
Morton, D. S., 91
Mosby,, 200
Moschetti, T. L., 86
Moser, J. C., 354
Moser, Robert, 189
Moses, C. O., 237
Moses, M. S., 364
Moskowitz,, 245
Moskowitz, P., 124, 125
Most, Michael, 21
Motta, A. T., 98
Moussavi, Massoum, 10, 13
Movshovich, R., 485
Mowry, C. D., 36
Mroczkowski, S. J., 143
Mughabghab,, 416
Muhleman, D. O., 577
Mukai, T., 26, 116
Mukku, Venkat R., 327
Mulcahy, T. M., 54
Mulhearn, P. J., 289
Muller, J., 467
Mulligan, J. B., 331
Munir, Z. A., 120
Munkholm, A., 461
Munson, D. E., 136, 140
Muntele, C. I., 33, 457
Murach, J. M., 266
Murayama, N., 113
Murchie, S. L., 204
Murchie, Scott L., 26
Murman, Scott M., 192
Murokh, A., 388, 435
Murphy, J. B., 475
Murphy, R. W., 43, 259
Murray, Keith E., 213
Murthy, G., 320, 326
Murthy, Gita, 325
Musumeci, P., 435
Muto, M., 502
Muyshondt,, 174
Muza, Stephen R., 312
Myers, R. E., 140
Myers, W. Neill, 32, 218

## N

Nagaitsev, S., 394
Nagy, Z., 487
Nahan, R., 253
Nakahata, M., 145, 260, 268
Nakano, Aiichiro, 54
Nakoaka, R. K., 123
Nakos, J. T., 159, 202
Nakotte, H., 90
Naleway, C. A., 66
Nanal, V., 413
Nanstad, R. K., 425
Narayanan, Ram M., 541
Narayanan, S., 261
Narheim, Bjorn, 30
Nash, K. L., 135
Nastasi, M., 35
Natesan, K., 74, 75, 109
Nath, S., 403
Natoli, J. Y., 441
Navarro, B. J., 316
Navarro, B.J., 321
Navidi, Meena, 324
Nayak, P. Pandurang, 550
Necker, C. T., 104
Neely, R., 150
Neil,, 435
Neilsen,, 96
Neilsen, M. K., 93
Nellums,, 165
Nelson,, 386
Netanyahu, Nathan S., 203
Netanyahuy, Nathan S., 243
Neukum, G., 205, 588, 595
Neumeyer, C., 395
New, Michael H., 311
NewMyer, David A., 23, 543
Newton,, 60
Neyman,, 131
Ng, K. Y., 503
Nguyen, L., 483
Ni, Q., 230
Nichols, A. L., 150
Nicolussi, G. K., 92, 564
Nieh, T. G., 94, 116
Nielan, P. E., 417
Nielsen, Paul H., 241
Niemann, R. C., 463
Niemczyk, M. P., 48
Niemczyk, Mary, 329
Nieplocha, J., 553
Nigam,, 201, 412
Nikolaev, Y. A., 425
Niles, Frederick A., 29
Nilsson, M., 221
Nimmo, F., 588
Ninov, V., 456
Nishi, M., 445
Nishiizumi, K., 573
Nitzan, R. L., 165
Nitzberg, Bill, 360
Noailles, L. D., 264
Noble, S. K., 589
Nocera, Daniel G., 136
Nodulman, L., 531, 537
Nolen, J., 516
Nolen, S. D., 389

Nolting, F., 381
Nonidez, W., 126
Noorishad, J., 226
Norberg, O., 579
Noreen, Eric D., 573
Norem, J., 518, 535
Norman, M. R., 487
Normann,, 250
Norseng, M. S., 454
Norsworthy, G., 257
Northam, Gary J., 554
Norton, D. P., 373, 456, 458
Norum, B. E., 391
Nowicki, A. W., 118
Nowlan, M. J., 266
Nuhn,, 490
Nukala, P. K., 225
Nunez, L., 81
Nunn, S. D., 115
Nusser, M. A., 220, 222
Nygren, R., 452
Nyquist, J. E., 237

## O

O, 41, 44, 175, 181, 344, 345, 348, 353
Obaldia, Nicanor, 311
Oberkampf, W. L., 343
Oberli,, 490
Oberst, J., 205
Oelgoetz, Peter A., 218
Ogata, S., 462
Ognibene, T. J., 436
Ohara,, 331
OHara, D., 324
OHare, J. J., 78
Ohnuki, S., 111
OHolleran, T., 127
Oide,, 490
Okamoto,, 490
Okamoto, P. R., 111
Okeefe, S., 303
Oldenburg, C., 44
Oliker, L., 357
Olivier, S. S., 430
Olkin, I., 370
Olsen, B., 394
Olsen, Karl Erik, 162
Olson, Lawrence E., 18
Olson, R. E., 376
Olsson, F., 213
Olynick, Dave, 189
Olynick, David R., 3
Orasanu, Judith, 543, 544, 545
Orland,, 496
Ormiston, Robert A., 17
Orr, R. D., 120
Orsini, S., 206
Orth, Reid N., 312
Ortiz, G., 468
Osborn, R., 473
Osborne, P. E., 73
Osgood, R. M., 247
Osleeb,, 342
Oslick, J., 572
Ostroumov, P. N., 514
Oswald, Lawrence, 115
Otahal, T. J., 347
Otero, I. J., 358
Ottoboni, V., 162
Ouzounov, Dimitar, 293
Overmyer,, 471
Ozawa, M., 287, 486
Ozyuzer, L., 474

## P

Paar, Christof, 363
Pacala, S. W., 303
Padmore, H., 438
Padture, Nitin P., 34
Paige,, 496
Pak, Hon, 311
Palmer, C. A., 143
Palmer, Grant, 189
Palmer, P. T., 275
Palmer, Peter T., 76
Palmer, Robert D., 541
Palumbo, P., 578
Panchal, C. B., 48
Pang, Y., 384
Pantelides, S. T., 458
Pantuso, J. G., 159
Pao, H. Y., 171
Papadimitriou, V., 400
Papanicolaou, George C., 367
Papazoglou,, 416
Papka, M. E., 346
Parazynski, Scott E., 325
Pardo, R. C., 518
Park, C., 373, 458
Park, Chung Sik, 31
Park, J. H., 90, 110
Parker, G. G., 156
Parker, T. J., 574
Parkhutik, V., 487
Parkinson, W. J., 370
Parmeter, J. E., 147
Parra, J. O., 230
Parrish, Clyde F., 27
Parsa,, 494, 525, 526
Parsa, Z., 499
Parsons, A. M., 225
Parsons, D. K., 421
Parsons, S. M., 132
Partridge, Harry, 76, 98, 412
Parzyszek, K., 553
Paschke, Timothy M., 62
Pasciak, J. E., 196
Pasky, S., 517
Patti, Anthony L., 329
Pattison, Tim, 551
Paul, J. H., 306
Paul, M., 566
Pauling,, 305
Paulus, M. J., 340
Paus, C., 400
Pawel, S. J., 103
Payne, T. L., 542
Peacock, K., 204
Peale, S. J., 587, 592, 598
Pearman, J. L., 236
Pearson, J., 487
Pearson, Jerome, 223
Pearson, Richard, 275
Pearton, S. J., 175, 467
Pedron, D., 478
Pellerano, F. A., 173, 182
Pellin, M. J., 92, 128
Pendleton, Yvonne, 564
Pendleton, Yvonne J., 562
Penney, Kent, 12
Pennycook, S. J., 456, 457
Pennyscook, S. J., 458
Penttila, S. I., 479
Peplow, D., 229
Pepper,, 555
Pereira, C., 268
Pereira, Joao A. Raposo, 284
Perez, J. M., 214
Perkins, C. J., 244
Pernambuco-Wise, P., 372
Pernice, M., 337
Persson, B., 148
Peters, T., 27
Peterson, D. W., 483
Peterson, H. A., 353
Peterson, Victor L., 563
Petkov, V., 461
Petrak, D. R., 111
Petrick, M., 253, 427
Petrini, F., 167
Petroff, Pierre M., 462

Pettersson, A., 221
Petuskey, William, 69
Peurrung, L. M., 75
Pfeiffer, Karl D., 296
Pfluger, J., 440
Pham, A. Q., 259
Phillips, D. S., 81
Phillips, Matthew, 551
Phillips, P. J., 340
Phillips, R. J., 571, 592, 598
Phillips, Roger J., 581
Picard, R., 276
Pickering, T. G., 326
Pieper, S. C., 528
Pierce, J. L., 123
Pierson,, 336
Piert, S., 308
Pieters, C. M., 589
Piette, M. A., 546
Pilat,, 492
Pillai, T. A. K., 111, 114
Piller, C., 488
Pinaud, F., 436
Pint, Bruce, 34
Piotrowiak, P., 77
Pisarski,, 496, 525
Plate, D., 491
Plummer, Dawson A., 249
Poggio, A., 171
Pohorille, Andrew, 311
Poker, D. B., 33, 457
Polk, K., 572
Pollina, R. J., 43, 234
Polzin, B. J., 53
Pomykala, J. A., 53
Poole, L., 253
Porter, J. L., 446, 512
Porter, K., 149
Pothen, Alex, 352
Potter, A. E., 579, 589, 590
Potter, J. E., 451
Potts, L. V., 590
Powell, M. D., 305
Powell, R. M., 228
Power, J., 388, 389, 519, 522
Power, J. G., 534, 535
Powers, William T., 208
Pozebanchuk, M., 217
Praphairaksit, N., 453
Predecki, Paul K., 50
Preece, D. S., 194, 235
Prentice, Andrew J. R., 590
Prestemon,, 488
Price, W. H., 41
Priestley, Kory, 239
Prinja, A. K., 335
Prothro, L. B., 229
Protopopescu, V., 408
Protopopescu, V. A., 370
Pruess, K., 44, 226
Prufert-Bebout, Lee, 307
Pruitt, S., 315
Psinakis, W. L., 236
Ptitsin,, 491, 492
Pueschel, R. F., 275, 287
Puesschel, R. F., 299
Pugh, R. D., 529
Puhl, J., 207
Pukhov, A., 448
Puskar, J. D., 94, 108
Pzekwas, Andrzej, 354

## Q

Qian,, 428
Qiang, J., 476
Qin, L. C., 488
Qiu,, 386
Qiu, Z. Q., 382
Quinlan, D. J., 338, 355
Quintana,, 202
Quintana, M. A., 262

## R

Rabas, T. J., 48
Radebaugh, R., 157
Radeka,, 525
Radeka, V., 181
Rader, D. J., 463
Radonyi, L., 160
Raitses, Y., 180
Rajic, N., 100
Rall, Jonathan A. R., 163
Ramirez, J., 315
Ramirez, Joel, 308
Ramos, Kim, 246
Ramsey, G. P., 510
Ramsey, J. M., 33
Rank, David, 558
Rathke, J., 392
Ray, R. L., 391
Raymond,, 373
Razis, Panos, 54
Read,, 493
Redmond, J. M., 482
Ree, F. H., 121
Reed, B. J., 10, 541
Reed, D. T., 130
Reeder, Robin, 209
Reese, C. C., 593
Regan, T., 381
Rehak, P., 498
Rehm, K. E., 503, 524
Rehn, L. E., 111
Reichle, D. E., 546
Reid, J. R., 294
Reidel, S. P., 229
Reifsnider, Kenneth, 50
Reilly, R. D., 108
Reinhart,, 139, 445
Reinhart, W. D., 103
Reinheimer, Alice, 172
Reinhold, J., 504
Reinovsky, R. E., 263
Reiss, Michael, 309
Reiss-Bubenheim, D., 321
Reiss-Bubenheim, Debra, 316
Reiten, J., 294
Reitsema, H., 559
Reitze,, 492
Relies, Daniel A., 310
Remer, L. A., 239
Remington, Roger W., 333
Remsberg,, 385
Ren, F., 175, 179, 467
Renfrow,, 201, 412
Renusch, D., 37
Repeta, D. J., 307
Ressler, H. E., 216
Ressouche,, 373
Rest, J., 105
Revercomb, H. E., 241
Reynolds, John R., 117
Rhykerd, C. L., 147
Ricca, Alessandra, 58
Rice, J. W., Jr., 574
Rice, Julia E., 415
Richardson, John, 195
Richardson, T. J., 251
Richmann, M. K., 130
Rickel, D., 454
Rickman, Jeffrey M., 95
Rider, Andrew, 117
Ridgeway, Gregory K., 310
Riewe,, 173
Riggan, Philip J., 284
Riggins,, 230
Rimondi, F., 383
Rindskopf, M. S., 234
Rischke,, 525
Rivenes, A., 357
Rizk, Yehia, 22
Roach,, 19

Roach, Pat, 156
Robbins, D. L., 442
Robert, John, 350
Roberts, C. D., 452
Roberts, J. J., 238
Roberts, M. L., 436
Roberts, P., 508
Roberts, W., 334
Robertson, Glen A., 28
Robinett, R. D., 156
Robino, C. V., 94
Robinson, M. S., 243, 578, 580, 591, 596
Rochau, G. A., 444
Rock, Paul B., 312
Rodler, Waldo E., Jr., 173
Rodriguez,, 60, 471
Rodriguez, Charley, 21
Rodriguez, D., 302
Rodriguez, J. A., 33
Rodriguez, M. A., 265
Roe, R., 257
Rogers, R. E., 131
Rohatgi, A., 184
Rohay, A. C., 229
Rohlsberger, R., 478
Rokhvarger, A., 124, 125
Romanovsky, Alexander, 86
Romero, V. J., 130
Romine, Peter L., 218
Ronzhim, A., 180
Roos, R. C., 244
Rooth, C. G. H., 303
Rosanov, Nikolay N., 211
Rosecrans, P. M., 91
Rosekind, Mark R., 330
Rosenmann, D., 486
Rosenthal, David, 361
Roser,, 385, 536
Roser, T., 429, 499
Ross, Muriel D., 321
Ross, P. N., 251
Rossi,, 201
Rostoker, N., 452
Rostov,, 60
Rosu, Grigore, 346
Rote, D. M., 154
Rothberg, Edward, 352
Rothman, D. H., 568
Rothschild, Lynn J., 316
Roush, Ted L., 557
Routbort, J. L., 118, 127
Rowe, M. W., 456
Roy,, 5
Rubenchik, A. M., 441
Rubinstein, F., 161
Rubinstein, R., 381
Ruby, D. S., 261, 264
Ruddle, C., 236
Ruett, U., 379
Ruggiero,, 489
Ruggiero, A. G., 376, 498
Ruggles, L. E., 446, 512
Rugh, J., 159
Ruiz, C. L., 446
Ruiz, Jose R., 543
Ruiz, Lorelei E., 544
Rule, D. W., 433
Rupp, T. D., 442
Russ, J. S., 381
Russ, W. R., 274
Russell, C. T., 591
Russell, Philip B., 287
Russell, R. W., 594
Russell, Stephen M., 62
Rustad, Gunnar, 208
Ruter, M., 440
Ruther, W. E., 47
Rutledge, C. Ken, 599
Rutqvist, J., 226
Ryan, S., 379
Ryan, S. M., 502
Ryder, P. L., 227
Ryne, R., 476
Rzepniewski, E., 461

## S

Sabatke, D. S., 378
Sabbagh, S. A., 450
Sachse, G. W., 285
Sahai, V., 91
Sahin, Ibrahin, 352
Sahu, Jubaraj, 189
Saimonson, Jay D., 275
Saini, Subhash, 352
Saito,, 386, 513
Salama, Farid, 563
Saletnik, Donald, 19
Salisbury, J. W., 571
Salmonson, J. D., 76
Samarth, N., 372
Samn, Sherwood, 367
Sampath, Sanjay, 34
Sampson,, 490
Sampson, T. E., 48
Sanders, Brian, 5
Sanders, Gerald B., 27
Sandford, Scott A., 563
Sandi, G., 91, 267
Sandord, T. W. L., 376
Santini, D., 270
Santini, D. J., 269
Santo, Andrew G., 30, 593
Sarholm, L., 148
Saricks, C. L., 154
Sarukkai, Sekhar R., 359
Sasaki,, 496
Sathaye, J., 283, 296
Sauer, L., 354
Savina, M., 212
Savina, M. R., 128
Sawyer, Christine, 323
Scanlan, S., 334
Scanlon, L. G., 42, 82, 91, 247
Scarpellini, Nanette M., 541
Schaaf, Michaela M., 2, 9, 10
Schaef, H. T., 120
Schaefer,, 513
Schaefer, E. D., 204
Schaefer, Henry F., III, 58
Schafer,, 386
Schaffner-Bielich,, 416
Schenkel,, 201
Schiavilla, R., 384
Schiff, Lewis B., 192
Schiffer, J. P., 63
Schlemm, C., 206
Schlueter, J. A., 38, 467
Schmidt, S., 452
Schneider, C. L., 142
Schneider, Steven J., 153
Schoelkopf, R. J., 173, 182
Schoenung, S., 250
Schoessow, P., 221, 470, 534, 535
Scholl, A., 381
Schorghofer, N., 568
Schramm,, 416
Schubert, G., 575
Schuerger, A. C., 314
Schultheiss, J., 392
Schultz, A. J., 90
Schultz, R. A., 596
Schulz, Mark J., 363
Schulz, W. W., 47
Schutz, A. E., 571
Schwab, M. J., 449
Schwam, D., 108
Schwank,, 179
Schwartz, D. F., 377
Schwartz, J., 414
Schwartz, S., 441
Schwartz, S. E., 277
Schwarz, R. B., 39, 81, 83
Schweitzer, D., 467

Schwenterly, S. W., 134
Schwinkendorf, W. E., 547
Scott, D., 409
Scott, E. R. D., 595
Scott, M., 269
Scoville, John, 567
Scribner, K. A., 325
Scurlock, J. M. O., 133
Seager, C. H., 60
Searson, Peter C., 68
Sedlet, J., 46
Seglie, Ernest A., 369
Seifert, S., 148, 415
Selenyi, E., 160
Selkowitz, S. E., 546
Semenov, V. V., 152
Sengoer, T., 398, 484
Serduke, F. J. D., 401
Sereno, N. S., 433, 506, 519, 527
Settergren, Daniel J., 16
Setzer, Alberto, 284
Seweryniak, D., 424
Shack, W. J., 47, 110
Shadwick, B. A., 367
Shafer, Kenneth W., 173
Shafer, Steven, 365
Shafto, Michael G., 333
Shams. Qamar A., 208
Shan, H., 357
Shaneyfelt,, 179
Shapira, Y., 338
Shapiro, D., 326
Shapiro, M. D., 491
Shapiro, S. M., 103
Sharma, R. P., 375
Sharma, Surendra, 31
Sharp, J. H., 306
Sharp, R., 150
Sharpe, J. J., 234
Shasharina, S., 359
Shastri, S. D., 461
Shea, T., 388
Sheehan, J., 149, 231
Sheehan, L., 441
Sheehan, L. M., 441
Sheffield, S. A., 442
Shepard, Alan, 574
Shepard, K. W., 488, 504, 514, 530, 534
Shepherd,, 335
Shepperd, W. D., 231
Shermer, Russ, 353
Sherstobitov, Vladimir E., 211
Sheth, R. K., 390
Shi, Y., 276
Shibata,, 497
Shih, Tsung-Ming A., 316
Shilling, Russell D., 548
Shilo, Mark, 21
Shin, D., 52
Shinn,, 435
Shipers, L. R., 366
Shirakabe, Y., 502
Shively, R. Jay, 330
Sholander, P., 362
Short, S. M., 486
Shoup, R. W., 398
Shramstad,, 51
Shu, D., 430, 538
Shum, C. K., 590
Shur,, 174
Shvets, G., 448
Sickafus, K., 84
Sickafus, K. E., 52, 476
Sidorowicz, K. V., 539
Siefken, L. J., 419
Siegal,, 471
Siemann,, 157
Sienicki, J. J., 87
Sigler, Jason, 23
Sigman, M. E., 80
Silberberg, Yaron, 349
Simmons, J. A., 372
Simon, H. D., 552
Simon, Horst, 352
Simon, Horst D., 195, 352, 359
Simon, Tom, 27
Simons, R. W., 553
Simpson, Carol, 17
Simpson, J. C., 160
Simpson, Janet P., 561
Simpson, L. J., 74
Simpson, W. W., 446, 512
Sims, William Herbert, III, 186
Simunovic, S., 115
Singh, Hanwant B., 285
Singh, J., 187
Singh, J. P., 39, 44, 357
Singleton, J., 461, 467
Sinha, S. K., 46
Sisterson, D. L., 235, 301
Sitler, Ruth L., 329
Siwajek,, 131
Skalski, J., 227, 228
Skanthakumar, S., 485
Skidmore, C. B., 81
Skinner, C. H., 445
Skinner, C. J., 564
Skinner, D. E., 266
Skocypec, R. D., 417
Skogloev, E., 565
Skoglund, P., 221
Skourikhine, A. N., 339
Slade, M. A., 587, 592
Slade, M. A., III, 575
Slate, J. L., 227
Slatter, Steven R., 16
Slavin, J. A., 291
Slayton, Donald, 574
Slayton, Donald K., 601
Sloan, Teresa Ann, 8
Smartt, H. A., 343
Smith,, 418, 489
Smith, Amie M., 599
Smith, C. A., 41, 123
Smith, D. A., 293
Smith, D. E., 592, 598
Smith, D. L., 110, 163, 183, 420
Smith, D. S., 135, 261
Smith, Dennis, 344, 353
Smith, Dennis A., 207
Smith, H. V., 519
Smith, J. L., 140
Smith, J. R., 215
Smith, L. L., 36
Smith, M. F., 108
Smith, P., 144
Smith, P. J., 337
Smith, R. A., 340
Smith, Roy M., 330
Smith, Russell, 10, 12
Smith, Russell L., 10
Smith, S. A., 335
Smith, Suzanne D., 332
Smith, W., Jr., 296
Smith-Cruz, Lisa L., 311
Smithpeter,, 165
Smolarkiewicz, P. K., 294
Smolsky, I., 459, 469
Smorchikova, I. P., 372
Snow, W. M., 83
Snyder, Erik L., 16
So, R. M. C., 187
Soderholm, L., 482, 485
Soderman, Paul T., 410
Sohal, M. S., 419
Sohlberg, K., 458
Sokolov, M. A., 425
Soliday, R., 517
Solomatov, V. S., 593
Solomon, S. C., 592, 598
Solomon, Sean C., 30, 581, 593
Soms, Leonid N., 211
Son,, 93
Son, S. F., 81
Song, J., 242

Song, J. J., 382
Song, M., 46, 112
Sonmez, F., 52
Sontag,, 305
Soo,, 33
Sood, A., 421
Sostero,, 536
Souers, P. C., 147
Southon, J. R., 436
Spampinato, P. T., 397
Spath, P. L., 133
Speck, J. S., 461
Speck, James S., 462
Spence, D., 516
Spencer, B. W., 87
Spencer, Charles F., Jr, 17
Spielman,, 391
Spielman, R. B., 398, 452
Spinhirne, James D., 163
Spinka, H., 374
Spires, S. V., 168
Spohnholtz, T., 128
Spolenak, R., 378
Sprague, A., 586
Sprague, A. L., 583, 594
Spudis, Paul D., 362
Squire, F. R., 134
Srinivas, S., 105
Srinivasan, G.R., 2
Srinivasan, Venkatesh, 332
Staehler, J. M., 123, 222
Stafford, Judith A., 347
Stahle, C. M., 173, 182
Standish, E. M., 592
Standish, E. M., Jr., 575
Stanek, R., 403
Stankovic, S., 90
Staple, Aaron, 567
Starr, R. D., 206
Starrs, T., 251
Stasevich, T. J., 508
Steele, M., 318
Steffan, C. E., 49
Steinvall, O., 170
Stenersen, Knut, 208
Stephens, A. G., 188
Stephenson, Lou A., 322
Stern,, 305
Sterner, U., 169
Stevens,, 253
Stevens, J. W., 244
Stevenson, Thomas R., 173, 182
Stodofsky, F., 270
Stodolsky, F., 86, 154
Stohr, J., 381
Stone, C. A., 554
Stone, Harold S., 203
Stone, L. S., 331
Stone, Robert B., 366
Storstenvik, Anders, 272
Stout, M. G., 107
Stovall, J., 403
Strain, R. V., 47, 110
Stranick, Stephan J., 68
Street, R. L., 286
Streets, D. G., 279, 280
Streiffer, S. K., 480
Stremel, Paul M., 2
Stricklin, V. E., 236
Striegnitz, J., 335
Struve,, 391
Struve, K. W., 398, 452
Stubbs, A., 60
Stubler,, 331
Studor,, 165
Stuecker, J. N., 156
Sturek, Walter B., 188
Sturek, Walter B., Sr, 3
Stute, Nicholas J., 548
Stutz, John, 369
Stutz, R. A., 545
Stygar, W. A., 398
Sud, Yogesh C., 281
Sullivan,, 342
Sullivan, J. P., 89
Sullivan, Z., 531, 533
Sumida, David S., 209
Summers, D. J., 396
Summons, Roger E., 291, 314
Sun, Degui, 179
Sun, J. G., 111, 114, 222
Sun, K., 57
Sun, Sidney, 332
Sundaram, M., 200
Sundelin, R., 406
Sunderesan, Mannur J., 363
Sunderland, P. B., 55, 57
Sunwoo, A., 160
Susan, D. F., 94
Suschev, V. G., 152
Sutherland, J. C., 431
Sutherland, S. F., 266
Suzuki, S., 486
Svec, W. A., 48
Svenes, Knut, 30
Svitek, J., 245
Swank, Jeff, 248
Swanson, Keith, 560
Swanson, L. H., 222
Sward, Ricky E., 344
Swartz, William H., 278
Sweatt, W. C., 378
Sweeney, M. D., 274, 275
Sweet, J. N., 483
Swegle,, 72
Sweider, D. R., 430
Swindeman, R., 138
Symington, J. A., 461, 467
Syphershers, M., 383
Szaloki, I., 233
Szoboszlay, Zoltan, 17
Szostak, Jack W., 311
Szweda, A., 114

## T

Tabita, F. R., 306
Taboada, John M., 179
Tai, C., 60
Taiwo, T. A., 425
Takacs,, 428
Takagi, A., 502
Talamas, E., 155
Talbot, Peter D., 6
Talbot, R., 285
Taleyarkhan, R. P., 408
Taljat, B., 138
Tallant, D. R., 60
Tamura, N., 378, 457
Tan, Zhiqiang, 354
Tanaka, K. L., 573
Tangyunyong,, 174
Tannenbaum, M. J., 374
Tanner,, 492
Tanre, D., 239
Tarman, T., 362
Tarry, Scott E., 2
Tata, X., 533
Tayloe, R., 380
Taylor, B., 185
Taylor, Eric S., 32
Taylor, F., 142
Taylor, G. J., 591, 595
Taylor, J., 300
Taylor, Kirk D., 555
Taylor, Will, 369
Taylor, WIlliam R., 248, 249
Taylor, William R., 248
Tayor, L. M., 358
Telschow, K. L., 408
Temi, Pasqiale, 558
Tepikian, S., 388
Terray, Eugene, 191
Terry, J. H., 476

Teskey, R., 233
Tetenbaum, M., 126, 472
Teter, D. F., 78, 449
Thacher, P. D., 253
Thackerary, M. M., 269
Thackeray, M. M., 90, 251
Thales, Marcelo Cordeiro, 239
Theofilis, Vassilios, 368
Thevuthasan, S., 85
Thieme, C. L., 472
Thissel, W., 53
Thiyagarajan, P., 113, 148, 212, 267, 415
Thoma, D. J., 449
Thomale, J. M., 301
Thomas,, 252
Thomas, D. K., 116
Thomas, G., 220
Thomas, H., 252
Thomas, N., 586
Thome, R. J., 449
Thompson, David J., 24
Thornhill,, 139, 445
Thornhill, T. G., 103
Thurman-Keup, R., 529
Thynell, Stefan T., 77
Tichler, J. L., 295
Tidman, Derek A., 377
Tidwell,, 228
Tiede, D. M., 415
Tielens, A. G. G. M., 564
Tierney, B., 166
Tierney, B. L., 165, 166
Tilley, R. Ian, 274
Timmerhaus, K. D., 157
Tisone, G. C., 36
Tobak, Murray, 563
Tobin, K. W., 469
Todosow,, 489
Tokarcik-Polsky, S., 194
Tome, C., 112
Tome, C. N., 104
Tompkins, M., 135
TonThat, D. M., 454
Torcellini, P. A., 155
Torczynski, J. R., 460
Torrey, J. M., 248, 249
Toscano, W. B., 321, 326
Totemeier, T. C., 65, 66
Toth, K. S., 456
Touryan, K., 255
Townsend, M. J., 230, 231
Toy, M. Y., 398
Tozer, S., 454
Traversat, Bernard, 360
Travis, B., 104
Traweek, Kasandra T., 312
Trbojevic,, 501
Trbojevic, D., 498
Treml, C. A., 221
Trevathan, Joseph R., 27
Trimble, Jay W., 333
Trombka, J. I., 206
Trott, W. M., 78
Trouw, F. R., 70
Trowbridge, John H., 191
Trucano, T. G., 343
Truman, C. R., 191
Trzaska, Rick, 431
Tsai, H., 110
Tsai, K., 315
Tsang, C. F., 44, 226
Tsao, T. C., 60
Tu, P., 259
Tuggle, D. G., 449
Tumas, W., 47
Tumer, Irem Y., 366
Tung, Chee, 3
Turcot,, 496
Turhollow, A., 152
Turney, Mary Ann, 328, 329
Turowski, Marek, 354
Twait, D., 214
Twitty, C., 600
Tzanos, C. P., 365

## U

Udagawa,, 79
Underwood, D. G., 515, 519
Urban, D. L., 55, 57
Urie, M. W., 32
Uselton, Samuel P., 355
Usmani, Q. N., 524
Ustugov, Vladimir I., 210

## V

Valdez, J. A., 52
Valdez, P. F., 338
Valek, B., 378
Valentine, T. E., 271
Valle, Christopher R., 8
Van Grieken, R., 233
Van Hauwaert,, 131
Van Orden, K. F., 334
VanBaal,, 496
vanDam, Tonie, 292
Vandegrift, G. F., 46
Vandemark, D., 305
VanderWijngaart, Rob F., 359
Vandor,, 132
Vandra, Kartik, 410
VanHoozer, W. R., 365
Vanier, P. E., 474
VanZandt, John, 356
Varelas, N., 384
Varga, K., 377, 472
Varley, N. R., 147
Vashishta, Priya, 54
Vasques, M., 318
Vassilevski, P. S., 196
Vastano, John A., 285
Vaughey, J., 112
Vause, Nancy, 548
Veal, B. W., 464
Veazey, G., 123
Veers, P. S., 270
Veil, J. A., 254, 277
Veirs, D. K., 41
Vekemans, B., 233
Venkatapathy, E., 194
Venkataraman,, 455
Venugopalan,, 512, 513, 526
Venugopalan, A., 387
Venugopalan, R., 507
Verdier, M., 182
Verhoef, Chris, 345
Vernik, Rudi, 551
Vernikos, J., 324
Vianco,, 96
Vilpors, Steven E., 298
Vincze, L., 233
Vine, E., 296
Vinokurov, N. A., 433
Viollier, Michel, 239
Visscher, Luuk, 371
Vitek, J. M., 22
Vizkelethy,, 201
Vlasek, Scott E., 2
Vo, D. T., 48
Vogelsang,, 386
Voie, Oyvind, 272
Volakis, John, 342
Volkov, V. V., 374
vonFrese, R. R., 590
Vorobieff, Peter, 191
Voss, J. E., 57
Voth, T. E., 96
Voulgaris, George, 191
Voyiadjis, George, 54
Vyas, A., 86

Vyas, A. D., 264, 269

## W

Wach, S. T., 77
Wachal, Jocelyn, 12
Wachs, D. M., 426
Wachtel,, 331
Wade, C., 318
Wade, C. E., 324
Wade, D. C., 87
Wadsworth, J., 116
Wagh, A. S., 123
Wagner, J. S., 36
Wagner, R., 205, 588
Wagner, R. J., 595
Wagoner, D. E., 396
Wahlquist, D. R., 158
Wakefield, C., 446
Walch, Stephen P., 79
Walker, G. K., 281
Wall,, 93
Wall, F. D., 89
Wallace, J. F., 108
Wallis, G. B., 196
Walraven,, 174
Walsh,, 179, 201, 412
Walsh, E. J., 305
Walsh, Jack, 549, 550
Walsh, R. P., 372
Walstrom, P., 508
Walther, H., 354
Wambsganss, M. W., 149
Wang,, 93
Wang, C. X., 508
Wang, H. H., 70
Wang, J. G., 116
Wang, Lie, 352
Wang, S., 200
Wang, T. F., 523
Wang, Tommy J., 327
Wang, X., 138, 432
Wang, X. J., 388, 389, 434, 436
Warberg, Erik Normann, 542
Ward, J. S., 247
Warell, J., 565, 586, 596
Warwick, T., 438
Was, G. S., 91, 109, 110
Washio, M., 388
Wasielewski, M. R., 48, 74, 121, 431
Watanabe,, 79
Watenpaugh, D. E., 320, 326
Watenpaugh, Donald E., 325
Watkins, Wendell R., 202
Watson, A. B., 353
Watson, Velvin, 197
Watters, T. R., 243, 578, 596
Waugh, Terry, 12
Weatherby, J. R., 235
Weaver, James, 317
Weber, W. J., 85
Webster, L., 559
Weckmann, Stephanie, 287
Weekley, Daniel L., 288
Weggel, R. J., 374
Wegrzyn,, 132, 133
Wei,, 21, 413, 491, 492
Wei, G. C., 172
Wei, J., 500
Wei, Y., 93
Weil, Max, 309
Weinstein, Leonard M., 208
Weinstock, Charles B., 347
Welch,, 50, 455
Welch, D. O., 459
Welch, Larry D., 209
Weldon, Keri J., 330
Weller, A., 402
Wendt, J. R., 372
Wenger, D. F., 512
Wenger, H., 251
Wennersten, Miriam D., 29
Werner, A., 402
Wessel, F. J., 452
Wessendorf, K. O., 185
Westenskow, G., 382
Westerman, John F., 248, 249
Westhagen, P., 228
Westphal, Douglas L., 295
Wetteland, C. J., 78
Wetteroth, T. A., 116
Whalen, R. T., 323
Whipple, K. X., 568
White,, 335
White, A. R., 523, 527, 531
White, M. M., 524
White, Michael E., 20
Whitten, W. B., 33
Wicklund, A. B., 503
Wiederrecht, G. P., 48, 431
Wielicki, Bruce, 239
Wieliczka, David, 15
Wiencek, T. C., 102
Wiener, T., 404
Wilbur, D., 138
Wilde, M. H., 268
Wilde, Norman, 347
Wildenschild, D., 238
Wiley, Victor, 7
Wilkenhoener, R., 149, 268
Wilkinson, George, 19
Wilkison, S. L., 243
Will, R., 233
Willen,, 412
Willett, J. C., 293
Williams,, 555
Williams, A. B., 358
Williams, B. D., 204
Williams, E. K., 33, 457
Williams, George M., 172
Williams, J. R., 194
Williams, Robin G., 293
Williamson, D., 479
Willis, K. J., 85
Wills, J. M., 476
Wills, K. S., 185
Wilson,, 386
Wilson, Gregory J., 186
Wilson, J. K., 597
Wilson, Lionel, 582
Wilson, S. R., 116
Winans, R., 267
Winans, R. E., 87, 91, 148, 415
Wine, P. H., 280
Winefordner, J. D., 39
Winfree, N. A., 103
Wingate, Robert T., 223
Winkler, P., 453
Winningham, J. D., 579
Winokur,, 173
Winter, R. M., 49
Winterstein, S. R., 270
Wire, G. L., 114
Wiringa, R. B., 423
Wise, M. B., 80
Wiser, R., 149
Witkover, R., 388, 389
Witt,, 252
Witt, C., 252
Woelk, K., 69
Wolf, U., 595
Wolinsky, I., 324
Wong, C. C., 39
Wong, C. M., 76
Wong, Carla M., 275
Wong, T., 485
Woo, Alex, 342
Wood, B. D., 194
Wood, J. R., 232
Wood, William, 345
Wood, William G., 347
Woodbury, Adam D., 363
Wooden, Diane H., 559
Woodruff, W. L., 424

Woodward, E. C., Jr., 409
Wooley, R., 142
Woolley, Colleen, 548
Workman, R. L., 393
Worrells, D. Scott, 543
Wortman, David J., 34
Wosnitza, J., 469
Wozniak, J., 143
Wright,, 95
Wright, A. D., 247
Wright, C. W., 305
Wright, J. K., 112
Wright, Patricia A., 549, 550
Wright, R. Q., 416
Wu, D. D., 396
Wu, Y. S., 226

## X

Xiong, D., 547
Xu,, 363
Xu, F., 56, 57
Xu, J., 33
Xu, K., 54
Xu, Y., 234
Xu, Z., 99

## Y

Yakimenko,, 501
Yakimenko, V., 388, 389, 436
Yakshinskiy, B. V., 597
Yamada, M., 390
Yan, Jerry C., 360
Yan, Y., 476
Yang,, 201
Yang, B., 506, 517, 518
Yang, H., 59
Yang, L. H., 90
Yang, P., 264
Yarrington, P., 417
Yashin, Vladimir E., 210
Yasuda, Hirotsugu, 15
Yates, N. A., 76
Yazaki,, 497
Yazaki, K., 377
Yeboah, Yaw D., 67
Yee, W., 142
Yin, Y., 404
Yokoi, H., 454
Yong, J., 408
Yost, R. A., 76
You, C. Y., 186, 465
You, H., 487
Young, C. J., 547, 553
Young, D. L., 477
Young, Gerald P., 115
Young, John P., 328
Young, K. M., 445
Young, L., 403
Yu,, 489
Yu, B., 181
Yu, Enchao, 354
Yu, J., 393
Yu, L. H., 432, 439
Yuan, Z.-G., 55, 57
Yugo, J. J., 532
Yul, D., 308
Yusuf, S. M., 465

## Z

Zacharaia, T., 138
Zacharia, T., 349
Zachos, C., 485
Zadorozhny,, 494
Zahnle, Kevin, 560
Zaidi, S. H., 261
Zaitseva, N. P., 459
Zakharov, V. E., 304
Zamonsky, O. M., 427
Zamudio, Stacy, 312
Zapol, P., 66, 83
Zaslavsky, B., 45
Zaug, J. M., 411
Zavorin, Ilya, 203
Zavorotny, V. U., 243
Zavorotny, Valery, 14
Zawada, L. P., 123
Zayas, J. R., 358
Zebker, H. A., 581
Zhang, A. P., 175, 467
Zhang, H., 225
Zhao,, 93, 180
Zhao, C. Y., 187
Zhao, L., 461
Zheludev,, 373
Zhou, C. Q., 427
Zhou, D., 488
Zilm, K. W., 142
Zimbelman, J. R., 291
Zimmermann,, 386, 455
Zinder, S. H., 153
Ziock,, 141
Zirkle-Yoshida, M., 308, 315
Zoback, M. D., 245
Zou, P., 485
Zschiesche,, 416
Zuber, M. T., 568, 592, 598
Zuk, K. J., 172
Zurbuchen, T. H., 585, 597
Zurek, A., 53
Zutavern, F. J., 175
Zweiback, J., 413
Zweibel,, 245
Zysko, Jan A., 30